EPA/635/R-08/013C
www.epa.gov/iris

TOXICOLOGICAL REVIEW

OF

ACRYLONITRILE

(CAS No. 107-13-1)

In Support of Summary Information on the Integrated Risk Information System (IRIS)

January, 2010

NOTICE

This document is an **Interagency Science Consultation draft**. This information is distributed solely for the purpose of pre-dissemination peer review under applicable information quality guidelines. It has not been formally disseminated by EPA. It does not represent and should not be construed to represent any Agency determination or policy. It is being circulated for review of its technical accuracy and science policy implications.

U.S. Environmental Protection Agency
Washington, DC

DISCLAIMER

This document is a preliminary draft for review purposes only. This information is distributed solely for the purpose of pre-dissemination peer review under applicable information quality guidelines. It has not been formally disseminated by EPA. It does not represent and should not be construed to represent any Agency determination or policy. Mention of trade names or commercial products does not constitute endorsement or recommendation for use.

CONTENTS —TOXICOLOGICAL REVIEW OF ACRYLONITRILE
(CAS No. 107-13-1)

LIST OF TABLES

LIST OF FIGURES

LIST OF ABBREVIATIONS AND ACRONYMS

ABS	AN butadiene styrene
ABT	1-aminobenzotriazole
ADAF	age-dependent adjustment factor
ADUR	AN-derived undialyzable radioactivity
AIC	Akaike's Information Criterion
ALT	alanine aminotransferase
AMAP	amplitude of the motor action potential
AN	acrylonitrile
ASAP	amplitude of the sensory action potential
AST	aspartate aminotransferase
ATP	adenosine triphosphate
ATPase	adenosine triphosphatase
ATSDR	Agency for Toxic Substances and Disease Registry
AUC	area under the curve
BAL	broncho alveolar lavage
BMC	benchmark concentration
BMCL	95% lower bound of the BMC
BMD	benchmark dose
BMDL	95% lower confidence limit of benchmark dose
BMDS	benchmark dose software
BMR	benchmark response
BrdU	bromodeoxyuridine
BSO	buthionine sulfoximine
BUN	blood urea nitrogen
BW	body weight
CA	chromosomal aberration
CAIII	carbonic anhydrase III
CAP	compound action potential
CASRN	Chemical Abstracts Service Registry Number
CEMA	2-cyanoethyl mercapturic acid
CEO	2-cyanoethylene oxide
CEVal	N-(2-cyanoethyl)valine
CF	correction factor
CHL	Chinese hamster lung
CHO	Chinese hamster ovary
CI	confidence interval
CNS	central nervous system
con-A	concanavalin-A
CSF	cancer slope factor
CV	coefficient of variation
CYP450	cytochrome P450
DEM	diethylmaleate
DEX	dexamethasone
dGMP	deoxyguanosine-5′-monophosphate
DMSO	dimethyl sulfoxide
DNA	deoxyribonucleic acid

DPOAE	distortion product otoacoustic emission
DTH	delayed-type hypersensitivity
EC	exposure concentration
ECG	electrocardiogram
EH	epoxide hydrolase
ERK	extracellular signal-regulated kinase
EROD	ethoxyresorufin-O-deethylase
FISH	fluorescence in situ hybridization
FSH	follicle stimulating hormone
GAPDH	glyceraldehyde-3-phosphate dehydrogenase
GD	gestation day
GEI	gastric erosion severity index
GI	gastrointestinal
GJIC	gap junction intercellular communications
GSH	reduced glutathione
GSSG	glutathione disulfide
GST	glutathione-S-transferase
GSTM	GST of the μ subclass
γ-GTP	γ-glutamyl transpeptidase
Hb	hemoglobin
HbCO	carboxyhemoglobin
HbO	oxyhemoglobin
HEC	human equivalent concentration
HED	human equivalent dose
HMPA	hexamethylphosphoramide
HPLC	high performance liquid chromatography
hprt	hypoxanthine guanine phosphoribosyl transferase
IC_{50}	median inhibitory concentration
Ig	immunoglobulin
i.p.	intraperitoneal
IPCS	International Programme on Chemical Safety
IRIS	Integrated Risk Information System
IUR	inhalation unit risk
i.v.	intravenous
KCN	potassium cyanide
LC_{50}	median lethal concentration
LD_{50}	median lethal dose
LDH	lactate dehydrogenase
LEC	95% lower bound of exposure concentration
LH	luteinizing hormone
LOAEL	lowest-observed-adverse-effect level
LPS	lipopolysaccharide
MCMC	Markov chain Monte Carlo
MCV	motor conduction velocity
MDA	malondialdehyde
mEH	microsomal epoxide hydrolase
MEK	mitogen-activated/ERK-activating kinase
MEL	melatonin
MetHb	methemoglobin

MN	micronucleus, micronuclei
MNU	methylnitrosourea
MP	microsomal protein
4MP	4-methylpyrazole
NAC	N-acetylcysteine
NADP(H)	nicotinamide adenine dinucleotide phosphate (reduced)
NAS	National Academy of Sciences
NCI	National Cancer Institute
NCTB	Neurobehavioral Core Test Battery
NHA	normal human astrocyte
NIHL	noise-induced hearing loss
NIOSH	National Institute for Occupational Safety and Health
NMR	nuclear magnetic resonance
NOAEL	no-observed-adverse-effect level
NRC	National Research Council
NTP	National Toxicology Program
OBN	octave band of noise
OHC	outer hair cell
OR	odds ratio
OTC	L-2-oxothiazolidine-4-carboxylic acid
8-oxodG	8-oxodeoxyguanosine, also referred to as 8-oxo-7,8-dihydro-2′deoxyguanosine and 8-hydroxy-2′-deoxyguanosine
PB	phenobarbital
PBN	phenyl-N-tertiary-butylnitrone
PBPK	physiologically based pharmacokinetic
PBTK	physiologically based toxicokinetic
PC	partition coefficient
PCR	polymerase chain reaction
PH	phorone
PHA	phytohemagglutinin
PK	protein kinase
PMA	phorbol 12-myristate 13-acetate
PND	postnatal day
POD	point of departure
PRL	prolactine
RBC	red blood cell
RfC	reference concentration
RfD	reference dose
RLC	rat liver cell
RNA	ribonucleic acid
ROS	reactive oxygen species
RR	relative risk
SAED	serially additive expected dose
s.c.	subcutaneous
SCE	sister chromatid exchange
SCV	sensory conduction velocity
SD	standard deviation
SDH	sorbitol dehydrogenase
SEER	Surveillance, Epidemiology and End Results

SG	USEPA Supplemental Guidance for Assessing Susceptibility from Early-Life Exposure to Carcinogens
SGPT	serum glutamate pyruvate transaminase
SHE	Syrian hamster embryo
SIR	standardized incidence ratio
SMR	standardized mortality ratio
SOD	superoxide dismutase
SRBC	sheep red blood cell
STS	sodium thiosulfate
TAU	taurine
TBARS	thiobarbituric acid-reactive substances
TCPO	1,1,1-trichloropropane-2,3-oxide
6-TG	6-thioguanine
TNF-α	tumor necrosis factor
TPO	3,3,3-trichloropropylene oxide
TRX	trolox
TWA	time-weighted average
UCL	upper confidence limit
UDS	unscheduled DNA synthesis
UF	uncertainty factor
U.S. EPA	U.S. Environmental Protection Agency
v/v	volume/volume
WBC	white blood cell
WHO	World Health Organization
WT	wild-type

FOREWORD

The purpose of this Toxicological Review is to provide scientific support and rationale for the hazard and dose-response assessment in IRIS pertaining to chronic exposure to acrylonitrile. It is not intended to be a comprehensive treatise on the chemical or toxicological nature of acrylonitrile.

The intent of Section 6, *Major Conclusions in the Characterization of Hazard and Dose Response*, is to present the major conclusions reached in the derivation of the reference dose, reference concentration and cancer assessment, where applicable, and to characterize the overall confidence in the quantitative and qualitative aspects of hazard and dose response by addressing the quality of data and related uncertainties. The discussion is intended to convey the limitations of the assessment and to aid and guide the risk assessor in the ensuing steps of the risk assessment process.

For other general information about this assessment or other questions relating to IRIS, the reader is referred to EPA's IRIS Hotline at (202) 566-1676 (phone), (202) 566-1749 (fax), or hotline.iris@epa.gov (email address).

AUTHORS, CONTRIBUTORS, AND REVIEWERS

CHEMICAL MANAGER

Diana Wong, Ph.D., DABT
National Center for Environmental Assessment
Office of Research and Development
U.S. Environmental Protection Agency
Washington, DC

AUTHORS

Diana Wong, Ph.D., DABT
Ted Berner, MS
John Fox
Rosemarie Hakim, Ph.D.
Karen Hogan, MS
Amanda Persad, Ph.D.
Leonid Kopylev, Ph.D.
Paul Schlosser, Ph.D.
National Center for Environmental Assessment
Office of Research and Development
U.S. Environmental Protection Agency
Washington, DC

Roglio Tornero-Valez, Ph.D.
Office of Research and Development
U.S. Environmental Protection Agency
Washington, DC

CONTRACTOR SUPPORT

Lutz W.D. Weber, Ph.D., DABT (First Draft)
George Holdsworth, Ph.D. (First Draft)
Janusz Z. Byczkowski, Ph.D., D.Sc., DABT (First Draft)
Donna Cragle, Ph.D. (First Draft)
Virginia H. Sublet, Ph.D. (First Draft)
Oak Ridge Institute for Science and Education
Oak Ridge Associated Universities
Oak Ridge, TN

Margaret Fransen, Ph.D. (Second Draft)
Michael Lumpkin, Ph.D. (Second Draft)
Jennifer Rhoades, B.S. (Second Draft)
Peter McClure, Ph.D., DABT (Second Draft)
Environmental Science Center
SRC, Inc.
North Syracuse, NY

INTERNAL EPA REVIEWERS

James Allen, Ph.D.
NHEERL
Office of Research and Development
U.S. Environmental Protection Agency
Research Triangle Park, NC

Dave Bayliss, Ph.D.
National Center for Environmental Assessment
Office of Research and Development
U.S. Environmental Protection Agency
Washington, DC

Jerry Blancato, Ph.D.
NERL
U.S. Environmental Protection Agency
Research Triangle Park, NC

Anthony DeAngelo, Ph.D.
NHEERL
Office of Research and Development
U.S. Environmental Protection Agency
Research Triangle Park, NC

Rob Dewoskin, Ph.D.
National Center for Environmental Assessment
Office of Research and Development
U.S. Environmental Protection Agency
Research Triangle Park, NC

Lynn Flowers, Ph.D., DABT
National Center for Environmental Assessment
Office of Research and Development
U.S. Environmental Protection Agency
Washington, DC

Kate Guyton, Ph.D., DABT
National Center for Environmental Assessment
Office of Research and Development
U.S. Environmental Protection Agency
Washington, DC

Karl Jensen, Ph.D.
NHEERL
Office of Research and Development

U.S. Environmental Protection Agency
Research Triangle Park, NC

Jennifer Jinot
National Center for Environmental Assessment
Office of Research and Development
U.S. Environmental Protection Agency
Washington, DC

Channa Keshava, Ph.D.
National Center for Environmental Assessment
Office of Research and Development
U.S. Environmental Protection Agency
Washington, DC

John Lipscomb, Ph.D.
National Center for Environmental Assessment
Office of Research and Development
U.S. Environmental Protection Agency
Cincinnati, OH

Robert MacPhail, Ph.D.
NHEERL
Office of Research and Development
U.S. Environmental Protection Agency
Research Triangle Park, NC

Jeff Ross, Ph.D.
NHEERL
Office of Research and Development
U.S. Environmental Protection Agency
Research Triangle Park, NC

Cheryl Scott
National Center for Environmental Assessment
Office of Research and Development
U.S. Environmental Protection Agency
Washington, DC

Lawrence Valcovic, Ph.D.
National Center for Environmental Assessment
Office of Research and Development
U.S. Environmental Protection Agency
Washington, DC

John Whalan
National Center for Environmental Assessment
Office of Research and Development
U.S. Environmental Protection Agency
Washington, DC

1. INTRODUCTION

This document presents background information and justification for the Integrated Risk Information System (IRIS) Summary of the hazard and dose-response assessment of acrylonitrile (AN). IRIS Summaries may include oral reference dose (RfD) and inhalation reference concentration (RfC) values for chronic and other exposure durations, and a carcinogenicity assessment.

The RfD and RfC, if derived, provide quantitative information for use in risk assessments for health effects known or assumed to be produced through a nonlinear (presumed threshold) mode of action (MOA). The RfD (expressed in units of mg/kg-day) is defined as an estimate (with uncertainty spanning perhaps an order of magnitude) of a daily exposure to the human population (including sensitive subgroups) that is likely to be without an appreciable risk of deleterious effects during a lifetime. The inhalation RfC (expressed in units of mg/m^3) is analogous to the oral RfD, but provides a continuous inhalation exposure estimate. The inhalation RfC considers toxic effects for both the respiratory system (portal of entry) and for effects peripheral to the respiratory system (extrarespiratory or systemic effects). Reference values are generally derived for chronic exposures (up to a lifetime), but may also be derived for acute (≤24 hours), short-term (>24 hours up to 30 days), and subchronic (>30 days up to 10% of lifetime) exposure durations, all of which are derived based on an assumption of continuous exposure throughout the duration specified. Unless specified otherwise, the RfD and RfC are derived for chronic exposure duration.

The carcinogenicity assessment provides information on the carcinogenic hazard potential of the substance in question and quantitative estimates of risk from oral and inhalation exposure may be derived. The information includes a weight-of-evidence judgment of the likelihood that the agent is a human carcinogen and the conditions under which the carcinogenic effects may be expressed. Quantitative risk estimates may be derived from the application of a low-dose extrapolation procedure. If derived, the oral slope factor is a plausible upper bound on the estimate of risk per mg/kg-day of oral exposure. Similarly, an inhalation unit risk is a plausible upper bound on the estimate of risk per $\mu g/m^3$ air breathed.

Development of the hazard identification and dose-response assessments for AN has followed the general guidelines for risk assessment as set forth by the National Research Council (NRC, 1983). U.S. Environmental Protection Agency (U.S. EPA) Guidelines and Risk Assessment Forum Technical Panel Reports that may have been used in the development of this assessment include the following: *Guidelines for the Health Risk Assessment of Chemical Mixtures* (U.S. EPA, 1986a), *Guidelines for Mutagenicity Risk Assessment* (U.S. EPA, 1986b), *Recommendations for and Documentation of Biological Values for Use in Risk Assessment* (U.S. EPA, 1988), *Guidelines for Developmental Toxicity Risk Assessment* (U.S. EPA, 1991), *Interim*

Policy for Particle Size and Limit Concentration Issues in Inhalation Toxicity (U.S. EPA, 1994a), *Methods for Derivation of Inhalation Reference Concentrations and Application of Inhalation Dosimetry* (U.S. EPA, 1994b), *Use of the Benchmark Dose Approach in Health Risk Assessment* (U.S. EPA, 1995), *Guidelines for Reproductive Toxicity Risk Assessment* (U.S. EPA, 1996), *Guidelines for Neurotoxicity Risk Assessment* (U.S. EPA, 1998a), *Science Policy Council Handbook*: *Risk Characterization* (U.S. EPA, 2000a), *Benchmark Dose Technical Guidance Document* (U.S. EPA, 2000b), *Supplementary Guidance for Conducting Health Risk Assessment of Chemical Mixtures* (U.S. EPA, 2000c), *A Review of the Reference Dose and Reference Concentration Processes* (U.S. EPA, 2002), *Guidelines for Carcinogen Risk Assessment* (U.S. EPA, 2005a), *Supplemental Guidance for Assessing Susceptibility from Early-Life Exposure to Carcinogens* (U.S. EPA, 2005b), *Science Policy Council Handbook: Peer Review* (U.S. EPA, 2006a), and *A Framework for Assessing Health Risks of Environmental Exposures to Children* (U.S. EPA, 2006b).

The literature search strategy employed for this compound was based on the Chemical Abstracts Service Registry Number (CASRN) and at least one common name. Any pertinent scientific information submitted by the public to the IRIS Submission Desk was also considered in the development of this document. The relevant literature was reviewed through June 2009.

2. CHEMICAL AND PHYSICAL INFORMATION

AN (CASRN 107-13-1) is a three-carbon alkene carrying a nitrile substituent group as part of the terminal carbon atom (carbon 1) (Figure 2-1). Synonyms for the compound include vinyl cyanide, propenenitrile, and cyanoethylene, and there are a variety of trade names. AN is a colorless, flammable, and volatile liquid with a weakly pungent onion- or garlic-like odor. Some physical and chemical properties are shown below (NLM, 2003; IPCS, 2002; ATSDR, 1990).

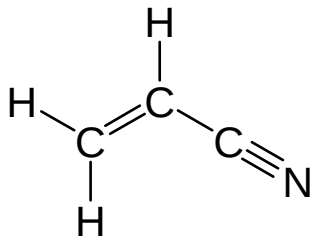

Figure 2-1. Chemical structure of AN.

Formula:	C_3H_3N
Molecular weight:	53.06
Melting point:	–83°C
Boiling point:	77.4°C
Density:	0.806 g/mL (at 20°C)
Log K_{ow}:	–0.92
Log K_{oc}:	–0.07
Vapor pressure:	100 mm Hg at 22.8°C
Henry's law constant:	8.8×10^{-5} atm-m^3/mol
Conversion factors:	1 ppm = 2.17 mg/m^3
	1 mg/m^3 = 0.46 ppm

AN is a commercially important chemical with a wide range of uses in the chemical industry. It is used in the production of acrylic and modacrylic fibers, plastics (AN butadiene styrene [ABS] and AN-styrene resins), and nitrile rubbers and as an intermediate in the production of other important chemicals, such as adiponitrile and acrylamide. AN is used in the plastics industry in the formation of surface coatings and adhesives. It is a chemical intermediate in the synthesis of antioxidants, pharmaceuticals, and dyes and, in general, for processes requiring the introduction of a cyanoethyl group into a molecule (NLM, 2003). AN is also used in clinical practice in the form of dialysis tubing (Mulvihill et al., 1992). AN was used occasionally as a fumigant insecticide for stored grain. A measure of the commercial importance of AN may be judged by the amount produced in a given year. The Agency for Toxic Substances and Disease Registry (ATSDR, [1990]) reports that 1,112,754 metric tons of AN were produced in the United States in 1987. Production had increased to 1,455,735 metric tons

by 1995 (ACS, 2003). Exposure of the general public to AN can potentially occur through migration of residual monomer in polymeric products via contact with food or water. Exposure to airborne AN is possible among members of the general population living in the vicinity of emission sources such as acrylic fiber or chemical manufacturing plants or waste sites (ATSDR, 1990). In addition, smokers are expected to be exposed to AN, which has been detected in cigarette smoke at levels of 3.2–15 mg per cigarette (IARC, 1999).

3. TOXICOKINETICS

Although only limited information on the toxicokinetics of AN in exposed humans is available, a substantial body of evidence has accumulated on the absorption, distribution, metabolism, and excretion of AN in experimental animals. The overall conclusion that can be drawn is that AN is rapidly and nearly completely absorbed, widely distributed among the tissues, and biochemically transformed into several discrete metabolic products that are excreted in the urine and, to a much lesser extent, in feces and expired air. Characterization of the excretory products of AN, with support from in vitro and in vivo kinetic data on its biotransformation, has contributed to a picture of how AN is rearranged into a series of metabolic products. Two primary processes appear to be involved: (1) interaction with reduced glutathione (GSH) and (2) cytochrome P450 (CYP450) 2E1-mediated formation of 2-cyanoethylene oxide (CEO). Each product of these processes can undergo further metabolic transformations. For example, CEO can be hydrolyzed to cyanide with further transformation to thiocyanate. Alternatively, CEO can itself interact with GSH, resulting in the formation of a number of metabolites, several of which have been identified in the urine of experimental animals.

Important data elements that have contributed to the EPA's current understanding of the toxicokinetics of AN are summarized in the following sections.

3.1. ABSORPTION

3.1.1. Studies in Humans

There are few data on the absorption of AN in humans. However, Jakubowski et al. (1987) provided some information on the topic by administering AN via inhalation to six male volunteers for 8 hours at concentrations of either 5 or 10 mg/m^3 from a chamber. Lung ventilation and retention of AN in the lungs of these individuals were measured by determining the concentrations of AN in the inhaled and expired air. A respiratory retention of 52% was estimated, based on 90 minutes to 8 hours of observation.

3.1.2. Studies in Animals

Most of the available information on the absorption of AN has come from studies in experimental animals. Young et al. (1977) carried out a series of experiments in which [1-^{14}C]-AN was administered to male Sprague-Dawley rats via the oral, inhalation, or intravenous (i.v.) route. Semiquantitative evidence of extensive absorption of AN has come from an inhalation experiment of Young et al. (1977) in which four rats/group were exposed nose only to 5 or 100 ppm AN vapor for 6 hours. Following the exposure, the animals were kept in metabolism cages and excreta were collected for 220 hours. Total recovered doses estimated

from total recovered radioactivity for the low and high exposure levels were 0.7 and 10.2 mg/kg [1-^{14}C]-AN, respectively. Substantial amounts of the recovered dose were found in urine, feces, and tissues, which indicated that AN has the capacity to be absorbed via the inhalation route (Table 3-1).

Table 3-1. Recovery of radioactivity from male Sprague-Dawley rats exposed to 5 or 100 ppm [1-^{14}C]-AN for 6 hours via inhalation

Site of recovery	5 ppm	100 ppm
	Percentage of recovered dose (mean ± standard deviation [SD])	
Urine	68.50 ± 9.38	82.17 ± 4.21
Feces	3.94 ± 0.97	3.15 ± 0.82
$^{14}CO_2$	6.07 ± 1.58	2.60 ± 0.83
Body	18.53 ± 4.68	11.24 ± 2.85
Cage wash	2.95 ± 3.95	0.85 ± 0.58
Total dose (mg/kg)	0.7	10.2

Source: Young et al. (1977).

In the gavage experiments of Young et al. (1977), animals were kept in metabolic cages after a single dose of either 0.1 or 10 mg/kg [1-^{14}C]-AN (vehicle not stated), and the fate of the radiolabel was monitored for 72 hours. As shown in Table 3-2, only about 5% of the administered radiolabel was recovered in the feces after 72 hours. By contrast, most of the administered radiolabel was recovered in the urine, carcass, and skin, with smaller fractions of the administered radiolabel expired as $^{14}CO_2$. These data suggest that at least 95% of administered AN was absorbed.

Table 3-2. Recovery of radioactivity after a single gavage dose of 0.1 or 10 mg/kg [1-^{14}C]-AN to male Sprague-Dawley rats

Recovery site	0.1 mg/kg	10 mg/kg
	Percent of dose	
Urine	34.22 ± 6.26	66.68 ± 10.6
Feces	5.36 ± 1.43	5.22 ± 1.17
Expired CO_2	4.56 ± 1.82	3.93 ± 1.79
Carcass	24.24 ± 5.02	16.04 ± 1.87
Skin	12.78 ± 1.17	10.57 ± 4.55
Total recovery	81.2	102.4

Source: Young et al. (1977).

Ahmed et al. (1983) administered a single oral dose of 46.5 mg/kg AN to male Sprague-Dawley rats in distilled water, using 50 μCi/kg of either [2,3-^{14}C]- or [1-^{14}C]-AN as a tracer.

Only 8–10% of administered radioactivity from the [2,3-^{14}C]-AN dose had been excreted in feces 72 hours after dosing, compared with 2% from orally administered [1-^{14}C]-AN during the same period. Thus, AN was readily absorbed at the gastrointestinal (GI) tract. The time course of radioactivity released from feces showed a major spike of [2,3-^{14}C]-AN-derived radiolabel after 72 hours. The delayed release suggests that at least a portion of this released radioactivity may have resulted from biliary elimination of absorbed AN. The major peak of released radiolabel from [1-^{14}C]-AN was at 24 hours postexposure, possibly indicative of a different metabolic fate for the nitrile portion of the molecule.

Kedderis et al. (1993a) administered [2,3-^{14}C]-AN orally to male F344 rats (0.09–28.8 mg/kg) and male B6C3F$_1$ mice (0.09–10 mg/kg). Three to five percent of the administered dose was recovered in the feces of rats after 72 hours. Between 2 and 8% of the dose was recovered in the feces of male B6C3F$_1$ mice. These data indicated the near-complete absorption of the compound when administered via the oral route.

3.2. DISTRIBUTION

The toxicokinetic experiments of Young et al. (1977) provided data on the deposition of radiolabel when male Sprague-Dawley rats were exposed to [1-^{14}C]-AN via inhalation, gavage, or i.v. injection. As shown in Table 3-1, an average of 11.24% of total recovered dose (10.2 mg/kg [1-^{14}C]-AN) was obtained in the tissues when a group of four rats were exposed to 100 ppm of [1-^{14}C]-AN for 6 hours via inhalation, and excreta were collected for 220 hours. Another group exposed to 5 ppm [1-^{14}C]-AN had an average of 18.53% of the recovered radiolabel (0.7 mg/kg [1-^{14}C]-AN) deposited in the tissues. When the fate of radiolabel administered by gavage was monitored, combining the recoveries of the administered radioactivity in carcass and skin gave a value of 37% for tissue deposition at the lower AN concentration (0.1 mg/kg) vs. 27% at the higher concentration (10 mg/kg) (Table 3-2), indicating possible metabolic saturation at the higher dose. The percentage of expired CO_2 was lower for the high-dose group than the low-dose group (3.93 vs. 4.56%), providing support for possible metabolic saturation.

Young et al. (1977) examined the distribution of the radiolabel among the major organs and tissues after oral and i.v. administration of [1-^{14}C]-AN. Radioactivity was detected at a range of tissues, including lungs, liver, kidneys, stomach, intestines, skeletal muscle, heart, spleen, brain, thymus, testes, skin, carcass, and blood cells. Of these, the stomach, red blood cells (RBCs), and skin appeared to be the most important deposition sites for radiolabeled AN or its metabolites, regardless of the route of administration, dose level, or time. Radioactivity found in the stomach was highest after either oral or i.v. route and was not due to unabsorbed AN since similar results were obtained with either i.v. or oral dosing.

In a follow-up time course experiment, Young et al. (1977) administered 10 mg/kg [1-^{14}C]-AN intravenously via the tail vein to three male Sprague-Dawley rats and examined the

distribution of radioactivity to the stomach and adrenal glands. The level of radioactivity in the stomach and its contents increased from 5 minutes to 24 hours postinjection. On the other hand, radioactivity was high in the adrenal gland at 5 minutes but decreased 13-fold in 24 hours. Radioactivity was observed in the bile of a single bile-duct-cannulated rat, indicating biliary excretion. Maximal radioactivity in bile was observed after 15 minutes but declined at later time points.

When both sexes of adult Sprague-Dawley rats (including some pregnant animals) and two cynomolgus monkeys were exposed orally (26 mg/kg) or intravenously (13 mg/kg) to single doses of [1-^{14}C]-AN, whole-body autoradiography from 20 minutes after injection primarily showed radioactivity in the bile, intestinal contents, and urine (Sandberg and Slanina, 1980). Other organs showing accumulation of isotope in the autoradiogram were blood, liver, kidney, lung, and adrenal cortex, in which the activity declined slowly during 24 hours. There also was uptake of the label in the stomach mucosa and hair follicles. Distribution of radioactivity in fetal tissue following i.v. and oral administration to pregnant rats was uniform and showed a low uptake compared to maternal tissue. An exception was found in the eye lens, in which the radioactivity exceeded that of the maternal blood (Sandberg and Slanina, 1980).

Jacob and Ahmed (2003a) used whole-body autoradiography to examine the distribution of 11.5 mg/kg [2-^{14}C]-AN administered orally or intravenously to male F344 rats 5 minutes and 8, 24, and 48 hours postexposure. Levels of radioactivity per gram of tissue were highest 5 minutes after oral dosing for stomach lumen and mucosa, small intestine lumen and mucosa, liver, nasal mucosa, spleen, and kidney; other tissues (including the lung, brain, spinal cord, thyroid, and testis) had peak levels at 8 hours. Covalently bound radioactivity was detected 48 hours later in stomach mucosa, blood, and hair follicles. Five minutes following i.v. administration, the highest levels of radioactivity per gram of tissue were detected in the lung, liver, spleen, small intestine lumen, kidney, epididymis, and adrenal gland. At 24 hours, tissues that showed peak levels included bone marrow, brain, lacrimal gland, and testis. Tissues with the highest level at 24 hours included the lung, liver, and bone marrow. The levels of covalent bound radioactivity (nCi/g) were higher 48 hours after i.v. exposure compared with oral exposure, with bound radioactivity retained in liver, spleen, bone marrow, lung, kidney, and adipose tissue ranging from 2.5 to 23 times higher following i.v. exposure. The only organs that retained higher levels of covalently bound radioactivity 48 hours following oral exposure were the stomach mucosa (3×) and heart blood (5.7×). The total radioactive dose retained in animals after i.v. and oral exposures were 70 and 38%, respectively. Jacob and Ahmed (2003a) concluded that the metabolism and distribution of AN is greatly influenced by the portals of entry, with a higher amount of AN metabolized and excreted following oral exposure compared with exposure by i.v. injection. Rapid delivery of AN after i.v. treatment resulted in fast conjugation and/or covalent interaction of the parent compound with biological molecules, resulting in minimal metabolism and excretion in urine or feces.

Sapota (1982) administered 40 mg/kg AN in saline, containing either 40 μCi/kg [1,2-^{14}C]-AN or [1-^{14}C]-AN to male Wistar rats, either via gavage or intraperitoneally. Tissue distribution of radioactivity as measured by liquid scintillation counting after intraperitoneal (i.p.) and oral administration showed that the highest specific radioactivity in tissue (nCi/g) was found in RBCs, liver, and kidneys. Tissue-wide recovery of the radiolabel from either [1,2-^{14}C]-AN or [1-^{14}C]-AN at 2, 8, and 24 hours after a single oral dose is shown in Table 3-3. Statistically significant differences were observed in the distribution of radioactivity from the two forms of labeled AN in RBCs, plasma, liver, and kidney at 8 and 24 hours after administration. More rapid loss of tissue radioactivity in the liver, kidneys, and brain was also observed after oral administration of [1-^{14}C]-AN than [1,2-^{14}C]-AN. These results suggested different pathways for disposition and biotransformation of the cyano and vinyl moieties of the AN molecule.

Table 3-3. Percentage recovery of radioactivity in tissues of male Wistar rats following a single oral dose of radiolabeled AN

Target organ/ tissue	Recovered radioactivity (percent of dose in tissue)					
	Distribution from [1-^{14}C]-AN			Distribution from [1,2-^{14}C]-AN		
	2 h	8 h	24 h	2 h	8 h	24 h
RBCs	5.36	4.82[a]	5.45	5.31	7.27[a]	6.72
Plasma	2.63	4.00[a]	0.50[a]	1.93	1.92[a]	1.70[a]
Liver	6.13	1.21[a]	1.00[a]	7.00	5.98[a]	2.67[a]
Kidney	1.17	0.27[a]	0.15[a]	0.82	0.77[a]	0.30[a]
Spleen	0.22	0.10	0.08	0.14	0.17	0.10
Lung	0.36	0.25	0.25	0.30	0.27	0.11
Brain	0.25	0.12[a]	0.09	0.24	0.25[a]	0.12
Total	16.1	10.8	7.5	15.7	16.6	11.7

[a]$p < 0.05$; significant difference between [^{14}CN]-AN and [1,2-^{14}C]-AN at the same time point.

Source: Sapota (1982).

In an in vivo study on the interaction of orally administered 46.5 mg/kg [1-^{14}C]-AN or 5 mg/kg K^{14}CN with rat blood, Farooqui and Ahmed (1982) reported that up to 94% of ^{14}C from AN in RBCs was covalently bound to cytoplasmic and membrane proteins. On the other hand, 90% of the radioactivity from K^{14}CN in erythrocytes was bound to the heme fraction of hemoglobin (Hb), indicating that CN^- liberated from potassium cyanide (KCN) interacted with heme. In addition, distribution of ^{14}C from erythrocytes of rats treated with [1-^{14}C]-AN showed that more than 40% of total radioactivity was localized in membrane residue, 20–35% in the globin fraction, and 11–25% in the heme fraction. In contrast, 70% of ^{14}C from K^{14}CN in red cells was localized in the heme fraction, 14–25% in globin, and 5–10% in cell membrane. The study authors concluded that KCN interacted with rat blood mainly through liberation of CN^-,

which was bound to heme. Since AN was found to be mainly covalently bound to cell membranes, AN might cause damage to RBCs by mechanisms other than the release of CN^-.

In male Wistar rats that received 40 mg/kg AN (about half the median lethal dose [LD_{50}]) by gavage in water, peak blood levels of AN (2 μg/mL) were detected 1.5 hours after dosing (Shibata et al., 2004). By 2.5 hours after dosing, blood levels of AN had dropped to less than 0.2 μg/mL. Ten hours after dosing, AN was still detectable in blood at 50 ng/mL.

Ahmed et al. (1983, 1982) studied the distribution of AN administered to male Sprague-Dawley rats by gavage with a dose equivalent to one-half the LD_{50} (46.5 mg/kg). In the first experiment (Ahmed et al., 1982), the dose additionally contained 50 μCi/kg [1-^{14}C]-AN. In the second experiment (Ahmed et al., 1983), both [2,3-^{14}C]-AN (both carbons in the vinyl moiety were radiolabeled) and [1-^{14}C]-AN were studied in rats administered an oral dose of 46.5 mg/kg.

Radioactivity from both forms of labeled AN or its metabolites initially was sequestered mainly in the stomach and stomach content, followed by the rest of the GI tract, including small and large intestines. The GI tract contained the highest levels of radioactivity up to 72 hours before beginning to decline, suggesting that AN or its metabolites were re-secreted in the stomach (Ahmed et al., 1983). In addition, radioactivity became widely distributed in all tissues within 1–6 hours after dosing, with liver, kidney, and blood showing higher radioactivity than muscle, fat, and bone (Ahmed et al., 1983, 1982). Heart, spleen, brain, and thymus showed maximum concentrations between 3 and 6 hours. By 24 hours after administration, the levels of radioactivity found in liver, kidney, and lung began to decline, resulting in 10- to several 100-fold reductions from peak concentrations over the course of the 10-day experiment. However, in several tissues, the decline of radioactivity was much lower: at 10 days postdosing, radiolabel concentrations had declined only 2.4-fold in skin, 2.9-fold in blood, 3.8-fold in spleen, and 4.9-fold in eyes, as compared with peak levels.

Two differently labeled AN preparations were administered to rats to elucidate potential differences in distribution and metabolism between the cyano and vinyl groups. One important finding of these studies was that radioactivity in blood was predominantly in the RBCs, especially for radioactivity from [2,3-^{14}C]-AN. Radioactivity from [1-^{14}C]-AN in plasma was higher than that from [2,3-^{14}C]-AN. For radioactivity from [1-^{14}C]-AN in RBCs, 40% was localized in membrane residue, 20–35% in the globin fraction, and 11–25% in the heme fraction. In contrast, 50% of radioactivity from [2,3-^{14}C]-AN was in the membrane fraction, 45% in the globin fraction, and only a trace amount in the heme fraction.

In addition, compared to [1-^{14}C]-AN administered to animals, the percentage of covalent binding of [2,3-^{14}C]-AN to proteins was significantly higher even 72 hours after dosing. Subcellular distribution of radioactivity from [2,3-^{14}C]-AN was also different from that derived from [1-^{14}C]-AN. For [2,3-^{14}C]-AN, the cytosol fraction attained the lowest covalent protein binding in tissues. The percentage of covalently bound radioactivity in tissues relative to the total increased four- to fivefold over that of the 1-hour level. At 72 hours after administration,

the highest bound radioactivity was in the mitochondrial fractions of kidney, spleen, lung, and heart. However, in liver, the microsomal fraction contained the highest radioactivity (Ahmed et al., 1983).

For [1-^{14}C]-AN, covalent binding to macromolecules in tissues remained unchanged over time. Cytosol contained the highest levels of total radioactivity in the six tissues (liver, kidney, spleen, brain, lung, and heart) selected for the study of subcellular distribution. Twenty to 40% of total radioactivity was bound to nuclear, mitochondrial, or microsomal fractions. Only 6–14% of total radioactivity was bound to cytosol over 6 hours (Ahmed et al., 1982).

Farooqui and Ahmed (1983a) demonstrated the irreversible binding of radiolabel from [2,3-^{14}C]-AN to proteins and nucleic acids in vivo. AN was administered by gavage as a bolus dose of 46.5 mg/kg (one-half LD_{50}) in distilled water to male Sprague-Dawley rats (3–4/group). Proteins were extracted by chloroform-isoamyl alcohol-phenol, and ribonucleic acid (RNA) and deoxyribonucleic acid (DNA) were isolated by hydroxyapatite chromatography. Protein binding at 1 hour after dosing was highest in spleen and stomach, followed by liver, brain, and kidney. Protein binding in spleen and stomach declined after 1 hour, whereas binding in liver, kidney, and brain increased. At 6 hours after dosing, protein binding fell to lower values in spleen and stomach but increased in other tissues. Binding plateaued in all tissues between 6 and 48 hours, with levels in spleen > liver > stomach > kidney > brain. Binding to RNA was highest in liver, stomach, and brain, with liver attaining a maximum by 6 hours and stomach and brain by 24 hours. The subsequent decline until 48 hours was also slow. DNA binding did not reach a maximum until 24 hours after dosing, with levels in brain > stomach > liver. Again, the decline of DNA-bound radioactivity during the following 24 hours was slow. Binding of AN to DNA in brain, stomach, and liver was 56, 45, and 5 μmol AN per mol DNA, respectively, at 24 hours. The study authors also calculated a covalent binding index for DNA, defined as the ratio of (μmol AN bound per mol DNA) to (mmol AN applied per kg body weight [BW]). The values for brain, stomach, and liver were 65, 52, and 6, respectively.

Silver et al. (1987) examined the distribution of 100 mg [1-^{14}C]-AN in female Sprague-Dawley rats after i.v. injection to investigate why this procedure induced acute hemorrhagic necrosis of the adrenal gland 2 hours after administration and why this damage was more prominent with i.v. injection than with oral administration. Total radioactivity was found to be highest in the blood, liver, kidney, duodenum, and adrenals 15–90 minutes following i.v. injection of the radiolabeled compound. (This result was largely in agreement with the whole-body autoradiographic findings of Sandberg and Slanina [1980] in rats and monkeys.) Total radiolabel in blood increased over this time period, whereas the total radiolabel in other organs remained constant or decreased with time. The level of covalently bound radiolabel in the adrenals was lower than that observed in blood, liver, kidney, forestomach, and glandular stomach.

Silver et al. (1987) also administered the same dose of [1-^{14}C]-AN in water by gavage to female Sprague-Dawley rats (four/group) and investigated the distribution of radiolabel up to 24 hours after dosing. Total radioactivity was highest during the first 8 hours after dosing in the blood, GI tract, liver, and kidney. At 24 hours after dosing, the highest total radioactivity was found in the blood, forestomach, and glandular stomach. The highest level of covalently bound radioactivity was found in these same tissues during the first 8 hours after dosing and remained highest in the blood and forestomach at 24 hours after dosing. The study authors concluded that their observations would not support a role of covalent binding in the hemorrhagic effect of AN on the adrenals. Rather, the initial high concentrations of radiolabel from AN might play a role in the action of AN on the adrenal gland. However, it should be noted that in both studies, the cyano carbon, not the vinyl carbons, was labeled.

The rapidity with which AN was biotransformed and distributed to the brain as its epoxide metabolite, CEO, was reported in two studies (Kedderis et al., 1993b; Roberts et al., 1991). Roberts et al. (1991) administered 4 mg/kg AN to male F344 rats and B6C3F$_1$ mice (three/group) and measured CEO levels in blood at 0.5, 1, 4, or 24 hours after dosing. Higher levels of CEO were found in rat blood than in mouse blood. In addition, CEO was cleared from mouse blood in 4 hours, but was cleared in rat blood in 24 hours. The dose dependence of CEO concentrations in blood was also evaluated. Blood CEO was measured 0.5 hours after oral dosing in F344 rats given either 0, 1, 4, 10, or 30 mg/kg AN and in B6C3F$_1$ mice given either 0, 1, 4, 8, or 10 mg/kg AN. Blood CEO concentrations increased with dose in rats and mice but at higher concentrations in rats at the same doses.

In the first experiment by Kedderis et al. (1993b), three male F344 rats and three male B6C3F$_1$ mice were administered 10 mg/kg AN in water by gavage. The rats were sacrificed 10 minutes after dosing, while the mice were sacrificed 5 minutes after dosing. CEO concentrations from blood and brains of rats and mice were measured. Higher CEO concentrations were found in the blood and brains of rats than in mice (13% higher in blood and 23% higher in brain). In addition, CEO concentration in rat blood 10 minutes after oral administration was about twice the concentration previously reported by Roberts et al. (1991) at 30 minutes after oral dosing of 4 mg/kg AN to three male F344 rats. On the other hand, CEO concentration in mice 5 minutes after oral administration was about 10 times higher than that reported at 30 minutes after oral dosing of 4 mg/kg AN to three male B6C3F$_1$ mice (Roberts et al., 1991). These results suggested that CEO was rapidly cleared in both rats and mice and that the clearance of CEO in mice was more rapid than in rats.

Kedderis et al. (1993b) also administered 3 mg/kg [2,3-^{14}C]-CEO orally to F344 rats and B6C3F$_1$ mice to determine the tissue distribution of radioactivity from labeled CEO after 2 and 24 hours. Radioactivity from labeled CEO was widely distributed in major organs of rats and mice 2 hours after administration, with the highest level of radioactivity found in the stomach and intestines of rats and mice. However, radioactivity detected in the stomach and intestines of

mice was only about 15 and 40%, respectively, of that detected in rats, suggesting that mice absorbed CEO more rapidly than rats (Kedderis et al., 1993b). By 24 hours, radioactivity decreased by 71–90% in all tissues, including the brain, liver, and lung. Stomach and intestines continued to retain the highest level of radioactivity, probably due to covalent binding of CEO to macromolecules in these organs.

Burka et al. (1994) monitored the tissue distribution of radiolabel derived from [2-^{14}C]-AN after oral dosing at 0.87 mmol/kg (46 mg/kg) to untreated, phenobarbital (PB)-pretreated, or SKF 525A pretreated male F344 rats (three/group). PB induces a number of CYP450 isozymes, including CYP2B1 and CYP2B2, whereas SKF 525A is a general inhibitor of CYP450. After 24 hours, about 10% of the administered dose in untreated rats was present in the blood with a further 4% sequestered in the tissues. In PB-pretreated rats, a 40% increase in AN-derived radioactivity was found in both the liver and glandular stomach when compared with rats treated with AN alone, with no changes in other tissues. However, AN-derived radioactivity in most tissues of SKF 525A pretreated rats were up to 278% higher, suggesting the involvement of CYP450 metabolism in the disposition of AN and/or its metabolites. (AN reacts more rapidly with tissue nucleophiles than CEO; hence, decreasing its oxidative metabolism to CEO would increase tissue binding of radiolabel.) Because PB pretreatment had little effect on tissue distribution, the isoforms of CYP450 induced by PB are probably not the ones involved in the metabolism of AN. It is known that AN is metabolized by CYP2E1, not CYP2B1 or CYP2B2, to CEO (see Section 3.3). PB might increase AN-derived radioactivity in the liver and stomach by inducing other enzymes, such as nicotinamide adenine dinucleotide phosphate (NADPH)-cytochrome CYP450 reductase.

Ahmed et al. (1996a) monitored the tissue distribution of AN-derived radioactivity in F344 rats (four/group) up to 48 hours following i.v. injection of 11.5 mg/kg of [2-^{14}C]-AN (50 μCi/kg). The study authors used whole-body autoradiography to chart a time course of tissue deposition and obtained the highest levels of activity in lung (998 nCi/mg), intestinal contents (752 nCi/mg), liver (713 nCi/mg), and spleen (539 nCi/mg) 5 minutes after dosing. Other tissues with high radiolabel at this time point were the kidney (283 nCi/mg), epididymis (266 nCi/mg), adrenal gland (241 nCi/mg), intestinal mucosa (245 nCi/mg), heart-blood (166 nCi/mg), bone-marrow (178 nCi/mg), thyroid (121 nCi/mg), adipose tissue (169 nCi/mg), and lacrimal gland (122 nCi/mg), while the brain, spinal cord, and testis had the lowest levels of radioactivity. At 8 hours after dosing, the contents of the large intestine, especially the cecum, had the highest level of radioactivity (852 nCi/mg). Radioactivity in brain (92 nCi/mg), lacrimal gland (294 nCi/mg), and thyroid (211 nCi/mg) peaked at 24 hours after dosing, while radioactivity level in bone marrow (698 nCi/mg) peaked at 48 hours. Covalent bound radioactivity, as determined after acid-extraction techniques on freeze-dried sections, was observed in the spleen, liver, bone marrow, and lung.

3.3. METABOLISM

A proposed scheme for the metabolic pathways of AN in mammals is shown in Figure 3-1. The scheme has been developed as a result of studies on the identification of urinary metabolites following acute exposure (Fennell and Sumner, 1994; Kedderis et al., 1993a; Fennell et al., 1991; Turner et al., 1989; Müller et al., 1987; Tardiff et al., 1987; Gut et al., 1985; Kopecky et al., 1980; Langvardt et al., 1980), measurements of the in vivo modulation of AN-induced toxicological and biochemical changes by enzyme inhibitors or inducers (Wang et al., 2002; Sumner et al., 1999; Burka et al., 1994; Kedderis et al., 1993c; Pilon et al., 1988a, b; Ghanayem and Ahmed, 1986; Ahmed and Abreu, 1981; Abreu and Ahmed, 1980), determination 1996a), and analysis of metabolites formed in vitro by subcellular fractions of liver, lung, and kidney in response to AN administration (Mostafa et al., 1999; Kedderis et al., 1995; Kedderis and Batra, 1993; of the subcellular distribution of metabolic products of AN (Nerland et al., 2001; Ahmed et al., Roberts et al., 1991, 1989; Hogy, 1986; Geiger et al., 1983; Ahmed and Abreu, 1981; Guengerich et al., 1981; Abreu and Ahmed, 1980).

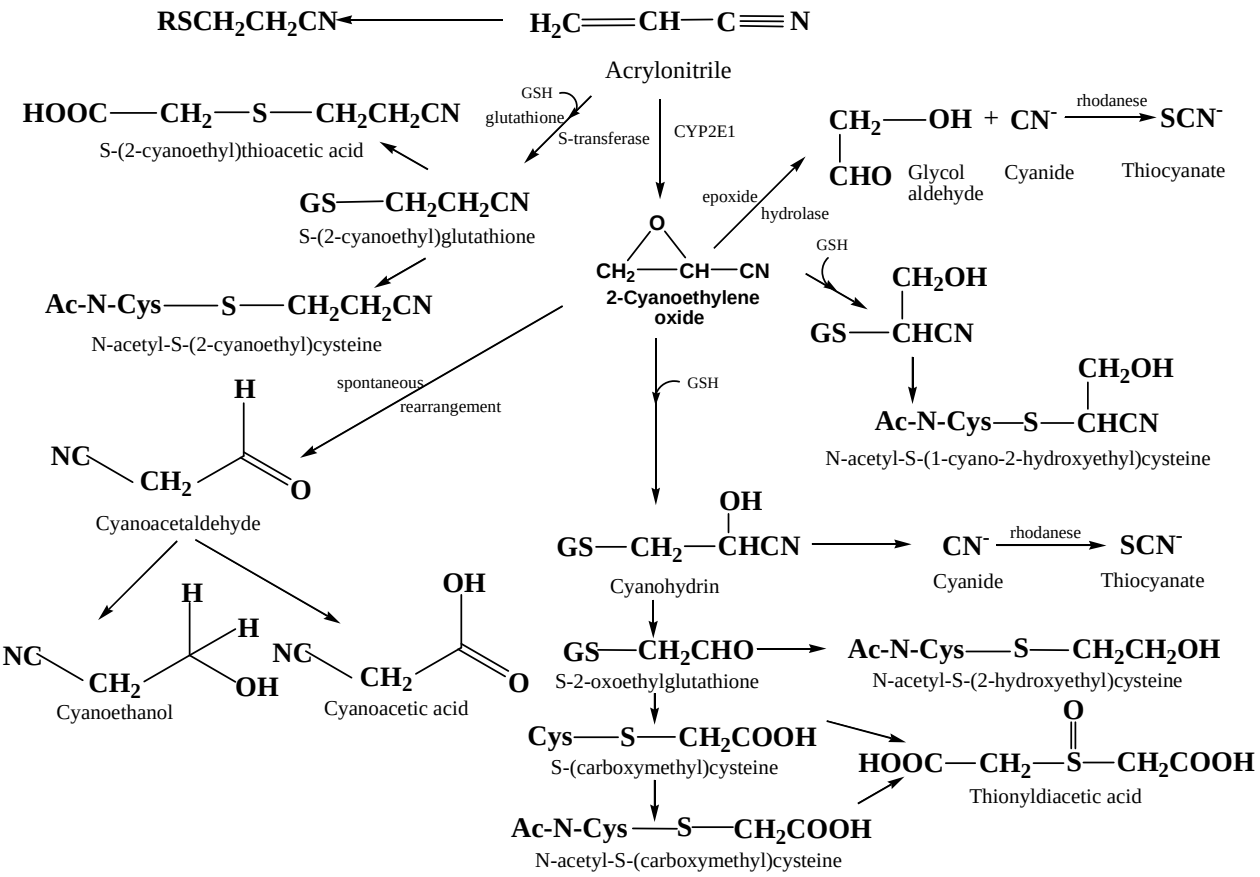

Source: National Toxicology Program (NTP) (2001).

Figure 3-1. Scheme for the metabolic transformation of AN.

Primary components of the scheme are formation of CEO by the action of mixed function oxidases (predominantly CYP4502E1), detoxification of AN by interaction with GSH, and covalent binding of AN reactive metabolite to other biological macromolecules.

In rats, CYP2E1 is present in the liver and widespread among other tissues. This isoform can be induced in the tongue, esophagus, forestomach squamous epithelia (Shimizu et al., 1990), and intestinal mucosa (Subramanian and Ahmed, 1995). It is present, albeit at levels 10–20 times lower than in liver, in such tissues as kidney and lung. It is also present in the brain (Geng and Strobel, 1993; Sohda et al., 1993). The formation of CEO has important implications for the toxicity of AN, because the intermediate has been proposed as the principal carcinogenic metabolite of AN. However, CEO can undergo a number of further transformations. These include the interaction with GSH to form a series of cysteine or N-acetyl cysteine derivatives and the production of cyanide via the action of epoxide hydrolase (EH). Subsequent detoxification of cyanide to thiocyanate is thought to occur under the action of rhodanese (Kopecky et al., 1980).

3.3.1. Oxidation of AN to CEO

Evidence for the oxidation of AN to CEO and its subsequent transformations came from a number of studies. Abreu and Ahmed (1980) studied the in vitro conversion of AN to cyanide in subcellular fractions of liver from Sprague-Dawley rats (also reported in Ahmed and Abreu [1981]). The metabolic activity was localized in the microsomal fraction and required NADPH, $MgCl_2$, and oxygen for maximal activity. Determination of the kinetic parameters (K_m and V_{max}) of the transformation of AN to cyanide pointed to a higher affinity and faster rate of product formation in microsomes from rats pretreated with CYP450-inducing agents, such as Aroclor 1254 and PB. (Six AN concentrations ranging from 10 to 300 mM were used for each preparation.) The K_m values calculated for the PB and Aroclor 1254 preparations were 54.8 and 40.9 mM, respectively, and were lower than the control (190 mM). Pretreatment of rats or addition to incubation mixtures with agents that inhibit CYP450 activity, such as SKF 525A or cobalt chloride, reduced the amount of cyanide formed by rat liver microsomes.

Abreu and Ahmed (1980) studied the effect on cyanide formation when 1,1,1-trichloro-propane-2,3-oxide (TCPO), a specific inhibitor of EH, was added to the microsomal incubation mixtures. Production of cyanide was dose-dependently reduced to 19% of control levels at TCPO concentration of 1×10^{-2} M. Abreu and Ahmed (1980) also tested the effect of sulfhydryl compounds on microsomal metabolism of AN, as measured by the rate of cyanide formation. Only cysteamine decreased cyanide formation; other sulfhydryl compounds, including GSH and cysteine, enhanced the rate of cyanide formation from AN.

Abreu and Ahmed (1980) suggested that probably more than one step was involved in the enzymatic conversion of AN to cyanide. The study authors proposed the initial product of AN oxidation to be CEO, which could then undergo a number of alternative transformations, one of

which would be non-enzymatic conversion to cyanide. That another transformation might involve EH was indicated by the decrease in cyanide formation following administration of the inhibitor TCPO. Because cyanide production was enhanced in the presence of sulfhydryl compounds, such as GSH, chemical interaction of CEO with GSH could lead to formation of cyanohydrin. Rearrangement of this cyanohydrin to an aldehyde could result in the release of cyanide. Cysteamine might diminish cyanide formation due to its inhibition of CYP450-dependent metabolism (Buckpitt et al., 1979).

Geiger et al. (1983) studied the conversion of AN to its metabolic products in isolated rat hepatocytes and demonstrated the formation of CEO and its hydrolysis to cyanide, which itself was transformed and detected as thiocyanate.

In vitro incubation of AN with liver microsomes isolated from male F344 rats pretreated with inhibitors or inducers of specific members of the CYP450 family of mixed function oxidases indicated that CYP2E1 is the major catalyst in the oxidation of AN to CEO (Kedderis et al., 1993c). The rate (V_{max}) at which rat liver microsomes oxidized AN to CEO was increased more than fivefold from V_{max} of 366 pmol CEO/minute-mg for untreated rats following acetone pretreatment, although K_m was increased from 11 to 19 μM. Because acetone is a potent inducer of CYP2E1, the data suggest that this isoform is a primary catalyst of AN epoxidation in rats. Treatment with β-naphthoflavone to induce CYP1A1 and CYP1A2 or with dexamethasone (DEX) to induce the CYP3A enzymes increased V_{max} only less than twofold, but K_m was increased by 3.5 and 5.2-fold, respectively, for AN epoxidation in these two pretreatment systems. Treatment with PB to induce CYP2B1 and CYP2B2 slightly decreased the V_{max} but increased the K_m in microsomes from rats. These studies demonstrated that other forms of CYP450 (CYP2B1, CYP2B2, and the 3A enzymes) can oxidize AN but with specific activities much lower than CYP2E1.

The effect of a number of CYP450 inhibitors on epoxidation of 1.2 mM AN by rat hepatic microsomes was investigated (Kedderis et al., 1993c). Neither SKF 525A nor metyrapone were effective inhibitors, retaining 87% of control activity. After treatment of rats with DEX or PB, SKF 525A became a more effective inhibitor, retaining 45 and 47% of control activity. Metyrapone also became a more effective inhibitor of epoxidation of AN after DEX treatment. The CYP450 ligand, 1-phenylimidazole, was a potent inhibitor of AN epoxidation (4% of control activity). Chlorzoxazone (27%), ethanol (42%), and diethyldithiocarbamate (17%) also inhibited this pathway. The changes in the degree of inhibition of epoxidation of AN following DEX and PB treatments could be interpreted as multiple CYP450 enzymes from rat hepatic microsomes were capable of oxidizing AN.

Antibodies to CYP2E1 (sheep or goat anti-rabbit CYP2E1) inhibited more than 85% of AN epoxidation in liver microsomes from untreated or acetone-treated rats but only 40 and 60% inhibition following DEX and PB treatment, respectively (Kedderis et al., 1993c), suggesting that CYP450 enzymes other than CYP2E1 might participate in the epoxidation. However, it

should be noted that the AN concentration in these in vitro studies was high (1 mM). Forms of CYP450 enzymes other than CYP2E1 might have been recruited to AN metabolism.

Kedderis et al. (1993c) also investigated the kinetics of the epoxidation of 1.2 mM AN by using human hepatic microsomes. K_m and V_{max} values for oxidation of AN by liver microsomes from six uninduced individuals ranged from 12 to 18 μM and from 129 to 315 pmol/minute-mg, respectively. Antibodies to CYP2E1 produced 58–70% inhibition of AN epoxidation catalyzed by the six human liver microsomal preparations. This suggests that, while CYP2E1 was the major catalyst of AN epoxidation in humans, other isoforms of CYP450 may also be involved.

Sumner et al. (1999) investigated the role of CYP450 in the metabolism of AN in mice. Three male wild-type (WT) mice and three to four male CYP450 2E1-null mice were treated orally with either 2.5 mg or 10 mg/kg of [1,2,3-^{13}C] AN. Urinary metabolites in samples collected over 24-h were characterized using ^{13}C nuclear magnetic resonance (NMR). In WT mice, urinary metabolites of CEO predominated, with metabolites derived from GSH conjugation at the 3-carbon of CEO accounting for 67–71%. Metabolites from GSH conjugation at the 2-carbon accounted for about 13%. Metabolites from direct GSH conjugation with the parent compound, AN, accounted for 15–21%. In the urine of CYP2E1-null mice, however, only metabolites from direct GSH conjugation were detected. Sumner et al. (1999) interpreted their data as indicating that CYP2E1 may be the only CYP450 involved in the metabolism of AN in mice.

Subramanian and Ahmed (1995), attempting to characterize the specific intestinal toxicity of AN, incubated microsomes isolated from male Sprague-Dawley rat intestinal mucosa in vitro with AN in the presence of NADPH. AN metabolism to cyanide was enhanced by the addition of sulfhydryl compounds such as GSH, cysteine, and D-penicillamine. AN metabolism to cyanide was also enhanced following the induction of microsomal proteins (MPs) by treating rats with PB (inducer of CYP2B1), β-naphthoflavone (inducer of CYP1A1), and 4-methylpyrazole (inducer of CYP2E1). AN metabolism to cyanide was inhibited to 8 and 20% of control, respectively, when dimethyl sulfoxide (DMSO) or ethanol (competitive inhibitors of CYP2E1) was added to the incubation mixtures.

Subramanian and Ahmed (1995) showed that the intestinal CYP450 isoform had a high affinity for AN, with a K_m of 1.1 μM and a V_{max} of 1,250 pmol/mg protein/minute. Addition of DMSO in varying concentrations (final 30 mM) increased the K_m of the reaction to 10 μM, but V_{max} remained unchanged. Since DMSO is a specific substrate and competitive inhibitor for CYP2E1, these studies indicated that CYP2E1 was the main CYP450 isoform that bio-activates AN in the intestine. In addition, anti-P450 3a immunoglobulin (Ig)G (which cross-reacts with rat CYP2E1) caused a concentration-dependent inhibition of the metabolism of AN to cyanide in the ethanol-induced intestinal microsomes (Subramanian and Ahmed, 1995). These results showed that CYP2E1 was the main intestinal mucosa enzyme metabolizing AN to cyanide.

Similarly, Abdel-Aziz et al. (1997) demonstrated the metabolism of AN to cyanide when AN was incubated in vitro with NADPH and a microsomal fraction prepared from Sprague-Dawley rat testis. The V_{max} of this reaction was 65 pmol CN^-/mg protein/minute, and the K_m was 88.6 µM AN. Addition of SKF 525A or benzimidazole (competitive inhibitors of CYP450) to the incubation mixture inhibited the formation of cyanide, whereas microsomes obtained from PB-treated rats increased activation of AN to cyanide. Thus, AN was metabolized in rat testis via CYP450 mixed function oxidase. Addition of GSH, L-cysteine, D-penicillamine, or 2-mercaptoethanol also enhanced the release of cyanide from AN.

The capability of rat kidney to metabolize AN to cyanide was demonstrated by Mostafa et al. (1999) in an in vitro study that investigated the mechanism by which AN caused renal toxicity. In renal subcellular fractions from Sprague-Dawley rats, the metabolism of AN to cyanide was highest in the microsomal fraction. An NADPH-generating system in the presence of magnesium ions was required for maximal activity. The V_{max} of this reaction was 118 pmol CN^-/mg protein/minute, and the K_m was 160 µM AN. Metabolism of AN to cyanide was increased when microsomes were obtained from PB-, ethanol-, 4-methylpyrazole-, and 3-methylcholanthrene-treated rats. On the other hand, addition of SKF 525A or benzimidazole to the incubation mixture inhibited AN metabolism. These data suggested that AN was metabolized in the kidney via a CYP450-dependent mixed function oxidase system. Addition of GSH, L-cysteine, cysteamine, D-penicillamine, or 2-mercaptoethanol to the incubation mixture enhanced AN metabolism.

Ahmed and Patel (1981) carried out a series of single-dose gavage experiments on male Sprague-Dawley rats and male Swiss mice at fractions of the LD_{50} values of AN and KCN. (The LD_{50} of AN is 93 mg/kg in rats and 27 mg/kg in mice; the LD_{50} of KCN is 10 mg/kg in rats and 8.5 mg/kg in mice.) Cyanide was measured and detected in blood, liver, kidney, and brain of both rats and mice 1 hour after administration in a dose-dependent manner. However, cyanide concentrations from metabolism of one LD_{50} AN in blood and tissues of rats were significantly lower than those produced from one LD_{50} of KCN. On the other hand, comparable concentrations of cyanide in blood and tissues were observed after one LD_{50} AN or KCN was administered to mice. Blood and liver contained higher amounts of cyanide per unit volume than kidney and brain (the other two organs evaluated).

Observed signs of toxicity were also different in rats and mice administered an LD_{50} of AN. Rats developed severe cholinomimetic signs including salivation, lacrimation, diarrhea, wheezing on expiration, and peripheral vasodilatation within 10 minutes after administration of 93 mg/kg AN. These signs were not observed in rats treated with KCN. Severe central nervous system (CNS) effects such as depression, convulsions, and asphyxia were observed in rats 10–20 minutes after treatment with 10 mg/kg KCN (LD_{50}). These CNS signs of cyanide toxicity were observed in AN-treated rats 2–3 hours after dosing. No physiological adverse effects were observed in rats receiving 0.25 LD_{50} AN. Mild salivation, diarrhea, and vasodilation were

observed after one-half LD_{50} AN in rats. However, in mice treated with equitoxic dose (LD_{50} 27 mg/kg) AN, CNS signs identical to those observed after KCN was administered were observed. These results demonstrated species differences in the toxicity and metabolism of AN.

Moreover, Ahmed and Patel (1981) showed that pretreatment of rats with Aroclor 1254 and PB increased AN metabolism to cyanide in rats, and pretreatment of rats with $CoCl_2$ or SKF 525A decreased blood cyanide concentrations. These results showed that the AN transformations demonstrated by Abreu and Ahmed (1980) in vitro also could take place in vivo. In addition, increased metabolism of AN to cyanide would increase CNS effects. However, acute AN toxicity was also manifested as cholinomimetic signs, which were not from cyanide.

Shibata et al. (2004) employed headspace gas chromatography to simultaneously measure blood levels of AN and its metabolite, hydrogen cyanide, following oral administration to rats. Plasma and urinary thiocyanate concentrations were also measured by the colorimetric method. Male Wistar rats that received 40 mg/kg AN (about half the LD_{50}) by gavage in water showed toxic signs such as tachycardia 1 hour later. Peak blood levels of AN (2 μg/mL) and cyanide (0.7 μg/mL) were detected 1.5 hours after dosing. By 2.5 hours after dosing, blood levels of AN had dropped to less than 0.2 μg/mL and blood levels of cyanide decreased to 0.1 μg/mL; at that time, thiocyanate was detected in plasma (20 μg/mL). Plasma thiocyanate concentrations rose over time, peaking at 5 hours (31.3 μg/mL). At the same time, excretion of thiocyanate in urine began to increase significantly. Ten hours after dosing, AN was still detectable in plasma at 50 ng/mL, but cyanide had decreased to a background level of about 5 ng/mL. The cumulative urinary elimination of thiocyanate gradually increased, and at 10 hours, about 1.2 mg thiocyanate was excreted into the urine. This amount was calculated to be 7% of the total administered AN. Urinary AN level was not measured.

The capacity for formation of CEO from AN has been demonstrated in F344 rat liver microsomes, lung microsomes, and isolated lung cells. The rate of CEO formation in rat lung was cell specific, with the Clara cell-enriched fraction having a rate of CEO formation 7 times greater than other cell fractions (Roberts et al., 1989). The overall rate of CEO formation was about 15 times greater in the livers than the lungs (Roberts et al., 1989).

Roberts et al. (1991) provided data on the kinetics of CEO formation in liver and lung microsomes isolated from male F344 rats, $B6C3F_1$ mice, and humans (Table 3-4). While CEO was produced in vitro by lung and liver microsomes in both rats and mice, the metabolite was produced at a greater rate in liver compared with lung and in mice vs. rats. These data potentially implicated the liver as the primary site of CEO formation after oral challenge with AN but suggested differences in the kinetics of CEO formation between species. The rate of CEO formation in microsomes isolated from human livers was comparable to that of F344 rats, but about 4 times lower than that of $B6C3F_1$ mice. The average rate of CEO formation in liver microsome samples from six human donors was 501 ± 112 pmol/minute-mg protein. (The almost eightfold variation in enzymatic activity among these human samples appeared to

correlate with the amount of CYP450 in each preparation.) However, after oral administration of AN, the concentration of CEO in mouse blood was about one-third that in rat blood at all doses and time points tested. Thus, blood CEO concentration did not correlate with rate of microsomal CEO formation, suggesting that species differences in detoxification of CEO might play a role in determining CEO concentrations in blood. The single human lung microsome sample tested in the study formed 0.55 pmol CEO/minute-mg protein, which was much lower than that for rat liver or lung microsomes.

Table 3-4. Apparent kinetic parameters of CEO formation from AN in B6C3F1 mice, F344 rats, and humans

Tissue	Species	V_{max} (pmol/min-mg protein)	K_m (μM)[a]
Liver	Mouse	2,801[a]	67
	Rat	667[a]	52
	Human	501[b]	Not available
Lung	Mouse	570[a]	1,229
	Rat	45[a]	1,854
	Human	0.55[c]	Not available

[a]Values are the mean of eight replicates.
[b]Value is the mean of six human donors.
[c]Value is from one human donor.

Source: Roberts et al. (1991).

Guengerich et al. (1981) used a reconstituted enzyme system containing purified rat liver CYP450 and NADPH-P450 reductase and a NADPH-generating system to oxidize AN in vitro to a metabolite that they identified colorimetrically as CEO. The extent of CEO accumulation was decreased by the addition of purified rat liver EH to the incubation medium. When 0.5 mM CEO was incubated with 30 μg/mL purified EH, the rate that CEO was hydrolyzed was 5.5 nmol/minute. The rate of disappearance of CEO (due to nonenzymatic hydrolysis) was 1.7 nmol/minute in the absence of EH or in the presence of inactivated EH. HCN was released at a rate of 1.5 nmol/minute during the hydrolysis of CEO by EH. (The rate of HCN release was 0.2 nmol/minute in the absence of EH.) The study authors suggested that the reason the HCN release was not stoichiometric with epoxide disappearance might be due to a finite level of cyanohydrin existing in solution. A K_m of 0.8 mM and a V_{max} of 300 nmol/minute-mg based on disappearance of CEO was estimated for the hydrolysis of CEO by purified rat liver microsomal EH. The half-life of CEO in 0.1 M potassium phosphate was estimated to be about 2 hours at 37°C (Guengerich et al., 1981).

Kopecky et al. (1980) also investigated the role of EH and the generation of hydrogen cyanide from AN metabolism. AN was incubated in vitro with liver microsomes isolated from female Wistar rats, with and without cofactors (NADP, Mg^{2+}, etc.) for 60 minutes. After the

incubation, the mixtures were adjusted to either pH 1.8 (acidic processing) or 6.3 (alkaline processing). Cyanide released, in the presence of cofactors, was found to be fourfold higher under alkaline processing condition than acidic processing condition. The role of EH in AN metabolism in rats was supported by the increase in cyanide released after alkaline processing, indicating the existence of a cyanohydrin intermediate (glycolaldehyde cyanohydrin) in the biotransformation of AN. (Cyanohydrins generally decompose spontaneously to hydrogen cyanide and a carbonyl compound at pH higher than 7.) Moreover, when 3,3,3-trichloro-propylene oxide (TPO), a potent inhibitor of EH, was added to the incubation mixture, the conversion of AN to cyanide was decreased by 70%. This result also provided evidence for the participation of the cyanohydrin in AN metabolism because the hydration of CEO to glycolaldehyde cyanohydrin was significantly inhibited by TPO.

Kedderis and Batra (1993) compared the rates of CEO hydrolysis, enhanced by liver cytosol and microsomes from rats, mice, and humans, to the background rate of non-enzymatic hydrolysis displayed by the chemical. [2,3-^{14}C]-CEO was incubated at pH 7.3 and 37°C for 5 minutes with liver cytosol or microsomes. [2,3-^{14}C]-CEO and its hydrolysis products were separated by high performance liquid chromatography (HPLC). The identity of the hydrolysis products could not be determined and did not correspond to aldehydes. Human hepatic microsomes enhanced the formation of hydrolysis products of CEO, whereas both human hepatic cytosol and liver cytosol and microsomes from F344 rats and B6C3F$_1$ mice had no effect on hydrolysis product formation from CEO. The study authors concluded that rodent hepatic microsomal and cytosolic EHs were not active toward CEO, contrary to conclusions developed by Guengerich et al. (1981) on rat purified microsomal EH and the conclusions by Kopecky et al. (1980).

One possible explanation that EH activity was not observed by Kedderis and Batra (1993) in microsomes from rats and mice was that their enzymatic reactions had not been optimized. No cofactors were used in the incubation mixture, and the incubation duration was only for 5 minutes. Both Kopecky et al. (1980) and Guengerich et al. (1981) used an NADPH-generating system in their incubation mixture.

Kedderis and Batra (1993) also showed that the heat-labile human EH activity was inhibited by the specific inhibitor, 1,1,1-trichloropropene oxide (median inhibitory concentration [IC_{50}] of 23 μM), indicating that EH was the catalyst in the hydrolysis of CEO. The half-life of CEO in sodium phosphate buffer (pH 7.3), as estimated from hydrolysis by human liver microsomes, was 99 minutes. Estimated K_m using liver microsomes from six individuals ranged from 0.6 to 3.2 mM. V_{max} ranged from 8.3 to 18.8 nmol hydrolysis products/minute-mg protein. The affinity of the human liver microsomal EH for CEO was relatively low, suggesting that the contribution of the hydrolysis pathway to the clearance of CEO would be small at low substrate concentrations. Increase in microsomal hydrolysis was observed after treatment of mice and rats

with PB or acetone, suggesting that CEO hydrolysis is inducible. However, treatment of rats and mice with AN did not induce hepatic EH activity towards CEO (Kedderis and Batra, 1993).

Studies that demonstrated that EH is present in rats and humans are also available. Immunoblot analysis of MPs was used by de Waziers et al. (1990) to measure EH in different organs and tissues of rats and humans. They reported that EH occurred in rat liver microsomes at 165 μg/mg protein and in human liver microsomes at 170 μg/mg protein. Therefore, the concentrations of EH in MP are similar in rats and humans. Guengerich et al. (1979) also reported that multiple forms of EH exist in rats and humans.

EH activity was demonstrated in mice in a recent study, contrary to the conclusion by Kedderis and Batra (1993). El Hadri et al. (2005) demonstrated that microsomal EH was present in WT mice, which metabolized AN administered by gavage to cyanide in a dose- and time-dependent manner. Blood cyanide levels in microsomal EH-null mice treated with a gavage dose of 0.047–0.38 mmol/kg AN were lower than levels in similarly treated WT mice. Blood cyanide level was also largely abolished in CYP2E1-null mice and in WT mice pretreated with a nonselective CYP inhibitor, 1-aminobenzotriazole (ABT), confirming that CYP2E1 was the key enzyme for the epoxidation of AN and the subsequent formation of cyanide. AN-treated CYP2E1- and mEH-null mice showed less severe symptoms of cyanide poisoning (labored breathing, lethargy, and trembling) than similarly treated WT mice (El Hadri et al., 2005). Significantly higher levels of AN-derived blood cyanide levels were observed in male mice than in female mice, suggesting gender-related differences in toxicity. Western blot analysis also demonstrated that expression of soluble EH was greater in male than female mice.

Detection and identification of urinary metabolites of AN from male F344 rats or $B6C3F_1$ mice exposed orally to [1,2,3- ^{13}C]-AN (10 or 30 mg/kg for rats, 10 mg/kg for mice), using ^{13}C NMR spectroscopy, also offered more information of its possible metabolic interactions (Fennel and Sumner, 1994; Fennel et al., 1991). As detailed in Section 3.4, some of the hypothetical metabolites of AN shown in Figure 3-1 were detected in the urine of animals exposed to AN. A major urinary metabolite in rats was N-acetyl-S-(2-cyanoethyl)cysteine, from conjugation of AN with GSH. Other metabolites, formed following oxidation of AN to CEO and subsequent conjugation to GSH, were identified as N-acetyl-S-(2-hydroxyethyl)cysteine, thiodiglycolic acid, S-carboxylmethylcysteine, and thionyldiacetic acid, all derived from addition of GSH to the 3-position of CEO. Thiocyanate was detected in urine as a metabolite of released cyanide. Moreover, N-acetyl-S-(1-cyano-2-hydroxyethyl)cysteine was formed after addition of GSH to the 2-position of CEO (Fennel and Sumner, 1994). These metabolites were also found in mouse urine.

Species differences in the extent of AN metabolism via oxidation to CEO, and subsequent conjugation of CEO with GSH, may exist. Fennell et al. (1991) and Fennell and Sumner (1994) noted differences in the relative abundance of these urinary metabolites in mice compared with rats. After oral administration of 10 mg/kg AN to mice, 80% of the urinary

metabolites were derived from CEO, most notably thiodiglycolic acid and S-(carboxymethyl)-cysteine. By contrast, these metabolites made up only 60% of metabolites in the urine from rats administered orally with 10 or 30 mg/kg AN. This difference indicated that more CEO was produced in the mouse than in rats. In addition, the ratio of metabolites derived from glutathione conjugation of CEO at the 2- and 3-positions determined the amount of cyanide released, since cyanide is released from CEO metabolites conjugated at the 3-position. This ratio was 0.43 in rats and 0.21 in mice, indicating that a greater percentage of the CEO produced in mice was metabolized to release cyanide. Thus, mice were likely to be exposed to a higher cyanide level produced from CEO, possibly accounting for the greater acute toxicity of AN in the mouse (Fennel and Sumner, 1994).

Wang et al. (2002) confirmed the central role of CYP2E1 in the metabolism of AN to cyanide via CEO. Male WT and CYP2E1-null mice were dosed by gavage with 0, 2.5, 10, 20, or 40 mg/kg AN, and cyanide was measured in blood and tissues. Expression of CYP2E1 and EH was monitored concurrently using Western blot techniques. Cyanide concentrations in blood and tissues of AN-treated WT mice increased dose dependently but remained at background levels in CYP2E1-null mice or control WT mice. Results from Western blots showed CYP2E1 to be well expressed in the liver, kidney, and lung of WT mice and not detected in tissues of CYP2E1-null mice. EH was equally expressed in both WT and CYP2E1 mice, supporting the hypothesis that CYP2E1-mediated oxidation of AN is an early step in the metabolism of AN to cyanide. The role of cyanide in the acute toxicity of AN was confirmed by the lack of acute symptoms of AN toxicity in CYP2E1-null compared with WT mice. Pretreatment of WT mice with a universal CYP450 inhibitor, ABT, likewise blocked cyanide formation and abolished the symptoms of acute toxicity. Wang et al. (2002) concluded that the metabolism of AN to CEO was exclusively catalyzed by CYP2E1.

3.3.2. Interaction of AN with GSH

A succession of research findings showed that AN conjugates with GSH, both non-enzymatically or by being catalyzed by glutathione transferase. Young et al. (1977) suggested that since the toxicity of AN was due to the parent compound (AN) or its oxidative metabolites, the cyanoethylation of sulfhydryl-containing compounds, such as GSH or cysteine, by AN represented a detoxification mechanism. This metabolic pathway was shown indeed to play a role in the detoxification of AN (Ghanayem and Ahmed, 1986; Ghanayem et al., 1985; Appel et al., 1981). The toxicity of AN would be expected to increase in severity as the GSH level becomes depleted (Benz et al., 1997a).

Kopecky et al. (1980) administered 0.75 mmol/kg AN or 0.5 mmol/kg [1-^{14}C]-AN to female Wistar rats by different routes (oral, i.p., subcutaneous [s.c.], and i.v.) and measured radioactivity and thiocyanate excreted in the urine. "Non-thiocyanate" metabolites excreted in urine constituted about two-thirds of the administered dose. Paper chromatography of the

metabolites in urine identified AN mercapturic acid as the key metabolite. Kopecky et al. (1980) proposed that there were at least two pathways for AN metabolism. The minor route was oxidative metabolism to cyanide, which was further metabolized to thiocyanate and other "non-thiocyanate" metabolites. The major route was conjugation with glutathione, catalyzed by glutathione S-alkenetransferases, to N-acetyl-S-(2-cyanoethyl)cysteine.

Further support for this proposition came from Geiger et al. (1983), who studied AN metabolism in isolated F344 rat hepatocytes. GSH levels and AN-protein binding were measured after incubating rat hepatocytes with [1-^{14}C]- or [2,3-^{14}C]-AN. GSH-adduct levels were determined by chromatographic procedures of aliquots of the trichloroacetic acid supernatant. Exposure to AN at 5 or 10 mM resulted in decrease of GSH levels to 15–20% of controls within 10 minutes. The primary radiolabeled product was S-(2-cyanoethyl)glutathione, and not S-(2-oxoethyl)GSH (the compound formed by reaction of CEO with GSH in the presence of purified GSH transferase).

Indirect evidence for the involvement of GSH in the metabolism of AN was provided by Langvardt et al. (1980, 1979), who used gas chromatography-mass spectrometry and gas chromatography-infrared spectroscopy to identify urinary components in male Sprague-Dawley rats 16 hours after exposure to [1-^{14}C]- or [2,3-^{14}C]-labeled AN by gavage. They identified two major components: the first was N-acetyl-S-(2-cyanoethyl)cysteine, which they assumed to be a product of AN conjugation with GSH, and the other was thiocyanate. A third metabolite, N-acetyl-S-(2-cyanoethyl)cysteine, was tentatively identified and was proposed by Langvardt et al. (1980) to have resulted from the action of GSH on the epoxide intermediate. The authors speculated that the detoxification of AN likely involved conjugation with GSH, and the toxicity of AN was likely affected by the status of GSH pools in target tissues, since a rapid and dose-dependent decrease in GSH stores in the liver, lungs, kidney, and adrenals was observed by Szabo et al. (1977) after i.v. injection of 1–15 mg/100 g AN to Sprague-Dawley rats. A sharp decrease in cerebral GSH concentrations occurred between 5 and 15 mg/100 g AN and correlated with the occurrence of mortality. On the other hand, oral dosing of 0.002–0.05% AN to rats for 21 days resulted in up to 25% increase in hepatic GSH and might represent a rebound phenomenon (Szabo et al., 1977).

Benz et al. (1997a) studied the time and dose dependence of the depletion of tissue GSH and tissue cyanide and the covalent binding to tissue after s.c. injection of 0, 20, 50 (LD_{10}), 80 (LD_{50}), or 115 mg/kg (LD_{90}) AN to male Sprague-Dawley rats. GSH levels in liver were the most sensitive marker of AN exposure and were depleted by 50% at 20 mg/kg, a dose without overt toxicity. At 50 mg/kg, the threshold dose for overt toxicity, GSH was depleted by ≥85% and followed by a rapid recovery of 60% at 4 hours. Liver GSH was depleted almost completely within 30 minutes when rats were injected with 80 mg/kg AN. The depletion was sustained through 120 minutes and followed by 40% recovery through the end of study period of 4 hours. Blood and brain GSH were more resistant to the GSH depleting effects of AN and were depleted

less extensively in a dose-dependent manner as the doses were in the toxic range. (The highest dose of 115 mg/kg depleted only 40% brain GSH at 2 hours.) In addition, brain GSH levels showed little capacity for recovery during the study period, unlike liver and kidney. Glandular and forestomach GSH were also dose-dependently depleted by AN treatment and were unable to recover within the study period.

GSH depletion was accompanied by a dose-dependent increase of cyanide in the blood and brain during the first 60 minutes. At the lowest dose of 20 mg/kg, blood and brain cyanide declined after 60 minutes. At the higher doses, blood and brain cyanide continued to increase to 120 minutes and then declined. Covalent binding of AN to tissue protein increased in all tissues rapidly during the first 30 minutes at all doses. At 20 mg/kg, covalent binding reached a plateau at 30 minutes. At the three higher doses, covalent binding continued to increase after 30 minutes and reached a plateau level by 2–4 hours. Benz et al. (1997a) concluded that when liver GSH was depleted, detoxification of AN was terminated. Acute AN toxicity became apparent, and a sustained increase in covalent binding to tissue protein was observed.

Further experiments by Ahmed and coworkers (Ahmed et al., 1983, 1982; Ghanayem and Ahmed, 1982) confirmed the involvement of hepatic GSH in AN metabolism. For example, when bile was collected from male Sprague-Dawley rats given a single oral dose of 46.5 mg/kg AN containing 12 μCi/kg [1-^{14}C]-AN, four metabolites were isolated and characterized in biliary extracts at 6 hours after treatment. The two main metabolites were S-cyanoethyl glutathione and N-acetyl-S-(2-cyanoethyl)cysteine (Ghanayem and Ahmed, 1982). Both were glutathione conjugates of AN. Pretreatment of rats with diethyl malate (a glutathione-depleting agent) significantly decreased or abolished all of the metabolites in the bile. The study authors proposed GSH conjugation as a major pathway of AN metabolism, probably catalyzed by glutathione transferases. The product, S-cyanoethyl glutathione, is further metabolized to N-acetyl-S-(2-cyanoethyl)cysteine. Nearly 27% of the administered dose was excreted in the bile after 6 hours (Ahmed et al., 1982).

Kedderis et al. (1995) compared the kinetics of AN and CEO interaction with GSH in vitro by measuring the formation of conjugates when [2,3-^{14}C]-labeled AN or CEO were incubated for a very short time (20 seconds for mice, 30 seconds for rats) with [glycine-2-^{3}H]-GSH in the presence of microsomal and cytosolic subcellular fractions of human, rat, or mouse liver. Because of the rapid non-enzymatic reaction of AN and CEO with GSH at pH 7.3, the steady-state kinetics of GSH conjugation were determined at pH 6.5. HPLC-mass spectrometry was used to separate and identify the conjugates, which included S-(2-cyanoethyl)-glutathione from AN; and S-(1-cyano-2-hydroxyethyl)glutathione and S-(2-cyano-2-hydroxy-ethyl)-glutathione from CEO. The apparent kinetic parameters for the conjugation reactions ($V_{max\ app}$ and $K_{m\ app}$) were estimated by fitting the Michaelis-Menten equation to the data, giving estimates of $V_{max\ app}$ for the conjugation reactions catalyzed by mouse cytosolic enzymes that were four to six times greater than those for rat cytosolic enzymes at pH 6.5 (Table 3-5). These

data suggest that mouse liver cytosolic glutathione-S-transferase (GST) has a greater capacity for conjugating AN and CEO than do rat liver enzymes. Initial velocity studies were also carried out with microsomes and cytosol from human liver, providing data to suggest that GSH conjugation of AN with human liver cytosol was broadly similar to that of rodent liver cytosol (Table 3-6).

Table 3-5. Apparent kinetic parameters for glutathione conjugation of AN and CEO at pH 6.5

Fixed substrate	Species	$V_{max\ app}$ (µmol/min-mg)[a]	$K_{m\ app}$ (GSH) (mM)[a]
AN	Rat	3.32 ± 0.29	17.47 ± 3.60
	Mouse	21.68 ± 1.75	23.39 ± 3.99
CEO	Rat	2.00 ± 0.20	9.36 ± 2.27
	Mouse	8.34 ± 0.75	15.12 ± 2.84

[a]Values are the means ± SDs of three determinations.

Source: Kedderis et al. (1995).

Table 3-6. Glutathione conjugation of AN and CEO with or without microsomal or cytosolic GST from rat, mouse, and human liver preparations

Species[a]	Substrate	Nanomoles of product		
		Non-enzymatic	Microsomal	Cytosolic
Rat	AN	25.5 ± 2.0	32.6 ± 1.9[b]	36.1 ± 3.0[b]
Mouse			31.3 ± 1.2[b]	36.6 ± 1.4[b]
Human			19.5–24.5[c]	25.2–34.4[c]
Rat	CEO	15.5 ± 1.3	16.6 ± 1.1	25.2 ± 1.1[b]
Mouse			18.9 ± 1.0[b]	25.9 ± 3.7[b]
Human			11.2–14.3[c]	12.6–14.5[c]

[a]Rodent values are means ± SDs of three determinations.
[b]Statistically significantly greater than the non-enzymatic reaction ($p < 0.05$) as calculated by the authors.
[c]Range of values for subcellular fractions prepared from six human subjects.

Source: Kedderis et al. (1995).

In the same report, Kedderis et al. (1995) described the determination of the initial velocities of non-enzymatic vs. enzymatic GSH conjugation of AN and CEO at pH 7.3 in the absence or presence of GST (Table 3-6). Both substrates reacted rapidly with GSH in a non-enzymatic reaction, and addition of hepatic microsomes or cytosol from rats and mice statistically significantly enhanced the rate of product formation from AN ($p < 0.05$). Initial velocities indicated that AN conjugated more effectively with GSH than did CEO. Hepatic cytosol enhanced the rate of product formation from CEO to a greater extent (up to 52% higher) than did microsomes, suggesting that rodent cytosolic GST is more active toward CEO than

microsomal GST. Under physiological conditions (pH 7.3), addition of liver cytosol from four out of six individuals similarly enhanced GSH conjugation with AN but not CEO. Human liver microsomes did not enhance the velocity of CEO or AN conjugation with GSH, suggesting that human microsomal GST forms do not catalyze this reaction (Table 3-6).

Similarly, Guengerich et al. (1981) studied the reaction of AN and CEO with glutathione in vitro. The pseudo first-order rate constant for disappearance of GSH at pH 7.7 (37°C) was 0.28/minute, when 0.5 mM was mixed with 0.1 M AN. The rate constant for the disappearance of GSH in the presence of 0.1 mM CEO was 0.11/minute.

Guengerich et al. (1981) also incubated [1-^{14}C]-AN or -CEO with GSH at pH 6.5 in the presence of cytosolic fraction from rat liver, human liver, or rat brain to determine GST activity. Rat liver cytosol showed GSH S-transferase activity towards AN, with a K_m of 33 mM and a V_{max} of 57 nmol/minute-mg protein. Human liver and rat brain cytosolic fraction had no activity towards AN. Rat liver also showed activity towards CEO, with activity in rat brain more than an order of magnitude lower.

The importance of sulfhydryl compounds in the detoxification of AN was shown in a number of studies, particularly by the demonstration that treatment with exogenous sulfhydryl compounds could protect the organism from the harmful effects of AN. Appel et al. (1981) reported that sulfhydryl compounds such as cysteine were effective antidotes for both orally and intraperitoneally administered lethal doses of AN in rats. N-acetyl-cysteine was ineffective when given intraperitoneally and less effective than cysteine when administered orally. The GSH-depleting effect of a single s.c. dose of AN administered to male Sprague-Dawley rats and the subsequent GI bleeding and gastric mucosal necrosis could be blocked by pretreatment with sulfhydryl-containing agents such as L-cysteine or cysteamine (Ghanayem and Ahmed, 1986; Ghanayem et al., 1985).

Benz et al. (1990) studied the effectiveness of D- or L-cysteine and N-acetyl-D-cysteine or N-acetyl-L-cysteine in the detoxification of acutely administered AN by determining the s.c. LD_{50} of AN in male Sprague-Dawley rats either administered AN alone or in combination with individual antidotes. The LD_{50} of AN alone was determined to be 74.7 mg/kg. The LD_{50} of AN when combined with other antidotes ranged from 93.3 mg/kg (with N-acetyl-D-cysteine) to 151.4 mg/kg (with L-cysteine). The antidote protective index ranged from 1.25 for N-acetyl-D-cysteine to 2.03 for L-cysteine. Thus, N-acetyl-D-cysteine was less effective than other antidotes in reducing acute lethality. Measurement of urinary N-acetyl-S-cyanoethyl cysteine, which was derived from conjugation with GSH pathway, following s.c. injection of 50 mg/kg AN alone or AN plus an antidote, indicated that none of the antidotes significantly increased the excretion of this metabolite.

Blood cyanide levels were also measured in rats at 0.5, 1, 2, 4, and 6 hours following s.c. injection of 50 mg/kg AN or AN plus an antidote. Benz et al. (1990) showed that all of the antidotes, except N-acetyl-D-cysteine, lowered blood cyanide levels. Since N-acetyl-D-cysteine

was the least effective antidote, the antidotal effectiveness of these cysteine enantiomers was related to their cyanide detoxification mechanism. Discussing these findings, Borak (1992) pointed out that, because both D- and L-cysteine provided equivalent protection against AN poisoning but only L-cysteine could be incorporated into GSH, the antidotal effects of these compounds may be unrelated to GSH repletion. In fact, since the potency of each antidote was proportional to their ability to lower cyanide levels, Borak (1992) suggested that their effects may be due to the ability of cysteine derivatives to serve as sulfur donors for the detoxification of cyanide via rhodanese-mediated transformation of cyanide to thiocyanate. The protection provided by these antidotes for cyanide poisoning from AN exposure, however, does not necessarily extend to other forms of AN-induced toxicity.

3.3.3. Covalent Binding of AN and Its Metabolites to Subcellular Macromolecules

When isolated hepatocytes from male F344 rats were incubated with 1 mM [2,3-^{14}C]-AN for 2 hours (Hogy, 1986; Geiger et al., 1983), a radiolabeled protein adduct was formed that could be characterized after the removal of residual AN and other low molecular weight products by dialysis. Analysis of the hydrolyzed non-dialyzable fraction indicated that about 75% of the radioactivity was contained in a single major peak that was chromatographically identified as S-(2-carboxyethyl)cysteine, the hydrolysis product of S-(2-cyanoethyl)cysteine, indicating direct cyanoethylation of cysteinyl residues by AN. When isolated hepatocytes were incubated with 2 mM [2,3-^{14}C]-AN for 60 minutes, Geiger et al. (1983) estimated the level of irreversible binding to protein to be 8.1 nmol/mg protein, a level of alkylation corresponding to modification of 1 in every 900 amino acid residues or roughly 1 of every 20 cysteine groups. In contrast to AN-protein binding, detection of binding of [2,3-^{14}C]-AN-derived radiolabel to DNA and RNA in hepatocytes was limited by the low level of radioactivity that could be incorporated into [^{14}C]-AN because of polymerization and microsynthesis problems and by the high level of protein binding. Therefore, hepatocytes were incubated with 2 mM [2,3-^{14}C]-AN for 60 minutes in the presence of extracellular calf thymus DNA (0.5 mg/mL) (Hogy, 1986; Geiger et al., 1983). RNA and both intracellular and extracellular DNA were isolated. The isolated RNA contained 53 pmol AN metabolites per mg RNA of which 9 pmol/mg RNA could be attributed to the contaminating protein. The isolated extracellular DNA contained 47 pmol AN adducts per mg DNA, of which 30 pmol/mg DNA could be attributed to protein. A portion of incubated extracellular DNA was further purified; alkylation of extracellular DNA was not observed at a detection limit at 3.5×10^5 bases (Geiger et al., 1983).

Hogy and Guengerich (1986) treated an F344 rat intraperitoneally with 0.6 mg/kg [2,3-^{14}C]-CEO to assess macromolecular binding in liver and brain 1 hour after treatment. DNA and RNA in liver and brain were isolated, and the amounts were estimated. Bound radioactivity was estimated by liquid scintillation counting. Covalent binding of CEO-derived radioactivity was detected in both liver and brain protein at rates of 1.1 and 1.0 alkylations per 10^6 amino

acids, respectively. However, no covalent binding to DNA or RNA could be detected at the level of 0.3 alkylations per 10^6 bases in liver and brain.

In another experiment by Hogy and Guengerich (1986), liver and brain DNA were isolated from three rats 2 hours after treatment with 50 mg/kg AN i.p. or 6 mg/kg CEO i.p. Using thin layer chromatography with fluorescent plates, the study authors were able to detect N^7-(2-oxoethyl)guanine at 0.014 and 0.032 alkylations per 10^6 DNA bases in liver for rats treated with CEO and AN, respectively. This DNA adduct was apparently derived from CEO, consistent with its recovery after AN and CEO treatment. The apparent lineage of this DNA adduct was different from the protein adduct, S-(2-cyanoethyl)cysteine, described previously, which was derived from AN.

N^7-(2-oxoethyl)guanine was only at the level of detection in rat brain DNA. In addition, 1,N^6-ethenoadenosine or 1,N^6-ethenodeoxyadenosine were not detected in liver DNA, using HPLC with fluorescence detector in the analyses of these two adducts. Binding of AN and/or CEO to DNA is also discussed in Section 4.5.1.2.1.

As discussed in Section 3.3.2, when 0, 20, 50, 80, or 115 mg/kg [2,3-^{14}C]-AN was injected subcutaneously into male Sprague-Dawley rats, GSH became almost completely depleted (>95%) in liver at 80 mg/kg within 30 minutes, while blood and brain GSH were more resistant to the depleting effect of AN. Brain and blood GSH were not affected at 20 mg/kg. The amount of cyanide in blood and brain increased dose dependently in the first hour after dosing (Benz et al., 1997a). Covalent binding to tissue proteins increased in a dose-dependent fashion during the first 30 minutes at all doses, with binding to blood proteins being 3–4 times greater than in any other tissue. Benz et al. (1997a) suggested that GSH depletion in liver was related to AN toxicity and covalent binding.

The effect of GSH depletion on the irreversible binding of AN to tissue macromolecules has been studied in male F344 rats exposed to 4 mg/kg [2,3-^{14}C]-AN either by inhalation (Pilon et al., 1988a) or gavage (Pilon et al., 1988b). Binding of radiolabel to tissue macromolecules was evaluated in control rats or rats depleted of GSH by an i.p. injection of phorone (PH)/ buthionine sulfoximine (BSO) about 30 minutes prior to AN exposure. GSH contents in control rats were as follows: liver (17.3 μmol/g), kidney (4.5 μmol/g), lung (3.1 μmol/g), stomach (5.3 μmol/g), brain (3.9 μmol/g), and blood (4.2 μmol/g). A significant depletion of GSH was produced in liver (43%), kidney (42%), and lung (22%) after PH/BSO treatment. No significant depletion of GSH was observed in blood, brain, or stomach 30 minutes after a combined PH/BSO treatment.

In the inhalation studies (Pilon et al., 1988a), three rats were exposed to initial AN concentrations of 0, 25, 50, 100, 500, or 750 ppm in a closed-circuit inhalation chamber for 240 minutes. AN was not replenished during the exposure, and the decrease in chamber AN concentration was monitored by taking samples every 10 minutes during the exposure. Uptake of AN vapor by control rats showed two distinct phases: an initial, rapid phase that lasted about

60 minutes, followed by a slower phase. An uptake rate of 4.82 mg/kg-hour was estimated for a concentration of 100 ppm using the uptake curve for the rapid phase. In GSH-depleted rats, the mortality rate was higher. The rate of AN uptake was increased in the rapid phase but decreased at 500 and 750 ppm. In the slow phase, uptake was similar to that in control rats for concentrations below 200 ppm, but was elevated at 500 and 750 ppm.

Radioactivity irreversibly associated with tissue macromolecules was measured in control rats 1, 2, 4, 6, 12, or 24 hours after the AN dose. In GSH-depleted rats, radioactivity was measured 1, 6, or 24 hours postexposure. In most tissues, the concentration of AN-derived undialyzable radioactivity (ADUR) reached a maximum in ≤1 hour in both control and GSH-depleted rats. (In the brain, ADUR levels reached a maximum in 2 hours.) The time course of ADUR levels showed a plateau from 1 to 6 hours in studied organs of control rats, followed by a decrease thereafter during the next 6 hours. This was then followed by an increase between 12 and 24 hours in the lung and kidney (but not in the brain, stomach, and liver). The time course of ADUR levels in blood showed high level 1 hour after AN administration, decreased from 6 to 12 hours, and increased from 12 to 24 hours, resulting in a maximum level at 24 hours.

Total radioactivity recovered from brain, stomach, liver, kidney, and blood decreased by 54% in GSH-depleted rats compared with controls at both 1 and 24 hours. In GSH-depleted rats, ADUR levels remained constant in all organs evaluated throughout the 24-hour postexposure period and were lower than those in controls. The kidney was the most affected organ, with an average 52% decrease in ADUR levels, followed by the liver (44%). ADUR levels in the brain, stomach, and lung of GSH-depleted rats were 31% lower when compared with controls. Blood ADUR levels were decreased by 50% in GSH-depleted rats.

Irreversible binding of ADUR with total nucleic acids (RNA + DNA) of brain, stomach, and liver was also evaluated in control and GSH-depleted rats 1 hour after an inhalation dose of 4 mg/kg (40 μCi) AN vapor. In control rats, ADUR in total nucleic acids was found to be highest in the brain (63 pmol AN equivalents/mg), followed by that in the stomach (20 pmol AN equivalents/mg) and the liver (12 pmol AN equivalents/mg). In GSH-depleted rats, ADUR in nucleic acids in the brain was about 50% lower than that in controls, but no change was detected in stomach or liver. ADUR in DNA could not be detected in any tissue of control or GSH-depleted rats. The study authors suggested that ADUR in DNA was not detected because the analytical method used was not sensitive enough to detect radiolabel bound to DNA. Nevertheless, a preferential binding of ADUR with brain RNA was observed in both control and GSH-depleted rats, with ADUR in brain RNA about 50% lower in GSH-depleted rats.

It is unlikely that the observed decrease in radiolabel binding in GSH-depleted rats treated with PH/BSO was due to treatment effect on CYP2E1. BSO is a selective inhibitor of GST; PH depletes GSH in liver, kidney, and lung but not in the blood or brain by conjugation

with GSH. PH was reported not to affect the hepatic microsomal mixed-function oxidase system (Younes et al., 1986).

In the oral studies on male F344 rats, total radioactivity recovered in the tissues examined was similar in control and GSH-depleted rats at both 1 and 24 hours. However, significantly higher recovered radioactivity was found in stomach, lung, and blood of GSH-depleted rats than of control rats 1 hour after dosing, while the radioactivity in kidney was lower in GSH-depleted rats (Pilon et al., 1988b).

The concentration of ADUR in brain reached a maximum in ≤1 hour for both control and GSH-depleted rats and remained constant for 24 hours. In GSH-depleted rats, 60–80% increase in ADUR was measured in brain at 1, 6, and 24 hours after dosing. The highest ADUR level was found in stomach and increased with time in control rats. ADUR levels in liver and kidney of control rats was characterized by an increase over the first 6 hours and a decrease between 5 and 24 hours. GSH-depletion resulted in an increase in ADUR levels in liver, lung, kidney, stomach, blood, and brain between 6 and 24 hours after the dose.

GSH depletion also caused a significant increase in ADUR levels in total nucleic acid (DNA + RNA) in both brain and stomach (one and a half- and threefold, respectively) 6 hours after the dose. No change was found in liver. ADUR associated with DNA was detected in stomach tissue of control rats only. Pilon et al. (1988b) suggested that ADUR levels reflected the relative concentration of covalently bound radioactivity in control and GSH-depleted rats and that the reaction of AN with protein and other macromolecules was responsible for the rapid increase in ADUR at ≤1 hour. The slower increase in ADUR in metabolically competent organs (liver, kidney, and lung) of control rats and all organs of GSH-depleted rats might represent the binding of CEO to macromolecules. Urinary excretion of thiocyanate, a final metabolite from the epoxide pathway of AN metabolism, was increased twofold in GSH-depleted rats. Since urinary thiocyanate is indicative of CEO formation, Pilon et al. (1988a) interpreted their results as indicating that more CEO was formed after GSH-depletion.

Farooqui and Ahmed (1983a) also reported covalent binding of [2,3-^{14}C]-AN to protein, DNA, and RNA of tissues of male Sprague-Dawley rats treated with a single oral dose of 46.5 mg/kg. DNA from tissue homogenate was isolated by extraction with chloroform/isoamyl alcohol/phenol and application of the aqueous extract to hydroxyapatite chromatography. DNA alkylation was higher in brain and stomach than that in the liver, with highest levels of covalent binding in the brain. The covalent binding indices for the liver, stomach, and brain at 24 hours after dosing were 5.9, 51.9, and 65.3, respectively.

Ahmed et al. (1992a) demonstrated the covalent binding of radiolabel from [2,3-^{14}C]-AN to testicular DNA after a single gavage of radiolabeled AN (46.5 mg/kg) to male Sprague-Dawley rats. In a time course study, bound activity was shown to be greatest after 30 minutes (8.93 ± 0.80 μmol AN bound per mol nucleotide). Using an identical experimental protocol, Ahmed et al. (1992b) demonstrated the capacity of AN to bind covalently to DNA in the lung.

Binding was associated with a 28–41% decrease in replicative DNA synthesis at time points up to 24 hours after dosing.

Jacob and Ahmed (2003a) used whole-body autoradiography to examine the distribution of [2-^{14}C]-AN administered orally or intravenously to male F344 rats. Two days after oral dosing, covalently bound radioactivity was retained at higher levels in the gastric mucosa, blood, and hair follicles. After i.v. injection, covalently bound radioactivity was retained in liver, spleen, bone marrow, adipose tissue, and lung. The amount of radioactivity associated with covalent binding was lower for oral dosing than for i.v. injection, which was consistent with the higher recovery of radioactivity excreted following oral dosing compared with injection (see Section 3.4.2).

Covalent binding of [2,3-^{14}C]-AN to tissue protein and globin was also studied in male Sprague-Dawley rats after a single s.c. injection of 1.2–115 mg/kg (Benz et al., 1997b). Covalent binding to tissue protein reached completion in 1–4 hours and was linear in the low dose range (1.2–50 mg/kg), with the relative order (in descending order) as follows: blood > kidney = liver > forestomach = brain > glandular stomach > muscle. Covalent binding to globin followed a similar dose-response curve. Benz et al. (1997b) also measured an N-(2-cyanoethyl)-valine (CEVal) adduct of globin at this dose range. This adduct was formed by reaction of AN with the NH_2-terminal residue of globin (Osterman-Golkar et al., 1994) and represented only 0.2% of total AN binding to globin. However, regression of tissue protein binding vs. globin total covalent binding or globin CEVal adduct indicated that both globin biomarkers could be used as surrogates for the amount of AN bound to tissue protein.

Using a similar dosing regimen, Nerland et al. (2001) employed sodium dodecyl sulfate-polyacrylamide gel electrophoresis to separate labeled proteins isolated from subcellular fractions of liver from treated rats. Binding of AN was found to be associated preferentially with GST of the μ subclass (GSTM). Within this subclass, GSTM1 was labeled about seven times more strongly than GSTM2, while, from the α-subclass, only GSTA3 was labeled (at about 1/35 the strength of GSTM1). No label was associated with GSTA1 or GSTA2. The site of binding was identified as exclusively cysteine 86. Since this particular cysteine residue in rGSTM1 appeared to have been targeted specifically, the study authors hypothesized that high reactivity at cysteine 86 was due to its potential interaction with histidine residue at position 84, which would lower the pk_a of cysteine 86, increasing reactivity towards sulfhydryl reagents. These data would suggest that tissue proteins containing cysteine residues with an abnormally low pk_a value would be likely targets for AN. In an in vivo experimental approach, Nerland et al. (2003) demonstrated that subcutaneously administered AN preferentially bound to the cysteine 186 residue of carbonic anhydrase III (CAIII) in rat liver.

A considerable body of evidence demonstrated the ability of AN to bind to intercellular proteins, in particular to Hb. Osterman-Golkar et al. (1994) reported a method for quantifying an N-terminal cyanoethyl-valine adduct, CEVal, the product of reaction between AN and the

N-terminal valine of Hb. The method was based on the N-alkyl Edman procedure involving the derivatization of globin with pentafluorophenyl isothiocyanate and gas chromatography-mass spectrometry analysis. Osterman-Golkar et al. (1994) showed that the method was applicable to experimental animals exposed to AN in drinking water and to humans exposed to AN in tobacco smoke. Hb from smokers (10–20 cigarettes/day) with a daily intake of 0.5–5 μg AN per kg BW contained about 90 pmol CEVal/g, whereas adduct levels in the Hb of nonsmokers were below the detection limit of about 20 pmol/g Hb. This utility was confirmed by Tavares et al. (1996) for occupationally exposed workers and for smokers.

A subsequent study by Bergmark (1997) showed that the Hb of smokers contained adducts of ethylene oxide and acrylamide as well as AN. In nonsmokers, the CEVal Hb adduct of AN was below the detection limit of <2 pmol/g of globin. In the 10 smokers studied, the levels of this adduct ranged from 25 to 178 pmol/g (mean 106 pmol/g) and correlated with the number of cigarettes smoked per day (correlation coefficient = 0.94).

Fennell et al. (2000) determined CEVal from blood samples of 16 nonsmokers and 32 smokers and reported that CEVal Hb adducts increased with increased cigarette smoking. The estimated CEVal level from smoking was 170 fmol per mg Hb per pack-day. Two participants in a smoking cessation program showed a gradual reduction of CEVal levels (Perez et al., 1999). Thus, the use of the Hb adduct CEVal may have utility as a biomarker to assess low-level exposure to AN (in the region of 50 ppb), even in a complex mixture of toxicants, although smoking would be a confounding variable. Fennell et al. (2000) also reported that the null genotypes for GSTM1 or GSTT1 had little effect on CEVal levels when compared to active genotypes.

Borba et al. (1996) measured CEVal as a marker of AN exposure in occupationally exposed workers in an acrylic fiber factory. The values for CEVal among the subjects were 8.5–70.5 pmol/g globin in controls, 635.2–4,603.5 pmol/g globin for continuous polymerization workers, and 93.9–4,746 pmol/g globin for maintenance workers. These findings pointed to the ready formation of AN adducts with Hb in an occupational setting.

CEVal Hb adduct was also used as a follow-up dose monitor after accidental exposure of four cleaning workers to AN in an AN-containing tank wagon (Bader and Wrbitzky, 2006). On day 25 after exposure, CEVal adduct levels in Hb ranged from 640 (blood sample partly hemolyzed) to 2,020 pmol/g globin for the three smokers and was 566 pmol/g globin for the nonsmoker, indicating residual AN adducts from the accidental exposure. On day 175, CEVal adduct levels were 81–276 pmol/g globin for the smokers and 2 pmol/g globin for the nonsmoker and represented background CEVal of the study participants according to their smoking status. For both the smokers and nonsmoker, the adduct concentrations in blood declined linearly with time. Linear regression analysis of the data estimated a total elimination interval of 148 days, longer than the standard lifespan of 126 days of erythrocytes. Linear regression analysis also allowed estimation of the initial adduct levels of the workers on the day of the accident and

estimation of the exposed AN concentrations based on the correlation from the former German exposure equivalent that 3 ppm AN yields 17,200 pmol/g globin.

3.4. ELIMINATION

3.4.1. Studies in Humans

In an inhalation study of six male volunteers exposed to 7.8–10 mg/m^3 AN for 8 hours (Jakubowski et al., 1987), 44–58% (mean = 52%) of the inhaled AN was absorbed, of which about 22% of absorbed AN was metabolized and excreted in the urine over 31 hours from the start of exposure as N-acetyl-S-(2-cyanoethyl)-L-cysteine (2-cyanoethyl mercapturic acid [CEMA]). Elimination followed first-order kinetics, with a half-life of about 8 hours. The authors concluded that individual urinary CEMA levels were not a useful measure for exposure to AN.

3.4.2. Studies in Animals

Three pathways are involved in the elimination of AN from an organism: exhalation, urinary excretion, or fecal excretion.

3.4.2.1. *Exhalation*

In a study by Young et al. (1977), male Sprague-Dawley rats were exposed to [1-^{14}C]-AN via inhalation (5 or 100 ppm) or a single oral dose (0.1 or 10 mg/kg). Exhalation of AN as CO_2 within 6 hours after dosing decreased with increasing dose, from 6.1 to 2.6% of the dose following inhalation exposure and from 4.6 to 3.9% after gavage (see Tables 3-1 and 3-2).

When Ahmed et al. (1983) administered a single oral dose of 46.5 mg/kg AN to male Sprague-Dawley rats in distilled water, using 50 μCi/kg of either [2,3-^{14}C]- or [1-^{14}C]-AN as tracer, the recovery of total dose in expired $^{14}CO_2$ varied from 2% for [2,3-^{14}C]-AN to 12% for [1-^{14}C]-AN 24 hours after dosing. Burka et al. (1994) administered 0.87 mmol/kg (46.2 mg/kg) [2-^{14}C]-AN by gavage to male F344 rats. About 2% of the dose was expired as volatile organic components, predominantly unchanged AN, while 11% was liberated as $^{14}CO_2$ 24 hours after dosing.

Jacob and Ahmed (2003a) compared excretion of 11.5 mg/kg [2-^{14}C]-AN administered orally or intravenously to male F344 rats. In the 48 hours after oral dosing, 61% of the radioactive dose was excreted, with 4% in exhaled CO_2, 4% in urine, and 53% in feces. Following i.v. administration, 30% of the dose was eliminated over 48 hours, with 2% in expired air, 8% in urine, and 21% in feces. In the 8 hours after oral dosing, 3% of the radioactive dose was in exhaled CO_2, 2% in urine, and 48% in feces. Following i.v. administration, 2% of the dose was in exhaled CO_2, 3% in urine, and 0.2% in feces. Jacob and Ahmed (2003a) concluded that these results indicated a significant difference in biological fate of AN following i.v. or oral treatment.

3.4.2.2. *Fecal Excretion*

Young et al. (1977) also investigated the fecal excretion of AN in male Sprague-Dawley rats. This route of excretion showed little dependence on the route of administration, amounting to 3–4% of the dose following inhalation exposure and about 5% following gavage within 6 hours of dosing. Young et al. (1977) also investigated the possibility of biliary excretion with subsequent reabsorption from the intestines in one male rat. A cannula was inserted between the common bile duct and the duodenum for sampling of bile, and [^{14}C]-AN was given intravenously. Based on the concentrations of radioactivity in bile, urine, RBCs, and plasma as a function of time, the rate of elimination from the bile was found to be faster than from other fluids during the first 6 hours after dosage. The initial half-life for excretion of radioactivity via bile was estimated to be about 15 minutes. One unidentified metabolite was excreted in the bile and underwent enterohepatic circulation to the GI tract, contributing partially to 5% of the dose excreted in feces.

Kedderis et al. (1993a) estimated that 3–5% of AN doses were excreted in feces of F344 rats (0.09–28.8 mg/kg orally), while 2–8% of the dose were recovered from the feces of B6C3F$_1$ mice (0.09–10 mg/kg orally). In either species, the differences in fecal excretion were not related to the administered dose. Farooqui and Ahmed (1982) administered a single oral dose of 46.5 mg/kg [1-^{14}C]-AN to male Sprague-Dawley rats, the highest percentage of ^{14}C excreted in feces (2%) occurred between 12 and 24 hours after dosing. At the end of 10 days, 2.5% of the dose was excreted in feces. In another study, male Sprague-Dawley rats were given a single gavage dose of 46.5 mg/kg [1-^{14}C]-AN; four radioactive peaks were identified in biliary extracts at 6 hours after treatment. The two major metabolites in bile were GSH conjugates of AN: S-cyanoethyl glutathione and N-acetyl-S-(2-cyanoethyl)cysteine (Ghanayem and Ahmed, 1982). Nearly 27% of the dose appeared in the bile after 6 hours (Ghanayem and Ahmed, 1982; Ahmed et al., 1982). The GI tract contained the highest level of radioactivity up to 72 hours, suggesting resecretion of AN metabolites to the stomach or binding of metabolites to the stomach mucosa (Ahmed et al., 1982).

3.4.2.3. *Urinary Excretion*

A substantial number of studies demonstrated the rapid urinary elimination of AN or its metabolites when AN was administered to experimental animals via the oral or inhalation routes (Burka et al., 1994; Fennell and Sumner, 1994; Kedderis et al., 1993a; Ahmed et al., 1983, 1982; Young et al., 1977). For example, when Young et al. (1977) exposed male Sprague-Dawley rats to radiolabeled AN via inhalation (5 or 100 ppm) or a single oral dose (0.1 or 10 mg/kg), most of the radiolabel was recovered in the urine, with much lower proportions of the initial dose in feces or expired air (see Table 3-1 and 3-2). Urinary excretion increased with dose, from 69 to 82% of

the dose following inhalation exposure and from 34 to 67% after gavage (Tables 3-1 and 3-2). Excreted dose in urine was mostly unidentified metabolites.

In another study, Sapota (1982) administered 40 mg/kg AN, containing either 40 μCi/kg [1,2-^{14}C]- or [1-^{14}C]-AN, in saline to male Wistar rats, either via gavage or intraperitoneally. In parallel to the depletion of radiolabel in tissues at 24 hours postexposure, 82–93% of the dose was eliminated from the body in the urine, with 3–7% exhaled unchanged in the breath in 24 hours, independent of the route of administration and the position of the radiolabel. However, when Farooqui and Ahmed (1982) administered an oral dose of 46.5 mg/kg [1-^{14}C]-AN to male Sprague-Dawley rats, 40% of the radioactivity was excreted in urine over 24 hours after dosing. At the end of 10 days, 61% of the total dose was excreted in urine. Similarly, when Ahmed et al. (1983) gave a single oral dose of 46.5 mg/kg AN to male Sprague-Dawley rats in distilled water, using 50 μCi/kg of either [2,3-^{14}C]- or [1-^{14}C]-AN as tracer, 40% of the radioactivity from [1-^{14}C]-AN but 60% of [2,3-^{14}C]-AN-derived radiolabel were detected in the urine in the initial 24 hours. Neither of the two studies provided details that might explain the discrepancy. However, the observed discrepancy might indicate the impact of different strains used in the studies.

The single gavage dose experiment of Burka et al. (1994), in which male F344 rats were placed in metabolic cages after receiving 0.87 mmol/kg (46.2 mg/kg) [2-^{14}C]-AN, resulted in 67% of the load being voided to the urine after 24 hours. This proportion of the recovered load was similar to the 55–56% value obtained when male F344 rats or B6C3F$_1$ mice were orally exposed to [1,2,3-^{13}C]-AN (Fennell and Sumner, 1994). However, Ahmed et al. (1996a) recovered only about 4% of the counts in 48-hour urine samples when F344 rats were injected intravenously with 11.5 mg/kg [2-^{14}C]-AN. About 27% of the load was eliminated via all routes combined. In this study, much higher levels of tissue binding were observed than in other studies.

Identification of the urinary metabolites derived from AN metabolism was attempted in several studies. Langvardt et al. (1980) administered [2,3-^{14}C]- and [1-^{14}C]-AN orally to male Sprague-Dawley rats, thereby specifically tracing the fate of the vinyl and cyano groups of AN. Two main urinary metabolites, thiocyanate and N-acetyl-S-(2-cyanoethyl)cysteine, were identified. Thiocyanate, formed from the epoxide metabolite CEO, was the predominant urinary metabolite following oral dosing with 30 mg/kg of [1-^{14}C]-AN and accounting for 54% of the injected radioactivity within 16 hours after dosing. On the other hand, thiocyanate only accounted for 1% of the urinary radioactivity after dosing with [2,3-^{14}C]-AN. The second metabolite, N-acetyl-S-(2-cyanoethyl)cysteine, a mercapturic acid derived from direct conjugation between AN and GSH, constituted 18% of the radiolabel derived from [1-^{14}C]-AN and 28% from [2,3-^{14}C]-AN. Another metabolite, tentatively identified as N-acetyl-3-carboxy-5-cyanotetrahydro-1,4-2H-thiazine, constituted 19% of the label from [1-^{14}C]-AN and 35% from [2,3-^{14}C]-AN. Evidently, this metabolite was formed from conjugation of CEO with GSH.

Langvardt et al. (1980) found another four minor metabolites that were not identified structurally.

Tardiff et al. (1987) monitored the urinary metabolites of AN-treated male Sprague-Dawley rats 24 hours after i.v. or i.p. single doses (0.6, 3, or 15 mg/kg) or inhalation exposure to 4, 20, and 100 ppm for 6 hours. Three major metabolites were measured: thiocyanate, N-acetyl-S-(2-hydroxyethyl)cysteine, and N-acetyl-S-(2-cyanoethyl)cysteine, that were also detected by Langvardt et al. (1980). These three excreted metabolites represented 50–54% of the administered dose in urine within 24 hours, independent of the dose. Tardiff et al. (1987) found that following i.p. or i.v. administration of AN, N-acetyl-S-(2-hydroxyethyl)cysteine and thiocyanate each represented between 5 and 10% of the urinary metabolites; the major metabolite was N-acetyl-S-(2-cyanoethyl)cysteine, representing 74–78% of the urinary metabolite when AN was administered intraperitoneally or intravenously. However, following inhalation exposure of AN, only 8% of the dose was excreted as N-acetyl-S-(2-cyanoethyl)-cysteine, and the major urinary metabolite was thiocyanate at 20 and 100 ppm. Moreover, N-acetyl-S-(2-hydroxyethyl)cysteine was excreted in larger amounts than N-acetyl-S-(2-cyano-ethyl)cysteine. These results also showed that the percentage of dose excreted as urinary thiocyanate increased with dose when AN was administered by inhalation. The study authors concluded that the route of administration of AN had an important influence on the pattern of metabolic excretion.

Shibata et al. (2004) investigated the urinary excretion of thiocyanate in male Wistar rats that received 40 mg/kg AN (about half the LD_{50}) by gavage in water. Urinary excretion of thiocyanate became measurable at the time of peak plasma thiocyanate levels, 5 hours after dosing. Excretion of urinary thiocyanate gradually increased so that at 10 hours after dosing, about 1.2 mg thiocyanate (7% of administered dose) had been excreted into urine.

Gut et al. (1981) administered [1-^{14}C]-AN to male Wistar rats (dose not given) by the oral, i.v., i.p., and s.c. routes. Total excretion of radioactivity after 48 hours was reported to be close to 100% following oral administration but 75–84% following the other routes of administration. The patterns of urinary radioactivity elimination were also different: after parenteral administrations, elimination of radioactivity was highest within the first 4 hours after dosing, with much smaller amounts for the remaining 44 hours. After oral dosing, between 6 and 8% of the dose was eliminated in urine for the time periods 4, 8, and 12 hours after dosing with much lower amounts thereafter. However, the major difference was found to be urinary thiocyanate elimination: 23% during the 48 hours after oral dosing and 4% following i.p., 4.6% following s.c., and 1.2% following i.v. administration.

In another study (Gut et al., 1985), male Wistar rats were exposed via inhalation to 57, 125, or 271 mg/m^3 AN for 12 hours. A constant ratio between thiocyanate and the sum of thioether compounds (AN mercapturic acids) in urine was found throughout the three doses. Average total amounts of thioethers excreted in urine during 12 hours of exposure were 24, 63,

or 83 μmol/kg for 57, 125, or 271 mg/m^3 AN, respectively. Average total amounts of thiocyanate excreted were 14, 24, and 49 μmol/kg for 57, 125, and 271 mg/m^3 AN, respectively. The ratio of thioethers to thiocyanate was about 2:4 during the 12 hours of exposure and was similar to that from oral exposure to AN. Thus, thioethers, not thiocyanate, were the major urinary metabolites following inhalation and oral exposure. These results were different from those reported by Langvardt et al. (1980) and Tardiff et al. (1987).

Müller et al. (1987) quantified four urinary metabolites and unchanged AN following inhalation exposure of male Wistar rats to 1–100 ppm of AN for 8 hours (thiocyanate was not measured). At 24 hours postexposure, N-acetyl-S-(2-cyanoethyl)cysteine was the primary urinary metabolite, followed by N-acetyl-S-(2-hydroxyethyl)cysteine, thiodiglycolic acid (also known as thiodiacetic acid), S-carboxyethyl-L-cysteine, and unchanged AN. The excretion pattern of AN and its metabolites was dependent on the inhalation exposure concentrations. The study authors proposed cyanoethyl mercapturic acid was the most sensitive indicator metabolite of AN exposure at levels of 5 ppm.

Fennell et al. (1991) also measured GSH-derived metabolites, but not thiocyanate, in the urine of male F344 rats (10 or 30 mg/kg) and male B6C3F$_1$ mice (10 mg/kg), following oral administration of [1,2,3-^{13}C]-AN. The results of this study are shown in Table 3-7. N-acetyl-S-(2-cyanoethyl)cysteine was formed by conjugation of AN with GSH, whereas the other metabolites were from reaction of CEO with GSH. The results support the finding that rats and mice differ in the way they metabolize AN, and mice evidently metabolize more AN through the CYP2E1-mediated formation of CEO.

Table 3-7. Urinary excretion of thioethers derived from AN

Metabolite (see Figure 3-2)	Rat (30 mg/kg)	Mouse (10 mg/kg)
	Percent of total metabolites	
N-acetyl-S-(2-cyanoethyl)cysteine	42.8 ± 4.8	20.5 ± 2.0
N-acetyl-S-(2-hydroxyethyl)cysteine	26.7 ± 1.8	22.3 ± 1.2
N-acetyl-S-(1-cyano-2-hydroxyethyl)cysteine	17.4 ± 2.2	13.9 ± 3.2
N-acetyl-S-(carboxymethyl)cysteine and thiodiacetic acid	7.4 ± 2.9	43.2 ± 3.5
Thionyldiacetic acid	5.7 ± 0.21	Not detected

Source: Fennell et al. (1991).

Kedderis et al. (1993a) studied the dose dependence of the urinary excretion of AN metabolites in male F344 rats and male B6C3F$_1$ mice. In rats during the 72 hours following oral doses of 0.09–28.8 mg/kg [2,3-^{14}C]-AN, 73–99% of the dose was excreted in urine, while 3–5% was found in feces. In mice receiving 0.09–10 mg/kg [2,3-^{14}C]-AN, 83–94% of the dose was excreted in urine and 2–8% in feces. Excretion of radioactivity by both routes was not dose dependent in either species.

The position of the radiolabel did not allow detection of thiocyanate. Radiochromatograms of urine from rats or mice identified five major peaks, two of which contained more than one compound. Following administration of [2,3-^{14}C]-CEO, two of the five peaks were not found, indicating that those peaks were derived from direct conjugation of AN without metabolic activation to CEO. The sum of the percent of total radioactivity from CEO conjugate-derived peaks was higher than that from the AN conjugate-derived peaks in both rats and mice. None of the metabolites appeared to be glucuronides. Kedderis et al. (1993a) detected four of the five metabolites shown in Table 3-7, but could not identify thionyldiacetic acid. In addition, S-(2-cyanoethyl)-thioacetic acid was detected in mouse urine only, likely a degradation product of N-acetyl-S-(2-cyanoethyl)cysteine.

The excretion of metabolites derived from CEO was approximately linear with the AN dose in both rats and mice. However, the urinary excretion of N-acetyl-S-(2-cyanoethyl)cysteine increased nonlinearly with increasing dose of AN, an effect that was much more pronounced in rats than in mice. This probably indicated the presence of a competing pathway, namely, epoxidation of AN, with the conjugation of AN with GSH. The fraction of the total dose recovered as metabolite from CEO was 0.5 in rats and 0.67 in mice. The study authors estimated that the ratio of AN epoxidation to GSH conjugation ranged from 4.8 to 1.3 as the AN dose increased in rats and from 5.7 to 2.7 as the dose increased in mice. Kedderis et al. (1993a) also pointed specifically to the species differences detected in this study—a roughly 10-fold higher excretion of thiodiglycolic acid (thiodiacetic acid) in mice as compared with rats and measurable excretion of S-(2-cyanoethyl)thioacetic acid in mice. This urinary metabolite could not be detected in rats at all.

Sumner et al. (1999) treated three male WT and four male CYP2E1-null mice (C57BL/GN × Sv129) orally to 0, 2.5, or 10 mg/kg [1,2,3-^{13}C]-AN and used NMR spectroscopy to characterize AN metabolites in urine samples collected over 24 hours. WT mice excreted metabolites derived from CEO (80–85% of total excreted) and from direct GSH conjugation with AN (15–21% of total excreted), with the largest percentage of metabolites from conjugation of GSH with the 3-carbon of CEO. CYP2E1-null mice displayed only metabolites derived from direct GSH conjugation with AN in their urine following administration of 2.5 or 10 mg/kg [1,2,3-^{13}C]-AN. This confirmed the role of CYP2E1in the oxidation of AN to CEO and its subsequent transformation to a range of other products. Since CYP2E1-null mice did not excrete metabolites that would be produced by oxidation by other CYP450s, CYP2E1 may be the only CYP450 enzyme involved in the metabolism of AN. In addition, CYP2E1-null mice excreted about the same percentage of administered dose as the WT mice, indicating CYP2E1-null mice compensated for the CYP2E1 deficiency by producing more metabolites from direct conjugation of AN with GSH.

Taken together, the animal data indicate that AN can be exhaled as parent compound at a low percentage of the administered dose, probably increasing at high doses (e.g., 10 mg/kg).

Fecal excretion amounts to about 5% of a given dose. The biliary pathway leading to fecal excretion has not been well characterized. To a small extent, similar to fecal excretion, AN is metabolized completely and exhaled as CO_2. Both pathways appear to be quite independent of the administered dose. Urinary excretion of AN metabolites has been well characterized but is not without contradictory findings. There appears to be little doubt that mice metabolize more AN via the CYP2E1-mediated oxidative pathway than do rats. To what extent this pathway is likely to be overcome by large doses, or what contribution the GSH conjugation makes with varying doses of AN and different species exposed, is not known.

3.5. PHYSIOLOGICALLY BASED TOXICOKINETIC MODELS

A physiologically based toxicokinetic (PBTK) model for AN was previously developed in rats (Kedderis et al., 1996; Gargas et al., 1995) and extended to describe the dosimetry of both AN and CEO in humans (Sweeney et al., 2003). The PBTK model structure consists of two parallel modules, one for AN and one for CEO, interlinked by the rate of oxidative metabolism of AN to CEO in the liver, essentially as described by Gargas et al. (1995). Each module consists of seven dynamic tissue compartments representing the lung, slowly perfused tissues, fat, well-perfused tissues, brain, stomach, and liver (Figure 3-2). All perfusion-limited tissue compartments are linked through blood flow, following an anatomically accurate, typical, physiologically based description (Andersen, 1991).

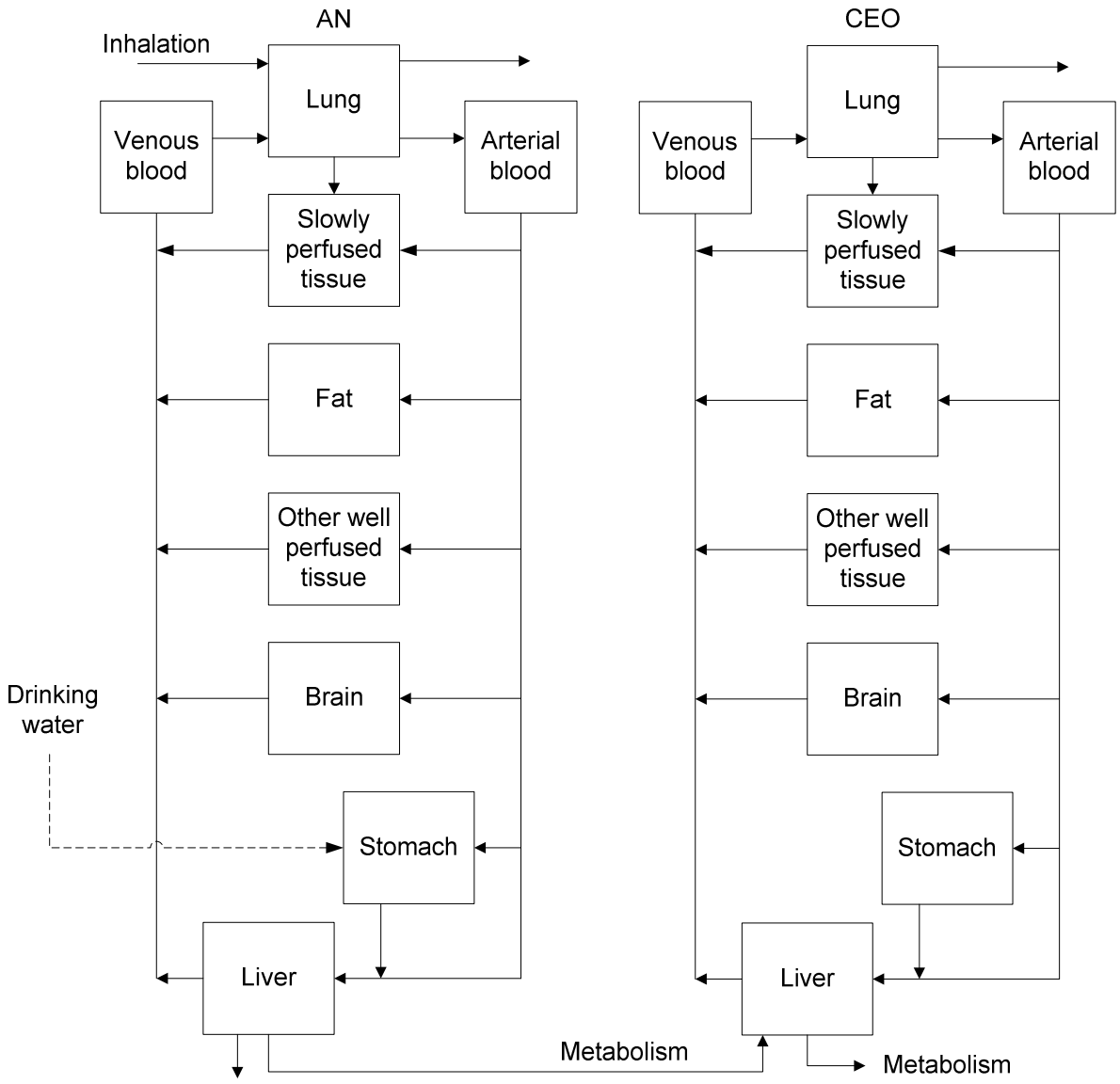

Source: Sweeney et al. (2003).

Figure 3-2. Structure of the PBTK model for AN and CEO.

Because AN and CEO are retained by the tissue in each compartment according to their tissue/blood partition coefficients (PCs) (which were measured in vitro), the concentrations of both chemicals in venous blood (leaving the tissue) are lower than those in arterial blood during the equilibration phase (except CEO in the liver). Therefore, the rate of change in the amounts of both chemicals in each tissue compartment is given by the difference between concentration in blood entering and exiting the tissue multiplied by the blood flow. Simple differential equations for each compartment, corrected for the non-enzymatic conjugation with GSH, are integrated over time, giving the amounts of AN and CEO present in the tissue (Kedderis et al., 1996) (see equation below). Therefore, knowing (from the literature) the actual volume of each tissue, concentrations of AN and CEO in each tissue can be calculated over time.

$$dA_i/dT = Q_i(CA–CV_i)–(K_{SO} \times CV_i \times GSH) \times V_i$$

where

Q_i = blood flow rate to the target tissue (i)
CA = concentration of AN in arterial blood
CV_i = concentration of AN in venous blood
K_{SO} = rate constant for the conjugation of AN with glutathione (GSH)
V_i = volume of the target tissue (i)

For the lung compartment, with two mass inputs (mixed venous blood and inhaled air) and two outputs (arterial blood and exhaled air), the amount of either chemical in alveolar air is in equilibrium with the amount in lung blood at the steady state. Thus, concentrations of AN and CEO in arterial blood can be calculated from simple mass balance equations. Such calculations take into account the alveolar ventilation rate and the rate of blood flow through the lung, a parameter made equal to cardiac output (both known from the literature) and corrected for binding to Hb and blood sulfhydryls.

For the liver compartment, with mass input from blood and two outputs (venous blood and metabolism, excluding biliary excretion that was not considered), the chemical mass transfer is given by the difference between concentrations in portal and venous blood multiplied by hepatic blood flow and corrected for: (1) metabolism of AN to yield CEO (calculated from the Michaelis-Menten equation, subtracted from the mass of AN, and added to the mass of CEO), (2) enzymatic hydrolysis of CEO (also described by the Michaelis-Menten equation), and (3) the first-order conjugation with GSH. A simplified scheme of the mass flow in the PBTK model for AN and CEO is shown in Figure 3-2 (Sweeney et al., 2003).

The model was initially calibrated in rats for three routes of AN administration—oral, i.v. (bolus), and inhalation (Kedderis et al., 1996)—by manually adjusting the metabolic parameters V_{max} and K_m for AN oxidation, first-order constants for AN- and CEO-GSH conjugation, and first-order constant for absorption of AN from the GI tract, guided by the approximate statistical likelihood calculation of SimuSolv. Absorption through the skin, which has been estimated at about 1% of that through the lung (Rogaczewska, 1975), was not considered in this model. Chemical-specific modeling parameters were either: (1) measured in vitro in rats (PC [Teo et al., 1994]; macromolecular interaction constants [Gargas et al., 1995]), (2) fitted to the experimental data by the model (metabolism parameters: V_{max} and K_m), or (3) estimated from the literature (CEO elimination constants).

The model assumed that rats do not have EH activity, based on data from Kedderis and Batra (1993). As discussed previously in Section 3.3.1, this assumption is probably incorrect, based on data from de Waziers et al. (1990), Guengerich et al. (1981), and Kopecky et al. (1980). This PBTK model did not scale allometrically EH activity to humans, whose liver microsomes display EH activity toward CEO (Kedderis and Batra, 1993). Instead, Kedderis (1997) estimated

this activity in humans in vivo based on the ratio of EH to CYP450 activity in subcellular hepatic fractions multiplied by the CYP450 activity in vivo. In addition, the human blood-to-air PC for AN was determined experimentally (Kedderis and Held, 1998). Because no in vivo pharmacokinetic data were available to validate the human model, human in vitro data were scaled to experimental data obtained from rats by using a "parallelogram approach."

The model by Kedderis et al. (1996) overestimates the oral exposure of venous blood CEO concentration by 3- to 10-fold. This is a systematic bias, which suggests that the model parameters need to be reevaluated or that the model is not capturing an important kinetic process for CEO clearance. In particular, for all tissues except the liver, the measured rise in CEO concentration for the first 10–15 minutes after oral and i.v. exposures is much slower than predicted by the model, and the model continues to overpredict the oral data for all measured time points, with the overprediction in the brain being the worst. Kedderis et al. (1996) suggested that the overestimation of CEO concentration in blood at early time points is "most likely due to a large intrahepatic first-pass effect." This hypothesis has not been further evaluated, but, even if correct, the model structure has not been revised to simulate this phenomenon. The model continues to overestimate CEO levels in blood (albeit to a lesser degree) at later time points when the hypothesized first-pass effect would be less of a contributing factor.

It should also be noted that Kedderis et al. (1996) did not compare their model predictions to data on the urinary elimination of AN-GSH and CEO-GSH conjugates and on total activity bound to Hb, as was done in a previous version of the model (Gargas et al., 1995). While fits to those data may have informed the parameters reported by Kedderis et al. (1996), this is clearly not the case in this instance. Also, the blood and tissue time-course data shown by Kedderis et al. (1996) do not include all of the points shown in the previous publication.

Since Kedderis and colleagues (1996) did not include EH activity in their rat model (but other evidence strongly indicates significant CEO hydrolysis be EH), did not perform a more global, numerical optimization of their parameters, may not have included the urinary and Hb data, and the subsequent model fits consistently overpredicted CEO pharmacokinetics in blood and brain to a large extent, the model parameterization was revised to hopefully improve the model characterization of the rat pharmacokinetic data and provide a more sound footing for human-rat dosimetry comparisons and hence risk extrapolation, at least making the results numerically reproducible. Guengerich et al. (1981) measured CEO hydrolysis with purified rat EH and obtained a V_{max} of 0.3 μmol/minute-mg protein and a K_m of 800 μM. Since the highest blood levels observed for CEO were ~2 μM (0.1 μg/mL), to a good approximation hydrolysis can then be described using a first-order rate constant of $0.3/800 = 3.75 \times 10^{-4}$ L/minute-mg EH protein. The EH content of rat liver was measured by de Waziers et al. (1990), who found 0.165 mg EH/mg MP and a value of 40 mg MP/g liver from Ploemen et al. (1997) can be applied.

Finally, the liver fraction for the rat as used in the model 40 g/kg BW was applied, assuming a standard 0.25 kg rat. The rate constant for a standard rat would then be k_{EH} = (3.75×10^{-4} L/minute-mg EH) × (0.165 mg EH/mg MP) × (40 mg MP/g liver) × (40 g liver/kg BW) × (0.25 kg BW) × (60 minutes/hour) = 1.49 L/hour. Because k_{EH} is effectively the ratio, V_{max}/K_m, for EH, and a V_{max} is expected to scale with BW across species while K_m is not expected to scale with BW, k_{EH} is expected to scale in the same way as a V_{max}. In particular, since k_{EH} is a total activity (rather than an activity per unit volume of liver), it is expected to scale as $BW^{0.7}$. Therefore, as for V_{max} values in general, one derives a scaled constant, k_{EHC} = $k_{EH}/(0.25\ kg)^{0.7}$ = 3.92 L/h-$kg^{0.7}$. Based on similar in vitro (Krause et al., 1997) and in vivo (Kemper et al., 2001) EH activity data for butadiene mono-epoxide, it is suspected that the in vivo enzymatic hydrolysis of CEO is also similar to in vitro values, further supporting this direct extrapolation.

Because of the close dose spacing used in the protein kinase (PK) studies and the limited data on metabolite disposition, we found that not all of the remaining parameters were readily identifiable from the in vivo PK data. Therefore, a value of K_m for AN oxidation to CEO from in vitro experiments with rat liver microsomes from Roberts et al. (1991) will be used:
52 μM × 0.05306 mg AN/μmol = 2.76 mg/L.

While the model predictions of AN and CEO blood levels after oral exposures tended to either match or exceed the measured levels, the model predictions of the Hb-binding data were below the measured levels, indicating that the corresponding binding constants that had been determined in vitro were too low. Since the data are only for total binding to Hb (AN plus CEO), the ratio of the AN:CEO binding constants from in vitro was held constant, but the absolute value of the constants was allowed to vary.

Given the values for K_m and the k_{EHC} obtained above, the parameters varied during model fitting were V_{max} (AN oxidation), k_{FC} (GST activity towards AN), k_{FC2} (GST activity towards CEO), k_A (oral absorption), and k_H (AN-Hb binding constant, with the CEO-Hb binding constant, k_{H2}, varied in direct proportion, so that k_H/k_{H2} remained equal to the ratio of the values measured in vitro). An approximate log likelihood function as described by Cole et al. (2001) was used as a measure of goodness of fit. During initial optimizations, it was assumed that the heteroscedasticity values for AN and CEO were distinct but that the same value held for each compound among all three tissues sampled (brain, liver, and blood). However, examination of the standard deviations (SDs) noted in the data of Kedderis et al. (1996) and Gargas et al. (1995) indicated that measurement error was approximately proportional to the signal strength, so the heteroscedasticities were set to two.

Initial attempts to fit the model to the entire data set by varying other model parameters were not satisfactory. While the results are not shown here in detail, a possible reason that the model could not entirely fit the data is that it assumes constant GSH levels in each tissue, while previous studies (e.g., Benz et al., 1997a) have shown significant GSH depletion at dose levels in

the range of those used in the PK studies. Since GSH depletion will be least significant at the lowest doses used, and the most interest is in the low-dose range for extrapolation, it was decided to reestimate the model parameters by using only the lowest concentration pharmacokinetic data: the oral doses at or below 3 mg/kg, i.v. dose of 3.4 mg/kg, and inhalation concentration of 186 ppm. Also, of the data used to estimate parameters, it was determined that the last AN blood measurement from both the 3 mg/kg oral data and the 3.4 mg/kg i.v. data appeared to be outliers since they were well above the otherwise log-linear clearance curve defined by the preceding data, so they too were not used in the estimation. (Model simulations of all exposure concentrations and doses will be shown as compared with the data, but only the data for the exposure values stated two sentences above were used for fitting.)

The following figures show the model fits obtained with the parameters of Kedderis et al. (1996) as compared with the EPA's revised parameters. (All parameter values are listed in Table C-1 of Appendix C.) The term “fits” is used here to describe the closeness of model simulations to the data, recognizing that only a subset of the data, as described in the preceding paragraph and indicated in the figure legends, was actually used in parameter estimation.) The most remarkable aspect of the revised fits is how close they are to identical to the original model fits. Results are nearly identical for most of the i.v., inhalation, and oral (Figures 3-3 to 3-5a) blood- and tissue-time-course data. The revised fits to the CEO blood- and tissue-time-course data after oral dosing are slightly worse than in the original model (Figure 3-6b), but then the fits to the urine and especially the Hb-binding data (Figure 3-6c) are considerably better than those obtained with the parameters of Kedderis et al. (1996). Since only a few of the fits were degraded slightly, while others were improved, the revised model parameters are considered to represent the overall data set at least as well as the original. The fact that the revised parameters are specifically defined by the low-dose data, which are closest to the range where the model will be applied and are obtained using an objective criteria and numerically reproducible methods (the approximate likelihood function with numerical optimization), gives further support for their use.

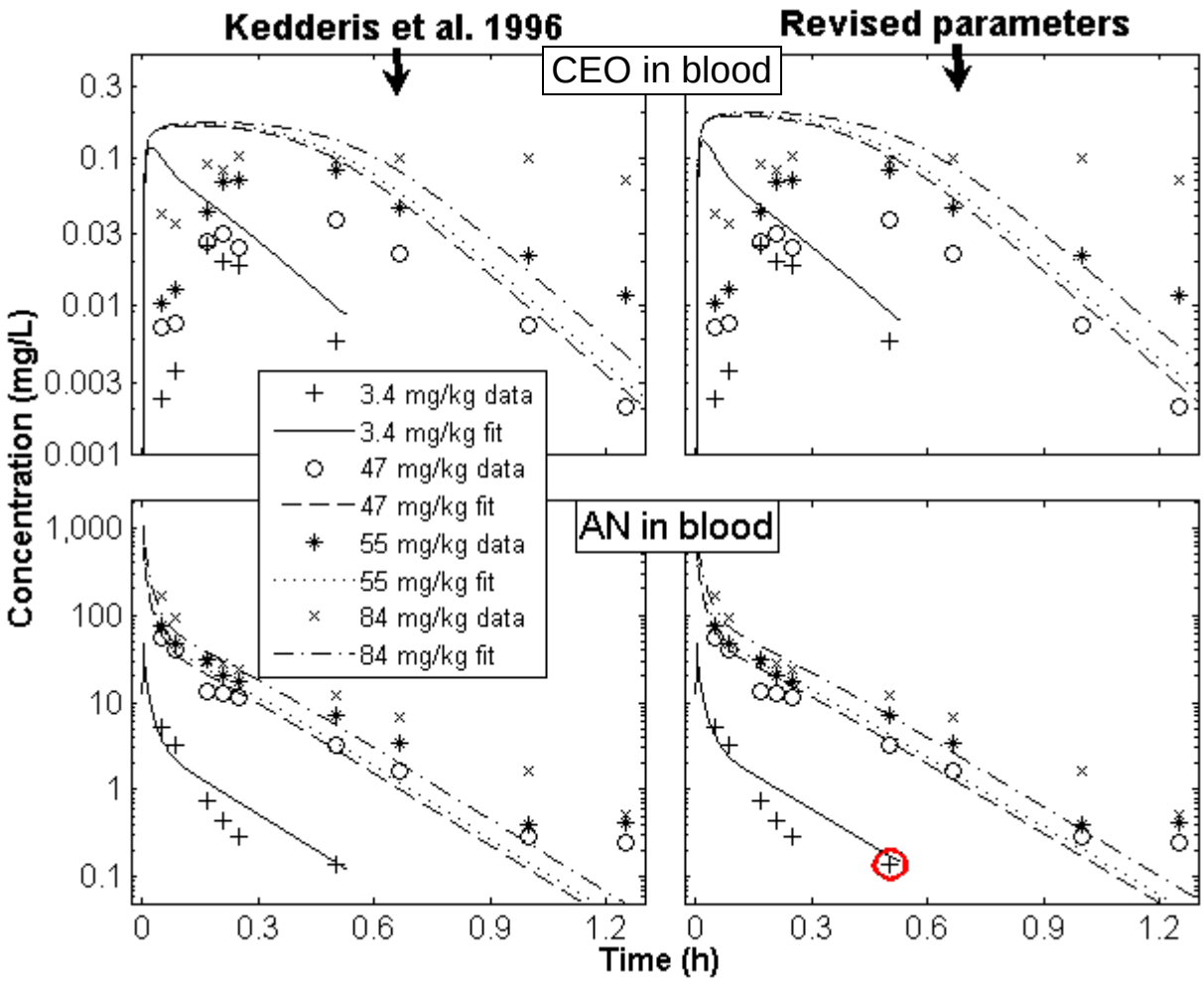

Note: Only 3.4 mg/kg data were used to estimate revised parameters, with circled point excluded.

Figure 3-3. Intravenous exposure, dosimetry, and model fits.

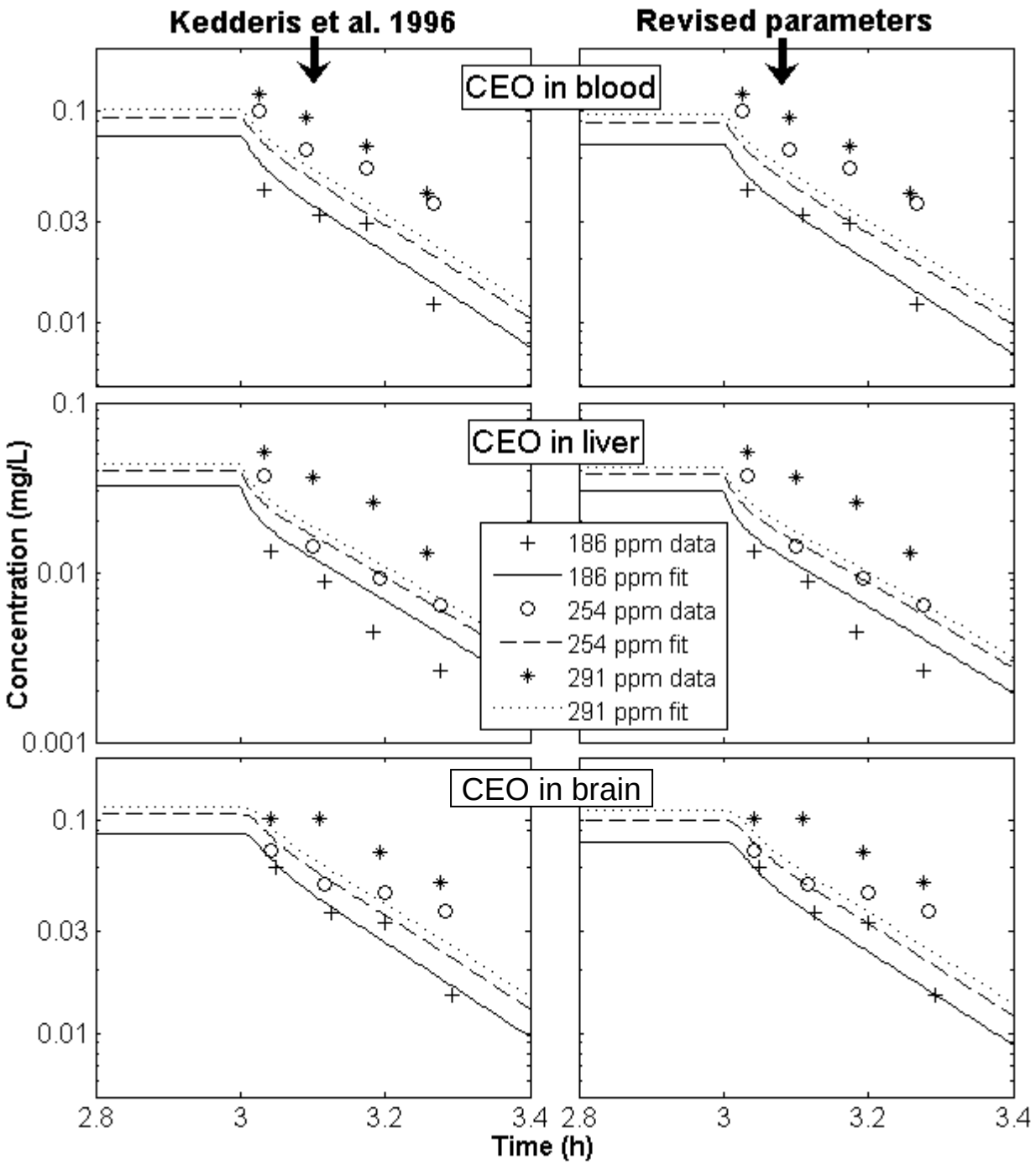

Note: Only 186 ppm data were used to estimate revised parameters.

Figure 3-4a. Inhalation exposure, CEO concentrations.

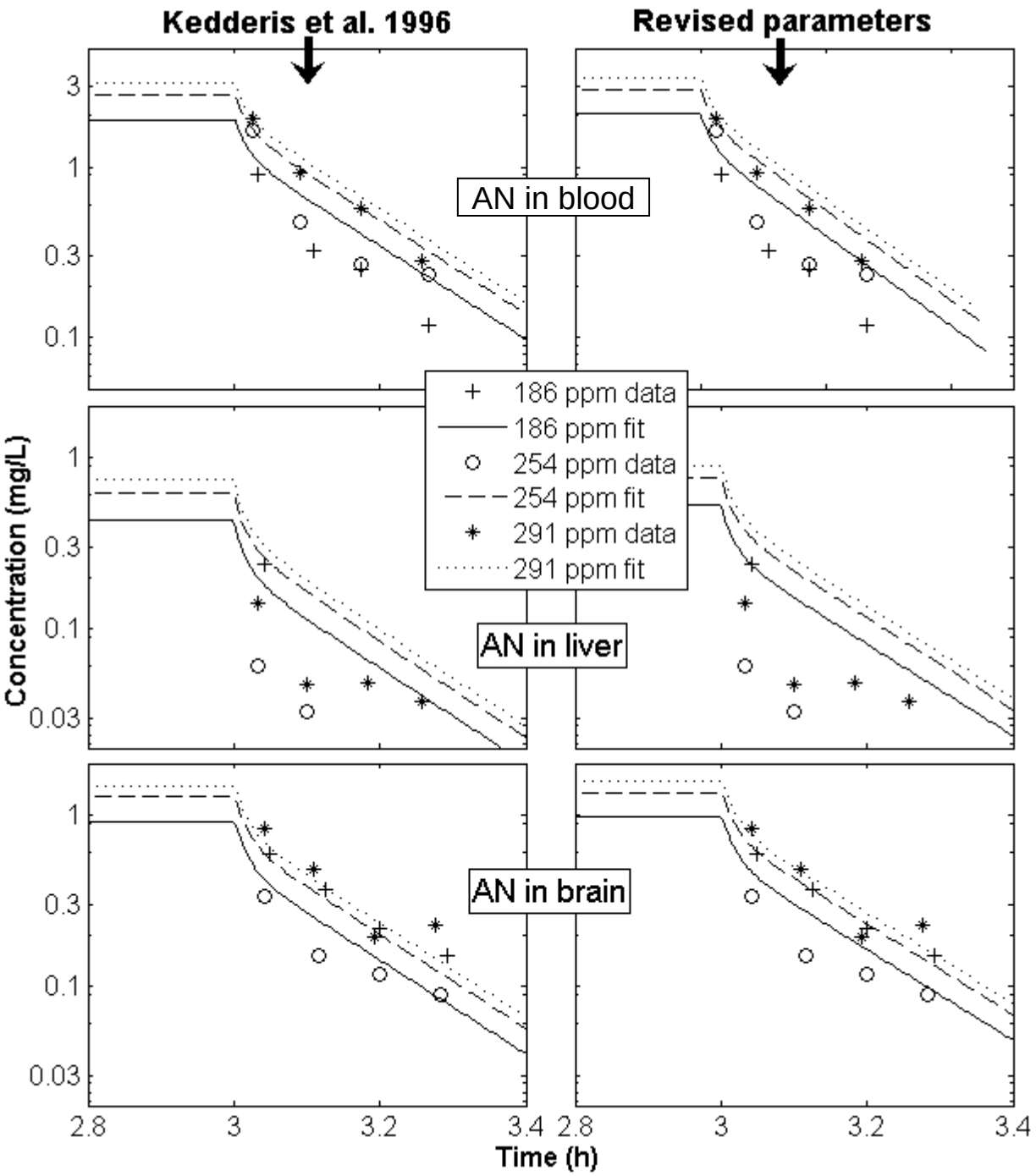

Note: Only 186 ppm data were used to estimate revised parameters.

Figure 3-4b. Inhalation exposure, AN concentrations.

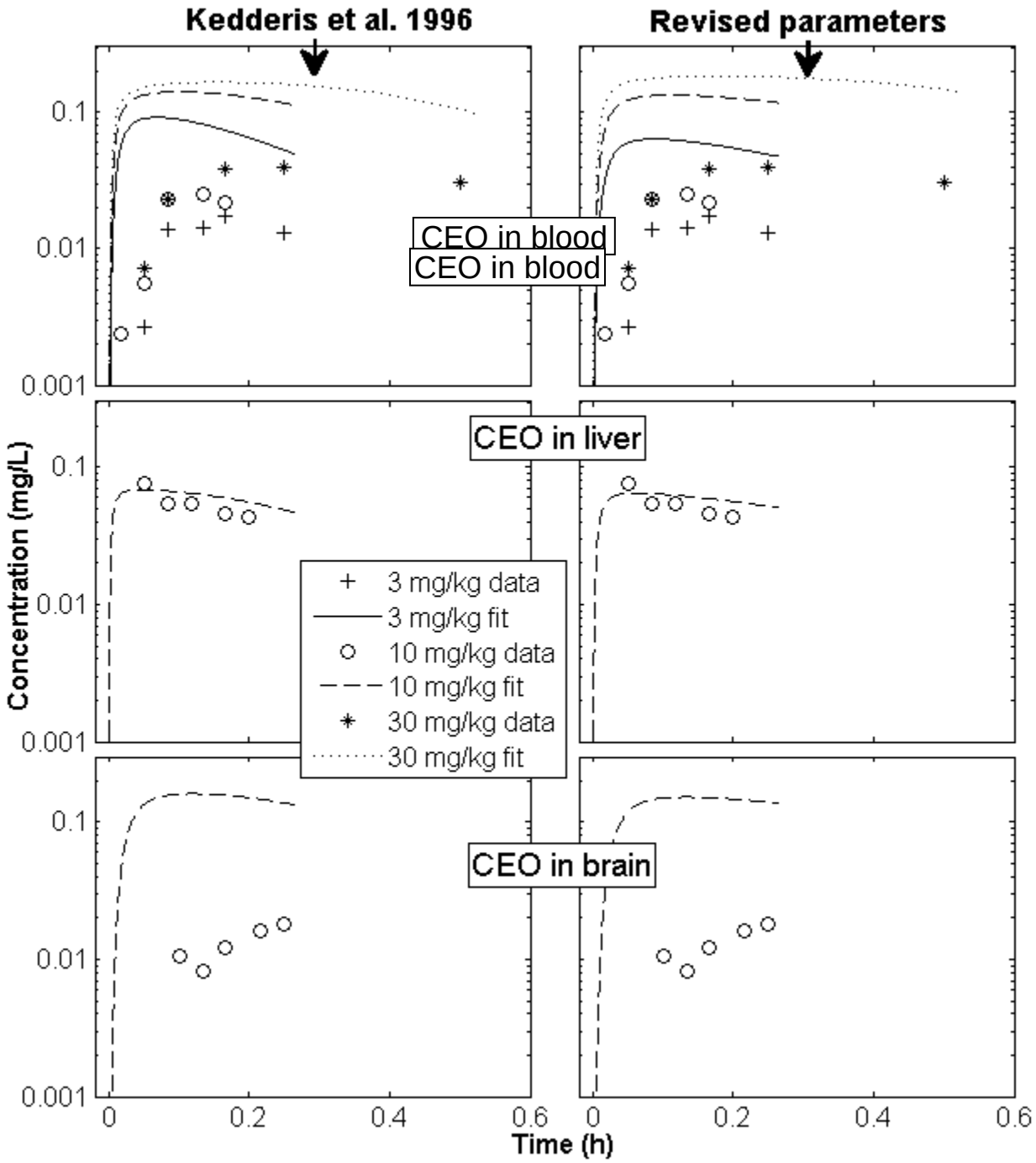

Note: Only 3 mg/kg data were used to estimate revised parameters.

Figure 3-5a. Oral exposure, CEO concentrations.

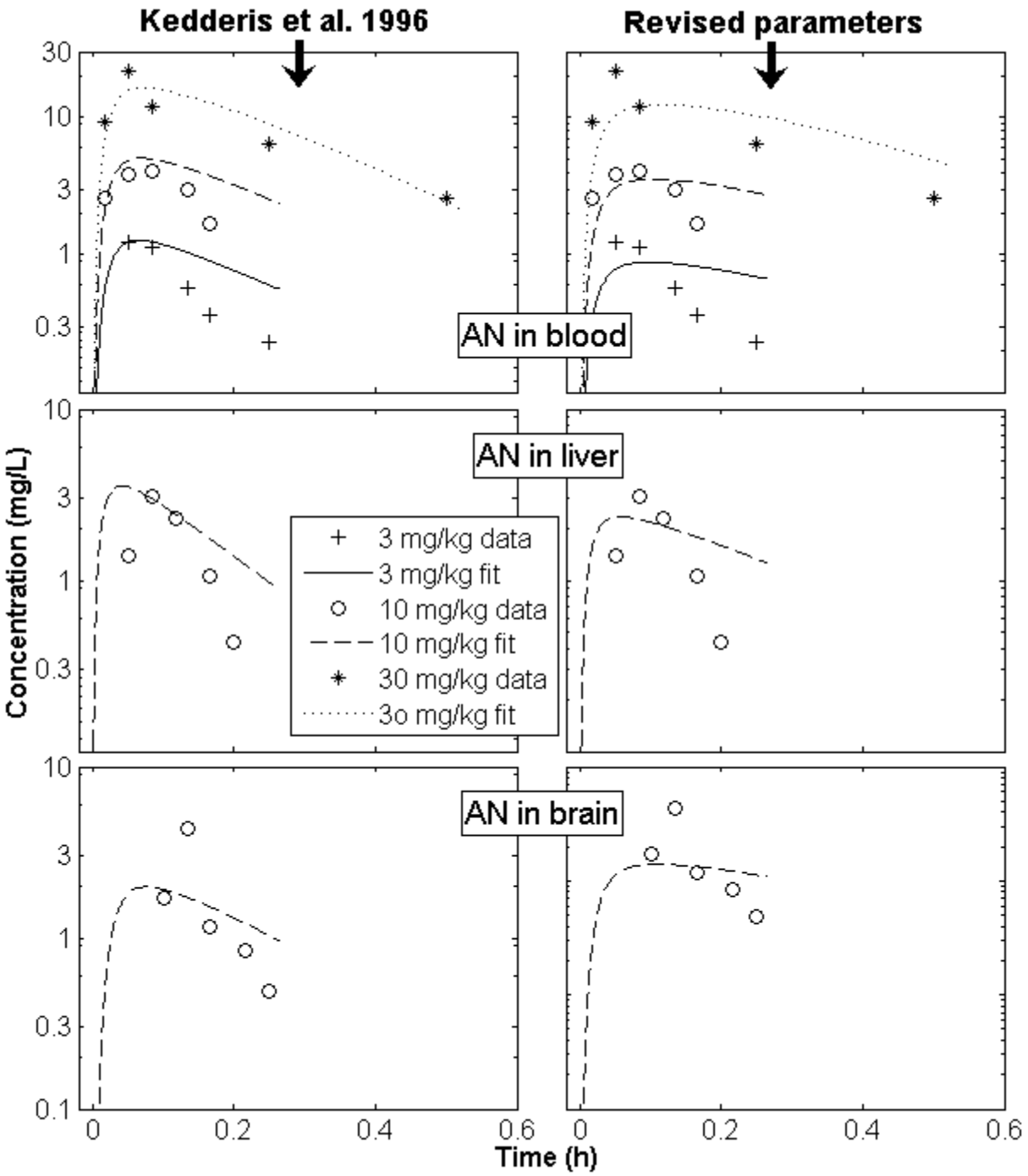

Note: Only 3 mg/kg data were used to estimate revised parameters.

Figure 3-5b. Oral exposure, AN concentrations.

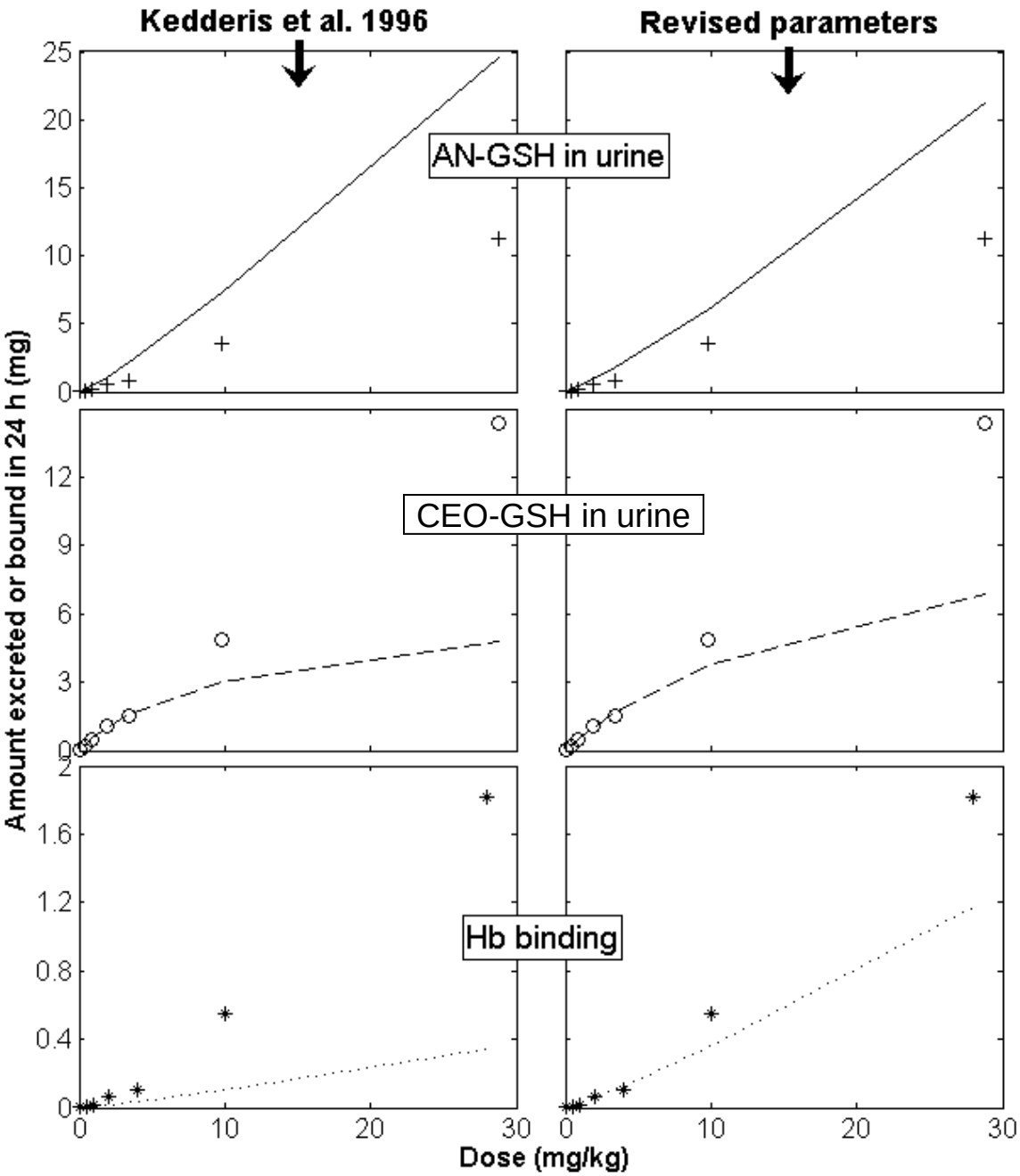

Note: points are data; lines are model fits or simulations. Only data for doses ≤2 mg/kg were used to estimate revised parameters.

Figure 3-5c. Oral exposure, urinary excretion, and Hb binding.

Since the human metabolic parameters were extrapolated from in vitro measurements by using the relationship between in vitro measured and in vivo estimated values from the rat (Sweeney et al., 2003), it is appropriate to update the human metabolic parameters and model in parallel with the EPA's update of those in the rat. For EH, Sweeney et al. (2003) used the in vivo:in vitro relationship for the CYP450-mediated metabolism, since there had been no parallel relationship for hydrolysis. As we are now choosing to extrapolate the rat EH from in vitro to in

vivo based only on enzyme content, microsomal content, liver fraction, and BW, a parallel approach for the human would be to do the same, rather than using a correction factor based on a different class of enzymes. In the case of humans, Kedderis and Batra (1993) measured EH activity in vitro by using hepatic microsomes, so we do not need to use the amount of enzyme per mg MP in the calculation. Kedderis and Batra (1993) determined a V_{max} and K_m EH-mediated hydrolysis of CEO using liver samples from six individual humans. The lowest estimated K_m in the group was 600 μM, so again, we choose to describe the metabolism as first order, using the ratio of V_{max}/K_m. The ratio of V_{max}/K_m was first calculated for each individual since V_{max} and K_m tend to be statistically correlated due to the way they are estimated, and an average value for the ratio was then determined to be 7.02×10^{-6} L/minute-mg MP. We can then apply the value of 56.9 mg MP per g liver from Lipscomb et al. (2003), the liver fraction of 25.7 g/kg BW, and the standard value of 70 kg for a human. The rate constant for a standard human is then k_{EH} = (7.02×10^{-6} L/minute-mg MP) × (56.9 mg MP/g liver) × (25.7 g liver per kg BW) × (70 kg BW) × (60 minutes/hour) = 43.1 L/hour, assuming it also scales as $BW^{0.7}$, $k_{EHC} = k_{EH}/(0.70 \text{ kg})^{0.7}$ = 2.20 L/hour-$kg^{0.7}$. Recall that the value for rats was estimated to be 3.92 L/hour-$kg^{0.7}$.

The original PBTK model for humans was assessed for its sensitivity to changes in key input parameters, and the expected variability in CEO concentrations in humans under different AN exposure scenarios was estimated (Sweeney et al., 2003). In addition to updating the CEO hydrolysis rate constant for the human model (and using a first-order equation for that reaction) as previously discussed, the ratio of V_{max} for the oxidation step as estimated in vivo vs. measured in vitro for the rat was used to estimate the human in vivo V_{maxC}, and the enzymatic GSH conjugation rate constants for AN (k_{FC}) was likewise estimated from the rat estimated in vivo vs. measured in vitro ratio (k_{FC2} was unchanged during the reestimation). Since the rat values for V_{maxC} and k_{FC} were revised, and these values were each one leg of the metabolic extrapolation "parallelogram," the human in vivo values should be accordingly varied. The result is that the ratio of revised/original human values for each of these constants is simply equal to the respective revised/original in vivo values for the rat constants; the revised human values are V_{maxC} = 22.1 mg/hour-$kg^{0.7}$ and k_{FC} = 77 $kg^{0.3}$/hour. Finally, since the original model extrapolation assumed that the oral absorption constant, k_A, and the Hb-binding constants, k_H and k_{H2}, were the same in humans as in rats, these assumptions were retained, updating the human parameters appropriately.

Appendix C provides model source codes written in acsXtreme (AEgis Technologies, Huntsville, AL) and Matlab (The Mathworks, Inc., Natick, MA) that were used to model AN/CEO pharmacokinetics with the PBTK models of Kedderis et al. (1996, as revised) and Sweeney et al. (2003) in this evaluation.

4. HAZARD IDENTIFICATION

4.1. STUDIES IN HUMANS—EPIDEMIOLOGY AND CASE REPORTS

4.1.1. Oral Exposure

No studies were identified that addressed the exposure of human beings to AN via the oral route.

4.1.2. Inhalation Exposure

4.1.2.1. *Acute Exposure*

In a study on six male volunteers, a single 8-hour inhalation exposure of 5–10 mg/m^3 AN produced no subjective symptoms, such as headache, nausea, or general weakness (Jakubowski et al., 1987).

A report by Chen et al. (1999) collated 144 acute AN poisoning cases that had occurred between 1977 and 1994 in China. Each case involved a brief workplace accidental exposure to a high concentration of AN. There were few reliable data on the levels of exposure in these cases, although transient concentrations of AN were thought to range from 40 to 560 mg/m^3 (18–258 ppm) for 60 cases and may have been over 1,000 mg/m^3 for the remaining 84 cases. All but 9 of the 144 subjects were males, ranging in age from 18 to 53 years old. Forty-two of the cases were considered to have resulted in severe acute AN poisoning, while the rest fell into the mild acute category.

Table 4-1 summarizes the incidence of symptoms and signs of toxicity that were evident in the 144 cases. Other changes in monitored biochemical or physiological parameters included transient increases in peripheral white blood cell (WBC) count to greater than 10×10^9/L in 66 cases and a number of apparent fluctuations in clinical chemistry parameters. Out of 120 subjects whose liver function was monitored, seven subjects showed abnormal increases in alanine aminotransferase (ALT) (slight), aspartate aminotransferase (AST), and cholylglycine (i.e., glycocholic acid). Up to 23 times the normal serum concentration of the latter compound was detected. The seven subjects with abnormal liver functions were poisoned at low concentrations in air (40–79 mg/m^3 [18–36 ppm]) but for a comparatively long duration of acute exposure (36 hours). Blood levels of GSH were depressed up to 50% in the severe cases, and urine thiocyanate was increased up to fourfold.

Table 4-1. Clinical signs in 144 subjects accidentally exposed to AN

Symptoms	Cases (%)	Symptoms	Cases (%)
Dizziness	144 (100)	Congestion of pharynx	105 (73)
Headache	144 (100)	Hoarseness	13 (9)
Feebleness	144 (100)	Pallor	108 (75)
Sore throat	87 (60)	Profuse diaphoresis	95 (66)
Chest tightness	144 (100)	Rough breathing sound	18 (13)
Cough	16 (11)	Rapid heart rate	36 (25)
Dyspnea	118 (82)	ECG abnormalities[a]	15 (10)
Nausea	133 (92)	High blood pressure	20 (13)
Vomiting	95 (66)	Low blood pressure	5 (4)
Abdominal pain	97 (68)	Liver tenderness	9 (7)
Numbness of the limbs	50 (40)	Hepatomegaly and splenomegaly	7 (5)
Fainting	104 (72)	Coma	7 (5)
Convulsion	46 (32)	Hyperactive knee jerk	137 (95)

[a]All 15 instances of electrocardiogram (ECG) abnormalities occurred in cases of severe poisoning.

Source: Chen et al. (1999).

These changes disappeared after poisoned subjects were removed from the accident site and underwent treatment that included amyl nitrite via inhalation and an i.v. injection of 3% sodium nitrite followed by 50% sodium thiosulfate (STS). Other treatments included infusion with glucose, adenosine triphosphate (ATP), coenzyme A, and DEX along with oxygen inhalation to prevent the development of cerebral edema and to protect brain and liver cells.

In a study that was possibly reflective of combined inhalation and dermal exposure to AN, Wilson et al. (1948) reported that workers exposed to AN vapors at 16–100 ppm (35–217 mg/m^3) for periods of 20–45 minutes while involved in cleaning operations in polymerizer facilities complained of dull headache, fullness in the chest, irritation of all mucous membranes (eyes, nose, and throat), and a feeling of apprehension and nervous irritability. Some workers also complained of intolerable itching of the skin but had no clinically demonstrable dermatitis. Workers who had direct skin contact with AN displayed a sequence of symptoms, including skin irritation and erythema, followed by bleb formation and then desquamation with slow healing (Wilson et al., 1948). An earlier report by Wilson (1944) reported the onset of nausea, vomiting, weakness, headache, fatigue, diarrhea, and an "oppressive feeling" in the upper respiratory passages following exposure to "mild concentrations" of the compound. Several cases of reversible mild jaundice and one case of slow-to-reverse severe jaundice were identified and associated with occasional liver tenderness and low-grade anemia, but it was unclear whether they were related to inhalation or dermal contact exposures to only AN or to a combination of AN with other industrial rubber manufacturing chemicals such as butadiene and styrene.

4.1.2.2. *Chronic Exposure*

4.1.2.2.1. *Cancer epidemiology*

Cohort studies

A retrospective cohort study involving workers at a DuPont textile fibers plant in Camden, South Carolina, was the first epidemiologic study addressing the potential carcinogenicity of AN (O'Berg, 1980). Shortly thereafter, reports from other cohorts of AN-exposed workers, based in Germany, the Netherlands, the United Kingdom, and the United States, were published. Other smaller-scaled occupational cohorts have also been utilized to better assess the association between AN exposure and adverse human health effects.

Early studies did not utilize quantitative measures of exposure nor were they able to control for smoking (an important consideration when lung cancer is an outcome of interest). These factors were being taken into account by the late 1980s. The following section provides a summary of some of the major cohort studies conducted both within and outside the United States.

The DuPont studies

Researchers from DuPont conducted a series of studies among male workers potentially exposed to AN (Symons et al., 2008; Wood et al., 1998; Chen et al., 1987; O'Berg et al., 1985; O'Berg, 1980). The original study was conducted in South Carolina, with a follow-up study a few years later. A second DuPont plant, located in Virginia, was the site for another cohort study. Finally, Wood et al. (1998) combined the cohorts from South Carolina and Virginia to further investigate the relationship between AN exposure and cancer. Most recently, Symons et al. (2008) updated this combined cohort, adding 11 years of follow-up for a total follow-up period of over 50 years.

The first epidemiologic study addressing the potential carcinogenicity of AN (O'Berg, 1980) examined cancer incidence and mortality in a cohort of 1,345 male workers from a DuPont textile plant who were potentially first exposed to AN between 1950 and 1966. The cohort was chosen from a larger group of more than 10,000 workers, based on examination of work history (wage roll employees and some salaried employees), recollection of plant supervisors (wage roll maintenance employees and salaried employees), and survey of salaried employees (salary roll employees). No individual or area exposure monitoring data were available during the period of study. Several surrogate measures of potential exposure were utilized in the analyses, including job title, initial period of first exposure, length of exposure, and payroll (assuming that wage roll employees have higher potential exposure than supervision or salary roll employees).

Workers were followed through the end of 1976, thus allowing a latency period of at least 10 years for all surviving members of the cohort. Cancer incidence was ascertained for all cohort members who were diagnosed during their employment, and cause of death was determined for all cohort members who died either while employed or after termination.

Comparison rates for cancer incidence and mortality were derived from similarly collected data in a company-wide cancer incidence and mortality registry system. Additional mortality information was supplied by the Social Security Administration, and death certificates were obtained for all known deaths. Other standard comparison rates were also utilized and presented; however, the company-wide data represented the most comparable control group.

After observing only one incident case of cancer in the 217 employees with <6 months of exposure, examination of the incidence data was concentrated on the 1,128 employees who had more than 6 months of exposure. Among this group, cancer incidence was stratified by interval of diagnosis: 1956–1964, 1965–1969, and 1970–1976. The cancer incidence was statistically significantly elevated only in the last interval with 19 cases observed compared to 10.1 expected (standardized incidence ratio [SIR] = observed ÷ expected = 1.88, 95% confidence interval [CI] = 1.17–2.88, $p < 0.01$), based on company-wide rates. Seventeen of the 19 cases were among wage roll employees, the remaining two were salary roll employees. The difference between the observed and expected number of cases among the wage employees was statistically significant (SIR = 2.05, 95% CI = 1.23–3.21, $p < 0.01$) (Table 4-2).

Table 4-2. Distribution of select incidence and mortalities among wage workers and all workers at an AN plant

	Wage workers				All workers			
Cause of disease/death	**Observed cases**	**SIR[a] (CI)**	**Observed deaths**	**SMR[a] (CI)**	**Observed cases**	**SIR[a] (CI)**	**Observed deaths**	**SMR[a] (CI)**
Less than 6 months of exposure								
All cancers	1	0.77 (0.04–3.19)	3	1.30 (0.33–3.55)	1	0.67 (0.03–3.29)	3	1.25 (0.32–3.40)
Respiratory cancer	0	0.00	1	1.11 (0.06–5.48)	0	0.00	1	1.11 (0.06–5.48)
Greater than 6 months of exposure								
All cancers (1956–1976)	20	1.30 (0.82–1.97)	15	1.16 (0.68–1.87)	24	1.26 (0.82–1.85)	17	1.13 (0.68–1.78)
All cancers (1970–1976)	17	2.05[b] (1.23–3.21)	11	1.41 (0.74–2.45)	19	1.88[b] (1.17–2.88)	13	1.44 (0.80–2.41)
Respiratory cancer (1956–1976)	8	2.35[b] (1.09–4.47)	6	1.30 (0.53–2.71)	8	1.95 (0.91–3.71)	7	1.35 (0.59–2.66)
Respiratory cancer (1970–1976)	6	2.86[b] (1.16–5.94)	5	1.61 (0.59–3.57)	6	2.40[b] (0.97–4.99)	6	1.71 (0.69–3.57)

[a]SIR and SMR standardized against company-wide rates.
[b]Statistically significant ($p < 0.05$).

SMR = standardized mortality ratio

Source: Amended from O'Berg et al. (1980).

Eight incident respiratory cancer cases were observed in the cohort of 1,345 workers. All eight of the respiratory cancers occurred in the group of employees who had >6 months of exposure, and all were among wage roll employees. Six of the eight respiratory cancers occurred in the 1970–1976 time interval compared to 2.1 expected based on company-wide rates (SIR = 2.86, 95% CI = 1.16–5.94, $p < 0.05$) (Table 4-2). The numbers were too small to perform any other cancer-specific analyses.

In order to consider the effects of latency and level of exposure, further analyses were performed looking at the group of workers who had first been exposed between 1950 and 1952, when AN was first used at the plant and when exposures were known to have been highest. Statistically significant differences between the number of observed and expected cases were found among the wage roll employees in the diagnosis interval from 1970 to 1976, with 17 cancers observed and 5.6 expected (SIR = 3.04, 95% CI = 1.83–4.78), with six of these cancer cases being respiratory cancers with an expected value of 1.5 (SIR = 4.0, 95% CI = 1.62–8.32). This group is presumed to have the longest latency and highest exposures to AN.

Other factors related to significant differences in cancer incidence between observed and expected cases among the wage roll employees during the time period 1970–1976 were: (1) being a mechanic (10 observed vs. 3.7 expected), (2) duration of exposure of more than 10 years (9 observed vs. 2.8 expected), and (3) exposure above "low level" (13 cancers observed vs. 5.5 expected), low level not defined. Similar relationships were found among respiratory cancers except for duration of exposure of more than 10 years.

Incidence data among wage roll employees were examined by duration of exposure, excluding exposures of <6 months. The duration categories were <5, 5–9, and ≥10 years. The SIRs for all cancers in these three duration of exposure categories were 0.7 (95% CI = 0.23–1.79), 1.2 (95% CI = 0.49–2.50), and 2.3 (95% CI = 1.18–4.14), respectively.

A total of 89 deaths was observed in the entire cohort of 1,345 workers by the end of 1976. The mortality analyses using company-wide rates for comparison did not show any large deviations between observed and expected numbers for all cancers or for respiratory cancers alone. Observed and expected numbers of cancer deaths between 1970 and 1976 for the wage roll employees with ≥6 months of exposure were not markedly different, with 11 cancers observed vs. 7.8 expected (standardized mortality ratio [SMR] = 1.41, 95% CI = 0.74–2.45) and 5 respiratory cancers observed vs. 3.1 expected (SMR = 1.61, 95% CI = 0.59–3.57) (Table 4-2). The excess mortality observed is of interest, since statistical significance may have been hindered by the small sample size.

The use of company-wide rates as a comparison may be problematic because the company-wide rates are based on other plants where exposure to carcinogenic agents may be possible. Additionally, company-wide rates include both exposed and unexposed workers, thus weakening the ability to observe increased risk among the exposed workers. The use of this population-based referent may hide true associations between AN and cancer. Additionally, the

number of incident cancer cases and cancer-specific mortalities was too small for further analysis. However, the fact that the cancer/respiratory cancer comparisons appeared to be stronger for workers with longer latency, longer exposure, jobs with higher exposure, and work during the early years of observation when exposures were highest added to the weight of the evidence.

Another potential limitation of this study was under-ascertainment of incident lung cancer cases. Two confirmed lung cancer cases that should have been included in the cohort were omitted because of clerical error. A validity check of a subsample of 465 employees revealed five more omissions, suggesting that a problem existed with ascertainment of lung cancer cases. The omission of these cases may have resulted in the underestimation of the risk estimate for the incidence of lung cancer. Also, subjective exposure assessment could have resulted in misclassification of exposure. If the exposure misclassification was random, it would bias the risk ratio toward the null value. If it was nonrandom because those assessing AN exposure believed it could cause illness, the effect on the risk estimate is unpredictable. However, other metrics used in this study, including duration of exposure, time of diagnosis, and job category, had internal validity and supported the finding of an association between AN exposure and cancer. Another limitation is the indication that workers may have been exposed to other chemicals in addition to AN. Lastly, there was no adjustment for smoking. The EPA AN health assessment (U.S. EPA, 1983) adjusted the results of this analysis based on smoking rates in the plant and among U.S. blue-collar workers, estimating that the expected number of cancer cases would be 15% higher and would reduce, but not eliminate, the association between AN and cancer in this study. Finally, the small sample size and limited follow-up restricted the ability to detect most cancers.

A second DuPont study extended the follow-up of the above cohort through 1983 for cancer incidence and 1981 for cancer mortality, adding 7 and 5 years of follow-up, respectively (O'Berg et al., 1985). The exposure assessment was not updated, and case ascertainment and calculation of expected incidence and mortality were unchanged from the above study. To evaluate dose-response relationships and latency, cumulative exposure was categorized into three groups (<2, 2–12, and ≥13 years), and latency was dichotomized into "less than 20 years" or "20 or more years." Men with <6 months of exposure were included in the analyses. As with the earlier study, DuPont cancer registry data were used as a comparison for the cancer incidence rates observed in the exposed cohort. DuPont and U.S. death rates were used as a comparison for the mortality data in the exposed cohort.

There were 43 incident cancer cases, including 10 lung cancer cases and 6 prostate cancer cases (Table 4-3). The authors did not comment on the problems with ascertainment of incident lung cancer cases described in the O'Berg (1980) study. Two additional cases of lung cancer were identified. No significant differences between observed all-cancer incidence or even lung cancer incidence and expected values were found among workers (Table 4-3). There was a

statistically significant association between AN exposure and prostate cancer incidence (SIR = 6 observed ÷ 1.8 expected = 3.3, 95% CI = 1.35–6.93). All prostate cancer cases were observed among wage workers who had at least 20 years of latency. No other significant relationship between latency and cumulative exposure was detected.

Table 4-3. Distribution of select incidence and mortalities among wage workers and all workers at an AN plant

Cause of disease/death	Wage workers				All workers			
	Observed cases	SIR[a,b] (CI)	Observed deaths	SMR[a] (CI)	Observed cases	SIR[a,b] (CI)	Observed deaths	SMR[a] (CI)
All causes	–	–	139	1.18 (1.00–1.39)	–	–	155	1.15 (0.98–1.34)
All cancers	37	1.25 (0.89–1.70)	31	1.15 (0.79–1.61)	43	1.17 (0.86–1.56)	36	1.14 0.81–1.56)
Lung cancer	10	1.67 (0.85–2.97)	12	1.17 (0.63–2.00)	10	1.39 (1.41–4.95)	14	1.21 (0.69–1.98)
Prostate	6	4.00[c] (1.62–8.32)	1	1.11 (0.05–5.48)	6	3.33[c] (1.35–6.93)	1	1.00 (0.05–4.93)

[a]SIR and SMR standardized against company-wide rates.
[b]Calculated based on observed and expected values provided.
[c]Statistically significant ($p < 0.05$).

Source: Amended from O'Berg et al. (1985).

A total of 155 deaths was reported, 36 of which were attributed to cancer. No significant differences between observed and expected deaths were reported among either wage workers or salary workers (Table 4-3). Twelve lung cancer deaths were observed vs. 10.2 expected (SMR = 1.17, 95% CI = 0.63–2.00), and 1 prostate cancer death was observed vs. 0.9 expected (SMR = 1.11, 95% CI = 0.05–5.48). The mortality comparisons were less elevated than the morbidity comparisons, indicating that a longer follow-up period may be needed. The observation that prostate cancer was elevated in the incidence data but not in the mortality data could reflect the fact that prostate cancer has a relatively high 5-year survival rate.

In summary, O'Berg et al. (1985) added approximately 7 years of follow-up to the previous DuPont cohort but did not aid in refining knowledge about the potential for a relationship between AN exposure and lung-cancer incidence. The population was exposed to chemicals other than AN, and these additional exposures were not accounted for in the analyses. The small number of lung cancer and prostate cancer cases made the interpretation of the stratified analyses difficult, and the observed numbers of cases were not different from expected numbers of cases in either the highest cumulative exposure group or the longest latency group. This study shares the same limitations as the O'Berg (1980) study. Smoking status, which was not available in O'Berg et al. (1985), may have acted as a confounder. As the numbers of

incident cases and cancer-specific deaths are small, and concomitant exposure to other chemicals is a potential limitation, this study does not provide a substantial basis for the evaluation of the relationship between AN exposure and cancer incidence.

Chen et al. (1987) assembled a cohort of 1,083 mostly white male workers from a DuPont plant in Waynesboro, Virginia, that produced the acrylic fiber Orlon®. The manufacturing process was similar to that at the Camden plant except there was greater distance between the process areas at the Waynesboro facility (Wood et al., 1998). Workers employed at the plant between 1944 and 1970 who had a potential for AN exposure were included. The cohort consisted of 805 wage roll employees and 278 salary roll employees. Potential exposure was based on the review of work histories. No quantitative information was available for exposure levels to AN; however, each job was classified as having either low, moderate, or high levels of AN exposure. Because data prior to 1957 were not available, the investigators analyzed only deaths between 1957 and 1981.

As with previous DuPont cohort studies, morbidity in the exposed cohort was compared with company-wide cancer incidence rates, while mortality was compared with company-wide rates and national rates. A total of 92 deaths was observed, with 21 attributed to cancer. For both wage workers and salary workers, the number of observed deaths was significantly lower than expected (Table 4-4). No excess of observed cancer deaths was observed in either worker category. Among the wage workers, the five observed lung cancer deaths were not statistically different than expected based on U.S. rates (SMR = observed ÷ expected = 0.59, 95% CI = 0.22–1.32). The significant deficit in observed deaths likely indicates, at least in part, the presence of a healthy worker effect, incomplete cohort identification, and possibly incomplete ascertainment of mortality data. It should be noted that death information was gathered for active and pensioned employees, and names of terminated employees were submitted to the Social Security Administration for identification of vital status. Vital status for 20 people (1.8%) was unknown. No lung cancer deaths were observed among the salary workers. As for other cause-specific deaths, no significant trends were detected among either wage or salary workers by time period or duration of exposure. Analyses by the level of AN exposure and cumulative exposure did not show significant differences between observed deaths and expected values.

Table 4-4. Distribution of select incidence and mortalities among wage and salary workers at an AN plant

Cause of disease/death	Wage workers			Salary workers			Total	
	Observed deaths	SMR_{US}[a] (CI)	SMR_{DuPont}[a] (CI)	Observed deaths	SMR_{US}[a] (CI)	SMR_{DuPont}[a,b] (CI)	Observed cases	SIR_{DuPont}[a,b] (CI)
All causes	68	0.57[b] (0.44–0.78)	0.77[b] (0.61–0.98)	24	0.41[b] (0.27–0.60)	0.66[b] (0.43–0.97)	–	–
All cancers	18	0.75 (0.44–1.16)	0.88 (0.54–1.37)	3	0.24[b] (0.06–0.66)	0.31[b] (0.08–0.85)	37	1.01
Lung cancer	5	0.59 (0.22–1.32)	0.66 (0.24–1.46)	0	Not determined	Not determined	5	0.72 (0.26–1.61)
Prostate cancer	1	1.11 (0.06–5.48)	1.11 (0.06–5.48)	1	2.0 (0.03–2.47)	2.0 (0.03–2.47)	5	2.63 (0.96–5.83)

[a]Calculated based on observed and expected values provided.
[b]Statistically significant ($p < 0.05$).

SMR_{DuPont} = SMR based on DuPont Registry; $SMR_{U.S.}$ = SMR based on U.S. statistics

Source: Amended from Chen et al. (1987).

Analyses of cancer incidence or morbidity reported 37 incident cancers in the cohort (Table 4-4). Twenty-seven were among the wage roll employees (vs. 26.0 expected) and 10 were among the salary roll employees (vs. 10.5 expected). No increase was noted in lung cancer incidence, with 5 cases observed in the total group vs. 6.9 expected (SIR = observed ÷ expected = 0.72, 95% CI = 0.26–1.61). The incidence of prostate cancer was increased, with 5 observed cases compared to 1.9 expected based on the company-wide database (SIR = 2.63, 95% CI = 0.96–5.83).

In summary, no statistically significant observed excess in overall cancer incidence or mortality was found among AN workers, but the presence of a healthy worker effect is likely. An increase in prostate cancer incidence was noted. As there is a general high rate of survival for prostate cancer cases, cancer incidence rather than mortality should be considered in the evaluation of AN exposure and disease. Some of the study's disadvantages that limit the interpretation of the results include the small sample size and number of cancer cases, subjective exposure assessment, lack of smoking information, and lack of stratification by latency and dose in the data analysis. There was the possibility of under-ascertainment of cases, particularly prostate cancer cases, by relying on the DuPont Cancer Registry as the source of information on cancer incidence. The results of this study support the findings of an excess in prostate cancer by O'Berg et al. (1985), but the aforementioned study limitations may have hindered the observation of an association between lung cancer and AN.

Wood et al. (1998) combined the Virginia and South Carolina cohorts described above (Chen et al., 1987; O'Berg et al., 1985) and analyzed 2,428 male workers with an added decade of follow-up. The exposure assessment was updated, taking into account plant histories,

descriptions of manufacturing processes, and changes that would affect exposures, a matrix of job titles, and work area names, documentation of personal protective equipment use, personal and area air sampling data from 1975, and descriptions of working conditions by long-term employees. Environmental air samples confirmed changes in plant processes, engineering, and ventilation. Exposure levels for the period before 1975 were estimated from information provided by a panel of "knowledgeable employees." Wood et al. (1998) estimated peak AN exposure in parts per million for a 40-hour workweek for each job title/work area combination and averaged this over a year. Peak exposure level categories, reported as the interval averages, were low (0.11 ppm), moderate (1.1 ppm), high (11 ppm), and very high (30 ppm). Other exposure variables analyzed included latency (<20 and ≥20 years of observation), duration of exposure (<5, 5–9, and ≥10 years), and cumulative exposure (<10, ≥10–<50, ≥50–<100, and ≥100 ppm-years). There was no information on exposure to other chemicals or on smoking status of the subjects.

The cohort included all employees who worked in exposed areas in either plant until the plants were closed. The DuPont Cancer Registry was used to identify incident cases of cancer among employees during employment. Thus, incident cancer cases occurring after tenure at DuPont would not have been identified. Vital status of past employees was determined through a review of the National Death Index (1979–1991) and the Social Security Administration (all years). Vital status of living employees was confirmed through pension records, motor vehicle records, and credit bureau reports. Expected numbers of deaths were derived from the DuPont mortality files and the U.S. population. The period of follow-up was extended through 1991 in the South Carolina plant and 1990 in the Virginia plant. At the end of the follow-up period, approximately 18% of the cohort was deceased (n = 454). The entire cohort had a total of 72,083 person-years of follow-up for the mortality analyses and 29,461 person-years for the morbidity analyses. More than half of the study population was born before 1930, and 82% were first exposed before 1971, thus allowing adequate follow-up to examine latency and adequate attained age to examine most cancer outcomes. A total of 37% of the population had a cumulative exposure level estimated at 50 or more ppm-years.

The SMR analysis revealed that the 454 deaths observed in the cohort were significantly below the expected number of deaths based on U.S. rates (SMR = 0.69, 95% CI = 0.62–0.75). There were 126 deaths from cancer, which include 46 lung cancer deaths, 27 digestive cancer deaths, and 11 prostate cancer deaths (Table 4-5). The SMR for all cancers was also significantly lower than expected (SMR = 0.78, 95% CI = 0.64–0.93), indicating a possible healthy worker effect. Incomplete ascertainment of the endpoint of death may have also played a role in the low SMR value, as only 18% of the cohort was deceased at the time of the follow-up. Among the site-specific cancer mortalities, an excess number of prostate cancer deaths was reported (SMR = 1.29, 95% CI = 0.64–2.30). A comparison of the cohort death rates with those derived from the DuPont mortality registry showed SMRs that were slightly different than those

derived from the U.S. data but did not provide any definitive differences. For all comparisons, there was no evidence of a relationship with any measure of exposure. For respiratory cancer, a nonsignificant excess of observed deaths was noted for the highest exposure level within the stratified analysis (SMR = 1.23 based on 23 observed deaths, 95% CI = 0.80–1.85).

Cancer incidence in the cohort was compared with company-wide incidence rates derived from the DuPont Cancer Registry. There were no significant elevations reported in any cancer-specific category (Table 4-5), although an excess in prostate cancer cases was reported. There were sufficient deaths in several categories to allow examination of the patterns of incidence by the four measures of exposure utilized in the mortality analyses. Specifically, all cancers, digestive organ cancers, respiratory system cancer, and prostate cancer were examined in the exposure analyses. There was no evidence of a relationship with any measure of exposure for all cancers, respiratory cancer, or digestive organ cancers.

Table 4-5. Distribution of select mortalities among exposed workers in two AN plants

Cause of disease/death	South Carolina cohort		Virginia cohort		Combined cohort			
	Observed deaths	SMR[a] (CI)	Observed deaths	SMR[a] (CI)	Observed deaths	SMR[a] (CI)	Observed cases	SIR[a] (CI)
All causes	271	0.76[b] (0.67–0.85)	185	0.60 (0.51–0.69)	454	0.69[b] (0.62–0.75)	–	–
All cancers	77	0.88 (0.69–1.10)	50	0.66 (0.49–0.87)	126	0.78b (0.64–0.93)	101	0.97 (0.79–1.18)
Lung cancer	35	1.06 (0.74–1.47)	11	0.40[b] (0.20–0.71)	46	0.76 (0.56–1.02)	17	0.81 (0.48–1.28)
Digestive cancer	12	0.57[b] (0.29–0.99)	15	0.81 (0.45–1.33)	27	0.69 (0.45–1.00)	22	0.89 (0.56–1.34)
Prostate cancer	5	1.23 (0.40–2.86)	6	1.32 (0.48–2.88)	11	1.29 (0.64–2.30)	12	1.58 (0.82–2.76)

[a]SIR and SMR standardized against company-wide rates.
[b]Statistically significant ($p < 0.05$).

Source: Amended from Wood et al. (1998).

In summary, this study provided better exposure assessment than previous studies of this group of workers. Additional follow-up and the combination of two small cohorts enhanced the information available for inclusion; however, the apparent healthy worker effect may have masked a relationship between AN exposure and death from or incidence of lung cancer or other cancers.

Symons et al. (2008) provided an update based on the combined Virginia and South Carolina cohorts from Wood et al. (1998), adding 11 years of follow-up. The exposure assessment was the same as described in Wood et al. (1998) with exposure being based on a job-

exposure matrix, documentation of personal protective equipment use, personal and area air sampling data, and descriptions of working conditions by long-term employees. Vital statistics were obtained through the DuPont Epidemiology Registry and verified by the National Death Index. New in this update was the assignment of mean intensity values based on estimated intensity categories ranging from <0.2 to >20 ppm. These intensity categories were coupled with duration of employment to determine cumulative exposure. For SMR calculations, the expected number of deaths were derived both the U.S. population and regional DuPont employees. To reduce potential bias associated with the healthy worker effect, the Occupational Mortality Analysis Program (OC-MAP) was utilized for SMR calculations. For the estimation of relative mortality risk via a hazard ratio, a log linear model for AN exposure was assumed for all-cause and cause-specific outcomes.

Of the 2,559 workers from Wood et al. (1998), 11 workers were found to be exposed to AN for <6 months and thus were excluded from the cohort in Symons et al. (2008). A total of 839 deaths (32%) were observed in this updated cohort of 2,548 male workers. Of these, 240 deaths were due to cancer, with 88 deaths being specific to lung cancer (Table 4-6). One quarter of the updated cohort were found to be in the mean intensity exposure group of <2.0 ppm, while, two-thirds were in the 2.0–19.9 ppm mean intensity exposure category. The number of deaths, especially cause-specific deaths, in these exposure groups was not reported.

Table 4-6. Distribution of select mortalities among exposed workers

Cause of death	South Carolina cohort		Virginia cohort		Combined cohort		
	Observed deaths	SMR[a] (95% CI)	Observed deaths	SMR[a] (95% CI)	Observed deaths	SMR[a] (95% CI)	SMR[b] (95% CI)
All causes	481	0.98 (0.89–1.07)	358	0.85[c] (0.76–0.95)	839	0.92[c] (0.86–0.98)	0.69[c] (0.64–0.74)
All cancers	144	1.00 (0.84–1.18)	96	0.81[c] (0.67–0.99)	240	0.92 (0.81–1.04)	0.73[c] (0.64–0.82)
Lung cancer	61	1.14 (0.88–1.49)	27	0.64[c] (0.42–0.93)	88	0.92 (0.75–1.14)	0.74[c] (0.60–0.91)
Prostate cancer	12	0.93 (0.48–1.63)	13	1.12 (0.60–1.92)	25	1.02 (0.66–1.51)	0.91 (0.59–1.35)

[a]Based on company regional rates.
[b]Based on U.S. population rates.
[c]Statistically significant ($p < 0.05$).

Source: Amended from Symons et al. (2008).

Symons et al. (2008) also reported hazard ratio estimates for 100-ppm years increase in cumulative exposure (Table 4-7). In addition to the variable 'exposure term' used in the crude model, the adjusted model utilized in generating hazard ratio estimates included 'birth period' (6-decade ordinal variable) and 'employment in South Carolina start-up group' (binary

indicator). The authors noted a slight significant increase in all-cause mortality associated with increasing cumulative exposure to AN in the crude model but did not find any other statistically significant findings. Colorectal and brain cancers had elevated hazard ratios but were not statistically significant in either the crude or adjusted models.

Table 4-7. Crude and adjusted hazard ratio estimates for 100 ppm-year increase in cumulative exposure

Cause of death	Crude		Adjusted[a]	
	Hazard ratio	95% CI	Hazard ratio	95% CI
All causes	1.12[b]	1.04–1.21	1.05	0.97–1.14
All cancers	1.07	0.92–1.24	1.00	0.86–1.17
Lung cancer	1.04	0.81–1.33	0.95	0.73–1.23
Prostate cancer	0.81	0.48–1.35	0.78	0.46–1.32
Colorectal cancer	1.13	0.74–1.71	1.16	0.75–1.81
Brain and CNS	1.37	0.59–3.16	1.03	0.38–2.78

[a]Model includes exposure term, birth period, and employment in South Carolina start-up group.
[b]Statistically significant ($p < 0.05$).

Source: Amended from Symons et al. (2008).

Hazard ratios estimates were also derived based on lagged cumulative exposure. Increasing exposure lags resulted in decreasing hazard ratios for all cancers, lung cancer, and colorectal cancer. However, an increase in hazard ratio estimates over lagged cumulative exposure was observed for brain and CNS cancer and lymphatic and hematopoietic cancer. It should be noted that the number of events for these cancers were small (Table 4-8).

Table 4-8. Hazard ratio estimated for select cancer mortality by lagged cumulative exposure for 100 ppm-year increase in cumulative exposure

Cause of death	5-Yr lag (n = 2,224)		10-Yr lag (n = 2,066)		15-Yr lag (n = 1,907)	
	Events	Hazard ratio (95% CI)	Events	Hazard ratio (95% CI)	Events	Hazard ratio (95% CI)
All cancers	210	1.03 (0.87–1.23)	199	0.98 (0.80–1.20)	179	0.94 (0.74–1.19)
Lung	75	0.95 (0.70–1.28)	72	0.84 (0.59–1.19)	63	0.80 (0.53–1.22)
Prostate	22	0.86 (0.48–1.53)	19	0.98 (0.50–1.92)	15	0.95 (0.41–2.22)
Colorectal	26	1.06 (0.64–1.76)	24	0.90 (0.49–1.66)	23	0.81 (0.40–1.66)
Brain and CNS	4	1.38 (0.43–4.47)	4	1.55 (0.44–5.47)	4	1.96 (0.49–7.84)
Lymphatic and hematopoietic	16	1.09 (0.59–2.01)	14	1.29 (0.66–2.54)	13	1.27 (0.57–2.86)

Source: Amended from Symons et al. (2008).

In summary, Symons et al. (2008) followed workers for over 50 years and, among the 33% mortality in the cohort, reported that no statistically significant observed excess in overall mortality was found among AN workers. Unlike the previous studies based on the DuPont cohort, Symons et al. (2008) did not provide cancer incidence data or address previous issues with this cohort such as smoking status and concomittent exposure to other chemicals. This update did attempt to reduce potential bias from the healthy worker effect with specialized statistical program. Differences between U.S. population-based SMRs and regional worker-based SMR indicated that there may still be a strong healthy worker effect. Although Symons et al. (2008) categorized workers in different mean intensity exposure and cumulative exposure groups, the authors did not report the observed number of cause-specific deaths in these categories or provide cause-specific SMR estimates. In deriving hazard ratio estimates, Symons et al. (2008) adjusted for workers 'employment in South Carolina start-up group.' Based on O'Berg (1980), it appears that workers in the South Carolina start-up group may have had higher levels of exposure to AN. Additionally, the metric derived by quantitation of AN exposure and SMR derivation of this subgroup would have been helpful for better assessing the relationship between AN exposure and lung cancer.

Overall summary

The DuPont cohort studies were the first to hypothesize an association between AN exposure and cancer, specifically lung and prostate cancer. It should be noted that the DuPont cohort studies are limited to male workers and lack appropriate unexposed worker comparison

groups to better assess the risk of developing cause-specific diseases, namely cancer. Even in the most recent cohort study by Symons et al. (2008), smoking and concomitant exposures were not adequately addressed in any of the DuPont cohort studies. Interestingly, the prostate cancer findings in the Wood et al. (1998) study revealed a closer association to duration of employment rather than exposure. This observation is echoed with brain and CNS cancer and lymphatic and hematopoietic cancer in Symons et al. (2008).

Excluding Symons et al. (2008), the DuPont cohort studies are the only studies that evaluate the association between AN exposure and cancer incidence rather than relying on a surrogate marker such as cause-specific death. For cancer incidence, the cohort studies appeared to only focus on data from the DuPont cancer registry rather than including data from state or national tumor registries that have known quality assurance and quality control procedures for diagnoses.

Symons et al. (2008) assessed risk based on mortality. As with the other DuPont studies, the reliance on mortality statistics from the U.S. population as a comparison group is less desirable given the potential for bias from the healthy worker effect. Symons et al. (2008) attempted to address this issue by employing DuPont regional workers as a comparison group instead of using company-wide statistics as in other DuPont studies. Information regarding other chemical exposures among regional workers would aid in reducing the uncertainty of exposure to other potential carcinogens in this comparison group.

As with its predecessor, Wood et al. (1998), the most recent DuPont cohort study Symons et al. (2008) may also suffer from exposure misclassification, as no exposure monitoring existed prior to 1975. This lack of information on exposure potential and level may also subject the studies to recall bias. However, given the shortcomings of each of the individual DuPont studies, there is still suggestive evidence that there may be an association between AN exposure and the incidence of cancer.

American Cyanamid Company

Collins et al. (1989) conducted a retrospective cohort study of 2,671 men who worked at two American Cyanamid Company plants in Louisiana and Florida from start-up (1951 for the Louisiana plant, 1957 for the Florida plant) through December 1973. One facility manufactured AN and other materials, and the other facility utilized large quantities of AN in the manufacturing of acrylic fiber. All 2,671 study subjects were followed through the end of 1983 for mortality, thus allowing at least 10 years of follow-up for the cohort. According to Collins et al. (1989) for exposure estimation, industrial hygiene monitoring, which began in 1977, was considered representative of previous exposure levels, with adjustments made for changes in practices and engineering controls. Any actual measurements that were available were also used to tailor job-specific exposure. The investigators created four exposure categories: 0–<0.01, 0.01–0.7, 0.7–7.0, and >7 ppm/year. Exposed workers were defined as

having a cumulative exposure of >0.01 ppm/year. Smoking information was only available for 58% of the workers. Each person in the cohort was coded as smoker (smoked for ≥3 months), nonsmoker (smoked for <3 months), or unknown (information not available). The authors used an internally standardized method of adjustment for age (<45, 45–54, 55–64, 75+ years), race (white, nonwhite), smoking status (smoker, nonsmoker, unknown), latency (<10, 10–19, 20+ years), and time period (<1965, ≥1965). In the calculation of the SMR, the expected number of cause-specific deaths was derived from U.S. general population data on men.

More than 50% of the exposed workers in this study were followed for at least 20 years. By the end of the study, a total of 237 deaths (92 from the unexposed group and 145 from the exposed group) were observed, and death certificates were located for 224 of these workers. From both groups combined, there were 65 cancers, including 23 respiratory cancers, of which 22 were lung cancers. For lung cancer, there was no significant elevation in the SMR for either the exposed or unexposed group (SMR in unexposed group = 1.08, 95% CI = 0.69–1.61; SMR in exposed group = 1.01, 95% CI = 0.74–1.35). A similar pattern was observed among the lung cancer deaths, with no significant elevations reported (SMR in unexposed group = 1.01, 95% CI = 0.44–2.01 [7 cancer deaths]; SMR in exposed group = 1.00, 95% CI = 0.58–1.61 [15 cancer deaths]). The SMRs for the AN exposure categories for lung cancer were 1.09 (95% CI = 0.51–2.08), 0.63 (95% CI = 0.10–2.06), 0.64 (95% CI = 0.20–1.53), and 1.41 (95% CI = 0.68–2.58) for categories 0–<0.01, 0.01–0.7, 0.7–7.0, and >7 ppm/year, respectively. Using an internally standardized method that adjusted for smoking, race, latency, age, and time period, the SMRs were 1.11 (95% CI = 0.52–2.11), 0.72 (95% CI = 0.12–2.36), 0.71 (95% CI = 0.23–1.72), and 1.22 (95% CI = 0.59–2.23), respectively, for the above exposure categories. None of these risk estimates or subsequent trend tests was statistically significant. No additional information was provided with regard to the nature of the trend test.

The inclusion of an analysis for the unexposed group compared to the U.S. population was helpful and allowed an evaluation of whether elevations in cancer rates in the exposed group were also observed in the unexposed group and thus were not likely to be related to exposure. It should be noted that indirect standardization (the use of age-specific mortality rates from the standard U.S. population to derive regional expected deaths) was used, thus hindering the ability to compare SMRs across groups. This study attempted to quantify exposure levels and control for smoking history. The study did allow for approximately 50% of the exposed cohort to have at least 20 years of follow-up, thus strengthening the possibility that a health effect might be detected. However, since the endpoint marker used was death, as recorded on the death certificates, and with less than 10% of the study cohort deceased by the end of the study, the study may have been premature in attempting to link AN exposure to cancer deaths. This study may have had insufficient power as portrayed by the observation of only 15 lung cancer deaths in the exposed group. It should also be noted that this study, as with many other cohorts assembled to assess the relationship between AN and cancer, consists of only men.

Because the results presented were adjusted by latency, duration of exposure, and time since exposure, relative risks (RRs) in these strata could not be readily compared with the results of the studies of Symons et al. (2008), Benn and Osborne (1998), Blair et al. (1998), Swaen et al. (1998), Wood et al. (1998), O'Berg et al. (1985), and O'Berg (1980). Unlike other studies that assumed early exposure levels were higher, Collins et al. (1989) assumed that AN exposure levels in 1977 were representative of the time frame prior to that date. This assumption may have led to exposure misclassification, resulting in a flattening of the dose-response gradient. Other limitations included low statistical power to evaluate lung or rarer cancers, particularly in subgroup analyses, incomplete smoking information, and use of SMRs rather than comparable unexposed controls. In summary, this study may have been premature in assessing the relationship between AN exposure to cancer deaths.

Synthetic chemical plant in the U.S.

Waxweiler et al. (1981) examined the mortality rates in a cohort of 4,806 chemical plant workers who were exposed to many potential carcinogens, including AN. The cohort was identified as all workers at the synthetic chemicals plant who were first employed between 1942 and 1973. These workers were followed through the end of 1973. Since the majority of the cohort (63%) were actually hired before 1954, this allowed for at least 20 years of latency and follow-up for the majority of the workers. However, it should be noted that some workers had less than 1 year of follow-up, latency, or exposure. The cohort was described as young, with only 30% of live workers being over 55 years of age.

Mortality rates in the plant cohort were compared to those derived from the U.S. white male population. Under the assumption that all workers were considered at risk from the first day of employment, no difference was noted between the observed deaths and the expected deaths (556 observed deaths vs. 550.2 expected deaths, SMR = 1.01, 95% CI = 0.93–1.10). The number of observed cancer deaths was higher than expected (109 observed vs. 92.5 expected, SMR = 1.18, 95% CI = 0.97–1.42). Upon stratification of cancer deaths, higher numbers of respiratory system and CNS cancers were observed among the workers (respiratory cancer SMR = 1.49, 95% CI = 1.09–1.99; CNS cancer SMR = 2.09, 95% CI = 1.02–3.84).

A secondary analysis was performed among workers who had at least 10 years of exposure. Waxweiler et al. (1981) noted similar findings, though actual values were not reported. The authors did note that there were 39 observed deaths from cancers of the respiratory system compared to 25 expected (SMR = 1.56, 95% CI = 1.12–2.11). A similar elevation had been observed by the authors in a previous publication (Waxweiler et al., 1976) that focused on the workers with high vinyl chloride monomer exposure; thus, the authors concluded that the excess lung cancer risk may not solely be due to exposure to a single chemical.

Serially additive expected dose (SAED) modeling was performed to determine whether exposure to chemicals, including AN, was associated with excess lung cancer risk. Job histories were used to assess the potential for exposure to 19 chemicals routinely used at the plant. Each job was assigned a qualitative exposure rating (from 0 for no exposure to 5 for intimate contact on the skin or high inhalation potential) for each year of the study. Thirty-five of the 80 (56%) job categories ranked had no exposure to AN, with another 30% reporting minimal to low levels of exposure. An exposure score was derived for each chemical for all workers by summing each exposure rating for each year. The exposure score for each cohort member dying from respiratory system cancers was compared to the score for a group of workers with a similar birth year and year of first hire (the "subcohort" from which the case arose). Scores in the nonrespiratory death subcohorts (expected scores) were subtracted from the observed scores in the respiratory cancer deaths to obtain an observed-minus-expected cumulative dose difference per lung-cancer case. For AN, this calculation resulted in a negative unit, reflecting that expected cumulative dose greatly exceeded the observed cumulative dose. No significant differences with regard to AN exposure were observed in this analysis.

While this study showed significant increased risks of death from lung and CNS cancer in a cohort of workers exposed to multiple carcinogens, limitations with the study design hindered the ability to assess the relationship between the observed deaths and exposure to AN. The population of workers was potentially exposed to multiple carcinogens, so any effect of exposure to AN may have been impossible to measure.

Rubber manufacturing plant

Delzell and Monson (1982) analyzed the mortality among workers from a rubber manufacturing plant in order to determine if potential exposure to AN might be associated with excess deaths. The study included 327 white males who had been employed at the plant for at least 2 years between January 1940 and July 1971. These employees were selected from over 15,000 workers because they worked in departments where AN exposure was most likely. Mortality information was gathered on both active and pensioned workers through July 1978, allowing at least 7 years of follow-up for most workers in the cohort. Workers without a record of death were assumed to be alive. Mortality rates were compared with the white male subset of the U.S. general population rates, stratifying by cause of death, age, and calendar time.

By mid-1978, a total of 74 deaths (~ 22%) were observed, 22 of which were from various types of cancers. The differences between the observed and expected deaths for all-cause and for cancer mortality were not statistically significant, with SMRs of 0.8 (95% CI = 0.7–1.0) and 1.2 (95% CI = 0.8–1.9), respectively. Nine lung cancer deaths were observed as compared to the 5.9 expected (SMR = 1.5, 95% CI = 0.7–2.9). The ability to detect statistical significance may have been hindered by the small number of deaths. The numbers of deaths from bladder, lymphatic, and hematopoietic cancers exceeded the expected values, but the number of deaths

were small. Lung cancer deaths were examined by duration of employment and latency. No trends were noted, and there were no deaths in the group employed for ≥15 years. However, 7 lung cancer deaths were observed as compared to the 4.1 expected in the group with 15 or more years of latency since first exposure.

This study was based on a small number of study participants, with less than a quarter reaching the study endpoint of death. The study provides no quantitative assessment as to the level of AN exposure. Mixed exposure is also an issue, since it is noted that butadiene, styrene, and vinyl pyridine were utilized at the plant during the exposure time frame. However, there is no information in the study as to whether the study participants were potentially exposed to these other agents. Finally, though lung cancer was specifically analyzed, no mention of data collection or adjustment for smoking history was reported. These shortcomings limit the weight that this study carries with regard to assessing the relationship between AN exposure and cancer mortality.

The Netherlands cohort

Three successive papers (Swaen et al., 2004, 1998, 1992) reported mortality analyses of a Dutch cohort consisting of 2,842 male workers employed ≥6 months from 1956 to 1979 in eight companies that produced AN, latex polymer, acrylic fiber, AN polymers, resins, or acrylamide. This cohort was compared to 3,961 workers at a neighboring plant during the same time frame who were not exposed to any known carcinogens in the normal work setting. Use of this reference population aided in minimizing the impact of a potential healthy worker effect.

In the original study (Swaen et al., 1992), exposure assessment for most companies was conducted using a job matrix model and air AN samples collected in 1978–1979. The exposure assessment took into account changes in the production process, industrial hygiene control measures, and work procedures over time. Potential for exposure misclassification was enhanced by the extrapolation of exposure monitoring data from one plant to the other seven plants, for which there were no exposure monitoring data. For all of the companies involved, most jobs were classified in the following ranges: 0–0.5, 0.5–1, 1–2, and 2–5 ppm. However, for some jobs, only two categories could be distinguished: 0–2 and 2–5 ppm. For all exposed workers in the study, a cumulative measure of exposure was derived by multiplying the average concentration for a particular exposure class by the number of years in that class. Although workers were characterized by duration of exposure and duration of follow-up, these variables were not used in the evaluation of the relationship between AN and cancer deaths.

Both the exposed and the unexposed groups were compared with national Dutch death rates to generate SMRs. No direct comparison of rates in the exposed and unexposed groups was followed for ≥20 years after entry into the cohort. Almost 24% of the exposed cohort was categorized in the highest category of cumulative exposure of ≥10 ppm-years, a cutoff higher than the ≥8 ppm used in the Blair et al. (1998) study.

Mortality information was collected for both groups through the end of 1987, allowing at least 8 years of follow-up for all surviving study members. A total of 134 deaths was observed in the exposed group (SMR = 0.78, 95% CI = 0.65–0.92) and 572 deaths in the unexposed group (SMR = 0.77, 95% CI = 0.71–0.84), undertaken, with the authors citing differences in age and calendar time between the groups as the rationale. Nearly half of the exposed group worked with AN for at least 5 years, and 26% of the unexposed group was both observations significantly lower than expected. As both exposed and unexposed workers were compared to a national rate, the lower observed deaths may be attributable to the healthy worker effect. Among the workers exposed to AN, no significant differences were noted between the number of observed and expected cancer deaths (i.e., 42 observed deaths vs. 50.8 expected, SMR = 0.83, 95% CI = 0.60–1.10). Analyses of site-specific cancer deaths in this group did not reveal any significant differences between the observed cancer deaths and the expected values. However, among the unexposed workers, the number of observed deaths from cancer of the trachea and lung was significantly lower than expected (i.e., 67 observed deaths vs. 93.3 expected deaths, SMR = 0.72, 95% CI = 0.56–0.90), likely indicating, at least in part, the presence of a healthy worker effect. Among exposed workers in the highest exposure category, the number of observed lung cancer deaths exceeded the number expected (SMR = 1.11, 95% CI = 0.48–2.19). Compelling evidence of the healthy worker effect is provided by the fact that the observed number of deaths among the unexposed group, regardless of disease category, is significantly lower than the expected estimates derived from the national population statistics.

In an updated analysis by Swaen et al. (1998), an additional 8 years of follow-up yielded 156 more deaths in the exposed cohort and 411 more deaths in the unexposed group, bringing the total number of observed deaths to 290 and 983, respectively. The exposure assessment was not updated because more recent exposures were considered to be negligible. For both groups, the total number of cancers observed was lower than expected. The exposed group had 97 deaths from neoplasms observed vs. 110.8 expected (SMR = 0.88, 95% CI = 0.71–1.06) and the unexposed group had 332 deaths observed vs. 400.4 expected (SMR = 0.83, 95% CI = 0.74–0.92). With the increased follow-up time, slight, but mainly statistically nonsignificant, increases in cancer of the brain, large intestine, prostate, and all leukemias for the exposed group were observed that were not previously evident. While these increases were based on small numbers, it is noteworthy that intestinal tract and brain are cancer target organs in rat studies.

The association between AN exposure and mortality, all-cancer mortality, and lung cancer mortality was examined by the following exposure variables: latency, peak exposure, cumulative exposure, respirator use, and exposure to other carcinogens. Overall, among workers exposed to AN, the number of observed deaths did not differ greatly from expected.

Swaen et al. (2004) revisited this cohort of AN workers and added 5 years of follow-up to the analysis, for a minimum of 22 years of follow-up. This updated study added 142 new deaths for the exposed cohort and 360 deaths to the unexposed cohort, bringing the total number of

observed deaths for 432 and 1,343, respectively. The number of deaths was 2.5-fold higher than in the original cohort study and accounted for over a quarter of the original study population. The exposure assessment was not updated from the first study.

SMR analyses were conducted for both the exposed and unexposed cohorts, using the Dutch general population rates as a comparison. The observed number of cancer deaths in the exposed group was not significantly different from the expected value (Table 4-9). The study found that number of respiratory cancer deaths in this group was higher than expected, 67 observed vs. 62.5 expected (SMR = 1.07, 95% CI = 0.83–1.36). Analyses by peak exposure, respirator use, and possible exposure to cocarcinogens were also performed, yielding no indication for elevated site-specific cancer risks in any of the subgroups. Additional analyses were performed by examining the SMRs for lung cancer by various measures of dose and latency (Table 4-10). An increasing SMR was noted with increasing levels of exposure (i.e., 0.92, 1.06, and 1.15 for low, medium, and high exposure, respectively).

Table 4-9. Distribution of select mortalities among AN-exposed and unexposed workers

Cause of death	Exposed workers				Unexposed workers			
	Observed	Expected	SMR	95% CI	Observed	Expected	SMR	95% CI
All causes	432	467.8	0.92	0.84–1.01	1,343	1,545.2	0.87	0.82–0.92[a]
All cancers	146	164.5	0.89	0.75–1.04	447	519.8	0.86	0.78–0.94[a]
Lung and trachea cancer	67	62.5	1.07	0.83–1.36	160	203.8	0.78	0.67–0.92[a]

[a]Statistically significant ($p < 0.05$).

Source: Amended from Swaen et al. (2004).

Table 4-10. Lung cancer mortality of AN-exposed workers stratified by cumulative dose and latency

	All cancer mortality				Lung cancer mortality			
Dose	**Observed**	**Expected**	**SMR**	**95% CI**	**Observed**	**Expected**	**SMR**	**95% CI**
Low (<1 ppm/yr)								
<10 Yrs latency	0	1.9	–	–	–	0.7	–	–
10–20 Yrs latency	7	7.5	0.93	0.37–1.91	3	2.9	1.03	0.21–2.97
≥20 Yrs latency	10	11.3	0.88	0.42–1.62	4	4.0	1.00	0.27–2.53
Total	17	20.7	0.82	0.48–1.31	7	7.6	0.92	0.37–1.89
Moderate (1–10 ppm/yr)								
<10 Yrs latency	8	8.4	0.95	0.41–1.87	1	3.2	0.31	0.40– 1.58
10–20 Yrs latency	31	32.1	0.96	0.66–1.37	16	12.4	1.29	0.74–2.09
≥20 Yrs latency	39	49.4	0.79	0.56–1.08	19	18.2	1.04	0.63–1.63
Total	78	89.9	0.87	0.69–1.08	36	33.8	1.06	0.75–1.47
High (>10 ppm/yr)								
<10 Yrs latency	8	6.0	1.33	0.57–2.62	3	2.5	1.20	0.24–3.44
10–20 Yrs latency	25	21.1	1.18	0.77–1.75	12	8.4	1.43	0.74–2.49
≥20 Yrs latency	18	26.3	0.68	0.40–1.08	9	10.0	0.90	0.41–1.70
Total	51	53.4	0.95	0.71–1.26	24	20.9	1.15[a]	0.75–1.68[a]

[a]Calculated based on reported data.

Source: Amended from Swaen et al. (2004).

In summary, as with previous analyses of this cohort, the interpretation of the results from this study is limited by the following: potential misclassification of AN exposure because of the use of current measures to derive past exposures and the use of subjective information about exposure, use of a population-based control group, pooling of data from factories with different kinds of AN production and exposures without adjusting for this, and lack of information on smoking.

Epidemiology studies based on this Dutch cohort provided better exposure assessment than studies using the SAED method or similar extrapolation tools. Here, exposure categories represented estimates based, in part, on actual measurements rather than ordinal ranking. The number of lung cancer deaths observed among the AN-exposed workers was higher than expected. However, the following biases regarding the Dutch cohort studies are possible: potential misclassification of AN exposure because of the use of current measures to estimate past exposures and the use of subjective information about exposure, use of a population-based control group, pooling of data from factories with different kinds of AN production and exposures without appropriate adjustment, and bias based on the lack of smoking information available. The low SMRs observed indicate the presence of a potential healthy worker effect, making it more difficult to detect an association with AN.

The Dutch studies cohort utilized an unexposed worker cohort for a "comparison" group. The use of this unexposed group was not fully explored by developing rates by age and calendar time in the unexposed group to be used as a basis for developing expected rates in the exposed group. Instead, the unexposed group was compared to national rates and then used as a "standard" to see if the patterns of SMRs generated in the exposed cohort looked similar to those generated in the unexposed cohort. Therefore, the true comparison group used in these studies was the national population. It should be noted that the lung cancer SMR among workers exposed to AN was found to be higher than that among unexposed workers. Direct comparison between the exposed and unexposed workers in terms of an RR was not derived, as the demographics between the exposed and unexposed workers may have differed. Though no explicit details were provided, it is noted that the number of person-years and crude mortality rate are higher in the unexposed workers (recruited from a different plant) than in the exposed workers. Thus, the expected number of deaths for each group, on which the SMRs are based, would be dependent on different distributions or standards, a situation in which comparing the SMRs between the exposed and unexposed groups would not be recommended. Additional support is provided with the increasing SMR with level of exposure; a progressive increase of 0.92 in the low exposure group to 1.15 in the high exposure group was reported.

Finally, the statistical measure used in all the Dutch cohort studies was the SMR. This statistic allows for the comparison of cause-specific deaths and not the incidence of disease. Using deaths as a surrogate for disease may underestimate the true relationship between AN exposure and cancer, especially when the majority of the cohort population is not deceased. As with other studies that evaluate AN exposure using SMRs, these Dutch studies were focused on determining if AN exposure may lead to an excess of cause-specific deaths; however, these studies lack the appropriate design to address the issue of AN exposure and the incidence of disease, namely site-specific cancers.

BASF plants in Germany

A mortality study was conducted among workers from 12 BASF plants in Germany (Thiess et al., 1980). Though none of these plants manufactured AN, this substance, along with styrene and butadiene, was used in many of their processes. The number of employees in each plant varied, ranging from 30 to 334 employees. The first uses of AN at these plants did not occur simultaneously but rather over a course of 14 years, from 1954 to 1968. A total of 1,469 active and former employees who had worked for >6 months processing AN were identified for mortality follow-up. The cohort was followed through May 15, 1978, and death certificates were obtained and coded for cause of death. There were 1,081 German workers in the cohort, and the vital status was traced for 98% of these workers. Tracing was less successful for the 388 foreign workers in the cohort, with only 56% follow-up.

No measurements of levels of AN exposure were available for use in this study. It was noted that prior to 1976, AN was handled manually, and as a result, there may have been increased exposure during that time (Thiess et al., 1980). In later years, closed systems were utilized, leading to reduced exposures. Although measurements were not available, this study assumed that workers were occasionally exposed to levels of ≥20 ppm for short periods, based on the manual handling of AN at specific work sites prior to 1976. Several other known carcinogens were used at some of the facilities and could have presented a confounding effect in terms of cancer outcomes. One plant (Plant 5) was subsequently excluded from the analysis because of the potential for concurrent exposure to β-naphthylamine.

The comparison rates used for the majority of the analyses were derived from mortality rates for the Federal Republic of Germany. The 1,469 workers accounted for a total of 15,350 person-years of follow-up. A total of 89 deaths were observed, a value lower than the 99 predicted deaths based on rates for the Federal Republic of Germany (SMR = 0.90, 95% CI = 0.72–1.10). A total of 27 cancer deaths was observed for the entire cohort, compared to the 20.5 expected deaths (SMR = 1.32, 95% CI = 0.89–1.89).

In the analysis that excludes Plant 5, the number of observed deaths dropped to 74, with the expected deaths at 78.8 (SMR = 0.94, 95% CI = 0.74–1.17). Among these deaths, 20 were attributed to cancer, with a calculated expected value of 16.1 deaths (SMR = 1.24, 95% CI = 0.78–1.88). In both analyses, the number of cancer deaths exceeded expected estimates, but the small sample size might have hindered the observation of statistically significant findings. When cause-specific cancer deaths were examined, a significant difference was noted between the observed and expected bronchial carcinoma (lung cancer) deaths, regardless of the inclusion of Plant 5 in the analysis (i.e., 11 observed deaths vs. 5.7 expected in the full cohort and 9 observed vs. 4.4 expected in the cohort without Plant 5).

Neoplasms of the lymphatic and hematopoietic organs were also observed to be elevated, but not significantly (i.e., 4 observed vs. 1.7 expected in the full cohort and 4 observed vs. 1.4 expected in the cohort without Plant 5). Because of the small number of deaths in this category, further stratification or examination was precluded. It should be noted that two of the four deaths in this category were from Hodgkin's disease, which is significantly different from the 0.3 deaths expected.

Analyses were conducted, excluding Plant 5, for the group of workers who were followed for at least 5 years before death or loss to follow-up. This comprised 944 workers, with only seven bronchial carcinomas reported. These carcinoma deaths were stratified by duration of exposure into three categories: 0–4, 5–9, and ≥10 years. There were no bronchial carcinomas in the 0–4 year exposure category, four in the 5–9-year exposure category and three in the highest exposure category. For the latter two categories, the observed number of deaths was higher than expected ($SMR_{4–9\ years}$ = 3.86, 95% CI = 1.23–9.31; $SMR_{\geq 10\ years}$ = 2.23, 95% CI = 0.57–6.07).

The study of BASF workers showed a significant excess in lung-cancer deaths in workers potentially exposed to AN. The follow-up time was not specifically quantified; however, examination of the exposure (1954–1968) and follow-up (5/15/1978) dates indicates that most workers in the cohort were followed for at least 9 years. The study is limited by the fact that only 6% of the study cohort was recorded as deceased; this observation is important since death certificates were used to determine if an association between AN exposure and certain cancers existed. An additional limitation of this study is the fact that the cohort was assembled from 12 different plants and some of the plants were acknowledged to have concurrent exposures to known carcinogens such as β-naphthylamine, vinyl chloride, or solvents. The study did not indicate when these overlaps in exposures could have occurred and how many workers at the plant could have been possibly exposed, and no information on the level of exposure was provided. This limitation coupled with a lack of ability to characterize the workers by job or exposure level makes this study less informative in trying to assess the relationship between cancer mortality and AN exposure.

Six factories in the United Kingdom

There have been two successive studies evaluating the mortality rates in a cohort of male workers potentially exposed to AN at six United Kingdom polymerization and spinning factories (Benn and Osborne, 1998; Werner and Carter, 1981). For both studies, workers were included if they were employed for at least 1 year between 1950 and 1968. Werner and Carter (1981) examined the mortality rates in a cohort of 1,111 men drawn from six factories in England, Wales, Scotland, and Northern Ireland. This cohort was followed through the end of 1978, allowing for a minimum 10-year follow-up for all surviving workers. The workers included in the study were deemed to have the potential for the highest level of AN exposure, since they were involved in either the AN polymerization process or spinning of acrylic fiber. However, no exposure monitoring data were available for the period of the study. Additionally, there was potential for concomitant exposure to styrene and butadiene in the work environment.

Each worker in the cohort was classified according to the length of time spent in a high-exposure job. This categorization resulted in 934 workers with ≥1 years and 177 workers with <1 year of potential for high exposure to AN. The remainder of the analyses focused on the 934 workers with ≥1 year in a job with potential for high exposure. Examination of the person-years distribution by age group in these 934 workers revealed that <2% of the person-years was observed in persons over age 65, while 65% of the person-years was observed in the 15–44-year age range. Thus, the follow-up time for this cohort may be inadequate to detect excess cancer deaths.

Among the 934 workers, 68 deaths were observed compared to the 72.4 expected based on mortality rates for the total male population of England and Wales (SMR = 0.93, 95% CI = 0.73–1.18). Of these observed deaths, 21 were attributed to cancer, with 9 specifically attributed

to cancer of the trachea, bronchus, and lung. The SMRs for all malignant neoplasms and cancer of the trachea, bronchus, and lung are 1.10 (95% CI = 0.72–1.70) and 1.20 (95% CI = 0.58–2.17), respectively. Incidentally, the number of observed stomach cancer deaths was significantly higher than expected (5 observed vs. 1.9 expected, SMR = 2.63, 95% CI = 0.96–5.83).

The distribution of cancer deaths was also examined by age at death (age groups: 15–44, 45–54, 55–64, and ≥65 years). No significant differences between the number of observed and expected all-cause deaths were found in any of the age groups. Of the 14 deaths observed in the 15–44-year age group, 3 deaths were attributed to cancer of the trachea, bronchus, and lung, a significant increase over the 0.7 expected value (SMR = 4.28, 95% CI = 1.09–11.66). No significant differences between observed and expected cancer-specific deaths were noticed in any of the other age groups.

All-cause deaths were also stratified based on the year of first exposure to determine if cancer risks were higher for those who were exposed in the early years of the factories' operations (usually a surrogate for longer and often higher exposure and longer latency) compared with more recent hires. Three time periods were examined: 1950–1958, 1959–1963, and 1964–1968, with the observed number of deaths being 35, 21, and 12, respectively. No significant differences between the number of observed and expected deaths were found. Observed and expected deaths from all cancer types, including cancer of the trachea, bronchus, and lung, were similar in all three time periods, with only a slight increase in the most recent time period (i.e., 1964–1968) (all-cancer SMR = 1.36, 95% CI = 0.55–2.83; cancer of the trachea, bronchus, and lung SMR = 1.87, 95% CI = 0.48–5.10).

In order to further examine latency, an analysis of cancer deaths by length of time since first exposure was performed. No increases in cancers of the stomach or cancers of the trachea, bronchus, and lung were noted with increasing time since first exposure. Similarly, the observed increases in cancers of the stomach and of the trachea, bronchus, and lung could not be related to duration of exposure, year of first exposure, or latency. It should be noted that the study power to examine these parameters was quite limited. Furthermore, 25% of the cohort (foreign workers, who may have had the highest exposure) were lost to follow-up, potentially introducing a bias resulting from an under-ascertainment of deaths. Another shortcoming of this study was that the comparison group selected to derive the expected values may not have been representative of the other regions and the comparisons may have been biased downwards by the healthy worker effect. This study was also limited by the short length of follow-up and small number of deaths observed. Aside from the shortcomings of this study, if an effect of AN were to be observed, one would expect cancer rates to be elevated in the group with the earliest years of first exposure, which represents the workers with the highest potential for greater exposure, longest follow-up, and longest latency. The fact that increases were observed in the most recent group (i.e., those first exposed between 1964 and 1968) weakens the argument that there was an

exposure effect demonstrated in this study, because the latter group probably had lower exposure levels and fewer than 15 years latency and follow-up.

In the update of the above study, Benn and Osborne (1998) expanded the sample to include workers employed in the same six AN polymerization and acrylic fiber spinning factories from 1969 to 1978 and extended follow-up through 1991, allowing for at least 13 years of follow-up. Added to the study were craftsmen with possible AN exposure, control laboratory workers, other possibly exposed workers, and unexposed workers. The sample size was 2,763 men employed for ≥1 year. The exposure assessment in this study was based on a threshold limit enacted by the British government in 1981, a few measurements from the late 1970s, and an exposure estimated for the period 1958–1977 by a chemist at one of the factories. The available exposure measurements were found to be lower than the calculated 8-hour time-weighted average (TWA) (0.4–2.7 vs. 20 ppm, respectively). Job titles were collapsed into three AN exposure categories: polymer workers and spinners—"high"; craftsmen, control laboratory workers, and others with possible AN exposure—"other or medium"; and all others into the "little or no" AN exposure group. No details were provided on how these categories were based on the previously described exposure estimates. Unlike the earlier study by Werner and Carter (1981), death rates for England and Wales were used to calculate expected deaths for the factories that were located in England and Wales. Scottish rates were used for the factories located in Scotland and Northern Ireland (rates for Northern Ireland were not available).

The 13 years of follow-up resulted in a total 409 observed deaths, a value significantly lower than the expected (SMR = 0.84, 95% CI = 0.76–0.93). This result demonstrates a likely healthy worker effect. Stratifying by cause of death, no significant differences were noted between observed and expected deaths (Table 4-11), except in the case of all-circulatory diseases, in which the number of observed deaths was significantly lower than expected (SMR = 0.86, 95% CI = 0.75–0.99). Upon stratification by the level of AN exposure, no significant excess in cause-specific mortality was observed (Table 4-11); however, an excess of lung, trachea, and bronchial cancers in the highest exposure group was found. In addition, linear regression analysis found a significant increasing trend between level of AN exposure and stomach cancer mortality. The distribution of cause-specific deaths was also examined by age of death, with age categorized in the same manner as by Werner and Carter (1981). No significant difference was found between the observed number of deaths in each age category and the expected value. This observation was also noted when all-cancer mortality was stratified by age group. Interestingly, among the youngest cohort of AN-exposed workers, the number of observed deaths from respiratory cancers was significantly higher than expected (5 observed vs. 0.8 expected, SMR = 6.10, 95% CI = 2.23–13.51).

Table 4-11. Distribution of select mortalities among AN-exposed and unexposed workers

	Exposure level											
Cause of death	**High**			**Possible**			**Little or none**			**Total**		
	O[a]	**E[a]**	**SMR**	**O[a]**	**E[a]**	**SMR**	**O[a]**	**E[a]**	**SMR**	**O[a]**	**E[a]**	**SMR**
All causes	170	181.2	0.94 (0.80–1.09)	97	124.7	0.78[b] (0.63–0.94)	142	179.6	0.79[b] (0.67–0.93)	409	485.5	0.84[b] (0.76–0.93)
All cancers	58	50.1	1.16 (0.89–1.49)	22	35.9	0.61[b] (0.39–0.91)	41	51.1	0.80 (0.58–1.08)	121	137.1	0.88 (0.74–1.05)
Lung, tracheal, bronchial cancer	27	19.1	1.41 (0.95–2.03)	7	13.3	0.52 (0.23–1.04)	19	19.1	0.99 (0.62–1.52)	53	51.5	1.03 (0.78–1.34)
Stomach cancer[c]	7	4.2	1.66 (0.73–3.30)	3	2.9	1.03 (0.26–2.81)	1	4.3	0.23 (0.01–1.15)	11	11.4	0.96 (0.51–1.68)
Circulatory disease	81	86.9	0.93 (0.74–1.15)	49	59.1	0.83 (0.62–1.09)	70	86.2	0.81 (0.64–1.02)	200	232.2	0.86[b] (0.75–0.99)

[a]O = observed deaths; E = expected deaths.
[b]Statistically significant ($p < 0.05$).
[c]Statistically significant trend ($p < 0.05$).

Source: Amended from Benn and Osborne (1998).

Data were also analyzed by stratifying by year of first exposure, time since first exposure, and length of exposure. The latter variables were divided into the following groups: <5, 5–10, 10–15, and >15 years. When cause-specific deaths, including all cancers and respiratory cancers, were examined within these categories, no significant differences were noted between observed and expected values. However, a significant increasing trend was noted for all deaths and circulatory diseases based on time since first exposure but not with length of exposure. The analysis that focused on cause-specific mortality and the year of first exposure differed from the previous study by Werner and Carter (1981) in that workers were divided into the following three groups: pre-1960, 1960–1968, and post-1968. No differences in all-cause or cancer deaths were noted between the observed and expected values, but a significant increase in respiratory cancer deaths was noted in the subgroup of workers that were exposed post-1968 (7 observed deaths vs. 2.6 expected deaths, SMR = 2.70, 95% CI = 1.18–5.32).

This study increased the number of observed deaths sixfold as compared with the number of deaths reported in the previous study by Werner and Carter (1981). The number of cancer deaths, including deaths from lung cancer, also rose proportionally. However, the number of observed deaths only represented less than 15% of the studied cohort and thus may have contributed to not finding an overall statistically significant association between lung cancer and

exposure to AN. As seen in the initial study, cancers of the trachea, bronchus, and lung (respiratory cancers) were elevated in the youngest age group. While significant, this statistic was based on five subjects in the younger age group. Also noted was the fact that there was a significant elevation of deaths from cancers of the trachea, bronchus, and lung in the workers who were first exposed in 1969 and later, rather than those first exposed prior to that year. Smoking history, an important confounder when assessing cause-specific lung cancer, was not addressed. The analyses on the high-exposure group included fewer than 800 workers from the total cohort; therefore, power to detect trends and excess deaths was limited in this part of the publication. Although not statistically significant, an increased SMR for lung, tracheal, and bronchial cancers was observed in the high exposure group (SMR = 1.41, 95% CI = 0.95–2.03, n = 27). The finding of an increase in stomach cancer in the high exposure group is interesting, but the small total number of stomach cancer deaths (n = 11) makes rigorous analysis difficult.

This study had no quantitative AN levels, use of a population reference group could have masked associations, and statistical power needed to detect rare cancers such as stomach cancer was low. There was no evidence of a dose-related trend between increasing AN exposure and respiratory cancer, which is not surprising given study deficiencies and the lack of quantitative exposure data.

Acrylic fiber factory in Italy

A retrospective cohort study was conducted with 671 male workers who had at least 12 months of exposure to AN (or mixed exposure to AN and dimethylacetamide) at an acrylic fiber factory in Venezia, Italy (Mastrangelo et al., 1993). Mortality patterns were examined to determine whether excess cancer cases were related to these exposures. Occupational exposure to AN occurred between 1959 and the end of 1988, with mortality tracked until the end of 1990, thus allowing at least 2 years of follow-up for every person in the cohort. Workers with past exposure to vinyl chloride or benzidine were excluded from the study cohort. Study participants were categorized based on their level of AN exposure as follows: (1) high exposure to AN only, (2) low exposure to AN plus exposure to dimethylacetamide, and (3) episodic exposure to AN plus exposure to dimethylacetamide. SMRs were calculated based on the observed deaths and the expected number of deaths in the general population. The expected death rate took into account age, gender, year, cause, and person-time.

No significant difference in all-cause mortality was observed during 1959–1990, with only 32 deaths (4.7% of total cohort) being reported. A total of 12 deaths from cancer was observed in the total cohort. This observation was slightly, but not significantly, higher than the 8.73 expected cancer deaths. None of these cancer deaths was observed among the 100 workers who were only exposed to high levels of AN. Of the 12 cancer cases, there were 2 lung cancer cases and 4 intestinal cancer cases. The lung cancer cases were observed among the 272 workers who had discontinuous but episodic exposure to AN and dimethylacetamide, and the number was

not significantly different than the expected number of lung cancer cases. The intestinal and colon cancer cases were equally distributed between the groups that had concomitant exposure to dimethylacetamide and were significantly higher than expected in both groups.

When analyses were stratified by duration of exposure and time since first exposure, no relationship was found with regard to all-cause mortality or all cancers. Among individuals exposed for 1–4 years, significant differences were noted between the number of observed testicular, rectal, intestinal, and colon cancer deaths and the expected values. However, the number of cancer-specific deaths was small, with only one or two deaths being attributed to the above cancer types.

In addition to questions about the comparison group, the ability of this study to greatly inform an assessment of the relationship between AN and cancer is quite limited due to its small sample size. The follow-up time is also short, as reflected by the fact that less than 5% of the cohort was deceased by the end of the follow-up period. These factors combined may contribute to the study's lack of sufficient power to determine if AN exposure is associated with cancer.

National Cancer Institute (NCI) cohort study

Many studies have investigated the relationship between AN exposure and cause-specific death using a cohort assembled by the NCI (Starr et al., 2004; Marsh et al., 2001, 1999; Blair et al., 1998). The studies were found to differ by the types of analyses used, comparison groups, cohort subsets, or years of follow-up.

Blair et al. (1998) assembled a cohort of 25,460 workers (18,079 white males, 4,293 white females, 2,191 nonwhite males, and 897 nonwhite females) who were employed in AN production or use beginning in the 1950s through 1983. The cohort included workers who were employed prior to 1984 and after the start-up of AN operations (between 1952 and 1965) at one of eight plants located in Alabama, Florida, Louisiana, Ohio, Texas, and Virginia. This method allowed for the examination of both AN-exposed workers and unexposed workers. Workers were followed through the end of 1989, allowing ≥6 years of follow-up.

Exposure was assessed for each plant by developing a quantitative estimate for each job, department, and time period. Sources used to develop the estimates were walk-through surveys, personal and area monitoring data, and interviews with longtime workers. The exposure assessment for this study was more detailed (Stewart et al., 1998) than for any previously published study. More than 10,000 estimates were developed for 3,662 job, department, and plant combinations for a 30-year period of time. Individual worker exposure estimates were developed, including estimates for workers whose exposures were difficult to estimate because of their movement through all areas of a plant (i.e., maintenance workers). The estimation methods were compared with actual data for validation.

SMR analyses were performed to compare observed mortality in both the exposed and unexposed groups to expected numbers of deaths based on U.S. race- and gender-specific death

rates. Subsequent analyses used the unexposed worker rates to develop internal comparison rate ratios adjusted for birth year, plant, calendar time, race, gender, wage, and salary status. These comparisons alleviate the healthy worker effect that is expected when using external general population rates. Smoking history was obtained on a sample of workers by using a case-cohort design to allow statistical adjustment for risk estimates calculated for known smoking-related cancers, such as lung cancer. A 10% sample of living workers was chosen at random to be interviewed regarding their smoking history. A 10% sample of persons deceased prior to 1983 was chosen, and next-of-kin interviews were attempted. Also, all brain and lung cancer deaths that were not chosen in the 10% sample of deceased persons were also selected for next-of-kin interview.

At the end of the study, the total person-years for the exposed workers was 348,642, while the person-years for the unexposed workers tallied 196,727. More than 66% of the members of the cohort had at least 20 years of follow-up. A total of 1,217 exposed workers and 702 unexposed workers were known to be deceased. For all-cause mortality, significant lower numbers of observed deaths than expected were reported for both AN-exposed and unexposed groups (Table 4-12). This pattern is also noted for all-cancer mortality among exposed workers; however, no statistically significant difference between observed and expected deaths was found among the unexposed workers. A similar observation was made for lung and tracheal cancer death, with SMR values for AN-exposed and unexposed workers being 0.9 (95% CI = 0.8–1.1) and 0.8 (95% CI = 0.6–1.1), respectively (Table 4-12). Interestingly, among the exposed workers, the numbers of observed deaths from pancreatic cancer, lymphosarcoma, and reticulosarcoma, as well as noncancer deaths like diabetes, cerebrovascular disease, and liver cirrhosis, were significantly lower than expected values. Upon comparison of the exposed workers to the unexposed workers, a small excess in lung and tracheal cancer deaths was observed (see RR in Table 4-12).

Table 4-12. Distribution of select mortalities among AN-exposed and unexposed workers

Cause of death	Exposed workers			Unexposed workers			RR (95% CI)
	Observed	SMR	95% CI	Observed	SMR	95% CI	
All causes	1,217	0.7	0.6–0.7[a]	702	0.7	0.7–0.8[a]	0.9 (0.8–1.0)
All cancers	326	0.8	0.7–0.9[a]	216	0.9	0.8–1.0	0.8 (0.7–1.0)
Lung and tracheal cancer	134	0.9	0.8–1.1	59	0.8	0.6–1.1	1.2 (0.9–1.6)
Pancreatic cancer	10	0.5	0.3–0.9[a]	13	1.2	0.7–2.1	0.4 (0.2–1.0)
Cerebrovascular disease	37	0.5	0.4–0.7[a]	23	0.5	0.4–0.8[a]	0.9 (0.5–1.6)

[a]Statistically significant ($p < 0.05$).

Source: Amended from Blair et al. (1998).

Data were stratified by time since first exposure (<10, ≥10–20, and ≥20 years) to examine any evidence of latency effects. Using the unexposed group for comparison, no significant increases in cancer deaths were observed among AN exposed workers in any of the latency intervals examined. The RRs for lung cancer mortality were increased for the longer latency periods; however, these RRs and the overall trend were not statistically significant. The RRs were 0.4, 1.6, and 1.3 in the <10-years exposure group, the ≥10–20-years group, and the ≥20 years group, respectively.

Cumulative exposure was examined by stratifying the data into five exposure groups: <0.13, ≥0.13–0.57, ≥0.57–1.5, ≥1.5–8.0, and ≥8.0 ppm-years. There was no evidence of a dose-response effect across the quintiles of exposure when death rates for all cancers combined were examined. Similarly, lung cancer death rates did not increase across the exposure categories with rate ratios of 1.1, 1.3, 1.2, 1.0, and 1.5, respectively. A sufficient number of lung cancer deaths were available to analyze the relationship between latency and cumulative exposure. Among the lung cancer deaths that occurred within 10 years since first exposure to AN, there was no significant increase in deaths with increasing exposure. This observation is also noted for lung cancer deaths occurring 11–19 years after first exposure to AN. For the workers with ≥20 years since first exposure, a statistically significant rate ratio of 2.1 (95% CI = 1.2–3.8) was reported in the highest cumulative exposure quintile; however, there was not a significant exposure-response trend ($p = 0.11$).

The risk of lung cancer mortality was also analyzed by other exposure variables, including duration, intensity, frequency of peak exposures, and cumulative exposures, considering different lag periods and adjustment factors. Most exposure variables showed a nonsignificant increase in lung cancer deaths among workers with the highest level of AN exposure, but none yielded a strong exposure-response gradient or statistically significant exposure-response trend. No exposure-response patterns were observed for duration of exposure at any intensity level.

Additional analyses focused on the workers with 20 or more years since first exposure in order to examine the factors that might contribute to increased risk of lung cancer at the highest cumulative exposure level in this group. The increased risk was not observed when analyses were restricted to workers first employed between 1960 and 1969. This could be because workers who were first employed between 1960 and 1969 would have at least 10 fewer years of follow-up than those hired before 1960 and would tend to be younger. Also, having a later hire date would allow workers in this group less time to work and accumulate exposure, so they would be less likely to be included in the highest quintiles of exposure. This is confirmed by the fact that 42 lung cancer cases were observed in the two highest quintiles for those first hired before 1960, and 9 were observed in the two highest quintiles for those first hired between 1960 and 1969. The increase in risk in the highest exposure quintile was evident in both wage and salary employees and for both fiber and nonfiber plants for this group that was followed for

20 or more years after first exposure. None of the trend tests for cumulative exposure in workers with 20 or more years since first exposure was significant.

Smoking history was sought on a 10% sample of study subjects. A total of 2,655 workers was identified for interview, and 1,890 (71%) of this group were interviewed. For lung cancer deaths, 64 next-of-kin interviews were conducted. Additional analyses were performed by controlling for smoking status. These analyses did not change previous results, although they did result in a slight reduction in the risk ratios in the highest quintile of exposure. Blair et al. (1998) stated that they assumed that if smoking data were available for the full cohort, then the smoking adjustment would yield the same proportion of effects in the full cohort as in the subcohort.

In summary, the sample size and follow-up time in this study were likely large enough to detect any substantial elevation of cause-specific cancer deaths. For lung and tracheal cancer deaths, an elevated RR of 1.2 (95% CI = 0.9–1.6) was observed in AN-exposed workers compared to the unexposed worker population. With lung cancer deaths as the surrogate for the development of lung cancer and less than 10% of the worker population being deceased at the time of the study evaluation, lung cancer risk may have been underestimated. The study authors state that increased risk with latency or cumulative exposure in separate analyses was not demonstrated. This observation could be attributable to the reduced level of power in the subgroup analyses. However, a statistically significant RR of 2.1 (95% CI = 1.2–3.81) was observed in the highest cumulative exposure quintile among workers with ≥20 years since first exposure. Overall, this study provides suggestive evidence with regard to AN exposure and lung cancer.

Marsh et al. (1999) added 7 years of follow-up and focused on analyzing a subset of the original cohort of Blair et al. (1998). The subcohort was comprised of 992 white male workers who had worked for ≥3 months between 1960 and 1996 at a chemical plant in Ohio. Analyses included the calculation of SMRs and RRs for categories of exposure and latency for lung cancer and the calculation of SMRs (based on regional mortality rates) and RRs for stomach, prostate, large intestine, and lymphohematopoietic cancers by cumulative exposure level.

Exposure assessment in this cohort mirrored that of the original cohort study by Blair et al. (1998) with the following modifications. A panel of industrial hygienists used all of the exposure data collected to assign calendar time-specific categories to each job title. The following categories were designated: <0.2, ≥0.2–2.0, 2.1–20.0, and >20.0 ppm. Job titles were also assessed for the potential for exposure to nitrogen products in a qualitative manner (potential, no potential). Marsh et al. (1999) mentioned that other known potential occupational hazards at the plant included asbestos, 1,3-butadiene, and depleted uranium; exposure to these chemicals was not assessed. However, in the exposure assessment by Stewart et al. (1998) on this cohort, these chemicals were not singled out as impactful potential occupational hazards. For AN exposure, the quantitative evaluations for each job title were used to compute three time-dependent measures of exposure for each worker who held any job where AN exposure was

possible. These measures included duration of exposure, cumulative exposure, and average intensity of exposure. Cumulative exposure was recorded in ppm-years, with workers being assigned to one of the following categories: >0–0.139, 0.14–0.579, 0.58–1.509, 1.51–7.999 ppm-years, and ≥8.000 ppm-years. Unlike the study by Blair et al. (1998), which measured person-year accumulation from the first day of employment at the plant to the end of 1989 or date of death or last date known to be alive, Marsh et al. (1999) extended their 1960–1988 job exposure matrix to include new job categories and monitoring data through 1996. Thus, the exposure assessment by Marsh et al. (1999) covers all jobs held from the beginning of the plant operation (1960) through the end of 1996.

The total cohort of 992 workers included 474 workers who never worked in a job where AN exposure was possible and 518 workers who were potentially exposed to AN in at least one of their jobs. A total of 110 deaths was observed in the cohort through the end of 1996. Smoking history was collected for 90.3% of the total cohort and 93.2% of the AN-exposed group. The prevalence of smokers was similar between the two groups with 58% of the unexposed workers being smokers and 62.5% of the exposed workers being smokers. However, the prevalence of smoking in the exposed group was associated with the level of cumulative AN exposure and increased with increasing levels of exposure.

Of the 110 deaths observed, 43 deaths were attributed to cancer. The observed number of cancer deaths did not differ from expected values based on the U.S. mortality rates or the regional death rates, with SMRs of 0.98 (95% CI = 0.71–1.32) and 0.97 (95% CI = 0.70–1.31), respectively. Fifteen of the observed cancer deaths were attributed to respiratory cancers, which showed a similar pattern of nonsignificant SMRs <1 (Table 4-13). With the exception of bladder tumors, none of the other site-specific cancers evaluated showed a significant difference between observed and expected values using either the U.S. mortality rates or the regional mortality rates. The number of bladder cancer deaths among workers was significantly higher than expected (SMR = 4.5, 95% CI = 1.23–11.53); however, all the deaths occurred among workers not exposed to AN.

Table 4-13. Distribution of mortality among AN-exposed workers

Cause of death	Exposed workers		Unexposed workers		Overall cohort			
	Ob	SMR (95% CI)	Ob	SMR (95% CI)	Ob	SMR_{US} (95% CI)	$SMR_{regional}$ (95% CI)	RR (95% CI)
All causes	41	0.58[a] 0.42–0.79	69	0.78[b] 0.60–0.98	110	0.64[a] 0.53–0.77	0.69[a] 0.57–0.83	0.74 0.5–1.1
All cancers	17	0.88 0.52–1.42	26	1.04 0.68–1.53	43	0.98 0.71–1.32	0.97 0.70–1.31	0.87 0.4–1.7
Respiratory cancer	9	1.28 0.58–2.42	6	0.64 0.24–1.40	15	0.88 0.49–1.43	0.92 0.51–1.51	1.98 0.6–6.9
Bladder and other urinary cancer	0	– 0.00–8.23	4	7.01[a] 1.91–17.96	4	4.50[a] 1.23–11.53	3.93[a] 1.07–10.06	Not determined

[a]Statistically significant ($p < 0.05$).

Ob = observed deaths

Source: Amended from Marsh et al. (1999).

For respiratory cancers, there were nine observed deaths in the exposed group and six in the unexposed group, leading to a risk ratio of 1.98 (95% CI = 0.6–6.9) (Table 4-13). This indicates that there was nearly 2 times the rate of lung cancer deaths in the exposed group as in the unexposed group. Respiratory cancer deaths were further examined using RR regression models that were able to adjust for age and calendar time as well as one other potential confounding factor, such as year of hire or smoking. Two variables were marginally associated with lung cancer risk in the total cohort (exposed and unexposed workers): duration of employment and time since first exposure. Smoking was not related to lung cancer risk; therefore, it is probable that there was misclassification of this risk variable, and use of smoking information in models of time-related exposure variables to control for a smoking effect was not possible. Regression analyses performed using categories of duration of exposure, cumulative exposure, and average exposure compared to no exposure were not more informative than previous analyses that compared exposed to unexposed rates. For each analysis, the exposed worker RR was approximately 2 times that for unexposed workers across all categories of exposure (Table 4-14). The risk ratios, derived in the regression analysis, increased with exposure level and time since first exposure, though the small numbers of observed deaths may have hindered the observation of a statistically significant increasing trend.

Table 4-14. Summary of relative regression analyses for cancer of the bronchus, trachea, and lung

Exposure measure	Category	Observed deaths	RR	95% CI
Duration (yrs)	Unexposed	6	1.00	
	>0–4.9	3	1.71	0.25–8.94
	5.0–13.9	3	2.28	0.35–11.38
	14.0+	3	2.15	0.34–10.70
Cumulative exposure (ppm-yrs)	Unexposed	6	1.00	
	>0–7.9	2	1.96	0.81–12.04
	8.0+	7	2.07	0.58–7.58
Cumulative exposure (ppm-yrs)	Unexposed	6	1.00	
	>0–7.9	2	1.97	0.18–12.10
	8.0–109.9	4	2.15	0.43–9.33
	110.0+	3	1.97	0.31–9.42
Average exposure (ppm)	Unexposed	6	1.00	
	>0–4.9	3	1.97	0.31–9.54
	5.0–11.9	3	1.70	0.26–8.26
	12.0+	3	2.64	0.42–12.67

Source: Amended from Marsh et al. (1999).

The risk ratio for all-cancer mortality and AN exposure derived by Marsh et al. (1999) was similar to the risk ratio derived in the larger-scale study by Blair et al. (1998). Despite the limitations of the small number of observed deaths and the focus on only white males, this study does indicate that there may be an association between AN exposure and increased risk in respiratory cancer deaths.

Marsh et al. (2001) performed a sensitivity analysis on data from the original cohort of Blair et al. (1998), examining dependency of lung cancer RR estimates on selection of referent populations. Exposure categorization from the Blair et al. (1998) study was retained for this analysis, but the comparison groups differed. Mortality analyses were performed using U.S. mortality rates and local county rates. SMRs were calculated for both AN-exposed and unexposed workers.

Upon comparison with U.S. and regional mortality rates, both exposed and unexposed workers were found to have significantly lower rates of all-cause mortality. Using the U.S. morality rates, the SMRs for the unexposed group and the exposed group were 0.75 (based on 702 deaths, 95% CI = 0.7–0.8) and 0.66 (based on 1,217 deaths, 95% CI = 0.6–0.7), respectively. The SMRs for all-cause mortality utilizing regional rates were nearly identical to those using U.S. rates. Additionally, the number of lung cancer deaths observed among workers, both exposed and unexposed, was significantly lower than regional estimates, with SMRs for each group of workers being 0.74 (95% CI = 0.6–0.9) and 0.68 (95% CI = 0.5–0.9), respectively, compared with U.S. population rates. These findings indicate a potential healthy worker effect.

Observed lung-cancer deaths were stratified by the cumulative exposure to AN and time since first exposure to derive RRs and regional-mortality-rate-based SMRs (Table 4-12). Workers with the highest cumulative exposures and at least 20 years of exposure were twice as likely to have lung cancer as unexposed workers (RR = 2.1, 95% C.I = 1.2–3.8). The numbers of observed and expected deaths in this highest exposure, longest duration category were about the same using external comparisons (SMR = 1.07, 95% CI = 0.7–1.6). This illustrates how the use of an external comparison population can mask an apparent association; the discrepancy is most likely attributable, at least in part, to the healthy worker effect. There was no evidence of a linear exposure-response relationship for lung cancer, based on the categories used to assess time since first exposure. SMRs in each category did appear to increase with increasing cumulative exposure category (Table 4-15).

Table 4-15. Distribution of observed lung cancer deaths among AN-exposed workers, using regional rates for comparison

Cumulative exposure (ppm-yrs)	Time since first exposure								
	Less than 10 yrs			10–19 Yrs			At least 20 yrs		
	Ob	RR (CI)	SMR (CI)	Ob	RR (CI)	SMR (CI)	Ob	RR (CI)	SMR (CI)
>0–0.13	7	0.4 (0.2–1.2)	0.72 (0.3–1.5)	9	0.5 (0.5–3.2)	0.71 (0.3–1.4)	11	1.1 (0.6–2.2)	0.56 (0.3–1.0)
0.13–0.57	3	0.4 (0.1–1.4)	0.63 (0.1–1.8)	12	2.6[a] (1.2–5.7)	1.18 (0.6–2.1)	11	1.0 (0.6–2.2)	0.57 (0.3–1.0)
0.57–1.50	2	0.4 (0.1–1.6)	0.70 (0.1–2.5)	10	2.0 (0.9–4.8)	1.01 (0.5–1.8)	16	1.2 (0.5–2.1)	0.71 (0.4–1.2)
1.50–8.00	2	0.4 (0.1–2.0)	0.87 (0.1–3.1)	7	1.2 (0.5–3.1)	0.66 (0.3–1.4)	18	1.2 (0.6–2.2)	0.61 (0.4–1.0)
≥8.00	1	0.4 (0.1–3.1)	0.81 (0.02–4.5)	4	0.9 (0.3–1.2)	0.54 (0.2–1.4)	21	2.1[a] (1.2–3.8)	1.07 (0.7–1.6)

[a]Statistically significant ($p < 0.05$).

Ob = observed deaths

Source: Amended from Marsh et al. (2001).

To look for plant-specific risks, the lung-cancer deaths in each of the eight study plants were analyzed separately by cumulative level of exposure. Only one plant showed an increased risk of lung-cancer deaths among the exposed workers, with the highest level of exposure (i.e., ≥8 ppm-years) having an SMR of 2.68 (based on 10 deaths, 95% CI = 1.3–4.9). There was no comparison of process differences in the plants, thus raising uncertainty as to whether workers at this plant were exposed to other potential carcinogens or if these findings were due to chance. In addition, the small number of observed lung-cancer deaths in the plant-specific exposure categories lowers the level of power this study had to discern trends in SMRs that might provide more information on the association between AN exposure and cancer.

In summary, Marsh et al. (2001) focused on external comparison groups rather than the available unexposed worker cohort. The use of an external comparison group, rather than a cohort more comparable to the exposed population (i.e., internal comparison group), may subject the relationship between exposure and lung cancer to biases such as the healthy worker effect. Internal comparison groups are generally preferred since they tend to be less influenced by the healthy worker effect, other sources of selection bias, and confounding (Checkoway et al., 1989). Marsh et al. (2001) mentioned potential occupational hazards such as asbestos, 1,3-butadiene, and depleted uranium not being assessed. Stewart et al. (1998) conducted an exposure assessment for the cohort of workers exposed to AN. Exposure to 340 substances other than AN was assessed qualitatively. 1,3-Butadiene and depleted uranium were not among the chemicals with exposures of >20,000 person-years. Additionally, Blair et al. (1998) did not observe any deaths from asbestosis or mesotheliomas, which would have been indicative of asbestos exposure. The reanalysis by Marsh et al. (2001), particularly the RR results, does support the association, found by Blair et al. (1998), between AN exposure and increased lung cancer mortality risk among workers with the highest exposure level, but the healthy worker effect, small sample sizes within subcategories, use of external controls, and short follow-up may limit the detection of stronger support for such an association.

Data from this cohort were reanalyzed employing semiparametric Cox regression models with time-dependent covariates to estimate additional risk of death from lung cancer for several different AN occupational exposure scenarios (Starr et al., 2004). The "cumulative exposure estimate" was a time-dependent covariate, and "plant worked" was a time-independent covariate. The analysis focused on the largest race-sex group (18,079 white males) from the original Blair et al. (1998) study. The Cox models allowed for the calculation of the cumulative risk of dying from a disease by a certain age. The outcome measurement used was the risk of dying from lung cancer by age 70 years. Baseline rates were developed for the unexposed worker population and for three different AN exposure scenarios: (1) early intense exposure, (2) long moderate exposure, and (3) late intense exposure. All scenarios provided 50 ppm-years of cumulative exposure by age 55 years. The increased number of lung cancers per 1,000 workers that would develop by age 70 was calculated as 0.77–1.56, 0.74–1.50, and 0.68–1.56, respectively (the ranges reflect the use of different plant-specific baseline rates). The upper bound of additional risk was in the range of 7.5–15.1 per 1,000 workers with the upper bound on the exposure parameter being 0.0048 per ppm-working year. It is important to note that this study analysis did not control for smoking. Also, based on the extent of exposure misclassification, any exposure-response association may have been underestimated.

In summary, the study by Blair et al. (1998) reported an elevated risk of lung cancer deaths among AN-exposed workers as compared to the unexposed workers, particularly among workers in the highest cumulative exposure quintile with ≥20 years since first exposure (RR = 2.1, 95% C.I. = 1.2–3.8). However, the short follow-up may have contributed to the study's

inability, overall, to demonstrate an increased risk associated with latency or cumulative exposure. Similar to Blair et al. (1998), Marsh et al. (1999) found an increased risk of lung cancer deaths among AN-exposed workers as compared to the unexposed workers, though the point estimate of 1.98 was not statistically significant. However, Marsh et al. (1999) only focused on a small subset of the NCI cohort. Though the small sample size and the study inclusion of only white males reduces the statistical power and generalizability of the study, the observation of the excess lung cancer risk in Marsh et al. (1999) does provide some weight with regard to hazard inferences.

Marsh et al. (2001) utilized primarily an external comparison group and, while they provide better stability of comparison rates than internal controls as used by Blair et al. (1998), a limitation of external controls as the referent population is the risk of having potential associations masked by a healthy worker effect or other factors that may be more similar within an occupational cohort than between the cohort and the general population. The results from Marsh et al. (2001) indicate the presence of such an effect dampening the observation of an association between AN and cancer.

Though the studies by Marsh et al. (2001) and Blair et al. (1998) have a relatively large cohort size, the number of observed deaths is small. These studies, though they rely on cancer-specific mortality ratios rather than cancer incidence as in the Wood et al. (1998) study, have several advantages to the Wood et al. (1998) study. The low SMR for overall mortality reported by Wood et al. (1998) suggests the potential presence of a number of biases, including the healthy worker effect, incomplete cohort identification, and incomplete ascertainment of the outcome measure. Furthermore, Blair et al. (1998) provide a better job exposure matrix than Wood et al. (1998). Although cancer incidence is typically preferred, mortality rates do serve as a good surrogate for incidence for some cancers like lung cancer. On the other hand, these mortality studies may miss associations with treatable cancers such as prostate cancer.

The small percentage of deaths in the NCI cohort suggest a young mean age, which can impact statistical power. Thus, the observation of a statistically significant elevation in SMR among those with the longest latency and high cumulative exposure is noteworthy. Additional follow-up of this cohort may be useful to further assess the association between AN exposure and cancer suggested by the excess in lung cancer deaths that has been observed among workers exposed to high levels of AN.

Case-control studies

A large case-control study conducted in seven European countries investigated the association between occupational exposure to vinyl chloride, AN, and styrene and the risk of lung cancer (Scélo et al., 2004). The study included new cases of lung cancer occurring between 1998 and 2002 in 15 centers in six Central and Eastern European countries and in Liverpool in the United Kingdom. Controls, consisting of subjects hospitalized in general public hospitals in

the same areas as cases, were frequency matched to cases based on age and gender. Controls had to have been hospitalized within 3 months of diagnosis of the case and could not have cancer or any tobacco-related diseases. A total of 3,403 cases and 3,670 controls met the study inclusion criteria; after exclusions and refusals to participate, the final study group included 2,861 cases and 3,118 controls.

In order to ascertain exposure and lifestyle information, such as tobacco consumption, each study participant was interviewed using a standard questionnaire. Exposure assessment was obtained from the work history portion of the questionnaire, where information was collected for each job held at ≥1 year. Experts evaluated the frequency and intensity of exposure to AN, among other agents, for each job held by each study subject. The following exposure models were constructed for analysis: (1) duration of exposure, (2) weighted duration of exposure (which considered both duration and frequency), and (3) cumulative exposure in ppm-years. Models included age, gender, center, tobacco consumption, and other occupational factors.

A total of 10,555 jobs were held by the 2,861 study participants with lung cancer, and a total of 11,174 jobs were held by the 3,118 controls. AN exposure was associated with 48 jobs held by the cases and 26 jobs held by the controls. Thirty-nine of the 2,861 cases and 20 of the 3,118 controls were characterized as being exposed to AN, resulting in a significant odds ratio (OR) of 2.20 (95% CI = 1.11–4.36) (i.e., cases were 2 times more likely to be exposed to AN than controls). However, it was found that more than half of the study participants that were exposed to AN were also exposed to styrene. Further analysis was conducted on individuals not exposed to styrene (17 cases and 10 controls). This resulted in a similar OR estimate but with a wider CI due to the smaller sample size (OR = 2.08, 95% CI = 0.82–5.27). Increasing linear trends for lung cancer were noted for both weighted duration of exposure ($p = 0.05$) and cumulative exposure ($p = 0.06$) (Table 4-16). Additional analyses employed a 20-year lag for exposures, which did not change the results appreciably. The authors reported an increased risk of exposure among lung cancer cases diagnosed before the age of 60 (43% of the cases), where the OR for ever being exposed was 2.79 (95% CI = 1.01–7.70), while the OR for ever being exposed among those over 60 years was 1.02 (95% CI = 0.35–2.92). An age-exposure interaction test yielded nonsignificant results.

Table 4-16. ORs of lung cancer for AN exposure

Exposure measure	Cases	Controls	OR	95% CI
Weighted duration of exposure (yrs)				
Not exposed	2,822	3,098	1.00	
0.01–1.00	13	9	2.03	0.72–5.73
1.01–2.25	9	5	2.73	0.73–10.20
>2.25	17	6	2.91	0.87–9.79
	Linear trend: p = 0.05			
Cumulative exposure (ppm-yrs)				
Not exposed	2,822	3,098	1.00	
0.01–0.46	13	9	2.03	0.72–5.73
0.47–1.61	10	4	2.76	0.68–11.22
>1.61	16	7	2.87	0.85–9.66
	Linear trend: p = 0.06			

Source: Amended from Scélo et al. (2004).

Because of the personal interviews conducted with each case and control, this study was able to provide an in-depth assessment of potential confounding factors, such as smoking history and lifestyle factors. The exposure assessment, though different than for the recent generation of cohort studies where actual plant measurements were possible, utilized reasonable and standardized methods to assign various levels of AN exposure to different jobs. As a multi-industry study, the possibility of exposure misclassification in this study was probably greater than in single-industry studies, though exposure misclassification is probably nondifferential with respect to disease and therefore would serve to lessen the outcome measures (ORs) calculated. The key observation in this study is the fact that, even after adjustment for confounding factors such as smoking history, an association between AN exposure and lung cancer incidence was observed. This observation adds to the weight of evidence in support of an association between AN and cancer.

Cross-sectional studies

A detailed cross-sectional study was conducted among workers at a Hungarian AN factory in June 2000 (Czeizel et al., 2004). Of the 888 employees, 72 employees did not work during the study time frame and 33 refused to participate. The remaining 783 employees were interviewed, with information gathered on demographics, lifestyle and habits, occupational exposures, and history of general and occupational diseases, among other factors. Medical records aided in the validation of the workers' responses. Workers were categorized into three groups based on level of contact with AN (i.e., direct exposure, indirect or sporadic exposure, and no exposure). Since the interviews were done with living current workers, cancer

information for any worker who had left the plant or died before the study was conducted was anecdotal.

It is known that 12 former workers from the factory had died from cancer between 1990 and 1999, and none of these deaths was due to lung cancer. Of the 783 workers interviewed, 12 workers were found in the interview sample that had cancer. Of these, only one lung-cancer case was identified. This worker, categorized as having direct exposure to AN, started working at the plant in 1973 and was diagnosed 15 years later. Five of the 12 cancer cases were among the group (n = 452) thought to have the highest level of exposure to AN, while 4 cancer cases were noted among workers with no exposure to AN. No significant association between AN exposure and the development of cancer was observed. The study mentioned three of its shortcomings: persons with serious disorders who died or had premature pensions were not included, updated information on occupational exposures was unavailable, and there was difficulty in identifying appropriate controls. It should be noted that workers were not exposed exclusively to AN but to a mixture of other chemicals as well. The small number of cancer incidences and the identified shortcomings hinder the reliability of this study in evaluating the association between AN exposure and the development of cancer.

Other supporting studies

In 2006, the Ohio Department of Health assessed the burden of cancer among residents of Addyston, Hamilton County, Ohio, who lived near a thermoplastics manufacturing plant that emitted AN and 1,3-butadiene into the environment (Ohio Department of Health, 2006). The study population consisted of invasive cancer cases identified through the Ohio Cancer Incidence Surveillance System between 1996 and 2003. The incidence of site-specific cancer was compared to the expected number of cases, the latter being derived from national background cancer incidence rates from NCI's Surveillance, Epidemiology and End Results (SEER) program in 1998–2002 and region-specific cancer incidence rates from 1993 to 2003. A total of 55 invasive cancer cases were identified among the 1,010 residents in the area, with an SIR = 1.8 (95% C.I. = 1.3–2.3) based on the 1998–2002 SEER age-specific incidence rates. Cancer of the lung and bronchus was the most common cancer identified (13 cases, 23.6%), followed by colorectal cancer (10 cases, 18.2%). The number of observed cancer cases in both instances was higher than expected (lung and bronchus SIR = 3.2, 95% C.I. = 1.7–5.4; colon and rectum SIR = 3.0, 95% C.I. = 1.5–5.6). SIRs based on the region-specific cancer incidence yielded similar results. Although cancer incidence in this cohort was higher than expected, the association between AN exposure and the incidence of lung cancer may be confounded by other risk factors, such as smoking, that were acknowledged but not controlled in the analyses.

Overall summary of epidemiology data

The early DuPont studies found potential increases in incidence and/or death from lung cancer and prostate cancer among persons possibly exposed to AN. These studies were the impetus for generating several additional studies spanning more than 20 years after the first publication. Exposure assessment was not fully explored until recently, though older studies did examine qualitative distributions of exposure. The cohorts ranged from a few hundred workers to over 25,000 workers. The follow-up period for many of the studies was short, not allowing half of the population to reach a terminal endpoint so that a health outcome such as cancer could be observed. However, over time, the cohort studies increased in power by increasing the number of workers, length of follow-up, and sophistication of the exposure assessment.

A composite of the major cohort studies reviewed, along with all-cancer SMRs, is provided in Table 4-17. Table 4-18 summarizes SMRs for lung cancer, a cancer type that has been assessed in most of the epidemiology studies reviewed. In both tables, the SMRs are based on the cohort population most likely to be exposed to AN, as the actual cohort sample size in many cases included an unexposed worker group. As in most studies, the number of deaths on which the SMRs are based is a fraction (≤33%) of the actual cohort studied; thus, the actual cohort size may not reflect the relative number of deaths in the SMR calculation. These SMRs were evaluated by the size of the exposed cohort, number of observed deaths, percentage of observed deaths within each study, and year of publication to determine if any of these factors was associated with increased SMR values. For both all-cancer mortality and lung-cancer mortality, no discernable association was observed between increased SMRs and the size of the exposed cohort, number of observed deaths, percentage of observed deaths within each study, or year of publication (data not shown).

Table 4-17. Derived all-cancer SMRs for major cohort studies on AN exposure

Reference	Study population	Comparison group	Potentially exposed cohort	Observed deaths	All-cancer SMR[a]
DuPont					
O'Berg (1980)	Male workers exposed to AN between 1950 and 1966 at a DuPont Plant in South Carolina and followed through 1976.	DuPont Registry	1,128[b]	17	1.13 (0.68–1.78)
O'Berg et al. (1985)	As above but updated extended to 1983	DuPont Registry	1,345	36	1.14 (0.81–1.56)
Chen et al. (1987)	Male workers exposed to AN between 1944 and 1970 at DuPont Plant in Virginia and followed through 1983.	White male subset of U.S. population	1,083	18[c]	0.75 (0.44–1.16)
Chen et al. (1987)	As above.	DuPont Registry	1,083	18[c]	0.88 (0.54–1.37)
Wood et al. (1998)	Combined O'Berg et al. (1985) and Chen et al. (1987)	U.S. general population	2,559	126	0.78[d] (0.64–0.93)
Wood et al. (1998)	As above.	DuPont Registry	2,559	126	0.86 (0.72–1.02)
Symons et al. (2008)	Update from Wood et al. (1998) with 11 yrs of follow-up	Regional Dupont workers	2,548	839	0.92 (0.81–1.04)
Symons et al. (2008)	As above.	U.S. general population	2,548	839	0.73[d] (0.64–0.82)
NCI					
Blair et al. (1998)	Workers employed in eight AN-producing facilities from 1950s to 1983, followed through 1989.	U.S. general population	25,460	326	0.80[d] (0.70 -0.90)
Blair et al. (1998)	As above.	Unexposed workers	25,460	326	RR = 0.80 (0.7–1.0)
Marsh et al. (1999)	Subset of Blair et al. (1998).	County mortality rates	518	17	0.88 (0.52–1.42)
Marsh et al. (1999)	As above.	Unexposed workers	518	17	RR = 0.87 (0.4–1.7)
Marsh et al. (2001)	Same as Blair et al. (1998)	Regional mortality rates	25,460	–	
American Cyanamid Company					
Collins et al. (1989)	Male workers at two plants employed between 1951 to 1973, followed through1983.	White male subset of U.S. population	1,774	43	1.01 (0.74–1.35)
Synthetic chemical plant					
Waxweiler et al. (1981)	Chemical plant workers employed between 1942 and 1973, followed through 1973.	White male subset of U.S. population	4,806	101	1.18 (0.97–1.43)

Table 4-17. Derived all-cancer SMRs for major cohort studies on AN exposure

Reference	Study population	Comparison group	Potentially exposed cohort	Observed deaths	All-cancer SMR[a]
Table 4-17. Derived all-cancer SMRs for major cohort studies on AN exposure					
Reference	**Study population**	**Comparison group**	**Potentially exposed cohort**	**Observed deaths**	**All-cancer SMR[a]**
Rubber industry					
Delzell and Monson (1982)	White male rubber chemical plant workers employed for at least 2 yrs between 1940 and mid-1971, followed through mid-1978.	White male subset of U.S. population	327	22	1.20 (0.77–1.79)
Netherlands cohort					
Swaen et al. (1992)	Male workers exposed to AN in eight factories for ≥6 mos before mid-1979, followed through 1987.	Dutch general population	2,842	42	0.83 (0.61–1.11)
Swaen et al. (1998)	As above, but followed through 1995.	Dutch general population	2,842	97	0.88 (0.72–1.07)
Swaen et al. (2004)	As above, but followed through 2000.	Dutch general population	2,842	146	0.89 (0.75–1.04)
BASF (Germany)					
Thiess et al. (1980)	Male workers from 12 plants followed through mid-1978.	German mortality rates	1,469	27	1.32 (0.89–1.89)
Six factories (U.K.)					
Werner and Carter (1981)	Male workers employed for at least 1 yr in one of six factories from 1950 to 1968, followed through 1978.	Male mortality rates in England and Wales	934	21	1.10 (0.70–1.65)
Benn and Osborne (1998)	As above but employed from 1969 to 1978, followed through 1991.	Mortality rates from different European countries	2,963	121	0.88 (0.73–1.05)
Acrylic fiber factory (Italy)					
Mastrangelo et al. (1993)		General population	671	12	1.37 (0.74–2.33)

[a]SMR may be calculated from article based on available data.
[b]Only workers employed for ≥6 mos.
[c]Based only on wage workers.
[d]Statistically significant ($p < 0.05$).

Table 4-18. Derived lung cancer SMRs for major cohort studies on AN exposure

Reference	Study population	Comparison group	Potentially exposed cohort	Observed lung cancer deaths	Lung cancer SMR[a]
DuPont					
O'Berg (1980)	Male workers exposed to AN between 1950 and 1966 at a DuPont Plant in South Carolina and followed through 1976.	DuPont Registry	1,128[b]	7	1.35 (0.59–2.66)
O'Berg et al. (1985)	As above, but updated and extended to 1983.	DuPont Registry	1,345	14	1.21 (0.69–1.98)
Chen et al. (1987)	Male workers exposed to AN between 1944 and 1970 at DuPont Plant in Virginia and followed through 1983.	White male subset of U.S. population	1,083	5[c]	0.59 (0.22–1.32)
Chen et al. (1987)	As above.	DuPont Registry	1,083	5[c]	0.66 (0.24–1.46)
Wood et al. (1998)	Combined O'Berg et al. (1985) and Chen et al. (1987).	U.S. general population	2,559	47	0.74[d] (0.55–0.98)
Wood et al. (1998)	As above.	DuPont Registry	2,559	47	0.89 (0.66–1.17)
Symons et al. (2008)	Update from Wood et al. (1998) with 11 yrs of follow-up	Regional Dupont workers	2,548	88	0.92 (0.75–1.14)
Symons et al. (2008)	As above.	U.S. general population	2,548	88	0.74[d] (0.60–0.91)
NCI					
Blair et al. (1998)	Workers employed in eight AN-producing facilities from 1950s to1983, followed through 1989.	U.S. general population	25,460	134	0.90 (0.8–1.1)
Blair et al. (1998)	As above.	Unexposed workers	25,460	134	RR = 1.2 (0.9–1.6)
Marsh et al. (1999)	Subset of Blair et al. (1998).	County mortality rates	518	9	1.32 (0.64–2.42)
Marsh et al. (1999)	As above.	Unexposed workers	518	9	RR = 1.98 (0.96–3.63)
Marsh et al. (2001)	Same as Blair et al. (1998).	Regional mortality rates	25,460	134	0.74[d] (0.62–0.87)
American Cyanamid Company					
Collins et al. (1989)	Male workers at two plants employed between 1951 and 1973, followed through 1983.	White male subset of U.S. population	1,774	15	1.00 (0.58–1.61)

Table 4-18. Derived lung cancer SMRs for major cohort studies on AN exposure

Reference	Study population	Comparison group	Potentially exposed cohort	Observed lung cancer deaths	Lung cancer SMR[a]
Table 4-18. Derived lung cancer SMRs for major cohort studies on AN exposure					
Reference	**Study population**	**Comparison group**	**Potentially exposed cohort**	**Observed lung cancer deaths**	**Lung cancer SMR[a]**
Synthetic chemical plant					
Waxweiler et al. (1981)	Chemical plant workers employed between 1942 and 1973, followed through 1973.	White male subset of U.S. population	4,806	42	1.49[d] (1.09–1.99)
Rubber industry					
Delzell and Monson (1982)	White male rubber chemical plant workers employed for at least 2 yrs between 1940 and mid-1971, followed through mid-1978.	White male subset of U.S. population	327	9	1.52 (0.74–2.79)
Netherlands cohort					
Swaen et al. (1992)	Male workers exposed to AN in eight factories for ≥6 mos before mid-1979, followed through 1987.	Dutch general population	2,842	16	0.82 (0.48–1.30)
Swaen et al. (1998)	As above, but followed through 1995.	Dutch general population	2,842	47	1.10 (0.82–1.45)
Swaen et al. (2004)	As above, but followed through 2000.	Dutch general population	2,842	67	1.07 (0.84–1.35)
BASF (Germany)					
Thiess et al. (1980)	Male workers from 12 plants followed through mid-1978.	German mortality rates	1,469	11	1.85 (0.97–3.22)
Six factories (U.K.)					
Werner and Carter (1981)	Male workers employed for ≥1 yr in one of six factories from 1950 to 1968, followed through 1978.	Male mortality rates in England and Wales	934	9	1.20 (0.58–2.20)
Benn and Osborne (1998)	As above but employed from 1969 to 1978, followed through 1991.	Mortality rates from different European countries	2,963	53	1.03 (0.78–1.34)
Acrylic fiber factory (Italy)					
Mastrangelo et al. (1993)		General population	671	2	0.77 (0.13–2.54)

[a]SMR may be calculated from article based on available data.
[b]Only workers employed for ≥6 mos.

Table 4-18. Derived lung cancer SMRs for major cohort studies on AN exposure

Reference	Study population	Comparison group	Potentially exposed cohort	Observed lung cancer deaths	Lung cancer SMR[a]

[c]Based only on wage workers.
[d]Statistically significant ($p < 0.05$).

To date, the largest cohort assessed in determining the relationship between AN and cancer is the NCI cohort. The NCI/National Institute for Occupational Safety and Health (NIOSH) cohort study of Blair et al. (1998) provides the strongest evidence for carcinogenicity, although this evidence is not conclusive. This study of 25,460 subjects in eight plants was designed to evaluate a relationship between AN exposure and site-specific cancer, including lung cancer, an a priori hypothesis. Both AN-exposed and unexposed subjects showed a favorable all-cause mortality rate compared to the all-cause mortality rate of the U.S. population. Although only 5% of the cohort had died, this study has a large number of observed deaths that could be analyzed. The study addressed known problems occurring with earlier studies by quantifying exposures, estimating the effect of smoking, and using an internal control group of unexposed workers.

The study by Blair et al. (1998) is of particular interest because a possible association between AN exposure and death from lung cancer was observed among workers in the highest level of AN exposure. Specifically, workers with at least 20 years since first exposure and exposed to a high level of AN were 2 times more likely to die of lung cancer than unexposed workers. However, though significance was found among workers exposed to high levels of AN, as with other studies, the exposure-response analysis in the Blair et al. (1998) study did not provide strong or consistent evidence for a causal association.

The observations of Swaen et al. (2004) of AN-exposed workers in the Netherlands and of Benn and Osborne (1998) of AN-exposed workers in the United Kingdom support the findings of Blair et al. (1998) and provide some evidence for carcinogenicity, although lung cancer SMRs in these studies were not statistically significant. Other supporting evidence comes from the observation that SMRs for lung cancer among subjects with the highest exposure (as compared to national mortality rates) were not only >1, but also larger than the SMRs for low- or no-exposed groups. Furthermore, the statistically significant increased OR for AN exposure in the lung-cancer case control study of Scélo et al. (2004) provides weight for this association. This study adjusted for effects related to individual smoking history and to a number of potential coexposures found in a subject's occupational setting. The finding of lung-cancer risk increasing with increasing exposure duration or with increasing cumulative exposure provides further evidence of an association with AN.

Within the body of epidemiologic literature examining a potential relationship between exposure to AN and cancer in occupational cohorts, the following shortcomings are noted: low power from small numbers of exposed subjects, lack of quantitative exposure information on individual study subjects leading to a greater potential for exposure misclassification bias, assessment of an insensitive outcome, and insufficient follow-up period for cancer latency. In addition, many of the studies used external comparison groups, and their results were subject to a downward bias from the healthy worker effect.

An alleged shortcoming of the Blair et al. (1998) study has been the observation that the AN-exposed workers experienced a lower rate of lung-cancer deaths than in the general population; however, this is likely a manifestation of the healthy worker effect. The use of internal controls by Blair et al. (1998) was to draw inferences about AN risks. With cancer mortality being used as a surrogate for developing cancer associated with AN exposure and with a low percentage of the cohort having died, there may be an underestimate of the risk associated with AN exposure. In addition, Selikoff and Seidman (1992) showed based on histopathological analysis of a comparably large industrial cohort (17,800 asbestos workers) that as much as 13.7% of lung cancer cases are misdiagnosed on death certificates, both as neoplasms and nonmalignant diseases, with about 3% as asbestos only diseases (mesothelioma and asbestosis). Therefore, Blair cohort may have as much as 10% of internal controls that are actually lung cancers. That would cause a strong bias against finding a statistically significant relationship. Finally, mortality data may be inadequate for assessing treatable cancers that could result from AN exposure. The earlier studies based on the DuPont cohort utilized cancer incidence as well as cancer mortality data. In these studies, although a better outcome measurement (i.e., cancer incidence) is used, observed rates are compared through an SIR with company-wide or national population statistics rates, rather than rates from an internal control group. Thus, a strong healthy worker effect may hinder the observation of a cancer effect of AN exposure. Even in the most recent DuPont cohort study (Symons et al. 2008) where an attempt was made to reduce the bias due to healthy worker effect, there may be bias from the health worker effect. It should be noted that unlike the other DuPont cohort studies, Symons et al. (2008), with over 50 years of follow-up, did not report cancer incidence. Though the outcome measure of mortality in the Blair et al. (1998) study is not as sensitive, this study has a relatively large number of lung-cancer deaths and does compare cause-specific deaths between exposed and unexposed workers as well as the general population. The resulting risk ratio may not achieve statistical significance (as mentioned above, several factors may have caused bias to the null), but the point estimate does indicate a potential excess in lung-cancer deaths among workers exposed to AN. Furthermore, the observed RR in the group of workers with the highest cumulative exposure and the longest time since first exposure was statistically significantly increased.

4.1.2.2.2. ***Epidemiological studies of AN in humans (noncancer effects).*** Sakurai et al. (1978) performed a cross-sectional health examination of 102 male workers exposed to AN in six acrylic fiber manufacturing factories in Japan in 1976. Also examined were 62 nonexposed matched control workers from polyester fiber manufacturing plants, power supply plants, or finishing branches of the acrylic fiber plants. The workers were selected by a random sampling process. By experimental design, all exposed subjects were shift workers who had been exposed to AN in the workplace for at least 5 years but had no history of exposure to other chemicals. All subjects underwent medical examinations, and blood and urine samples were collected for

chemical analysis. Clinical chemistry analyses included urinary protein and other parameters, including Hb, total cholesterol, AST, ALT, alkaline phosphatase, cholinesterase, γ-glutamyl transpeptidase (γ-GTP), and lactate dehydrogenase (LDH). Parameters that measured liver injury were a focus of the clinical examinations because a previous epidemiological study of 576 Japanese acrylic fiber manufacturing workers exposed to <5 or <20 ppm AN between 1960 and 1970 had reported an increase in subjective symptoms and mild injury to the liver in exposed workers (Sakurai and Kusumoto, 1972). AN and thiocyanate concentrations in urine were also measured to evaluate individual exposure levels.

Levels of AN in the air (Sakurai et al., 1978) were measured as 8-hour TWA from "spot" samples (from stationary air samplers) and from exposed subjects wearing personal samplers. As shown in Table 4-19, the factories and exposed workers were classified into three groups (A, B, and C), according to their level of AN exposure. SDs for the means and ranges of the exposure concentrations were not reported. Mean exposure durations for workers in the three groups of factories were 10.3 years (SD = 4.5) for group A, 10.8 years (SD = 4.4) for group B, and 12.6 years (SD = 2.1) for group C.

Table 4-19. Industrial AN exposure, levels of AN and thiocyanate in urine, and prevalence of physical signs of adverse effects in workers exposed to AN at six acrylic fiber factories in Japan

Factory group (n = number of factories)	Mean 8-hr TWA AN concentration (ppm)		AN in urine (µg/L)	Thiocyanate in urine (µg/L)	Percentage of exposed vs. control workers with physical signs of adverse effects		
	Spot samples	Personal samples			Reddening of pharynx or conjunctiva	Palpable liver	Rashes or pigmentation of skin
A (n = 2)	2.1 (n = 116)	0.1 (n = 11)	3.9 (n = 35)	4.50 (n = 19)	19.4 (n = 31) vs. 18.2 (n = 22)	16.1 (n = 31) vs. 9.1 (n = 22)	9.7 (n = 31) vs. 9.1 (n = 22)
B (n = 3)	7.4 (n = 394)	0.5 (n = 37)	19.7 (n = 51)	5.78 (n = 58)	11.3 (n = 53) vs. 10.0 (n = 30)	15.1 (n = 53) vs. 10.0 (n = 30)	3.8 (n = 53) vs. 0 (n = 30)
C (n = 1)	14.1 (n = 98)	4.2 (n = 14)	359.6 (n = 22)	11.41 (n = 14)	50.0 (n = 18) vs. 30.0 (n = 10)	38.9 (n = 18) vs. 30.0 (n = 10)	11.0 (n = 18) vs. 0 (n = 10)
Control	–	–	0 (n = 22)	4.00 (n = 52)	–	–	–

Source: Sakurai et al. (1978).

Although there were some differences in mean age between the groups (38.1 years for group C, 33.9 years for group B, and 30.5 years for group A), the age distributions of exposed and control subjects were broadly similar (Sakurai et al., 1978). No statistically significant differences in mean clinical chemistry parameters were found between exposed workers and controls. Medical histories of exposed workers and controls suggested a transient AN-related

increase in such symptoms as irritation of the conjunctiva and upper respiratory tract, runny nose, and skin irritation (for example, at the scrotum). Physical examination of subjects suggested a slight increase in the incidence of palpable liver, reddening of the conjunctiva and pharynx, and occurrence of skin rashes (see Table 4-19). However, the incidences of these findings among the groups did not rise to the level of statistical significance. Likewise, there were no AN-related changes in blood pressure or neurological findings.

EPA determined 4.2 ppm (average 8-hour TWA from the high exposure group) as an equivocal lowest-observed-adverse-effect level (LOAEL) for physical signs of eye or throat irritation, liver enlargement, or skin irritation in male workers with average durations of 10–12 years of occupational exposure to airborne AN. Limitations to this LOAEL are that workplace air concentrations across the 10–12 years of exposure were not available, workers who underwent medical examinations were not necessarily the same as those whose air and urine were sampled, and no survey of self-reported symptoms was conducted.

A later study of Japanese acrylic fiber workers by some of the same investigators (Muto et al., 1992) included a survey of self-reported symptoms. A strength of the LOAEL is the concurrence between the urinary biomarkers of exposure and the measured air concentrations (see Table 4-19).

Muto et al. (1992) performed another cross-sectional health examination of male workers in seven Japanese acrylic fiber manufacturing plants in 1988. The seven factories included the six factories studied in the 1976 cross-sectional health examination of Japanese acrylic fiber workers (Sakurai et al., 1978). Exposed workers selected for the study were 157 male shift workers with at least 5 years of experience on production lines. The mean years of exposure for these workers was 17 ± 6.6 years. A nonexposed control group consisted of 537 male shift workers in polyester fiber plants, power supply plants, or finishing branches in the acrylic fiber plants. Controls were similar to exposed workers in average age (42.2 years, controls; 41.9 years, exposed), percentage who drank alcohol (76.5%, controls; 77.1%, exposed), and percentage who smoked (58.1%, controls; 58.6%, exposed). Subjects underwent a medical examination that documented past illnesses, work history, exposure to AN, smoking and drinking habits, subjective symptoms, physical condition, urinalysis, hematology, liver function blood variables (total bilirubin, AST, ALT, and γ-GTP), and chest X-rays. Prevalences of workers with abnormal values for the medical examination parameters were analyzed statistically (protein, sugar, or urobilinogen in urine; blood specific gravity >1.055, Hb <14 g/dL, hematocrit >40%, and RBC count $<10^3/mm^3$; and bilirubin >1.0 mg/dL, AST >40 enzyme activity units, ALT >35 units, and γ-GTP >80 units). Exposure of workers (reported as 8-hour TWA concentrations) was assessed by data from workplace area air samples and from personal air samples collected over a 2-day period for 142 of the 157 exposed workers. Overall, the mean AN exposure concentrations for the exposed workers were 0.53 ± 0.52 ppm (range, 0.01–2.80 ppm) based on stationary air samples and 0.62 ± 0.90 ppm (range, 0.01–5.70 ppm) based on

personal air samples. The mean AN exposure measurements were lower than the exposure measurements made in 1976 (see Table 4-19), suggesting that workplace air concentrations in the plants had declined over the 12-year period between the studies.

Prevalences of subjective symptoms that were statistical significantly different between the exposed and control groups included "heaviness in stomach" and decreased libido, with the symptom described as heaviness in stomach as most significant (Muto et al., 1992). Reported prevalences for heaviness of stomach were 29.3% in the exposed group vs. 18.7% in the control group. No significant differences were found in prevalences for other GI effects such as anorexia, nausea, vomiting, heartburn, or stomachache.

When workers were grouped into those from factories with mean TWA AN concentrations below 0.3 ppm (four factories; mean stationary and personal air concentrations of 0.27 and 0.19 ppm, respectively; Group A) or above 0.3 ppm (three factories; mean stationary and personal air concentrations of 0.84 and 1.13 ppm, respectively; Group B), statistically significant increased prevalences for the following symptoms (compared with controls) were found for the workers in the factories with higher exposure levels (Group B): decreased libido (54.9 vs. 40.2% for controls), poor memory (76.1 vs. 64.0% for controls), irritability (35.2 vs. 24.1% for controls), reddening of conjunctiva (21.1 vs. 11.7% for controls), and eye pain or lacrimation (32.4 vs. 19.2% for controls). There were no statistically significant differences between the exposed and control groups in the prevalences of clinically observed physical signs (skin rashes or reddening of conjunctiva) or abnormal findings in urinalytic, hematological, liver function, or blood pressure variables. Prevalences of chest X-ray abnormalities were likewise not different between exposed and control groups.

The mean 8-hour TWA personal air concentration of workers in the Group B factories, 1.13 ppm, was judged by EPA to be a LOAEL for small but statistically significant increased prevalences of several subjectively reported symptoms (e.g., poor memory and irritability) in the absence of statistically significant increases in the prevalences of physical signs or abnormal values for a number of urinalytic, hematological, liver function, or blood pressure variables (Muto et al., 1992). The average 8-hour TWA personal air concentration in the Group A factories, 0.19 ppm, was judged to be a no-observed-adverse-effect level (NOAEL). Like the NOAEL identified in the earlier cross-sectional health examination of Japanese acrylic fiber workers (Sakurai et al., 1978), a limitation to the Muto et al. (1992) NOAEL is that the exposure assessments were cross-sectional in nature. Historical measurements of air concentrations were not available.

Kaneko and Omae (1992) performed a cross-sectional health questionnaire study of exposed and nonexposed workers from seven acrylic fiber manufacturing plants in Japan. The questionnaire for surveying subjective symptoms was administered to 1,220 exposed male workers and 757 nonexposed male workers who were either from the same factory or a close-by factory of the same company. The selected study population included 504 exposed individuals

and 249 unexposed controls. Subjects who were excluded from the study were workers with administrative or nonshift jobs, a history of exposure to other chemicals, ages not able to be matched, or incomplete information on the questionnaire. Workplace air concentrations of AN were measured on 2 consecutive days in each factory by using a portable gas chromatograph. Factories were grouped into three exposure groups with the following mean workplace air concentrations: Group L = 1.8 ppm, Group M = 7.4 ppm, and Group H = 14.1 ppm. Further information on the exposure measurements was not reported (e.g., SD of means, ranges of values, or whether or not the reported concentrations represented 8-hour TWA concentrations). Mean durations of exposure in the three groups were 5.6, 7.0, and 8.6 years for the L, M, and H groups, respectively. All subjects filled in a detailed questionnaire (232 questions in all) that was intended to detect neurological condition and subjective symptoms.

The neurological statuses, as assessed with two different analytical methods (Fukamachi's criteria and Cornell Medical Index profiles), of the AN-exposed workers were slightly higher than those of control workers, although the differences were not statistically significant. Subjective symptoms with significantly higher prevalences in the L, M, and H groups, compared with the nonexposed groups, included headaches, tongue trouble, choking, lump in throat, fatigue, general malaise, heavy arms, and heavy sweating. The numbers of subjective symptoms that were significantly more prevalent in exposed workers were as follows: 8 in group L, 19 in group M, and 14 in group H. Only the prevalence of one subjective symptom, "often feel a choking lump in the throat," had a tendency to increase with increasing length of exposure to AN in all factories and in group L. EPA identified 1.8 ppm as an equivocal LOAEL (Group L mean air concentration) for statistically significantly increased prevalences of subjective symptoms.

In a translated study from China, Chen et al. (2000) examined the health effects of occupational exposure to AN in 224 workers at an acrylic fiber plant. The exposed group consisted of 180 males and 44 females, with an average age of 38.6 years (range 19–57 years) and an average of 13 years of service. The average AN concentration in the work areas at the plant was reported to be 1.04 mg/m^3 (0.48 ppm). All subjects were given a physical examination. The results of these investigations and of subjects' hematological and clinical chemistry parameters were compared with those of unexposed controls. Reported symptoms that had significantly higher incidence in exposed subjects than in unexposed controls included headache and dizziness (41 vs. 21%), poor memory (30 vs. 13%), feelings of choking in the chest (13 vs. 8%), and loss of appetite (13 vs. 7%). However, of the other parameters evaluated in this study, all hematological data and all but one of the clinical chemistry parameters gave closely similar values to those of controls. The exception was the serum activity of γ-GTP that was significantly higher ($p < 0.05$) in exposed subjects than in controls (44.32 ± 32.21 vs. 40.22 ± 31.06 IU/L). The study authors identified 0.48 ppm as a LOAEL for statistically significantly increased prevalences of subjective symptoms (including headache, dizziness, poor

memory, and loss of appetite) in workers employed in an acrylic fiber manufacturing plant for an average of 13 years, without significant changes in most hematological and clinical chemistry variables except for γ-GTP activity.

Lu et al. (2005a) employed the World Health Organization (WHO)-recommended Neurobehavioral Core Test Battery (NCTB), which includes seven components, to evaluate neurobehavioral effects of workers exposed to AN in a Chinese plant. The subjects included 81 workers (68 males and 13 females) in the AN-monomer department, 94 workers (67 males and 27 females) in the acrylic fibers department, and 174 workers (130 males and 44 females) in the administrative or embroidery departments with no AN exposure. The monomer and fiber workers represented 96% of the eligible exposed workers in the two departments. Periodic short-term area sampling between 1997 and 1999 indicated that the geometric means of AN exposure were 0.11 ppm (range 0.00–1.70 ppm for 390 samples) in the monomer department and 0.91 ppm (range 0.00–8.34 ppm for 570 samples) in the fiber department; no personal sampling data were collected. As categorized by duration of employment, 23% of monomer workers were exposed for 1–10 years, 42% for 11–20 years, and 35% for more than 20 years; and 47% of fiber workers were exposed for 1–10 years, 23% for 11–20 years, and 30% for more than 20 years. Mean durations of employment were not reported for the exposed groups. Monomer workers were also potentially exposed to cyanide and fiber workers to methyl methacrylate and heat, but levels of exposure to these possible confounders were not monitored. The exposed workers were frequency matched on age (within 5 years) and years of education (within 1 year) with the unexposed workers. Exposed workers (mean age 40.8 years; range 25–53) were slightly older than unexposed workers (mean age 36.4 years; range 21–53); the percentage of females and years of education were roughly similar across groups. All subjects were interviewed for demographic data, general health status, and lifestyle. All tests were conducted by three specially trained physicians using a Chinese operational guide of the NCTB.

Results of the analysis revealed that exposure to AN had adverse effects for some components of the NCTB, indicating neuropsychological impairment; scores from the following tests were statistically significantly different ($p < 0.05$) from controls in analyses of covariance that took into account age, sex, and education level. In the Profile of Mood States test, all scores for negative moods (anger, confusion, depression, fatigue, and tension) were significantly higher in the exposed groups than in the unexposed group and higher for monomer workers (41–68% higher than controls) than for fiber workers (20–44% higher than controls). Simple Reaction Time, a test of attention and visual response speed, was longer in the two exposed groups than in the unexposed group: 16% longer for monomer workers and 10% longer for fiber workers. Exposed workers performed more poorly (by 21% for monomer workers and 24% for fiber workers) in the backward sequence of the Digit Span test, a measure of auditory memory, but fiber workers had better performance in the forward sequence than unexposed workers. Both groups of exposed workers also had a 4% poorer performance in the Benton Visual Retention

test, a measure of visual perception and memory; scores in the Pursuit Aiming II test, which assesses fine motor skills and perceptual speed, were 14% lower for monomer workers and 10% lower for fiber workers compared with controls. Exposure to AN had no significant effect on scores for manual dexterity in the Santa Ana test or for perceptual speed in the Digital Symbol test. In examining effects by duration of AN exposure, there was no statistical relationship for mood scores and duration of exposure. However, there was an insignificant decrease in Simple Reaction performance with duration of exposure for both monomer and fiber workers. Inverse relationships were found between performance and duration in both the Digital Symbol test and total scores of the Digit Span test in the two exposed groups. Decreased performance with duration of exposure was also found in the Pursuit Aiming II test for exposed monomer workers.

Lu et al. (2005a) mentioned several limitations of this study. One was that the cited exposure data represented estimates of previous exposure levels and no contemporaneous personal monitoring data were available. Furthermore, as the NCTB was developed for populations in Europe and North America, it is not known to what extent cultural differences may have affected results of the Profile of Mood States test, shown to be sensitive to cultural differences. In addition, the study authors could not rule out the possibility that examiner drift may have affected the results. Selection bias among volunteers in different groups was mentioned as a possible confounding effect, but was discounted on the basis that the participation among exposed workers was so high. Moreover, largest measures of neurobehavioral effect occurred on the acrylic fiber workers, who had lower average exposure level.

EPA determined the results from this study were consistent with the designation of the average exposure levels for the monomer workers, 0.11 ppm, and the fiber workers, 0.91 ppm, as LOAELs for small deficits in neurobehavioral tests of mood, attention and response speed, auditory memory, and motor steadiness but not in tests of manual dexterity or perceptual motor speed.

The toxicity of AN in an occupational setting has been the subject of a number of other reports from China, which were collectively submitted to the U.S. EPA as a Toxic Substances Control Act Test Submissions report (Acrylonitrile Group, 2000). While these studies are discussed below for hazard identification purposes, some reports lack sufficient detail to support reported findings of AN-related toxicity. For example, Wang et al. (2000) reported on the disease incidence of 1,121 AN-exposed workers compared with 489 unexposed controls in a university in the same area. Subjects in the exposed group were stated to have a higher incidence of disease of the digestive system (16.95 vs. 8.28%) and the liver (8.12 vs. 1.84%) than in the control group. The highest prevalence rate of 12.5% for liver disease was found in workers exposed to AN over 20 years. The prevalence rate of chronic disease also increased with duration of exposure. However, the report contained no diagnostic information on these conditions and no information on the levels of AN to which the subjects had been exposed.

Dong and Pan (1995) surveyed reproductive outcomes in 150 male and 105 female workers at a chemical fiber plant in China. The concentration of AN in the air in work areas of the plant ranged from 0.53 to 15.5 mg/m^3 (0.24–7.1 ppm; midpoint = 3.7 ppm). Controls in the study were 110 male and 121 female workers who had not been exposed to AN. The report compared the reproductive outcomes for the wives of male workers to the wives of male controls (Table 4-20) and for all female workers at the plant vs. female controls (Table 4-21). As shown in Table 4-20, the rates of premature delivery, spontaneous abortion, threatened abortion, stillborn fetuses, and sterility in the wives of male exposed workers all were higher than those in wives of male controls, with some differences achieving statistical significance.

Table 4-20. Comparison of reproductive outcomes in wives of exposed and control males at a chemical fiber plant

Parameter	Exposed group[a] (n = 150)	Controls[a] (n = 110)
Average age	20.97 ± 6.85[b]	30.04 ± 3.37
Average working yrs	3.19 ± 5.35	8.53 ± 3.89
Pregnancies	168	113
Sterility (%)	9 (5.00)[c]	2 (1.82)
Life births	159[b]	113
Normal births	141	104
Premature deliveries (%)	18 (10.71[d])[c]	4 (3.54)
Late deliveries (%)	6 (3.57)	4 (3.54)
Spontaneous abortion (%)	8 (4.76)[c]	1 (0.88)
Threatened abortion (%)	5 (2.98)[c]	1 (0.88)
Stillborn fetuses (%)	4 (2.38)	0 (0)
Low birth weight	5 (3.14)	4 (3.84)

[a]Numbers in parentheses are in %.
[b]Given as 7.74 in the report.
[c]Significantly different from controls ($p < 0.05$ by Fisher's exact test), as calculated by U.S. EPA.
[d]Significantly different from controls ($p < 0.001$ by Student's t-test), as calculated by U.S. EPA.

Source: Dong and Pan (1995).

Table 4-21. Comparison of reproductive outcomes between exposed and control females at a chemical fiber plant

Outcome	Exposed group[a] (n = 105)	Control group[a] (n = 151)
Average age	29.36 ± 5.12[b]	20.68 ± 4.05
Average number of working yrs	10.19 ± 8.22	10.12 ± 4.34
Number of pregnancies	112	124
Number of alive newborns	105	125
Normal births	101	113
Immature deliveries (%)	8 (7.14)	5 (4.03)
Late deliveries (%)	8 (7.14)	6 (4.84)

Table 4-21. Comparison of reproductive outcomes between exposed and control females at a chemical fiber plant

Outcome	Exposed group[a] (n = 105)	Control group[a] (n = 151)
Spontaneous abortions (%)	1 (0.89)	0 (0)
Threatened abortions (%)	3 (2.68)	5 (4.03)
Stillborn fetuses (%)	5 (4.46)[c]	0 (0)
Mortality of newborns (%)	3 (2.86)	0 (0)
Sterility (%)	3 (2.86)	1 (0.83)

[a]Numbers in parentheses are in %.
[b]Significantly different from controls ($p < 0.001$ by Student's t-test).
[c]Significantly different from controls ($p < 0.05$), as calculated by the study authors.

Source: Dong and Pan (1995).

Effects on the reproductive outcome in exposed female workers at the plant were not as striking as in males, when compared with controls (Table 4-21) (Dong and Pan, 1995). However, the rate of stillborn fetuses in the exposed group was far higher than that of the control group (5/112 vs. 0/124, $p < 0.05$). It is unclear how much these differences may be related to the fact that in the first comparison (Table 4-20), the exposed males were significantly younger than the controls ($p < 0.001$ by Student's t-test, as calculated by the reviewers), whereas in the second case (Table 4-21), the exposed childbearing females were significantly older than the controls ($p < 0.001$). The results from this study identify the midpoint of the range of average workplace air concentrations of AN, 3.7 ppm, as a LOAEL for increased prevalences of adverse reproductive outcomes in male and female workers employed for averages of about 3 and 10 years, respectively. The adverse outcomes showing statistically significantly increased prevalences compared with controls were premature deliveries (18/150 vs. 4/110 in controls), threatened abortion (5/150 vs. 1/110 in controls), and sterility (9/150 vs. 2/110 in controls) for the male exposed workers and their wives and increased prevalence of stillborn fetuses in female exposed workers (4/105 vs. 0/151 in controls).

In a follow-up to the study by Dong and Pan (1995), Dong et al. (2000b) expanded the cohort to include the years 1994 and 1995, resulting in 548 exposed male workers (496 controls) and 391 exposed female workers (427 controls). Average employment durations for the exposed males and females were 11.0 ± 4.5 and 10.4 ± 3.8 years, respectively. The average ages of the male and female workers were 33.8 and 32.4 years, respectively. The age, length of service, and lifestyle of the controls were similar to the exposed workers.

The reported range of AN concentrations in the workplace air, 0.11–15.5 mg/m^3 (0.05–7.14 ppm, midpoint = 3.6 ppm), was not markedly different from that reported in the initial study. In the follow-up study, however, Dong et al. (2000b) also evaluated birth defects. The general trend of results was a slightly higher percentage of abnormal findings in the exposed cohort, as compared with the initial study, and an incidence of 15.7% birth defects, as compared

with 6.1% in controls. This difference was not statistically significant. There were, however, some statistically significant findings in the reproductive outcome of exposed females. In the initial study, Dong and Pan (1995) had reported a significant increase in stillbirths (4.5% in exposed vs. 0% in controls). In the expanded cohort, this value was lower, 2.7 vs. 0.68%, but still statistically significant at the $p < 0.05$ level. There was also a significantly ($p < 0.05$) increased incidence of birth defects (21.3 vs. 4.8%), decreased incidence of low birth weights (3.5 vs. 4.8%), and highly significant ($p < 0.01$) increase in premature deliveries (8.2 vs. 3.9%). The results from the follow-up study identify the midpoint of the range of workplace air concentrations, 3.6 ppm, as a LOAEL for statistically significantly increased prevalences of adverse reproductive outcomes (increased stillbirths, birth defects, and premature deliveries) in female exposed workers employed for an average of 11 years.

Dong et al. (2000a) also carried out an industrial hygiene survey of 68 male and 25 female workers at a Chinese chemical plant, as compared with 58 male and 38 female workers who had not been exposed to AN. The average age of exposed subjects was 27.9 years, and their years of employment at the plant ranged from 1 to 15 years. The average age of controls was 32.3 years. All subjects in the study answered lifestyle questions, including medical and occupational history, smoking and drinking history, and subjective symptoms. They also were given a physical examination, including clinical examinations, chest X-rays, liver and gallbladder ultrasound, electrocardiogram (ECG), clinical chemistry, and blood and urine tests. Air samples were collected from two workplace areas over a 3-year period and analyzed for AN, HCN, and acetonitrile concentrations. Annual average AN concentration was not provided in the report, but measured AN concentrations were over 2 mg/m^3 at all times, with the highest concentration reaching 22.79 mg/m^3.

Exposed workers reported the occurrence of headache, dizziness, sleeping disorders, and a feeling of choking in the chest at a significantly higher prevalence than nonexposed workers. Without presenting details, Dong et al. (2000a) referred to ultrasound tests of six individuals in the exposed group, which appeared to show diffuse changes in the liver. In this group, there was also a higher incidence of trembling of eyes, face, and fingers than in controls. However, all of the blood pressure, hematological, and clinical chemistry parameters under evaluation (including liver function tests) for exposed subjects were within the normal range and closely similar to those of controls. Although the results indicated that increased prevalences of symptoms were reported by exposed workers compared with nonexposed workers, the reported exposure information was inadequate to designate a LOAEL for this study.

Li (2000) surveyed reproductive outcomes in 379 female workers in a Chinese AN manufacturing company and in 511 unexposed control workers from a bed sheet factory and a biological research institute in 1991. The average age and duration of employment of the (20.8 vs. 7.14%), premature deliveries (11.62 vs. 4.72%), and congenital defects (25.4 vs. 4.2 exposed workers were 33.95 years (22.75–54.83 years) and 14.10 years (3.25–34.45 years), respectively.

Average age and employment duration of the control workers were reported to be similar to the exposed group. Monthly workplace air concentration data for 1989 and 1990 were provided by the factory. The average AN air concentration was reported as 16.35 mg/m^3 (7.5 ppm, range = 0–152.88 mg/m^3 [0–70 ppm]). Statistically significant increased prevalences of the following reproductive outcomes were found, compared with controls: sterility (2.64 vs. 0.78%), pregnancy complications %). Li (2000) also divided the exposed group into female workers with and without exposed male partners. Prevalence rates for several adverse reproductive outcomes (pregnancy complications, premature delivery, late delivery, stillbirths, and congenital deficits) were statistically significantly elevated in females with exposed partners, compared with those with nonexposed partners. This study identifies the average workplace AN air concentration, 7.5 ppm, as a LOAEL for increased prevalences of adverse reproductive outcomes in female AN manufacturing workers employed for an average of 14 years.

Xiao (2000a) reported on the fasting serum activities of serum glutamate pyruvate transaminase (SGPT, also known as ALT) in 372 workers exposed to AN for 1–31 years in a chemical factory in China and compared the levels with those in 186 unexposed workers. Individuals with SGPT level ≥19 μmol/L-minute were considered positive. The percentage of individuals with SGPT activity exceeding the benchmark level was compared between the groups. Significantly higher percentage of positive individuals were found in the exposed group compared with controls (41.13 vs. 4.8%), with exposed males being more severely affected than exposed females (50.23 vs. 27.82%). No data were provided on the level of AN exposure.

Xiao (2000b) also reported on the levels of whole blood cholinesterase in 237 workers exposed to AN in a chemical factory in comparison with those in 184 unexposed workers. AN measurements were provided for three separate workshops, although it is not evident from the report whether the measurements were taken as spot samples or from personal samplers. A colorimetric method was used to measure cholinesterase activity. The average AN concentrations in air for the three workshops were 7, 3.3, and 3 ppm, respectively. The authors reported that the levels of whole blood cholinesterase in AN-exposed workers from the three workshops were more than 50% lower than in controls. Health examination results showed there was also an apparent increase in the incidence of symptoms related to lowered cholinesterase activity in exposed subjects compared with controls. These symptoms included neurological disorder, excessive sweating, trembling, and discomfort in the chest.

In an article published in a Chinese journal, Ding et al. (2003) evaluated mitochondrial DNA damage in a group of 47 Chinese workers randomly selected from 1,020 active workers in the chemistry department of a petrochemical company. These workers were exposed to AN at a geometric mean concentration of 0.25 mg/m^3 (0.11 ppm) (median 0.36 mg/m^3 [0.17 ppm], range 0–3.70 mg/m^3) for an average of 17.3 ± 3.8 years. An unexposed control group of 47 persons was selected from the teachers and staff of a college, with an average length of employment of 18.7 ± 4.1 years. DNA was extracted from peripheral blood samples from each subject and

evaluated using the polymerase chain reaction (PCR) with specific primer pairs to detect deletions in mitochondrial DNA. Deletions in mitochondrial DNA were detected in 8/47 exposed workers compared with 0/47 nonexposed workers. A deletion rate of 0.00225 ± 0.00171 was calculated based on optical densities from gel scans of the deletion fragment compared with a fragment synthesized by using primer pairs to a conserved region of mitochondrial DNA; this deletion rate was statistically significantly different ($p < 0.05$) from the rate of 0 for the controls. For studying the effects of aging, a group of 12 healthy nonexposed retirees from governmental organizations (average age 79.15 ± 3.80 years) and a group of 12 healthy nonexposed high school students (average age 14.23 ± 1.52 years) were also examined. Deletion fragments were detected in 3/12 elderly subjects and 0/12 young subjects. The deletion rate for the elderly was calculated as 0.00193 ± 0.00086, which was not significantly different from that calculated for AN-exposed workers. The study authors suggested that exposure to AN might have an effect on the molecular process(es) of aging. Limitations of this study included the lack of reporting for the criteria of selection for the controls and the gender composition of each group. The results identified the mean workplace AN air concentration, 0.11 ppm, as a LOAEL for increased prevalence of workers with deletions in peripheral blood mitochondrial DNA compared with controls.

Ivanescu et al. (1990) used a radioimmunoassay to measure serum levels of testosterone in three groups of male workers exposed to AN in a chemical factory. Blood samples were taken from 39 subjects in May 1975, from 109 subjects in March 1976, and from 149 subjects in May 1977. Subjects were between 19 and 40 years old and had been employed at the facility from 6 months to 10 years. Controls in the study consisted of 145 unexposed men. The three groups of exposed subjects had average serum testosterone concentrations ranging from 3.5 to 4.1 ng/mL. This compared with average values ranging from 5.4 to 7.3 ng/mL in different subsets of the 145 control subjects. Although the time of blood sampling during the day was variable in this study and the circadian rhythm of testosterone was unknown, testosterone concentrations in sera of exposed groups were much lower than in control groups of the same month. However, no data were presented in the report on the level of exposure to AN or other chemicals.

An epidemiological report by Czeizel et al. (2000, 1999) examined the incidence of congenital abnormalities and indicators of germinal mutations in the vicinity of an AN-using factory in Hungary. The study used the incidence of congenital abnormalities from the Hungarian Congenital Abnormality Registry in 46,326 infants born between 1980 and 1996 in 30 settlements within a 25-km radius of an AN-using factory. A number of time-space-specific clusters of abnormalities were identified among the subjects, including pectus excavatum in the Tata community between 1990 and 1992 (OR = 78.5, 95% CI = 8.4–729.6), undescended testis in Nyergesujfalu between 1980 and 1983 (OR = 8.6, CI = 1.4–54.3) and at Esztergom between

1981 and 1982 (OR = 4.2, CI = 1.3–13.5), and clubfoot in Tata between 1980 and 1981 (OR = 5.5, CI = 1.5–20.3).

The relationship between the findings of clusters of abnormalities and AN exposure was uncertain because there were no exposure data in the report. Consequently, it was not known by how much the mothers of affected infants were exposed to the compound, if at all. Furthermore, when the incidence of congenital abnormalities was considered for infants born throughout the entire duration of the study, there were no increased incidences of congenital abnormalities compared with infants born throughout Hungary.

The study authors stated that there was a technological change at the AN factory in 1984 that resulted in greater environmental protection, implying that releases of AN to the environment were lower than before the change. This suggests that the cluster of pectus excavatum obtained at Tata between 1990 and 1992 was unlikely to have been due to AN exposure. However, the high incidence of undescended testis in Nyergesujfalu between 1980 and 1983 may have been an environmental phenomenon, because the region-wide incidence of this congenital abnormality appeared to decrease with increasing distance from the factory. In general, however, it is difficult to draw conclusions about a link between maternal exposure to AN and the incidence of congenital abnormalities from the data in this study because of a lack of exposure data.

Wu et al. (1995) (in the English translation of the abstract of an article in Chinese) reported findings on 477 female workers exposed to AN and 527 controls studied using the retrospective cohort method. Statistically significant increases in the incidence of pernicious vomiting, anemia, preterm delivery, and birth defects were found in exposed women. However, the authors also emphasized several confounding factors in their study, such as illness, medicine taking, and X-ray exposure during pregnancy.

Other reports of chronic occupational exposure to AN described additional health effects. Babanov et al. (1959) (as cited in IPCS, 1983) reported nonspecific changes in skin and pale mucous membranes in addition to vocal cord inflammation in workers exposed to 0.6–6.0 mg/m^3 (0.3–3 ppm) AN in air for approximately 3 years.

Depression, lowered arterial pressure, diffuse dermographia, and increased sweating in AN production workers was described by Ageeva (1970) (as cited in IPCS, 1983). Stamova et al. (1976) (as cited in IPCS, 1983) reported that workers in a polyacrylic fiber plant showed increased incidence of skin diseases when exposed to air concentrations of 10–25 mg/m^3 (5–12 ppm) AN. An increase in other "neurasthenic" complaints and diseases was also reported. However, the presence of other industrial chemicals and uncertainty in the length of exposure were potential confounding factors in these responses.

Borba et al. (1996) measured CEVal-Hb adducts as a marker of AN exposure in three groups of occupationally exposed workers in an acrylic fiber factory in Portugal. The groups comprised 20 administrative workers who were not exposed to AN in the same plant,

14 individuals employed in the continuous polymerization department, and 10 equipment maintenance workers. Considered a measure of the biologically effective dose, CEVal values were 8.5–70.5 pmol/g Hb in controls, 635.2–4,603.5 pmol/g Hb for continuous polymerization workers, and 93.9–4,746 pmol/g Hb for maintenance workers. These findings pointed to the ready formation of AN adducts with Hb in exposed workers. Unfortunately, the report lacked critical information about the levels and duration of exposure to AN undergone by the workers of the different groups and whether such exposure and the adduct formation that resulted were associated with symptoms of ill health.

Borba et al. (1996) also monitored several internal exposure markers for the three groups of workers. The induction of CYP450 species was determined by the excretion of D-glucaric acid (an end product of the glucuronic pathway) in the urine, and formation of malondialdehyde (MDA) (a final product of lipid peroxidation) in RBCs was determined as a surrogate measure of oxidative stress. The study authors found no indication of AN-induced CYP450 induction, but a significant increase was seen for the oxidative stress marker in the group of maintenance workers. Smoking had no influence on these metrics. Borba et al. (1996) also investigated markers for genotoxicity (viz., gene reversion activity of urine extracts, chromosomal aberrations (CAs), and sister chromatid exchanges [SCEs]). These are discussed in the genotoxicity section (Section 4.5.2).

4.1.3. Dermal Exposure

4.1.3.1. *Acute Exposure*

A case report by Vogel and Kirkendall (1984) described a 24-year-old ship's officer who was accidentally sprayed with AN when a valve burst while he was unloading the chemical. Because the man's face, eyes, and body were covered with AN, it is likely that he was exposed via the oral and inhalation routes as well as to the skin and eyes. Immediate responses to exposure included dizziness, flushing, and nausea with vomiting. During hospitalization, acute toxicological impacts included a rapid pulse rate (100 beats/minute) and a respiratory rate of 16/minute. The subject displayed erythema and mild conjunctivitis, tachycardia, and striking hematological changes (WBC count of 26,400 cells/cm^3, of which 76% was polymorphonuclear leukocytes, 10% lymphocytes, and 7% each basophiles and monocytes). Methemoglobin (MetHb) concentration was 10.3% on admission. The patient received nitrite/thiosulfate treatment, underwent dialysis, and, overall, showed steady recovery over his 5-day hospitalization.

There are a number of additional case studies of the toxic effects of AN resulting from acute exposure after accidental spillage in the workplace. These support the designation of AN as a skin irritant. In several cases, erythemas were shown to result from direct dermal contact with solutions of AN (Davis et al., 1973 [as cited in IPCS, 1983]; Zeller et al., 1969; Wilson et al., 1948; Dudley and Neal, 1942). The lesions were followed by delayed blistering and burns,

typically 1 or 2 days following exposure (Davis et al., 1973 [as cited in IPCS, 1983]; Zeller et al., 1969; Babanov et al., 1959; Dudley and Neal, 1942). In some cases, clinically diagnosed dermatitis was associated with irritation (Bakker et al., 1991; Davis et al., 1973 [as cited in IPCS, 1983]). For example, Davis et al. (1973) (as cited in IPCS, 1983) reported a wide range of dermal effects from AN contact, including skin dermatitis, local irritation, erythema, swelling, blistering, and burns. However, dermatitis has not always resulted from AN-induced skin irritation (Zeller et al., 1969; Babanov et al., 1959; Wilson et al., 1948; Dudley and Neal, 1942).

When Dudley and Neal (1942) investigated the effects of AN exposures to laboratory animals, an accident in their laboratory resulted in a case of occupational exposure. Symptoms similar to those described later by Wilson et al. (1948) were reported for a male laboratory worker who spilled small quantities of liquid AN on his hands. Diffuse erythema on hands and wrists was evident after 24 hours, with subsequent blistering on the fingertips on day 3. Both hands became slightly swollen, erythematous, itching, and painful. By day 10 after exposure, the skin of the fingers had cracked and peeled and the skin was dry and scaly with large areas of tender new skin.

Zeller et al. (1969) identified 137 cases of accidental exposure to nitriles when reviewing industrial hygiene data from Germany on accidental exposures to chemical agents in an occupational setting over a 15-year period. Of the 137 cases, 66 cases related to AN exposure, of which 50 cases resulted from direct skin contact and the remaining 16 to inhalation or exposure to AN vapors. All 66 cases were judged to be minor and did not require hospitalization. However, up to 3 weeks of recuperation was required as a result of direct skin contact with the compound. Typically, the first symptoms appeared between 5 minutes to 24 hours after initial dermal contact with AN. For the most part, the workers complained of burning sensations of the skin, followed by reddening of the exposed area and the formation of blisters at any point during the first 24 hours. In one case, AN was thought to have diffused through the leather of a shoe on which it was spilled, resulting in a delay before blisters appeared and delayed healing. There was no indication of resorptive damages from the dermal exposure in any of the 50 cases.

In another study (Babanov et al., 1959), blistering was also observed on workers' legs within 6–8 hours of contact with spilled AN, while a diluted (5%), heated (50°C) solution of AN caused serious skin burns.

A fatal case of dermal contact exposure with AN was described by Lorz (1950), when application of a delousing agent containing AN resulted in the death of a 10-year-old girl. Following dermal application of the delousing agent to the scalp, the girl's head was wrapped in a cloth and she went to bed. Symptoms of nausea, headaches, and dizziness were followed by repeated vomiting and coma. Cramps and increasing cyanosis were followed by death 4 hours after application. A similar case of fatal poisoning was reported by Grunske (1949) in which a 3-year-old girl died after reentry into a home that had been treated with an AN-containing

fumigant. In both of these cases, exposure was likely to have occurred via inhalation as well as the dermal route.

4.1.3.2. *Chronic Exposure*

In addition to the known skin irritation effects of acute exposures to high-concentration liquids and vapors, various chronic dermal exposure effects were reported. There was limited evidence that skin sensitization resulted in dermal allergies to AN. Therefore, an intrinsic capacity of AN to act as a skin sensitizing agent was suggested.

The abstract of a Japanese language report by Hashimoto and Kobayasi (1961) discussed the case of a chemical laboratory worker who developed skin lesions through contact with AN. Although much of the detail remained uncertain, including period and duration of exposure and the influence of other chemicals on the subject's condition, the lesions apparently spread across the subject's body from the contact site, consistent with a direct contact allergic reaction.

Bakker et al. (1991) reported that 10 employees at an acrylic fiber factory complained of skin irritation. While five of the subjects developed irritant dermatitis, the other five subjects gave positive patch tests with AN, suggesting an allergic reaction. This finding also supported the designation of AN as a sensitizing agent.

Prolonged dermal contact for 6 weeks to methyl methacrylate, a copolymer of AN, resulted in an allergic skin sensitization reaction in the case of a 27-year-old man who had his finger splinted for a torn ligament (Balda, 1975). The unpolymerized AN of the Plexidur copolymer resulted in strong skin irritation response, with erythema and formation of scaly skin and scattered blisters. Patch testing confirmed that the allergic sensitization was to AN and not to a copolymer or the polymerization catalyst, benzoyl peroxide. A contributing factor may have been the man's prior hyperhydrosis episode of the hands that led to blister formation.

Very few studies hinted at a possible desensitization or adaptive effect for prolonged chronic exposures. Based on investigations carried out over a period from 1965 to 1971, Zotova (1975) reported complaints of poor health, which included skin irritation, in workers at an AN manufacturing facility. Gincheva et al. (1977) (as cited in IPCS, 1983) did not find changes in the health status of a group of 23 men exposed to 4.2–7.2 mg/m^3 (2–3.3 ppm) of AN for exposure durations of 3–5 years. Details of the study were not provided.

4.1.4. Ocular Exposure

Secondary routes of exposure to AN include ocular exposure to either AN liquid or vapor. For example, in the Wilson et al. (1948) study, subjects exposed to AN at concentrations varying from 16 to 100 ppm (35–217 mg/m^3) for 20–45 minutes demonstrated irritation of all mucous membranes, including the eyes, nose, and throat. In other studies, blepharoconjunctivitis was reported in workers exposed to the compound (Delivanova et al., 1978). Of 302 workers

examined over 2 years (138 in 1976 and 164 in 1978), 42 had severe cases of blepharoconjunctivitis related to AN exposure.

In the case report by Vogel and Kirkendall (1984), the mucous membranes of the eyes of the 24-year-old man had been sprayed with AN. Among other symptoms, mild conjunctivitis but no apparent corneal clouding was observed. Eye irritations and nasal discharge also were reported in workers exposed to relatively high levels of AN at an acrylic fiber plant (Sakurai, 2000; Sakurai et al., 1978).

A synopsis of noncancer outcomes of exposure to AN is provided in Table 4-22.

Table 4-22. Epidemiology studies of noncancer outcomes among cohorts of workers exposed to AN

Reference	Study population	Exposure assessment	Toxic effects/outcome
Muto et al. (1992)	157 Male workers employed in seven Japanese acrylic fiber plants with average of 17 yrs employment; 537 unexposed controls	Mean 8-hr TWAs: Group A factories = 0.19 ppm; Group B factories = 1.13 ppm	Increased prevalences of subjective symptoms in Group B factories, such as heaviness of the stomach, decreased libido, poor memory, irritability, conjunctival reddening, and eye irritation; not in Group A; no significantly increased prevalences of physical signs or abnormal values in urinalytic, hematological, liver function, or blood pressure variables in Group A or B compared with control
Sakurai et al. (1978)	102 Male workers in six Japanese acrylic fiber plants with averages of 10–12 yrs of employment; 62 matched controls	Mean 8-hr TWAs: Group A factories = 0.1 ppm; Group B factories = 0.5 ppm; Group C factories = 4.2 ppm	Statistically insignificant increase in the incidence of palpable liver, reddening of the conjunctiva and pharynx, and skin rashes compared with controls; survey of subjective symptoms not performed
Kaneko and Omae (1992)	502 Male workers in seven Japanese acrylic fiber plants with averages of 5.6, 7.0, and 8.6 yrs of employment at low-, medium-, and high-level workplace exposure; 249 unexposed matched controls	Group L factories = 1.8 ppm; Group M factories = 7.4 ppm; Group H factories = 14.1 ppm: air concentrations reported as "means" without other information	Statistically significant increased prevalences of subjective symptoms, such as headaches, tongue trouble, choking lump in chest, fatigue, general malaise, heavy arms, and heavy sweating in workers in Groups L, M, and H factories, compared with controls
Chen et al. (2000)	224 Workers (180 males and 44 females) in an acrylic fiber plant with average of 13 yrs of employment; 224 unexposed controls	0.48 ppm	Statistically significant increased prevalences of subjective symptoms, such as headache, dizziness, poor memory, choking feeling in the chest, and loss of appetite, compared with controls; increase in serum γ-GTP but not in other clinical chemistry or hematological variables

Table 4-22. Epidemiology studies of noncancer outcomes among cohorts of workers exposed to AN

Reference	Study population	Exposure assessment	Toxic effects/outcome
Lu et al. (2005a)	Chinese acrylic fiber workers: 81 monomer workers (68 male and 13 female); 94 fiber workers (67 male and 27 female); 174 unexposed workers	Mean 8-hr TWAs: Monomer work areas = 0.11 ppm (0–1.7 ppm); fiber manufacture work areas = 0.91 ppm (0–8.34 ppm)	Small but statistically significant deficits in tests of neurobehavior in monomer and fiber workers compared with controls; significant deficits in tests of mood (increased scores for anger, confusion, depression, fatigue, and tension), attention and response speed, auditory memory, and motor steadiness; not in tests of manual dexterity or perceptual motor speed
Dong and Pan (1995)	255 Workers in a Chinese chemical fiber plant (150 males and 105 females) with averages of 3.2 and 10.2 yrs of employment; 231 unexposed controls	Workplace air concentrations = 0.24–7.1 ppm; midpoint = 3.7 ppm	Statistically significant increased prevalences of adverse reproductive outcomes (premature delivery [10.7 vs. 3.5%, wives of exposed males], stillbirths [4.5 vs. 0%, exposed females], and sterility [5.0 vs. 1.8%, exposed males]) compared with controls
Dong et al. (2000b)	548 Male and 391 female workers in a Chinese chemical fiber plant with averages of 11.0 and 10.4 yrs of employment; 496 male and 427 female unexposed controls	Workplace air concentrations = 0.05–7.14 ppm; midpoint = 3.6 ppm	Statistically significantly increased prevalences of adverse reproductive outcomes (increased stillbirths [2.7 vs. 0%], birth defects [21.3 vs. 4.8%], and premature deliveries [8.2 vs. 3.9%]) in female workers compared with controls
Dong et al. (2000a)	93 Workers at a Chinese chemical fiber plant; 96 unexposed controls	Unclear presentation of exposure data	Increased prevalences of subjective symptoms (headache, dizziness, sleeping disorders, and a feeling of choking in the chest) compared with controls
Li (2000)	379 Female AN manufacturing workers employed an average of 14 yrs; 511 unexposed controls	Average workplace air concentration = 7.5 ppm; range = 0–70 ppm	Statistically significant increased prevalences of adverse reproductive outcomes (sterility [2.6 vs. 0.8%], pregnancy complications [20.8 vs. 7.1%], premature deliveries [11.6 vs. 4.7%], and congenital defects [25.4 vs. 4.2%]) in female exposed workers compared with controls
Xiao (2000a)	372 Workers exposed to AN in a chemical factory; 186 unexposed controls	No data	Increase in the serum ALT activity
Xiao (2000b)	237 Workers exposed to AN in a chemical factory; 184 unexposed controls	Workshop A = 7 ppm; workshop B = 3.3 ppm; workshop C = 3 ppm	Reduction in whole blood cholinesterase activity; subjective symptoms such as neurological disorder, sweating, trembling, and discomfort in the chest
Ivanescu et al. (1990)	39 Subjects (May 1975), 109 subjects (March 1976), 149 subjects (May 1977)	No data	Reduced serum testosterone
Czeizel et al. (2000, 1999)	Case control study of babies born with congenital abnormalities in the vicinity of an AN-using factory	No data	Incidence of undescended testis possibly related to proximity to the AN-using facility

Table 4-22. Epidemiology studies of noncancer outcomes among cohorts of workers exposed to AN

Reference	Study population	Exposure assessment	Toxic effects/outcome
Wu et al. (1995)	477 Female AN workers; 527 workers	No data	Increased vomiting, anemia, preterm delivery, and birth defects in pregnant females
Babanov et al. (1959)	Unstated number of exposed subjects	0.3–3.0 ppm	Changes to skin and mucous membranes, vocal cord inflammation
Ageeva (1970) (as cited in IPCS, 1983)	Unstated number of exposed workers	No data	Diffuse dermographia and increased sweating
Stamova et al. (1976) (as cited in IPCS, 1983)	Unstated number of exposed AN workers	5–12 ppm	Skin reactions
Delivanova et al. (1978)	302 Exposed workers	No data	Blepharoconjunctivitis

4.2. SUBCHRONIC AND CHRONIC STUDIES AND CANCER BIOASSAYS IN ANIMALS—ORAL AND INHALATION

AN has been demonstrated to be a multiple-site carcinogen in rat and mouse bioassays. Chronic oral exposure to AN-induced tumors in the brain or spinal cord, Zymbal gland in the ear canal, the forestomach, and, to a lesser degree and less consistently, in the female mammary gland and the tongue in several oral bioassays with F344 rats (Johannsen and Levinskas, 2002b; Bigner et al., 1986; Biodynamics, 1980b) and Sprague-Dawley rats (Johannsen and Levinskas, 2002a; Quast, 2002; Biodynamics, 1980a, b; Quast et al., 1980a). In addition, oral exposure for up to 46 weeks led to increases in brain astrocytomas and Zymbal gland in female Sprague-Dawley rats (Friedman and Beliles, 2002; Litton Bionetics, 1992). Lifetime inhalation cancer bioassays with Sprague-Dawley rats found exposure-related increased incidences of brain tumors, Zymbal gland tumors, intestinal tumors, malignant mammary gland tumors, and tongue tumors (Dow Chemical Co., 1992a; Maltoni et al., 1988, 1977; Quast et al., 1980b). In mice, a single gavage lifetime bioassay identified the forestomach and the Harderian gland as sites of tumor development, but elevated incidences of brain, Zymbal gland, or mammary gland tumors were not found (NTP, 2001). Thus, consistent target organs for the carcinogenicity of AN include the forestomach, CNS, and Zymbal gland in rats and the forestomach and ocular Harderian gland in mice. Exposure-related increased incidences of tongue and mammary gland tumors have been observed, but the responses have not been observed as consistently across studies as the responses in the forestomach, CNS, and Zymbal gland in rats.

Evidence from two studies of exposure to AN starting in early-life suggests increased susceptibility to the carcinogenicity of AN compared with chronic exposure during adulthood only. The evidence for carcinogenicity in these studies, a three-generation reproductive/ developmental study of AN in drinking water (Friedman and Beliles, 2002) and an inhalation

bioassay (Maltoni et al., 1988), is presented in Sections 4.2.1.2.8. and 4.2.2.2, respectively. The evidence for early-life susceptibility is discussed in Section 4.8.1.

Oral toxicity studies in rats and mice identified the forestomach as the most sensitive target organ for the noncancer toxicity of oral exposure to AN. Hyperplasia of the forestomach epithelium occurred at lower oral doses than doses producing other noncancer effects. Increases in other nonneoplastic lesions were observed in the kidney, Harderian gland, and ovary. Available data include results from several oral toxicity and cancer bioassays of chronically exposed rats (see the first paragraph for references) and one oral toxicity and cancer bioassay in mice (NTP, 2001).

Results from a single chronic inhalation toxicity study in rats (Quast et al., 1980b) identified the nasal epithelium as a sensitive noncancer toxicity target of AN. Hyperplasia of mucus-secreting cells and flattening of the respiratory epithelium developed with chronic exposure to concentrations as low as 20 ppm. A limited number of other subchronic studies in rats identified impaired sensory nerve conduction (Gagnaire et al., 1998) and mild developmental effects in the presence of maternal toxicity (Saillenfait et al., 1993; Murray et al., 1978) (see Section 4.3) as other noncancer effects associated with repeated inhalation exposure to AN.

4.2.1. Oral Exposure

4.2.1.1. *Subchronic Studies*

Single studies in dogs and mice are the only well-documented standard bioassays for the subchronic toxicity of AN in experimental animals by the oral route (NTP, 2001; Quast et al., 1975). A full report of a study in rats is not available (Humiston et al., 1975 [as cited in Quast, 2002]). Additional subchronic studies have evaluated only functional effects of AN exposure in specific organs, such as the adrenals (Szabo et al., 1984) and the brain (Gagnaire et al., 1998). These endpoint-specific studies are discussed in Section 4.4.1.

Humiston et al. (1975) (as cited in Quast, 2002) exposed groups of Sprague-Dawley rats (10/sex/group) to AN in drinking water at concentrations of 0, 35, 85, 210, or 500 ppm for 90 days. Reported intakes of AN for males/females, respectively, were 0/0, 4/5, 8/10, 17/22, or 38/42 mg/kg-day. Water consumption was decreased in a dose-related manner in both sexes, with females more affected than males. However, the lowest dose affecting males was not identified in the summary; in females exposed at 35 ppm, 9 of 26 measured intervals showed statistically significant decreases compared with controls. In the 210 and 500 ppm groups, there were significant decreases in water consumption, food consumption, and BW, but no information was provided as to the magnitude of these changes. Exposure to AN had no effect on hematology, clinical chemistry, or histopathologic findings; urinalysis results were also unaffected by treatment, except for an increase in specific gravity that was correlated with increasing dose. Apparently, a number of treatment-related effects was observed in the 85 ppm group, but neither their identity nor the magnitude of change were specified. The summary

provided by Quast (2002) did not provide sufficient detail to accurately identify NOAEL or LOAEL values from the study by Humiston et al. (1975) (as cited in Quast, 2002).

Szabo et al. (1984) evaluated the effect of subchronic oral exposure to AN on the structure and function of the adrenal gland and intestinal tract in rats. Female Sprague-Dawley rats (three to four per group) were exposed for 7, 21, or 60 days to AN in drinking water at concentrations of 0, 1, 20, 100, and 500 ppm, representing approximate daily doses of 0, 0.2, 4, 20, and 100 mg/kg. Other groups of rats received equivalent doses of AN by gavage for the same duration. Water and food intakes were monitored continuously and BWs were recorded every fourth day. At the end of the studies, blood samples were taken to measure plasma corticosterone and aldosterone, and a complete necropsy was carried out on all survivors. The adrenals, thyroid, liver, and one kidney were weighed. Samples of liver, kidney, lung, brain, and the entire adrenal and thyroid glands were measured for levels of nonprotein sulfhydryls in tissue homogenates. Adrenals, "other" endocrine organs, stomach, duodenum, liver, kidney, lung, and heart were evaluated for histopathology.

BWs were reduced by about 25% in rats exposed to 500 ppm in drinking water up to 60 days, but no reduction in BW was observed in rats receiving the equivalent dose of 100 mg/kg-day by gavage (Szabo et al.,1984). Water intake was reduced in rats exposed to 500 ppm in drinking water but increased at the equivalent gavage dose. Adrenal weights were slightly lower than in controls in the 7- and 21-day exposure groups, but significant increases in relative adrenal weights were observed after 60 days of exposure to 500 ppm in drinking water or to ≥0.2 mg/kg-day by gavage. The kidneys were enlarged in rats exposed to 100 or 500 ppm AN in drinking water for 60 days or 500 ppm for 21 days.

Histopathological lesions included adrenocortical hyperplasia in all rats exposed by gavage at ≥0.2 mg/kg-day for 60 days. Enlarged kidneys and hyperplasia of the gastric mucosa at the junction of the glandular stomach and forestomach was observed in rats exposed to 100 or 500 ppm in drinking water for 21 or 60 days. No incidence data were provided for these lesions. Plasma corticosterone levels were significantly decreased by both 500 ppm AN in drinking water or by gavage in the 21-day study. Even the lowest concentration of 1 ppm AN by gavage resulted in a 50% reduction in corticosterone. Plasma aldosterone concentration was reduced, starting from 20 ppm AN. In the 60-day study, significant suppression of plasma corticosterone was observed after exposure to 100 or 500 ppm AN in drinking water and in all exposure levels given by gavage.

Levels of nonprotein sulfhydryls (glutathione) were increased by 20–50% in the 7- and 21-day studies but were significantly reduced by 20–30% in the adrenals after 60 days of gavage exposure to 4–60 mg/kg-day. Increases in nonprotein sulfhydryl concentrations in duodenal mucosa were observed in the 100 or 500 ppm AN exposure groups in the 7- and 21-day studies and in all doses after 60 days, but not in the control group of rats that received water by gavage. For the drinking water study, a NOAEL of 20 ppm (4 mg/kg-day) and a LOAEL of 100 ppm

(20 mg/kg-day) were identified for enlarged kidneys and increases in regional hyperplasia of the gastric mucosa in female rats exposed for 60 days. For the gavage study, no NOAEL was identified, but a LOAEL of 0.2 mg/kg-day was identified for adrenocortical hyperplasia in rats exposed for 60 days.

In a separate experiment, Szabo et al. (1984) evaluated age-dependency in the sensitivity of Sprague-Dawley rats to the action of AN on the adrenals. Groups of weanling rats (40 g) and adult rats (190 g) were treated with 0, 0.002% (20 ppm), 0.01% (100 ppm), or 0.05% (500 ppm) of AN in drinking water for 21 days, or were given by the corresponding amount of AN by daily gavage for 21 days. The animals were sacrificed, and plasma and adrenals were collected as in the previous experiments. Young, immature rats treated with AN were found to have lower (up to 66%) levels of plasma corticosterone and aldosterone than adult rats. These differences were statistically significant with 0.01% AN given by gavage or 0.05% AN in drinking water.

Quast et al. (1975) exposed beagles (four/sex/group) to 0, 100, 200, and 300 ppm AN (purity >99%) in drinking water for 6 months; the reported calculated doses were approximately 0, 10, 16, and 17 mg/kg-day in males, respectively, and 0, 8, 17, and 18 mg/kg-day in females, respectively. Dogs were evaluated daily for clinical signs and weighed weekly; food and water consumption were calculated from the consumption by groups of dogs penned together. Routine hematology examinations were conducted on all samples taken from all dogs 20 days before exposure and on days 83, 130, and 179. Blood and urine samples for standard biochemical analyses were collected from all dogs 8 days before exposure, on days 84, 135, and 176, and at termination (day 182 for males and day 183 for females). Serum samples were collected from all dogs on day 155 to determine total protein concentrations and evaluate the percentages of specific Igs by electrophoresis. Ophthalmic examinations were conducted pretest and at 85, 112, and 175 days. All dogs were subjected to gross necropsy at which time organ weights were recorded for brain, heart, liver, kidneys, and testes; a full set of tissues from all dogs was examined for histopathology. Samples of liver and kidney were analyzed for nonprotein free sulfhydryl content.

The following treatment-related effects were observed in dogs exposed to AN in drinking water for 6 months (Quast et al., 1975). No mortality was observed in the control or 100 ppm groups, but dogs exposed at 200 ppm (2/4 males and 3/4 females) and 300 ppm (3/4 males and 2/4 females) either died prematurely or were euthanized in a moribund condition. Signs of toxicity manifested in these dogs included reduced consumption of food and water, decreased BW, roughened hair coat, and a nonproductive cough. These dogs subsequently exhibited lethargy, weakness, emaciation, respiratory distress, and terminal depression. Decreased water consumption was observed throughout the study in males at 300 ppm and sporadically in females at ≥200 ppm. Food consumption was reduced in males at 300 ppm and females at ≥100 ppm. A supplemental study was conducted on eight female dogs treated with 100 ppm AN for 5 weeks, and no reduction in food or water consumption was observed.

Substantial reductions in BW were observed among dogs that died (200 and 300 ppm); group mean weights among surviving male and female dogs were not statistically significantly different from controls. RBC and Hb counts were reduced by 19–21% in males exposed to 200 ppm for 83 days but not at later time points; females exposed at 300 ppm exhibited 22–26% decreases in RBC counts after 83 and 130 days of exposure. No treatment-related changes in hematology parameters were evident after 179 days of exposure. Exposure to AN had no effect on urinalysis, clinical chemistry, ophthalmoscopic examinations, nonprotein free sulfhydryl content in liver or kidney, or the electrophoretic behavior of serum proteins. Statistically significant alterations in organ weight, such as increases in relative kidney weights in males treated at 100 and 200 ppm, were not biologically significant (less than 10% change). Histopathologic changes were observed in the esophagus (focal erosions and/or ulcerations in the middle one-third, dilations, and thinning of the walls) and tongue (increased thickness of epithelium lining of the dorsal surface) of male and female dogs treated at 200 and 300 ppm. Lesions of the lung were attributed to parasitic nematode infection that was present in all dogs. In this study, a NOAEL of 100 ppm (8–10 mg/kg-day) and a LOAEL of 200 ppm (16–17 mg/kg-day) were identified for early mortality and histopathological lesions of the esophagus and tongue in male and female dogs.

In a comparative study of the neurotoxicity of nitriles, Gagnaire et al. (1998) administered AN (>99% purity) at doses of 0, 12.5, 25, or 50 mg/kg-day to male Sprague-Dawley rats (12/group plus 10 controls) by gavage in olive oil, 5 days/week for 12 weeks. BWs were measured weekly. After 3, 6, 9, and 12 weeks of treatment and after an 8-week recovery period (week 20), rats were evaluated for electrophysiological parameters, with testing occurring 16 hours after dosing (or 48 hours for testing after weekends). Electrical stimulation of the tail nerve was used to assess four neurological properties, the motor conduction velocity (MCV), sensory conduction velocity (SCV), and amplitudes of the sensory and motor action potentials (ASAPs and AMAPs).

One high-dose rat died during the first week of treatment, but no other mortality was observed. High-dose rats showed reduced BW gain that became significant after the fourth week of treatment, leading to a terminal BW 17% lower than in controls. BWs of mid-dose rats became significantly lower than controls after the fifth week, resulting in a terminal weight approximately 7% lower than controls (as estimated by visual inspection of the data graph); this weight change was not considered biologically significant. Five of 11 high-dose rats exhibited significant weakness of the hind limbs that somewhat improved during the recovery period. Rats exposed to AN showed acute signs of behavioral abnormalities, including salivation, locomotor hyperactivity, and fur wetting within 1 hour of dosing. Gagnaire et al. (1998) attributed these findings to cholinomimetic effects possibly caused by AN-induced changes in muscarinic acetylcholine receptors or by alterations in hepatic metabolism. Exposure to AN had no effect on MCV or AMAP except for a 40% increase in AMAP observed in high-dose rats at the 9-week

time point. The most consistent effect of AN was a significant reduction in SCV compared with that in controls (Table 4-23), ranging from 7.5 to 15% between weeks 6 and 12 ($p < 0.05$ to $p < 0.001$); this effect abated following the cessation of exposure, but a 10.6% reduction compared with controls ($p < 0.001$) was observed after 8 weeks of recovery (week 20). A 25% reduction in ASAP was also observed in high-dose rats at week 20, but no effect on this parameter was observed during the treatment period. A NOAEL of 25 mg/kg-day and a LOAEL of 50 mg/kg-day were identified in the study by Gagnaire et al. (1998), based on reduced BW and neurotoxic effects (weakness of the hind limbs and reduced SCV) in male rats exposed to AN by gavage.

Table 4-23. Effect on SCV in male Sprague-Dawley rats exposed to AN via gavage for 12 weeks

Group (mg/kg)	SCV (m/s)[a]					
	Exposure (weeks)					Recovery
	0	3	6	9	12	20
0	34.2 ± 0.7	43.2 ± 0.6	45.2 ± 1.3	48.4 ± 1.1	46.6 ± 0.8	53.8 ± 1.5
12.5	34.9 ± 0.5	42.6 ± 0.9	45.7 ± 0.7	47.8 ± 0.7	46.7 ± 0.9	51.8 ± 0.9
25	34.6 ± 0.8	40.0 ± 1.0	45.5 ± 0.6	46.0 ± 0.9	44.4 ± 0.9	51.3 ± 0.7
50	35.8 ± 1.1	42.2 ± 1.1	41.8 ± 1.3[b]	44.0 ± 1.2[c]	39.8 ± 0.6[c]	48.1 ± 0.7[c]

[a]Values are means ± SDs, n = 12 for treated rats and n = 10 for controls.
[b]Statistically significant compared with controls ($p < 0.05$), as calculated by the authors.
[c]Statistically significant compared with controls ($p < 0.001$), as calculated by the authors.

Source: Gagnaire et al. (1998).

In a comparative study on the effects of nine compounds related to acrylamide (Barnes, 1970), AN was administered by gavage over a period of 7 weeks to six young adult albino rats of the Porton strain as 15 daily doses of 30 mg/kg, followed by 7 doses of 50 mg/kg, and finally 13 doses of 75 mg/kg. The time-adjusted average dose administered over the course of the study was 36 mg/kg-day. Rats were weighed weekly, and their gait and stance when walking on a sloping nonslippery surface including an ascent up a sloping wooden board were evaluated. Treated rats were also held by the tail in front of a sloping bar, and tested for the ability to grasp the bar with the front paws, and then grasp it with the hind feet, a reflex typically lost early in rats with peripheral neuropathies. No data were provided for this experiment, but the study author reported that there was no evidence of adverse effects.

In a recent study that explored the neurobehavioral effects of AN in rats (Rongzhu et al., 2007), male Sprague-Dawley rats (10/group) were exposed to 0, 50, or 200 ppm AN in drinking water. The study authors estimated AN doses to be 0, 4.03, and 13.46 mg/kg-day. Three neurobehavioral tests, including the open field test, rotarod test, and spatial water maze, were conducted to evaluate locomotor activities, motor coordination, and learning and memory,

respectively, prior to initiation of exposure and at 4, 8, and 12 weeks of exposure. Thiocyanate levels in urine were measured in a minimum of five rats from each group at week 12 and were reported to be 2.79, 6.10, and 25.03 mg/g creatinine, respectively.

Beginning from the sixth week of AN administration, three rats in the 50 ppm AN group and five rats in the 200 ppm AN group showed behavioral changes. The coat appearance in all treated rats was soiled, and the main changes were head twitching, trembling, circling, backwards pedaling, and decreased home-cage activities. The two treatment groups also showed less BW gain than the control group. In the open field test, there were no significant differences in start-up latency among the exposed and unexposed groups. The 200 ppm group consistently had higher locomotor activity than the control group, from pretreatment to 12 weeks of exposure. There were also no changes in the number of rearing and grooming episodes. Therefore, there were no uniform changes in exploration and locomotion. In the rotarod test, the maximal and the total and falling latency in the 50 and 200 ppm groups were significantly decreased in a dose- and time-dependent manner. In the spatial water maze test, rats in the 200 ppm group had significantly increased training time and training duration, compared with the control and 50 ppm groups. However, these two parameters in the exposed groups returned to close to control level at the end of the experiment. Rongzhu et al. (2007) suggested that this reversible phenomena may be caused by tolerance. The study authors concluded that oral exposure to AN induced neurobehavioral alterations. The neurochemical mechanisms need to be further investigated. The LOAEL for neurobehavioral alterations is 4 mg/kg-day.

In a range-finding study for a 2-year bioassay (see Section 4.2.1.2), the National Toxicology Program (NTP) (2001) treated $B6C3F_1$ mice (10/sex/group) with 0, 5, 10, 20, 40, or 60 mg/kg-day AN (purity >99%) by gavage in water, 5 days/week for 14 weeks; adjusted for intermittent exposure (5 days/7 days), the intakes were 0, 3.6, 7.1, 14.3, 28.6, and 42.9 mg/kg-day. Clinical findings were recorded on day 8 and once weekly thereafter. BWs were recorded before treatment, weekly, and at study termination. Necropsies were performed on all animals, at which time organ weights were recorded for heart, right kidney, liver, lung, spleen, right testis, and thymus. Hematology analysis was conducted on all mice surviving at the end of the study. Complete histopathologic analyses were conducted on all control mice and those treated with 40 and 60 mg/kg-day; males receiving 20 mg/kg-day were also examined. At the end of the study, 10 males/group in the groups receiving 0, 5, 10, and 20 mg/kg-day were selected for reproductive evaluations; the left cauda, left epididymis, and left testis were weighed and sperm samples were evaluated for sperm counts and motility. Also, 10 females/group in the groups receiving 0, 10, 20, and 40 mg/kg-day were evaluated for vaginal cytology (estrous cycle and stage length) in the last 12 days of the study before termination.

The following effects were observed in mice exposed by gavage to AN. Aside from one control male at week 9, there were no deaths at exposures up to and including 20 mg/kg-day. Mortality at the two highest doses comprised 9/10 males and 3/10 females at 40 mg/kg-day and

all mice treated at 60 mg/kg-day. All deaths occurred on the first day, except for one male in the 40 mg/kg-day group. Slight (2–8%) decreases in BW in treated mice compared with controls were not biologically significant. Survivors (seven females and one male) receiving 40 mg/kg-day exhibited lethargy and abnormal breathing immediately after dosing "for several days" but then appeared to develop tolerance to AN.

Sporadic, statistically significant alterations in hematological parameters included reductions in platelet counts by 20% in males at 20 mg/kg-day, in leukocyte and lymphocyte counts (~30% in males at 20 mg/kg-day and ~37% in females at 40 mg/kg-day), and in Hb and RBC counts by 10% in females at 40 mg/kg-day; other statistically significant changes of doubtful biological significance in females included reductions in RBC counts by 4% in groups treated with 5–20 mg/kg-day and in hematocrit by 6% in the 40 mg/kg-day group. Some of these hematological effects may have been secondary to stomach ulceration observed in some mice.

Absolute and relative heart weights were increased by 20 and 30%, respectively, in males at 20 mg/kg-day. The absolute weights of the left cauda epididymides were increased by 15% in groups exposed at 10 and 20 mg/kg-day. However, no histopathological findings were reported in these organs. The only treatment-related lesions were in the forestomach of females at 40 mg/kg-day: 4/7 with chronic active inflammation (associated with hyperplasia) and 5/7 with focal epithelial hyperplasia. Two females in this group exhibited focal ulceration of the forestomach associated with the hyperplasia. No other treatment-related histopathology was observed. Exposure to AN produced no effects on sperm motility in males at ≤20 mg/kg-day. There were no differences in vaginal cytology parameters in females at ≤40 mg/kg-day. A NOAEL of 20 mg/kg-day and a LOAEL of 40 mg/kg-day were identified in the NTP (2001) bioassay, based on hyperplastic lesions in the forestomach of female mice.

4.2.1.2. *Chronic Studies*

The chronic toxicity and/or carcinogenicity of AN have been evaluated in drinking water or gavage studies in rats and a gavage study in mice (Johannsen and Levinskas, 2002a, b; Quast, 2002; Biodynamics, 1980a, b; Quast et al., 1980a). Studies by Gallagher et al. (1988), Maltoni et al. (1988, 1977), and Bigner et al. (1986) were cancer bioassays that did not investigate nonneoplastic lesions caused by oral exposure to AN. In addition, a three-generation reproductive toxicity assay involving up to 46 weeks of exposure to AN (Friedman and Beliles, 2002; Litton Bionetics, 1992) provided evidence of AN carcinogenicity. These studies are discussed below.

4.2.1.2.1. *Quast (2002) and Quast et al. (1980a).* Quast (2002) and Quast et al. (1980a) conducted a 2-year toxicity and carcinogenicity study in Sprague-Dawley rats (48/sex/group) exposed to AN (purity >99%) in drinking water at concentrations of 35, 100, or 300 ppm; groups of 80/sex receiving untreated drinking water served as controls. Additional interim-sacrifice

groups of 10/sex/dose were exposed for 1 year and analyzed under the same protocol as the main study. The reported intakes of AN were 0, 3.4, 8.5, and 21.3 mg/kg-day for male rats and 0, 4.4, 10.8, and 25.0 mg/kg-day for female rats. Rats were observed daily for clinical signs of toxicity and were weighed and examined monthly for palpable masses. Food and water consumptions were determined for 30 rats/sex/group weekly for the first 3 months of the study and for 1 week during each of the following months: 4, 5, 6, 7, 9, 11, 12, 15, 18, 21, and 24. Hematology examinations and urinalysis were conducted on 10 rats/sex in the control and the highest dose group on days 45, 87, 180, and 355. Additional hematology examinations were conducted on 10 rats/sex from all groups on days 544 (males) and 545 (females) and at study termination on day 724 (males and females); an additional urinalysis was conducted on 10 rats/sex from all groups on day 181 to evaluate a dose response for increased urine specific gravity observed previously at the highest dose group. Clinical chemistry examinations were conducted on 10 rats/sex from the control and highest dose groups on days 46 and 356, on 10 rats/sex from all groups on days 88, 180, and 550, and on all survivors on day 746. All rats, whether dying prematurely, sacrificed in a moribund condition, or sacrificed on schedule, were subjected to a gross necropsy, which included an ophthalmologic examination. Necropsies of rats on scheduled sacrifice included organ weight determinations for brain, heart, liver, kidneys, and testes. Complete histopathologic examinations were conducted for rats in the control and 300 ppm groups in the 1-year interim and 2-year studies, and, based on those results, a set of 22 tissues was examined microscopically in nearly all rats exposed at 35 and 100 ppm; tumors and other lesions identified at gross necropsy were also examined microscopically.

Noncancer results

Exposure to AN in drinking water reduced survival, BW, and consumption of food and water by Sprague-Dawley rats in a dose-related manner (Quast, 2002; Quast et al., 1980a). In male rats exposed at 300 ppm, survival was significantly reduced compared with controls ($p < 0.05$), beginning at 16 months, and none survived after 22 months; survival in other treated male groups was not significantly different from controls. In female rats, exposure at 300, 100, and 35 ppm resulted in significantly reduced survival beginning at 10, 12, and 18 months, respectively, with no high-dose females surviving past month 22; at 24 months, survival was 25, 8.3, 2.1, and 0% for the control and low- to high-dose groups, respectively. The magnitude, time of onset, and duration of significantly lower BWs in exposed rats compared with controls were dose related. Only the 17–22 and 17–18% decreases observed in males and females, respectively, at 300 ppm were biologically significant. Reductions only reached ~8–9% in the 100 ppm groups and ~6–9% in the 35 ppm groups.

The study authors mentioned that BW comparisons near the end of the study tended to be confounded by geriatric changes, few surviving rats, and excessive tumor growth in exposed rats. Food intake (g/rat/day) was significantly lower in 100 and 300 ppm groups compared with

controls beginning during the first week of the study and only in females at 35 ppm. Significantly lower feed intake values for males and females, respectively, compared with controls were measured on 12/24 and 16/24 occasions at 300 ppm, 8/24 and 11/24 times at 100 ppm, and 9/24 times in females only at 35 ppm. The largest difference in high-dose rats was a 25% reduction of feed intake in males after 6 months and a 27% reduction in females after 9 months. Feed intakes during the last weeks of the study were not significantly different among the different groups.

Water intake was reduced during the first 10 days by 36% in males and 38% in females exposed to 300 ppm AN and remained significantly lower for all 26 measurements throughout the study. Significantly lower water consumption was also measured 24/26 times for males and 23/26 times for females at 100 ppm and 13/26 times for males and 21/26 times for females at 35 ppm. Male and female rats in the 100 and 300 ppm dose groups showed a lack of normal grooming later in the study. In addition, signs of nervous system dysfunction (erratic movements, trembling, circling, and limb weakness) were observed in the higher dose groups rats in the absence of end-stage kidney disease or pituitary tumors. These signs of nervous system dysfunction when they occurred in controls were correlated with end-stage kidney disease or pituitary tumors and occurred more frequently in males than in females. The study authors were unable to detect microscopic tumors or lesions that would correlate with the observed clinical signs.

AN had no primary effect on hematological parameters, except for lowered RBC counts associated with blood loss from ulcerated tumors or nutritional anemia during the later stages of the study. The only effect of AN on urinalysis was a slight, but statistically significant increase (1.3–3.0%) in urine specific gravity noted for 300 ppm group males at five time points (45–355 days) and females at all six time points (45–545 days). Significant increase in urine specific gravity was also observed in 100 ppm male and female rats on day 181 and day 544 (females only). The lack of significant effect in treated males on days 544 and 724 was attributed by Quast (2002) to higher incidence of advanced chronic renal disease in controls that resulted in an inability to concentrate urine normally. All 300 ppm male and female rats were dead by day 724. No toxicological significant alterations were observed in clinical chemistry parameters or in absolute or relative organ weights in the few treated rats surviving at termination.

Lesions of the forestomach were the most prominent nonneoplastic histopathologic effects observed in Sprague-Dawley rats (Quast, 2002; Quast et al., 1980a). In the 1-year interim sacrifice, the only treatment-related noncancer lesion was squamous cell hyperplasia of the forestomach, which was observed in 10/10 males and 9/10 females in the 300 ppm group and 4/10 males and 7/10 females in the 100 ppm group. At 2 years, the incidence of forestomach lesions (hyperplasia and/or hyperkeratosis of the squamous epithelium) was dose related and significantly elevated in males at ≥100 ppm and in females at ≥35 ppm; incidences were 15/80, 15/47, 44/48, and 45/48 for males and 20/80, 23/48, 41/48, and 47/48 for females in the 0, 35,

100, and 300 ppm dose groups, respectively. Minimal progressive chronic nephropathy was also elevated in females treated at ≥100 ppm; incidences were 37/80, 24/48, 37/48, and 38/48 for control to high-dose groups. In males, minimal progressive nephropathy was elevated only in the 300 ppm group. However, significant increase in severe progressive nephropathy was observed in males in the 35 and 100 ppm groups; incidences were 11/80, 13/47, 13/48, and 10/48 for control to high-dose groups. Gliosis of the brain, with or without perivascular cuffing, was significantly increased in the low- and middle-dose females (8/48 and 13/48, respectively, vs. 2/80 in controls), although the incidence (5/48) did not reach statistical significance in the high-dose females. In males, it was present in one rat exposed at 100 ppm and three rats exposed at 200 ppm. A NOAEL was not identified in this drinking water study. A LOAEL of 4.4 mg/kg-day was identified for increases in forestomach lesions, decreased survival, and gliosis in brain in female rats exposed to 35 ppm AN in drinking water. Table 4-24 summarizes incidence of nonneoplastic lesions in Sprague-Dawley rats exposed to AN in drinking water for 2 years.

Table 4-24. Incidence of nonneoplastic lesions in Sprague-Dawley rats exposed to AN in drinking water for 2 years

AN in drinking water (ppm)		**0**	**35**	**100**	**300**
Male rats	***Dose (mg/kg-d)***	**0**	**3.4**	**8.5**	**21.3**
Forestomach hyperplasia and/or hyperkeratosis		15/80 (19%)	15/47 (32%)	44/48 (92%)[a]	45/48 (94%)[a]
Kidneys—chronic progressive nephropathy					
Severity:	minimal	10/80 (12%)	4/47 (9%)	7/48 (15%)	16/48 (33%)[a]
	moderate	10/80 (12%)	5/47 (11%)	10/48 (21%)	16/48 (33%)[a]
	severe	11/80 (14%)	13/47 (28%)[a]	13/48 (27%)[a]	10/48 (21%)
Female rats	***Dose (mg/kg-d)***	**0**	**4.4**	**10.8**	**25.0**
Forestomach hyperplasia and/or hyperkeratosis		20/80 (25%)	23/48 (48%)[a]	41/48 (85%)[a]	47/48 (98%)[a]
Kidneys—chronic progressive nephropathy					
Severity:	minimal	37/80 (46%)	24/48 (50%)	37/48 (77%)[a]	38/48 (79%)[a]
	moderate	17/80 (21%)	13/48 (27%)	8/48 (17)	5/48 (10%)
	severe	13/80 (16%)	9/48 (19%)	1/48 (2%)	4/48 (8%)
Brain—gliosis and perivascular cuffing		2/80 (3%)	8/48 (17%)[a]	13/48 (27%)[a]	5/48 (10%)

[a]Statistically significant at $p < 0.05$.

Source: Quast (2002).

Cancer results

The drinking water study by Quast (2002) and Quast et al. (1980a) provided evidence of the carcinogenicity of AN in male and female Sprague-Dawley rats. Tumor findings in the 1-year sacrifices included forestomach papillomas in males: 1/10 at 100 ppm and 7/10 at 300 ppm. In females, the occurrence was 5/10 at 300 ppm. Also observed after 1 year of exposure were microscopic tumors of the CNS (brain) in 2/10 males and 4/10 females at 100 ppm and 1/10 males and 2/10 females at 300 ppm. Carcinoma of Zymbal gland and benign and malignant tumors of the mammary gland, also observed after 1 year of exposure, were considered by the study authors to be related to treatment.

Histopathologic examinations after 2 years of exposure revealed statistically significant and dose-dependent increase in incidences of several types of tumors (Table 4-25). Squamous cell papillomas or carcinomas of the forestomach were significantly elevated in males and females exposed at ≥100 ppm. Carcinomas of Zymbal gland were significantly increased in males at 300 ppm and in females at ≥35 ppm.

Table 4-25. Selected tumor incidences in response to AN administered to Sprague-Dawley rats in drinking water for up to 2 years

	Incidence of tumor formation							
	Male rats				**Female rats**			
	Exposure concentration (ppm)							
	0	**35**	**100**	**300**	**0**	**35**	**100**	**300**
	Dose (mg/kg-d)							
Tissue type	**0**	**3.4**	**8.5**	**21.3**	**0**	**4.4**	**10.8**	**25.0**
Astrocytomas only	1/80	8/47[a]	19/48	23/48[a]	1/80	17/48[a]	22/48[a]	24/48[a]
Combined astrocytomas/glial cell proliferation	1/80	12/47[a]	22/48[a]	30/48[a]	1/80	20/48[a]	25/48[a]	31/48[a]
Tongue (papilloma or carcinoma)	1/80	2/47	4/48	5/48[a]	0/80	1/48	2/48	12/48[a]
Forestomach (papilloma or carcinoma)	0/80	2/47	23/48[a]	39/48[a]	1/80	1/48	12/48[a]	30/48[a]
Zymbal gland (carcinoma or adenoma)	3/80	4/47	3/48	16/48[a]	1/80	5/48[a]	9/48[a]	18/48[a]
Small intestine (mucous cystadenocarcinoma)	ND[b]	ND	ND	ND	0/80	1/48	4/48[a]	4/48[a]
Mammary gland (malignant)	ND	ND	ND	ND	1/80	1/48	3/48	10/48[a]
Mammary gland (malignant or benign)	ND	ND	ND	ND	58/80	42/48[a]	42/48[a]	35/48

[a]Significantly different from controls ($p < 0.05$), as calculated by the study authors.
[b]ND = not determined.

Sources: Quast (2002); Quast et al. (1980a).

An increase in papillomas or carcinomas of the tongue in males at 300 ppm was also considered to be related to exposure. Increases were also observed in the incidences of malignant tumors of the mammary gland. The incidence of malignant or benign mammary tumors was significantly increased in the low- and high-dose females but decreased in the high-dose group. Quast (2002) noted that the lower mammary tumor incidence in the 300 ppm group was likely due to the marked early mortality in this group, despite the earlier occurrence of these tumors. The incidence of mammary tumors increased considerably in controls during the latter portion of the study, when few high-dose females survived.

Two diagnostic categories—focal or multifocal glial cell proliferation (suggestive of early tumors), and focal or multifocal glial cell tumor (astrocytomas)—were used by Quast (2002) for tumors present in the brain or spinal cord. These diagnoses were mutually exclusive and primarily based on the size of the lesion, with glial cell proliferation a smaller-sized lesion than astrocytoma. For enumerating the astrocytomas of the CNS, the incidence of glial proliferation was combined with the incidence of astrocytomas and was elevated in both males and females in all exposed groups (Table 4-25).

Distribution of astrocytomas in the various regions of nervous tissue in male and female Sprague-Dawley rats is shown in Table 4-26. No tumors were found from 0 to 12 months in any location in either male or female rats. As noted by Quast (2002), the sections of cerebral cortex contained most of the tumors because of the cortex's larger size. However, astrocytomas were also found in the cerebellum, brain stem, and spinal cord in male and female rats. Smaller-sized lesions (glial cell proliferation) had a distribution similar to astrocytomas.

Table 4-26. Histopathologic location of astrocytomas in the CNS of male Sprague-Dawley rats administered AN in drinking water for 2 years

Age at sacrifice	Location of astrocytomas[a]							
	Male rats				Female rats			
	Cerebral cortex	Cerebellum	Brain stem	Spinal cord	Cerebral cortex	Cerebellum	Brain stem	Spinal cord
0 ppm								
13–18 mos	0/23	0/23	0/23	0/22	0/11	0/11	0/10	0/11
19–24 mos	1/43	0/43	0/43	0/43	0/48	0/48	0/47	0/46
Terminal kill	0/7	0/7	0/7	0/7	1/20	0/20	0/20	0/20
35 ppm								
13–18 mos	2/14	0/14	1/14	0/14	1/13	0/13	1/13	0/13
19–24 mos	5/26	1/26	1/25	0/26	5/30	2/29	6/30	0/30
Terminal kill	1/5	0/5	1/5	0/5	3/4	0/4	2/4	0/4
100 ppm								
13–18 mos	3/16	1/16	2/16	1/16	5/19	2/20	1/19	1/19
19–24 mos	13/26	0/26	6/26	1/26	12/24	1/24	9/24	1/24
Terminal kill	2/5	0/5	0/5	0/5	0/1	0/1	1/1	0/1
300 ppm								
13–18 mos	10/26	0/26	2/26	1/26	11/23	2/23	4/23	3/22
19–24 mos	11/18	2/18	4/18	2/18	8/11	2/11	3/11	2/11
Terminal kill	0/0	0/0	0/0	0/0	0/0	0/0	0/0	0/0

[a]No astrocytomas were found in any locations from 0 to 12 mos.

Sources: Quast (2002); Quast et al. (1980a).

4.2.1.2.2. ***Johannsen and Levinskas (2002a) and Biodynamics (1980a): drinking water study.*** Johannsen and Levinskas (2002a) and Biodynamics (1980a) carried out another 2-year drinking water study of AN in Sprague-Dawley rats. Groups of 100 rats/sex/group were exposed to 0, 1, or 100 ppm AN (100% purity) in drinking water; as calculated by the study authors, average daily doses were 0, 0.09, and 8.0 mg/kg-day , respectively, for males and 0, 0.15, and 10.7 mg/kg-day, respectively, for females. Ten rats/sex/group were selected from these groups for interim evaluations at 6, 12, and 18 months and at study term, leaving a maximum of 70/sex/group for lifetime exposure. Although the study was designed to last 24 months, because of high mortality among high-dose rats, surviving males were necropsied after 22 months and females at 19 months to ensure that a sufficient number of animals would be available for clinical and pathological analyses. Rats were observed daily for morbidity and mortality and examined and palpated weekly to detect growths. All rats received ophthalmoscopic examinations in the period before treatment started and again at the time of necropsy.

BWs were recorded weekly for the first 14 weeks, biweekly between weeks 16 and 26, and monthly thereafter. Food intake and water consumption were recorded over 3-day periods

for about 25 rats/sex/group at the same intervals at which BWs were recorded. Ten rats/sex from each group were selected for hematological, clinical chemical, and urinalysis examinations at 6, 12, and 18 months and at study termination (22 months for males and 19 months for females). All rats, whether dying prematurely, sacrificed in a moribund condition, or sacrificed on schedule, were subjected to a gross necropsy that included preservation of 40 tissues and organs, gross lesions, and tissue masses for possible histopathological examination. At interim and terminal necropsies, weights were recorded for selected organs (brain, pituitary, adrenal, gonads, heart, kidney, and liver) in 10 rats/sex/group. Interim gross necropsies were performed after 6, 12, and 18 months on 10 rats/sex/group and on the remaining rats at termination. For the scheduled interim and terminal sacrifices, complete histopathologic examinations were conducted on 10 rats/sex from the control and 100 ppm groups; on all other rats, a limited set of tissues was examined microscopically that included potential target organs (brain, ear canal, spinal cord, and stomach) and any tissue masses observed at necropsy.

Noncancer results

Treatment-related noncancer effects were observed in Sprague-Dawley rats exposed to AN for 19–22 months (Johannsen and Levinskas, 2002a; Biodynamics, 1980a). Statistically significant increases in early deaths were observed in high-dose male and female rats after 10 months and became particularly severe during the last 5 months of the study. Reduction in survival compared with controls was not significant in high-dose males at termination (22 months) but was significant in high-dose female rats terminated at 19 months. Food and water consumption in high-dose rats was lower than in controls throughout the study. Reduction in mean BW compared with controls was observed in high-dose males and females throughout the study (a significant 10% reduction in males and an insignificant 8% reduction in females at term). Slight reductions in hematocrit, RBC count, and Hb values compared with controls were observed during the study in high-dose groups but were generally not statistically significant; 3–6% reductions in Hb values in high-dose males were statistically significant at the 6- and 18-month interim time points. Exposure to AN had no effect on clinical chemistry or urinalysis parameters or ophthalmoscopic examinations; there were no treatment-related clinical signs except for some neurological symptoms at the time of terminal necropsy in a few rats with astrocytomas of the brain or spinal cord. The only significant treatment-related effects on organ weights were lower absolute pituitary weights in high-dose males at 12 months and in females at termination. Significant increase in mean relative kidney and liver weights observed in high-dose males and females were considered by the study authors to reflect the reduced BWs rather than target organ effects, since this effect did not occur at other study intervals.

Statistically significant increases in nonneoplastic lesions related to exposure to AN included renal transitional cell hyperplasia in high-dose females at termination (Table 4-27). Significant increase in squamous metaplasia of the uterus was observed in high-dose females at

12 months compared with controls (5/10 vs. 0/10), and in low-dose females at 18 months (3/3 vs. 2/10). This effect was not significant in high-dose females at 18 months (4/10), and was not observed at terminal sacrifice.

Table 4-27. Incidence of nonneoplastic lesions in Sprague-Dawley rats exposed to AN in drinking water for 2 years

AN in drinking water (ppm)	0[a]	1	100
Male rats ***Dose (mg/kg-d)***	**0**	**0.09**	**8.0**
Kidney transitional cell hyperplasia	1/15	2/18	0/12
Forestomach squamous cell hyperplasia			
Incidence at termination[b]	14/19	24/26	14/15
Severity: mild	5	4	1
moderate	7	14[c]	8[c]
severe	2	6[c]	5[c]
Forestomach squamous cell hyperplasia			
Incidence in early deaths or unscheduled sacrifices	36/46	31/37	37/42
Severity: mild	9	10	4
moderate	17	15	18[c]
severe	10	6	15[c]
Female rats ***Dose (mg/kg-d)***	**0**	**0.15**	**10.7**
Kidney transitional cell hyperplasia	2/27	1/18	8/14[d]
Forestomach squamous cell hyperplasia			
Incidence at termination[b]	39/48	40/57	17/17
Severity: mild	12	8	4
moderate	18	25	9
severe	9	7	4
Incidence in early deaths or unscheduled sacrifices	14/20	6/12	33/43
Severity: mild	4	1	1
moderate	7	2	21[d]
severe	3	3	11[d]

[a]Drinking water control.
[b]Males exposed for 22 mos, females for 19 mos.
[c]Significantly different from controls as calculated by authors ($p \leq 0.05$).
[d]Significantly different from controls as calculated by authors ($p \leq 0.01$).

Sources: Johannsen and Levinskas (2002a); Biodynamics (1980a).

In addition, the incidence of squamous cell hyperplasia was increased in high-dose males and females at terminal sacrifice and in spontaneous deaths in high-dose groups (Table 4-27). The severity of squamous cell hyperplasia of the forestomach was significantly greater (characterized as moderate or severe) than in controls in male rats at termination after exposure to 1 or 100 ppm AN; a significant increase in severity in high-dose males was also observed at 12 months (not shown) but not at 18 months. Increased incidences in forestomach hyperplasia

characterized as moderate or severe were also observed in high-dose rats of both sexes that died prematurely or were sacrificed in a moribund condition. A NOAEL for nonneoplastic effects was not identified in this study. A LOAEL of 1 ppm (0.09 mg/kg-day) was identified for increased severity of squamous cell hyperplasia of the forestomach in male Sprague-Dawley rats exposed to AN in drinking water for 2 years (22 months).

Cancer results

Significant increases in the cumulative incidences of neoplasms of the CNS, ear canal (Zymbal gland), and forestomach were observed in Sprague-Dawley rats exposed to 100 ppm AN in drinking water for 2 years (Johannsen and Levinskas, 2002a; Biodynamics, 1980a). Statistically significant, dose-dependent increases were observed for astrocytomas of the brain in both sexes and astrocytomas of the spinal cord in females. The astrocytomas varied from discrete solid masses to localized areas of diffuse infiltrations of neoplastic cells. In addition, adenomas of Zymbal gland (ear canal) in both sexes, carcinomas of Zymbal gland in both sexes, and squamous cell papillomas of the forestomach in females were increased. Intestinal adenocarcinomas were also found in high-dose male and female rats (see Table 4-28).

Table 4-28. Selected tumor incidences in Sprague-Dawley rats exposed to AN in drinking water for up to 2 years

Tissue type	Tumor incidence[a]					
	Male rats			Female rats		
	Exposure concentration (ppm)					
	0	1	100	0	1	100
	Dose (mg/kg-d)					
	0	0.09	7.98	0	0.15	10.7
CNS						
Brain (astrocytomas)	2/78	3/75	23/77[b]	0/79	1/80	32/77[b]
Spinal cord (astrocytomas)	ND[c]	ND	ND	0/76	0/79	7/78[b]
Total	2/78	3/75	23/77[b]	0/79	1/80	39/78[b]
Zymbal gland						
Carcinomas	1/80	0/71	14/83[b]	0/79	0/75	7/78[b]
Adenomas	0/80	0/71	5/83	1/79	0/75	5/78
Total	1/80	0/71	19/83[b]	1/79	0/75	12/78[b]
Forestomach						
Carcinomas	0/78	1/78	3/77	0/80	0/79	0/79
Papillomas	3/78	2/78	8/77	1/80	4/79	7/79[b]
Total	3/78	3/78	11/77[b]	1/80	4/79	7/79[b]
Intestine						
Adenocarcinomas	0/40	0/34	2/41	0/78	0/79	2/70

[a]Denominators are calculated from the total number of animals examined (as reported in Table 4 of Johannsen and Levinskas, 2002a) minus the animals scheduled for sacrifice at 6 and 12 mos. Thus, incidences are for animals scheduled for the 18-mo, spontaneous deaths and terminal sacrifices (22 mos for males and 19 mos for females). For Zymbal gland tumors in the 100 ppm male, one carcinoma and adenoma occurred in the 12-mo sacrifice; therefore, adjustment to the denominator was only made for the 6-mo sacrifice.
[b]Significantly different from controls ($p < 0.05$), Fisher's exact test.
[c]ND = no data collected.

Sources: Johannsen and Levinskas (2002a); Biodynamics (1980a).

Johannsen and Levinskas (2002a) reported that most of the tumors occurred in rats after 12 months of exposure. CNS astrocytomas were not detected at the 6- or 12-month interim sacrifices (at which about 10 rats of each gender were sacrificed from each group). However, brain astrocytomas and Zymbal gland carcinomas were detected in high-dose females as early as after 6 months of exposure. One each of Zymbal gland carcinoma, adenoma, and squamous cell carcinoma of the forestomach was detected at the 12-month interim sacrifice in high-dose males. This finding was consistent with findings in the other drinking water bioassay with Sprague-Dawley rats, indicating that some male and female rats exposed to 300 ppm AN developed tumors after only 7–12 months of exposure (Quast, 2002). Mammary gland carcinomas were detected in female rats scheduled for the terminal sacrifice but not in male or female rats scheduled for sacrifice at 6, 12, or 18 months. Incidences of female rats (scheduled for the

terminal sacrifice) with mammary gland carcinomas, however, did not show exposure-related increases: 13/80, 4/79, and 14/79 for the control, 1 ppm, and 100 ppm female groups, respectively.

4.2.1.2.3. ***Johannsen and Levinskas (2002a) and Biodynamics (1980b): gavage study.*** In parallel to the chronic drinking water study in Sprague-Dawley rats, Johannsen and Levinskas (2002a) and Biodynamics (1980b) conducted a lifetime study in which groups of Sprague-Dawley rats (100 rats/sex/group) received 0, 0.1, or 10 mg/kg-day AN by gavage in water for 7 days/week. The doses were selected to match the daily intake levels in the drinking water study. The schedule and protocols used in the gavage study for observations of clinical signs, measurements of food and water consumption and BW, clinical biochemistry analyses, and gross necropsy and histopathologic analyses were identical to those in the drinking water study.

Ingestion of 10 mg/kg-day AN resulted in increased mortality after 12 months and was significantly higher in males at termination and in females beginning at month 14 compared with controls. The study was terminated after 20 months of exposure because of high treatment-related deaths, with a decreased survival of about 30 and 50% in males and females compared with their respective controls. BWs showed a significant reduction of about 6% in high-dose males compared with controls, beginning on week 12 and reaching 13% by termination; there were no BW effects in exposed females.

Exposure to AN had no effect on food consumption in either sex or on water consumption in males; high-dose females had slightly increased water consumption during the first 12 months only. Small reductions in hematocrit, Hb, and RBC counts were observed in high-dose males at 12 and 18 months and reached statistical significance at terminal sacrifice (hematocrit, 15%; Hb, 19%; and RBC counts, 18%). Significant increases in absolute mean liver weights were observed in the high-dose males and females and low-dose males at the 18-month interval. Relative liver weights for high-dose males and females were significantly increased in most intervals and might be reflective of lower BWs. Absolute and relative kidney weights of high-dose males were increased significantly at 18 months and increased insignificantly in both males and females at study term. The adrenal gland of high-dose males was the organ that showed the most significant weight increase of 43% at termination.

Noncancer results

Nonneoplastic histopathological effects were observed in male and female Sprague-Dawley rats exposed to 10 mg/kg-day AN by gavage for 20 months (Table 4-29). A significant increase in epidermal inclusion cysts was observed in male and female rats, most notably in animals dying spontaneously. Significant increases in renal transitional cell hyperplasia were observed in high-dose females at 12-month sacrifice and in high-dose males after 18 months. In addition, there was a significant increase in the severity of squamous cell hyperplasia of the

forestomach in high-dose males and females. This effect was most noticeable among rats dying early or at scheduled sacrifices after at least 12 months. High-dose rats showed a significant elevation in the incidence of moderate or severe hyperplasia. In this gavage study, a NOAEL of 0.1 mg/kg-day and a LOAEL of 10 mg/kg-day were identified for increased severity of forestomach lesions (squamous cell hyperplasia) in male and female rats.

Table 4-29. Incidence of nonneoplastic lesions in Sprague-Dawley rats exposed to AN by gavage for 20 months

Dose (mg/kg-d)	0[a]	0.1	10
Male rats			
Skin: Epidermal inclusion cysts (in spontaneous deaths)	2/59	4/68	8/56[b]
Kidney: Transitional cell hyperplasia (18 mos)	3/11	0/8	10/10[c]
Heart: Cardiomyopathy (18 mos)	3/11	No data	8/10[b]
Forestomach: Squamous cell hyperplasia			
Incidence at terminal sacrifice	10/10	No data	8/10
Severity: mild	2		0
moderate	5		2
severe	3		6
Incidence in early deaths or unscheduled sacrifices	46/58	46/67	49/56
Severity: mild	18	11	2
moderate	19	26	13[c]
severe	9	10	34[c]
Female rats			
Skin: Epidermal inclusion cysts (in spontaneous deaths)	0/10	No data	4/10[b]
Kidney: Transitional cell hyperplasia (12 mos)	0/10	0/1	4/10[b]
Heart: Cardiomyopathy (18 mos)	4/10	No data	3/10
Forestomach squamous cell hyperplasia			
Incidence at terminal sacrifice	8/10	No data	9/10
Severity: mild	1		1
moderate	5		3
severe	2		5
Incidence in early deaths or unscheduled sacrifices	47/57	63/69	53/59
Severity: mild	12	12	0
moderate	23	38	14[c]
severe	12	13	39[c]

[a]Water vehicle control.
[b]Significantly different from controls as calculated by the study authors ($p < 0.05$).
[c]Significantly different from controls as calculated by the study authors ($p \leq 0.01$).

Sources: Johannsen and Levinskas (2002a); Biodynamics (1980a).

Cancer results

The carcinogenic effects of AN on Sprague-Dawley rats exposed via gavage were similar to those in the drinking water studies (Johannsen and Levinskas, 2002a; Biodynamics, 1980b). Significant increase in tumor incidences were observed in male and female rats dosed with 10 mg/kg-day and included carcinomas of Zymbal gland, astrocytomas of the brain, and tumors of the squamous epithelium of the forestomach (papillomas and carcinomas in males and papillomas in females) (Table 4-30). Adenocarcinomas of the intestine were also observed in high-dose male rats that died or were killed after at least 12 months of exposure. Increases in carcinomas of the mammary gland were observed in high-dose females that died prematurely.

Table 4-30. Cumulative incidence of tumors in response to AN administered to Sprague-Dawley rats by gavage for up to 2 years

Tissue type	Tumor incidence[a]					
	Male rats (mg/kg-d)			Female rats (mg/kg-d)		
	0	0.1	10	0	0.1	10
Brain astrocytomas	2/80	0/79	16/77[b]	1/80	2/78	17/80[b]
Spinal cord astrocytomas	0/74	0/73	1/77	0/80	0/75	1/79
Zymbal gland papillomas	0/76	0/73	3/76	0/65	0/74	0/74
Zymbal gland carcinomas	1/76	0/73	10/76[b]	0/65	0/74	9/74[b]
Zymbal gland adenomas	0/76	1/73	5/76[b]	1/65	0/74	5/74
Forestomach carcinomas	0/79	0/77	18/79[b]	0/79	0/79	1/79
Forestomach papillomas	2/79	6/77	19/79[b]	2/79	4/79	14/79[b]
Intestine adenocarcinomas	0/80	0/80	6/80[b]	0/40	0/40	1/41
Mammary gland carcinomas	0/80	0/78	0/80	5/80	6/80	21/80[b]

[a]Denominators are calculated from the total number of animals examined (as reported in Table 4 of Johannsen and Levinskas, 2002a) minus the animals scheduled for sacrifice at 6 and 12 mos; thus, incidences are for animals scheduled for the 18-mo, spontaneous death, and terminal sacrifices (20 mos).
[b]Significantly different from controls ($p < 0.05$), as calculated by the study authors.

Sources: Johannsen and Levinskas (2002a); Biodynamics (1980a).

4.2.1.2.4. ***Johannsen and Levinskas (2002b); Biodynamics (1980c).*** A 2-year drinking water assay was conducted in F344 rats (Johannsen and Levinskas, 2002b; Biodynamics, 1980c). Groups of rats (100/sex/group) were given AN (100% purity) in drinking water at concentrations of 0, 1, 3, 10, 30, or 100 ppm; two groups of 100/sex served as untreated controls. The study authors reported the equivalent average daily doses of AN as 0, 0.1, 0.3, 0.8, 2.5, and 8.4 mg/kg-day for males and 0, 0.1, 0.4, 1.3, 3.7, and 10.9 mg/kg-day for females. Rats were observed twice daily for overt signs of toxicity and examined and palpated weekly to detect growths. Ophthalmoscopic examinations were carried out before testing and again at the time of necropsy. BWs were recorded weekly for the first 14 weeks, biweekly between weeks 16 and 26, and monthly thereafter. Food intake and water consumption were recorded over a 3-day period at the

same intervals that BWs were recorded for about 25 rats/sex/group for all groups. At intervals of 6, 12, and 18 months and at study termination (26 months for males and 23 months for females), 10 rats/sex/group from each exposed and control group were sacrificed for clinical pathology and microscopic evaluation.

At 6, 12, and 18 months and at termination, 10 rats/sex from the 100 ppm group and 5 rats/sex from each of the control groups were selected for hematology, clinical chemistry, and urinalysis examinations. Lower dose group rats were evaluated as needed to determine possible dose-response relationships. All rats, whether dying prematurely, sacrificed in a moribund condition, or sacrificed on schedule, were subjected to a gross necropsy that included preservation of 40 tissues and organs, all gross lesions, and tissue masses for possible histopathologic examination. At interim and terminal sacrifice, weights were recorded for selected organs (brain, pituitary, adrenal, gonads, heart, kidney, and liver) for 10 rats/sex from treated groups and 5 rats/sex from each control group. For the interim sacrifices, complete histopathologic examinations were conducted on 10 rats/sex from the 100 ppm group and 5 rats/sex from the two control groups. Potential target organs (e.g., brain, ear canal, spinal cord, and stomach), gross lesions, and tissue masses were examined microscopically in all study animals. All surviving females were terminated after 23 months and all males after 26 months. Terminal necropsies included complete microscopic examinations for 10 rats/sex exposed to 100 ppm AN and 5/sex/group for the two control groups. Potential target organs and suspicious lesions were examined in all animals in other dose groups.

Noncancer results

Treatment-related noncancer effects were observed in F344 rats exposed to AN in drinking water for 2 years (Johannsen and Levinskas, 2002b; Biodynamics, 1980c). Statistically significantly early deaths ($p < 0.05$), compared with controls, were observed in male and female rats exposed to 100 ppm, beginning after 14 months of exposure. A statistically significant decrease in survival was also observed in female rats exposed to 30 ppm but not to 10 ppm, beginning after 18 months of exposure. Exposure to AN did not result in any overt neurological impairments or ophthalmoscopic findings.

Statistically significant decrease in BWs (~12% lower than controls, $p < 0.01$) were observed in male and female rats exposed to 100 ppm AN. A statistically significant decrease in BWs of less than 5% was found in male rats exposed to 30 ppm AN and was not biologically significant. Total food consumption (g/week) was reduced compared with controls in rats exposed at 100 ppm (more prominently in female rats after week 13), but consumption on a BW basis (g/kg) for both 100 ppm male and female rats was not significantly different from that for controls. Total water consumption (mL/week) was significantly lower in the 100 ppm male and female rats compared with controls. No differences in food and water consumption from controls were found for groups exposed to ≤30 ppm AN. Hematological analyses revealed slight

reductions in Hb, hematocrit, and RBC counts in the 100 ppm group, beginning at 12 months, with Hb significantly lower in female rats at 12 and 18 months (13% at 18 months). Hematocrit in 100 ppm female rats was 4% lower at 12 months. However, no statistically significant differences from controls were noted at termination.

Serum alkaline phosphatase levels were significantly elevated by 80 and 65% ($p < 0.05$), respectively, in 100 ppm females at 18 and 23 months. Results of clinical chemistry for the 30 and 10 ppm groups were not reported. However, the study authors noted that female rats in these dose groups also showed significant elevation of this enzyme. A significant 33% increase in SGPT was also observed in 100 ppm female rats at 18 months but not at other intervals. The only treatment-related urinalysis finding was a slight increase in urine specific gravity in 100 ppm males at 18 and 26 months. No significant dose-related changes were observed for absolute organ weights; elevations in relative organ weights (kidney, brain, liver, adrenal, testis, heart, and pituitary in females) sporadically observed at 100 ppm at intervals throughout the study were attributed by the study authors to lower BWs rather than target-organ toxicity.

Unlike Sprague-Dawley rats exposed to AN in drinking water (see above, Quast [2002]), F344 rats did not show forestomach lesions at the 6- or 12-month sacrifices. In rats exposed for periods >1 year, treatment-related nonneoplastic effects were observed in the forestomach (Table 4-30) and skin. The incidence of squamous cell hyperplasia or hyperkeratosis of the forestomach was elevated in male and female rats exposed to 3, 10, and 30 ppm but not to 100 ppm. Johannsen and Levinskas (2002b) suggested that, because the lesions were observed more frequently in late surviving animals, the reduced survival in 100 ppm group may have been the reason that no significant increase was observed for that dose group. Because these forestomach lesions were not observed in rats examined during the 6- or 12-month sacrifices, no such incidence data are listed in Table 4-31. An increase in epidermal inclusion cysts of the skin, observed in 4/50 male rats treated at 100 ppm but in no other group, was also considered by the study authors to be treatment related. A NOAEL of 1 ppm (0.1 mg/kg-day) and a LOAEL of 3 ppm (0.3 and 0.4 mg/kg-day for males and females, respectively) were identified for increases in squamous cell lesions (hyperplasia and/or hyperkeratosis) of the forestomach in male and female F344 rats exposed to AN in drinking water for 2 years.

Table 4-31. Incidences of nontumorous lesions in F344 rats exposed to AN in drinking water for 2 years

AN in drinking water (ppm)	0[a]	1	3	10	30	100
Male rats Dose (mg/kg-d)	**0**	**0.1**	**0.3**	**0.8**	**2.5**	**8.4**
Forestomach squamous cell hyperplasia or hyperkeratosis[b]	11/159	3/80	18/75[c]	13/80[d]	17/80[c]	9/77
Foci of cellular alteration in liver	7/94	5/31	11/51	8/45	14/50[c]	6/68
Epidermal inclusion cysts	0/61	0/12	0/12	0/11	0/17	4/50[d]
Chronic nephropathy, bilateral	118/149	57/58[d]	62/64[c]	52/54[d]	57/60[d]	42/62
Atrophy of seminiferous tubules, bilateral	150/172	72/75[d]	68/84	64/74	78/78[c]	64/87
Female rats Dose (mg/kg-d)	**0**	**0.1**	**0.4**	**1.3**	**3.7**	**10.9**
Forestomach squamous cell hyperplasia or hyperkeratosis[b]	4/156	2/80	16/80[c]	23/74[c]	13/80[c]	5/74
Foci of cellular alteration in liver	1/84	2/20	4/39[d]	3/49	0/40	1/70
Chronic nephropathy, bilateral	52/68	10/19	21/26	20/29	23/26	18/50

[a]Drinking water control.
[b]Males exposed for 18–26 mos, females for 18–23+ mos; excludes rats sacrificed at 6 or 12 mos. These incidences were further adjusted to exclude (from the denominators) rats that died between 0 and 12 mos in the study. Rats dying during this time period were determined from page 6 of Appendix H and Table 1 in Biodynamics (1980c) and Table 8 in Johannsen and Levinskas (2002b). Unscheduled deaths between 0 and 12 mos in the study occurred in two female controls, two males at 3 ppm, three females at 10 ppm, and three males and three females at 100 ppm.
[c]Significantly different from vehicle control as calculated by study authors ($p \leq 0.01$).
[d]Significantly different from vehicle control as calculated by study authors ($p \leq 0.05$).

Sources: Johannsen and Levinskas (2002a); Biodynamics (1980a).

Other microscopic findings included increase in chronic nephropathy and atrophy of seminiferous tubules, which were significant at 1 ppm. However, the study authors did not consider these effects to be related to treatment, but rather to be due to the sample selection procedure that only tissues showing questionable or suspicious lesions were selected for microscopic examination for the intermediate dose groups (1–30 ppm), resulting in the selection of tissues from more aged animals.

Cancer results

Increases in tumor incidences (Table 4-32) were observed in multiple organs, following chronic exposure of F344 rats to AN in drinking water (Johannsen and Levinskas, 2002b; Biodynamics, 1980c). No tumors were detected in rats sacrificed after only 6 months of exposure. One female rat exposed to 100 ppm for 12 months had an adenocarcinoma of the mammary gland that the study authors considered to be possibly related to treatment. Treatment-related tumors, appearing at the 18-month interim sacrifice, included brain astrocytomas (one/sex/group) in male and female rats exposed to 30 and 100 ppm, squamous cell papillomas of the ear canal (Zymbal gland) in 2/9 males at 100 ppm and 1/9 females at 30 ppm, and squamous cell carcinomas of the latter organ in one female at 100 ppm. AN-related neoplastic

lesions were observed at terminal sacrifice in the brain, spinal cord, forestomach, ear canal (Zymbal gland), and mammary gland (females only). Significant dose-related elevations in astrocytomas were observed in the brains of male and female rats exposed to 30 and 100 ppm and in the spinal cord of male rats exposed to 100 ppm (see Table 4-32). Dose-related increases in squamous cell adenomas/carcinomas of the ear canal (Zymbal gland) were observed in males exposed to 30 and 100 ppm and in females at 10–100 ppm. Increased incidences of squamous cell papillomas or carcinomas of the forestomach, observed in males exposed to 3 and 10 ppm and in both sexes exposed to 30 ppm, were considered by the study authors to be likely treatment related despite the lack of a dose response. Fibroadenomas of the mammary gland were slightly increased in females treated with 10 and 30 ppm. Other lesions considered by the study authors to be possibly treatment related included a single case of squamous cell carcinoma of the salivary gland in one male at 100 ppm and squamous cell papillomas of the tongue in female rats (one/group) exposed to 10 and 30 ppm.

Table 4-32. Selected tumor incidences in F344 rats exposed to AN in drinking water for 2 years

AN in drinking water (ppm)	0[a]	1	3	10	30	100
Male rats[b] ***Dose (mg/kg-d)***	**0**	**0.1**	**0.3**	**0.8**	**2.5**	**8.4**
Brain astrocytoma Total[c]	2/200[c]	2/100	1/100	2/100	10/99[e]	21/99[e]
Adjusted[d]	2/160[d]	2/80	1/78	2/80	10/79[e]	21/76[e]
Spinal cord astrocytoma	1/196	0/99	0/92	0/98	0/99	4/93[f]
	1/156	0/79	0/70	0/78	0/79	4/70[f]
Ear canal (Zymbal gland) squamous cell papilloma/adenoma and carcinoma	2/189	1/97	0/93	2/88	7/94[e]	16/93[e]
	1/147	1/76	0/73	0/67	2/71[e]	14/68[e]
Forestomach squamous cell papilloma/carcinoma	0/199	1/100	4/97[f]	4/100[f]	4/100[f]	1/101
	0/159	1/80	4/78[f]	3/80[f]	4/80[f]	1/77
Mammary gland fibroadenoma	2/48	1/4	2/7	2/12	0/7	2/45
Mammary gland carcinoma	1/48	0/4	0/7	0/12	0/7	0/45
Female rats[b] ***Dose (mg/kg-d)***	**0**	**0.1**	**0.4**	**1.3**	**3.7**	**10.9**
Brain astrocytoma	1/199	1/100	2/101	4/95	6/100[e]	23/98[e]
	1/157	1/80	2/80	4/75	6/80[e]	23/76[e]
Spinal cord astrocytoma	0/197	0/97	0/99	1/92	0/96	1/91
	0/155	0/78	0/79	1/72	0/77	1/69
Ear canal (Zymbal gland) squamous cell papilloma/adenoma and carcinoma	0/193	0/94	2/92	4/90[e]	5/94[e]	10/86[e]
	0/157	0/73	0/73	0/70[e]	2/73[e]	8/62[e]
Forestomach squamous cell papilloma/carcinoma	1/199	1/100	2/100	2/97	4/100[f]	2/97
	1/157	1/80	2/79	2/77	4/80[f]	2/75
Mammary gland fibroadenoma	12/65	5/14	6/14	9/16[e]	10/22[f]	9/49
	12/156	5/80	6/80	8/79	9/80	9/73
Mammary gland carcinoma	1/65	2/14	0/14	0/16	3/22	2/49
	3/156	4/80	0/80	1/78	3/80	6/73

[a]Drinking water control.
[b]Males exposed for 26 mos, females for 23+ mos.
[c]Total cumulative number of rats with lesion.
[d]The denominators for incidences excluded rats from the 6- and 12-mo sacrifices and rats that died before the appearance of the first tumor for each of three tumor sites: CNS, Zymbal gland, and forestomach. The termination history reports in Appendix C and the individual animal histopathology reports in Appendix H of the Biodynamics (1980b) report were examined to determine time of death and tumor occurrence for each of the F344 rats. Times of first detection of tumors were 419 d for forestomach tumors, 495 d for CNS tumors, and 475 d for Zymbal gland tumors. Due to the limited number of mammary glands examined in most groups, the adjusted denominators represented the number of animals that were exposed for more than 12 mos for each group; mammary gland tumor incidences are for animals scheduled for the 18-mo and terminal sacrifices.
[e]Significantly different from vehicle control as calculated by study authors (cumulative only) ($p \leq 0.01$).
[f]Significantly different from vehicle control as calculated by study authors (cumulative only) ($p \leq 0.05$).

Sources: Johannsen and Levinskas (2002a); Biodynamics (1980a).

4.2.1.2.5. ***NTP (2001).*** NTP (2001) evaluated the toxicity and carcinogenicity of AN (>99% purity) given by gavage in water to $B6C3F_1$ mice (50/sex/dose) at doses of 0, 2.5, 10, and 20 mg/kg-day, 5 days/week for 2 years. Adjusted for discontinuous exposure (5 days/7 days), the intakes were 0, 1.8, 7.1, and 14.3 mg/kg-day. The doses were chosen based on results of the

14-week assay described in Section 4.2.1.1. Mice were observed twice daily for clinical signs that were recorded on day 29, every 4 weeks, and at study termination. BWs were recorded before the start of the exposure period, then every 4 weeks, and at study termination. Five male and five female mice were evaluated at 2 weeks and 3, 12, and 18 months for urinalysis parameters. All mice were subjected to gross necropsies and complete histopathologic examinations.

Noncancer results

Survival was significantly reduced in male and female mice treated with 20 mg/kg-day; 38/50, 42/50, 39/50, and 14/50 males and 39/50, 32/50, 39/50, and 23/50 females survived to 104–105 weeks with increasing dose. Despite a tendency for BWs in high-dose mice to be slightly lower compared with controls after 30 weeks of treatment, AN had no significant effect on terminal BWs; no treatment-related clinical signs were observed.

Exposure to AN significantly increased the incidences of nonneoplastic lesions in male and female mice compared with control mice (Table 4-33). Statistically significant increases in the incidences of mild focal or multifocal epithelial hyperplasia of the forestomach were observed in males treated with 10 or 20 mg/kg-day and in focal or multifocal epithelial hyperplasia of the forestomach in females treated with 20 mg/kg-day. The hyperplastic lesions were often accompanied by focal hyperkeratosis and occasionally associated with chronic inflammation. The incidence of hyperkeratosis (diffuse or focal) of the forestomach was statistically significantly elevated in males treated at 20 mg/kg-day. AN-treated males showed a higher incidence of hyperplasia of the Harderian gland, but only the increase observed at 10 mg/kg-day was statistically significantly different from the control. No significant increase was found in treated females (Table 4-33). Statistically significant elevations were observed in the incidences for ovarian cysts in females treated with 2.5–20 mg/kg-day and for ovarian atrophy in females treated with 10–20 mg/kg-day; for both ovarian lesions, the highest incidences were observed at 10 mg/kg-day. A NOAEL was not identified for noncancer effects in this gavage study. A LOAEL of 1.8 mg/kg-day (adjusted for continuous exposure) was identified for increased incidence of ovarian cysts in female mice. A NOAEL of 1.8 mg/kg-day and a LOAEL of 7.1 mg/kg-day were identified for increased incidences of forestomach hyperplasia in male mice.

Table 4-33. Incidence and severity of nonneoplastic lesions in B6C3F$_1$ mice exposed by gavage to AN for 2 years

Adjusted dose (mg/kg-d)[a]	0[b]	1.8	7.1	14.3
Males				
Number of male mice examined	50	50	50	50
Forestomach hyperkeratosis, diffuse/focal	2[c] (2.5)[d]	3 (2.0)	7 (1.7)	12[f](1.8)
Forestomach epithelial hyperplasia, focal	2 (3.0)	4 (2.3)	8[e] (2.0)	9[f](1.9)
Harderian gland hyperplasia	1 (2.0)	4 (2.3)	7[e] (3.4)	4 (2.3)
Females				
Number of female mice examined	50	50	50	50
Forestomach hyperkeratosis, diffuse/focal	2 (1.5)	1 (2.0)	2 (2.0)	4 (2.0)
Forestomach epithelial hyperplasia, focal, or multifocal	2 (1.5)	2 (3.0)	5 (1.8)	7[e] (1.6)
Harderian gland hyperplasia	5 (3.0)	4 (3.3)	6 (2.2)	8 (3.5)
Ovarian atrophy	6 (3.0)	8 (3.9)	45[f] (4.0)	40[f] (4.0)
Ovarian cyst	12 (2.3)	20[e] (2.3)	27[f] (2.1)	19[e] (2.1)

[a]Doses administered 5 d/wk.
[b]Vehicle control.
[c]Number of mice with lesion.
[d]Average severity grade of lesions in affected mice: 1 = minimal, 2 = mild, 3 = moderate, 4 = marked.
[e]Significantly different from vehicle control as calculated by authors ($p \leq 0.05$).
[f]Significantly different from vehicle control as calculated by authors ($p \leq 0.01$).

Source: NTP (2001).

Cancer results

In mice exposed to AN, treatment-related carcinogenic effects (Table 4-34) were observed in the forestomach, Harderian gland, and, less consistently, lung and ovary of treated female mice (NTP, 2001). Histopathologic examination revealed significantly increased incidences of forestomach squamous cell papillomas and in overall incidence of papillomas or carcinomas in male and female mice treated with 10 or 20 mg/kg-day. Forestomach squamous cell carcinomas alone were significantly increased in males at ≥10 mg/kg-day and in females at 20 mg/kg-day. Incidences of Harderian gland adenoma and adenomas or carcinomaswere significantly elevated in males at ≥2.5 mg/kg-day and in females at ≥10 mg/kg-day. The overall incidence of alveolar/bronchiolar adenomas or carcinomas was significantly elevated in females treated at 10 mg/kg-day but not at the highest dose. Increase in benign or malignant granulosa cell tumor of the ovary was observed in females treated with 10 mg/kg-day AN. However, the increase was not statistically significant. Significant positive trends ($p \leq 0.001$) were observed in both male and female mice for the incidences of forestomach squamous cell papilloma or carcinoma and Harderian gland adenoma or carcinoma; there was also a significant positive trend ($p = 0.029$) for alveolar/bronchiolar adenoma or carcinoma in treated females. An inverse relationship between tumor latency and dose was observed for forestomach squamous cell papillomas or carcinomas in females and for Harderian gland adenomas or carcinomas in males.

Table 4-34. Incidences of selected neoplastic lesions in B6C3F$_1$ mice exposed by gavage to AN for 2 years

Adjusted Dose (mg/kg-d)[a]	Control[b]	1.8	7.1	14.3
Males[c]				
Number of mice examined	50	50	50	50
Forestomach				
Squamous cell papilloma (includes multiple)	3	4	19[d]	25[d]
Squamous cell carcinoma	0	0	8[d]	9[d]
Squamous cell papilloma or carcinoma	3	4	26[e]	32[e]
Harderian gland				
Adenoma (includes bilateral)	5	16[d]	24[d]	27[d]
Carcinoma	1	1	4	3
Adenoma or carcinoma	6	16[f]	27[e]	30[e]
Females[c]				
Number of mice examined	50	50	50	50
Forestomach				
Squamous cell papilloma (includes multiple)	3	6	24[d]	19[d]
Squamous cell carcinoma	0	1	1	11[d]
Squamous cell papilloma or carcinoma	3	7	25[e]	29[e]
Harderian gland				
Adenoma (includes bilateral)	10	10	25[d]	23[d]
Carcinoma	1	0	3	2
Adenoma or carcinoma	11	10	26[e]	25[e]
Lung				
Alveolar/bronchiolar adenoma or carcinoma	6	6	14[g]	9
Ovary				
Benign or malignant granulosa cell tumor	0	0	4	1

[a]Doses administered 5 d/wk.
[b]Vehicle control.
[c]Number of mice with tumor.
[d]Significantly different from vehicle control as calculated by authors ($p \leq 0.01$).
[e]Significantly different from vehicle control as calculated by authors ($p \leq 0.001$).
[f]Significantly different from vehicle control as calculated by authors ($p = 0.014$).
[g]Significantly different from vehicle control as calculated by authors ($p = 0.039$).

Source: NTP (2001).

4.2.1.2.6. ***Gallagher et al. (1988).*** In a cancer bioassay, groups of 20 male Sprague-Dawley-derived CD rats were exposed to 0, 20, 100, or 500 ppm AN in drinking water for 2 years (Gallagher et al.,1988). As calculated from the reported AN concentration and average daily drinking water consumption data, the intakes of AN were 0, 1.5, 7.1, and 28 mg/kg-day. Rats were weighed weekly, and feed intake and water consumption were measured for 1 week each month. All rats, whether dying prematurely or sacrificed at termination, were subjected to a

complete gross necropsy. Tissues exhibiting gross lesions and a selection of organs (liver, stomach, adrenal, kidney, heart, brain, pituitary, and lung) were examined for histopathology.

Significantly reduced survival compared with controls was observed in the high-dose group after 1 year of exposure but not in the other treatment groups. The last high-dose rat died shortly before the scheduled termination. BWs were significantly reduced in high-dose rats after 8 months and in mid-dose rats after 16 months; compared with terminal BWs of the control group, reductions of >50% at 500 ppm and >20% at 100 ppm were estimated from the data graph. Exposure to AN had no effect on food consumption, but water consumption was reduced in a dose-related fashion (by 7.5, 11.3, and 30% in the low- to high-dose groups). A NOAEL of 1.5 mg/kg-day and a LOAEL of 7.1 mg/kg-day were identified for reduced BW in rats exposed to AN for 2 years. This study was limited as to its usefulness for noncancer risk assessment because few tissues were evaluated for histopathology and noncancer histopathology was not reported.

Gallagher et al. (1988) reported dose-related increases for the incidences of tumors of the forestomach and ear canal (Zymbal gland). Four of 20 high-dose rats (20%) had papillomas of the squamous epithelium of the forestomach, a tumor type not observed in the other groups. Squamous carcinomas of Zymbal gland were observed in 1/20 (5%) mid-dose rats and 9/20 (45%) high-dose rats but not in low-dose rats or controls. This study provided evidence of the carcinogenicity of AN to the forestomach and Zymbal gland in male rats. Limitations of the study in evaluation of AN carcinogenicity included small group sizes, lack of testing in females, and only limited tissues were evaluated in gross and histopathological examination.

4.2.1.2.7. ***Bigner et al. (1986).*** In an interim (18-month) report of a 2-year drinking water study (Bigner et al., 1986), F344 rats were exposed to AN at targeted concentrations of 0 ppm (51 males and 49 females), 100 ppm (50 rats/sex), and 500 ppm (two subgroups, with a total of 197 males and 203 females). One group of the 500 ppm rats, 147 males and 153 females, was allocated for studies of morphology, tumor biology, and karyotyping, leaving the remaining rats for studies of comparative survival and tumor incidences. By using reference average BWs for F344 rats in a chronic-duration study and an allometric equation deriving drinking water consumption from BW (U.S. EPA, 1988), the average daily doses of AN were calculated as 0, 12.9, and 64.5 mg/kg-day for males and 0, 14.8, and 74.2 mg/kg-day for females. Rats were observed twice daily for neurological signs and death and were weighed weekly. Complete gross necropsies were conducted on all rats. Brains were evaluated for tumors using light and electron microscopy. The only endpoints related to noncancer effects reported for this study were mortality, BW, and clinical signs. Incomplete quantitative data were provided for mortality, which was reported to show dose-response effect in both sexes, occurring earlier in 100 and 500 ppm females than in males. A total of 215 high-dose rats died between month 6 and 18, whereas only “a few” male and female controls were reported to have died by month 18. No

quantitative results were provided for the magnitude or statistical significance of BW reductions that affected high-dose male rats by the third week and high-dose females "slightly" later. BW reductions in the mid-dose group occurred in males after 2 months and females sometime during the second year. The incidences of neurological clinical signs (paralysis, head tilt, circling, and seizures) were dose related, affecting a total of 45/400 rats treated at 500 ppm, 4/100 rats at 100 ppm, and 0/100 controls exposed for 12–18 months. The reported data were insufficient to accurately identify a NOAEL or LOAEL for noncancer effects in this study. A final report of this study was not located.

In 215 rats in the 500 ppm group that died between months 6 and 18, the types of tumors frequently found included s.c. papillomas, papillomas of the forestomach, and tumors in Zymbal gland, but no incidence data were provided for these lesions (Bigner et al., 1986). A statistically significant increase in tumors of the brain bearing similarity to astrocytomas was observed in rats exposed to 500 ppm AN, with 49 primary brain tumors observed among the 215 rats dying between months 6 and 18; incidences in other treatment groups were not reported. The tumors were observed mostly in the cerebral cortex (about 75%) and also in the brain stem and cerebellum. When the brain tumors were classified according to size, 10/49 of these tumors were larger than 5 mm, 28/49 were between 1 and 5 mm in diameter, and 11/49 were detected only microscopically. Although this study provided support for the carcinogenic effect of AN at multiple sites in rats, the lack of numerical results rendered it inadequate for the purpose of quantifying cancer risk.

4.2.1.2.8. ***Maltoni et al. (1988, 1977).*** Maltoni et al. (1988, 1977) reported a cancer bioassay (designated BT203) in which groups of Sprague-Dawley rats (40/sex) received 5 mg/kg AN by gavage in olive oil, 3 days/week for 52 weeks; a control group of 75/sex received olive oil alone on the same schedule. After the exposure period, rats were maintained without further treatment for the rest of their natural lives (the study ending on week 131). Rats were examined 3 times daily for their general health status and were subjected to a clinical examination for gross changes every 2 weeks. Rats were weighed every 2 weeks during the first year and monthly thereafter. All rats were examined by gross necropsy. All tissues with gross lesions and a limited set of 12 tissues/organs from each rat were examined microscopically. No statistically significant increases in tumors were observed in treated rats in this study. However, slight decrease in tumor latency or increase incidence were observed for some types of tumors identified in other studies on AN. For example, a carcinoma of Zymbal gland was noted in 1/40 exposed males (latency 84 weeks) and 1/75 control females (latency 90 weeks). Papillomas and acanthomas of the forestomach were observed in 1/40 exposed males (latency 92 weeks), 4/40 exposed females (average latency 97.5 weeks), and 1/ 75 control females (latency 54 weeks). Maltoni et al. (1977) recognized the increase in forestomach tumors as treatment related. Gliomas (a category that includes astrocytomas) appeared in 1/40 treated females

(latency of 33 weeks), 2/75 control females (average latency 104 weeks), and 1/74 control males (latency 98 weeks). The major limitation of this study as a cancer bioassay was the relatively short exposure period and the small number of animals in each group. The dose was also low for a single exposure group study.

4.2.1.2.9. ***Friedman and Beliles (2002); Litton Bionetics (1992).*** In a three-generation reproductive toxicity study in Sprague-Dawley rats, Friedman and Beliles (2002) and Litton Bionetics (1992) provided further evidence of the possible carcinogenicity of AN (methods and reproductive/developmental findings of this study are presented in Section 4.3.2). In this study, 15 males and 30 females per dose level (F0 parents) were exposed to 0, 100, and 500 ppm AN in drinking water for 100 days prior to mating for 6 days. As calculated by the study authors, the concentrations were equivalent to doses of 0, 11, and 37 mg/kg-day for males and 0, 20, and 40 mg/kg-day for females. A subset of F0, F1, and F2 females underwent two cycles each of breeding, then were held for a further 20 weeks after weaning of the second litter prior to termination.

Considering each generation separately, F1b female breeders in the 500 ppm group showed statistically significant increased incidences of brain and Zymbal gland tumors, while increased incidences of tumors in F0 or F2b female breeders in the 100 or 500 ppm groups compared with controls were consistent with the F1b responses, but not statistically significant (Table 4-35). These were relatively small groups, however, with low power to detect responses as high as 10% statistically significant. Across all of the generations, there was a statistically significant increasing trend in both tumor types, supporting the conclusion that exposure to AN for up to 51 weeks at 100 or 500 ppm in drinking water was associated with increased tumor incidence in female Sprague-Dawley rats.

Table 4-35. Incidence of tumors in female Sprague-Dawley rats exposed to AN in drinking water for up to 46 weeks

Generation	Tumor incidence in rats					
	Brain astrocytomas			Zymbal gland		
	Exposure concentration (ppm)					
	0	100	500	0	100	500
	Dose (mg/kg-d)					
	0	20	40	0	20	40
F0	0/19	1/20	2/24	0/19	0/20	2/24
F1b	0/20	1/19	4/17[a]	0/20	2/19	3/17[a]
F2b	0/20	1/20	1/20	0/20	0/20	3/20
Total	0/59[b]	3/59	7/61[a]	0/59[b]	2/59	8/61[a]

[a]Significantly different from controls ($p < 0.05$), as calculated by the authors.
[b]Statistically significant by Cochran-Armitage trend test, $p < 0.01$.

Sources: Friedman and Beliles (2002); Litton Bionetics (1992).

Table 4-36 summarizes the noncancerous effects observed in chronic oral studies of AN in rats and mice. Table 4-37 summarizes the cancerous effects observed in chronic oral studies of AN in rats and mice.

Table 4-36. Summary of chronic oral toxicity studies of AN: noncancer effects in rats and mice

Strain number/sex	Exposure route/ duration[a]	Doses	Effects	NOAEL/ LOAEL[a]	References	Comments
Rats						
F344 100/sex/group Unexposed controls = 200/sex	Drinking water/ 2 yrs	M: 0, 0.1, 0.3, 0.8, 2.5, 8.4 mg/kg-d; F: 0, 0.1, 0.4, 1.3, 3.7, 10.9 mg/kg-d	Squamous cell hyperplasia/ hyperkeratosis of the forestomach; decreased survival in high-dose groups, increase in epidermal inclusion cysts of the skin	NOAEL = 0.1 mg/kg-d; LOAEL = 0.3 mg/kg-d (M) 0.4 mg/kg-d (F)	Johannsen and Levinskas (2002b); Biodynamics (1980c)	10 rats/sex/group were taken from exposed and control groups for interim sacrifice at 6, 12, and 18 mos

Table 4-36. Summary of chronic oral toxicity studies of AN: noncancer effects in rats and mice

Strain number/sex	Exposure route/ duration[a]	Doses	Effects	NOAEL/ LOAEL[a]	References	Comments
Sprague-Dawley 100/sex/group	Drinking water: 22 months (M); 19 months (F)	M: 0, 0.09, 8.0 mg/kg-d; F: 0, 0.15, 10.7 mg/kg-d	Squamous cell hyperplasia of the forestomach, decreased survival in high-dose groups, reduction in absolute/relative pituitary weight (F)	LOAEL = 0.09 mg/kg-d (M)	Johannsen and Levinskas (2002a); Biodynamics (1980a)	10 rats/sex/group were taken from exposed and control groups for interim sacrifice at 6, 12, and 18 mos
Sprague-Dawley 100/sex/group	Gavage/ 20 months	0, 0.1, 10 mg/kg-d	Squamous cell hyperplasia of the forestomach, small reductions in hematocrit, Hb, and RBC count in high-dose males, increase in absolute/relative liver weight in high-dose groups	NOAEL = 0.1 mg/kg-d; LOAEL = 10 mg/kg-d	Johannsen and Levinskas (2002a); Biodynamics (1980b)	10 rats/sex/group were taken from exposed and control groups for interim sacrifice at 6, 12, and 18 mos
Sprague-Dawley 48/sex/group; Controls: 80/sex	Drinking water/ 2 yrs	M: 0, 3.4, 8.5, 21.3 mg/kg-d; F: 0, 4.4, 10.8, 25.0 mg/kg-d	Hyperplasia/ hyperkeratosis of the forestomach, reduced survival and BW, minimal progressive nephropathy, gliosis of the brain	LOAEL = 4.4 mg/kg-d (F)	Quast (2002); Quast et al. (1980a)	
F344 50/sex low-dose; 197 males and 203 females high-dose. Controls: 51-males and 49-females:	Drinking water/ lifetime	M: 0, 12.9, 64.5 mg/kg-d; F: 0, 14.8, 74.2 mg/kg-d	Neurological signs	No data	Bigner et al. (1986)	Doses calculated using default assumptions (U.S. EPA, 1988); noncancer effects not evaluated in the study

Table 4-36. Summary of chronic oral toxicity studies of AN: noncancer effects in rats and mice

Strain number/sex	Exposure route/ duration[a]	Doses	Effects	NOAEL/ LOAEL[a]	References	Comments
Mice						
$B6C3F_1$ 50/sex/group	Gavage/ 2 yrs	0, 2.5, 10, 20 mg/kg-d, 5 d/wk; continuous exposure-adjusted doses: 0, 1.8, 7.14, 14.3 mg/kg-d	Reduced survival in high dose group; hyperkeratosis/ hyperplasia of the forestomach; ovarian cysts and atrophy (F)	LOAEL: 1.8 mg/kg-d (F); NOAEL = 1.8 mg/kg-d; (M) LOAEL = 7.1 mg/kg-d (M)	NTP (2001)	

[a]M = male; F = female.

Table 4-37. Summary of chronic oral toxicity studies of AN: cancer effects in rats and mice

Strain number/sex	Exposure route/ Duration	Doses[a]	Effects[a]	References	Comments
Rats					
F344 100/sex/group Unexposed controls = 200/sex	Drinking water/ 2 yrs	Males: 0, 0.1, 0.3, 0.8, 2.5, and 8.4 mg/kg-d; females: 0, 0.1, 0.4, 1.3, 3.7, and 10.9 mg/kg-d	Males: increase in brain astrocytomas and Zymbal gland tumors, increase in forestomach tumors; females: increase in brain astrocytomas, Zymbal gland tumors, and forestomach tumors	Johannsen and Levinskas (2002b); Biodynamics (1980c)	10 rats/sex/group were taken from exposed and control groups for interim sacrifice at 6, 12, and 18 months
Sprague-Dawley 100/sex/group	Drinking water/ 22 months (M); 19 months (F)	Males: 0, 0.09, and 8.0 mg/kg-d; females: 0, 0.15, and 10.7 mg/kg-d	Significant increases in incidences of tumors of the CNS, Zymbal gland, and forestomach	Johannsen and Levinskas (2002a); Biodynamics (1980a)	10 rats/sex/group were taken from exposed and control groups for interim sacrifice at 6, 12, and 18 months
Sprague-Dawley 100/sex/group	Gavage/ 20 months	0, 0.1, and 10 mg/kg-d	Increase in brain astrocytomas, and tumors of Zymbal gland, forestomach, and intestine. Carcinomas of the mammary gland in females	Johannsen and Levinskas (2002a); Biodynamics (1980b)	10 rats/sex/group were taken from exposed and control groups for interim sacrifice at 6, 12, and 18 months
Sprague-Dawley 48/sex/group; Controls: 80/sex	Drinking water/ 2 yrs	Males: 0, 3.4, 8.5, and 21.3 mg/kg-d; females: 0, 4.4, 10.8, and 25.0 mg/kg-d	Increases in CNS tumors, squamous cell papillomas or carcinomas of the forestomach, carcinomas of Zymbal gland, as well as benign and malignant tumors of the mammary gland	Quast (2002); Quast et al. (1980a)	

Table 4-37. Summary of chronic oral toxicity studies of AN: cancer effects in rats and mice

Strain number/sex	Exposure route/ Duration	Doses[a]	Effects[a]	References	Comments
F344 50/sex low-dose; 197 males and 203 females high-dose. Controls: 51 males and 49 females	Drinking water/ lifetime	M: 0, 12.9, and 64.5 mg/kg-d; females: 0, 14.8, and 74.2 mg/kg-d	Tumors found included brain astrocytomas, Zymbal gland tumors, and papillomas of the forestomach	Bigner et al. (1986)	Doses calculated using default assumptions (U.S. EPA, 1988); no tumor incidence data were provided
Sprague-Dawley 40/sex Control: 75/sex	Gavage/ 3 ds/week for 52 weeks; rats maintained without treatment until natural death (study ended week 131)	0, 5 mg/kg in olive oil	Treatment-related increase in forestomach tumors	Maltoni et al. (1977)	Study limitations: single dose, short exposure period, and small number of animals in each group
Sprague-Dawley 20 M/group	Drinking water/2 yrs	0, 1.5, 7.1, and 28 mg/kg-d	Increase in tumors of the forestomach and Zymbal gland	Gallagher et al. (1988)	Study limitations: small group size, lack of testing in females, and only limited tissues were examined for histopathology.
Sprague-Dawley 15 M/group, 30 F/group	Drinking water/ 46 weeks (three-generation reproduction/ developmental study)	0, 11, 37 mg/kg-d (M); 0, 20, and 40 mg/kg-d (F)	Increase in incidences of brain and Zymbal gland tumors	Friedman and Beliles (2002); Litton Bionetics (1992)	Study suggested increased susceptibility to the carcinogenicity of AN from early-life exposure (see Section 4.8.1).
Mice					
B6C3F$_1$ 50/sex/group	Gavage/ 2 yrs	0, 2.5, 10, and 20 mg/kg-d, 5 d/wk, continuous exposure-adjusted doses: 0, 1.8, 7.14, and 14.3 mg/kg-d	Increase in tumors of the forestomach and of Harderian gland in males and females	NTP (2001)	Overall incidence of alveolar/bronchiolar adenomas or carcinomas was significantly elevated in females at 10 mg/kg-d, but not at 20 mg/kg-d.

[a]M = male; F = female.

4.2.2. Inhalation Exposure

4.2.2.1. *SubchronicSubchronic Studies*

The only subsubchronic study of inhalation effects of AN in animals was a comparative study of the neurotoxicity of nitriles (Gagnaire et al., 1998). Groups of 12 male Sprague-Dawley rats were exposed (whole body) to AN vapor at concentrations of 25, 50, or 100 ppm, 6 hours/day, 5 days/week for 24 weeks. A control group of 10 male rats was exposed to filtered air. BWs were measured weekly. Following 4, 8, 12, 16, 20, and 24 weeks of exposure and an 8-week recovery period (week 32), rats were evaluated for the same electrophysiological parameters that were tested in parallel experiments on orally exposed rats (see Section 4.2.1.1). As in the companion study, electrophysiological testing was performed at least 16 hours after daily exposure (waiting period was 48 hours for weekends). Electrical stimulation of the tail nerve was used to assess MCVs, SCVs, ASAPs, and AMAPs. No mortality was observed during the treatment period, but, during the first and second week of the recovery period, 2/12 rats in the 100 ppm group died and one rat each in the 100 and 25 ppm groups was euthanized in week 31 because of tumors in the neck. BW gain in the 100 ppm group was significantly lower than in controls in weeks 4, 8, 16, and 21–24, such that the BW was 11% lower at the end of week 24.

Rats exposed to AN did not develop weakness of the hind limbs or disturbances in gait. After 1 or 2 weeks of exposure, rats exposed at ≥50 ppm exhibited clinical signs of gross toxicity (wet fur and excessive salivation but not hyperactivity). Excessive salivation was attributed by the study authors to a cholinomimetic effect of AN. Exposure to AN had no effect on neurophysiological parameters during the first 8 weeks and no effect on the AMAP at any time during the study. Statistically significant concentration-dependent SCV reductions of ~9% compared with controls were observed in the 100 ppm group from weeks 12–24 (Table 4-38). In week 12, an ~7% reduction was observed in the 50 ppm group, and in week 24 the SCV was reduced by 5% in the 25 ppm group (not biologically significant) and by >8% in the 50 and 100 ppm groups. The ASAP was significantly reduced by 14.5–20% in the 50 ppm group and by 29–30% in the 100 ppm group from weeks 16–24. After recovery in week 32, a 21% reduction in ASAP persisted in the 100 ppm group. Sporadic reductions in MCV were observed in 100 ppm rats beginning in week 16 (11% reduction) but were not concentration dependent in week 24 or after recovery in week 32. A LOAEL of 25 ppm was identified for reductions in SCV in rats exposed to AN by inhalation for 24 weeks. A NOAEL was not identified.

Table 4-38. Effect on SCV in male Sprague-Dawley rats exposed to AN via inhalation for 24 weeks

Exposure (ppm)	SCV (m/s)[a]					
	Exposure (weeks)					Recovery
	0	12	16	20	24	32
0	35.0 ± 0.5	49.7 ± 0.8	49.9 ± 1.0	50.3 ± 0.5	53.3 ± 1.0	53.4 ± 0.6
25	35.2 ± 0.4	48.2 ± 0.7	47.8 ± 1.0	50.2 ± 0.7	50.5 ± 0.8[b]	51.8 ± 0.8
50	35.3 ± 0.6	46.3 ± 0.8[c]	48.0 ± 1.1	50.5 ± 0.6	49.1 ± 0.5[d]	51.3 ± 1.0
100	35.8 ± 0.5	45.3 ± 1.0[c]	46.2 ± 0.7[b]	48.1 ± 0.7[b]	48.4 ± 1.0[d]	50.4 ± 0.8

[a]Values are means ± SDs (n = 12 for treated, n = 10 for controls).
[b]Statistically significant compared with controls ($p < 0.05$) as calculated by the study authors.
[c]Statistically significant compared with controls ($p < 0.01$) as calculated by the study authors.
[d]Statistically significant compared with controls ($p < 0.001$) as calculated by the study authors.

Source: Gagnaire et al. (1998).

4.2.2.2. *Chronic Studies*

Two chronic inhalation bioassays in rodents were available: Dow Chemical (1992a)/ Quast et al. (1980b) and Maltoni et al. (1988, 1977).

4.2.2.2.1. *Dow Chemical (1992a) and Quast et al. (1980b).* Dow Chemical (1992a) and Quast et al. (1980b) evaluated the effects of AN in Sprague-Dawley rats (100/sex/group) exposed by inhalation at concentrations of 0, 20, or 80 ppm (0, 43.4, or 173.6 mg/m^3) 6 hours/day, 5 days/week for 2 years. Additional groups of 7 and 13 rats/sex/group were exposed and sacrificed at 6 and 12 months, respectively. BWs were determined 10 times during the first 3 months and monthly thereafter. Rats were observed daily for clinical signs and mortality, and beginning after 6 months, were examined for palpable masses and dental condition. Moribund animals or those with ulcerating tumors were sacrificed and subjected to gross necropsy. Hematology and urinalysis examinations were conducted on 10 rats/sex/group on days 174/175, 365/366, 616/617, and 727/727 for males/females, respectively. The hematology determinations of male rats was also conducted on day 183 to verify observations made on day 174. Clinical chemistry analyses were conducted on 10 rats/sex/group on days 176, 372, and 735. Water consumption was determined for representative male and female rats in each group for the first 8 months. At terminal sacrifice, all rats received an ophthalmologic examination and necropsy during which organ weights were recorded for brain, heart, liver, kidneys, and testes. Complete histologic examinations were carried out on all rats in the control and 80 ppm groups at terminal sacrifice. More than 80% of rats in the 20 ppm group were examined for gross lesions, and 23 selected organs and all tissues with grossly recognized tumors were collected for histopathology examination. Because there were signs of upper respiratory tract irritation in the nasal turbinate, about 10 rats/sex/group from the terminal sacrifice were evaluated by light

microscopy. In addition, because of brain lesions observed during drinking water studies, nine sections from various regions of the CNS of all rats were examined microscopically.

Noncancer results

Inhalation exposure to AN resulted in significant concentration-related noncancer effects compared with controls (Quast et al., 1980b). Statistically significant ($p < 0.05$) decreases in survival with respect to controls were observed in males after 6 months of exposure at 80 ppm and in females after 10 months of exposure at 80 ppm or 22 months at 20 ppm. The numbers of rats surviving at termination (out of 100/sex) were 18, 14, and 4 males and 22, 9, and 1 females in the control, 20 ppm, and 80 ppm groups, respectively. BWs were decreased by about 10–15% in male and female rats after 9 months of exposure to 80 ppm AN. A significant decrease of less than 10% was also observed in 20 ppm female rats. By the end of the study, BWs in 20 and 80 ppm females were not significantly different from those in controls.

Hb and RBC counts were significantly lower (by ~9%) in rats exposed to 80 ppm for 4–8 months but not later. However, the study authors considered these changes to be a secondary effect of reduced growth, tumor formation, and hemorrhage, resulting from exposure and not due to bone marrow toxicity. Statistically significant increases in water consumption were observed in both exposed groups of male and female rats during the first 6 months of the study and were consistent with slightly decreased urine specific gravity measured in 80 ppm groups during that period. No significant effects on urinalysis parameters were observed after 6 months. Exposure to AN had no consistent significant effect on clinical chemistry parameters or results of ophthalmoscopic examinations. A significant elevation (about 26%) in blood urea nitrogen (BUN) was observed in the 20 and 80 ppm female rats on day 176. SGPT was also elevated by 57% in the 80 ppm females at that time. However, no significant findings of these parameters were found upon subsequent evaluation at a later time interval. Hence, Quast et al. (1980b) considered these changes as secondary responses and not indications of direct renal or hepatotoxicity from AN exposure. Significant increases in relative weights of brain, heart, and testes of male rats exposed at 80 ppm were considered by the study authors to be a consequence of the reduction in BW.

Gross pathological examinations found statistically significantly findings in the nasal turbinates, lungs, teeth (malocclusion), and liver of the 80 ppm rats. Gross observation of male rats indicated significant increase in minimal chronic nephropathy in the 80 ppm group (40/100 vs. 24/100). Significant increase in pneumonia, atelectasis, or edema was found in the 20 and 80 ppm males (14/100, 27/100, and 30/100 for 0, 20, and 80 ppm groups, respectively). Gross observations of nontumorous changes included enlarged liver in female rats, with incidence of 2/100, 9/100, and 7/100 in 0, 20, and 80 ppm groups, respectively. (The increased incidence in the 20 ppm group was statistically significant.)

Statistically significant increases in the incidence of histopathologic lesions of the nasal turbinates were observed in all rats exposed at 80 ppm and most rats in the 20 ppm group. These effects were considered by the study authors to be the result of irritant effects of AN (Table 4-39). These lesions appeared in rats sacrificed after at least 13 months (usually 19 months) of exposure. These inflammatory and degenerative changes included hyperplasia, flattening, focal erosion, and squamous metaplasia of the respiratory epithelium and hyperplasia of mucus secreting cells. Flattening of the respiratory epithelium in females and hyperplasia of mucus-secreting cells in males were both significantly increased at the 20 ppm exposure level.

Table 4-39. Incidence of histopathological lesions of the nasal turbinates in Sprague-Dawley rats exposed to AN via inhalation for 2 years

Response	Concentration (ppm)		
	0	20	80
	Incidence		
Males			
Suppurative rhinitis	0/11	1/12	5/10[a]
Hyperplasia of respiratory epithelium	0/11	4/12	10/10[a]
Focal erosion of mucous lining	0/11	0/12	4/10[a]
Squamous metaplasia of the respiratory epithelium	0/11	1/12	7/10[a]
Hyperplasia of mucus-secreting cells	0/11	7/12[a]	8/10[a]
Focal inflammation	0/11	1/12	1/10
Flattening of the respiratory epithelium	0/11	2/12	3/10
Females			
Suppurative rhinitis	1/11	0/10	2/10
Hyperplasia of respiratory epithelium	0/11	2/10	5/10[a]
Focal erosion of mucous lining	0/11	1/10	1/10
Squamous metaplasia of the respiratory epithelium	0/11	2/10	5/10[a]
Hyperplasia of mucus-secreting cells	0/11	2/10	8/10[a]
Focal inflammation	2/11	6/10	7/10[a]
Flattening of the respiratory epithelium	1/11	7/10[a]	8/10[a]

[a]Statistically significant ($p < 0.05$), as calculated by the study authors.

Source: Quast et al. (1980b).

Increase in acute suppurative pneumonia was observed in the lungs of the 80 ppm male rats during the 7–12-month time interval. A nonsignificant increase was also observed in the 20 ppm group.

Other histopathological observations included an increase in the incidence of gliosis and perivascular cuffing in the brain of high-dose rats (either sex) and, in males only, minimal chronic focal progressive nephrosis and formation of keratinized cysts in the thyroid gland (Table 4-40). Incidences of focal necrosis of the liver were increased in 20 and 80 ppm female

rats. The incidence of AN-related hyperplasia and hyperkeratosis of the nonglandular portion of the stomach did not achieve statistical significance in either sex but was statistically significant ($p < 0.05$) by Fisher's exact test when the data were combined. There were concentration-related increases in the incidences of several lesions that were secondary to other effects of AN exposure (numerical data not provided here). These included hepatocellular atrophy without fatty changes and atrophy of mediastinal fat in 80 ppm male rats, attributed by the study authors to the decreased feed intake of the rats at the end of the study, and extramedullary hematopoiesis of the spleen in females, a consequence of the reductions in RBC and Hb counts. An increase in lymphoid hyperplasia in males at 80 ppm was interpreted by the study authors to be secondary to tumors of the ear canal and inflammatory changes in the nasal turbinates. A NOAEL was not identified in this study. A LOAEL of 20 ppm was identified for increased lesions of the nasal turbinates (hyperplasia of mucus-secreting cells in males and flattening of the respiratory epithelium in females) and focal necrosis in liver of female rats exposed to AN vapor for 2 years.

Table 4-40. Incidence of dose-related noncancerous histopathological lesions in Sprague-Dawley rats exposed to AN via inhalation for 2 years

Response	Concentration (ppm)		
	0	20	80
	Incidence		
Males			
Focal nephrosis (progressive)	22/100	24/100	48/100[a]
Minimal chronic nephropathy	24/100	21/100	40/100[a]
Thyroid cyst	4/95	9/97	13/96[a]
Gliosis and perivascular cuffing (brain)	1/100	2/99	7/99[a]
Acute suppurative pneumonia	0/100	4/100	10/100[a]
Pulmonary changes	15/100	26/100[a]	20/100
Hyperplasia of the nonglandular epithelium (stomach)	8/98	7/100	16/99
Females			
Gliosis and perivascular cuffing (brain)	0/100	2/100	8/100[a]
Focal necrosis in liver	3/100	16/100[a]	10/100[a]
Vasculization of spinal myelin (minimal)	42/100	67/100[a]	47/100
Hyperplasia of the nonglandular epithelium (stomach)	2/99	3/99	7/97

[a]Statistical significance ($p < 0.05$), as calculated by the study authors.

Source: Quast et al. (1980b).

Cancer results

In rats chronically exposed to AN vapor, there were significant increases in tumors at multiple sites, several of which also had been affected in oral exposure bioassays (Quast et al., 1980b). In males and females exposed to 80 ppm AN, there were increased incidences of

astrocytomas of the brain as well as glial cell proliferation that was considered an earlier stage in the progression to astrocytomas. The incidence data in Table 4-41 combine the incidences of astrocytomas and glial cell proliferation. The incidence of CNS tumors was also significantly increased in females exposed to 20 ppm AN and insiginificantly increased in males exposed to 20 ppm AN. Carcinomas of Zymbal gland were significantly elevated in the 80 ppm rats of both sexes. Other tumor increases observed in the 80 ppm groups were squamous cell papillomas or carcinomas in the tongue and carcinomas of the intestinal tract of males and adenocarcinomas of the mammary gland in females. An increase was observed in forestomach tumors in 80 ppm male rats and nasal turbinate tumors in 80 ppm female rats. Both types of tumors were considered by the study authors to be treatment related, although the increase was not statistically significant. Table 4-41 presents incidences of AN-induced target organ-specific tumor formation. All tumors were found in exposed rats that died or were sacrificed after 12 months of exposure, with the exception of one male rat with a CNS tumor and three female rats with mammary gland adenocarcinomas that died between 7 and 12 months.

Table 4-41. Cumulative incidence of tumors in Sprague-Dawley rats exposed to AN via inhalation for up to 2 years

Tissue	Males (ppm)			Females (ppm)		
	0	20	80	0	20	80
All brain/CNS[a]	0/96	4/93	22/82[b]	0/93	8/99[b]	20/89[b]
Zymbal gland	2/96	4/93	11/82[b]	0/93	1/98	11/89[b]
Intestinal tract	4/96	3/93	17/82[b]	Not increased		
Mammary gland (adenocarcinomas)	0/100	0/100	1/100	9/93	8/98	20/99[b]
Mammary gland (total, benign and malignant)	4/100	5/100	7/100	88/100	95/100	85/100
Forestomach (squamous cell papilloma)	1/98	1/100	4/99	0/99	0/99	1/97
Tongue	1/95	0/14	7/82[b]	0/96	0/9	1/91
Nasal turbinate (carcinoma in respiratory epithelial region)	Not increased			0/11	0/98	2/10

[a]Incidence data include all brain/CNS tumors (astrocytomas and glial cell proliferation). Male tumor incidence data are from Tables 22, 25, and 26 of the Quast et al. (1980b) report; female tumor incidence data are from Tables 31, 34, and 35 in the same report. For all incidence data, the denominators excluded rats dying earlier than 12 mos in the study. These data were ascertained from Tables 22, 25, 31, 34, and 35 in the original study report by Quast et al. (1980b).
[b]Significantly different from controls ($p < 0.05$) as calculated by the study authors.

Sources: Dow Chemical (1992a); Quast et al. (1980b).

An apparent decrease in the incidence of tumors of the pituitary, adrenals, thyroid, and pancreas of male and female treated rats, and testes of males, was observed when compared with controls.

4.2.2.2.2. ***Maltoni et al. (1988, 1977).*** The following studies by Maltoni et al. (1988, 1977) were cancer bioassays that did not investigate nonneoplastic effects in rats exposed to AN vapor. These study authors reported a number of experiments in which Sprague-Dawley rats were exposed to AN by inhalation. In the first (designated BT201 by the authors), 30 rats/sex/group were exposed to 0, 5, 10, 20, and 40 ppm 4 hours/day, 5 days/week for 52 weeks; the animals then were allowed to complete their natural life spans, with the final deaths occurring in week 136 (Maltoni et al., 1977). Rats were examined 3 times weekly for general health status and subjected to a clinical examination for gross changes every 2 weeks. Rats were weighed every 2 weeks during the exposure period and monthly thereafter. All rats were subjected to gross necropsy. Histopathologic examinations were conducted on all gross lesions and a selection of about 12 organs and tissues, including the Zymbal glands, interscapular brown fat, salivary glands, tongue, lungs, liver, kidneys, spleen, stomach, intestine, bladder, and brain.

Exposure to AN had no significant effect on survival or BWs in male or female rats. A moderate increase in gliomas, forestomach tumors, Zymbal gland carcinomas, and mammary tumors was found in the treated group. However, increases in the incidences of these tumors in exposed rats were not statistically significant and could be due to the small number of animals in each dose group. For example, gliomas were found in 20 and 40 ppm males at 1/30 and 2/30, respectively, and not in controls and other exposure groups. The average latency of the gliomas was shorter at the higher concentration (63.5 vs. 84 weeks). Forestomach papillomas and acanthomas were found in males at 0/30, 1/30, 2/30, and 3/30 for 0, 5, 10, and 40 ppm, respectively. In females, forestomach tumor incidences were 0/30, 1/30, 2/30, and 1/30 for the 0, 5, 10, and 20 ppm groups. The average latency of forestomach tumors ranged from 103 to 124 weeks. Zymbal gland carcinomas were also found at 1/30 in the 10 ppm group for male and female and 1/30 for the female 20 ppm group. No Zymbal gland carcinomas were found in the control and other dose groups.

Moreover, a possible treatment-related effect of AN in the mammary gland of females was observed, as indicated by the following incidences of benign or malignant tumors in relation to exposure level: 5/30 (controls), 10/30 (5 ppm), 7/30 (10 ppm), 10/30 (20 ppm), and 7/30 (40 ppm) (Maltoni et al., 1977). Slight discrepancies in the incidence of tumors of the mammary gland were reported for controls and highest-exposed females in a subsequent report of this study (Maltoni et al., 1988). In the later study, the incidence of tumors in control females was listed as 20%, an incidence of 6/30, whereas that of highest-concentration females was listed as 26.7%, an incidence of 8/30. In the later report, taking both sexes together, the incidences of encephalic gliomas were 3/60 and 2/60 in the 40 and 20 ppm groups, respectively, and none in the control and lower-dose groups. Although this cancer study was consistent with other studies in the identification of tumor sites associated with exposure to AN, it was limited in that the exposure concentrations were too low, the number of animals per group was too small, and the exposure duration was too short to result in statistically significant increases in specific tumor

types. However, this study demonstrated that rats with less-than-lifetime exposure and allowed to recover to their natural life span developed the same tumor types as rats with lifetime exposure to AN.

The later report by Maltoni et al. (1988) described two additional lifetime exposure experiments in which Sprague-Dawley rats were exposed to AN by inhalation beginning during the gestation period. In the first experiment (designated BT4003), 54 adult pregnant females, beginning on gestation day 12, were exposed to 60 ppm AN for 4 hours/day, 5 days/week for 7 weeks and then 7 hours/day, 5 days/week for 97 weeks. A group of 60 unexposed adult females served as controls. Gestation was permitted to proceed normally and the offspring were exposed on the same schedule as the dams. The exposed offspring included 67 males and 54 females, whereas the controls were 158 males and 149 females.

Overall, there was a statistically significant treatment-related increase in the percentage of dams with malignant tumors at all sites (37 vs. 15%). Increased incidences in exposed dams compared with controls were observed for several sites, but none of these was statistically significant: Zymbal gland carcinomas (5.5 vs. 1.7%), mammary gland carcinomas (5.5 vs. 3.3%), benign or malignant mammary gland tumors (69 vs. 40%), extrahepatic angiosarcomas (1.8 vs. 0%), and encephalic gliomas (5.5 vs. 0%). No hepatomas were observed in exposed or unexposed dams. These site-specific results are summarized in Table 4-42.

Table 4-42. Comparison of carcinogenic effects of chronic exposure to AN at 60 ppm starting either in utero or in adulthood, in Sprague-Dawley rats

Stage during exposure	Exposure protocol	Sex[a]	Number of rats at start[b]	Percent with tumor				
				Brain tumors (encephalic gliomas)	Zymbal gland carcinomas	Hepatomas	Malignant mammary tumors	Extra-hepatic angio-sarcomas
Adult only	Chronic[c]	F	54	5.5	5.5	0.0	5.5	1.8
	Unexposed controls	F	60	0.0	1.7	0.0	3.3	0.0
Starting at GD 12	Chronic	M F	67 54	16.4 18.5	14.9[c] 1.8	7.5 1.8	0.0 16.7[d]	4.4 5.5[e]
	Subchronic[d]	M F	60 60	5.0 3.3	6.7 1.7	1.7 0.0	0.0 6.7	5.0 1.7
	Unexposed controls	M F	158 149	1.3 1.3	1.3 0.0	0.6 0.0	1.9 5.4	0.6 0.0

[a]F = female; M = male.
[b]Animals were allowed to live until spontaneous death.
[c]Chronic: 4 hrs/d, 5 d/wk for 7 wks (starting during gestation), followed by 7 hrs/d for 97 wks.
[d]Statistically significantly higher than correspondng control incidence, $p < 0.05$.
[e]Subchronic: 4 hrs/d, 5 d/wk for 7 wks (starting during gestation), followed by 7 hrs/d for 8 wks.

Source: Maltoni et al. (1988).

In contrast, chronically exposed male and female offspring showed statistically significant increases in the incidences of specific types of tumors: malignant tumors of the mammary gland in females (16.7 vs. 5.4%; $p < 0.05$), extrahepatic angiosarcomas in females (5.5 vs. 0%; $p < 0.05$), hepatomas in males (7.5 vs. 0.6%; $p < 0.05$), Zymbal gland carcinomas in males (14.9 vs. 1.3%; $p < 0.01$), and encephalic gliomas (16.4% in males and 18.5% in females vs. 1.3% for controls of both sexes; $p < 0.01$) (see Table 4-42). Higher responses in the exposed offspring at these sites relative to the dams suggests some early-life susceptibility to AN carcinogenity. These results are discussed further in Section 4.8.1.

The second exposure experiment (BT4006) involving gestational exposure of Sprague-Dawley rats started with the same exposure conditions as for experiment BT4003, except that exposure of the offspring (127 males and 114 females) ended after 15 weeks (Maltoni et al., 1988). Exposure in this group of offspring was for 4 hours/day, 5 days/week for 7 weeks starting on GD 12, followed by 7 hours/day, 5 days/week for 8 weeks. All animals were kept under observation until spontaneous death, at which time they were examined for the presence of tumors. The control group of offspring was the one used in experiment BT4003 (158 males and 149 females). There was a statistically significant increase in the total incidence of malignant tumors in exposed offspring compared with controls for both males (31.7 vs. 17.1%, $p < 0.05$) and females (35.0 vs. 17.4%, $p < 0.01$). Increases in the following tumors were observed when compared with controls: Zymbal gland tumors in males and females (4.2 vs. 0.7%); extrahepatic angiosarcomas in males (5.0 vs. 0.6%); encephalic gliomas in males and females (4.2 vs. 1.3%); and hepatomas in males (1.7 vs. 0.6%) (see Table 4-42). However, these increases were not statistically significant.

4.3. REPRODUCTIVE/DEVELOPMENTAL STUDIES—ORAL AND INHALATION

In contrast to the extensive information on cancer and noncancer effects of AN in experimental animals and exposed human populations, there are comparatively few data that address the reproductive and developmental toxicity and teratogenic action of AN.

4.3.1. Studies in Humans

There have been some preliminary translated reports of surveys of the reproductive history of women occupationally exposed to AN in chemical factories in China. While these studies pointed to a possible link between occupational exposure to AN and adverse effects on pregnancy, in some cases, there was insufficient information in the reports to assess the validity of these claims. However, there are studies with usable data. As described in Section 4.1.2.2, Dong and Pan (1995) provided data on exposure and reproductive outcomes in 150 male and 106 female workers employed at a chemical fiber plant. These subjects, routinely exposed to AN concentrations ranging from 0.53 to 15.5 mg/m^3 (0.24–7.1 ppm), were compared with 110 male and 121 female workers who had not been exposed to AN. The results of the study

were divided into two sections, one dealing with a comparison of the reproductive outcome for female employees, exposed vs. unexposed, and the second comparing the reproductive outcome of the wives of exposed male employees to that of the wives of unexposed male controls. In the former case, there were few differences in reproductive performance between exposed females and controls (see Table 4-21 for details), although the incidence of stillborn fetuses in the exposed group was significantly greater than in controls (5/112 vs. 0/124). However, it should be noted that there was a statistically significant age difference between the groups (29.36 ± 5.12 in exposed females vs. 20.68 ± 4.05 in female controls). The wives of exposed male workers at the plant had poorer reproductive outcomes than the wives of male controls, even though they were significantly younger than their counterparts. For example, there were differences in the incidence of live births as a proportion of the total number of pregnancies (159/168 vs. 113/113), spontaneous abortions (8/168 vs. 1/113), threatened abortions (5/168 vs. 1/113), stillborn fetuses (4/168 vs. 0/113), and sterility (9/150 vs. 2/110). These data suggested a potential AN-related impact on the sperms and reproductive performance of exposed males.

An elevated incidence of complications in pregnancy was reported also by Li (2000) in 379 female workers exposed to an average AN concentration of 7.5 ppm for ≥1 year. When compared with 511 unexposed controls, exposed subjects had a higher rate of overall complications (20.8 vs. 7.14%) and premature deliveries (11.62 vs. 4.72%). Exposed subjects were subdivided to create a category where both partners had been exposed to AN. Overall rates of complications, premature delivery, overdue delivery, and deficiency were greater than in cases where only the female partner was exposed.

In another Chinese study, Wu et al. (1995) reported statistically significant increases in the incidence of pernicious vomiting, anemia, preterm delivery, and birth defects in 477 females exposed to AN in the workplace compared with 527 controls.

The epidemiological report and follow-up by Czeizel et al. (2000, 1999) examined the environmental distribution of congenital abnormalities in 30 settlements within a 25 km radius of an AN factory, drawing on data from the Hungarian Congenital Abnormality Registry covering 46,326 infants born between 1980 and 1996. A number of time-space-specific clusters of abnormalities were identified among the subjects, the most striking of which was the incidence of pectus excavatum in the community of Tata between 1990 and 1992. This effect was associated with an OR of 78.5 and a 95% CI of 8.4–729.6. Other clusters of congenital abnormalities in the vicinity of the factory were undescended testis in the community of Nyergesujfalu between 1980 and 1983 (OR = 8.6, CI = 1.4–54.3) and at Esztergom between 1981 and 1982 (OR = 4.2, CI = 1.3–13.5) and clubfoot in the Tata community between 1980 and 1981 (OR = 5.5, CI = 1.5–20.3).

As set forth in Section 4.1.2.2, the relationship between the findings of clusters of abnormalities and AN is uncertain because there are no exposure data in the report (Czeizel et al., 2000, 1999). Consequently, it is not known by how much the mothers of affected infants

were exposed to the compound if at all. Furthermore, when the incidence of these and other abnormalities was considered for infants born throughout the duration of the study, there were no overall increased incidences of congenital abnormalities within the study area compared with infants born throughout Hungary.

The study authors stated that there was a technological change at the AN factory in 1984 that resulted in greater environmental protection, implying that releases of the compound to the environment were less after 1984 than before the change. This suggested that the cluster of pectus excavatum obtained at Tata between 1990 and 1992 was unlikely to have been due to AN exposure. However, the high incidence of undescended testis in Nyergesujfalu between 1980 and 1983 may have been an environmental phenomenon, because the region-wide incidence of this congenital abnormality appeared to decrease with increasing distance from the factory. In general, however, it was difficult to draw conclusions about a link between maternal exposure to AN and the incidence of congenital abnormalities from the data in this study because of a lack of exposure data.

Ivanescu et al. (1990) reported lower serum testosterone level in male workers exposed to AN in a chemical factory (see Section 4.1.2.2.2).

Xu et al. (2003) performed conventional sperm analysis according to WHO guidelines and investigated DNA strand breakage and sex chromosome aneuploidy in spermatozoa of 30 AN-exposed workers compared with 30 unexposed controls. The mean concentration of AN at exposure sites was reported to be 0.8 ± 0.25 mg/m^3 (0.37 ppm). Sperm density was significantly lower in the exposed group (75×10^6/mL) than in the control group (140×10^6/mL). Sperm number per ejaculum was 205×10^6 in the exposed group, significantly lower than the 280×10^6 spermatozoa in the control. However, there were no significant differences between the groups in semen volume, sperm motility, viability, or morphology. Xu et al. (2003) used single cell gel electrophoresis (comet assay) to monitor the incidence of DNA strand breakage of sperm cells. The rate of comet sperm nuclei was 28.7% in the exposed group, significantly higher than in the control group (15.0%). Mean comet tail length was 9.8 μm in exposed workers but 4.3 μm in control workers. The frequency of sex chromosome aneuploidy in sperm cells was analyzed using fluorescence in situ hybridization (FISH). Sex chromosome disomy was found to be 0.69% in the exposed group, significantly higher than 0.35% in controls. XY-bearing sperm was the most common sex chromosome disomy, with an average rate of 0.37% in exposed vs. 0.20% in controls. XX- and YY-bearing sperm accounted for an additional 0.09 and 0.23% of sperm in exposed vs. 0.05 and 0.10% in controls, respectively. Xu et al. (2003) concluded that AN exposure affected semen quality among occupationally exposed persons by the induction of DNA strand breakage and sex chromosome nondisjunction.

4.3.2. Studies in Animals

4.3.2.1. *Oral Studies*

Assessments of reproductive/developmental effects of AN in orally exposed animals are derived from standard toxicity assays in rats and mice, standard developmental toxicity assays in female rats, and a three-generation reproductive toxicity assay in male and female rats.

4.3.2.1.1. ***Standard toxicity assays: reproductive organ pathology.*** As described in Section 4.2.1, standard 2-year oral toxicity assays in rats revealed no evidence for increased reproductive histopathology in males or females exposed to AN at doses as high as 8–25 mg/kg-day (Johannsen and Levinskas, 2002a, b; Quast, 2002; Biodynamics 1980a, b, c; Quast et al., 1980a). In addition, there was no evidence for adverse effects of AN on functional reproductive parameters (sperm morphology, estrous cycle) or the histology of reproductive organs in male $B6C3F_1$ mice treated with AN by gavage 5 days/week at 20 mg/kg-day or in females at 40 mg/kg-day for 14 weeks (NTP, 2001). In this subchronic study, the weights of the left cauda epididymides were significantly elevated compared with controls in male mice exposed to 10 and 20 mg/kg-day, but this effect was not considered biologically significant in the absence of histopathology. In the companion 2-year gavage assay (NTP, 2001), no reproductive histopathology was observed in male mice treated 5 days/week with AN at doses as high as 20 mg/kg-day, but effects were observed in females (Table 4-33). The incidence of ovarian cysts was significantly elevated at 2.5, 10, and 20 mg/kg-day, and the incidence of atrophy of the ovary increased at 10 and 20 mg/kg-day. Atrophy was severe and was characterized by lack of histologically evident follicle and corpus luteum development with a predominance in interstitial tissue. The lowest dose of 2.5 mg/kg-day in this study was identified as the LOAEL for ovarian cysts and atrophy.

4.3.2.1.2. ***Developmental toxicity assays.*** Dow Chemical (1992b) and Murray et al. (1978) evaluated developmental effects in pregnant female Sprague-Dawley rats (29–39/group) that received 10, 25, or 65 mg/kg AN by gavage in water on GDs 6–15; an additional group of 43 controls received water alone. Dams were observed daily for clinical signs and weighed on GDs 6, 10, 16, and 21. Food and water consumption were monitored at 3-day intervals on GDs 6–21, at which point all animals were sacrificed and maternal liver weights were recorded. Among the reproductive parameters evaluated were the numbers and positions of live, dead, and resorbed fetuses and the number of implantation sites. Developmental toxicity was evaluated by the weight, sex ratio, and crown-rump length of the fetuses. One-third of the fetuses in each litter were evaluated for visceral malformations and soft tissue abnormalities; the rest were examined for skeletal alterations.

Maternal toxicity of AN was most evident in the high-dose group. Systemic effects observed only at this dose included a single maternal death on GD 6, an increase in clinical signs

(hyperexcitability and excessive salivation) during the dosing period, BW gain reduced 46% compared with controls by GD 15 (22% by GD 21), water consumption significantly increased by an unspecified amount on GDs 6–20, and a statistically significant 11% increase in absolute (but not relative) liver weight compared with controls. Food consumption was significantly reduced by an unspecified amount compared with controls in high- and mid-dose dams on GDs 6–8. At necropsy, most (number not specified) dams dosed with 65 mg/kg-day and 3/33 dams dosed with 25 mg/kg-day displayed a thickening of the nonglandular portion of the stomach. Pregnancy rate was significantly decreased among dams given 65 mg/kg-day AN, with only 20 of 29 dams producing litters. Uterine staining revealed implantation sites in four additional dams. A NOAEL for maternal toxicity was identified as 10 mg/kg-day AN, and 25 mg/kg-day was the LOAEL for hyperplasia of forestomach.

Exposure to AN had no statistically significant effect on the average numbers of implantations/dam, live fetuses/litter, or resorptions/litter; the average sex ratio of litters was not reported. At 65 mg/kg-day, there were statistically significant reductions in fetal BW (by 7.4%) and crown-rump length (by 1.8%) compared with controls. The high-dose group also showed a significant increase in external malformations (short tail in 6/17 litters and short trunk in 3/17 litters); there was also a significant increase in skeletal malformations (missing vertebrae) (Table 4-43). The defect ranged in severity from the absence of a single lumbar vertebra to the absence of all sacral and lumbar vertebrae and most thoracic vertebrae. Although the incidence of malformations at 25 mg/kg-day was not statistically significant (Table 4-43), a minimal LOAEL of 25 mg/kg-day was identified for fetal malformation in Sprague-Dawley rats. The NOAEL for fetal toxicity was 10 mg/kg-day.

Table 4-43. Incidence of fetal abnormalities among litters of Sprague-Dawley rats following maternal exposure to AN on GDs 6–15

Type of malformation	AN (mg/kg-d)			
	0	10	25	65
	Number of fetuses affected/number of litters examined			
External and skeletal malformations	443/38	388/35	312/29	212/17
Visceral malformations	154/38	135/35	111/29	71/17
	Number of fetuses (litters) affected			
External malformations				
Short tail	1 (1)	0 (0)	2 (2)	8 (6)[a]
Short trunk	0 (0)	0 (0)	0 (0)	3 (3)[a]
Imperforate anus	0 (0)	0 (0)	0 (0)	2 (2)
Visceral abnormalities				
Right side aortic arch	0 (0)	0 (0)	1 (1)	1 (1)
Missing kidney, unilateral	1 (1)	0 (0)	0 (0)	1 (1)
Anteriorly displaced ovaries	0 (0)	0 (0)	1 (1)	1 (1)
Skeletal malformations				
Missing vertebrae	1 (1)	0 (0)	2 (2)	8 (6)[a]
Missing two vertebrae and two ribs	7 (1)	0 (0)	7 (2)	0 (0)
Hemivertebrae	0 (0)	0 (0)	0 (0)	0 (0)
Total malformed	8 (2)	0 (0)	10 (4)	8 (6)[a]

[a]Significantly different from controls ($p < 0.05$), as determined by the study authors.

Source: Murray et al. (1978).

Behavioral teratogenicity of AN was examined in the progeny of pregnant Wistar rats (15/group) that received 0 or 5 mg/kg-day AN by gavage on GDs 5–21 (Mehrotra et al., 1988). Dams were weighed at intervals, and food and water intakes and the length of gestation were recorded. At parturition (postnatal day [PND] 0), litters were culled to four males and four females. On PND 1, pups were sexed and examined for gross external anomalies; litters with fewer than two/sex were rejected. Eight pups from four litters were examined for behavioral abnormalities, including tests for spontaneous locomotion and passive avoidance. Excised brains of 21-day-old pups were assayed for biogenic amines (noradrenaline, dopamine, and 5-hydroxytryptamine) and for the activities of Na^+,K^+-adenosine triphosphatase (ATPase), monoamine oxidase, and acetylcholinesterase.

Exposure to AN at 5 mg/kg-day had no significant effect on BW or food and water intakes in dams or on reproductive parameters such as gestational length, number of viable offspring, or pup sex ratio. No AN-induced effects were observed on postnatal morphological development, pup BWs, developmental indices (eye opening or incisor eruption), or tests of neurological impairment (righting reflex, cliff avoidance, and grip strength). The levels of biogenic amines were significantly altered in specific brain regions as a result of exposure.

Levels of 5-hydroxytryptamine were increased by 32% in the pons medulla and decreased by 44% in the corpus striatum and 30% in the hippocampus. Levels of noradrenaline were decreased by 40% in the pons medulla and increased by 81% in the hippocampus. Gestational exposure to AN resulted in a statistically significant 49% reduction in brain levels of monoamine oxidase in 21-day-old pups; levels of acetylcholinesterase and Na^+,K^+-ATPase were not significantly affected. The biological significance of the enzyme and neurotransmitter changes was unclear, given that no treatment-related behavioral effects were observed. However, Mehrotra et al. (1988) noted that alterations in the levels of biogenic amines may become more prominant after prolonged exposure or exposure to higher doses of AN.

In a study comparing developmental toxicities of aliphatic nitriles in vitro and in vivo, Saillenfait and Sabaté (2000) administered a single dose of 0 or 100 mg/kg AN by gavage in olive oil to groups of four pregnant Sprague-Dawley rats on GD 10. Dams were sacrificed on GD 12, and the numbers of uterine implantation sites and fetuses with heartbeats were recorded. Viable fetuses were examined for defects of the allantois, trunk, and misdirected caudal extremity (left-sided), which the investigators had found to be typical in embryos exposed to sodium cyanide. Maternal effects of all of the nitriles (including AN) included increases in clinical signs (piloerection, prostration, and/or tremors) and unspecified maternal BW loss between GDs 10 and 12. AN exposure had no effect on the numbers of implants/litter or live embryos/litter, but significantly increased the incidence of overall poor and abnormal development and the incidence of misdirected allantois or allantois, trunk, and caudal extremity misdirected (Table 4-44). The study authors suggested that maternal production of the metabolite cyanide may have contributed to the developmental toxicity of AN since the characteristic defects that occurred in embryos exposed to cyanide were found in AN-exposed embryos. The single applied dose of 100 mg/kg is a LOAEL for maternal and fetal effects.

Table 4-44. Morphological alterations in GD 12 fetuses of Sprague-Dawley rats exposed to 100 mg/kg AN on GD 10

Response	Group (number of litters examined)	
	Control (n = 4)	100 mg/kg (n = 4)
Implants/litter	13.25 ± 1.71	13.75 ± 0.96
Live embryos/litter	13.0 ± 1.83	12.5 ± 1.0
Total embryos examined	52	50
Allantois, trunk, and/or caudal extremity misdirected		
Embryos affected/embryos examined	0/52	13/46[a]
Litters affected/litters examined	0/4	3/4

[a]Significantly different from controls ($p < 0.01$) as calculated by the reviewers (Fisher's exact test).

Source: Saillenfait and Sabaté (2000).

4.3.2.1.3. ***Reproductive toxicity assay.*** Friedman and Beliles (2002) and Litton Bionetics (1992) conducted a three-generation reproductive study in Sprague-Dawley rats (groups of 15 males and 30 females) exposed to 100 or 500 ppm AN in drinking water for 100 days before mating. Groups of 10 male and 20 female controls received untreated drinking water. As calculated by the study authors, the concentrations were equivalent to average doses of 0, 11, and 37 mg/kg-day for males and 0, 20, and 40 mg/kg-day for females. The calculated average doses, averaged across sexes, were 0, 16, and 39 mg/kg-day. Rats were observed daily, especially for signs of neurotoxicity (e.g., abnormal gait). Water consumption in the F0 generation was measured twice a week, food intake was measured weekly, and BWs were recorded every 2 weeks. After 100 days of exposure, rats were paired for mating for 6 days; females not bred after 6 days were mated to another proven breeding male from the same exposure group. The offspring (F1a) of the first mating were examined on PNDs 0, 4, and 21. Litters were culled to 10 pups on PND 4 to achieve an equal sex ratio. Litter BWs were recorded on PND 4 and individual pup weights were recorded on PND 21. Two weeks after removal of the F1a offspring, F0 females were remated to produce the F1b litter, and those not used in breeding F1a were also mated to produce F1b pups to ensure a sufficient number of offspring for the F2 generation, although these animals should have been discarded according to the original study design. The original study design stipulated discarding F1a pups (those not scheduled for breeding) at weaning, but, because of high mortality in the 500 ppm group, they were retained to ensure sufficient time-mated females to use as foster mothers (one-half of each high-dose litter was fostered onto untreated females). All F0 males used for breeding were discarded after the second mating, and those not used in breeding were discarded when the F1a litter were weaned.

At weaning (21 days), one male and one female from the unfostered F1b litter (or from the F1a litter, if needed) were selected as potential breeders for the F2 generation. All F1 offspring exposed to AN were checked daily for mortality, and necropsies were performed on all animals either found dead or killed in a moribund condition. The F0 dams and females not producing a litter were exposed for an additional 20 weeks after weaning the F1b pups. After that period, they were sacrificed and the sciatic nerve, gastrocnemius muscle, brain, and gross lesions were examined for histopathology. F1a and F1b rats were sacrificed in week 95 of the study and necropsied for the examination of papillomas in the stomach and intestines. The protocol for the subsequent generations (F1b parents and F2a and F2b offspring; F2b parents and F3a and F3b offspring) was as described for the first generation. F2 females, after an additional 20 weeks of exposure following the weaning of the F3b litters, were necropsied, and sciatic nerve, gastrocnemius muscle, brain, stomach, and gross lesions were evaluated for histopathology. F3b rats (10/sex) in the control and 500 ppm groups were randomly selected for histologic examination.

The following discussion of results does not include cancer data from this study, which were presented separately in Section 4.2.1.2. In F0 parents, BWs were lower than controls after

4 weeks of exposure to 500 ppm, the reduction reaching 22% in males and 17% in females by week 10. This BW reduction was accompanied reduction in food intake by ~18% in 500 ppm males and 8% in 500 ppm females for the first 10 weeks. Water consumption was reduced in males and females by about 50% at the high dose and 20–25% at the low dose for the first 10 weeks. Reduced water consumption and possibly BWs may have been a result of reduced palatability of treated water. Exposure to AN had no effect on the incidence of neurological or other clinical signs, male or female fertility indices, or the duration of mating or gestation of F0 parents.

Compared with controls, no significant changes in fertility index or gestational index were observed in any of the exposed generations (Table 4-45) (Friedman and Beliles, 2002; Litton Bionetics, 1992). However, poor fertility among controls for the F1b (50–60%) and F2b (60–70%) parents might have limited the capability of this study to detect differences in fertility between control and treated rats (Table 4-45). The durations of mating and gestation were also unaffected, except the mating duration of F2b rats for F3a generation. Significant decreased viability and lactation indices were observed in the 500 ppm F0 parents for the F1a generation, due to the deaths of pups between 1–4 and 5–21 days, respectively. Significant decreases in viability index were also observed in 100 and 500 ppm F0 parents for the F1b generation and in 500 ppm F2b parents for the F3a generation (Table 4-45). In addition, decreases of about 10–40% in pup weights were observed in the F1a, F1b, F2a, F2b, F3a, and F3b generations in the 500 ppm groups (Table 4-46). Overall, the results identified a drinking water concentration of 100 ppm (16 mg/kg-day) as a minimal reproductive toxicity LOAEL for decrease in lactation index in F2a generations. Although no effects on fertility were observed in this three-generation study, poor fertility among controls in F1b and F2b parents might have limited the sensitivity of this assessment. The study also identified a LOAEL of 100 ppm for reduced viability in F0 parents.

Table 4-45. Group-specific reproductive indices in three generations of Sprague-Dawley rats receiving AN in drinking water

Generation/group	Male[a,b]	Female[c,d]	Gestation index[e]	Viability index[f]	Lactation index[g]
	Fertility index				
F0 parents for F1a					
Control	10/10	18/20	18/18	185/186	138/150
100 ppm	8/10	16/20	16/16	197/201	139/150
500 ppm	10/10	16/20	16/16	166/177[h]	95/143[h]
F0 parents for F1b					
Control	10/10	16/20	16/16	186/186	137/150
100 ppm	10/10	17/20	17/17	182/202[h]	132/139
500 ppm	13/15	22/28	22/22	99/109[h]	87/99
F1b parents for F2a					
Control	5/10	10/20	10/10	107/109	91/91
100 ppm	7/10	11/20	11/11	116/124	95/104[h]
500 ppm	8/10	14/20	14/14	133/140	107/114[h]
F1b parents for F2b					
Control	6/10	10/20	10/10	101/101	82/82
100 ppm	5/10	8/20	8/8	93/97	70/73
500 ppm	8/10	14/20	14/14	138/138	123/123
F2b parents for F3a					
Control	6/10	14/20	14/14	161/161	128/131
100 ppm	9/10	13/20	13/13	157/158	124/124
500 ppm	10/10	15/20	15/15	157/166[h]	134/135
F2b parents for F3b					
Control	9/10	14/20	14/14	170/176	106/108
100 ppm	10/10	15/20	15/15	198/198	117/119
500 ppm	10/10	17/20	17/17	170/178	115/125

[a]Doses in males: 0, 11, or 37 mg/kg-d for 0, 100, or 500 ppm as calculated by the study authors.
[b]Fertility index in males = number of males producing a litter/number mated.
[c]Doses in females: 0, 20, or 40 mg/kg-d for 0, 100, or 500 ppm, as calculated by the study authors.
[d]Fertility index in females = number of pregnant females/number mated.
[e]Gestation index = number of litters born/number of pregnant females.
[f]Viability index = number of pups that survived to PND 4/number of pups born alive.
[g]Lactation index = number of pups surviving to weaning/number of pups alive on PND 4.
[h]Significantly lower than controls ($p < 0.05$), as calculated by the study authors.

Sources: Friedman and Beliles (2002); Litton Bionetics (1992).

Table 4-46. Group-specific pup weights in three generations of Sprague-Dawley rats receiving AN in drinking water

Generation-concentration	Weight (g)	
	D 4	D 21 (males)
F1a-control	11	42
F1a-100 ppm	10	40
F1a-500 ppm	9[a]	28[a]
F1b-control	10	39
F1b-100 ppm	9	36
F1b-500 ppm	10	34[a]
F2a-control	11	39
F2a-100 ppm	10	39
F2a-500 ppm	9[a]	30
F2b-control	11	53
F2b-100 ppm	10	46
F2b-500 ppm	9	30[a]
F3a-control	10	43
F3a-100 ppm	9	43
F3a-500 ppm	8[a]	30[a]
F3b-control	10	50
F3b-100 ppm	10	47
F3b-500 ppm	8[a]	32[a]

[a]Significantly different from controls ($p < 0.05$), as calculated by the study authors.

Sources: Friedman and Beliles (2002); Litton Bionetics (1992).

4.3.2.1.4. ***Male exposure reproductive toxicity studies.*** Tandon et al. (1988) evaluated reproductive toxicity in male CD-1 mice that received 0, 1, or 10 mg/kg-day AN by gavage in saline for 60 days. The testes of six mice/group were examined histopathologically, and homogenates of pooled testes (four testes) in each group were assayed for the activities of sorbitol dehydrogenase (SDH), acid phosphatase, LDH, glucose-6-phosphatase dehydrogenase, and β-glucuronidase.

Exposure to AN decreased the epididymal sperm count by 21 and 45% at the low- and high-dose group, respectively. However, the decrease was statistically significant ($p < 0.05$) only with the 10 mg/kg-day group. Histopathological examination of the testes did not reveal changes in the low-dose group. In high-dose mice, degenerative changes were seen in 40% of seminiferous tubules. In addition, the testes of mice dosed with 10 mg/kg-day showed a 12% increase in the activity of LDH, a 22% decrease in the activity of SDH, a 37% increase in the activity of β-glucuronidase, and a 16% decrease in the activity of acid phosphatase compared with controls. AN exposure had no effect on the activity of testicular glucose-6-phosphatase dehydrogenase. The study authors suggested that the changes in the activities of LDH and SDH were related to the AN-induced degeneration of germinal epithelium. In this study, a NOAEL of

1 mg/kg-day and a LOAEL of 10 mg/kg-day were identified for the toxicological effects of AN on the testes of male CD-1 mice.

In a range-finding acute toxicity study for a dominant lethal assay, groups of 10 male F344 rats received 45, 60, 68, 75, or 90 mg/kg-day AN by gavage in 0.9% saline daily for 5 days (Working et al., 1987). Rats were observed for a total of 42 days from the first administration. No deaths were observed in groups receiving 45 or 60 mg/kg-day. In the higher dose groups, the study was terminated early on account of mortality: 40% at 68 mg/kg-day (terminated on day 6), 30% at 75 mg/kg-day (terminated on day 4), and 30% at 90 mg/kg-day (terminated on day 2). As a result of this range-finding study, 60 mg/kg-day was selected as the maximum tolerated dose for the dominant lethal assay. In this assay, groups of 50 male F344 rats received AN by gavage at 0 or 60 mg/kg-day in 0.9% saline for 5 days. BWs of males were recorded three times during the week of treatment and then weekly during the mating period of 10 weeks; males were caged with a different female each week for 6 days. A transient reduction in mean BW (~4%) compared with controls was observed in rats on treatment days 3 and 5 and on the fourth post-treatment day; BW gain in treated rats was equivalent to controls beginning the second week of observation. AN exposure in males had no effect on the incidence of pre- or postimplantation losses, indicating a negative result in the dominant lethal assay. AN also had no effect on the fertility of exposed males in any postexposure week.

4.3.2.2. *Inhalation Exposure*

Information about reproductive/developmental toxicity in animals exposed to AN by inhalation comes from a standard chronic toxicity assay in rats, developmental toxicity assays in rats, and a dominant lethal assay in male mice.

4.3.2.2.1. ***Standard toxicity assays*****.** As described in Section 4.2.2.2, no reproductive histopathology was observed in male or female Sprague-Dawley rats that were exposed to AN at concentrations as high as 80 ppm 6 hours/day, 5 days/week for up to 2 years (Dow Chemical Co., 1992a; Quast et al., 1980b).

4.3.2.2.2. ***Developmental toxicity assays.*** Haskell Laboratory (1992a) and Murray et al. (1978) evaluated developmental toxicity in groups of 30 pregnant Sprague-Dawley rats exposed (whole body) to 0, 40, or 80 ppm AN vapor for 6 hours/day on GDs 6–15. The parameters examined were the same as those for the oral exposure study by these authors described in Section 4.3.2.1. Inhalation exposure to 40 or 80 ppm AN did not result in deaths, changes in appearance, gastric thickening, or increase in terminal liver weight in dams. Maternal BW gain was significantly reduced during GDs 6–15 by 47% in the 40 ppm group and by 58% in the 80 ppm group (a reduction of about 20% in both groups for GDs 6–21). Both exposure groups exhibited significant (unspecified) decreases in food consumption on GDs 6–9 (but not later intervals) and

increases in water consumption on GDs 9–20. In this study, a NOAEL for maternal effects was not identified, but a LOAEL of 40 ppm was identified for reduced BW gain in dams.

Gestational exposure to AN had no significant effect on any of the reproductive parameters (pregnancy rates, numbers of implantations, live fetuses, or resorptions) and no effect on fetal BW or crown-rump length measurements. Furthermore, no single major malformation occurred at significantly higher incidence in AN-exposed rats vs. controls. However, as shown in Table 4-47, there was an increase in the incidence of total major malformations when they were considered collectively ($p < 0.06$) for the high-dose group (present in 6/35 litters). Malformations observed in litters of 80 ppm group included short tail, missing vertebrae, short trunk, omphalocele, and hemivertebra. In this study, a NOAEL of 40 ppm and a LOAEL of 80 ppm were identified for increases in total malformations in rats.

Table 4-47. Incidence of fetal malformations among litters of Sprague-Dawley rats exposed to AN by inhalation

Type of malformation	AN concentration (ppm)		
	0	**40**	**80**
	Number of fetuses/number of litters examined		
External and skeletal malformations	421/33	441/36	406/35
Visceral malformations	140/33	148/36	136/35
	Number of fetuses (litters) affected		
External malformations			
Short tail	0 (0)	0 (0)	2 (2)
Short trunk	0 (0)	0 (0)	1 (1)
Imperforate anus	0 (0)	0 (0)	0 (0)
Omphalocele	0 (0)	1 (1)	1 (1)
Visceral abnormalities			
Right-sided aortic arch	0 (0)	0 (0)	0 (0)
Missing kidney, unilateral	0 (0)	0 (0)	0 (0)
Anteriorly displaced ovaries	0 (0)	0 (0)	1 (1)
Skeletal malformations			
Missing vertebrae	0 (0)	0 (0)	2 (2)
Missing two vertebrae and two ribs	8 (1)	2 (1)	7 (2)
Hemivertebrae	0 (0)	0 (0)	1 (1)
Total malformed	8 (1)	3 (2)	11 (6)[a]

subchronic

[a]Significantly different from control, as calculated by the study authors ($p = 0.06$).

Source: Murray et al. (1978).

Saillenfait et al. (1993) included AN in a survey of the relative developmental toxicities of inhaled aliphatic mononitriles in rats. Pregnant Sprague-Dawley rats (20–21/group) were exposed (whole body) for 6 hours/day to 0, 12, 25, 50, and 100 ppm AN vapor on GDs 6–20.

Dams were observed daily throughout pregnancy and BWs were recorded on GDs 0, 6, and 21. All subjects were sacrificed on GD 21, and the uteri were weighed and opened to assess the numbers of implantations, resorption sites, and live and dead fetuses. The fetuses were examined for external abnormalities and then split into two equal groups for examination of skeletal or visceral anomalies.

AN exposure did not cause premature deaths in the dams, but exposure to ≥25 ppm caused concentration-related, statistically significant reductions (by 16–45%) in overall BW gain and concentration-related losses in absolute BW (exclusive of gravid uterus weight) in dams. In this study, 12 ppm is a NOAEL and 25 ppm is a LOAEL for reduced BW in dams.

AN exposure had no effect on reproductive parameters (pregnancy rate, average number of implantations, numbers of live fetuses, incidences of nonsurviving implants, or resorptions per litter). Concentration-dependent, statistically significant reductions in average fetal weight (by 5–15% compared with controls) were observed at ≥25 ppm. There were no significant increases in the incidences of external, visceral, or skeletal anomalies in the exposed groups and one control fetus. In this study, a NOAEL of 12 ppm and a LOAEL of 25 ppm were identified for significantly reduced fetal BW.

In a dominant lethal assay for AN, Zhurkov et al. (1983) continuously exposed male ICR mice (20/group, whole body) to AN at concentrations of 0, 20, or 100 mg/m^3 (0, 9.1, or 46 ppm) for 5 days. After exposure, each male was mated to two unexposed females for 8 weeks. Females were sacrificed between GDs 13 and 15, and a number of reproductive and developmental parameters were monitored, including the percentage of pregnant females, number of corpora lutea, implantations, and live and dead fetuses per female as well as total and pre- and postimplantation mortality. Exposure to AN did not result in any dominant lethal effect on male germ cells nor did it cause adverse pre- or postimplantation outcomes. The highest exposure level in this study, 46 ppm, was a NOAEL for reproductive toxicity. This study was limited by sparse descriptions of methods and a lack of quantitative reporting of results.

4.3.2.3. *Intraperitoneal Administration*

In a translated study in Chinese, the effect of AN on spermatogenesis was examined in groups of male Kunming mice (10 3–4-week-old pubertal and five 6–8-week-old adult mice per group) treated by i.p. injection (Liu et al., 2004). The animals received AN (>99% purity) at doses of 1.25, 2.5, or 5.0 mg/kg-day (1/24, 1/12, or 1/6 of the LD_{50}) for 5 days. Negative controls received physiological saline (10 mL/kg) daily for 5 days, whereas positive controls received a single injection of 40 mg/kg CP (not identified but presumably cyclophosphamide). On day 35, mice were sacrificed, the left testicle was selected from five mice per group, and testicular cell suspensions were evaluated using flow cytometry.

The following dose-related effects observed in the 2.5 and 5.0 mg/kg-day groups were statistically significantly different from the negative control group ($p < 0.05$); the same effects

were observed in positive controls (Liu et al., 2004). AN decreased the percentage of haploid testicular cells (indicative of completed spermatogenic meiosis) by 14.3 and 15% in mid- and high-dose adult mice, but a slight reduction was not statistically significant in pubertal mice. The percentage of apoptotic testicular cells was significantly increased by 58.7 and 74.8% in mid- and high-dose pubertal mice and by 81.5 and 108% in mid- and high-dose adult mice. The percentages of spermatogenic epithelial cells in G_0/G_1 phase were significantly reduced by 18 and 20% in mid- and high-dose pubertal mice and by 35.5 and 40.5% in mid- and high-dose adult mice. The percentage of spermatogenic epithelial cells in G_2/M phase was significantly elevated in adult mice by 31.4 and 32.8% at the mid- and high doses, respectively. AN exposure had no effect on the percentage of spermatogenic epithelial cells in S phase. The NOAEL and LOAEL for suppression of spermatogenesis were 1.25 and 2.5 mg/kg-day, respectively.

The teratogenic effects of AN were investigated in groups of pregnant golden hamsters that were exposed via an i.p. injection on GD 8 (Willhite et al., 1981). The actual numbers of dams per group were not reported, but data were presented for 3–6 litters in the exposed groups and 12 litters for the controls injected with sodium chloride. Dose levels were 0, 0.09, 0.19, 0.47, 1.23, and 1.51 mmol/kg (equivalent to 0, 5, 10, 25, 65, and 80 mg/kg). No adverse clinical symptoms were observed in the dams exposed to up to 1.23 mmol/kg (65 mg/kg) AN by GD 14, when the dams were sacrificed. No malformations were observed in the offspring. In contrast, dams exposed to 1.51 mmol/kg (80 mg/kg) showed intense dyspnea, gasping, incoordination, hypothermia, salivation, and convulsions for 1–5 hours after injection. Additionally, several fetal abnormalities and malformations were observed at this exposure level, including encephaloceles and fused or bifurcated ribs. Coadministration of 8.06 mmol/kg STS and 1.51 mmol/kg AN induced neither maternal toxicity nor fetal malformations. Coadministration of 8.06 mmol/kg STS and a higher dose of AN (1.88 mmol/kg, 100 mg/kg) prevented toxic symptoms in dams but not the teratological effects in fetuses. The study authors concluded that the teratogenic action of AN was related to the metabolic release of cyanide.

The effect of AN on rat liver cytochrome P-450 and serum hormone levels were studied in male Sprague-Dawley rats (4/group) injected with 33 mg/kg AN (i.p.) for 3 consecutive days (Nilsen et al., 1980). Control animals were treated with 0.9% sodium chloride. Blood were collected immediately after the animals were sacrificed and serum luteinizing hormone (LH), follicle stimulating hormone (FSH), and prolactine (PRL) were measured by radioimmunoassay. Serum corticosterone levels and liver microsomal cytochrome P-450 were also determined.

A significant increase (3%) in BW was reported in the AN treated group when compared with controls (Nilsen et al., 1980), but relative liver weight was not increased. A significant decrease in liver microsomal content of CYP450 was observed. Serum corticosterone measured 24 hours after the last AN injection was decreased by 70%, while FSH levels were increased by 118%. Serum PRL levels were decreased by 63% when compared with the controls, while

serum LH levels were unchanged. Nilsen et al. (1980) suggested that the increase in FSH might be secondary to impaired spermatogenesis in the testes of treated rats.

4.3.3. In Vitro Studies

The embryotoxicity of AN was evaluated in cultures of whole rat embryos by Saillenfait and coworkers in a series of studies (Saillenfait et al., 2004, 1992; Saillenfait and Sabaté, 2000). As described initially in Saillenfait et al. (1992), the experimental system involved incubating day 10 embryos from pregnant Sprague-Dawley rats for 26 hours in whole organ culture in a medium containing AN at concentrations of 76–760 μmol/L. The growth-related parameters evaluated were functional yolk-sac circulation, yolk-sac diameter, crown-rump length, head length, number of somites, number of malformed embryos, incidences of abnormal brain, malformed caudal extremities, delayed yolk-sac circulation, and defective flexion. The effects of metabolic activation on the embryotoxicity of AN were evaluated by the inclusion of S9 and cofactors (NADPH, glucose-6-phosphate) for CYP450-dependent biotransformation in the incubation system.

Exposure to AN induced concentration-related effects on growth and development. Functional yolk-sac circulation (circulating erythrocytes) was reduced at ≥304 μM and was completely absent at 760 μM. Crown-rump length was reduced at 304 μM and could not be measured at higher concentrations. A concentration-dependent increase in the incidence of malformations was observed following in vitro exposure of day 10 fetuses to AN at 152 μM and above. AN at 152 and 304 μM induced malformations in 53 and 100% of the exposed embryos, respectively. Malformations primarily consisted of a shortened caudal extremity (significant at 152 μM) and a reduction of the brain (achieving significance at 304 μM). Other general malformations were delayed development of the yolk-sac circulation and defective flexion. Furthermore, growth retardation and severity of malformations induced by 304 μM AN were enhanced by the presence of S9 and cofactors, suggesting a role for oxidative biotransformation in AN embryotoxicity. Addition of 0.1–2.2 mM GSH in the incubation medium reduced the embryotoxic effects of AN in this system.

Similarly, a later experiment by this research group (Saillenfait and Sabaté, 2000) demonstrated that day 10 rat embryos exposed to AN for 46 hours in vitro showed concentration-related effects on growth, development, and morphology. Reduced growth (reduced yolk sac diameter and crown-rump length) occurred at 100 μM. The head length and somite number were reduced at 125 μM. Abnormal development (reduced prosencephalon and mesencephalon) and maxillary process defects occurred at ≥125 μM AN. Defects of the rhombencephalon and the auditory system were observed less frequently. These effects were characteristic of those developed by embryos exposed to sodium cyanide in culture. Addition of microsomes and NADPH to the culture medium containing 150 or 175 μM AN enhanced the observed growth

retarding and dysmorphogenic effects, especially in increasing the incidence of rhombencephalon and auditory system defects.

Saillenfait et al. (2004) evaluated the effects of eight aliphatic nitriles on the viability and differentiation of cultured limb bud cells from Sprague-Dawley rat embryos on GD 13. Limb bud micromass cultures were exposed for 5 days to AN at concentrations between 0.01 and 0.45 mM (0.5 and 23.9 μg/mL), with or without microsomal activation, after which they were evaluated for cytotoxicity (neutral red uptake assay) and differentiation of chondrocytes (number and total surface of foci with Alcian blue staining were used as indicator of cell differentiation). The concentrations that inhibited cell viability and cell differentiation by 50% of concurrent untreated controls were determined.

The IC_{50} values were 0.24 mM (13 μg/mL) for cytotoxicity (viability) and 0.33–0.38 mM (18–20 μg/mL) for differentiation (total surface of foci and number of foci), respectively. The ratios of IC_{50} for cytotoxicity and differentiation were 0.6 for number of foci and 0.7 for total surface of foci. Microsomal activation had no effect on the results with AN. In parallel experiments, the IC_{50} for cytotoxicity in cultured 3T3 cells (differentiated mouse fibroblast cell line) exposed to AN was 0.065 mM. The relative potency of the tested nitriles in this limb bud cell culture system matched previously published results for cultured whole embryos, but not necessarily for in vivo teratogenicity (false negative results were obtained for two of the eight nitriles). Saillenfait et al. (2004) characterized the response of AN in the micromass culture assay as equivocal, since it depended on the criteria used to define a positive result. According to one criterion, AN might be considered to have teratogenic potency because its IC_{50} was less than 50 μg/mL. However, under the "twofold rule" that defines a positive result by a value >2 for the ratio (IC_{50} for cytotoxicity)/(IC_{50} for differentiation), AN would be classified as having poor potential developmental hazard. As suggested by comparison of the IC_{50} for cytotoxicity, embryonic rat limb bud cells were not more vulnerable to AN than differentiated 3T3 mouse fibroblasts. These suggestive results are consistent with the observations in vivo (see Section 4.3.2) that fetal toxicity from AN occurs only at exposure levels that cause maternal toxicity.

4.4. OTHER DURATION- OR ENDPOINT-SPECIFIC STUDIES

4.4.1. Acute Toxicity Data

Closely similar values have been reported for the oral LD_{50} in rats: 78 mg/kg (Benesh and Cherna, 1959), 93 mg/kg (Smyth and Carpenter, 1948), 90 mg/kg (Sprague-Dawley rats) (Younger Labs, 1992), and 81 mg/kg (male CF Nelson rats) (Vernon et al., 1990). Lower value has been published for the oral LD_{50} in mice: 25 mg/kg (H-strain, sex not stated) (Benesh and Cherna, 1959) and 36 and 48 mg/kg in male and female mice, respectively (strain not stated) (Tullar, 1947, as cited in IPCS, 1983). These findings indicate that mice are more susceptible to the acute toxicity of AN than are rats. Published LD_{50} values for guinea pigs (56 mg/kg)

(Jedlicka et al., 1958) and rabbits (93 mg/kg) (Paulet and Desnos, 1961) are in the same narrow range as those for rats and mice. For the inhalation route, median lethal concentration (LC_{50}) values in rats of 217 ppm (470 mg/m^3) (Knobloch et al., 1971) and 333 ppm (777 mg/m^3) (Haskell Laboratory, 1992b) have been reported. However, exposing Sprague-Dawley rats to 1,008 ppm AN for 1 hour failed to produce mortality (Younger Labs, 1992). A 4-hour LC_{50} value of 946 ppm (2,053 mg/m^3) was reported for Sprague-Dawley rats following nose-only exposure (WIL Research Laboratories, 2005); no mortality was observed in male or female rats at exposures as high as 775 ppm (1,682 mg/m^3) in this study. However, ataxia, labored respiration, and hypoactivity were observed at this exposure concentration and higher. LC_{50} values (duration not reported) of 138 ppm (300 mg/m^3) in mice and 456 ppm (990 mg/m^3) in guinea pigs have been reported (Knobloch et al., 1971).

As set forth in the English abstract of an article in Polish, Knobloch et al. (1971) investigated the acute and subacute toxicity of AN in BN mice, Wistar rats, and guinea pigs (strain not given). For rats, s.c. and i.p. LD_{50} values of 80 and 100 mg/kg, respectively, were reported. For mice, the LD_{50} was 34 mg/kg.

An earlier subacute study examined the effect of oral AN administration on the liver of sodium PB-pretreated (400 μmol/kg) or Aroclor 1254-pretreated (300 μmol/kg) male and female Sprague-Dawley rats that received 100 or 500 ppm AN in drinking water for 21 days (Silver et al., 1982). Other pretreated animals were given 0, 50, 75, 100, or 150 mg/kg AN by gavage for up to 3 days. Some liver-related biochemical changes were noted as a result of AN exposure, including a dose-dependent reduction in hepatic nonprotein sulfhydryl concentrations (maximal reduction of 81% at the highest dose of 150 mg/kg). Serum SDH activity was increased by fourfold 24 hours after administration of 150 mg/kg AN. On the other hand, SGPT activity was not significantly altered. Pretreatment with PB or Aroclor 1254 resulted in only a slight enhancement of AN-induced elevation of serum SDH or SGPT activities. In the experiment in which female rats were pretreated with either vehicle, PB or Aroclor 1254, and treated with 100 ppm or 500 ppm AN for 21 days, there was a 60% increase in serum SDH activity in animals receiving 500 ppm AN in drinking water.

In the 3-day studies, there was some evidence of focal superficial necrosis of the liver in rats receiving high gavage doses (100 or 150 mg/kg). This effect was associated with the presence of hemorrhagic gastritis and distention of the forestomach. However, while the biochemical and pathology changes implied a limited perturbation of the liver by AN, light microscopy showed only minor changes in the histopathology of the organ and no ultrastructural changes to the liver were evident when evaluated by electron microscopy. Silver et al. (1982) concluded that liver did not appear to be a target organ in the acute or subacute toxicity of AN.

Dudley and Neal (1942) exposed several species of laboratory animals—rat, guinea pig, rabbit, cat, dog, rhesus monkey—to AN vapor for 0.5–8 hours at concentrations ranging from 0.063 to 5.3 mg/L (30–2,445 ppm). In rats (Osborne Mendel, sex not stated), 1,260 ppm was

found to be an effective lethal concentration when administered for 4 hours. During or after an 8-hour exposure, 320 ppm AN was fatal. A 4-hour exposure to 260 ppm AN was fatal in rabbits (strain and sex not stated), while 1,160 ppm appeared to be a fatal concentration in guinea pigs. Other lethal concentrations were 600 ppm for 1.5 hours in cats and 110–165 ppm for 3 hours in dogs (breed not given, male and female), while Rhesus monkeys (males and females) tolerated 90 ppm AN with only minor, transitory adverse effects (skin redness, sleepiness). In all species except guinea pig, AN caused an initial respiratory stimulation, followed by rapid, shallow breathing, nasal exudate, and watering eyes. In rats, the most striking symptom was reddening of the skin in the less prominently haired regions (nose, ear, feet). Reddening of the skin was also observed in the other species, again with the exception of guinea pigs. The study authors concluded that, in five of the six species investigated, AN-induced symptoms resembled cyanide poisoning. By contrast, AN acted as a severe pulmonary irritant in guinea pigs. Consistent with these findings, sodium nitrite (a cyanide antidote) protected five of the species studied, but not guinea pigs, from AN toxicity. The study authors postulated that guinea pigs may metabolize AN differently than rats, rabbits, cats, dogs, or monkeys, possibly by transformation to acrolein rather than cleavage of the cyano group. However, Dudley and Neal (1942) were unable to extract any cyanide from the tissues of animals that had succumbed to AN exposure.

Knobloch et al. (1971) evaluated the acute toxicity of AN via inhalation exposure (duration not given) in three species. The LC_{50} in mice was 0.30 mg/L (138 ppm), in rats 0.47 mg/L (217 ppm), and in guinea pigs 0.99 mg/L (456 ppm). These values confirmed the roughly twofold species difference between rats and guinea pigs, but were about threefold lower than values reported by Dudley and Neal (1942).

Two studies by Gut et al. (1985, 1984) evaluated the subchronic toxicity of AN in rats when administered via inhalation. In both studies, male Wistar rats were exposed to 280 mg/m^3 AN by inhalation 8 hours/day for 5 days (Gut et al., 1985, 1984). As shown in Table 4-48, BW was decreased in rats exposed to AN for 5 days. The absolute weight of liver decreased, while brain weight remained unchanged. Hence, the relative liver weight was significantly decreased, while relative brain weight increased due to the BW decrease. However, there were no significant histopathological changes in the lungs, livers, kidneys, or adrenals. The concentrations of glucose, pyruvate, and lactate were elevated in the brain and blood of exposed rats (Table 4-48). Treatment-related reductions in the concentrations of serum cholesterol and triglycerides were found in test animals. The study authors considered the increase in blood glucose concentration to be the most sensitive indicator of AN exposure under these experimental conditions (Gut et al., 1984).

Table 4-48. Effects of AN on organ weight, clinical chemistry, and biochemical parameters when administered to male Wistar rats via inhalation

Parameter (units)	Controls (n)	AN (n)
BW (g)	341 ± 18 (8)	287 ± 24[a] (8)
Relative liver weight (g/100 g BW)	3.39 ± 0.29 (8)	2.79 ± 0.08[a] (8)
Relative brain weight (g/100 g BW)	0.564 ± 0.06 (8)	0.647 ± 0.076[a] (8)
Serum triglyceride (mmol/L)	2.36 ± 0.51 (10)	1.47 ± 0.47[b] (10)
Serum cholesterol (mg/dL)	72.3 ± 8.5 (10)	54.6 ± 12.9[b] (10)
Pyruvate (mmol/L)		
Blood	0.080 ± 0.012	0.128 ± 0.028[a] (5)
Brain	0.039 ± 0.007	0.068 ± 0.014[a] (5)
Lactate (mmol/L)		
Blood	2.259 ± 0.577 (5)	4.032 ± 1.061[a] (5)
Brain	6.002 ± 0.258 (5)	8.034 ± 0.471[a] (5)
Glucose (mmol/L)	4.10 ± 0.21	10.22 ± 1.26[c] (5)

[a]Significantly different from controls ($p < 0.05$).
[b]Significantly different from controls ($p < 0.001$).
[c]Significantly different from controls ($p < 0.01$).

Source: Gut et al. (1984).

Gut et al. (1984) further examined the dose-response effects of AN on blood glucose levels by giving food-deprived male Wistar rats a single 12-hour exposure of 0, 57, 125, or 271 mg/m^3 AN. Blood glucose levels were dose-dependently increased at the end of the exposure period (4.33 ± 0.64 at 57 mg/m^3; 10.88 ± 3.74 at 271 mg/m^3 vs. 3.46 ± 0.29 mg/m^3 in controls) but declined to normal or below normal levels 24 hours after exposure (1.79 ± 0.84 at 271 mg/m^3 vs. 4.73 ± 0.34 mg/m^3 in controls). The simultaneous increase in the pyruvate and lactate concentrations suggests that AN affected carbohydrate metabolism on the level of glycolysis as well as on the citric acid cycle level.

In a subsequent study using exposure regimens identical to those in Gut et al. (1984), Gut et al. (1985) monitored AN-induced changes in sulfhydryl concentrations in the liver and brain and the appearance of thioethers (AN-mercapturic acid) and thiocyanate in the urine. GSH concentrations in the liver were significantly reduced compared with controls (3.86 ± 0.41 vs. 7.66 ± 0.58 μmol/g) in rats exposed to AN for five consecutive daily 8-hour exposures at 280 mg/m^3. No GSH depletion was evident in the brain. The protein sulfhydryl level remained unchanged in the brain but was increased by 17% in the liver, although not statistically significant. One out of 15 treated animals died, and the study authors suggested that GSH depletion could have been responsible.

Urinary excretion of thioethers and thiocyanate was proportional to the inhaled concentration. The ratio between urinary thioethers and thiocyanate in exposed rats was about 2:4 and was not influenced by the exposed AN concentrations (Gut et al., 1985).

Bhooma et al. (1992) evaluated the effect of AN on the procoagulant activity in pulmonary alveolar macrophages of rats. Six male Wistar rats/group were exposed to 100 ppm AN 5 hours/day for 5 days. Animals were sacrificed at 1–28 days after the last exposure. The lungs were lavaged, and alveolar macrophages were collected from the broncho alveolar lavage (BAL) fluid. Procoagulant activity (the ability of a cell or cell products to accelerate the conversion of fibrinogen to fibrin) in macrophage and BAL fluid was determined. The procoagulant activity in the isolated macrophages from exposed animals was about 10-fold higher than in controls 1 day after AN exposure and then slowly declined to control levels by day 28 after exposure. Procoagulant activity of BAL fluid remained unaltered in rats sacrificed up to 7 days after exposure but was elevated in those sacrificed 14 and 28 days after exposure. The study authors noted that acute lung injury often resulted in deposition of fibrin in alveolar spaces (Bachofen and Weibel, 1977) and that fibrin and its degradation products have been implicated in contributing to pulmonary inflammation (Malik et al., 1979; Cuterman et al., 1977). Since this study showed macrophage-associated procoagulant activity in the lung following inhalation to AN, the study authors suggested the alveolar macrophages participated in the pulmonary deposition of fibrin.

Other experimental studies have used acute dosing protocols to study toxicological effects of AN on various target organs. These studies are summarized in the following sections.

4.4.1.1. *Effects of AN on the GI Tract*

Two studies have reported GI hemorrhage and gastric erosion in rats administered with single doses of AN. In the first report (Ghanayem and Ahmed, 1983), a single dose of 50 mg/kg AN was administered to Sprague-Dawley rats (orally or s.c.). GI bleeding was observed 3 hours after treatment, with no significant difference in the amount of GI blood loss resulting from s.c. or oral administration. Thus, AN-induced GI bleeding was not a result of direct irritation of AN on the GI tract. A time-course study of a single 50 mg/kg dose of AN administered by the s.c. route indicated that the amount of blood recovered from the stomach was significantly higher than that of controls at 1, 2, and 3 hours after treatment, while the amount recovered from the intestinal contents was significantly higher than in controls at 2 and 3 hours. Dose-response study of s.c. administration of AN and GI bleeding indicated that significantly higher GI bleeding than in controls occurred at 40, 50, and 70 mg/kg AN, with the maximum at 50 mg/kg AN.

Pretreatment of rats with the CYP450 enzyme inducer, PB, decreased the AN-induced GI blood loss by 55%, whereas pretreatment with Aroclor 1254 increased blood loss by 240% (Ghanayem and Ahmed, 1983). In contrast, pretreatment of rats with CYP450 inhibitors, cobalt

chloride or SKF 525A, prior to AN administration produced significant decreases in blood loss of 10 and 40%, respectively. Pretreatment of rats with diethylmaleate (DEM), a known depletor of GSH, prior to AN administration produced no significant change in GI bleeding. In addition, s.c. administration of a sublethal dose (6 mg/kg) of KCN did not induce GI bleeding when compared with controls, whereas 50 mg/kg AN produced significant GI bleeding. The study authors concluded that metabolic activation of AN to a reactive metabolite other than cyanide (probably CEO) by CYP450 was a prerequisite for AN to induce gastric hemorrhage.

In the second paper, Ghanayem et al. (1985) studied the mechanism of AN-induced gastric mucosal necrosis in the glandular stomach. Male Sprague-Dawley rats were treated with a single s.c. dose of AN (50 or 30 mg/kg), and the glandular stomach was removed and evaluated for histopathology and GSH concentrations. The liver was also removed for GSH determination. Gastric erosion severity index (GEI) was obtained for each exposure group by multiplying the mean severity score by the incidence of gastric necrosis in the group. Calculated GEI was found to be dose and time dependent: higher at 50 mg/kg than 30 mg/kg AN 3 hours after administration and in rats killed 3 hours as compared with rats killed 1 hour after the same dose of AN.

Subcutaneous administration of 30, 40, or 50 mg/kg AN also caused a significant decrease in hepatic GSH concentration 3 hours after treatment, with greater decrease at lower dose (30 mg/kg) than in high dose (50 mg/kg). A significant decrease in gastric GSH concentrations was observed 3 hours after treatment at 40 and 50 mg/kg AN. Pretreatment of rats with various metabolic modulators (CYP450 monooxygenase and GSH) before administration showed that there was a significant inverse relationship between gastric GSH concentration and AN-induced gastric erosions. P450 inducers (Na PB and Aroclor 1254) alone increased GSH levels in the liver. Pretreatment of rats with these P450 inducers inhibited AN-induced gastric necrosis, and partially blocked AN-induced gastric GSH depletion. SKF 525A, a CYP450 inhibitor, caused a slight depletion of gastric and hepatic GSH and potentiated the AN-induced gastric necrosis and GSH depletion. In contrast, cobaltous chloride, another inhibitor of CYP450 enzyme, inhibited AN-induced gastric necrosis and increased both the hepatic and gastric GSH concentrations. In rats treated with DEM, a depletor of GSH and AN, or DEM + cysteamine + AN, GEIs were increased up to fivefold when compared with rats treated with AN alone. Mucosal erosion severity in these two groups was also greatly increased, with more than 50% of rats showing severe or extensive lesions. Pretreatment of rats with sulfhydryl-containing compounds (cysteine or cysteamine) protected against AN-induced gastric necrosis and blocked the depletion of gastric GSH.

In addition, AN-induced gastric erosions could be prevented by pretreatment with atropine, a muscarinic receptor blocker, suggesting the involvement of muscarinic receptors in the AN-induced gastric mucosal necrosis (Ghanayem et al., 1985). Activation of acetylcholine muscarinic receptors is known to increase gastric acid secretion and cause gastric erosions.

Because muscarinic receptors are known to contain sulfhydryl groups in their active site (Ikeda et al., 1980; Aronstam et al., 1978), Ghanayem et al. (1985) hypothesized that AN inactivated critical sulfhydryl groups and caused gastric erosions by locally modulating muscarinic acetylcholine receptors in the stomach.

More recently, Ahmed et al. (1996a) showed accumulation of AN-derived radioactivity in intestinal contents and intestinal mucosa following i.v. injection of 2-[^{14}C]-AN to rats. A recent study by Jacob and Ahmed (2003a) also demonstrated that AN and or its metabolites accumulated and covalently interacted in GI mucosa of male F344 rats treated either i.v. or orally with 2-[^{14}C]-AN. These studies supported the hypothesis that AN-induced injury of the GI mucosa is not due to direct irritation by AN but by metabolic incorporation and macromolecular interaction of AN in these tissues.

4.4.1.2. *Effects of AN on the Kidney*

The acute nephrotoxic effect of AN was investigated in single exposure studies in rats and hamsters by inhalation or i.p. administration. Intraperitoneal injection of Chinese hamsters with 30 mg/kg AN increased kidney weight and renal GSH concentration 24 hours after injection (Zitting et al., 1981). Kidney deethylation activity was also decreased. Rouisse et al. (1986) administered i.p. doses (0, 10, 20, 40, 60, or 80 mg/kg) of AN to male F344 rats (six/dose group). Urinary volume was increased two- to threefold during the 24-hour period following administration for all dose groups. Urinary glucose was about 6 times higher in the 20 mg/kg group than in controls, and 40–60 times higher in the higher dose groups. Urinary excretion of N-acetyl-β-D-glucosaminidase was increased at the highest doses, up to 80% over controls in the 80 mg/kg group. An increased number of lysosomes or dense bodies in renal proximal tubules was seen under the light or electron microscope. In the inhalation study, a similar array of toxicological and clinical chemistry effects relating to kidney structure and function was observed in male rats (seven/group) exposed to 200 ppm AN for 4 hours (Rouisse et al., 1986).

4.4.1.3. *Effects of AN on the Adrenal Gland*

An experimental model for the toxicity of AN investigated the capacity of single i.v. doses of AN to induce acute hemorrhagic necrosis of the adrenal gland (Szabo et al., 1976). This condition has a parallel in man, the Waterhouse-Friderichsen syndrome, which is characterized by thrombocytopenia, disseminated intravascular coagulation, and the appearance of fibrin degradation products in the circulation (Szabo et al., 1976). The condition has been induced in female Sprague-Dawley rats by a single injection of 150 mg/kg AN into the jugular vein (Szabo et al., 1980) and typically has been marked by massive “bilateral apoplexy,” a usually fatal hemorrhagic necrosis of the adrenal glands that occurs in 90–100% of the rats within 90–150 minutes. Thrombocytopenia and a range of associated clinical signs, including tremors, cyanosis, and ultimately respiratory failure, were observed. Light and electron microscopy

showed that an early event in the onset of this condition was damage to the vascular endothelium of the adrenal cortex, with parenchymal injury as a late event. However, these AN-induced lesions could be prevented by pretreatment with the α-adrenergic antagonist phenoxybenzamine, the α,β-blocker labetalo, or the 11-β-hydoxylase inhibitor metyrapone. Elevation of tissue sulfhydryl levels by cysteine or GSH reduced the adrenal apoplexy. Dopamine concentrations in the adrenals increased over time. Because depletion of catecholamines by reserpine, or medullectomy, could prevent the chemically induced adrenocortical necrosis, the study authors proposed that cortical damage resulting from AN was associated with vasoactive amines released from the medulla and/or with metabolites of AN.

4.4.1.4. *Effects of AN on Neurological Endpoints*

Neurotoxic effects were induced in male Sprague-Dawley rats receiving single gavage or s.c. doses of 20, 40, or 80 mg/kg AN (Ghanayem et al., 1991). Two distinct phases of neurological response were evident. The early phase was cholinomimetic in nature, with signs such as salivation, lacrimation, polyuria, miosis, vasodilatation, gastric secretion, and diarrhea. The second phase developed 4–5 hours later with toxic signs, including depression, convulsions, and respiratory failure, followed by death at the higher doses. These CNS effects were observed in rats treated with 40 and 80 mg/kg and were similar to those caused by cyanide. Pretreatment of animals with 1 mg/kg atropine, an acetylcholine muscarinic antagonist, abolished the cholinomimetic toxicity, implicating an involvement of the cholinergic system in some aspects of acute AN neurotoxicity. Since effects were observed even at the lowest dose, a NOAEL was not identified, and 20 mg/kg was the LOAEL.

In another study, male Sprague-Dawley rats that were administered s.c. doses of 112 mg/kg AN (LD_{90}) showed a biphasic response consisting of an early phase with tremors and seizures about 100 minutes after dose administration, followed by severe clonic convulsions that preceded death at about 3–4 hours (Benz and Nerland, 2005). The effects of preadministered inhibitors of oxidative metabolism by CYP450 (80 mg/kg SKF 525A, 75 mg/kg 1-benzylimidazole, or 100 or 200 mg/kg metyrapone) and an alternative CYP450 substrate, ethanol (5,000 mg/kg), on the acute convulsions were examined. Although blood levels of cyanide, and the development of the first phase of tremors and seizures, were inhibited by 1-benzylimidazole or ethanol, treatment with these two agents did not prevent the terminal convulsions or the death of rats injected with 112 mg/kg AN. Ethanol, being a CNS depressant, decreased the incidence of terminal convulsion (5/17 vs. 15/17). These results suggested that the initial phase of the acute neurotoxically lethal effects may have been due to cyanide, which is released via the CYP450 metabolic pathway for AN, and that the second phase was mediated by the parent compound.

Because ethanol showed some effect on lessening the second phase response to AN (although it did not prevent lethality), several anticonvulsants were examined for their ability to

counteract the acute neurotoxicity and lethality of 112 mg/kg AN. Administration of PB (25 mg/kg) or phenytoin (150 mg/kg) (but not 144 mg/kg valproic acid) markedly inhibited the lethal response to 112 mg/kg AN: 9/10 rats died following administration of AN alone or AN plus valproic acid, whereas 1/10 and 2/10 rats died following administration of AN plus PB or AN plus phenytoin, respectively. The protection by phenytoin and PB against convulsion and lethality was not due to inhibition of metabolism of AN to cyanide, since only phenytoin was able to lower blood cyanide levels (by about 32%), and was much less effective than 1-benzylimidazole or ethanol (97 and 94%, respectively).

4.4.1.5. *Effects of AN on Hearing*

AN is one of a number of organic compounds that have been shown to promote noise-induced hearing loss (NIHL) in rats (Fechter, 2004; Fischel-Ghodsian et al., 2004). The ototoxicity of AN was examined in several experiments in male Long-Evans rats exposed by s.c. injection (Fechter et al., 2003). The AN used in these experiments was stabilized to minimize the accumulation of peroxides. Ten rats were anesthetized and surgically prepared for the assessment of the compound action potential (CAP), which represents the synchronous neural activity elicited by primary auditory neurons (spiral ganglion cells) and directly measures auditory threshold sensitivity. Auditory thresholds at each test frequency were measured for each rat under anesthesia on 20 different occasions before treatment with AN to determine baseline auditory thresholds. Auditory thresholds for 11 test frequencies between 2 and 40 kHz were recorded at 5-minute intervals up to 100 minutes postinjection with AN. The acute effect of 50 mg/kg s.c. AN on auditory sensitivity was studied in five rats; five control rats were injected only with water. In a second study, the effects of AN on permanent NIHL were evaluated in six experimental groups (six rats each) that received the following: no treatment; 50 mg/kg AN alone, two injections of 50 mg/kg-day AN on 2 consecutive days, noise alone (108 dB octave-band noise for 8 hours), single injection of 50 mg/kg AN immediately followed by noise, and exposure to noise after a second injection of AN.

The acute study showed that exposure to 50 mg/kg AN s.c. alone elevated auditory threshold temporily and produced a 10–20 dB loss in auditory threshold sensitivity (temporary threshold shift) in the stimulus range of 8–40 kHz (Fechter et al., 2003). This transient loss reached a maximum within 10–20 minutes after injection but returned to control levels within 75–100 minutes. In the study on permanent auditory threshold shifts, when rats were tested 3 weeks following AN and AN + noise treatment, exposure to AN alone did not produce a persistent loss in auditory threshold sensitivity. AN-treated rats had slightly reduced auditory threshold compared with controls, indicating slightly increased sensitivity (within 5 dB of controls), but the difference was not statistically significant. Noise treatment alone elevated auditory thresholds by less than 20 dB at all tested frequencies. However, rats given two injections of AN followed by noise in the high frequency range of 12–40 kHz exhibited auditory

impairments averaging 27 dB (maximally 40 dB) compared with controls; this shift was statistically significant compared with other groups (controls, noise alone, AN alone, or no treatment). Rats given a single injection before exposure to noise showed an average 11 dB threshold shift in the high-frequency range (12 and 40 kHz). This study demonstrates that exposure to AN exacerbated NIHL.

Fechter et al. (2003) also assessed blood cyanide and glutathione levels in brain, liver, and paired cochleae in additional groups of rats exposed to AN. Groups of five rats given 20, 50, or 80 mg/kg s.c. AN produced peak levels of cyanide, a metabolite of AN, in the blood at 1 hour (for 20 and 50 mg/kg) and 2 hours (for 80 mg/kg) following injection. Cyanide levels returned to baseline values within 2, 3, and 4 hours, respectively. Since AN produced maximal auditory threshold impairment within 20 minutes of administration, before blood cyanide level peaked at 1 hour, the acute ototoxic effect of AN was not likely associated with elevated cyanide levels.

When rats were given a single injection of 50 mg/kg, maximal reductions in glutathione levels (measured between 15 minutes and 8 hours postinjection) were detected in the brain by 15 minutes (–50%), in the liver by 1 hour (–80%), and in the cochlea by 2 hours (–45%). Cochlear glutathione levels remained depressed for about 4 hours. Recovery of glutathione levels to near control levels was achieved in all tissues by 8 hours. Since AN induced transient cochlear function loss that peaked within 10–20 minutes after injection and recovered within 75–100 minutes, the acute ototoxic effect of AN could not be associated with GSH level in the cochlea. Fechter et al. (2003) concluded that, while AN-induced oxidative stress in the cochlea may play a role by which AN promotes NIHL, the acute ototoxic effect of AN might reflect other unidentified toxic action of AN in the cochlea.

Fechter et al. (2004) extended their evaluation of the potentiation effect of AN exposure on NIHL. Two experiments were conducted: the first experiment studied the effects of a single AN exposure on permanent NIHL, while the second one evaluated the effects with five daily AN and noise exposures. In both experiments, six male Long-Evans rats were assigned to each treatment group: AN alone, noise alone, AN + noise, and untreated controls. AN exposed groups were given s.c. injections of 50 mg/kg-day AN, with or without 4 hours of exposure to noise (105 dB), and then assessed for auditory threshold sensitivity 4 weeks later.

In the single-day treatment study, AN alone did not alter the auditory threshold, but a single AN exposure in combination with noise significantly elevated auditory thresholds by an average of 10 dB above the effect of noise alone. Noise exposure alone increased auditory thresholds compared with controls by an average of 10 dB in the range of 12–40 kHz (Fechter et al., 2004). In the 5 consecutive-day treatment study, AN plus noise treatment exacerbated the impairment induced by noise alone by an average of 30–45 dB at frequencies between 20 and 40 kHz and by no more than 10 dB at frequencies <16 kHz. Similar to the single-exposure study, repeated AN exposure had no effect on auditory thresholds assessed 4 weeks later. Repeated noise exposure elevated auditory thresholds about 17 dB above control rats.

When the reactive-oxygen scavenger phenyl-N-tertiary-butylnitrone (PBN) (100 mg/kg i.p.) was injected twice daily for 5 days prior to exposure to noise alone and rats were assessed 4 weeks later, PBN reduced the magnitude of hearing loss. When PBN was injected daily prior to the injection of AN and again following noise exposure, the magnitude of hearing loss was equivalent to that exhibited by rats treated by noise alone. (No significant difference was found between rats receiving noise alone and those receiving PBN plus noise.) These results indicated that reactive oxygen species (ROS) were responsible for the ototoxic effects of AN. These findings are consistent with the suggestion that mitochondria injury within cochlear cells, primarily or secondarily through oxidative stress, may be a common feature of ototoxicity induced by chemicals and noise (Fischel-Ghodsian et al., 2004).

Results from a recent study indicated that hearing loss from AN and noise exposure involves histologic damage to hair cells on the surface of the organ of Corti (Pouyatos et al., 2005). Groups of five male Long-Evans rats were given s.c. injections of 0 or 50 mg/kg-day AN for 5 consecutive days, with or without exposure 30 minutes later to noise for 4 hours/day (95 or 97 dB octave-band noise at 8 kHz). Hearing dysfunction of these rats were then assessed by: (1) distortion product otoacoustic emissions (DPOAEs) before exposure, as well as 1 hour and 4 weeks postexposure; (2) CAP for auditory threshold sensitivity 4 weeks after the last treatment; and (3) number of hair cells on surface preparation of the organ of Corti 4 weeks after treatment. Permanent effects on these endpoints (i.e., effects observed 4 weeks following the last treatment) were only observed in rats exposed to both AN and noise and not in rats exposed to AN or noise alone. Permanent effects from combined exposure to AN and noise included auditory threshold shifts (13–16 dB between 7 and 40 kHz), a decrease in DPOAE amplitudes (up to 25 dB at 19 kHz), and significant outer hair cell (OHC) loss in the cochleae. With the AN plus 97 dB treatment, average OHC loss was 20, 16, and 9% in the first, second, and third rows, respectively, in the areas corresponding to frequencies ranging from 13 to 47 kHz. Similar effects were found in the AN plus 95 dB treatment group. This study demonstrated AN could potentiate NIHL at noise levels that are relevant to human exposure.

Pouyatos et al. (2007) further proposed that AN exacerbated NIHL by decreasing antioxidant defenses of hair cell. This hypothesis was tested in a study in which the capability of specific antioxidants in the protection of the cochlea of male Long-Evans rats treated with 50 mg/kg AN s.c. 30 minutes prior to the daily noise exposure of 97 dB sound pressure level 4 hours/day for 5 days. Sixty-five Long-Evans rats (2–12/group) were exposed to different combinations of noise, AN, and antioxidants; AN alone or AN + STS (150 mg/kg i.p.), a CN inhibitor; AN + 4-methylpyrazole (4MP,100 mg/kg i.p.), a drug that blocks CN generation by competing with CYP2E1; AN + L-N-acetylcysteine (L-NAC) (4 × 400 mg/kg, orally), a pro-GSH drug; noise (97 dB octave band of noise [OBN]/8 kHz) alone; noise and STS, 4MP, or L-NAC; or noise plus AN and antioxidants. To evaluate auditory impairment, DPOAEs and CAPs were measured prior to experimental treatment and 3 days and 4 weeks after treatment. At

the end of exposure, cochleae were harvested for histologic examination. Additional rats (n = 64) were used to measure cochlear and liver GSH and blood CN levels at different time points after treatment.

At 3 days postexposure, similar auditory loss was found in animals exposed to AN + noise, STS + AN + noise, 4MP +AN + noise, and L-NAC + AN + noise. The maximum shifts averaged 25–30 dB between 12 and 32 kHz. At 4 weeks postexposure, animals exposed to L-NAC + AN + noise recovered to baseline levels above 25 kHz. However, at lower frequencies, L-NAC did not prevent auditory loss caused by AN + noise exposure. Animals received combined exposure to AN + noise, and AN + noise + STS or AN + noise + 4MP showed little change in producing auditory loss.

In addition, the cochleae from rats exposed to AN and noise demonstrated substantial damage in the basal half of the organ of Corti. Mean OHC loss averaged 35% in the three rows in the region corresponding to frequencies above 12 kHz. Neither STS nor 4MP pretreatment protected against OHC loss caused by AN + noise. However, pretreatment with L-NAC reduced the OHC loss caused by AN + noise in the region corresponding to 25 kHz and above.

Liver GSH level was depleted by 63% 1 hour after AN injection. Cotreatment with STS or 4MP reduced GSH level about 80% at 1 hour and 52% at 3 hours. However, with L-NAC pretreatment, GSH level was reduced only by 23 and 20% at 1 and 3 hours, respectively. Similarly, whereas AN treatment depleted cochlear GSH levels to undetectable levels at 1 hour, STS pretreatment had no effect on GSH depletion. 4MP pretreatment only slightly reduced GSH depletion. However, L-NAC pretreatment not only protected but induced an increase in GSH levels above control levels. Pouyatos et al. (2007) concluded that, since L-NAC cotreatment reduced auditory loss and OHC loss from AN + noise treatment, GSH is involved in the protection of the cochlea against ROS generated by moderate noise levels. However, CN did not appear to be involved in this potentiation.

4.4.2. Immunological Effects of AN

A case study by Balda (1975) described a human subject who developed contact dermatitis following the use of a Plexidur finger splint. Investigators obtained a positive result in a patch test with AN, which is one of the constituents of the polymer Plexidur. This observation suggested that AN might induce immunological response in exposed subjects.

The immunotoxicity of AN was evaluated in groups of six male CD-1 mice given a single oral dose in water or repeated oral doses for 5 or 14 days (Ahmed et al., 1993). In each of these experiments, a positive control group received a single immunosuppressive dose of 225 mg/kg of cyclophosphamide i.p. In the first experiment, mice given a single gavage dose of 0 or 13.5 mg/kg AN in water were evaluated 3 or 5 days later for BW, relative organ weights (thymus, spleen, liver, and kidney), number of viable splenocytes, and total and differential WBC counts in spleen cells suspension (Ahmed et al., 1993). AN slightly reduced BWs in mice

(6–7%) after 3 and 5 days, but the difference was not biologically significant. In treated mice, relative spleen weights were increased by 50% after 5 days, whereas relative thymus weights were decreased by 42% after 5 days; relative liver weight was decreased by 11% on day 3 but was 9% higher than controls on day 5. AN treatment reduced total leucocytes by 42–57%, lymphocytes by 39 and 65%, monocytes by 38 and 50%, and neutrophils by 67 and 73% on days 5 and 3, respectively.

In the second experiment, mice received 0 or 6.75 mg/kg-day of AN in water on 5 consecutive days and were evaluated on day 6 (Ahmed et al., 1993). In mice treated for 5 days, BWs were reduced by 27%, relative liver weights were decreased by 10%, and relative spleen weights were increased by 25%. Total splenocytes were decreased by 51%, with total blood leucocytes and lymphocytes reduced by 48 and 68%, respectively; circulating monocytes were increased by 88%. The immunotoxic effects of AN in both studies were comparable to effects elicited by the known immunosuppressant cyclophosphamide.

In a third experiment, groups of male CD-1 mice (six/group) were treated with AN by gavage in water for 14 days (Ahmed et al., 1993). There were a total of nine groups: three groups dosed with AN at 1.35, 2.7, or 5.4 mg/kg-day only, three groups dosed the same way but immunized with sheep red blood cells (SRBCs) on day 9 of exposure, and three concurrent control groups (normal, SRBC-immunized, and a positive control group treated intraperitoneally with cyclophosphamide [225 mg/kg] 1 day before immunization). Mice were evaluated for total BW, relative organ weights (thymus, spleen, liver, and lung), number of splenocytes, total and differential WBC counts in spleen cell suspensions, and histopathology of lymph nodes, lung, and intestinal Peyer's patches. Subsets of spleen lymphocytes (T and B cells) were enumerated by flow cytometry. Spleen cells from mice immunized with SRBCs were evaluated in a plaque-forming cell assay.

In nonimmunized mice, AN decreased BW by 12–15% and increased relative thymus weights by 43% at 2.7 mg/kg-day and relative lung weights by 39% at 5.4 mg/kg-day. AN increased splenocyte viability by 49–264% in a dose-independent manner. AN also caused dose-independent increases of 126–293% in relative spleen weight at all doses. Total leukocyte counts/spleen were increased by 171, 119, and 107% at the low to high doses; lymphocyte counts/spleen were significantly reduced by 25–45% at all doses, while monocyte and neutrophil counts/spleen were increased concomitantly by as much as 78-fold. Reductions in lymphocyte subsets were observed at all doses: T-cells by 40–53%, B-cells by 32–36%, T-helper cells by 40–59%, and T-suppressor cells by 49–62%. Histological examination revealed severe enlargement of mesenteric lymph nodes and intestinal Peyer's patches, abscesses and massive necrotic damage in the lung, and swellings in the brachial lymph nodes in mice treated with AN at all doses but more aggressive in the 5.4 mg/kg group. No incidence data were reported for these lesions. Some of the mice treated with 5.4 mg/kg-day died rapidly. Microbiological

examination revealed the swelling in the lymph nodes was related to migration of normal intestinal flora, which the study authors attributed to immunosuppressive effects of AN.

In the SRBC-immunized mice, AN treatment did not affect the BW. The relative weight of lung, liver, and thymus showed inconsistent and dose-independent increases. The viable spleen cells showed 77% increases only in the 2.7 mg/kg group. The lymphocytic count showed dose-independent decreases. However, the neutrophilic and monocytic counts showed large increases at all doses. Decreases in lymphocyte subsets were found in all three doses of AN: T-cells by 42–45%, B-cells by 37–50%, T-helper by 43–54%, and T-suppressors by 40–48%. The IgM antibody plaque forming cell response was decreased by 55, 23, and 65 after treatment with 1.35, 2.7, and 5.4 mg/kg AN, respectively. The lowest dose used in this study, 1.35 mg/kg-day, was a LOAEL for immunotoxicity (suppression of humoral and cell-mediated immunity) in mice treated for 14 days.

Hamada et al. (1998) further investigated the immunotoxicity of AN by administering 2.7 mg/kg-day AN (1/10 the LD_{50}) to male CD-1 mice orally for either 5, 10, or 15 days. All mice were injected with 100 mg/kg bromodeoxyuridine (BrdU) i.p. 1 hour before sacrifice. An immunohistochemical assessment of the number of cells capable of producing IgA in different intestinal compartments as a result of AN administration was conducted. Uptake of ^{3}H-thymidine into splenocytes derived from treated animals and stimulated with different mitogens—phytohemagglutinin (PHA), concanavalin-A (con-A), or lipopolysaccharide (LPS)—was measured. The rate of proliferation of gut epithelial cells of different intestinal compartments was determined by the incorporation of BrdU in newly synthesized DNA of S-phase cells.

The mitogenic response of mouse splenocytes to PHA, con-A, and LPS was affected by AN exposure as shown by a significant decrease in [^{3}H]-thymidine incorporation (Table 4-49). The decreases were 68–79% with con-A and 35–57% with LPS, depending on the time intervals. However, uptake of [^{3}H]-thymidine by splenocytes after stimulation with PHA was markedly reduced only after 15 days of exposure. These results suggested that AN induced systemic suppression of humoral immunity (by the decrease in mitogen response to LPS) and cell-mediated immunity (by the inhibition of mitogen response to con-A and PHA).

Table 4-49. Time course of the effect of AN administration on [^{3}H]-thymidine uptake into mouse splenocytes under the influence of different mitogens in vitro

Mitogens	Control	D of AN treatment		
		5	10	15
PHA[a]	1,331 ± 163	1,203 ± 265	1,434 ± 35	898 ± 32[b]
con-A[a]	14,927 ± 972	4,756 ± 532[b]	4,792 ± 946[b]	3,198 ± 448[b]
LPS[a]	1,225 ± 112	803 ± 87[b]	486 ± 2[b]	522 ± 31[b]

[a]Values are counts/min, mean ± standard error of the mean; n = 4.
[b]Significantly different from controls ($p < 0.05$) as calculated by the authors.

Source: Hamada et al. (1998).

Inhibition of [^{3}H]-thymidine uptake by stimulated spleen lymphocytes may indicate a systemic immunosuppression by AN. Such an effect could also occur locally, as indicated by a reduction in the number of IgA-producing cells in all intestinal compartments following AN administration. The counts of IgA-producing cells were reduced by 56–77% in the duodenum, 44–67% in the jejunum, and 60–62% in the ileum. Another local effect of AN was demonstrated by the increased incorporation of BrdU into epithelial cells of the duodenum (threefold) and ileum (1.6-fold) of AN-treated animals. This result indicated that the rate of cell proliferation was markedly increased following oral AN administration, even as a result of short-term treatment. The study authors considered this to be the result of a regenerative response to chemically induced intestinal injury and suggested that AN-induced immunosuppressive effect systemically and locally in the gut, as well as increases in the rate of cell proliferation, may contribute to carcinogenicity of AN in the gut.

Summary

AN caused contact dermatitis in a human subject exposed via the use of Plexidur finger splint. In mice, AN suppressed cell-mediated and humoral immunity systemically and locally in the intestine. Table 4-50 summarizes immunotoxicity studies of AN.

Table 4-50. Summary of immunotoxicity studies of AN

Test species	Endpoint/effect	Exposure concentration/condition	Exposure duration	Results	References
Human subject	Contact dermatitis	Use of a Plexidur finger splint	ND	Positive patch test	Balda, 1975
Male CD-1 mice (n = 6)	Immunosuppressive Effect	Study 1: Single dose of 0 or 13.5 mg/kg AN in water (oral) 225 mg/kg cyclophosphamide as positive control	3 or 5 d	Increased relative spleen by 50%, decreased relative thymus weight by 42%, reduction in total leucocytes, lymphocytes, monocytes, and neutrophils.	Ahmed et al., 1993
		Study 2: 0 or 6.75 mg/kg-d AN in water 225 mg/kg cyclophosphamide as positive control.	5 d	Increased relative spleen weights by 25%; decreased total spenocytes by 51%; reduction in total blood leucocytes and lymphocytes by 48 and 68%, respectively.	
		Study 3: a. Three groups dosed with 1.35, 2.7, or 5.4 mg/kg-d AN b. Three groups dosed with 1.35, 2.7, or 5.4 mg/kg-d AN, but immunized with SRBCs on d 9 of exposure c. Three concurrent control groups (normal, SRBC-immunized) d. a positive control group treated intraperitoneally with cyclophosphamide (225 mg/kg) 1 d before immunization	14 d	In nonimmunized mice: increased spleen weight at all doses, increased total leukocyte counts, reduced lymphocyte counts/spleen, and increased monocyte and neutrophil counts/spleen. Enlargement of mesenteric lymph nodes and intestinal Peyer's patches, swellings in the brachial lymph nodes for all dose groups. In the SRBC-immunized mice: viable spleen cells showed 77% increase in the 2.7 mg/kg group. Decreases in lymphocyte count, increases in neutrophilic and monocytic counts, and decreases in plaque forming cell response were observed. The LOAEL for immunotoxicity was 1.35 mg/kg-d.	

Table 4-50. Summary of immunotoxicity studies of AN

Test species	Endpoint/effect	Exposure concentration/condition	Exposure duration	Results	References
Male CD-mice	Systemic and local immunosuppression	2.7 mg/kg-d AN orally	5, 10, or 15 d	Decrease ^{3}H-thymidine incorporation into splenocytes in: (1) mice treated with mitogens con-A or LPS, suggesting systemic suppression of cell-mediated immunity, and (2) mice treated with mitogen PHA, suggesting systemic suppression of humoral immunity. Local immunosuppression in the gut, as indicated by: (1) reduction in the number of IgA-producing cells in all intestinal compartments, and (2) increased proliferation of epithelial cells of the duodenum.	Hamada et al., 1998.

4.5. MECHANISTIC DATA AND OTHER STUDIES IN SUPPORT OF THE MODE OF ACTION

4.5.1. Mode-of-Action Studies

Studies have been conducted with the primary purpose of evaluating the potential mechanisms by which AN and/or its metabolites produce noncancer and cancer effects in experimental animals. Studies that investigated potential mechanisms for noncancer effects include GI hemorrhaging, effects on Hb and metabolism in RBCs, neurotoxicity, oxidative stress, and immunotoxicity. Studies that investigated the potential mechanisms for the carcinogenicity of AN include formation of DNA adducts, oxidative stress, intercellular communication, and cell proliferation. In addition, genotoxicity studies are described in Section 4.5.2.

4.5.1.1. *Noncancer Endpoints*

4.5.1.1.1. *GI hemorrhaging.* Ghanayem and Ahmed (1983) administered AN to male Sprague-Dawley rats by both s.c. or oral routes, in each case observing significant gastric bleeding (see Section 4.4.1.1). The response appeared to peak at 50 mg/kg, the effect being maximal at 2 hours after a 50 mg/kg s.c. dose. Different CYP450 inducers had different effects: Aroclor 1254 more than doubled the effect, while PB reduced the bleeding by half. CYP450

inhibitors SKF 525A and cobalt chloride were even more effective, with cobalt chloride reducing gastric bleeding to almost untreated levels. GSH depletion by DEM did not prevent hemorrhaging. The effect was not due to cyanide release from AN, since KCN administration (6 mg/kg) did not induce bleeding. The results indicated that the gastric hemorrhaging was caused by metabolic activation of AN to a reactive metabolite other than cyanide (probably CEO).

As described in Section 4.4.1.1, the follow-up study by Ghanayem et al. (1985) demonstrated that pretreatment of rats with sulfhydryl-containing compounds or atropine protected the rats from AN-induced lesions. The findings suggested that modulation of muscarinic receptors by AN increased gastric acid secretion and caused gastric mucosal erosions.

4.5.1.1.2. ***Effects on Hb and metabolism in RBCs*.** Farooqui and Ahmed (1983b) studied the effect of AN on Hb and metabolism in RBCs both in vivo and in vitro. Male Sprague-Dawley rats (three/group) were administered a single oral dose of 80 mg/kg aqueous AN, and blood was collected 1 hour after treatment. Other groups of animals were sacrificed at 3, 6, and 24 hours after dosing. Mean cell Hb concentration, hematocrit, and platelet counts were reduced to 78, 79, and 71% of the controls 1 hour after dosing. GSH levels were lowered significantly within 1 hour. Among the metabolic intermediates measured, a reduction in the intracellular concentration of 2,3-diphosphoglyceric acid and increases in intracellular levels of ATP, pyruvate, and lactate were observed. The increase in the levels of pyruvate and lactate, which were end products of glycolysis, suggested an increase in the metabolic rate in RBCs as a result of exposure to AN (Table 4-51). A significant decrease in the activity of 2,3-diphosphoglycerate mutase, an erythrocyte enzyme, was found in treated animals (3.61 ± 0.21 IU/g Hb in treated animals after 1 hour vs. 4.57 ± 0.23 IU/g Hb in controls). In general, the intermediates studied returned to normal values between 6 and 24 hours.

Table 4-51. Effect of AN on RBC metabolic intermediates following a single oral dose

Intermediates (µmol/mL blood)	Control	AN treatment			
		1 hr	3 hrs	6 hrs	24 hrs
2,3-Diphosphoglycerate	3.6 ± 0.3	2.8 ± 0.2[a]	3.0 ± 0.4	3.2 ± 0.3	3.7 ± 0.5
Adenosine triphosphate	0.49 ± 0.04	0.60 ± 0.05[a]	0.64 ± 0.06[a]	0.66 ± 0.06[a]	0.58 ± 0.05
Pyruvate	58 ± 6	227 ± 21[a]	187 ± 13[a]	175 ± 16[a]	167 ± 11[a]
Lactate	1,478 ± 131	9,932 ± 211[a]	1,889 ± 129[a]	1,955 ± 160[a]	2,079 ± 151[a]
GSH	1.39 ± 0.11	0.28 ± 0.02[a]	0.34 ± 0.04[a]	0.47 ± 0.05[a]	1.27 ± 0.15

[a]Significantly different from controls ($p < 0.05$) as calculated by the study authors.

Source: Farooqui and Ahmed (1983b).

In another study, male Sprague-Dawley rats were treated with single oral doses of 46.5 mg/kg [2,3-^{14}C]-AN (Farooqui and Ahmed, 1983b). RBC GSH concentrations were lowered to 10% of controls in 1 hour, followed by a slow recovery of 10% in 5 hours. Extensive covalent binding of AN to Hb (about 1.7 μmol equivalents of AN bound/mL RBCs) in 1 hour was also observed.

For the in vitro study, isolated RBCs from male Sprague-Dawley rats were incubated with 5 mmol/L AN at 37°C to investigate the ability of AN to interact covalently with Hb and deplete GSH, and the effect of such depletion on Hb (Farooqui and Ahmed, 1983b). GSH in the supernatant and in the RBCs was estimated by measuring nonprotein sulfhydryl groups. In addition, the levels of Hb and MetHb and GSH conjugates with AN were monitored.

Incubation of rat RBCs with AN caused a depletion of more than 85% of intracellular GSH within 1 hour. No hemolysis occurred during the incubation period. In addition, GSH was not detected in the incubation media. Most of the GSH in the RBCs was converted to a GSH-AN conjugate, S-cyanoethyl GSH. This conjugate was present in the RBCs after 24 hours, suggesting that it was not metabolized further at least for 24 hours. Moreover, about 6% of Hb was converted to MetHb in 1 hour and 8% in 3 hours (Farooqui and Ahmed, 1983b). MetHb levels in controls during this time period were 0.61–0.87%.

The rate and extent of MetHb reduction to Hb in AN-treated RBCs was also determined to investigate if this protective mechanism against such oxidative damage to Hb was affected. Incubation of nitrite-treated RBCs (for conversion of Hb in RBCs to MetHb) with AN resulted in a significant decrease in MetHb reduction, with a 70% decrease in RBCs treated with 10 mM AN when compared with controls. In the same experiment, AN initiated hemolysis of RBCs at a concentration of <0.1 M.

Farooqui and Ahmed (1983b) suggested that the effects of AN on RBC metabolism were related to the availability of GSH. Oxidative stress induced by depletion of GSH as a result of AN exposure may have stimulated the rate of RBC metabolism, based on increase in the end products of glycolysis. Another possible explanation could be the impaired permeability of the erythrocyte membrane due to extensive covalent binding of AN, resulting in the retention of metabolic products. Since the levels of ATP and 2,3-diphosphoglycerate were altered and these two intermediates regulate the oxygen dissociation curve, it was concluded that chronic exposure to AN may lead to methemoglobinemia, damage to the RBC membrane, and impaired delivery of oxygen to tissues.

Farooqui et al. (1990) provided in vitro data on the effect of AN on lipid metabolism in RBCs. Three types of RBC preparations from male Sprague-Dawley rats were incubated with AN: those containing oxyhemoglobin (HbO), those containing MetHb, and those containing carboxyhemoglobin (HbCO). HbO-containing RBCs were taken directly from the RBC pellet; MetHb-containing RBCs were produced by incubating packed RBCs with 0.5% sodium nitrite; while RBCs containing HbCO were prepared by blowing carbon monoxide over a 20%

suspension (volume/volume [v/v]) of RBCs until the visible spectrum of red cell lysate reached a maximum at 570 nm. All preparations of RBCs were incubated for 1 hour with 10 mM AN and variable additions of glucose. Following incubation, supernatants were removed and used to estimate lipid peroxidation by measuring the concentration of conjugated dienes, while the red cell pellets were used to determine Hb. In another set of experiments, isolated rat red cell membranes were incubated with 25 mM AN at different temperatures. Total and Na^+/K^+-ATPase activity were measured in control and AN-incubated red cell membranes.

Incubation of HbO-containing RBCs with AN resulted in the formation of MetHb, loss of intact Hb, and membrane lipid peroxidation. The availability of glucose to HbO-RBC incubation reduced the formation of MetHb by 33% and the loss of intact HbO by 33% but increased lipid peroxidation by 35%. As a positive control, HbO-containing RBCs were incubated with 0.1 mM t-butyl hydroperoxide, a strong GSH depleter. The formation of MetHb and non-intact Hb in the positive control was 3 and 5 times higher than that in AN-incubated RBCs. Incubation of MetHb-containing RBCs with AN also resulted in the loss of intact Hb and membrane lipid peroxidation. However, availability of glucose resulted in only 13% increase in peroxidation of membrane lipids. Lipid peroxidation was about 3 times higher in incubations of HbCO-containing RBCs with AN, with or without glucose, than the other two RBC preparations. The extent of lipid peroxidation in RBCs and isolated RBC membranes was dependent on the concentrations of AN.

Farooqui et al. (1990) also demonstrated an inverse relationship between GSH concentrations and lipid peroxidation in RBCs incubated with AN. A 75% reduction in GSH levels in RBCs was observed as a result of AN incubation for 2 hours, with the half-life of GSH depletion being less than 22 minutes. The concentration of lipid peroxides increased by 274% over control levels during the same period.

In addition, Farooqui et al. (1990) showed that Na^+/K^+-ATPase activity was reduced in the isolated RBC membranes incubated with AN (release of inorganic phosphate: 87.9 ± 9.1 vs. 145.6 ± 13.1 nmol/mg protein per hour at 37°C; and 4.3 ± 0.7 vs. 87.9 ± 9.1 nmol/mg protein per hour at 15°C). The degree of AN-induced inhibition of ATPase was temperature dependent. The K_m of Na^+/K^+-ATPase (3.5 mM at 37°C) was barely affected by the AN treatment, while the V_{max} was significantly lower (–36%) than that of controls. This noncompetitive inhibition of Na^+/K^+-ATPase by AN was proposed to be the result of changes in the physicochemical properties of RBC membrane macromolecules subsequent to irreversible binding of AN to membrane proteins.

In summary, Farooqui et al. (1990) demonstrated that AN induced GSH depletion, elevated lipid peroxidation, and enhanced concentration of MetHb in RBC, as well as inhibited Na^+/K^+-ATPase activity in RBC membrane.

4.5.1.1.3. ***Neurotoxicity.*** Campian et al. (2002) evaluated the capacity of AN to inactivate the important glycolytic enzyme, glyceraldehyde-3-phosphate dehydrogenase (GAPDH) in vitro in order to elucidate the mechanism for the acute toxicity of AN. GAPDH was incubated with AN (final concentrations ranged from 50 to 400 μM), and the activity of GAPDH was assayed at different time points. An irreversible inhibition of GAPDH activity was obtained. Incubation of GAPDH with 200 μM AN resulted in 90% loss of activity in about 60 minutes. The second-order rate constant for inhibition of GAPDH activity was measured as 0.2 M^{-1} s^{-1} at pH 7.4 and 37°C.

The site of AN incorporation was identified by using matrix-assisted laser desorption ionization time-of-flight mass spectrometry to analyze tryptic digests of control and AN-labeled GAPDH (Campian et al., 2002). Inactivation of GAPDH was due to covalent binding of AN to cysteine 149 at the active site of the enzyme. This finding demonstrated the specificity of AN binding to cysteine residues and, more widely, implied the ability of AN to impair glycolytic ATP production in vivo. Campian et al. (2002) speculated that the combination of glycolytic ATP production impairment with inhibition of mitochondrial ATP synthesis by the AN metabolite cyanide could result in metabolic arrest. This might have profound consequences for the toxicity of AN in sensitive tissues such as the brain.

In a followup study (Campian et al., 2008), male Sprague-Dawley rats (3-5/group) were injected subcutaneously with LD_{90} (115 mg/kg) AN and the brains of treated rats were frozen when respiration ceased via head immersion (HI) in liquid nitrogen or funnel freezing (FF) technique. Only minor decreases in ATP of 5% (FF) and 21% (HI) were found when respiration ceased, although phosphocreatine was decreased by 74% (FF) and 80% (HI), possibly due to inhibition of creatine kinase by AN. Campian et al. (2008) concluded that no toxicological relevant depletion of ATP occurred when respiration ceased in AN treated rats. Hence, the acute lethality of AN was not due to brain metabolic arrest.

Dorman et al. (1996) investigated the mechanisms by which AN and CEO exert neurotoxic effects in primary dissociated cerebrocortical cell cultures prepared from GD16-18 CD rats. Mature 7-day old cultures were exposed to 0-10 mM AN or 1-2 mM CEO for 8 h at 37°C. Cytotoxicity was evaluated by measuring leakage of LDH, GSH depletion, inhibition of acetylcholinesterase (AChE) and histopathology.

Both AN and CEO induced dose-dependent increased in cytoxicity. Significant increase in LDH-leakage was observed in neural cultures following 8 h exposure to 2.5-10 mM AN or 0.125 – 1 mM CEO. Significant reduction in GSH only occurred following exposure to 5 mM AN. Thus, Dorman et al. (1996) concluded that GSH depletion probably played a limited role in the development of AN toxicity. No change in AN-induced cytotoxicity was observed following cotreatment with the cytochrome P-450 inhibitor 1-phenylimidazole, indicating minimal metabolism of AN to CEO in the neural cells. AChE inhibition was not observed following 8 h exposure up to 2.5 mM AN. Widespread necrosis of the small, round cholinergic neurons was

present in the cultures treated with 2.5 mM AN or 0.125 mM CEO for 8 h. Astrocytes, pyramidal neurons, and bipolar neurons were mostly unaffected. On the other hand, treatment of cell cultures with ≥0.6 mM cyanide resulted in extensive loss of cytochrome oxidase activity in the large pyramidal neurons without a concomitant increase in LDH leakage. Dorman et al. (1996) concluded that AN may selectively destroy cholinergic neurons and induce neurotoxicity in rats, and that AN metabolism to cyanide was not a prerequisite for the development of AN-induced neurotoxicity.

Satayavivad et al. (1998) provided some evidence for the alterations of central muscarinic functions from subchronic exposure to AN. Either 0, 1, or 25 mg/kg AN was injected subcutaneously to male Wistar rats (10/group) 5 days/week for 8 weeks. The authors studied the impact of AN on motor behavioral activities by using a computerized system to chart the movements of rats within the cage. The system provided information on a total of 11 motor behavioral parameters, such as distance traveled/time interval, resting time, time spent moving, and number of clockwise and counterclockwise rotations. This test model can be used to detect subtle changes of central muscarinic receptors during exposure to cholinomimetic agents. Evaluations were carried out on each animal on day 5 of weeks 1, 2, 4, 6, and 8, 1 hour after treatment with AN.

Both doses of AN were associated with marked decreases in all motor activities and a concomitant increase in the resting time of treated rats compared with controls (Satayavivad et al., 1998). There was a decrease in all motor parameter values at weeks 1 and 2, but most of these effects were diminished by weeks 4 and 6. However, the effects of the high dose of AN were more pronounced and longer lasting. Thus, the incidence of clockwise and counterclockwise rotations in high-dose rats was reduced compared with controls throughout the study (for example, 0.7 ± 0.3 [high dose], 2.6 ± 0.8 [low dose], and 2.8 ± 0.4 [controls] counterclockwise rotations/10-minute study period after 8 weeks). The effects of intramuscular injection of the muscarinic receptor antagonist, atropine, and the reversible acetylcholinesterase inhibitor, physostigmine, with and without concurrent AN administration, also were evaluated in this system. Atropine administration (10 mg/kg) was associated with increases in motor activity that were enhanced by AN treatment at 25 mg/kg. Physostigmine (0.5 mg/kg) caused reductions in motor activity irrespective of AN administration. Satayavivad et al. (1998) concluded that AN possesses cholinomimetic effects, one of which might include the down-regulation of muscarinic receptors. This would explain the marked increase in the response to atropine. Since AN did not inhibit the activity of acetylcholinesterase, the cholinomimetic effect of AN might be mediated by the release of acetylcholine from nerve endings.

Jacob and Ahmed (2003b) studied AN-induced neurotoxicity by exposing proliferating normal human astrocytes (NHAs) in culture to 25–400 μM AN for 12 hours. Assessment was then made on cell viability, levels of endogenous antioxidants, GSH, catalase, levels of ROS, and secretion of tumor necrosis factor (TNF-α), a cellular marker for oxidative stress and oxidative

damage to nuclear DNA. Treatment with 25–50 μM AN had no significant effect on viability of the astrocytes. At 100–400 μM AN, 15–42% reduction in cell viability was observed (as indicated by trypan blue exclusion). Reduced viability was further substantiated by 8–40% increased cytotoxicity (as indicated by leakage of LDH). The morphology of astrocytes was normal at concentrations up to 200 μM, but cells exposed to 400 μM AN showed a larger number of swollen nuclei and enlarged membrane structures.

Intracellular levels of GSH were not affected at 25 and 50 μM AN. However, a significant dose-dependent decrease in GSH was observed at 100, 200, and 400 μM AN (18, 28, and 35% lower than controls, respectively). A concomitant increase in levels of oxidized GSH (glutathione disulfide [GSSG]) was observed (Jacob and Ahmed, 2003b). The ratio of GSH to GSSG was reduced from the control value of 37–18, 7, 3, and 2 at 50, 100, 200, and 400 μM AN, respectively. Compared to control level, catalase activity increased 21% at 100 μM AN, but declined to 37% below control levels at 400 μM.

Significant increases in measures of oxidative stress (four- to sevenfold increase in the generation of ROS) and oxidative DNA damage (greater than twofold increase in 8-oxodeoxyguanosine [8-oxodG]), were observed at 200–400 μM AN. Treatment at 400 μM significantly increased the release of the inflammatory cytokine, TNF-α, by 30% compared with controls. The observation that compromised antioxidant defense mechanisms (depletion of glutathione, increase in GSSG, inhibition of catalase) occurred at the same exposure concentration as reduced cell viability supported the hypothesis that oxidative stress in astrocytes was a possible mechanism for neurotoxic effects of AN exposure.

In a translated Chinese study (Lu et al., 2005b), levels of monoamine neurotransmitters and their metabolites were measured in the striatum and cerebellum of the brains of male Sprague-Dawley rats (n = 10 per group, 7 selected randomly for measurement) exposed to 0, 50, or 200 ppm AN in drinking water for 12 weeks. The study authors estimated the administered doses to be 4.0 and 13.5 mg/kg-day for the 50 and 200 ppm groups, respectively. Monoamine oxidase activity in the cerebral cortex was also measured.

Compared with control values, average dopamine levels in the striatum were decreased by 76 and 64% in the 50 and 200 ppm groups, respectively, and by 46 and 18% in the cerebellum. The decreases in dopamine levels were statistically significant only in the striatum. No statistically significant exposure-related changes were observed in average levels of the dopamine metabolite, 3,4-dihydroxyphenylacetic acid, in the striatum or the cerebellum except for increased levels (by about 32%) for the 50 ppm group in the cerebellum compared with controls. Average concentrations of serotonin were decreased by about 38 and 49% in the striatum in the 50 and 200 ppm groups, respectively, and by about 41 and 68% in the cerebellum. These changes were statistically significant only in the striatum. No statistically significant exposure-related changes were observed in average levels of the serotonin metabolite, 5-hydroxyindoleacetic acid, in the striatum or the cerebellum, in average levels of

norepinephrine in the two brain regions, or in average activities of monoamine oxidase. The observed changes in the endpoints examined in this study are of uncertain biological relevance; as such, the study does not identify NOAELs or LOAELs suitable for health hazard identification or dose-response assessment. However, the striatum and cerebellum are major centers for movement control, balance, and coordination. Thus, an abnormality in the neurotransmitters will cause malfunction in the movement coordination of an organism. The study authors suggested that a decrease in dopamine will reduce the environmental adaptability of rats and provide neurotransmitter evidence for the effect of AN exposure on neurobehavior. Serotonin plays a role in the maintenance of sleep and the emotional and psychological states of the body. Thus, reduced serotonin level in the exposed groups may also have neurobehavioral effect.

4.5.1.1.4. ***Oxidative stress.*** Farooqui and Ahmed (1983b) demonstrated that exposure of rats to AN resulted in depletion of GSH and induction of oxidative stress in RBCs (see Section 4.5.1.1.2). Farooqui et al. (1990) provided in vitro data that AN induced GSH depletion, lipid peroxidation, and enhanced concentration of MetHb in rat RBCs.

In another study, the cytotoxic effect of AN-potentiated oxidative stress in rat alveolar macrophages was investigated (Bhooma and Venkataprasad, 1997). When alveolar macrophages isolated from male Wistar rats were incubated with 200 nM to 20 μM AN at 37°C for up to 4 hours, a dose-dependent loss of viability was observed. Incubation of alveolar macrophages with 10 μM AN increased the release of H_2O_2 by 44% when compared with controls. This effect was abolished by the addition of antioxidant enzymes superoxide dismutase (SOD) or catalase to the incubation medium. In addition, while exposure of alveolar macrophages to 10 μM AN resulted in 42% viability, addition of SOD exerted a marked protective effect with a resultant viability of 79%. Thus, cell injury induced by AN is mediated by the production of highly toxic OH radicals.

The role of oxidative stress and lipid peroxidation in the induction of the toxic effects of AN was studied by a number of other research groups. In a study designed to evaluate the possible role of free-radical-mediated lipid peroxidation in the etiology of AN-induced acute adrenal necrosis, Silver and Szabo (1982) monitored the formation of MDA and conjugated diene concentrations in the adrenal glands and other tissues (brain, liver, stomach, duodenum) of female Sprague-Dawley rats treated with an i.v. dose of 150 mg/kg AN. Controls received i.v. injections of aqueous 0.1% Tween 80. Rats were killed at 15, 30, 60, or 90 minutes after injection of AN, and the liver, adrenal glands, brain, stomach, and duodenum were removed. While no effects on the monitored parameters were observed in the mitochondria or microsomes from adrenal gland, brain, duodenal mucosa, or glandular stomach mucosa of rats 30 minutes after injection of AN, conjugated diene concentrations were elevated by 60% in hepatic microsomes and 30 and 40% in gastric mitochondria and microsomes. Therefore, although lipid

peroxidation is unlikely to be involved in the pathogenesis of AN-induced adrenal necrosis, AN can cause lipid peroxidation in other target organs.

The cytotoxicity and oxidative stress induced by AN were examined in cultured colonocytes from male and female Sprague-Dawley rats (Mohamadin et al., 2005). These cells were exposed to AN in the concentration range of 0.1–2.0 mM for 60 minutes or incubated with 1.0 mM (the concentration that reduced viability by 50%) for different time intervals up to 180 minutes and then assayed for LDH leakage, cellular GSH levels, and lipid peroxidation. Cell viability was reduced (assessed by trypan blue exclusion method) after 60-minute exposure to 0.5 mM AN and higher; incubation with 1.0 mM reduced viability as early as 60 minutes and by 72% at 180 minutes. Concentration-dependent increases in plasma membrane damage, as assessed by leakage of LDH, and enhanced lipid peroxidation (production of thiobarbituric acid-reactive substances [TBARS]) were observed following 60-minute exposures at all levels (0.1–2 mM); exposure to 1.0 mM AN produced a 2.5-fold increase in leakage after 60 minutes.

Significant reductions in glutathione levels resulted from 60-minute exposure to ≥1.0 mM AN. The time course study revealed that, by 30 minutes, exposure to 1.0 mM AN caused a significant decrease in GSH concentration that kept decreasing until 180 minutes, when the experiment was terminated. In additional experiments, AN-induced membrane damage and lipid peroxidation were reduced, but not totally abolished, by cotreatment with thiol-containing compounds (GSH, N-acetyl-L-cysteine (NAC), and dithiothreitol (DTT)), antioxidant enzymes (SOD and catalase), as well as the iron chelator desferrioxamine (DFO) and the hydroxyl radical scavenger DMSO. Mohamadin et al. (2005) suggested that the observed protective effects of GSH, NAC, and DTT could be attributed to direct interaction with ROS, direct binding to toxic metabolites, and/or enhancement of cellular GSH synthesis, while depletion of iron by DFO could indirectly prevent cell damage by inhibiting the generation of hydroxyl radical. Pretreatment of colonocytes with either SOD or catalase inhibited LDH leakage by about 23 and 54%, respectively, when compared with colonocytes treated with AN alone. These antioxidant enzymes reduced TBARS production that was induced by AN by 17 and 45%, respectively. Since these antioxidants could not restore the normal level of LDH leakage or TBARS production, Mohamadin et al. (2005) concluded that in addition to lipid peroxidation, other factors contributed to AN-induced cytotoxicity.

Mahalakshmi et al. (2003) evaluated the potential protective effect of taurine (TAU) against AN-induced oxidative stress in rat brain. Male Wistar rats (six/group) were exposed to 0 or 100 ppm AN (average intake 8–10 mg/kg-day) in drinking water for 14 or 28 days. Additional groups of rats received TAU (10 g/kg in diet) alone or along with AN treatment for 14 or 28 days. AN had no effect on BW gain or weights of liver or brain. AN treatment for 14 days increased levels of TBARS by about 13% in plasma and 30% in brain and increased levels of lipid hydroperoxides by 38% in plasma and 31% in brain; values after 28 days were similar, except for a 45% increase in lipid hydroperoxides in plasma. AN exposure also

increased the percentage of DNA fragmentation detectable in brain by 60 and 81% after 14 and 28 days, respectively. TAU completely prevented the AN-induced increases in levels of TBARS and lipid hydroperoxides in plasma and brain, but afforded only partial protection from AN-induced increases in DNA fragmentation, which was significantly increased to 30 and 19% after 14 and 28 days, respectively. These results demonstrated that, even as TAU completely prevented the formation of ROS and oxidative stress, DNA fragmentation still occurred. Thus, other factors in addition to oxidative stress caused DNA fragmentation as a result of AN exposure.

AN significantly reduced activity levels of enzymatic antioxidants after 14 days (28-day values were similar to 14-day values but slightly lower): SOD (50% lower in hemolysate, 30% lower in brain), catalase (50% in hemolysate, 62% in brain), glutathione peroxidase (39% in hemolysate, 60% in brain), and GST (20% in hemolysate and brain). TAU also partially protected against these AN-induced reductions of enzymatic antioxidant activities, resulting in reductions of less than 11% in rats treated with AN and TAU for 14 days when compared with controls. For rats treated with AN and TAU for 28 days, there was insignificant reduction of <5%. AN exposure for 14 days also lowered levels of nonenzymatic antioxidants, such as ascorbic acid (by 30% in plasma and brain), α-tocopherol (by 40% in plasma and brain), and GSH (by 45% in plasma and 28% in brain); reductions were slightly greater for the 28-day exposure. In animals treated with TAU and AN for 14 days, the AN-related reductions in nonenzymatic antioxidants were less than 10% compared with controls. These experiments demonstrated that oral exposure to AN in drinking water increased oxidative stress in the brain and that TAU partly protected against AN-induced oxidative stress by increasing the activities of enzymatic antioxidants and replenishing nonenzymatic antioxidants.

However, Carrera et al. (2007) were not able to reproduce the results obtained by Mahalakshimi et al. (2003) when oxidative stress parameters were measured in Wistar rats treated with AN in vivo. Male Wistar rats (12/group) were treated with 0 or 200 ppm AN in drinking water for 14 days. The estimated daily dose was 30 mg/kg-day, using water factor of 0.15 L/kg-day (USEPA, 1988). Brains were excised and homogenized, and lipid peroxidation (as measured by nmol MDA/mg protein), catalase activity, GSH levels, and proteins in brain tissue were measured. No differences were found in lipid peroxidation products, catalase activity, and reduced and oxidized GSH levels in the control and treated rats. Carrera et al. (2007) concluded that there was no evidence of oxidative damage in the brain of AN-treated rats at the studied dose of AN.

In another study (El-Sayed et al., 2008), the effect of hesperidin (HES), an antioxidant flavonoid, on AN-induced oxidative stress in rat brain was investigated. Male Swiss rats (8/group) were treated with 50 mg/kg-day AN via oral gavage for 28 days (Group II). Control rats received distilled water (Group I). Group III rats received 200 mg/kg-day HES i.p. for 28 days. Group IV rats received 200 mg/Kg-day HES i.p. 24 h before starting AN treatment and

concomitantly with AN treatment. At study termination, brain GSH content, MDA content, and enzymatic antioxidant parameters: SOD, CAT, glutathione peroxidase (GSH-Px), and GST were measured. Histopathological examination was conducted on brain samples from two rats in each group.

Brain lipid peroxides levels measured as MDA was increased by 107% in the AN-treated rats, accompanied by a 63% decrease in brain GSH content as compared with controls (El-Sayed et al., 2008). On the other hand, pretreatment of rats with HES prior to AN administration resulted in 55% reduction in brain MDA content and 183% increase in brain GSH content when compared with the AN-treated group. In addition, significant decreases in enzymatic antioxidant parameters were found in the brain of AN-treated rats, with SOD, CAT, GSH-Px, and GST decreased by 43%, 64%, 52%, & 43%, respectively, when compared with controls. Pretreatment with HES and coadministration with AN attenuated the reduction of enzymatic antioxidants levels, resulting in elevations of SOD, CAT, GSH-Px, and GST by 73%, 169%, 197%, and 71%, respectively, when compared with the AN-treated group.

Histopathological examination of brain sections indicated damage to neuronal cells of the brain in AN-treated rats, as manifested by edema and interstitial neuronal atrophy with perineuronal vacuolation. Pretreatment of the rats with HES nearly normalized the histopathological changes induced by AN. This study indicated that treatment of rats with 50 mg/Kg-day AN via oral gavage induced oxidative stress in the brain, and that pretreatment with the antioxidant HES might have protective role against AN-induced oxidative stress in the brain.

Zhang et al. (2002) studied the mechanisms by which AN induced oxidative stress and found evidence that CYP450 metabolism is required for AN to affect the activities of antioxidant enzymes, such as catalase, xanthine oxidase, or SOD. Syrian hamster embryo (SHE) cells were incubated for 4, 24, and 48 hours with subcytolethal doses of AN (0, 25, 50, or 75 μg/mL), and the effects of AN on enzymatic and nonenzymatic antioxidants were monitored. All three concentrations of AN increased ROS (hydroxyl radicals, measured as 2,3-dihydroxybenzoic acid formation from salicylic acid) levels in SHE cells at all time points, with concurrent depletion of GSH after 4 hours of treatment, ranging from 80 to 66% reduction. GSH levels in all AN-treatment groups returned to control values after 24 hours of treatment and increased only in the SHE cells treated with 75 μg/mL AN after 48 hours of treatment.

Inhibition of the antioxidant enzymes was temporal. Decreased catalase activity was observed following treatment with 50 and 75 μg/mL AN for 4 hours at 72 and 52%, respectively. However, catalase activity was increased with 25, 50, and 75 μg/mL AN treatment for 24 hours by 82, 138, and 182%, respectively. Similar increases were observed with 48 hours of treatment. SOD activity was decreased only in SHE cells treated with 75 μg/mL AN for 4 hours.

The activity of xanthine oxidase, the enzyme that generates the superoxide radical and hydrogen peroxide via the oxidation of hypoxanthine or xanthine by oxygen, was also monitored. Xanthine oxidase activity was increased by 47% in SHE cells treated with 75 μg/mL

AN for 24 hours. After 48 hours of treatment, both 50 and 75 μg/mL AN significantly increased xanthine oxidase activity. The addition of 0.5 mM of ABT (a suicide inhibitor of CYP450) to the system prevented the AN-induced decrease in catalase activity after 4 and 24 hours. Cotreatment of AN with ABT also blocked the increase in xanthine oxidase in SHE cells after 48 hours of treatment. ABT alone had no effect on catalase or xanthine oxidase activity. In addition, AN had no effect on catalase or SOD activities in the absence of metabolic source (SHE cell homogenate). Thus, AN-induced oxidative stress in SHE cells involved decrease of antioxidants and activation of the oxidant enzyme xanthine oxidase. Taken together, these data suggest that AN induced oxidative stress via its oxidative metabolism.

Nerland et al. (2003) proposed another mechanism by which AN might induce oxidative stress in their study on the covalent binding site of AN to rat liver CAIII. Two-dimensional polyacrylamide gel electrophoresis and autoradiography were used to locate proteins in male rat liver cytosol that were radiolabeled after s.c. administration of 115 mg/kg of [2,3-^{14}C]-AN to male Sprague-Dawley rats. The intensely labeled spots in the autoradiogram were identified as CAIII. Analysis of the trypic fragment established that only cysteine 186 in the CAIII was labeled. Thus, AN selectively bound to the cysteine 186 residue of CAIII in rat liver. Nerland et al. (2003) also showed that over 50% of rat CAIII had participated in scavenging the toxicant AN. CAIII has been proposed to protect cells against oxidative stress by scavenging reactive xenobiotics, thereby reducing covalent binding to more critical macromolecules. Thus, AN exposure would impair this protective function by covalently binding to cysteine 186 of CAIII.

In another study, the cytotoxicity of AN was related to disturbances in intracellular ionic homeostasis and induction of oxidative stress. Mikhutkina et al. (2004) investigated the role of disturbance in cell Ca^{2+} homeostasis in AN-induced blebbing of thymocyte plasma membrane and apotosis. Blebbing of cell membrane develops in the initial stage of cell damage and is a sign of apoptosis and necrosis. A component of apoptogenic and necrogenic factors on the cell is Ca^{2+} imbalance, a result of disturbed activity of ion channels and intracellular Ca^{2+} stores. Exhaustion of intracellular Ca^{2+} stores increases the activity of store-activated (capacitance) Ca^{2+} channels that allow influx of Ca^{2+} into cells. Exhaustion of Ca^{2+} stores is a stimulus for apoptosis.

When exposed to 5 mM AN in vitro for 1 hour, thymocytes isolated from male albino mice exhibited twofold increases in the incidence of blebbing of the plasma membrane, followed by apoptosis (as detected by the expression of phosphatidylserine on the outer membrane) and necrosis (as indicated by membrane permeability to propidium iodide) (Mikhutkina et al., 2004). The initial and terminal blebbing of the plasma membrane peaked by the 15th and 45th minutes of incubation. The dynamics of terminal blebbing correlated with the accumulation of MDA in the incubation medium. Cotreatment with compounds (e.g., caffeine and procaine) that regulate activity of intracellular Ca^{2+} stores modulated the cytotoxic effect of AN, suggesting to Mikhutkina et al. (2004) that AN induced the release of Ca^{2+} from the endoplasmic reticulum.

Preincubation of thymoctyes with 10 μM isoptin, a blocker of voltage-dependent ion channels, decreased AN-induced apoptosis and necrosis but increased the number of cells in AN-induced secondary necrosis and decreased the intensity of oxidative stress (as indicated by the levels of MDA). This effect was related to the ability of isoptin (an antioxidant) to suppress AN-induced generation of free radicals. Cotreatment of AN with 10 μM SKF 96365, a blocker of calcium release-activated channels that were dependent on the activity of voltage-dependent ion channels, increased the apoptogenic, but not the necrogenic, activity of AN. (SKF96365 had low prooxidant activity.) The cells treated with SKF 96365 and AN developed intensive blebbing at various periods of incubation. Mikhutkina et al. (2004) interpreted the results to be that isoptin, via K^+ channels, only partially inhibited store-activated Ca^{2+} entry into cells through calcium release-activated channels and in turn, protected cells from apoptosis. However, secondary necrosis (the process associated with cells unable to form apoptotic bodies) developed in thymocytes with suppressed blebbing. On the other hand, direct inhibition of these channels with SKF 96365 completely blocked Ca^{2+} entry and promoted progression of apoptosis. The results of these experiments suggested that AN caused disturbances in intracellular calcium balance that led to plasma membrane blebbing, apoptosis, and necrosis of thymocytes.

A recent study on the effects of AN on primary-cultured astrocytes from Wistar male rats (Carrera et al., 2007) indicated that AN-induced cellular damage was not due to oxidative stress, since antioxidants did not prevent AN-induced toxicity. In this study, primary cultured rat astrocytes were treated for 1 hour with or without trolox (TRX) (100 μM), TAU (5 mM), NAC (20 mM), estradiol (10 μM), or melatonin (MEL) (10^{-3} M, 10^{-5} M, or 10^{-7} M). They were then exposed to 2.5 mM AN (which induced about 40% cell death) for 24 hours. Cell viability was determined by measuring the activity of LDH released by damaged cells into the medium. GSH levels were also measured.

Among the antioxidants included in this study, only NAC, a sulfhydryl donor, prevented the decrease of the number of viable cells in the culture. None of the other antioxidants prevented cell death induced by AN treatment. Moreover, 10^{-5} M MEL and TAU increased the toxicity of AN in astrocytes. Treatment of astrocytes for 4 hours with AN partially depleted intracellular GSH, whereas pretreatment with 20 mM NAC recovered GSH content to the control levels. Carrera et al. (2007) concluded that protective effect of NAC was due to increase in the intracellular pool of GSH, GSH conjugation with AN, decreasing the availability of AN for being metabolized to CEO and cyanide, halting the toxicity of AN. Carrera et al. (2007) also concluded cellular toxicity induced by AN could not be prevented only by antioxidants.

Oxidative stress summary

The role of oxidative stress in AN-induced cytotoxicity was evaluated in both in vitro and in vivo studies (Mohamadin et al., 2005). AN was reported to induce oxidative stress and decreased the viability of NHAs in cell cultures (Jacob and Ahmed, 2003b) and cultured rat

colonocytes (Mohamadin et al., 2005). However, other causes contributed to AN-induced cytotoxicity as antioxidants could not restore the normal level of LDH leakage or TBARS production.

Zhang et al. (2002) studied the mechanisms by which AN induced oxidative stress in SHE cells and suggested that AN induced oxidative stress via its oxidative metabolism. Other proposed mechanisms by which AN might induce oxidative stress included covalent binding of AN to cysteine 186 of rat liver CAIII (Nerland et al., 2003), and disturbances in intracellular ionic homeostasis (Mikhutkina et al., 2004).

Drinking water studies in Wistar rats yielded contradictory results. Mahalakshmi et al. (2003) reported exposure to 8–10 mg/kg-day AN significantly reduced enzymatic antioxidant (SOD, glutathione peroxidase, catalase) levels in rat brain after 14 or 28 days, and that TAU prevented the AN-induced increases in levels of TBARS and lipid hydroperoxides in plasma and brain. However, Carrera et al. (2007) were unable to reproduce the results obtained by Mahalakshimi et al. (2003) in another 14-day drinking water study in Wistar rats. No differences were found in lipid peroxidation products, catalase activity, and reduced and oxidized GSH levels in the control and treated rats. Carrera et al. (2007) concluded that there was no evidence of oxidative damage in the brain of rats treated with 30 mg/kg-day AN for 14 days.

In an oral gavage study of male Swiss albino rats, treatment of rats with 50 mg/Kg-day for 28 days induced increased levels of MDA in the brain, and decreased brain GSH content and enzymatic antioxidant levels (El-Sayed et al., 2008). Pretreatment with HES (200 mg/Kg, i.p.) attenuated the effects of AN treatment.

4.5.1.1.5. ***Immunotoxicity.*** Zabrodskii et al. (2000) studied the mechanisms for cell and humoral immunosuppressive effect of AN. CBA mice were treated by a single s.c. injection at one-half the LD_{50} (28 mg/kg) of AN. One day after treatment, mice were tested for delayed-type hypersensitivity (DTH) reactions: α-naphthylbutyrate esterase activity in splenocytes, number of antibody-producing cells in spleen, and the paw edema test. AN treatment suppressed primary cell immune response, as demonstrated by a 61% reduction of the DTH reaction (edematous paw weight). Secondary DTH response (the number of esterase-positive splenocytes) was reduced by 28%. Humoral immune response was also decreased, as shown by a 56% reduction of the number of antibody-producing cells. The cholinesterase reactivator, bispyridinium dioxime (dipyroxime), rehabilitated paw swelling completely but only partially restored the numbers of antibody-producing cells and esterase-positive splenocytes.

The role of cytochrome c oxidase a3 in the mitochondrial respiration enzyme system of immunocompetent cells was evaluated using hydrogen cyanide, a metabolite of AN, and its antidote anticyan. Anticyan, an agent that converts Hb to MetHb, also improved the DTH effects of AN but less efficiently than dipyroxime. A combination of both agents reversed the immunotoxic effects of AN completely. Zabrodskii et al. (2000) suggested that AN-induced

immunotoxic effects were the result of its anticholinesterase activity targeted at T lymphocytes and general toxicity associated with inhibition of cytochrome c oxidase a3 of the immunocytes.

4.5.1.2. *Cancer Effects*

4.5.1.2.1. ***Formation of DNA adducts.*** There is evidence that AN and its epoxide metabolite, CEO, can form a number of different DNA adducts in vitro. For example, Solomon and Segal (1985) demonstrated the direct, nonenzymatic alkylation of calf thymus DNA by AN. Following a 40-day incubation of AN at 37°C and pH 7.4, the reaction products were identified as cyanoethyl adducts of guanine and thymine and carboxyethyl adducts of adenine and cytosine. The major adducts were 1-carboxyethyl adenosine (26%), 7-cyanoethyl-guanine (26%), imidazole ring-opened 7,9-bis cyanoethyl guanine (19%), 3-cyanoethyl thymine (16%), and N^6-cyanoethyl adenine (8%).

CEO formed a number of DNA adducts more quickly when incubated with DNA in vitro (Solomon et al., 1993; Yates et al., 1993; Hogy and Guengerich, 1986). When calf thymus DNA was incubated with CEO at pH 7.0–7.5 and 37°C for 3 hours (Solomon et al., 1993), N^7-(oxoethyl)guanine (110 nmol/mg DNA), N^3-(2-hydroxy-2-carboxyethyl)deoxyuridine (80 nmol/mg DNA), and smaller amounts of adenine and thymine adducts were produced. Therefore, the adducts formed from CEO were different than those formed from AN. The order of reactivity with CEO was guanine > cytosine > adenine > thymine. In addition to reacting with N7 of guanine, forming N^7-(oxoethyl)guanine, CEO reacted to a great extent with the cytosine residue, resulting in the detection of a major adduct, N^3-(2-hydroxy-2-carboxyethyl)deoxyuridine. Solomon et al. (1993) proposed that the uracil adduct was formed from an initial cytosine adduct from hydrolytic deamination of cytosine to uracil.

Yates et al. (1993) also characterized an adduct formed when calf thymus DNA was incubated with 150 mM CEO at 37°C for 3 hours. The adduct was identified as N^3-(2-cyano-2-hydroxyethyl)deoxythymidine. This adduct was also formed when 150 mM [2,3-^{14}C]-CEO reacted with 10 mM deoxythymidine in vitro (Yates et al., 1993). Subsequent degradation of this adduct yielded N^3-(2,2-dihydroxyethyl)deoxythymidine.

Similarly, Guengerich et al. (1981) showed that when 1 mM [1-^{14}C]-AN and [2,3-^{14}C]-AN were incubated at 37°C with 1.5 mg/mL calf thymus DNA in the presence of rat liver microsomes or a reconstituted CYP450 system, DNA adducts were formed as measured by irreversible binding of radioactive label to DNA. Formation of DNA adducts was enhanced by the presence of NADPH. Only trace levels of DNA adducts were detected when incubated with rat brain microsomes, and the reaction was not NADPH dependent, probably due to insignificant metabolism of AN by brain microsomes. Guengerich et al. (1981) also showed nonenzymatic irreversible binding of labeled CEO to calf thymus DNA. The extent of binding for [2,3-^{14}C]-labeled CEO was three- to fivefold greater than that for [1-^{14}C]-labeled CEO. Moreover, when 100 mM CEO was incubated with 50 mM adenosine for 24 hours at 37°C,

1,N^6-ethenoadenosine was formed. In another experiment, an unidentified product was formed when CEO was incubated with cytidine.

Data from Peter et al. (1983a) showed the extent of irreversible binding of AN or its metabolites to DNA to be lower after purification of isolated DNA and RNA by column chromatography on hydroxyapatite. In their in vitro incubation experiment, [2,3-^{14}C]-AN was incubated with rat-liver microsomes, NADPH and DNA or RNA. Irreversible AN binding was found to be 3 nmol/hour per mg DNA, when ethanol precipitation or phenol extraction of DNA was used. When the isolated DNA was further purified by column chromatography on hydroxyapatite, irreversible binding was found to be 0.15 nmol/hour per mg DNA. Peter et al. (1983a) also administered [2,3-^{14}C]-AN intraperitoneally to male Wistar rats and measured the incorporation of radioactivity into hepatic RNA bases. The amount of radiolabel from AN associated with hepatic DNA was lower than that from labeled vinyl chloride.

However, when hepatic DNA from these treated rats was isolated and hydrolyzed, chromatography on PEI-cellulose showed two ^{14}C peaks that did not correspond to known standards. Thus, Peter et al. (1983a) concluded that AN or its metabolites could alkylate DNA, although these DNA adducts had not yet been identified.

Yates et al. (1994) also characterized the products formed when 150 mM CEO reacted with 50 mg/mL nucleotides for 3 hours at 37°C in vitro. The reaction of CEO with 5′-monophosphates of deoxyguanosine, deoxyadenosine, deoxycytidine, or deoxythymidine resulted in the formation of at least one adduct for each nucleotide. These CEO-nucleotide adducts were characterized as 2-cyano-2-hydroxyethyl phosphodiesters. The reaction of deoxyguanosine-5′-monophosphate (dGMP) also produced a second adduct, N^7-(2-cyano-2-hydroxyethyl)-dGMP. Yates et al. (1994) suggested that the cyano-hydroxyethyl-phosphodiester adduct could induce single and double DNA strand breaks (as observed when CEO was incubated with pBR322 plasmid DNA) via interaction of the adduct's β-hydroxyl-group with the DNA phosphate backbone.

Irreversible binding of AN or its metabolites to DNA in vivo has also been studied. Farooqui and Ahmed (1983a) investigated the ability of [2,3-^{14}C]-AN or its metabolites to bind to macromolecules in rats in vivo. [2,3-^{14}C]-AN was administered in a single dose to male Sprague-Dawley rats (three to four per group) via gavage at a dose of 46.5 mg/kg in water. Animals were sacrificed at 1, 6, 24, and 48 hours after dosing. Organs, including liver, kidney, brain, spleen, and stomach, were dissected out and frozen rapidly. Nucleic acids extracted from the homogenates were applied to the hydroxyapatite column for separation of RNA and DNA fractions. Radioactivity was detected in the extracts of RNA and DNA from liver, stomach, and brain. Bound radioactivity (as pmol equivalent AN/mg DNA) to DNA in the brain was the highest at 24 hours (119 pmol/mg DNA), followed by stomach (81 pmol/mg DNA), and liver (25 pmol/mg DNA). Bound radioactivity in all three organs plateaued at 24 hours and remained unchanged thereafter. RNA from liver showed the highest amount of radioactivity, followed by

brain and stomach. Bound radioactivity in liver RNA peaked at 6 hours after dosing, whereas RNA from the brain and stomach showed maximal radioactivity at 24 hours. Binding to proteins was extensive and time dependent. In the first hour after oral dosing, the highest protein binding occurred in spleen and stomach, followed by liver, kidney, and brain. After 6 hours, protein binding plateaued until 48 hours. At 6 hours, the highest protein binding occurred in the spleen, followed by liver, stomach, and kidney, with brain having the lowest protein binding. The study authors developed numerical indices for the AN-derived DNA alkylation; covalent binding indices were 5.9, 51.9, and 65.3 for liver, stomach, and brain, respectively, after 24 hours.

Ahmed et al. (1992a) demonstrated the covalent binding of radiolabel from [2,3-^{14}C]-AN to testicular DNA after a single oral dose of 46.5 mg/kg of [2,3-^{14}C]-AN to male Sprague-Dawley rats. In a time course study, bound activity was shown to be greatest after 30 minutes (8.93 ± 0.80 μmol AN bound/mol nucleotide), with covalent binding index of 10.15. Using an identical experimental protocol, Ahmed et al. (1992b) demonstrated the capacity of AN to bind covalently to DNA in the lung. Covalent binding of radioactivity to DNA increased with time and was maximum at 12 hours after a single oral dose, with a covalent binding index of 3.48. Binding was associated with a 55–72% decrease in replicative DNA synthesis at time points up to 24 hours after dosing.

Hogy (1986) and Hogy and Guengerich (1986) studied the in vivo interaction of AN and CEO with DNA. Three male F344 rats were administered AN (50 mg/kg, i.p.); three more rats were administered CEO (6 mg/kg, i.p.). The rats were sacrificed after 2 hours, and the brain and livers were removed and frozen. DNA and RNA were isolated from these tissues. For detection of N^7-(2-oxoethyl)guanine, DNA samples were reductively tritiated with NaB^3H_4; the adduct was released by neutral thermal hydrolysis and purified by thin-layer chromatography for subsequent quantitation by liquid scintillation counting. N^7-(2-oxoethyl)guanine was detected in liver DNA at 3.1×10^7 nucleotides per alkylation in AN-treated rats and 6.9×10^7 nucleotides per alkylation in CEO-treated rats (Table 4-52). For brain DNA, N^7-(2-oxoethyl)guanine was detected at 2.4×10^8 nucleotides per alkylation in AN-treated rats and at 1.1×10^9 nucleotides per alkylation for CEO-treated rats. The values obtained from the brain DNA samples were near the limit of detection. Thus, the presence of these adducts in the brain could not be unequivocally verified.

Table 4-52. Detection of N^7-(2-oxoethyl)guanine after i.p. administration of 50 mg/kg AN or CEO to male F344 rats

Compound	Formation of N^7-(2-oxoethyl)guanine			
	Liver		Brain	
	fmol/mg DNA	Nucleotides/alkylation	fmol/mg DNA	Nucleotides/alkylation
AN	109 ± 71	3.1×10^7	14	2.4×10^8
CEO	48 ± 15	6.9×10^7	3	1.1×10^9

Source: Hogy (1986).

In the same study (Hogy, 1986; Hogy and Guengerich, 1986), rat DNA samples were also analyzed by HPLC with a fluorescence detector for 1,N^6-ethenoadenosine and 1,N^6-ethenodeoxyadenosine. These adducts were not detected with limits of detection estimated to be 3 pmol/mg DNA and 1 pmol/mg RNA, respectively.

In another study, Prokopczyk et al. (1988) administered 50 or 100 mg/kg s.c. AN to male F344 rats (10/group). DNA was isolated from liver and brain after 2 hours (50 mg/kg group) or 6 hours (100 mg/kg AN). An HPLC assay with fluorescence detector was used to detect 7-(2-cyanoethyl)guanine (detection limit: 1 per 5×10^4 guanine) and O^6-cyanoethylguanine (detection limit: 1 per 7×10^4 guanine). Neither adduct was detected. These two adducts were not formed when CEO was incubated with calf thymus DNA in vitro (Solomon et al., 1993).

4.5.1.2.2. ***Oxidative stress.*** Jiang et al. (1998) evaluated the ability of AN to induce oxidative stress in the brain cortex of rats. Male Sprague-Dawley rats (at least nine/group) were exposed to 0, 5, 50, 100, or 200 ppm AN in drinking water for either 14, 28, or 90 days. These concentrations were selected from those used in chronic bioassays (see Section 4.2.1.2). As calculated by the study authors, average daily doses of 0, 0.6, 5.1, 8.9, or 15.0 mg/kg-day were ingested over the 90-day treatment period by the control to high-dose groups, respectively. At study termination, brains and livers were weighed. The livers and brain cortexes from six rats/group were evaluated for the following oxidative endpoints: oxidative DNA damage (8-hydroxy-2′-deoxyguanosine levels), lipid peroxidation (MDA levels), levels of nonenzymatic antioxidants (glutathione and vitamin E), and the activities of enzymatic antioxidants (catalase, SOD, and glutathione peroxidases). 8-Hydroxy-2′-deoxyguanosine has also been referred to as 8-oxo-7,8-dihyro-2′-guanosine (Murata et al., 2001) and 8-oxodeoxyguanosine (Whysner et al., 1998a) and will be referred to as 8-oxodG in this document. ROS formation—as measured by the formation of 2,3-dihydrobenzoic acid from salicylic acid in brain cortex and liver—were evaluated in three rats/group injected with salicylic acid in saline 12 hours before termination.

In rats exposed to AN at concentrations as high as 200 ppm for up to 90 days, no effects were noted on viability. A statistically significant reduction of 9% in BW was observed in the 200 ppm group after 90 days. No differences were observed in brain or liver weights nor were

any of the measures of oxidative damage or antioxidant levels in the liver for all groups at any sampling times. AN exposure resulted in statistically significant increases in oxidative stress parameters and decreases in antioxidants levels in the brain cortex. Levels of hydroxy free radicals (ROS) were significantly elevated in a dose-related manner in the 50–200 ppm groups, beginning at 14 days and persisting until the 90-day time point; at 200 ppm, the increase was approximately fivefold over controls. Levels of 8-oxodG in the cellular DNA of brain cortex were significantly elevated (three- to fourfold compared with controls) in a dose-related manner in the 100 and 200 ppm groups, beginning at 14 days of exposure, and two- to threefold in the 50 ppm group, beginning after 28 days of exposure. MDA levels were significantly increased (1.5-fold) in the 200 ppm group after 14 days but at no other time point.

Slight but significant decreases in levels of vitamin E (about 20%) and glutathione (about 20%) in the brain cortex were observed in the 50–200 ppm groups but were statistically significant only at the 14-day time point. Statistically significant, dose-dependent reductions (by up to 60%) in catalase activity were observed in brain cortex at all exposure levels after 14 days, at ≥100 ppm after 28 days, and at ≥50 ppm after 90 days; the transient effect at 5 ppm was not considered to be biologically significant. Reductions in SOD levels in the brain (by up to 30% at 200 ppm) were dose related and statistically significant at ≥50 ppm after 14 days and at 200 ppm after 28 or 90 days. In this study, a NOAEL of 5 ppm (0.6 mg/kg-day) and a LOAEL of 50 ppm (5.1 mg/kg-day) were identified for increases in levels of oxidative damage (increased ROS and DNA damage) and reductions in the antioxidant enzymes catalase and SOD in the brain of rats exposed to AN in drinking water. Jiang et al. (1998) suggested that observed oxidative stress in rat brain cortex following AN treatment could be induced by: (1) direct generation of free radicals from AN or its metabolites, (2) binding of AN or its metabolites to free radical scavengers (e.g., GSH, vitamin E), (3) modulation of the activity and/or synthesis of antioxidant enzymes (e.g., SOD, catalase), and/or (4) interference with electron flow through the respiratory chain via inhibition of cytochrome C oxidase by the cyanide ion, a metabolite of AN. However, these potential mechanisms need to be further investigated.

In a follow up study, Pu et al. (2009) examined the potential for AN to induce oxidative DNA damage in rats. These investigators also examined whether blood could serve as a surrogate for the biomonitoring of oxidative stress induced by AN in target tissues (in particular brain) of exposed populations. Male Sprague-Dawley rats (9/group) were treated with 0, 3, 30, 100 or 200 ppm AN in drinking water for 28 days. N-acetyl cysteine (NAC), an acetylated precursor of glutathione, was coadministered at a dietary concentration of 0.3% to one group of rats receiving 200 ppm AN in drinking water to evaluate its protective effect against potential AN-induced oxidative stress. At the end of treatment, animals were sacrificed and blood samples were collected immediately. The alkaline comet assay was used as a measure of direct DNA damage in 3 rats/group, and the formamidopyrimidine DNA glycosylase (fpg)-modified comet assay was used as a measure oxidative DNA damage in brain cortex and white blood cells

(WBCs) of different treatment groups. 8-oxodG levels in brain tissues and WBCs were also measured by HPLC with electrochemical detection. 2,3-DHBA was measured in WBCs and brain tissues for the presence of ROS.

Pu et al. (2009) observed no increase in DNA damage in rat WBC and brain tissue following exposure to AN with or without NAC coadministration using the alkaline comet assay. Dose-dependent increases in DNA damage were observed in rat WBC and brain following exposure to AN using the fpg-modified alkaline comet assay. These increases in DNA damage were not observed in WBC and brain of rats exposed to 200 ppm AN and NAC. Pu et al. (2009) interpreted the results as indicative of oxidative DNA damage in AN-exposed rats, and further that the absence of oxidative DNA damage in rats coadministered NAC reflected the antioxidant action of NAC. Significant increases in the level of 8-oxodG were found in WBC and brain of rats treated with 100 and 200 ppm AN; no increase was observed in rats treated with 200 ppm AN and NAC. 2,3-DHBA, a measure of ROS formation, was increased in the WBC of rats treated with AN in a dose-dependent manner, but was not detectable in the brain of treated rats. In addition, the ratios of reduced to oxidized glutathione (GSH/GSSG) were reported to be significantly lower in rats treated with 30, 100 and 200 ppm AN, but not in a dose dependent manner. Pu et al. (2009) concluded that AN induced oxidative stress and DNA damage in male Sprague-Dawley rats and that the fpg-modified comet assay in WBC correlated with target tissue oxidative DNA damage.

EPA identified certain issues with study design and choice of analytical methods that raise questions about the interpretation of the findings by Pu et al. (2009). First, Pu et al. (2009) stated that direct DNA damage was not detected in rat WBC and brain of AN-exposed rats based on results in the standard alkaline comet assay. The standard comet assay detects single and double strand breaks, cross link, oxidative DNA damage, apurinic/pyrimidinic sites and DNA repair (Smith et al., 2006; Collins, 2007). The induction of other types of DNA damage not detected by the comet assay cannot be precluded.

Second, Pu et al. (2009) utilized the fpg-modified comet assay to detect oxidative DNA damage induced by AN; however, this assay is not specific for the detection of oxidative DNA damage, as this assay also detects alkylation DNA damage (Speit et al., 2004; Smith et al., 2006). The fpg-modified comet assay has been shown to be especially sensitive for the detection of DNA damage by N-7 guanine alkylation, which was responsible for the observed DNA damage by alkylating agents methylmethanesulfonate (MMS) and ethylmethanesulfonate (EMS) (Speit et al., 2004). N-7 guanine adduct was detected in liver and brain (at the limit of detection) of AN-treated rats (see Section 4.5.1.2.1). Thus, the observed DNA damage using the fpg-modified comet assay in Pu et al. (2009) cannot necessarily be attributed to oxidative DNA damage, but could also be due to N-7 guanine alkylation.

Third, NAC was used by Pu et al. (2009) to demonstrate the effect of an antioxidant to protect against observed DNA damage. It should be noted that NAC is a precursor of

glutathione. Glutathione conjugates with AN to N-acetyl-S-(2-cyanoethyl)cysteine, which can then be excreted in the urine. Glutathione conjugation is therefore a detoxification pathway for AN. Thus, the reduction in DNA damage in AN-treated rats coadministered with NAC observed by Pu et al. (2009) may, in fact, reflect increased detoxification of AN and reduced availability of AN for oxidation to CEO. The protective effect of NAC on AN toxicity was demonstrated by Carrera et al. (2007) (see Section 4.5.1.1.4). Fourth, Pu et al. (2009) reported that the ratios of reduced to oxidized glutathione (GSH/GSSH) were decreased in the brain cortex of rats treated with AN in drinking water at concentrations of 30, 100, and 200 ppm for 28 days. This reduction was not dose related; the GSH/GSSG ratio was similar in all three exposure groups [Figure 8 in Pu et al. (2009)]. GSH/GSSG provided the redox status in the brain cortex. It should be noted that in the 2-year drinking water study in Sprague-Dawley rats involving AN drinking water concentrations of 30, 100, and 300 pmm (Quast, 2002), the incidence of tumors increased with increasing exposure. The absence of a dose-related decrease in GSH/GSSG ratio observed by Pu et al. (2009) does not parallel the dose-related increase in tumor incidence observed in AN-exposed rats by Quast (2002). Thus, the GSH/GSSG ratio is not concordant with an oxidative stress mode of action for the carcinogenicity of AN. Fifth, no ROS was detected in the brain of AN exposed rats in Pu et al. (2009), as no 2,3-DHBA was detected in the brain of AN-treated rats.

Whysner et al. (1998a) also evaluated oxidative DNA damage (increased levels of 8-oxodG) in the brains of male Sprague-Dawley and F344 rats exposed to AN in drinking water for durations of either 21 or 94 days. In the first experiment, male Sprague-Dawley rats (20/group) were exposed to 0, 3, 30, or 300 ppm AN in drinking water for 21 days (Whysner et al.,1998a). Based on default values for the BW of male Sprague-Dawley rats in a subchronic study (0.267 kg) and an allometric equation linking water consumption to BW (U.S. EPA, 1988), the average intakes of AN were calculated as approximately 0, 0.43, 4.3, and 43 mg/kg-day for the control to high-dose groups, respectively. At termination, brains, livers, and forestomachs were excised from five rats/group each for DNA isolation. These tissues were analyzed for GSH, cyst(e)ine, and 8-oxodG levels in nuclear DNA. TBARS levels in brains were determined for another five rats/group. Brain homogenate from another five rats/group were analyzed for cytochrome oxidase activity (in the mitochondria fraction), catalase (in supernatant), and glutathione peroxidase (in homogenate). Tissues from another five rats/group were examined for histopathology, but results were to be published separately.

In rats exposed to 30 or 300 ppm AN, statistically significant increases in 8-oxodG levels in nuclear DNA were measured in brains (approximately twofold increase compared with control values for both dose groups) and livers (approximately 1.4-fold increase for both dose groups when compared with controls). Also observed in the 300 ppm dose group were approximately twofold increases in the levels of glutathione and cyst(e)ine in the forestomach, and approximately 50% increase in cyst(e)ine level in the brain. There were no exposure-related

effects on levels of glutathione in the brain and liver or on levels of cytochrome oxidase, catalase, glutathione peroxidase, or TBARS in the brain. However, glutathione level in the forestomach was increased about 1.8-fold in the 300 ppm dose group compared with controls. In this study, a NOAEL of 3 ppm (0.43 mg/kg-day) and a LOAEL of 30 ppm (4.3 mg/kg-day) were identified for increased oxidative DNA damage in the brains and livers of Sprague-Dawley rats. Whysner et al. (1998a) concluded that the formation of 8-oxodG from AN exposure did not involve disruption of antioxidant defense or lipid peroxidation. In addition, the absence of effect on brain cytochrome oxidase activity in exposed rats indicated lack of inhibition by cyanide, a metabolite of AN. Thus, Whysner et al. (1998a) concluded that cyanide-induced metabolic hypoxia did not appear to be involved in the generation of ROS by AN administered in drinking water.

Whysner et al. (1998a) conducted a parallel 21-day drinking water study in male F344 rats (10/group). Concentrations of AN in drinking water were of 0, 1, 3, 10, 30, or 100 ppm. Based on default values for the BW of male F344 rats in a subchronic study (0.18 kg) and an allometric equation linking water consumption to BW (U.S. EPA, 1988), the average doses of AN were estimated at 0, 0.16, 0.47, 1.6, 4.7, and 15.6 mg/kg-day in the control to high-dose groups. An additional group of rats received 5 mg methylnitrosourea (MNU) per kg/week via i.v. injection. At termination, rat brains were evaluated for levels of 8-oxodG in nuclear DNA, cytochrome oxidase, glutathione, and cyst(e)ine. Levels of all these parameters in the brains of AN-exposed rats and MNU-exposed rats were not significantly different from controls. The levels of 8-oxodG in the brains of 3–100 ppm AN dose groups were the same, about 1.3-fold higher than control values. However, the increases were not statistically significant. The highest drinking water concentration of 100 ppm AN (15.6 mg/kg-day) was a NOAEL for oxidative effects in the brains of F344 rats (i.e., oxidative stress was not demonstrated in the brains of F344 rats even at the highest dose of 15.6 mg/kg-day).

In the subchronic experiment by Whysner et al. (1998a), male Sprague-Dawley rats (10 rats/group) were exposed to 0 or 100 ppm AN in drinking water for 3, 10, 31, or 94 days. Two additional groups of Sprague-Dawley rats (six/group) were exposed to 5 mg MNU/kg/week or 5 mg MNU/kg/week + 100 ppm AN. Brains were assayed for levels of 8-oxodG, cytochrome oxidase, and glutathione. Levels of 8-oxodG were also measured in the livers of rats exposed for 3, 10, or 94 days.

No effects on brain levels of cytochrome oxidase or glutathione were observed in any dose group up to 94 days. The 8-oxodG levels were significantly increased by 77% following exposure to 100 ppm AN for 3, 10, and 94 days. Administration of 5 mg/kg MNU (a DNA-reactive carcinogen that produces glial cell tumors in rats) did not increase the level of 8-oxodG in the brain of treated rats but increased 8-oxodG in the liver after 10 days. However, coadministration of 100 ppm AN and MNU increased the 8-oxodG level in the brain after 31 and 94 days when compared with controls. Whysner et al. (1998a) proposed that AN-induced

generation of ROS and resultant oxidative DNA damage represented one possible mode of action for the neoplastic process in the rat brain. However, as discussed in Section 4.7.3.3.1, results from this study did not support the proposed oxidative stress mode of action.

The ability of AN to induce oxidative stress and oxidative DNA damage was also studied in a rat glial cell line and cultured rat hepatocytes in vitro (Kamendulis et al., 1999a). In parallel experiments, DITNC1 rat astrocytes and rat hepatocytes were incubated with sublethal concentrations (up to 1 mM) AN in vitro for 4 or 24 hours. The 8-oxodG levels in total cellular (nuclear and mitochondrial) DNA, generation of ROS (measured as increase in generation of 2,3-dihydroxybenzoic acid in salicylic acid), levels of the lipid peroxidation product MDA, GSH, and antioxidant enzymes activity were measured at the end of the incubation period.

In rat astrocytes, significant increases (up to 3.8-fold) in the production of 8-oxodG over control was observed after 4 hours and up to 3.9-fold after 24 hours. No increase in 8-oxodG formation was observed in rat hepatocytes at all AN concentrations and time examined. The induction of 8-oxodG by AN in rat astrocytes was reversible. Following removal of AN after 24 hours of treatment, 8-oxodG levels returned to control values at all studied concentrations in 24 hours. Intercellular production of ROS was found to be increased 2- to 2.6-fold after 4 and 24 hours at 0.1 and 1.0 mM AN. No increase in ROS generation was found in rat hepatocytes at any AN concentration or exposure duration. On the other hand, no significant change in MDA formation (as indicator of lipid peroxidation) was found in either cell type following treatment with AN.

A significant decrease in cellular GSH levels was observed in rat astrocytes treated with 0.1 and 1.0 mM AN for 4 hours (25–36% of control) and 24 hour (43–61% of control) and in SOD activity in astrocytes treated for 4 hours with 1 mM AN (39% reduction over control) and for 24 hours with 0.1 and 1 mM AN (38–40% reduction over control). In contrast, no significant decrease in catalase and glutathione peroxidase activities was observed in treated astrocytes. Cotreatment with L-2-oxothiazolidine-4-carboxylic acid (OTC), a precursor to GSH biosynthesis, or with vitamin E, an antioxidant, reduced 8-oxodG and ROS formation induced by AN treatment. These effects were not evident in isolated hepatocytes treated with AN. Results from this study were in agreement with results from the in vivo study by Jiang et al. (1998) on rat brain cortex. Kamendulis et al. (1999a) suggested that, since the formation of 8-oxodG and ROS observed after AN treatment in this study was temporal, dose dependent, and reversible following removal of AN in the culture medium, these are established properties of tumor-promoting agents. Kamendulis et al. (1999a) proposed that AN-induced astrocytomas in rats were produced via tumor promotion mechanisms.

Jacob and Ahmed (2003b) also demonstrated the ability of AN to induce oxidative stress and oxidative DNA damage in NHA culture (see Section 4.5.1.1.3).

Pu et al. (2006) measured direct and oxidative DNA damage in cultured D1 TNC1 rat astrocytes treated with 0–2.5 mM AN for 24 hours. Direct DNA damage was measured by the

comet assay, and oxidative DNA damage was measured with a modified comet assay that included enzymatic digestion with formamidopyrimidine glycosylase. 7-Ethoxyresorufin-O-deethylase (EROD) and CYP2E1 activities in the astrocytes were measured.

At 2.5 mM AN, a 40% decrease in cell viability was observed. No increase in direct DNA damage (measured as increase in tail moment) was observed at any AN concentration. Hydrogen peroxide (20 μM) was used as positive control, and significant increase in DNA damage was found. On the other hand, a threefold increase in oxidative DNA damage was observed in astrocytes treated with 1 mM AN. Supplementation of 1 mM AN with three different antioxidants—vitamin E (150 μM), TRX (water-soluble analog of vitamin E, 150 μM), and epigallocathechin-3 gallate (a polyphenol from green tea, 5 μM)—reduced AN-induced oxidative DNA damage by 65, 54, and 65%, respectively.

As expected, only low level CYP2E1 activity was measured in the astrocytes and was about 10% of that measured in mouse liver. EROD (an indicator of CYP1A) activity was measured in rat astrocytes and was about 500-fold higher than that for CYP2E1. In addition, a 90% reduction in the activities of EROD and CYP2E1 was observed when the astrocytes were cotreated with AN and 0.5 mM ABT for 24 hours. Cotreatment of astrocytes with 1 mM AN and 0.5 mM ABT also prevented the increase in oxidative DNA damage induced by AN, indicating the metabolism of AN by P450 was required for the production of oxidative stress. GSH depletion induced by 4 and 24 hours of treatments with DL-buthionine [S,R]-sulfoximine, a selective inhibitor of γ-glutamylcysteine synthetase, enhanced the oxidative DNA damage induced by AN by 44–160% over control). On the other hand, cotreatment with 2.5 mM OTC, a precursor for glutathione biosynthesis, reduced AN-induced oxidative DNA damage by 63–85%. Exposure to 0.1–0.5 mM cyanide also increased oxidative DNA damage (Pu et al., 2006).

EPA has identified issues in the study design, analytical methods, and data interpretation in Pu et al. (2006). First, as mentioned previously in the discussion of Pu et al. (2009), the alkaline comet assay measures DNA strand breaks and alkali-labile sites, and is not limited to the detection of direct DNA damage only. For the alkaline comet assay, Pu et al. (2006) used hydrogen peroxide as a positive control, demonstrating that this assay is not limited to detecting direct DNA damage, but also oxidative DNA damage. Second, Pu et al. (2006) used the fpg-modified comet assay for detection of oxidative DNA damage. As discussed previously, the fpg-modified comet assay is not specific for the detection of oxidative DNA damage. Third, CYP2E1 level in astrocytes was known to be low and was found to be about 10% that found in the mouse liver. Since bioactivation of AN to CEO via CYP2E1 is needed for direct DNA damage to be detected, it is not surprising that direct DNA damage could not be detected in astrocytes treated with AN (although oxidative DNA damage could have been detected in the alkaline comet assay). As discussed previously in Section 3, CEO is a relatively stable reactive metabolite, with a half-life of about 2 hours; therefore, most of the CEO detected in rat brain is presumed to be formed in the liver of rats treated with AN and transported to the rat brain.

Hence, direct DNA damage could not be detected in this in vitro study. Another weakness in this study concerns the selection of the positive control. A carcinogen that needs bioactivation via CYP2E1 to form a reactive metabolite and induce DNA damage would have served as a better positive control than hydrogen peroxide, which does not require bioactivation. Therefore, the findings reported in this in vitro study are not anticipated to predict what can occur in vivo.

Murata et al. (2001) investigated the enhancing effect of AN on the formation of 8-oxodG in calf thymus DNA, induced by hydrogen peroxide (H_2O_2) and Cu(II). Calf thymus DNA was incubated with various concentrations of H_2O_2 plus $CuCl_2$ in the presence or absence of AN for 30 minutes. The level of Cu(II)-mediated 8-oxodG formation increased with increasing concentration of H_2O_2. The addition of AN (0.1–0.5%) enhanced the formation of 8-oxodG by hydrogen peroxide and Cu(II) in a dose-dependent manner, whereas AN itself did not cause DNA damage. The enhancing effect of AN was more marked in double-stranded than in single-stranded DNA. Further experiments with [^{32}P]-labeled DNA showed that addition of AN enhanced the site-specific DNA damage at guanine residues, particularly at the 5′-site of the GG and GGG sequences while H_2O_2/Cu(II) induced piperidine-labile sites at thymine, cytosine, and guanine residues. Electron spin resonance spectroscopy showed that a nitrogen-centered radical was generated from AN during incubation with hydrogen peroxide and Cu(II). Murata et al. (2001) proposed that AN enhanced H_2O_2-mediated DNA damage via nitrogen-centered radical formation. Thus, AN may enhance endogenous oxidative stress, although AN itself does not have the ability to induce oxidative DNA damage.

4.5.1.2.3. ***Intercellular communication.*** Kamendulis et al. (1999b) investigated the effect of AN on gap junction intercellular communication (GJIC) in D1 TNC1 astrocytes (a rat astrocyte transformed cell line) and primary rat hepatocytes in culture. Noncytolethal concentrations of AN (0.01–1.0 mmol/L) were incubated with D1 TNC1 astrocytes or primary rat hepatocytes. GJIC was determined by microinjection of lucifer yellow CH into cells. Dye coupling was quantitated by determining the number of recipient cells in contact with microinjected cells that showed communication. The reversibility of AN inhibition of GJIC was also evaluated by replacement of AN with fresh medium.

Following 2 hours of treatment, AN at 0.1 and 1 mmol/L inhibited GJIC in D1 TNC1 astrocytes, which were putative target cells. After treatments for 4 and 24 hours, all concentrations of AN (0.01–1.0 mmol/L) inhibited GJIC. The inhibitory effect of AN in this system was dose dependent at all time points, reversible by removal of AN, and partially suppressed by the presence of antioxidants such as vitamin E (0.1 mmol/L). After treatment with both vitamin E and AN for 24 hours, inhibition of GJIC was reduced by 23%. On the other hand, AN did not inhibit GJIC in primary cultured hepatocytes at all concentrations and durations of treatment.

AN also caused a concentration-dependent decrease in cellular GSH content in both D1 TNC1 astrocytes and rat hepatocytes (Kamendulis et al., 1999b). Cotreatment with 5 mmol/L OTC, a precursor of GSH synthesis, reduced inhibition of GJIC by AN in D1 TNC1 astrocytes following 4 and 24 hours of exposure, with the greatest reduction observed at 1.0 mmol/L AN (up to 68%). However, depleting GSH by L-BSO (an inhibitor of intracellular GSH synthesis) alone without AN did not affect GJIC in rat astrocytes. Thus, depletion of GSH alone in astrocytes was not sufficient for the observed decrease in GJIC by AN.

Inhibition of intercellular communication by AN was implied in an inhibition of metabolic cooperation assay. Two studies (Elmore et al., 1985; Umeda et al., 1985) evaluated AN by using the Chinese hamster V79 cells, which are 6-thioguanine (6-TG) sensitive and 6-TG-resistant cloned cells that are the hypoxanthine guanine phosphoribosyl transferase ($hprt^-$**)** mutant of the V79 cell line. The $hprt^-$ mutant cannot phosphorylate several purine analogues, including 6-TG, and are therefore resistant to cell killing by the purine analogue. When the WT cells are cultured at a density that permits frequent contact with the mutant cells, metabolic cooperation (i.e., gap junction formed between these cells) allows the transfer of nutrients and phosphorylated purine analogue from the WT cells to the mutant cells and decreases probability of recovery of the mutant cells in purine analog selective medium. The principle of the assay is based on the fact that recovery of 6-TG-resistant cells cocultivated with 6-TG-sensitive cells in 6-TG-containing medium increased by addition of compounds that inhibit metabolic cooperation. This assay evaluates if the test agent can modulate gap junctional communication.

AN inhibited gap junction formation slightly and dose dependently (Umeda et al., 1985). Average recovery of the mutant cells was 22% in the control, 33% at 1 mM AN, and 39% at 2 mM AN. Umeda et al. (1985) considered AN as positive in the metabolic cooperation assay. In the study by Elmore et al. (1985), AN produced positive responses at noncytotoxic concentrations of 10–50 μg/mL after incubation for 3 days.

4.5.1.2.4. ***Cell proliferation.*** Ghanayem et al. (1997) examined the effects of AN on forestomach cell proliferation and apoptosis in male F344 rats (12/group) administered either 0, 0.22, or 0.43 mmol/kg (0, 11.67, or 22.8 mg/kg) by gavage for 6 weeks. Six rats from each dose group were used to assess BrdU incorporation in the stomach, the remaining six rats from each group were used to assess BrdU incorporation in hepatocytes. Proliferation of forestomach squamous epithelial cells was evaluated with light microscopy by determining the number of cells (nuclei) per unit length muscularis and by quantitating BrdU-stained cells.

AN was shown to induce a dose-dependent increase in epithelial cell proliferation in the forestomach, as determined by the incorporation of BrdU into S-phase DNA. The increase in forestomach mucosal cell proliferation was significant at both the low and high doses of AN. No cellular proliferation was detected in the liver and glandular stomach, which are not target organs of AN carcinogenicity.

There was an associated increase in the thickness (hyperplasia) of the forestomach squamous mucosa, also possibly indicative of enhanced cell proliferation. Forestomach hyperplasia (expressed as the increase in the total number of epithelial cells per mm muscularis) was significant in the high-dose group and was about 60% above vehicle-treated controls. Hyperplasia in the low-dose group was only 7% above controls and was statistically insignificant. The effects of AN on cellular proliferation in the forestomach of treated rats were also evaluated by quantitative determination of BrdU incorporation into S-phase DNA, using immunohistochemical staining. The increase in forestomach mucosal cell proliferation was significant at both the low- and high-dose groups. In addition, the effect of AN on apoptosis was determined by in situ end labeling of tissue sections. Apoptotic bodies were observed in the forestomach of rats treated with high-dose AN. No increase in apoptosis was detected in the liver or glandular stomach of control or treated rats. Thus, AN induced a significant increase in forestomach apoptosis at the high dose, coupled with an increase in hyperplasia.

Ghanayem et al. (1997) proposed that disruption of the normal balance between cell proliferation and apoptosis in favor of enhanced forestomach cell proliferation (as reflected by hyperplasia of the forestomach epitheilium) probably contributed to the pathogenesis of AN-induced forestomach tumors. This suggestion was supported by the observations that cell proliferation in forestomach squamous mucosa of treated rats occurred at doses that caused forestomach tumors in rats and that cell proliferation was selective and only occurred in the target organ forestomach but not in liver.

In a recent study, Chantara et al. (2006) evaluated whether AN induced extracellular signal-regulated kinase (ERK) activation in human neuroblastoma SK-N-SH cells. The activation of ERKs belonging to the mitogen-activated PK family has been implicated to play crucial roles in cell proliferations and is involved in many steps of tumor progression (Fang and Richardson, 2005; Platanias, 2003; Seger and Krebs, 1995). Dysfunction of the ERK signaling pathways was shown to play a pivotal role in the development of many cancers, including leukemia and colon cancer. Active forms of ERK1/2 were found to be dually phosphorylated at threonine and tyrosine. To investigate whether AN could activate ERK, the effect of AN on the activation-association phosphorylation of ERK1/2 was measured in SK-N-SH cells. Treatment with 400 μg/mL AN for 1 hour increased the activation-associated phosphorylation of ERK1/2. Further increase in ERK1/2 phosphorylation was observed with 3 and 24 hours of incubation. Furthermore, increase in ERK phosphorylation was found to be dependent on AN concentration. When SK-N-SH cells were treated with specific mitogen-activated/ERK-activating kinase (MEK) inhibitors, PD98059 (10 μM) and U0126 (10 μM), for 1 hour prior to treatment with 400 μg/mL AN for 24 hours, activation of ERK by AN was significantly abolished. Thus, Chantara et al. (2006) concluded that AN induced ERK1/2 phosphorylation in SK-N-SH cells via activation of MEK.

The role of muscarinic receptors in AN-mediated ERK activation was also investigated by pretreating SK-N-SH cells with or without 10 μM atropine, a muscarinic receptor antagonist, followed by incubation with AN for 24 hours. Carbachol, a muscarinic receptor agonist, was used as a positive control. Previous studies suggested that expression of muscarinic receptors can induce cell proliferation by activating the ERK1/2 pathway (Jiménez and Montiel, 2005). The results showed that 1 mM carbachol induced ERK1/2 activation, and this effect was reduced by atropine pretreatment. However, AN-induced ERK activation was not significantly altered by atropine pretreatment, suggesting that muscarinic receptor stimulation may not be directly involved in the observed AN-induced ERK activation (Chantara et al., 2006).

Chantara et al. (2006) also investigated whether oxidative stress generated by various stimuli might result in activation of ERK by studying the effects of antioxidants on AN-induced ERK activation. Three non-enzymatic antioxidants were used: NAC, ascorbic acid, and water-soluble vitamin E (TRX) were used. When SK-N-SH cells were pretreated with 20 mM NAC for 10 minutes or 1 mM ascorbic acid or 1 mM TRX for 1 hour prior to addition of 400 μg/mL AN for 24 hours, no reduction in AN-induced ERK activation was found. Therefore, Chantara et al. (2006) concluded that the activation of ERK by AN observed in SK-N-SH cells was not mediated via an oxidative stress-dependent mechanism.

To determine if AN-induced ERK activation was mediated via PKC, PKC was inhibited via several methods. In addition to applying the PKC inhibitors, GF109203X (bisindolymalcimide) and rottlerin, PKC was also depleted by prolonged incubation of the cells with phorbol 12-myristate 13-acetate (PMA). Inhibition of PKC by GF109203X significantly reduced the increase in ERK1/2 phosphorylation to 26% of that caused by AN alone. Similarly, rottlerin and prolonged treatment with PMA reduced the activation of ERK by AN. Therefore, the study authors concluded that PKC played an important role in AN-induced ERK activation in SK-N-SH cells. In summary, this study demonstrated that AN activated ERK1/2 in a PKC-dependent manner and that oxidative stress and muscarinic receptor activation were probably not involved in ERK1/2 activation by AN.

4.5.2. Genotoxicity Studies

The following subsections provide a summary of the results of AN and its reactive metabolite, CEO, in in vitro and in vivo mutagenicity/genotoxicity assays. The overall conclusion that can be drawn from these studies is that AN is genotoxic after metabolic activation to CEO. Table 4-53, which provides a summary of studies on the mutagenicity/ genotoxicity of AN, is at the end of this section.

4.5.2.1. *Studies in Humans*

Seven studies have examined the genotoxicity of AN in vivo in humans who may have been occupationally exposed to AN.

Xu et al. (2003) measured the incidence of DNA strand breakage and sex chromosome aneuploidy in the sperm of 30 workers exposed to AN for 2.8 years. The mean AN concentration at operation sites was 0.8 mg/m^3. Thirty sperm donors of the same approximate age range from the general population were recruited as controls. Lower sperm density was noted in exposed workers compared with controls (75×10^6/mL vs. 140×10^6/mL). DNA strand breakage was detected in AN-exposed workers by using single-cell gel electrophoresis, with the rate of comet sperm higher in the exposed workers than in the controls (28.7 vs. 15%). The frequency of sex chromosome disomy was 0.69% in the exposed group and was >0.35% in the control group. There were also significant differences in the frequencies of XX-, YY-, and XY-bearing sperm between the exposed and control groups.

Fan et al. (2006), in an article translated from Chinese, evaluated the application of a micronucleus test by using buccal mucosal cells to detect genetic damages in AN-exposed workers. The low concentration (average concentration 0.522 mg/m^3 AN) exposed group consisted of 41 healthy male workers with direct contact with AN in a chemical plant that produced AN (by the oxidation of propylene, ammonia, and air) in Shanghai. Since the entire propylene-ammonia oxidation process was carried out in a closed system of pipes and automated technology, the chance of contact with AN was primarily at the time of on-site sampling and pipe inspection. The average age of this exposed group was 37.4 years, and the range and average exposure duration were 1–33 and 15.7 years, respectively.

The intermediate (average concentration 1.998 mg/m^3) exposed group consisted of 47 healthy male workers in an acrylic fiber factory in Shanghai. AN was used as a raw material in the synthesis of polyacrylonitrile by polymerization. The average age of workers was 39.8 years, and the range and average exposure duration were 1–33 and 17.2 years, respectively. The control group consisted of 31 healthy male workers with no exposure to any known mutagen or AN and living in the same community. Their average age was 37.2 years, and the average working duration was 16.7 years. The rates of alcohol consumption and cigarette smoking were similar in the exposed and control groups.

Buccal mucosal cells were collected from second scrapings from the mucous membrane on the inside of both cheeks of study subjects after rinsing their mouths with clean water. Blood samples were also collected for measurement of micronuclei (MN) in peripheral blood lymphocytes. The rates of occurrence of MN in buccal mucosal cells in the intermediate concentration exposed, low concentration exposed, and control groups were 4, 3.68, and 2.03%, respectively. The rates of MN in the low and intermediate concentration groups were significantly higher than in the control group ($p < 0.05$). The rates of occurrence of MN in peripheral blood lymphocytes in the intermediate and low concentration exposed and control groups were 4.23, 2.44, and 2.48%, respectively. The rate of occurrence of MN in blood lymphocytes in the intermediate exposed group was significantly different from that in the control group ($p < 0.05$).

To investigate the relationship between AN exposure and the rate of occurrence of MN and to eliminate the possibility of the presence of other confounding factors, a multivariate linear regression analysis was conducted. The results indicated that the cumulative exposed amount of AN, the recent exposed amount of AN, and the extent of cigarette smoking were important factors in the rate of occurrence of MN in buccal mucosal cells and blood lymphocytes. Fan et al. (2006) concluded that the micronucleus test of buccal mucosal cells could replace the micronucleus test of lymphocytes in the peripheral blood as a screening test for genetic damage in AN-exposed workers.

Borba et al. (1996) evaluated urinary genotoxicity of three groups of workers in an AN fiber production plant (exposed group 1: 14 workers in the continuous polymerization section; exposed group 2: 10 equipment maintenance workers; control group: 20 administrative workers from the same plant). Urine extracts were used in the Ames test (using TA 98, +S9) to assess gene reversion activity. No differences in urinary genotoxicity were found in the three groups. Additionally, there were no significant differences in the incidence of SCE in peripheral lymphocytes among the groups. However, the maintenance workers had a higher incidence of CAs in lymphocytes, consisting of chromatid and chromosomal gaps and chromatid and chromosomal breaks, than the controls ($p < 0.003$). These effects were also increased in production workers but not to statistically significant levels, possibly due to the comparatively low number of subjects in the study. The significantly higher incidence of CAs in maintenance workers were in agreement with the highly significant levels of Hb adducts and CEVal in the same population (see Section 4.1.2.2). The maintenance workers also had significantly higher levels of erythrocyte MDA, an indicator of lipid peroxidation, than the other two group of workers.

Ding et al. (2003) compared deletion frequencies of mitochondrial DNA in peripheral lymphocytes in 47 workers exposed to a mean workplace concentration of 0.11 ppm AN and 47 nonexposed workers using PCR techniques (this study is described more fully in Section 4.1.2.2). No deletions were detected in the nonexposed group, but a deletion frequency of 17% was detected in the exposed group. In a separate experiment on presumably nonexposed individuals, no deletions in mitochondrial DNA were detected in samples from 12 high school students, whereas the deletion frequency was 25% in samples from 12 elderly persons. Consistent with the hypothesis that damage to mitochondrial DNA contributes to degenerative diseases related to aging, the study authors suggested that occupational exposure to AN may induce mitochondria DNA deletion in cells that are related to aging.

Using the FISH technique with probes for chromosomes 1 and 4, Beskid et al. (2006) examined patterns of CAs in cultured lymphocytes from blood samples of 61 AN-exposed male workers involved in the polymerization of Indian rubber and 49 nonexposed control subjects. Stationary monitoring in the workplaces indicated AN air concentrations of 0.05–0.3 mg/m^3 for a group of 39 exposed workers sampled in 2000 and 0.05–0.7 mg/m^3 for another group of

22 exposed workers sampled in 2003. A 38% increase in frequency of aberrant cells in AN-exposed workers was found to be statistically insignificant. However, the number of reciprocal translocations increased by 53% ($p < 0.05$) in the AN-exposed group. In addition, a significant increase in a relative number of insertions was found in the AN-exposed group. Furthermore, chromosomal specificity was observed in lymphocytes with aberrations on chromosome #1 and #4. In the AN-exposed group, the proportion of cells with aberrations on chromosome #1 decreased significantly (58.8 vs. 73.8% in the control subjects, adjusted to age and smoking), but aberrations on chromosome #4 increased (47.0 vs. 29.4% in the controls).

In an earlier study by the same research group, the frequency of CAs in peripheral blood samples was studied in 45 male rubber polymerization workers exposed for the last 3 months to 0.05–0.3 mg AN/m^3, 23 matched controls living in the same region (control group I), and 33 unexposed controls from Prague (control group II) (Šrám et al., 2004). Subjects were interviewed and completed questionnaires on demographic data, occupational and environmental exposures, smoking habits, medications, X-ray examinations, viral infections, and alcohol consumption within the 3 months before sampling. Cytogenetic analysis was conducted using two methods. Conventional chromosomal analysis was used to quantify CAs (chromatid plus chromosome breaks and chromatid plus chromosome exchanges), the number of aberrant cells (those with breaks and exchanges, gaps not included), and the aberration frequency (number of breaks per cell). The FISH technique, using probes for chromosomes 1 and 4, was employed to quantify translocations. Conventional analysis did not detect any differences in the frequency of CAs in exposed workers compared with either control group. FISH detected no differences in the frequencies of aberrations or translocations in exposed workers compared with matched controls (control group I), but the frequencies in both groups were significantly elevated compared with unexposed controls from Prague (control group II). Šrám et al. (2004) concluded that occupational exposure to 0.05–0.3 mg/m^3 AN did not present a significant genotoxic risk and attributed higher frequencies in the exposed group and control group I to undetermined factors present in the region in which the petrochemical industries are located but absent in Prague.

Thiess and Fleig (1978) surveyed 18 workers at a plant that was used for manufacturing copolymers of styrene and AN, styrene, AN, and butadiene and also for synthesis of organic intermediates. The workers had been exposed to AN, on average, for 15.3 years and could have been exposed simultaneously to styrene, ethylbenzene, butadiene, and other chemicals. The control group consisted of 18 workers who had not been exposed to AN. Atmospheric monitoring conducted between 1963 and 1974 revealed AN concentration of about 5 ppm, with the possibility of higher peak values occurring in connection with special tasks. Between 1975 and 1977, exposure to AN had been reduced to an average of 1.5 ppm. The incidence of CAs in the lymphocytes was measured in these 18 workers and in age-matched nonexposed controls. The numbers of aberrant metaphases (gaps and iso-gaps included) were 5.5 ± 2.5% in exposed

workers and 5.1 ± 2.3% in controls. When gaps were not included, the numbers dropped to 1.8 ± 1.3% in exposed workers and 2.0 ± 1.6% in controls. The differences were statistically not significant. This study is of limited value because of mixed exposure in the exposed group, small group size, and uncertainty in exposure levels.

4.5.2.2. *In Vivo Tests in Mammals*

Rats

Oral administration of up to 40 mg/kg AN or i.v. administration of up to 98 mg/kg AN to male Sprague-Dawley rats did not induce MN in bone marrow and peripheral blood, respectively (Morita et al., 1997). However, Wakata et al. (1998) demonstrated induction of MN in bone marrow polychromatic erythrocytes of Sprague-Dawley rats (four/group) treated 2 times with 124.8 mg/kg AN i.v. and sampled 24 hours after treatment. A negative result was obtained in peripheral blood. In another study (Rabello-Gay and Ahmed, 1980), male Sprague-Dawley rats treated orally with 16 daily doses of 40 mg/kg-day AN showed no increase in CAs in the bone marrow over controls.

Irreversible binding of radioactivity from [2,3-^{14}C]-AN to DNA in brain, stomach, and liver of male Sprague-Dawley rats was reported 24 hours after a single oral dose of 46.5 mg/kg (Farooqui and Ahmed, 1983a). DNA alkylation was significantly higher in the target organs, brain and stomach (119 and 81 pmol/mg DNA at 24 hours, respectively), than in the liver (25 pmol/mg DNA). The covalent binding indices in the liver, stomach, and brain at 24 hours after dosing were 5.9, 51.9, and 65.3, respectively. Similarly, covalent binding of [2,3-^{14}C]-AN or its metabolite to testicular (Ahmed et al., 1992a), lung (Ahmed et al., 1992b), and gastric tissue DNA (Abdel-Rahman et al., 1994b) has been reported in male Sprague-Dawley rats treated with a single oral dose of 46.5 mg/kg AN. Maximum covalent binding of radioactivity to gastric DNA occurred at 15 minutes after dosing and occurred at 0.5 and 12 hours for testicular and lung DNA, respectively. Alkylation of hepatic DNA was also reported when a single dose of 0.2 mmol [2,3-^{14}C]-AN was administered to male Wistar rats intraperitoneally (Peter et al., 1983a). Two ^{14}C peaks that did not cochromatograph with any known standards were observed when the DNA hydrolysate from rat livers was chromatographed on PEI-cellulose column.

In another study, 0.6 mg/kg [2,3-^{14}C]-CEO was administered to one F344 rat intraperitoneally (Hogy and Guengerich, 1986), and the rat was sacrificed after 1 hour. Covalent binding to both liver and brain protein was found, but no covalent binding to nucleic acids could be detected at the level of 0.3 alkylations per 10^6 bases. In the same study, three male F344 rats were administered 50 mg/kg AN i.p., and three other rats were administered 6 mg/kg CEO i.p. (Hogy and Guengerich, 1986). The rats were sacrificed after 2 hours. N^7-(2-oxoethyl)guanine was measured in liver DNA at the level of 0.032 and 0.014 alkylations/10^6 bases for CEO- and AN-treated rats, respectively. In the brains of treated rats, the levels of N^7-(2-oxoethyl)guanine were not above the limit of detection. Since DNA adduct was detected in liver DNA, covalent

binding to DNA had to occur. The method used in the study was not sensitive enough to detect low levels of alkylation of nucleic acids, probably because of the small amount of DNA sample from one rat, and the DNA isolation protocol (DNA extract purified by hydroxylapatite column chromatography and DNA fraction dialyzed against water and lyophilized then treated with RNAase and proteinase K) and method for correction for contaminating protein via quantitative amino acid analysis in the DNA sample may have allowed a more stringent determination of DNA-bound material.

When the alkaline comet assay was used to detect DNA lesions, Sekihashi et al. (2002) demonstrated DNA damage in the forestomach, colon, kidney, bladder, and lung of Wistar rats treated with a single dose of 30 mg/kg AN i.p. but not in the brain or bone marrow.

Oral exposure to 100 ppm AN in drinking water for 14 or 28 days significantly increased the level of cellular DNA fragmentation in the brain of male Wistar rats (Mahalakshmi et al., 2003). Other aspects of this study are discussed in Section 4.5.1.1.4.

AN-induced unscheduled DNA synthesis (UDS) was demonstrated in several studies in rats. In a study by Hogy and Guengerich (1986), male F344 rats (12/group) received a single sublethal dose of 50 mg/kg AN in saline by gavage, followed by hydroxyurea to arrest replicative DNA synthesis but allowing excision repair DNA synthesis. Two hours after dosing, the animals received s.c. methyl [^{3}H]-labeled thymidine. This dose was repeated after 2 hours, and half the dose was given again after 2 more hours for a total dose of 3.0 mCi/kg of BW. The animals were sacrificed 2 hours after the last methyl [^{3}H]-labeled thymidine. A significant occurrence of UDS was found in the livers but not in the brains of AN-treated rats.

Hogy and Guengerich (1986) also studied the effect of treatment on DNA synthesis over 4 hours in the liver and brain of male F344 rats 48 hours after an oral dose of 50 mg/kg AN. DNA synthesis was decreased in the brain but not in the liver; replicative indices were 0.29 and 1.30, respectively. Thus, the carcinogenicity of AN in rat brain is not likely from cytotoxicity, followed by an increased rate of DNA replication and leading to a greater chance of error during the rapid DNA synthesis.

UDS was demonstrated in lung (Ahmed et al.,1992a), testis (Ahmed et al., 1992b), and gastric tissue (Abdel-Rahman et al., 1994a) of AN-treated male Sprague-Dawley rats (12/group). Animals received a single oral dose of 46.5 mg/kg AN in saline, with or without hydroxyurea cotreatment to block the endogenous deoxynucleotide pool. [^{3}H]-Thymidine was administered 0.5, 6, or 24 hours after AN dosing, and animals were sacrificed 2 hours later. The replicative index for DNA synthesis (i.e., the ratio of DNA synthesis in treated animals over controls) was significantly reduced at all three time points in lung, while DNA repair in the lung was increased by twofold at 0.5 hour and 1.6-fold at 6 hours following AN oral treatment. Similarly, DNA synthesis was inhibited in testes at 0.5 and 24 hours after treatment (but increased at 6 hours), whereas DNA repair increased at 1.5- and 33-fold at 0.5 and 24 hours after treatment. For gastric tissue, DNA replicative synthesis was inhibited 6 hours after AN administration but was

rebounded and followed by a twofold increase at 24 hours. A threefold increase in UDS was observed at 24 hours after dosing.

On the other hand, Butterworth et al. (1992) followed the incorporations of [^{3}H]-thymidine into the hepatocytes isolated from male F344 rats gavaged with either a single dose of 75 mg/kg AN or five daily doses of 60 mg/kg AN. Single-dosed animals were sacrificed 2 or 12 hours after dosing. Multiple-dosed animals were sacrificed 4 hours after the last dose. Hepatocytes were isolated and plated on cover slips and incubated with [^{3}H]-thymidine. Autoradiography was used to detect UDS. No sign of AN-induced UDS was found in hepatocytes from exposed rats. In addition, no UDS was found in the in vivo spermatocyte DNA repair assay with AN, using cells isolated from the seminiferous tubules of the same treated rats (Butterworth et al., 1992). The difference in results from Butterworth et al. (1992) and Hogy and Guengerich (1986) regarding UDS in rat liver may be due to differences in methodology in that incorporation of [^{3}H]-thymidine actually took place in vitro in the study by Butterworth et al. (1992).

AN also produced negative results for dominant lethal assay in male F344 rats (Working et al., 1987). In this assay, groups of 50 male F344 rats received AN by gavage at 0 or 60 mg/kg-day in 0.9% saline for 5 days. AN exposure in males had no effect on the incidence of pre- or postimplantation losses, indicating a negative result to germ cells.

Mice

When the alkaline comet assay was used to detect DNA lesions, Sekihashi et al. (2002) demonstrated DNA damage in the forestomach, colon, bladder, lung, and brain of male ddY mice treated with 20 mg/kg AN i.p. DNA damage was not detected in the liver, kidney, or bone marrow.

Sharief et al. (1986) determined that AN caused a slight increase on SCE frequencies in bone marrow cells of male C57B1/6 mice (four/dose group). No increase in SCE frequencies was observed in mice administered a single dose of up to 30 mg/kg AN intraperitoneally. Higher doses were lethal to most of the animals. An increase in SCE frequency (2 × control) was observed in the only surviving mouse at the 45 mg/kg dose group. However, Fahmy (1999) reported AN-induced SCEs in bone marrow cells of male Swiss mice (five/group) treated with 7.5 mg/kg or 10 mg/kg AN i.p. 8 hours following BrdU treatment and with colchicines 2 hours prior to sacrifice. The lowest dose of 5 mg/kg i.p. produced no significant effect on SCE frequency.

Earlier CA studies in mice have been largely negative. Rabello-Gay and Ahmed (1980) showed that AN did not produce increases in CAs in bone marrow cells of male Swiss mice (six/group) when given orally for 4, 15, or 30 days at doses up to 21 mg/kg-day or by i.p. injection at doses up to 20 mg/kg-day for the same duration. No increase in the incidence of CAs compared with controls was observed in bone marrow cells of NMRI mice that were

injected intraperitoneally with 20 or 30 mg/kg AN (Leonard et al., 1981). No increase in CAs in bone marrow cells and spermatogonia was observed in ICR mice treated with 20 or 100 mg/m^3 AN for 5 days (Zhurkov et al., 1983). However, Fahmy (1999) reported AN-induced CAs in mouse spermatocytes after single oral doses of 15.5 or 31 mg/kg or three or five successive oral doses of 7.75 mg/kg (1/8 LD_{50}) in male Swiss mice. In addition, AN induced CAs in mouse bone marrow cells and spleen cells after a single oral dose of 7.75 mg/kg or three or five successive doses of 7.75 mg/kg. The aberrations were mainly of chromatid type (gaps, breaks, fragments, and deletions), with metaphases carrying one aberration only being dominant.

Leonard et al. (1981) also reported AN did not induce MN in polychromatic erythrocytes of male NMRI mice injected intraperitoneally with 20 or 30 mg/kg AN. Marginal, but statistically significant, increases in MN were observed in bone marrow polychromatic erythrocytes but not in peripheral blood when AN at doses of 5.6–45 mg/kg was administered to male CD-1 mice (five/group) via i.p. administration. Oral or i.v. injection yielded negative results (Morita et al., 1997).

Treatment with AN produced negative results for dominant lethal assays in male mice. The dominant lethal assay was used to detect CAs in meiotic and postmeiotic male germ cells. Groups of five male NMRI mice were injected intraperitoneally with 0 or 30 mg/kg AN in saline or isopropyl methanesulfonate (positive control) and then mated to untreated females (three per male) for 5 weeks (Leonard et al., 1981); females were replaced after 7, 14, 21, and 28 days, and the uterine contents were examined 17 days after mating. No evidence for dominant lethal effects was observed.

4.5.2.3. *Short-term Tests: Bacteria, Fungi, Drosophila, Others*

There are a large number of reports of short-term genotoxicity test results on AN that have been made available through the auspices of the International Programme on Chemical Safety (IPCS). The IPCS coordinated the investigation of eight organic carcinogens known to be either inactive or difficult to detect in the Salmonella assay, including AN, benzene, diethylhexylphthalate, diethylstilbestrol, hexamethylphosphoramide (HMPA), PB, safrole, and o-toluidine, as well as two noncarcinogens in rodent bioassays (benzoin and caprolactam). Most of the available short-term genotoxicity tests were employed, and the work was carried out at some of the major research and testing laboratories throughout the world. The purpose of this endeavor was to evaluate the efficacy of these tests, to evaluate the strengths and weaknesses of such tests, and to identify the assay systems to complement the widely used Salmonella assay. All of the results from these studies have been compiled in a 750-page collection (Ashby et al., 1985), and a 56-page synopsis of the results is available on the Internet (IPCS, 1985). The conclusion from these evaluations was that AN, along with HMPA, o-toluidine, and safrole, belonged to a group of genotoxins that were detected by most of the eukaryotic assays studied and could easily be found to be nonmutagenic in the Salmonella assay because of protocol

deficiencies associated with the overall metabolic capacity of the assay system. While several of these studies have been cited in this section, an overview of the findings as they pertain to AN follows.

AN, at concentrations not overtly toxic in a given assay, was found in 42 of 68 tests to positively cause genotoxicity in bacteria, fungi, *Drosophila melanogaster* (mutation, gene reversion, mitotic crossing over, aneuploidy), and mammalian cell culture assay systems, both human and animal (single-strand breaks, UDS, CAs, SCEs, MN, and transformation). Among the eight carcinogens studied, AN gave the most positive results, inducing genotoxicity responses in 62% of all tests (42 out of 68 tests; 25 were negative and 1 was questionable). That number of positive responses rose to 81% when a more stringent selection of assays was applied (IPCS, 1985). Other studies, covering all assay types used in that collaborative study, are listed in the two subsections on short-term assays (Sections 4.5.2.3 and 4.5.2.4).

4.5.2.3.1. ***Bacterial tests.*** A number of research groups have examined the capacity of AN to induce gene reversion in the Ames test. One of the first published papers was Milvy and Wolff (1977), which reported positive results of AN on *Salmonella typhimurium* strains TA 1535, 1538, and 1978 in the presence of S9 and an NADPH generating system. The first strain is sensitive to base substitution mutagens, and the latter two strains are sensitive to frameshift mutagens. Negative results were obtained when metabolic activation was excluded from the system. Gene mutation by exposure of bacteria to an atmosphere containing AN was found to occur at concentrations as low as 57 ppm (equivalent to 2 μL of AN), lower than exposure in solution or spotting AN to a "lawn" of bacteria on a plate. This could be because AN vaporized readily in solution such that the actual exposure concentrations in solution or by spotting were uncertain. The findings of Milvy and Wolff (1977) were criticized by Venitt (1978) in a letter to the editor. While not disagreeing with the overall conclusion, Venitt (1978) considered the study authors to have calculated mutation frequency incorrectly from the data. Venitt (1978) confirmed AN to be mutagenic in TA 1535 but not in the frameshift strains TA 1538 and 1978.

Among other reports of AN activity in the Ames test, Lijinsky and Andrews (1980) found AN at doses of 100–1,000 μg per plate to be positive in *S. typhimurium* TA 1535 in the presence of S9 but negative in TA 98, 100, 1537, and 1538 in the plate incorporation assay. Similarly, Brams et al. (1987) reported AN (50–750 μg/L) to be negative for gene reversion in TA 97, 98, and 100 using plate incorporation assay, irrespective of metabolic activation. The study authors accounted for these negative results with inadequate experimental conditions. Previously, they had demonstrated that AN was mutagenic in TA 1530, 1535, and 1950 when 0.2% gaseous AN was injected into the dessicator where the plates were incubated for 1 hour in the presence of S9 (the plate agar contained 200 μg AN/plate) (de Meester et al., 1978). A lower mutagenic activity was also detected with strains reversed by frameshift mutation (TA 98, 1978, 100), and assays

conducted by the plate incorporation method gave negative results (de Meester et al., 1978; Dow Chemical Co., 1976).

Jung et al. (1992) provided data from three laboratories that examined the ability of AN to induce gene reversion in TA 102 in the plate incorporation assay, with uniformly negative results. Hakura et al. (2005) reported that AN induced dose-dependent increases in the number of revertants per plate in strain TA 100 exposed to concentrations ranging from 806 to 12,100 μg per plate in the presence of rat or human liver S9 preparations, but the maximum response at 12,100 μg per plate was slightly less than twofold higher than the number of revertants per plate observed in the negative controls.

Although the methodologies of the experiments may have been different, the positive finding of mutagenicity by de Meester et al. (1978) for AN in TA 98 and 100 is in agreement with data from Khudoley et al. (1987) that AN (concentration not provided) was positive in TA 98 and 100 (with two- to fivefold increase in frequency of induced mutants), irrespective of the presence of S9. Zhurkov et al. (1983) reported AN to dose-dependently induce mutations in *S. typhimurium* TA 1535 but not in TA 1538. The presence of complete S9 fraction was required for this effect, but a 9,000 × g microsomal supernatant without cofactors gave inconsistent results. The concentrations tested were between 0.1 and 10,000 μg per dish. The highest concentration was overtly toxic to the bacteria.

Other tests of the mutagenicity of AN in bacterial systems were negative. For example, Nakamura et al. (1987) employed the SOS test to evaluate the capacity of AN to induce expression of the umu gene in *S. typhimurium* TA 1535/pSK1002. This strain contains a umuC-lacZ fused gene, such that a forward mutation results in umu gene expression and the transcription of the lac operon and can be demonstrated phenotypically by a twofold increase in β-galactosidase activity. AN, at concentrations up to 2,820 μg/mL, and seven other known mutagens gave negative results in this system. Similarly, AN was negative in the SOS chromotest in *Escherichia coli* PQ37 (Brams et al., 1987). It should be noted that only 4 out of 14 compounds that were positive in the Ames assay were positive in the SOS chromotest kit used. Thus, some technical issues were responsible for the poor performance of the test kit (Brams et al., 1987).

Venitt et al. (1977) tested AN for mutagenicity in a gene reversion assay (2–3 days at 37°C), using the tryptophan-dependent *E. coli* WP2 series of bacteria as indicator organisms. Doses of 75 and 150 μmol per plate of AN produced a dose-related increase in the number of revertant colonies ($trp^- \rightarrow trp^+$) compared with untreated bacteria in WP2 (which is DNA repair proficient), WP2 *uvrA* (which lacks excision repair), and WP2 *uvrApolA* (which lacks both excision repair and DNA polymerase 1) without a need for S9 fraction. The study authors confirmed these results by using a simplified "fluctuation" assay in which they obtained a dose-dependent increase in mutation rate induced by 0.4–2 mM AN (20- to 40-fold lower than the levels in plate test) in *E. coli* WP2. An exponential dose response was seen at lower

concentrations, 0.1–0.4 mM, with mutant WP2 uvrApolA, which lacked both excision repair and DNA polymerase-1. The effective mutagenic concentration range for AN was lowered by an order of magnitude when an error-prone DNA-repair plasmid, pKM101, was introduced into *E. coli* WP2. The study authors concluded from these results that AN caused non-excisable mis-repair DNA damage that ultimately gave rise to DNA strand breaks. Venitt et al. (1977) hypothesized that AN might react with thymine residues in DNA since AN has been shown to cyanoethylate ring N atoms of minor tRNA nucleosides and ribothymidine and thymidine (Ofengand, 1967).

Lambotte-Vandepaer et al. (1985, 1981, 1980) collected urine from male Wistar rats (two/group) and NMRI mice (five/group) that had been administered a single dose of AN (30 mg/kg intraperitoneally). The urine samples were evaluated for potential induction of gene reversion in *S. typhimurium* TA 1530. Positive results were obtained in rats and mice in the absence of S9. Mutagenic activity in urine was abolished by the presence of S9 in rats and decreased in mice, a finding that suggests that the mutagenic agent in urine can be inactivated metabolically. Pretreatment with PB (induces CYP450 monooxygenase), $CoCl_2$ (inhibits CYP450 monooxygenase), and DEM (depletes GSH), before AN treatment, slightly decreased the mutagenic response in urine from mice and completely abolished the response in urine from rats. However, the study authors were unable to identify the genotoxic compound in urine.

4.5.2.3.2. ***Fungi.*** Available studies that employed fungi in short-term assays on the mutagenicity/genotoxicity of AN produced mostly positive results. AN induced mitotic gene conversion in both stationary-phase and log-phase cultures at the his_4 and trp_5 loci of *Saccharomyces cerevisiae* JD1, in the presence of metabolic activation by S9. Negative results were obtained without metabolic activation (Brooks et al., 1985; Shell Oil, 1984a). AN did not induce chromosome loss in *S. cerevisiae* D61.M (Whittaker et al., 1990) but elicited respiratory deficiency, reflecting antimitochondrial activity.

4.5.2.3.3. ***Drosophila.*** A range of in vivo experimental systems used the fruit fly, *D. melanogaster*, to examine the mutagenicity/genotoxicity of AN. Drosophila can biotransform certain procarcinogens to their reactive metabolites and are used in short-term tests for identifying carcinogens and in studies on the mechanism of mutagenesis of chemicals (Vogel et al., 1999).

Osgood et al. (1991) used the Drosophila ZESTE system to monitor the potential for AN to induce sex chromosome aneuploidy, following inhalation exposure of adult females to 2.7 ppm for up to 70 minutes. AN induced chromosome loss after exposure for 50 and 70 minutes. AN was mostly nontoxic at the tested dose, with only 13% killed after a 70-minute exposure. Similarly, in a Drosophila somatic recombination and mutation assay, Drosophila larvae were exposed to 5–20 mM AN in water for 9–11 days, and hatching females were scored

for twin mosaic spots and single mosaic light spots in their eyes (Vogel, 1985). These genetic markers might arise from many types of genetic alterations. Mitotic recombination and chromosome breakage would result in mosaic twin spots, whereas deletions and gene mutations would give rise to mosaic single light spots. AN was positive for the induction of mosaic single spots at 5 mM (LC_{50} concentration was 10 mM) and negative for twin spots. Since the classification of single spots or twin spots might be subjected to personal bias, the total of twin and single spots was also reported, and AN gave positive result.

AN was shown to be mutagenic by having marginally positive effects in somatic mutation/recombination assay on wing spots of Drosophila, with gas exposure of larva to 0.5–1 μL/1,150 mL for 0.5 or 1 hour (Würgler et al.,1985). AN gave negative results in a sex-linked recessive lethal mutation test on postmeiotic and meiotic germ cells of male *D. melanogaster*, exposed either by feeding of 420 ppm AN or injected with 3,500 ppm AN (Foureman et al., 1994).

The in vitro effect of AN on taxol-purified microtubules from Drosophila and mouse brain was evaluated by Sehgal et al. (1990). (Taxol promoted the formation and stability of microtubules.) Microtubules assist in the movement of chromosomes in both mitosis and meiosis. Polymerization and depolymerization of microtubules occur in cell division to separate the chromosomes from the metaphase plate during anaphase. In this study, the assembly and disassembly of microtubules was monitored spectrophotometrically in vitro. Previous results from in vivo assays monitoring induced sex chromosome aneuploidy indicated that effective aneuploidogens affected microtubule assembly. When taxol-purified *D. melanogaster* microtubule was incubated at 37°C to allow polymerization, addition of 5 or 50 mM AN resulted in 28 and 64% inhibition of microtubule assembly, respectively. When taxol-purified mouse brain microtubules were incubated with 5 or 50 mM AN, 74 and 96% inhibitions of microtubule assembly were observed, respectively. Thus, these results indicated that AN was an aneuploidogen in vitro. On the other hand, taxol significantly affects microtubule depolymerization assay, probably by stabilizing the formed microtubules. None of the tested aneuploidogens, including colchicine, promoted disassembly to taxol-purified microtubules.

4.5.2.3.4. ***Other short-term tests.*** Yates et al. (1994) reported on the ability of CEO to induce single- and double-strand DNA breaks in supercoiled DNA plasmid pBR322 DNA. Supercoiled DNA (1 μg) was incubated for 3 hours at 37°C with ≥50 mM CEO and then subjected to agarose gel electrophoresis. The study authors reported that CEO non-enzymatically induced DNA strand breaks in a dose- and time-dependent manner, but detailed data were not provided. Peter et al. (1983b) found that AN did not induce strand breaks in SV40 phage DNA in vitro, whereas synthetic glycidonitrile (i.e., CEO) was effective in the same system (both agents were incubated with DNA at 1 mmol/L for 17 hours in the dark, at 37°C, in a buffered solution without any enzyme addition).

4.5.2.4. *Mammalian Cell Short-term Tests*

4.5.2.4.1. ***Mutations.*** A number of research groups have examined the ability of AN to induce forward mutations in human lymphoblast cell lines and the well-known mouse lymphoma L5178Y $Tk^{+/-}$ system.

Crespi et al. (1985) used two human lymphoblast cell lines, *Tk*6 (which does not contain CYP450 activities) and AHH-1 (which is metabolically competent) to assess AN mutagenicity at the thymidine kinase ($Tk^{+/-}$) locus and the hprt locus, respectively. *Tk*6 cell cultures were treated with 0–40 μg/mL AN for 3 hours with and without externally added metabolic activation (rat liver S9). On the third day after treatment, the cultures were plated in a selective medium containing 2 μg/mL trifluorothymidine. After incubation for 12 days, the plates were scored for the presence of mutant colonies. Similarly, AHH-1 cell cultures were treated with AN for 28 hours, and the cultures were plated on the 6th and 7th day after treatment in a selective medium containing 0.6 μg/mL 6-TG. AN induced dose-dependent mutations at the $Tk^{+/-}$ locus in *Tk*6 cells in the presence, but not in the absence, of S9. AN induced mutations at the hprt locus in AHH-1 cells. The lowest AN concentrations that were mutagenic in these test systems were 40 μg/mL with *Tk*6 cells +S9 and 25 μg/mL with AHH-1 cells.

Similarly, Recio and Skopek (1988a, b) assessed the mutagenicity of AN and its epoxide metabolite, CEO, at the $Tk^{+/-}$ locus in *Tk*6 human lymphoblast cells in the presence and absence of rat liver S9. In the presence of S9, 2-hour incubations with 1.4 mM AN induced mutations at the $Tk^{+/-}$ locus as demonstrated by the presence of mutant clones when plated in trifluoro-thymidine selection medium after treatment, but, in the absence of S9, no mutagenic activity was observed over the concentration range of 0.4–1.5 mM (Recio and Skopek, 1988b). In contrast, 2-hour incubation with CEO at concentrations as low as 100 and 150 μM induced a mutagenic response (without metabolic activation) at the $Tk^{+/-}$ locus (Recio and Skopek, 1988b). On a molar basis, CEO was as mutagenic in this system as the well-known mutagen, ethyl methanesulfonate (Recio and Skopek, 1988a).

Two classes of CEO-induced $Tk^{-/-}$ mutant phenotypes were identified that differed in their growth rates: Tk_n with normal growth rate and Tk_s with slower growth rates. Southern blot analysis of DNA of these two classes indicated that the phenotypes differed genotypically (Recio and Skopek, 1988b). Ninety-six percent (25/26) of Tk_s mutants had lost a 14.8 kb DNA fragment corresponding to the active *Tk* allele, whereas only 8% (1/12) of CEO induced Tk_n mutant clones and 22% (2/9) of spontaneous Tk_n mutant clones had lost the 14.8 kb fragment (Recio and Skopek, 1988a, b). Recio and Skopek (1988a) suggested that Tk_s mutants resulted from large-scale DNA structural alterations involving the active *Tk* allele. CEO induced predominantly Tk_n mutants. Southern blot analysis of CEO-induced Tk_n mutants indicated the majority of these mutants were below the detection limit of <2 kb. Thus, CEO-induced alterations are relatively small DNA alterations. Recio and Skopek (1988a) suggested that

CEO-induced Tk_n mutants resulted from point mutations or small insertion/deletions that occurred during the replication or repair of CEO-modified DNA. Karyotypic analysis on two Tk_n mutants and 16 Tk_s mutants indicated that the majority of *Tk* mutants were not accompanied by abnormalities of the chromosome on which the *Tk* gene resides (chromosome 17).

CEO also induced mutations at the hprt locus in *Tk*6 cells (Recio and Skopek, 1988a). Characterization of the hprt mutations by cDNA sequencing analysis indicated that several hprt mutations were formed. A major (8/14) type of CEO-induced mutation was the specific loss of exons from the coding region of hprt. Remaining mutants (6/14) were single base substitutions (point mutation) resulting from amino acid changes (A:T base pairs and G:C base pairs).

The mutagenicity of AN was evaluated in the mouse lymphoma L5178Y $Tk^{+/-}$ forward mutation assay by a number of laboratories. Oberly et al. (1996) demonstrated that AN (activated with S9) was mutagenic at 40 μg/mL in this assay because of producing a more than twofold increase in mutant frequency when compared to the mutant frequency of the solvent controls. Earlier results in the mouse lymphoma L5178Y *Tk*+/- system from several studies all pointed to the capacity of AN at 12.5–200 μg/mL to induce forward mutations at the $Tk^{+/-}$ with or without S9 (Lee and Webber, 1985; Myhr et al., 1985; Amacher and Turner, 1985; Rudd, 1983). Garner and Campbell (1985) also reported that AN induced mutations to ouabain and 6-TG resistance in the mouse lymphoma L5178 Y cells in the presence of S9. However, negative results were obtained by Styles et al. (1985) in the mouse lymphoma L5178Y $Tk^{+/+}$ cell line (Na^+/K^+ ATPase locus, ouabain was used for mutant selection) and $Tk^{+/-}$ cell line (trifluorothymidine was used for mutant selection). Using P388F mouse lymphoma $Tk^{+/-}$cell line in the presence of S9, Anderson and Cross (1985) also obtained forward mutations to 5-iodo-2-deoxyuridine resistance with AN. However, negative results were obtained by Lee and Webber (1985) in Chinese hamster V79/HGPRT assay in which AN did not induce 8-azaguanine resistance mutation with or without S9.

4.5.2.4.2. *Other DNA effects*

UDS

AN, at concentrations up to 2.5 mg/mL, was negative for induction of UDS in HeLa cells with or without the presence of S9, using the scintillometric method (Martin and Campbell, 1985). However, an increase in UDS, as measured by uptake of [^{3}H]-thymidine, was reported in cultured human lymphocytes treated with 5×10^{-1} M AN and S9 (Perocco et al., 1982). Negative results were reported for the ability of AN to induce DNA repair synthesis (measured by incorporation of [^{3}H]-thymidine and autoradiographic techniques) in rat hepatocyte primary culture (Probst and Hill, 1985; Williams et al., 1985). However, no UDS, as measured by autoradiography, was observed in any of the cultures treated with the eight tested carcinogens (Probst and Hill, 1985). Similarly, only one of the eight carcinogens tested by Williams et al. (1985) induced DNA repair synthesis as determined by autoradiography of [^{3}H]-thymidine

incorporation (AN was negative in this assay). Thus, IPCS (1985) concluded the rat hepatocyte autoradiographic UDS assay was an insensitive assay for determination of genotoxicity of these chemicals and should be avoided for use as a complement to the Ames assay.

Butterworth et al. (1992) used incorporation of [^{3}H]-thymidine and autoradiographic techniques to study the effect of AN and CEO on unscheduled DNA repair in vitro in rat hepatocytes, and human mammary epithelial cells. AN and CEO were negative for the induction of DNA repair in hepatocytes in vitro. There was some indication of a statistically insignificant response at 0.1 mM CEO. However, CEO was toxic to the hepatocyte culture at 1 mM, the next higher tested concentration. As noted previously, IPCS (1985) has determined that rat hepatocyte autoradiographic UDS assay is insensitive for genotoxicity testing of AN and a group of seven other carcinogens. However, CEO, but not AN, was positive for UDS in human mammary epithelial cells in vitro (Butterworth et al., 1992).

DNA strand breaks

DNA single-strand breaks were measured by the alkaline elution method in the following studies. DNA single-strand breaks were induced in [^{14}C]-thymidine-labeled cultured adult human bronchial epithelial cells treated with 200 or 500 μg/mL AN for 20 hours (Chang et al., 1990). These concentrations were below the cytotoxic concentration of 600 μg/mL AN. DNA single-strand breaks were also reported in cultured rat hepatocytes treated with 65.8 μg/mL AN for 3 hours (Bradley, 1985). Higher concentrations of 197 or 658 μg/mL AN resulted in cytotoxicity. In another study, AN induced DNA single-strand breaks in cultured Chinese hamster ovary (CHO) cells treated with 3.7×10^{3} or 5.3×10^{4} μg/mL AN (7×10^{-2} or 1×10^{-1} M AN) with or without S9 mix for 1 hour (Douglas et al., 1985). These concentrations were above the cytotoxic concentrations of 5.31 and 53.1 μg/mL AN (10^{-5} and 10^{-4} M) with and without S9 mix, respectively. Thus, the observed DNA strand break effect was relatively weak in CHO cells. Lakhanisky and Hendrickx (1985) reported that AN (concentrations not reported) did not in induce DNA strand breaks in cultured CHO cells with or without S9. Therefore, cultured CHO cells may not be a sensitive assay system to test for DNA strand breaks induced by AN when compared with other cell cultures. On the other hand, DNA strand breaks was reported in SHE cells treated with AN. Parent and Casto (1979) observed incubation of [^{3}H]-thymidine-labeled primary SHE cells with 200 or 400 μg/mL AN for 18 hours caused a shift in the sedimentation pattern of the labeled cellular DNA when subjected to alkaline sucrose gradient.

4.5.2.4.3. ***Cytogenic effects.*** AN induced SCE in cultured adult human bronchial epithelial cells treated with noncytotoxic concentrations of 150 or 300 μg/mL AN for 20 hours (Chang et al., 1990). An increase in frequency of SCE was observed in human lymphocytes from two different donors incubated for 1 hour with 5×10^{-4} M AN and S9 mix. No increase in SCE was observed without the S9 mix metabolizing system. (Perocco et al., 1982). AN was negative for the

induction of SCEs in CHO cells (Ved Brat and Williams, 1982). However, when CHO cells were cocultured with freshly isolated rat hepatocytes, Ved Brat and Williams (1982) observed that AN at 10^{-4} M produced a greater than twofold increase in SCEs in the CHO cells, suggesting that the rat hepatocytes metabolized AN to its reactive metabolite, which was then transported into the CHO cells. Other cytogenetic findings in CHO cells included positive results for the induction of SCEs at 2 mM AN with S9 (Natarajan et al., 1985) and CA at 4 mM AN with or without S9, while Douglas et al. (1985) reported that AN at 10^{-1} M induced the formation of MN. AN was reported to induce CAs in Chinese hamster lung (CHL) fibroblasts in culture without metabolic activation at nontoxic concentrations of 12.5 μg/mL (Ishidate and Sofuni, 1985). AN induced structural CAs in Chinese hamster liver fibroblast cell line (CH1-L) at the lowest concentration of 2.5 μg/mL and higher (Danford, 1985).

Sasaki et al. (1980) found that 0.0053 mg/mL AN induced chromosome breaks in a pseudodiploid Chinese hamster cell line (Don-6). AN was negative at concentrations up to 10 μg/mL for the induction of CAs, SCEs, and polyploidy in cultured epithelial-like cells from rat liver (RL4 cell line) (Priston and Dean, 1985; Shell Oil Co., 1984b). Mangir et al. (1991) reported that CHO cells treated with AN demonstrated a growth and RNA synthesis rate that is similar to that for agents that cause damage to nuclear DNA in cells. Growth and RNA synthesis of CHO cells was inhibited with 0.001% (v/v) AN and completely inhibited at 0.005% (v/v) AN.

Kodama et al. (1989) conducted cytogenetic analyses on eight spontaneous and eight CEO-induced Tk_s mutant clones in *Tk*6 human lymphoblastoid cultures that had lost the 14.8 kb polymorphic band corresponding to the active *Tk* allele. These CEO-induced $Tk^{-/-}$ mutants were reported in the Recio and Skopek (1988a, b) studies. No chromosomal abnormalities were found in the eight spontaneous mutants. On the other hand, a visible abnormality on chromosome 17 was found in one of the CEO-induced tk_s mutants and was marked by duplication of the long arm of chromosome 17, with break points at q11 and q21. The latter break point was close to the *Tk* locus, suggesting the observed aberration might be associated with $Tk^{-/-}$ phenotype.

4.5.2.4.4. ***Transformation assays.*** Parent and Casto (1979) studied the capacity of AN to induce transformations in primary SHE cells in culture by monitoring the incidence of microscopically observed foci of morphologically transformed cells. In two experiments, SHE cell cultures were exposed to 25–200 μg/mL AN for 18 hours, after which AN was removed and cultures were subsequently inoculated with 200 focus-forming units of simian adenovirus SA7 and incubated for 3 hours. Colonies of surviving cells were counted after 8 days, and virus-transformed foci were counted after 21 days. Pretreatment of cells with AN prior to viral inoculation resulted in only slight enhancement of 1.8-fold in SA7 foci. In another experiment, SHE cells were treated with the same concentrations of AN 5 hours after viral inoculation. This resulted in an enhancement ratio that was markedly increased (8.9 at AN concentration of 200 μg/mL vs. 1.0 in controls).

When SHE cells were treated for 6 days with 12–100 μg/mL AN without added SA7 virus, foci of morphologically transformed cells were observed at 50 μg/mL AN (two foci/six dishes) and 100 μg/mL AN (three foci/nine dishes).

The ability of AN to induce transformation in SHE cells was also evaluated by Barrett and Lamb (1985). AN was considered to give a positive response according to the criterion of inducing four or more transformed colonies per 2,000 surviving colonies. With a relative survival of unity, the lowest concentration of AN (0.01 μg/mL) generated morphologically transformed colonies at a rate of 4/1,149.

Lawrence and McGregor (1985) evaluated the ability of 10 potential carcinogens, including AN, to induce morphological transformation in cultured embryonic mouse fibroblasts (C3H/10T1/2, Clone 8) in the presence or absence of S9. Positive response was obtained at 16 μg/mL AN in the presence of S9, while responses were uniformly negative in its absence.

Banerjee and Segal (1986) studied whether AN (0–200 μg/mL) could produce in vitro transformation of C3H/10T1/2 and NIH/3T3 mouse fibroblast cells in culture. AN was cytotoxic at the higher concentrations, with cell survival dropping below 75% at ≥50 μg/mL in C3H/10T1/2 and NIH/3T3 cells. Optimal transformation rates were obtained at AN concentrations of 12.5 μg/mL in C3H/10T1/2 cells. AN-induced transformation was observed at concentrations between 3 and 100 μg/mL in NIH/3T3 cells.

Matthews et al. (1985) evaluated whether AN induced morphological transformation and mutation to ouabain resistance in Balb/c-3T3 cells in culture with or without exogenous metabolic activation. For activation transformation assay, Balb/c-3T3 cells were cocultured with lethally X-irradiated primary F344 rat liver cells (RLCs). The RLC-3T3 cocultures were treated with 0–25 μg/mL AN for 48 hours. The cocultures were then treated biweekly for 3 weeks with 0.05 μg/mL 12-*O*-tetradecenoyl-phorbol-13-acetate beginning 1–2 days after completion of AN treatment. For nonactivation transformation assay, 3T3 cell cultures were incubated with 0–20 μg/mL AN for 72 hours. For RLC-3T3 cocultures, significant increase in relative transformation activity was found in coculture treated with 8.8 μg/mL AN (noncytotoxic concentration). At 16.7 μg/mL AN, relative cell survival was only 22%, and no significant increase in transformation activity was found. No significant increase in transformation activity was observed in AN-treated 3T3 cell cultures without RLCs.

For ouabain resistance (Oua^r) mutation assay, 3T3 cell cultures were treated with 0–150 μg/mL AN with or without S9 mix for 4 and 24 hours, respectively. After the treatment, AN was removed and the cultures were refed and maintained for 5–6 days for expression and selection, using 2 mM cardiac glycoside ouabain. The appearance of ouabain-resistant (Qua^r) variants would indicate a mutation arose in the gene controlling the synthesis of cell membrane Na^+/K^+ ATPase (Corsaro and Migeon, 1978). Significant increase in relative Oua^r frequency was observed at 50 μg/mL AN with S9 activation.

Yuan and Wong (1991) used a nonfocus transfection-transformation assay to study the capacity of the oxidative metabolite CEO to bring about functional changes in a plasmid that would be indicative of a compound-induced mutation. A new plasmid that had been constructed by ligating a human c-HA-*ras*-1 protooncogene to a pSV2neo mammalian vector was reacted with CEO in vitro and then transfected into NIH3T3 cells. Cells were selected for neomycin resistance and/or abnormal growth characteristics, the latter serving to discriminate between colonies arising from *ras* mutations and those from cells that were not transfected (or that were transfected with nonplasmid DNA). Although CEO-modified *ras* gave rise to two neomycin resistant clones, they were probably not indicative of a *ras* mutation because their normal growth rate and monolayer density were similar to negative control. Southern blot analysis of transformant DNA also supported this conclusion. For example, when anti-benzo(a)pyrene-7,8-dihydrodiol-9,10-epoxide transformant DNA was examined in this system as a positive control, a fragment of 411 base pairs was revealed, indicating a *ras* mutation at codon 11 or 12. However, both CEO-derived clones and untreated control showed the WT band of 355 base pairs.

4.5.2.4.5. ***Genotoxicity summary.*** All identified studies concerning the mutagenicity or genotoxicity of AN are compiled in Table 4-53. The overall weight of evidence from in vitro and in vivo studies is adequate to support direct mutagenicity for the AN metabolite, CEO.

Table 4-53. Summary of studies on the mutagenicity/genotoxicity of AN

Test system	Endpoint/effect	Exposure concentration	Exposure duration	Result[a]	Reference
Humans					
AN-exposed workers n = 30	DNA strand breaks; nondisjunction of sex chromosomes in sperm	0.8 mg/m^3	2.8 yrs	+	Xu et al. (2003)
AN-exposed workers: 31 controls, 41 low, 47 intermediate	Increase in MN in buccal mucosal cells (low and intermediate groups) and blood lymphocytes (intermediate group) of AN-exposed workers.	Low = 0.522 mg/m^3 Intermediate = 1.998 mg/m^3	Low = 1–33 yrs (average 15.7 yrs) Intermediate = 1–33 yrs (average 17.2 yrs)	+	Fan et al. (2006)
AN-exposed polymerization workers: 14 Maintenance workers: 10 controls: 20	CAs in lymphocytes	ND[b]	ND	Maintenance workers: + Production workers: (+)	Borba et al. (1996)
AN-exposed workers: 47; 47 controls	Deletion of mitochondrial DNA in lymphocytes	0.11 ppm	17.3 yrs	+	Ding et al. (2003)

Table 4-53. Summary of studies on the mutagenicity/genotoxicity of AN

Test system	Endpoint/effect	Exposure concentration	Exposure duration	Result[a]	Reference
AN-exposed workers Group 1 = 39 Group 2 = 22 Unexposed controls = 49	CAs (detected by FISH) in cultured lymphocytes from peripheral blood samples	Group 1 = 0.05–0.3 mg/m^3 Group 2 = 0.05–0.7 mg/m^3	3 mos	(+) Significant increase in the number of reciprocal translocations and relative number of insertions. Increase in frequency of aberrant cells not significant.	Beskid et al. (2006)
AN-exposed workers (n = 45) Matched controls = 23, unexposed controls = 33	CAs in cultured lymphocytes in peripheral blood samples	0.05–0.3 mg/m^3	3 mos	–	Srám et al. (2004)
AN-exposed workers (n = 18); controls = 18	CAs in lymphocytes	5 ppm, reduced to 1.5 ppm between 1975 and 1977 (possible exposure to other chemicals)	15.3 yrs	–	Thiess and Fleig (1978)
Rats					
Sprague-Dawley (male) (4/group)	MN	125 mg/kg i.v.	Two treatments	Bone marrow: + Peripheral blood: –	Wakata et al. (1998)
Sprague-Dawley (male)	MN in bone marrow	10–40 mg/kg oral	Single dose	–	Morita et al. (1997)
	MN in peripheral blood	24.5–98 mg/kg i.v.	Single dose	–	Morita et al. (1997)
Sprague-Dawley (male) n = 3	CAs in bone marrow	40 mg/kg oral	16 d	–	Rabello-Gay and Ahmed (1980)
Sprague-Dawley (male) n = 3–4/group	Binding to DNA in stomach, brain, and liver	46.5 mg/kg oral	Single dose	+	Farooqui and Ahmed (1983a)
Sprague-Dawley n = 4/group	Binding to testicular DNA	46.5 mg/kg oral	Single dose	+	Ahmed et al. (1992a)
Sprague-Dawley (male) n = 4/group	Binding to lung DNA	46.5 mg/kg oral	Single dose	+	Ahmed et al. (1992b)
Sprague-Dawley (male) n = 3/group	Binding to gastric tissue DNA	46.5 mg/kg oral	Single dose	+	Abdel-Rahman et al. (1994b)
Wistar (male)	Alkylation of hepatic DNA	0.2 mmol i.p.	Single dose	+	Peter et al. (1983a)
F344 n = 1	Binding to liver and brain DNA	0.6 mg/kg CEO i.p.	Single dose	–	Hogy and Guengerich (1986)

Table 4-53. Summary of studies on the mutagenicity/genotoxicity of AN

Test system	Endpoint/effect	Exposure concentration	Exposure duration	Result[a]	Reference
F344 n = 3	DNA adduct formation	50 mg /kg AN i.p. or 6 mg/kg CEO i.p.	Single dose	Liver: + Brain: (+)	Hogy (1986); Hogy and Guengerich (1986)
Wistar	DNA damage in forestomach, colon, kidney, bladder, and lung but not in brain or bone marrow	30 mg/kg i.p.	Single dose	+	Sekihashi et al. (2002)
Wistar, male	Fragmentation of brain DNA	100 ppm AN in drinking water	14 or 28 d	+	Mahalakshmi et al. (2003)
F344 n = 12/group	UDS in liver but not brain	50 mg/kg gavage	Single dose	+	Hogy and Guengerich (1986)
Sprague-Dawley	UDS in lung	46.5 mg/kg oral	Single dose	+	Ahmed et al. (1992a)
	UDS in gastric tissue	46.5 mg/kg oral	Single dose		Abdel-Rahman et al. (1994a)
	UDS in testis	46.5 mg/kg oral	Single dose		Ahmed et al. (1992b)
F344	UDS in isolated hepatocytes or spermatocytes	a. 75 mg/kg b. 60 mg/kg oral	a. Single dose b. five daily doses	–	Butterworth et al. (1992)
F344 n = 50	Dominant lethal mutations	60 mg/kg	5 d	–	Working et al. (1987)
Mice					
ddY	DNA damage in forestomach, colon, bladder, lung, and brain	20 mg/kg i.p.	Single dose	+	Sekihashi et al. (2002)
C57B1/6 n = 1–4/group	SCEs in bone marrow	10–45 mg/kg	Single dose	(+) positive at toxic dose of 45 mg/kg	Sharief et al. (1986)
Swiss	SCEs in bone marrow	7.5 or 10 mg/kg i.p.	Single dose	+	Fahmy (1999)
	CAs in spermatocytes, bone marrow, and spleen cells	a. 15.5 or 31 mg/kg oral b. 7.75 mg/kg	a. Single dose b. three or five doses	+	Fahmy (1999)
Swiss n = 3–6/group	CAs in bone marrow	7, 14, or 21 mg/kg-d oral or 10, 15, or 20 mg/kg-d i.p.	4, 15, or 30 d	–	Rabello-Gay and Ahmed (1980)
NMRI male n = 4/group	CAs in bone marrow	20 or 30 mg/kg i.p.	Single dose	–	Leonard et al. (1981)
C57B1/6 n = 1–4/group	CAs in bone marrow	10–45 mg/kg	Single dose	–	Sharief et al. (1986)
NMRI male n = 4–5/group	MN in erythrocytes	20 or 30 mg/kg i.p.	Single dose	–	Leonard et al. (1981)

Table 4-53. Summary of studies on the mutagenicity/genotoxicity of AN

Test system	Endpoint/effect	Exposure concentration	Exposure duration	Result[a]	Reference
CD-1	MN in bone marrow	0–45 mg/kg i.p. 0–32 mg/kg oral 0–40 mg/kg i.v.	Single dose	i.p.: (+) oral and i.v.: –	Morita et al. (1997)
CD-1	MN in peripheral blood	5.6–45 mg/kg i.p. or 10–40 mg/kg i.v.	Single dose	–	Morita et al. (1997)
ICR	CAs in bone marrow cells and spermatogonia	100 or 20 mg/m^3	5 d	–	Zhurkov et al. (1983)
NMR1 n = 5/group	Dominant lethal mutation	30 mg/kg i.p.	Single dose	–	Leonard et al. (1981)
Short-term assays—bacteria				**(–S9 / +S9)**	
S. typhimurium TA 1535	Gene reversion (His$^+$ revertant)	5–20 µL AN solution	0.5 h	–/+	Milvy and Wolff (1977)
TA 1535	Gene reversion	2–300 µL AN vapor	0.5–4 h	–/+	Milvy and Wolff (1977)
TA 1538	Gene reversion	200 µL AN vapor	2 h	–/+	Milvy and Wolff (1977)
TA 1978	Gene reversion	5–10 µL AN solution	0.5 h	–/+	Milvy and Wolff (1977)
TA 1535	Gene reversion	100–1,000 µg AN plate incorporation assay	ND	–/+	Lijinsky and Andrews (1980)
TA 1537, 1538, 98, 100	Gene reversion	Plate incorporation assay	ND	–/–	Lijinsky and Andrews (1980)
TA 1535	Gene reversion	0.1– 1,000 µg/dish	ND	–/+	Zhurkov et al. (1983)
TA 1538	Gene reversion	0.1– 10,000 µg/dish	ND	–/–	Zhurkov et al. (1983)
TA 97, 98, 100	Gene reversion	50–750 µg/mL plate incorporation assay	48 h	–/–	Brams et al. (1987)
TA 102	Gene reversion	Up to 5,000 µg/plate	ND	–/–	Jung et al. (1992)
TA 98, 100, 1535, 1537, 1538	Gene reversion	0.1–5,000 µg/plate	2 d	–/–	Dow Chemical Co. (1977)
TA 1530, 1535, 1950, 1538, 100, 98, 1978	Gene reversion	0.2% AN vapor (200 µg/plate)	1 h	–/+ (weaker response with TA 100, 98, and 1978)	de Meester et al. (1978); Dow Chemical Co. (1976)
TA 98, 100	Gene reversion	ND, plate incorporation assay	ND	+/+	Khudoley et al. (1987)
TA 100	Gene reversion	806–12,100 µg/plate	48 h	–/(+)	Hakura et al. (2005)

Table 4-53. Summary of studies on the mutagenicity/genotoxicity of AN

Test system	Endpoint/effect	Exposure concentration	Exposure duration	Result[a]	Reference
TA 1535/pSK1002	*umu* gene expression (increased β-galactosidase activity)	ND, 0.1 mL AN in 2.5 mL culture medium	2 h	–/–	Nakamura et al. (1987)
TA 1530	Gene reversion	0.1 mL 24-hr urine from rats and mice treated with a single dose 30 mg/kg AN i.p. (plate incorporation assay)	48 h	+	Lambotte-Vandepaer et al. (1985, 1981, 1980)
E. coli WP2 series	Gene reversion ($trp^- \rightarrow trp^+$)	75 or 150 μmol/ plate	2–3 d	+[c]	Venitt et al. (1977)
E. coli PQ37	SOS chromotest	ND	2 h	–/–	Brams et al. (1987)
Short-term assays—fungi					
S. cerevisiae JD1	Mitotic gene conversion	250 or 500 μg/mL	18 h	–/+	Brooks et al. (1985); Shell Oil Co. (1984a)
S. cerevisiae D61.M	Chromosome loss	0.8 or 1.36 mg/mL	16 h	–/–	Whittaker et al. (1990)
Short-term assays—fruit fly					
Adult female Drosophila ZESTE system	Sex chromosome loss	Inhalation exposure to 2.7 ppm AN	50 min or 70 min	+	Osgood et al. (1991)
Mosaic eye in hatching females	Somatic recombination and mutation	Treatment of larvae with 5–20 mM AN	Single dose, incubate for 9–11 d	(+)	Vogel (1985)
Germ cells of male *D. melanogaster*	Sex-linked recessive lethal	Feeding: 420 ppm or injection: 3,500 ppm	Feeding: 3 d	–	Foureman et al. (1994)
Wing spots of Drosophila *(mwh*+/+*flr* +/mei-9)	Somatic mutation and recombination	Gas exposure of larvae to 0.5–1 μL/1,150 mL	0.5 or 1 h	(+)	Würgler et al. (1985)
D. melanogaster ZESTE (inhibition of taxol-purified microtubule assembly in vitro)	Aneuploidy	5 mM	Microtubule assembly monitored for 80 min	+	Sehgal et al. (1990)
Other short-term assays					
Supercoiled plasmid DNA pBR322	CEO induced DNA strand breaks	50 mM CEO incubated with 1.1 μg supercoiled pBR322 plasmid DNA	3 h	+	Yates et al. (1994)

Table 4-53. Summary of studies on the mutagenicity/genotoxicity of AN

Test system	Endpoint/effect	Exposure concentration	Exposure duration	Result[a]	Reference
SV40 phage DNA	CEO induced DNA strand breaks, but not AN	1 mM CEO incubated with 5,000 dpm [^{3}H]-thymidine labelled SV–40 phage DNA	17 h	+	Peter et al. (1983b)
In vitro mammalian cell assays					
Human lymphoblasts *Tk*6	Gene-locus mutations at the *Tk* (thymidine kinase) locus ($Tk^{+/-} \rightarrow Tk^{-/-}$)	40 µg/mL AN	3 h	–/+	Crespi et al. (1985)
	Mutation at *Tk* locus	1.4 mM AN	2 h	–/+	Recio and Skopek (1988a, b)
	Mutation at *Tk* locus	100 µM and 150 µM CEO	2 h	+	Recio and Skopek (1988a, b)
	Abnormality at chromosome 17 in 1 of 8 CEO-induced tk_s mutant clones	NA[b]	NA	+	Kodama et al. (1989)
	CEO-induced mutations at the hprt locus	NA	NA	+	Recio and Skopek (1988a)
Human lymphoblasts AHH-1	Gene-locus mutations at the hypoxanthine guanine phosphoribosyl transferase locus	25 µg/mL AN	28 h	+	Crespi et al. (1985)
L5178Y mouse lymphoma cells	Mutation at $Tk^{+/-}$ locus	30 and 40 µg/mL AN	ND	+	Oberly et al. (1996)
	Mutation at $Tk^{+/-}$ locus	10–40 µg/mL AN	4 h	+/+	Rudd (1983)
	Mutation to ouabain or 6-TG resistance	12.5–200 µg/mL AN	2 h	+/+	Garner and Campbell (1985)
	Induction of $Tk^{-/-}$ *mutants*	80–225 µg/mL AN	2 h	+/+	Lee and Webber (1985)
	Induction of $Tk^{-/-}$ *mutants*	30 nL/mL AN	4 h	+/+	Myhr et al. (1985)
	Induction of $Tk^{-/-}$ *mutants*	5–69 µg/mL AN	3 h	+/+	Amacher and Turner (1985)
L5178Y $Tk^{+/+}$	Mutation to ouabain resistance (Na^+/K^+ ATPase locus)	12.5–100 µg/mL AN	2 h	–	Styles et al. (1985)
L5178Y $Tk^{+/-}$	Mutation to trifluorothymidine resistance	12.5–100 µg/mL AN	2 h	–	Styles et al. (1985)

Table 4-53. Summary of studies on the mutagenicity/genotoxicity of AN

Test system	Endpoint/effect	Exposure concentration	Exposure duration	Result[a]	Reference
P388F mouse lymphoma $tk^{+/-}$	Mutation to 5-iodo-2-deoxyuridine resistance	80–160 μg/mL AN	24–48 h	–/+	Anderson and Cross (1985)
V79/hprt	Induction of 8-azaguanine resistance	50–200 μg/mL AN	2 h	–/–	Lee and Webber (1985)
HeLa cells	UDS	2.5 mg/mL AN	2.5 h	–/–	Martin and Campbell (1985)
Human lymphocytes	UDS	5×10^{-1} M	4 h	–/+	Perocco et al. (1982)
Primary cultures of F344 rat hepatocytes	UDS	0.026–53 μg/mL AN	20 h	–	Probst and Hill (1985)
Primary cultures of F344 rat hepatocytes	UDS	10^{-1}–10^{2} μg/mL AN	18–20 h	–	Williams et al. (1985)
Primary F344 rat hepatocyte	UDS	0.01–1 mM AN	17–19 h	–	Butterworth et al. (1992)
Primary F344 rat hepatocyte	UDS	0.01–0.1 mM CEO	17–19 h	–	Butterworth et al. (1992)
Human mammary epithelial cell	UDS	0.1 mM CEO	24 h	+	Butterworth et al. (1992)
Human bronchial epithelial cells	DNA single-strand breaks	200 and 500 μg/mL AN	20 h	+	Chang et al. (1990)
Rat hepatocytes	DNA single-strand breaks	65.8 μg/mL AN	3 h	+	Bradley (1985)
CHO cells	DNA single-strand breaks	7×10^{-2}–1×10^{-1} M AN	1 h	+/+	Douglas et al. (1985)
CHO cells	DNA single-strand breaks	ND	ND	–/–	Lakhanisky and Hendrickx (1985)
SHE cells	DNA single-strand breaks	200 or 400 μg/mL AN	18 h	+	Parent and Castro (1979)
Human bronchial epithelial cells	SCEs	150 and 300 μg/mL AN	20 h	+	Chang et al. (1990)
Human lymphocytes	SCEs	5×10^{-4} M	1 h	–/+	Perocco et al. (1982)
CHO cells	SCEs	10^{-7}–10^{-4} M AN	3 h	–[d]	Ved Brat and Williams (1982)
CHO cells cocultured with freshly isolated rat hepatocytes	SCEs	10^{-4} M AN	3 h	+[d]	Ved Brat and Williams (1982)
CHO cells	SCEs	2 mM AN	1 h	–/+	Natarajan et al. (1985)
CHO cells	CAs	4 mM AN	1 h	+/+	Natarajan et al. (1985)
CHL fibroblast	CAs	12.5 μg/mL AN	24 and 48 h	+[d]	Ishidate and Sofuni (1985)

Table 4-53. Summary of studies on the mutagenicity/genotoxicity of AN

Test system	Endpoint/effect	Exposure concentration	Exposure duration	Result[a]	Reference
CH1-L liver fibroblast	CAs	2.5 μg/mL AN	36 h	+	Danford (1985)
Chinese hamster cell line Don-6	CAs	1×10^{-4} M or 0.0053 mg/mL	26–30 h	+	Sasaki et al. (1980)
CHO cells	MN	10^{-1} M AN	1 h	+/+	Douglas et al. (1985)
Rat liver (RL4) cells	CAs, polyploidy, SCEs	1.25, 2.5, 5.0, or 10 μg/mL AN	2 h	–[d]	Priston and Dean (1985); Shell Oil Co. (1984b)
CHO cells	Inhibition of cell growth and RNA synthesis	0.001, 0.002, and 0.005% (v/v) AN	8 d	+[d]	Mangir et al. (1991)
In vitro mammalian cell transformation					
SHE cells	Cell transformation	50 or 100 μg/mL AN	6 d	+	Parent and Castro (1979)
SHE cells	Enhancement of viral transformation	100 or 200 μg/mL AN	18 hrs before SA7 or 5 hrs after SA7 inoculation	+	Parent and Castro (1979)
SHE cells	Cell transformation	0.01–1 μg/mL AN	7 d	+	Barett and Lamb (1985)
Mouse fibroblasts NIH/3T3 cells	Cell transformation	12.5–200 μg/mL AN	48 h	+	Banerjee and Segal (1986)
Mouse fibroblasts C3H/10T1/2 cells	Cell transformation	3–100 μg/mL AN	48 h	+	Banerjee and Segal (1986)
Mouse fibroblasts C3H/10T1/2 cells	Cell transformation	16 μg/mL AN	24 h	–/(+)	Lawrence and McGregor (1985)
Balb/c-3T3 cells	Cell transformation	8.8 μg/mL AN	48 h	–/+[e]	Matthews et al. (1985)
Balb/c-3T3 cells	Ouabain-resistant mutants	50 μg/mL AN	24 h	–/+	Matthews et al. (1985)
NIH 3T3 cells	Cell transformation after transfection with CEO modified *ras* DNA	NA	14 h	–	Yuan and Wong (1991)

[a]NA = not applicable; ND = not determined.
[b]+ = Positive;– = negative; (+) = borderline positive.
[c]S9 activation not needed.
[d]S9 not included in the assay.
[e]With or without coculture with lethally X-irradiated primary F344 RLCs.

In vitro evidence indicates that AN can be directly mutagenic, most likely through the formation of CEO-DNA adducts. In short-term tests with bacteria, AN induced mutations in a majority of test systems, most often requiring exogenous metabolic activation (Table 4-53). In

mouse lymphoma cell assays, AN induced mutations at the *Tk* locus in most assays (Table 4-53). In human lymphoblast *Tk*6 cells devoid of CYP450 activity, AN induced multiple mutations at the *Tk* locus only in the presence of metabolic activation (Recio and Skopek, 1988a, b; Crespi et al., 1985). CEO was mutagenic in *Tk*6 cells at 10-fold lower concentrations than AN itself and was as mutagenic in this test system as the well-known mutagen, ethyl methanesulfonate (Recio and Skopek, 1988a, b). CEO also induced multiple mutations at the hprt locus in *Tk*6 cells (Recio and Skopek, 1988a). CEO induced UDS in cultured human mammary epithelial cells but not in cultured rat hepatocytes (Butterworth, 1992).

Supporting evidence for the direct mutagenicity of AN and its metabolites comes from in vivo studies (Table 4-53). Increases in the occurrence of MN in buccal mucosal cells and blood lymphocytes were recently reported in AN exposed workers in China (Fan et al., 2006). Three studies of AN workers reported genotoxic effects such as DNA strand breaks, nondisjunction of sex chromosomes, and CAs (Beskid et al., 2006; Xu et al., 2003; Borba et al., 1996), whereas an earlier study did not find elevated frequency of CAs in exposed workers (Thiess and Fleig, 1978). Increases in cytogenetic aberrations such as MN were found in assays of exposed rats (Wakata et al., 1998) and a single assay of mice (Fahmy, 1999), but were not evident in other rat and mouse assays (Morita et al., 1997; Zhurkov et al., 1983; Leonard et al., 1981; Rabello-Gay and Ahmed, 1980). Comet assays found DNA damage in forestomach, colon, bladder, lung, and brain in mice, following single i.p. injections of 20 mg/kg AN, and in forestomach, colon, kidney, bladder, and lung of rats injected with 30 mg/kg (Sekihashi et al., 2002).

UDS was detected by following the time course of ^{3}H-thymidine incorporation into DNA in lung, testis, and gastric tissue, following administration of single oral doses of 46.5 mg/kg AN to Sprague-Dawley rats (Ahmed et al., 1996b, 1992a, b; Abdel-Rahman et al., 1994a). Autoradiographic techniques did not detect UDS following incubation of primary cultures of hepatocytes or spermatocytes from F344 rats given single oral doses of 75 mg/kg or five daily doses of 60 mg/kg-day AN (Butterworth et al., 1992). Dominant lethal effects (from mutations in germ cells) were not found in mice given single i.p. doses of 30 mg/kg AN (Leonard et al., 1981) or rats given five oral doses of 60 mg/kg (Working et al., 1987). DNA binding by AN or its metabolites was indicated by elevated levels of radioactivity in DNA from several tissues in rats given single oral doses of 46.5 mg/kg radiolabeled AN (Abdel-Rahman et al., 1994b; Ahmed et al., 1992a, b; Farooqui and Ahmed, 1983a).

In the *European Union Risk Assessment Report on Acrylonitrile* (EC 2004), AN was regarded as "genotoxic or at least mutagenic, despite the recent publication of Whysner et al. (1998a) which argues for a possible nongenotoxic mechanism for the tumour induction in experimental animals."

4.5.2.5. Indirect Genotoxicity

As discussed in Section 4.5.1.2.2, studies are available that investigated the indirect

genotoxicity of AN resulting from oxidative stress. These studies measured 8-oxodG levels in DNA as biomarkers of oxidative DNA damage from AN exposure. 8-OxodG is mutagenic (Kamiat et al., 1992; Moriya et al., 1991; Wood et al., 1990) and causes GC → TA transversions during DNA replication.

In vitro studies

Zhang et al. (2000) studied AN-induced morphological transformation in SHE cells. SHE cell culture was treated in vitro for up to 7 days with 0–75 μg/mL AN in 12.5 μg/mL increments (75 μg/mL was cytotoxic, with 50% reduction in cell colony number). After 7 days of exposure, there was a dose-dependent increase in morphological transformation at 50, 62.5, and 75 μg/mL, reaching a transformation frequency of 1.3% at 75 μg/mL. After a 24-hour AN exposure, an increase in transformation was not observed at all concentrations. Levels of 8-oxodG in DNA isolated from cells incubated with 75 μg/mL were increased to 192 and 186% of control after 2 and 3 days, indicating an association between cell transformation and oxidative DNA damage. However, no increase in 8-oxodG was observed after 1 or 7 days. AN-induced morphological transformation was inhibited by cotreatment with the antioxidants α-tocopherol (100 μM: up to 65% inhibition) and (-)-epigallocathechin-3-gallate (5 μM: up to 87% inhibition) for 7 days. Cotreatment with antioxidants also inhibited the formation of 8-oxodG in SHE cell DNA from treatment with 75 μg/mL AN.

In a later study by the same research group, Zhang et al. (2002) investigated the time course of SHE cell morphological transformation in the presence of 75 μg/mL AN. The results indicated that statistically significant increases in morphological transformation frequency could not be observed until after 2 consecutive days of exposure; a plateau at a transformation frequency of about 2% was reached after 4–5 days of exposure. In another experiment, coadministration of 0.5 mmol/L ABT, a nonspecific suicidal CYP450 inhibitor, for 7 days significantly reduced the rate of cell transformation from about 1.25% to about 0.3% (shown graphically), demonstrating the need for metabolic activation of AN in this test system.

Zhang et al. (2002) also showed that AN (25, 50, and 75 μg/mL) increased the amount of ROS (measured by 2,3-dihydroxybenzoic acid production) in the SHE cells after 4, 24, and 48 hours of treatment. At the same time, xanthine oxidase (which generates the superoxide radical and hydrogen peroxide via oxidation of hypoxanthine or xanthine by oxygen) activity was increased by 47% in SHE cells after 24 hours of treatment with 75 μg/mL AN. After 48 hours of treatment, xanthine oxidase activity was increased in both 50 and 75 μg/mL (80%) AN groups. This increase in xanthine oxidase activity was blocked by cotreatment with 0.5 mM ABT. On the other hand, antioxidant GSH was depleted 66–80% by all doses of AN (25, 50, and 75 μg/mL) after 4 hours of treatment and returned to control levels after 24 hours. At 48 hours, a significant increase in GSH was observed with the 75 μg/mL group but not in other dose groups. Antioxidant enzyme catalase activity was significantly decreased after 4 hours of treatment with

50 and 75 μg/mL AN but increased after 24 and 48 hours of treatment. Cotreatment with ABT prevented the decrease and increase in activity of catalase at 4 and 24 hours after treatment, respectively. A transient decrease in SOD activity was also observed after 4 hours of treatment with 75 μg/mL AN.

The effect of AN on catalase and SOD activities was also studied in a cell-free system (Zhang et al., 2002). Catalase and SOD activities were determined in samples containing purified catalase or SOD incubated with 75 μg/mL AN in the presence or absence of SHE cell homogenate. In the absence of a metabolic source of SHE cell homogenate, no inhibition of catalase activity was seen following incubation up to 60 minutes with AN. In the presence of SHE cell homogenate, AN significantly decreased catalase activity in a time-dependent manner after 10 minutes of incubation. Similarly, a significant time-dependent decrease in SOD activity was observed following 30 minutes incubation with AN. The study authors concluded that morphological transformation of SHE cells is caused by oxidative stress as a result of oxidative metabolism of AN.

Kamendulis et al. (1999a) also investigated oxidative DNA damage induced by AN in DITNC1, a rat glial astrocyte cell line, and primary rat hepatocytes exposed to AN in vitro (see Section 4.5.1.2.2). AN was cytotoxic at concentrations ≥2.5 mmol/L (133 μg/mL) (as measured by the release of LDH from the cells) to both cell lines, following ≥4 hours of exposure. Concentrations of 0.01, 0.1, and 1.0 mmol/L AN (0.53, 5.3, and 53 μg/mL, respectively) caused a dose-dependent increase in formation of 8-oxodG in astrocytes but not in hepatocytes. Corresponding increases in ROS formation were also observed in astrocytes only. However, no oxidative lipid damage (as evaluated by formation of MDA, a product of lipid peroxidation) was found in either cell type following treatment with AN at all exposure concentrations or durations. The formation of 8-oxodG in rat astrocytes was reversible. Following treatment with AN for 24 hours and removal of AN for 24 hours afterwards, 8-oxodG levels returned to control values in all concentrations examined. Kamendulis et al. (1999a) concluded that this demonstrated property was consistent with tumor promoting agents.

Pu et al. (2006) investigated oxidative DNA damage induced by AN in D1TNC1 rat astrocyte cell line using the fpg-modified comet assay. Increase in oxidative DNA damage was observed in astrocytes treated with 1 mM AN for 24 h. No increase in oxidative DNA damage was observed in astrocytes treated with 0.005 – 0.75 mM AN for 24 hours.

Jacob and Ahmed (2003b) investigated oxidative stress in cultured NHA (4631) treated with up to 400 μM AN for 12 hours. AN was cytotoxic at concentrations >50 μM. Cell viability was 85, 78, and 58%, respectively, at AN concentrations of 100, 200, and 400 μM. Significant increases in measures of oxidative stress were observed at cytotoxic concentrations of 200–400 μM AN: the production of ROS was increased four- to sevenfold, whereas 8-oxodG levels were increased more than twofold.

Esmat et al. (2007) investigated cytoxicity in rat (strain not known) primary glial cells exposed to 0–5.0 mM AN up to 12 hours. Cell membrane integrity was evaluated by trypan blue exclusion and LDH leakage. About 50% membrane damage in primary glial cells was observed in incubations containing 1.0 mM AN for 3 hours. Thus, subsequent studies on AN-induced oxidative stress were performed using 1 mM AN for 3 hours incubation. AN increased MDA levels (indicator of lipid peroxidation) to about ninefold compared with control incubations and depleted GSH level to about 7% of controls., while no change in total glutathione level was observed. AN induced CN^- formation by glial cells and decreased ATP level by about 90% as compared with the control. Pretreatment with 5 mM NAC (an acetylated precursor of cysteine and GSH, and an antioxidant), reduced MDA level by 40% as compared with glial cells treated with AN alone and raised GSH and total glutathione level in cell extract to about 2.5-fold of control and AN alone treated group. Pretreatment with NAC also caused reduction of CN^- induced by AN to about 15% as compared wth the AN alone treated group, and raised ATP level to about sixfold, as compared with the AN alone treated group.

It should be noted that NAC stimulated GSH synthesis, enhanced glutathione-S-transferase activity, and was a powerful nucleophile capable of scavenging free radicals (De Vries and De Flora, 1993). Observed increases in GSH and total glutathione and decrease in CN^- formation with NAC pretreatment in Esmat et al. (2007) would suggest that most of the administered AN could be detoxified via conjugation via the GSH pathway (consistent with findings by Carerra et al., 2007), as less AN was available for oxidation to CN^-. Esmat et al. (2007) concluded that AN toxicity was at least partly mediated by oxidative stress.

In vivo studies

As described in Section 4.5.1.2.2, Jiang et al. (1998) reported increases in measures of oxidative stress in the brain cortices but not the livers of male Sprague-Dawley rats exposed to AN in drinking water at concentrations of 50–200 ppm for up to 90 days. Increases in ROS and oxidative DNA damage (increased levels of 8-oxodG) and concomitant decreases in antioxidant enzymes (catalase, SOD) were observed in the brain cortices of exposed rats. Transient small decreases in the antioxidants vitamin E and glutathione were also observed in the brain cortices of AN-exposed rats only at 14 days. A transient increase in MDA level was observed only at the highest dose group after 14 days but not at other time points.

Pu et al. (2009) reported oxidative DNA damage in WBC and brain of male Sprague-Dawley rats treated with 100-200 ppm AN; however, EPA has identified issues with this study (see Section 4.5.1.2.2).

In another study, Whysner et al. (1998a) examined the ability of AN to induce oxidative DNA damage in the brain, liver, and forestomach of rats by exposing male Sprague-Dawley and F344 rats up to 300 ppm AN in drinking water for 21 days (see Section 4.5.1.2.2). As shown in Table 4-54, elevated levels of 8-oxodG were found in DNA from the brain and liver of Sprague-

Dawley rats. However, 8-oxodG levels in the forestomach of exposed Sprague-Dawley rats and the brain of exposed F344 rats were not statistically significantly elevated compared with controls. Significant increase in 8-oxodG levels was found in the liver of exposed Sprague-Dawley rats, although the liver is not a target organ for carcinogenicity in adult rats.

Table 4-54. Formation of 8-oxodG in DNA from tissues of male Sprague-Dawley and F344 rats exposed to AN in drinking water for 21 days

Dose group	Formation of 8-oxodG (mol/10^5 mol dG)			
	Sprague-Dawley rats			F344 rats
	Liver	Forestomach	Brain	Brain
Control	0.67 ± 0.22	0.68 ± 0.14	0.62 ± 0.08	0.79 ± 0.37
3 ppm	0.72 ± 0.06	1.77 ± 0.55	0.86 ± 0.41	1.07 ± 0.41
30 ppm	0.95 ± 0.19[a]	1.59 ± 0.30	1.35 ± 0.49[a]	1.03 ± 0.38
300 ppm	0.96 ± 0.15[a]	1.44 ± 1.22	1.29 ± 0.10[a]	1.06 ± 0.48[b]

[a]Significantly different from controls ($p < 0.05$) as calculated by the study authors.
[b]Exposure was at 100 ppm.

Source: Whysner et al. (1998a).

Whysner et al. (1998a) also exposed male Sprague-Dawley rats to 100 ppm AN in drinking water for up to 94 days. (This dose was carcinogenic in Sprague-Dawley rats in a chronic study [Johannsen and Levinskas, 2002a; Biodynamics, 1980b].) The rats were divided into four groups and were exposed to distilled water, 100 ppm AN, 5 mg MNU (a DNA-reactive carcinogen that produces glial cell tumors in rats) per week, or 100 ppm AN plus 5 mg MNU per week. Levels of 8-oxodG in brain and liver of rats exposed to 100 ppm AN were significantly greater than those in controls after 10 days (1.31 ± 0.52 in brains of exposed rats vs. 0.65 ± 0.22 mol per 10^5 mol dG in controls and 0.70 ± 0.20 in livers of exposed rats vs. 0.49 ± 0.10 mol per 10^5 mol dG in controls). Administration of 5 mg/kg MNU alone did not increase the level of 8-oxodG in the brain of treated rats but increased 8-oxodG in the liver after 10 days. However, coadministration of 100 ppm AN and MNU increased 8-oxodG level in the brain after 31 days and 94 days when compared with the MNU-only group.

Whysner et al. (1998a) suggested that AN-induced tumors may be produced by a mode of action involving 8-oxodG. However, several findings in this study did not support this proposed mode of action. First, no significant increase in 8-oxodG levels were found in the brain DNA of F344 rats exposed to AN in the 21-day study whereas AN was carcinogenic to F344 rats in a chronic drinking water study (Johannsen and Levinskas, 2002b). Second, although a significant increase in 8-oxodG levels was found in the brain DNA of Sprague-Dawley rats exposed to AN for 21 days, no dose-dependent increase was observed above 30 ppm, which was not the dose producing the highest occurrence of tumors in the chronic bioassay. Third, no increase in

8-oxodG levels were found in the forestomach DNA of exposed rats. The forestomach was a target organ for AN carcinogenicity. Finally, increase in 8-oxodG levels was found in liver DNA of exposed rats. Liver was not a target organ for AN carcinogenicity in adult rats. Therefore, there was no association between 8-oxodG levels and tumorigenicity in target organs.

Results of indirect mutagenicity/genotoxicity studies of AN are summarized in Table 4-55.

Table 4-55. Summary of studies on the indirect mutagenicity or genotoxicity of AN

Test system	Endpoint/effect	Exposure concentration	Exposure duration	Result	Reference
In vitro mammalian cell assays					
SHE cells	Cell transformation	50–75 μg/mL AN	7 d	+	Zhang et al. (2000)
SHE cells	8-oxodG in DNA	75 μg/mL AN	Increased after 2 and 3 d but not after 1 or 7 d	(+)	Zhang et al. (2000)
SHE cells	ROS	25–75 μg/mL AN	4–48 h	+	Zhang et al. (2002)
DITNC1rat glial astrocytes	8-oxodG in DNA	0.01–1 mM AN (0.53–53 μg/mL)	4 or 24 h	+[a]	Kamendulis et al. (1999a)
D1TNC1 rat astrocytes	DNA damage in fpg-comet assay	1 mM	24 h	+	Pu et al. (2006)
Rat hepatocytes	8-oxodG in DNA	0.01–1 mM AN	4 or 24 h	–	Kamendulis et al. (1999a)
NHAs	8-oxodG in DNA	200–400 μM AN	12 h	+	Jacob and Ahmed (2003b)
NHAs	ROS	200–400 μM AN	12 h	+	Jacob and Ahmed (2003b)
In vivo studies in rats					
Male Sprague-Dawley rats	8-oxodG in brain cortex DNA	0–200 ppm AN in drinking water	100 and 200 ppm: + after 14–90 d 50 ppm: + after 28 and 90 d	+	Jiang et al. (1998)
Male Sprague-Dawley rats	8-oxodG in liver DNA	0–200 ppm AN in drinking water	14–90 d	–	Jiang et al. (1998)
Male Sprague-Dawley rats	8-oxodG in WBC and brain DNA	100 or 200 ppm AN in drinking water	28 days	+	Pu et al. (2009)
Male Sprague-Dawley rats	8-oxodG in brain DNA	30 or 300 ppm AN in drinking water	21 d	+	Whysner et al. (1998a)
Male Sprague-Dawley rats	8-oxodG in liver DNA	30 or 300 ppm AN in drinking water	21 d	+	Whysner et al. (1998a)
Male Sprague-Dawley rats	8-oxodG in forestomach DNA	0–300 ppm AN in drinking water	21 d	–	Whysner et al. (1998a)
Male F344 rats	8-oxodG in brain DNA	0–100 ppm AN in drinking water	21 d	–	Whysner et al. (1998a)
Male Sprague-Dawley rats	8-oxodG in brain DNA	100 ppm AN in drinking water	3–94 d	+	Whysner et al. (1998a)

[a]The formation of 8-oxodG was reversible. Following treatment with AN for 24 hrs and removal of AN for 24 hrs afterwards, 8-oxodG levels returned to control values.

+ = Positive;– = negative; (+) = borderline positive.

4.6. SYNTHESIS AND EVALUATION OF MAJOR NONCANCER EFFECTS AND MODE OF ACTION—ORAL AND INHALATION

4.6.1. Oral

No studies are available regarding noncancer health effects in humans following acute, subchronic, or chronic oral exposure to AN.

The chronic oral noncancer toxicity database for AN consists of results from four rat toxicity and cancer bioassays (one with F344 rats and three with Sprague-Dawley rats) (see Table 4-56 for references), one toxicity and cancer bioassay with $B6C3F_1$ mice (NTP, 2001), and a three-generation developmental/reproductive toxicity study with Sprague-Dawley rats (Friedman and Beliles, 2002; Litton Bionetics, 1992). NOAELs and LOAELs for noncancer effects in these studies are summarized in Table 4-56. Also included in Table 4-56 are summaries of results from a 12-week gavage study of nerve conduction velocities in male Sprague-Dawley rats (Gagnaire et al., 1998), a 60-day gavage study of testicular toxicity in male CD-1 mice (Tandon et al., 1988), a 14-week gavage toxicity bioassay in $B6C3F_1$ mice (NTP, 2001), a developmental toxicity study in Sprague-Dawley rats exposed by gavage during GDs 6–15 (Murray et al., 1978), and a neurobehavioral study of Sprague-Dawley rats exposed to AN in drinking water for up to 12 weeks (Rongzhu et al., 2007).

Table 4-56. Noncancer effects in animals repeatedly exposed to AN by the oral route

Reference *Species*	Exposure conditions, mg/kg-d	NOAEL (mg/kg-d)	LOAEL (mg/kg-d)	Effect
Johannsen and Levinskas (2002b); Biodynamics (1980c) *F344 rat*	0, 0.1, 0.3, 0.8, 2.5, 8.4 (M) 0, 0.1, 0.4, 1.3, 3.7, 10.9 (F) DW, 2 yrs; sacrifices at 6, 12, and 18 mos and termination (99 wks or 699–706 d [F]; 107 wks or 770–777 d [M])	0.1(M) 0.1 (F)	0.3[a] (M) 0.4[a] (F)	Forestomach squamous cell hyperplasia and hyperkeratosis, increased incidence
		2.5 (M) 1.3 (F)	8.4[b](M) 3.7[b] (F)	Decreased survival after 18 mos
		2.5 (M) 3.7 (F)	8.4[a] (M) 10.9[a] (F)	Decreased BW (>10% compared with control)
		0.4 (F)	1.3[b] (F)	Increase in serum alkaline phosphatase (F only)
		2.5 (M)	8.4[b] (M)	Increase in epidermal inclusion cysts (M only)
Johannsen and Levinskas (2002a); Biodynamics (1980a) *Sprague-Dawley rat*	0, 0.09, 8.0 (M) 0, 0.15, 10.7 (F) DW, 22 mos (M); 19 mos (F); sacrifices at 6, 12, and 18 mos and termination	ND (M) 0.15 (F)	0.09[b](M) 10.7[a] (F)	Forestomach squamous cell hyperplasia, increased severity
		8.0 (M) 0.15 (F)	ND (M) 10.7[a] (F)	Renal transitional cell hyperplasia (F only)
		0.09 (M) 0.15 (F)	8.0[b] (M) 10.7[a] (F)	Decreased survival at 10 mos (M + F); decreased BW (10/8% [M/F])

Table 4-56. Noncancer effects in animals repeatedly exposed to AN by the oral route

Reference *Species*	Exposure conditions, mg/kg-d	NOAEL (mg/kg-d)	LOAEL (mg/kg-d)	Effect
Johannsen and Levinskas (2002a); Biodynamics (1980b) *Sprague-Dawley rat*	0, 0.1, 10 (M + F) Gavage, 7 d/wk for 20 mos; sacrifices at 6, 12, and 18 mos and termination	0.1 (M + F)	10[a] (M + F)	Forestomach squamous cell hyperplasia, increased severity
		0.1	10[a]	Renal transitional cell hyperplasia at some but not all sacrifices
		0.1	10[a]	Decreased survival after 14 mos (M + F); decreased BW (6–13% compared with controls [M only]).
Quast (2002); Quast et al. (1980a) *Sprague-Dawley rat*	0, 3.4, 8.5, 21.3 (M) 0, 4.4, 10.8, 25.0 (F) DW, 2 yrs	3.4 (M) ND (F)	8.5[b](M) 4.4[b](F)	Forestomach squamous cell hyperplasia and hyperkeratosis, increased incidence
		ND (F)	4.4[b](F)	Gliosis in brain with or without perivascular cuffing in females; not significant in males
		ND (M) 4.4 (F)	3.4[b] (M) 10.8[b] (F)	Chronic nephropathy
		8.5 (M) ND (F)	21.3[b](M) 4.4[b] (F)	Decreased survival after 300 (F) or 480 (M) d
		8.5 (M) 10.8 (F)	21.3[b] (M) 25.0[b] (F)	Decreased BW (>10% compared with control); clinical signs of nervous system dysfunction
NTP (2001) *B6C3F$_1$ mouse*	0, 2.5, 10, 20 (M + F) Gavage, 5 d/wk for 2 yrs Adjusted doses: 0, 1.8, 7.1, 14.3 mg/kg-d (M + F)	1.8 (M) 7.1 (F)	7.1[b] (M) 14.3[b] (F)	Forestomach squamous cell hyperplasia and hyperkeratosis, increased incidence
		1.8 (M) 14.3 (F)	7.1[b] (M) ND (F)	Increased incidence of Harderian gland hyperplasia
		ND (F)	1.8[b] (F)	Increased incidence of ovarian cysts or ovarian atrophy
		7.1 (M + F)	14.3[a] (M + F)	Decreased survival after 15 wks
NTP (2001) *B6C3F$_1$ mouse*	0, 5, 10, 20, 40 60 (M + F) Gavage, 5 d/wk for 14 wks. Adjusted doses: 0, 3.6, 7.1, 14.3, 28.6, and 42.9 (M + F)	28.6 (M) 14.3 (F)	ND (M) 28.6[a] (F)	Forestomach inflammation, ulceration, and epithelial hyperplasia, increased incidence in F only No histopathology data for 60 mg/kg groups
		14.3 (M + F)	28.6[b] (M + F)	Increased mortality
Tandon et al. (1988) *CD-1 mouse*	0, 1, 10 (M only) Gavage, for 60 d	1	10[b]	45% decreased sperm count; 40% of seminiferous tubules examined degenerated

Table 4-56. Noncancer effects in animals repeatedly exposed to AN by the oral route

Reference *Species*	Exposure conditions, mg/kg-d	NOAEL (mg/kg-d)	LOAEL (mg/kg-d)	Effect
Friedman and Beliles (2002); Litton Bionetics (1992) *Sprague-Dawley rat*	0, 11, 37 (M) 0, 20, 40 (F) DW, three-generation reproduction study	ND	11[b] (M) 20[b] (F)	Decreased viability for F1b pups; no changes in fertility index or pregnancy outcome for F1a, F1b, F2a, F2b, F3a, or F3b generations
		ND	11[b] (M) 20[b] (F)	LOAEL for decreased lactation index in F1b parents for F2a pups; small deficits in postnatal pup weights (10–40%, variable across generations) and postnatal survival (about 10%, variable across generations) in higher dosed groups
Murray et al. (1978) *Sprague-Dawley rat*	0, 10, 25, 65 (F only) Gavage GDs 6–15	10	25	Maternal effects: forestomach hyperplasia, 11% increased liver weight, 22% decrease in BW gain
		10	25	Fetal effects: missing vertebrae in 6/17 litters, 7% decreased BW
Gagnaire et al. (1998) *Sprague-Dawley rat*	0, 12.5, 25, 50 (M only) Gavage, 5 d/wk for 12 wks	25	50[a]	SCV decreased beginning wk 6 (-7.5%), –17.8% by wk 12; -10.6% after 8 wks recovery; decreased BW after 4 wks (-17% at wk 12); hind limb weakness in 5/11 surviving high-dose rats after wk 9
Rongzhu et al. (2007) *Sprague-Dawley rat*	0, 4, 13.5 (M only) DW for 0, 4, 8, 12 wks	ND	4[b]	Neurobehavioral alterations, as indicated by decreased motor coordination, increased training duration, head twitching, trembling, circling, backwards pedaling, and decreased home-cage activities
Szabo et al., (1984) *Sprague-Dawley rats*	0, 0.2, 4, 20, and 100 mg/kg-day (F only) DW for up to 60 days	4 (F)	20 (F)	Enlarged kidneys, increase in regional hyperplasia of the gastric mucosa
Szabo et al. (1984) *Sprague-Dawley rats*	0, 0,2, 4, 20 or 100 mg/kg-day (F only) Daily gavage for up to 60 days	ND	0.2 (F)	Adrenocortical hyperplasia
Quast et al. (1975) *Beagle dog*	0, 10, 16, 17 (M) 0, 8, 17, 18 (F) DW for 6 months	10 (M) 8 (F)	16 (M) 17 (F)	Early mortality, histopathological lesions of the esophagus and tongue.

[a]significantly different from controls ($p < 0.01$).
[b]significantly different from controls ($p < 0.05$).

DW = drinking water; F = female; M = male; ND = not determined

Forestomach lesions (epithelial hyperplasia and hyperkeratosis) were the most consistently observed noncancer effect associated with chronic oral exposure of rats and mice to AN and were associated with the lowest LOAELs in AN-exposed rats (Table 4-56). The lowest LOAELs were 0.09 and 10.7 mg/kg-day for increased severity of forestomach lesions in male and female Sprague-Dawley rats exposed by drinking water (Johannsen and Levinskas, 2002a; Biodynamics, 1980a), 0.3 and 0.4 mg/kg-day for increased incidence of forestomach lesions in male and female F344 rats exposed in drinking water (Johannsen and Levinskas, 2002b; Biodynamics, 1980c), and 8.5 and 4.4 mg/kg-day for increased incidence of forestomach lesions in male and female Sprague-Dawley rats exposed in drinking water (Quast, 2002; Quast et al., 1980a). Increased incidences of animals with hyperplasia or hyperkeratosis of the forestomach were also observed in $B6C3F_1$ mice exposed by gavage (5 days/week) for 2 years to 10 mg/kg-day (males) or 20 mg/kg-day (females) (NTP, 2001), female $B6C3F_1$ mice exposed to 40 mg/kg-day by gavage (5 days/week) for 14 weeks (NTP, 2001), and pregnant Sprague-Dawley rats exposed to 25 mg/kg-day by gavage on GDs 6–15 (Murray et al., 1978). Other effects observed in orally exposed animals generally were observed at higher doses (Table 4-56).

Kidney effects included increased incidence of renal transitional cell hyperplasia in Sprague-Dawley rats exposed by gavage or in drinking water to about 10 mg/kg-day but not 0.1 mg/kg-day (Johannsen and Levinskas, 2002a; Biodynamics, 1980a) and increased incidence of chronic nephropathy in Sprague-Dawley rats exposed to drinking water doses of 3.4 mg/kg-day (males) or 10.8 mg/kg-day (females) (Quast 2002; Quast et al., 1980a).

Decreased survival was observed after 18 months in F344 rats exposed to drinking water at 8.4 mg/kg-day (males) and 3.7 mg/kg-day (females) (Johnannsen and Levinskas, 2002b) and in Sprague-Dawley rats exposed to drinking water at 21.2 mg/kg-day (males) and 4.4 mg/kg-day (females) (Quast, 2002). In another drinking water study of Sprague-Dawley rats, decreased survival was observed at 8.0 mg/kg-day (males) and 10.7 mg/kg-day (females).

Increased incidences of ovarian lesions (cysts or atrophy) were observed in female mice exposed to gavage doses of 2.5, 10, or 20 mg/kg-day (NTP, 2001), but exposure-related ovarian lesions were not observed in the chronic rat bioassays. In a reproductive toxicity study in Sprague-Dawley rats exposed to 0, 100, or 500 ppm AN in drinking water (11 or 37 mg/kg-day [males]; 20 or 40 mg/kg-day [females]), small deficits in postnatal pup weights and pup survival without effects on fertility or pregnancy success were observed in three generations exposed to either 100 or 500 ppm (Friedman and Beliles, 2002; Litton Bionetics, 1992) (see Table 4-56). Other reproductive effects observed in animals were a reduction of epididymal sperm counts and degeneration of seminiferous tubules in CD-1 mice exposed to 10 mg/kg-day by gavage for 60 days (Tandon et al., 1988), but no exposure-related lesions in male reproductive organs were found in $B6C3F_1$ mice exposed by gavage to up to 40 mg/kg-day for 14 weeks or up to 20 mg/kg-day for 2 years (NTP, 2001). Likewise, no effects on sperm motility parameters were found in male $B6C3F_1$ mice exposed to up to 20 mg/kg-day for 14 weeks (NTP, 2001).

The only oral developmental toxicity study (Murray et al., 1978) identified 10 and 25 mg/kg-day as a NOAEL and LOAEL for maternal effects (increased incidence of forestomach hyperplasia, 10% increased absolute liver weight, and 22% decreased BW gain) and developmental effects (7% decrease in fetal BW and missing vertebrae associated with short tails in 6/17 litters, compared with 1/38 in the controls). The study involved daily gavage exposure on GDs 6–15.

Neurological effects in animals associated with chronic oral exposure to AN were observed in: (1) a report of gross clinical signs of neurological impairment in about 10% of Sprague-Dawley rats (paralysis, head tilt, circling, and seizures) exposed to drinking water concentrations of 500 ppm (providing doses of about 65 and 74 mg/kg-day for males and females) but not in rats exposed to 100 ppm (13 and 15 mg/kg-day, males and females) (Bigner et al., 1986); (2) decreases (8–15%) in SCV in tail nerves and hind-limb weakness in male Sprague-Dawley rats exposed by gavage to 50 mg/kg-day (5 days/week) for 6–12 weeks but not in rats exposed to 25 mg/kg-day (Gagnaire et al., 1998); and (3) neurobehavioral alterations in male Sprague-Dawley rats exposed to 4 and 13.46 mg/kg-day AN for 4, 8, or 12 weeks (head twitching, trembling, circling, backwards pedaling, decreased home-cage activities, decreased motor coordination, and learning and memory) (Rongshu et al., 2007). These studies indicated that neurological impairment in AN-exposed rats occurred at higher administered doses than doses associated with hyperplasia and hyperkeratosis in forestomach squamous epithelial cells.

4.6.2. Inhalation

Table 4-57 lists the NOAELs and LOAELs from four cross-sectional health examinations and surveys of subjective symptoms in Japanese and Chinese acrylic fiber workers (Chen et al., 2000; Kaneko and Omae, 1992; Muto et al., 1992; Sakurai et al., 1978), a cross-sectional examination of performance of acrylic fiber workers in a battery of neurobehavioral tests (Lu et al., 2005a), a study on the effect of AN exposure on the sperm cells of AN production plant workers (Xu et al., 2003), and three cross-sectional surveys of reproductive outcomes in Chinese acrylic fiber or AN manufacturing workers (Dong et al., 2000b; Li, 2000; Dong and Pan, 1995). More detailed descriptions of these studies are in Section 4.1.2.2. Each of these epidemiologic studies measured AN concentrations in workplace air samples and compared results of the examinations and surveys in exposed workers with unexposed workers of similar age. The human LOAELs and NOAELs in Table 4-57 are mean or midpoint values of the range of concentrations determined for various groups of exposed workers. Table 4-57 also lists NOAELs and LOAELs identified in the animal toxicity studies involving repeated inhalation exposure to AN.

Table 4-57. Noncancer effects in human workers and animals repeatedly exposed to AN by inhalation

Reference/ Study subjects	Exposure conditions[a]	NOAEL[a] ppm	LOAEL ppm	Effect
Muto et al. (1992) Acrylic fiber workers	Male workers with average 17 yrs of occupational exposure compared with unexposed workers	0.19	1.13	Statistically significantly increased prevalences of subjective symptoms (e.g., heaviness of stomach, poor memory, irritability) but no increases in prevalences of physical signs or abnormal values in urinalytic, hematological, liver function, or blood pressure variables compared with controls.
Sakurai et al. (1978) Acrylic fiber workers	Male workers with average 10–12 yrs of occupational exposure compared with unexposed workers	ND	4.2	Statistically insignificant increase in incidence of palpable liver, reddening of the conjunctiva and pharynx, and the occurrence of skin rashes compared with unexposed controls. No survey of subjective symptoms.
Kaneko and Omae (1992) Acrylic fiber workers	Male workers with average 5.6, 7.0, or 8.6 yrs of occupational exposure in three groups of factories (mean AN concentrations at 1.8, 7.4, and 14.1 ppm) were compared with unexposed workers	ND	1.8	Statistically significantly increased prevalences of subjective symptoms (e.g., headaches, tongue trouble, choking lump in chest, fatigue) were found in workers from all three groups of factories when compared with controls.
Chen et al. (2000) Acrylic fiber workers	Male and female workers with average 13 yrs of occupational exposure compared with unexposed workers	ND	0.48	Statistically significantly increased prevalences of subjective symptoms (e.g., headache, dizziness, poor memory, choking feeling in chest, loss of appetite) compared with controls.
Lu et al. (2005a) Acrylic fiber workers	Male and female workers with >1 yr of occupational exposure (average duration not available) compared with unexposed workers	ND	0.11	Small, but statistically significant, deficits in tests of neurobehavior in monomer workers and fiber workers (average air concentrations of 0.11 ppm for monomer workers and 0.91 ppm for fiber workers) compared with controls.
Xu et al. (2003) AN production workers	Male workers with 2.8 yrs of occupational exposure in a AN production plant, compared with controls of approximate age range in the general population.	ND	0.37	Statistically significant decrease in sperm density and sperm number in exposed workers, statistically significant increase in DNA strand breakage and sex chromosome aneuploidy in sperm cells of exposed workers compared with controls
Dong and Pan (1995) Acrylic fiber workers	Male and female workers with average 3.2 and 10.2 yrs of occupational exposure compared with unexposed controls	ND	3.7	Statistically significant increased prevalences of adverse reproductive outcomes (premature delivery [10.7 vs. 3.5%, in wives of exposed males], stillbirths [4.5 vs. 0%, in exposed females], and sterility [5.0 vs. 1.8%, in exposed males]) compared with controls.
Dong et al. (2000b) Acrylic fiber workers	Male and female workers with average 11 and 10.4 yrs of occupational exposure compared with unexposed controls	ND	3.6	Statistically significantly increased prevalences of adverse reproductive outcomes (increased stillbirths [2.7 vs. 0%], birth defects [21.3 vs. 4.8%], and premature deliveries [8.2 vs. 3.9%]) in female workers compared with controls.

Table 4-57. Noncancer effects in human workers and animals repeatedly exposed to AN by inhalation

Reference/ Study subjects	Exposure conditions[a]	NOAEL[a]	LOAEL	Effect
		ppm		
Li (2000) AN manufacturing workers	Female workers with average 14 yrs of occupational exposure compared with unexposed controls	ND	7.5	Statistically significant increased prevalences of adverse reproductive outcomes (sterility [2.6 vs. 0.8%], pregnancy complications [20.8 vs. 7.1%], premature deliveries [11.6 vs. 4.7%], and congenital defects [25.4 vs. 4.2%]) in female exposed workers compared with controls.
Quast et al. (1980b) Sprague-Dawley rats (M + F)	0, 20, 80 ppm, 6 hrs/d, 5 d/wk for 2 yrs	ND	20	Statistically significant increase in incidence of lesions in nasal epithelia at 20 ppm in males and females; focal necrosis in liver of females. At 80 ppm, other lesions occurred at increased incidences—gliosis and perivascular cuffing in brain in both sexes, hepatic necrosis in females, focal nephrosis and thyroid cysts in males, and hyperplasia in nonglandular stomach.
Gagnaire et al. (1998) Sprague-Dawley rats (M only)	0, 25, 50, 100 ppm, 6 hrs/d, 5 d/wk for 24 wks	ND	25	Statistically significant deficits (5% decreased compared with controls) in sensory conduction velocity of the tail nerve.
Murray et al. (1978) Pregnant Sprague-Dawley rats	0, 40, or 80 ppm, 6 hrs/d on GDs 6–15	ND 40	40 80	Maternal weight gain decreased by >20% compared with controls. No increased incidence of litters with a single malformation; 6/35 litters with short tail, short trunk, missing vertebrae, or missing ribs vs. 1/33 in controls.
Saillenfait et al. (1993) Pregnant Sprague-Dawley rats	0, 12, 25, 50, 100 ppm, 6 hrs/d on GDs 6–20	12 12	25 25	Statistically significant decreased maternal weight gain compared with controls. Statistically significant decreased fetal BW, >5% decreased compared with controls. No exposure-related increased incidences of litters with fetal anomalies.

[a]ND = cannot be determined

In acute AN poisoning cases involving humans (Chen et al., 1999), first aid treatment of victims generally included antidotes for cyanide poisoning and pure oxygen to overcome respiratory distress caused by damage to the lung. Other clinical symptoms following such poisoning included blood chemistry changes indicative of slight liver damage. In an analysis of 144 case reports of acute AN poisoning, Chen et al. (1999) estimated that exposure levels were in the 18–258 ppm range (40–560 mg/m^3) for 60 cases and >460 ppm (>1,000 mg/m^3) for the remaining 84 cases. Subjective symptoms reported for 92–100% of the cases included dizziness, headache, chest tightness, feebleness, and hyperactive knee jerk. Sore throat, dyspnea, vomiting, abdominal pain, fainting, and congestion of the pharynx were reported in 60–87% of cases. Other less frequently reported symptoms or effects (5–32% of cases) included numbness of

limbs, convulsion, rapid heart rate, cough, hoarseness, rough breathing sound, coma, and abnormal liver function (Chen et al., 1999).

In the cross-sectional studies of AN-exposed workers, subjective symptoms that were reported with increased prevalences compared with unexposed workers included dizziness, headache, chest tightness, and poor memory, indicating respiratory irritation and neurological effects. Average workplace air concentrations associated with increased prevalences of these subjective symptoms were 1.13 ppm (Muto et al., 1992), 1.8 ppm (Kaneko and Omae, 1992), and 0.48 ppm (Chen et al., 2000) (see Table 4-57). No statistically significant increases in the prevalences of subjective symptoms were found in a group of acrylic fiber workers whose average workplace air concentration was 0.19 ppm (Muto et al., 1992). The studies by Muto et al. (1992) and Sakurai et al. (1978) included clinical physical examinations, but no statistically significant increases in prevalences of physical signs (such as reddened conjunctiva or pharynx) or abnormal values in clinical chemistry variables (including activities of liver enzymes) were found in exposed workers (more details of results from these studies can be found in Section 4.1.2.2.2 and Table 4-22).

To provide support that neurological effects are the most sensitive identified class of effects from repeated inhalation exposure to AN, statistically significant deficits in several neurobehavioral tests were measured in exposed workers in a Chinese acrylic fiber manufacturing plant with mean workplace air concentrations of 0.11 ppm (range 0.00–1.70 ppm) and 0.91 ppm (range 0.00–8.34 ppm) in two different process areas. Deficits in exposed workers compared with nonexposed workers were noted in a Profile of Mood States test (20–68% higher for negative moods such as anger and confusion), a Simple Reaction Time test of attention and response speed (10–16% deficits), and the backward sequence of the Digit Span test of auditory memory (21–24% deficits).

Statistically significant increases in the prevalences of adverse reproductive outcomes were associated with mean workplace air concentrations of 3.7 ppm (Dong and Pan, 1995), 3.6 ppm (Dong et al., 2000a), and 7.5 ppm (Li, 2000), indicating that reproductive effects from occupational exposure may occur at higher exposure levels than those associated with mild neurobehavioral effects. However, statistically significant decrease in sperm density and number, statistically significant increase in DNA strand breakage and sex chromosome aneuploidy in sperm cells were reported in workers exposed to 0.37 ppm AN with average 2.8 years of exposure (Xu et al., 2003). An epidemiological study conducted in the area surrounding an AN-using plant in Hungary reported increased ORs for several congenital malformations (e.g., undescended testis), but no exposure data were provided in this study (Czeizel et al., 2000, 1999).

Exposure levels associated with adverse effects in Sprague-Dawley rats were higher than the workplace air concentrations associated with adverse effects in AN-exposed workers (Table 4-57). The lowest exposure level in the 2-year inhalation bioassay, 20 ppm, produced

increased incidence of lesions in nasal epithelia (hyperplasia of mucus-secreting cells in males and flattening of the respiratory epithelium in females). At 80 ppm, further increases in incidences of nasal lesions of a wider variety were observed as well as statistically significant increases in the incidences of histopathological lesions at other sites, including gliosis and perivascular cuffing in the brain of males and females, focal nephrosis and thyroid cysts in males, hepatic necrosis in females, and hyperplasia and hyperkeratosis of the nonglandular portion of the stomach in both sexes combined (Quast et al., 1980b). Other effects in Sprague-Dawley rats associated with repeated inhalation exposure to AN included deficits in sensory nerve conduction in the tail nerve of rats exposed to 25 ppm AN (Gagnaire et al., 1998) and developmental effects. Statistically significantly increased incidence of litters with missing vertebrae, missing ribs, or anteriorly displaced ovaries were observed in rats exposed to 80 ppm, but not 40 ppm, 6 hours/day on GDs 6–15 (Murray et al., 1978). In another study involving 6 hours/day inhalation exposure of Sprague-Dawley rats on GDs 6–20, developmental effects were restricted to a statistically significant decrease in fetal weight gain per litter, compared with controls, associated with exposure to 25 ppm (5% decrease), 50 ppm (8% decrease), or 100 ppm (15% decrease); no effects on fetal weight gain were observed at 12 ppm (Saillenfait et al., 1993).

4.6.3. Mode-of-Action Information

The precise modes of action whereby AN induces noncancer effects are unknown. However, a general understanding of the processes by which AN is metabolized within the body allows some conclusions to be drawn about the range of processes that might be involved in bringing about one or more of its toxic responses. Relevant metabolic processes are likely to include partitioning between detoxification and oxidative activation sub-pathways, conversion of AN to one or more toxic metabolites, depletion of GSH, the association of AN metabolism with the onset of oxidative stress, and the ability of CEO, the reactive metabolite of AN, to covalently bind to macromolecules, such as proteins. In addition, other processes related to the parent compound AN, such as its cholinomimetic effects, may also be involved.

4.6.3.1. *GI Effects*

The relationship between AN metabolism and GI hemorrhage in rats was suggested by Ghanayem and Ahmed (1983). GI bleeding was observed 3 hours after a single dose of 50 mg/kg AN was administered to Sprague-Dawley rats orally or subcutaneously, with no significant difference in the amount of GI blood loss resulting from either route of administration. Thus, AN-induced GI bleeding was not a result of direct irritation of AN on the GI tract.

Pretreatment of rats with CYP450 enzyme inducer Aroclor 1254 increased blood loss by 240% (Ghanayem and Ahmed, 1983). In contrast, pretreatment of rats with CYP450 inhibitors

cobalt chloride or SKF 525A prior to AN administration produced significant decreases in blood loss of 10 and 40%, respectively. Pretreatment of rats with DEM, a known depletor of GSH, prior to AN administration produced no significant change in GI bleeding. In addition, administration of a sublethal dose (6 mg/kg s.c.) of KCN did not induce GI bleeding when compared with controls. Therefore, Ghanayem and Ahmed (1983) concluded that metabolic activation of AN by CYP450 to a reactive metabolite other than cyanide (probably CEO) was a prerequisite for AN to induce gastric hemorrhage.

Ahmed et al. (1996a) showed irreversibly bound AN-derived radioactivity in intestinal mucosa following a single i.v. injection of 2-[^{14}C]-AN to male F344 rats. A recent study by Jacob and Ahmed (2003a) also demonstrated that AN and or its metabolites accumulated and covalently interacted in GI mucosa of male F344 rats treated either by i.v. or orally with 2-[^{14}C]-AN. These studies supported the hypothesis that AN-induced injury of the GI mucosa is not due to direct irritation by AN but by metabolic activation and macromolecular interaction of AN metabolite in these tissues.

Ghanayem et al. (1985) also studied the mechanism of AN-induced gastric mucosal necrosis in the glandular stomach in male Sprague-Dawley rats. Subcutaneous administration of 40 or 50 mg/kg AN caused a significant decrease in hepatic and gastric GSH concentration 3 hours after treatment, and induced gastric necrosis. Pretreatment of rats with various metabolic modulators (CYP450 monooxygenase and GSH) before administration showed that there was a significant inverse relationship between gastric GSH concentration and AN-induced gastric erosions. Pretreatment of rats with sulfhydryl-containing compounds (cysteine or cysteamine) protected against AN-induced gastric necrosis and blocked the depletion of gastric GSH.

In addition, AN-induced gastric erosions could be prevented by pretreatment with atropine, a muscarinic receptor blocker, suggesting the involvement of muscarinic receptors in the AN-induced gastric mucosal necrosis (Ghanayem et al., 1985). Activation of acetylcholine muscarinic receptors is known to increase gastric acid secretion and cause gastric erosions. Because muscarinic receptors are known to contain sulfhydryl groups in their active site (Ikeda et al., 1980; Aronstam et al., 1978), Ghanayem et al. (1985) hypothesized that AN inactivated critical sulfhydryl groups and caused gastric erosions by locally modulating muscarinic acetylcholine receptors in the stomach.

4.6.3.2. *Neurological Effects*

Increased prevalence of subjective symptoms of neurological effects was associated with average workplace air concentrations of 1.13 ppm (Muto et al., 1992), 1.8 ppm (Kaneko and Omae, 1992), and 0.48 ppm (Chen et al., 2000), and small deficits in performance in a battery of neurobehavioral tests were observed in workers from factories with average workplace air concentrations of 0.11 and 0.91 ppm (Lu et al., 2005a). In a case of acute severe accidental AN poisoning (AN concentration at 62 mg/m^3) of a worker (Fei and Xu, 2006), impairment of the

CNS, including diffused damage to the cerebral cortex layer (pyramidal system) and damage to the subcortical layer (extrapyramidal system), was observed. In addition to poisoning symptoms (dizziness, headache, difficulty breathing, confusion, convulsion, etc.), cerebral focal damage was also detected in the patient, suggesting Parkinson's syndrome (static tremor, muscle rigidity, increased muscle tension and lead-pipe rigidity, slow motor activity). The clinical symptoms were related to those induced by adverse effects on the cholinergic system and dopaminergic system.

Neurotoxicological effects of AN in animals included cholinomimetic effects on the peripheral and central muscarinic systems in Sprague-Dawley rats after administration of nonlethal oral doses of 20, 40, or 80 mg/kg (Ghanayem et al., 1991) and the development of brain lesions in Sprague-Dawley rats (gliosis and perivascular cuffing) following chronic inhalation exposure to 80 ppm (Quast et al., 1980b) or chronic drinking water exposure to 4.4 mg/kg-day (females only).

The neurobehavioral effect of AN was suggested to be related to changes in brain monoamine neurotransmitter levels (Lu et al., 2005b). In a 12-week drinking water study of male Sprague-Dawley rats (Lu et al., 2005b), dopamine levels were decreased by 76 and 46% in rats exposed to 50 ppm AN, in the striatum and cerebellum, respectively. Serotonin levels were decreased by 38 and 41% in the striatum and cerebellum, respectively, for rats exposed to 50 ppm AN. In the case of acute severe AN poisoning, the development of Parkinson's syndrome and other CNS impairment in the exposed worker would suggest involvement of the cholinergic system and dopaminergic system (Fei and Xu, 2006).

The cholinomimetic effects were thought to be due to an effect of AN on muscarinic receptors, since atropine sulfate (which blocks both central and peripheral muscarinic receptors) protected animals against these effects (Ghanayem et al., 1991). In an earlier study on AN-induced gastric mucosal necrosis (Ghanayem et al., 1985), it was reported that pretreatment with atropine and sulfhydryl-containing chemicals protected against such lesions. Since muscarinic receptors contain sulfhydryls in their active sites (Aronstam et al., 1978) and sulfhydryl-depleting chemicals are known to potentiate chemically induced activation of muscarinic receptors (Hedlund and Bartfai, 1979), Ghanayem et al. (1991) speculated that depletion and/or inactivation of endogenous sulfhydryls by AN and/or its metabolite may cause configurational changes of muscarinic receptor binding affinity that, in turn, lead to the development of acetylcholine-like (cholinomimetic) toxic effects. It is unlikely that these cholinomimetic effects are due to inhibition of acetylcholinesterase activity. Rajendran and Muthu (1981) reported that AN did not inhibit the activity of acetylcholinesterase. In addition, Satayavivad et al. (1998) reported that AN had no effect on decreased motor activity induced by physostigmine (an inhibitor of acetylcholinesterase). Thus, Satayavivad et al. (1998) proposed that the cholinomimetic effect of AN might be mediated by the release of acetylcholine from nerve endings.

In addition, Ghanayem et al. (1991) proposed that lipid peroxidation may at least partly be involved in AN-induced cholinergic overstimulation. In noting that AN enhanced lipid peroxidation and inhibited Na^+,K^+-ATPase in RBCs in vitro, Farooqui et al. (1990) speculated that disruption of the lipid microenvironment in membranes by either or both of these processes might impact the muscarinic receptor function and induce cholinergic overstimulation.

For acute CNS effects, the signs were similar to those produced by cyanide. Ghanayem et al. (1991) proposed that the free cyanide liberated from AN during its metabolism may contribute to these effects. It is well established that cyanide causes CNS dysfunction by inhibition of cellular respiration via inactivation of tissue cytochrome c oxidase, which is the terminal electron acceptor in cellular energy production (Klaassen, 2001). Intraperitoneal injection of 30 mg/kg AN in Chinese hamsters decreased cerebral succinate dehydrogenase and cytochrome oxidase activities (Zitting et al., 1981). These authors suggested that the observed biochemical effects were likely due to the formation of cyanide from AN.

The neurotoxicity of AN may also result from the covalent binding of AN or its metabolites to enzymes. There is abundant evidence that important proteins bearing cysteine residues (e.g., enzymes such as GSTM1) can bind AN, thereby possibly impairing their functions and creating metabolic imbalances leading to toxicity. For example, AN was shown to covalently bind to the important glycolytic enzyme GAPDH in vitro (Campian et al., 2002). AN specifically targeted and bound to cysteine 149 in the active center of this enzyme, causing irreversible inhibition of its activity. This suggested that AN might impair glycolytic ATP production in vivo. Campian et al. (2002) speculated that the combination of glycolytic impairment with inhibition of mitochondrial ATP synthesis by cyanide released from AN could result in metabolic arrest. However, Campian et al. (2008) demonstrated in male Sprague-Dawley rats that acute lethality of AN was not due to brain metabolic arrest (see Section 4.5.1.1.3),

4.6.3.3. *Reproductive/Developmental Effects*

As discussed in Section 4.5.2.1, lower sperm density was noted in workers exposed to 0.8 mg/m^3 AN compared with controls of approximate age range from the general population (75×10^6/mL vs. 140×10^6/mL) (Xu et al., 2003). DNA strand breakage was also detected in AN-exposed workers using single-cell gel electrophoresis, with the rate of comet sperm higher in the exposed workers than in the control (28.7 vs. 15%). The frequency of sex chromosome disomy was 0.69% in exposed groups and was higher than 0.35% in the control group. There were also significant differences in the frequencies of XX-, YY-, and XY-bearing sperm between exposed and control groups.

AN-induced effects on the male reproductive system are restricted to a report that treatment of CD-1 mice for 60 days with gavage doses of 10 mg/kg-day produced degeneration of the seminiferous tubules and altered testicular activities of several enzymes (SDH, acid

phosphatase, LDH, and β-glucuronidase) (Tandon et al., 1988). Exposure-related increases in the incidence of lesions in male reproductive organs were not observed in 14-week or 2-year gavage bioassays with $B6C3F_1$ mice (NTP, 2001) or in the 2-year bioassays with Sprague-Dawley or F344 rats (see Table 4-56).

The potential male reproductive effect of AN may involve the distribution and metabolism of AN to CEO in the testis and interaction of CEO with tissue protein and DNA. Radiolabeled AN distributed to the rat testis after oral and i.v. administration (Ahmed et al., 1996a; Young et al., 1977). The testis has the capability to bioactivate AN (Abdel-Aziz et al., 1997). Thus, CEO can either be formed in the liver and transported to the testis or be formed in the testis in situ. AN has been reported to interact with testicular DNA in rats treated with a single 46.5 mg/kg oral dose (Ahmed et al., 1992b). Covalent binding of [2,3-^{14}C]-AN-derived radioactivity to testicular DNA was maximal at 0.5 hours following administration, while DNA synthesis in testicular tissue was decreased (80% of control). In addition, testicular DNA repair was increased 1.5-fold at 0.5 hour and more than threefold at 24 hours after treatment (Ahmed et al., 1992b). Alkylating agents have the potential to produce infertility via destruction of dividing primary spermatogonia (Heinrichs and Juchau, 1980). Thus, any effect of AN on male reproductive tissue may be due to its interference with testicular DNA synthesis and repair processes. The consequence may be reproductive abnormalities as well as impact on altered heritability in offspring.

No mechanistic studies are available to elucidate the mode of action whereby AN induced ovarian atrophy and cysts in female mice chronically exposed by gavage to doses as low as 2.5 mg/kg-day (NTP, 2001).

The mild developmental effects associated with gestational exposure to 80 ppm AN by inhalation or 65 mg/kg-day by gavage (Murray et al., 1978) may be associated with the release of cyanide during maternal metabolism of AN. Concurrent administration of thiosulfate, a cyanide antagonist, was shown to protect against the malformations induced by i.p. injection of 80 mg/kg AN in hamsters (Willhite et al., 1981). However, Saillenfait et al. (1993) tested for relative developmental toxicities of eight aliphatic mononitriles and proposed that factors other than cyanide liberation from the nitrile may be involved, since teratogenicity of inhaled aliphatic mononitriles in rats could not be predicted based on the presence of a vinyl moiety in their molecular structure.

4.6.3.4. *Hematological Effects*

Farooqui and Ahmed (1983b) conducted work to elucidate the mechanism of the hematological effects of AN. Their findings pointed to substantial AN-induced covalent binding of CEO to RBCs, GSH depletion, increase in rate of RBC metabolism, and increase in the formation of two metabolic intermediates, ATP and 2,3-diphosphoglycerate, that regulate the oxygen dissociation curve. These authors suggested that chronic exposure to AN may lead to

methemoglobinemia, damage to RBC membranes, and impaired delivery of oxygen to the tissues.

Oxidative stress and lipid peroxidation were also suggested as additional factors aiding in the destruction of RBCs, evidenced by a significant decrease of Na^+,K^+-ATPase activity in isolated RBC membranes (Farooqui et al., 1990).

AN-Hb adducts have been measured and used as a marker of exposure in humans. AN can bind to amino acid residues other than cysteine. Thus, MacNeela et al. (1992) identified the N-terminal cyanoethyl-valine adduct of Hb (CEVal), the formation of which may have implications for the efficiency of oxygen transport to the tissues.

4.6.3.5. *Immunological Effects*

Zabrodskii et al. (2000) suggested a potential mechanism of action for the AN-induced DTH. They found that, in mice, AN reduced the number of esterase-positive splenocytes, the number of antibody-producing cells, and the inflammatory response induced by injection of SRBCs in the paws of animals. Treatment of the animals with an esterase activity-restoring drug restored the paw-response completely but not the numbers of immune-competent cells. However, a combination of the esterase-restoring drug and a cyanide-trapping drug restored immune function completely. Therefore, the study authors concluded that the immunotoxic effect of AN was due to combined inhibition of esterase and cytochrome c oxidase a_3 activities.

4.6.3.6. *Covalent Binding to Sulfhydryl Groups*

The capacity of AN to bind to proteins may be an important determinant of its toxicological effects. AN has been shown to have high affinity for cysteine residues on proteins and polypeptides. There is abundant evidence that AN will bind to the cysteine-bearing tripeptide, GSH, even without the contribution of enzymes such as GST. As discussed in Chapter 3, the formation of 2-(cyanoethyl)glutathione and the appearance of 2-(cyanoethyl)cysteine and N-acetyl 2-(cyanoethyl)cysteine in the urine have been taken as an indication of the ready interaction of AN and GSH. However, the presence of excess AN can cause GSH to become depleted. This will tend to channel AN into an oxidative reaction with CYP2E1 and result in formation of CEO and other products. Perturbing the balance between detoxification of AN with GSH and oxidation by CYP2E1 (for example, by blockade of CYP2E1) may facilitate the binding of AN to other cysteine-bearing proteins when GSH levels are low.

AN also has been shown to bind to the cysteine 186 residue of the enzyme CAIII in rat liver in vivo. Nerland et al. (2003) pointed out that this enzyme may play a role in protecting cells from oxidative stress. AN binding to this component, with possible conformational changes in tertiary structure and functionality, might abolish this protective ability and increase cell vulnerability to oxidative stress. In a similar study, Nerland et al. (2001) demonstrated that

AN can bind also with high selectivity to cysteine 86 of GSTM1. However, in this case, the binding did not exert an effect on the catalytic activity of the enzyme.

4.7. EVALUATION OF CARCINOGENICITY—SYNTHESIS OF HUMAN, ANIMAL, AND OTHER SUPPORTING EVIDENCE, CONCLUSIONS ABOUT HUMAN CARCINOGENICITY, AND LIKELY MODE OF ACTION

4.7.1. Summary of Overall Weight of Evidence

Following *EPA's Guidelines for Carcinogen Risk Assessment* (U.S. EPA, 2005a), AN is "likely to be carcinogenic to humans," based predominantly on consistent results showing that lifetime inhalation or oral exposure caused a statistically significantly increased incidence of tumors at multiple tissue sites in rats and mice. The most consistently observed tissue sites with tumors were the brain, forestomach, Zymbal gland in the ear canal in rats, and forestomach and ocular Harderian gland in mice. In addition, rats exposed during gestation and throughout adulthood showed higher incidences of brain tumors, Zymbal gland tumors, and extrahepatic angiosarcomas than did rats with exposure throughout adulthood only; hepatomas, which were not observed in exposed adult rats, were reported in rats exposed during gestation and throughout adulthood. Epidemiological studies of AN-exposed workers provide no strong evidence that mortality from any type of cancer is causally related to occupational exposure to AN, but limited evidence from the largest and best-designed epidemiologic study (Blair et al., 1998) indicated that workers with the longest duration and highest exposures to AN had a small, but statistically significant, increased risk for dying from lung cancer.

The available weight of evidence is adequate for a direct mutagenic mode of action involving DNA modification by reactive metabolite CEO. Other modes of action, including oxidative stress and inhibition of intercellular communication, may also contribute. Currently, no mechanistic explanations are available for the fact that AN induces brain tumors in rats but not in mice, although this may be related to higher CEO levels in rat brains and the more rapid clearance of CEO in mice than in rats (see Section 3.2). Mouse liver GST has a greater capacity for conjugating AN or CEO than rat liver GST (see Section 3.3.2). The modes of action involved in tumors induced by AN at other sites in animals (e.g., forestomach squamous epithelium in rats and mice and Zymbal gland in rats) have not received adequate investigation.

The mutagenic mode of action for AN-induced tumors is considered to be relevant to humans.The metabolism of AN in rats and humans is similar and there is evidence for mutagenicity of AN in exposed humans.

4.7.2. Synthesis of Human, Animal, and Other Supporting Evidence

Section 4.1.2.2 presents an historical perspective and evaluation of the epidemiologic studies of possible relationships between occupational exposure to AN and elevated risks for cancer. The early studies were of small cohorts with limited follow-up periods and limited

assessment of actual exposures. Elevations for incidence and death from lung cancer and incidence of prostate cancer were sufficiently consistent among the early studies to provoke the conduct of several additional studies over a 20-year period. The later studies had increased power due to increased number of workers, longer periods of follow-up, increased sophistication and quantification of exposure assessments, or inclusion of information on smoking habits. Small excess risks for lung and prostate cancer were identified in a few of these studies, but consistently and statistically significantly elevated risks were not observed across studies (see Tables 4-3 and 4-9). Other studies reported small excess risks for other types of cancer (e.g., bladder, colon, and brain cancers), but these findings were even less consistent across studies than the findings for lung and prostate cancer (see Tables 4-8, 4-11, 4-12 and 4-13).

The most informative study in the later generation of studies was the large, well-documented study by Blair et al. (1998). This study was strong because it examined a large cohort and attempted to adjust for known problems with earlier studies by quantifying exposures, estimating the effect of smoking, and using an internal control group of unexposed workers. The AN-exposed cohort as a whole experienced fewer deaths from lung cancer than those expected from the experience of the general U.S. population (probably reflecting a healthy worker effect), but when the exposed workers were grouped into quintiles of cumulative exposure, the lung cancer rate in the highest quintile of exposure (>8 ppm-years) for those who were followed for 20 or more years was about two times the rate in the unexposed group of workers (RR = 2.1; 95% CI = 1.2–3.8). Conclusions regarding the association between AN exposure and other cancer types (stomach, brain, breast) are limited due to the small number of site-specific cancer deaths (Blair et al., 1998).

As concluded in Section 4.1.2.2, there is no strong evidence from the body of epidemiologic studies that mortality from any type of cancer is causally related to exposure to AN at the levels that have been measured in workplaces utilizing this chemical. However, based on these epidemiology studies, there is suggestive evidence of a possible association between occupational exposure to AN and increased risk of lung cancer.

In rat and mouse bioassays, AN has been demonstrated to be a multiple-site carcinogen. Chronic oral exposure to AN induced tumors in the brain or spinal cord, Zymbal gland in the ear canal, the forestomach, and, to a lesser degree and less consistently, the female mammary gland, tongue, and intestine in several oral bioassays with F344 rats (Johanssen and Levinskas, 2002b; Biodynamics, 1980c) and Sprague-Dawley rats (Johannsen and Levinskas, 2002a; Quast, 2002; Biodynamics, 1980a, c; Quast et al., 1980a). In addition, lifetime inhalation cancer bioassays with Sprague-Dawley rats found exposure-related increased incidences of brain tumors, Zymbal gland tumors, intestinal tumors, malignant mammary gland tumors, and tongue tumors (Dow Chemical Co., 1992a; Maltoni et al., 1988, 1977; Quast et al., 1980b). Strong evidence exists for dose-response relationships for the carcinogenic responses in the CNS, Zymbal gland, and the forestomach of rats, especially in the lifetime drinking water studies with multiple exposure

levels. The lowest drinking water concentrations associated with significant increased incidence of forestomach and brain tumors were 3 and 30 ppm, respectively, corresponding to daily doses of about 0.3 and 2.5 mg/kg-day in F344 rats (Johanssen and Levinskas, 2002b; Biodynamics, 1980c).

With chronic inhalation exposure of Sprague-Dawley rats, increased incidences of brain tumors occurred at air concentrations of 20 and 80 ppm, whereas the incidences of Zymbal gland tumors, mammary gland adenocarcinomas and intestinal tumors were increased only at the 80 ppm level (Quast et al., 1980b). In mice, a single gavage lifetime bioassay identified the forestomach and the Harderian gland as sites of tumor development, but elevated incidences of brain, Zymbal gland, or mammary gland tumors were not found (NTP, 2001). A significant increase in lung tumors was found in the female mid-dose group of exposed mice but not in the female high-dose group or in any of the male exposed groups. NTP (2001) concluded that the evidence for carcinogenicity in the mouse lung was equivocal; this conclusion is consistent with the small magnitude of the increase, lack of a monotonic dose-response relationship, and lack of a demonstrated carcinogenic response in exposed male mice. No consistent evidence was found for carcinogenicity in the rat lung or the prostate or bladder tumors in rats or mice.

Results from two rat studies provide evidence that chronic exposure starting during early-life periods may result in increased susceptibility to the carcinogenicity of AN, compared with lifetime exposure during adulthood only (see Sections 4.2.2.2.2 and 4.2.1.2.8 for more details).

The possible human relevance of the rodent carcinogenic responses to AN is not fully understood. The brain is the only organ for which there is a direct human counterpart among rodent organs showing strong carcinogenic responses to AN, but the forestomach squamous epithelium and Zymbal gland have analogous tissues in humans. Although humans do not have a forestomach, the human esophagus is lined with squamous epithelial cells morphologically similar to those in which tumors develop in rats, with the exception that the rat cells are keratinized and the human cells are not (Cohen, 2004; Wester and Kroes, 1988). Likewise, although humans do not have a Zymbal gland, a sebaceous gland in the ear canal, they do have sebaceous glands. In contrast, humans and other primates do not have tissue analogous to the Harderian gland, an ocular gland in rodents that secretes lipids and porphyrins (Cohen, 2004; Sheldon, 1994; Albert et al., 1986). However, given that mutagenic modes of carcinogenic action are plausible for AN or its metabolites (see Section 4.6.3), formation of tumors in these organs may be indicative of a more generic carcinogenic hazard (Cohen, 2004). Chemicals with a mutagenic mode of action are frequently observed to cause cancers in many sites in one species, as well as to have different sites of tumor formation in different species. Therefore, it is reasonable to consider the tumor responses in these rodent organs as indicators of AN-induced carcinogenicity in humans. In addition, the National Academy of Sciences (NAS) (2008) in its *Science and Decisions: Advancing Risk Assessment,* stated on page 134 that "…the target organ in a rodent species, such as the forestomach or Zymbal gland, may not have an exact human

counterpart. However, the presence of carcinogenic action in tissues for which there is no correspondence in humans or that may be regulated differently in humans does not mean that the toxicity or tumor finding in animals is irrelevant. That the rodent tissue is sensitive to the toxicant signifies that the toxicant MOAs operate in a mammalian system that has characteristics in common with similar or even not obviously related tissues in humans or human subpopulations…it is typically impossible to rule out the relevance of an effect seen in a particular rodent tissue unless there is detailed mechanistic information on why humans would not be affected…In general, tissues that are responsive to a toxicant should be considered relevant to human risk assessment unless mechanistic information demonstrates that the processes occurring in the tissues could not occur in humans."

4.7.3. Mode-of-Action Information

The U.S. EPA (2005a) *Guidelines for Carcinogen Risk Assessment* defines mode of action as a sequence of key events and processes, starting with the interaction of an agent with a cell, proceeding through operational and anatomical changes, and resulting in cancer formation. Mode of action is distinct from "mechanism of action," a term that implies greater understanding and description of events, including those at the molecular level. Toxicokinetic processes leading to the formation or distribution of the active agent (i.e., parent material or metabolite) to the target tissue are not part of the mode of action. Examples of possible modes of carcinogenic action include mutagenic, mitogenic, anti-apoptotic (inhibition of programmed cell death), cytotoxic with reparative cell proliferation, and immunologic suppression.

AN has been demonstrated to be a multiple-site carcinogen in rats and mice, inducing tumors in the forestomach, brain, and Zymbal gland in two strains of rats following chronic oral exposure; in the forestomach and Harderian gland in a mouse strain following chronic oral exposure; and in the forestomach, brain, Zymbal gland, intestinal tract, and tongue in one rat strain following chronic inhalation exposure. Carcinogenic responses have also been reported less consistently across studies in the female mammary gland and small intestine. Several hypothesized modes of action by which AN causes cancer in the brain of rats have been investigated to varying degrees and are discussed within the context of the modified Hill criteria of causality as recommended in the most recent Agency guidelines (U.S. EPA, 2005a). These discussions are followed by discussion of possible modes of action involved in the development of forestomach tumors and hepatomas in rats and lung cancer in humans. Modes of action by which AN may induce tumors in the Zymbal gland, Harderian gland, mammary gland, and tongue have not been investigated. The generic mutagenic modes of action probably apply to these organs also, unless there is information to indicate otherwise.

4.7.3.1. *Hypothesized Mode of Action: Direct Mutagenic Mode-of-Action*

Key Events

This mode of action hypothesizes that AN is first activated by CYP2E1 (mostly in the liver but also at other sites, such as intestinal mucosa or squamous epithelium of the forestomach) to its reactive metabolite, CEO. CEO is then distributed to target organs (e.g., rat brain) where it reacts with DNA, forming DNA adducts. DNA adduct formation results in genetic damage, especially the formation of point mutations. Other types of DNA damage by CEO are also observed in vivo, including DNA strand breaks, SCEs, and MN formation. Mutagenicity is a well-established cause of carcinogenicity.

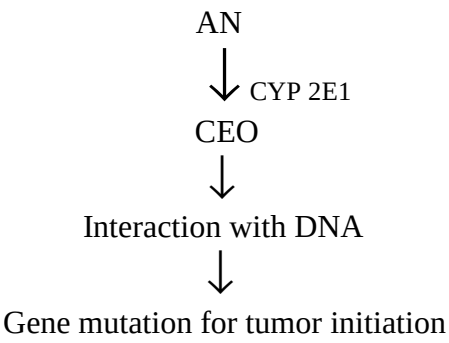

Following these key events, tumor growth may be promoted by any one or combination of a number of cell-signaling pathways, leading to enhanced cell proliferation or inhibition of programmed cell death.

4.7.3.2. *Experimental Support for the Hypothesized Mode of Action*

4.7.3.2.1. *Strength, consistency, specificity of association.* The evidence that supports a mutagenic mode of action is strong and consistent (as summarized in Table 4-53). In addition to positive findings in blood lymphocytes, buccal mucosal cells, and sperm in five epidemiologic studies, DNA alkylation by AN was found in numerous tissues in rats or mice (brain, liver, testes, forestomach, colon, kidney, bladder, and lung) treated with a single dose of AN. AN or its reactive metabolite CEO yielded positive results in in vitro mutation assays using bacteria, fungi, and insects, as well as animal and human cell cultures. The mutagenicity/genotoxicity is *specific* and occurs in the absence of cytotoxicity or other overt toxicity. Although the temporal relationship of adduct formation and mutagenicity with carcinogenicity has not been adequately explored, these effects are seen in short-term assays (before tumor formation). Dose-response concordance is observed between mutagenic doses in vivo and tumorigenic doses in rats and mice. A mutagenic mode of action also comports with notions of biological *plausibility* and *coherence* because AN is metabolized to an epoxide intermediate. Such agents are generally capable of forming DNA adducts, which in turn have the potential to cause genetic damage,

including mutations, and mutagenicity, in its turn, is a well-established cause of carcinogenicity. This chain of key events is consistent with current understanding of the biology of cancer.

The possible association between a direct mutagenic action of CEO, the epoxide metabolite of AN, and brain tumors in rats is supported by the detection of CEO in rat brains after oral administration of 10 mg/kg AN to rats (Kedderis et al., 1993b), reported binding of CEO to brain DNA after oral administration of [2,3-^{14}C]-AN to rats (Farooqui and Ahmed, 1983a), results from studies of in vitro DNA reactivity, positive results from in vitro tests of mutagenicity and cytogenetic effects, and positive results from in vivo studies of DNA damage and repair assays and other genotoxic endpoints in rats and mice. Studies that demonstrate the mutagenicity of AN in occupational exposed workers are also available.

In the following subsections, experimental evidence supporting the mutagenic mode of action of AN using different test systems is summarized.

In vitro DNA binding

AN itself reacts very slowly with DNA in vitro at very high, nonphysiological concentrations (>1 M) (Solomon et al., 1984), but CEO forms different adducts in vitro with DNA (Solomon et al., 1993; Yates et al., 1993) or nucleotides (Yates et al., 1994) more rapidly (see Section 4.5.1.2.1). When calf thymus DNA was incubated with CEO for 3 hours (Solomon et al., 1993), the main adducts formed included N^7-(oxoethyl)guanine, N^3-(2-hydroxy-2-carboxy-ethyl)deoxyuridine, and smaller amounts of adenine and thymine adducts. Yates et al. (1993) also identified the formation of N^3-(2-cyano-2-hydroxylethyl)deoxythymidine when CEO was incubated with calf thymus DNA in vitro.

Mutations in bacteria

In short-term tests with bacteria, AN induced mutations in a majority of test systems, often requiring the presence of exogenous metabolic systems (Table 4-53). AN induced mutation in *S. typhimurium* strains TA 1530, 1535, 1538, 1937, and 1950 with strong response when AN was tested in the vapor phase in the presence of S9. AN induced a weak response for TA 98, 100, and 1978. Thus, AN induced gene reversion mainly by base substitution and induced lower mutagenic activity with strains reversed by frameshift mutation. AN also produced a dose-related increase in the number of revertant colonies compared with untreated bacteria in *E. coli* WP2 (which is DNA repair proficient), WP2uvrA (which lacks excision repair), and WP2 *uvrApolA* (which lacks both excision repair and DNA polymerase 1) without a need for S9 fraction (Venitt et al., 1977).

Mutations in fungi and Drosophila

As shown in Table 4-53, AN induced mitotic gene conversion in *S. cerevisiae* JD1 (Brooks et al., 1985). AN also induced sex chromosome loss in the adult female Drosophila

ZESTE system (Osgood et al., 1991), as well as somatic recombination and mutation in hatching Drosophila with exposure in the larvae stage (Vogel, 1985; Würgler et al., 1985).

Mutations in mammalian cell culture

AN also induced mutations in mammalian cells in vitro. In the mouse lymphoma cell assay, AN induced forward mutations at the $Tk^{+/-}$ locus in most assays (Table 4-53). In human lymphoblastoid *Tk*6 cells devoid of CYP450 activity, AN induced mutations at the *Tk* locus only in the presence of an exogenous S9 metabolic system (Crespi et al., 1985), and CEO was effective at 10-fold lower concentrations than AN (Recio and Skopek, 1988a, b).

Characterization of the Tk^{-} mutants in human lymphoblastoid *Tk*6 cultures by Recio and Skopek (1988b) identified two classes of CEO-induced $Tk^{-/-}$ mutant phenotypes that differed in their growth rates. CEO-induced predominantly Tk_n mutant with normal growth rate and Tk_s with slower growth rate. Southern blot analysis of CEO-induced Tk_n mutants indicated that the majority of these mutants were below the detection limit of <2 kb. Thus, CEO-induced alterations are relatively small DNA alterations. Recio and Skopek (1988a) suggested that CEO induced Tk_n mutants resulted from point mutations or small insertions/deletions that occurred during the replication or repair of CEO-modified DNA. Kodama et al. (1989) conducted cytogenetic analyses of eight CEO-induced Tk_s mutant clones reported in Recio and Skopek (1988a, b). A visible abnormality on chromosome 17 was found in one of the CEO-induced Tk_s mutants and was marked by duplication of the long arm of chromosome 17, with break points at q11 and q21. The latter break point was close to the *Tk* locus, suggesting that the observed aberration might be associated with $Tk^{-/-}$ phenotype.

CEO also induced mutations at the hprt locus in *Tk*6 cells (Recio and Skopek, 1988a). Characterization of the hprt mutations by cDNA sequencing analysis indicated that several hprt mutations were formed. The majority of CEO-induced mutations were the specific loss of exons from the coding region of hprt. Remaining mutants were single base substitutions (point mutation) resulting from amino acid changes (A:T base pairs and G:C base pairs).

Cytogenetic effects in vitro

Additional evidence of mutagenicity included AN-induced cytogenetic changes, such as SCEs or CAs in a majority of assays with CHO or CHL cells (Natarajan et al., 1985; VedBrat and Williams,1982; Ishidate et al., 1981) and human lymphocytes in vitro (Perocco et al., 1982) but not in epithelial-like cells from rat liver (RL4 cell line) (see Table 4-53). AN also induced DNA single-strand breaks in rat hepatocytes (Bradley, 1985) and CHO cells (Douglas et al., 1985). Of note is that AN induced SCEs and DNA single-strand breaks in human bronchial epithelial cells in culture without S9 (Chang et al., 1990), indicating that human bronchial epithelial cells have the metabolic capabilities to activate AN to CEO.

DNA repair in vitro

In DNA repair assays, neither AN nor CEO induced UDS in cultured rat hepatocytes (Butterworth et al., 1992; Probst and Hill, 1985; Williams et al., 1985) (as measured by incorporation of [^{3}H]-thymidine and autoradiographic techniques) or in HeLa cells with or without the presence of S9 (using liquid scintillation spectrometry) (Martin and Campbell, 1985). However, IPCS (1985) concluded that the rat hepatocyte autoradiographic UDS assay was too insensitive for determination of genotoxicity of the eight tested carcinogens, including AN. On the other hand, CEO, but not AN, induced UDS in human mammary epithelial cells in vitro (Butterworth et al., 1992).

DNA repair in vivo

Unscheduled DNA repair activity was detected by following the time course of [^{3}H]-thymidine incorporation into DNA isolated from lung (Ahmed et al., 1992a), testis (Ahmed et al., 1992b), and gastric tissue (Ahmed et al., 1996b; Abdel-Rahman et al., 1994a) after exposure of Sprague-Dawley rats to single oral doses of 46.5 mg/kg AN. In a study by Hogy and Guengerich (1986), UDS was found in the liver of male F344 rats administered 50 mg/kg AN or 6 mg/kg CEO i.p. but was not found in the brain. The absence of detected UDS in the brain could reflect the absence of DNA damage. Alternatively, this absence could reflect differences in the repair rate of CEO-DNA adducts and could account for the observed target organ specificity of AN in rat brain but not liver. Since the difference in DNA repair rates in brain and liver is well known (Kleihues et al., 1977), the second explanation may be more sound. In another study, UDS activity was not detected by autoradiographic techniques following incubation of primary cultures of hepatocytes or spermatocytes from F344 rats given single oral doses of 75 mg/kg or five daily doses of 60 mg/kg-day with [^{3}H]-thymidine (Butterworth et al., 1992). This difference in results from those by Hogy and Guengerich (1986) was probably due to differences in methodology.

DNA binding in vivo

Several studies examining the amounts of radioactivity in DNA fractions of tissues following acute in vivo exposure of rats to radiolabeled AN provide evidence of in vivo DNA reactivity of AN or its metabolites. Maximal amounts of radioactivity covalently bound to hydroxyapatite-purified DNA from the liver, stomach, and brain showed the following order 24 hours after male Sprague-Dawley rats were given single oral doses of 46.5 mg/kg [2,3-^{14}C]-AN: brain (≈120 pmol AN equivalent/mg DNA) > stomach (≈80 pmol/mg) > liver (≈25 pmol/mg) (Farooqui and Ahmed, 1983a). Other studies from the same group of investigators found elevated covalent binding of radioactivity in gastric, testicular, and lung DNA from similarly exposed rats (Abdel-Rahman et al., 1994b; Ahmed et al., 1992a, b). The results from these studies provided some evidence of associations between covalent DNA

binding following acute exposure and sites of tumor development following chronic exposure. The methods to isolate DNA in these studies may not have been stringent enough to exclude covalent binding of radiolabel to proteins (Whysner et al., 1998b; Geiger et al., 1983); however, the degree to which these alternative processes may have contributed to the measured amounts of radioactivity in the DNA fractions is unknown. When 0.6 mg/kg [2,3-^{14}C]-CEO was administered to one F344 rat i.p., covalent binding to both liver and brain protein was found, but no covalent binding to both liver and brain nucleic acids could be detected at the level of 0.3 alkylations per 10^6 base (Hogy and Guengerich, 1986). However, the N^7-(2-oxoethyl) guanine adduct was detected in liver DNA of F344 rats treated with 6 mg/kg CEO or 50 mg/kg AN i.p. in the same experiment. Thus, covalent binding of CEO to DNA had to occur. No DNA binding was detected in the Hogy and Guengerich (1986) study, presumably due to the small DNA sample from one rat, low CEO concentration (0.6 vs. 6 mg/kg CEO), stringent DNA isolation procedure, and overcorrection of protein binding.

DNA adducts in vivo

Limited attempts to detect CEO-DNA adducts in brain tissues following acute in vivo exposure protocols have been largely unsuccessful, but in vitro studies indicate that the formation of other DNA adducts from AN and its metabolites are possible (Yates et al., 1994; Solomon et al., 1993; Hogy and Guengerich, 1986; Solomon et al., 1984). N^7-(2-oxoethyl)-guanine, a CEO-DNA adduct formed in vitro following incubation of calf thymus DNA with CEO, was detected in DNA isolated from the livers of male F344 rats, following single i.p. administration of doses of 50 mg/kg AN or 6 mg/kg CEO, but was found only equivocally at detection limit in DNA isolated from the brains of exposed rats (Hogy and Guengerich, 1986). In another study, 7-(2-cyanoethyl)guanine and O^6-(2-cyanoethyl)deoxyguanosine adducts were not detected in DNA isolated from the liver or brain of male F344 rats given s.c. or i.v. injections of 50 or 100 mg/kg AN (Prokopczyk et al., 1988). The DNA samples were analyzed for the presence of the two adducts using HPLC with fluorescence detection. The detection limits were 20 μmol/mol guanine for 7-(2-cyanoethyl)guanine and 15 μmol/mol guanine for O^6-(2-cyano-ethyl)deoxyguanosine. These detection limits may be not sensitive enough. More importantly, these two DNA adducts were not formed from incubation of CEO with calf thymus DNA in vitro. Hence, the limitations of these studies were that not all the major adducts formed in in vitro incubation of CEO with DNA were measured.

As discussed previously, the main adducts found after 3 hours of incubation of CEO with calf thymus DNA were N^7-(oxoethyl)guanine, N^3-(2-hydroxy-2-carboxyethyl)deoxyuridine (Solomon et al., 1993), and N^3-(2-cyano-2-hydroxylethyl)deoxythymidine (Yates et al., 1993). Yet only N^7-(oxoethyl)guanine has been measured in available studies. Thus, it is highly likely that the actual adducts formed from interaction of CEO with brain DNA have not yet been looked for. It is also likely that the analytical methods used to measure DNA adducts in

available studies were not sensitive enough for their detection. In addition, DNA adducts were measured only in single-dose studies not repeated-dose studies.

DNA damage in rats and mice

Evidence of DNA damage after AN exposure in rats and mice is available. Comet assays showed DNA damage in various tissues in both rats and mice exposed to AN (Sekihashi et al., 2002). Single i.p. injections of 20 mg/kg AN induced DNA damage in forestomach, bladder, and brain but not in colon, liver, kidney, or bone marrow of ddY mice, whereas single doses of 30 mg/kg induced DNA damage in forestomach, colon, kidney, bladder, and lung but not in brain or bone marrow of Wistar rats (Sekihashi et al., 2002).

Increased frequencies of MN in bone marrow were found in Sprague-Dawley rats, following i.v. injection of 98 or 124 mg/kg AN (Wakata et al., 1998) but were not found in Sprague-Dawley rats following administration of oral doses up to 40 mg/kg (Morita et al., 1997) or in male CD-1 mice following administration of oral, i.p., or i.v. doses up to 45 mg/kg (Morita et al., 1997). Increases in CAs in bone marrow cells were not found in Swiss albino mice exposed to oral doses up to 20 mg/kg-day for 4, 15, or 30 days (Rabello-Gay and Ahmed, 1980); in Sprague-Dawley rats given 16 daily doses of 40 mg/kg-day (Rabello-Gay and Ahmed, 1980); in NMRI mice given single i.p. doses of 30 mg/kg (Leonard et al., 1981); or in ICR mice exposed in inhalation chambers to 20 or 100 mg/m^3 for 5 days (Zhurkov et al., 1983). In contrast, Fahmy (1999) reported that increased CAs occurred in spermatocytes of Swiss mice following single oral doses of 15.5 or 31 mg/kg AN or five daily doses of 7.75 mg/kg and in spleen cells and bone marrow cells after a single oral dose of 7.75 mg/kg.

Dominant lethal mutations in rats and mice

Dominant lethal mutations were not increased by treating male NMRI mice with single i.p. doses of 30 mg/kg AN (Leonard et al., 1981) or male F344 rats with five oral doses of 60 mg/kg-day AN (Working et al., 1987), indicating no AN-induced germ cell mutations.

Chromosomal mutations in humans

There is sufficient evidence of AN-induced mutagenicity in occupationally exposed workers. Fan et al. (2006) reported significant increase in the occurrence of MN in buccal mucosal cells of workers exposed to 0.52 or 1.99 mg/m^3 AN for an average duration of 15.7–17.2 years and significant increase in MN in peripheral blood lypmphocytes in workers exposed to 1.99 mg/m^3 AN for an average of 17.2 years. The workers in the Fan et al. (2006) study were exposed to higher concentrations than those in a previous study by Srám et al. (2004), in which the exposure concentration range was 0.05–0.3 mg/m^3 AN, thus explaining the negative results reported in Srám et al. (2004) or in other studies where exposure concentrations were not reported. Evidence of CAs in AN-exposed workers was also reported by Borba et al. (1996), and

DNA strand breakage and sex chromosome aneuploidy in the sperm of AN-exposed workers were reported by Xu et al. (2003). In addition, Beskid et al. (2006) reported an increase in the number of reciprocal translocations and the relative number of insertions in the chromosomes of cultured lymphocytes of AN-exposed male workers.

Therefore, the overall in vitro and in vivo evidence in support of the direct mutagenicity of CEO is strong, consistent, and specific.

4.7.3.2.2. ***Dose-response concordance.*** Chronic exposures of rats to AN in drinking water concentrations ≥30 ppm (≥2.5 mg/kg-day) or air concentrations ≥20 ppm were associated with significantly increased incidences of brain tumors. No published studies are available that have measured CEO-DNA adducts or other endpoints pertinent to mutagenicity in brain tissues following acute-, subchronic-, or chronic-duration oral or inhalation exposures of rats to AN, mainly because in vivo DNA adduct studies were conducted before the Solomon et al. (1993) and Yates et al. (1993) studies that reported on DNA adducts formed from CEO in vitro. Hence, these DNA adduct studies were not looking for the adducts formed in vitro from CEO. The available studies that looked for CEO-DNA adducts in brain or other tissues involved single i.p. (Hogy and Guengerich, 1986), s.c., or i.v. (Prokopczyk et al., 1988) administration protocols at dose levels (50 or 100 mg/kg-day AN) that were higher than the chronic oral doses associated with brain tumors in rats (0.3 to 40 mg/kg-day). However, no repeated-dose studies have been conducted for detection of DNA adducts. The single oral dose of 46.5 mg/kg used in studies that demonstrated UDS in the lung, gastric tissue, and testis of treated Sprague-Dawley rats (Abdel-Rahman et al., 1994b; Ahmed et al., 1992a, b) was comparable to the high dose of 40 mg/kg-day used in studies by Friedman and Beliles (2002), providing evidence that the dose that caused DNA repair was carcinogenic.

A study in mice by Fahmy (1999) showed that increased CAs occurred in spermatocytes of Swiss mice, following single oral doses of 15.5 or 31 mg/kg AN or five daily doses of 7.75 mg/kg, and in spleen cells, and bone marrow cells after a single oral dose of 7.75 mg/kg. Fahmy (1999) also reported increases in SCEs in bone marrow cells of male Swiss mice after a single i.p. dose of 7.5 or 10 mg/kg of AN. These doses were all in the range of, or comparable to, the tumorigenic doses in $B6C3F_1$ mice of 2.5–20 mg/kg-day in a 2-year bioassay.

The single doses employed by Sekihashi et al. (2002) that demonstrated DNA damage in forestomach, colon, kidney, bladder, and lung of rats treated with 30 mg/kg i.p. and in colon, bladder, lung, and brain of male ddY mice treated with 20 mg/kg i.p. were also within the range of tumorigenic doses in the 2-year bioassay.

Therefore, the doses that demonstrated DNA damage or chromosome mutations in single-dose studies are in concordance with tumorigenic doses in chronic bioassays.

4.7.3.2.3. ***Temporal relationships.*** Currently available examinations of DNA damage, chromosome mutations, SCEs, UDS, or CEO-DNA adducts in brain or other tissues are restricted to single-dose acute administration protocols. Studies designed to examine temporal relationships of key events, such as the presence of CEO-DNA adducts in brain tissue, are not available. Nevertheless, results from the rat bioassays indicated that most AN tumors occur after 12–14 months of exposure or longer. Thus, the observed mutagenic effects of AN occurred before tumor formation and provide support for a mutagenic mode of action.

4.7.3.2.4. ***Biological plausibility and coherence.*** The hypothesis that the key primary event in AN induction of brain tumors is the formation of CEO-DNA adducts that lead to mutations that initiate tumor formation is plausible based on in vitro and in vivo evidence for the direct mutagenicity of the AN metabolite, CEO. However the available data do not establish that this is the only mode of action by which AN may induce brain tumors in rats. Notably lacking in the database are studies designed to detect a range of DNA adducts or mutations associated with tumor initiation in brain tissues following prolonged oral or inhalation exposures at levels that induced brain tumors in the chronic rat bioassays. In vitro studies by Solomon et al. (1993) reported that CEO interacted with calf thymus DNA and, in addition to N^7-(oxoethyl)guanine, formed N^3-(2-hydroxy-2-carboxyethyl)deoxyuridine from an initial cytosine adduct. Other adenine and thymine adducts were also formed. Yates et al. (1993) demonstrated that CEO reacted calf thymus DNA formed N^3-(2-cyano-2-hydroxylethyl)-deoxythymidine. Yet, only N^7-(oxoethyl)guanine has been measured in exposed rats in available studies (Hogy, 1986).

The available data do not provide an explanation of why AN induces brain tumors in F344 and Sprague-Dawley rats but not in $B6C3F_1$ mice. Kedderis et al. (1993b) reported that when male F344 rats and male $B6C3F_1$ mice were administered 10 mg/kg AN in water by gavage, higher CEO concentrations were found in blood and brains of rats than in mice (13% higher in blood, 23% higher in brain). Higher CEO concentrations in rat brain may at least partially explain why tumors were only found in the brains of exposed rats but not in mice. In addition, the clearance of CEO in mice was more rapid than in rats (Roberts et al., 1991). It may also be that mice are more efficient in repairing DNA damage since DNA damage has been detected in the brain of ddY mice exposed to 20 mg/kg AN, i.p. (Sekihashi et al., 2002). It has been noted that the $B6C3F_1$ mouse is generally insensitive to chemically induced neurogenesis in NTP carcinogenesis bioassays (Radovsky & Mahler,1999).

The difference in susceptibility to AN induction of brain tumors between mice and rats is similar to that observed for glycidol, an aliphatic epoxide structurally similar to CEO (Irwin et al., 1996). Glycidol is a direct acting alkylating agent, which induces tumors at a variety of sites in both rats and mice. However, although significant induction of gliomas was observed in both sexes of F344 rats after glycidol treatment, no brain tumors were induced in $B6C3F_1$ mice. Ethylene oxide also shows a similar pattern of tumorigenesis, inducing brain tumors in both

sexes of exposed rats (Garmin et al., 1985; 1986), but no brain tumors in exposed mice (NTP, 1987). Thus, induction of brain tumors in rats but not in mice by known genotoxic carcinogenic appears to reflect primarily a species difference in inherent susceptibility to brain tumorigenesis.

There have been no investigations to attempt to explain the apparent susceptibility of early-life plus chronic adult exposures compared with adult-only exposures. It is possible that mutations are established more effectively in rapidly dividing tissues such as the fetal brain, since the higher rate of cell division increases the number of cells in S phase (Slikker et al., 2004), which tends to make the cell population more vulnerable to the genotoxic effects of chemicals. It is also possible that the lack of key DNA repair mechanisms in embryonic tissues may be involved. However, DNA repair was not found in adult rat brain after administration of 6 mg/kg CEO i.p. (Hogy and Guengerich, 1986). It would appear that the rapid cell division in earlier stages of development is a determining factor for the greater mutagenic and subsequent carcinogenic sensitivity of perinatal life (Slikker et al., 2004).

Data for another chemical, ethylene oxide, that causes brain tumors (gliomas) in rats show a different accumulation pattern for N^7-(2-oxoethyl)guanine adducts than that observed following i.p. administration of AN or CEO. In rats exposed to 500 ppm ethylene oxide for 1 day, higher levels of N^7-(2-oxoethyl)guanine adducts were detected in DNA from brain than in DNA from liver (Walker et al., 1990), whereas N^7-(2-oxoethyl)guanine adducts were detected in brain at detection limit and only at low levels in the liver of rats given single i.p. injections of 50 mg/kg AN or 6 mg/kg CEO (Hogy and Guengerich, 1986). Whysner et al. (1998b) suggested that these and other results indicated that glioma formation from chronic exposure to AN may not involve the formation of N^7-(2-oxoethyl)guanine adducts; however, several alternative explanations are possible. The lack of unequivocal detection of CEO-DNA adducts in rat brain may indicate that the detection limits of the methods used were not sensitive enough. More sensitive methods of detection, such as liquid chromatography-mass spectrometry (Poirier, 2004), have not been used in AN-induced DNA adduct studies. Alternatively, the stringent methods used to isolate purified DNA (without associated proteins) in the experiments by Hogy and Guengerich (1986) may have caused the loss of adducts or inhibited the recovery of adducted DNA (Meek et al., 2003). Another possibility is that N^7-(2-oxoethyl)guanine adduct may not be involved in mutations leading to AN-induced brain tumors, and other, as yet uninvestigated, DNA adducts that were reported by Solomon et al. (1993) and Yates et al. (1993) may be involved. Still another possibility is that CEO-DNA adducts and resultant mutations in target tissues may occur only after prolonged exposure to AN. Notably absent from the available mode-of-action database are experiments designed to detect a range of possible DNA adducts in target tissues following repeated oral or inhalation exposure at exposure levels producing tumors in the chronic bioassays.

Guengerich et al. (1986) discussed the findings in which AN was metabolized by liver microsomes but not brain microsomes to form CEO. N^7-(2-oxoethyl)guanine DNA adducts were

detected in liver but not the brain, yet AN induced tumors in the rat brain with chronic exposure but not in the adult rat liver. In addition, AN-induced UDS was demonstrated in rat liver but not brain (Hogy and Guengerich, 1986). Guengerich et al. (1986) proposed that AN was metabolized in the liver to CEO. Since CEO formed by liver microsomes from AN has a half-life of about 2 hours in neutral buffer, it can be transported easily via blood from liver to the brain. Although DNA adducts have not yet been detected unequivocally in rat brains, CEO has been measured in rat brains (Kedderis et al., 1993b) and shown to bind to brain DNA (Farooqui and Ahmed, 1983b). Liver cells are efficient in repairing DNA damage via UDS, while brain cells do not have this capability. This could help to explain why the rat brain is a target tissue of AN carcinogenicity but the adult rat liver is not. It should be noted that hepatomas were found in rats that were exposed to AN during gestation and extending through adulthood (Maltoni et al., 1988). It is conceivable that the rat fetal and neonatal liver do not have sufficient capability to repair DNA damage.

Meek et al. (2003) noted that there are several aspects of the development of AN-induced tumors that are characteristic of tumors induced by compounds or metabolites that directly interact with DNA. These comparisons add support to the evidence of a direct mutagenic mode of carcinogenic action.

- *Tumors are systemic and occur at multiple sites.* Exposure-related increased incidences were found for forestomach tumors, CNS tumors, and Zymbal gland tumors in chronic oral exposure bioassays with F344 rats and Sprague-Dawley rats (which also showed exposure-related increased incidence of tongue tumors); for forestomach and Harderian gland tumors in a chronic oral exposure bioassay with $B6C3F_1$ mice; for brain tumors, Zymbal gland tumors, intestinal tumors, and tongue tumors in a chronic inhalation exposure bioassay with Sprague-Dawley rats; and for brain tumors, Zymbal gland tumors, hepatomas, and extrahepatic angiosarcomas in a chronic inhalation bioassay with Sprague-Dawley rats exposed during gestation and extending throughout adulthood. Particularly noteworthy is that Zymbal gland tumors in rats commonly occur with carcinogens that are also mutagens. Of the 27 chemicals associated with site-specific tumor induction in this gland found in NTP database, 23 were mutagenic in the Salmonella assay. The NTP database indicated that these chemicals were multisite carcinogens.
- *Tumors sometimes occur at nontoxic doses or concentrations.* Elevated incidences for CNS tumors occurred in Sprague-Dawley (Quast, 2002; Quast et al., 1980a) and F344 (Johannsen and Levinskas, 2002b; Biodynamics, 1980c) rats chronically exposed to drinking water concentrations (30 or 35 ppm) that did not induce elevated incidences of nonneoplastic CNS lesions in interim sacrifices at 6, 12, or 18 months.
- *Tumors sometimes occur after less-than-lifetime exposure durations.* In an inhalation study by Maltoni et al. (1977), Sprague-Dawley rats were exposed to 0–40 ppm AN via

inhalation for 52 weeks. The animals were then allowed to complete their natural life spans, with the final deaths occurring in week 136 (Maltoni et al., 1977). Gliomas were developed in 20 and 40 ppm males at 84 and 63.5 weeks, respectively, and not in other dose groups. In addition, forestomach papillomas and acanthomas (latency 103–124 weeks) and Zymbal gland carcinomas (latency 77–102 weeks) were developed in exposed rats. Thus, these tumors were developed long after exposure was terminated, indicating the carcinogenic effect from AN exposure was not reversible. Although the incidence of these tumors did not reach statistical significance, development of these tumors does not support the hypothesis that AN-induced tumors are due to the promoting action of AN alone.

- *Tumors developed as early as 7–12 months following AN exposure.* In the Sprague-Dawley chronic drinking water bioassay, the number of high-dose (300 ppm) female rats dying or sacrificed with CNS tumors were 1/1 during months 0–6, 5/13 during months 7–12, 14/23 during months 13–18, and 11/11 during months 19–24 (Quast, 2002). At the lower exposure levels in this study (35 and 100 ppm), nearly all of the tumors in female rats were detected after 13 months of exposure. In all groups of exposed Sprague-Dawley male rats, all but one tumor were detected after 13 months of exposure (Quast, 2002). In the F344 chronic drinking water bioassay, the time of first detection of a rat with a brain tumor was 481 days for male rats and 495 days for female rats, approximately 16 months (Johannsen and Levinskas, 2002b; Biodynamics, 1980c). In the three-generation reproductive toxicity study involving 46 weeks of exposure to AN in drinking water, brain tumors were detected in 0/19, 1/20, and 2/24 F0 breeding females exposed to 0, 100, or 500 ppm, respectively. In the other generations, incidences of brain tumors were 0/20, 1/19, and 4/17 for the F1 breeding females and 0/20, 1/20, and 1/20 for the F2 breeding females (Friedman and Beliles, 2002). Statistically significantly elevated incidences of brain tumors occurred in Sprague-Dawley rats exposed by inhalation to 60 ppm AN during gestation and extending chronically throughout adulthood, but rats exposed during gestation followed by a subchronicsubchronic-duration exposure during adulthood showed an elevated incidence of brain tumors that was not statistically significant when compared only with control (Maltoni et al., 1988). The weight of the available evidence indicates that most AN-induced brain tumors require at least a half-lifetime duration of exposure to develop, but associations with shorter durations of exposure have been observed, specifically in female Sprague-Dawley rats exposed to 300 ppm in drinking water.
- *The ratio of benign to malignant tumors is small.* The brain tumors noted in AN-exposed Sprague-Dawley or F344 rats were astrocytomas, which were malignant tumors. Most of the Zymbal gland tumors were also malignant tumors.

4.7.3.2.5. ***Human relevance.*** The metabolic scheme of AN in rats and humans is similar. Humans are known to be able to activate AN to its reactive metabolite, CEO. As discussed in Section 4.5.2.1, studies that demonstrate the mutagenicity of AN in humans are available. There is sufficient evidence for mutagenicity of AN in exposed humans, and the direct mutagenic mode of action of AN-induced carcinogenicity is considered to be relevant to humans.

4.7.3.3. ***Other Possible Modes of Action***

Other modes of action may contribute, along with the direct mutagenic mode of action, to tumorigenesis. These additional modes of action are evaluated in the following subsections. The results of these evaluations indicate that these modes of action are not likely to be prinicipal modes of action or to contribute to the carcinogenicity in a significant manner.

4.7.3.3.1. ***Oxidative stress***

Key events

This mode of action hypothesizes that ROS are generated either directly from the oxidant or are indirectly produced via activation of endogenous sources when the oxidant or its metabolite is distributed to the target organ. Oxidative stress is induced. These free radical ROS can interact with DNA and produce DNA damage leading to gene mutation for tumor initiation. ROS can also interact with lipids via lipid peroxidation, resulting in cell damage.

One of the most prevalent biomarkers of oxidative DNA damage is 8-oxodG. This DNA lesion has been found to produce mutations involving GC→TA transversions due to base mispairing and AT→CG transversions due to misincorporation during DNA synthesis (Cheng et al., 1992). G-C base pairs provide a common target for activating point mutations (e.g., in both *p53* and retinoblastoma tumor suppressor genes and in the *ras* family of oncogenes). Thus, G-C base pairs in both tumor suppressor genes and oncogenes may represent a vulnerable target for mutation by oxidative stress (Guyton and Kensler, 1993). The induction of base changes in the DNA sequence of these genes may be the basis for tumor initiation by the oxidant.

Another role that oxidants may play in carcinogenesis is tumor promotion. ROS generating systems are known to possess some of the biochemical actions of tumor promoters, such as promoting a rapid and sustained decrease in antioxidant defenses, including SOD, catalase, and glutathione peroxidase activities (O'Connell et al., 1986; Slaga et al., 1981). Tumor growth may also be promoted by oxidative stress via modification of gene expression through induction of gene transcription factors (e.g., NF_KB or transcription factor protein [AP-1]) or change in DNA methylation status by ROS. Signal transduction pathways, including AP-1 and NF_KB, are known to be activated by ROS, and they lead to the transcription of genes involved in cell growth regulatory pathway. Oxidative DNA damage can also result in DNA hypomethylation by interfering with the ability of methyltransferases to interact with DNA, allowing the expression of normally quiescent genes and promoting tumor growth. ROS can

also induce the release of calcium from intracellular stores, resulting in the activation of kinases, including PKC (Larsson and Cerrutti, 1989), which is known to regulate many intracellular processes, including those related to growth and differentiation. Hence, any one or a combination of these events may lead to enhanced cell proliferation or inhibition of programmed cell death.

The plausibility of an indirect mutagenicity mode of action for AN-induced tumors is evaluated in the following discussion.

Strength, consistency, specificity of association

Experimental data for indirect mutagenicity of AN are discussed in Section 4.5.2.5 and summarized in Table 4-55. These studies are only briefly discussed here.

In vitro studies

There is some in vitro experimental evidence that supports an indirect mutagenic mode of action for AN. When SHE cells were treated in vitro with 0–75 μg/mL AN in 12.5 μg/mL increments, there was a dose-dependent increase in morphological transformation at 50, 62.5, and 75 μg/mL after 7 days of exposure (Zhang et al., 2000). Levels of 8-oxodG isolated from cells incubated with 75 μg/mL AN were increased to 192 and 186% of control after 2 and 3 days. However, no increase in 8-oxodG was observed after 1 or 7 days.

AN-induced oxidative stress in SHE cells was confirmed in a later study by Zhang et al. (2002). AN at 25, 50, or 75 μg/mL increased the amount of ROS in SHE cells after 4, 24, and 48 hours of treatment and increased xanthine oxidase activity 24 and 48 hours after treatment with 75 μg/mL AN. AN also caused temporal changes in GSH levels and antioxidant enzyme catalase and SOD activities. The involvement of CYP450 metabolism of AN in the production of oxidative stress was indicated by the observation that inclusion of a nonspecific suicidal inhibitor of CYP450 enzyme, ABT (0.5 mM), in the medium resulted in a significant reduction (about 77%) in the cell transformation activity of 75 μg/mL AN (Zhang et al., 2002).

In another study, when cultured rat astrocytes were exposed for 4 or 24 hours to 0.01, 0.1, or 1 mM AN, up to a 3.9-fold increase in 8-oxodG was found in cellular DNA of the rat astrocytes (Kamendulis et al., 1999a). No increase in 8-oxodG was found in rat hepatocytes exposed to 0.01, 0.1, or 1 mM AN for 4 or 24 hours (Kamendulis et al., 1999a). Pu et al. (2006) also reported a 3-fold increase in oxidative DNA damage (as measured by the fpg-modified comet assay) in cultured D1TNC1 rat astrocytes treated with 1 mM AN for 24 hours. When NHAs were treated with 200–400 μM AN for 12 hours, a four- to sevenfold increase in the generation of ROS and a greater than twofold increase in 8-oxodG were observed (Jacob and Ahmed, 2003b).

In vivo studies

Three studies on rats are available that investigated oxidative DNA damage in the brain after exposure to AN in drinking water (Jiang et al., 1998; Whysner et al., 1998a). A two- to threefold increase in 8-oxodG levels was found in cellular DNA from brain cortex of Sprague-Dawley rats exposed to 50, 100, or 200 ppm AN in drinking water for 28 or 90 days (Jiang et al., 1998). Levels of 8-oxodG in DNA increased with increasing exposure levels in this study. At 90 days, levels of 8-oxodG were more than twofold higher in DNA from 50 ppm rat brain cortex compared with controls (Jiang et al., 1998). In addition, no increased levels of 8-oxodG were found in the liver DNA of exposed rats at all dose levels following 14, 28, or 90 days of exposure (Jiang et al., 1998). The liver is not a target organ for AN-induced carcinogenicity in adult rats. In a follow-up study, Pu et al. (2009) reported an increase in 8-oxodG levels in brain DNA of male Sprague-Dawley rats exposed to 100 or 200 ppm AN in drinking water for 28 days. However, EPA has identified issues with Pu et al. (2009) (see Section 4.5.1.2.1); therefore, this study was not discussed separately here.

In another study, levels of 8-oxodG in brain nuclear DNA were increased by about twofold in Sprague-Dawley rats exposed to 30 or 300 ppm AN in drinking water for 21 days and by about 1.5-fold in rats exposed to 100 ppm AN for 94 days (Whysner et al., 1998a). However, no significant increase in 8-oxodG levels was found in F344 rats exposed to 10, 30, or 100 ppm for 21 days (Whysner et al., 1998a). (A statistically insignificant increase of about 30% was found in the 3–100 ppm AN dose groups.) Levels of 8-oxodG in liver DNA were increased by about 1.4-fold in Sprague-Dawley rats exposed to 30 or 300 ppm for 21 days and by about 1.3- and 2-fold following exposure to 100 ppm for 10 and 94 days, respectively (Whysner et al., 1998a). Levels of 8-oxodG in liver DNA were not measured in F344 rats in this study. No significant increase in 8-oxodG levels in DNA of forestomach (a target organ of AN carcinogenicity) were found in Sprague-Dawley rats exposed to 3–300 ppm AN (see Table 4-54).

Several inconsistencies can be found in the results of Jiang et al. (1998) and Whysner et al. (1998a). While a dose-related increase in 8-oxodG levels in brain cortex DNA of Sprague-Dawley rats exposed up to 200 ppm AN was reported by Jiang et al. (1998), a twofold increase in 8-oxodG levels in brain DNA was found for Sprague-Dawley rats exposed to either 30 or 300 ppm in the study by Whysner et al. (1998a). Thus, there was no increase in 8-oxodG level with a 10-fold increase in exposure concentration in Sprague-Dawley rats (Whysner et al., 1998a). While 8-oxodG levels were measured via different sample preparation methods in these two studies (i.e., 8-oxodG level was measured in nuclear DNA in whole brain in Whysner et al. [1998a] and in cellular DNA from brain cortex in Jiang et al. [1998]), 8-oxodG level measured in Sprague-Dawley rats exposed to 3 or 30 ppm AN for 21 days in Whysner et al. (1998a) was comparable to that measured in Sprague-Dawley rats exposed to 5 or 50 ppm AN for 28 days in Jiang et al. (1998) ($0.86/10^5$ and $1.35/10^5$ dG vs. $1.8/10^5$ and $2.5/10^5$ dG). Thus, inconsistencies

in the two studies regarding 8-oxodG levels in rat brain are not likely due to differences in sample preparation.

Inconsistencies were also found in 8-oxodG levels in livers in the two rat studies. Jiang et al. (1998) reported no increase in 8-oxodG levels in liver DNA of exposed rats, but Whysner et al. (1998a) reported a 1.4-fold increase in 8-oxodG levels in liver DNA of Sprague-Dawley rats exposed to 30 or 300 ppm for 21 days and a 1.3- and twofold increase following exposure to 100 ppm AN for 10 and 94 days, respectively. Moreover, the increase in 8-oxodG levels in brain DNA was not much higher than that in liver DNA (see Table 4-55). The rat brain is a target organ for AN-induced carcinogenicity but not adult rat liver. In addition no significant increase in 8-oxodG levels in forestomach DNA was found. Thus, no specificity is indicated regarding increased 8-oxodG levels (oxidative DNA damage) in target organ DNA and tumor formation.

Inconsistencies were also found regarding AN-induced disruption of antioxidant defense. While Jiang et al. (1998) reported increases in ROS and concomitant persistent decreases in antioxidant enzyme catalase activity in the brain cortex of Sprague-Dawley rats exposed to 50–200 ppm AN in drinking water after 14, 28, and 90 days, as well as decrease in SOD activity and GSH level in all dose groups after 14 days of treatment, Whysner et al. (1998a) reported no changes in catalase and glutathione peroxidase activities and GSH levels in the brains of Sprague-Dawley rats treated with 3, 30, or 300 ppm AN in drinking water for 21 days. Whysner et al. (1998a) did report a dose-related increase in cysteine levels in the brains of Sprague-Dawley rats exposed to AN for 21 days, and the increase was significant for the 300 ppm dose groups. However, no changes in GSH and cysteine levels were found in the brains of F344 rats exposed to 0, 1, 3, 10, 30, or 300 ppm AN in the drinking water for 21 days (Whysner et al., 1998a). Since F344 rats exposed to these dose levels of AN also developed brain tumors in chronic bioassay, the formation of these tumors cannot be explained by oxidative stress resulting from disruption of antioxidant defense. Whysner et al. (1998a) also found no changes in cytochrome oxidase activities in the brain mitochondria of both exposed Sprague-Dawley rats and F344 rats. Cyanide, a metabolite of AN, is a noncompetitive inhibitor of cytochrome oxidase. No change in cytochrome oxidase activity indicated that no metabolic hypoxia occurred in brain mitochondria as a result of inhibition of the enzyme by cyanide. Therefore, cyanide-induced metabolic hypoxia did not appear to be involved in the mechanism of ROS generation by AN.

Moreover, Whysner et al. (1998a) reported no changes in TBARS in the brains of all groups of AN-exposed Sprague-Dawley rats, indicating the absence of lipid peroxidation, another biomarker of oxidative stress and oxidative lipid damage. Jiang et al. (1998) reported significant increase in MDA only in the brain cortex of rats exposed to 200 ppm AN for 14 days and not in other dose groups at 14 days. No increase was found in all dose groups at 28 and 90 days. Since lipid peroxidation is another biomarker of oxidative stress, there is no strong evidence for occurrence of significant oxidative stress in the brain of AN-exposed rats.

In addition, Chantara et al. (2006) demonstrated that AN induced ERK activation via PKC in SK-N-SH neuroblastoma cells. However, oxidative stress was found not to be involved in AN-induced ERK1/2 activation, which played a crucial role in cell proliferation and tumor progression. Thus, the potential tumor promotion effect of AN has not been related to oxidative stress.

Dose-response concordance

Levels of 8-oxodG in DNA from brain cortex of Sprague-Dawley rats (Jiang et al., 1998) or rat astrocytes (Kamendulis et al., 1999a) increased with increasing in vivo (50, 100, 200 ppm) or in vitro (0.01, 0.1, 1.0 mM) exposure levels. However, 8-oxodG in DNA from brain of F344 rats exposed to 1–100 ppm AN were not significantly increased. In addition, 8-oxodG levels in DNA from brain of F344 rats did not show a dose-response relationship (see Table 4-54), and no correlation can be found between 8-oxodG levels in brain DNA of these rats and brain tumor incidence of F344 rats exposed to the same concentration of AN in drinking water for 2 years (Table 4-58). Thus, experimental data do not support the hypothesis that brain tumors from F344 rats are the result of oxidative DNA damage.

Table 4-58. 8-OxodG in brain DNA and brain tumor incidence in male F344 rats exposed to AN in drinking water

Dose group (ppm)	8-oxodG (mol/10^5 mol dG)[a]	Incidence of brain astrocytomas[b]
0	0.79 ± 0.37	2/160
1	0.84 ± 0.25	2/80
3	1.07 ± 0.41	1/78
10	1.04 ± 0.30	2/80
30	1.03 ± 0.38	10/79
100	1.06 ± 0.48	21/76

[a]Data are from 21-d drinking water study by Whysner et al. (1998a).
[b]Data are from 2-yr drinking water study by Biodynamics (1980b) and Johannsen and Levinskas (2002b). The denominators for incidence of brain astrocytomas excluded rats from the 6- and 12-mo interim sacrifices and rats that died before the appearance of the first tumor for this site.

Moreover, although Whysner et al. (1998a) demonstrated a significant increase in levels of 8-oxodG in brain DNA of Sprague-Dawley rats exposed to AN for 21 days, no correlation can be found between 8-oxodG levels in brain and tumor incidence in the 2-year bioassay (Table 4-59). Therefore, dose-response data on Sprague-Dawley rats from Whysner et al. (1998a) did not support oxidative DNA damage as the mode of action for AN-induced brain tumor formation.

Table 4-59. 8-OxodG in brain DNA and brain tumor incidence in male Sprague-Dawley rats exposed to AN in drinking water

Dose group (ppm)	8-oxodG (mol/10^5 mol dG)[a]	Incidence of brain astrocytomas[b]
0	0.62 ± 0.08	1/80
1	0.86 ± 0.41	ND
3	1.35 ± 0.49	ND
10	ND	8/47
30	ND	19/48
100	1.29 ± 0.10	23/48

[a]Data are from 21-d drinking water study by Whysner et al. (1998a).
[b]Data are from 2-yr drinking water study by Quast (2002).

ND = cannot be determined

Temporal relationships

The detection of increased 8-oxodG levels in brains of Sprague-Dawley rats exposed for subchronic durations (Jiang et al., 1998; Whysner et al., 1998a) is temporally consistent with oxidative DNA damage being a plausible key precursor event in the development of later-appearing tumors. However, no significant increase in 8-oxodG levels in the brain of exposed F344 rats was found.

Biological plausibility and coherence

The demonstration of AN-induced oxidative DNA damage in rat brain cortexes following subchronic-duration exposure to AN at dose levels producing brain tumors with chronic exposure would have provided support for the involvement of an indirect mutagenic mode of action in AN carcinogenicity. However, no increase in oxidative DNA damage was found in F344 rats exposed to AN in drinking water. Brain tumors were found in F344 rats at similar frequencies as Sprague-Dawley rats in chronic bioassays. Thus, brain tumors in F344 rats cannot be explained by oxidative DNA damage, and the predicted greater sensitivity of Sprague-Dawley rats vs. F344 rats based on 8-oxodG levels measured in short-term studies is not reflected in cancer bioassays. In addition, the presence of increased oxidative DNA damage in the livers of Sprague-Dawley rats exposed to AN in drinking water in one study (Whysner et al., 1998a) but not in another (Jiang et al., 1998) also raised the question regarding a significant association between oxidative DNA damage and tumor formation.

The origin of oxidative stress is unclear. Proposed molecular mechanisms that may be involved in AN induction of oxidative stress in the brain (or other toxicity targets) include direct generation of free radicals by AN (or its metabolites), stimulation by AN or its metabolites of systems that generate free radicals, binding of AN to free radical scavengers (e.g., GSH, vitamins C or E) and depletion of stores of these antioxidants, inhibition of the expression or activities of

antioxidant enzymes, and interference of mitochondrial respiratory electron flow via cyanide inhibition of cytochrome c oxidase (Zhang et al., 2002; Jiang et al., 1998). As discussed previously, some of these potential mechanisms have been ruled out.

As with the direct mutagenic mode of action, there are no data currently available to indicate how or if this indirect mutagenic mode of action may explain the occurrence of brain tumors in rats but not in mice, following chronic exposure to AN.

Human relevance

Humans possess the biochemical pathways for the key steps of this proposed mode of action. This hypothetical mode of action, if it occurs, is considered to be relevant to humans.

Conclusion

While plausible, this postulated mode of action is not supported by in vivo studies in rats. Studies on oxidative DNA damage or oxidative lipid damage in the brain of exposed rats do not provide sufficient evidence to support this mode of action. In addition, Chantara et al. (2006) demonstrated AN-induced ERK activation via PKC in SK-N-SH neuroblastoma cells. Oxidative stress was found to be not involved in AN-induced ERK1/2 activation, which played a crucial role in cell proliferation and tumor progression. Therefore, while this mode of action may play a role, it is not likely to be the principal mode of action for AN-induced carcinogenicity.

4.7.3.3.2. *Other modes of action for brain tumors*

Key events

Other hypothesized modes involve actions by AN or its metabolites to directly or indirectly alter the expression of genes (either at the level of translation, post-translation, or protein activity), leading to the loss of control of cell growth and the ultimate promotion of initiated cells into brain tumors. Possible modes of AN carcinogenic action include stimulation of cell proliferation (mitogenic), cytotoxicity with subsequent reparative cell proliferation (cytotoxic), inhibition of programmed cell death (anti-apoptotic), and inhibition of GJIC.

Studies specifically designed to examine these possible modes of action are restricted to a study of GJIC in rat astrocytes (Kamendulis et al., 1999b).

Strength, consistency, and specificity of association

No studies are available that examine cellular proliferation indices in brain cells following in vivo exposure to tumor-producing doses of AN. In in vitro studies with rat astrocytes, indices of cytolethality after 24 hours of exposure occurred at higher AN concentrations (2.5, 5.0, and 10.0 mM) than increased 8oxodG levels in DNA (0.01, 0.1, and 1.0 mM) (Kamendulis et al., 1999a). The available data do not support a prominent role for cytotoxic or mitogenic modes of action in AN-induced rat brain tumors.

Inhibition of GJIC has been shown to correlate with tumor promotion activity (i.e., the loss of control of growth) and to be induced by various chemical agents thought to operate via other modes of carcinogenic action, such as phorbol esters and PB (Kamendulis et al., 1999b). Exposure of rat astrocytes to 0.01, 0.1, or 1 mM AN for 4–48 hours statistically significantly inhibited GJIC compared with controls (Kamendulis et al., 1999b). The inhibition was reversible and prevented by the presence of an antioxidant, α-tocopherol, or a precursor for the synthesis of glutathione, OTC, in the culture medium. The results are consistent with the involvement of AN-induced oxidative stress in the inhibition of GJIC. The inhibitory concentrations were the same as those that produced oxidative DNA damage in a companion experiment (Kamendulis et al., 1999a). The specificity of the inhibitory response to rat astrocytes was demonstrated by the lack of inhibition of GJIC in rat hepatocytes exposed to 0.01, 0.1, or 1.0 mM AN (Kamendulis et al., 1999b).

Dose-response concordance

The inhibition of GJIC in rat astrocytes increased with increasing sublethal concentrations in the range of 0.01–1 mM (Kamendulis et al., 1999b). A concordance of these concentrations to dose levels associated with brain tumors is not available.

Temporal relationships

The acute nature of the observed inhibition of GJIC is consistent with the hypothesis that this action may be one of a number of precursor events involved in tumor promotion.

Biological plausibility and coherence

Other potential modes of action for AN-induced brain tumors have not been adequately studied. The involvement of inhibition of GJIC by oxidative stress induced by AN or its metabolites is plausible, based on the limited evidence with rat astrocytes (Kamendulis et al., 1999b). However, the available histopathology data from interim sacrifices of the chronic rat bioassays do not support the involvement of a mode of action involving brain cell cytotoxicity followed by reparative cell proliferation.

4.7.3.3.3. ***Conclusions about modes of action for brain tumors.*** Data gaps still exist in the current understanding of the mode of action for carcinogenicity of AN. However, there is sufficient experimental evidence to support direct mutagenicity as the principal mode of action. Key events are the generation of direct DNA damage by the AN metabolite, CEO, and interaction with DNA. There is in vitro and in vivo evidence to support the occurrence of key events in the brain following AN exposure. Other modes of action may contribute, along with direct mutagenesis, to tumorigenesis. For example, AN-induced ERK activation via PKC may play a role in cell proliferation and tumor progression. However, limited experimental evidence does

not support them as alternatives. Available data are inadequate to establish an oxidative stress mode of action for AN-induced carcinogenicity.

The available data do not provide an explanation for AN induction of brain tumors in F344 and Sprague-Dawley rats but not in $B6C3F_1$ mice. However, it should be noted that generally mice are much less susceptible than rats in developing brain tumors resulting from exposure to chemical carcinogens (Rice and Wilbourn, 2000; Radovsky and Mahler, 1999). Hence, this species difference in response is not limited to AN alone. In addition, there have been no investigations to attempt to explain the apparent susceptibility of early-life plus chronic adult exposures compared with adult-only exposures. It is possible that a higher rate of cell division in the fetal brain and the resultant greater sensitivity to direct mutagenic damage may be involved (Slikker et al., 2004). Possible differences between early-life and adult stages of rat development in pertinent physiologic processes, such as distribution of AN or its metabolites to the brain, levels of antioxidants, activities of antioxidant enzymes, or repair of DNA damage, have not been investigated to explain this apparent susceptibility of early-life stages to AN carcinogenicity.

Possible differences between rats and humans in distribution of AN or its metabolites to the brain, susceptibility to oxidative stress, or repair of DNA damage have not been investigated. Identified differences between rats and humans in AN disposition are restricted to the finding of higher rates of metabolic oxidation of AN in human vs. rat hepatic microsomes, presumably due to a more active EH in humans (Kedderis and Batra, 1993; Kedderis et al., 1993c). The relevance of this apparent difference in AN metabolism to possible species differences in susceptibility to AN carcinogenicity in the brain is not understood. Within the framework of the hypothesized direct mutagenic mode of action, the balance between the formation of CEO by CYP2E1 and its hydrolysis by EH is thought to be important in determining the levels of CEO that might be available to bind DNA or GSH. Experimental comparison of this balance in human and rat brain tissues is not available.

4.7.3.4. *Possible Modes of Action for Forestomach Tumors*

There is evidence to suggest that, once delivered to forestomach epithelial cells, AN or its metabolites shift the normal balance between cell proliferation and apoptosis, leading to hyperplasia and eventually, with continued exposure and sustained net cellular proliferation, to tumor formation. Sustained increased cellular proliferation is viewed as the key precursor event in this hypothesized mode of carcinogenic action. Exposure of male F344 rats to gavage doses of about 12 and 23 mg/kg-day AN for 6 weeks produced minimal to mild hyperplasia and hyperkeratinization of the squamous mucosa of the forestomach but not the epithelium of the glandular stomach or the liver (Ghanayem et al., 1997). The early induction of hyperplasia by AN doses that resulted in forestomach tumors in chronic rat bioassays is temporally consistent with the involvement of sustained cell proliferation in the development of these tumors. A dose-

related increase in cell proliferation (as determined by BrdU incorporation into DNA) was observed in the forestomach epithelium, but no increases were found in the glandular stomach or the liver, which are not targets of AN toxicity or carcinogenicity from chronic exposure to AN during adulthood. At the high-dose level, an increase in apoptotic cells was found. These results suggest that AN stimulation of cellular proliferation overcame the apparent stimulation of apoptosis at the higher dose, since hyperplasia was observed. Whether or not the stimulation of cellular proliferation was due to a reparative response to cytotoxicity or to a direct mitogenic action is uncertain. Acute administration of a higher dose of AN (50 mg/kg) caused gastric mucosal necrosis in rats, which was shown to involve CYP-mediated metabolism of AN (Ghanayem et al., 1985; Ghanayem and Ahmed, 1983). Whether or not these findings relate to the stimulation of cellular proliferation and development of hyperplasia at the lower doses is uncertain.

Possible direct or indirect mutagenic modes of action for forestomach tumors, such as those investigated for brain tumors, have not been investigated. However, DNA damage, as detected by the comet assay, was reported in the stomach of rats and mice exposed by i.p. injection (Sekihashi et al., 2002). No significant oxidative DNA damage (levels of 8-oxodG) was measured in the forestomach of rats exposed to 3, 30, or 300 ppm in drinking water for 21 days (Whysner et al., 1998a). In addition, AN was reported to bind to DNA in the stomach of rats following a single oral dose of 46.5 mg/kg (Farooqui and Ahmed, 1983a). Given that a mutagenic MOA is hypothesized for AN induced brain tumors in rats, that mutagenic carcinogens usually cause tumors in multiple sites, and evidence of DNA damage in the forestomach of AN treated rats, direct mutagenicity is a likely mode of action for AN-induced forestomach tumors.

4.7.3.5. *Possible Modes of Action for Hepatomas*

Although adult female Sprague-Dawley rats exposed to 60 ppm AN by inhalation during adulthood did not develop hepatomas, these tumors were found in 5/67 male offspring and 1/54 female offspring exposed during gestation and extending throughout adulthood (Maltoni et al., 1988). In unexposed offspring in this study, hepatomas were found in 1/158 males and 0/149 females. This apparent susceptibility of early-life stages to the initiation of liver tumors may be suggestive of a direct mutagenic mode of action in which embryonic DNA repair mechanisms are inadequate to repair AN-induced DNA damage during this stage of development when cells are rapidly dividing. N^7-(2-oxoethyl)guanine-DNA adducts have been measured in the livers of adult rats following i.p. exposure to AN (Hogy and Guengerich, 1986). Increased levels of 8-oxodG have also been measured in DNA from the livers of adult Sprague-Dawley rats exposed to AN in drinking water for 21 or 94 days (Whysner et al., 1998a). Thus, indirect mutagenic mode of action may also contribute. However, possible modes of action for the

development or initiation of liver tumors during early stages of development have not been investigated.

4.7.3.6. *Possible Modes of Action for Tumors of Intestines, Tongue, Zymbal Gland, and Harderian Gland*

Based on analogy to other direct-acting mutagens that cause tumors at multiple sites in animal bioassays, it is possible that a direct mutagenic mode of action may be involved in the formation of AN-induced tumors at these sites in rats and mice. Although possible modes of carcinogenic actions of AN at these sites have not been investigated, direct mutagenic mode of action is the most likely mode of action. CYP2E1 enzymes occur in intestinal mucosa, and CEO can form in intestine and bind to DNA. In addition, there is no evidence that AN would have a tissue specificity that would lead to mutagenesis in brain but not other organs. Moreover, AN appears to act systemically with DNA damage, and tumors occur in multiple tissues of treated animals. The direct mutagenic mode of action is considered relevant to all tumor sites

4.7.3.7. *Possible Modes of Action for Lung Cancer*

Evidence of a possible association between occupational exposure to AN and lung cancer is found in some studies, including the best available epidemiologic study that workers in the highest exposure category (>8 ppm-years) with more than 20 years of employment displayed a twofold increased risk for lung cancer compared with unexposed workers (Blair et al., 1998). Human bronchial epithelium has CYP2E1 metabolic activities. In a short-term mutagenicity assay, AN induced SCEs and DNA single-strand breaks in human bronchial epithelial cells without the addition of S9 mix (Chang et al., 1990). Thus, a direct mutagenic mode of action is supported for potential AN-induced lung cancer.

In contrast, there is no convincing evidence of lung cancer in rodents chronically exposed by the oral or inhalation routes. The possible mode of action by which AN may induce lung tumors in humans and not in rodents has not been investigated but may involve species differences in inhalation rates and anatomical features of the respiratory tract.

4.8. SUSCEPTIBLE POPULATIONS AND LIFE STAGES

4.8.1. Possible Childhood Susceptibility

Evidence that children may be more susceptible to the acute or chronic toxicity of AN is restricted to a report that children died after sleeping in rooms fumigated with a commercial form of AN called Ventox, whereas adults sharing the same rooms only experienced skin or eye irritation (Grunske, 1949; see Section 4.1.3.1).

Animal studies specifically designed to examine whether or not early-life stages of development are more susceptible than adult stages to the induction of noncancer or cancer-related effects by AN include a lifetime inhalation cancer bioassay in Sprague-Dawley rats (Maltoni et al., 1988) and a three-generation drinking water reproductive toxicity bioassay in

Sprague-Dawley rats that provides evidence of increased tumor incidences in F1 and F2 female breeders after 46 weeks of exposure starting in utero (Friedman and Beliles, 2002). In addition, a subacute study on Sprague-Dawley rats (Szabo et al., 1984) also found weanling rats to be more susceptible than adult rats to the action of AN on the adrenals (see Section 4.2.1.1).

Results from the lifetime inhalation bioassay showed that rats that were chronically exposed starting in utero had higher incidences of tumors at several sites (brain, Zymbal gland, mammary gland, liver, and blood vessels) compared with rats chronically exposed during adulthood only (Maltoni et al., 1988; see Section 4.2.2.2.2 for details). For example, brain tumors occurred in 5.5% of rat dams chronically exposed to 60 ppm AN compared with no brain tumors in unexposed controls (Table 4-42). In contrast, 16.4% of male and 18.5% of female offspring of the exposed dams had brain tumors compared with 1.3% of male and 1.3% of unexposed female rats exposed starting in utero, otherwise under the same exposure protocol as the dams. The responses for brain tumors (male and female offspring), extrahepatic angiosarcomas (female offspring), Zymbal gland (male offspring), and mammary gland (female offspring) with chronic exposure were about threefold higher than those observed in female rats exposed only during adulthood (Table 4-42). In addition, although none of the exposed or unexposed dams had hepatomas, 5/67 male offspring with early-life plus chronic exposure had hepatomas compared with 1/158 unexposed male offspring; hepatomas were observed in 1/54 exposed female offspring compared with 0/149 unexposed female offspring. Rats with early-life plus subchronic (8-week) adult exposure did not show elevated incidences for these tumors compared with adults with chronic adult exposure (Table 4-42).

Comparison of the results from the two chronic phases of this experiment indicated that, compared with chronic exposure to 60 ppm during only adult stages of development, chronic exposure to 60 ppm AN starting during gestation increased the risk for development of extrahepatic angiosarcomas and malignant mammary gland tumors in females, hepatomas and Zymbal gland carcinomas in males, and encephalic gliomas in males and females. Although testing in adult male rats was not included in this study, the increase in hepatomas in male offspring may indicate differences in detoxification and DNA repair mechanisms between fetal and adult livers.

In the drinking water bioassay involving 46-week exposures of each of three generations of female breeder Sprague-Dawley rats, there were slightly increased incidences of tumors in F0 or F2b female breeders in the 100 or 500 ppm groups compared with controls, which were not statistically significant, while F1b female breeders in the 500 ppm group showed statistically significantly increased incidences of brain and Zymbal gland tumors compared with control, at 24 (4/17) vs. 0 and 18 (3/17) vs. 0%, respectively (Friedman and Beliles, 2002). Compared with the 500 ppm F0 breeders that were exposed starting in adulthood, there was an approximate twofold increase in Zymbal gland tumor incidence and a threefold increase in brain tumor incidence in the 500 ppm F1b female breeders, exposed starting in utero (Table 4-35). The

results provide evidence for the increased susceptibility to the carcinogenicity of AN during early-life exposure, positive evidence being in the F1 generation. Increases in tumor incidence in the F2 generation were not as pronounced and were not statistically significant.

As discussed in Sections 4.5.1 and 4.6.3, toxic effects from acute or chronic exposure to AN have been associated with inhibition of glutathione-mediated detoxification of AN by conjugation (e.g., glutathione depletion), transformations in the CYP2E1 metabolic pathway to CEO and cyanide, and oxidative stress. Differences in enzymatic activities (e.g., CYP2E1, EH, DNA repair enzymes, or antioxidant enzymes such as catalase or SOD) or pool sizes of reactive oxygen scavengers (e.g., levels of vitamin E or C) or glutathione between early-life and adult stages may result in life stage differences in susceptibility to AN toxicity.

For CYP2E1, immunoreactive CYP2E1 protein has been detected in human liver microsomes as early as the second trimester (GDs 93–186) (Johnsrud et al., 2003). CYP2E1 enzyme activity increases shortly after birth but less in neonates than in older infants, children, and adults (Johnson, 2003; Johnsrud et al., 2003; Vieira et al., 1996). However, in the fetal brain, CYP2E1 activity is seen as early as 50 days gestation, with increasing levels seen to at least the end of the first trimester (Brzezkinski et al., 1999). In rats, CYP2E1 protein is not significantly expressed in fetal hepatic tissues, although an elevation of CYP2E1 mRNA was seen within a few hours after birth, coincident with the transcriptional activation of the gene (Borlakoglu et al., 1993). Moreover, only neonates expressed small quantities of the CYP2E1 protein, despite the large quantities of CYP2E1 mRNA found in perinatal and neonatal rats.

For EH, fetal immunoreactive enzyme content in human livers averages only 25% of that found in adults with corresponding less enzyme activity (Cresteil et al., 1985). EH activity in fetal liver and adrenal glands are about threefold higher than in kidney and lung with only a weak correlation with gestational age between 10 and 25 weeks. Overall, EH activity in fetal tissue is about 30–40% of that in adults (Pacifici and Rane, 1983b; Pacifici et al., 1983a). In another study (Omiecinski et al., 1994), human microsomal EH (mEH) was detected in fetal liver as early as 7.2 weeks, although at a much lower level of mEH protein, and demonstrated a linear increase with gestational age to a level at 77 weeks that is about half of that observed in adult liver. However, mEH activity in the fetal lung did not correlate with increasing age. Lung mEH activity from days 85 to 130 of gestation was maintained at consistent levels, at about the same level as fetal hepatic EH at 53 days, and varied only by threefold. In addition, Omiecinski et al. (1994) reported that mEH activities in liver or lung, from either fetal or adult tissues, did not correlate with corresponding mRNA levels.

The overall balance of pertinent enzymatic activities (AN metabolizing enzymes and antioxidant enzymes) and pool sizes of reactive oxygen scavengers and glutathione will determine the relative susceptibility of an individual or a life stage. The relatively high activity of CYP2E1 in the brain compared to the liver of the developing human fetus, and low EH activity for detoxification raise concern for increased susceptibility in early life to lung tumors,

and brain tumors from AN exposure, as seen in rats. Additional research examining age-dependent changes in these physiological variables and responses to AN may help to provide explanations for the observed susceptibility of early-life stages in rats to the carcinogenicity of AN, and is outside the scope of this assessment.

The importance of CYP2E1 metabolism in the acute toxicity and lethality of AN has been demonstrated by the lack of lethality or gross signs of intoxication in CYP2E1-null male mice given single gavage doses up to 40 mg/kg, whereas all WT male mice given doses of 40 mg/kg died within 3 hours of administration (Wang et al., 2002). This type of research approach (i.e., the comparison of pertinent endpoints in WT and CYP2E1-null animals) may be useful in helping to better understand the physiologic basis of the apparent susceptibility of early-life stages to the carcinogenicity of AN, which was demonstrated in the rat study by Maltoni et al. (1988).SubchronicSubchronic

4.8.2. Possible Geriatric Susceptibility

Age-related reductions in antioxidant or glutathione pool sizes may increase susceptibility of elderly people to the tissue-damaging actions of AN and reactive metabolites, but specific studies of the possible increased susceptibility of aged people or rats to AN are not available. A 35% decrease in glutathione levels in the liver of aged F344 rats compared with younger animals was associated with an age-related decrease in the levels and activity of γ-glutamylcysteine ligase, a key enzyme in the synthesis of glutathione (Suh et al., 2004). In Wistar rats, the liver and kidney of 22-month-old rats showed significant decreases, compared with 10-week-old rats, in glutathione and glutathione peroxidase and increased levels of biomarkers of lipid peroxidation (Martin et al., 2003). In another study with F344 rats (Tian et al., 1998), activities of several antioxidant enzymes in several tissues displayed an age-dependent decline. Enzymatic activities showing significant decline with age included SOD in the heart, kidney, and serum; glutathione peroxidase in the serum and kidney; and catalase activities in the brain, liver, and kidney. These changes indicated a lower resistance to oxidative stress in older animals.

The possible toxicological impact of an age-related decline in glutathione could be offset by an age-related decline in CYP2E1-mediated metabolism of AN leading to reactive metabolites (CEO), cyanide, or ROS. Many studies have reported that hepatic enzymatic activities of CYP2E1 are lower in elderly human subjects (>65 years) compared with younger adults (see Tanaka, 1998, for review). Decreased hepatic CYP2E1 enzyme activities have also been reported in aged rats. For example, hepatic CYP2E1 enzyme activities were decreased by 46% in 18-month-old rats compared with 8-month-old rats, whereas no age-related changes in CYP2E1 mRNA or protein content were evident (Wauthier et al., 2004). Such age-related declines in CYP2E1 enzyme activities may lead to lower tissue levels of reactive metabolites or cyanide but also may lead to elevated levels or increased residence time of AN in aged tissues compared with younger tissues. No definitive conclusions about the possible susceptibility of

the elderly to AN toxicity can be drawn without more specific studies designed to examine the effects of age on susceptibility to AN toxicity.

As studied in a small number of individuals (n = 47), long-term occupational exposure to AN increased the deletion rate in mitochondrial DNA to a level equivalent to that seen in a group of elderly nonexposed subjects (n = 12) (Ding et al., 2003) (see Section 4.1.2.2). The study authors suggested that AN may have an effect on the molecular processes of aging.

4.8.3. Possible Gender Differences

No reports of gender differences in susceptibility of humans to AN toxicity are available. No consistent gender-related differences in carcinogenic responses were observed in rats or mice, following chronic oral exposure to AN, or in rats, following chronic inhalation exposure. With oral exposure, male and female groups showed similarly increased incidences of brain astrocytomas (rats: Quast, 2002; Bigner et al., 1986; Biodynamics, 1980a, b, c; Quast et al., 1980a), forestomach tumors (rats: Quast, 2002; Bigner et al., 1986; Biodynamics, 1980a, b, c; Quast et al., 1980a; mice: NTP, 2001), Zymbal's gland tumors (rats: Quast, 2002; Bigner et al., 1986; Biodynamics, 1980a, b, c; Quast et al., 1980a), and Harderian gland tumors (mice: NTP, 2001). Following inhalation exposure to 80 ppm AN for 2 years, male and female exposed groups of rats showed similarly increased incidences of brain/CNS tumors and Zymbal's gland tumors compared with the respective control groups (Quast et al., 1980b).

No marked gender-related differences in noncarcinogenic responses were observed in the rat chronic oral toxicity study reported by Quast (2002). Groups of male and female rats were exposed to AN in drinking water at concentrations of 0, 35, 100, or 300 ppm. At the 1-year interim sacrifice, the only exposure-related noncancer histopathologic finding was an increase in the incidence of forestomach squamous cell hyperplasia in rats exposed to concentrations of 100 ppm (4/10 males, 7/10 females) or 300 ppm (10/10 males, 9/10 females). At the 2-year sacrifice, incidences of stomach lesions (nonglandular hyperplasia and/or hyperkeratosis) were similar in male (15/80, 15/47, 44/48, and 45/80 for the control through high-concentration groups, respectively) and female (20/80, 23/48, 41/48, and 47/48) rats at the same exposure level (Quast, 2002). These data, however, give some indication that the forestomach epithelium of female rats may have been slightly more susceptible than that of male rats: at the 1-year sacrifice, 7/10 100 ppm females (70%) had lesions compared with 4/10 100 ppm males (40%); at 2 years, 23/48 35 ppm females (48%) had lesions compared with 15/47 35 ppm males (32%).

In contrast to the lack of apparent gender differences in carcinogenic or noncarcinogenic responses in rodents with chronic exposure, male mice appear to be more susceptible to the acute oral toxicity of AN than female mice (Chanas et al., 2003; NTP, 2001).

In a 14-week study, groups of 10 male and 10 female mice were given 0, 5, 10, 20, 40, or 60 mg/kg AN in deionized water by gavage 5 days/week (NTP, 2001). Exposure-related mortalities were restricted to the first week of the study and occurred in the 40- and 60-mg/kg

groups. Both male and female groups showed mortality, but only at 40 mg/kg was the incidence of deaths higher in male mice compared with females (9/10 and 10/10, males, and 3/10 and 10/10, females, at 40 and 60 mg/kg, respectively).

In a subsequent study, groups of three to four male and three to four female WT or CYP2E1-null mice (mixed 129/Sv and C57BL) were given single gavage doses of 0, 2.5, 10, 20, or 40 mg/kg in tap water and sacrificed 1 or 3 hours later (Chanas et al., 2003). All male WT mice exposed to 40 mg/kg died within 3 hours, showing gross signs typical of cyanide poisoning (rapid shallow breathing, cyanosis, trembling, and convulsions). In contrast, exposed female WT mice showed milder gross signs of poisoning, and none died within the 3-hour period. One hour after dose administration, concentrations of cyanide in blood were statistically significantly elevated, compared with vehicle controls, in WT male mice given doses ≥2.5 mg/kg. At doses ≥10 mg/kg, female WT mice also showed elevated cyanide levels in blood, compared with controls, but cyanide levels were <50% that in male WT mice. Exposed CYP2E1-null mice of both genders showed no elevation in blood cyanide concentrations compared with vehicle controls. Cyanide levels in brain and kidney tissues were also higher in WT males compared with females; cyanide levels in liver and lung tissues showed less distinct differences between male and female mice.

Expression of hepatic, renal, and pulmonary CYP2E1, soluble EH, and microsomal EH were measured in male and female WT mice using Western blot analysis (Chanas et al., 2003). In the liver, WT males showed greater expression of EH, both soluble and microsomal, than did females; CYP2E1 levels were similar in males and females. In the kidney, male WT mice showed markedly higher levels of CYP2E1 (about fourfold), moderately higher levels of soluble EH (about twofold), and comparable levels of microsomal EH compared with female mice. Higher CYP2E1 and soluble EH in the kidney of male mice provided explanation for higher blood cyanide levels in the kidney and acute lethality in male mice. In the lung, no gender differences in the expression of these enzymes were apparent. The results indicated that male mice were more susceptible than female mice to the acute toxicity and lethality of AN and that this difference was associated with higher blood, kidney, and brain levels of cyanide in males shortly after dose administration. Chanas et al. (2003) noted that another possible explanation was that female mice had greater detoxification capability of converting cyanide to thiocyanate, as demonstrated by excretion of greater amount of thiocyanate in urine than males after repeated administration of equal doses of AN (NTP, 2001).

In a subsequent study, male mice (mixed 129/Sv and C57BL) showed higher blood levels of cyanide than female mice 1 hour after gavage administration of 0.047, 0.095, 0.19, or 0.38 mmol/kg (2.5, 5, 10, or 20 mg/kg) AN (El Hadri et al., 2005). This difference between genders was evident in WT mice and in microsomal EH-null (mEH-null) mice, but blood levels of cyanide were lower in exposed mEH-null mice, compared with comparably exposed WT mice. As in the previous experiments reported by Chanas et al. (2003), exposure to AN induced

no elevation of blood levels of cyanide in CYP2E1-null mice of either gender. Western blot analysis revealed no gender differences in expression of CYP2E1 in the liver of WT or mEH-null mice or in expression of mEH in WT or CYP2E1-null mice. However, expression of soluble EH in the liver was greater in WT males, compared with females. No gender differences in expression of this enzyme was observed in mEH-null mice or in CYP2E1-null mice.

The effect of gender on the expression of CYP2E1 and EH have been investigated in humans and rats. Gender was reported to have no influence on the level of CYP2E1 in human liver (George et al., 1995). Sex-related patterns in the activity of hepatic EH activity was studied in Sprague-Dawley rats (Chengelis, 1988). At week 4, epoxide activity in both male and female rats was equivalent (3.5–4.0 nmol/minute per mg protein, or 85–100 nmol/minute per g liver). However, there were consistent increases in activity in males from week 4 to 78, while activity in females actually decreased, but returned to week 4 levels during the later stages (week 78–103). EH activity in male liver peaked at week 78 (about 10 nmol/minute per mg protein, or 350 nmol/minute per g liver). There was a sharp decline in EH activity in aged male rats to about 6 nmol/minute per mg protein, or 200 nmol/minute per g liver at 104 weeks. Cornet et al. (1994) studied gender-related changes in microsomal and cytosolic EH activity in male and female Brown Norway rats. At 15 week, microsomal EH activity was about the same for male and female rats at 4.5 nmol/mg protein/minute. The microsomal EH activity decreased strongly as a function of age in female rats, and in the 125-week-old females, the activity was only half of that found in 15-week-old rats. However, there was no age-related change in males, although the activity in the 83- and 125-week age groups was significantly lower than that in 28-week-old males. The activity of EH activity was higher in males than in females in these aged animals. In another study that compared hepatic microsomal EH in different strains of adult rats (170–250 g) (Oesch et al., 1983), EH activities in females were found to be 71–88% of those in males in all strains. Denlinger and Vesell (1989) studied the hormonal regulation on the developmental pattern of EH in F344 rats, and found that EH activities in males increased gradually until puberty, when activities in males rose rapidly to be from 1.5- to twofold higher than those in females. The higher activity in males was not seen if the males were castrated 24 hours after birth. When castrated males and females were injected with testosterone propionate (0.5 mg s.c.) on days 1, 3, and 5 postpartum, increased mEH an cEH activities were observed at adulthood. Thus, Denlinger and Vesell (1989) concluded that full adult expression of EH activities depends on hormonal influences exerted neonatally.

Gender-related differences were also observed in cytosolic EH activity of Brown Norway rats (Cornet et al., 1994). Significant gender-related differences in the cytosolic EH activity were found in 15-, 28-, and 83-week-old rats with the male animals showing the highest values. In the oldest animals and in 56-week-old rats comparable cytosolic EH activities were found in both genders.

In summary, the available data from animal studies provide no evidence of consistent or marked gender differences in susceptibility to noncancer or cancer-related effects from chronic exposure to AN. There is evidence that male mice are more susceptible than female mice to the acute, cyanide-induced toxicity and lethality of AN, but whether or not this apparent gender dimorphism extends to other species is uncertain at the present time.

4.8.4. Genetic Polymorphisms

4.8.4.1. *CYP450*

In humans, CYP2E1 exists in several modifications that differ in amino acid sequence (alleles). Human variability in their susceptibility to the toxic effects of AN likely exists since CYP2E1 activities may fluctuate between one person and another.

Microsomal CYP2E1 activities varied from 6- to 20-fold in human livers (Lucas et al., 1993). Environmental factors, diet habits, and/or genetic factors may account for the observed interindividual variations observed. In addition, CYP2E1 is elevated in obese overfed rats (Salazar et al., 1988) and diabetic rats (Song et al., 1987), suggesting induction by increased plasma levels of ketone bodies (Bellward et al., 1988). Moreover, CYP2E1 is elevated in lymphocytes from poorly controlled insulin-dependent diabetics (Song et al., 1990). Thus, obese and diabetic individuals may have elevated levels of CYP2E1.

Besides induction, polymorphism of the human CYP2E1 gene may have an impact on AN metabolism in humans. Stephens et al. (1994) compared two restriction fragment length polymorphic sites of the CYP2E1 gene (Rsa 1 and Dra 1), in 695 African-American, European-American, and Taiwanese subjects. Rare alleles at these two loci have been associated with a reduced risk for lung cancer in Japanese and Swedish populations. Stephens et al. (1994) demonstrated that rare alleles (c2 and C) at the Rsa 1 and Dra 1 sites were at least twice as frequent in Taiwanese populations (28 and 24%, respectively) compared with African-Americans (1–8%) or European-Americans (4–11%), raising the possibility of differential susceptibility to chemically induced cancers across ethnic groups. However, when Carrière et al. (1996) measured the allele frequencies for Ras 1, Dra 1, and Taq 1 polymorphic sites in liver CYP2E1 from kidney donors (n = 93) in Geneva, they failed to find a correlation between frequencies of rare alleles and CYP2E1 activity. This implied that observed differences in enzyme activity in humans were more likely to be the result of different levels of induction by environmental factors or other genetic factors.

McCarver et al. (1998) identified a 100-bp insertion mutation in the regulatory region of CYP2E1 gene. Associated with an elevated CYP2E1 metabolic activity, this insertion mutation appears to be present only in obese people or persons who had recently consumed alcohol. The incidence of this mutation was seen in 31% of 65 African-American samples but only in 6.9% of 58 Caucasian samples (McCarver et al., 1998). If tumor formation is determined by the activity

of CYP2E1, this mutation might put affected individuals at a higher risk of cancer from tumorigenic agents that are metabolized by CYP2E1.

Thier et al. (2002) were unable to detect any influence of six genetic CYP2E1 polymorphisms ($G_{-1259}C$, $A_{-316}G$, $T_{-297}A$, $G_{-35}T$, $G_{4804}A$, and $T_{7668}A$) on the formation of N-(cyanoethyl)valine Hb adducts of AN. Conversely, in a study confined to a cohort of individuals from ethnic minorities (African-Americans and Mexican-Americans), Wu et al. (1998) observed an increased incidence of the CYP2E1 DraI DD genotype in peripheral WBC DNA in 126 patients with untreated lung cancer compared with 193 unaffected controls. This could imply an etiological association between the CYP2E1 DraI polymorphism and tumor formation in the lung. Altered toxicokinetic characteristics of CYP2E1 in persons exposed to AN might result in some persons being more vulnerable than others to the tumorigenic effects of the compound, with concomitant changes to the rate and amount of formation of the toxic metabolite and associated changes in susceptible individuals.

Kim et al. (1996), investigating the differences in CYP2E1 activities between 20 Caucasian and 20 Japanese men, pointed out that the significantly lower activity of CYP2E1 in Japanese men might account for the lower rate of some cancers in Japanese compared to Caucasian men.

4.8.4.2. *Glutathione S-transferases*

Thier et al. (1999) studied the formation of Hb adducts of AN (N-[cyanoethyl]valine, N-[methyl]valine, and N-[hydroxyethyl]valine) in a group of 59 people occupationally exposed to the chemical. They reported their findings in relation to subjects' smoking habits and their genetic status with respect to the GST isozymes GSTM1 and GSTT1. Included in the study was an evaluation of smoking habits, since elevated adduct levels of AN in Hb have been reported in smokers. There was no correlation between adduct levels and either the subjects' status of GST isozymes or smoking habit. Thus, neither GSTM1 nor GSTT1 appears as a major AN-metabolizing isoenzyme in humans. However, in a follow-up study with the same group of 59 workers, Thier et al. (2001) reported that polymorphism of the GSTP1 gene at codon 104 was associated with a higher level of N-(cyanoethyl) valine adducts, while GSTM3 variants had no effect on Hb adduct formation. Any potential effect arising from such polymorphisms on the health risk to AN-exposed humans awaits to be evaluated. However, Zielinska et al. (2004) reported an increase in the frequency of the GSTP1b/b genotype in children with cancer (OR = 5.7, CI = 2.4–13.8).

4.8.4.3. *EH*

Two major polymorphisms of mEH have been identified in human population (Hasset et al., 1997). One is a polymorphism in exon 3 that changes the tyrosine residue 113 (Tyr113) to histidine (His113), and the other is an A→G substitution in exon 4 that changes the histidine

residue 139 (His 139) to arginine (Arg139). In vitro expression studies demonstrated that with the Tyr113His polymorphism, the corresponding mEH enzymatic activity is decreased by about 40% (Hasset et al., 1997). On the other hand, the His139Arg polymorphism results in increased enzyme activity. Population studies have demonstrated that the low activity 113His allele correlates with an increased risk for lung cancer (Benhamou et al., 1998), colon cancer (Harrison et al., 1999), hepatocellular carcinoma developed after aflatoxin exposure (McGlynn et al., 1995), and chronic obstructive pulmonary disease (Smith and Harrison, 1997).

The mEH genotypes was shown to play a significant role in human sensitivity to the genotoxic effects of exposure to 1,3-butadiene (Abdel-Rahman et al., 2003, 2001). The carcinogenic and mutagenic effects of 1,3-butadiene are thought to be due to its epoxide metabolites, and the hydrolytic pathway involving mEH is the main detoxification pathway for 1,3-butadiene-reactive intermediates in humans (Jackson et al., 2000). In a study of 49 nonsmoking workers from two styrene-butadiene rubber plants, the hprt gene mutation assay was used as a biomarker of genotoxic effect of BD (Abdel-Rahman et al., 2003, 2001). Abdel-Rahman et al. (2003, 2001) evaluated the effect of polymorphisms in both exon 3 and exon 4 of the mEH gene as modifiers of individual susceptibility to the mutagenic response associated with exposure to 1,3-butadiene, and found a progressive increase in hprt mutant frequency with declining mEH activity in the high exposure group (>150 ppb). The highest frequency of hprt mutant lymphocytes occurred in the group with the mEH low-activity genotype. Individuals with low mEH activity had three- and twofold increases in hprt mutant frequency compared to individuals with high and intermediate mEH activity, respectively. In the low exposure group, there was no difference in hprt mutant frequency between high-, intermediate-, and low-activity individuals. Although there are no studies that evaluate the role played by mEH genotypes in human sensitivity to the toxicity of AN, since EH is involved in the hydrolysis of CEO and its elimination, polymorphisms in exon 3 and exon 4 of the mEH gene are likely to have a role in human susceptibility.

5. DOSE-RESPONSE ASSESSMENTS

5.1. ORAL REFERENCE DOSE (RfD)

5.1.1. Choice of Principal Study and Critical Effect

As previously discussed in Section 4, no human studies currently exist that involve oral exposures to AN. The primary route of AN exposure in humans is via inhalation. The available animal oral toxicity studies, however, identify forestomach lesions (i.e., squamous cell epithelial hyperplasia and hyperkeratosis) as the most sensitive, prevalent, and consistent noncancer effect associated with chronic oral exposure to AN (see Table 4-56 and Figure 5-1). Although, benchmark dose (BMD) modeling of dose-response data is preferred, several of the endpoints under consideration (i.e., incidences of chronic nephropathy, ovarian cysts, and gliosis in the brain in rodents) were not amenable to modeling because either there was no evidence of a dose response or the response was not a monotonically increasing function of dose. A NOAEL/LOAEL approach was used as a common basis for comparison. Using this approach, forestomach lesions were selected as the critical effect on which to base the derivation of the RfD. Although, anatomically, humans do not possess a forestomach, they do have comparable squamous cell epithelial tissues in their oral cavity and in the upper two-thirds of their esophagus (IARC, 1999). Moreover, the forestomach lesions observed in animals were not likely due to the direct irritating effect of AN on gastric tissue. GI bleeding has been observed with single s.c. or oral administration of AN in rats (Ghanayem and Ahmed, 1983) that likely resulted from the distribution of AN metabolites from blood into the GI mucosa. Jacob and Ahmed (2003a) have also demonstrated that AN or its metabolites accumulated and covalently interacted with the GI mucosa of F344 rats treated either orally or intravenously with 2-[^{14}C]-AN, supporting the theory of metabolic incorporation and macromolecular interaction of AN or its metabolites with gastric tissue.

Two 2-year drinking water studies, one in Sprague-Dawley rats (Quast, 2002; Quast et al., 1980a) and the other in F344 rats (Johannsen and Levinskas, 2002b; Biodynamics 1980c), and a 2-year gavage study in B6C3F$_1$ mice (NTP, 2001) provided the best available dose-response data on which to base the RfD (Table 5-1 for rats and Table 5-2 for mice). In Sprague-Dawley rats, significantly elevated incidences of hyperplasia and hyperkeratosis in squamous epithelium of the forestomach occurred in both males and females exposed to AN in drinking water at the two highest concentrations administered (i.e., 100 and 300 ppm) with incidences approaching 100% at the highest dose. Female Sprague-Dawley rats also exhibited statistically significantly elevated incidences at the lowest concentration of AN administered (i.e., 35 ppm). In F344 rats, both males and females exposed to 3, 10, and 30 ppm AN in drinking water exhibited statistically significantly elevated incidences of forestomach lesions with incidences of approximately 20–30%. Male and female F344 rats exposed to the lowest and highest

concentrations of AN in drinking water (i.e., 1 and 100 ppm) did not show statistically significantly elevated incidences of forestomach lesions.

Table 5-1. Incidences of forestomach lesions (hyperplasia or hyperkeratosis) in Sprague-Dawley and F344 rats exposed to AN in drinking water for 2 years

Sex	Administered concentration (ppm in drinking water)	Administered dose[a] (mg/kg-d)	Predicted internal dose metrics[b]		Incidence of forestomach lesions[c]
			AN-AUC in rat blood (mg/L)	CEO-AUC in rat blood (mg/L)	
Sprague-Dawley rats (Sources: Quast, 2002; Quast et al., 1980a)					
Male	0	0	0	0	15/80 (19%)
	35	3.4	2.06×10^{-2}	1.83×10^{-3}	15/47 (32%)
	100	8.5	5.36×10^{-2}	4.36×10^{-3}	44/48 (92%)[c]
	300	21.3	1.46×10^{-1}	9.70×10^{-3}	45/48 (94%)[c]
Female	0	0	0	0	20/80 (25%)
	35	4.4	2.37×10^{-2}	2.07×10^{-3}	23/48 (48%)[c]
	100	10.8	6.18×10^{-2}	4.87×10^{-3}	41/48 (85%)[c]
	300	25.0	1.56×10^{-1}	1.01×10^{-2}	47/48 (98%)[c]
F344 rats[d] (Sources: Johannsen and Levinskas, 2002b; Biodynamics, 1980c)					
Male	0	0	0	0	11/159 (7%)
	1	0.08	4.33×10^{-4}	4.06×10^{-5}	3/80 (4%)
	3	0.25	1.35×10^{-3}	1.27×10^{-4}	18/75 (24%)[c]
	10	0.83	4.52×10^{-3}	4.19×10^{-4}	13/80 (16%)[c]
	30	2.48	1.37×10^{-2}	1.23×10^{-3}	17/80 (22%)[c]
	100	8.37	4.85×10^{-2}	3.97×10^{-3}	9/77 (12%)
Female	0	0	0	0	4/156 (3%)
	1	0.12	5.73×10^{-4}	5.32×10^{-5}	2/80 (3%)
	3	0.36	1.72×10^{-3}	1.59×10^{-4}	16/80 (20%)[c]
	10	1.25	6.02×10^{-3}	5.49×10^{-4}	23/74 (31%)[c]
	30	3.65	1.79×10^{-2}	1.58×10^{-3}	13/80 (16%)[c]
	100	10.90	5.63×10^{-2}	4.46×10^{-3}	5/74 (7%)

[a]Administered doses were averages calculated by the study authors based on animal BW and drinking water intake.
[b]The EPA-modified rat physiologically based pharmacokinetic (PBPK) model of Keddaris et al. (1996) was employed to predict a rat internal dose (i.e., either AN-AUC or CEO-AUC concentration in blood, where AUC = area under the curve) resulting from the ingestion of the specified administered dose of AN consumed in six bolus episodes/d.
[c]Indicates significantly different (at $p < 0.05$) from control incidence by Fisher's exact test.
[d]Incidences for F344 rats do not include animals from the 6- and 12-mo sacrifices and were further adjusted to exclude (from the denominators) rats that died between 0 and 12 mos in the study. Rats dying during this time period were determined from page 6 of Appendix H and Table 1 in Biodynamics (1980c) and Table 8 in Johannsen and Levinskas (2002b). Unscheduled deaths between 0 and 12 mos in the study occurred in two female controls, two males at 3 ppm, three females at 10 ppm, and three males and three females at 100 ppm.

Table 5-2. Incidences of forestomach lesions (hyperplasia or hyperkeratosis) in male and female B6C3F$_1$ mice administered AN via gavage for 2 years

Lesion site and type	Dose (mg/kg-d)[a]			
	0	2.5	10	20
Males				
Forestomach hyperplasia or hyperkeratosis	2/50 (4%)	4/50 (8%)	10/50[a] (20%)	13/50[b] (26%)
Females				
Forestomach hyperplasia or hyperkeratosis	2/50 (4%)	2/50 (4%)	5/50 (10%)	8/50[a] (16%)

[a]Significantly elevated above vehicle control as determined by EPA using Fisher's exact test ($p \leq 0.05$).
[b]Significantly elevated above vehicle control as determined by EPA using Fisher's exact test ($p \leq 0.01$).

Source: NTP (2001).

In B6C3F$_1$ mice, males exhibited statistically significantly elevated incidences of forestomach lesions (hyperplasia or hyperkeratosis) at the two highest doses administered (i.e., 10 and 20 mg/kg-day), while females showed statistically significantly elevated incidences of forestomach lesions at the highest dose only.

While the Johannsen and Levinskas (2002b) drinking water study with F344 rats was selected as the principal study on which to base the RfD, candidate RfDs were also developed from studies in Sprague-Dawley rats (Quast, 2002) and B6C3F$_1$ mice (NTP, 2001) for comparison purposes. The Johannsen and Levinskas (2002b) study was selected as the principal study primarily because it employed five doses of AN, ranging from 1 to 100 ppm, and thus tested a more complete range of doses, especially in the low-dose region, than did either the Quast (2002) study in Sprague-Dawley rats or the NTP (2001) study in B6C3F$_1$ mice, which both employed three doses (i.e., 35, 100, and 300 ppm in rats and 2.5, 10, and 20 mg/kg-day in mice). In addition, Johannsen and Levinskas (2002b) and Quast (2002) are both drinking water studies, which are preferred over the NTP (2001) gavage study in B6C3F$_1$ mice because drinking water exposure is more relevant to humans. Finally, of these three studies[1], the Johannsen and Levinskas (2002b) study identified the lowest LOAELs based on an increased incidence of nonneoplastic stomach lesions (i.e., 0.3 mg/kg-day for males and 0.4 mg/kg-day for females). Therefore, hyperplasia or hyperkeratosis in F344 rats was selected as critical effect for derivation of RfD.

[1]Although SD male rats in the Johannsen and Levinskas (2002a) study exhibited the lowest LOAEL (0.1 mg/kg-d) for all endpoints across all studies considered for RfD derivation (see Figure 5-1), this study experienced significant mortality, especially in the high-dose groups, rendering the results of this study highly suspect, and thus, it was deemed not suitable for RfD derivation.

5.1.2. Methods of Analysis—Including Use of PBTK Modeling

Candidate RfDs for AN were derived from the incidence of forestomach lesions in Sprague-Dawley rats, F344 rats, and $B6C3F_1$ mice using a BMD approach. Incidences of forestomach lesions from chronic drinking water studies in male and female Sprague-Dawley rats (Quast, 2002) and F344 rats (Johannsen and Levinskas, 2002b) provided four sets of dose-response data from which to derive candidate RfDs (see Table 5-1), while incidences of forestomach lesions from a chronic gavage study in male and female $B6C3F_1$ mice provided an additional two sets of dose-response data (see Table 5-2). The incidence data from rats in Table 5-1 were not combined across strains for purposes of dose-response modeling because response levels were different across the two strains. As described further below, dose-response modeling of the incidence of forestomach lesions after 2 years of AN exposure was carried out using BMD modeling. For rats, in addition to administered dose, two alternative internal dose metrics (AN in blood and CEO in blood), as estimated by PBTK modeling, were employed in BMD modeling. In mice, only administered dose was employed as a dose metric for BMD modeling purposes.

5.1.2.1. *PBTK Modeling*

In deriving candidate RfDs from the rat studies, internal dose metrics generated using PBTK models developed by EPA (see Section 3.5; Appendix C) based on the rat and human PBTK models of Kedderis et al. (1996) and Sweeney et al. (2003), respectively, were employed. The EPA-modified PBTK models included many realistic features, each of them leading to a different dose metric. The primary features of interest were estimated daily average internal concentrations of AN or CEO in blood (area under the curve [AUC] expressed on a 24-hour basis) and estimates based on continuous versus episodic exposure, with episodic exposure more realistically reflecting how rats (and humans) actually consume drinking water.

As indicated above, two potentially useful chemical markers of internal exposure were selected (i.e., the concentration in blood of the parent compound, AN, and its reactive metabolite, CEO). These two internal dose metrics were evaluated under an episodic exposure pattern because rats (and humans) consume drinking water in an episodic manner. In addition, for rats and mice, the externally administered AN dose was also used for deriving candidate RfDs for purposes of comparison with the candidate RfDs derived based on internal doses of AN and CEO estimated from the PBTK model.

For this assessment, internal dose metrics were evaluated for use in cross-species extrapolation from rats because of the following:

- The rat and human PBTK models incorporated species differences in physiological processes influencing the disposition of AN and CEO and were developed with rat in vivo toxicokinetic data, human in vitro metabolic data, and rat-to-human allometric

scaling (Section 3.5; Appendix C; Sweeney et al., 2003; Kedderis et al., 1996). As such, approaches using these models were expected to provide more accurate bases for extrapolation of dose-response relationships from rats to humans than approaches based on administered animal dose alone.

- For oral exposures, PBTK model predictions of AN or CEO concentrations in blood appear to provide a more accurate basis for extrapolation than predictions based on forestomach AN-AUC or forestomach CEO-AUC concentrations because the stomach compartment in the PBTK model was not calibrated with measurements of AN or CEO in the stomach epithelium, the site of the forestomach lesions. Thus, more research is needed before a more physiologically meaningful stomach compartment can be incorporated into the model. Blood AN concentrations predicted by the rat PBTK model were fairly close to measured AN concentrations in rats following oral exposure, but the model consistently predicted higher CEO concentrations in blood than was reported in studies of orally exposed rats (see Figure 3 in Kedderis et al., 1996).

Given the relative uncertainties in the PBTK predictions noted above, especially for CEO, both internal dose metrics (AN and CEO in blood) were used in deriving candidate RfDs based on the rat data, in addition to administered dose. The concentration of AN administered in the bioassay, in terms of mg/kg-day, was used as input into the EPA-modified rat PBTK model of Kedderis et al. (1996) in order to predict a rat internal dose (either AN-AUC or CEO-AUC concentration in blood) resulting from the ingestion of the total daily administered dose of AN consumed in six bolus episodes per day. The resulting predicted AN-AUC or CEO-AUC concentrations in rat blood are shown in Table 5-1 for male and female SD and F344 rats.

5.1.2.2. *BMD Modeling*

The incidences of forestomach lesions observed following 2 years of AN exposure in male and female SD and F344 rats were modeled using AN and CEO in blood, expressed in mg/L, as internal dose metrics. In addition, incidences of these same lesions were modeled in male and female SD and F344 rats, as well as male and female $B6C3F_1$ mice, employing administered dose. For $B6C3F_1$ mice, administered doses were multiplied by 5/7 to convert 5 day/week gavage exposures to 7 day/week continuous exposures. In all cases, all of the dichotomous dose-response models available in EPA's BMD Software (BMDS, version 2.0) (i.e., the gamma, logistic, log-logistic, probit, log-probit, multistage, Weibull, and quantal-linear models) were fit to these incidence data. Because the incidence of forestomach lesions in male and female F344 rats did not increase monotonically across all administered concentrations, however, only incidence data from the three lowest concentrations (i.e., 0, 1, and 3 ppm) were ultimately used in dose-response modeling. Although the incidence of forestomach lesions did

increase from 20 to 31% at 3 and 10 ppm, respectively, in female F344 rats, this dose-response relationship could still not be adequately described by any of the existing dichotomous dose-response models in BMDS, and thus, the 10 ppm dose group was dropped in females prior to modeling. For the same reason, the incidence data from the highest dose group in male Sprague-Dawley rats needed to be dropped prior to BMD modeling.

In most cases, several models fit the data equally well (i.e., exhibited χ^2 goodness-of-fit *p* values >0.1). Of those models exhibiting adequate fit, the selected model was the one with the lowest Akaike's Information Criterion (AIC) value. $BMDL_{10}$ and $BMDL_{05}$ estimates were then derived from this selected model. If more than one model shared the lowest AIC, the mean $BMDL_{10}$ and $BMDL_{05}$ were calculated, as per the EPA's *Benchmark Dose Technical Guidance Document* (U.S. EPA, 2000b). Appendix B-1 provides additional details regarding the BMD modeling results used in the derivation of the RfD.

Although $BMDL_{10}$ values were derived for comparison purposes, a benchmark response (BMR) of 5% extra risk was selected as the point of departure (POD) for deriving the RfD based on both biological and statistical considerations. Biologically, the endpoint selected on which to base the RfD derivation (i.e., forestomach lesions—hyperplasia or hyperkeratosis) is considered severe. Although the severity of the hyperplasia observed was generally not reported, Johannsen and Levinskas (2002b) concluded that, "This [forestomach] lesion has been described as progressing from hyperplasia and hyperkeratosis to papilloma, and ultimately to carcinoma, following chronic oral exposure...." Statistically, the dose at 5% extra risk identifies a POD near the lower end of the observed data. Consequently, 5% extra risk appears to be a reasonable choice for the POD for RfD derivation.

For the two internal dose metrics selected (AN and CEO in blood), once the $BMDL_{10}$ and $BMDL_{05}$ estimates (or their means) were derived from the selected model(s), these estimates, expressed as rat internal AUCs (in mg/L), were then input into the EPA-modified human PBTK model of Sweeney et al. (2003) in order to predict the human equivalent administered dose of AN that would result in a human 24-hour blood AN-AUC or CEO-AUC equivalent to the corresponding rat AUC, again assuming six bolus ingestion episodes per day. The resulting predicted 95% lower bounds on the human equivalent administered dose of AN, expressed in mg/kg-day, represent potential PODs for deriving candidate RfDs. In the case of administered dose, the $BMDL_{10}$ and $BMDL_{05}$ estimates (or their means) are already expressed as human equivalent doses (HEDs) in mg/kg-day, and are thus used directly as potential PODs for deriving candidate RfDs. The $BMDL_{10}$ and $BMDL_{05}$ estimates and their corresponding PODs across the three dose metrics are presented in Tables 5-3, 5-4, and 5-5 for Sprague-Dawley rats, F344 rats, and $B6C3F_1$ mice, respectively.

Table 5-3. Candidate RfDs based on BMD modeling of the incidence of forestomach lesions (hyperplasia or hyperkeratosis) in male and female Sprague-Dawley rats exposed to AN in drinking water for 2 years

Sex	Endpoint	Dose metric	BMR[a]	BMDL[b]	POD[c] (mg/kg-d)	UF	Candidate RFD[d] (mg/kg-d)
Male	Forestomach lesions	Administered dose (mg/kg-d)	5%	0.72 mg/kg-d	0.72	100	7.20×10^{-3}
			10%	1.27 mg/kg-d	1.27	100	1.27×10^{-2}
		Predicted AN in blood (mg/L)	5%	4.32×10^{-3} mg/L	1.27	30	4.23×10^{-2}
			10%	7.72×10^{-3} mg/L	2.17	30	7.23×10^{-2}
		Predicted CEO in blood (mg/L)	5%	3.90×10^{-4} mg/L	3.86×10^{-2}	30	1.29×10^{-3}
			10%	6.82×10^{-4} mg/L	6.75×10^{-2}	30	2.25×10^{-3}
Female	Forestomach lesions	Administered dose (mg/kg-d)	5%	0.64 mg/kg-d	0.64	100	6.39×10^{-3}
			10%	1.24 mg/kg-d	1.24	100	1.24×10^{-2}
		Predicted AN in blood (mg/L)	5%	1.76×10^{-3} mg/L	5.35×10^{-1}	30	1.78×10^{-2}
			10%	3.62×10^{-3} mg/L	1.07	30	3.57×10^{-2}
		Predicted CEO in blood (mg/L)	5%	2.88×10^{-4} mg/L	2.84×10^{-2}	30	9.48×10^{-4}
			10%	5.58×10^{-4} mg/L	5.51×10^{-2}	30	1.84×10^{-3}

[a]BMR refers to the 95% lower confidence limit on the administered or PBPK-predicted internal dose in the rat associated with a 5 or 10% extra risk for the incidence of forestomach lesions.

[b]All dichotomous models in EPA's BMDS (version 2.0) were fit to the incidence of forestomach lesions (hyperplasia or hyperkeratosis) in Sprague-Dawley rats using the data presented in Table 5-1. For BMD modeling, three different dose metrics were employed: (1) administered animal dose expressed in mg/kg-d, (2) AN in blood (predicted) expressed in mg/L, and (3) CEO in blood (predicted) expressed in mg/L. Adequate fit of a model was achieved if the χ^2 goodness-of-fit statistic yielded a *p*-value >0.1. Of those models exhibiting adequate fit, the selected model was the model with the lowest AIC value. $BMDL_{10}$ and $BMDL_{05}$ estimates were derived from the selected model. If more than one model shared the lowest AIC, the mean $BMDL_{10}$ and $BMDL_{05}$ were calculated and are presented, as per the EPA's *Benchmark Dose Technical Guidance Document* (U.S. EPA, 2000b). Appendix B-1 provides additional details regarding these BMD modeling results.

[c]For administered dose, the POD is the $BMDL_{05}$ or $BMDL_{10}$ based on BMD modeling using administered animal dose as the dose metric. For the internal dose metrics (AN and CEO in blood), the PODs are PBPK model-derived human equivalent administered doses of AN that would result in a human 24-hr blood AN-AUC or CEO-AUC equivalent to the corresponding rat $BMDL_{05}$ or $BMDL_{10}$ values, assuming AN ingestion in six bolus episodes/d.

[d]RfD = POD/UF.

Sources: Quast (2002); Quast et al. (1980a).

Table 5-4. Candidate RfDs based on BMD modeling of the incidence of forestomach lesions (hyperplasia or hyperkeratosis) in male and female F344 rats exposed to AN in drinking water for 2 years

Sex	Endpoint	Dose metric	BMR[a]	BMDL[b]	POD[c] (mg/kg-d)	UF	Candidate RFD[d] (mg/kg-d)
Male	Forestomach lesions	Administered dose (mg/kg-d)	5%	9.97×10^{-2} mg/kg-d	9.97×10^{-2}	100	9.97×10^{-4}
			10%	0.151 mg/kg-d	0.151	100	1.51×10^{-3}
		Predicted AN in blood (mg/L)	5%	5.39×10^{-4} mg/L	1.66×10^{-1}	30	5.55×10^{-3}
			10%	8.14×10^{-4} mg/L	2.50×10^{-1}	30	8.35×10^{-3}
		Predicted CEO in blood (mg/L)	5%	5.06×10^{-5} mg/L	5.00×10^{-3}	30	1.67×10^{-4}
			10%	7.65×10^{-5} mg/L	7.56×10^{-3}	30	2.52×10^{-4}
Female	Forestomach lesions	Administered dose (mg/kg-d)	5%	0.117 mg/kg-d	0.117	100	1.17×10^{-3}
			10%	0.209 mg/kg-d	0.209	100	2.09×10^{-3}
		Predicted AN in blood (mg/L)	5%	5.58×10^{-4} mg/L	1.72×10^{-1}	30	5.74×10^{-3}
			10%	9.97×10^{-4} mg/L	3.06×10^{-1}	30	1.02×10^{-2}
		Predicted CEO in blood (mg/L)	5%	5.17×10^{-5} mg/L	5.11×10^{-3}	30	1.70×10^{-4}
			10%	9.23×10^{-5} mg/L	9.12×10^{-3}	30	3.04×10^{-4}

[a]BMR refers to the 95% lower confidence limit on the administered or PBPK-predicted internal dose in the rat associated with a 5 or 10% extra risk for the incidence of forestomach lesions.
[b]All dichotomous models in EPA's BMDS (version 2.0) were fit to the incidence of forestomach lesions (hyperplasia or hyperkeratosis) in F344 rats using the data presented in Table 5-1. For BMD modeling, three different dose metrics were employed: (1) administered animal dose expressed in mg/kg-d, (2) AN in blood (predicted) expressed in mg/L, and (3) CEO in blood (predicted) expressed in mg/L. Adequate fit of a model was achieved if the χ^2 goodness-of-fit statistic yielded a *p*-value >0.1. Of those models exhibiting adequate fit, the selected model was the model with the lowest AIC value. $BMDL_{10}$ and $BMDL_{05}$ estimates were derived from the selected model. If more than one model shared the lowest AIC, the mean $BMDL_{10}$ and $BMDL_{05}$ were calculated and are presented, as per the EPA's *Benchmark Dose Technical Guidance Document* (U.S. EPA, 2000b). Appendix B-1 provides additional details regarding these BMD modeling results.
[c]For administered dose, the POD is the $BMDL_{05}$ or $BMDL_{10}$ based on BMD modeling using administered animal dose as the dose metric. For the internal dose metrics (AN and CEO in blood), the PODs are PBPK model-derived human equivalent administered doses of AN that would result in a human 24-hr blood AN-AUC or CEO-AUC equivalent to the corresponding rat $BMDL_{05}$ or $BMDL_{10}$ values, assuming AN ingestion in six bolus episodes/d.
[d]RfD = POD/UF.

Sources: Johannsen and Levinskas (2002b); Biodynamics (1980c).

Table 5-5. Candidate RfDs based on BMD modeling of the incidence of forestomach lesions (hyperplasia or hyperkeratosis) in male and female B6C3F$_1$ mice exposed to AN via gavage for 2 years

Sex	Endpoint	Dose metric	BMR[a]	BMDL[b] (mg/kg-d)	POD[c] (mg/kg-d)	UF	Candidate RfD[d] (mg/kg-d)
Male	Forestomach lesions	Administered dose (mg/kg-d)	5%	1.43	1.43	100	1.43×10^{-2}
			10%	3.01	3.01	100	3.01×10^{-2}
Female	Forestomach lesions	Administered dose (mg/kg-d)	5%	3.02	3.02	100	3.02×10^{-2}
			10%	6.20	6.20	100	6.20×10^{-2}

[a]BMR refers to the 95% lower confidence limit on the administered dose in the mouse associated with either a 5 or 10% extra risk for the incidence of forestomach lesions.
[b]All dichotomous models in EPA's BMDS (version 2.0) were fit to the incidence of forestomach lesions (hyperplasia or hyperkeratosis) in B6C3F$_1$ mice using the data presented in Table 5-2. For BMD modeling, administered animal dose, expressed in mg/kg-d, was employed. Adequate fit of a model was achieved if the χ^2 goodness-of-fit statistic yielded a *p*-value >0.1. Of those models exhibiting adequate fit, the selected model was the model with the lowest AIC value. $BMDL_{10}$ and $BMDL_{05}$ estimates were derived from the selected model. If more than one model shared the lowest AIC, the mean $BMDL_{10}$ and $BMDL_{05}$ were calculated and are presented, as per the EPA's *Benchmark Dose Technical Guidance Document* (U.S. EPA, 2000b). Appendix B-1 provides additional details regarding these BMD modeling results.
[c]The POD is the $BMDL_{05}$ or $BMDL_{10}$ based on BMD modeling using administered animal dose as the dose metric. No internal dose metrics were employed for mice because of the absence of a PBPK model for this species.
[d]RfD = POD/UF.

Source: NTP (2001).

5.1.3. RfD Derivation—Including Application of Uncertainty Factors (UFs)

In Tables 5-3 and 5-4, the candidate PODs based on the internal dose metrics (i.e., CEO-AUC in blood and AN-AUC in blood) were divided by a composite UF of 30 to account for two areas of uncertainty. An UF of 3 (i.e., $10^{0.5}$) was used to account for uncertainty associated with extrapolating from rats to humans. A factor of 3 was chosen instead of the default value of 10, because toxicokinetic uncertainty was decreased by the application of the rat and human PBTK models. The applied factor of 3 was selected to account for any remaining toxicokinetic uncertainties in the dosimetric extrapolation, and possible differences in the response of rat and human target tissues to AN or its metabolites (i.e., toxicodynamic differences). A default UF of 10 was then used to account for uncertainty associated with extrapolation to individuals or groups within the human population who may be especially sensitive or susceptible to the noncancer toxicity of AN.

The candidate PODs based on administered dose in Tables 5-3, 5-4, and 5-5 were divided by a composite UF of 100 to again account for two areas of uncertainty. First, a UF of 10 was used to account for uncertainty associated with extrapolating from rats to humans because no PBTK model was employed, and thus, a default factor of 10 was needed to account for both toxicokinetic and toxicodynamic uncertainties. Secondly, as above, a default UF of 10 was used to account for uncertainty associated with extrapolation to individuals or groups within the human population who may be especially sensitive or susceptible to the noncancer toxicity of AN. Considerations in selecting individual UFs are discussed in greater detail below.

A default UF of 10 was used to account for uncertainty associated with extrapolation to individuals or groups within the human population who may be especially sensitive or susceptible to the noncancer toxicity of AN. As discussed in Section 4.8, available data on AN are inadequate to reliably identify populations that may be especially susceptible to the noncancer toxicity of AN. There is one human case report indicating that children are more susceptible to AN toxicity. These data at least suggest that juvenile populations may be especially susceptible to the noncancerous effects of AN exposure.

An UF to account for extrapolation from subchronic to chronic exposure was not necessary because of the availability of chronic oral studies in both rats and mice.

An UF to account for LOAEL to NOAEL extrapolation was not applied because the BMR selected for BMD modeling, a 5% extra risk of forestomach lesions, was judged to have minimal biological significance.

A database deficiency UF was not used in the development of the RfD. Although studies of health effects in humans exposed to AN by the oral route are not available, the animal oral toxicity database is particularly robust. As discussed in Section 4.6.1, there are nine rat toxicity and cancer bioassays, one toxicity and cancer bioassay with $B6C3F_1$ mice, a three-generation (46-week) developmental/reproductive rat toxicity study with Sprague-Dawley rats, a 12-week gavage study of nerve conduction velocities in male Sprague-Dawley rats, a 14-week gavage

toxicity bioassay in B6C3F$_1$ mice, a developmental toxicity study in Sprague-Dawley rats exposed by gavage during GDs 6–15, and a 90-day study of oxidative stress indicators in the brain and liver of F344 rats. These animal data identify forestomach lesions as the most sensitive, prevalent, and consistent noncancer effect in animals associated with repeated oral exposure to AN, and thus provide evidence that an RfD based on this effect will be protective for other potential noncancer effects, including neurological, reproductive, and developmental effects. In addition, the data for forestomach lesions in rats and mice provide an adequate characterization of the dose-response relationship for the development of these lesions with chronic exposure, which, coupled with the application of the PBTK models for cross-species dosimetric extrapolation, adds to the confidence in the estimation of a chronic oral human dose expected to be without risk in the general population for the development of gastric lesions.

For the purpose of this assessment, CEO-AUC in blood is considered to be the most appropriate dose metric to use in deriving an RfD. CEO is believed to be the reactive metabolite most likely responsible for the noncancer (and cancer) effects observed following AN exposure. Results from acute exposure studies in rats indicate that CEO plays a key role in the mode of action by which AN elicits stomach lesions. Research has shown that pretreatment with inhibitors of CYP2E1 inhibited the development of GI ulceration, following acute exposure of rats to AN, and doses of KCN equivalent to toxic doses of AN did not induce GI bleeding in a similar manner to AN (Ghanayem et al., 1985; Ghanayem and Ahmed, 1983). For oral exposures, then, the use of CEO-AUC as the internal dose metric for cross-species extrapolation is recommended. Therefore, while the PBTK model does not predict CEO in blood as accurately as it predicts AN in blood, CEO in blood provides the most biologically relevant dose metric for modeling the incidence of forestomach lesions and for extrapolating from orally exposed rats to humans.

In comparing the candidate RfDs for the preferred dose metric of predicted CEO in blood across Tables 5-3 and 5-4, the candidate RfDs based on the forestomach lesion incidence data in F344 rats are about an order of magnitude lower than those candidate RfDs based on forestomach lesion incidence data in Sprague-Dawley rats. This comparison confirms what had previously been predicted (i.e., F344 rats are more sensitive to AN exposure than Sprague-Dawley rats). Moreover, these same candidate RfDs in F344 rats are approximately two orders of magnitude lower than the candidate RfDs based on administered dose in B6C3F$_1$ mice. Therefore, for the critical endpoint (i.e., forestomach lesions), F344 rats are the most sensitive species and strain. Consequently, the RfD is 2×10^{-4} mg/kg-day. This RfD is consistent with the candidate RfDs derived for both male (1.67×10^{-4} mg/kg-day) and female (1.70×10^{-4} mg/kg-day) F344 rats using predicted CEO in blood as the dose metric and based on the incidence of forestomach lesions following chronic oral exposure to AN.

5.1.4. Oral Data Array for Noncancer Endpoints

LOAELs based on selected animal studies presented in Table 4-56 are arrayed for comparison in Figure 5-1, and provide a perspective on the RfD developed in the previous section from data in F344 rats (Johannsen and Levinskas, 2002b). Figure 5-1 should be interpreted with caution, however, because the LOAELs across studies are not necessarily comparable due to the lack of any indication regarding the confidence in the data sets from which the LOAELs were derived. In addition, the nature, severity, and incidence of effects at a LOAEL are also likely to vary. For example, the incidence of forestomach squamous cell hyperplasia in male and female F344 rats at the LOAEL were both 17% (see Figure 5-1), while in Sprague-Dawley rats, the incidence of the same lesions at the LOAEL in males and females were 73 and 23%, respectively. Figure 5-1 provides a graphical comparison of organ-specific LOAELs from chronic studies in experimental animals. The predominant noncancer effect of chronic oral exposure to AN is hyperplasia and hyperkeratosis of squamous cell epithelial tissue in the forestomach. The LOAELs for this endpoint are lower than those observed for chronic nephropathy, gliosis, ovarian cysts, or developmental effects. Therefore, the RfD based on hyperplasia and hyperkeratosis of squamous cell epithelial tissue in the forestomach should be protective of other effects resulting from oral exposure to AN.

Figure 5-1. Comparison of LOAELs for noncancer effects across target organs following oral exposure to AN in animals.

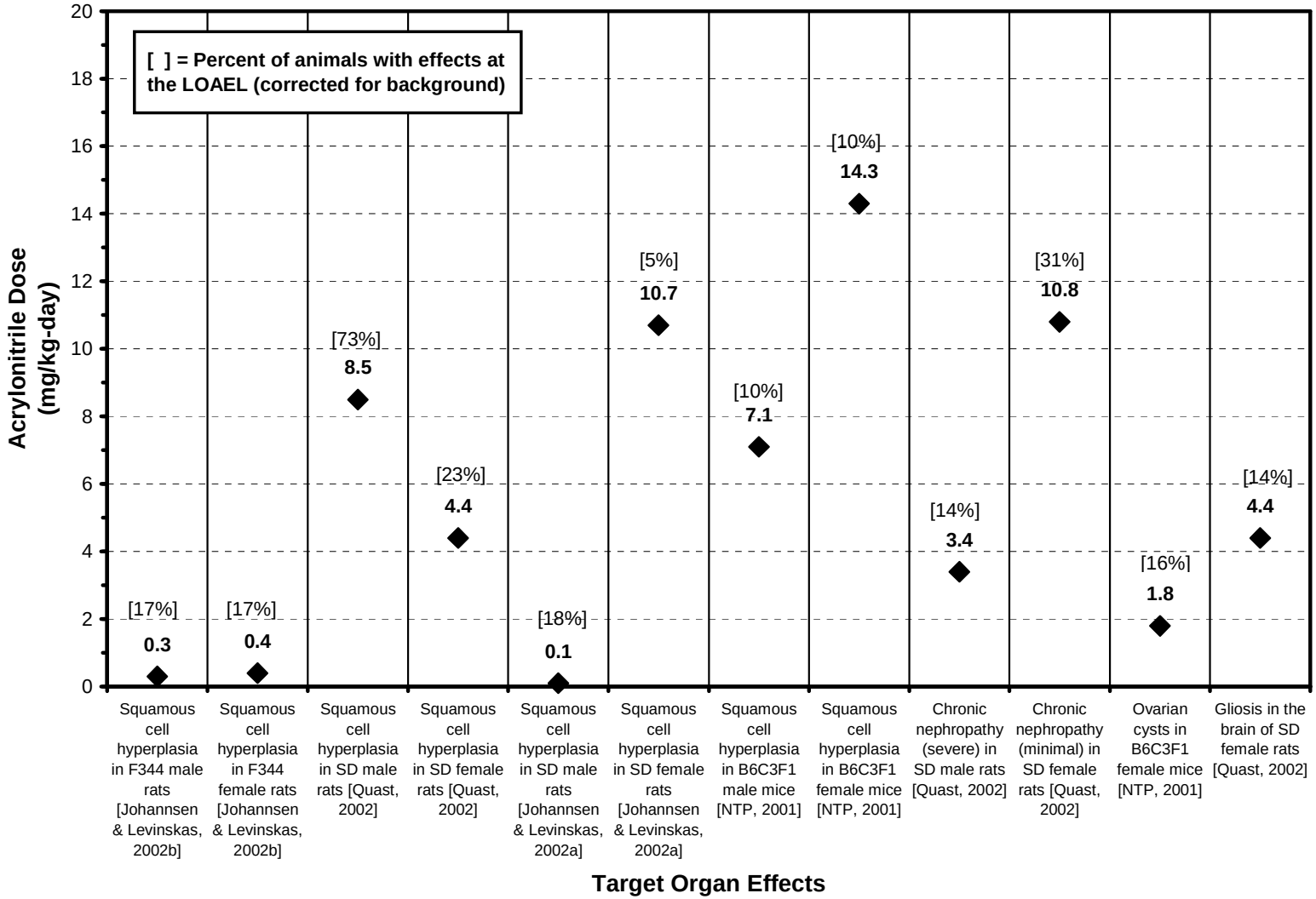

5.1.5. Previous RfD Assessment

No RfD was derived in the previous IRIS assessment of AN.

5.2. INHALATION RfC

5.2.1. Choice of Principal Study and Critical Effect

As discussed in Section 4.1.2, results from several cross-sectional health examinations and surveys of AN-exposed workers (Chen et al., 2000; Kaneko and Omae, 1992; Muto et al., 1992; Sakurai et al., 1978) and a study of the performance on a battery of neurobehavioral tests by exposed workers (Lu et al., 2005a) identified increased prevalence of subjective neurological symptoms (e.g., headache, poor memory, and irritability) and small performance deficits in neurobehavioral tests as the critical effects from chronic occupational inhalation exposure to AN. An increased prevalence of subjective symptoms was associated with average workplace air concentrations of 1.13 ppm (Muto et al., 1992), 1.8 ppm (Kaneko and Omae, 1992), and 0.48 ppm (Chen et al., 2000). Deficits in the neurobehavioral tests were associated with average workplace air concentrations of 0.11 ppm for a group of workers designated as monomer workers and 0.91 ppm for a group of workers designated as fiber workers (Lu et al., 2005a).

Cross-sectional epidemiologic surveys of reproductive outcomes in AN-exposed workers found increased prevalence of adverse reproductive outcomes associated with somewhat higher average workplace air concentrations of 3.7 ppm (Dong and Pan, 1995), 3.6 ppm (Dong et al., 2000a), and 7.5 ppm (Li, 2000). Adverse outcomes with statistically significantly increased prevalence compared with unexposed workers included the following:

- *Premature deliveries*—10.7% in unexposed wives of exposed males vs. 3.5% in controls (implying the sperm of exposed males may be affected) (Dong and Pan, 1995); 8.2% in exposed females vs. 3.9% in controls (Dong et al., 2000b); and 11.6% in exposed females vs. 4.7% in controls (Li, 2000)

- *Stillbirths*—4.5% in exposed females vs. 0% in controls (Dong and Pan, 1995); 2.7% in exposed females vs. 0% in controls (Dong et al., 2000b)

- *Sterility*—5.0% in wives of exposed males vs. 1.8% in wives of controls (Dong and Pan, 1995); 2.6% in exposed females vs. 0.8% in controls (Li, 2000)

- *Birth defects*—21.3% in exposed females vs. 4.8% in controls (Dong et al., 2000b); 25.4% in exposed females vs. 4.2% in controls (Li, 2000)

- *Pregnancy complications*—20.8% in exposed females vs. 7.1% in controls (Li, 2000)

Exposure levels associated with adverse effects in the available animal inhalation toxicity studies were higher than the workplace air concentrations associated with adverse effects in AN-exposed workers (see Table 4-57). With repeated inhalation exposure to AN, effects noted with the lowest exposure levels were as follows:

- Increased incidence of nasal epithelial lesions in Sprague-Dawley rats exposed for 2 years to 20 ppm AN (Quast et al., 1980b)

- Deficits in sensory nerve conduction in the tail nerve of Sprague-Dawley rats exposed for 12 weeks to AN concentrations ≥50 ppm, but not 25 ppm (Gagnaire et al., 1998)

- Increased incidence of litters with short tail, short trunk, missing vertebrae, or anteriorly displaced ovaries (combined) in Sprague-Dawley rats exposed to AN concentrations of 80 ppm, but not 40 ppm, on GDs 6–15 (Murray et al., 1978)

- Decreased fetal weight gain per litter in Sprague-Dawley rats exposed to AN concentrations ≥25 ppm, but not to 12 ppm, on GDs 6–20 (Saillenfait et al., 1993)

The cross-sectional study of neurobehavioral performance in acrylic fiber workers by Lu et al. (2005a) was selected as the principal study for deriving the RfC because it is the best available study that identified neurobehavioral effects in workers exposed to AN. Previous occupational studies by Kaneko and Omae (1992) and Muto et al. (1992) reported subjective neurological symptoms (e.g., poor memory and irritability) in exposed workers. Lu et al. (2005a) utilized the WHO-recommended NCTB administered by trained physicians to evaluate these neurobehavioral effects systematically. Hence, the results were more reliable when compared with those based on self reporting. In addition, neurobehavioral effects were also reported in AN-treated rats (Rongzhu et al., 2007; Ghanayem et al. 1991). Confounding by other workplace exposures is not considered likely.

The distribution of employment duration for the monomer workers was 1–10 years, 23%; 11–20 years, 42%; and >20 years, 35%. For fiber workers, the distribution was 1–10 years, 47%; 11–20 years, 23%; and >20 years, 30%. Geometric mean workplace AN air concentrations were 0.11 ppm for the monomer operations areas (range 0–1.70 ppm based on 390 stationary air samples collected between 1997 and 1999) and 0.91 ppm for the acrylic fiber operations areas (range 0.00–8.34 ppm based on 570 samples). For monomer workers, the following statistically significant deficits, compared with unexposed controls, were measured:

- 41–68% higher scores for negative moods (i.e., anger, confusion, depression, fatigue, and tension) in the Profile of Mood States Test.

- 16% longer times in the Simple Reaction Time Test of attention and visual response speed.

- 21% lower scores in the backward sequence of the Digit Span Test of auditory memory.

- 4% lower scores in the Benton Visual Retention Test, a measure of visual perception and memory.

- 14% lower scores in the Pursuit Aiming II Test, a measure of motor steadiness.

Statistically significant deficits were not found in the Santa Ana Test for manual dexterity or in the Digital Symbol Test for perceptual motor speed. Fiber workers showed deficits of a similar magnitude in many of the same tests (20–44% higher in Profile of Mood States Test, 10% longer in the Simple Reaction Time Test, 24% lower score in the backward sequence of the Digit Span Test, 4% lower scores in the Benton Visual Retention Test, and 10% lower scores in the Pursuit Aiming II Test), with the exception that scores in the forward sequence of the Digit Span Test were significantly better than those of unexposed workers.

Lu et al. (2005a) reported that air in these workplaces also presented potential exposures to cyanide in the monomer operations areas and methyl methacrylate in the fiber areas, but measurements of these chemicals in air samples were not made. Cyanide is a breakdown product of AN. Its concentration in the monomer plant should be low compared with AN. Methyl methacrylate was generally used as a minor component in the production of acrylic fiber. With an RfC of 0.7 mg/m^3 (U.S. EPA, 1998b), its toxicity is much lower than that for AN. Therefore, potential exposure to these confounders was determined to be an insufficient limitation to preclude using Lu et al. (2005a) to identify neurological effects as potential health hazards from occupational exposure to AN and derive an RfC for chronic inhalation exposure to AN. Both groups of workers showed deficits, despite being exposed to different potentially confounding chemicals, and the results from this study are consistent with the increased prevalence of subjective symptoms in other studies of AN-exposed workers.

An RfC based on the results from the chronic inhalation bioassay with Sprague-Dawley rats (Quast et al., 1980b) was also derived for comparison purposes. As discussed in Section 4.6.2, statistically significant increased incidence of inflammatory and degenerative nasal lesions (i.e., hyperplasia of mucus-secreting cells in males and flattening of respiratory epithelium in females) occurred in rats exposed to the lowest level of AN in this two-year bioassay, 20 ppm (6 hours/day, 5 days/week), and represent the critical effects in animals exposed to AN chronically by inhalation. At the higher exposure level, 80 ppm, other nasal lesions with elevated incidences were suppurative rhinitis and focal erosion of the mucous lining

in females and hyperplasia of respiratory epithelium in males and females. Other lesions with elevated incidences at the 80 ppm exposure level were gliosis and perivascular cuffing in the brain of males and females, focal nephrosis and thyroid cysts in males, and hepatic necrosis in females (which was also elevated at 20 ppm).

5.2.2. Methods of Analysis

A NOAEL/LOAEL approach to the human data was used to derive the RfC. The performance deficits measured in monomer and fiber workers were judged to be adverse and the geometric mean of the range of air concentrations measured for the monomer work areas, 0.11 ppm (0.24 mg/m^3), was selected as the POD for deriving the RfC.

For the animal data, a BMD approach was used. Dose-response models available in EPA's BMDS (version 1.3.2) were fit to incidence data for flattening of the respiratory epithelium in female rats and hyperplasia of mucus-secreting cells in male rats. Prior to modeling, animal exposure data were converted to human equivalent concentrations (HECs) using U.S. EPA (1994) methods for extrathoracic respiratory effects from a category 1 gas (Table 5-6). A BMR of 10% extra risk was selected as the POD for deriving the RfC based on both biological and statistical considerations. Biologically, the endpoints selected on which to derive the RfC (i.e., flattening of the respiratory epithelium in female rats and hyperplasia of mucus-secreting cells in male rats) are relatively benign. Statistically, the dose at 10% extra risk identifies a POD near the lower end of the data range. Thus, a BMR of 10% extra risk was selected for this analysis consistent with the U.S. EPA (. Benchmark concentrations (BMCs) and the 95% lower bounds on the BMCs ($BMCL_{10}$s) for the best-fitting models are shown in Table 5-6. Potential PODs for the animal-based RfC are the $BMCL_{10}$s of 0.082 and 0.059 mg/m^3 for nasal effects in male and female rats, respectively. More detailed information on these BMD modeling results is presented in Appendix B-2.

Table 5-6. Results of dose-response analyses of incidence data for selected nasal lesions in male and female Sprague-Dawley rats exposed by inhalation to AN for 2 years

Nasal lesion	Administered concentration (mg/m^3)	HEC (mg/m^3)[a]	Lesion incidence	BMC_{10} (mg/m^3)[b]	$BMCL_{10}$ (mg/m^3)[b]	Candidate RfC (mg/m^3)[c]
Hyperplasia of mucus-secreting cells in males	0	0	0/11 (0%)	0.187	0.082	3×10^{-3}
	43.4	2.1	7/12 (58%)[d]			
	173.6	8.5	8/10 (80%)[d]			
Flattening of respiratory epithelium in females	0	0	1/11 (9.1%)	0.162	0.059	2×10^{-3}
	43.4	2.1	7/10 (70%)[d]			
	173.6	8.5	8/10 (80%)[d]			

[a]HEC as per U.S. EPA (1994) methods for a category 1 gas producing an upper respiratory effect.
Sample calculation: 43.4 $mg/m^3 \times$ 6h/24h $\times$ 5d/7d $\times$ $RGDR_{ET}$ = 2.1 mg/m^3, where $RGDR_{ET}$ = 0.275 = $[VE/SA_{ET}]$ rat ÷ $[VE/SA_{ET}]$ human; VE = minute volume = 0.281 L/min rat, 13.8 L/min human; SA_{ET} = extrathoracic surface area = 15 cm^2 rat, 200 cm^2 human.
[b]BMC_{10} and $BMCL_{10}$ refer to the BMD model-predicted air concentration and its 95% lower confidence limit, associated with a 10% extra risk for having nonneoplastic nasal lesions. BMC_{10}s and $BMCL_{10}$s are estimated from the best-fitting model among those fit to the data. More detailed information on the BMD modeling results is presented in Appendix B-2.
[c]RfC = $BMCL_{10}$/UF, where the UF is 30.
[d]Statistically significantly different from control value as reported by Quast et al., 1980b.

Source: Quast et al. (1980b).

5.2.3. RfC Derivation—Including Application of UFs

The LOAEL of 0.11 ppm (0.24 mg/m^3) from Lu et al. (2005a) for statistically significant performance deficits in neurobehavioral tests of mood, attention and speed, auditory memory, visual perception and memory, and motor steadiness in humans occupationally exposed to AN via inhalation was used for derivation of the RfC. Since the LOAEL was from an occupational study, the adjusted LOAEL for continuous exposure was obtained by multiplying the study LOAEL by a factor of 0.36 (5 days/7 days $\times$ 10 m^3/day ÷ 20 m^3/day). This adjusted LOAEL ($LOAEL_{ADJ}$) of 0.03 ppm (0.086 mg/m^3) was divided by a composite UF of 100 to arrive at an RfC of 9×10^{-4} mg/m^3. This two-step calculation is illustrated below:

1. $LOAEL_{ADJ}$ = 0.24 $mg/m^3 \times 0.36$ = 0.086 mg/m^3
2. RfC = 0.086 mg/m^3 ÷ 100 = 0.00086 mg/m^3 or 0.9 $\mu g/m^3$

An UF of 10 was used for extrapolating from a LOAEL to a NOAEL. The RfC is derived from an occupational study. A default UF of 10 was used to account for sensitive or susceptible members of the general population, including children. A database UF was not

applied since the database for AN is robust, and occupational exposure studies exist that evaluated reproductive effects in AN-exposed workers.

Comparative animal-based RfCs of 3×10^{-3} mg/m^3 (or 3 μg/m^3) and 2×10^{-3} mg/m^3 (or 2 μg/m^3) were derived by dividing the $BMDL_{10}$s of 0.082 mg/m^3 and 0.059 mg/m^3 for nasal lesions in male and female rats, respectively, by UFs of 30 (3 for extrapolating from rats to humans using the default U.S. EPA [1994] dosimetric adjustment and 10 to protect sensitive subpopulations). These candidate RfCs are displayed in Table 5-6. Extrapolating the results from animal toxicity studies to derive an RfC has inherently greater uncertainty than using the results from the cross-sectional studies of health effects in human workers; however, the human-based and animal-based RfCs differ by about twofold. For this assessment, the human-based RfC of 9×10^{-4} mg/m^3 or 0.9 μg/m^3 is the recommended value.

5.2.4. Inhalation Data Array for Noncancer Endpoints

LOAELs based on selected studies included in Table 4-57 are arrayed in Figure 5-2 and provide perspective on the RfC derived from Lu et al. (2005a). Figure 5-2 should be interpreted with caution because the LOAELs across studies are not necessarily comparable, due to inherent limitations in NOAEL/LOAEL determination (U.S. EPA, 2000b), nor is the confidence in the data sets from which the LOAELs were derived the same. The nature, severity, and incidence of effects occurring at a LOAEL are likely to vary. The text in Section 5.2.1 should be consulted for a more complete understanding of the issues associated with each data set and the rationale for the selection of the critical effect and principal study used to derive the RfC. The most sensitive endpoint is the neurobehavioral effects identified in Lu et al. (2005a) and this endpoint provides the basis for the derivation of the RfC.

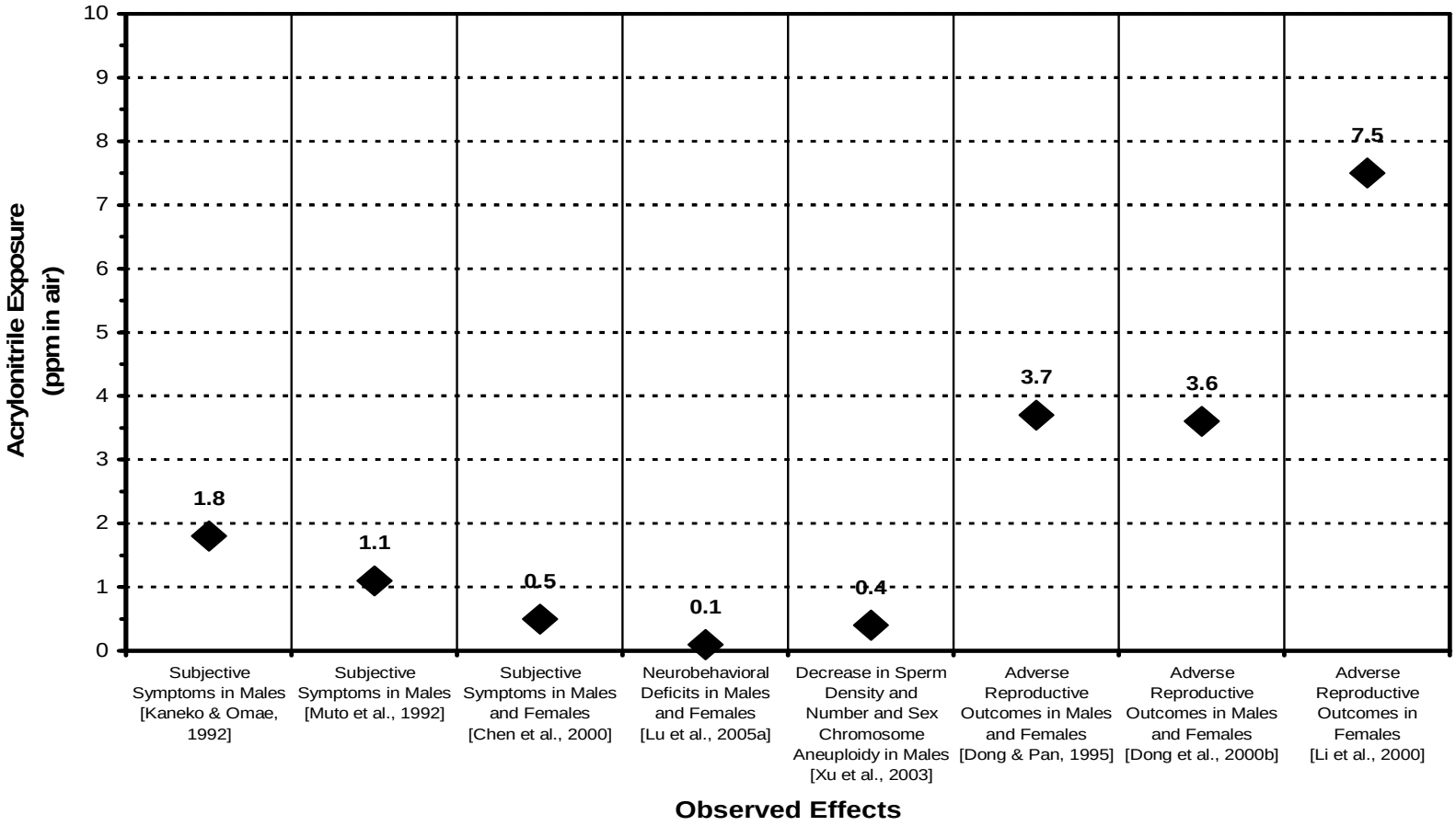

Figure 5-2. Comparison of LOAELs for noncancer effects in human workers following inhalation exposure to AN.

5.2.5. Previous Inhalation Assessment

Previously, EPA derived an RfC of 2×10^{-3} mg/m^3 from the low exposure level (i.e., 20 ppm AN, duration-adjusted to a $LOAEL_{HEC}$ of 1.9 mg/m^3) in the Quast et al. (1980b) animal study, which was identified as a LOAEL for the onset of hyperplasia of the mucus-secreting cells. The $LOAEL_{HEC}$ was adjusted with a combined UF of 1,000 to derive the RfC. This composite UF was made up of 10 for intraspecies variability; 3 for interspecies variability, where dosimetric adjustments had already been applied to account for part of this area of uncertainty; 3 for extrapolation from a minimally adverse LOAEL to a NOAEL; and 10 for database deficiencies. The latter UF was applied because of the lack of an inhalation bioassay in a second species and the absence of reproductive data by the inhalation route where an oral study existed that showed reproductive effects.

New pertinent information, available since the previous RfC was developed, includes: (1) several cross-sectional health examinations and surveys of subjective symptoms and reproductive outcomes in AN-exposed workers; (2) a published cross-sectional study of performance in a battery of neurobehavioral tests by AN-exposed workers (Lu et al., 2005a) (the principal study for the current RfC); (3) toxicokinetic information and the development of PBTK models for AN; and (4) two inhalation developmental toxicity studies in rats.

5.3. UNCERTAINTIES IN THE ORAL RfD AND INHALATION RfC

The following discussion identifies uncertainties associated with the RfD or RfC for AN. As presented earlier in this chapter (Sections 5.1.2 and 5.1.3; and 5.2.2 and 5.2.3), the UF approach, following EPA methodology for RfC and RfD development (U.S. EPA, 2002, 1994), was applied to a POD. For the RfD, the POD was determined as $BMDL_{05}$ of internal dose estimated from rats and subsequently converted to a HED. For the RfC, a LOAEL was derived from an epidemiologic study for neurobehavioral effects. Factors accounting for uncertainties associated with a number of steps in the analyses were adopted to account for extrapolating from the POD, the starting point in the analysis, to a no-adverse-effect level (LOAEL to NOAEL) given insufficient data in the principal study for BMD modeling, to a diverse population of varying susceptibilities. These extrapolations are carried out with default approaches instead of data on AN, given the paucity of experimental AN data to inform individual steps.

Selection of principal study and critical effect for reference value determination

Hyperplasia and hyperkeratosis of squamous epithelium of the forestomach was selected as the critical effect for RfD. This effect is the most prevalent, consistent, and most sensitive effect in rats and mice. Since GI bleeding occurs after s.c. injection of AN in rats, this effect is probably not due to local irritation on gastric tissues, but is likely due to binding of CEO to GI mucosa. Although humans do not possess a forestomach, humans do have comparable squamous cell epithelial tissues in their oral cavity and the upper two-thirds of their esophagus (IARC, 1999). Thus, there is little uncertainty that this effect is relevant to humans.

For derivation of the RfC, both a 2-year rat inhalation study and epidemiologic studies are available. To reduce uncertainty in extrapolating from animals to humans, epidemiologic studies are preferred. Several earlier cross-sectional health surveys of AN-exposed workers reported subjective neurological symptoms. In addition, adverse reproductive outcomes were also found in cross-sectional epidemiologic surveys of AN-exposed workers in China. Neurobehavioral effects of AN-exposed workers were selected as the critical effect since this effect was observed from several occupational studies with workers chronically exposed to AN via the inhalation route.

Lu et al. (2005a) mentioned several limitations of this study. One was that the cited exposure data represented estimates of previous exposure levels and no contemporaneous personal monitoring data were available. Furthermore, as the NCTB was developed for populations in Europe and North America, it is not known to what extent cultural differences may have affected results of the Profile of Mood States Test, shown to be sensitive to cultural differences. In addition, the study authors could not rule out the possibility that examiner drift may have affected the results. Selection bias among volunteers in different groups was mentioned as a possible confounding effect, but was discounted on the basis that the participation among exposed workers was so high. Moreover, the largest measures of neurobehavioral effects occurred in the acrylic fiber workers, who had lower average AN exposure levels.

Animal to human extrapolation

No human oral exposure studies are available for derivation of the RfD. For derivation of the RfD, extrapolating dose-response data from animals to humans is a source of uncertainty. A PBTK model, which has its own associated uncertainties, was used to address toxicokinetic differences between animals and humans. Uncertainties of the PBTK model are discussed as part of the overall uncertainty discussion (Section 5.4.4.5), with quantitative details given in Appendix D. Residual uncertainties pertaining to unknown interspecies differences in pharmacodynamics were addressed by application of a UF of 3.

A human occupational exposure study (Lu et al., 2005a) was used for derivation of the RfC, eliminating uncertainty associated with extrapolation from animals to humans. An RfC was also derived from a two-year inhalation study of rats based on increased incidence of inflammatory and degenerative nasal lesions. This alternative RfC was, at most, threefold higher than the RfC derived from Lu et al. (2005a).

Dose-response modeling

BMD modeling was used to estimate the POD for the RfD. While models with better biological support may exist, the selected models provided adequate mathematical fits to the experimental data sets. BMD modeling has advantages over a POD based on a NOAEL or

LOAEL because NOAELs/LOAELs are a reflection of the particular exposure concentration or dose at which a study was conducted, they do not make use of the dose-response curve, and they do not address the variability of the study population. NOAELs and LOAELs also are less amenable to quantitative uncertainty analysis.

The RfC was based on a LOAEL identified from an occupational epidemiology study. As stated above, there are several reasons to prefer a POD obtained from BMD modeling. However, the available data only supported a LOAEL. A UF to address extrapolation to a less adverse response level was applied.

Intrahuman variability

Heterogeneity among humans is another source of uncertainty. Uncertainty related to human variation needs consideration, also, in extrapolation from a small subset of presumably healthy humans (i.e., workers) to a larger, more diverse general population. Available data from animal studies provide no evidence of gender differences in susceptibility to toxicity of AN, although no data are available regarding possible gender differences in susceptibility. Human genetic polymorphisms in CYP2E1 activities likely contribute to variability in human susceptibility to the toxic effects of AN (see Section 4.8.4.1). A UF of 10 was used to account for intrahuman variability for derivation of RfD and RfC. A factor of 10 has been found to be generally sufficient to account for human variability in response to chemical exposure (Renwick and Lazarus, 1998).

5.4. CANCER ASSESSMENT

5.4.1. Choice of Study/Data—with Rationale and Justification

As previously discussed in Section 4.1.2.2, evidence of a possible association between exposure to AN and cancer in humans has been found in some studies. The best available occupational epidemiologic study (Blair et al., 1998) reported that workers exposed to AN via inhalation in the highest cumulative exposure category (i.e., >8 ppm-years) with more than 20 years of employment displayed a twofold increased risk of death from lung cancer compared with unexposed workers (RR = 2.1, 95% CI = 1.2–3.8). To date, Blair et al. (1998) is largest cohort study to assess the relationship between AN and cancer, following 25,460 workers in eight AN-producing facilities, with two-thirds of this cohort having a follow-up period of over 20 years. The large sample size and the duration of follow-up time in this study provides a good opportunity to detect any substantial elevation of case-specific cancer deaths. The findings from Blair et al. (1998) are not inconsistent with other studies evaluating carcinogenic endpoints from AN exposure. However, Blair et al. (1998) addressed known problems with earlier studies by quantifying exposures, examining potential confounding from smoking, and employing an internal control group of unexposed workers. And although only 5% of the cohort had died by the time of analysis, this study has a large number of observed deaths that can be used to assess

the relationship between AN-exposure and cancer based on cancer mortality. Also, Blair et al. (1998) utilized a detail job-exposure matrix as part of the exposure assessment. For these reasons, data from Blair et al. (1998) were chosen to derive an inhalation unit risk (IUR) for AN. Additionally, the use of epidemiology data for the derivation of the IUR, versus using data from an animal bioassay, reduces uncertainty inherent to animal to human extrapolation.

Sections 4.6.1 and 4.6.2 summarized the current animal data on AN indicating that it is a multiple-site carcinogen in chronic oral and inhalation bioassays with rats and mice. The best available animal studies for evaluating the dose-response relationship between AN exposures and forestomach, CNS, Zymbal gland, tongue, and mammary gland tumors were two chronic drinking water studies, one with Sprague-Dawley rats exposed to 0, 35, 100, or 300 ppm AN in drinking water for 2 years (Quast, 2002; Quast et al., 1980a) and the other with F344 rats exposed to 0, 1, 3, 10, 30, or 100 ppm AN in drinking water for 2 years (Johannsen and Levinskas, 2002b; Biodynamics, 1980c). In addition, data from another bioassay with Sprague-Dawley rats exposed to AN in drinking water at concentrations of 0, 1, or 100 ppm for 2 years were also considered (Johannsen and Levinskas, 2002a; Biodynamics, 1980a). In the absence of definitive human studies demonstrating the carcinogenicity of chronic oral exposure to AN, developing an oral cancer slope factor (CSF) from these animal studies is reasonable, especially because the application of the AN PBTK models described in Chapter 3 can decrease the toxicokinetic uncertainty in the interspecies extrapolation and in the mode of action of carcinogenicity of AN in rodents versus humans.

Animal data from the only available chronic inhalation cancer bioassay with multiple exposure levels (Dow Chemical Co., 1992a; Quast et al., 1980b) were also used to develop an IUR to compare with the one derived from AN-exposed workers (Blair et al., 1998). In this animal study, male and female Sprague-Dawley rats were exposed to 0, 20, or 80 ppm AN in air, 6 hours/day, 5 days/week, for 2 years. At 80 ppm, significantly increased incidences of astrocytomas and glial cell proliferation and Zymbal gland tumors in males and females, malignant mammary gland tumors (adenocarcinomas) in females, as well as intestinal and tongue tumors in males, were found. At 20 ppm, male and female rats showed increased incidences of astrocytomas and glial cell proliferation and Zymbal gland tumors. IUR estimates were derived based on dose-response data for these tumors using the AN PBTK models previously described to dosimetrically extrapolate from rats to humans.

5.4.2. Dose-Response Data

5.4.2.1. *Human Occupational Data*

An analysis of the lung cancer mortality and AN exposure data from the Blair et al. (1998) study was conducted to derive an IUR estimate for AN. This analysis used the approach described by Starr et al. (2004) in which the risk of death from lung cancer in AN-exposed workers was characterized using a semi-parametric Cox regression model with time-dependent

covariates. The Cox regression model has several advantages in that it allows inclusion of individual exposure histories and utilizes internal controls, thus avoiding confounding by the "healthy worker" effect. In contrast to the analysis done by Starr et al. (2004), the analysis conducted for this assessment included the entire cohort (not just white male workers), and the final model only had cumulative exposure as a covariate. Starr et al. (2004) included a second covariate in their final model, plant of employment. This analysis is further described in Appendix B-7.

5.4.2.2. *Rat Oral Data*

Incidence data for forestomach, CNS, Zymbal gland, tongue, and mammary gland tumors in Sprague-Dawley and F344 rats exposed to AN in drinking water for 2 years were used to develop site-specific oral CSFs for AN (Tables 5-7–5-9). Tumor incidences in F344 rats were adjusted to exclude animals dying before the first appearance of each tumor type, which ranged from day 419 to 495. No early mortality adjustments were made to the cumulative tumor incidences from the Sprague-Dawley bioassay (Quast, 2002) because CNS and Zymbal gland tumors were seen in some high-dose female rats as early as 7 months (210 days) after exposure began, and no differences in survival were observed across the dose groups during the first 6 months of the study.

Table 5-7. Incidence of CNS tumors in Sprague-Dawley and F344 rats exposed to AN in drinking water for 2 years

Sprague-Dawley rats (Quast, 2002; Quast et al., 1980a)[a]				
Sex	**AN drinking water concentration (ppm)**	**Glial cell proliferation[b]**	**Astrocytomas**	**Overall CNS tumors**
Male	0	0/80	1/80	1/80
	35	4/47[c]	8/47[c]	12/47[c]
	100	3/48	19/48	22/48[c]
	300	7/48[c]	23/48[c]	30/48[c]
Female	0	0/80	1/80	1/80
	35	3/48	17/48[c]	20/48[c]
	100	3/48	22/48[c]	25/48[c]
	300	7/48[c]	24/48[c]	31/48[c]

F344 rats (Johannsen and Levinskas, 2002b; Biodynamics, 1980c)[d]						
Sex	**AN drinking water concentration (ppm)**	**Glial cell proliferation[b]**		**Astrocytomas**		**Overall CNS tumors**
		Brain	**Spinal cord**	**Brain**	**Spinal cord**	
Male	0	0/160	0/156	2/160	1/156	3/160
	1	0/80	0/79	2/80	0/79	2/80
	3	0/78	0/70	1/78	0/70	1/78
	10	0/80	0/78	2/80	0/78	2/80
	30	0/79	0/79	10/79[c]	0/79	10/79[c]
	100	0/76	0/70	21/76[c]	4/70[c]	25/76[c]
Female	0	0/157	0/155	1/157	0/155	1/157
	1	0/80	0/78	1/80	0/78	1/80
	3	0/80	0/79	2/80	0/79	2/80
	10	0/77	0/72	4/75	1/72	5/75
	30	0/80	0/87	6/80[c]	0/77	6/80[c]
	100	0/76	0/69	23/76[c]	1/69	24/76[c]

[a]Incidence denominators were calculated from the total number of animals examined from the beginning of the study. Numerators for CNS tumor incidences (glial cell proliferation, astrocytomas, or overall incidence of glial cell proliferation or astrocytomas) for these Sprague-Dawley rats were reported as combined brain and spinal cord lesions by Quast et al. (1980a).

[b]Glial cell proliferation is a smaller-sized lesion, either focal or multifocal, than astrocytomas, suggestive of an early tumor.

[c]Statistically significantly different from controls ($p < 0.05$) as calculated by the study authors.

[d]The denominators for incidences in these F344 rats exclude rats from the 6- and 12-mo sacrifices and unscheduled deaths prior to the 12-mo sacrifice. Numerators for the overall incidences were the number of rats with astrocytomas in brain or spinal cord. Reviews of summaries of individual animal pathology reports for this study (Appendix H, Biodynamics, 1980c) indicated that five of the seven F344 rats showing spinal cord astrocytomas also showed a brain astrocytoma; thus, the number was not always as great as the sum of the numerators for the incidences of these lesions in the two tissues (e.g., 21/76 male 100-ppm brain tissues had astrocytomas and 4/70 male 100-ppm spinal cord tissues had astrocytomas, but all four rats with astrocytomas also had brain astrocytomas). Because the response to AN was predominately in brain tissue and a few spinal cord tissue samples were missing in each exposure group, denominators for the overall incidences were taken as the number of rats examined for brain lesions

Table 5-8. Incidence of mammary gland tumors in F344 and Sprague-Dawley rats exposed to AN in drinking water for 2 years

Sex	AN drinking water concentration (ppm)	Benign mammary gland tumors[a]	Malignant mammary gland tumors[b]	Benign and/or malignant mammary gland tumors
F344 rats (Johannsen and Levinskas, 2002b; Biodynamics, 1980c)[c,d]				
Male	0	No statistically significantly elevated incidences of mammary gland tumors were found in exposed groups compared with controls.		
	1			
	3			
	10			
	30			
	100			
Female	0	12/156	3/156	14/156
	1	5/80	4/80	8/80
	3	6/80	0/80	6/80
	10	8/79	1/78	9/80
	30	9/80	3/80	12/80
	100	9/73	6/73[e]	14/73[e]
Sprague-Dawley rats (Quast, 2002; Quast et al., 1980a)[f]				
Male	0	Not reported	Not reported	Not reported
	35			
	100			
	300			
Female	0	52/80	1/80	58/80
	35	35/48	1/48	42/48[e]
	100	33/48	3/48	42/48[e]
	300	22/48	10/48[e]	35/48

[a]Incidence includes fibroadenomas for F344 rats and fibroadenomas/adenofibromas/adenomas for Sprague-Dawley rats.
[b]Incidence includes adenocarcinomas and carcinomas.
[c]The denominators for tumor incidences in F344 rats excluded rats from the 6- and 12-mo sacrifices and rats that died prior to 12 mos. Mammary gland tumor incidences are for animals scheduled for the 18-mo and terminal sacrifices. Microscopic examinations were only conducted on mammary glands showing gross signs of tumors—the inclusion of all rats living for >52 wks in the denominators assumes that rats without gross signs of tumors were also without microscopic neoplastic changes.
[d]Animals with multiple tumor types within a tissue were counted only once.
[e]Statistically significantly different from controls (at $p < 0.05$) via Fisher's exact test.
[f]Denominators were calculated from the total number of animals examined from the beginning of the study. Incidences were reported as total number of rats with benign-only, malignant-only, or benign and/or malignant tumors.

Table 5-9. Tumor incidences Sprague-Dawley and F344 in rats exposed to AN in drinking water for 2 years

Sex	AN drinking water concentration (ppm)	Forestomach tumors	CNS tumors	Zymbal gland tumors	Tongue tumors	Intestinal tumors	Mammary gland tumors
Sprague-Dawley rats (Quast, 2002; Quast et al., 1980a)							
Male	0	0/80	1/80	3/80	1/80	Not reported	Not reported
	35	2/47	12/47[a]	4/47	2/47		
	100	23/48[a]	22/48[a]	3/48	4/48		
	300	39/48[a]	30/48[a]	16/48[a]	5/48[a]		
Female	0	1/80	1/80	1/80	0/80	0/80	58/80
	35	1/48	20/48[a]	5/48[a]	1/48	1/48	42/48[a]
	100	12/48[a]	25/48[a]	9/48[a]	2/48	4/48[a]	42/48[a]
	300	30/48[a]	31/48[a]	18/48[a]	12/48[a]	4/48[a]	35/48
F344 rats (Johannsen and Levinskas, 2002b; Biodynamics, 1980c)[b]							
Male	0	0/159	3/160	1/147	Not examined		3/159
	1	1/80	2/80	1/76			2/80
	3	4/78[a]	1/78	0/73			2/78
	10	3/80[a]	2/80	0/67			2/80
	30	4/80[a]	10/79[c]	2/71[c]			0/80
	100	1/77	25/76[c]	14/68[c]			2/77
Female	0	1/157	1/157	0/157	Not examined		14/156
	1	1/80	1/80	0/73			8/80
	3	2/79	2/80	0/73			6/80
	10	2/77	5/75	0/70			9/80
	30	4/80[a]	6/80[c]	2/73[c]			12/80
	100	2/75	24/76[c]	8/62[c]			14/73[a]

[a]Significantly different from controls ($p < 0.05$).
[b]The denominators for tumor incidences in F344 rats excluded rats from the 6- and 12-mo sacrifices and unscheduled deaths prior to the 12-mo sacrifice. Numerators for the incidences of CNS tumors were derived by adding the number of rats with brain or spinal astrocytomas; denominators were taken as the greater of the number of rats examined for brain or spinal cord lesions after the 12-mo sacrifice. Numerators for Zymbal gland tumor incidences included squamous cell papillomas and carcinomas designated to occur in the ear canal. Mammary gland tumor incidences are for fibroadenomas and adenocarcinomas in animals sacrificed or found dead after 12 mos. Tongues were not routinely histopathologically examined for tumors in this bioassay.
[c]Significantly different from controls ($p < 0.01$).

As previously noted, a second 2-year AN drinking water study employing Sprague-Dawley rats has been conducted (Johannsen and Levinskas, 2002a; Biodynamics, 1980a). To determine whether these data should also be employed in the cancer assessment, an analysis was performed to evaluate the statistical validity of pooling tumor incidence data from the two Sprague-Dawley rat chronic AN drinking water studies. The first study (Quast, 2002; Quast et al., 1980a) exposed animals to AN drinking water concentrations of 0, 35, 100, and 300 ppm, while the second study (Johannsen and Levinskas, 2002a) employed AN drinking water concentrations of 0, 1, and 100 ppm. The dichotomous multistage model in BMDS was fit to the tumor incidence data from three sites (i.e., forestomach, CNS, and Zymbal gland) in each sex across both studies, using administered animal dose expressed in mg/kg-day. A statistical test described by Stiteler et al. (1993), which employs a maximum likelihood ratio statistic distributed as a χ^2, was then used to test the null hypothesis that the two data sets are compatible with a common dose-response model. If the null hypothesis is not rejected, this provides evidence that the results from the two studies may be pooled.

As discussed in more detail in Appendix B-5, the statistical tests indicated that some, but not all, of the data sets from the two studies were consistent with a common dose-response model. More specifically, the results of this analysis showed that forestomach and Zymbal gland tumors in both male and female Sprague-Dawley rats were not compatible with a common dose-response model, while CNS tumors in male and female Sprague-Dawley rats were compatible with a common dose-response model. Because of these conflicting results, it was decided that the results from the two Sprague-Dawley rat drinking water studies would not be pooled. Therefore, the final dose-response analysis for deriving the oral slope factor for AN focused on the two rat drinking water studies containing the most dose groups (i.e., the Sprague-Dawley rat bioassay reported by Quast [2002] and the F344 rat bioassay reported by Johannsen and Levinskas [2002b]).

5.4.2.3. *Rat Inhalation Data*

Incidence data for intestinal, CNS, Zymbal gland, tongue, and mammary gland tumors in Sprague-Dawley rats exposed to AN via inhalation were used for deriving site-specific IURs for AN (Table 5-10). With the exception of one male in the 80 ppm exposure group that died with a CNS tumor after 7–12 months on study, all of the remaining tumors occurred in rats that died or were sacrificed after at least 12 months of AN exposure. Denominators for the incidences in Table 5-10 excluded animals that died without a tumor before 12 months on study because these animals were not exposed long enough to be at risk for tumor development. Although a statistically significantly elevated incidence in tongue tumors was observed in male rats at 80 ppm, tongues from only 14 of the males in the 20 ppm exposure group were examined. No data on the incidence of tongue tumors in female rats were presented in the original study report by Quast et al. (1980b).

Table 5-10. Incidences of intestinal, CNS, Zymbal gland, tongue, and mammary gland tumors in Sprague-Dawley rats exposed to AN via inhalation for 2 years

Sex	AN air concentration (ppm)	Intestinal tumors[a]	CNS tumors[a,b]	Zymbal gland tumors[a]	Tongue tumors[a]	Mammary gland adenocarcinomas[a]
Male	0	4/96	0/96	2/96	1/95	–
	20	3/93	4/93	4/93	0/14	–
	80	17/82[c]	22/82[c]	11/82[c]	7/82[c]	–
Female	0	–	0/93	0/93	–	9/93
	20	–	8/99[c]	1/98	–	8/98
	80	–	20/89[c]	11/89[c]	–	20/99[c]

[a]For all incidence data, the denominators excluded rats dying earlier than 12 mos in the study. These data were ascertained from Tables 22, 25, 31, 34, and 35 in the original study report by Quast et al. (1980b).
[b]Incidences for CNS tumors (brain and spinal cord) in Sprague-Dawley rats listed in this table, as reported by Quast et al. (1980b), include both glial cell proliferation and astrocytomas.
[c]Statistically significantly different from controls ($p < 0.05$) as calculated by the study authors.

Sources: Dow Chemical (1992a); Quast et al. (1980b).

5.4.3. Dose-Response Modeling

5.4.3.1. *Human Occupational Data*

A Cox regression model was developed based on an analysis of the Blair et al. (1998) lung cancer mortality data for AN-exposed workers. This model yielded a regression coefficient (β) estimate of 1.2×10^{-3} with an associated estimated standard error of 2.47×10^{-3} and a corresponding p value of 0.61. The 95% upper confidence limit (UCL) on the parameter estimate, β, was 5.3×10^{-3}. The parameter estimate, β, in this model was about threefold greater than the same parameter estimate in the final model developed by Starr et al. (2004), but the UCL was similar. The Cox regression model described above was used to predict an AN exposure concentration (EC) and its associated 95% lower confidence limit (LEC), associated with a 10^{-2} (1%) risk of dying from lung cancer at age 80 (EC_{01} and LEC_{01}, respectively). Conversions of occupational exposures to continuous environmental exposures were performed to account for differences in the number of days exposed per year (240 vs. 365 days) and in the amount of air inhaled during an 8-hour workday versus a 24-hour day (10 and 20 m^3/day, respectively). The resulting AN exposure estimates (by age 80) were EC_{01} = 0.992 ppm (or 2.2 mg/m^3) and LEC_{01} = 0.238 ppm (or 0.524 mg/m^3). The IUR estimate was then derived by linear extrapolation from the LEC_{01}. The corresponding unit risk was calculated to be 4.2×10^{-2} ppm^{-1} or 2×10^{-2} per mg/m^3. As previously noted, Appendix B-7 provides more details on this Cox regression analysis.

5.4.3.2. *Rat Oral Data*

Within each rat strain, sex, and tumor site, the multistage model, employing EPA's BMDS (version 1.4.1), was fit to the tumor incidence data from the bioassays in Sprague-Dawley (Quast, 2002) and F344 (Johannsen and Levinskas, 2002b) rats shown in Table 5-9 using two internal dose metrics, CEO concentration in blood (AUC/24 hours) and AN concentration in blood (AUC/24 hours). As already discussed, CEO is a DNA-reactive epoxide metabolite thought to play a key role in the carcinogenic mode of action of AN. The EPA-modified PBTK model employed consistently predicted higher CEO concentrations in blood and brain than were reported in studies of orally exposed rats (see Figures 3 and 4 in Kedderis et al., 1996). In contrast, AN concentrations in blood, brain, and liver predicted by the same PBTK model were fairly close to measured AN concentrations in rats following oral exposure. Ultimately, CEO levels in blood were chosen as the internal dose metric of choice for the oral cancer dose-response assessment because CEO is believed to be the most biologically relevant dose metric, and it is also consistent with the dose metric employed in derivation of the RfD. As with the RfD, CEO concentration in blood represents a reasonable internal dose metric for extrapolating from orally exposed rats to humans.

The AN concentrations in drinking water (in ppm) employed in the Quast (2002) and Johannsen and Levinskas (2002b) rat studies were converted to AN administered doses (in mg/kg-day) by the study authors, using water intake data recorded during the study. These administered doses of AN were then used as input into the EPA-modified rat PBTK model of Kedderis et al. (1996) in order to predict a rat internal dose (either CEO-AUC or AN-AUC concentration in blood) resulting from the ingestion of a total daily dose of AN equivalent to the administered dose consumed in six bolus episodes per day that reflect the daily drinking water consumption pattern of rats. The resulting predicted CEO-AUC or AN-AUC concentrations in rat blood were then employed in dose-response modeling. Table 5-11 displays the relationship between AN drinking water concentrations (in ppm), administered animal doses (in mg/kg-day), and two internal dose metrics (i.e., CEO in blood and AN in blood, both expressed in mg/L) predicted from the PBTK model.

Table 5-11. Four different dose metrics, two external and two internal, based on doses employed in studies of Sprague-Dawley and F344 rats exposed to AN in drinking water for 2 years

Species, strain (reference)	Sex	External dose		Predicted internal dose[a]	
		Concentration in drinking water (ppm)	Administered dose[b] (mg/kg-d)	CEO in blood (mg/L)	AN in blood (mg/L)
Rat, Sprague-Dawley (Quast, 2002)	Male	0	0	0	0
		35	3.4	1.83×10^{-3}	2.06×10^{-2}
		100	8.5	4.36×10^{-3}	5.36×10^{-2}
		300	21.3	9.70×10^{-3}	1.46×10^{-1}
	Female	0	0	0	0
		35	4.4	2.07×10^{-3}	2.37×10^{-2}
		100	10.8	4.87×10^{-3}	6.18×10^{-2}
		300	25.0	1.01×10^{-2}	1.56×10^{-1}
Rat, F344 (Johannsen and Levinskas, 2002b)	Male	0	0	0	0
		1	0.08	4.06×10^{-5}	4.33×10^{-4}
		3	0.25	1.27×10^{-4}	1.35×10^{-3}
		10	0.83	4.19×10^{-4}	4.52×10^{-3}
		30	2.48	1.23×10^{-3}	1.37×10^{-2}
		100	8.37	3.97×10^{-3}	4.85×10^{-2}
	Female	0	0	0	0
		1	0.12	5.32×10^{-5}	5.73×10^{-4}
		3	0.36	1.59×10^{-4}	1.72×10^{-3}
		10	1.25	5.49×10^{-4}	6.02×10^{-3}
		30	3.65	1.58×10^{-3}	1.79×10^{-2}
		100	10.90	4.46×10^{-3}	5.63×10^{-2}

[a]The EPA-modified rat PBPK model of Keddaris et al. (1996) was employed to predict a rat internal dose (i.e., either AN-AUC or CEO-AUC concentration in blood) resulting from the ingestion of an administered dose of AN consumed in six bolus episodes/d.
[b]Administered doses were averages calculated by the study authors based on animal BW and drinking water intake.

Employing the internal dose metrics in Table 5-11 (i.e., CEO in blood and AN in blood), successive stages of the multistage model, starting with stage 1 and ending with the stage equal to the number of dose groups minus one, were fit to the tumor incidence data at a particular site for each rat strain and sex. Then, all stages of the multistage model that did not show a significant lack of fit (i.e., $p > 0.1$) were compared using AIC. The stage of the multistage model with the lowest AIC was selected as the "best-fit" model. For most tumor sites, the one-stage model exhibited the best fit.

A BMR of 10% extra risk was selected for all tumor sites, consistent with the *Guidelines for Carcinogen Risk Assessment* (U.S. EPA, 2005a), which recommend identifying the POD near the lower end of the observed data. Using the best-fit model, the resulting BMD_{10}s and

$BMDL_{10}$s were estimated for each tumor site within each rat strain and sex. A summary of the results of this BMD modeling is shown in Table 5-12. Additional details regarding dose-response modeling used in the derivation of the oral CSFs are provided in Appendix B-3.

Table 5-12. BMD modeling results using tumor incidence data from male and female Sprague-Dawley and F344 rat studies in which animals were exposed to AN in drinking water for 2 years

Strain/species	Sex	BMD modeling results[a]			
		Tumor site	Dose metric	BMD_{10} (mg/L)	$BMDL_{10}$ (mg/L)
Sprague-Dawley rats	Male	Forestomach	CEO	1.87×10^{-3}	1.44×10^{-3}
			AN	2.26×10^{-2}	1.70×10^{-2}
		CNS	CEO	8.87×10^{-4}	7.16×10^{-4}
			AN	8.82×10^{-3}	6.64×10^{-3}
		Zymbal gland	CEO	5.46×10^{-3}	3.15×10^{-3}
			AN	8.94×10^{-2}	4.26×10^{-2}
		Tongue	CEO	8.78×10^{-3}	4.90×10^{-3}
			AN	1.29×10^{-1}	6.97×10^{-2}
	Female	Forestomach	CEO	3.29×10^{-3}	2.38×10^{-3}
			AN	4.22×10^{-2}	2.49×10^{-2}
		CNS	CEO	5.79×10^{-4}	4.51×10^{-4}
			AN	7.12×10^{-3}	5.55×10^{-3}
		Zymbal gland	CEO	2.40×10^{-3}	1.78×10^{-3}
			AN	3.41×10^{-2}	2.52×10^{-2}
		Tongue	CEO	6.70×10^{-3}	4.74×10^{-3}
			AN	9.67×10^{-2}	6.10×10^{-2}
		Mammary gland	CEO	5.50×10^{-4}	2.98×10^{-4}
			AN	7.05×10^{-3}	3.77×10^{-3}

Table 5-12. BMD modeling results using tumor incidence data from male and female Sprague-Dawley and F344 rat studies in which animals were exposed to AN in drinking water for 2 years

Strain/species	Sex	BMD modeling results[a]			
		Tumor site	Dose metric	BMD_{10} (mg/L)	$BMDL_{10}$ (mg/L)
F344 rats	Male	Forestomach	CEO	6.03×10^{-4}	3.55×10^{-4}
			AN	6.48×10^{-3}	3.81×10^{-3}
		CNS	CEO	1.16×10^{-3}	8.74×10^{-4}
			AN	1.37×10^{-2}	1.03×10^{-2}
		Zymbal gland	CEO	2.73×10^{-3}	2.19×10^{-3}
			AN	3.31×10^{-2}	2.59×10^{-2}
	Female	Forestomach	CEO	3.65×10^{-3}	1.69×10^{-3}
			AN	4.13×10^{-2}	1.90×10^{-2}
		CNS	CEO	1.39×10^{-3}	1.05×10^{-3}
			AN	1.70×10^{-2}	1.28×10^{-2}
		Zymbal gland	CEO	3.78×10^{-3}	2.97×10^{-3}
			AN	5.41×10^{-2}	3.35×10^{-2}
		Mammary gland	CEO	3.58×10^{-3}	1.97×10^{-3}
			AN	4.51×10^{-2}	2.45×10^{-2}

[a]The multistage model in EPA's BMDS (version 1.4.1) was fit to each set of tumor incidence data from the Sprague-Dawley and F344 rat bioassays, as shown in Table 5-9, using the two internal dose metrics, CEO in blood and AN in blood, expressed in mg/L. An adequate fit of the MS model was achieved if the χ^2 goodness-of-fit statistic yielded $p > 0.1$. In the case of CNS tumors in Sprague-Dawley female rats, an adequate fit of the multistage model to the data could not be achieved; therefore, the best fitting of the other models available in BMDS (assessed by AIC), the log-logistic model, was used. Numbers in parentheses indicate the number of dose groups dropped in order to obtain an adequate fit (starting with the highest dose group). Appendix B-3 provides further details on these BMD modeling results.

Sources: Johannsen and Levinskas (2002b) (F344); Quast (2002) (Sprague-Dawley).

After completion of the dose-response modeling, the $BMDL_{10}$s estimated for each tumor site within each rat strain and sex for each internal dose metric were input into the EPA-modified human PBTK model of Sweeney et al. (2003) in order to predict the human equivalent administered dose of AN that corresponds to the estimated $BMDL_{10}$, assuming six bolus ingestion episodes of AN per day. The resulting predicted human equivalent administered dose of AN, expressed in mg/kg-day, are shown in the third column of Table 5-13 for the internal dose metric CEO in blood and Table 5-14 for the internal dose metric AN in blood. Finally, for each rat strain, sex, and tumor site, the site-specific oral CSFs shown in the last column of Table 5-13 (based on CEO concentration in blood) and Table 5-14 (based on AN concentration in blood) were derived by dividing the BMR (i.e., 10% or 0.1) by the human equivalent administered dose of AN (in mg/kg-day), displayed in the third column of Tables 5-13 and 5-14.

Table 5-13. Site-specific oral CSFs for AN based on BMD modeling of tumor incidence data in rats and predicted CEO levels in blood (AUC/24 hours) of rats and humans assuming episodic exposure to AN

Rat strain, gender **Tumor site**	**Rat $BMDL_{10}$[a] (mg/L)**	**$BMDL_{10/HED}$[b] (mg/kg-d)**	**CSF[c] $(mg/kg\text{-}d)^{-1}$**
Sprague-Dawley males			
Forestomach	1.44×10^{-3}	0.142	0.704
CNS	7.16×10^{-4}	0.071	1.410
Zymbal gland	3.15×10^{-3}	0.312	0.320
Tongue	4.90×10^{-3}	0.486	0.206
Sprague-Dawley females			
Forestomach	2.38×10^{-3}	0.236	0.424
CNS	4.51×10^{-4}	0.045	2.222
Zymbal gland	1.78×10^{-3}	0.176	0.567
Tongue	4.74×10^{-3}	0.470	0.213
Mammary gland	2.98×10^{-4}	0.029	3.390
F344 males			
Forestomach	3.55×10^{-4}	0.035	2.850
CNS	8.74×10^{-4}	0.086	1.160
Zymbal gland	2.19×10^{-3}	0.217	0.462
F344 females			
Forestomach	1.69×10^{-3}	0.167	0.599
CNS	1.05×10^{-3}	0.104	0.963
Zymbal gland	2.97×10^{-3}	0.294	0.340
Mammary gland	1.97×10^{-3}	0.195	0.514

[a]Rat $BMDL_{10}$ refers to the estimated 95% lower confidence limit on the internal dose of CEO in blood in the rat associated with a 10% extra risk for the incidence of tumors at the specified site in the associated strain and sex. This value is taken from the last column of Table 5-12.
[b]PBTK model-derived HED of AN that would result in a human 24-hr blood CEO-AUC equivalent to the rat CEO-AUC presented in the previous column of the table, assuming AN ingestion in six bolus episodes/d.
[c]$CSF = BMR/BMDL_{10/HED}$ or $0.1/BMDL_{10/HED}$.

Sources: Johannsen and Levinskas (2002b) (F344); Quast (2002) (Sprague-Dawley).

Table 5-14. Site-specific oral CSFs for AN based on BMD modeling of tumor incidence data in rats and predicted AN levels in blood (AUC/24 hours) of rats and humans assuming episodic exposure to AN

Rat strain, gender Tumor site	Rat $BMDL_{10}$[a] (mg/L)	$BMDL_{10/HED}$[b] (mg/kg-d)	CSF[c] $(mg/kg\text{-}d)^{-1}$
Sprague-Dawley males			
Forestomach	1.70×10^{-2}	4.30	0.023
CNS	6.64×10^{-3}	1.89	0.053
Zymbal gland	4.26×10^{-2}	8.59	0.012
Tongue	6.97×10^{-2}	11.85	0.008
Sprague-Dawley Females			
Forestomach	2.49×10^{-2}	5.82	0.017
CNS	5.55×10^{-3}	1.60	0.062
Zymbal gland	2.52×10^{-2}	5.87	0.017
Tongue	6.10×10^{-2}	10.90	0.009
Mammary gland	3.77×10^{-3}	1.11	0.090
F344 males			
Forestomach	3.81×10^{-3}	1.12	0.089
CNS	1.03×10^{-2}	2.82	0.036
Zymbal gland	2.59×10^{-2}	5.99	0.017
F344 females			
Forestomach	1.90×10^{-2}	4.71	0.021
CNS	1.28×10^{-2}	3.38	0.030
Zymbal gland	3.35×10^{-2}	7.26	0.014
Mammary gland	2.45×10^{-2}	5.75	0.017

[a]Rat $BMDL_{10}$ refers to the estimated 95% lower confidence limit on the internal dose of AN in blood in the rat associated with a 10% extra risk for the incidence of tumors at the specified site in the associated strain and sex. This value is taken from the last column of Table 5-12.
[b]PBTK model-derived HED of AN that would result in a human 24-hr blood AN-AUC equivalent to the rat AN-AUC presented in the previous column of the table, assuming AN ingestion in six bolus episodes/d.
[c]$CSF = BMR/BMDL_{10/HED}$ or $0.1/BMDL_{10/HED}$.

Sources: Johannsen and Levinskas (2002b) (F344); Quast (2002) (Sprague-Dawley).

In comparing Tables 5-13 and 5-14, the CEO-based site-specific oral CSF estimates in Table 5-13 are higher than those based on AN blood levels in Table 5-14. This occurs because the $V_{max}C/K_m$ for AN oxidation to CEO is estimated to be about 10 times higher in humans than in the rat. AN enzymatic GSH conjugation is estimated to be 1.5 times higher in the rat, but the 2^{nd}-order removal constant for non-enzymatic reaction of AN and GSH is assumed to be the same and the GSH tissue levels are roughly the same (and lower in the larger tissue groups). The result, for example, with a steady oral "infusion" of 30 mg/kg-day, is that AN is removed somewhat faster overall, leading to physiologically based pharmacokinetic (PBPK) predicted

steady-state blood level of 0.114 mg/L AN in humans vs. 0.151 in the rat, but a much higher portion of this goes to CEO in the human yielding a CEO blood level of 0.297 vs. 0.013 mg/L in the rat. Thus, AN:CEO = 11.4 in the rat and 0.385 in the human, and so the CEO-based risk estimates are approximately 50 times higher than the AN-based estimates.

For comparative purposes, in Table 5-15, the $BMDL_{10}$ estimates generated from the BMD modeling of the incidence of tumors in male and female Sprague-Dawley and F344 rats using administered animal dose (modeling results not shown) were converted to human equivalent administered doses of AN using BW scaling to the ¾ power. Then, as in Tables 5-13 and 5-14, oral CSFs were derived by dividing the BMR (i.e., 10% or 0.1) by the human equivalent administered dose of AN (in mg/kg-day).

Table 5-15. Site-specific oral CSFs for AN based on BMD modeling of tumor incidence data in rats and BW scaling to the ¾ power to convert from rat to human administered doses

Rat strain, gender **Tumor site**	**Rat $BMDL_{10}$[a] (mg/kg-d)**	**$BMDL_{10/HED}$[b] (mg/kg-d)**	**CSF[c] $(mg/kg\text{-}d)^{-1}$**
Sprague-Dawley males			
Forestomach	2.76	0.812	0.123
CNS	1.48	0.436	0.229
Zymbal gland	5.17	1.52	0.066
Tongue	10.4	3.04	0.033
Sprague-Dawley females			
Forestomach	4.81	1.27	0.079
CNS	0.99	0.262	0.382
Zymbal gland	4.19	1.11	0.090
Tongue	8.30	2.19	0.046
Mammary gland	0.66	0.174	0.575
F344 males			
Forestomach	0.70	0.193	0.517
CNS	1.81	0.493	0.203
Zymbal gland	3.43	0.932	0.107
F344 females			
Forestomach	3.89	0.926	0.108
CNS	2.52	0.602	0.166
Zymbal gland	6.64	1.59	0.063
Mammary gland	4.77	1.14	0.088

[a]Rat $BMDL_{10}$ is the estimated 95% lower confidence limit on the administered dose of AN in the rat associated with a 10% extra risk for the incidence of tumors at the specified site in the associated strain and sex. This value is generated from the "best-fit" dose-response model in BMDS (version 1.4.1).
[b]The HED of AN equal to the rat $BMDL_{10}$ in the previous column converted through use of BW scaling to the ¾ power.
[c]$CSF = BMR/BMDL_{10/HED}$ or $0.1/BMDL_{10/HED}$.

Sources: Johannsen and Levinskas (2002b) (F344); Quast (2002) (Sprague-Dawley).

5.4.3.3. *Rat Inhalation Data*

Within each sex and for each tumor site, the multistage model, employing EPA's BMDS (version 1.4.1), was fit to the tumor incidence data from the AN inhalation bioassay in Sprague-Dawley rats (Quast et al., 1980b) shown in Table 5-10 using the internal dose metric, CEO concentration in blood (AUC/24 hours). In contrast to the approach used for oral exposure, only one internal dose metric was selected on which to base site-specific IURs (i.e., CEO in blood), because, in contrast to oral exposure, the EPA-modified PBTK model adequately predicted measured blood and brain concentrations of CEO in rats exposed to AN via inhalation (Kedderis et al., 1996). Furthermore, as mentioned previously, CEO is the DNA-reactive metabolite thought to be key in the carcinogenic mode of action of AN.

Prior to dose-response modeling, the AN concentrations in air (in ppm) administered in the Quast et al. (1980b) rat study were input into the EPA-modified rat PBTK model of Kedderis et al. (1996) in order to predict a rat internal dose (CEO-AUC concentration in blood) resulting from inhalation exposure to the administered air concentration of AN. The resulting predicted CEO-AUC concentrations in rat blood were then employed in dose-response modeling. Table 5-16 displays the relationship between AN concentrations in air (expressed in ppm) and the internal dose metric, CEO in blood (expressed in mg/L), predicted from the PBTK model.

Table 5-16. Two different dose metrics, one external and one internal, based on administered air concentrations of AN employed in a 2-year bioassay in Sprague-Dawley rats

Species, strain	Sex	Exposed AN concentration in air (ppm)	Predicted CEO concentration in blood[a] (mg/L)
Rat, Sprague-Dawley	Male	0	0
		20	2.17×10^{-3}
		80	8.20×10^{-3}
	Female	0	0
		20	2.18×10^{-3}
		80	8.24×10^{-3}

[a]See Table 5-11.

Source: Quast et al. (1980b).

After completion of the dose-response modeling, the BMC_{10}s and $BMCL_{10}$s estimated within each sex for each tumor site using CEO in blood as the dose metric from Table 5-17 were input into the EPA-modified human PBTK model of Sweeney et al. (2003) in order to predict the HEC of AN in air that corresponds to the estimated BMC_{10} and $BMCL_{10}$ in animals. The resulting predicted 95% lower bounds of the HECs ($BMCL_{10/HEC}$) of AN in air, expressed in

mg/m^3, are shown in the third column of Table 5-18 for the internal dose metric CEO in blood. Finally, for each sex and tumor site, the site-specific IURs shown in the last column of Table 5-19 (based on CEO concentration in blood) were derived by dividing the BMR (i.e., 10% or 0.1) by the $BMCL_{10/HEC}$.

Table 5-17. BMD modeling results using tumor incidence data from male and female Sprague-Dawley rats exposed to AN via inhalation for 2 years and CEO concentration in blood predicted from an EPA-modified PBTK model

Strain, species	Sex	BMD modeling results			
		Tumor site	Dose metric	BMC_{10} (mg/L)	$BMCL_{10}$ (mg/L)
Rat, Sprague-Dawley	Male	Intestine	CEO	6.06×10^{-3}	4.47×10^{-3}
		CNS	CEO	3.14×10^{-3}	2.31×10^{-3}
		Zymbal gland	CEO	7.26×10^{-3}	4.40×10^{-3}
	Female	Tongue	CEO	9.48×10^{-3}	6.39×10^{-3}
		CNS	CEO	3.21×10^{-3}	2.39×10^{-3}
		Zymbal gland	CEO	7.90×10^{-3}	5.09×10^{-3}
		Mammary gland	CEO	7.31×10^{-3}	4.33×10^{-3}

[a]The multistage model in EPA's BMDS (version 1.4.1) was fit to each set of tumor incidence data from the Sprague-Dawley rat bioassay, as shown in Table 5-10, using the internal dose metric, CEO in blood, expressed in mg/L. An adequate fit of the multistage model was achieved if the χ^2 goodness-of-fit statistic yielded $p > 0.1$. Appendix B-4 provides further details on these BMD modeling results.

Source: Quast et al. (1980b).

Table 5-18. Site-specific IURs for AN based on BMD modeling of tumor incidence data in Sprague-Dawley rats and PBTK modeling of CEO levels in blood (AUC/24 hours) of rats and humans

Gender **Tumor site**	**Rat $BMCL_{10}$[a] (mg/L)**	**$BMCL_{10/HEC}$[b] (mg/m^3)**	**IUR[c] $(mg/m^3)^{-1}$**
Males			
Intestine	4.47×10^{-3}	6.00	0.017
CNS	2.31×10^{-3}	3.10	0.032
Zymbal gland	4.40×10^{-3}	5.91	0.017
Tongue	6.39×10^{-3}	8.58	0.012
Females			
CNS	2.39×10^{-3}	3.21	0.031
Zymbal gland	5.09×10^{-3}	6.83	0.015
Mammary gland	4.33×10^{-3}	5.81	0.017

[a]Rat $BMCL_{10}$ refers to the estimated 95% lower confidence limit on the concentration of CEO in blood of the rat associated with a 10% extra risk for the incidence of tumors at the specified site based on BMD modeling. This value is taken from the last column of Table 5-17.
[b]PBTK model-derived HEC of AN in air that would result in a human 24-hr blood CEO-AUC concentration equivalent to the rat $BMCL_{10}$ in the previous column of the table assuming continuous exposure to AN. The human PBTK model employed did not contain the human in vitro to in vivo modifying factor for CEO hydrolysis proposed by Sweeney et al. (2003).
[c]IUR = $BMR/BMCL_{10/HEC}$ or $0.1/BMCL_{10/HEC}$.

Table 5-19. Site-specific IURs for AN based on BMD modeling of tumor incidence data in Sprague-Dawley rats exposed to AN via inhalation

Gender **Tumor site**	**Rat $BMCL_{10}$[a] (ppm)**	**$BMCL_{10/HEC}$[b] (mg/m^3)**	**IUR[c] $(mg/m^3)^{-1}$**
Males			
Intestine	42.68	93.58	1.07×10^{-3}
CNS	22.23	48.74	2.05×10^{-3}
Zymbal gland	42.53	93.25	1.07×10^{-3}
Tongue	59.41	130.26	7.68×10^{-4}
Females			
CNS	22.89	50.19	1.99×10^{-3}
Zymbal gland	48.74	106.87	9.36×10^{-4}
Mammary gland	37.82	82.92	1.21×10^{-3}

[a]Rat $BMCL_{10}$ refers to the estimated 95% lower confidence limit on the concentration of AN in air associated with a 10% extra risk for the incidence of tumors at the specified site based on BMD modeling.
[b]The HEC of AN in air equivalent to the rat $BMCL_{10}$ in the previous column of the table generated through use of the following conversion equation: mg/m^3 = [ppm × molecular weight]/24.20, where molecular weight = 53.06.
[c]IUR = $BMR/BMCL_{10/HEC}$ or $0.1/BMCL_{10/HEC}$.

5.4.4. Cancer Risk Values

5.4.4.1. *Oral CSFs*

Because AN has been demonstrated to produce tumors at multiple sites in rats, the estimation of risk based on only one tumor site may underestimate the overall carcinogenic potential of AN. Under the assumption that AN causes tumors by a mutagenic mode of action, estimates of the composite risk of etiologically distinct tumor types in each rat strain/sex combination considered in Section 5.4.3.2 were derived employing the Bayesian approach described in Appendix B-6. This approach is consistent with the recommendations of the NRC (1994) and the *Guidelines for Carcinogen Risk Assessment* (U.S. EPA, 2005a), which recommends "adding risk estimates derived from different tumor sites (NRC, 1994) as an option for "how best to represent the human cancer risk." This composite risk is associated with the potential for developing tumors, not at all of the sites, but at any combination of the sites observed in male or female rats. For this analysis, the etiologically distinct tumor sites associated with AN exposure were assumed to be statistically independent. This assumption cannot currently be verified, but if not correct could lead to an overestimate of risk. NRC (1994) concluded that a general assumption of statistical independence of tumors within animals was not likely to introduce substantial error in assessing carcinogenic potency from rodent bioassay data.

Table 5-20 presents the estimated human equivalent oral CSFs for both site-specific risks and composite risks from multiple tumor types from each rat strain and sex exposed to AN via drinking water based on the internal dose metric, CEO concentration in blood (AUC over 24 hours).

Table 5-20. Estimated human equivalent oral CSFs for composite risk based on tumor incidence in AN-exposed rats and predicted CEO-AUC levels in blood

Rat strain and gender Tumor sites included	Site-specific oral CSF[a] $(mg/kg\text{-}d)^{-1}$	Oral CSF for composite risk across sites $(mg/kg\text{-}d)^{-1}$
Sprague-Dawley Male		
Forestomach	0.704	2.8
CNS	1.410	
Zymbal gland	0.320	
Tongue	0.206	
Sprague-Dawley Female		
Forestomach	0.424	5.0
CNS	2.222	
Zymbal gland	0.567	
Tongue	0.213	
Mammary gland	3.390	
F344 Male		
Forestomach	2.850	3.1
CNS	1.160	
Zymbal gland	0.462	
F344 Female		
Forestomach	0.599	1.9
CNS	0.963	
Zymbal gland	0.340	
Mammary gland	0.514	

[a]These site-specific oral CSFs are taken from the last column of Table 5-13.

In Sprague-Dawley rats, males showed statistically significantly increased incidences of tumors at four sites (i.e., forestomach, CNS, Zymbal gland, and tongue), while females showed statistically significantly increased incidences of tumors at five sites (i.e., forestomach, CNS, Zymbal gland, tongue, and mammary gland), following chronic oral exposure to AN. The composite oral CSF based on tumor incidences in male Sprague-Dawley rats chronically exposed to AN (using CEO concentration in blood) is estimated to be 2.8 per mg/kg-day, about twice as high as the estimated slope factor resulting from the most sensitive single site in this strain and sex. For female Sprague-Dawley rats, the composite oral CSF (based on CEO concentration in blood) was 5.0 per mg/kg-day, approximately 50% higher than the estimated slope resulting from the most sensitive single site in this strain and sex.

In F344 rats, males showed statistically significant increased incidences of tumors at three sites (i.e., forestomach, CNS, and Zymbal gland), while females showed statistically significant increased incidences of tumors at four sites (i.e., forestomach, CNS, Zymbal gland, and mammary gland), following oral exposure to AN in drinking water for 2 years. Again, under

the assumption that the tumors at these sites are statistically independent, the composite oral CSF in F344 males (based on CEO concentration in blood) was 3.1 per mg/kg-day, slightly higher than the estimated slope factor of 2.8 per mg/kg-day based on tumors in the forestomach alone, the most sensitive single site in this strain and sex. For female F344 rats, the composite oral CSF (based on CEO concentration in blood) was 1.9 per mg/kg-day, about twice the estimated slope factor of 0.96 per mg/kg-day from tumors of the CNS, the most sensitive single site in this strain and sex.

The slope factors obtained from male and female Sprague-Dawley rats and F344 rats ranged from 2 to 5 $(mg/kg\text{-}day)^{-1}$. While female Sprague-Dawley rats had the highest slope factor due to increase in mammary gland tumor risk, the increase in mammary gland tumor risk in female F344 rats was not as high. There is no information as to which rat strain may be most similar to humans. Both strains of rats developed same tumors in response to AN exposure. For the purpose of this assessment, the slope factor of 5 per mg/kg-day is recommended for use in humans because it is the value obtained from the most sensitive species, strain, and sex (i.e., female Sprague-Dawley rats). This slope factor should not be used with exposures greater than 0.04 mg/kg-day (the lowest POD supporting the composite risk) because above this level the slope factor cannot be expected to be an adequate approximation to the dose-response relationship. The fitted dose-response relationship and pharmacokinetic models should be used to estimate risk above this exposure level. See Section 5.6 regarding the application of age-dependent adjustment factors (ADAFs).

Previous IRIS Assessment

In the previous IRIS assessment completed in 1991, EPA derived an oral CSF of 5×10^{-1} $(mg/kg\text{-}day)^{-1}$ by application of the linearized multistage model to incidence data from rats with astrocytomas, Zymbal gland carcinomas, or forestomach papillomas or carcinomas from the three 2-year drinking water studies in rats considered under the current assessment (Biodynamics, 1980a,c; Quast et al., 1980a). At that time, no PBTK models were available for generating internal dose metrics or informing interspecies extrapolation; therefore, interspecies extrapolation was accomplished using $BW^{2/3}$ scaling. The final slope factor of 5×10^{-1} $(mg/kg\text{-}day)^{-1}$ was the geometric mean of the slope factors derived from each of these three studies, i.e., 4×10^{-1} $(mg/kg\text{-}day)^{-1}$ (Biodynamics, 1980a), 4×10^{-1} $(mg/kg\text{-}day)^{-1}$ (Biodynamics, 1980c), and 10×10^{-1} $(mg/kg\text{-}day)^{-1}$ (Quast et al., 1980a).

5.4.4.2. *Inhalation Unit Risk*

Employing human data, the EC_{01} and LEC_{01}, defined as the AN exposure concentration and its associated 95% lower confidence limit, respectively, that result in a 1% increase in the risk of dying from lung cancer at age 80 were estimated from the Cox regression model derived from the Blair et al. (1998) occupational epidemiology study. These EC_{01} and LEC_{01} values

were 0.992 and 0.238 ppm, respectively (or 2,187 and 524 μg/m^3, respectively). From the LEC_{01}, an IUR of 4.2×10^{-2} ppm^{-1} or 2×10^{-2} (mg/m^3)$^{-1}$ was derived.

For inhalation exposures to AN in animals, as with oral exposures, estimates of composite risk addressing multiple tumor sites (within strain and sex) based on BMD modeling results from a chronic inhalation rodent bioassay in Sprague-Dawley rats (Dow Chemical 1992a; Quast et al., 1980b) were generated. These estimates were derived employing the same Bayesian approach described in Appendix B-6 for oral exposures.

Table 5-21 presents the human equivalent IURs for both site-specific risks and composite risks from multiple tumor types observed in each sex of Sprague-Dawley rat exposed to AN using the internal dose metric, CEO concentration in blood (AUC for 24 hours).

Table 5-21. Estimated human equivalent composite IURs based on tumor incidence in AN-exposed rats and predicted CEO-AUC levels in blood

Rat strain and gender Tumor sites included	**Site-specific IUR** [a] (mg/m^3)$^{-1}$	**Composite IUR** (mg/m^3)$^{-1}$
Sprague-Dawley male		
Intestine	0.017	6.8×10^{-2}
CNS	0.032	
Zymbal gland	0.017	
Tongue	0.012	
Sprague-Dawley female		
CNS	0.031	5.7×10^{-2}
Zymbal gland	0.015	
Mammary gland	0.017	

[a]These site-specific IURs are taken from the last column of Table 5-18.

From the inhalation bioassay, male rats showed statistically significant elevated tumor incidences at four sites (i.e., intestine, CNS, Zymbal gland, and tongue), while female rats showed statistically significant elevations at three tumor sites (i.e., CNS, Zymbal gland, and mammary gland), when exposed to AN via inhalation for 2 years. Under the assumption that tumors at these sites are statistically independent, the estimated composite IUR in male rats was 6.8×10^{-2} per mg/m^3, approximately 2 times higher than the site-specific IUR estimate of 3.2×10^{-2} per mg/m^3 based on the most sensitive single site in males (i.e., CNS). For female rats, the composite IUR was 5.7×10^{-2} per mg/m^3, about 2 times higher than the site-specific estimate of 3.1×10^{-2} per mg/m^3 from the most sensitive single site in females (i.e., CNS). These unit risks should not be used with exposures greater than 3 mg/m^3 (the lowest POD supporting the composite risk), because above this level the unit risk cannot be expected to be an adequate approximation of the dose-response relationship. The fitted dose-response relationship and pharmacokinetic models should be used to estimate risk above this exposure level.

The IUR recommended for use in estimating cancer risks associated with chronic inhalation exposures to AN during adult stages of development is 2×10^{-2} per mg/m^3 (or 2×10^{-5} per μg/m^3)—the value based on human data (i.e., the occupational epidemiology study by Blair et al., 1998). See Section 5.4.4.3 regarding the application of ADAFs.

Previous IRIS assessment

In the previous IRIS assessment, an IUR was also derived based on human data. This IUR was based on an increase in lung cancer incidence in humans occupationally exposed to AN, as described by O'Berg (1980). A value of 6.8×10^{-5} per μg/m^3 was derived by the application of an RR model, which was adjusted for smoking and was based on a continuous lifetime equivalent of occupational exposure to AN.

5.4.4.3. *Quantitative Analysis of Early Life Exposure Scenarios*

The mode of action for carcinogenicity of AN is determined to be mutagenic (Section 4.7.3.1), which raises concern for increased early life cancer susceptibility. Consistent with this possibility, two studies in Sprague-Dawley rats provide evidence of increased cancer susceptibility associated with chronic AN exposure that begins in early periods of development—a chronic-duration inhalation cancer bioassay (Maltoni et al., 1988) and a three-generation drinking water reproductive toxicity study (Friedman and Beliles, 2002). This evidence was summarized in Section 4.8.1. According to the *Supplemental Guidance for Assessing Susceptibility from Early-Life Exposure to Carcinogens* (U.S. EPA, 2005b), "when developing quantitative estimates of cancer risk, the Agency recommends integration of age-specific values for both exposure and toxicity/potency where such data are available and appropriate" (also see Box 5 in Figure 3 in U.S. EPA [2005b]). The available evidence is considered below.

5.4.4.3.1. ***Summary of Maltoni et al. (1988)***. Maltoni et al. (1988) exposed pregnant Sprague-Dawley rats to 60 ppm AN by inhalation for 104 weeks (see Section 4.2.2.2.2 for a complete description). In addition, the offspring of these dams were exposed to AN starting at GD 12 for a total of either 15 or 104 weeks. All animals were observed until natural death.

As noted in Section 4.2.2.2.2, Maltoni et al. (1988) reported statistically significant increases in tumor incidences for both male and female offspring exposed for 104 weeks compared with their controls. Female offspring showed statistically significant increases in malignant mammary tumors, encephalic gliomas, and extra-hepatic angiosarcomas, while male offspring showed statistically significant increases in encephalic gliomas, Zymbal gland carcinomas, and hepatomas. While there were no statistically significant increases for the exposed dams, their responses were slightly increased over background for most of these sites—mammary tumors at 2.3% extra risk, encephalic gliomas at 5.6%, extra-hepatic angiosarcomas at

1.9%, and Zymbal gland tumors at 3.8%. No hepatomas were observed in the dams. These results are summarized in Table 5-22. Note that there were no concurrently exposed or control adult male rats with which to compare the male offspring incidences; comparisons with the female adult data involve assuming that adult male responses would have been concordant. Although this profile of responses is similar to that seen for the female rats in Quast et al. (1980b),[2] the Quast study was not considered to be a suitable baseline for analyzing the male offspring responses.

For offspring exposed for a total of 15 weeks, although there were no statistically significantly elevated tumor incidences at any of the evaluated sites, the responses at these sites were elevated over respective controls and were consistent with a linear or even supralinear increase in response with increasing length of exposure to 60 ppm. Figure 5-3 shows the responses for both sets of offspring and the dams for the sites with statistically significant responses after chronic exposure. Note that while the extra-hepatic angiosarcoma response in the male offspring was not statistically significant for either exposure group, the responses were of a similar magnitude to the response of the female offspring exposed for 104 weeks. Although the study did not have sufficient power to find individual group responses of about 5% and below statistically significant, the mostly statistically significant trends and their consistency across sites, as well as across sexes for the angiosarcomas, add weight to the overall conclusion of increased early-life susceptibility to the carcinogenicity of AN.

[2]Assuming a continuous equivalent lifetime exposure concentration of 12.1 ppm for the administered concentration in the Maltoni et al. (1988) study, dose-response relationships developed from the Quast et al. (1980b) inhalation study (without considering pharmacokinetics) predict a similar incidence profile for the adult female rats, at about 2% extra risk predicted vs. 2.3% observed for mammary tumors, 10 vs. 5.6% observed for gliomas, and 0% predicted vs. 1.9% observed for extra-hepatic angiosarcomas. The differences between the female adult rats in the two studies are not large and can be explained by differences between animal colonies and husbandry practices, including diet. This analysis provides some assurance that any early-life susceptibility estimates derived from Maltoni et al. (1988) are compatible with the unit risks derived from the Quast et al. (1980b) bioassay.

Table 5-22. Tumor incidences in Sprague-Dawley rats following inhalation exposure to 60 ppm AN for 104 weeks, starting either in utero (GD 12) or as adults at 13 wks of age

Tumor site	Age at start of exposure	Length of exposure to 60 ppm								Trend test *p*-value[b]	Ratio of GD 12 and 13-week groups' extra risks at 104 weeks
		0 weeks (control)		15 weeks			104 weeks				
		x/n[a]	%	x/n[a]	%	Extra risk	x/n[a]	%	Extra risk		
Female rats											
Malignant mammary tumors	GD 12	8/149	5.4	4/60	6.7	1.4	9/54	16.7	11.9	0.008	5.1
	13 wks	2/60	3.3	–	–	–	3/54	5.6	2.3	>0.05	
Encephalic gliomas	GD 12	2/149	1.3	2/60	3.3	2.0	10/54	18.5	17.4	<0.001	3.1
	13 wks	0/60	0.0	–	–	–	3/54	5.6	5.6	>0.05	
Extrahepatic angiosarcomas	GD 12	0/149	0.0	1/60	1.7	1.7	3/54	5.6	5.6	0.005	3.0
	13 wks	0/60	0.0	–	–	–	1/54	1.9	1.9	>0.05	
Male rats											
Encephalic gliomas	GD 12	2/158	1.3	3/60	5.0	3.8	11/67	16.4	15.3	<0.001	*2.8*
	13 wks[c]	*0/60*	*0.0*	–	–	–	*3/54*	*5.6*	*5.6*	*>0.05*	
Zymbal gland carcinomas	GD 12	2/158	1.3	4/60	6.7	5.5	10/67	14.9	13.8	<0.001	*3.5*
	13 wks	*1/60*	*1.7*	–	–	–	*3/54*	*5.6*	*3.8*	*>0.05*	
Hepatomas	GD 12	1/158	0.6	1/60	1.7	1.0	5/67	7.5	6.9	0.002	*NA*
	13 wks	*0/60*	*0.0*	–	–	–	*0/54*	*0.0*	*0.0*	*>0.05*	
Extrahepatic angiosarcomas	GD 12	1/158	0.6	3/60	5.0	4.4	3/67	4.5	3.9	>0.05	*2.1*
	13 wks	*0/60*	*0.0*	–	–	–	*1/54*	*1.9*	*1.9*	*>0.05*	

[a]x = number of animals with specified tumor, n = number of animals at start of exposure.
[b]Cochran-Armitage trend test for datasets with 3 or more groups (early-life exposures); Fisher's exact test otherwise (adult exposures).
[c]Values in italics rely on adult female rat data; no male rats were exposed starting at age 13 wks in this study.

Source: Maltoni et al. (1988).

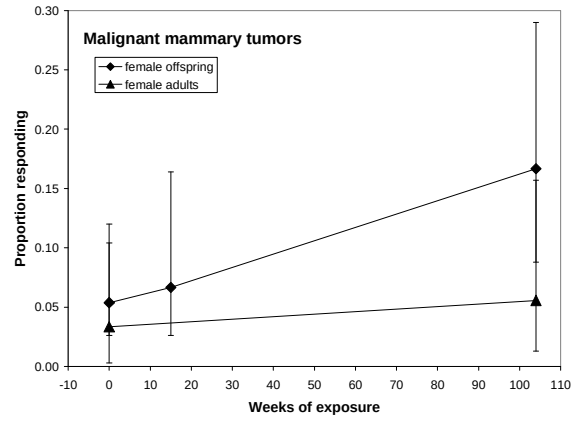

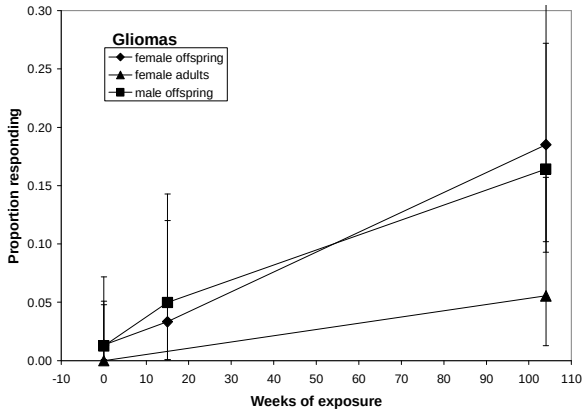

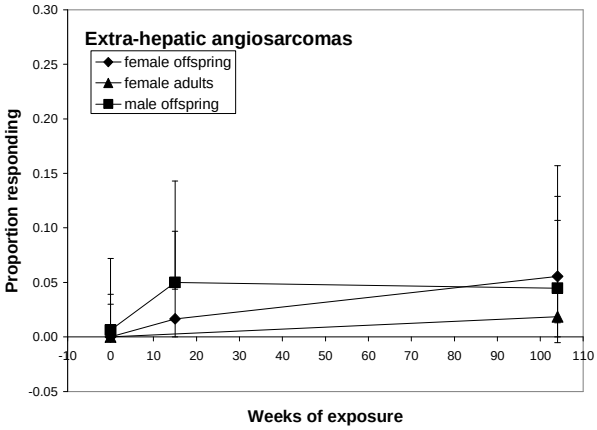

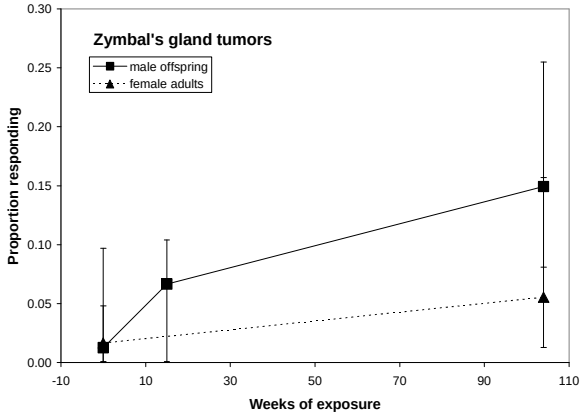

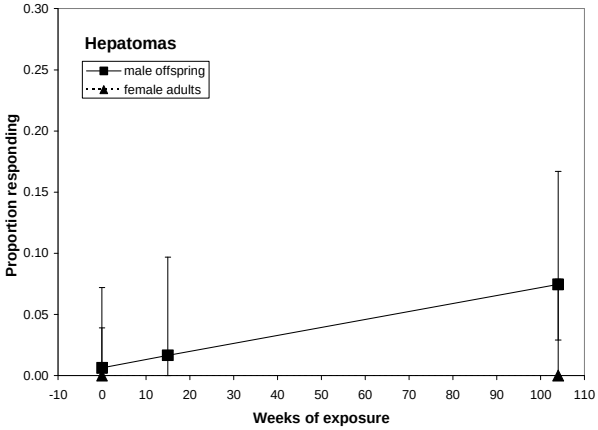

Error bars denote 95% CIs for each response.

Figure 5-3. Comparison of tumor responses to inhalation exposure of acrylonitrile, by age at start of exposure (offspring at GD 12, adults at 13 weeks), sex, and length of exposure, for Sprague-Dawley rats (Maltoni et al., 1988).

Figure 5-3 shows linear trends with increasing length of exposure among the offspring for malignant mammary tumors (females), gliomas (males and females), extrahepatic angiosarcomas (females) and hepatomas (males), while supralinear trends are suggested for extrahepatic angiosarcomas and Zymbal gland tumors in males. Linear trends suggest that offspring responses to the 15-week exposure are proportional to offspring responses resulting from the chronic exposure; that is, that the expected response is about 1/7 (15 weeks/104 weeks) of the response to chronic exposure starting in utero. The overall response after 104 weeks of exposure is markedly higher than that of the chronically exposed adult rats, suggesting that once the susceptible process (or processes) has started it continues well into adulthood. For each site, the ratios of the extra risk associated with chronic exposure starting at GD 12 relative to starting at age week 13 ranged from about 3 to 5 for individual sites in female rats, supported by a factor of 3 for gliomas in male rats (see Table 5-22).

In contrast, the supralinear trends suggest greater than proportional susceptibility in the early-life period which decreases over time, or which does not occur after the early-life period, as possibly illustrated by the male offspring angiosarcomas. On the other hand, the 15-week period used in this study includes a nontrivial period that cannot be considered early-life, given that rats are generally considered sexually mature by about 8 weeks of age. Consequently the magnitude of the early-life sensitivity, at least for two tumor sites, may be underestimated by these data without further characterization of the most sensitive timeframe. The low numbers of responses from the 15-week exposures (1–4 offspring and 0–3 adults responding per site) likely impact the resolution of early-life susceptibility estimates for these sites. From an overall point of view, however, note that the 15-week responses considered collectively are generally similar to the female adult responses following 104 weeks of exposure. Because these early-life responses result from sevenfold less exposure, they demonstrate approximately 7 times (or approximately one order of magnitude) more sensitivity than the adult responses.

5.4.4.3.2. ***Summary of Friedman and Beliles (2002).*** Supporting evidence of increased early-life susceptibility was also seen in the three-generation reproduction study reported by Friedman and Beliles (2002). There were statistically significant increases in Zymbal gland carcinomas and astrocytomas after approximately 51 weeks of exposure to 500 ppm AN in drinking water for F1 Sprague-Dawley female rats relative to F1 controls, while the incidences for F0 female rats were not significantly elevated at 500 ppm. The incidences for F2 female rats, exposed in utero like the F1 females, were not considered to be significantly elevated. Section 4.2.1.2.8 provides details of the study design, and Table 5-23 summarizes the results.

Table 5-23. Tumor incidences in female Sprague-Dawley rats exposed to AN in drinking water for approximately 46 weeks, starting either in utero or at 5 weeks of age

Tumor site	Generation	Tumor incidence, and percent, at AN in drinking water, ppm			Trend test *p*-value[a]	Ratio of early life + adult to adult extra risks at 500 ppm
		0	100	500		
Brain astrocytomas	F0 (adult exposure)	0/19 (0%)	1/20 (5%)	2/24 (8%)	0.247	–
	F1b	0/20 (0%)	1/19 (5%)	4/17 (24%)	0.005	2.8
	F2b	0/20 (0%)	1/20 (5%)	1/20 (5%)	0.506	–
	F1b + F2b	0/40 (0%)	2/39 (5%)	5/37 (14%)	0.007	1.8
Zymbal gland	F0 (adult exposure)	0/19 (0%)	0/20 (0%)	2/24 (8%)	0.036	–
	F1b	0/20 (0%)	2/19 (11%)	3/17 (18%)	0.088	2.1
	F2b	0/20 (0%)	0/20 (0%)	3/20 (15%)	0.007	1.9
	F1b + F2b	0/40 (0%)	2/39 (5%)	6/37 (16%)	0.005	2.0

[a]Cochran-Armitage test for linear trend.

Sources: Friedman and Beliles (2002); Litton Bionetics (1992).

Ratios of extra risks of astrocytomas and Zymbal gland tumors were estimated for the 500 ppm F1b and F2b groups if there was a statistically significant linear trend. These results suggest an increased early-life cancer susceptibility of about two- to threefold at the high dose. However, these results do not support a quantitative estimate of relative susceptibility because several factors contribute to underestimating any susceptibility. First, with only 20 animals per treatment group, this study had limited power to detect tumor increases, relative to the Maltoni et al. (1988) study and most other carcinogencity studies, with the consequence that any increased susceptibility at the low dose (100 ppm) may be less readily apparent. For example, an apparent effect of 0/20 is consistent with a tumor response as high as 17%, the 95% UCL on a response of 0/20.

Second, while it is notable that tumors were observed as early as they were, after no more than 51 weeks without another year of follow-up, these data do not inform lifetime risk estimates adequately. Although cancer incidence is expected to increase with increasing age (Doll, 1971), dose-response relationships starting at different ages may not be parallel. Given the short exposure and follow-up in this study, the data from this group are better considered as supporting early-life susceptibility qualitatively.

5.4.4.3.3 ***Analysis to support estimation of early-life susceptibility adjustment factors.*** In summary, two data sets support the conclusion of increased susceptibility to carcinogenicity with AN exposure in early life. One data set conducted by Maltoni et al. (1988), in female rats with

chronic exposure starting in early life or starting as adults, provides a sufficient basis for developing quantitative estimates of susceptibility. Due to the lack of adult male referent groups (control or exposed), the male offspring data provide support for early-life susceptibility. The female data supported point estimates for susceptibility adjustment factors of 5, based on malignant mammary tumors, and 3, based on gliomas or extra-hepatic angiosarcomas. In other words, cancer potency for specific tumor sites following chronic exposure to 60 ppm AN appears to be three- to fivefold higher if exposure starts in early-life rather than during adulthood.

Before recommending ADAFs based on these data, important considerations include the impact of experimental variability and overall risk encompassing multiple tumors. Given the incomplete understanding of the operant modes of action, it is unknown whether the tumor types observed in the Maltoni et al. (1988) study are independent of each other. They were not reported as metastases, which would clearly not be independent. Under the assumption that these tumor sites are independent, an analysis was undertaken focusing on overall risk as well as characterizing the impact of experimental variability.

A Monte Carlo analysis was conducted to obtain the distribution of the ratio of combined extra risk from the three tumor sites for the chronically exposed female offspring to the analogous combined extra risk from adult-only exposure. For each simulation, the outcome in each control and dose group was simulated by drawing a binomial B(n,p) random variable with n equal to the number of animals in the group and p obtained by dividing number of animals with tumor in the original dataset by the total number of animals. Since data for only one dose group was available for each tumor site, the individual binomial probabilities for this simulation run were estimated by dividing the number of animals with tumors by the total number of animals, rather than by fitting a dose-response model to the responses for each pair of control and exposed group. Then the risks from the three individual tumor sites were combined assuming independence of different tumor outcomes, as noted above. The standard formula for the probability of the union of multiple sets was used to compute the combined probability of tumor (dose d = 60 ppm was the same for all three tumor types):

$$P_{AorBorC}(d) = P_A(d) + P_B(d) + P_C(d) - P_A(d) * P_B(d) - P_A(d) * P_C(d) - P_B(d) * P_C(d) + P_A(d) * P_B(d) * P_C(d). \quad (1)$$

Then the combined extra risk was computed as:

$$ER_{AorBorC}(d) = [P_{AorBorC}(d) - P_{AorBorC}(0)]/ [1 - P_{AorBorC}(0)]. \quad (2)$$

Only the individual extra risks where probabilities in the control group did not exceed the probability in dose group were retained, in order not to create negative estimates of extra risk. If

only two tumor results were combined in a particular realization, the combined probability in equation (1) was adapted for two tumors

$$P_{AorB}(d) = P_A(d) + P_B(d) - P_A(d) * P_B(d).$$

Finally, the ratio of the extra risks is given by:

$$ER_{AorBorC}(d \mid \text{adult \& early-life}) / ER_{AorBorC}(d \mid \text{adult only}) \quad (3)$$

was calculated and retained for each simulation. The simulation was repeated 10,000 times and results are summarized in the first row of 5-24. Simulations were done in R language (www.r-project.org).

Because some of the control groups did not have any observed tumors, the approach above assigns no variability to such groups. As historic background rates are not available, a sensitivity analysis was conducted to evaluate if assigning a small probability of tumor (1/2n) to these control groups and the resulting variability influences the distribution of the ratio (eq 3). The simulations were performed as described above. Results are summarized in the second row of Table 5-24.

Table 5-24. Overall extra risks of multiple tumor incidence, for chronic exposure beginning either in early-life or in adulthood; based on Sprague-Dawley rats exposed to AN

Treatment of 0% tumors in referent groups	Start of exposure period	Number of simulations with k tumors retained			Percentiles of the distribution of the ratio of extra risks			
		k = 3	k = 2	k = 1	5th	Median	Mean[a]	95th
Zero background as observed	Adult	7,578	2,422	0	0.037	0.095	0.100	0.178
	Early-life	9,903	97	0	0.204	0.314	0.314	0.423
	Ratio				1.543	3.232	4.219 (9,957)	9.628
Zero background replaced by 1/2n[b]	Adult	5,483	3,923	574	0.021	0.085	0.089	0.166
	Early-life	9,685	314	1	0.199	0.311	0.311	0.421
	Ratio				1.610	3.594	6.373 (9,929)	15.627

[a]For calculation of means, the figure in parentheses indicates the number of finite ratios; the other percentiles were based on 10,000 simulations.
[b]For n = 60, 1/2n = 1/120 = 0.0083.

Source: Maltoni et al. (1988).

Extra risks for chronic exposure starting in early-life are not sensitive to the assumption regarding background probabilities, as shown by the similar percentiles for both cases. But the

extra risks for adult-only exposure decrease slightly when some variability at 0% response is assumed, resulting in slightly higher ratios. Because the second analysis is more realistic, allowing a background response in two of the sites and addressing plausible variability, it is used to derive the data-specific adjustment factors. Ninety-five percent of the values fell between 1.6 and 15.6.

Note that the analogous composite adjustment factor resulting from the default factors in the SG for chronic exposure beginning in early life is 1.7; the analysis provides a distribution of adjustment factors with about 95% of the possible values being larger than the default adjustment factors. The median and mean ratios, at 3.6 and 6.4, respectively, are far enough apart to indicate a nonsymmetrical distribution. The median of 3.6 is a better estimate of central tendency in this case.

Recommended early life susceptibility factors. The derived early-life susceptibility factor of 3.6 is to be used in assessing oral or inhalation exposures to AN that begin at birth (or earlier) and extend to or beyond 70 years of age. When exposures involving shorter periods of early-life exposure to AN are assessed, a modification consistent with the SG framework is recommended, as outlined in this section.

The available information for identifying appropriate ADAF(s) to apply to specific early-life periods is limited. While U.S. EPA's SG (U.S. EPA, 2005b) separates the pre-adult period into two age ranges, 0−<2 and 2−<16 years, the Maltoni et al. (1988) study design did not address age periods corresponding to these windows of human susceptibility. The offspring exposed for 15 weeks were about 14 weeks old at the time their exposure stopped (estimated by subtracting 9 days (GDs 21−12) from 15 weeks); female rats reach sexual maturity at about 8 weeks (35 days), so 14 weeks in rats would correspond to a higher age in humans than 16 years. Therefore, the Maltoni et al. (1988) data can support only one ADAF for the entire pre-adult window.

An ADAF for the pre-adult window can be derived from the derived lifetime estimate by treating it as a weighted sum of ADAFs for separate windows of susceptibility, consistent with the general framework in the SG for applying the default ADAFs, using a simplification of the SG framework for estimating human risk from exposure including early-life periods:

$$\text{ADAF for lifetime exposure starting at birth} = 3.6 = [ADAF_P \times t_P + ADAF_A \times (70\ \text{yr} - t_P)]/70, \quad (4)$$

where the subscripts P and A denote pre-adult and adult, respectively, and t_P = duration (in years) of exposure during the pre-adult period. By convention, $ADAF_A$ must be 1. With two unknowns, $ADAF_P$ and t_P, one value must be inferred so that the other can be estimated. Because the Maltoni et al. (1988) data from offspring exposed for 15 weeks are consistent with a 10-fold increased sensitivity relative to rats exposed only as adults (see Figure 5-3 and accompanying text), and the default ADAF of 10 in the SG for the most sensitive period (0–

<2 years of age) is also 10, an $ADAF_P$ of 10 seems a reasonable starting point. Substituting these two ADAFs in (eq 4) and solving for t_P leads to an empirical age cutpoint of 20 years.

This cutpoint is necessarily somewhat arbitrary—it is not an assertion that 14 weeks of age in a rat is equivalent to 20 years in a human—but appears to be a straightforward interpretation of the available data. Other interpretations are possible, such as that sensitivity at the earliest ages (i.e., before 2 years of age) could be relatively higher than later pre-adult ages, but further manipulation of the AN-specific data to align more closely with the SG early-life periods and relative sensitivities (i.e., that the earlier period might be about 3 times more sensitive that the second pre-adult period) is judged to be too speculative.

Illustrations of applying the derived ADAFs for estimating human cancer risk from lifetime exposures starting at birth are provided in Table 5-25.

Table 5-25. Application of ADAFs for estimating human cancer risk from 70-year oral or inhalation exposures to AN from ages 0 to 70

Age Group (yrs)	Duration adjustment	ADAF	Age group risk
For oral exposure to 0.01 mg/kg-d, with oral slope factor of 5 $(mg/kg\text{-}day)^{-1}$ for adult lifetime exposure:			
0–<20	20 yrs/70 yrs = 0.29	10	0.14[a]
20–70	50 yrs/70 yrs = 0.71	1	0.04
Total: 0–70	70 yrs/70 yrs = 1	3.6	0.18
For inhalation exposure to 1 mg/m^3, with IUR of 2×10^{-2} $(mg/m^3)^{-1}$ [or 2×10^{-5} $(\mu g/m^3)^{-1}$] for adult lifetime exposure:			
0–<20	0.29	10	0.057
20–70	0.71	1	0.014
Total: 0–70	1	3.6	0.072

[a]Age group risk = duration adjustment × ADAF × exposure × CSF or unit risk.

Equation (4) provides the framework for estimating risks from exposures involving shorter early-life periods. Two examples are provided:

- If calculating the cancer risk for a 30-year exposure to a constant oral exposure level of 0.01 mg/kg-day from ages 0 to 30, the duration adjustments would be 20/70 and 10/70, and the age group risks would be 0.14 and 0.01, resulting in a total risk estimate of 0.15.

- If calculating the cancer risk for a 30-year exposure to a constant oral exposure level of 0.01 mg/kg-day from ages 20–50, the duration adjustments would be 0/70 and 30/70, and the age group risks would be 0 and 0.02, resulting in a total risk estimate of 0.02.

5.4.4.3.4. ***Uncertainties in early-life susceptibility estimates.*** Unlike many of the studies supporting the default adjustment factors recommended in the SG, the available early-life studies for AN include gestational exposure. The pharmacodynamics and pharmacokinetics of AN during the perinatal period are not well understood, nor are the time frame and nature of the response leading to the apparent susceptibility; it is possible that gestational exposure is a necessary component of the increased susceptibility.

Regarding the level of exposure, it is not known whether perinatal exposure was comparable to adult exposure. If perinatal exposure was greater than adult exposure, the apparent susceptibility would be at least partly attributable to higher exposure; if lower, the apparent susceptibility would be underestimated.

Other uncertainties associated with the recommended data-derived early-life susceptibility adjustment factor include: (1) whether the relative susceptibility is dose-dependent, leading to different values for other parts of the dose-response range; (2) whether the relative susceptibility estimated from female data characterizes the relative susceptibility for males; note particularly the observation of hepatomas in male offspring exposed chronically beginning in early life; (3) the relevance of extrapolating these results to humans; and (4) possible underestimation of risk associated with the lack of knowledge of individual times of death if tumors in the exposed animals tended to occur earlier than in control animals or if tumors in the animals exposed perinatally tended to occur earlier than in those exposed starting at age 13 weeks.

Some uncertainty in cancer risk estimates can generally be characterized by fitting a dose-response model to the incidence data in order to provide a CI on the risk estimate. In this case, however, there was only one exposed group for each exposure pattern. Other methods for characterizing the statistical uncertainty in these data are currently being investigated.

5.4.5. Uncertainties in Cancer Risk Values Risk estimates have inherent uncertainties. This subsection discusses the uncertainties that may be associated with cancer risk values for oral and inhalation cancer assessments.

5.4.5.1. ***Oral Cancer Assessment***

Uncertainties related to the oral cancer assessment are discussed below and summarized in Table 5-26 and Figure 5-4.

Table 5-26. Summary of uncertainty in the AN oral cancer risk assessment

Consideration/ approach	Impact on cancer risk estimate	Decision	Justification
Low-dose extrapolation procedure	The selected model does not represent all possible models one might fit, and other models could conceivably be selected to yield more extreme results consistent with the observed data, both higher and lower than those included in this assessment.	Multistage model to determine POD, linear low-dose extrapolation from POD.	Available mode of action data support direct mutagenicity as the key mode of action and low-dose linear extrapolation approach. EPA's *Guidelines for Carcinogen Risk Assessment* (U.S. EPA, 2005a): mutagens "are assessed with a linear approach." Mutagenic mode of action functions systemically at multiple tumor sites.
PBTK model	Oral slope factor based on PBTK modeling and internal CEO levels is about sixfold higher than slope factor based on the default approach.	EPA-revised model was used.	The revised PBTK model includes EH activity in rats and provides better estimates of internal dose.
Dose metric	Alternatives could decrease oral slope factor (e.g., use of AN-AUC instead of CEO-AUC could lower slope factor by 30-fold).	CEO-AUC was used.	CEO is the reactive metabolite that binds to DNA and initiates tumor formation. AN is not the causal agent for cancer.
Statistical uncertainty at POD	Oral slope factor will be reduced 1.3-fold if BMD used as POD instead of BMDL.	BMDL (approach for calculating reasonable upper bound).	Limited size of bioassay results in sampling variability; BMDL is lower 95% confidence limit of BMD.
Bioassay	Oral slope factor would be the same if study on F344 rats were used (Johannsen and Levinskas, 2002b).	Quast (2002) study on Sprague-Dawley rats was used.	Quast (2002) has separate interim sacrifice groups and examined more endpoints than the Biodynamics (1980c) data sets.
Species/gender combination	Human risk could decrease or increase, depending on relative sensitivity.	Oral slope factor derived from study on female Sprague-Dawley rats.	It was assumed that humans are as sensitive as the most sensitive rodent gender/species tested; true correspondence is unknown. The carcinogenic response occurs across species. Generally, direct site concordance is not assumed; consistent with this view, some rodent tumors are not found in humans (e.g., Zymbal's gland tumors, Harderian gland tumors) and rat and mouse tumor types also differ.
Human population variability in metabolism and response/sensitive subpopulations	Low-dose risk increase to an unknown extent.	Considered qualitatively.	Increased early life susceptibility demonstrated in rat studies. Variability in human susceptibility likely exists due to differences in microsomal CYP2E1 activities and possibly GST activity.

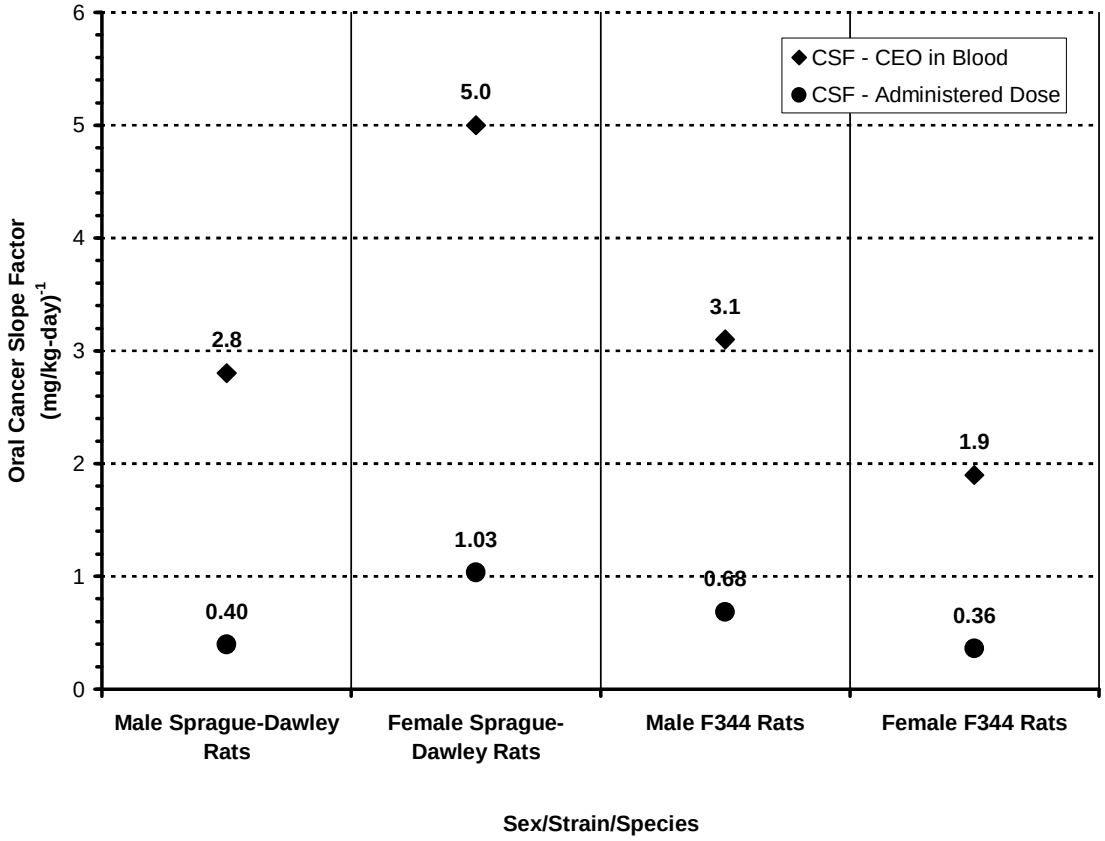

Figure 5-4. Comparison of composite oral CSFs derived from tumor incidence data in four different sex/strain/species of rats exposed chronically to AN. For each sex/strain/species combination, two different dose metrics were employed: (1) CEO concentration in blood, and (2) human equivalent administered dose.

Choice of study

Several bioassays by the oral route are available. The 2-year drinking water studies of Sprague-Dawley rats (Quast, 2002; Quast et al., 1980a) and F344 rats (Johannsen and Levinskas, 2002a; Biodynamics, 1980a) were selected as principal studies. These two studies have sufficient numbers of animals, investigate a thorough set of endpoints, and are considered well conducted. The tumor types observed and incidence of treatment-related tumors were similar in these two studies. Moreover, cancer risk estimates from these two studies differed only by a factor of 1.5. Similarities in these results increase the level of confidence of estimated cancer risk. The Quast (2002) study of Sprague-Dawley rats investigated more endpoints and is therefore a slightly stronger study.

PBTK model

Use of the PBTK model to extrapolate from rodents to humans also introduces some uncertainty. An extensive quantitative analysis of the PBPK model uncertainty is presented in Appendix D. Briefly, PBPK models are computational tools used to predict chemical/drug disposition and are comprised of three distinct types of information: physiological, physicochemical, and biochemical. The physiological data are independent of chemical-specific data, and describe such parameters as organ volumes and blood flows. Physicochemical parameters are chemical-specific and specify parameters, such as PCs or permeability. Biochemical parameters define the rates of chemical transformation or binding. Because the physiological data are considered to be well-characterized, analysis focused on uncertainties in the chemical-specific parameters employed in the PBPK model used to predict AN dosimetry in humans, which is adapted from that of Sweeney et al. (2003). (Only a small number of (metabolic) parameters were changed in the EPA's adaptation.) Uncertainty analysis and characterization of the human model lead to the following conclusions.

- Blood:air and tissue:air PCs as measured directly (in rodents) vs. estimated by a computational tool were compared, and the impact on model predictions of peak AN and peak CEO levels in brain and blood was found to be less than 30% (difference between predictions using the alternate sets of PCs).
- Comparison of model predictions to the limited human data of Jakubowski et al. (1987) shows that the model over-predicts the inhalation respiratory retention measured (predicted ~ 70%; measured 44–58%). This over-prediction may be due to the fact that the model does not fully describe the exposure apparatus (which can introduce additional airway "dead-space") or that the model does not describe gas absorption/desorption in the conducting airways that can reduce uptake rates. However, since the error (if any) is in the direction of over-prediction of uptake, the error is health-protective.
- Once absorbed, the model predicts that 8.4% of AN is converted to CEO and then hydrolyzed, while 30% is converted to CEO and then conjugated with GSH. These values bracket the observation of 16.3% of retained AN being excreted in urine as "CEO" (after acid extraction). Thus, this limited observation is in line with model predictions subsequent to AN predictions, though the exact level of agreement or error cannot be determined due to the distinction between observed quantity (CEO in urine) and what the model predicts (CEO metabolic rates).
- The PBTK model over-predicts CEO levels in the rat at early time-points after i.v. injection (Figure 3-3) and in blood and brain at all time points measured after oral exposure (Figure 3-5a). Kedderis et al. (1996) suggest that the overestimation of CEO by the rat model at the early time points (which also occurs in the EPA's revision) may be due to an intrahepatic first pass effect, as occurs with other epoxides formed in situ from

their parent olefins (Filser and Bolt, 1984). However, this explanation is unlikely and a more plausible explanation is that the model does not account for time-dependence in GSH levels. Inclusion of GSH dynamics would be a much more significant and intensive change to the model structure than single variation implemented here (addition of EH to the rat model with parameter re-estimation) and so has not been considered.

- Parametric sensitivity analysis of human predictions showed a shift in importance between the EH and GSH pathways for CEO elimination from being approximately equal in the implementation of Sweeney et al. (2003) to lower significance for EH (now low but significant) and high significance for GSH with the revised parameters. The oxidation of AN to CEO has a significant effect on AN predictions but only a small effect on CEO in both model versions, reflecting the high dependence of CEO concentrations on CEO metabolic removal. Not surprisingly, brain:tissue PCs significantly affect predictions in brain tissue, and the rate constant for oral absorption affects peak AN concentrations in blood, but not the AUC. While the human parameters are largely derived from human in vitro data, which gives a much higher confidence than would occur had they only been extrapolated from rats, the high dependence of CEO concentrations on GSH conjugation rates, together with the hypothesis above regarding the lack of GSH dynamics in the model, point to that pathway description in particular as being the greatest source of quantitative uncertainty.
- Estimated coefficients of variation for predicted concentrations in brain and blood after inhalation exposure are ~0.6–0.7 for AN and 0.9–1.2 for CEO; after oral exposure these are 0.8–0.9 for AN and 0.7–1.0 for CEO. Based on these values, the human model predictions are expected to be accurate to within a factor of approximately 3, which is the standard assumption for pharmacokinetic variability among humans.

It can be noted that the oral CSFs are larger when based on blood levels of CEO versus blood levels of AN. The VmaxC/Km for AN oxidation in humans is estimated to be about 10 times higher than in the rat. AN enzymatic GSH conjugation is estimated to be 1.5 times higher in the rat, but the 2nd-order removal constant is the same and the GSH tissue levels are roughly the same (and lower in the larger tissue groups). The result, for example, with a steady oral "infusion" of 30 mg/kg-day, is that AN is removed somewhat faster overall, leading to steady-state blood level of 0.114 mg/L in the human vs. 0.151 in the rat. However, a much higher portion of this goes to CEO in the human yielding a CEO blood level of 0.297 vs. 0.013 mg/L in the rat. Thus, CEO:AN = 0.088 in the rat and 2.6 in the human so that the CEO-based risk estimate is higher than the AN-based estimate.

Dose metric

AN is activated by CYP2E1 into its reactive metabolite, CEO, which binds to DNA and initiates tumor formation. Therefore, AUC CEO concentration in blood was selected as the internal dosimetric for PBTK modeling. AN is not anticipated to be the causal agent for carcinogenesis. Uncertainty in the risk estimate related to the dose metric is primarily associated with PBTK model estimation.

Statistical uncertainty at the POD

Parameter uncertainty within the chosen model reflects the sample size of the cancer bioassay. For the multistage model applied to this data set, there is a relatively small degree of uncertainty at the $BMDL_{10}$ (the POD for linear low-dose extrapolation), which is approximately 1.4-fold lower than the BMD_{10} (Appendix B, Table B-37). The highest value was selected in order to provide a reasonable upper-bound risk estimate.

With regard to the combined risk estimate, under the assumption of independence of the tumor type/site considered, no additional uncertainty is added to the estimated POD. Each combined estimate is a statistically rigorous restatement of the statistical uncertainty associated with the risk estimates derived from the individual sites. The only assumption in the combining tumors approach is independence of tumors. This assumption is consistent with NRC (1994) recommendations.

Choice of low dose extrapolation approach

The mode of action is a key consideration in deciding how risks should be estimated for low-dose exposure. The mode of action for cancer effects of AN is discussed extensively in Section 4.7.3.1 and is determined to be mainly due to direct mutagenicity. Other modes of action are plausible, but the evidence suggests they may not be key to the carcinogenicity of AN. The pattern of tumors is consistent with DNA-reactive chemicals. When the mode of action is determined to be direct mutagenicity, a linear approach is used to estimate low-exposure risk, in accordance with EPA's *Guidelines for Carcinogen Risk Assessment* (U.S. EPA, 2005a).

Choice of species/gender

No human cancer epidemiology study via the oral route is available. Cancer risk is estimated for both male and female rats, and cancer risk for the strain and gender with the highest risk, Sprague-Dawley females, was selected. Mammary gland tumors were observed in female rats of both studies. Although a cancer bioassay in $B6C3F_1$ mice is also available, the exposure was via gavage and no PBTK model is available for mice. It was assumed that humans are as sensitive overall as rats, although the true correspondence is unknown. Site concordance is not assumed, nor is it necessary (U.S. EPA, 2005a).

Human population variability

Heterogeneity among humans is another source of uncertainty, in that human risk can be higher or lower than that estimated from rats, depending on relative sensitivity. Human genetic polymorphisms in CYP2E1 activities likely contribute to variability in susceptibility to the toxic effects of AN (see Section 4.8.4.1). In addition, increased early-life susceptibility was demonstrated in two studies in rats exposed gestationally (see Section 5.4.4.3).

5.4.5.2. *Inhalation Cancer Assessment*

Uncertainties related to the IUR assessment are discussed below and summarized in Table 5-27 and Figure 5-5.

Table 5-27. Summary of uncertainty in the AN inhalation cancer risk assessment

Consideration/ approach	Impact on cancer risk estimate[a]	Decision	Justification
Choice of study	Cancer risk estimate could increase because only lung cancer deaths evaluated.	Lung cancer mortality and exposure data from Blair et al. (1998) study was used to derive IUR.	IUR derived from best available cancer epidemiological study of AN exposed workers has fewer inherent uncertainties than IUR derived from rat study (Quast et al., 1980b).
Low-dose extrapolation procedure	The selected model does not represent all possible models one might fit, and other models could conceivably be selected to yield more extreme results consistent with the observed data, both higher and lower than those included in this assessment.	Low-dose linear.	EPA's *Guidelines for Carcinogen Risk Assessment* (U.S. EPA, 2005a): mutagens "are assessed with a linear approach."
Statistical uncertainty at POD	IUR would be reduced fourfold if BMD used as POD instead of BMDL.	BMDL, approach for calculating reasonable upper bound.	Limited size of study results in sampling variability; BMCL is lower 95% confidence limit on EC_{01}.
Choice of species/gender	IUR estimated from exposed male and female workers.	IUR estimated from entire cohort was used.	No apparent gender difference between male and female workers; male and female rats were also similar.
Human population variability in metabolism and response/sensitive subpopulations	Low-dose risk for general population can increase to an unknown extent due to underestimation of human variability (healthy worker effect).	Semi-parametric Cox regression model with time-dependent covariates was used. The Cox model allows inclusion of individual exposure histories and utilizes internal controls, thus avoiding confounding by the healthy worker effect.	Increased early-life susceptibility demonstrated in rat studies. Human variability in susceptibility likely exists due to differences in microsomal CYP2E1 activities, and possibly GST activity.

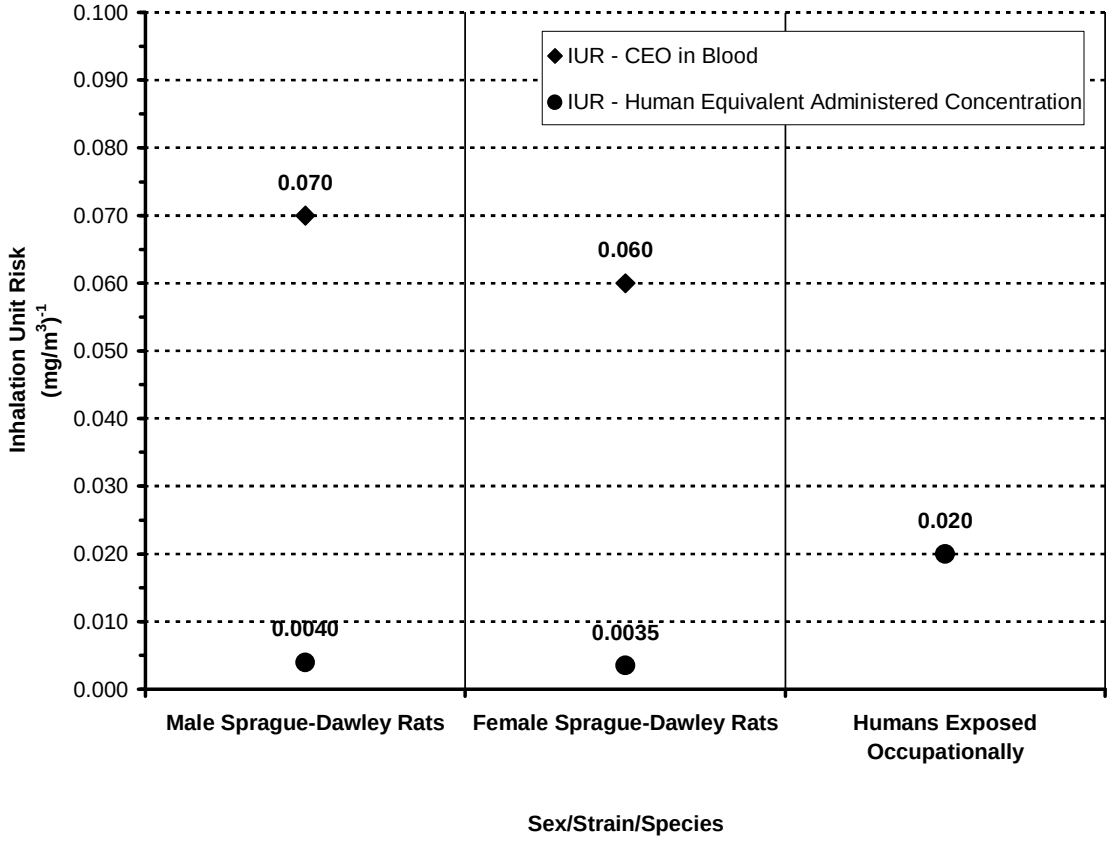

Figure 5-5. Comparison of composite IURs derived from: (1) tumor incidence data in male and female Sprague-Dawley rats exposed chronically to AN, and (2) neurological effects in humans exposed to AN occupationally. In deriving the animal-based IURs, two different dose metrics were employed: (1) predicted CEO concentration in blood, and (2) human equivalent administered AN concentration in air.

Choice of study

As mentioned previously, the Blair et al. (1998) cohort study is the largest cohort assessment of the relationship between AN exposure and cancer. This study had the distinct advantage of quantifying exposure and using an internal control group of unexposed workers, all factors identified as shortcomings in previous studies. Information on smoking history, a potential confounder when lung cancer is the outcome of interest, was available, but only for a small subset within the Blair et al. (1998) cohort. Blair et al. (1998) limited their analysis to the white male population and noted that adjustment for smoking reduced the risk of lung cancer slightly. The data used in this assessment to derive the IUR included the entire cohort; consequently, the smoking history data were incomplete for this analysis, leading to an area of uncertainty surrounding this risk estimate.

Another source of uncertainty stems from the use of only lung cancer mortality for the derivation of the IUR. As previously described, other studies reported small, but not consistent, excess risks for other types of cancer (prostate, bladder, brain cancers) associated with AN exposure. Thus, basing the IUR on only lung cancer mortality may underestimate the carcinogenic potential of AN. Further, as the IUR is based on mortality rather than lung cancer incidence, though in the case of lung cancer mortality is a good surrogate of lung cancer incidence, there may be potential for underestimation of carcinogenic potential with this approach. Additional uncertainties related to the statistical analysis of these data are further discussed in Appendix B-7. Briefly, uncertainties of the statistical approach include: (1) Cox model that was fit to the data is not a biologically based model; (2) the estimator of the cumulative hazard does not account for the covariate path and hence is only an approximation; and (3) the estimate of risk is obtained using the first-order "linearized" approximation. However, obtained results are consistent with assumptions of the first-order approximation validity.

Other uncertainties associated with the NCI/NIOSH cohort include nondifferential exposure misclassification, lung cancer misdiagnosis among the internal controls, the relatively short follow-up period (reflected by the relatively small proportion of mortality within the cohort), and the extrapolation of continuous environmental exposure from 8-hour occupational exposure without consideration of potential recovery mechanisms between daily exposures. The nondifferential exposure misclassification contributes to an underestimation of risk, while the impacts of short follow-up and extrapolation to a continuous exposure scenario are unclear. Nonetheless, the NCI/NIOSH cohort provides the most robust data set in terms of sample size and exposure assessment for the derivation of the IUR.

Statistical uncertainty at the POD

Parameter uncertainty within the chosen model reflects the limited sample size of the cancer bioassay. For the results relying on the cohort study, the EC_{01} is approximately fourfold higher than the LEC_{01}.

For the multistage model applied to the rat data, in support of the human-based results, there is a reasonably small degree of uncertainty at the 10% incidence level (the POD for linear low-dose extrapolation). Composite BMC_{10}s for overall cancer risk are approximately 1.3-fold higher than their corresponding $BMCL_{10}$s for both male and female rats.

With regard to the combined risk estimate, under the assumption of independence of the tumor type/site considered no additional uncertainty is added to the estimated POD. Each combined estimate is a statistically rigorous restatement of the statistical uncertainty associated with the risk estimates derived from the individual sites. This assumption is consistent with NRC (1994) recommendations.

Low-dose extrapolation procedure

As discussed previously, the key mode of action for carcinogenicity of AN is determined to be direct mutagenicity. A linear approach is used to estimate low-exposure risk, in accordance with EPA's *Guidelines for Carcinogen Risk Assessment* (U.S. EPA, 2005a). Nonlinear low-dose extrapolation approach is not used since data do not support other modes of action at this time.

Choice of species/gender

A human study was selected for quantification of IUR. Both male and female workers were evaluated. A 2-year inhalation study of male and female rats was used for comparison. Estimates of IURs from the human study and from the rat studies were similar. IURs estimated from male and female rats were also similar, although there was a suggestion of higher cancer risk in females associated with mammary gland tumors.

Human population variability

Heterogeneity among humans is another source of uncertainty. Uncertainty related to human variation needs consideration, also, in extrapolation from a small subset of human population to a larger, more diverse population. The study population in Blair et al. (1998) was AN-exposed workers in the United States. To counter the healthy worker effect, internal controls were used in the study. Available data from animal studies provide no evidence of gender differences in susceptibility to toxicity of AN, although no data is available regarding possible gender differences in susceptibility. Polymorphisms in the CYP2E1 gene that affect enzyme activity likely contribute to the variability of human susceptibility towards the toxic effect of AN (see Section 4.8.4.1).

6. MAJOR CONCLUSIONS IN THE CHARACTERIZATION OF HAZARD AND DOSE-RESPONSE

6.1. HUMAN HAZARD POTENTIAL

AN (CASRN 107-13-1) is a colorless, flammable, and volatile liquid with a weakly pungent onion- or garlic-like odor. It is a commercially important chemical used in the manufacture of acrylic and modacrylic fibers, plastics (ABS and AN-styrene resins), and nitrile rubbers and as an intermediate in the synthesis of other chemicals, such as adiponitrile and acrylamide. Exposure to airborne AN is possible for people living in the vicinity of emission sources such as acrylic fiber or chemical manufacturing plants or waste sites.

AN is rapidly and nearly completely absorbed, widely distributed to tissues, and biochemically transformed into metabolites that are excreted in the urine and, to a much lesser extent, in feces and expired air. Two major metabolic pathways for AN have been identified: detoxification of AN by conjugation with GSH, forming the urinary metabolite N-acetyl-S-(2-cyanoethyl)cysteine, and oxidation of AN to its epoxide metabolite, CEO, via CYP2E1. CEO can bind to tissue macromolecules, such as proteins and DNA. CEO can be hydrolyzed to cyanide with further transformation to thiocyanate, which is excreted in urine. Alternatively, CEO can interact with GSH, resulting in the formation of a number of other urinary metabolites.

There are no studies directly identifying health hazards in humans following oral exposures of any duration, but results from a robust array of studies in rats and mice identify noncancer lesions in the gastric squamous epithelium and tumors in multiple tissues as potential health hazards to humans exposed to AN by the oral route for chronic durations. Results from cross-sectional epidemiologic studies of AN-exposed workers identify increased prevalences of neurological symptoms and adverse reproductive outcomes in occupationally exposed workers as potential health hazards from chronic inhalation exposure. Cancer is another potential human health hazard from chronic inhalation exposure, as indicated by increased incidences of tumors at several tissue sites in rat chronic inhalation bioassays. Studies of AN-exposed workers have provided no strong evidence that mortality from any type of cancer is casually related to occupational exposure, but limited evidence from the best-designed epidemiologic study found a small, but statistically significant, increased risk for dying from lung cancer in workers with the longest durations and highest exposures to AN.

The animal toxicity database identifies hyperplasia and hyperkeratosis of the squamous epithelium of the forestomach as the most sensitive noncancer effects associated with repeated oral exposure to AN. Following chronic oral exposure, these lesions have been observed in rats at drinking water concentrations as low as 1–3 ppm (0.09–0.3 mg/kg-day) (Johannsen and Levinskas, 2002a, b; Biodynamics, 1980a, b). Other effects have been observed in repeatedly exposed animals, generally at higher exposure levels. These include ovarian atrophy in female

mice exposed to doses ≥2.5 mg/kg-day for 2 years (NTP, 2001); chronic nephropathy in male and female rats exposed for 2 years to 3.4 and 10.8 mg/kg-day AN, respectively (Quast et al., 1980a); gliosis in the brain of female Sprague-Dawley rats at 4.4 mg/kg-day (Quast et al., 1980a); decreased sperm count in male mice exposed to 10 mg/kg-day for 60 days (Tandon et al., 1988); hind-limb weakness and decreased sensory nerve conduction velocity in male rats exposed to 50 mg/kg-day AN for 12 weeks (Gagnaire et al., 1998); and neurobehavioral effects in male rats exposed to 4 mg/kg-day AN in drinking water for 8 or 12 weeks (Rongzhu et al., 2007). No changes in fertility index or pregnancy success were found in a three-generation study of rats exposed to drinking water doses as high as 39 mg/kg-day (Friedman and Beliles, 2002; Litton Bionetics, 1992). Mild developmental effects were observed at 11 and 20 mg/kg-day (small deficits in postnatal pup weight or survival) in this three-generation rat study and at 25 mg/kg-day (increased litters with pups with missing vertebrae) but not at 10 mg/kg-day in rat fetuses exposed on GDs 6–15 (Murray et al., 1978).

Repeated inhalation exposure to AN in the workplace has been associated with increased prevalence of subjective neurological symptoms, such as headache, poor memory, and irritability (Chen et al., 2000; Kaneko and Omae, 1992; Muto et al., 1992; Sakurai et al., 1978) and small performance deficits in neurobehavioral tests of mood, attention and speed, auditory memory, visual perception and memory, and motor steadiness (Lu et al., 2005a). Such effects have been associated with average workplace air concentrations of 0.1 or 0.9 ppm and appear to be the most sensitive noncancer effects from repeated inhalation exposure to AN. Adverse reproductive outcomes, such as increased prevalences of premature deliveries, stillbirths, sterility, birth defects, and pregnancy complications, have been associated with occupational exposure to average workplace concentrations ranging from 3.6 to 7.5 ppm (Dong et al., 2000a; Li, 2000; Dong and Pan, 1995). SubchronicSubchronic and chronic inhalation toxicity studies in rats identified other noncancer effects at higher exposure levels, including nasal epithelial lesions in rats exposed to concentrations of 20 or 80 ppm for 2 years (Quast et al., 1980b), decreased nerve conduction velocity and hind-limb weakness in rats exposed to ≥25 ppm AN (Gagnaire et al., 1998), increased incidence of rat fetuses with missing vertebrae, missing ribs, or anteriorly displaced ovaries following exposure of pregnant Sprague-Dawley rats to 80 ppm on GDs 6–15 (Murray et al., 1978), and decreased rat fetal weight gain following exposure of pregnant Sprague-Dawley rats to concentrations ≥25 ppm on GDs 6–20 (Saillenfait et al., 1993).

The genotoxicity of AN has been evaluated in multiple systems in vitro and in vivo. In addition to positive findings in blood lymphocytes, buccal mucosal cells, and sperm in five epidemiologic studies, DNA alkylation by AN was found in numerous tissues in rats or mice (brain, liver, testes, forestomach, colon, kidney, bladder, and lung) treated with a single dose of AN. AN or its reactive metabolite, CEO, yielded positive results in in vitro mutation assays using bacteria, fungi, and insects, as well as animal and human cell cultures. The weight of evidence from these studies suggests that AN is mutagenic after metabolic activation to CEO.

Following EPA *Guidelines for Carcinogen Risk Assessment* (U.S. EPA, 2005a), AN is "likely to be carcinogenic to humans," based predominantly on consistent results showing that lifetime inhalation or oral exposure caused statistically significantly increased incidence of tumors at multiple tissue sites in rats and mice. Lifetime oral exposure to AN caused increased incidences of tumors at multiple tissue sites, including the brain, forestomach, and Zymbal gland, in several rat studies and the forestomach and Harderian gland in a gavage study in mice (NTP, 2001). Lifetime inhalation bioassays with Sprague-Dawley rats found exposure-related increases in the incidences of brain tumors, Zymbal gland tumors, intestinal tumors, tongue tumors, and malignant mammary gland tumors (Dow Chemical Co., 1992a; Maltoni et al., 1988, 1977; Quast et al., 1980b). Also, there is some association between AN exposure and lung cancer deaths in occupationally exposed workers. Rats exposed during gestation and through adulthood displayed higher incidences of tumors at several tissue sites than did rats exposed throughout adulthood only (Friedman and Beliles, 2002; Maltoni et al., 1988). The latter results suggest that exposure to AN during gestation and childhood may present increased risk of developing cancer compared with exposure during adulthood alone.

Although data gaps still exist in the current understanding of the mode of action for carcinogenicity of AN, there is adequate experimental evidence to support a direct mutagenic mode of action as the key mode of action for AN-induced tumors. Other modes of action may contribute, but limited data do not appear supportive at this time. Indirect mutagenicity via oxidative DNA damage is plausible, but oxidative stress was not supported by experimental evidence as a key mode of action.

6.2. DOSE-RESPONSE

6.2.1. Oral RfD

The available oral toxicity studies in animals identify nonneoplastic forestomach lesions (i.e., squamous cell epithelial hyperplasia and hyperkeratosis) as the most sensitive noncancer effect associated with chronic oral exposure to AN. These lesions are expected to be relevant to humans because, although humans do not possess a forestomach, they do have comparable squamous cell epithelial tissue in their oral cavity and in the upper two-thirds of their esophagus.

A 2-year drinking water study with F344 rats (Johanssen and Levinskas, 2002b) was selected as the principal study on which to base the RfD because it provided the best available dose-response data. This study included five drinking water exposure levels ranging from 1 to 100 ppm, and it also identified the lowest administered-dose LOAEL of the available chronic animal toxicity studies based on an increased incidence of forestomach lesions (i.e., LOAELs of 0.3 and 0.4 mg/kg-day for males and females, respectively, with associated NOAELs of 0.1 mg/kg-day for both sexes).

An RfD of 2×10^{-4} mg/kg-day (or 0.2 µg/kg-day) is derived for use in humans because it is the lowest value derived based on the observed critical effect in the selected principal study

(i.e., incidence of nonneoplastic forestomach lesions in F344 rats in a 2-year drinking water study). This RfD was derived using a BMD approach based on incidence data for forestomach lesions in male and female F344 rats exposed chronically to AN via drinking water and pharmacokinetic data from EPA-modified rat and human PBTK models (Section 3.5; Appendix C; Sweeney et al., 2003; Kedderis et al., 1996).

The RfD derivation process involved first fitting all available dichotomous models in BMDS (version 2.0) to the incidence data for male and female rats, separately, employing two different internal dose metrics (i.e., AN in blood and CEO in blood). These two internal dose metrics were derived by converting administered rat doses of AN to internal rat doses (either AN or CEO in blood) using the rat PBTK model of Kedderis et al. (1996), as modified by EPA (Section 3.5; Appendix C). Then, for each sex, the BMDL associated with both a 5 and 10% extra risk for gastric epithelial lesions was derived based on the best-fitting model. This BMDL based on rat internal dose was then converted to the human equivalent administered dose of AN by using the human PBTK model of Sweeney et al. (2003) (with EPA-modified parameters; Section 3.5; Appendix C). As discussed in more detail in Section 5.1, CEO in blood was selected as the best available internal dose metric for cross-species extrapolation with oral exposure, while 5% extra risk was chosen as the most appropriate BMR level. The human equivalent administered dose of AN represents a POD for noncancer effects and was then divided by a UF of 30 (3 to account for uncertainty in extrapolating from rats to humans with dosimetric adjustment and 10 to account for variation in response from average humans to sensitive humans) to arrive at an RfD.

Confidence in the principal study selected for the RfD is high. The principal study, Johannsen and Levinskas (2002b), was selected from eight chronic rat studies and one gavage study in exposed mice. The study employed five exposure levels of AN, ranging from 1 to 100 ppm, and thus provided a more complete description of the dose-response relationship in the low-dose region than did either the Quast (2002) study in Sprague-Dawley rats or the NTP (2001) study in $B6C3F_1$ mice, which started at higher dose levels, and both employed only three dose groups. Johannsen and Levinskas (2002b) identified the lowest LOAELs based on an increased incidence of hyperplasia and hyperkeratosis in squamous epithelium of forestomach (0.4 mg/kg-day for males and 0.4 mg/kg-day for females). No human exposure study is available for derivation of the RfD. Overall confidence in the RfD is medium, reflecting these considerations.

6.2.2. Inhalation RfC

Results from several cross-sectional epidemiologic studies of AN-exposed workers identified increased prevalence of neurological symptoms and small performance deficits in neurobehavioral tests as the critical effects resulting from chronic inhalation exposure to AN. The cross-sectional study of neurobehavioral performance measures in acrylic fiber workers by

Lu et al. (2005a) was selected as the principal study for RfC derivation because it identified the lowest reliable exposure level in humans associated with adverse neurological effects.

A NOAEL/LOAEL approach was used to derive the RfC from the human data. The average workplace AN air concentration of 0.11 ppm for workers in the monomer work areas of the acrylic fiber plant was selected as the LOAEL or POD for RfC derivation. This LOAEL of 0.11 ppm (0.24 mg/m^3) for small, but statistically significant, performance deficits in neurobehavioral tests of mood, attention and speed, auditory memory, visual perception and memory, and motor steadiness was divided by a UF of 100 (10 for extrapolating from a LOAEL to a NOAEL and 10 to account for extrapolating from healthy workers to sensitive humans), after conversion to an equivalent continuous exposure of 0.086 mg/m^3, to arrive at an RfC for AN of 0.9 $\mu g/m^3$.

As discussed in more detail in Section 5.2, comparative animal-based RfCs for AN of 3×10^{-3} mg/m^3 (or 3 $\mu g/m^3$) and 2×10^{-3} mg/m^3 (or 2 $\mu g/m^3$) were derived based on PODs from BMD modeling of nasal lesions observed in male and female rats, respectively, exposed to AN via inhalation for 2 years (Quast et al., 1980b). In deriving these RfCs, the PODs were divided by a composite UF of 30 (3 for extrapolating from rats to humans using the default U.S. EPA (1994) dosimetric adjustment and 10 to account for variation from average humans to sensitive humans). These animal-based RfCs are quite consistent with the human-based value. However, the human-based value of 0.9 $\mu g/m^3$ is selected as the RfC, because extrapolating from animals has greater associated uncertainty than extrapolating from humans.

The principal study is given medium confidence because it is the best available study that identified neurobehavioral effects of AN in occupationally exposed workers. Previous occupational studies by Kaneko and Omae (1992) and Muto et al. (1992) reported subjective neurological symptoms in exposed workers. Lu et al. (2005a) utilized the WHO-recommended NCTB administered by trained physicians to evaluate these neurobehavioral effects systemically. Hence, the results were more reliable when compared with those based on self reporting. The confidence in the principal study is medium because there are several limitations in the study. One was that the cited exposure data represented estimates of previous exposure levels and no contemporaneous personal monitoring data were available. In addition, the study authors could not rule out the possibility that examiner drift may have affected the results. Moreover, largest measures of neurobehavioral effect occurred on the acrylic fiber workers, who had lower average exposure level.

Confidence in the database is medium to high. An RfC based on the results from a chronic inhalation study with Sprague-Dawley rats was also derived for comparison. Statistically significant increased incidence of inflammatory and degenerative nasal lesions occurred in rats exposed to the lowest level in this 2-year bioassay. The alternative RfC derived from the rat study is only about threefold higher than the RfC derived from the occupational exposure study. Overall confidence in the RfC is medium to high, reflecting these

considerations.

6.2.3. Oral CSF

Incidence data for forestomach, CNS, Zymbal gland, tongue, and mammary gland tumors in male and female Sprague-Dawley (Quast, 2002) and F344 (Johanssen and Levinskas, 2002a) rats were used to develop site-specific oral CSFs for AN, employing EPA-modified rat and human PBTK models for cross-species dosimetric extrapolation (Section 3.5; Appendix C; Sweeney et al., 2003; Kedderis et al., 1996). These animal studies were selected for the development of oral CSFs because human data are not available, and these studies are the best available chronic bioassays for characterizing the dose-response relationships for these AN-induced tumors. Weight-of-evidence evaluation following U.S. EPA (2005a) guidelines determined that a direct mutagenic mode of action, most likely via the reactive AN metabolite CEO, was the principal mode of action. Consequently, a linear low-dose extrapolation approach was used in the development of the oral CSFs.

As discussed in more detail in Section 5.4, CEO in blood and AN in blood were both evaluated as internal dose metrics for use in cross-species extrapolation with oral exposure. The multistage dose-response model in BMDS (version 1.4.1) was fit to the male and female rat tumor incidence data, using internal animal dose expressed as either CEO or AN in blood. Rat administered doses were converted to rat internal doses (either CEO or AN in blood) by using the rat PBTK model of Kedderis et al. (1996), as modified by EPA (Section 3.5; Appendix C). For each of these two dose metrics, the resulting best-fit model for each endpoint was then used to derive a 95% lower confidence limit on the dose associated with 10% extra risk (i.e., a $BMDL_{10}$). These BMDLs, based on internal rat doses, were then converted to human equivalent administered doses of AN using the human PBTK model of Sweeney et al. (2003), as modified by EPA (Section 3.5; Appendix C). The site-specific oral CSFs based on incidence data from each tumor site were derived by linear extrapolation from the human equivalent administered doses down to the origin (oral CSF = $0.1/BMDL_{10/HED}$). Within rat strain and sex, an oral slope factor for the composite risk across these tumor sites, based on CEO in blood, was then estimated by employing the procedure described in Section 5.4.4.1.

The highest composite slope factor of 5 per mg/kg-day is recommended for use in humans because it has the highest potency based on the observed critical effect in the selected principal study (i.e., incidence of tumors in male and female Sprague-Dawley rats). This slope factor is recommended for estimating composite cancer risks in humans who experience chronic oral exposures to AN during adulthood. This slope factor should not be used with exposures greater than 0.04 mg/kg-day (the lowest POD supporting the composite risk) because above this level, the slope factor cannot be expected to be an adequate approximation to the dose-response relationship. The fitted dose-response relationship and pharmacokinetic models should be used to estimate risk above this exposure level.

Results from a chronic rat inhalation cancer bioassay (Maltoni et al., 1988) and a three-generation rat drinking water reproductive toxicity study (Friedman and Beliles, 2002) indicate that AN exposure during gestation and early periods of development may increase risks for cancer by at least threefold compared with chronic AN exposures during adulthood only. A chemical-specific early life susceptibility factor of 3.6 was developed for assessing cancer risks associated with lifetime exposure beginning at birth, based on the incidence data in the Maltoni et al. (1988) bioassay for mammary tumors, brain tumors, and extra-hepatic angiosarcomas in female rats.

6.2.4. Cancer Inhalation Unit Risk

An analysis of the human lung cancer mortality data from the Blair et al. (1998) cohort study of AN-exposed workers was conducted to derive an IUR estimate for AN based on human data. This analysis employed the approach presented by Starr et al. (2004) and is further described in Appendix B-7. In brief, the risk of death from lung cancer in AN-exposed workers was characterized by using a semi-parametric Cox regression model with a cumulative exposure metric (i.e., ppm-working years) as the only time-dependent covariate. In contrast to the analysis by Starr et al. (2004), the entire cohort was included in the analysis conducted for this assessment (not just white male workers), and the final model only included cumulative exposure as the covariate.

The Cox regression model described above was used to estimate an AN exposure level and its associated 95% lower confidence limit corresponding to a 1% risk of dying from lung cancer by age 80 (i.e., EC_{01} and LEC_{01}, respectively). Conversion of occupational exposures to continuous environmental exposures was accomplished by adjusting for differences in the amount of air inhaled during an 8-hour workday versus a 24-hour day (10 and 20 m^3/day, respectively). The IUR estimate was derived by linear extrapolation from the LEC_{01}. The predicted EC_{01} and LEC_{01} derived from the Cox regression model based on the Blair et al. (1998) data were 0.992 and 0.238 ppm (2,168 and 524 $\mu g/m^3$) AN, respectively. From the LEC_{01}, an IUR estimate of 0.042 per ppm (2×10^{-5} per $\mu g/m^3$) was derived.

Some uncertainty is associated with this IUR estimate because of the study on which it is based. More specifically, no adjustment for smoking was applied in the Blair et al. (1998) study. The investigators collected smoking information on only about 10% of the exposed and unexposed members of the cohort and found similar incidences of smoking in the two groups. Because their statistical analysis compared exposed and unexposed groups of workers, Blair et al. (1998) noted that the adjustment for smoking made only a slight difference in the results of their analysis. Other uncertainties associated with the Blair et al. (1998) data set included nondifferential exposure misclassification and a relatively short follow-up period, an average of 21 years. Additionally, the outcome of the study was lung cancer mortality, not lung cancer

incidence. Additional uncertainties related to the statistical analysis of these data are discussed further in Appendix B-7.

Tumor incidence data from the best available animal inhalation study (Dow Chemical Co., 1992a) were selected for describing the dose-response relationship between intestinal, CNS, Zymbal's gland, tongue, and mammary gland tumors and AN exposure. These dose-response relationships were used to derive animal-based IURs for AN for comparative purposes. As with the animal-based oral slope factor, a direct mutagenic mode of action, most likely via the reactive AN metabolite CEO, was assumed, because available information was inadequate to establish AN's mode of carcinogenic action in these tissues in animals. Consequently, a linear low-dose extrapolation approach was used in the development of the animal-based IURs.

Based on the assumption that the epoxide metabolite, CEO, is critical to AN's carcinogenic mode of action, the selected internal dose metric was CEO in blood. In contrast to oral exposure, the EPA-modified PBTK model adequately predicted measured blood and brain concentrations of CEO in rats exposed to AN by inhalation (Kedderis et al., 1996). The multistage model was fit to the rat tumor incidence and CEO concentration in blood predicted by the PBTK model of Kedderis et al. (1996), as modified by EPA (Section 3.5; Appendix C). The best-fitting stage of the model was used to derive 95% lower bounds on rat internal blood concentrations of CEO associated with 10% extra risk ($BMCL_{10}$s). The human PBTK model of Sweeney et al. (2003) (parameters modified; Section 3.5; Appendix C), was then used to calculate human equivalent administered concentrations of AN, corresponding to the rat $BMCL_{10}$s. These human equivalent administered concentrations of AN were used as the POD for the IUR estimates via linear extrapolation down to the origin (i.e., $IUR = 0.1/BMCL_{10/HEC}$).

The IUR estimates for multiple tumor sites were derived within each rat sex by employing the procedure described in Section 5.4.4.1. The resulting composite IUR estimates were 7×10^{-2} and 6×10^{-2} per mg/m^3 (7×10^{-5} and 6×10^{-5} per $\mu g/m^3$) and were derived based on tumor incidence data from male and female Sprague-Dawley rats, respectively. These unit risks should not be used with exposures greater than 3 mg/m^3 (the lowest POD supporting the composite risk), because above this level, the slope factor cannot be expected to be an adequate approximation of the dose-response relationship. The fitted dose-response relationship and pharmacokinetic models should be used to estimate risk above this exposure level.

Given that the IUR of 2×10^{-5} per $\mu g/m^3$ is based on human data and is consistent with the IUR derived from the animal data, it is the IUR recommended for estimating cancer risks associated with chronic inhalation exposures to AN during adult stages of development.

As described for the oral slope factor, a chemical-specific early-life adjustment factor of 3.6 was developed for assessing cancer risks associated with lifetime exposure beginning at birth, based on the multisite tumor incidence data for female rats in the Maltoni et al. (1988) bioassay.

7. REFERENCES

Abdel-Aziz, AH; Abdel-Naim, AB; Hamada, FM; et al. (1997) In-vitro testicular bioactivation of acrylonitrile. Pharmacol Res 35:129–134.

Abdel-Rahman, SZ; Nouraldeen, AM; Abo-Elwafa, AA; et al. (1994a) Acrylonitrile-induced reversible inhibition of uridine uptake by isolated rat intestinal epithelial cells. Toxicol Vitro 8:139–143.

Abdel-Rahman, SZ; Nouraldeen, AM; Ahmed, AE. (1994b) Molecular interaction of [2,3-^{14}C]acrylonitrile with DNA in gastric tissue of rat. J Biochem Toxicol 9:191–198.

Abdel-Rahman, SZ; Ammenheuser, MM; Ward, JB. (2001) Human sensitivity to 1,3-butadiene: role of microsomal epoxide hydrolase polymorphisms. Carcinogenesis 22:415–423.

Abdel-Rahman, SZ; El-Zein, RA; Ammenheuser, MM; et al. (2003) Variability in human sensitivity to 1,3 butadiene: influence of the allelic variants of the microsomal epoxide hydrolase gene. Environ Mole Mutagen41:40–146.

Abreu, ME; Ahmed, AE. (1980) Metabolism of acrylonitrile to cyanide. In vitro studies. Drug Metab Dispos 8:376–379.

Acrylonitrile Group. (2000) Initial submission: letter from Acrylonitrile Group to USEPA re 4 unpublished surveys of Chinese chemical industry worker exposure to acrylonitrile, w/attachments and dated 4/26/00. Submitted under TSCA Section 8E; EPA Document No. 88-000000150; NTIS No. OTS0559911.

ACS (American Chemical Society). (2003) Online information sheet. Available online at http://pubs.acs.org/hotartcl.cenear.960624/prod.html.

Ahmed, AE; Abreu, ME. (1981) Microsomal metabolism of acrylonitrile in liver and brain. Adv Exp Med Biol 136(Pt. B):1229–1238.

Ahmed, AE; Patel, K. (1981) Acrylonitrile: in vivo metabolism in rats and mice. Drug Metab Dispos 9:219–222.

Ahmed, AE; Farooqui, MYH; Upreti, RK; et al. (1982) Distribution and covalent interactions of [1-^{14}C]acrylonitrile in the rat. Toxicology 23:159–175.

Ahmed, AE; Farooqui, MYH; Upreti, RK; et al. (1983) Comparative toxicokinetics of 2,3-^{14}C-and 1 ^{14}C acrylonitrile in the rat. J Appl Toxicol 3:39–47.

Ahmed, AE; Abdel-Aziz, AH; Abdel-Rahman, SZ; et al. (1992a) Pulmonary toxicity of acrylonitrile: covalent interaction and effect on replicative and unscheduled DNA synthesis in the lung. Toxicology 76:1–14.

Ahmed, AE; Abdel-Rahman, SZ; Nouraldeen, AM. (1992b) Acrylonitrile interaction with testicular DNA in rats. J Biochem Toxicol 7:5–11.

Ahmed, AE; Hamada, FMA; Abdel-Aziz, AH; et al. (1993) Immunotoxicity of acrylonitrile: flow cytometric study of spleen lymphocyte subsets and the plaque forming cells response in immunized mice. J Biomed Sci Ther 9:139–161.

Ahmed, AE; Jacob, S; Ghanayem, BI. (1996a) Comparative disposition of acrylonitrile and methacrylonitrile: quantitative whole-body autoradiographic studies in rats. Fundam Appl Toxicol 33:49–59.

Ahmed, AE; Nouraldeen, AM; Abdel-Rahman, SZ; et al. (1996b) Role of glutathione modulation in acrylonitrile-induced gastric DNA damage in rats. Arch Toxicol 70:620–627.

Albert, DM; Frayer, WC; Black, HE; et al. (1986) The Harderian gland: its tumors and its relevance to humans. Trans Am Ophthalmol Soc 84:321–341.

Amacher, E; Turner, G. (1985) Tests for gene mutational activity in the L5158Y/TK assay system. Prog Mutat Res 5:487–496.

Andersen, ME. (1991) Physiological modeling of organic compounds. Ann Occup Hyg 35:309–321.

Anderson, D; Cross, MF. (1985) Suitability of the P388F mouse lymphoma system for detecting potential carcinogens and mutagens. Food Chem Toxicol 23:115–118.

Appel, KE; Peter, H; Bolt, HM. (1981) Effect of potential antidotes on the acute toxicity of acrylonitrile. Int Arch Occup Environ Health 49:157–163.

Aronstam, RS; Abood, LG; Hoss, W. (1978) Influence of sulfhydryl reagents and heavy metals on the functional state of the muscarinic acetylcholine receptor in rat brain. Mol Pharmacol 14:575–586.

Ashby, J; de Serres, F; Draper, M; et al. (1985) Evaluation of short-term tests for carcinogens. Prog Mutat Res 5:1–752

ATSDR (Agency for Toxic Substances and Disease Registry). (1990) Toxicological profile for acrylonitrile. Public Health Service, U.S. Department of Health and Human Services, Atlanta, GA. Available online at http://www.atsdr.cdc.gov/toxprofiles. (accessed April 21, 2009).

Babanov, GP; Kijuchikov, VN; Kaarajeva, NI; et al. (1959) Clinical symptoms of chronic poisoning by acrylonitrile. Vrach Delo 8:833–836.

Bachofen, M; Weibel, ER. (1977) Alterations of the gas exchange apparatus in adult respiratory insufficiency associated with septicemia. Am Rev Respir Dis 116:589–615.

Bader, M; Wrbitzky, R. (2006) Follow-up biomonitoring after accidental exposure to acrylonitrile—implications for protein adducts as a dose monitor for short-term exposures. Toxicol Lett 162(2–3):125–131.

Bakker, JG; Jongen, SM; Van Neer, FC; et al. (1991) Occupational contact dermatitis due to acrylonitrile. Contact Dermatitis 24:50–53.

Balda, BR. (1975) Acrylonitrile as a contact allergen. Hautarzt 26:599–601 (German).

Banerjee, S; Segal, A. (1986) In vitro transformation of C3H/10T1/2 and NIH/3T3 cells by acrylonitrile and acrylamide. Cancer Lett 32:293–304.

Barnes, JM. (1970) Observations on the effects on rats of compounds related to acrylamide. Brit J Ind Med 27:147–149.

Barrett, JC; Lamb, PW. (1985) Tests with the Syrian hamster embryo cell transformation assay. Prog Mutat Res 5:623–628.

Bellward, GD; Chang, T; Rodrigues, B; et al. (1988) Hepatic cytochrome P-450j induction in the spontaneously diabetic BB rat. Mol Pharmacol 33(2):140–143.

Benesh, V; Cherna, V. (1959) Acrylonitrile: acute toxicity and mechanism of action. J Hyg Epidemiol Microbiol Immunol 3:106–116.

Benhamou, S; Reinikainen, M; Bouchardy, C; et al. (1998) Association between lung cancer and microsomal epoxide hydrolase genotypes. Cancer Res 58:5291–5293.

Benn, T; Osborne, K. (1998) Mortality of United Kingdom acrylonitrile workers—an extended and updated study. Scand J Work Environ Health 24:17–24.

Benz, FW; Nerland, DE. (2005) Effect of cytochrome P450 inhibitors and anticonvulsants on the acute toxicity of acrylonitrile. Arch Toxicol 79:610–614.

Benz, FW; Nerland, DE; Pierce, WM; et al. (1990) Acute acrylonitrile toxicity: studies on the mechanism of the antidotal effect of D- and L-cysteine and their N-acetyl derivatives in the rat. Toxicol Appl Pharmacol 102:142–150.

Benz, FW; Nerland, DE; Li, J; et al. (1997a) Dose dependence of covalent binding of acrylonitrile to tissue protein and globin in rats. Fundam Appl Toxicol 36:149–156.

Benz, FW; Nerland, DE; Corbett, D; et al. (1997b) Biological markers of acute acrylonitrile intoxication in rats as a function of dose and time. Fundam Appl Toxicol 36:141–148.

Bergmark, E. (1997) Hemoglobin adducts of acrylamide and acrylonitrile in laboratory workers, smokers and nonsmokers. Chem Res Toxicol 10:78–84.

Beskid, O; Dusek, Z; Solansky, I; et al. (2006) The effects of exposure to different clastogens on the pattern of chromosomal aberrations detected by FISH whole chromosome painting in occupationally exposed individuals. Mutat Res 594(1–2):20–29.

Bhooma, T; Venkataprasad, N. (1997) Acrylonitrile potentiates oxidative stress in rat alveolar macrophages. Bull Environ Contam Toxicol 58:71–78.

Bhooma, T; Padmavathi, B; Devaraj, SN. (1992) Effect of acrylonitrile on the procoagulant activity of rat lung. Bull Environ Contam Toxicol 48:321–326.

Bigner, DD; Bigner, SH; Burger, PC; et al. (1986) Primary brain tumours in F344 rats chronically exposed to acrylonitrile in their drinking water. Food Chem Toxicol 24:129–137.

Biodynamics. (1980a) Initial submission: 24-month oral toxicity/carcinogenicity study with acrylonitrile administered to Spartan rats in drinking water (final report) with cover letter dated 072492. Submitted under TSCA Section 8E; EPA Document No. 88-920005779; NTIS No. OTS0544562.

Biodynamics. (1980b) Initial submission: Twenty-four month oral toxicity/carcinogenicity study of acrylonitrile administered by intubation to Spartan rats (final report) with cover letter dated 072492. Submitted under TSCA Section 8E; EPA Document No. 88-920005775; NTIS No. OTS0544558.

Biodynamics. (1980c) Initial submission: 24-month oral toxicity/carcinogenicity study with acrylonitrile administered in drinking water to F344 rats (final report) with cover letter dated 072492. Submitted under TSCA Section 8E; EPA Document No. 88-920005777; NTIS No. OTS0544560 (summary only). Full report available from National Institute for Occupational Safety and Health, Centers for Disease Control and Prevention, U.S. Department of Health and Human Services, Cincinnati, OH, 1-800-356-4674.

Blair, A; Stewart, PA; Zaebst, DD; et al. (1998) Mortality of industrial workers exposed to acrylonitrile. Scand J Work Environ Health 24(Suppl 2):25–41.

Borak, J. (1992) Acute acrylonitrile toxicity: reconsideration of mechanisms and antidotes. The OEM Report 6:19–21.

Borba, H; Monteiro, M; Proenca, MJ; et al. (1996) Evaluation of some biomonitoring markers in occupationally exposed populations to acrylonitrile. Teratog Carcinog Mutagen 16:205–218.

Borlakoglu, JT; Scott, A; Henderson, CJ et al. (1993) Expression of P450 isoenzymes during rat liver organogenesis. Int J Biochem 25:1659–1668.

Bradley, MO. (1985) Measurement of DNA single-strand breaks by alkaline elution in rat hepatocytes. Prog Mutat Res 5:353–357.

Brams, A; Buchet, JP; Crutzen-Fayt, MC; et al. (1987) A comparative study, with 40 chemicals, of the efficiency of the Salmonella assay and the SOS chromotest (kit procedure). Toxicol Lett 38:123–133.

Breslow, NE. (1974) Covariance analysis of censored survival data. Biometrics 30:89–99.

Brooks, TM; Gonzalez, LP; Calvert, R; et al. (1985) The induction of mitotic gene conversion in the yeast *Saccharomyces cerevisiae* strain JD1 Prog Mutat Res 5:225–228.

Brzezinski, MR; Boutelet-Bochan, H; Person, RE; et al. (1999) Catalytic activity and quantitation of cytochrome P450 2E1 in prenatal human brain. J Pharm Exp Therap 289(3):1648–1653.

Buckpitt, AR; Rollins, DE; Mitchell, JR. (1979) Varying effects of sulfhydryl nucleophiles on acetaminophen oxidation and sulfhydryl adduct formation. Biochem Pharmacol 28:2941–2946.

Burka, LT; Sanchez, IM; Ahmed, AE; et al. (1994) Comparative metabolism and disposition of acrylonitrile and methacrylonitrile in rats. Arch Toxicol 68:611–618.

Butterworth, BE; Eldridge, SR; Sprankle, CS; et al. (1992) Tissue-specific genotoxic effects of acrylamide and acrylonitrile. Environ Mol Mutagen 20:148–155.

Campian, EC; Cai, J; Benz, FW. (2002) Acrylonitrile irreversibly inactivates glyceraldehyde-3-phosphate dehydrogenase by alkylating the catalytically active cysteine-149. Chem Biol Interact 140:279–291.

Campian, EC; Benz, FW. (2008) The acute lethality of acrylonitrile is not due to brain metabolic arrest. Toxicology 253: 104-109.

Carrera, MP; Antolin, I; Martin, V; et al. (2007) Antioxidants do not prevent acrylonitrile-induced toxicity. Toxicol Lett 169:236–244.

Carrière, V; Berthou, F; Baird, S; et al. (1996) Human cytochrome P450 2E1 (CYP2E1) from genotype to phenotype. Pharmacogenetics 6:203–211.

Chanas, B; Wang, H; Ghanayem, BI. (2003) Differential metabolism of acrylonitrile to cyanide is responsible for the greater sensitivity of male vs female mice: role of CYP2E1 and epoxide hydrolases. Toxicol Appl Pharmacol 193:293–302.

Chang, CM; Hsia, MT; Stoner, GD; et al. (1990) Acrylonitrile-induced sister-chromatid exchanges and DNA single-strand breaks in adult human bronchial epithelial cells. Mutat Res 241:355–360.

Chantara, W; Watcharasit, P; Thiantanawat, A; et al. (2006) Acrylonitrile-induced extracellular signal-regulated kinase (ERK) activation via protein kinase C (PKC) in SK-N-SH neuroblastoma cells. J Appl Toxicol 26:517–523.

Checkoway, H; Pearce, NE; Crawford-Brown, D. (1989) Research methods in occupational epidemiology. New York, NY: Oxford University Press.

Chen, JL; Walrath, J; O'Berg, MT; et al. (1987) Cancer incidence and mortality among workers exposed to acrylonitrile. Am J Ind Med 11:157–163.

Chen, Y; Chen, C; Jin, S; et al. (1999) The diagnosis and treatment of acute acrylonitrile poisoning: a clinical study of 144 cases. J Occup Health 41:172–176.

Chen, Y; Chen, C; Zhu, P. (2000) Study on the effects of occupational exposure to acrylonitrile in workers. China Occup Med J 18(3). Available online at http://www.ilib2.com/A-ISSN~1006-9070(2007)03-0001-04.htm (accessed date April 22, 2009).

Cheng, KC; Cahill, DS; Kasai, H; et al. (1992) 8-Hydroxyguanine, an abundant form of oxidative DNA damage, causes G----T and A----C substitutions. J Biol Chem 267(1):166–172.

Chengelis, CP. (1988) Age- and sex-related changes in epoxide hydrolase, UDP-glucuronosyl transferase, glutathione S-transferase, and PAPS sulphotransferase in Sprague-Dawley rats. Xenobiotica 18:1225–1237.

Cohen, SM. (2004) Human carcinogenic risk evaluation: an alternative approach to the two-year rodent bioassay. Toxicol Sci 80:225–229.

Cole, CE; Tran, HT; Schlosser, PM (2001) Physiologically based pharmacokinetic modeling of benzene metabolism in mice through extrapolation from in vitro to in vivo. J Toxicol Environ Health 62:439–465.

Collins, AR. (2007) Investigating oxidative DNA damage and its repair using the comet assay. Mutation Research/Reviews in Mutation Research 681: 24-32.

Collins, JJ; Page, LC; Caporossi, JC; et al. (1989) Mortality patterns among employees exposed to acrylonitrile. J Occup Med 31:368–371.

Cornet, M; Mertens, K; Callaerts, A; et al. (1994) Age- and gender-related changes in the hepatic metabolism of 2-methylpropene and relationship to epoxide metabolizing enzymes. Mech Ageing Develop74:103–115.

Corsaro, CM; Migeon, BR. (1978) Gene expression in euploid human hybrid cells: ouabain resistance is codominant. Somatic Cell Genet 4:531–540.

Cox, DR. (1972) Regression models and life-tables (with discussion). J R Stat Soc [Ser B] 34:187–220.

Crespi, CL; Ryan, CG; Seixas, GM; et al. (1985) Tests for mutagenic activity using mutation assays at two loci in the human lymphoblast cell lines YK6 and AHH-1. Prog Mutat Res 5:497–516.

Cresteil, T; Beaune, P; Kremers, P; Celier, C; et al. (1985) Immunoquantification of epoxide hydrolase and cytochrome P-450 isozymes in fetal and adult human liver microsomes. Eur J Biochem 151:343–350.

Cuterman, A; Manwaring, D; Curreri, PW. (1977) The role of fibrinogen degradation products in the pathogenesis of respiratory distress syndrome. Surgery 82:703–709.

Czeizel, AE; Hegedus, S; Timar, L. (1999) Congenital abnormalities and indicators of germinal mutations in the vicinity of an acrylonitrile producing factory. Mutat Res 427:105–123.

Czeizel, AE; Hegedus, S; Timar, L. (2000) Corrigendum to “Congenital abnormalities and indicators of germinal mutations in the vicinity of an acrylonitrile producing factory.” Mutat Res 453:105–106.

Czeizel, AE; Szilvasi, R; Timar, L; et al. (2004) Occupational epidemiological study of workers in an acrylonitrile using factory with particular attention to cancers and birth defects. Mutat Res 547:79–89.

Danford, N. (1985) Tests for chromosomal aberrations and aneuploidy in the Chinese hamster fibroblast cell line CH1-L. Prog Mutat Res 5:397–411.

de Waziers, I; Cugnenc, PH; Yang, CS; et al. (1990) Cytochrome P 450 isoenzymes, epoxide hydrolase and glutathione transferases in rat and human hepatic and extrahepatic tissues. J Pharmacol Exp Ther 253(1):387−94.

de Meester, C; Poncelet, F; Roberfroid, M; et al. (1978) Mutagenicity of acrylonitrile. Toxicology 11:19–27.

Delivanova, S; Popovski, P; Orusev, T. (1978) Blepaharoconjunctivitis in workers in the manufacture of synthetic polyacrylonitrile fibers. God Zb Med Fak Skopje 24:279–282.

Delzell, E; Monson, RR. (1982) Mortality among rubber workers: VI. Men with potential exposure to acrylonitrile. J Occup Med 24:767–769.

Denlinger, CL; Vesell, ES (1989) Hormonal regulation of the developmental pattern of epoxide hydrolases. Biochem Pharmacol 38:603–610.

De Vries, N ; De Flora, S (1993) N-Acetyl-L-cysteine. J. Cell Biochem 17F : S270-S277.

Ding, S; Lai-ji, MA; Fan, W; et al. (2003) Study on mitochondrial DNA damage in peripheral blood nucleate cells of the workers exposed to acrylonitrile. Chinese J Indust Hyg Occup Disease 21:99–101. (Chinese).

Doll, R. (1971) The age distribution of cancer: implications for models of carcinogenesis. J R Stat Soc [Ser A] 134:133–166.

Dong, D; Pan, J. (1995) Acrylonitrile effect on worker's reproductive system. Petrochem Safe Technol Mag 5:30–31

Dong, D; Tao, D; Yang, Y. (2000a) Study of occupational harmfulness to acrylonitrile workers. Industrial Health Department of Safety and Technology, Daqing Petrochemical General Plant. Submitted under TSCA Section 8E; EPA Document No. 89-000000313; NTIS No. OTS0559911.

Dong, D; Wang, D; Ai, X; et al. (2000b) Study of acrylonitrile hazardous effects on workers' reproductive system. Submitted under TSCA Section 8E; EPA Document No. 89-000000313; NTIS No. OTS0559911.

Douglas, GR; Blakey, DH; Liu-Lee, VW; et al. (1985) Alkaline sucrose sedimentation, sister chromatid exchange and micronucleus assays in CHO cells. Prog Mutat Res 5:359–366.

Dow Chemical Co. (1976) Interim Report. In vitro microbiological mutagenicity studies of Dow Chemical Company Compounds. Submitted under TSCA Section FYI; EPA Document No. FYI-OTS-0677-0150; NTIS No. OTS0000150-0.

Dow Chemical Co. (1977) Teratologic evaluation of acrylonitrile monomer given to rats by gavage. Submitted under TSCA SectionFYI; EPA Document No. FYI-OTS-0677-0150; NTIS No. OTS0000150-0.

Dow Chemical Co. (1992a) Initial submission: 2-year toxicity and oncogenicity study with acrylonitrile following inhalation exposure in rats (final report) with cover letter dated 080392. Submitted under TSCA Section 8E; EPA Document No. 88-9200006574; NTIS No. OTS0545173.

Dow Chemical Co. (1992b) Initial submission: teratologic evaluation of gavaged acrylonitrile monomer in rats with cover letter dated 08/10/92. Submitted under TSCA Section 8E; EPA Document No. 88-920010410; NTIS No. OTS0555785.

Dudley, HC; Neal, PA. (1942) Toxicology of acrylonitrile (vinyl cyanide). I. A study of the acute toxicity. J Ind Hyg Toxicol 24:27–36.

Bureau, Institute for Health and Protection, European Commission and Joint Research Centre, Dublin, Ireland; EINECS (European Inventory of Existing Commerical Chemical Substances) No. 203-466-5. Available online at http://ecb.jrc.ec.europa.eu/DOCUMENTS/Existing- EC (European Communities). (2004) European Union risk assessment report: acrylonitrile. European Chemicals Chemicals/RISK_ASSESSMENT/REPORT/acrylonitrilereport029.pdf (accessed April 20, 2009).

El-Sayed, EM; Abo-Salem, OM; Abd-Ellah, MF et al. (2008) Hesperidin, an antioxidant flavonoid, prevents acrylonitrile-induced oxidative stress in rat brain. J Biochem Molecular Toxicol 22: 268-273.

El Hadri, L; Chanas, B.; Ghanayem, BI. (2005) Comparative metabolism of methacrylonitrile and acrylonitrile to cyanide using cytochrome P4502E1 and microsomal epoxide hydrolase-null mice. Toxicol Appl Pharmacol 205:116–125.

Elmore, E; Korytynski, EA; Smith, MP. (1985) Tests with the Chinese hamster V79 inhibition of metabolic cooperation assay. Prog Mutat Res 5:597–612.

Esmat, M; El-Demerdash, E; El-Mesallamy, H; et al. (2007) Toxicity and oxidative stress of acrylonitrile in rat primary glial cells: preventive effects of N-acetylcysteine. Toxicol Lett 171:111–118.

Fahmy, MA. (1999) Evaluation of the genotoxicity of acrylonitrile in different tissues of male mice. Cytologia 64:1–9.

Fan, W; Wang, WL; Ding, S; et al. (2006) [Application of micronucleus test of buccal mucosal cells in assessing the genetic damage of workers exposed to acrylonitrile.] Zhonghua Lao Dong Wei Sheng Zhi Ye Bing Za Zhi 24(2):106–108. (Chinese)

Fang, JY; Richardson, BC. (2005) The MAPK signaling pathways and colorectal cancer. Lancet Oncol 6:322–327.

Farooqui, MY; Ahmed, AE. (1982) Molecular interactions of acrylonitrile and potassium cyanide with rat blood. Chem Biol Interact 38:145–159.

Farooqui, MY; Ahmed, AE. (1983a) In vivo interactions of acrylonitrile with macromolecules in rats. Chem Biol Interact 47:363–371.

Farooqui, MY; Ahmed, AE. (1983b) The effects of acrylonitrile on hemoglobin and red cell metabolism. J Toxicol Environ Health 12:695–707.

Farooqui, MY; Mumtaz, MM; Ghanayem, BI; et al. (1990) Hemoglobin degradation, lipid peroxidation, and inhibition of Na+/K(+)-ATPase in rat erythrocytes exposed to acrylonitrile. J Biochem Toxicol 5:221–227.

Fechter, LD. (2004) Promotion of noise-induced hearing loss by chemical contaminants. J Toxicol Environ Health A 67:727–740.

Fechter, LD; Sjaak, FL; Najeeb, K; et al. (2003) Acrylonitrile produces transient cochlear function loss and potentiates permanent noise-induced hearing loss. Toxicol Sci 75:117–123.

Fechter, LD; Gearhart, C; Shirwany, NA. (2004) Acrylonitrile potentiates noise-induced hearing loss in rat. JARO 5:90–98.

Fei, N; Xu, LZ. (2006) [Parkinson's syndrome after acute severe acrylonitrile poisoning in one patient.] Zhonghua Lao Dong Wei Sheng Zhi Ye Bing Za Zhi 24(5):309–310. (Chinese)

Fennell, TR; Sumner, SCJ. (1994) Identification of metabolites of carcinogens by ^{13}C NMR spectroscopy. Drug Metab Rev 26:469–481.

Fennell, TR; Kedderis, GL; Sumner, SCJ. (1991) Urinary metabolites of [1,2,3-13C]acrylonitrile in rats and mice detected by carbon-13 nuclear magnetic resonance spectroscopy. Chem Res Toxicol 4:678–687.

Fennell, TR; MacNeela, JP; Morris, RW; et al. (2000) Hemoglobin adducts from acrylonitrile and ethylene oxide in cigarette smokers: effects of glutathione S-transferase T1-null and M1-null genotypes. Cancer Epidemiol Biomarkers Prev 9:705–712.

Filser, JG; Bolt, HM. (1984) Inhalation pharmacokinetics based on gas uptake studies. VI. Comparative evaluation of ethylene oxide and butadiene monoxide as exhaled reactive metabolites of ethylene and 1,3-butadiene in rats. Arch Toxicol 55:219–223.

Fischel-Ghodsian, N; Kopke, RD; Ge, X. (2004) Mitochondrial dysfunction in hearing loss. Mitochondrion 4:675–694.

Foureman, P; Mason, JM; Valencia, R; et al. (1994) Chemical mutagenesis testing in drosophila. IX. Results of 50 coded compounds tested for the National Toxicology Program. Environ Mol Mutagen 23:51–63.

Friedman, MA; Beliles, RP. (2002) Three-generation reproduction study of rats receiving acrylonitrile in drinking water. Toxicol Lett 132:249–261.

Gagnaire, F; Marignac, B; Bonnet, P. (1998) Relative neurotoxicological properties of five unsaturated aliphatic nitriles in rats. J Appl Toxicol 18:25–31.

Gallagher, GT; Maull, EA; Kovacs, K; et al. (1988) Neoplasms in rats ingesting acrylonitrile for two years. J Am Coll Toxicol 7:603–615.

Gargas, ML; Andersen, ME; Teo, SK; et al. (1995) A physiologically based dosimetry description of acrylonitrile and cyanoethylene oxide in the rat. Toxicol Appl Pharmacol 134:185–194.

Garner, RC; Campbell, J. (1985) Tests for the induction of mutations to ouabain or 6-thioguanine resistance in mouse lymphoma L5178Y cells. Prog Mutat Res 5:525–529.

Garmin, RH; Snellings, WM; Maronpot, RR. (1985) Brain tumors in F344 rats associated with chronic inhalation exposure to ethylene oxide. Neurotoxicol 6: 117-138.

Garmin, RH; Snellings, WM; Maronpot, RR (1986) Frequency, size and location of brain tumours in F344 rats chronically exposed to ethylene oxide. Food Chem Toxicol 24: 145-153.

Geiger, LE; Hogy, LL; Guengerich, FP. (1983) Metabolism of acrylonitrile by isolated rat hepatocytes. Cancer Res 43:3080–3087.

Geng, J; Strobel, HW. (1993) Identification of cytochromes P.450 1A2, 2A1, 2C7, 2E1 in rat glioma C6 cell line by RP PCR and specific restriction enzyme digestion. Biochem Biophys Res Commun 197:1179–1184.

George, J; Byth, K; Farrell, GC. (1995) Age but not agender selectively affects expression of individual cytochrome P450 proteins in human liver. Biochemical Pharmacol 50:727–730.

Ghanayem, BI; Ahmed, AE. (1982) In vivo biotransformation and biliary excretion of 1-^{14}C-acrylonitrile in rats. Arch Toxicol 50:175–185.

Ghanayem, BI; Ahmed, AE. (1983) Acrylonitrile-induced gastrointestinal hemorrhage and the effects of metabolism modulation in rats. Toxicol Appl Pharmacol 68:290–296.

Ghanayem, BI; Ahmed, AE. (1986) Prevention of acrylonitrile-induced gastrointestinal bleeding by sulfhydryl compounds, atropine and cimetidine. Res Commun Chem Pathol Pharmacol 53:141–144.

Ghanayem, BI; Boor, PJ; Ahmed, AE. (1985) Acrylonitrile-induced gastric mucosal necrosis: role of gastric glutathione. J Pharmacol Exp Ther 232:570–577.

Ghanayem, BI; Farooqui, MY; Elshabrawy, O; et al. (1991) Assessment of the acute acrylonitrile-induced neurotoxicity in rats. Neurotoxicol Teratol 13:499–502.

Ghanayem, BI; Elwell, MR; Eldridge, SR. (1997) Effects of the carcinogen, acrylonitrile, on forestomach cell proliferation and apoptosis in the rat: comparison with methacrylonitrile. Carcinogenesis 18:675–680.

Grunske, F. (1949) Health care and occupational medicine: ventox and ventox intoxication. Dtsch Med Wochenscher 74:1081–1083. (as cited in ATSDR, 1990).

Guengerich, FP; Wang, P; Mason, PS; et al. (1979) Rat and human microsomal epoxide hydratase. Immunological characterization of various forms of the enzyme. J Biol Chem 254(23):12255–12259.

Guengerich, FP; Geiger, LE; Hogy, LL; et al. (1981) In vitro metabolism of acrylonitrile to 2-cyanoethylene oxide, reaction with glutathione, and irreversible binding to proteins and nucleic acids. Cancer Res 41:4925–4933.

Guengerich, FP; Hogy, LL; Inskeep, PB; et al. (1986) Metabolism and covalent binding of vic-dihaloalkanes, vinyl halides and acrylonitrile. IARC Sci Publ 70:255–260.

Gut, I: Kopecky, J; Filip, J. (1981) Acrylonitrile-^{14}C metabolism in rats: effect of the route of administration on the elimination of thiocyanate and other radioactive metabolites in urine and feces. J Hyg Epidemiol Microbiol Immunol 25:12–16.

Gut, I; Nerudova, J; Frantik, E; et al. (1984) Acrylonitrile inhalation in rats: I. Effect on intermediary metabolism. J Hyg Epidemiol Microbiol Immunol 28:369–376.

Gut, I; Nerudova, J; Stiborova, A; et al. (1985) Acrylonitrile inhalation in rats: II. Excretion of thioethers and thiocyanate in urine. J Hyg Epidemiol Microbiol Immunol 29:9–13.

Guyton, KZ; Kensler, TW. (1993) Oxidative mechanisms in carcinogenesis. Brit Med Bull 49:523–544.

Hakura, A; Shimada, H; Nakajima, M; et al. (2005) Salmonella/human S9 mutagenicity test: a collaborative study with 58 compounds. Mutagenesis 20:217–228.

Hamada, FM; Abdel-Aziz, AH; Abd-Allah, AR; et al. (1998) Possible functional immunotoxicity of acrylonitrile (VCN). Pharmacol Res 37:123–129.

Harrison, DJ; Hubbard, AL; MacMillan, J; et al. (1999) Microsomal epoxide hydrolase gene polymorphism and susceptibility to colon cancer. Br J Cancer 79:168–171.

Hashimoto, K; Kobayasi, T. (1961) A case of acute dermatitis caused by contact with acrylonitrile. Q J Labor Res 9:21–24.

Haskell Laboratory. (1992a) Initial submission: teratological evaluation of inhaled acrylonitrile monomer in rats with cover letter dated 090192. Submitted under TSCA Section 8E; EPA Document No. 88-920008569; NTIS No. OTS0570857.

Haskell Laboratory. (1992b) Initial submission: acute inhalation toxicity in rats with acrylonitrile (inhibited), methyacrylonitrile (inhibited), and acetonitrile with cover letter dated 101592. Submitted under TSCA Section 8E; EPA Document No. 88-920009947; NTIS No. OTS0571605.

Hassett, C; Lin, J; Carty, CL; et al. (1997). Human hepatic microsomal epoxide hydrolase: comparative analysis of polymorphic expression. Arch Biochem 337:275–283.

Hedlund, B; Bartfai, T. (1979) The importance of thiol- and disulfide groups in agonist and antagonist binding to the muscarinic receptor. Mol Pharmacol 15:531–544.

Heinrichs, WL; Juchau, MR. (1980) Extrahepatic drug metabolism: the gonads. In: Gram, TE, ed. Extrahepatic metabolism of drugs and other foreign compounds. New York, NY: SP Medical and Scientific Books, pp. 319–332.

Hogy, LL. (1986) Metabolism of acrylonitrile and interactions with DNA (adduct, carcinogen, epoxide). Ph.D. thesis submitted to Vanderbilt University, Nashville, TN. Available from ProQuest, Ann Arbor, MI, Document No. 8616356.

Hogy, LL; Guengerich, FP. (1986) In vivo interaction of acrylonitrile and 2-cyanoethylene oxide with DNA in rats. Cancer Res 46:3932–3938.

IARC (International Agency for Research on Cancer). (1999) Predictive value of rodent forestomach and gastric neuroendocrine tumours in evaluating carcinogenic risks to humans, views and expert opinions of an IARC Working Group. Technical Publication No. 39. Lyon, France: International Agency for Research on Cancer.

Ikeda, SR; Aronstam, RS; Eldefrawi, ME. (1980) Nature of regional and chemically induced differences in the binding properties of muscarinic acetylcholine receptors from rat brain. Neuropharmacology 19:575–585.

IPCS (International Programme on Chemical Safety). (1983) Acrylonitrile. Environmental health criteria. Vol. 28. Geneva, Switzerland: World Health Organization. Available online at http://www.inchem.org/documents/ehc/ehc/ehc28.htm (accessed April 21, 2009)

IPCS (International Programme on Chemical Safety). (1985) Summary report of the evaluation of short-term tests from carcinogens (collaborative study on in vitro tests). Environmental health criteria. Vol. 47. Available online at http://www.inchem.org/documents/ehc/ehc/ehc47.htm (accessed April 21, 2009)

IPCS (International Programme on Chemical Safety). (2002) Acrylonitrile. Concise international chemical assessment document. Vol. 39. Geneva, Switzerland: World Health Organization. Available online at http://www.inchem.org/documents/cicads/cicads/cicad39.htm (accessed April 21, 2009).

Irwin, RD; Eustis, SL; Stefanski, S et al. (1996). Carcinogenicity of glycidol in F344 rats and B6C3F1 mice. J. of Applied Toxicology 16: 201-209.

Ishidate, M, Jr; Sofuni, T. (1985) The in vitro chromosomal aberration test using Chinese hamster lung (CHL) fibroblast cells in culture. Prog Mutat Res 5:427–432.

Ishidate, M, Jr; Sofuni, T; Yoshikawa, K. (1981) Chromosomal aberration tests in vitro as a primary screening tool for environmental mutagens and/or carcinogens. Gann 27:95–108.

Ivanescu, M; Berinde, M; Simionescu, L. (1990) Testosterone in sera of workers exposed to acrylonitrile. Revue Roum Med - Ser Endocrinol 28:187–192.

Jackson, MA; Stack, FH; Rice, JM; et al. (2000) A review of the genetic and related effects of 1,3-butadiene in rodents and humans. Mutat Res 463:181–213.

Jacob, S; Ahmed, AE. (2003a) Effect of route of administration on the disposition of acrylonitrile: quantitative whole-body autoradiographic study in rats. Pharmacol Res 48:479–488.

Jacob, S; Ahmed, AE. (2003b) Acrylonitrile-induced neurotoxicity in normal human astrocytes: oxidative stress and 8-hydroxy-2'-deoxyguanosine formation. Toxicol Mech Methods 13:169–179.

Jakubowski, M; Linhart, I; Pielas, G; et al. (1987) 2-Cyanoethylmercapturic acid (CEMA) in the urine as a possible indicator of exposure to acrylonitrile. Br J Ind Med 44:834–840.

Jedlicka, V; Pasek, A; Gola, J. (1958) Pesticides in foods. III. Acrylonitrile as a food insecticide. Hyg Epidemiol Microbiol Immunol. 1:116–125.

Jiang, J; Xu, Y; Klaunig, J E. (1998) Induction of oxidative stress in rat brain by acrylonitrile (ACN). Toxicol Sci 46:333–341.

Jiménez, E; Montiel, M. (2005) Activation of MAP kinase by muscarinic cholinergic receptors induces cell proliferation and protein synthesis in human breast cancer cells. J Cell Physiol 204:678–686.

Johannsen, FR; Levinskas, GJ. (2002a) Comparative chronic toxicity and carcinogenicity of acrylonitrile by drinking water and oral intubation to Spartan Sprague-Dawley rats. Toxicol Lett 132:197–219.

Johannsen, FR; Levinskas, GJ. (2002b) Chronic toxicity and oncogenic dose-response effects of lifetime oral acrylonitrile exposure to F344 rats. Toxicol Lett 132:221–247.

Johnson, TN. (2003) The development of drug metabolising enzymes and their influence on the susceptibility to adverse drug reactions in children. Toxicology 192:37–48.

Johnsrud, EK; Koukouritaki, SB; Divrkaran, K; et al. (2003) Human hepatic CYP2E1 expression during development. J Pharmacol Exp Ther 307:402–407.

Jung, R; Engelhart, G; Herbolt, B; et al. (1992) Collaborative study of mutagenicity with *Salmonella typhimurium* TA102. Mutat Res 278:265–270.

Kamendulis, LM; Jiang, J; Xu, Y; et al. (1999a) Induction of oxidative stress and oxidative damage in rat glial cells by acrylonitrile. Carcinogenesis 20:1555–1560.

Kamendulis, LM; Jiang, J; Zhang, H; et al. (1999b) The effect of acrylonitrile on gap junctional intercellular communication in rat astrocytes. Cell Biol Toxicol 15:173–183.

Kamiat, H; Miura, K; Ishikawa, H; et al. (1992) C-Ha-ras containing 8-hydroxyguanine at codon 12 induces point mutations at the modified and adjacent positions. Cancer Res 52:3483–3485.

Kaneko, Y; Omae, K. (1992) Effect of chronic exposure to acrylonitrile on subjective symptoms. Keio J Med 41:25–32.

Kedderis, GL. (1997) Development of a physiologically based dosimetry description for acrylonitrile (ACN) in humans. Toxicologist 36(1, Pt. 2):31.

Kedderis, GL; Batra, R. (1993) Species differences in the hydrolysis of 2-cyanoethylene oxide, the epoxide metabolite of acrylonitrile. Carcinogenesis 14:685–689.

Kedderis, GL; Held, SD. (1998) Refinement of the human dosimetry description for acrylonitrile (ACN). Toxicologist 42(1-S):142.

Kedderis, GL; Sumner, SC; Held, SD; et al. (1993a) Dose-dependent urinary excretion of acrylonitrile metabolites by rats and mice. Toxicol Appl Pharmacol 120:288–297.

Kedderis, GL; Batra, R; Held, SD; et al. (1993b) Rodent tissue distribution of 2-cyanoethylene oxide, the epoxide metabolite of acrylonitrile. Toxicol Lett 69:25–30.

Kedderis, GL; Batra, R; Koop, DR. (1993c) Epoxidation of acrylonitrile by rat and human cytochromes P450. Chem Res Toxicol 6:866–871.

Kedderis, GL; Batra, R; Turner, MJ, Jr. (1995) Conjugation of acrylonitrile and 2-cyanoethylene oxide with hepatic glutathione. Toxicol Appl Pharmacol 135:9–17.

Kedderis, GL; Teo, SK; Batra, R; et al. (1996) Refinement and verification of the physiologically based dosimetry description for acrylonitrile in rats. Toxicol Appl Pharmacol 140:422–435.

Kemper, RA; Krause, RJ; Elfarra, AA. (2001) Metabolism of butadiene monoxide by freshly isolated hepatocytes from mice and rats: different partitioning between oxidative, hydrolytic, and conjugation pathways. Drug Metab Dispos 29:830–836.

Khudoley, VV; Mizgireuv, I; Pliss, GB. (1987) The study of mutagenic activity of carcinogens and other chemical agents with *Salmonella typhimurium* assays: testing of 126 compounds. Arch Geschwulstforsch 57:453–462.

Kim, RB; Yamazaki, H; Chiba, K; et al. (1996) In vivo and in vitro characterization of CYP2E1 activity in Japanese and Caucasians. J Pharmacol Exp Ther 279:4–11.

Klaasen, CD, ed. (2001) Casarett and Doull's toxicology: the basic science of poisons. 6th edition. New York, NY: McGraw-Hill Companies, Inc.

Kleihues, P; Bucheler, J. (1977) Long-term persistence of O6-methylguanine in rat brain DNA. Nature 269(5629):625–626.

Knobloch, K; Szendzikowski, S; Czajkowska, T; et al. (1971) Experimental studies on acute and subacute toxicity of acrylonitrile. Med Pr 22:257–269.

Kodama, Y; Boreiko, CJ; Skopek, TR; et al. (1989) Cytogenetic analysis of spontaneous and 2-cyanoethylene oxide-induced tk-/- mutants in TK6 human lymphoblastoid cultures. Environ Mol Mutagen 14:149–154.

Kohn, MC; Melnick, RL. (2000) The privileged access model of 1,3-butadiene disposition. Environ Health Perspect 108(Suppl 5):911–917.

Kopecky, J; Gut, I; Nerudova, J; et al. (1980) Two routes of acrylonitrile metabolism. J Hyg Epidemiol Microbiol Immunol 24:356–362.

Kopylev, L; Chen, C; White, P. (2007) Towards quantitative uncertainty assessment for cancer risks: central estimates and probability distributions of risk in dose-response modeling. Regul Toxicol Pharmacol 49(3):203–207.

Krause, RJ; Sharer, JE; Elfarra, AA. (1997) Epoxide hydrolase-dependent metabolism of butadiene monoxide to 3-butene-1,2-diol in mouse, rat and human liver. Drug Metab Dispos 25:1013–1015.

Lakhanisky, Th; Hendrickx, B. (1985) Induction of DNA single-strand breaks in CHO cells in culture. Prog Mutat Res 5:367–370.

Lambotte-Vandepaer, M; Duverger-van Bogaert, M; de Meester, C; et al. (1980) Mutagenicity of urine from rats and mice treated with acrylonitrile. Toxicology 16:67–71.

Lambotte-Vandepaer, M; Duverger-van Bogaert, M; de Meester, C; et al. (1981) Identification of two urinary metabolites of rats treated with acrylonitrile; influence of several inhibitors on the mutagenicity of those urines. Toxicol Lett 7:321–327.

Lambotte-Vandepaer, M; Duverger-van Bogaert, M; Rollmann, B. (1985) Metabolism and mutagenicity of acrylonitrile: an in vivo study. Environ Mutagen 7:655–662.

Langvardt, PW; Putzig, CL; Young, JD; et al. (1979) Isolation and identification of urinary metabolites of vinyl-type compounds: application to metabolites of acrylonitrile and acrylamide. Toxicol Appl Pharmacol 48:A161.

Langvardt, PW; Putzig, CL; Braun, WH; et al. (1980) Identification of the major urinary metabolites of acrylonitrile in the rat. J Toxicol Environ Health 6:273–282.

Larsson, R; Cerutti, P. (1989) Translocation and enhancement of phosphotransferase activity of protein kinase C following exposure in mouse epidermal cells to oxidants. Cancer Res 49:5627–5632.

Lawrence, N; McGregor, DB. (1985) Assays for the induction of morphological transformation in C3H/10T1/2 cells in culture with and without S9-mediated metabolic activation. Prog Mutat Res 5:651–658.

Lee, CG; Webber, TD. (1985) The induction of gene mutations in the mouse lymphoma L5178Y/TK$^{+/-}$ assay and the Chinese hamster V79/HGPRT assay. Prog Mutat Res 5:547–554.

Leonard, A; Garny, V; Poncelet, F; et al. (1981) Mutagenicity of acrylonitrile in mouse. Toxicol Lett 7:329–334.

Li, Z. (2000) Study on reproductive organs in female workers exposed to acrylonitrile. Lanzhou Medical College. Submitted under TSCA Section 8E; EPA Document No. 88-000000150; NTIS No. OTS0559911.

Lijinsky, W; Andrews, AW. (1980) Mutagenicity of vinyl compounds in *Salmonella typhimurium*. Teratog Carcinog Mutagen 1:259–267.

Lipscomb, JC; Fisher, JW; Confer, PD; et al. (1998) In vitro extrapolation for trichloroethylene metabolism in humans. Toxicol Appl Pharmacol 152(2):376–387.

Lipscomb, JC; Teuschler, LK; Swartout, J; et al. (2003) The impact of cytochrome P450 2E1-dependent metabolic variance on a risk-relevant pharmacokinetic outcome in humans. Risk Anal 23(6):1221–1238.

Litton Bionetics. (1992) Initial submission: three-generation reproduction study of rats receiving acrylonitrile in drinking water (final report) with attachments and cover letter dated 043092. Submitted under TSCA Section 8E; EPA Document No. 88-920002178; NTIS No. OTS0536313.

Liu, X; Xiao, W; Wang, Z; et al. (2004) Effect of acrylonitrile on spermatogenesis in mice. J Hyg Res 33:345–346.

Lorz, H. (1950) On the percutaneous poisoning by acrylonitrile (Ventox). Dtsch Med Wochenschr 75:1087–1088.

Lu, R; Ziqiang C; Fusheng J; et al. (2005a) Neurobehavioral effects of occupational exposure to acrylonitrile in Chinese workers. Environ Toxicol Pharmacol 19:695–700.

Lu, R; Chen, Z; Fusheng, J. (2005b) [Effect of acrylonitrile on monoamine neurotransmitters and their metabolites in the brains of rats.] Chinese J Prev Med 39:122–126. (Chinese)

Lucas, D; Berthou, F; Dreano, Y; et al. (1993) Comparison of levels of cytochromes P-450, CYP1A2, CYP2E1, and their related monooxygenase activities in human surgical liver samples. Alcohol Clin Exp Res 17(4):900–905.

MacNeela, JP; Osterman-Golkar, SM; Turner, MJ; et al. (1992) 2-Cyanoethylvaline in hemoglobin as a dosimeter for exposure to acrylonitrile. Proc Am Assoc Cancer Res 33:147.

Mahalakshmi, K; Pushpakiran, G; Anuradha, CV. (2003) Taurine prevents acrylonitrile-induced oxidative stress in rat brain. Pol J Pharmacol 55:1037–1043.

Malik, AB; Lee, BC; van der Zee, H; et al. (1979) The role of fibrin in the genesis of pulmonary edema after embolization in dogs. Circ Res 45(1):120–125.

Maltoni, C; Ciliberti, A; Di, MV. (1977) Carcinogenicity bioassays on rats of acrylonitrile administered by inhalation and by ingestion. Med Lav 68:401–411.

Maltoni, C; Ciliberti, A; Cotti, G; et al. (1988) Long-term carcinogenicity bioassays on acrylonitrile administered by inhalation and by ingestion to Sprague-Dawley rats. Ann NY Acad Sci 534:179–202.

Mangir, M; Al, BI; Lochmann, E-R; et al. (1991) A test system for the rapid detection of nuclear and cytoplasmic damage in Chinese hamster ovary cells. Chemosphere 23:777–784.

Marsh, GM; Gula, MJ; Youk, AO; et al. (1999) Mortality among chemical plant workers exposed to acrylonitrile and other substances. Am J Ind Med 36:423–436.

Marsh, GM; Youk, AO; Collins, JJ. (2001) Reevaluation of lung cancer risk in the acrylonitrile cohort study of the National Cancer Institute and the National Institute for Occupational Safety and Health. Scand J Work Environ Health 27:5–13.

Martin, CN; Campbell, J. (1985) Tests for the induction of unscheduled DNA repair synthesis in HeLa cells. Prog Mutat Res 5:375–379.

Martin, C; Dutertre-Catella, H; Radionoff, M; et al. (2003) Effect of age and photoperiodic conditions on metabolism and oxidative stress related markers at different circadian stages in rat liver and kidney. Life Sci 73(3):327–335.

Mastrangelo, G; Serena, R; Marzia, V. (1993) Mortality from tumours in workers in an acrylic fibre factory. Occup Med 43:155–158.

Matthews, EJ; DelBalzo, T; Rundell, JO. (1985) Assays for morphological transformation and mutation to ouabain resistance of Balb/c-3T3 cells in culture. Prog Mutat Res 5:639–650.

McCarver, DG; Byun, R; Hines, RN; et al. (1998) A genetic polymorphism in the regulatory sequences of human CYP2E1: association with increased chlorzoxazone hydroxylation in the presence of obesity and ethanol intake. Toxicol Appl Pharmacol 152:276–281.

McGlynn, KA; Rosvold, EA; Lustbader, ED; et al. (1995) Susceptibility to hepatocellular carcinoma is associated with genetic variation in the enzymatic detoxification of aflatoxin B1. Proc Natl Acad Sci USA 92:2384–2387.

Meek, ME; Bucher, JR; Cohen, SM; et al. (2003) A framework for human relevance analysis of information on carcinogenic modes of action. Crit Rev Toxicol 33:591–653.

Mehrotra, J; Khanna, VK; Husain, R; et al. (1988) Biochemical and developmental effects in rats following in utero exposure to acrylonitrile: a preliminary report. Ind Health 26:251–255.

Mikhutkina, SV; Salmina, AB; Sychev, AV; et al. (2004) Blebbing of thymocyte plasma membrane and apoptosis are related to impairment of capacitance Ca^{2+} entry into cells. Bull Exp Biol Med 6:551–555.

Milvy, P; Wolff, M. (1977) Mutagenic studies with acrylonitrile. Mutat Res 48:271–278.

Mohamadin, AH; El-Demerdash, E; El-Beshbishy, HA; et al. (2005) Acrylonitrile-induced toxicity and oxidative stress in isolated rat colonocytes. Environ Toxicol Pharmacol 19:371–377.

Morita, T; Asano, N; Awogi, T; et al. (1997) Evaluation of the rodent micronucleus assay in the screening of IARC carcinogens (groups 1,2A and 2B): The summary report of the 6th collaborative study by CSGMT/JEMS MMS. Collaborative study of the micronucleus group test. Mammalian Mutagenicity Study Group. Mutat Res 389:3–122.

Moriya, M; Du, C; Bodepudi, V; et al. (1991) Site-specific mutagenesis using a gapped duplex vector: a study of translesion synthesis past 8-oxodeoxyguanine in *E. coli*. Mutat Res 254:281–288.

Mostafa, AM; Abdel-Naim, AB; Abo-Salem, O; et al. (1999) Renal metabolism of acrylonitrile to cyanide: in vitro studies. Pharmacol Res 40:195–200.

Müller, G; Verkoyen, C; Soton, N; et al. (1987) Urinary excretion of acrylonitrile and its metabolites in rats. Arch Toxicol 60:464–466.

Mulvihill, J; Cazenave, JP; Mazzucotelli, JP; et al. (1992) Minimodule dialyser for quantitative ex vivo evaluation of membrane haemocompatibility in humans: comparison of acrylonitrile copolymer cuprophan and polysulphone hollow fibres. Biomaterials 13:527–536.

Murata, M; Ohnishi, S; Kawanishi, S. (2001) Acrylonitrile enhances H2O2-mediated DNA damage via nitrogen-centered radical formation. Chem Res Toxicol 14:1421–1427.

Murray, FJ; Schwetz, BA; Nitschke, KD; et al. (1978) Teratogenicity of acrylonitrile given to rats by gavage or by inhalation. Food Cosmet Toxicol 16:547–551.

Muto, T; Sakurai, H; Omae, K; et al. (1992) Health profiles of workers exposed to acrylonitrile. Keio J Med 41:154–160.

Myhr, B; Bowers, L; Kaspary, WJ. (1985) Assays for the induction of gene mutations at the thymidine kinase locus in L5178Y mouse lymphoma cells in culture. Prog Mutat Res 5:555–568.

Nakamura, S; Oda, Y; Shimada, T; et al. (1987) SOS-inducing activity of chemical carcinogens and mutagens in *Salmonella typhimurium* TA1535-psk-1002: examination with 151 chemicals. Mutat Res 192:239–246.

NAS (2008) Science and decisions: advancing risk assessment. National Academy of Sciences.

Natarajan, AT; Bussmann, CJM; van Kesteren-van Leeuwen, AC; et al. (1985) Tests for chromosomal aberrations and sister chromatid exchanges in cultured Chinese hamster ovary (CHO) cells. Prog Mutat Res 5:433–437.

Nerland, DE; Cai, J; Pierce, WM, Jr; et al. (2001) Covalent binding of acrylonitrile to specific rat liver glutathione S-transferases in vivo. Chem Res Toxicol 14:799–806.

Nerland, DE; Cai, J; Benz, FW. (2003) Selective covalent binding of acrylonitrile to Cys 186 in rat liver carbonic anhydrase III in vivo. Chem Res Toxicol 16:583–589.

Nilsen, OG; Toftgard, R; Eneroth, P. (1980) Effects of arylonitrile on rat liver cytochrome P-450, benzo(A)pyrenemetabolism and serum hormone levels. Toxicol Lett 6:399–404.

NLM (National Library of Medicine). (2003) Acrylonitrile. HSDB (Hazardous Substances Data Bank). National Institutes of Health, Bethesda, MD. Available on-line at http://toxnet.nlm.nih.gov (accessed April 21, 2009).

NRC (National Research Council). (1983) Risk assessment in the federal government: managing the process. Washington, DC: National Academy Press.

NRC (National Research Council). (1994) Science and judgment in risk assessment. Washington, DC: National Academy Press.

NTP (National Toxicology Program). (1987) Toxicology and carcinogenesis studies of ethylene oxide (CAS No. 75-21-8) in mice (inhalation studies). Tech. report Series No. 326. Available from the National Institute of Environmental Health Sciences, Research Triangle Park, NC

NTP (National Toxicology Program). (2001) Toxicology and carcinogenesis studies of acrylonitrile (CAS No. 107-13-1) in B6C3F1 mice (gavage studies). Public Health Service, U.S. Department of Health and Human Services; NTP TR 506. Available from the National Institute of Environmental Health Sciences, Research Triangle Park, NC Available online at http://ntp.niehs.nih.gov/ntpweb/index.cfm?objectid=D16D6C59-F1F6-975E-7D23D1519B8CD7A5#tr500 (accessed April 21, 2009).

O'Berg, MT. (1980) Epidemiologic study of workers exposed to acrylonitrile. J Occup Med 22:245–252.

O'Berg, MT; Chen, JL; Burke, CA; et al. (1985) Epidemiologic study of workers exposed to acrylonitrile: an update. J Occup Med 27:835–840.

Oberly, TJ; Hoffman, WP; Garriott, ML. (1996) An evaluation of the twofold rule for assessing a positive response in the L5178Y TK(+/-) mouse lymphoma assay. Mutat Res 369:221–232.

O'Connell, JF; Klein-Szanto, AJP; DiGiovanni, DM; et al. (1986) Enhanced malignant progression of mouse skin tumors by the free-radical generator benzoyl peroxide. Cancer Res 46:2863–2865.

Oesch, F; Zimmer, A; Glatt, HR. (1983) Microsomal epoxide hydrolase in different rat strains. Biochem Pharmacol 32:1783–1788.

Ofengand, J. (1967) The function of pseudouridylic acid in transfer ribonucleic acid. I. The specific cyanoethylation of pseudouridine, inosine, and 4-thiouridine by acrylonitrile. J Biol Chem 242(21):5034–5045.

Ohio Department of Health. (2006) Cancer incidence among residents of Addyston Village, Hamilton County, Ohio 1993–2003. Hamilton County General Health District, Cincinnati, OH and the Ohio Department of Health, Columbus, OH. Final report. May 25, 2006.

Omiecinski, CJ; Alcher, L; Swenson, L. (1994) Developmental expression of human microsomal epoxide hydrolase. J Pharmacol Exp Ther 269:417–23.

Osgood, C; Bloomfield, M; Zimmering, S. (1991) Aneuploidy in drosophila. IV. Inhalation studies on the induction of aneuploidy by nitriles. Mutat Res 259:165–176.

Osterman-Golkar, SM; MacNeela, JP; Turner, MJ; et al. (1994) Monitoring exposure to acrylonitrile using adducts with N-terminal valine in hemoglobin. Carcinogenesis 15:2701–2707.

Pacifici, GM; Peng, D; Rane, A (1983) Epoxide hydrolase and aryl hydrocarbon hydroxylase in human fetal tissues: activities in nuclear and microsomal fractions and in isolated hepatocytes. Pediatr Pharmacol 3:189–197.

Pacifici, GM; and Rane, A (1983b) Epoxide hydrolase in human fetal liver. Pharmacology 26: 241-248.

Parent, RA; Casto, BC. (1979) Effect of acrylonitrile on primary Syrian golden hamster embryo cells in culture: transformation and DNA fragmentation. J Natl Cancer Inst 62:1025–1029.

Paulet, G; Desnos, J. (1961) Acrylonitrile, toxicity, mechanism of action, therapeutic uses. Arch Int Pharmacodyn 131:54–83.

Perez, HL; Segerback, D; Osterman-Golkar, S. (1999) Adducts of acrylonitrile with hemoglobin in nonsmokers and in participants in a smoking cessation program. Chem Res Toxicol 12:869–873.

Perocco, P; Pane, G; Bolognesi, S; et al. (1982) Increase of sister chromatid exchange and unscheduled synthesis of deoxyribonucleic acid by acrylonitrile in human lymphocytes in vitro. Scand J Work Environ Health 8:290–293.

Peter, H; Appel, KE; Berg, R; et al. (1983a) Irreversible binding of acrylonitrile to nucleic acids. Xenobiotica 13:19–25.

Peter, H; Schwarz, M; Mathiasch, B; et al. (1983b) A note on synthesis and reactivity towards DNA of glycidonitrile, the epoxide of acrylonitrile. Carcinogenesis 4:235–237.

Pilon, D; Roberts, AE; Rickert, DE. (1988a) Effect of glutathione depletion on the irreversible association of acrylonitrile with tissue macromolcules after oral administration to rats. Toxicol Appl Pharmacol 95:311–320.

Pilon, D; Roberts, AE; Rickert, DE. (1988b) Effect of glutathione depletion on the uptake of acrylonitrile vapors and on its irreversible association with tissue macromolcules. Toxicol Appl Pharmacol 95:265–278.

Platanias, LC. (2003) Map kinase signaling pathways and hematologic malignancies. Blood 101(12):4667–4679.

Ploemen, JP; Wormhoudt, LW; Haenen, GR; et al. (1997) The use of human in vitro metabolic parameters to explore the risk assessment of hazardous compounds: the case of ethylene dibromide. Toxicol Appl Pharmacol 143(1):56–69.

Poirier, MC. (2004) Chemical-induced DNA damage and human cancer risk. Nature 4:630–637.

Poulin, P; Theil, FP. (2002) Prediction of pharmacokinetics prior to in vivo studies. 1. Mechanism-based prediction of volume of distribution. J Pharm Sci 91:129–156.

Pouyatos, B; Gearhart, CA; Fechter, LD. (2005) Acrylonitrile potentiates hearing loss and cochlear damage induced by moderate noise exposure in rats. Toxicol Appl Pharmacol 204:46–56.

Pouyatos, B; Gearhart, C; Nelson-Miller, A; et al. (2007) Oxidative stress pathways in the potentiation of noise-induced hearing loss by acrylonitrile. Hear Res 224:61–74.

Priston, RAJ; Dean, BJ. (1985) Tests for the induction of chromosomal aberrations, polyploidy and sister chromatid exchanges in rat liver (RL_4) cells. Prog Mutat Res 5:387–395.

Probst, GS; Hill, LE. (1985) Tests for the induction of DNA-repair synthesis in primary cultures of adult rat hepatocytes. Prog Mutat Res 5:381–386.

Prokopczyk, B; Bertinato, P; Hoffman, D. (1988) Cyanoethylation of DNA in vivo in 3-(methylnitrosamino)-propionitrile, an Areca-derived carcinogen. Cancer Res 48:6780–6784.

Pu, X; Kamendulis, LM; Klaunig, JE. (2006) Acrylonitrile-induced oxidative DNA damage in rat astrocytes. Environ Mol Mutagen 47:631–638.

Pu, X; Kamendulis, LM; Klaunig, JE (2009) Acrylonitrile-induced oxidative stress and oxidative DNA damage in male Sprague-Dawley rats. Toxicological Sciences 111: 64-71.

Quast, JF. (2002) Two-year toxicity and oncogenicity study with acrylonitrile incorporated in the drinking water of rats. Toxicol Lett 132:153–196.

Quast, JF; Humiston, CG; Schwetz, BA; et al. (1975) A six-month oral toxicity study incorporating acrylonitrile in the drinking water of purebred beagle dogs. Dow Toxicology Research Laboratory, Midland, MI.

Quast, JF; Wade, C; Humiston, C; et al. (1980a) Two-year toxicity and oncogenicity study with acrylonitrile incorporated in the drinking water of rats. Dow Chemical Co., Toxicology Research Laboratory, Midland, MI.

Quast, JF; Schuetz, MF; Balmer, TS; et al. (1980b) A two-year toxicity and oncogenicity study with acrylonitrile following inhalation exposure of rats. Dow Chemical Co., Toxicology Research Laboratory, Midland, MI.

Rabello-Gay, MN; Ahmed, AE. (1980) Acrylonitrile: in vivo cytogenetic studies in mice and rats. Mutat Res 79:249–255.

Radovsky, A & Mahler, JF (1999) Nervous system. In: Maronpot, RR, Boorman, GA, and Gaul, BW ed. Pathology of the Mouse – Reference and Atlas, St. Louis, MO, Cache River Press: 445-470.

Rajendran, S; Muthu, M. (1981) Effect of acrylonitrile on trehalase, phosphorylase and acetylcholinesterase activities in Tribolium castaneum Herbst and Trogoderma granarium Everts. Experientia 37(8):886–887.

Recio, L; Skopek, TR. (1988a) The cellular and molcular analysis of acrylonitrile-induced mutations in human cells. CIIT Activities 8:1–6.

Recio, L; Skopek, TR. (1988b) Mutagenicity of acrylonitrile and its metabolite 2-cyanoethylene oxide in human lymphoblasts in vitro. Mutat Res 206:297–305.

Rice, JM; Wilbourn, JD. (2000) Tumors of the nervous system in carcinogenic hazard identification. Toxicol Pathol 28:202–214.

Renwick, AG ; Lazarus, NR. (1998) Human variability and noncancer risk assessment--an analysis of the default uncertainty factor. Regul Toxicol Pharmacol 27(1, Pt. 1):3–20.

Roberts, AE; Lacy, SA; Pilon, D; et al. (1989) Metabolism of acrylonitrile to 2-cyanoethylene oxide in F344 rat liver microsomes, lung microsomes, and lung cells. Drug Metab Dispos 17:481–486.

Roberts, AE; Kedderis, GL; Turner, MJ; et al. (1991) Species comparison of acrylonitrile epoxidation by microsomes from mice, rats and humans: relationship to epoxide concentrations in mouse and rat blood. Carcinogenesis 12:401–404.

Rogaczewska, T. (1975) Percutaneous absorption of acrylonitrile vapour in animals. Med Pr 19:349–353.

Rongzhu, L; Suhua, W; Guangwei, X; et al. (2007) Neurobehaviroal alterations in rats exposed in acrylonitrile in drinking water. Hum Exp Toxicol 26:179–184.

Rouisse, L; Chakrabarti, S; Tuchweber, B. (1986) Acute nephrotoxic potential of acrylonitrile in F344 rats. Res Commun Chem Pathol Pharmacol 53:347–360.

Rudd, CJ. (1983) L5178Y tk+/ mouse lymphoma forward mutation assay of acrylonitrile. Prepared by SRI International, Menlo Park, CA, for the Environmental Research Center, U.S. Environmental Protection Agency, Research Triangle Park, NC; SRI Project LSU-3447, EPA Contract No. 68-02-3703.

Saillenfait, AM; Sabaté, JP. (2000) Comparative development toxicities of aliphatic nitriles: in vivo and in vitro observations. Toxicol Appl Pharmacol 163:149–163.

Saillenfait, AM; Langonne, I; Sabaté, JP; et al. (1992) Embryotoxicity of acrylonitrile in whole-embryo culture. Toxicol In Vitro 6:253–260.

Saillenfait, AM; Bonnet, P; Guenier, JP; et al. (1993) Relative developmental toxicities of inhaled aliphatic mononitriles in rats. Fundam Appl Toxicol 20:365–375.

Saillenfait, AM; Sabaté, JP; Gaspard, C. (2004) Effects of aliphatic nitriles in micromass cultures of rat embryo limb bud cells. Toxicol In Vitro 18:311–318.

Sakurai, H. (2000) Carcinogenicity and other health effects of acrylonitrile with reference to occupational exposure limits. Ind Health 38:165–180.

Sakurai, H; Kusumoto, M. (1972) Epidemiological study of health impairment among acrylonitrile workers. J Sci Labor 48:273–282.

Sakurai, H; Onodera, M; Utsunomiya, T; et al. (1978) Health effects of acrylonitrile in acrylic fibre factories. Br J Ind Med 35(3):219−225.

Salazar, DE; Sorge, CL; Corcoran, GB. (1988) Obesity as a risk factor for drug-induced organ injury. VI. Increased hepatic P-450 concentration and microsomal ethanol oxidizing activity in the obese overfed rat. Biochem Biophys Res Commun 157:315–320.

Sandberg, EC; Slanina, P. (1980) Distribution of [1-^{14}C] acrylonitrile in rat and monkey. Toxicol Lett 6:187–191.

Sapota, A. (1982) The disposition of [^{14}C]acrylonitrile in rats. Xenobiotica 12:259–264.

Sasaki, M; Sugimura, K; Yoshida, MA; et al. (1980) Cytogenetic effects of 60 chemicals on cultured human and Chinese hamster cells. La Kromosomo II-20:574–584.

Satayavivad, J; Thiantanawat, A; Tuntawiroon, J; et al. (1998) Alterations of central muscarinic functions during subchronic exposure to acrylonitrile in rats. Res Commun Biol Psychol Psychiat 23:29–42.

Scélo, G; Constantinescu, V; Csiki, I; et al. (2004) Occupational exposure to vinyl chloride, acrylonitrile and styrene and lung cancer risk (Europe). Cancer Causes Control 15:445–452.

Seger, R; Krebs, EG. (1995) The MAPK signaling cascade. FASEB J 9:726–735.

Sehgal, A; Osgood, C; Zimmering, S. (1990) Aneuploidy in drosophila. III: Aneuploidogens inhibit in vitro assembly of taxol-purified Drosophila microtubules. Environ Mol Mutagen 16:217–224.

Sekihashi, K; Yamamoto, A; Matsumura, Y; et al. (2002) Comparative investigation of multiple organs of mice and rats in the comet assay. Mutat Res 517:53–75.

Selikoff, IJ; Seidman, H. (1992) Use of death certificates in epidemiological studies, including occupational hazards: Variations in discordance of different asbestos-associated disease on best evidence ascertainment. Am J Ind Med 22:481–492

Sharief, Y; Brown, AM; Backer, LC; et al. (1986) Sister chromatid exchange and chromosome aberration analyses in mice after in vivo exposure to acrylonitrile, styrene, or butadiene monoxide. Environ Mutagen 8:439–448.

Sheldon, W. (1994) Tumours of the Harderian gland. IARC Sci Pub 111:101–103.

Shell Oil Co. (1984a) The induction of mitotic gene conversion in the yeast, *Saccharomyces cerevisiae* JD1, by ten selected compounds in the IPCS collaborative study on short-term tests. Submitted under TSCA Section 8D; EPA Document No. 86-870001635; NTIS No. OTS0516216.

Shell Oil Co. (1984b) Induction of chromosome aberrations, polyploidy and sister chromatid exchanges in rat liver cells by chemical carcinogens. Submitted under TSCA Section 8D; EPA Document No. 86-870001636; NTIS No. OTS0515712.

Shibata, M; Inoue, K; Yoshimura, Y; et al. (2004) Simultaneous determination of hydrogen cyanide and volatile aliphatic nitriles by headspace gas chromatography, and its application to an in vivo study of the metabolism of acrylonitrile in the rat. Arch Toxicol 78:301–305.

Shimizu, M; Lasker, JM; Tsutsumi, M; et al. (1990) Immunohistochemical localization of ethanol inducible P-450IIE1 in the rat alimentary tract. Gastroenterology 99:1044–1053.

Silver, EH; Szabo, S. (1982) Possible role of lipid peroxidation in the actions of acrylonitrile on the adrenals, liver and gastrointestinal tract. Res Commun Chem Pathol Pharmacol 36:33–43.

Silver, EH; McComb, DJ; Kovacs, K; et al. (1982) Limited hepatotoxic potential of acrylonitrile in rats. Toxicol Appl Pharmacol 64:131–139.

Silver, EH; Szabo, S; Cahill, M; et al. (1987) Time-course studies of the distribution of [1-^{14}C]acrylonitrile in rats after intravenous administration. J Appl Toxicol 7:303–306.

Slaga, TJ; Klein-Szanto, AJP; Triplett, LL; et al. (1981) Skin tumor promoting activity of benzoyl peroxide, a widely used free radical generating compound. Science 213:1023–1025.

Slikker, W; Mei, N; Chen, T. (2004) N-ethyl-N-nitrosourea (ENU) increased brain mutations in prenatal and neonatal mice but not in the adults. Toxicol Sci 81:112–120.

Smith, CA; Harrison, DJ. (1997) Association between polymorphism in gene for microsomal epoxide hydrolase and susceptibility to emphysema. Lancet 350:630–633.

Smith, CC; O'Donovan, MR; and Martin, EA (2006). hOGG1 recognizes oxidative damage using the comet assay with greater specificity than FPG or ENDOIII. Mutagenesis 21: 185-190.

Smyth, HF; Carpenter, CP. (1948) Further experience with the range-finding test in the industrial toxicology laboratory. J Ind Hyg Toxicol 30:63–68.

Sohda, T; Shimizu, M; Kamimura, S; et al. (1993) Immunohistochemical demonstration of ethanol-inducible P450 2E1 in rat brain. Alcohol Alcohol Suppl. 1B:69–75.

Solleveld, HK; Bigner, DA; Averill, DA et al. (1986) Brain tumors in man and animals: report of a workshop. Environ Health Perspect 68: 155-173.

Solomon, JJ; Segal, A. (1985) Direct alkylation of calf thymus DNA by acrylonitrile. Isolation of cyanoethyl adducts of guanine and thymine and carboxyethyl adducts of adenine and cytosine. Environ Health Perspect 62:227–230.

Solomon, JJ; Cote, IL; Wortman, M; et al. (1984) In vitro alkylation of calf thymus DNA by acrylonitrile. Isolation of cyanoethyl-adducts of guanine and thymidine and carboxyethyl-adducts of adenine and cytosine. Chem-Biol Interact 51:167–190.

Solomon, JJ; Singh, US; Segal, A. (1993) In vitro reactions of 2-cyanoethylene oxide with calf thymus DNA. Chem-Biol Interact 88:115–135.

Song, BJ; Matsunaga, T; Hardwick, JP; et al. (1987) Stabilization of cytochrome P450j messenger ribonucleic acid in the diabetic rat. Mol Endocrinol 1(8):542–547.

Song, BJ; Veech, RL; Saenger, P. (1990) Cytochrome P-450IIE1 is elevated in lymphocytes from poorly controlled insulin-dependent diabetics. J Clin Endocrinol Metab 71:1036–1040.

Speit, G; Schutz, P; Bonzheim, I. et al. (2004) Sensitivity of the FPG protein towards alkylation damage in the comet assay. Toxicology letters 146: 151-158.

Spiegelhalter, D; Thomas, A; Best, N; et al. (2003) WinBUGS user manual. Version 1.4. Available online at www.mrc-bsu.cam.ac.uk/bugs/winbugs/manual14.pdf (accessed April 21, 2009) .

Srám, RJ; Beskid, O; Binkova, B; et al. (2004) Cytogenetic analysis using fluorescence in situ hybridization (FISH) to evaluate occupational exposure to carcinogens. Toxicol Lett 149:335–344.

Starr, TB; Gause, C; Youk, AD; et al. (2004) A risk assessment for occupational acrylonitrile exposure using epidemiology data. Risk Anal 24:587–601.

Stephens, EA; Taylor, JA; Japlan, N; et al. (1994) Ethnic variation in the CYP2E1 gene: polymorphism analysis of 695 African-Americans, European-Americans and Taiwanese. Pharmacogenetics 4:185–192.

Stewart, PA; Zaebst, D; Zey, JN; et al. (1998) Exposure assessment for a study of workers exposed to acrylonitrile. Scand J Work Environ Health 24:42–53.

Stiteler, WM; Knauf, LA; Hertzberg, RC; et al. (1993) A statistical test of compatibility of data sets to a common dose-response model. Regul Toxicol Pharmacol 18:392–402.

Stricker, EM; Hoffman, ML; Riccardi, CJ. (2003) Increased water intake by rats maintained on high NaCl diet: analysis of ingestive behavior. Physiol Behav 79:621–631.

Styles, JA; Clay, P; Cross, MF. (1985) Assays for the induction of gene mutations at the thymidine kinase and the Na^+/K^+ ATPase loci in two different mouse lymphoma cell lines in culture. Prog Mutat Res 5:587–596.

Subramanian, U; Ahmed, AE. (1995) Intestinal toxicity of acrylonitrile: in vivo metabolism by intestinal cytochrome P450 2E1. Toxicol Appl Pharmacol 135:1–8.

Suh, JH; Shenvi, SV; Dixon, BM; et al. (2004) Decline in transcriptional activity of Nrf2 causes age-related loss of glutathione synthesis, which is reversible with lipoic acid. Proc Natl Acad Sci USA 101:3381–3386.

Sumner, SC; Fennell, TR; Moore, TA; et al. (1999) Role of cytochrome P450 2E1 in the metabolism of acrylamide and acrylonitrile in mice. Chem Res Toxicol 12:1110–1116.

Swaen, GM; Bloemen, LJ; Twisk, J; et al. (1992) Mortality of workers exposed to acrylonitrile. J Occup Med 34:801–809.

Swaen, GM; Bloemen, LJ; Twisk, J; et al. (1998) Mortality update of workers exposed to acrylonitrile in the Netherlands. Scand J Work Environ Health 24(Suppl 2):10–16.

Swaen, GM; Bloemen, LJ; Twisk, J; et al. (2004) Mortality update of workers exposed to acrylonitrile in the Netherlands. J Occup Environ Med 46:691–698.

Sweeney, LM; Gargas, ML; Strother, DE; et al. (2003) Physiologically based pharmacokinetic model parameter estimation and sensitivity and variability analyses for acrylonitrile disposition in humans. Toxicol Sci 71:27–40.

Symons, JM; Kreckmann, KH; Sakr, CJ; et al. (2008) Mortality among workers exposed to acrylonitirled in fiber production: an update. J Occup Environ Med 50:550–560.

Szabo, S; Reynolds, ES; Kovacs, K. (1976) Animal model of human disease. Waterhouse-Friderichsen syndrome. Animal model: acrylonitrile-induced adrenal apoplexy. Am J Pathol 82:653–656.

Szabo, S; Bailey, KA; Boor, PJ; et al. (1977) Acrylonitrile and tissue glutathione: differential effect of acute and chronic interactions. Biochem Biophys Res Commun 79:32–37.

Szabo, S; Huttner, I; Kovacs, K; et al. (1980) Pathogenesis of experimental adrenal hemorrhagic necrosis ("apoplexy"): ultrastructural, biochemical, neuropharmacologic, and blood coagulation studies with acrylonitrile in the rat. Lab Invest 42:533–546.

Szabo, S; Gallagher, GT; Silver, EH; et al. (1984) Subacute and chronic action of acrylonitrile on adrenals and gastrointestinal tract: biochemical, functional and ultrastructural studies in the rat. J Appl Toxicol 4:131–140.

Tanaka, E. (1998) In vivo age-related changes in hepatic drug-oxidizing capacity in humans. J Clin Pharm Ther 23:247–255.

Tandon, R; Saxena, DK; Chandra, SV; et al. (1988) Testicular effects of acrylonitrile in mice. Toxicol Lett 42:55–63.

Tardiff, R; Talbot, D; Gerin, M; et al. (1987) Urinary excretion of mercapturic acids and thiocyanate in rats exposed to acrylonitrile: influence of dose and route of administration. Toxicol Lett 39:255–261.

Tavares, R; Borba, H; Monteiro, M; et al. (1996) Monitoring of exposure to acrylonitrile by determination of N-(2-cyanoethyl)valine at the N-terminal position of haemoglobin. Carcinogenesis 17:2655–2660.

Teo, SK; Kedderis, GL; Gargas, ML. (1994) Determination of tissue partition coefficients for volatile tissue-reactive chemicals: acrylonitrile and its metabolite 2-cyanoethylene oxide. Toxicol Appl Pharmacol 128:92–96.

Therneau, TM; Grambsch, PM. (2000) Modeling survival data: extending the Cox model. New York: Springer-Verlag.

Thier, R; Lewalter, J; Kempkes, M; et al. (1999) Haemoglobin adducts of acrylonitrile and ethylene oxide in acrylonitrile workers, dependent on polymorphisms of the glutathione transferases GSTT1 and GSTM1. Arch Toxicol 97:197–202.

Thier, R; Balkenhol, H; Lewalter, J; et al. (2001) Influence of polymorphisms of the human glutathione transferases and cytochrome P450 2E1 enzyme on the metabolism and toxicity of ethylene oxide and acrylonitrile. Mutat Res 482:41–46.

Thier, R; Lewalter, J; Selinske, S; et al. (2002) Possible impact of human CYP2E1 polymorphisms on the metabolism of acrylonitrile. Toxicol Lett 128:249–255.

Thiess, AM; Fleig, I. (1978) Analysis of chromosomes of workers exposed to acrylonitrile. Arch Toxicol 41:149–152.

Thiess, AM; Frentzel-Beyme, R; Link, R; et al. (1980) Mortality study in chemical personnel of various industries exposed to acrylonitrile. Zentralbl Arbeitsmed Arbeitsschutz Prophyl Ergonomie 30:259–267.

Tian, L; Cai, Q; Wei, H. (1998) Alterations of antioxidant enzymes and oxidative damage to macromolecules in different organs of rats during aging. Free Radic Biol Med 24(9):1477–1484.

Turner, MJ, Jr; Held, SD; Kedderis, GL. (1989) Identification of mercapturic acid metabolites of acrylonitrile by tandem mass spectrometry. In: Proceedings of the 37th ASMS conference on mass spectrometry and allied topics; May 21–26, 1989; Miami Beach, FL. East Lansing, MI: American Society for Mass Spectrometry, pp. 1361–1362.

Umeda, M; Noda, K; Tanaka, K. (1985) Assays for inhibition of metabolic cooperation by a microassay method Prog Mutat Res 5:619–622.

U.S. EPA (Environmental Protection Agency). (1983) Health assessment document for acrylonitrile [final report]. Environmental Criteria and Environmental Assessment Office, Office of Health and Environmental Assessment, Office of Research and Development, Research Triangle Park, NC; EPA-600/8-82-007F. Available online at http://nepis.epa.gov/Exe/ZyPurl.cgi?Dockey=3000170U.txt (accessed April 21, 2009).

U.S. EPA (Environmental Protection Agency). (1986a) Guidelines for the health risk assessment of chemical mixtures. Federal Register 51(185):34014–34025.

U.S. EPA (Environmental Protection Agency). (1986b) Guidelines for mutagenicity risk assessment. Federal Register 51(185):34006–34012.

U.S. EPA (Environmental Protection Agency). (1988) Recommendations for and documentation of biological values for use in risk assessment. Environmental Criteria and Assessment Office, Office of Health and Environmental Assessment, Cincinnati, OH; EPA/600/6-87/008. Available from the National Technical Information Service, Springfield, VA; PB88-179874/AS, and online at http://cfpub.epa.gov/ncea/cfm/recordisplay.cfm?deid=34855 (accessed April 21, 2009).

U.S. EPA (Environmental Protection Agency). (1991) Guidelines for developmental toxicity risk assessment. Federal Register 56(234):63798–63826. Available online at http://www.epa.gov/ncea/raf/rafguid.htm (accessed April 21, 2009).

U.S. EPA (Environmental Protection Agency). (1994) Methods for derivation of inhalation reference concentrations and application of inhalation dosimetry. Environmental Criteria and Assessment Office, Office of Health and Environmental Assessment, Cincinnati, OH; EPA/600/8-90/066F. Available from the National Technical Information Service, Springfield, VA, PB2000-500023, and online at http://cfpub.epa.gov/ncea/raf/recordisplay.cfm?deid=71993 (accessed April 21, 2009).

U.S. EPA (Environmental Protection Agency). (1995) Use of the benchmark dose approach in health risk assessment. Risk Assessment Forum, Washington, DC; EPA/630/R-94/007. Available from the National Technical Information Service, Springfield, VA, PB95-213765, and online at http://cfpub.epa.gov/ncea/raf/raf_pubtitles.cfm?detype=document&excCol=archive (accessed April 21, 2009).

U.S. EPA (Environmental Protection Agency). (1996) Guidelines for reproductive toxicity risk assessment. Federal Register 61(212):56274–56322.

U.S. EPA (Environmental Protection Agency). (1998a) Guidelines for neurotoxicity risk assessment. Federal Register 63(93):26926–26954.

U.S. EPA (Environmental Protection Agency). (1998b) Toxicological review of methyl methacrylate. Integrated Risk Information System (IRIS), National Center for Environmental Assessment, Washington, DC. Available online at http://www.epa.gov/iris (accessed April 21, 2009).

U.S. EPA (Environmental Protection Agency). (2000a) Science policy council handbook: risk characterization. Office of Science Policy, Office of Research and Development, Washington, DC. EPA100B00002.

U.S. EPA (Environmental Protection Agency). (2000b) Benchmark dose technical guidance document [external review draft]. Risk Assessment Forum, Washington, DC; EPA/630/R-00/001. Available online at http://oaspub.epa.gov/eims/eimscomm.getfile?p_download_id=4727 (accessed April 23, 2009).

U.S. EPA (Environmental Protection Agency). (2002) A review of the reference dose concentration and reference concentration processess. Risk Assessment Forum, Washington, DC; EPA/630/P-02/002F. Available online at http://cfpub.epa.gov/ncea/raf/raf_pubtitles.cfm?detype=document&excCol=archive (accessed April 22, 2009).

U.S. EPA (Environmental Protection Agency). (2005a) Guidelines for carcinogen risk assessment. Federal Register 70(66):17765–18717. Available online at http://www.epa.gov/cancerguidelines (accessed April 22, 2009).

U.S. EPA (Environmental Protection Agency). (2005b) Supplemental guidance for assessing susceptibility from early-life exposure to carcinogens. Risk Assessment Forum, Washington, DC; EPA/630/R-03/003F. Available online at http://www.epa.gov/cancerguidelines (accessed April 22, 2009).

U.S. EPA (Environmental Protection Agency). (2006a) Science policy council handbook: peer review. 3rd edition. Office of Science Policy, Office of Research and Development, Washington, DC; EPA/100/B-06/002. Available online at http://www.epa.gov/OSA/spc/2peerrev.htm (accessed April 22, 2009).

U.S. EPA (Environmental Protection Agency). (2006b) A framework for assessing health risk of environmental exposures to children. National Center for Environmental Assessment, Washington, DC; EPA/600/R-05/093F. Available online at http://cfpub.epa.gov/ncea/cfm/recordisplay.cfm?deid=158363 (accessed April 22, 2009).

Ved Brat, SV; Williams, GM. (1982) Hepatocyte-mediated production of sister chromatid exchange in co-cultured cells by acrylonitrile: evidence for extra cellular transport of a stable reactive intermediate. Cancer Lett 17:213–216.

Venitt, S. (1978) Letter on acrylonitrile mutagenicity. Mutat Res 57:107–109.

Venitt, S; Bushell, CT; Osborne, M. (1977) Mutagenicity of acrylonitrile (cyanoethylene) in *Escherichia coli*. Mutat Res 45:283–288.

Vernon, P; Dulak, L; Deskin, R. (1990) Acute toxicologic evaluation of acrylonitrile. J Am Coll Toxicol 1:114–115.

Vieira, I; Sonnier, M; Cresteil, T. (1996) Developmental expression of CYP2E1 in the human liver. Hypermethylation control of gene expression during the neonatal period. Eur J Biochem 238:476–483.

Vogel, EW. (1985) The Drosophila somatic recombination and mutation assay (SRM) using the white-coral somatic eye color system. Prog Mutat Res 5:313–317.

Vogel, RA; Kirkendall, WM. (1984) Acrylonitrile (vinyl cyanide) poisoning: a case report. Tex Med 80:48–51.

Vogel, EW; Graf, U; Frei, H; et al. (1999) The results of assays in Drosophila as indicators of exposure to carcinogens. IARC Sci Publ 146:427–470.

Wakata, A; Miyamae, Y; Sato, S; et al. (1998) Evaluation of the rat micronucleus test with bone marrow and peripheral blood: summary of the 9th collaborative study by CSGMT/JEMS.MMS. Environ Mol Mutagen 32:84–100.

Walker, VE; Fennell, TR; Boucheron, JA; et al. (1990) Macromelecular adducts of ethylene oxide: a literature review and a time-course study on the formation of 7-(2-hydroxyethyl)guanine following exposures of rats by inhalation. Mutat Res 233:151–164.

Wang, W; Xia, Z; Jin, F; et al. (2000) Investigation of prevalence rate in workers exposed to acrylonitrile. Chin J Ind Hyg. Submitted under TSCA Section 8E; EPA Document No. 89-000000313; NTIS No. OTS0559911.

Wang, H; Chanas, B; Ghanayem, BI. (2002) Cytochrome P450 2E1 (CYP2E1) is essential for acrylonitrile metabolism to cyanide: comparative studies using CYP2E1-null and wild-type mice. Drug Metab Dispos 30:911–917.

Wauthier, V; Verbeeck, RK; Calderon, PB. (2004) Age-related changes in the protein and mRNA levels of CYP2E1 and CYP3A isoforms as well as in their hepatic activities in Wistar rats. What role for oxidative stress? Arch Toxicol 78:131–138.

Waxweiler, RJ; Stringer, W; Wagoner, J; et al. (1976) Neoplastic risk among workers exposed to vinyl chloride. Ann N Y Acad Sci 271:40–48.

Waxweiler, RJ; Smith, AH; Falk, H; et al. (1981) Excess lung cancer risk in a synthetic chemicals plant. Environ Health Perspect 41:159–165.

Werner, JB; Carter, JT. (1981) Mortality of United Kingdom acrylonitrile polymerization workers. Brit J Ind Med 38:247–253.

Wester, PW; Kroes, R. (1988) Forestomach carcinogens: pathology and relevance to man. Toxicol Pathol 16:165–171.

Whittaker, SG; Zimmermann, FK; Dicus, B; et al. (1990) Detection of induced mitotic chromosome loss in *Saccharomyces cerevisiae*--an interlaboratory assessment of 12 chemicals. Mutat Res 241:225–242.

Whysner, J; Steward, RE, III; Chen, D; et al. (1998a) Formation of 8-oxodeoxyguanosine in brain DNA of rats exposed to acrylonitrile. Arch Toxicol 72:429–438.

Whysner, J; Ross, PM; Conaway, CC; et al. (1998b) Evaluation of possible genotoxic mechanisms for acrylonitrile tumorigenicity. Regul Toxicol Pharmacol 27:217–239.

Willhite, CC; Ferm, VH; Smith, RP. (1981) Teratogenic effects of aliphatic nitriles. Teratology 17:317–323.

Williams, GM; Tong, C; Ved Brat, S. (1985) Tests with the rat hepatocyte primary culture/DNA-repair test. Prog Mutat Res 5:341–345.

WIL Research Laboratories. (2005) Acute inhalation toxicity study of acrylonitrile in albino rats. Prepared by WIL Research Laboratories, LLC, Ashland, OH for Shanghai SECCO Petrochemical Company, Ltd., Shanghai, China. Submitted under TSCA Section 8E; EPA Document No. 8EHQ-0805-16067.

Wilson, RH. (1944) Health hazards encountered in the manufacture of synthetic rubber. J Am Med Assoc 124:701–703.

Wilson, RH; Hough, GV; McCormick, W. (1948) Medical problems encountered in the manufacture of American-made rubber. Ind Med 17:199–207.

Wood, ML; Diadaroglu, M; Gajewski, E; et al. (1990) Mechanistic studies of ionizing radiation and oxidative mutagenesis: genetic effects of single 8-hydroxyguanine (7-hydro-8-oxoguanine) residue inserted at a unique site in a viral genome. Biochemistry 29:7024–7032.

Wood, SM; Buffler, PA; Burau, K; et al. (1998) Mortality and morbidity of workers exposed to acrylonitrile in fiber production. Scand J Work Environ Health 24(Suppl 2):54–62.

Working, PK; Bentley, KS; Hurtt, ME; et al. (1987) Comparison of the dominant lethal effects of acrylonitrile and acrylamide in male F344 rats. Mutagenesis 2:215–220.

Wu, W; Su, J; Huang, M. (1995) An epidemiological study on reproductive effects in female workers exposed to acrylonitrile. Zhonghua Yu Fang Yi Xue Za Zhi (China Preventative Medicine Magazine) 29:83–85 (Chinese).

Wu, X; Amos, CI; Kemp, BL; et al. (1998) Cytochrome P450 2E1 DraI polymorphisms in lung cancer in minority populations. Cancer Epidemiol Biomarkers Prev 7:13–18.

Würgler, FE; Graf, U; Frei, H. (1985) Somatic mutation and recombination test in wings of *Drosophila melanogaster*. Prog Mutat Res 5:325–40.

Xiao, W. (2000a) Study of the toxic effects of acrylonitrile on liver. Lanzhou Medical College. Submitted under TSCA Section 8E; EPA Document No. 89-000000313; NTIS No. OTS0559911.

Xiao, W. (2000b) Effects of acrylonitrile on activity of blood cholinesterase. Lanzhou Medical College. Submitted under TSCA Section 8E; EPA Document No. 89-000000313; NTIS No. OTS0559911.

Xu, DX; Zhu, QX; Zheng, LK; et al. (2003) Exposure to acrylonitrile induced DNA strand breakage and sex chromosome aneuploidy in human spermatozoa. Mutat Res 537:93–100.

Yates, JM; Sumner, SC; Turner, MJ; et al. (1993) Characterization of an adduct and its degradation product produced by the reaction of cyanoethylene oxide with deoxythymidine and DNA. Carcinogenesis 14:1363–1369.

Yates, JM; Fennell, TR; Turner, MJ, Jr; et al. (1994) Characterization of phosphodiester adducts produced by the reaction of cyanoethylene oxide with nucleotides. Carcinogenesis 15:277–283.

Younes, M; Sharma, SC; Siegers, CP. (1986) Glutathione depletion by phorone organ specificity and effect on hepatic microsomal mixed-function oxidase system. Drug Chem Toxicol 9:67–73.

Young, JD; Slaurer, R; Karbowski, R. (1977) The pharmacokinetic and metabolism profile of ^{14}C-acrylonitrile given to rats by three routes. Prepared for the Manufacturing Chemical Association by the Toxicology Research Lab, Dow Chemical, Midland, MI.

Younger Labs. (1992) Initial submission: toxicological investigation of acrylonitrile (AN) with cover letter dated 081992. Submitted under TSCA Section 8E; EPA Document No. 88-920008086; NTIS No. OTS0546081.

Yuan, B; Wong, JL. (1991) Inactivity of acrylonitrile epoxide to modify a Ha-ras DNA in a non-focus transfection-transformation assay. Carcinogenesis 12:787–791.

Zabrodskii, PF; Kirichuk, VF; Germanchuk, VG; et al. (2000) Mechanisms of immunotoxic effects of acrylonitrile. Bull Exp Biol Med 5:463–465.

Zeller, H; Hoffman, H; Thiess, AM; et al. (1969) Toxicity of nitriles. Results of animal experiments and industrial experiences during 15 years. Zbl Arbeitsmd Arbeitsschutz 19:225–237.

Zhang, H; Kamendulis, LM; Jiang, J; et al. (2000) Acrylonitrile-induced morphological transformation in Syrian hamster embryo cells. Carcinogenesis 21:727–733.

Zhang, H; Kamendulis, LM; Klaunig, JE. (2002) Mechanisms for the induction of oxidative stress in Syrian hamster embryo cells by acrylonitrile. Toxicol Sci 67:247–255.

Zhurkov, VS; Shram, RY; Dugan, AM. (1983) Analysis of the mutagenic activity of acrylonitrile. Gig Sanit (1):71–72.

Zielinska, E; Zubowska, M; Bodalski, J. (2004) Polymorphism within the glutathione S-transferase P1 gene is associated with increased susceptibility to childhood malignant diseases. Pediatr Blood Cancer 43:552–559.

Zitting, A; Tenhunen, R; Savolainen, H. (1981) Effect of intraperitoneally injected acrylonitrile on liver, kidney and brain. Acta Pharmacol Toxicol 49:412–415.

Zotova, LV. (1975) Working conditions in the production of acrylonitrile and their influence on the workers' organism. Gig Tr Prof Zabol 8:8–11.

APPENDIX A. SUMMARY OF EXTERNAL PEER REVIEW AND PUBLIC COMMENTS AND DISPOSITION

APPENDIX B. BENCHMARK DOSE CALCULATIONS

APPENDIX B-1. NONCANCER ORAL DOSE-RESPONSE ASSESSMENT (RfD): BENCHMARK DOSE MODELING RESULTS EMPLOYING THE INCIDENCE OF FORESTOMACH LESIONS (HYPERPLASIA AND HYPERKERATOSIS) IN MALE AND FEMALE SPRAGUE-DAWLEY RATS, F344 RATS, AND B6C3F$_1$ MICE CHRONICALLY EXPOSED ORALLY TO AN FOR 2 YEARS

As previously discussed in Section 4, no human studies currently exist that involve oral exposures to AN. The available animal oral toxicity data, however, identify forestomach lesions (i.e., squamous cell epithelial hyperplasia and hyperkeratosis) as the most sensitive, prevalent, and consistent noncancer effect associated with chronic oral exposure to AN. Therefore, this endpoint was selected as the critical effect on which to base derivation of the RfD.

Two 2-year drinking water studies, one in Sprague-Dawley rats (Quast, 2002; Quast et al., 1980a) and the other in F344 rats (Johannsen and Levinskas, 2002b; Biodynamics 1980c), and a 2-year gavage study in B6C3F$_1$ mice (NTP, 2001) provided the best available dose-response data on which to base the RfD. Candidate RfDs for AN were derived from the incidence of forestomach lesions in Sprague-Dawley rats, F344 rats, and B6C3F$_1$ mice using a BMD approach. Incidences of forestomach lesions from chronic drinking water studies in male and female Sprague-Dawley rats (Quast, 2002) and F344 rats (Johannsen and Levinskas, 2002b) provided four sets of dose-response data from which to derive candidate RfDs, while incidences of forestomach lesions from a chronic gavage study in male and female B6C3F$_1$ mice provided an additional two sets of dose-response data. These six data sets are presented in Tables B-1 (for rats) and B-2 (for mice).

Table B-1. Incidences of forestomach lesions (hyperplasia or hyperkeratosis) in Sprague-Dawley and F344 rats exposed to AN in drinking water for 2 years

Sex	Administered concentration (ppm in drinking water)	Administered dose[a] (mg/kg-d)	Predicted internal dose metrics[b]		Incidence of forestomach lesions[c]
			AN-AUC in rat blood (mg/L)	CEO-AUC in rat blood (mg/L)	
Sprague-Dawley rats (Sources: Quast, 2002; Quast et al., 1980a)					
Male	0	0	0	0	15/80 (19%)
	35	3.4	2.06×10^{-2}	1.83×10^{-3}	15/47 (32%)
	100	8.5	5.36×10^{-2}	4.36×10^{-3}	44/48 (92%)[c]
	300	21.3	1.46×10^{-1}	9.70×10^{-3}	45/48 (94%)[c]
Female	0	0	0	0	20/80 (25%)
	35	4.4	2.37×10^{-2}	2.07×10^{-3}	23/48 (48%)[c]

Table B-1. Incidences of forestomach lesions (hyperplasia or hyperkeratosis) in Sprague-Dawley and F344 rats exposed to AN in drinking water for 2 years

Sex	Administered concentration (ppm in drinking water)	Administered dose[a] (mg/kg-d)	Predicted internal dose metrics[b]		Incidence of forestomach lesions[c]
			AN-AUC in rat blood (mg/L)	CEO-AUC in rat blood (mg/L)	
	100	10.8	6.18×10^{-2}	4.87×10^{-3}	41/48 (85%)[c]
	300	25.0	1.56×10^{-1}	1.01×10^{-2}	47/48 (98%)[c]
F344 rats[d] (Sources: Johannsen and Levinskas, 2002b; Biodynamics, 1980c)[d]					
Male	0	0	0	0	11/159 (7%)
	1	0.08	4.33×10^{-4}	4.06×10^{-5}	3/80 (4%)
	3	0.25	1.35×10^{-3}	1.27×10^{-4}	18/75 (24%)[c]
	10	0.83	4.52×10^{-3}	4.19×10^{-4}	13/80 (16%)[c]
	30	2.48	1.37×10^{-2}	1.23×10^{-3}	17/80 (22%)[c]
	100	8.37	4.85×10^{-2}	3.97×10^{-3}	9/77 (12%)
Female	0	0	0	0	4/156 (3%)
	1	0.12	5.73×10^{-4}	5.32×10^{-5}	2/80 (3%)
	3	0.36	1.72×10^{-3}	1.59×10^{-4}	16/80 (20%)[c]
	10	1.25	6.02×10^{-3}	5.49×10^{-4}	23/74 (31%)[c]
	30	3.65	1.79×10^{-2}	1.58×10^{-3}	13/80 (16%)[c]
	100	10.90	5.63×10^{-2}	4.46×10^{-3}	5/74 (7%)

[a]Administered doses were averages calculated by the study authors based on animal BW and drinking water intake.
[b]The EPA-modified rat PBPK model of Keddaris et al. (1996) was employed to predict a rat internal dose (i.e., either AN-AUC or CEO-AUC concentration in blood) resulting from the ingestion of the specified administered dose of AN consumed in six bolus episodes/d.
[c]Indicates significantly different (at $p < 0.05$) from control incidence by Fisher's exact test performed by Syracuse Research Corporation.
[d]Incidences for F344 rats do not include animals from the 6- and 12-mo sacrifices and were further adjusted to exclude (from the denominators) rats that died between 0 and 12 mos in the study. Rats dying during this time period were determined from page 6 of Appendix H and Table 1 in Biodynamics (1980c) and Table 8 in Johannsen and Levinskas (2002b). Unscheduled deaths between 0 and 12 mos in the study occurred in two female controls, two males at 3 ppm, three females at 10 ppm, and three males and three females at 100 ppm.

Table B-2. Incidences of forestomach lesions (hyperplasia or hyperkeratosis) in male and female B6C3F$_1$ mice administered AN via gavage for 2 years

Lesion site and type	Dose (mg/kg-d)[a]			
	0	2.5	10	20
Males				
Forestomach hyperplasia or hyperkeratosis	2/50 (4%)	4/50 (8%)	10/50[a] (20%)	13/50[b] (26%)
Females				
Forestomach hyperplasia or hyperkeratosis	2/50 (4%)	2/50 (4%)	5/50 (10%)	8/50[a] (16%)

[a]Significantly elevated above vehicle control as determined by EPA using Fisher's exact test ($p \leq 0.05$).
[b]Significantly elevated above vehicle control as determined by EPA using Fisher's exact test ($p \leq 0.01$).

Source: NTP (2001).

The incidences of forestomach lesions observed following 2 years of AN exposure in male and female SD and F344 rats were modeled using AN and CEO in blood, expressed in mg/L, as internal dose metrics. In addition, incidences of these same lesions were modeled in male and female SD and F344 rats, as well as male and female B6C3F$_1$ mice, employing administered dose. In all cases, all of the dichotomous dose-response models available in EPA's BMDS software (version 2.0) (i.e., the gamma, logistic, log-logistic, probit, log-probit, multistage, Weibull, and quantal-linear models) were fit to these incidence data. Because the incidence of forestomach lesions in male and female F344 rats did not increase monotonically across all administered concentrations, however, only incidence data from the three lowest concentrations (i.e., 0, 1, and 3 ppm) were used in dose-response modeling. Similarly, in male Sprague-Dawley rats, the incidence data from the highest dose group needed to be dropped prior to BMD modeling. In most cases, several models fit the data equally well (i.e., exhibited χ^2 goodness-of-fit *p* values greater than 0.1). Of those models exhibiting adequate fit, the selected model was the one with the lowest AIC value. BMDL$_{10}$ and BMDL$_{05}$ estimates were derived from the selected model. If more than one model shared the lowest AIC, the mean BMDL$_{10}$ and BMDL$_{05}$ were calculated, as per the EPA's *Benchmark Dose Technical Guidance Document* (U.S. EPA, 2000b).

In this appendix, detailed results of the dose-response modeling for forestomach lesions in male and female SD and F344 rats, and B6C3F$_1$ mice are presented. For each species, strain, and sex, summaries of the dose-response data (i.e., animal administered and internal doses and incidence data) are presented (Table B-1 for rats and Table B-2 for mice). Then, again for each species, strain, and sex, Tables B-3 (Sprague-Dawley rats), B-4 (F344 rats), and B-5 (B6C3F$_1$ mice) summarize the results of the dose-response modeling. Each of these tables is then

followed by the standard output from EPA's BMDS, version 2.0, for the dose-response models that did not exhibit statistically significant lack of fit.

Table B-3. Summary of the BMD modeling results based on the incidence of forestomach lesions (hyperplasia or hyperkeratosis) in male and female Sprague-Dawley rats exposed to AN in drinking water for 2 years

Sex	Endpoint	Dose metric	Selected model(s)[a]	χ^2 *p*-value	AIC	$BMDL_{10}$[b]	$BMDL_{05}$[b]
Male	Forestomach lesions	Estimated administered dose (mg/kg-d)	Two-stage multistage (1)	0.18	169.45	1.27	7.20×10^{-1}
		Predicted AN in blood (mg/L)	Two-stage multistage (1)	0.24	169.01	7.72×10^{-3}	4.32×10^{-3}
		Predicted CEO in blood (mg/L)	Two-stage multistage (1)	0.12	170.09	6.82×10^{-4}	3.90×10^{-4}

Table B-3. Summary of the BMD modeling results based on the incidence of forestomach lesions (hyperplasia or hyperkeratosis) in male and female Sprague-Dawley rats exposed to AN in drinking water for 2 years

Sex	Endpoint	Dose metric	Selected model(s)[a]	χ^2 *p*-value	AIC	$BMDL_{10}$[b]	$BMDL_{05}$[b]
Female	Forestomach lesions	Estimated administered dose (mg/kg-d)	gamma	0.38	212.77	6.87×10^{-1}	3.34×10^{-1}
			logistic	**0.45**	**211.31**	**1.24**	**6.39×10^{-1}**
			log-logistic	0.98	212.03	1.41	9.17×10^{-1}
			log-probit	0.74	212.14	1.38	9.61×10^{-1}
			one-stage multistage	0.31	212.40	6.30×10^{-1}	3.07×10^{-1}
			Weibull	0.31	213.07	6.74×10^{-1}	3.28×10^{-1}
			quantal linear	0.31	212.40	6.30×10^{-1}	3.07×10^{-1}
		Predicted AN in blood (mg/L)	gamma	0.32	212.96	3.76×10^{-3}	1.83×10^{-3}
			logistic	0.23	212.00	7.07×10^{-3}	3.64×10^{-3}
			log-logistic	0.98	212.03	6.93×10^{-3}	4.36×10^{-3}
			log-probit	0.70	212.18	7.02×10^{-3}	4.88×10^{-3}
			one-stage multistage	**0.42**	**211.79**	**3.62×10^{-3}**	**1.76×10^{-3}**
			Weibull	0.28	213.19	3.72×10^{-3}	1.81×10^{-3}
			quantal linear	**0.42**	**211.79**	**3.62×10^{-3}**	**1.76×10^{-3}**
		Predicted CEO in blood (mg/L)	gamma	0.51	212.45	3.53×10^{-4}	1.74×10^{-4}
			logistic	**0.69**	**210.72**	**5.58×10^{-4}**	**2.88×10^{-4}**
			log-logistic	0.87	212.06	7.25×10^{-4}	4.87×10^{-4}
			probit	0.33	211.86	5.87×10^{-4}	3.00×10^{-4}
			log-probit	0.86	212.06	7.17×10^{-4}	5.15×10^{-4}

[a]All dichotomous models in EPA's BMDS (version 2.0) were fit to the incidence of forestomach lesions (hyperplasia or hyperkeratosis) in Sprague-Dawley rats using the data presented in Table B-1. For BMD modeling, three different dose metrics were employed: (1) administered animal dose (estimated) expressed in mg/kg-d, (2) AN in blood (predicted) expressed in mg/L, and (3) CEO in blood (predicted) expressed in mg/L. Adequate fit of a model was achieved if the χ^2 goodness-of-fit statistic yielded a *p*-value > 0.1. The numbers in parentheses indicate the number of dose groups dropped in order to obtain an adequate fit, starting with the highest dose group. Of those models exhibiting adequate fit, the selected model was the model with the lowest AIC value, and is indicated in bold in the table.

[b]$BMDL_{10}$ and $BMDL_{05}$ estimates were derived from the selected model. If more than one model shared the lowest AIC, the mean $BMDL_{10}$ and $BMDL_{05}$ were calculated, as per the EPA's *Benchmark Dose Technical Guidance Document* (U.S. EPA, 2000b).

Sources: Quast (2002); Quast et al. (1980a).

SD Male Rats: Forestomach lesions (administered dose)

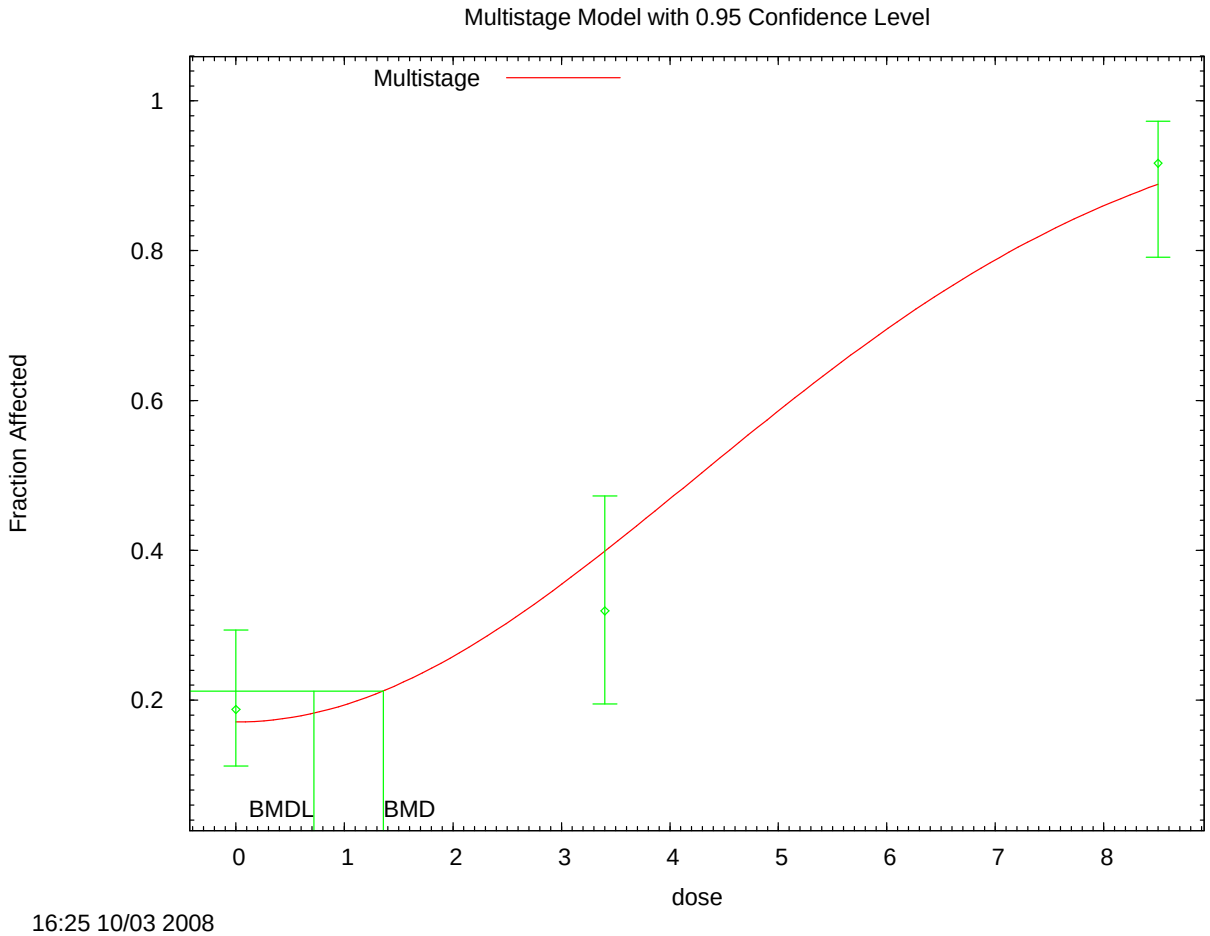

16:25 10/03 2008

```
=================================================================
        Multistage Model. (Version: 3.0;  Date: 05/16/2008)
        Input Data File: C:\USEPA\BMDS2\Temp\tmpAB.(d)
        Gnuplot Plotting File:  C:\USEPA\BMDS2\Temp\tmpAB.plt
                                                Fri Oct 03 16:25:01 2008
=================================================================

BMDS Model Run
~~~~~~~~~~~~~~~~~~~~~~~~~~~~~~~~~~~~~~~~~~~~~~~~~~~~~~~~~~~~~~~~~~~~~

  The form of the probability function is:

  P[response] = background + (1-background)*[1-EXP(
               -beta1*dose^1-beta2*dose^2)]

  The parameter betas are restricted to be positive


  Dependent variable = Response
  Independent variable = DOSE

Total number of observations = 3
Total number of records with missing values = 0
Total number of parameters in model = 3
Total number of specified parameters = 0
Degree of polynomial = 2


Maximum number of iterations = 250
Relative Function Convergence has been set to: 1e-008
```

Parameter Convergence has been set to: 1e-008

Default Initial Parameter Values
Background = 0.110075
Beta(1) = 0
Beta(2) = 0.0325391

Asymptotic Correlation Matrix of Parameter Estimates

(*** The model parameter(s) -Beta(1)
have been estimated at a boundary point, or have been specified by the user,
and do not appear in the correlation matrix)

	Background	Beta(2)
Background	1	-0.37
Beta(2)	-0.37	1

Parameter Estimates

Variable	Estimate	Std. Err.	95.0% Wald Confidence Interval Lower Conf. Limit	Upper Conf. Limit
Background	0.170685	*	*	*
Beta(1)	0	*	*	*
Beta(2)	0.0278185	*	*	*

* - Indicates that this value is not calculated.

Analysis of Deviance Table

Model	Log(likelihood)	# Param's	Deviance	Test d.f.	P-value
Full model	-81.807	3			
Fitted model	-82.7268	2	1.83969	1	0.175
Reduced model	-119.21	1	74.8052	2	<.0001

AIC: 169.454

Goodness of Fit

Dose	Est._Prob.	Expected	Observed	Size	Scaled Residual
0.0000	0.1707	13.655	15.000	80	0.400
3.4000	0.3987	18.741	15.000	47	-1.114
8.5000	0.8889	42.666	44.000	48	0.613

Chi^2 = 1.78 d.f. = 1 P-value = 0.1825

```
   Benchmark Dose Computation

Specified effect =           0.05

Risk Type        =      Extra risk

Confidence level =           0.95

              BMD =        1.35789

             BMDL =       0.719865

             BMDU =        1.59564

Taken together, (0.719865, 1.59564) is a 90     % two-sided confidence
interval for the BMD
```

SD Male Rats: Forestomach lesions (AN in blood)

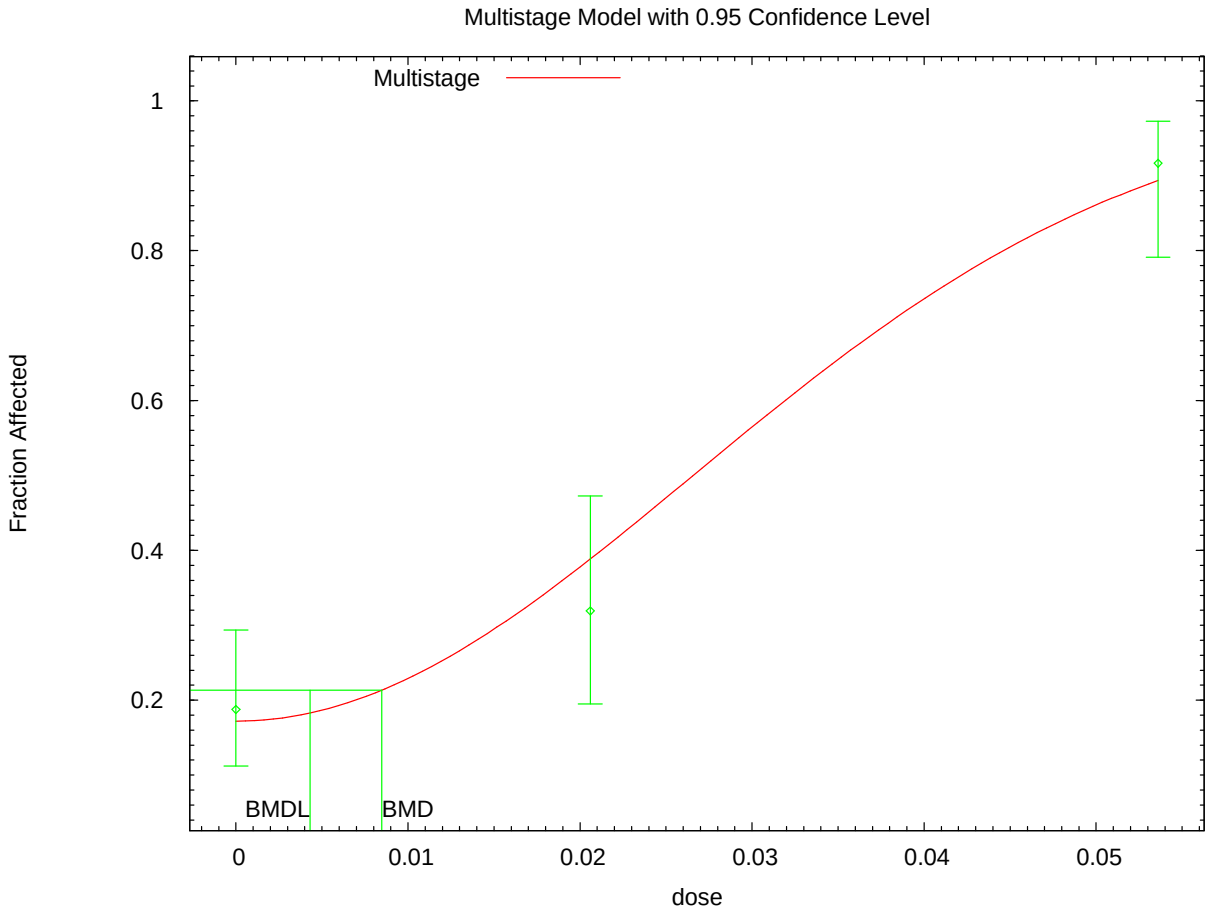

11:55 10/06 2008

```
=================================================================
        Multistage Model. (Version: 3.0;  Date: 05/16/2008)
        Input Data File: C:\USEPA\BMDS2\Temp\tmpBB.(d)
        Gnuplot Plotting File:  C:\USEPA\BMDS2\Temp\tmpBB.plt
                                                Mon Oct 06 11:55:17 2008
=================================================================

BMDS Model Run
~~~~~~~~~~~~~~~~~~~~~~~~~~~~~~~~~~~~~~~~~~~~~~~~~~~~~~~~~~~~~~~~~~~~~

  The form of the probability function is:

  P[response] = background + (1-background)*[1-EXP(
               -beta1*dose^1-beta2*dose^2)]

  The parameter betas are restricted to be positive


  Dependent variable = Response
  Independent variable = DOSE

Total number of observations = 3
Total number of records with missing values = 0
Total number of parameters in model = 3
Total number of specified parameters = 0
Degree of polynomial = 2


Maximum number of iterations = 250
Relative Function Convergence has been set to: 1e-008
Parameter Convergence has been set to: 1e-008
```

Default Initial Parameter Values
Background = 0.121757
Beta(1) = 0
Beta(2) = 815.045

Asymptotic Correlation Matrix of Parameter Estimates

(*** The model parameter(s) -Beta(1)
have been estimated at a boundary point, or have been specified by the user,
and do not appear in the correlation matrix)

	Background	Beta(2)
Background	1	-0.36
Beta(2)	-0.36	1

Parameter Estimates

Variable	Estimate	Std. Err.	95.0% Wald Confidence Interval Lower Conf. Limit	Upper Conf. Limit
Background	0.172109	*	*	*
Beta(1)	0	*	*	*
Beta(2)	714.086	*	*	*

* - Indicates that this value is not calculated.

Analysis of Deviance Table

Model	Log(likelihood)	# Param's	Deviance	Test d.f.	P-value
Full model	-81.807	3			
Fitted model	-82.5048	2	1.39565	1	0.2375
Reduced model	-119.21	1	74.8052	2	<.0001

AIC: 169.01

Goodness of Fit

Dose	Est._Prob.	Expected	Observed	Size	Scaled Residual
0.0000	0.1721	13.769	15.000	80	0.365
0.0206	0.3885	18.261	15.000	47	-0.976
0.0536	0.8936	42.892	44.000	48	0.519

Chi^2 = 1.35 d.f. = 1 P-value = 0.2445

```
   Benchmark Dose Computation

Specified effect =           0.05

Risk Type        =      Extra risk

Confidence level =           0.95

              BMD =      0.0084753

            BMDL =      0.0043156

            BMDU =      0.0099743

Taken together, (0.0043156, 0.0099743) is a 90     % two-sided confidence
interval for the BMD
```

SD Male Rats: Forestomach lesions (CEO in blood)

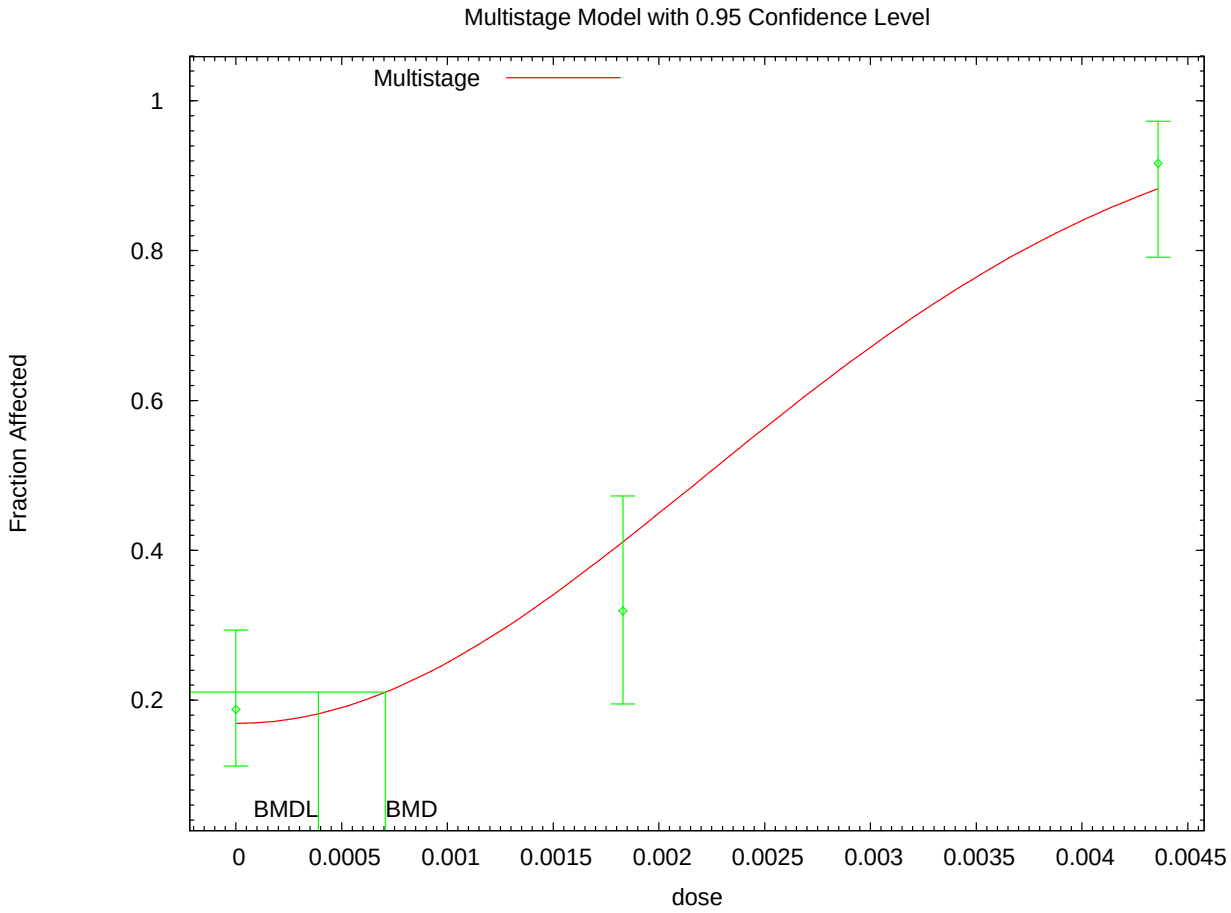


```
=================================================================
        Multistage Model. (Version: 3.0;  Date: 05/16/2008)
        Input Data File: C:\USEPA\BMDS2\Temp\tmpCC.(d)
        Gnuplot Plotting File:  C:\USEPA\BMDS2\Temp\tmpCC.plt
                                                Mon Oct 06 12:07:44 2008
=================================================================

BMDS Model Run
~~~~~~~~~~~~~~~~~~~~~~~~~~~~~~~~~~~~~~~~~~~~~~~~~~~~~~~~~~~~~~~~~~~~~

  The form of the probability function is:

  P[response] = background + (1-background)*[1-EXP(
               -beta1*dose^1-beta2*dose^2)]

  The parameter betas are restricted to be positive


  Dependent variable = Response
  Independent variable = DOSE

Total number of observations = 3
Total number of records with missing values = 0
Total number of parameters in model = 3
Total number of specified parameters = 0
Degree of polynomial = 2


Maximum number of iterations = 250
```

```
 Relative Function Convergence has been set to: 1e-008
 Parameter Convergence has been set to: 1e-008


                  Default Initial Parameter Values
                     Background =    0.0947166
                        Beta(1) =            0
                        Beta(2) =       124268


           Asymptotic Correlation Matrix of Parameter Estimates

           ( *** The model parameter(s)  -Beta(1)
                 have been estimated at a boundary point, or have been specified by the user,
                 and do not appear in the correlation matrix )

             Background      Beta(2)

Background            1        -0.37

   Beta(2)        -0.37            1



                                Parameter Estimates

                                                        95.0% Wald Confidence Interval
      Variable         Estimate        Std. Err.     Lower Conf. Limit   Upper Conf. Limit
     Background         0.169148            *                 *                   *
        Beta(1)                0            *                 *                   *
        Beta(2)           102914            *                 *                   *

* - Indicates that this value is not calculated.


                        Analysis of Deviance Table

       Model      Log(likelihood)  # Param's  Deviance  Test d.f.   P-value
     Full model         -81.807         3
    Fitted model       -83.0465         2       2.47897      1          0.1154
  Reduced model         -119.21         1       74.8052      2         <.0001

           AIC:         170.093

                                 Goodness  of  Fit
                                                                      Scaled
     Dose     Est._Prob.    Expected    Observed     Size       Residual
  ---------------------------------------------------------------------------
    0.0000     0.1691        13.532    15.000          80        0.438
    0.0018     0.4114        19.334    15.000          47       -1.285
    0.0044     0.8825        42.362    44.000          48        0.734

 Chi^2 = 2.38      d.f. = 1        P-value = 0.1228



   Benchmark Dose Computation

Specified effect =           0.05

Risk Type        =      Extra risk

Confidence level =           0.95

              BMD =    0.000705982

             BMDL =    0.000390266

             BMDU =    0.000828151

Taken together, (0.000390266, 0.000828151) is a 90     % two-sided confidence
interval for the BMD
```

SD Female Rats: Forestomach lesions (administered dose)

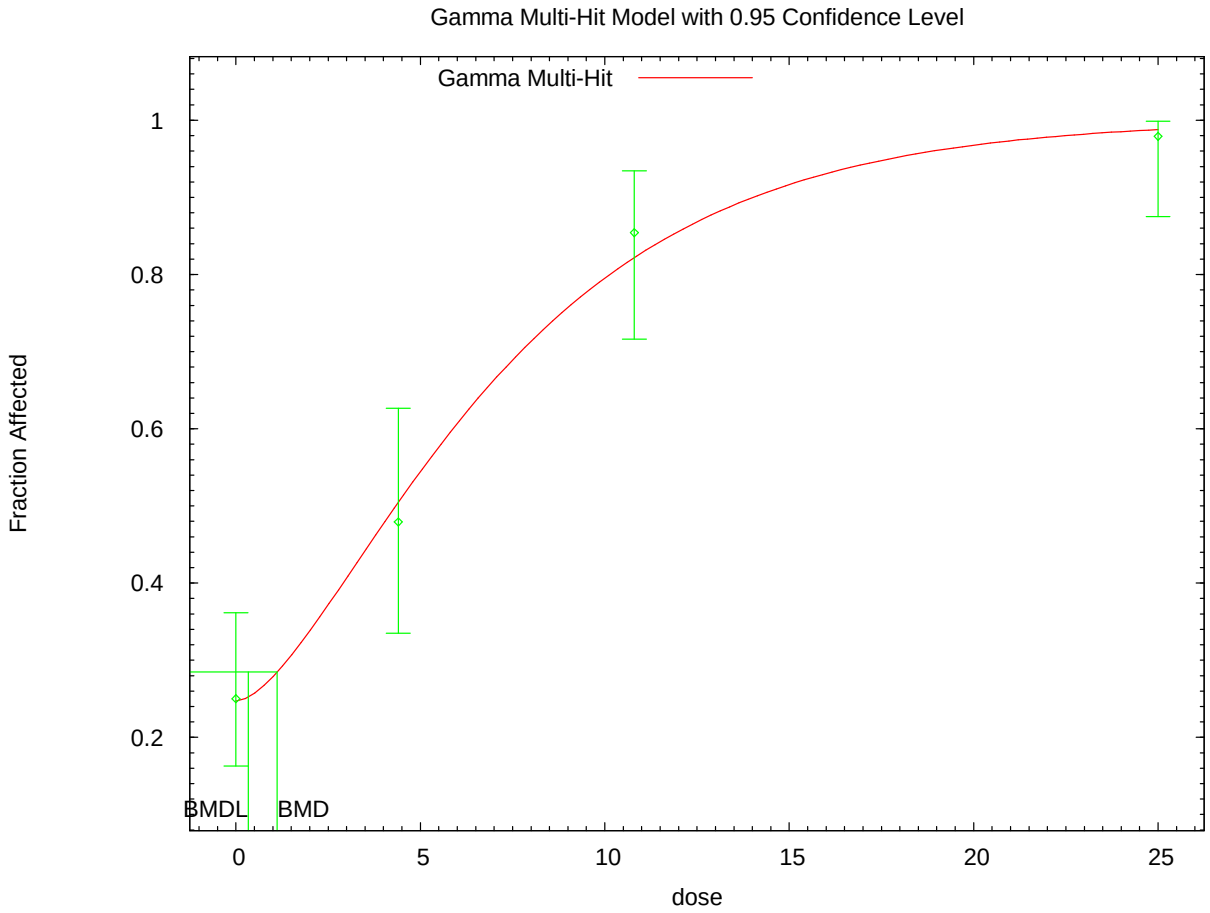

14:42 10/06 2008

```
=================================================================
        Gamma Model. (Version: 2.13;  Date: 05/16/2008)
        Input Data File: C:\USEPA\BMDS2\Temp\tmpD9.(d)
        Gnuplot Plotting File:  C:\USEPA\BMDS2\Temp\tmpD9.plt
                                                Mon Oct 06 14:42:46 2008
=================================================================

BMDS Model Run
~~~~~~~~~~~~~~~~~~~~~~~~~~~~~~~~~~~~~~~~~~~~~~~~~~~~~~~~~~~~~~~~~~~~~

  The form of the probability function is:

  P[response]= background+(1-background)*CumGamma[slope*dose,power],
  where CumGamma(.) is the cummulative Gamma distribution function


  Dependent variable = Response
  Independent variable = DOSE
  Power parameter is restricted as power >=1

  Total number of observations = 4
  Total number of records with missing values = 0
  Maximum number of iterations = 250
  Relative Function Convergence has been set to: 1e-008
  Parameter Convergence has been set to: 1e-008


                Default Initial (and Specified) Parameter Values
                   Background =     0.253086
                        Slope =     0.194377
```

Power = 1.66787

Asymptotic Correlation Matrix of Parameter Estimates

	Background	Slope	Power
Background	1	0.13	0.25
Slope	0.13	1	0.95
Power	0.25	0.95	1

Parameter Estimates

Variable	Estimate	Std. Err.	95.0% Wald Confidence Interval Lower Conf. Limit	Upper Conf. Limit
Background	0.247085	0.0476211	0.153749	0.340421
Slope	0.22327	0.0913548	0.0442181	0.402322
Power	1.72213	0.704799	0.340745	3.10351

Analysis of Deviance Table

Model	Log(likelihood)	# Param's	Deviance	Test d.f.	P-value
Full model	-103.017	4			
Fitted model	-103.386	3	0.738711	1	0.3901
Reduced model	-152.026	1	98.0188	3	<.0001

AIC: 212.772

Goodness of Fit

Dose	Est._Prob.	Expected	Observed	Size	Scaled Residual
0.0000	0.2471	19.767	20.000	80	0.060
4.4000	0.5044	24.212	23.000	48	-0.350
10.8000	0.8219	39.451	41.000	48	0.584
25.0000	0.9879	47.420	47.000	48	-0.555

Chi^2 = 0.78 d.f. = 1 P-value = 0.3785

Benchmark Dose Computation

Specified effect = 0.05

Risk Type = Extra risk

Confidence level = 0.95

BMD = 1.12

BMDL = 0.334344

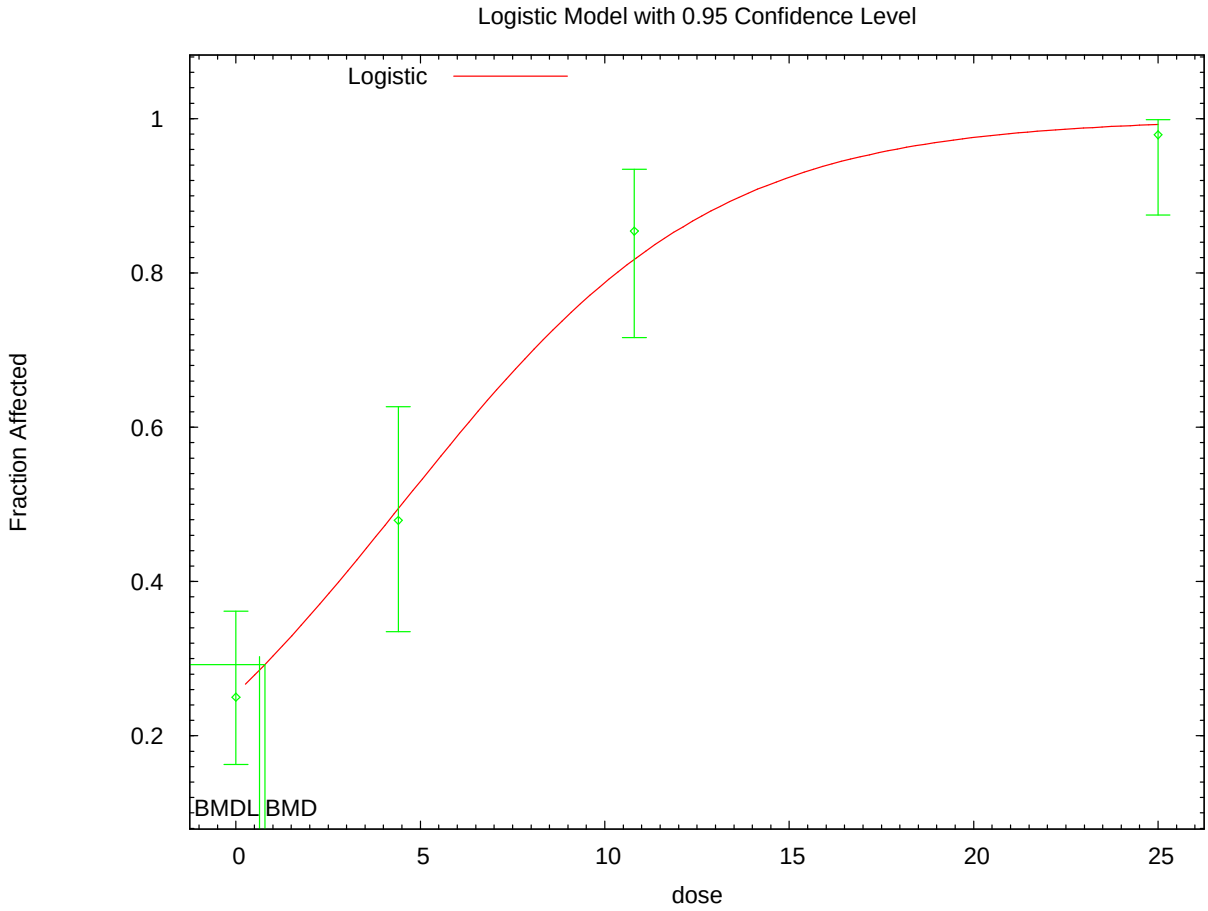

14:44 10/06 2008

```
================================================================
        Logistic Model. (Version: 2.12; Date: 05/16/2008)
        Input Data File: C:\USEPA\BMDS2\Temp\tmpDB.(d)
        Gnuplot Plotting File:  C:\USEPA\BMDS2\Temp\tmpDB.plt
                                                Mon Oct 06 14:44:22 2008
================================================================

BMDS Model Run
~~~~~~~~~~~~~~~~~~~~~~~~~~~~~~~~~~~~~~~~~~~~~~~~~~~~~~~~~~~~~~~~~~~~~~~

  The form of the probability function is:

  P[response] = 1/[1+EXP(-intercept-slope*dose)]


  Dependent variable = Response
  Independent variable = DOSE
  Slope parameter is not restricted

  Total number of observations = 4
  Total number of records with missing values = 0
  Maximum number of iterations = 250
  Relative Function Convergence has been set to: 1e-008
  Parameter Convergence has been set to: 1e-008


                Default Initial Parameter Values
                   background =            0   Specified
                    intercept =    -0.808992
                        slope =     0.180053


         Asymptotic Correlation Matrix of Parameter Estimates
```

(*** The model parameter(s) -background
have been estimated at a boundary point, or have been specified by the user,
and do not appear in the correlation matrix)

	intercept	slope
intercept	1	-0.66
slope	-0.66	1

Parameter Estimates

Variable	Estimate	Std. Err.	95.0% Wald Confidence Interval Lower Conf. Limit	Upper Conf. Limit
intercept	-1.07104	0.225024	-1.51208	-0.630006
slope	0.23795	0.0368793	0.165668	0.310232

Analysis of Deviance Table

Model	Log(likelihood)	# Param's	Deviance	Test d.f.	P-value
Full model	-103.017	4			
Fitted model	-103.655	2	1.27604	2	0.5283
Reduced model	-152.026	1	98.0188	3	<.0001

AIC: 211.31

Goodness of Fit

Dose	Est._Prob.	Expected	Observed	Size	Scaled Residual
0.0000	0.2552	20.416	20.000	80	-0.107
4.4000	0.4940	23.711	23.000	48	-0.205
10.8000	0.8174	39.235	41.000	48	0.659
25.0000	0.9924	47.637	47.000	48	-1.062

Chi^2 = 1.62 d.f. = 2 P-value = 0.4456

Benchmark Dose Computation

Specified effect = 0.05

Risk Type = Extra risk

Confidence level = 0.95

BMD = 0.78799

BMDL = 0.639403

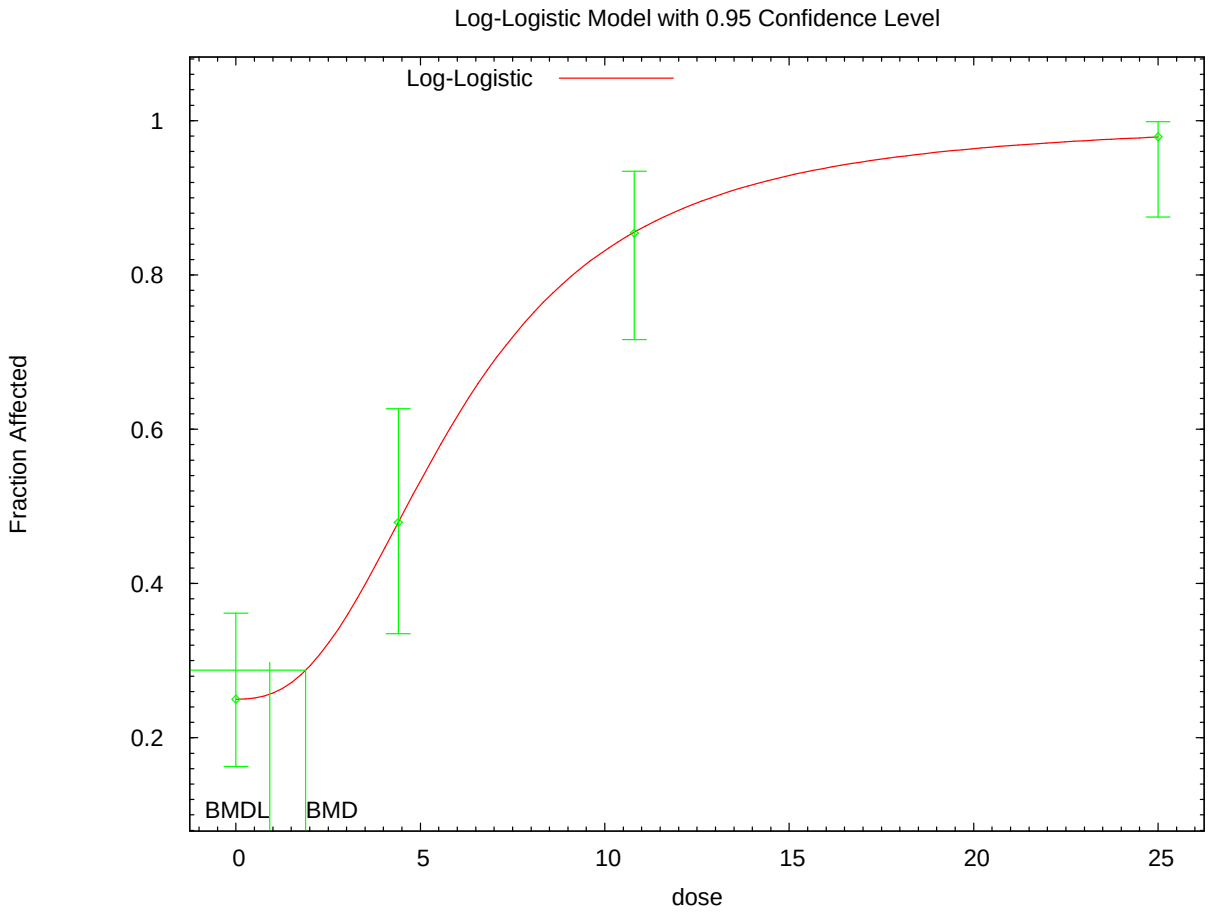

14:46 10/06 2008

```
==========================================================================
        Logistic Model. (Version: 2.12; Date: 05/16/2008)
        Input Data File: C:\USEPA\BMDS2\Temp\tmpDD.(d)
        Gnuplot Plotting File:  C:\USEPA\BMDS2\Temp\tmpDD.plt
                                                Mon Oct 06 14:46:39 2008
==========================================================================

BMDS Model Run
~~~~~~~~~~~~~~~~~~~~~~~~~~~~~~~~~~~~~~~~~~~~~~~~~~~~~~~~~~~~~~~~~~~~~~~~~~

  The form of the probability function is:

  P[response] = background+(1-background)/[1+EXP(-intercept-slope*Log(dose))]


  Dependent variable = Response
  Independent variable = DOSE
  Slope parameter is restricted as slope >= 1

  Total number of observations = 4
  Total number of records with missing values = 0
  Maximum number of iterations = 250
  Relative Function Convergence has been set to: 1e-008
  Parameter Convergence has been set to: 1e-008


  User has chosen the log transformed model


               Default Initial Parameter Values
                  background =         0.25
                   intercept =     -4.55921
                       slope =      2.51883
```

Asymptotic Correlation Matrix of Parameter Estimates

	background	intercept	slope
background	1	-0.3	0.2
intercept	-0.3	1	-0.96
slope	0.2	-0.96	1

Parameter Estimates

Variable	Estimate	Std. Err.	95.0% Wald Confidence Interval Lower Conf. Limit	Upper Conf. Limit
background	0.250085	*	*	*
intercept	-4.54432	*	*	*
slope	2.51011	*	*	*

* - Indicates that this value is not calculated.

Analysis of Deviance Table

Model	Log(likelihood)	# Param's	Deviance	Test d.f.	P-value
Full model	-103.017	4			
Fitted model	-103.017	3	0.000749029	1	0.9782
Reduced model	-152.026	1	98.0188	3	<.0001

AIC: 212.034

Goodness of Fit

Dose	Est._Prob.	Expected	Observed	Size	Scaled Residual
0.0000	0.2501	20.007	20.000	80	-0.002
4.4000	0.4785	22.970	23.000	48	0.009
10.8000	0.8550	41.041	41.000	48	-0.017
25.0000	0.9788	46.981	47.000	48	0.019

Chi^2 = 0.00 d.f. = 1 P-value = 0.9782

Benchmark Dose Computation

Specified effect = 0.05

Risk Type = Extra risk

Confidence level = 0.95

BMD = 1.89151

BMDL = 0.917407

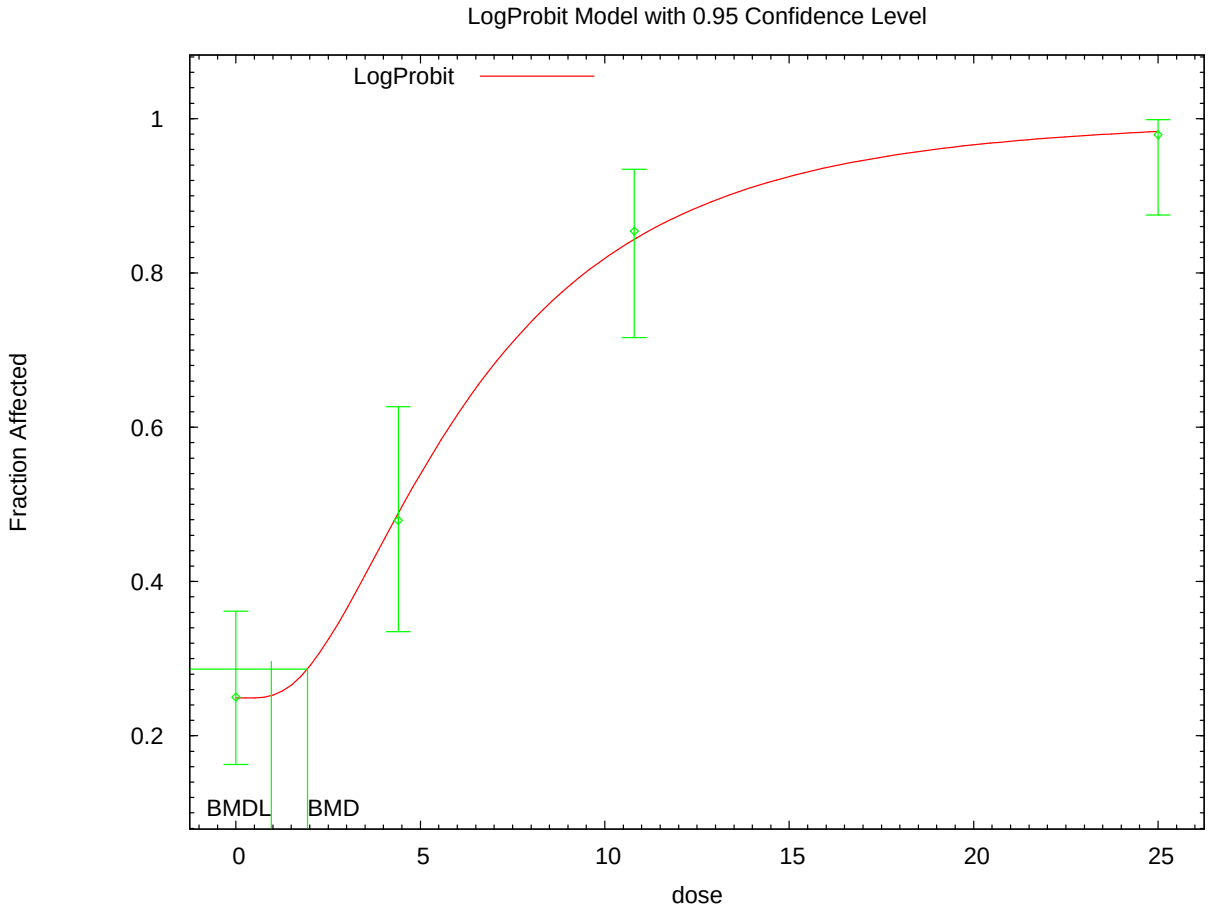

14:50 10/06 2008

```
================================================================
        Probit Model. (Version: 3.1;  Date: 05/16/2008)
        Input Data File: C:\USEPA\BMDS2\Temp\tmpDE.(d)
        Gnuplot Plotting File:  C:\USEPA\BMDS2\Temp\tmpDE.plt
                                                Mon Oct 06 14:50:13 2008
================================================================

BMDS Model Run
~~~~~~~~~~~~~~~~~~~~~~~~~~~~~~~~~~~~~~~~~~~~~~~~~~~~~~~~~~~~~~~~~~~~~~~

  The form of the probability function is:

  P[response] = Background
              + (1-Background) * CumNorm(Intercept+Slope*Log(Dose)),

  where CumNorm(.) is the cumulative normal distribution function


  Dependent variable = Response
  Independent variable = DOSE
  Slope parameter is restricted as slope >= 1

  Total number of observations = 4
  Total number of records with missing values = 0
  Maximum number of iterations = 250
  Relative Function Convergence has been set to: 1e-008
  Parameter Convergence has been set to: 1e-008


  User has chosen the log transformed model

                Default Initial (and Specified) Parameter Values
```

```
                    background =         0.25
                     intercept =     -2.53925
                         slope =      1.39624


          Asymptotic Correlation Matrix of Parameter Estimates

            background    intercept        slope

background            1        -0.31         0.21

 intercept        -0.31            1        -0.96

     slope         0.21        -0.96            1


                              Parameter Estimates

                                                        95.0% Wald Confidence Interval
      Variable         Estimate        Std. Err.     Lower Conf. Limit   Upper Conf. Limit
    background         0.248842        0.0480048           0.154755             0.34293
     intercept         -2.58881         0.657292           -3.87708            -1.30054
         slope          1.42762         0.288071            0.86301             1.99223


                       Analysis of Deviance Table

       Model      Log(likelihood)  # Param's  Deviance  Test d.f.   P-value
    Full model         -103.017         4
   Fitted model         -103.07         3      0.106572      1          0.7441
  Reduced model        -152.026         1       98.0188      3         <.0001

          AIC:          212.14


                              Goodness  of  Fit
                                                                    Scaled
    Dose     Est._Prob.    Expected    Observed     Size       Residual
  ---------------------------------------------------------------------------
    0.0000     0.2488        19.907    20.000          80        0.024
    4.4000     0.4876        23.406    23.000          48       -0.117
   10.8000     0.8427        40.448    41.000          48        0.219
   25.0000     0.9832        47.192    47.000          48       -0.216

 Chi^2 = 0.11      d.f. = 1        P-value = 0.7415


   Benchmark Dose Computation

Specified effect =           0.05

Risk Type        =      Extra risk

Confidence level =           0.95

             BMD =        1.93713

            BMDL =       0.961058
```

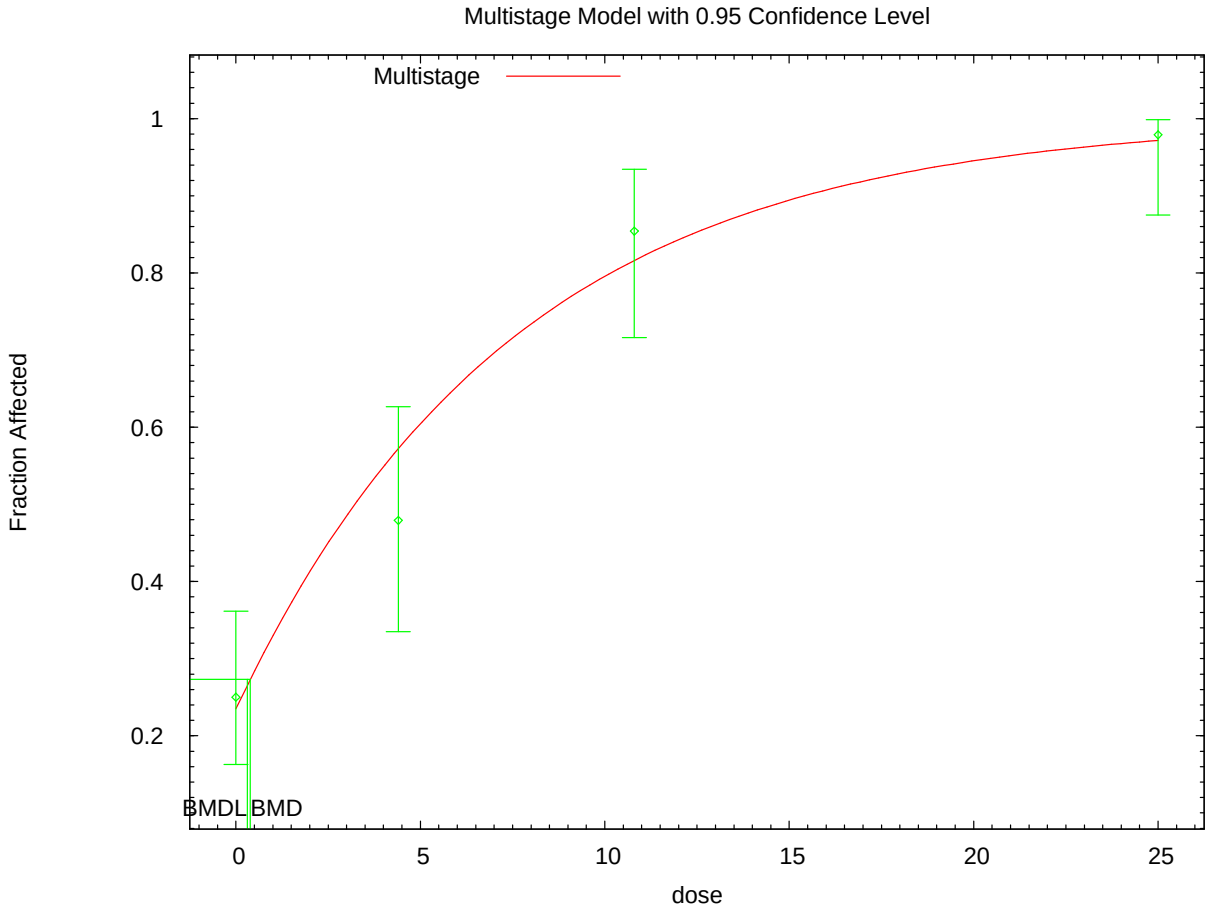

14:52 10/06 2008

```
================================================================================
        Multistage Model. (Version: 3.0;  Date: 05/16/2008)
        Input Data File: C:\USEPA\BMDS2\Temp\tmpDF.(d)
        Gnuplot Plotting File:  C:\USEPA\BMDS2\Temp\tmpDF.plt
                                                  Mon Oct 06 14:52:05 2008
================================================================================

BMDS Model Run
~~~~~~~~~~~~~~~~~~~~~~~~~~~~~~~~~~~~~~~~~~~~~~~~~~~~~~~~~~~~~~~~~~~~~~~~~~~~~~~~

  The form of the probability function is:

  P[response] = background + (1-background)*[1-EXP(
               -beta1*dose^1)]

  The parameter betas are restricted to be positive


  Dependent variable = Response
  Independent variable = DOSE

Total number of observations = 4
Total number of records with missing values = 0
Total number of parameters in model = 2
Total number of specified parameters = 0
Degree of polynomial = 1


Maximum number of iterations = 250
Relative Function Convergence has been set to: 1e-008
Parameter Convergence has been set to: 1e-008
```

Default Initial Parameter Values
Background = 0.18073
Beta(1) = 0.14774

Asymptotic Correlation Matrix of Parameter Estimates

	Background	Beta(1)
Background	1	-0.46
Beta(1)	-0.46	1

Parameter Estimates

Variable	Estimate	Std. Err.	95.0% Wald Confidence Interval Lower Conf. Limit	Upper Conf. Limit
Background	0.235056	*	*	*
Beta(1)	0.131634	*	*	*

* - Indicates that this value is not calculated.

Analysis of Deviance Table

Model	Log(likelihood)	# Param's	Deviance	Test d.f.	P-value
Full model	-103.017	4			
Fitted model	-104.199	2	2.36383	2	0.3067
Reduced model	-152.026	1	98.0188	3	<.0001

AIC: 212.397

Goodness of Fit

Dose	Est._Prob.	Expected	Observed	Size	Scaled Residual
0.0000	0.2351	18.804	20.000	80	0.315
4.4000	0.5714	27.425	23.000	48	-1.291
10.8000	0.8154	39.139	41.000	48	0.692
25.0000	0.9715	46.633	47.000	48	0.318

Chi^2 = 2.35 d.f. = 2 P-value = 0.3095

Benchmark Dose Computation

Specified effect = 0.05

Risk Type = Extra risk

Confidence level = 0.95

BMD = 0.389667

BMDL = 0.306761

BMDU = 0.505425

Taken together, (0.306761, 0.505425) is a 90 % two-sided confidence interval for the BMD

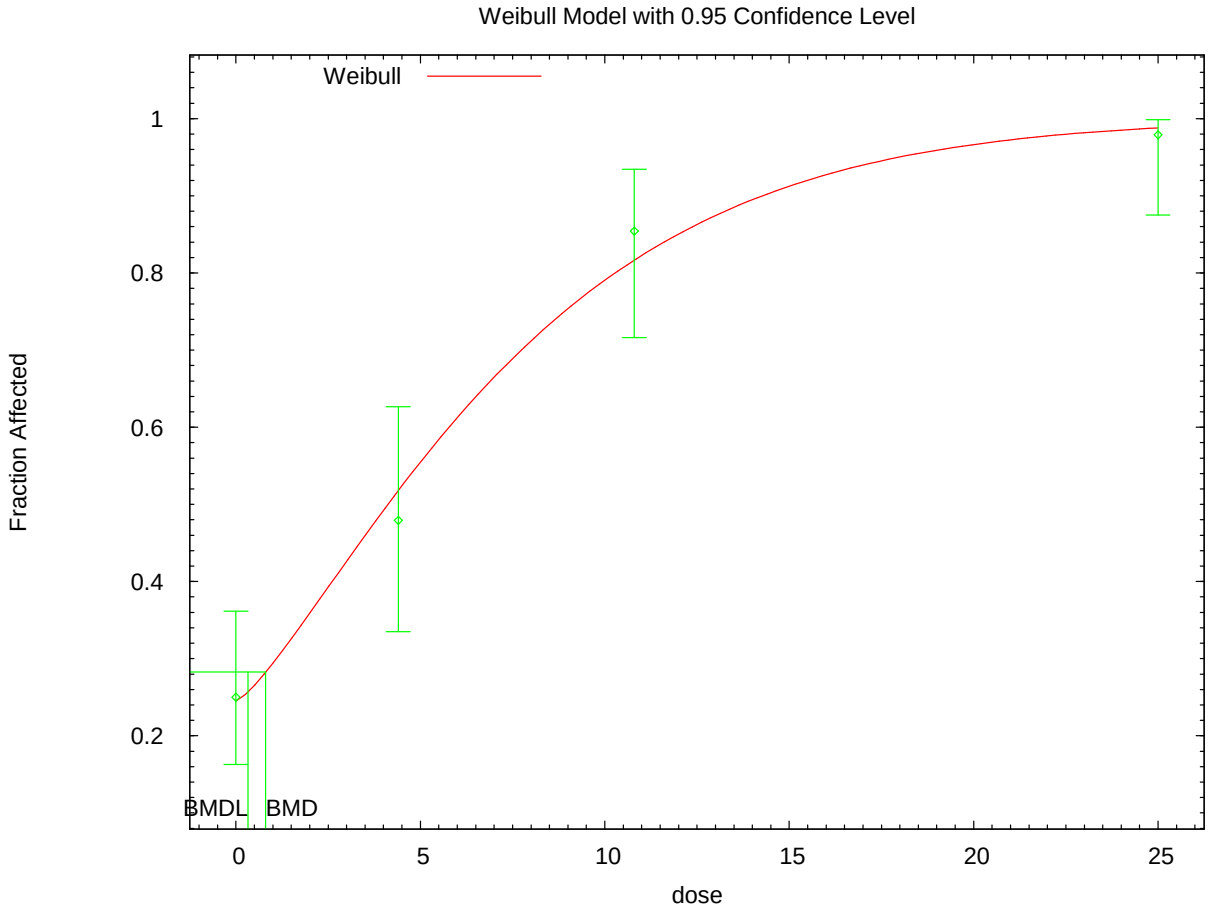

14:55 10/06 2008

```
 ================================================================
         Weibull Model using Weibull Model (Version: 2.12;  Date: 05/16/2008)
         Input Data File: C:\USEPA\BMDS2\Temp\tmpE2.(d)
         Gnuplot Plotting File:  C:\USEPA\BMDS2\Temp\tmpE2.plt
                                                 Mon Oct 06 14:55:23 2008
 ================================================================

 BMDS Model Run
~~~~~~~~~~~~~~~~~~~~~~~~~~~~~~~~~~~~~~~~~~~~~~~~~~~~~~~~~~~~~~~~~~~~~~~~

   The form of the probability function is:

   P[response] = background + (1-background)*[1-EXP(-slope*dose^power)]


   Dependent variable = Response
   Independent variable = DOSE
   Power parameter is restricted as power >=1

   Total number of observations = 4
   Total number of records with missing values = 0
   Maximum number of iterations = 250
   Relative Function Convergence has been set to: 1e-008
   Parameter Convergence has been set to: 1e-008


                  Default Initial (and Specified) Parameter Values
                     Background =     0.253086
                          Slope =    0.0679496
                          Power =      1.19621


           Asymptotic Correlation Matrix of Parameter Estimates
```

	Background	Slope	Power
Background	1	-0.31	0.23
Slope	-0.31	1	-0.97
Power	0.23	-0.97	1

Parameter Estimates

Variable	Estimate	Std. Err.	95.0% Wald Confidence Interval Lower Conf. Limit	Upper Conf. Limit
Background	0.245056	0.0471325	0.152678	0.337434
Slope	0.0673284	0.0436908	-0.018304	0.152961
Power	1.27711	0.255412	0.776514	1.77771

Analysis of Deviance Table

Model	Log(likelihood)	# Param's	Deviance	Test d.f.	P-value
Full model	-103.017	4			
Fitted model	-103.534	3	1.03516	1	0.3089
Reduced model	-152.026	1	98.0188	3	<.0001

AIC: 213.069

Goodness of Fit

Dose	Est._Prob.	Expected	Observed	Size	Scaled Residual
0.0000	0.2451	19.604	20.000	80	0.103
4.4000	0.5170	24.816	23.000	48	-0.525
10.8000	0.8150	39.118	41.000	48	0.700
25.0000	0.9876	47.404	47.000	48	-0.526

Chi^2 = 1.05 d.f. = 1 P-value = 0.3051

Benchmark Dose Computation

Specified effect = 0.05

Risk Type = Extra risk

Confidence level = 0.95

BMD = 0.808158

BMDL = 0.327975

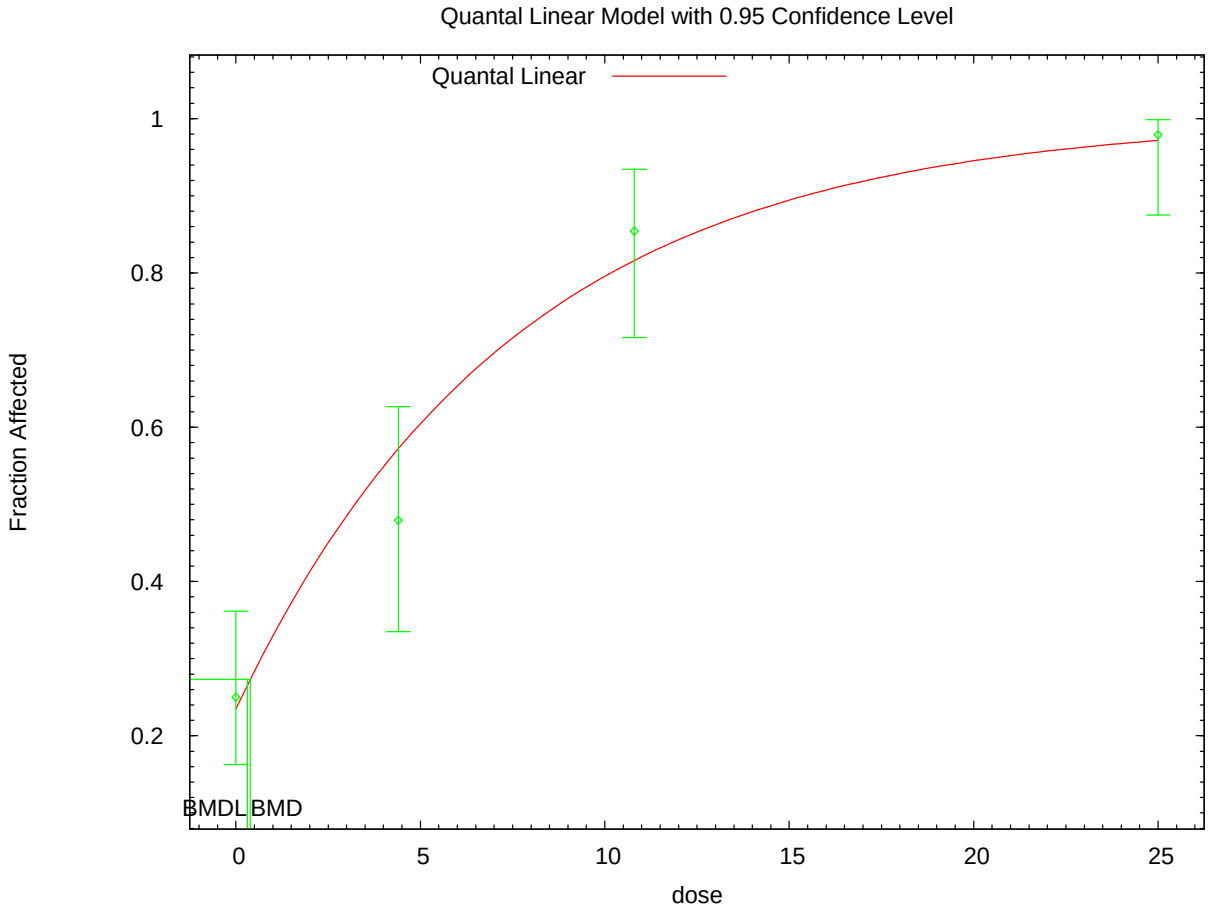

14:57 10/06 2008

```
 ======================================================================
         Quantal Linear Model using Weibull Model (Version: 2.12;  Date: 05/16/2008)
         Input Data File: C:\USEPA\BMDS2\Temp\tmpE4.(d)
         Gnuplot Plotting File:  C:\USEPA\BMDS2\Temp\tmpE4.plt
                                                Mon Oct 06 14:57:14 2008
 ======================================================================

 BMDS Model Run
~~~~~~~~~~~~~~~~~~~~~~~~~~~~~~~~~~~~~~~~~~~~~~~~~~~~~~~~~~~~~~~~~~~~~~~~~~~~

   The form of the probability function is:

   P[response] = background + (1-background)*[1-EXP(-slope*dose)]


   Dependent variable = Response
   Independent variable = DOSE

   Total number of observations = 4
   Total number of records with missing values = 0
   Maximum number of iterations = 250
   Relative Function Convergence has been set to: 1e-008
   Parameter Convergence has been set to: 1e-008


                  Default Initial (and Specified) Parameter Values
                     Background =     0.253086
                          Slope =     0.127782
                          Power =            1   Specified


           Asymptotic Correlation Matrix of Parameter Estimates
```

(*** The model parameter(s) -Power
have been estimated at a boundary point, or have been specified by the user,
and do not appear in the correlation matrix)

	Background	Slope
Background	1	-0.31
Slope	-0.31	1

Parameter Estimates

Variable	Estimate	Std. Err.	95.0% Wald Confidence Interval Lower Conf. Limit	Upper Conf. Limit
Background	0.235057	0.0449515	0.146954	0.323161
Slope	0.131633	0.019868	0.0926927	0.170574

Analysis of Deviance Table

Model	Log(likelihood)	# Param's	Deviance	Test d.f.	P-value
Full model	-103.017	4			
Fitted model	-104.199	2	2.36383	2	0.3067
Reduced model	-152.026	1	98.0188	3	<.0001

AIC: 212.397

Goodness of Fit

Dose	Est._Prob.	Expected	Observed	Size	Scaled Residual
0.0000	0.2351	18.805	20.000	80	0.315
4.4000	0.5714	27.425	23.000	48	-1.291
10.8000	0.8154	39.139	41.000	48	0.692
25.0000	0.9715	46.633	47.000	48	0.318

Chi^2 = 2.35 d.f. = 2 P-value = 0.3095

Benchmark Dose Computation

Specified effect = 0.05

Risk Type = Extra risk

Confidence level = 0.95

BMD = 0.389668

BMDL = 0.306761

SD Female Rats: Nonneoplastic forestomach lesions (AN in blood)

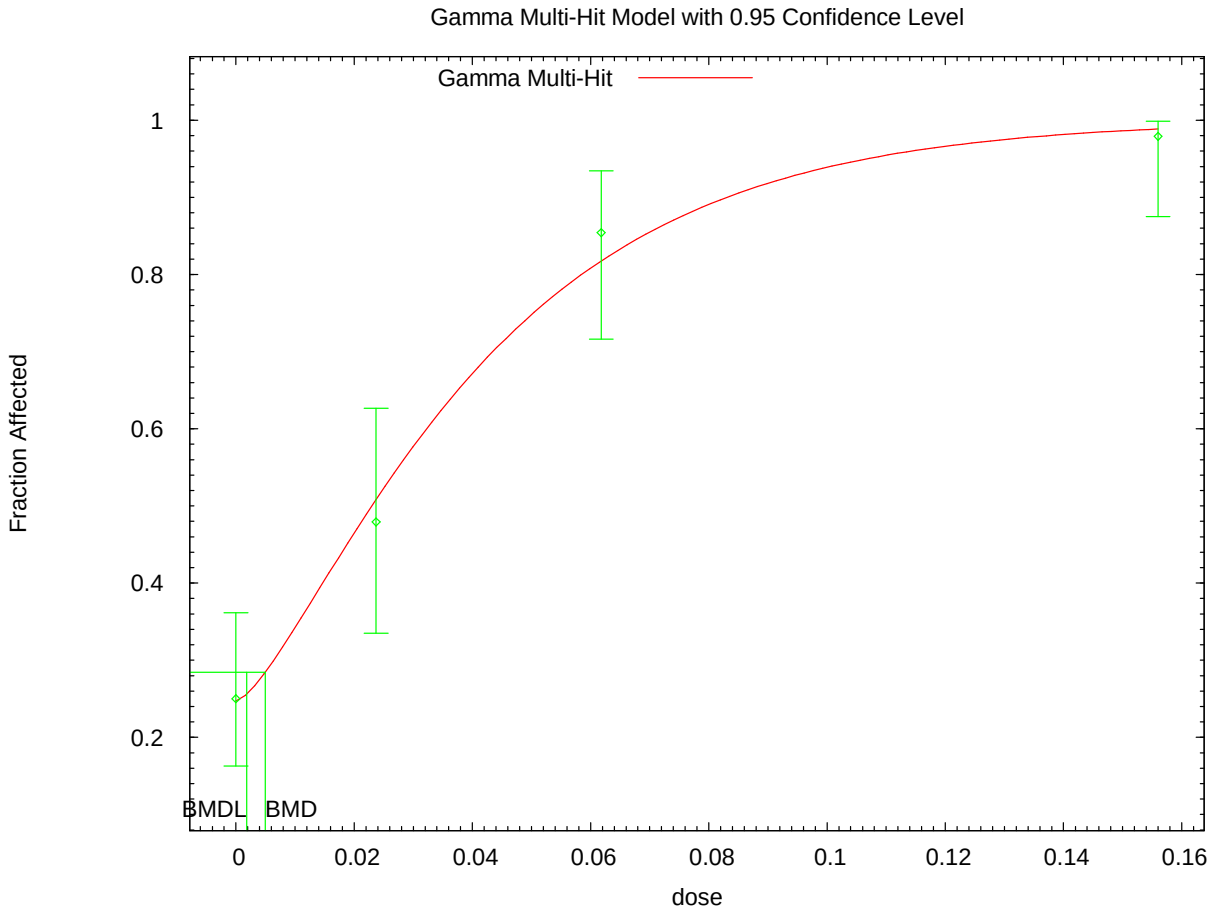

15:59 10/06 2008

```
 ======================================================================
         Gamma Model. (Version: 2.13;  Date: 05/16/2008)
         Input Data File: C:\USEPA\BMDS2\Temp\tmpF1.(d)
         Gnuplot Plotting File:  C:\USEPA\BMDS2\Temp\tmpF1.plt
                                                 Mon Oct 06 15:59:50 2008
 ======================================================================

 BMDS Model Run
~~~~~~~~~~~~~~~~~~~~~~~~~~~~~~~~~~~~~~~~~~~~~~~~~~~~~~~~~~~~~~~~~~~~~~~~~~

   The form of the probability function is:

   P[response]= background+(1-background)*CumGamma[slope*dose,power],
   where CumGamma(.) is the cummulative Gamma distribution function


   Dependent variable = Response
   Independent variable = DOSE
   Power parameter is restricted as power >=1

   Total number of observations = 4
   Total number of records with missing values = 0
   Maximum number of iterations = 250
   Relative Function Convergence has been set to: 1e-008
   Parameter Convergence has been set to: 1e-008


                  Default Initial (and Specified) Parameter Values
                     Background =     0.253086
```

Slope = 28.0854
Power = 1.40734

Asymptotic Correlation Matrix of Parameter Estimates

	Background	Slope	Power
Background	1	0.12	0.24
Slope	0.12	1	0.94
Power	0.24	0.94	1

Parameter Estimates

Variable	Estimate	Std. Err.	95.0% Wald Confidence Interval Lower Conf. Limit	Upper Conf. Limit
Background	0.24677	0.0475578	0.153558	0.339981
Slope	32.9782	13.6708	6.18402	59.7725
Power	1.45925	0.592225	0.298512	2.61999

Analysis of Deviance Table

Model	Log(likelihood)	# Param's	Deviance	Test d.f.	P-value
Full model	-103.017	4			
Fitted model	-103.482	3	0.931283	1	0.3345
Reduced model	-152.026	1	98.0188	3	<.0001

AIC: 212.965

Goodness of Fit

Dose	Est._Prob.	Expected	Observed	Size	Scaled Residual
0.0000	0.2468	19.742	20.000	80	0.067
0.0237	0.5082	24.395	23.000	48	-0.403
0.0618	0.8175	39.238	41.000	48	0.658
0.1560	0.9886	47.454	47.000	48	-0.617

Chi^2 = 0.98 d.f. = 1 P-value = 0.3220

Benchmark Dose Computation

Specified effect = 0.05

Risk Type = Extra risk

Confidence level = 0.95

BMD = 0.00495567

BMDL = 0.00183293

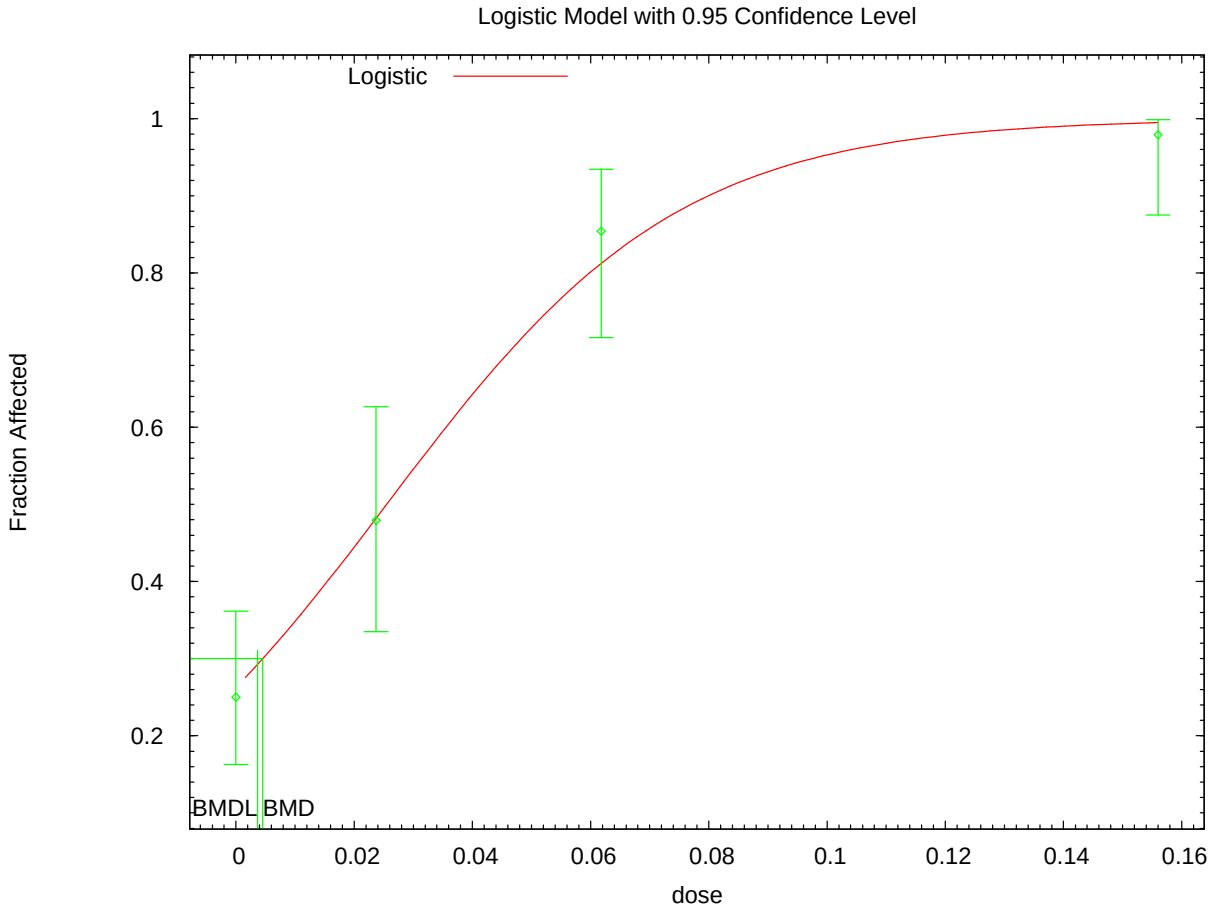

16:01 10/06 2008

```
 ================================================================
         Logistic Model. (Version: 2.12; Date: 05/16/2008)
         Input Data File: C:\USEPA\BMDS2\Temp\tmpF2.(d)
         Gnuplot Plotting File:  C:\USEPA\BMDS2\Temp\tmpF2.plt
                                                Mon Oct 06 16:01:31 2008
 ================================================================

 BMDS Model Run
~~~~~~~~~~~~~~~~~~~~~~~~~~~~~~~~~~~~~~~~~~~~~~~~~~~~~~~~~~~~~~~~~~~~~~~~

   The form of the probability function is:

   P[response] = 1/[1+EXP(-intercept-slope*dose)]


   Dependent variable = Response
   Independent variable = DOSE
   Slope parameter is not restricted

   Total number of observations = 4
   Total number of records with missing values = 0
   Maximum number of iterations = 250
   Relative Function Convergence has been set to: 1e-008
   Parameter Convergence has been set to: 1e-008


                  Default Initial Parameter Values
                     background =            0   Specified
                      intercept =    -0.712868
                          slope =      28.3794


           Asymptotic Correlation Matrix of Parameter Estimates
```

(*** The model parameter(s) -background
have been estimated at a boundary point, or have been specified by the user,
and do not appear in the correlation matrix)

	intercept	slope
intercept	1	-0.65
slope	-0.65	1

Parameter Estimates

Variable	Estimate	Std. Err.	95.0% Wald Confidence Interval Lower Conf. Limit	Upper Conf. Limit
intercept	-1.0292	0.221998	-1.46431	-0.594092
slope	40.4482	6.53178	27.6462	53.2503

Analysis of Deviance Table

Model	Log(likelihood)	# Param's	Deviance	Test d.f.	P-value
Full model	-103.017	4			
Fitted model	-104.001	2	1.9683	2	0.3738
Reduced model	-152.026	1	98.0188	3	<.0001

AIC: 212.002

Goodness of Fit

Dose	Est._Prob.	Expected	Observed	Size	Scaled Residual
0.0000	0.2632	21.059	20.000	80	-0.269
0.0237	0.4824	23.153	23.000	48	-0.044
0.0618	0.8131	39.030	41.000	48	0.729
0.1560	0.9949	47.757	47.000	48	-1.539

Chi^2 = 2.98 d.f. = 2 P-value = 0.2258

Benchmark Dose Computation

Specified effect = 0.05

Risk Type = Extra risk

Confidence level = 0.95

BMD = 0.00450626

BMDL = 0.00363943

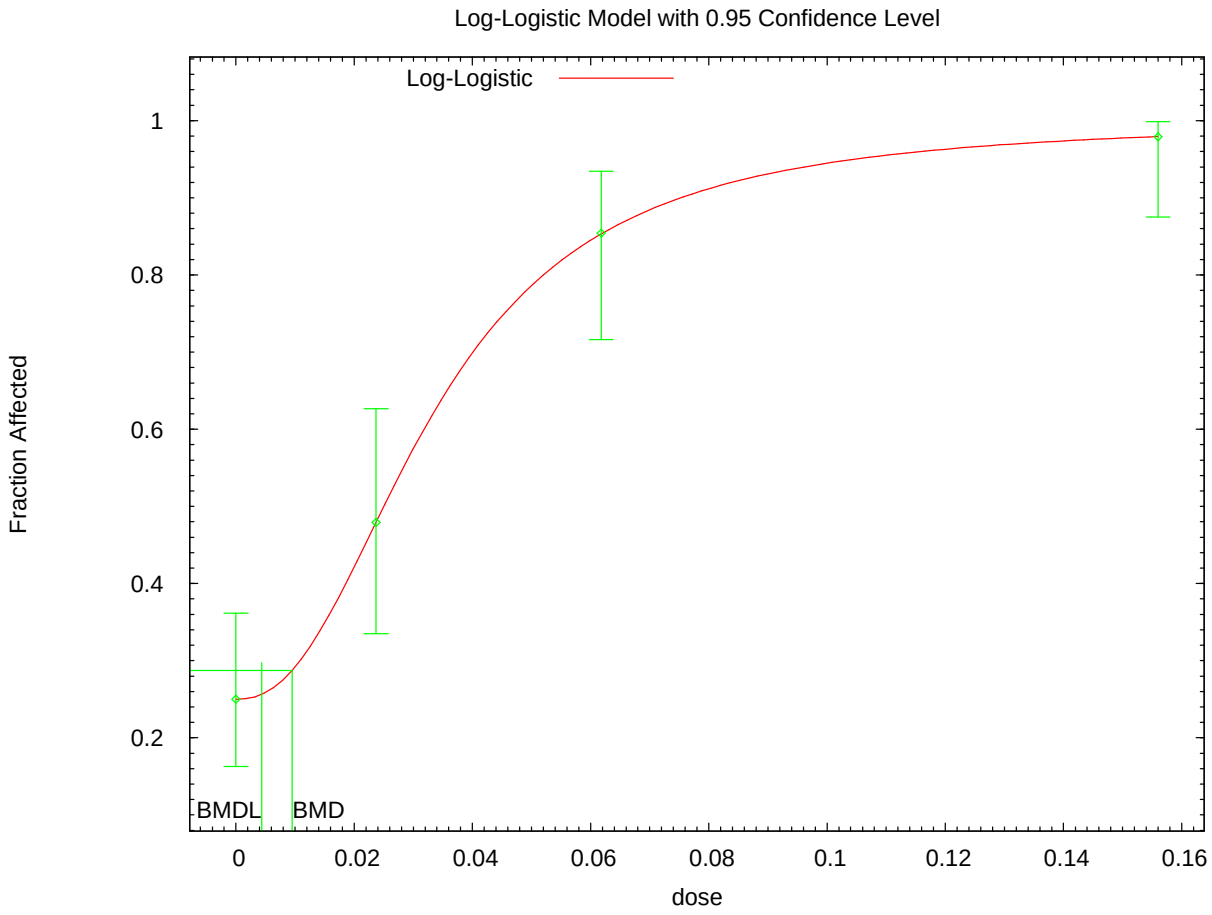

16:03 10/06 2008

```
=================================================================
        Logistic Model. (Version: 2.12; Date: 05/16/2008)
        Input Data File: C:\USEPA\BMDS2\Temp\tmpF3.(d)
        Gnuplot Plotting File:  C:\USEPA\BMDS2\Temp\tmpF3.plt
                                                Mon Oct 06 16:03:04 2008
=================================================================

BMDS Model Run
~~~~~~~~~~~~~~~~~~~~~~~~~~~~~~~~~~~~~~~~~~~~~~~~~~~~~~~~~~~~~~~~~~~~~

  The form of the probability function is:

  P[response] = background+(1-background)/[1+EXP(-intercept-slope*Log(dose))]


  Dependent variable = Response
  Independent variable = DOSE
  Slope parameter is restricted as slope >= 1

  Total number of observations = 4
  Total number of records with missing values = 0
  Maximum number of iterations = 250
  Relative Function Convergence has been set to: 1e-008
  Parameter Convergence has been set to: 1e-008


  User has chosen the log transformed model


               Default Initial Parameter Values
                  background =         0.25
                   intercept =      7.87595
                       slope =      2.32252
```

Asymptotic Correlation Matrix of Parameter Estimates

	background	intercept	slope
background	1	0.11	0.2
intercept	0.11	1	0.98
slope	0.2	0.98	1

Parameter Estimates

Variable	Estimate	Std. Err.	95.0% Wald Confidence Interval Lower Conf. Limit	Upper Conf. Limit
background	0.249911	*	*	*
intercept	7.9009	*	*	*
slope	2.32966	*	*	*

* - Indicates that this value is not calculated.

Analysis of Deviance Table

Model	Log(likelihood)	# Param's	Deviance	Test d.f.	P-value
Full model	-103.017	4			
Fitted model	-103.017	3	0.000533199	1	0.9816
Reduced model	-152.026	1	98.0188	3	<.0001

AIC: 212.034

Goodness of Fit

Dose	Est._Prob.	Expected	Observed	Size	Scaled Residual
0.0000	0.2499	19.993	20.000	80	0.002
0.0237	0.4797	23.025	23.000	48	-0.007
0.0618	0.8535	40.966	41.000	48	0.014
0.1560	0.9795	47.017	47.000	48	-0.017

Chi^2 = 0.00 d.f. = 1 P-value = 0.9816

Benchmark Dose Computation

Specified effect = 0.05

Risk Type = Extra risk

Confidence level = 0.95

BMD = 0.00951077

BMDL = 0.00435683

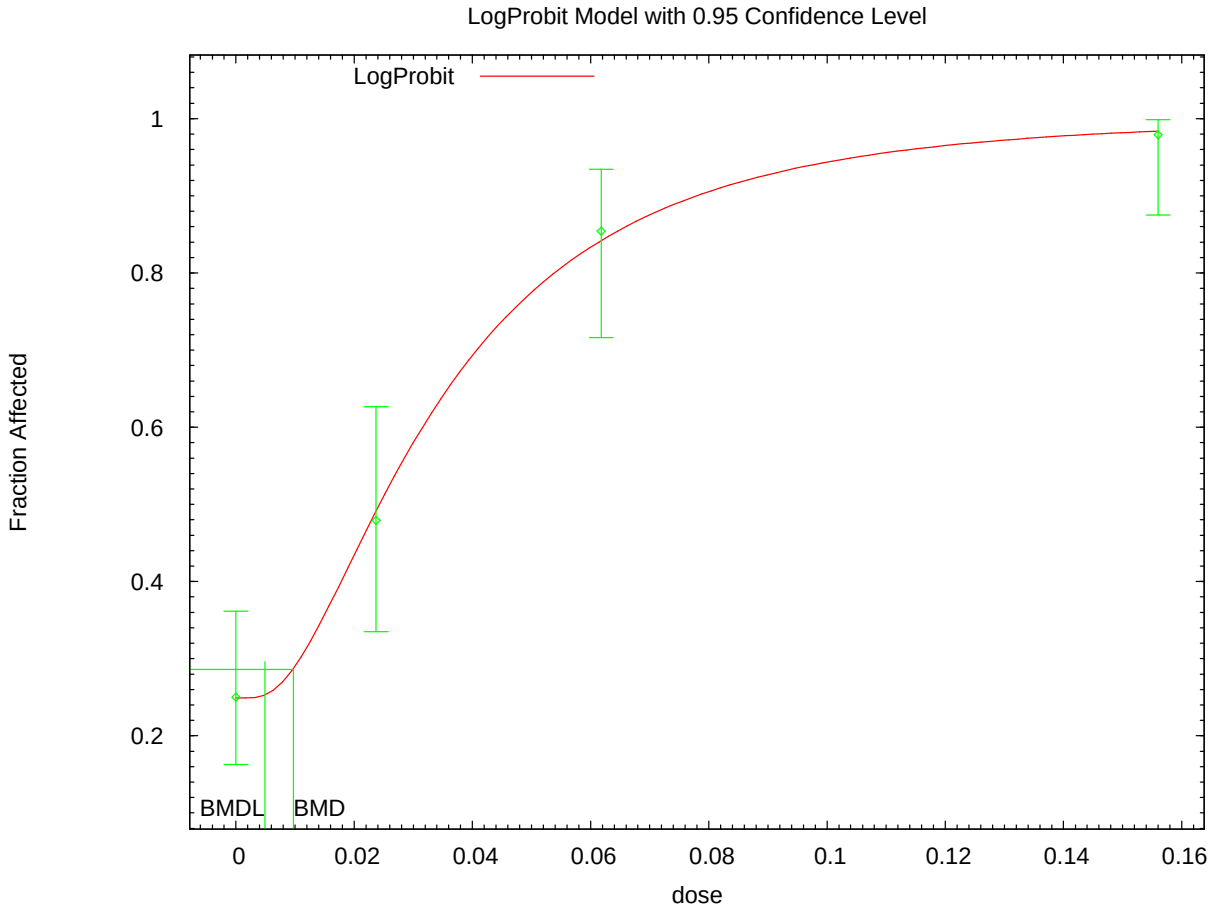

16:04 10/06 2008

```
================================================================
        Probit Model. (Version: 3.1;  Date: 05/16/2008)
        Input Data File: C:\USEPA\BMDS2\Temp\tmpF5.(d)
        Gnuplot Plotting File:  C:\USEPA\BMDS2\Temp\tmpF5.plt
                                                Mon Oct 06 16:04:48 2008
================================================================

BMDS Model Run
~~~~~~~~~~~~~~~~~~~~~~~~~~~~~~~~~~~~~~~~~~~~~~~~~~~~~~~~~~~~~~~~~~~~~~~~

  The form of the probability function is:

  P[response] = Background
              + (1-Background) * CumNorm(Intercept+Slope*Log(Dose)),

  where CumNorm(.) is the cumulative normal distribution function


  Dependent variable = Response
  Independent variable = DOSE
  Slope parameter is restricted as slope >= 1

  Total number of observations = 4
  Total number of records with missing values = 0
  Maximum number of iterations = 250
  Relative Function Convergence has been set to: 1e-008
  Parameter Convergence has been set to: 1e-008


  User has chosen the log transformed model

               Default Initial (and Specified) Parameter Values
```

```
                  background =         0.25
                   intercept =      4.35171
                       slope =      1.28667


          Asymptotic Correlation Matrix of Parameter Estimates

            background    intercept        slope

background            1         0.12         0.21

 intercept         0.12            1         0.97

     slope         0.21         0.97            1


                              Parameter Estimates

                                                        95.0% Wald Confidence Interval
      Variable         Estimate        Std. Err.     Lower Conf. Limit   Upper Conf. Limit
     background         0.248635        0.0479558            0.154644            0.342627
      intercept          4.47618         0.818254             2.87243             6.07993
          slope          1.32091         0.267134            0.797338             1.84448


                       Analysis of Deviance Table

       Model      Log(likelihood)  # Param's  Deviance  Test d.f.   P-value
     Full model         -103.017         4
   Fitted model          -103.09         3       0.14675      1          0.7017
  Reduced model         -152.026         1       98.0188      3         <.0001

           AIC:          212.18


                              Goodness  of  Fit
                                                                    Scaled
    Dose     Est._Prob.    Expected    Observed     Size       Residual
  ---------------------------------------------------------------------------
    0.0000     0.2486        19.891    20.000          80        0.028
    0.0237     0.4892        23.484    23.000          48       -0.140
    0.0618     0.8406        40.348    41.000          48        0.257
    0.1560     0.9838        47.222    47.000          48       -0.253

 Chi^2 = 0.15      d.f. = 1        P-value = 0.6982


   Benchmark Dose Computation

Specified effect =           0.05

Risk Type        =      Extra risk

Confidence level =           0.95

             BMD =     0.00971634

            BMDL =     0.00488108
```

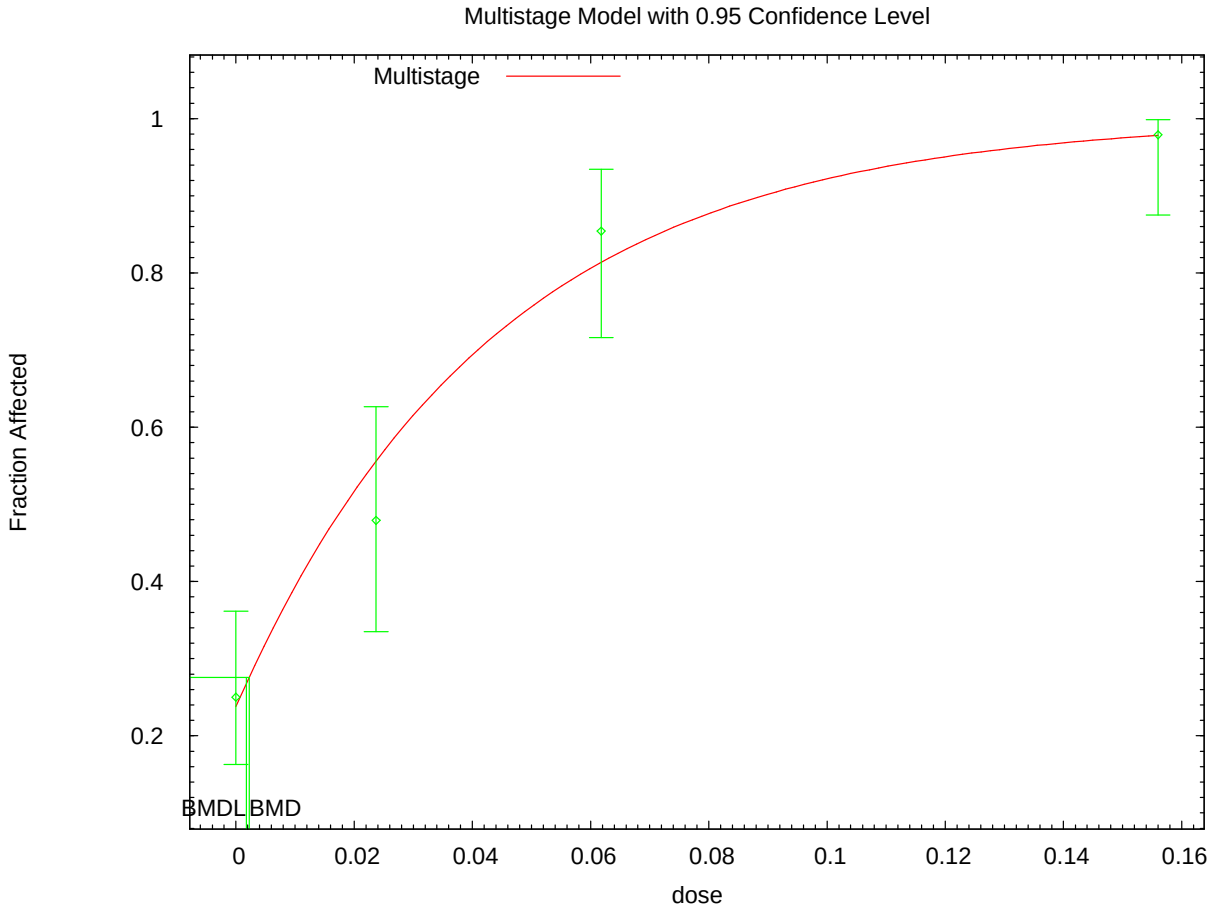

16:06 10/06 2008

```
=====================================================================
        Multistage Model. (Version: 3.0;  Date: 05/16/2008)
        Input Data File: C:\USEPA\BMDS2\Temp\tmpF7.(d)
        Gnuplot Plotting File:  C:\USEPA\BMDS2\Temp\tmpF7.plt
                                                Mon Oct 06 16:06:24 2008
=====================================================================

BMDS Model Run
~~~~~~~~~~~~~~~~~~~~~~~~~~~~~~~~~~~~~~~~~~~~~~~~~~~~~~~~~~~~~~~~~~~~~~~

  The form of the probability function is:

  P[response] = background + (1-background)*[1-EXP(
               -beta1*dose^1)]

  The parameter betas are restricted to be positive


  Dependent variable = Response
  Independent variable = DOSE

Total number of observations = 4
Total number of records with missing values = 0
Total number of parameters in model = 2
Total number of specified parameters = 0
Degree of polynomial = 1


Maximum number of iterations = 250
Relative Function Convergence has been set to: 1e-008
Parameter Convergence has been set to: 1e-008
```

Default Initial Parameter Values
Background = 0.2349
Beta(1) = 23.4597

Asymptotic Correlation Matrix of Parameter Estimates

	Background	Beta(1)
Background	1	-0.46
Beta(1)	-0.46	1

Parameter Estimates

Variable	Estimate	Std. Err.	95.0% Wald Confidence Interval Lower Conf. Limit	Upper Conf. Limit
Background	0.237678	*	*	*
Beta(1)	22.7713	*	*	*

* - Indicates that this value is not calculated.

Analysis of Deviance Table

Model	Log(likelihood)	# Param's	Deviance	Test d.f.	P-value
Full model	-103.017	4			
Fitted model	-103.895	2	1.75601	2	0.4156
Reduced model	-152.026	1	98.0188	3	<.0001

AIC: 211.789

Goodness of Fit

Dose	Est._Prob.	Expected	Observed	Size	Scaled Residual
0.0000	0.2377	19.014	20.000	80	0.259
0.0237	0.5556	26.670	23.000	48	-1.066
0.0618	0.8134	39.042	41.000	48	0.725
0.1560	0.9782	46.951	47.000	48	0.048

Chi^2 = 1.73 d.f. = 2 P-value = 0.4207

Benchmark Dose Computation

Specified effect = 0.05

Risk Type = Extra risk

Confidence level = 0.95

BMD = 0.00225254

BMDL = 0.00176165

BMDU = 0.00294313

Taken together, (0.00176165, 0.00294313) is a 90 % two-sided confidence interval for the BMD

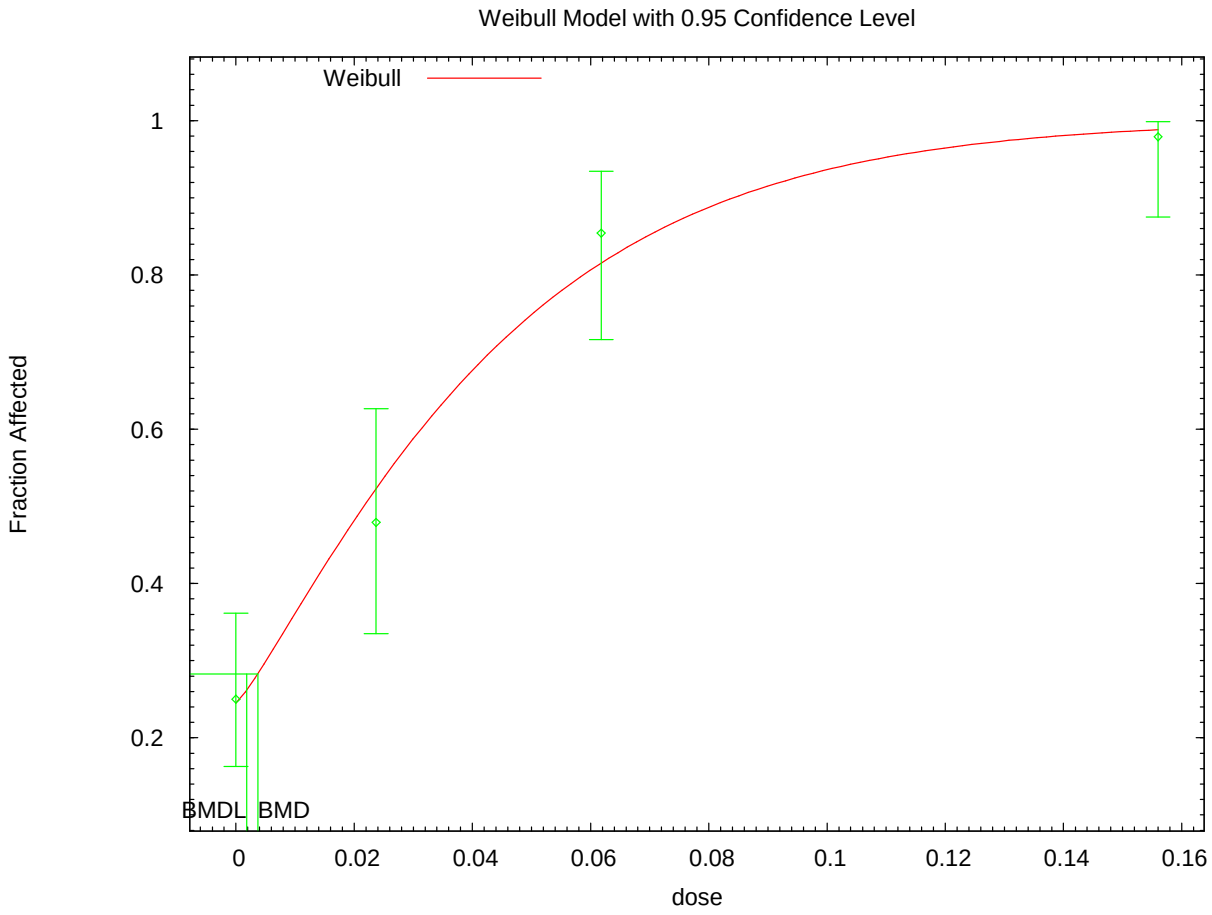

16:08 10/06 2008

```
=================================================================
        Weibull Model using Weibull Model (Version: 2.12;  Date: 05/16/2008)
        Input Data File: C:\USEPA\BMDS2\Temp\tmpF9.(d)
        Gnuplot Plotting File:  C:\USEPA\BMDS2\Temp\tmpF9.plt
                                                Mon Oct 06 16:08:23 2008
=================================================================

BMDS Model Run
~~~~~~~~~~~~~~~~~~~~~~~~~~~~~~~~~~~~~~~~~~~~~~~~~~~~~~~~~~~~~~~~~~~~~

  The form of the probability function is:

  P[response] = background + (1-background)*[1-EXP(-slope*dose^power)]


  Dependent variable = Response
  Independent variable = DOSE
  Power parameter is restricted as power >=1

  Total number of observations = 4
  Total number of records with missing values = 0
  Maximum number of iterations = 250
  Relative Function Convergence has been set to: 1e-008
  Parameter Convergence has been set to: 1e-008


                Default Initial (and Specified) Parameter Values
                   Background =     0.253086
                        Slope =      24.7803
                        Power =      1.10265


          Asymptotic Correlation Matrix of Parameter Estimates
```

	Background	Slope	Power
Background	1	0.14	0.23
Slope	0.14	1	0.97
Power	0.23	0.97	1

Parameter Estimates

Variable	Estimate	Std. Err.	95.0% Wald Confidence Interval Lower Conf. Limit	Upper Conf. Limit
Background	0.244833	0.0470971	0.152525	0.337142
Slope	36.5794	23.8993	-10.2624	83.4211
Power	1.17393	0.234182	0.71494	1.63291

Analysis of Deviance Table

Model	Log(likelihood)	# Param's	Deviance	Test d.f.	P-value
Full model	-103.017	4			
Fitted model	-103.595	3	1.15727	1	0.282
Reduced model	-152.026	1	98.0188	3	<.0001

AIC: 213.191

Goodness of Fit

Dose	Est._Prob.	Expected	Observed	Size	Scaled Residual
0.0000	0.2448	19.587	20.000	80	0.107
0.0237	0.5195	24.938	23.000	48	-0.560
0.0618	0.8125	38.998	41.000	48	0.740
0.1560	0.9879	47.417	47.000	48	-0.550

Chi^2 = 1.18 d.f. = 1 P-value = 0.2783

Benchmark Dose Computation

Specified effect = 0.05

Risk Type = Extra risk

Confidence level = 0.95

BMD = 0.00371148

BMDL = 0.00181169

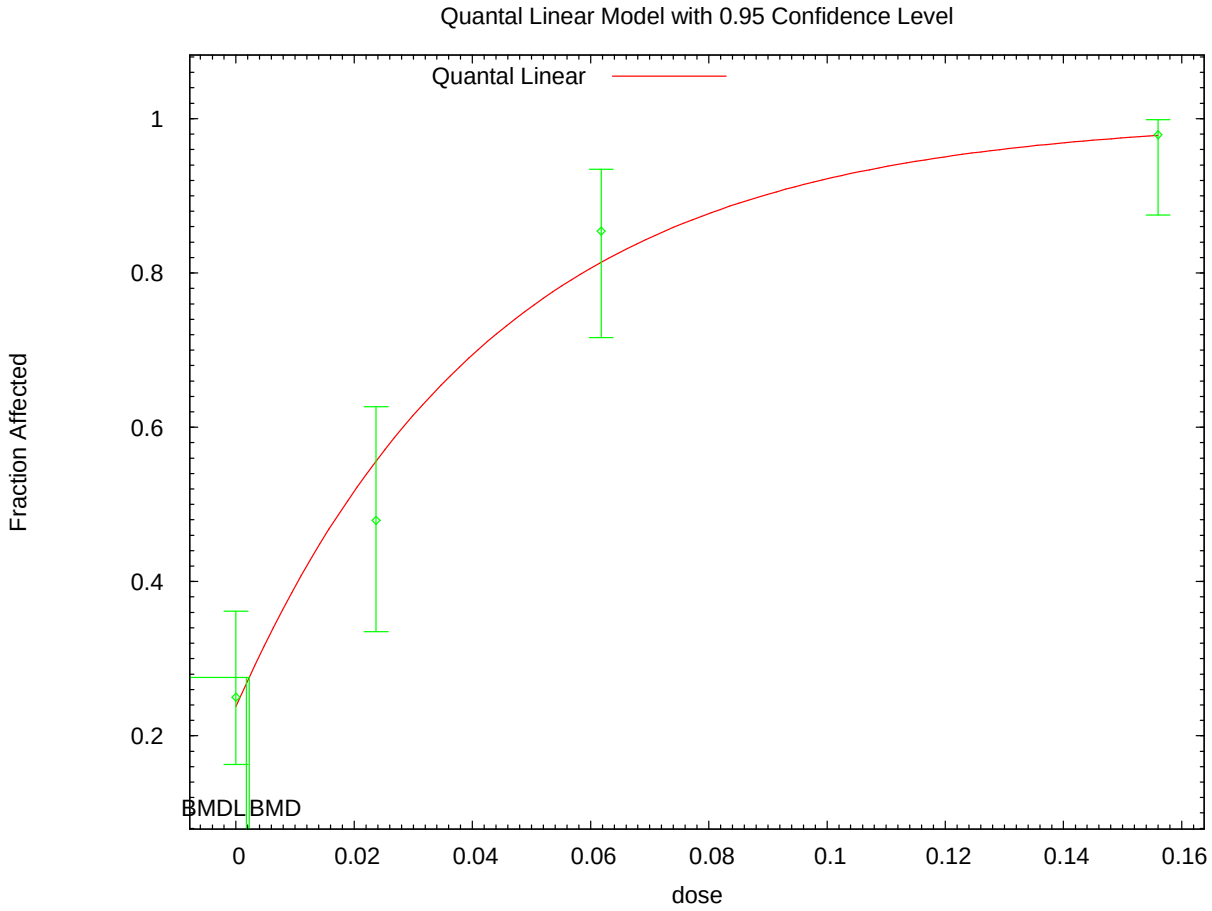

16:10 10/06 2008

```
================================================================================
        Quantal Linear Model using Weibull Model (Version: 2.12;  Date: 05/16/2008)
        Input Data File: C:\USEPA\BMDS2\Temp\tmpFA.(d)
        Gnuplot Plotting File:  C:\USEPA\BMDS2\Temp\tmpFA.plt
                                                  Mon Oct 06 16:10:19 2008
================================================================================

BMDS Model Run
~~~~~~~~~~~~~~~~~~~~~~~~~~~~~~~~~~~~~~~~~~~~~~~~~~~~~~~~~~~~~~~~~~~~~~~~~~~~~~~~

  The form of the probability function is:

  P[response] = background + (1-background)*[1-EXP(-slope*dose)]


  Dependent variable = Response
  Independent variable = DOSE

  Total number of observations = 4
  Total number of records with missing values = 0
  Maximum number of iterations = 250
  Relative Function Convergence has been set to: 1e-008
  Parameter Convergence has been set to: 1e-008


                 Default Initial (and Specified) Parameter Values
                    Background =     0.253086
                         Slope =      20.4779
                         Power =            1   Specified


          Asymptotic Correlation Matrix of Parameter Estimates
```

(*** The model parameter(s) -Power
have been estimated at a boundary point, or have been specified by the user,
and do not appear in the correlation matrix)

	Background	Slope
Background	1	-0.31
Slope	-0.31	1

Parameter Estimates

Variable	Estimate	Std. Err.	95.0% Wald Confidence Interval Lower Conf. Limit	Upper Conf. Limit
Background	0.237678	0.0452051	0.149078	0.326278
Slope	22.7713	3.5337	15.8454	29.6972

Analysis of Deviance Table

Model	Log(likelihood)	# Param's	Deviance	Test d.f.	P-value
Full model	-103.017	4			
Fitted model	-103.895	2	1.75601	2	0.4156
Reduced model	-152.026	1	98.0188	3	<.0001

AIC: 211.789

Goodness of Fit

Dose	Est._Prob.	Expected	Observed	Size	Scaled Residual
0.0000	0.2377	19.014	20.000	80	0.259
0.0237	0.5556	26.670	23.000	48	-1.066
0.0618	0.8134	39.042	41.000	48	0.725
0.1560	0.9782	46.951	47.000	48	0.048

Chi^2 = 1.73 d.f. = 2 P-value = 0.4207

Benchmark Dose Computation

Specified effect = 0.05

Risk Type = Extra risk

Confidence level = 0.95

BMD = 0.00225254

BMDL = 0.00176165

SD Female Rats: Nonneoplastic forestomach lesions (CEO in blood)

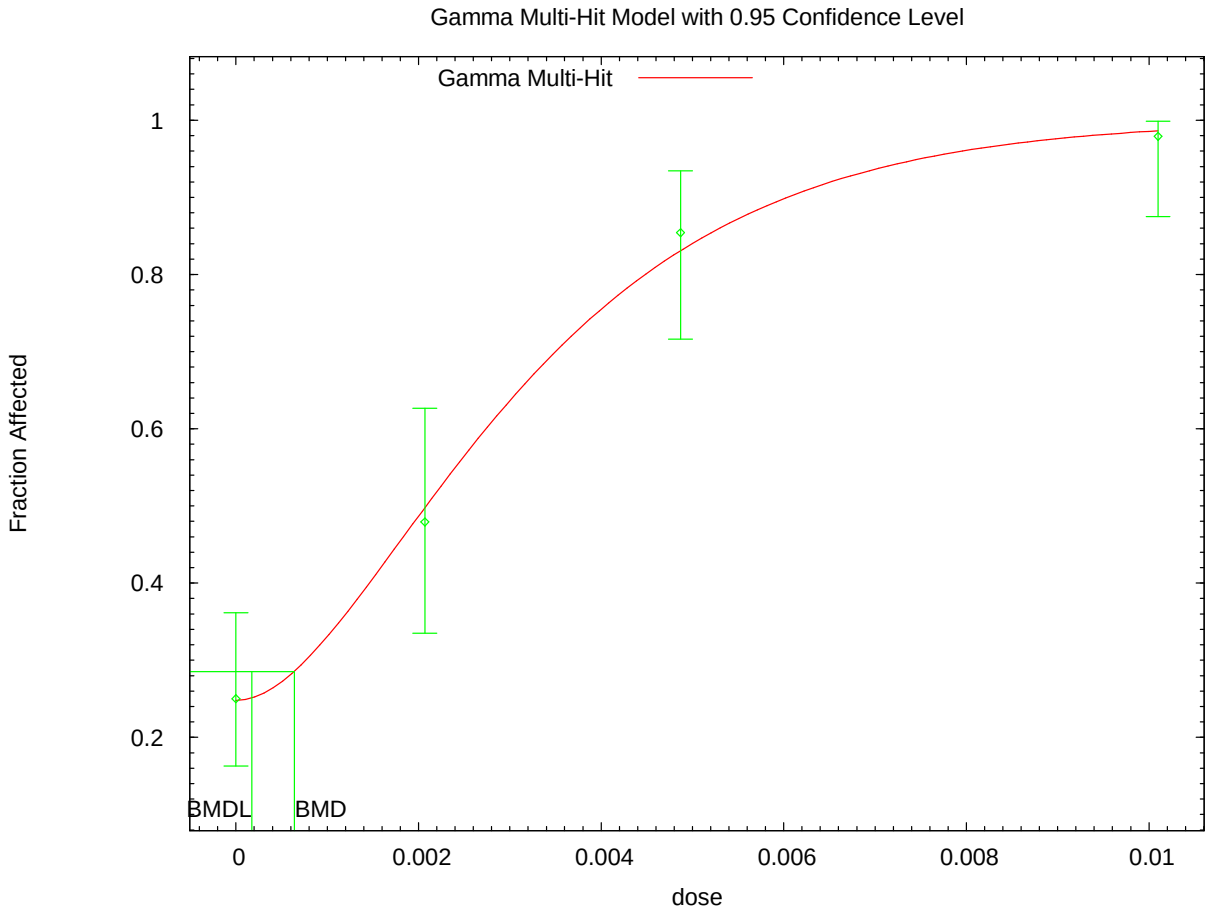

09:34 10/07 2008

```
 ======================================================================
         Gamma Model. (Version: 2.13;  Date: 05/16/2008)
         Input Data File: C:\USEPA\BMDS2\Temp\tmp1E.(d)
         Gnuplot Plotting File:  C:\USEPA\BMDS2\Temp\tmp1E.plt
                                                 Tue Oct 07 09:34:01 2008
 ======================================================================

 BMDS Model Run
~~~~~~~~~~~~~~~~~~~~~~~~~~~~~~~~~~~~~~~~~~~~~~~~~~~~~~~~~~~~~~~~~~~~~~~~~~

   The form of the probability function is:

   P[response]= background+(1-background)*CumGamma[slope*dose,power],
   where CumGamma(.) is the cummulative Gamma distribution function


   Dependent variable = Response
   Independent variable = DOSE
   Power parameter is restricted as power >=1

   Total number of observations = 4
   Total number of records with missing values = 0
   Maximum number of iterations = 250
   Relative Function Convergence has been set to: 1e-008
   Parameter Convergence has been set to: 1e-008


                  Default Initial (and Specified) Parameter Values
                     Background =     0.253086
```

Slope = 550.799
Power = 2.0706

Asymptotic Correlation Matrix of Parameter Estimates

	Background	Slope	Power
Background	1	0.15	0.26
Slope	0.15	1	0.96
Power	0.26	0.96	1

Parameter Estimates

Variable	Estimate	Std. Err.	95.0% Wald Confidence Interval Lower Conf. Limit	Upper Conf. Limit
Background	0.24778	0.0477681	0.154157	0.341404
Slope	600.839	241.065	128.36	1073.32
Power	2.07213	0.851839	0.402552	3.7417

Analysis of Deviance Table

Model	Log(likelihood)	# Param's	Deviance	Test d.f.	P-value
Full model	-103.017	4			
Fitted model	-103.226	3	0.419043	1	0.5174
Reduced model	-152.026	1	98.0188	3	<.0001

AIC: 212.453

Goodness of Fit

Dose	Est._Prob.	Expected	Observed	Size	Scaled Residual
0.0000	0.2478	19.822	20.000	80	0.046
0.0021	0.4972	23.867	23.000	48	-0.250
0.0049	0.8304	39.860	41.000	48	0.438
0.0101	0.9863	47.341	47.000	48	-0.423

Chi^2 = 0.44 d.f. = 1 P-value = 0.5092

Benchmark Dose Computation

Specified effect = 0.05

Risk Type = Extra risk

Confidence level = 0.95

BMD = 0.000640233

BMDL = 0.000173836

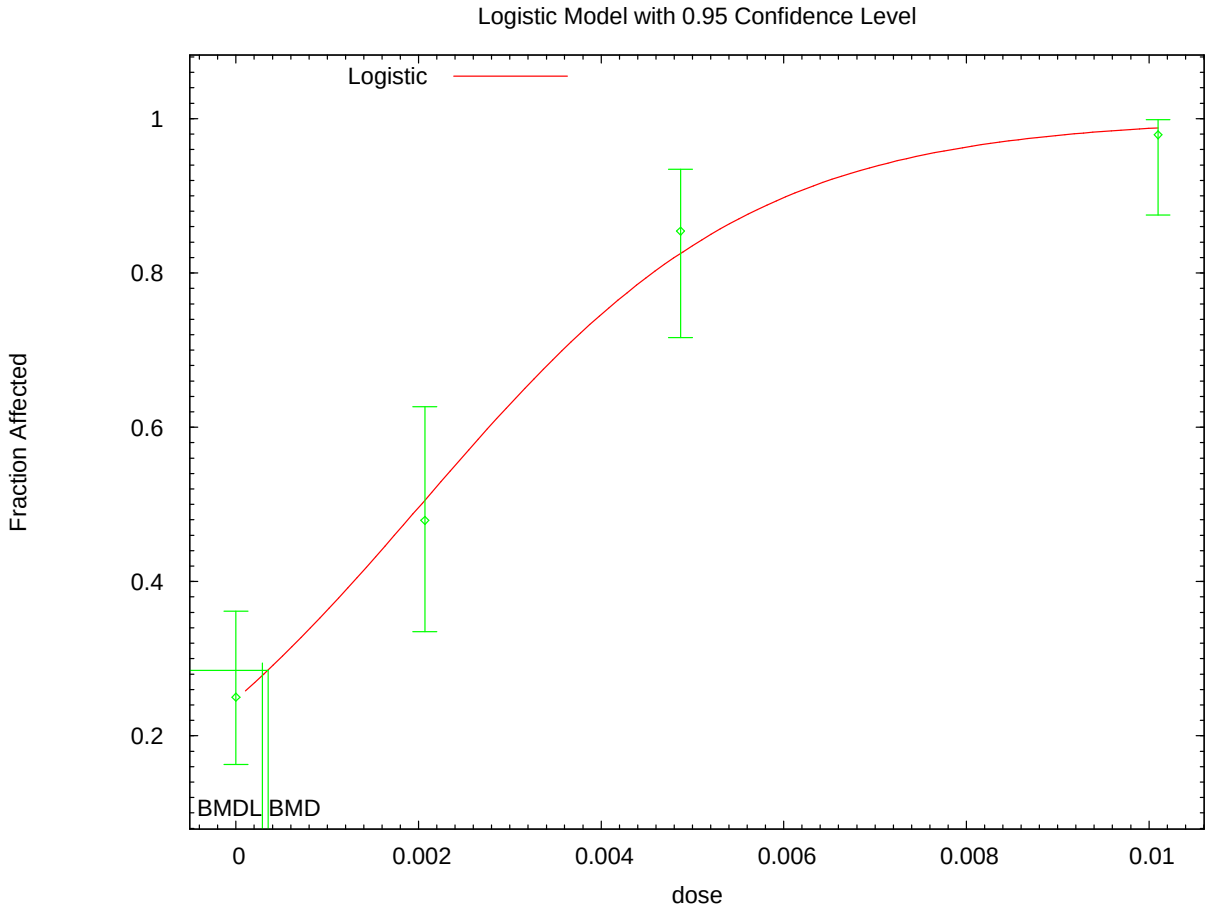

09:32 10/07 2008

```
================================================================
        Logistic Model. (Version: 2.12; Date: 05/16/2008)
        Input Data File: C:\USEPA\BMDS2\Temp\tmp110.(d)
        Gnuplot Plotting File:  C:\USEPA\BMDS2\Temp\tmp110.plt
                                                Mon Nov 10 10:51:57 2008
================================================================

BMDS Model Run
~~~~~~~~~~~~~~~~~~~~~~~~~~~~~~~~~~~~~~~~~~~~~~~~~~~~~~~~~~~~~~~~~~~~~~~

  The form of the probability function is:

  P[response] = 1/[1+EXP(-intercept-slope*dose)]


  Dependent variable = Response
  Independent variable = DOSE
  Slope parameter is not restricted

  Total number of observations = 4
  Total number of records with missing values = 0
  Maximum number of iterations = 250
  Relative Function Convergence has been set to: 1e-008
  Parameter Convergence has been set to: 1e-008


                Default Initial Parameter Values
                   background =            0   Specified
                    intercept =    -0.929208
                        slope =      452.992


          Asymptotic Correlation Matrix of Parameter Estimates
```

(*** The model parameter(s) -background
have been estimated at a boundary point, or have been specified by the user,
and do not appear in the correlation matrix)

	intercept	slope
intercept	1	-0.66
slope	-0.66	1

Parameter Estimates

Variable	Estimate	Std. Err.	95.0% Wald Confidence Interval Lower Conf. Limit	Upper Conf. Limit
intercept	-1.11487	0.227873	-1.56149	-0.668246
slope	547.334	80.7582	389.05	705.617

Analysis of Deviance Table

Model	Log(likelihood)	# Param's	Deviance	Test d.f.	P-value
Full model	-103.017	4			
Fitted model	-103.359	2	0.684912	2	0.71
Reduced model	-152.026	1	98.0188	3	<.0001

AIC: 210.718

Goodness of Fit

Dose	Est._Prob.	Expected	Observed	Size	Scaled Residual
0.0000	0.2470	19.757	20.000	80	0.063
0.0021	0.5045	24.217	23.000	48	-0.351
0.0049	0.8250	39.600	41.000	48	0.532
0.0101	0.9880	47.425	47.000	48	-0.565

Chi^2 = 0.73 d.f. = 2 P-value = 0.6946

Benchmark Dose Computation

Specified effect = 0.05

Risk Type = Extra risk

Confidence level = 0.95

BMD = 0.000352967

BMDL = 0.000287581

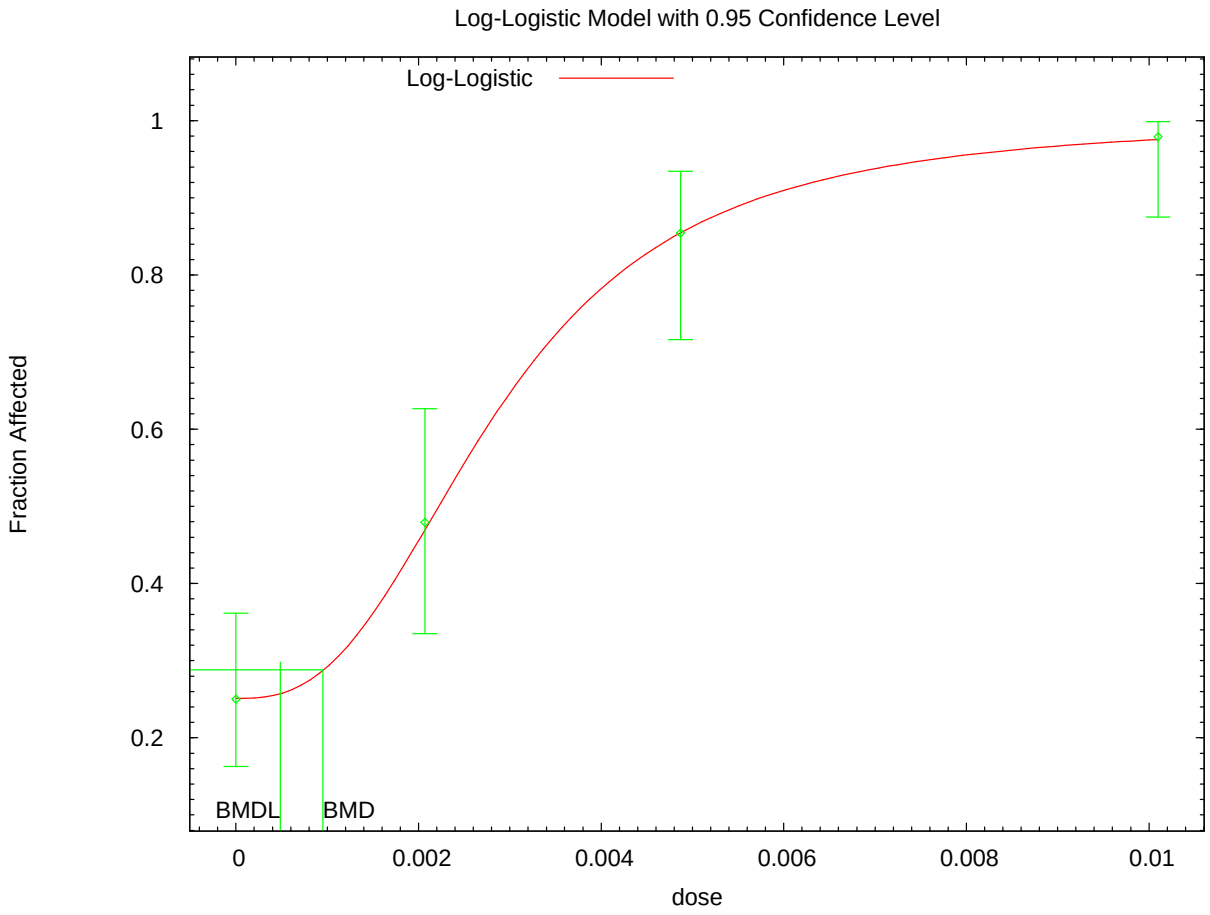

09:30 10/07 2008

```
================================================================================
        Logistic Model. (Version: 2.12; Date: 05/16/2008)
        Input Data File: C:\USEPA\BMDS2\Temp\tmp16.(d)
        Gnuplot Plotting File:  C:\USEPA\BMDS2\Temp\tmp16.plt
                                                  Tue Oct 07 09:30:55 2008
================================================================================

BMDS Model Run
~~~~~~~~~~~~~~~~~~~~~~~~~~~~~~~~~~~~~~~~~~~~~~~~~~~~~~~~~~~~~~~~~~~~~~~~~~~~~~~~

  The form of the probability function is:

  P[response] = background+(1-background)/[1+EXP(-intercept-slope*Log(dose))]


  Dependent variable = Response
  Independent variable = DOSE
  Slope parameter is restricted as slope >= 1

  Total number of observations = 4
  Total number of records with missing values = 0
  Maximum number of iterations = 250
  Relative Function Convergence has been set to: 1e-008
  Parameter Convergence has been set to: 1e-008


  User has chosen the log transformed model


               Default Initial Parameter Values
                  background =         0.25
                   intercept =      16.1818
                       slope =      2.75711
```

Asymptotic Correlation Matrix of Parameter Estimates

	background	intercept	slope
background	1	0.17	0.21
intercept	0.17	1	0.99
slope	0.21	0.99	1

Parameter Estimates

Variable	Estimate	Std. Err.	95.0% Wald Confidence Interval Lower Conf. Limit	Upper Conf. Limit
background	0.250617	*	*	*
intercept	15.839	*	*	*
slope	2.69969	*	*	*

* - Indicates that this value is not calculated.

Analysis of Deviance Table

Model	Log(likelihood)	# Param's	Deviance	Test d.f.	P-value
Full model	-103.017	4			
Fitted model	-103.03	3	0.027282	1	0.8688
Reduced model	-152.026	1	98.0188	3	<.0001

AIC: 212.061

Goodness of Fit

Dose	Est._Prob.	Expected	Observed	Size	Scaled Residual
0.0000	0.2506	20.049	20.000	80	-0.013
0.0021	0.4757	22.833	23.000	48	0.048
0.0049	0.8592	41.243	41.000	48	-0.101
0.0101	0.9766	46.875	47.000	48	0.119

Chi^2 = 0.03 d.f. = 1 P-value = 0.8699

Benchmark Dose Computation

Specified effect = 0.05

Risk Type = Extra risk

Confidence level = 0.95

BMD = 0.000951374

BMDL = 0.000486765

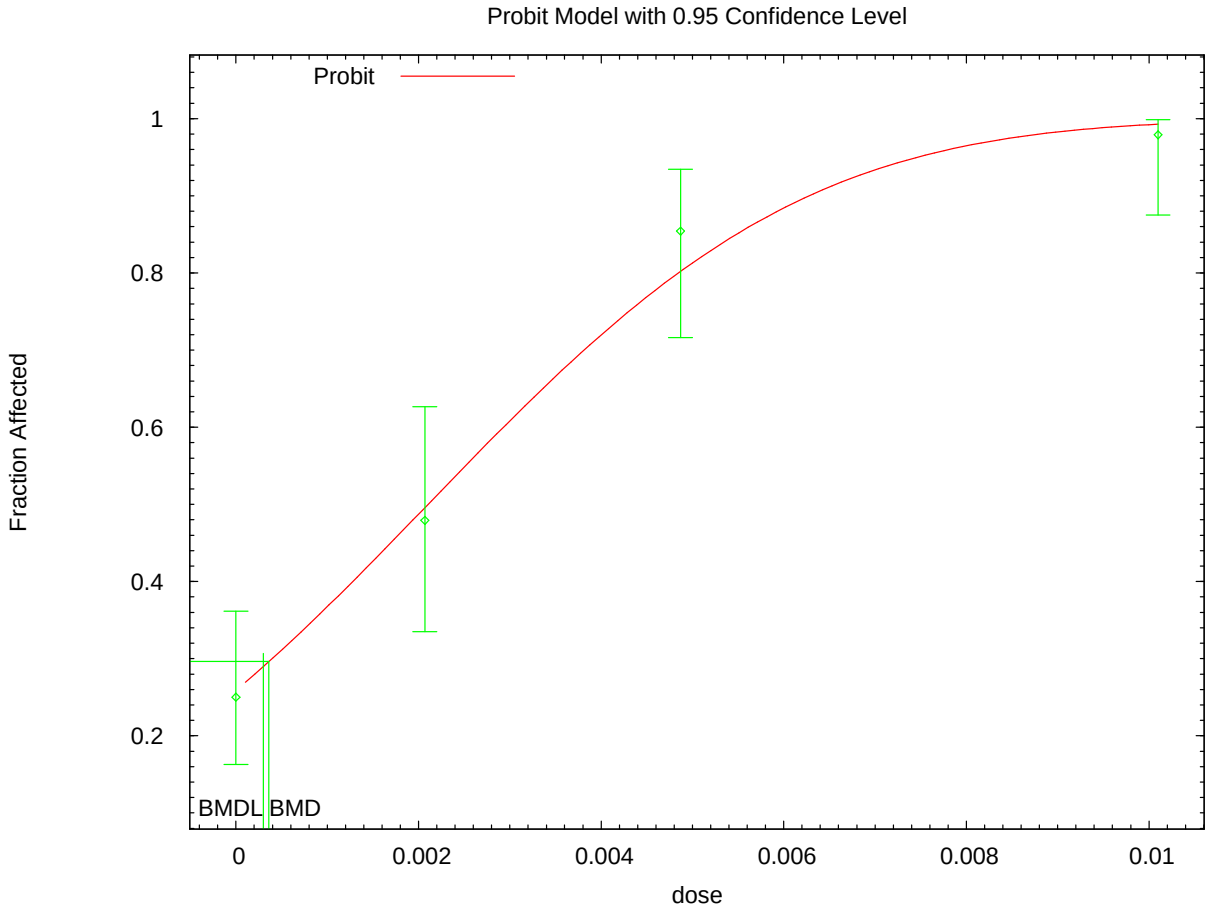

09:47 10/07 2008

```
================================================================================
        Probit Model. (Version: 3.1;  Date: 05/16/2008)
        Input Data File: C:\USEPA\BMDS2\Temp\tmp21.(d)
        Gnuplot Plotting File:  C:\USEPA\BMDS2\Temp\tmp21.plt
                                                  Tue Oct 07 09:47:22 2008
================================================================================

BMDS Model Run
~~~~~~~~~~~~~~~~~~~~~~~~~~~~~~~~~~~~~~~~~~~~~~~~~~~~~~~~~~~~~~~~~~~~~~~~~~~~~~~~

  The form of the probability function is:

  P[response] = CumNorm(Intercept+Slope*Dose),

  where CumNorm(.) is the cumulative normal distribution function


  Dependent variable = Response
  Independent variable = DOSE
  Slope parameter is not restricted

  Total number of observations = 4
  Total number of records with missing values = 0
  Maximum number of iterations = 250
  Relative Function Convergence has been set to: 1e-008
  Parameter Convergence has been set to: 1e-008


                Default Initial (and Specified) Parameter Values
                   background =            0   Specified
                    intercept =    -0.580731
                        slope =      266.006
```

Asymptotic Correlation Matrix of Parameter Estimates

(*** The model parameter(s) -background
have been estimated at a boundary point, or have been specified by the user,
and do not appear in the correlation matrix)

	intercept	slope
intercept	1	-0.65
slope	-0.65	1

Parameter Estimates

Variable	Estimate	Std. Err.	95.0% Wald Confidence Interval Lower Conf. Limit	Upper Conf. Limit
intercept	-0.645576	0.132116	-0.904519	-0.386633
slope	306.891	41.902	224.765	389.018

Analysis of Deviance Table

Model	Log(likelihood)	# Param's	Deviance	Test d.f.	P-value
Full model	-103.017	4			
Fitted model	-103.929	2	1.82488	2	0.4015
Reduced model	-152.026	1	98.0188	3	<.0001

AIC: 211.858

Goodness of Fit

Dose	Est._Prob.	Expected	Observed	Size	Scaled Residual
0.0000	0.2593	20.742	20.000	80	-0.189
0.0021	0.4959	23.803	23.000	48	-0.232
0.0049	0.8021	38.499	41.000	48	0.906
0.0101	0.9929	47.661	47.000	48	-1.139

Chi^2 = 2.21 d.f. = 2 P-value = 0.3315

Benchmark Dose Computation

Specified effect = 0.05

Risk Type = Extra risk

Confidence level = 0.95

BMD = 0.000360199

BMDL = 0.000300191

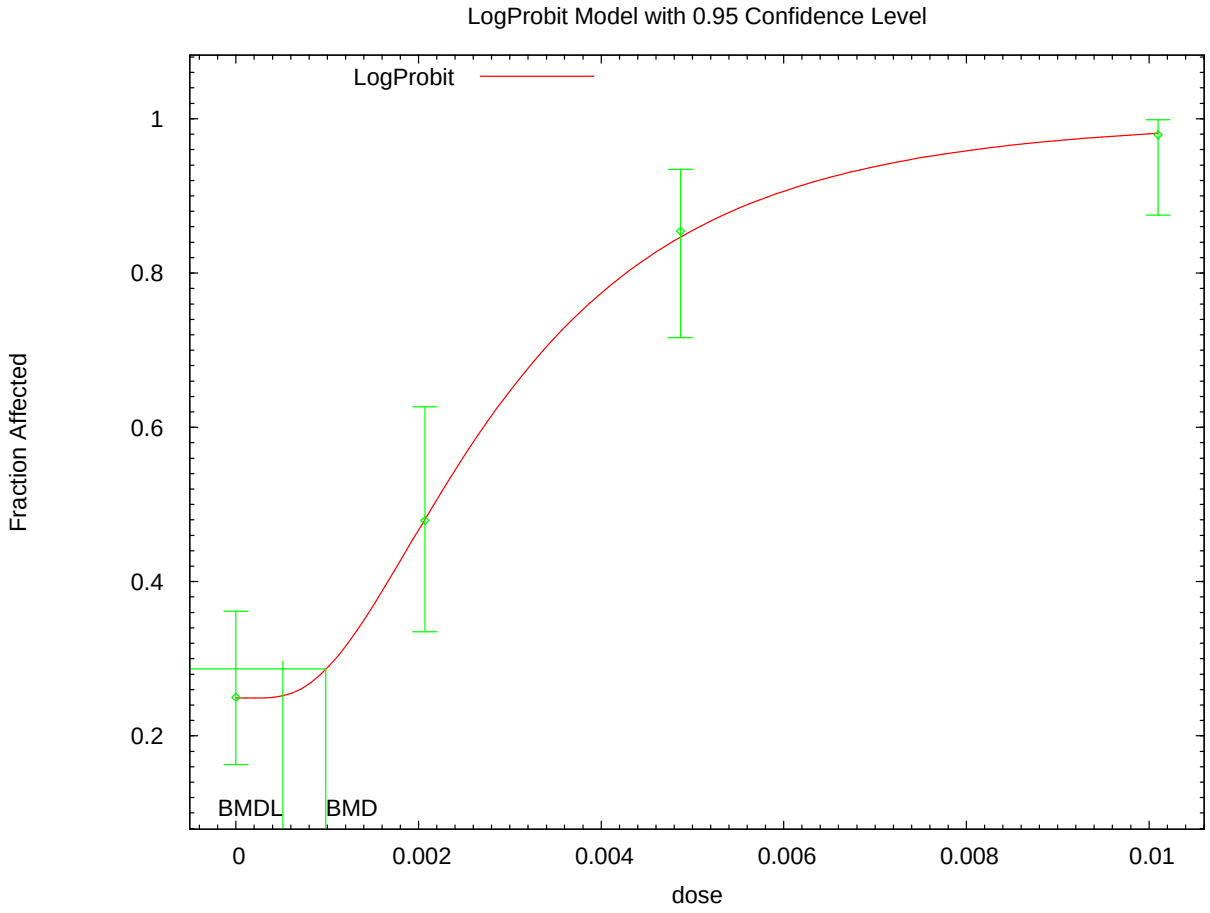

09:38 10/07 2008

```
 ================================================================
         Probit Model. (Version: 3.1;  Date: 05/16/2008)
         Input Data File: C:\USEPA\BMDS2\Temp\tmp1F.(d)
         Gnuplot Plotting File:  C:\USEPA\BMDS2\Temp\tmp1F.plt
                                                Tue Oct 07 09:38:17 2008
 ================================================================

 BMDS Model Run
~~~~~~~~~~~~~~~~~~~~~~~~~~~~~~~~~~~~~~~~~~~~~~~~~~~~~~~~~~~~~~~~~~~~~~~~

   The form of the probability function is:

   P[response] = Background
               + (1-Background) * CumNorm(Intercept+Slope*Log(Dose)),

   where CumNorm(.) is the cumulative normal distribution function


   Dependent variable = Response
   Independent variable = DOSE
   Slope parameter is restricted as slope >= 1

   Total number of observations = 4
   Total number of records with missing values = 0
   Maximum number of iterations = 250
   Relative Function Convergence has been set to: 1e-008
   Parameter Convergence has been set to: 1e-008



   User has chosen the log transformed model
```

Default Initial (and Specified) Parameter Values
background = 0.25
intercept = 8.97119
slope = 1.53079

Asymptotic Correlation Matrix of Parameter Estimates

	background	intercept	slope
background	1	0.18	0.22
intercept	0.18	1	0.99
slope	0.22	0.99	1

Parameter Estimates

Variable	Estimate	Std. Err.	95.0% Wald Confidence Interval Lower Conf. Limit	Upper Conf. Limit
background	0.249403	0.0481401	0.15505	0.343756
intercept	9.07823	1.71894	5.70916	12.4473
slope	1.54835	0.310846	0.939107	2.1576

Analysis of Deviance Table

Model	Log(likelihood)	# Param's	Deviance	Test d.f.	P-value
Full model	-103.017	4			
Fitted model	-103.031	3	0.0292544	1	0.8642
Reduced model	-152.026	1	98.0188	3	<.0001

AIC: 212.063

Goodness of Fit

Dose	Est._Prob.	Expected	Observed	Size	Scaled Residual
0.0000	0.2494	19.952	20.000	80	0.012
0.0021	0.4834	23.203	23.000	48	-0.059
0.0049	0.8482	40.715	41.000	48	0.115
0.0101	0.9814	47.106	47.000	48	-0.113

Chi^2 = 0.03 d.f. = 1 P-value = 0.8634

Benchmark Dose Computation

Specified effect = 0.05

Risk Type = Extra risk

Confidence level = 0.95

BMD = 0.000982443

BMDL = 0.000515017

Table B-4. Summary of the BMD modeling results based on the incidence of forestomach lesions (hyperplasia or hyperkeratosis) in male and female F344 rats exposed to AN in drinking water for 2 years

Sex	Endpoint	Dose metric	Selected model(s)[a]	χ^2 *p*-value	AIC	$BMDL_{10}$[b]	$BMDL_{05}$[b]
Male	Forestomach lesions	Estimated administered dose (mg/kg-d)	**gamma (3)**	**0.32**	**193.27**	**1.51×10^{-1}**	**9.97×10^{-2}**
			two-stage multistage (3)	0.14	194.76	1.40×10^{-1}	8.02×10^{-2}
		Predicted AN in blood (mg/L)	**gamma (3)**	**0.32**	**193.27**	**8.14×10^{-4}**	**5.39×10^{-4}**
			two-stage multistage (3)	0.14	194.77	7.56×10^{-4}	4.34×10^{-4}
		Predicted CEO in blood (mg/L)	**gamma (3)**	**0.32**	**193.27**	**7.65×10^{-5}**	**5.06×10^{-5}**
			two-stage multistage (3)	0.14	194.76	7.10×10^{-5}	4.07×10^{-5}
Female	Forestomach lesions	Estimated administered dose (mg/kg-d)	logistic (3)	0.32	141.06	2.31×10^{-1}	1.54×10^{-1}
			two-stage multistage (3)	**0.39**	**140.80**	**2.09×10^{-1}**	**1.17×10^{-1}**
			probit (3)	0.26	141.38	2.18×10^{-1}	1.40×10^{-1}
		Predicted AN in blood (mg/L)	logistic (3)	0.32	141.06	1.11×10^{-3}	7.34×10^{-4}
			two-stage multistage (3)	**0.39**	**140.80**	**9.97×10^{-4}**	**5.58×10^{-4}**
			probit (3)	0.26	141.38	1.04×10^{-3}	6.69×10^{-4}
		Predicted CEO in blood (mg/L)	logistic (3)	0.32	141.07	1.02×10^{-4}	6.78×10^{-5}
			two-stage multistage (3)	**0.39**	**140.81**	**9.23×10^{-5}**	**5.17×10^{-5}**
			probit (3)	0.26	141.40	9.63×10^{-5}	6.19×10^{-5}

[a]All dichotomous models in EPA's BMDS (version 2.0) were fit to the incidence of forestomach lesions (hyperplasia or hyperkeratosis) in F344 rats using the data presented in Table B-1. For BMD modeling, three different dose metrics were employed: (1) administered animal dose (estimated) expressed in mg/kg-d, (2) AN in blood (predicted) expressed in mg/L, and (3) CEO in blood (predicted) expressed in mg/L. Adequate fit of a model was achieved if the χ^2 goodness-of-fit statistic yielded a *p*-value > 0.1. The numbers in parentheses indicate the number of dose groups dropped in order to obtain an adequate fit, starting with the highest dose group. Of those models exhibiting adequate fit, the selected model was the model with the lowest AIC value, and is indicated in bold in the table.

[b]$BMDL_{10}$ and $BMDL_{05}$ estimates were derived from the selected model. If more than one model shared the lowest AIC, the mean $BMDL_{10}$ and $BMDL_{05}$ were calculated, as per the EPA's *Benchmark Dose Technical Guidance Document* (U.S. EPA, 2000b).

Sources: Johannsen and Levinskas (2002b); Biodynamics (1980c).

F344 Male Rats: Forestomach lesions (administered dose)

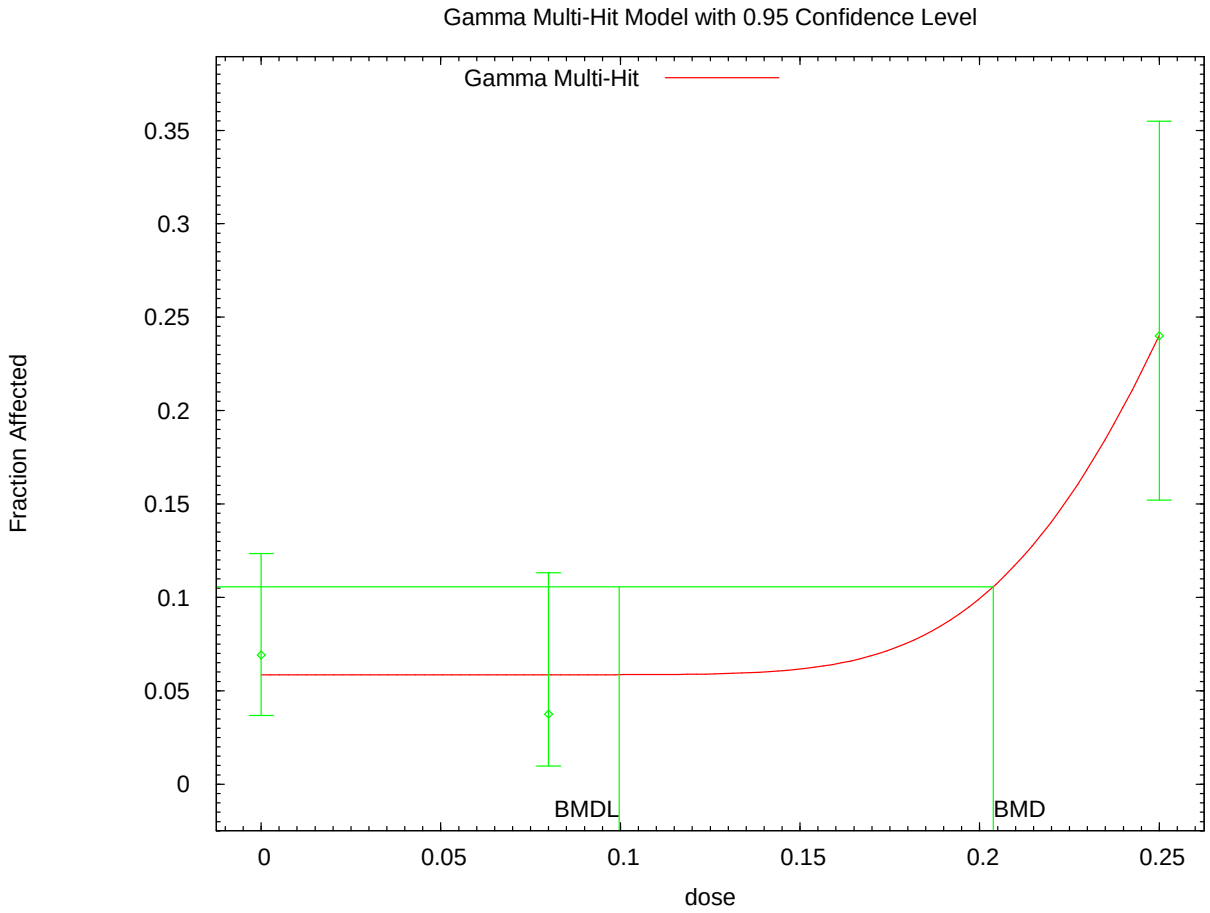


```
 ======================================================================
         Gamma Model. (Version: 2.13;  Date: 05/16/2008)
         Input Data File: C:\USEPA\BMDS2\Temp\tmp104.(d)
         Gnuplot Plotting File:  C:\USEPA\BMDS2\Temp\tmp104.plt
                                                 Tue Oct 07 14:10:45 2008
 ======================================================================

 BMDS Model Run
~~~~~~~~~~~~~~~~~~~~~~~~~~~~~~~~~~~~~~~~~~~~~~~~~~~~~~~~~~~~~~~~~~~~~~~~~~

   The form of the probability function is:

   P[response]= background+(1-background)*CumGamma[slope*dose,power],
   where CumGamma(.) is the cummulative Gamma distribution function


   Dependent variable = Response
   Independent variable = DOSE
   Power parameter is restricted as power >=1

   Total number of observations = 3
   Total number of records with missing values = 0
   Maximum number of iterations = 250
   Relative Function Convergence has been set to: 1e-008
   Parameter Convergence has been set to: 1e-008


                  Default Initial (and Specified) Parameter Values
                     Background =     0.071875
```

```
                          Slope =      5.59733
                          Power =      2.91574


          Asymptotic Correlation Matrix of Parameter Estimates

          ( *** The model parameter(s)  -Power
                have been estimated at a boundary point, or have been specified by the user,
                and do not appear in the correlation matrix )

            Background        Slope

Background            1        -0.24

     Slope        -0.24            1
```

Parameter Estimates

Variable	Estimate	Std. Err.	95.0% Wald Confidence Interval Lower Conf. Limit	Upper Conf. Limit
Background	0.0585772	0.0151899	0.0288055	0.0883489
Slope	57.0862	2.86678	51.4674	62.705
Power	18	NA		

NA - Indicates that this parameter has hit a bound implied by some inequality constraint and thus has no standard error.

Analysis of Deviance Table

Model	Log(likelihood)	# Param's	Deviance	Test d.f.	P-value
Full model	-94.1158	3			
Fitted model	-94.6364	2	1.04132	1	0.3075
Reduced model	-103.388	1	18.5446	2	<.0001

AIC: 193.273

Goodness of Fit

Dose	Est._Prob.	Expected	Observed	Size	Scaled Residual
0.0000	0.0586	9.314	11.000	159	0.569
0.0800	0.0586	4.686	3.000	80	-0.803
0.2500	0.2400	18.000	18.000	75	0.000

Chi^2 = 0.97 d.f. = 1 P-value = 0.3250

Benchmark Dose Computation

Specified effect = 0.05

Risk Type = Extra risk

Confidence level = 0.95

BMD = 0.203802

BMDL = 0.0996986

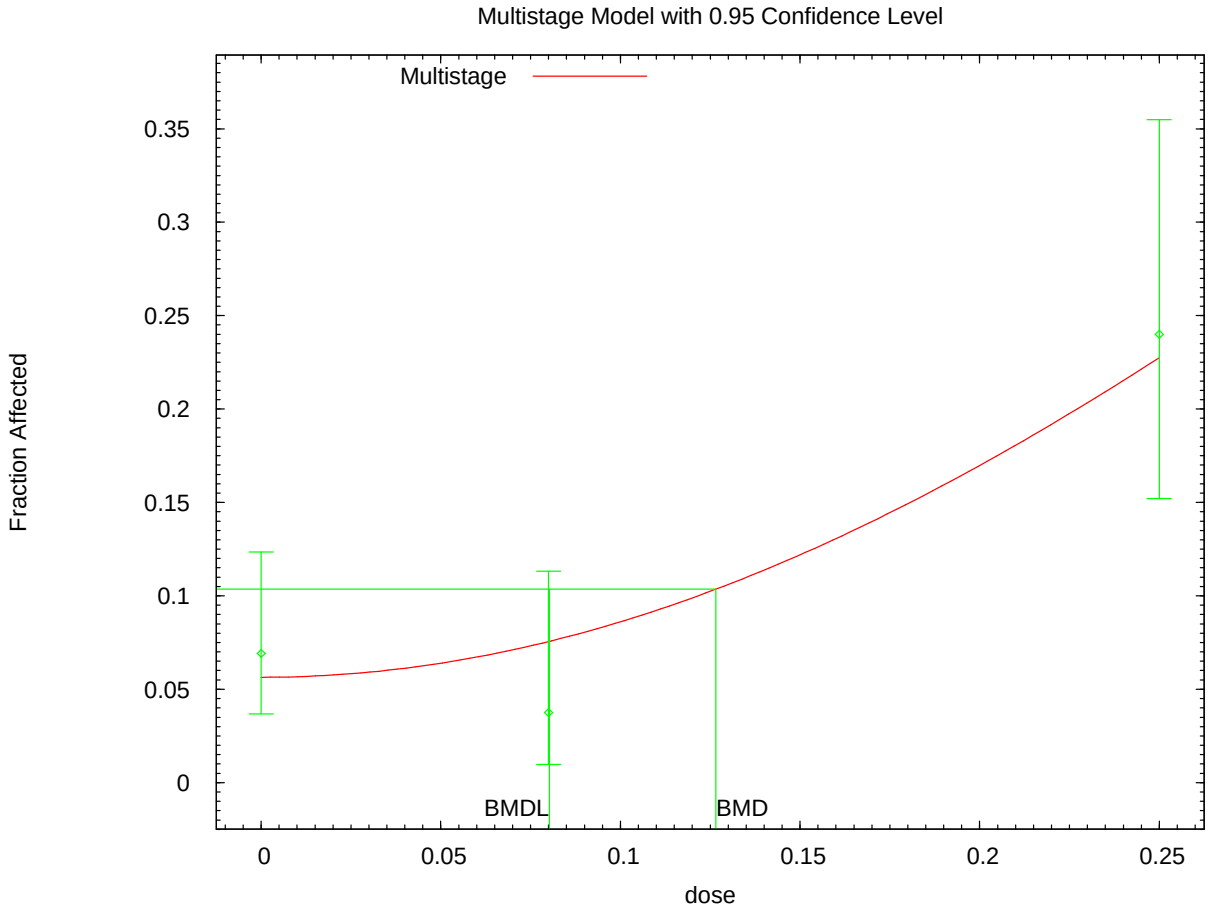

14:12 10/07 2008

```
=====================================================================
        Multistage Model. (Version: 3.0;  Date: 05/16/2008)
        Input Data File: C:\USEPA\BMDS2\Temp\tmp105.(d)
        Gnuplot Plotting File:  C:\USEPA\BMDS2\Temp\tmp105.plt
                                                Tue Oct 07 14:12:49 2008
=====================================================================

BMDS Model Run
~~~~~~~~~~~~~~~~~~~~~~~~~~~~~~~~~~~~~~~~~~~~~~~~~~~~~~~~~~~~~~~~~~~~~~~

  The form of the probability function is:

  P[response] = background + (1-background)*[1-EXP(
               -beta1*dose^1-beta2*dose^2)]

  The parameter betas are restricted to be positive


  Dependent variable = Response
  Independent variable = DOSE

Total number of observations = 3
Total number of records with missing values = 0
Total number of parameters in model = 3
Total number of specified parameters = 0
Degree of polynomial = 2


Maximum number of iterations = 250
Relative Function Convergence has been set to: 1e-008
Parameter Convergence has been set to: 1e-008
```

Default Initial Parameter Values
Background = 0.0438965
Beta(1) = 0
Beta(2) = 3.62384

Asymptotic Correlation Matrix of Parameter Estimates

(*** The model parameter(s) -Beta(1)
have been estimated at a boundary point, or have been specified by the user,
and do not appear in the correlation matrix)

	Background	Beta(2)
Background	1	-0.49
Beta(2)	-0.49	1

Parameter Estimates

Variable	Estimate	Std. Err.	95.0% Wald Confidence Interval Lower Conf. Limit	Upper Conf. Limit
Background	0.0563684	*	*	*
Beta(1)	0	*	*	*
Beta(2)	3.20151	*	*	*

* - Indicates that this value is not calculated.

Analysis of Deviance Table

Model	Log(likelihood)	# Param's	Deviance	Test d.f.	P-value
Full model	-94.1158	3			
Fitted model	-95.381	2	2.53038	1	0.1117
Reduced model	-103.388	1	18.5446	2	<.0001

AIC: 194.762

Goodness of Fit

Dose	Est._Prob.	Expected	Observed	Size	Scaled Residual
0.0000	0.0564	8.963	11.000	159	0.701
0.0800	0.0755	6.041	3.000	80	-1.287
0.2500	0.2275	17.062	18.000	75	0.258

Chi^2 = 2.21 d.f. = 1 P-value = 0.1368

Benchmark Dose Computation

Specified effect = 0.05

Risk Type = Extra risk

Confidence level = 0.95

BMD = 0.126576

BMDL = 0.0802271

BMDU = 0.173506

Taken together, (0.0802271, 0.173506) is a 90 % two-sided confidence interval for the BMD

F344 Male Rats: Forestomach lesions (AN in blood))

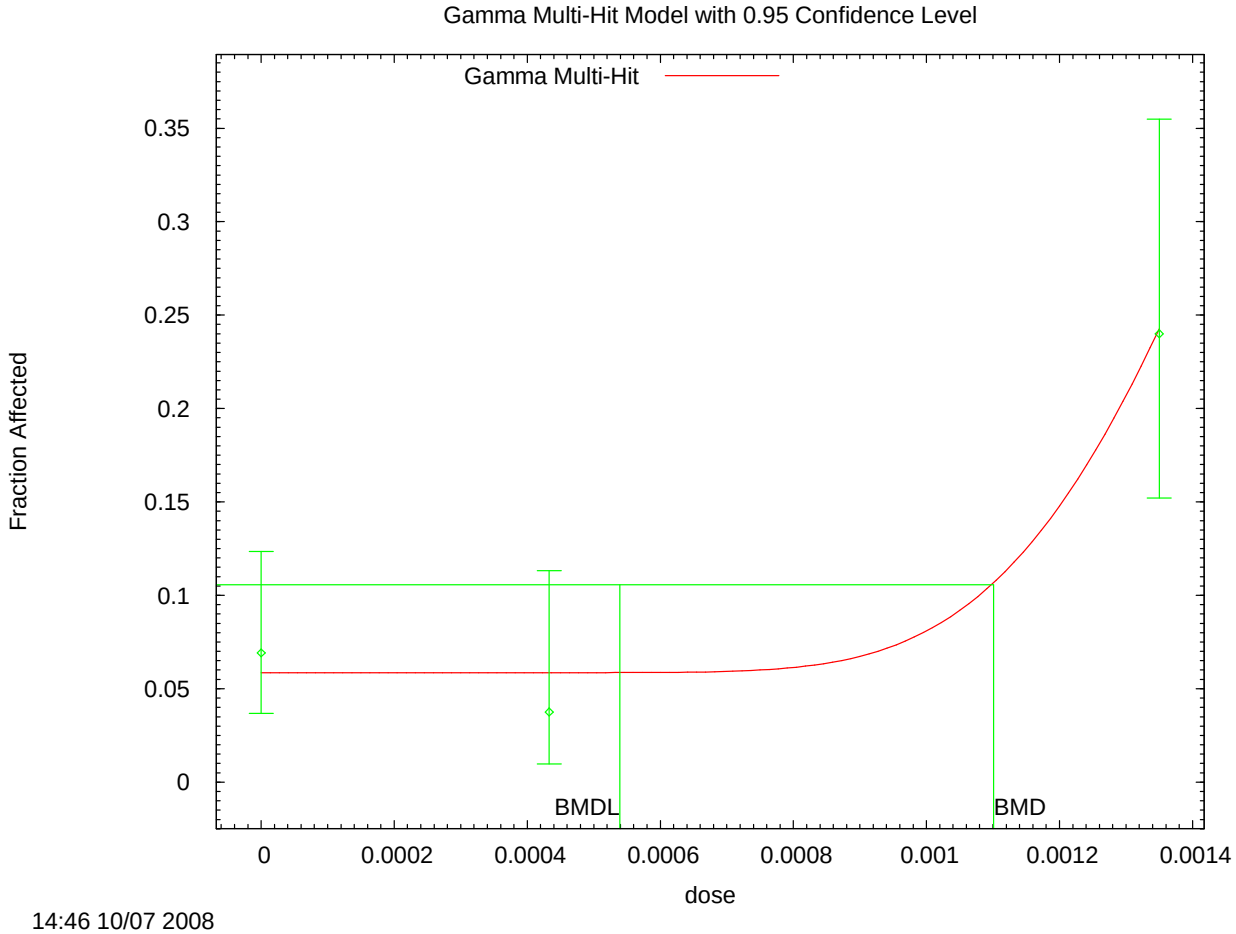

14:46 10/07 2008

```
 ======================================================================
         Gamma Model. (Version: 2.13;  Date: 05/16/2008)
         Input Data File: C:\USEPA\BMDS2\Temp\tmp107.(d)
         Gnuplot Plotting File:  C:\USEPA\BMDS2\Temp\tmp107.plt
                                                Tue Oct 07 14:46:28 2008
 ======================================================================

 BMDS Model Run
~~~~~~~~~~~~~~~~~~~~~~~~~~~~~~~~~~~~~~~~~~~~~~~~~~~~~~~~~~~~~~~~~~~~~~~~

   The form of the probability function is:

   P[response]= background+(1-background)*CumGamma[slope*dose,power],
   where CumGamma(.) is the cummulative Gamma distribution function


   Dependent variable = Response
   Independent variable = DOSE
   Power parameter is restricted as power >=1

   Total number of observations = 3
   Total number of records with missing values = 0
   Maximum number of iterations = 250
   Relative Function Convergence has been set to: 1e-008
   Parameter Convergence has been set to: 1e-008


                  Default Initial (and Specified) Parameter Values
                     Background =     0.071875
                          Slope =       1039.5
```

Power = 2.92132

Asymptotic Correlation Matrix of Parameter Estimates

(*** The model parameter(s) -Power
have been estimated at a boundary point, or have been specified by the user,
and do not appear in the correlation matrix)

	Background	Slope
Background	1	-0.24
Slope	-0.24	1

Parameter Estimates

Variable	Estimate	Std. Err.	95.0% Wald Confidence Interval Lower Conf. Limit	Upper Conf. Limit
Background	0.0585772	0.01519	0.0288053	0.088349
Slope	10571.5	530.886	9531.01	11612
Power	18	NA		

NA - Indicates that this parameter has hit a bound
implied by some inequality constraint and thus
has no standard error.

Analysis of Deviance Table

Model	Log(likelihood)	# Param's	Deviance	Test d.f.	P-value
Full model	-94.1158	3			
Fitted model	-94.6364	2	1.04133	1	0.3075
Reduced model	-103.388	1	18.5446	2	<.0001

AIC: 193.273

Goodness of Fit

Dose	Est._Prob.	Expected	Observed	Size	Scaled Residual
0.0000	0.0586	9.314	11.000	159	0.569
0.0004	0.0586	4.686	3.000	80	-0.803
0.0014	0.2400	18.000	18.000	75	0.000

Chi^2 = 0.97 d.f. = 1 P-value = 0.3250

Benchmark Dose Computation

Specified effect = 0.05

Risk Type = Extra risk

Confidence level = 0.95

BMD = 0.00110053

BMDL = 0.00053936

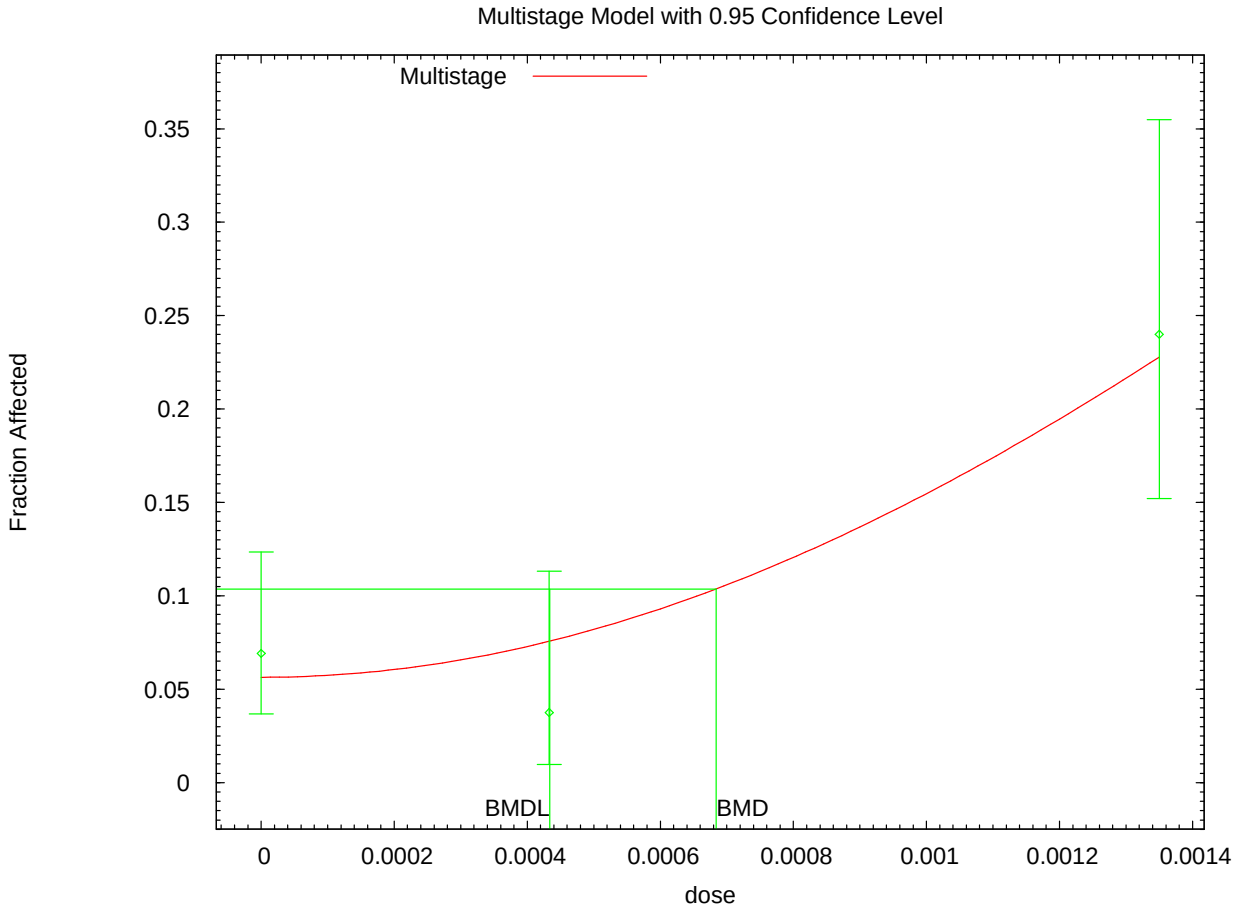

14:54 10/07 2008

```
=====================================================================
        Multistage Model. (Version: 3.0;  Date: 05/16/2008)
        Input Data File: C:\USEPA\BMDS2\Temp\tmp10C.(d)
        Gnuplot Plotting File:  C:\USEPA\BMDS2\Temp\tmp10C.plt
                                                Tue Oct 07 14:54:25 2008
=====================================================================

BMDS Model Run
~~~~~~~~~~~~~~~~~~~~~~~~~~~~~~~~~~~~~~~~~~~~~~~~~~~~~~~~~~~~~~~~~~~~~~~

  The form of the probability function is:

  P[response] = background + (1-background)*[1-EXP(
               -beta1*dose^1-beta2*dose^2)]

  The parameter betas are restricted to be positive


  Dependent variable = Response
  Independent variable = DOSE

Total number of observations = 3
Total number of records with missing values = 0
Total number of parameters in model = 3
Total number of specified parameters = 0
Degree of polynomial = 2


Maximum number of iterations = 250
Relative Function Convergence has been set to: 1e-008
Parameter Convergence has been set to: 1e-008
```

Default Initial Parameter Values
Background = 0.043854
Beta(1) = 0
Beta(2) = 124287

Asymptotic Correlation Matrix of Parameter Estimates

(*** The model parameter(s) -Beta(1)
have been estimated at a boundary point, or have been specified by the user,
and do not appear in the correlation matrix)

	Background	Beta(2)
Background	1	-0.49
Beta(2)	-0.49	1

Parameter Estimates

Variable	Estimate	Std. Err.	95.0% Wald Confidence Interval Lower Conf. Limit	Upper Conf. Limit
Background	0.0563637	*	*	*
Beta(1)	0	*	*	*
Beta(2)	109747	*	*	*

* - Indicates that this value is not calculated.

Analysis of Deviance Table

Model	Log(likelihood)	# Param's	Deviance	Test d.f.	P-value
Full model	-94.1158	3			
Fitted model	-95.3848	2	2.53803	1	0.1111
Reduced model	-103.388	1	18.5446	2	<.0001

AIC: 194.77

Goodness of Fit

Dose	Est._Prob.	Expected	Observed	Size	Scaled Residual
0.0000	0.0564	8.962	11.000	159	0.701
0.0004	0.0756	6.047	3.000	80	-1.289
0.0014	0.2274	17.057	18.000	75	0.260

Chi^2 = 2.22 d.f. = 1 P-value = 0.1363

Benchmark Dose Computation

Specified effect = 0.05

Risk Type = Extra risk

Confidence level = 0.95

BMD = 0.000683652

BMDL = 0.000433678

BMDU = 0.000937168

Taken together, (0.000433678, 0.000937168) is a 90 % two-sided confidence interval for the BMD

F344 Male Rats: Forestomach lesions (CEO in blood)

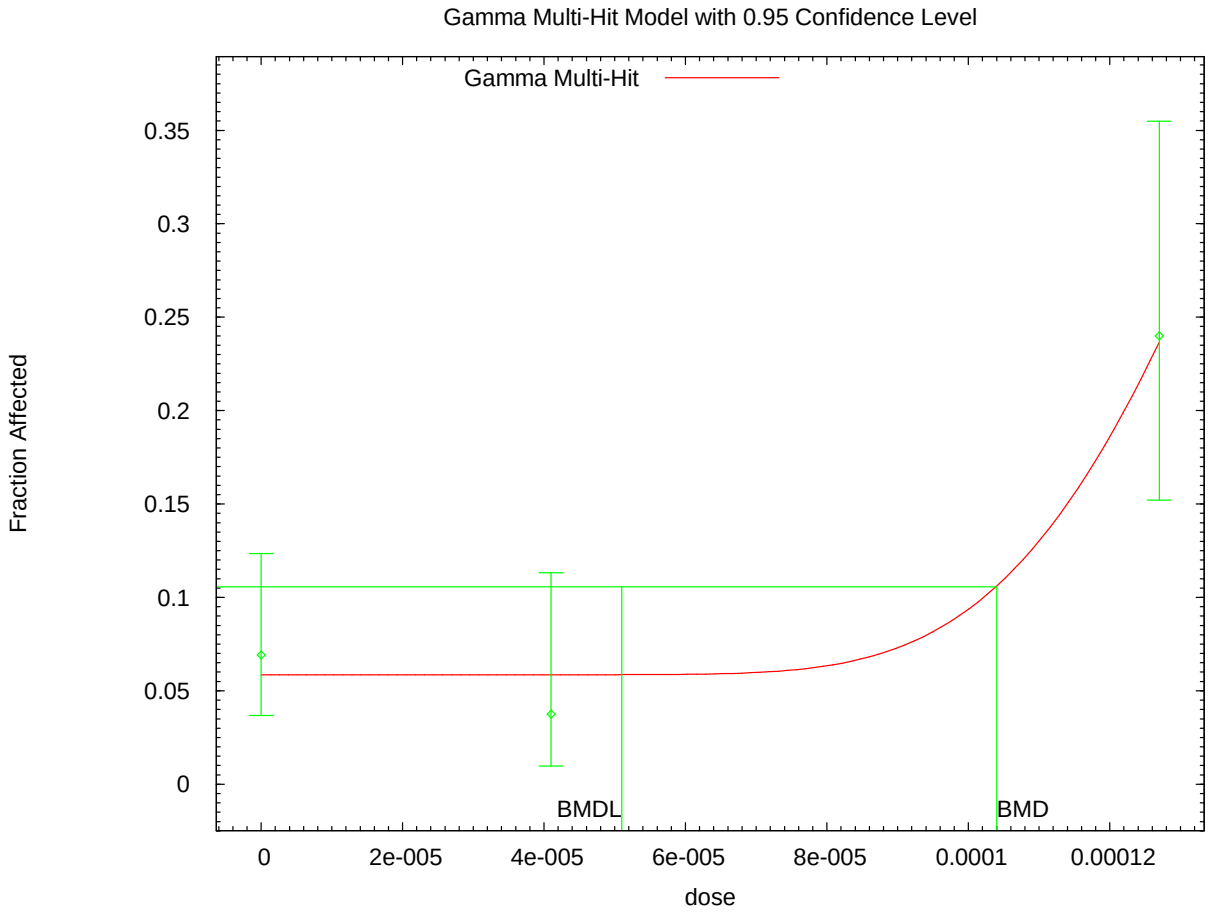

16:32 10/07 2008

```
 ======================================================================
         Gamma Model. (Version: 2.13;  Date: 05/16/2008)
         Input Data File: C:\USEPA\BMDS2\Temp\tmp115.(d)
         Gnuplot Plotting File:  C:\USEPA\BMDS2\Temp\tmp115.plt
                                                Tue Oct 07 16:32:49 2008
 ======================================================================

 BMDS Model Run
~~~~~~~~~~~~~~~~~~~~~~~~~~~~~~~~~~~~~~~~~~~~~~~~~~~~~~~~~~~~~~~~~~~~~~~~~~

   The form of the probability function is:

   P[response]= background+(1-background)*CumGamma[slope*dose,power],
   where CumGamma(.) is the cummulative Gamma distribution function


   Dependent variable = Response
   Independent variable = DOSE
   Power parameter is restricted as power >=1

   Total number of observations = 3
   Total number of records with missing values = 0
   Maximum number of iterations = 250
   Relative Function Convergence has been set to: 1e-008
   Parameter Convergence has been set to: 1e-008


                  Default Initial (and Specified) Parameter Values
                     Background =     0.071875
```

Slope = 11005
Power = 2.91337

Asymptotic Correlation Matrix of Parameter Estimates

(*** The model parameter(s) -Power
have been estimated at a boundary point, or have been specified by the user,
and do not appear in the correlation matrix)

	Background	Slope
Background	1	-0.24
Slope	-0.24	1

Parameter Estimates

Variable	Estimate	Std. Err.	95.0% Wald Confidence Interval Lower Conf. Limit	Upper Conf. Limit
Background	0.0585772	0.0151899	0.0288055	0.0883489
Slope	112374	5643.28	101314	123435
Power	18	NA		

NA - Indicates that this parameter has hit a bound
implied by some inequality constraint and thus
has no standard error.

Analysis of Deviance Table

Model	Log(likelihood)	# Param's	Deviance	Test d.f.	P-value
Full model	-94.1158	3			
Fitted model	-94.6364	2	1.04132	1	0.3075
Reduced model	-103.388	1	18.5446	2	<.0001

AIC: 193.273

Goodness of Fit

Dose	Est._Prob.	Expected	Observed	Size	Scaled Residual
0.0000	0.0586	9.314	11.000	159	0.569
0.0000	0.0586	4.686	3.000	80	-0.803
0.0001	0.2400	18.000	18.000	75	0.000

Chi^2 = 0.97 d.f. = 1 P-value = 0.3250

Benchmark Dose Computation

Specified effect = 0.05

Risk Type = Extra risk

Confidence level = 0.95

BMD = 0.000103532

BMDL = 5.06073e-005

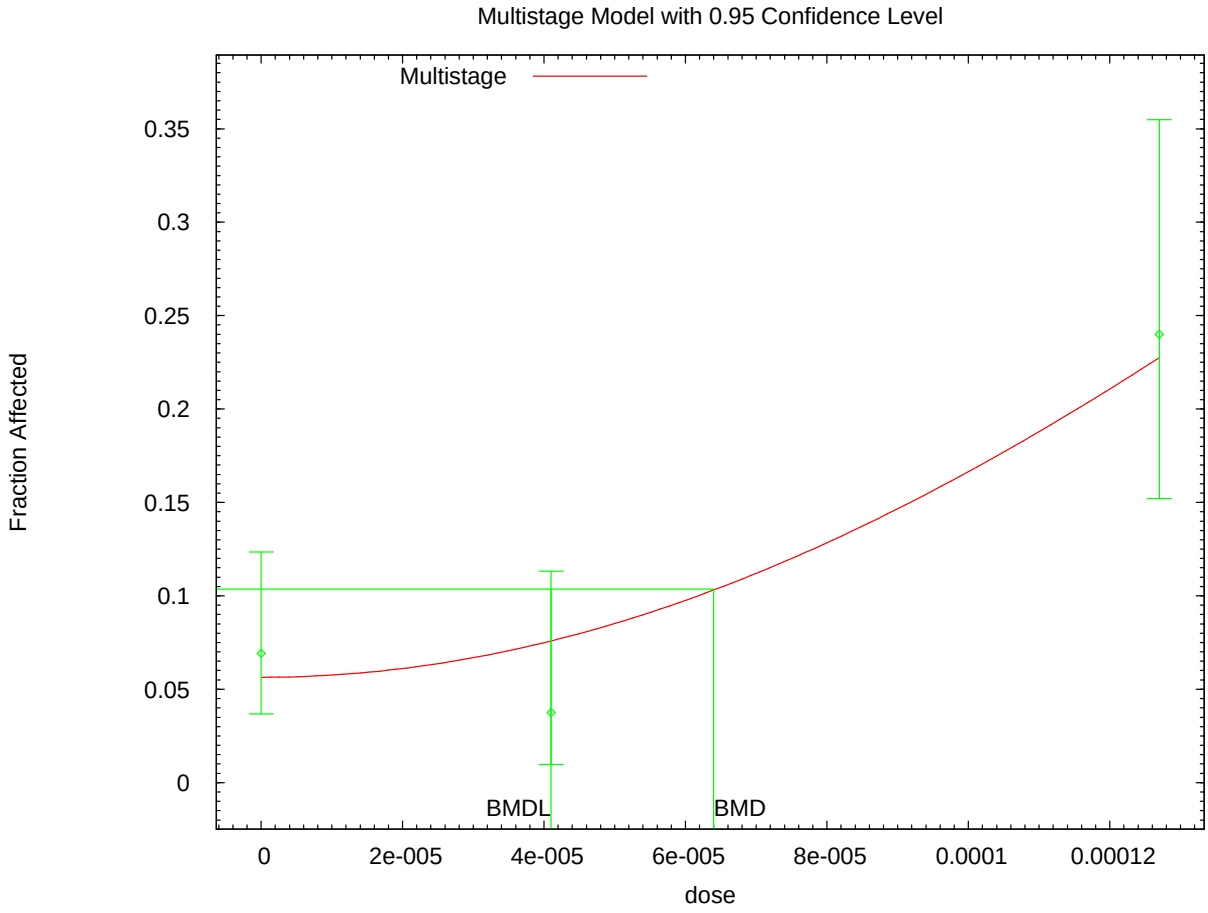

16:39 10/07 2008

```
=====================================================================
        Multistage Model. (Version: 3.0;  Date: 05/16/2008)
        Input Data File: C:\USEPA\BMDS2\Temp\tmp11A.(d)
        Gnuplot Plotting File:  C:\USEPA\BMDS2\Temp\tmp11A.plt
                                                Tue Oct 07 16:39:04 2008
=====================================================================

BMDS Model Run
~~~~~~~~~~~~~~~~~~~~~~~~~~~~~~~~~~~~~~~~~~~~~~~~~~~~~~~~~~~~~~~~~~~~~~~

  The form of the probability function is:

  P[response] = background + (1-background)*[1-EXP(
               -beta1*dose^1-beta2*dose^2)]

  The parameter betas are restricted to be positive


  Dependent variable = Response
  Independent variable = DOSE

Total number of observations = 3
Total number of records with missing values = 0
Total number of parameters in model = 3
Total number of specified parameters = 0
Degree of polynomial = 2


Maximum number of iterations = 250
Relative Function Convergence has been set to: 1e-008
Parameter Convergence has been set to: 1e-008
```

Default Initial Parameter Values
Background = 0.0439146
Beta(1) = 0
Beta(2) = 1.40418e+007

Asymptotic Correlation Matrix of Parameter Estimates

(*** The model parameter(s) -Beta(1)
have been estimated at a boundary point, or have been specified by the user,
and do not appear in the correlation matrix)

	Background	Beta(2)
Background	1	-0.49
Beta(2)	-0.49	1

Parameter Estimates

Variable	Estimate	Std. Err.	95.0% Wald Confidence Interval Lower Conf. Limit	Upper Conf. Limit
Background	0.0563704	*	*	*
Beta(1)	0	*	*	*
Beta(2)	1.2408e+007	*	*	*

* - Indicates that this value is not calculated.

Analysis of Deviance Table

Model	Log(likelihood)	# Param's	Deviance	Test d.f.	P-value
Full model	-94.1158	3			
Fitted model	-95.3793	2	2.52713	1	0.1119
Reduced model	-103.388	1	18.5446	2	<.0001

AIC: 194.759

Goodness of Fit

Dose	Est._Prob.	Expected	Observed	Size	Scaled Residual
0.0000	0.0564	8.963	11.000	159	0.700
0.0000	0.0755	6.038	3.000	80	-1.286
0.0001	0.2275	17.064	18.000	75	0.258

Chi^2 = 2.21 d.f. = 1 P-value = 0.1371

Benchmark Dose Computation

Specified effect = 0.05

Risk Type = Extra risk

Confidence level = 0.95

BMD = 6.42953e-005

BMDL = 4.07373e-005

BMDU = 8.81314e-005

Taken together, (4.07373e-005, 8.81314e-005) is a 90 % two-sided confidence interval for the BMD

F344 Female Rats: Forestomach lesions (administered dose)

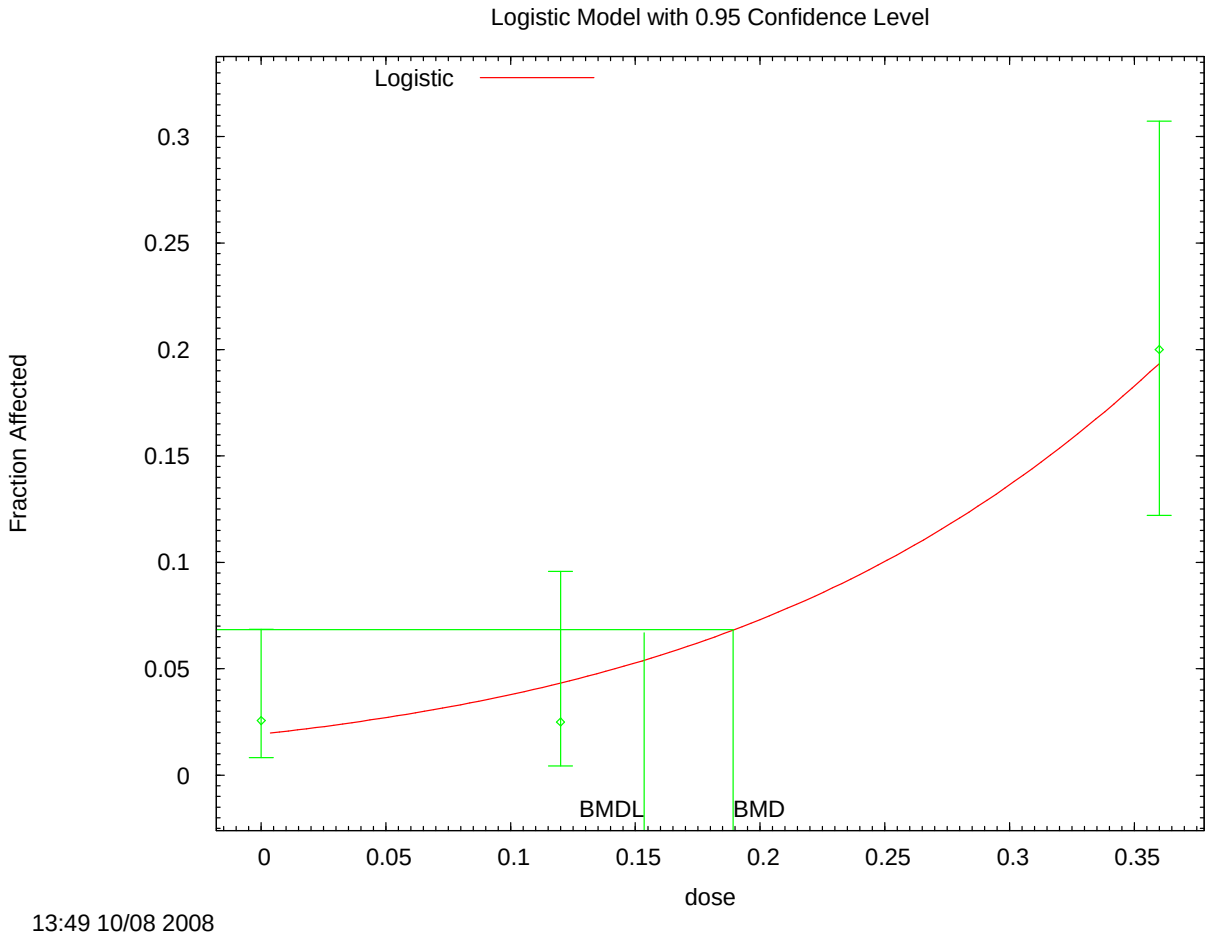

13:49 10/08 2008

```
 ======================================================================
         Logistic Model. (Version: 2.12; Date: 05/16/2008)
         Input Data File: C:\USEPA\BMDS2\Temp\tmpA62.(d)
         Gnuplot Plotting File:  C:\USEPA\BMDS2\Temp\tmpA62.plt
                                                 Wed Oct 08 13:49:00 2008
 ======================================================================

 BMDS Model Run
~~~~~~~~~~~~~~~~~~~~~~~~~~~~~~~~~~~~~~~~~~~~~~~~~~~~~~~~~~~~~~~~~~~~~~~~~~

   The form of the probability function is:

   P[response] = 1/[1+EXP(-intercept-slope*dose)]


   Dependent variable = Response
   Independent variable = DOSE
   Slope parameter is not restricted

   Total number of observations = 3
   Total number of records with missing values = 0
   Maximum number of iterations = 250
   Relative Function Convergence has been set to: 1e-008
   Parameter Convergence has been set to: 1e-008


                  Default Initial Parameter Values
                     background =            0   Specified
                      intercept =     -3.79894
                          slope =      6.38252
```

Asymptotic Correlation Matrix of Parameter Estimates

(*** The model parameter(s) -background
have been estimated at a boundary point, or have been specified by the user,
and do not appear in the correlation matrix)

	intercept	slope
intercept	1	-0.88
slope	-0.88	1

Parameter Estimates

Variable	Estimate	Std. Err.	95.0% Wald Confidence Interval Lower Conf. Limit	Upper Conf. Limit
intercept	-3.92594	0.477082	-4.86101	-2.99088
slope	6.94669	1.60094	3.80891	10.0845

Analysis of Deviance Table

Model	Log(likelihood)	# Param's	Deviance	Test d.f.	P-value
Full model	-67.9873	3			
Fitted model	-68.5288	2	1.08303	1	0.298
Reduced model	-79.8392	1	23.7038	2	<.0001

AIC: 141.058

Goodness of Fit

Dose	Est._Prob.	Expected	Observed	Size	Scaled Residual
0.0000	0.0193	3.017	4.000	156	0.571
0.1200	0.0434	3.474	2.000	80	-0.809
0.3600	0.1939	15.509	16.000	80	0.139

Chi^2 = 1.00 d.f. = 1 P-value = 0.3175

Benchmark Dose Computation

Specified effect = 0.05

Risk Type = Extra risk

Confidence level = 0.95

BMD = 0.189157

BMDL = 0.153543

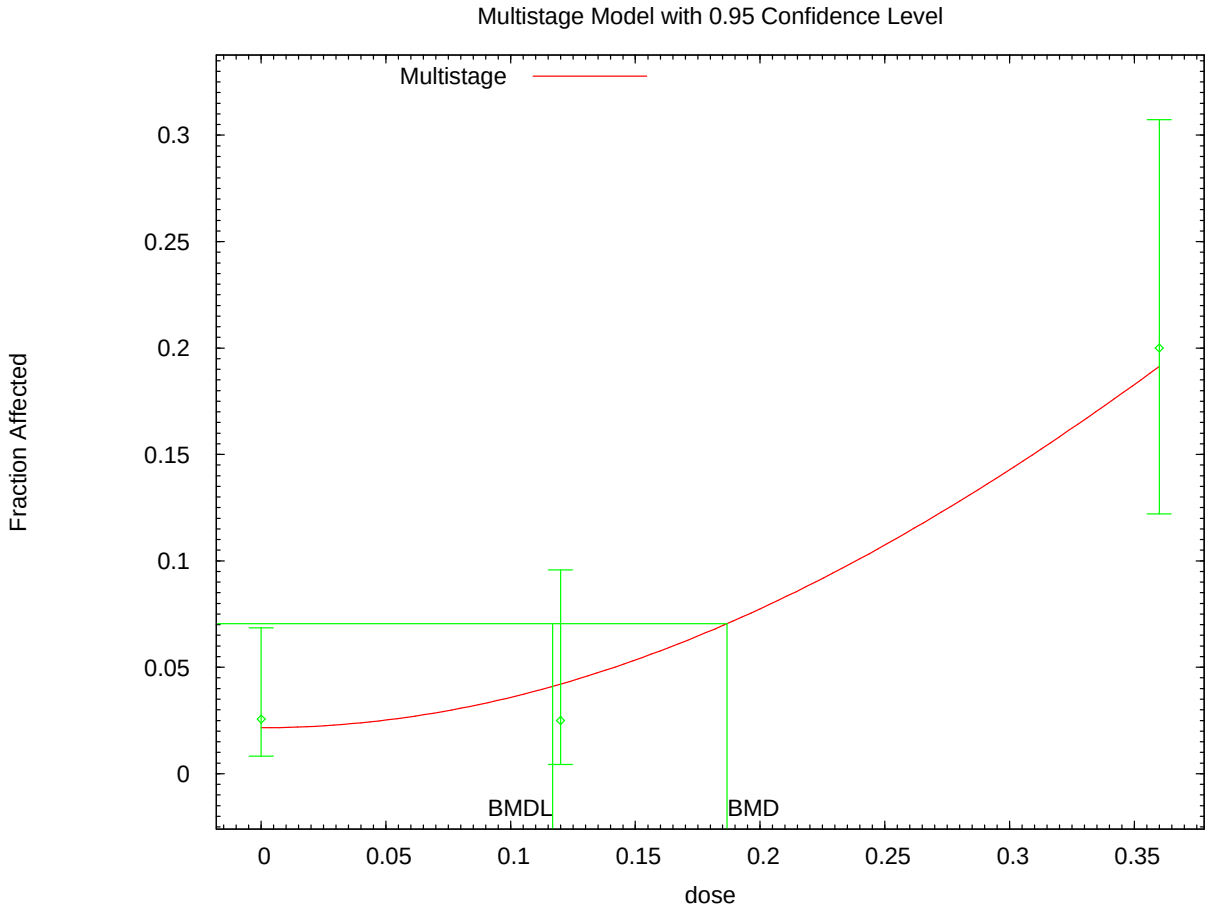

13:58 10/08 2008

```
=====================================================================
        Multistage Model. (Version: 3.0;  Date: 05/16/2008)
        Input Data File: C:\USEPA\BMDS2\Temp\tmpA65.(d)
        Gnuplot Plotting File:  C:\USEPA\BMDS2\Temp\tmpA65.plt
                                                Wed Oct 08 13:58:05 2008
=====================================================================

BMDS Model Run
~~~~~~~~~~~~~~~~~~~~~~~~~~~~~~~~~~~~~~~~~~~~~~~~~~~~~~~~~~~~~~~~~~~~~~~

  The form of the probability function is:

  P[response] = background + (1-background)*[1-EXP(
               -beta1*dose^1-beta2*dose^2)]

  The parameter betas are restricted to be positive


  Dependent variable = Response
  Independent variable = DOSE

Total number of observations = 3
Total number of records with missing values = 0
Total number of parameters in model = 3
Total number of specified parameters = 0
Degree of polynomial = 2


Maximum number of iterations = 250
Relative Function Convergence has been set to: 1e-008
Parameter Convergence has been set to: 1e-008
```

Default Initial Parameter Values
Background = 0.0147377
Beta(1) = 0
Beta(2) = 1.59649

Asymptotic Correlation Matrix of Parameter Estimates

(*** The model parameter(s) -Beta(1)
have been estimated at a boundary point, or have been specified by the user,
and do not appear in the correlation matrix)

	Background	Beta(2)
Background	1	-0.51
Beta(2)	-0.51	1

Parameter Estimates

Variable	Estimate	Std. Err.	95.0% Wald Confidence Interval Lower Conf. Limit	Upper Conf. Limit
Background	0.0216322	*	*	*
Beta(1)	0	*	*	*
Beta(2)	1.47012	*	*	*

* - Indicates that this value is not calculated.

Analysis of Deviance Table

Model	Log(likelihood)	# Param's	Deviance	Test d.f.	P-value
Full model	-67.9873	3			
Fitted model	-68.401	2	0.827463	1	0.363
Reduced model	-79.8392	1	23.7038	2	<.0001

AIC: 140.802

Goodness of Fit

Dose	Est._Prob.	Expected	Observed	Size	Scaled Residual
0.0000	0.0216	3.375	4.000	156	0.344
0.1200	0.0421	3.370	2.000	80	-0.763
0.3600	0.1914	15.308	16.000	80	0.197

Chi^2 = 0.74 d.f. = 1 P-value = 0.3901

Benchmark Dose Computation

Specified effect = 0.05

Risk Type = Extra risk

Confidence level = 0.95

BMD = 0.18679

BMDL = 0.116832

BMDU = 0.243753

Taken together, (0.116832, 0.243753) is a 90 % two-sided confidence
interval for the BMD

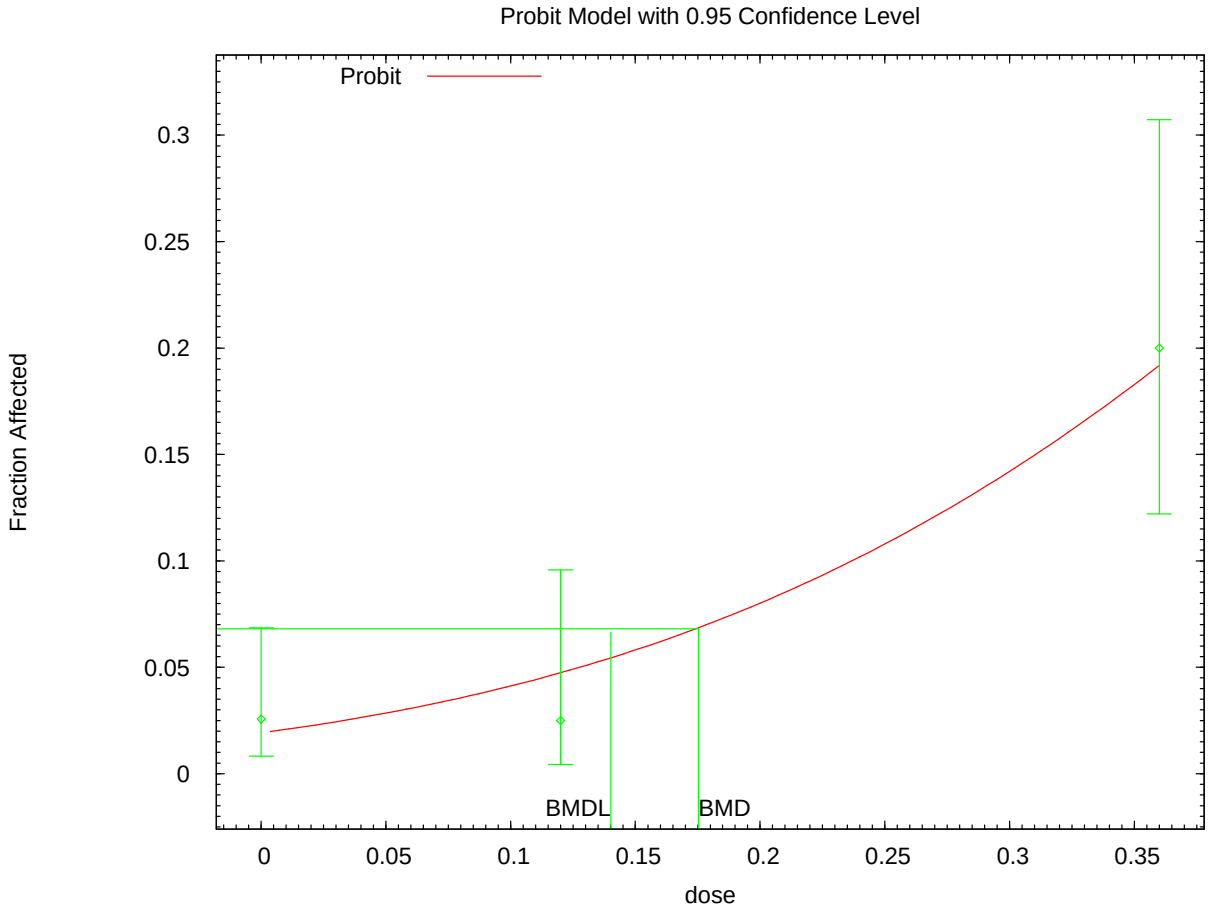

14:01 10/08 2008

```
================================================================
        Probit Model. (Version: 3.1;  Date: 05/16/2008)
        Input Data File: C:\USEPA\BMDS2\Temp\tmpA66.(d)
        Gnuplot Plotting File:  C:\USEPA\BMDS2\Temp\tmpA66.plt
                                              Wed Oct 08 14:01:52 2008
================================================================

BMDS Model Run
~~~~~~~~~~~~~~~~~~~~~~~~~~~~~~~~~~~~~~~~~~~~~~~~~~~~~~~~~~~~~~~~~~~~

  The form of the probability function is:

  P[response] = CumNorm(Intercept+Slope*Dose),

  where CumNorm(.) is the cumulative normal distribution function


  Dependent variable = Response
  Independent variable = DOSE
  Slope parameter is not restricted

  Total number of observations = 3
  Total number of records with missing values = 0
  Maximum number of iterations = 250
  Relative Function Convergence has been set to: 1e-008
  Parameter Convergence has been set to: 1e-008


                Default Initial (and Specified) Parameter Values
                   background =            0   Specified
                    intercept =     -2.03888
                        slope =      3.08079
```

Asymptotic Correlation Matrix of Parameter Estimates

(*** The model parameter(s) -background
have been estimated at a boundary point, or have been specified by the user,
and do not appear in the correlation matrix)

	intercept	slope
intercept	1	-0.81
slope	-0.81	1

Parameter Estimates

Variable	Estimate	Std. Err.	95.0% Wald Confidence Interval Lower Conf. Limit	Upper Conf. Limit
intercept	-2.0746	0.1976	-2.46189	-1.68732
slope	3.33316	0.739981	1.88282	4.78349

Analysis of Deviance Table

Model	Log(likelihood)	# Param's	Deviance	Test d.f.	P-value
Full model	-67.9873	3			
Fitted model	-68.6922	2	1.40991	1	0.2351
Reduced model	-79.8392	1	23.7038	2	<.0001

AIC: 141.384

Goodness of Fit

Dose	Est._Prob.	Expected	Observed	Size	Scaled Residual
0.0000	0.0190	2.966	4.000	156	0.606
0.1200	0.0470	3.760	2.000	80	-0.930
0.3600	0.1909	15.270	16.000	80	0.208

Chi^2 = 1.28 d.f. = 1 P-value = 0.2588

Benchmark Dose Computation

Specified effect = 0.05

Risk Type = Extra risk

Confidence level = 0.95

BMD = 0.175274

BMDL = 0.140136

F344 Female Rats: Forestomach lesions (AN in blood)

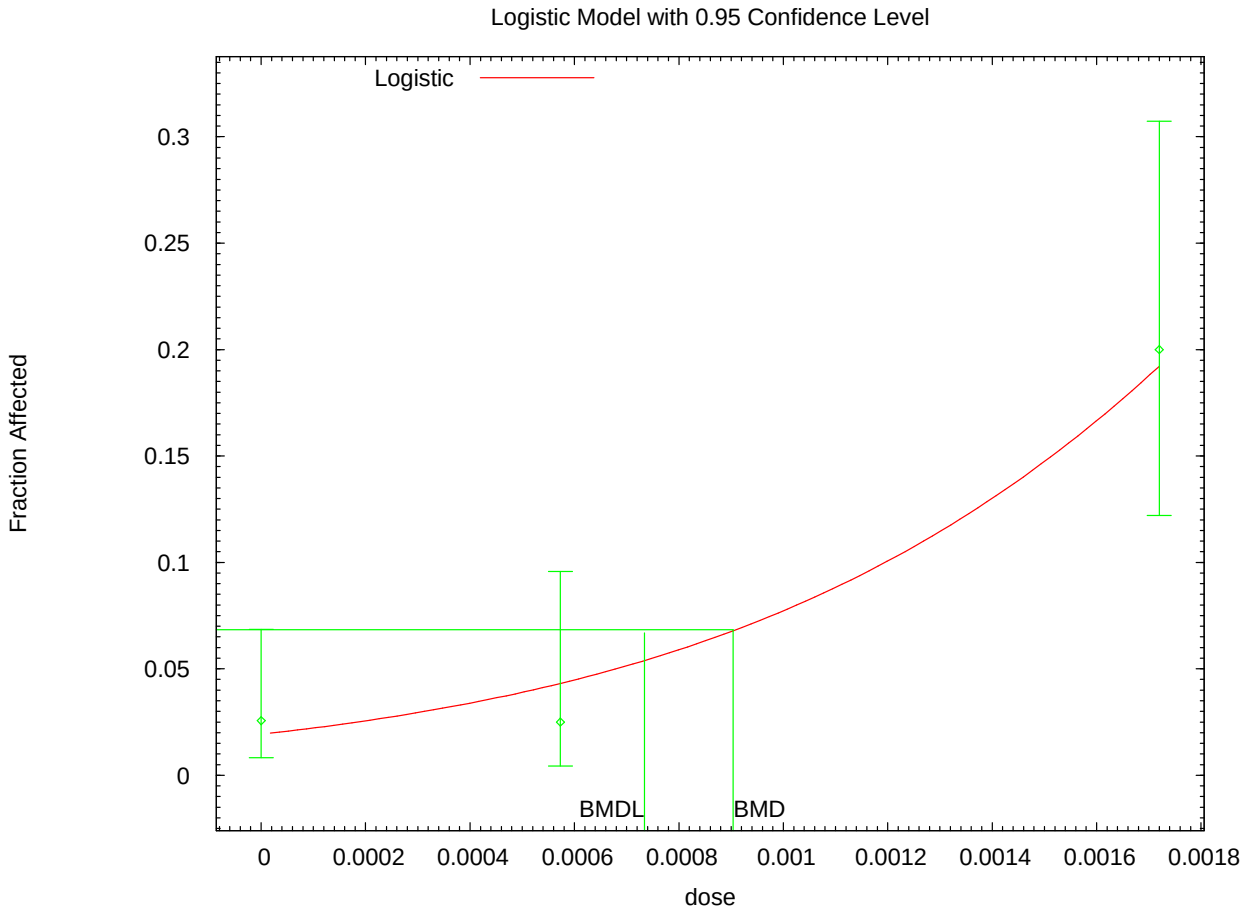

16:01 10/08 2008

```
 ======================================================================
         Logistic Model. (Version: 2.12; Date: 05/16/2008)
         Input Data File: C:\USEPA\BMDS2\Temp\tmpA6F.(d)
         Gnuplot Plotting File:  C:\USEPA\BMDS2\Temp\tmpA6F.plt
                                                 Wed Oct 08 16:01:43 2008
 ======================================================================

 BMDS Model Run
~~~~~~~~~~~~~~~~~~~~~~~~~~~~~~~~~~~~~~~~~~~~~~~~~~~~~~~~~~~~~~~~~~~~~~~~~~~

   The form of the probability function is:

   P[response] = 1/[1+EXP(-intercept-slope*dose)]


   Dependent variable = Response
   Independent variable = DOSE
   Slope parameter is not restricted

   Total number of observations = 3
   Total number of records with missing values = 0
   Maximum number of iterations = 250
   Relative Function Convergence has been set to: 1e-008
   Parameter Convergence has been set to: 1e-008


                  Default Initial Parameter Values
                     background =            0   Specified
                      intercept =     -3.79881
```

slope = 1335.91

Asymptotic Correlation Matrix of Parameter Estimates

(*** The model parameter(s) -background
have been estimated at a boundary point, or have been specified by the user,
and do not appear in the correlation matrix)

	intercept	slope
intercept	1	-0.88
slope	-0.88	1

Parameter Estimates

Variable	Estimate	Std. Err.	95.0% Wald Confidence Interval Lower Conf. Limit	Upper Conf. Limit
intercept	-3.92577	0.477035	-4.86074	-2.9908
slope	1453.89	335.047	797.213	2110.57

Analysis of Deviance Table

Model	Log(likelihood)	# Param's	Deviance	Test d.f.	P-value
Full model	-67.9873	3			
Fitted model	-68.5281	2	1.0816	1	0.2983
Reduced model	-79.8392	1	23.7038	2	<.0001

AIC: 141.056

Goodness of Fit

Dose	Est._Prob.	Expected	Observed	Size	Scaled Residual
0.0000	0.0193	3.018	4.000	156	0.571
0.0006	0.0434	3.473	2.000	80	-0.808
0.0017	0.1939	15.509	16.000	80	0.139

Chi^2 = 1.00 d.f. = 1 P-value = 0.3178

Benchmark Dose Computation

Specified effect = 0.05

Risk Type = Extra risk

Confidence level = 0.95

BMD = 0.00090371

BMDL = 0.000733555

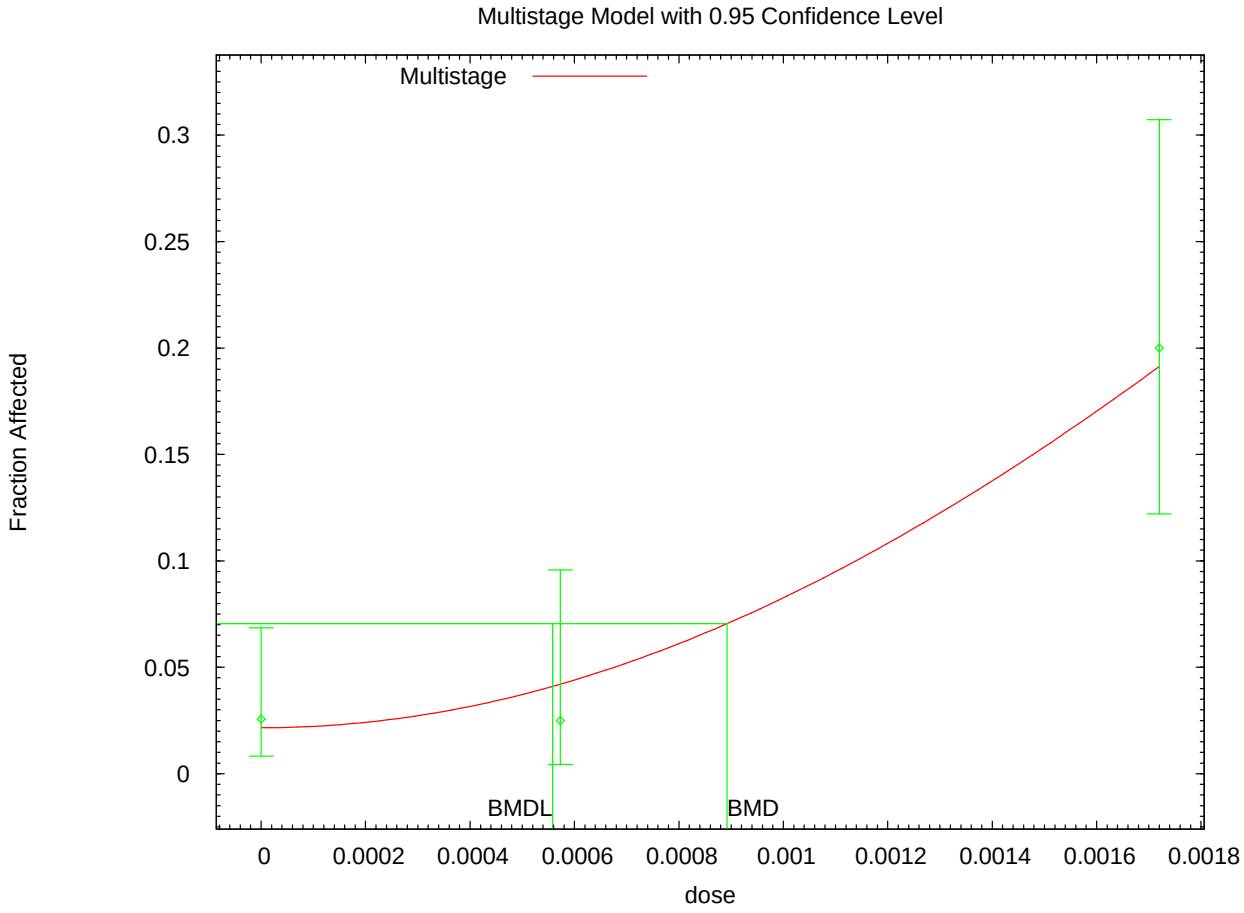

16:07 10/08 2008

```
=====================================================================
        Multistage Model. (Version: 3.0;  Date: 05/16/2008)
        Input Data File: C:\USEPA\BMDS2\Temp\tmpA72.(d)
        Gnuplot Plotting File:  C:\USEPA\BMDS2\Temp\tmpA72.plt
                                                Wed Oct 08 16:07:08 2008
=====================================================================

BMDS Model Run
~~~~~~~~~~~~~~~~~~~~~~~~~~~~~~~~~~~~~~~~~~~~~~~~~~~~~~~~~~~~~~~~~~~~~~~

  The form of the probability function is:

  P[response] = background + (1-background)*[1-EXP(
               -beta1*dose^1-beta2*dose^2)]

  The parameter betas are restricted to be positive


  Dependent variable = Response
  Independent variable = DOSE

Total number of observations = 3
Total number of records with missing values = 0
Total number of parameters in model = 3
Total number of specified parameters = 0
Degree of polynomial = 2


Maximum number of iterations = 250
Relative Function Convergence has been set to: 1e-008
Parameter Convergence has been set to: 1e-008
```

Default Initial Parameter Values
Background = 0.0147497
Beta(1) = 0
Beta(2) = 69935.2

Asymptotic Correlation Matrix of Parameter Estimates

(*** The model parameter(s) -Beta(1)
have been estimated at a boundary point, or have been specified by the user,
and do not appear in the correlation matrix)

	Background	Beta(2)
Background	1	-0.51
Beta(2)	-0.51	1

Parameter Estimates

Variable	Estimate	Std. Err.	95.0% Wald Confidence Interval Lower Conf. Limit	Upper Conf. Limit
Background	0.021634	*	*	*
Beta(1)	0	*	*	*
Beta(2)	64407.8	*	*	*

* - Indicates that this value is not calculated.

Analysis of Deviance Table

Model	Log(likelihood)	# Param's	Deviance	Test d.f.	P-value
Full model	-67.9873	3			
Fitted model	-68.4002	2	0.825863	1	0.3635
Reduced model	-79.8392	1	23.7038	2	<.0001

AIC: 140.8

Goodness of Fit

Dose	Est._Prob.	Expected	Observed	Size	Scaled Residual
0.0000	0.0216	3.375	4.000	156	0.344
0.0006	0.0421	3.369	2.000	80	-0.762
0.0017	0.1914	15.310	16.000	80	0.196

Chi^2 = 0.74 d.f. = 1 P-value = 0.3905

Benchmark Dose Computation

Specified effect = 0.05

Risk Type = Extra risk

Confidence level = 0.95

BMD = 0.000892403

BMDL = 0.000558013

BMDU = 0.00116455

Taken together, (0.000558013, 0.00116455) is a 90 % two-sided confidence interval for the BMD

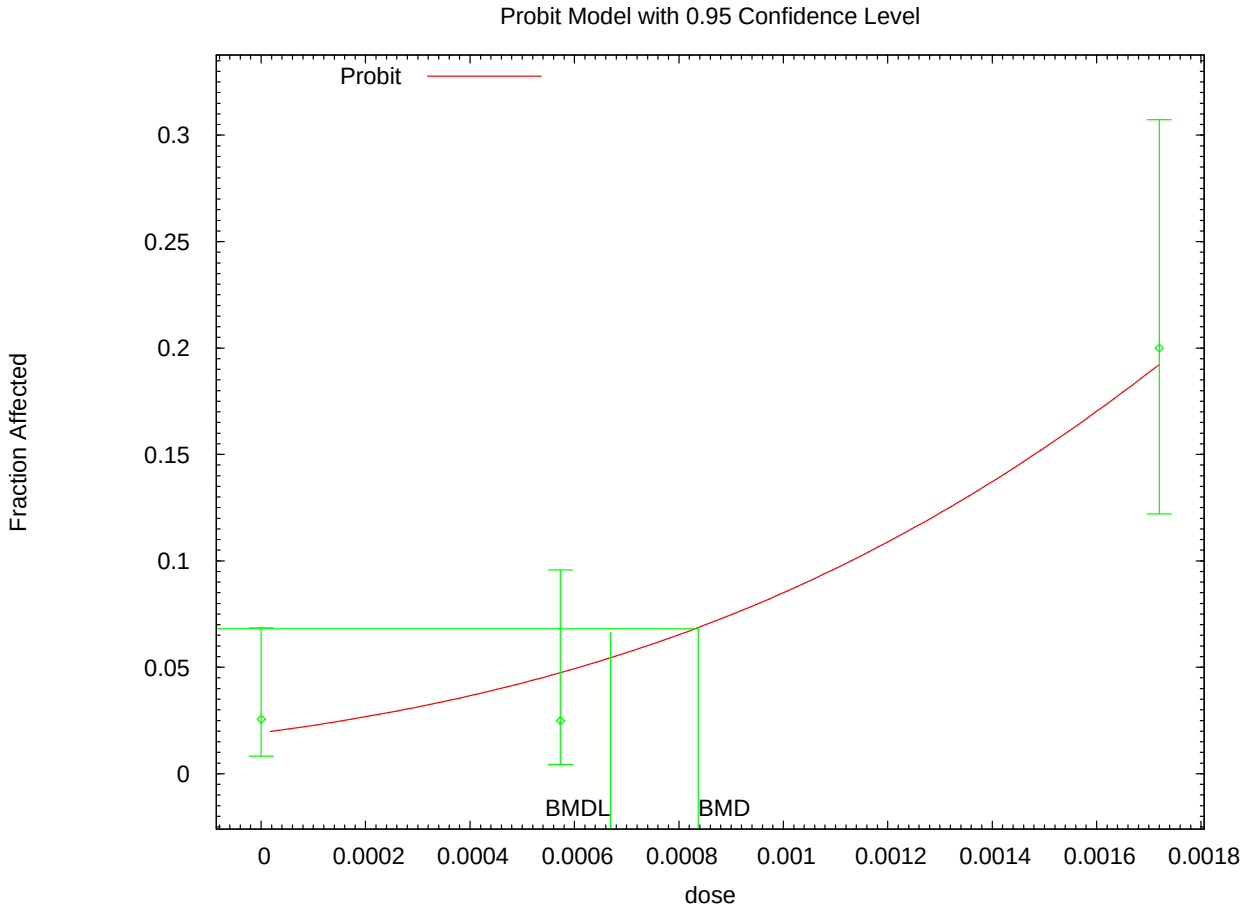

16:11 10/08 2008

```
=====================================================================
        Probit Model. (Version: 3.1;  Date: 05/16/2008)
        Input Data File: C:\USEPA\BMDS2\Temp\tmpA73.(d)
        Gnuplot Plotting File:  C:\USEPA\BMDS2\Temp\tmpA73.plt
                                                Wed Oct 08 16:11:23 2008
=====================================================================

BMDS Model Run
~~~~~~~~~~~~~~~~~~~~~~~~~~~~~~~~~~~~~~~~~~~~~~~~~~~~~~~~~~~~~~~~~~~~~~~

  The form of the probability function is:

  P[response] = CumNorm(Intercept+Slope*Dose),

  where CumNorm(.) is the cumulative normal distribution function


  Dependent variable = Response
  Independent variable = DOSE
  Slope parameter is not restricted

  Total number of observations = 3
  Total number of records with missing values = 0
  Maximum number of iterations = 250
  Relative Function Convergence has been set to: 1e-008
  Parameter Convergence has been set to: 1e-008


                Default Initial (and Specified) Parameter Values
                   background =            0   Specified
                    intercept =     -2.03885
                        slope =      644.864
```

Asymptotic Correlation Matrix of Parameter Estimates

(*** The model parameter(s) -background
have been estimated at a boundary point, or have been specified by the user,
and do not appear in the correlation matrix)

	intercept	slope
intercept	1	-0.81
slope	-0.81	1

Parameter Estimates

Variable	Estimate	Std. Err.	95.0% Wald Confidence Interval Lower Conf. Limit	Upper Conf. Limit
intercept	-2.07454	0.197583	-2.4618	-1.68729
slope	697.628	154.868	394.091	1001.16

Analysis of Deviance Table

Model	Log(likelihood)	# Param's	Deviance	Test d.f.	P-value
Full model	-67.9873	3			
Fitted model	-68.6913	2	1.40812	1	0.2354
Reduced model	-79.8392	1	23.7038	2	<.0001

AIC: 141.383

Goodness of Fit

Dose	Est._Prob.	Expected	Observed	Size	Scaled Residual
0.0000	0.0190	2.966	4.000	156	0.606
0.0006	0.0470	3.759	2.000	80	-0.929
0.0017	0.1909	15.271	16.000	80	0.207

Chi^2 = 1.27 d.f. = 1 P-value = 0.2590

Benchmark Dose Computation

Specified effect = 0.05

Risk Type = Extra risk

Confidence level = 0.95

BMD = 0.000837374

BMDL = 0.000669495

F344 Female Rats: Forestomach lesions (CEO in blood)

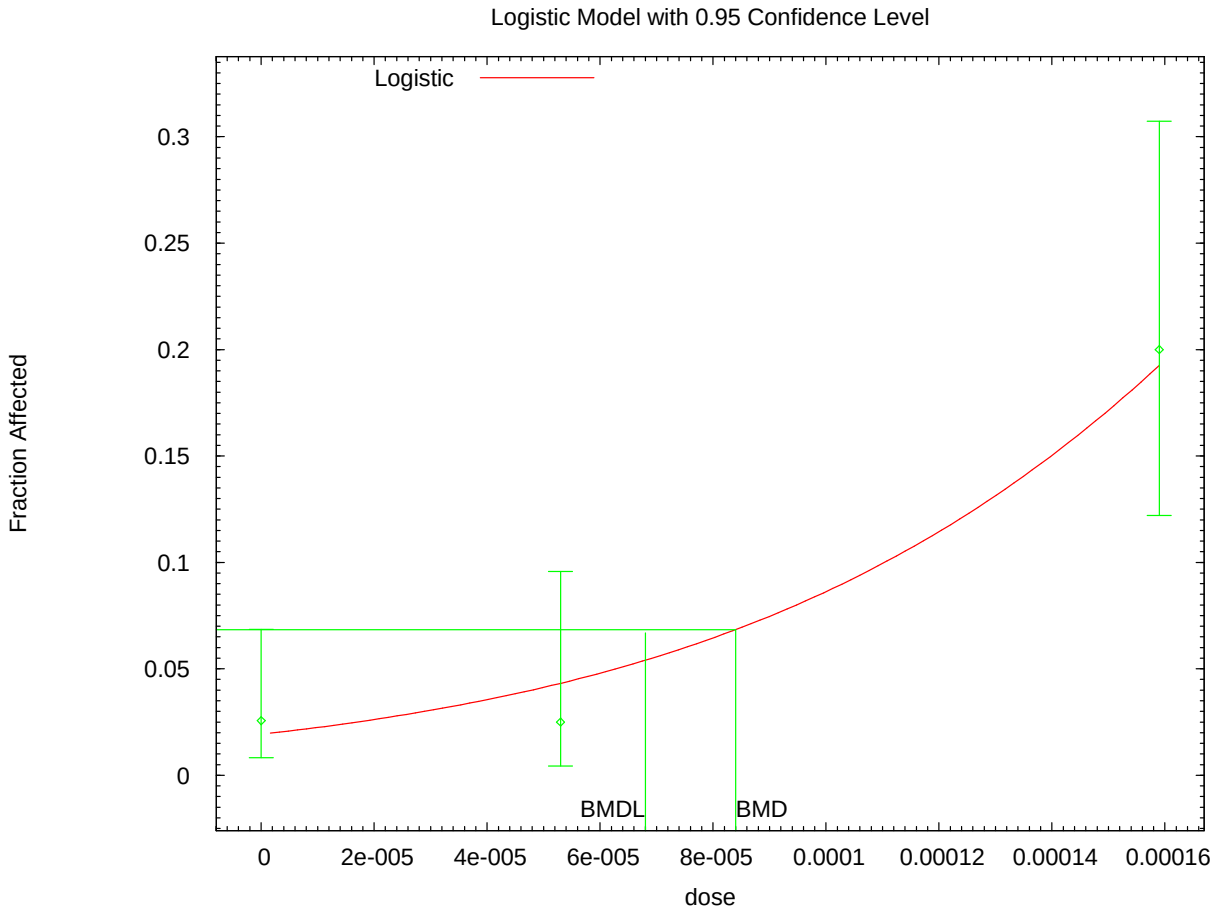

09:45 10/09 2008

```
 ======================================================================
         Logistic Model. (Version: 2.12; Date: 05/16/2008)
         Input Data File: C:\USEPA\BMDS2\Temp\tmp10.(d)
         Gnuplot Plotting File:  C:\USEPA\BMDS2\Temp\tmp10.plt
                                                 Thu Oct 09 09:45:26 2008
 ======================================================================

 BMDS Model Run
~~~~~~~~~~~~~~~~~~~~~~~~~~~~~~~~~~~~~~~~~~~~~~~~~~~~~~~~~~~~~~~~~~~~~~~~~~

   The form of the probability function is:

   P[response] = 1/[1+EXP(-intercept-slope*dose)]


   Dependent variable = Response
   Independent variable = DOSE
   Slope parameter is not restricted

   Total number of observations = 3
   Total number of records with missing values = 0
   Maximum number of iterations = 250
   Relative Function Convergence has been set to: 1e-008
   Parameter Convergence has been set to: 1e-008


                  Default Initial Parameter Values
                     background =            0   Specified
                      intercept =     -3.79973
```

slope = 14448.5

Asymptotic Correlation Matrix of Parameter Estimates

(*** The model parameter(s) -background
have been estimated at a boundary point, or have been specified by the user,
and do not appear in the correlation matrix)

	intercept	slope
intercept	1	-0.88
slope	-0.88	1

Parameter Estimates

Variable	Estimate	Std. Err.	95.0% Wald Confidence Interval Lower Conf. Limit	Upper Conf. Limit
intercept	-3.92703	0.4774	-4.86272	-2.99135
slope	15733	3627.17	8623.9	22842.1

Analysis of Deviance Table

Model	Log(likelihood)	# Param's	Deviance	Test d.f.	P-value
Full model	-67.9873	3			
Fitted model	-68.5334	2	1.09233	1	0.296
Reduced model	-79.8392	1	23.7038	2	<.0001

AIC: 141.067

Goodness of Fit

Dose	Est._Prob.	Expected	Observed	Size	Scaled Residual
0.0000	0.0193	3.014	4.000	156	0.573
0.0001	0.0435	3.482	2.000	80	-0.812
0.0002	0.1938	15.504	16.000	80	0.140

Chi^2 = 1.01 d.f. = 1 P-value = 0.3155

Benchmark Dose Computation

Specified effect = 0.05

Risk Type = Extra risk

Confidence level = 0.95

BMD = 8.35696e-005

BMDL = 6.78392e-005

14:46 10/09 2008

```
=====================================================================
        Multistage Model. (Version: 3.0;  Date: 05/16/2008)
        Input Data File: C:\USEPA\BMDS2\Temp\tmpFC.(d)
        Gnuplot Plotting File:  C:\USEPA\BMDS2\Temp\tmpFC.plt
                                                Thu Oct 09 14:46:41 2008
=====================================================================

BMDS Model Run
~~~~~~~~~~~~~~~~~~~~~~~~~~~~~~~~~~~~~~~~~~~~~~~~~~~~~~~~~~~~~~~~~~~~~~~

  The form of the probability function is:

  P[response] = background + (1-background)*[1-EXP(
               -beta1*dose^1-beta2*dose^2)]

  The parameter betas are restricted to be positive


  Dependent variable = Response
  Independent variable = DOSE

Total number of observations = 3
Total number of records with missing values = 0
Total number of parameters in model = 3
Total number of specified parameters = 0
Degree of polynomial = 2


Maximum number of iterations = 250
Relative Function Convergence has been set to: 1e-008
Parameter Convergence has been set to: 1e-008
```

Default Initial Parameter Values
Background = 0.0146597
Beta(1) = 0
Beta(2) = 8.18648e+006

Asymptotic Correlation Matrix of Parameter Estimates

(*** The model parameter(s) -Beta(1)
have been estimated at a boundary point, or have been specified by the user,
and do not appear in the correlation matrix)

	Background	Beta(2)
Background	1	-0.51
Beta(2)	-0.51	1

Parameter Estimates

Variable	Estimate	Std. Err.	95.0% Wald Confidence Interval Lower Conf. Limit	Upper Conf. Limit
Background	0.0216202	*	*	*
Beta(1)	0	*	*	*
Beta(2)	7.53198e+006	*	*	*

* - Indicates that this value is not calculated.

Analysis of Deviance Table

Model	Log(likelihood)	# Param's	Deviance	Test d.f.	P-value
Full model	-67.9873	3			
Fitted model	-68.4062	2	0.837895	1	0.36
Reduced model	-79.8392	1	23.7038	2	<.0001

AIC: 140.812

Goodness of Fit

Dose	Est._Prob.	Expected	Observed	Size	Scaled Residual
0.0000	0.0216	3.373	4.000	156	0.345
0.0001	0.0423	3.380	2.000	80	-0.767
0.0002	0.1913	15.301	16.000	80	0.199

Chi^2 = 0.75 d.f. = 1 P-value = 0.3873

Benchmark Dose Computation

Specified effect = 0.05

Risk Type = Extra risk

Confidence level = 0.95

BMD = 8.25232e-005

BMDL = 5.17106e-005

BMDU = 0.000107687

Taken together, (5.17106e-005, 0.000107687) is a 90 % two-sided confidence interval for the BMD

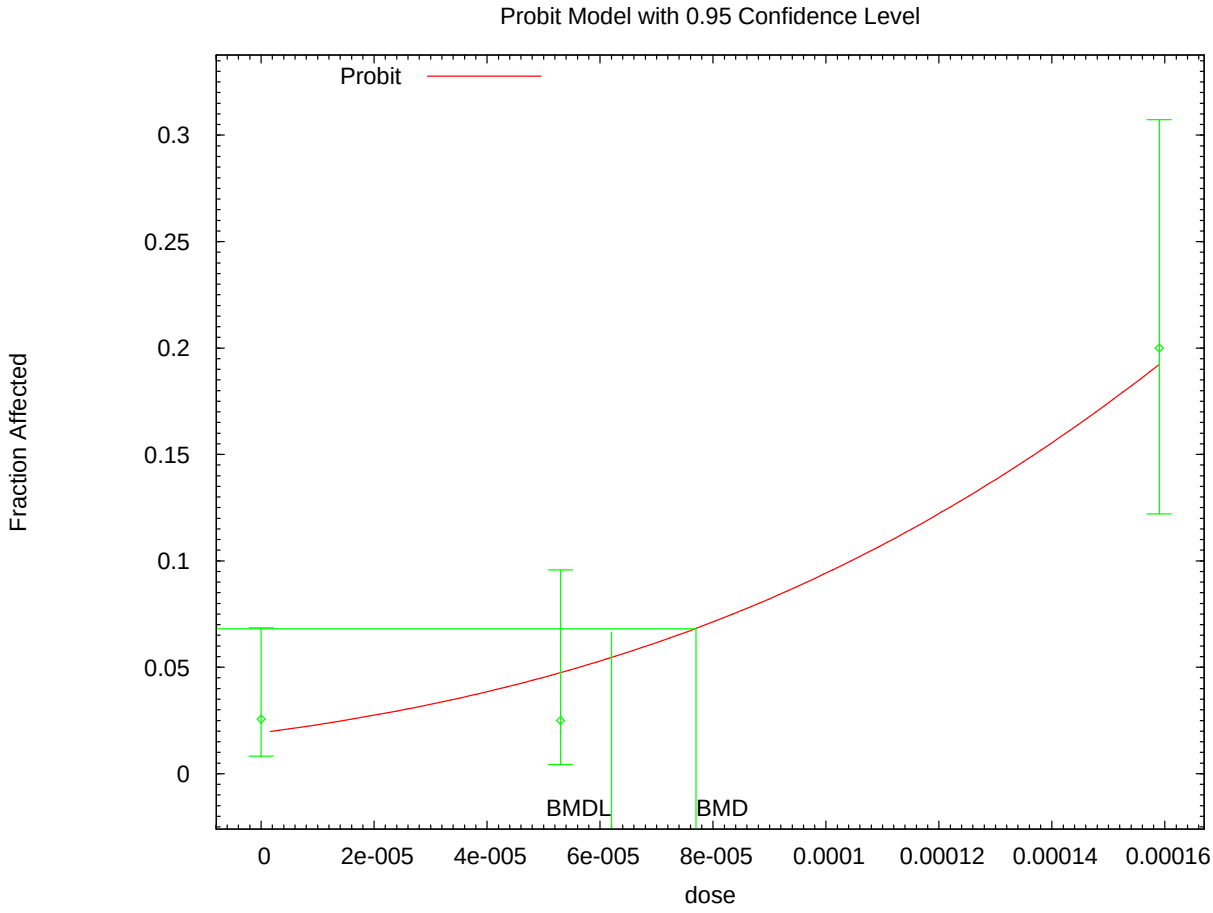

14:50 10/09 2008

```
================================================================
        Probit Model. (Version: 3.1;  Date: 05/16/2008)
        Input Data File: C:\USEPA\BMDS2\Temp\tmpFD.(d)
        Gnuplot Plotting File:  C:\USEPA\BMDS2\Temp\tmpFD.plt
                                                Thu Oct 09 14:50:46 2008
================================================================

BMDS Model Run
~~~~~~~~~~~~~~~~~~~~~~~~~~~~~~~~~~~~~~~~~~~~~~~~~~~~~~~~~~~~~~~~~~~~~~~~

  The form of the probability function is:

  P[response] = CumNorm(Intercept+Slope*Dose),

  where CumNorm(.) is the cumulative normal distribution function


  Dependent variable = Response
  Independent variable = DOSE
  Slope parameter is not restricted

  Total number of observations = 3
  Total number of records with missing values = 0
  Maximum number of iterations = 250
  Relative Function Convergence has been set to: 1e-008
  Parameter Convergence has been set to: 1e-008


                Default Initial (and Specified) Parameter Values
                   background =            0   Specified
                    intercept =     -2.03906
                        slope =      6972.11
```

Asymptotic Correlation Matrix of Parameter Estimates

(*** The model parameter(s) -background
have been estimated at a boundary point, or have been specified by the user,
and do not appear in the correlation matrix)

	intercept	slope
intercept	1	-0.81
slope	-0.81	1

Parameter Estimates

Variable	Estimate	Std. Err.	95.0% Wald Confidence Interval Lower Conf. Limit	Upper Conf. Limit
intercept	-2.075	0.197714	-2.46251	-1.68749
slope	7547.46	1676.24	4262.09	10832.8

Analysis of Deviance Table

Model	Log(likelihood)	# Param's	Deviance	Test d.f.	P-value
Full model	-67.9873	3			
Fitted model	-68.6981	2	1.42158	1	0.2331
Reduced model	-79.8392	1	23.7038	2	<.0001

AIC: 141.396

Goodness of Fit

Dose	Est._Prob.	Expected	Observed	Size	Scaled Residual
0.0000	0.0190	2.963	4.000	156	0.608
0.0001	0.0471	3.769	2.000	80	-0.934
0.0002	0.1908	15.264	16.000	80	0.209

Chi^2 = 1.29 d.f. = 1 P-value = 0.2569

Benchmark Dose Computation

Specified effect = 0.05

Risk Type = Extra risk

Confidence level = 0.95

BMD = 7.74403e-005

BMDL = 6.19187e-005

Table B-5. Summary of the BMD modeling results based on the incidence of forestomach lesions (hyperplasia or hyperkeratosis) in male and female $B6C3F_1$ mice exposed to AN via gavage for 2 years

Sex	Endpoint	Dose metric	Selected model(s)[a]	χ^2 *p*-value	AIC	$BMDL_{10}$[b]	$BMDL_{05}$[b]
Male	Forestomach lesions	Estimated administered dose (mg/kg-d)	gamma	0.80	156.45	3.45	1.68
			logistic	0.37	158.01	6.37	3.72
			log-logistic	**0.87**	**156.30**	**3.01**	**1.43**
			probit	0.42	157.74	5.96	3.42
			log-probit	0.33	158.23	5.53	3.85
			one-stage multistage	0.80	156.45	3.45	1.68
			Weibull	0.80	156.45	3.45	1.68
			quantal linear	0.80	156.45	3.45	1.68
Female	Forestomach lesions	Estimated administered dose (mg/kg-d)	gamma	0.74	116.17	6.24	3.04
			logistic	0.87	114.33	8.95	5.60
			log-logistic	0.75	116.17	5.98	2.83
			probit	0.90	114.28	8.51	5.19
			log-probit	0.81	114.48	8.12	5.65
			one-stage multistage	**0.92**	**114.24**	**6.20**	**3.02**
			Weibull	0.74	116.18	6.24	3.04
			quantal linear	**0.92**	**114.24**	**6.20**	**3.02**

[a]All dichotomous models in EPA's BMDS (version 2.0) were fit to the incidence of forestomach lesions (hyperplasia or hyperkeratosis) in $B6C3F_1$ mice using the data presented in Table B-2. For BMD modeling, animal dose (estimated), expressed in mg/kg-d, was employed. Adequate fit of a model was achieved if the χ^2 goodness-of-fit statistic yielded a *p*-value > 0.1. Of those models exhibiting adequate fit, the selected model was the model with the lowest AIC value, and is indicated in bold in the table.

[b]$BMDL_{10}$ and $BMDL_{05}$ estimates were derived from the selected model. If more than one model shared the lowest AIC, the mean $BMDL_{10}$ and $BMDL_{05}$ were calculated, as per the EPA's *Benchmark Dose Technical Guidance Document* (U.S. EPA, 2000b).

Source: NTP (2001).

B6C3F$_1$ Male Mice: Forestomach lesions (administered dose)

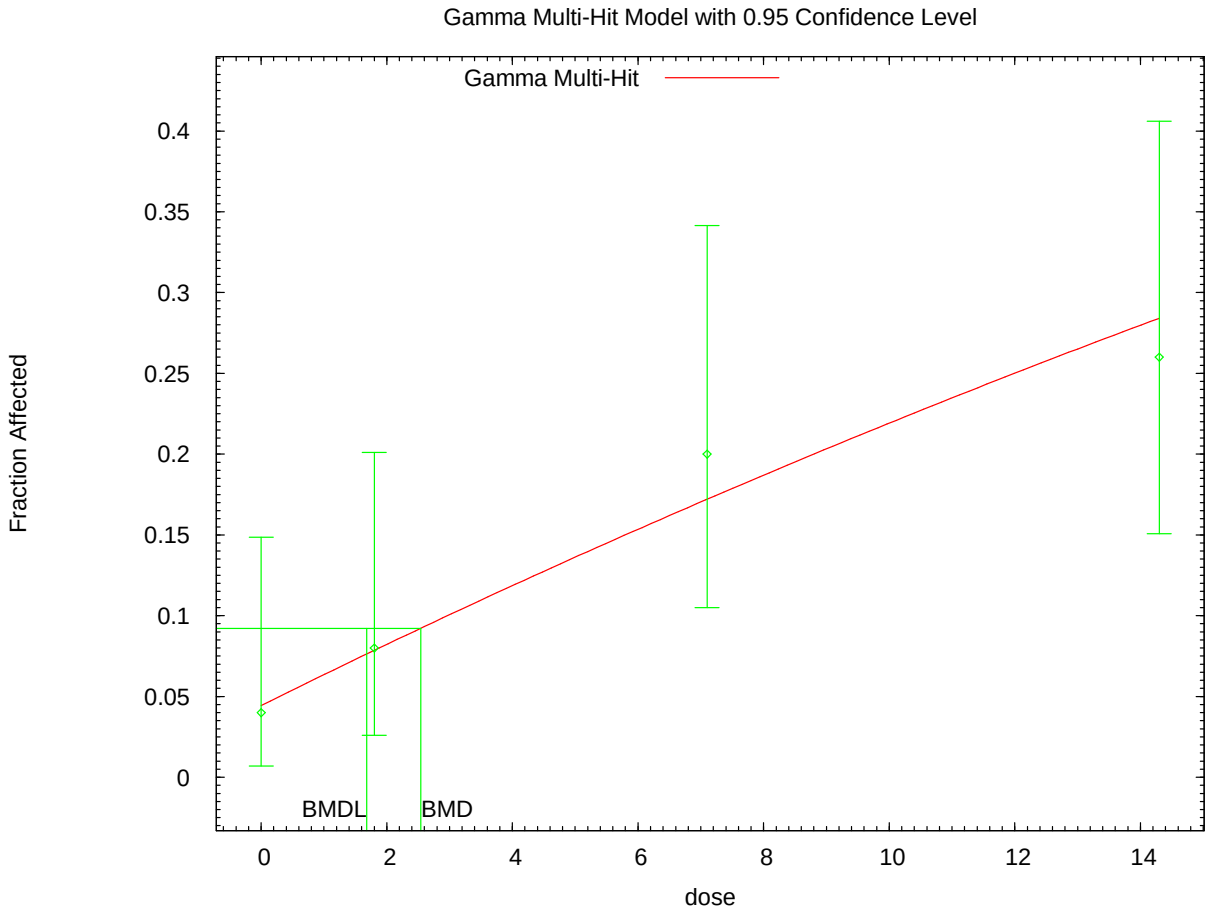

13:51 11/14 2008

```
 ================================================================
         Gamma Model. (Version: 2.13;  Date: 05/16/2008)
         Input Data File: C:\USEPA\BMDS2\Temp\tmp111.(d)
         Gnuplot Plotting File:  C:\USEPA\BMDS2\Temp\tmp111.plt
                                                Fri Nov 14 13:51:24 2008
 ================================================================

 BMDS Model Run
~~~~~~~~~~~~~~~~~~~~~~~~~~~~~~~~~~~~~~~~~~~~~~~~~~~~~~~~~~~~~~~~~~~~~~~~

   The form of the probability function is:

   P[response]= background+(1-background)*CumGamma[slope*dose,power],
   where CumGamma(.) is the cummulative Gamma distribution function


   Dependent variable = Response
   Independent variable = DOSE
   Power parameter is restricted as power >=1

   Total number of observations = 4
   Total number of records with missing values = 0
   Maximum number of iterations = 250
   Relative Function Convergence has been set to: 1e-008
   Parameter Convergence has been set to: 1e-008


                  Default Initial (and Specified) Parameter Values
                     Background =    0.0490196
```

Slope = 0.0449456
Power = 1.3

Asymptotic Correlation Matrix of Parameter Estimates

(*** The model parameter(s) -Power
have been estimated at a boundary point, or have been specified by the user,
and do not appear in the correlation matrix)

	Background	Slope
Background	1	-0.53
Slope	-0.53	1

Parameter Estimates

Variable	Estimate	Std. Err.	95.0% Wald Confidence Interval Lower Conf. Limit	Upper Conf. Limit
Background	0.0444165	0.025521	-0.00560381	0.0944368
Slope	0.0201613	0.00593774	0.00852351	0.031799
Power	1	NA		

NA - Indicates that this parameter has hit a bound
implied by some inequality constraint and thus
has no standard error.

Analysis of Deviance Table

Model	Log(likelihood)	# Param's	Deviance	Test d.f.	P-value
Full model	-76.0086	4			
Fitted model	-76.2255	2	0.433714	2	0.805
Reduced model	-82.7874	1	13.5576	3	0.003574

AIC: 156.451

Goodness of Fit

Dose	Est._Prob.	Expected	Observed	Size	Scaled Residual
0.0000	0.0444	2.221	2.000	50	-0.152
1.8000	0.0785	3.924	4.000	50	0.040
7.1000	0.1719	8.593	10.000	50	0.527
14.3000	0.2838	14.188	13.000	50	-0.373

Chi^2 = 0.44 d.f. = 2 P-value = 0.8019

Benchmark Dose Computation

Specified effect = 0.05

Risk Type = Extra risk

Confidence level = 0.95

BMD = 2.54415

BMDL = 1.68095

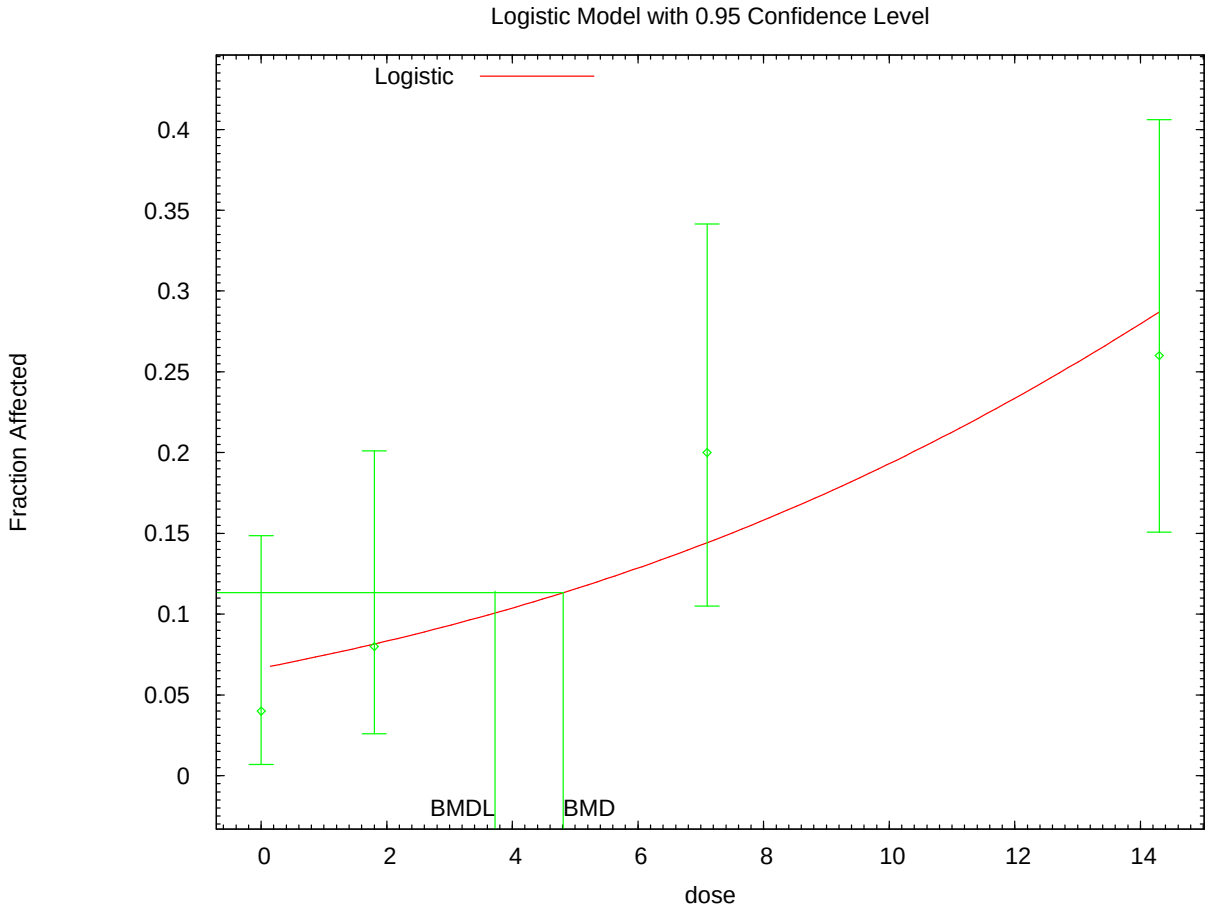

14:00 11/14 2008

```
================================================================
        Logistic Model. (Version: 2.12; Date: 05/16/2008)
        Input Data File: C:\USEPA\BMDS2\Temp\tmp113.(d)
        Gnuplot Plotting File:  C:\USEPA\BMDS2\Temp\tmp113.plt
                                                Fri Nov 14 14:00:33 2008
================================================================

BMDS Model Run
~~~~~~~~~~~~~~~~~~~~~~~~~~~~~~~~~~~~~~~~~~~~~~~~~~~~~~~~~~~~~~~~~~~~

  The form of the probability function is:

  P[response] = 1/[1+EXP(-intercept-slope*dose)]


  Dependent variable = Response
  Independent variable = DOSE
  Slope parameter is not restricted

  Total number of observations = 4
  Total number of records with missing values = 0
  Maximum number of iterations = 250
  Relative Function Convergence has been set to: 1e-008
  Parameter Convergence has been set to: 1e-008


                Default Initial Parameter Values
                   background =            0   Specified
                    intercept =     -2.67373
                        slope =     0.130289


          Asymptotic Correlation Matrix of Parameter Estimates
```

(*** The model parameter(s) -background
have been estimated at a boundary point, or have been specified by the user,
and do not appear in the correlation matrix)

	intercept	slope
intercept	1	-0.83
slope	-0.83	1

Parameter Estimates

Variable	Estimate	Std. Err.	95.0% Wald Confidence Interval Lower Conf. Limit	Upper Conf. Limit
intercept	-2.63925	0.372305	-3.36896	-1.90955
slope	0.121074	0.0365284	0.04948	0.192669

Analysis of Deviance Table

Model	Log(likelihood)	# Param's	Deviance	Test d.f.	P-value
Full model	-76.0086	4			
Fitted model	-77.0042	2	1.99121	2	0.3695
Reduced model	-82.7874	1	13.5576	3	0.003574

AIC: 158.008

Goodness of Fit

Dose	Est._Prob.	Expected	Observed	Size	Scaled Residual
0.0000	0.0667	3.333	2.000	50	-0.756
1.8000	0.0816	4.078	4.000	50	-0.040
7.1000	0.1443	7.217	10.000	50	1.120
14.3000	0.2874	14.372	13.000	50	-0.429

Chi^2 = 2.01 d.f. = 2 P-value = 0.3660

Benchmark Dose Computation

Specified effect = 0.05

Risk Type = Extra risk

Confidence level = 0.95

BMD = 4.80697

BMDL = 3.72464

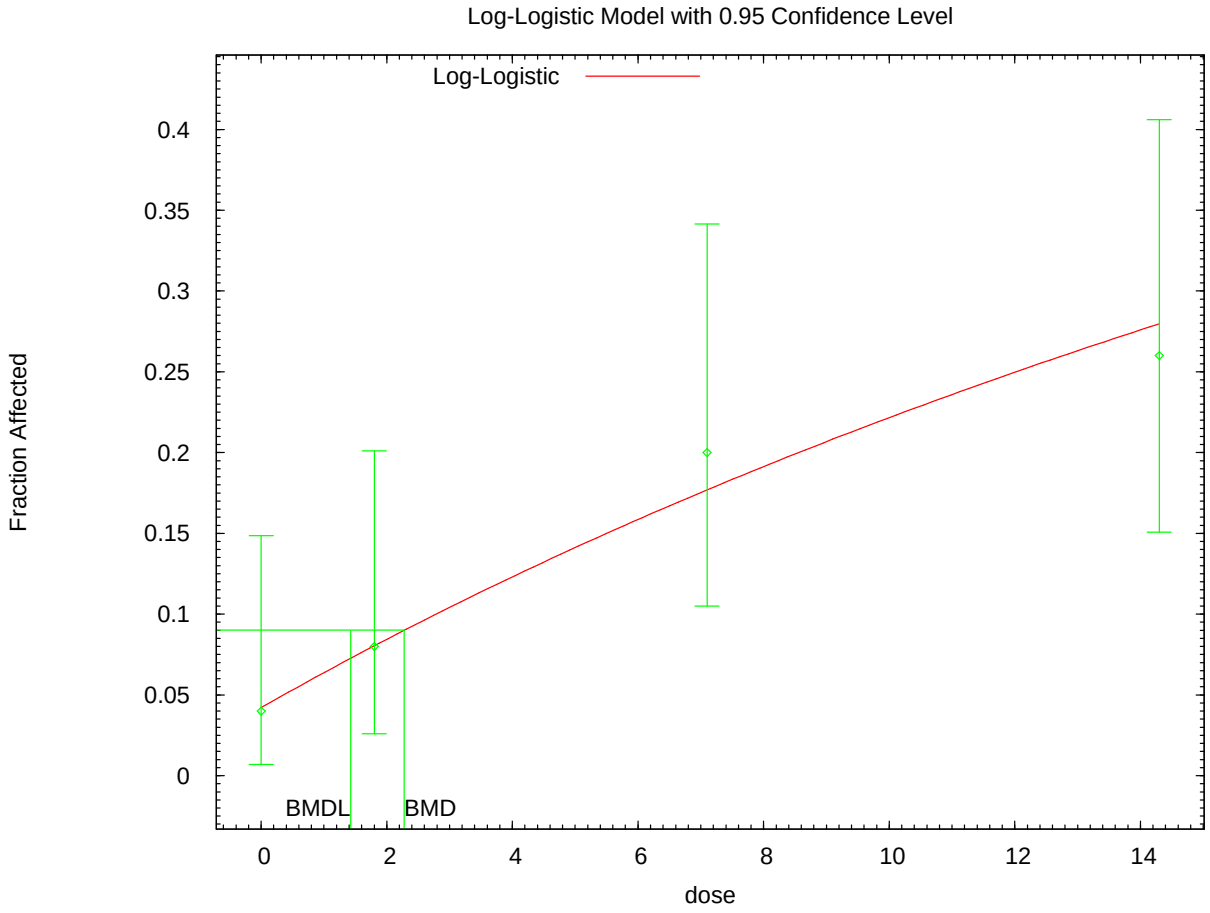

14:04 11/14 2008

```
=================================================================
        Logistic Model. (Version: 2.12; Date: 05/16/2008)
        Input Data File: C:\USEPA\BMDS2\Temp\tmp116.(d)
        Gnuplot Plotting File:  C:\USEPA\BMDS2\Temp\tmp116.plt
                                                Fri Nov 14 14:04:51 2008
=================================================================

BMDS Model Run
~~~~~~~~~~~~~~~~~~~~~~~~~~~~~~~~~~~~~~~~~~~~~~~~~~~~~~~~~~~~~~~~~~~~~

  The form of the probability function is:

  P[response] = background+(1-background)/[1+EXP(-intercept-slope*Log(dose))]


  Dependent variable = Response
  Independent variable = DOSE
  Slope parameter is restricted as slope >= 1

  Total number of observations = 4
  Total number of records with missing values = 0
  Maximum number of iterations = 250
  Relative Function Convergence has been set to: 1e-008
  Parameter Convergence has been set to: 1e-008


  User has chosen the log transformed model


               Default Initial Parameter Values
                  background =         0.04
                   intercept =     -3.73286
                       slope =            1
```

Asymptotic Correlation Matrix of Parameter Estimates

(*** The model parameter(s) -slope
have been estimated at a boundary point, or have been specified by the user,
and do not appear in the correlation matrix)

	background	intercept
background	1	-0.54
intercept	-0.54	1

Parameter Estimates

Variable	Estimate	Std. Err.	95.0% Wald Confidence Interval Lower Conf. Limit	Upper Conf. Limit
background	0.0421528	*	*	*
intercept	-3.76687	*	*	*
slope	1	*	*	*

* - Indicates that this value is not calculated.

Analysis of Deviance Table

Model	Log(likelihood)	# Param's	Deviance	Test d.f.	P-value
Full model	-76.0086	4			
Fitted model	-76.1489	2	0.280564	2	0.8691
Reduced model	-82.7874	1	13.5576	3	0.003574

AIC: 156.298

Goodness of Fit

Dose	Est._Prob.	Expected	Observed	Size	Scaled Residual
0.0000	0.0422	2.108	2.000	50	-0.076
1.8000	0.0804	4.021	4.000	50	-0.011
7.1000	0.1772	8.862	10.000	50	0.422
14.3000	0.2802	14.009	13.000	50	-0.318

Chi^2 = 0.28 d.f. = 2 P-value = 0.8674

Benchmark Dose Computation

Specified effect = 0.05

Risk Type = Extra risk

Confidence level = 0.95

BMD = 2.27602

BMDL = 1.42584

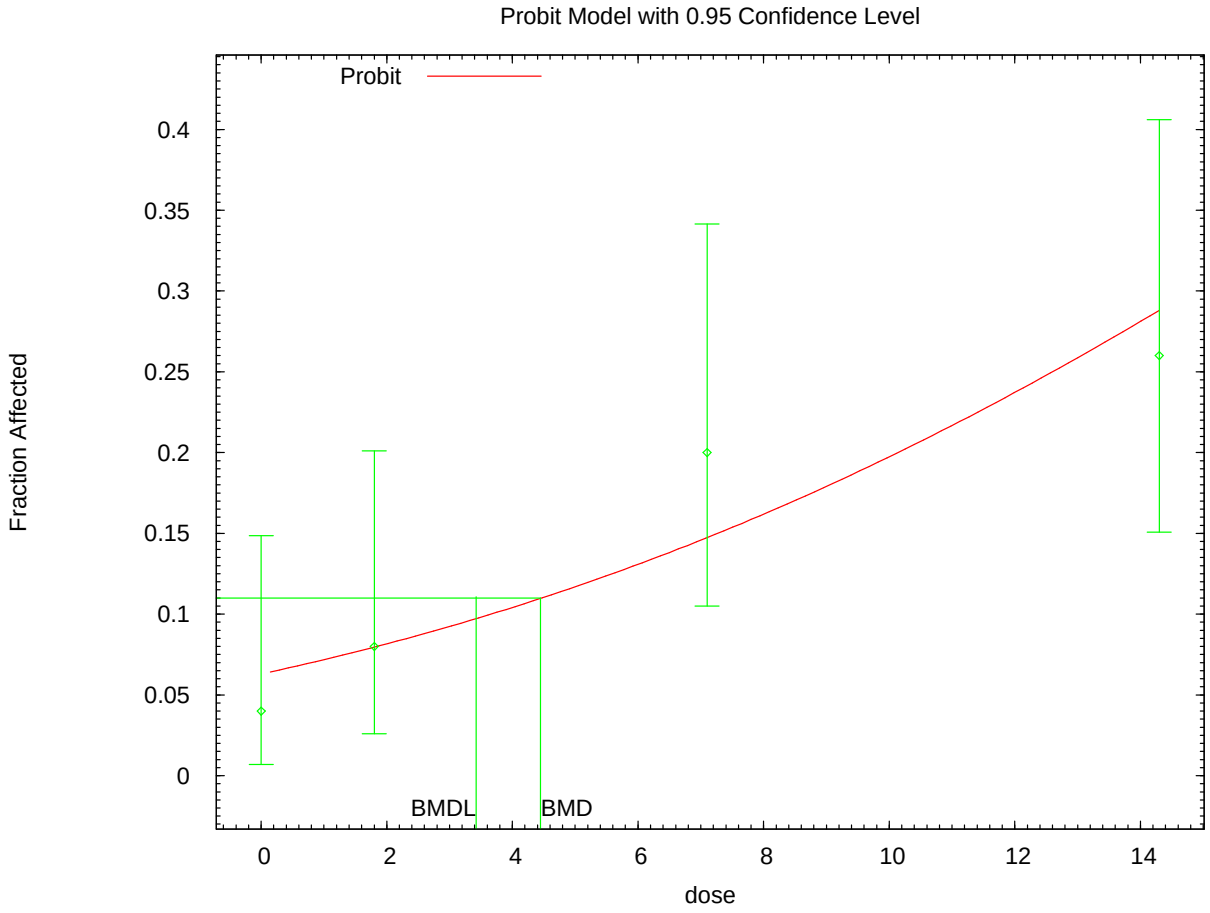

14:27 11/14 2008

```
=================================================================
        Probit Model. (Version: 3.1;  Date: 05/16/2008)
        Input Data File: C:\USEPA\BMDS2\Temp\tmp124.(d)
        Gnuplot Plotting File:  C:\USEPA\BMDS2\Temp\tmp124.plt
                                                Fri Nov 14 14:27:57 2008
=================================================================

BMDS Model Run
~~~~~~~~~~~~~~~~~~~~~~~~~~~~~~~~~~~~~~~~~~~~~~~~~~~~~~~~~~~~~~~~~~~~~

  The form of the probability function is:

  P[response] = CumNorm(Intercept+Slope*Dose),

  where CumNorm(.) is the cumulative normal distribution function


  Dependent variable = Response
  Independent variable = DOSE
  Slope parameter is not restricted

  Total number of observations = 4
  Total number of records with missing values = 0
  Maximum number of iterations = 250
  Relative Function Convergence has been set to: 1e-008
  Parameter Convergence has been set to: 1e-008


                Default Initial (and Specified) Parameter Values
                   background =            0   Specified
                    intercept =     -1.57644
                        slope =    0.0736548
```

Asymptotic Correlation Matrix of Parameter Estimates

(*** The model parameter(s) -background
have been estimated at a boundary point, or have been specified by the user,
and do not appear in the correlation matrix)

	intercept	slope
intercept	1	-0.8
slope	-0.8	1

Parameter Estimates

Variable	Estimate	Std. Err.	95.0% Wald Confidence Interval Lower Conf. Limit	Upper Conf. Limit
intercept	-1.52854	0.189536	-1.90002	-1.15706
slope	0.0679152	0.0200887	0.028542	0.107288

Analysis of Deviance Table

Model	Log(likelihood)	# Param's	Deviance	Test d.f.	P-value
Full model	-76.0086	4			
Fitted model	-76.8681	2	1.71884	2	0.4234
Reduced model	-82.7874	1	13.5576	3	0.003574

AIC: 157.736

Goodness of Fit

Dose	Est._Prob.	Expected	Observed	Size	Scaled Residual
0.0000	0.0632	3.159	2.000	50	-0.674
1.8000	0.0798	3.991	4.000	50	0.005
7.1000	0.1477	7.385	10.000	50	1.042
14.3000	0.2886	14.432	13.000	50	-0.447

Chi^2 = 1.74 d.f. = 2 P-value = 0.4189

Benchmark Dose Computation

Specified effect = 0.05

Risk Type = Extra risk

Confidence level = 0.95

BMD = 4.44923

BMDL = 3.4216

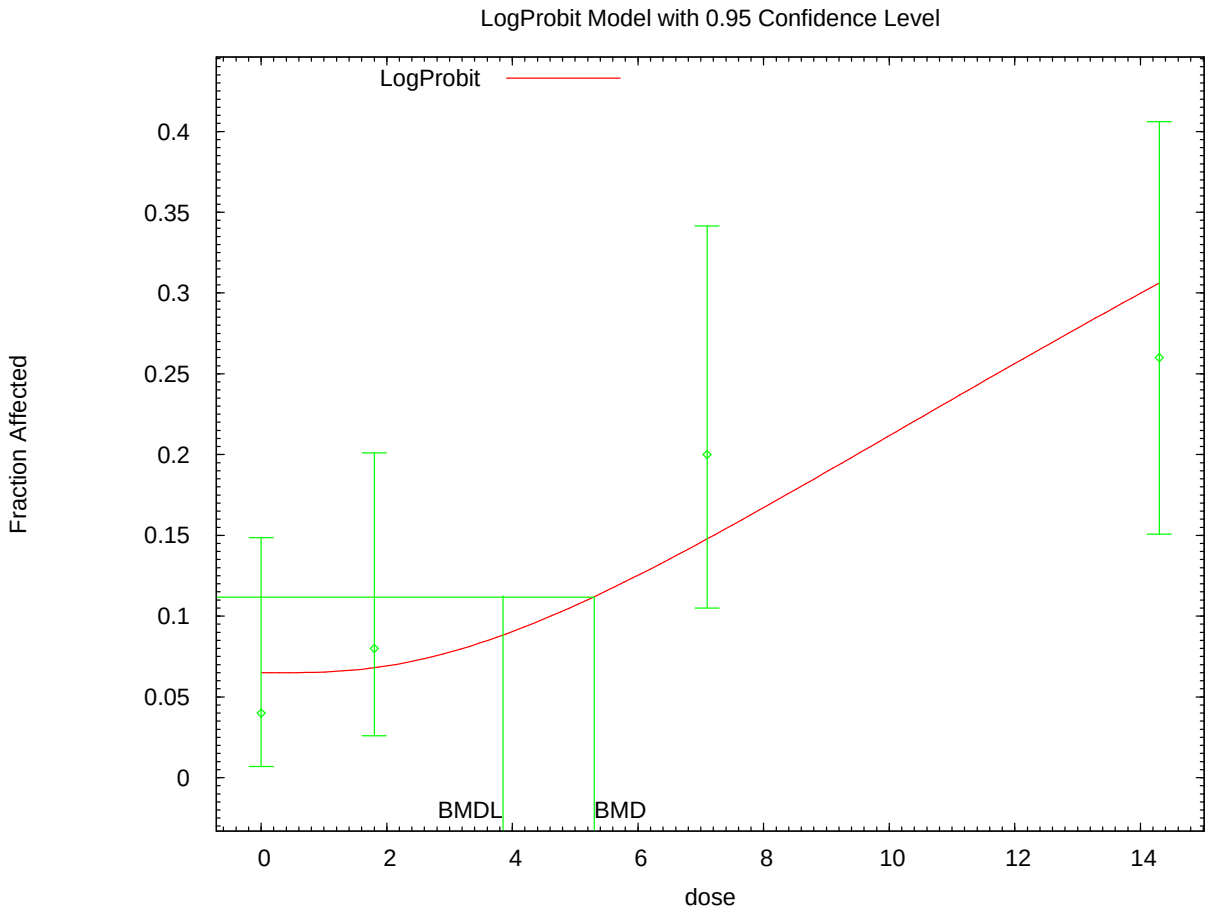

14:16 11/14 2008

```
=====================================================================
        Probit Model. (Version: 3.1;  Date: 05/16/2008)
        Input Data File: C:\USEPA\BMDS2\Temp\tmp11E.(d)
        Gnuplot Plotting File:  C:\USEPA\BMDS2\Temp\tmp11E.plt
                                                Fri Nov 14 14:16:36 2008
=====================================================================

BMDS Model Run
~~~~~~~~~~~~~~~~~~~~~~~~~~~~~~~~~~~~~~~~~~~~~~~~~~~~~~~~~~~~~~~~~~~~~~~

  The form of the probability function is:

  P[response] = Background
              + (1-Background) * CumNorm(Intercept+Slope*Log(Dose)),

  where CumNorm(.) is the cumulative normal distribution function


  Dependent variable = Response
  Independent variable = DOSE
  Slope parameter is restricted as slope >= 1

  Total number of observations = 4
  Total number of records with missing values = 0
  Maximum number of iterations = 250
  Relative Function Convergence has been set to: 1e-008
  Parameter Convergence has been set to: 1e-008


  User has chosen the log transformed model

                Default Initial (and Specified) Parameter Values
```

```
                    background =         0.04
                     intercept =     -3.00109
                         slope =            1


          Asymptotic Correlation Matrix of Parameter Estimates

          ( *** The model parameter(s)  -slope
                have been estimated at a boundary point, or have been specified by the user,
                and do not appear in the correlation matrix )

            background    intercept

background            1        -0.53

 intercept        -0.53            1
```

Parameter Estimates

Variable	Estimate	Std. Err.	95.0% Wald Confidence Interval Lower Conf. Limit	Upper Conf. Limit
background	0.0650367	0.0264604	0.0131753	0.116898
intercept	-3.3131	0.219612	-3.74353	-2.88267
slope	1	NA		

NA - Indicates that this parameter has hit a bound
implied by some inequality constraint and thus
has no standard error.

Analysis of Deviance Table

Model	Log(likelihood)	# Param's	Deviance	Test d.f.	P-value
Full model	-76.0086	4			
Fitted model	-77.1132	2	2.20909	2	0.3314
Reduced model	-82.7874	1	13.5576	3	0.003574

AIC: 158.226

Goodness of Fit

Dose	Est._Prob.	Expected	Observed	Size	Scaled Residual
0.0000	0.0650	3.252	2.000	50	-0.718
1.8000	0.0680	3.402	4.000	50	0.336
7.1000	0.1473	7.367	10.000	50	1.051
14.3000	0.3053	15.263	13.000	50	-0.695

Chi^2 = 2.21 d.f. = 2 P-value = 0.3304

Benchmark Dose Computation

```
Specified effect =          0.05

Risk Type        =      Extra risk

Confidence level =          0.95

             BMD =       5.30287

            BMDL =       3.84888
```

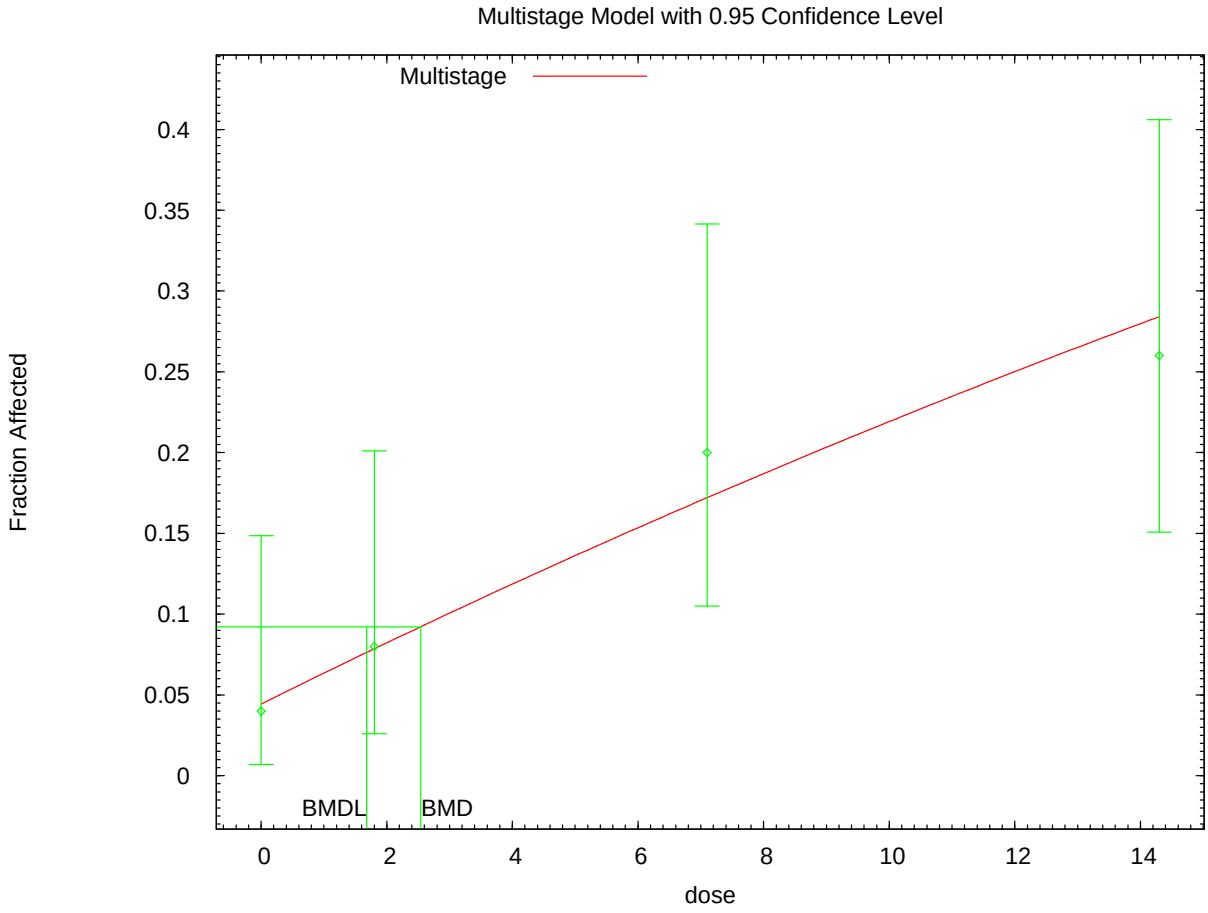

14:22 11/14 2008

```
=====================================================================
        Multistage Model. (Version: 3.0;  Date: 05/16/2008)
        Input Data File: C:\USEPA\BMDS2\Temp\tmp121.(d)
        Gnuplot Plotting File:  C:\USEPA\BMDS2\Temp\tmp121.plt
                                                Fri Nov 14 14:22:26 2008
=====================================================================

BMDS Model Run
~~~~~~~~~~~~~~~~~~~~~~~~~~~~~~~~~~~~~~~~~~~~~~~~~~~~~~~~~~~~~~~~~~~~~~~

  The form of the probability function is:

  P[response] = background + (1-background)*[1-EXP(
               -beta1*dose^1)]

  The parameter betas are restricted to be positive


  Dependent variable = Response
  Independent variable = DOSE

Total number of observations = 4
Total number of records with missing values = 0
Total number of parameters in model = 2
Total number of specified parameters = 0
Degree of polynomial = 1


Maximum number of iterations = 250
Relative Function Convergence has been set to: 1e-008
Parameter Convergence has been set to: 1e-008
```

Default Initial Parameter Values
Background = 0.0536508
Beta(1) = 0.018443

Asymptotic Correlation Matrix of Parameter Estimates

	Background	Beta(1)
Background	1	-0.71
Beta(1)	-0.71	1

Parameter Estimates

Variable	Estimate	Std. Err.	95.0% Wald Confidence Interval Lower Conf. Limit	Upper Conf. Limit
Background	0.0444165	*	*	*
Beta(1)	0.0201613	*	*	*

* - Indicates that this value is not calculated.

Analysis of Deviance Table

Model	Log(likelihood)	# Param's	Deviance	Test d.f.	P-value
Full model	-76.0086	4			
Fitted model	-76.2255	2	0.433714	2	0.805
Reduced model	-82.7874	1	13.5576	3	0.003574

AIC: 156.451

Goodness of Fit

Dose	Est._Prob.	Expected	Observed	Size	Scaled Residual
0.0000	0.0444	2.221	2.000	50	-0.152
1.8000	0.0785	3.924	4.000	50	0.040
7.1000	0.1719	8.593	10.000	50	0.527
14.3000	0.2838	14.188	13.000	50	-0.373

Chi^2 = 0.44 d.f. = 2 P-value = 0.8019

Benchmark Dose Computation

Specified effect = 0.05

Risk Type = Extra risk

Confidence level = 0.95

BMD = 2.54415

BMDL = 1.68095

BMDU = 4.75191

Taken together, (1.68095, 4.75191) is a 90 % two-sided confidence interval for the BMD

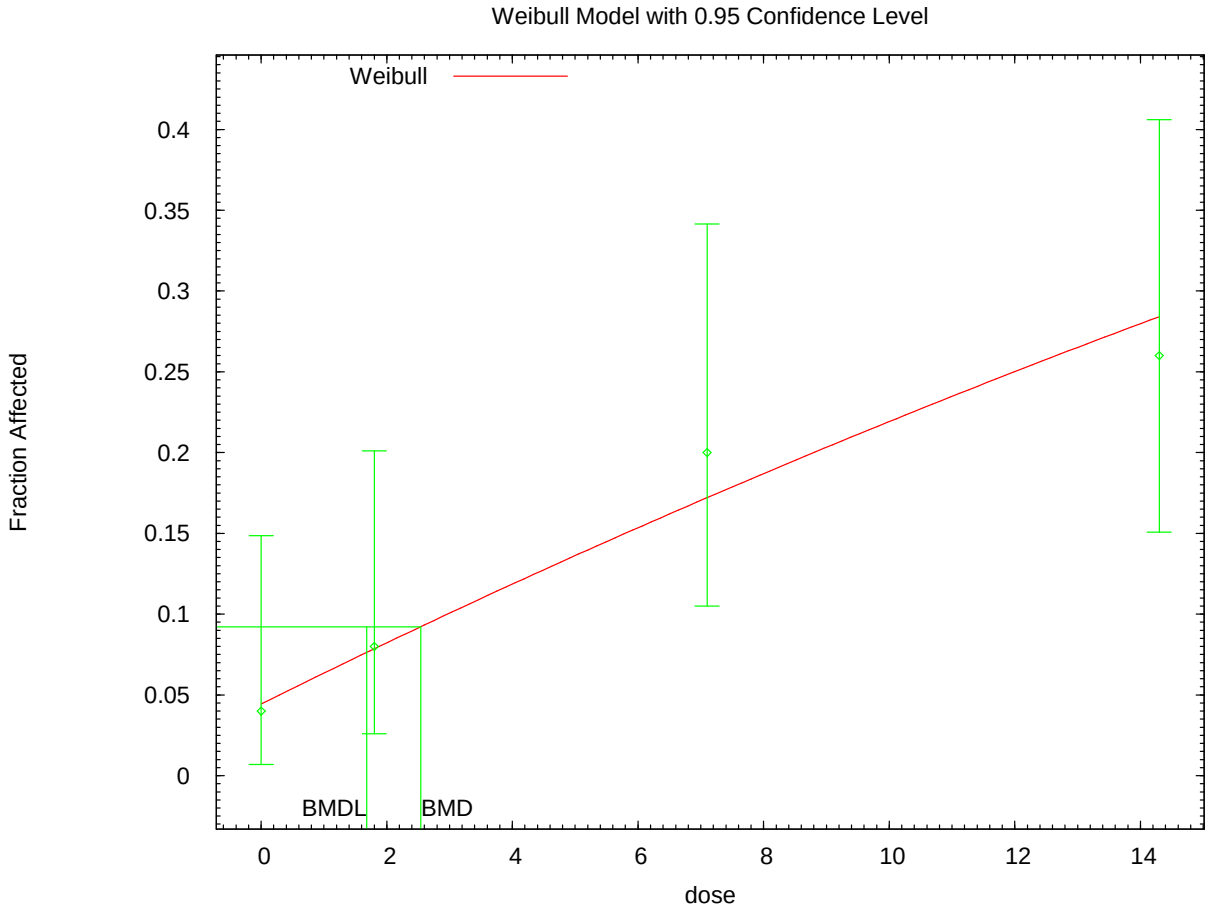

14:36 11/14 2008

```
================================================================
        Weibull Model using Weibull Model (Version: 2.12;  Date: 05/16/2008)
        Input Data File: C:\USEPA\BMDS2\Temp\tmp127.(d)
        Gnuplot Plotting File:  C:\USEPA\BMDS2\Temp\tmp127.plt
                                                Fri Nov 14 14:36:13 2008
================================================================

BMDS Model Run
~~~~~~~~~~~~~~~~~~~~~~~~~~~~~~~~~~~~~~~~~~~~~~~~~~~~~~~~~~~~~~~~~~~~~~~

  The form of the probability function is:

  P[response] = background + (1-background)*[1-EXP(-slope*dose^power)]


  Dependent variable = Response
  Independent variable = DOSE
  Power parameter is restricted as power >=1

  Total number of observations = 4
  Total number of records with missing values = 0
  Maximum number of iterations = 250
  Relative Function Convergence has been set to: 1e-008
  Parameter Convergence has been set to: 1e-008


                Default Initial (and Specified) Parameter Values
                   Background =    0.0490196
                        Slope =    0.0179876
                        Power =            1


          Asymptotic Correlation Matrix of Parameter Estimates
```

(*** The model parameter(s) -Power
have been estimated at a boundary point, or have been specified by the user,
and do not appear in the correlation matrix)

	Background	Slope
Background	1	-0.53
Slope	-0.53	1

Parameter Estimates

Variable	Estimate	Std. Err.	95.0% Wald Confidence Interval Lower Conf. Limit	Upper Conf. Limit
Background	0.0444162	0.0255203	-0.00560266	0.0944351
Slope	0.0201613	0.00593763	0.00852374	0.0317988
Power	1	NA		

NA - Indicates that this parameter has hit a bound
implied by some inequality constraint and thus
has no standard error.

Analysis of Deviance Table

Model	Log(likelihood)	# Param's	Deviance	Test d.f.	P-value
Full model	-76.0086	4			
Fitted model	-76.2255	2	0.433714	2	0.805
Reduced model	-82.7874	1	13.5576	3	0.003574

AIC: 156.451

Goodness of Fit

Dose	Est._Prob.	Expected	Observed	Size	Scaled Residual
0.0000	0.0444	2.221	2.000	50	-0.152
1.8000	0.0785	3.924	4.000	50	0.040
7.1000	0.1719	8.593	10.000	50	0.527
14.3000	0.2838	14.188	13.000	50	-0.373

Chi^2 = 0.44 d.f. = 2 P-value = 0.8019

Benchmark Dose Computation

Specified effect = 0.05

Risk Type = Extra risk

Confidence level = 0.95

BMD = 2.54415

BMDL = 1.68095

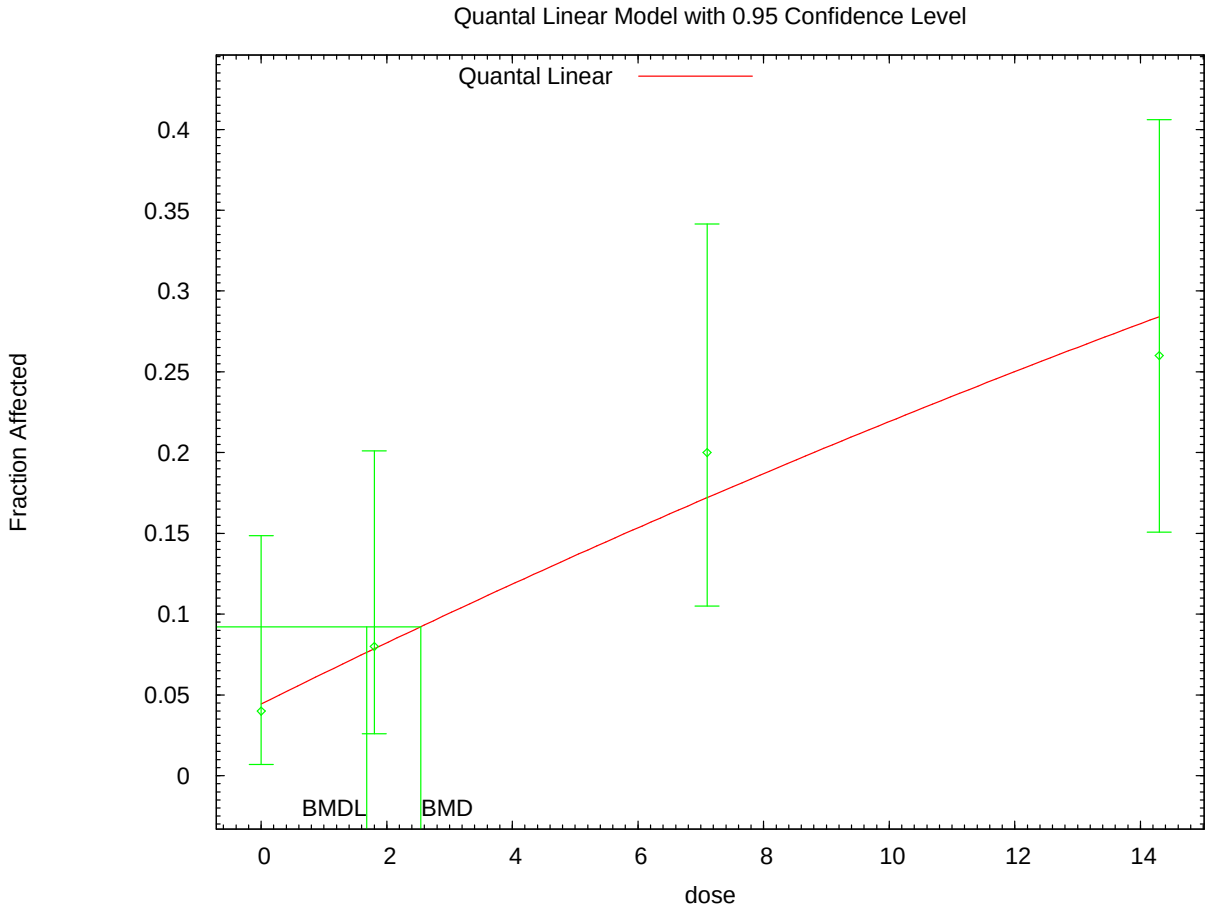

14:42 11/14 2008

```
=================================================================
        Quantal Linear Model using Weibull Model (Version: 2.12;  Date: 05/16/2008)
        Input Data File: C:\USEPA\BMDS2\Temp\tmp12A.(d)
        Gnuplot Plotting File:  C:\USEPA\BMDS2\Temp\tmp12A.plt
                                                Fri Nov 14 14:42:54 2008
=================================================================

BMDS Model Run
~~~~~~~~~~~~~~~~~~~~~~~~~~~~~~~~~~~~~~~~~~~~~~~~~~~~~~~~~~~~~~~~~~~~~

  The form of the probability function is:

  P[response] = background + (1-background)*[1-EXP(-slope*dose)]


  Dependent variable = Response
  Independent variable = DOSE

  Total number of observations = 4
  Total number of records with missing values = 0
  Maximum number of iterations = 250
  Relative Function Convergence has been set to: 1e-008
  Parameter Convergence has been set to: 1e-008


                Default Initial (and Specified) Parameter Values
                   Background =    0.0490196
                        Slope =    0.0179876
                        Power =            1   Specified


          Asymptotic Correlation Matrix of Parameter Estimates
```

(*** The model parameter(s) -Power
have been estimated at a boundary point, or have been specified by the user,
and do not appear in the correlation matrix)

	Background	Slope
Background	1	-0.53
Slope	-0.53	1

Parameter Estimates

Variable	Estimate	Std. Err.	95.0% Wald Confidence Interval Lower Conf. Limit	Upper Conf. Limit
Background	0.0444162	0.0255203	-0.00560266	0.0944351
Slope	0.0201613	0.00593763	0.00852374	0.0317988

Analysis of Deviance Table

Model	Log(likelihood)	# Param's	Deviance	Test d.f.	P-value
Full model	-76.0086	4			
Fitted model	-76.2255	2	0.433714	2	0.805
Reduced model	-82.7874	1	13.5576	3	0.003574

AIC: 156.451

Goodness of Fit

Dose	Est._Prob.	Expected	Observed	Size	Scaled Residual
0.0000	0.0444	2.221	2.000	50	-0.152
1.8000	0.0785	3.924	4.000	50	0.040
7.1000	0.1719	8.593	10.000	50	0.527
14.3000	0.2838	14.188	13.000	50	-0.373

Chi^2 = 0.44 d.f. = 2 P-value = 0.8019

Benchmark Dose Computation

Specified effect = 0.05

Risk Type = Extra risk

Confidence level = 0.95

BMD = 2.54415

BMDL = 1.68095

B6C3F$_1$ Female Mice: Forestomach lesions (administered dose)

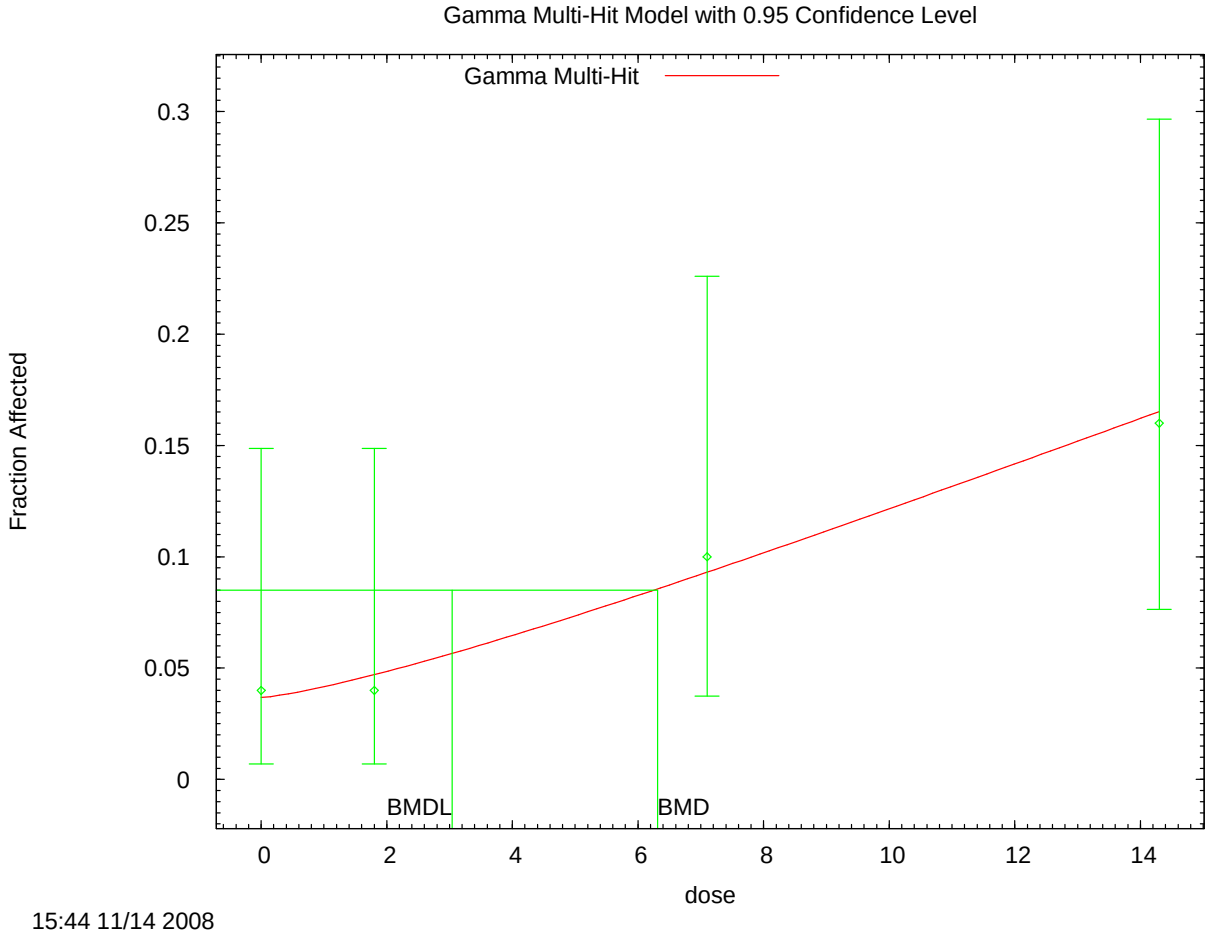

15:44 11/14 2008

```
 ================================================================
         Gamma Model. (Version: 2.13;  Date: 05/16/2008)
         Input Data File: C:\USEPA\BMDS2\Temp\tmp131.(d)
         Gnuplot Plotting File:  C:\USEPA\BMDS2\Temp\tmp131.plt
                                                Fri Nov 14 15:44:47 2008
 ================================================================

 BMDS Model Run
~~~~~~~~~~~~~~~~~~~~~~~~~~~~~~~~~~~~~~~~~~~~~~~~~~~~~~~~~~~~~~~~~~~~~~~

   The form of the probability function is:

   P[response]= background+(1-background)*CumGamma[slope*dose,power],
   where CumGamma(.) is the cummulative Gamma distribution function


   Dependent variable = Response
   Independent variable = DOSE
   Power parameter is restricted as power >=1

   Total number of observations = 4
   Total number of records with missing values = 0
   Maximum number of iterations = 250
   Relative Function Convergence has been set to: 1e-008
   Parameter Convergence has been set to: 1e-008


                  Default Initial (and Specified) Parameter Values
                     Background =    0.0490196
                          Slope =    0.0133015
```

Power = 1.18093

Asymptotic Correlation Matrix of Parameter Estimates

	Background	Slope	Power
Background	1	0.39	0.47
Slope	0.39	1	0.99
Power	0.47	0.99	1

Parameter Estimates

Variable	Estimate	Std. Err.	95.0% Wald Confidence Interval Lower Conf. Limit	Upper Conf. Limit
Background	0.0367793	0.0231276	-0.00854987	0.0821085
Slope	0.0180646	0.0405793	-0.0614694	0.0975986
Power	1.28374	1.22475	-1.11674	3.68421

Analysis of Deviance Table

Model	Log(likelihood)	# Param's	Deviance	Test d.f.	P-value
Full model	-55.0321	4			
Fitted model	-55.0866	3	0.109064	1	0.7412
Reduced model	-58.1629	1	6.26165	3	0.09955

AIC: 116.173

Goodness of Fit

Dose	Est._Prob.	Expected	Observed	Size	Scaled Residual
0.0000	0.0368	1.839	2.000	50	0.121
1.8000	0.0468	2.342	2.000	50	-0.229
7.1000	0.0924	4.618	5.000	50	0.187
14.3000	0.1639	8.197	8.000	50	-0.075

Chi^2 = 0.11 d.f. = 1 P-value = 0.7429

Benchmark Dose Computation

Specified effect = 0.05

Risk Type = Extra risk

Confidence level = 0.95

BMD = 6.31104

BMDL = 3.03872

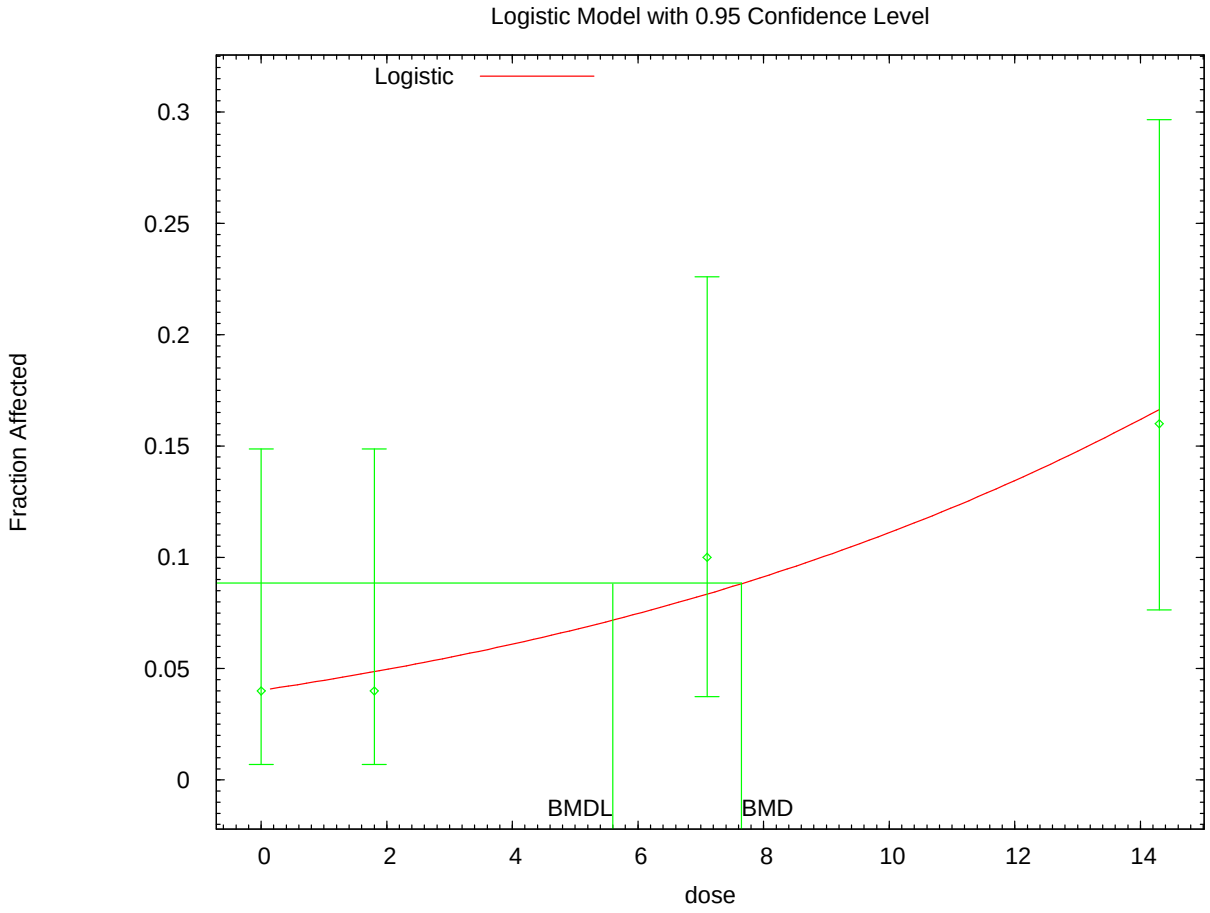

15:48 11/14 2008

```
================================================================
        Logistic Model. (Version: 2.12; Date: 05/16/2008)
        Input Data File: C:\USEPA\BMDS2\Temp\tmp134.(d)
        Gnuplot Plotting File:  C:\USEPA\BMDS2\Temp\tmp134.plt
                                              Fri Nov 14 15:48:45 2008
================================================================

BMDS Model Run
~~~~~~~~~~~~~~~~~~~~~~~~~~~~~~~~~~~~~~~~~~~~~~~~~~~~~~~~~~~~~~~~~~~~

  The form of the probability function is:

  P[response] = 1/[1+EXP(-intercept-slope*dose)]


  Dependent variable = Response
  Independent variable = DOSE
  Slope parameter is not restricted

  Total number of observations = 4
  Total number of records with missing values = 0
  Maximum number of iterations = 250
  Relative Function Convergence has been set to: 1e-008
  Parameter Convergence has been set to: 1e-008


                Default Initial Parameter Values
                   background =            0   Specified
                    intercept =     -3.00612
                        slope =     0.102222


          Asymptotic Correlation Matrix of Parameter Estimates
```

(*** The model parameter(s) -background
have been estimated at a boundary point, or have been specified by the user,
and do not appear in the correlation matrix)

	intercept	slope
intercept	1	-0.84
slope	-0.84	1

Parameter Estimates

Variable	Estimate	Std. Err.	95.0% Wald Confidence Interval Lower Conf. Limit	Upper Conf. Limit
intercept	-3.16594	0.471287	-4.08965	-2.24224
slope	0.108988	0.0453905	0.0200238	0.197951

Analysis of Deviance Table

Model	Log(likelihood)	# Param's	Deviance	Test d.f.	P-value
Full model	-55.0321	4			
Fitted model	-55.1666	2	0.269	2	0.8742
Reduced model	-58.1629	1	6.26165	3	0.09955

AIC: 114.333

Goodness of Fit

Dose	Est._Prob.	Expected	Observed	Size	Scaled Residual
0.0000	0.0405	2.023	2.000	50	-0.017
1.8000	0.0488	2.441	2.000	50	-0.289
7.1000	0.0838	4.189	5.000	50	0.414
14.3000	0.1669	8.347	8.000	50	-0.132

Chi^2 = 0.27 d.f. = 2 P-value = 0.8725

Benchmark Dose Computation

Specified effect = 0.05

Risk Type = Extra risk

Confidence level = 0.95

BMD = 7.64457

BMDL = 5.59724

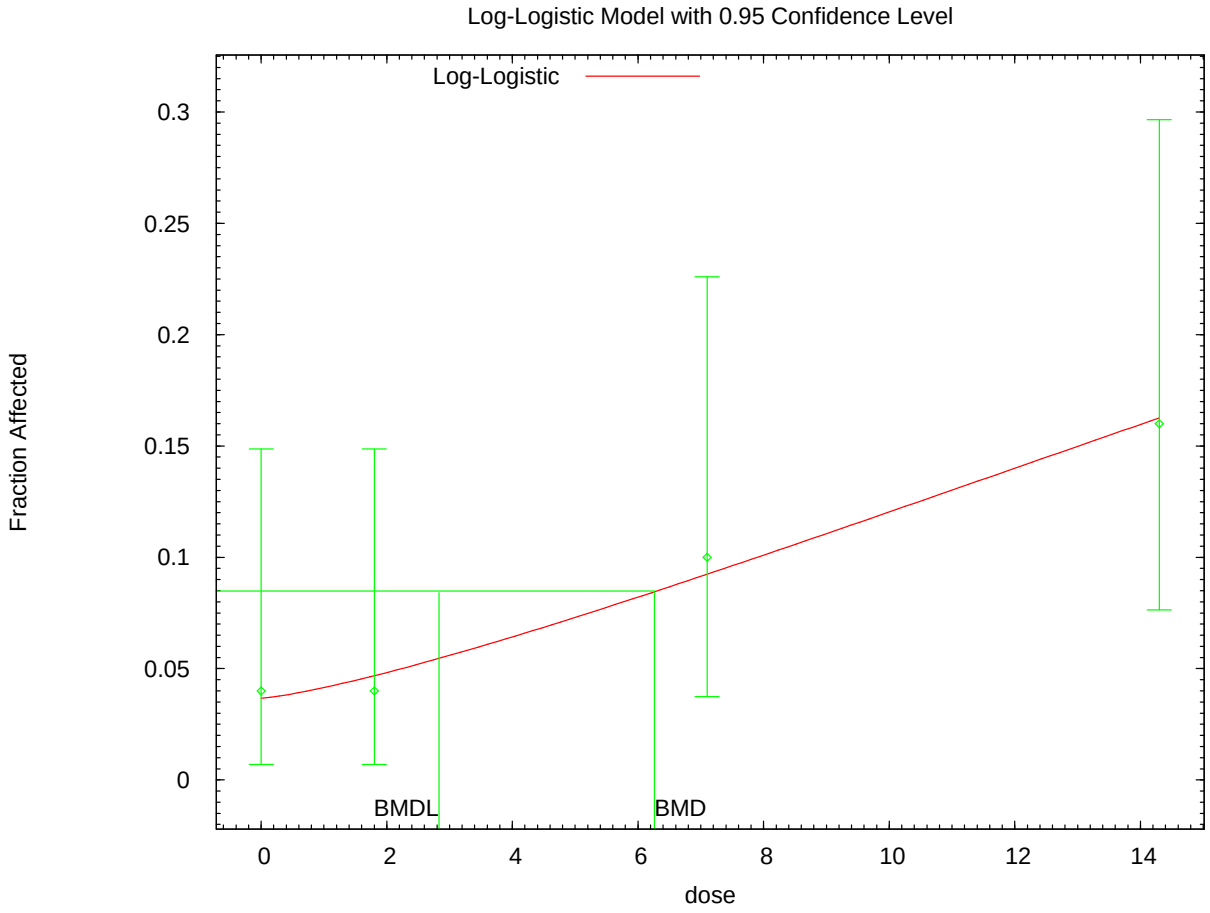

15:51 11/14 2008

```
=================================================================
        Logistic Model. (Version: 2.12; Date: 05/16/2008)
        Input Data File: C:\USEPA\BMDS2\Temp\tmp137.(d)
        Gnuplot Plotting File:  C:\USEPA\BMDS2\Temp\tmp137.plt
                                                Fri Nov 14 15:51:59 2008
=================================================================

BMDS Model Run
~~~~~~~~~~~~~~~~~~~~~~~~~~~~~~~~~~~~~~~~~~~~~~~~~~~~~~~~~~~~~~~~~~~~~

  The form of the probability function is:

  P[response] = background+(1-background)/[1+EXP(-intercept-slope*Log(dose))]


  Dependent variable = Response
  Independent variable = DOSE
  Slope parameter is restricted as slope >= 1

  Total number of observations = 4
  Total number of records with missing values = 0
  Maximum number of iterations = 250
  Relative Function Convergence has been set to: 1e-008
  Parameter Convergence has been set to: 1e-008


  User has chosen the log transformed model


               Default Initial Parameter Values
                  background =         0.04
                   intercept =     -5.35004
                       slope =      1.30201
```

Asymptotic Correlation Matrix of Parameter Estimates

	background	intercept	slope
background	1	-0.53	0.46
intercept	-0.53	1	-0.98
slope	0.46	-0.98	1

Parameter Estimates

Variable	Estimate	Std. Err.	95.0% Wald Confidence Interval Lower Conf. Limit	Upper Conf. Limit
background	0.0366811	*	*	*
intercept	-5.29891	*	*	*
slope	1.2835	*	*	*

* - Indicates that this value is not calculated.

Analysis of Deviance Table

Model	Log(likelihood)	# Param's	Deviance	Test d.f.	P-value
Full model	-55.0321	4			
Fitted model	-55.0846	3	0.104995	1	0.7459
Reduced model	-58.1629	1	6.26165	3	0.09955

AIC: 116.169

Goodness of Fit

Dose	Est._Prob.	Expected	Observed	Size	Scaled Residual
0.0000	0.0367	1.834	2.000	50	0.125
1.8000	0.0468	2.340	2.000	50	-0.228
7.1000	0.0928	4.639	5.000	50	0.176
14.3000	0.1637	8.186	8.000	50	-0.071

Chi^2 = 0.10 d.f. = 1 P-value = 0.7477

Benchmark Dose Computation

Specified effect = 0.05

Risk Type = Extra risk

Confidence level = 0.95

BMD = 6.26147

BMDL = 2.83097

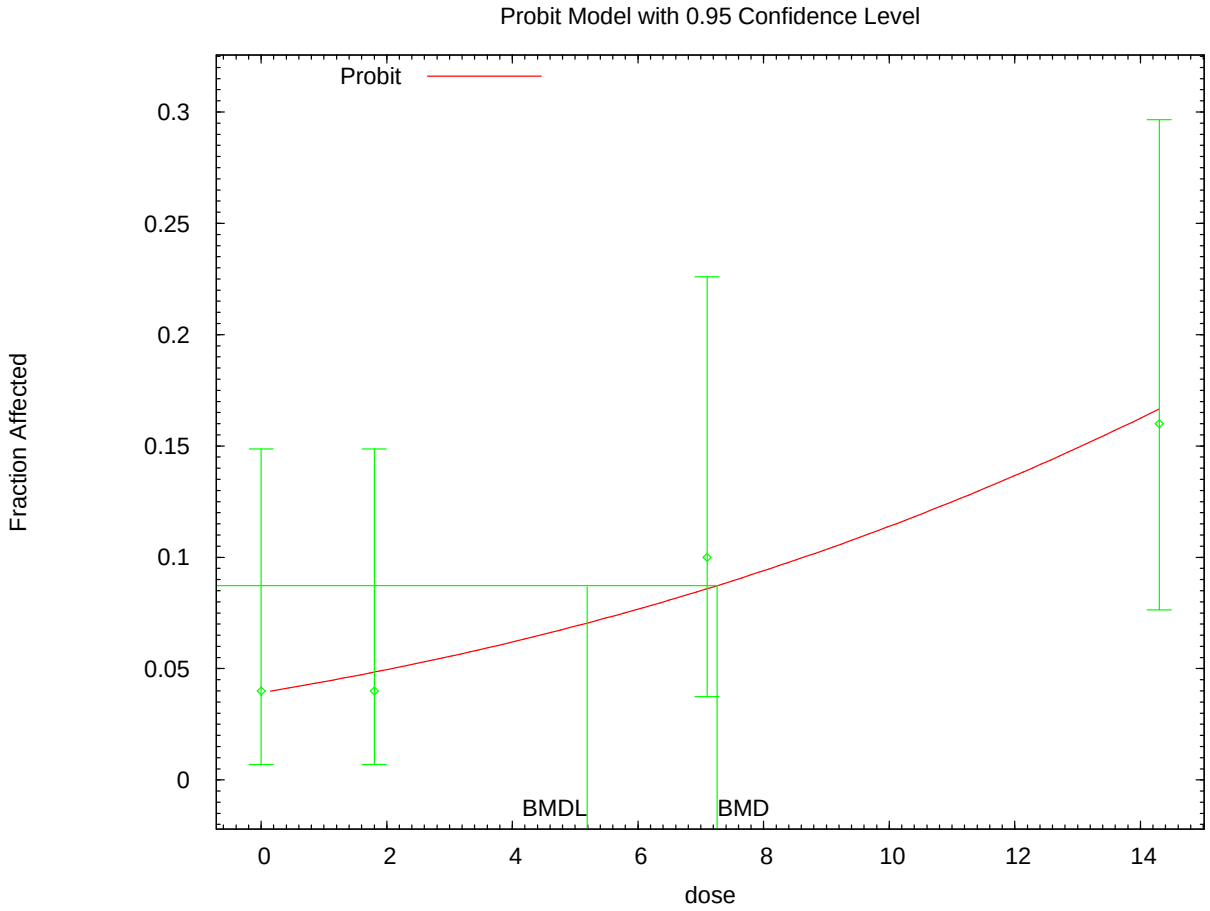


```
================================================================
       Probit Model. (Version: 3.1;  Date: 05/16/2008)
       Input Data File: C:\USEPA\BMDS2\Temp\tmp140.(d)
       Gnuplot Plotting File:  C:\USEPA\BMDS2\Temp\tmp140.plt
                                    Fri Nov 14 16:05:36 2008
================================================================

BMDS Model Run
~~~~~~~~~~~~~~~~~~~~~~~~~~~~~~~~~~~~~~~~~~~~~~~~~~~~~~~~~~~~~~~~

   The form of the probability function is:

  P[response] = CumNorm(Intercept+Slope*Dose),

  where CumNorm(.) is the cumulative normal distribution function


  Dependent variable = Response
  Independent variable = DOSE
  Slope parameter is not restricted

  Total number of observations = 4
  Total number of records with missing values = 0
  Maximum number of iterations = 250
  Relative Function Convergence has been set to: 1e-008
  Parameter Convergence has been set to: 1e-008


                Default Initial (and Specified) Parameter Values
                   background =           0   Specified
```

```
                    intercept =     -1.75537
                        slope =    0.0561083


          Asymptotic Correlation Matrix of Parameter Estimates

          ( *** The model parameter(s)  -background
                have been estimated at a boundary point, or have been specified by the user,
                and do not appear in the correlation matrix )

             intercept        slope

intercept            1         -0.8

    slope         -0.8            1


                                Parameter Estimates

                                                        95.0% Wald Confidence Interval
      Variable         Estimate        Std. Err.     Lower Conf. Limit   Upper Conf. Limit
     intercept          -1.7601         0.219358           -2.19003            -1.33017
         slope        0.0553914        0.0228374          0.0106309            0.100152


                       Analysis of Deviance Table

      Model      Log(likelihood)  # Param's  Deviance  Test d.f.   P-value
    Full model         -55.0321         4
  Fitted model         -55.1419         2      0.219734      2           0.896
 Reduced model         -58.1629         1       6.26165      3         0.09955

          AIC:          114.284


                               Goodness  of  Fit
                                                                    Scaled
    Dose     Est._Prob.    Expected    Observed     Size       Residual
  ---------------------------------------------------------------------------
   0.0000     0.0392         1.960     2.000          50         0.029
   1.8000     0.0484         2.421     2.000          50        -0.277
   7.1000     0.0858         4.292     5.000          50         0.357
  14.3000     0.1665         8.326     8.000          50        -0.124

 Chi^2 = 0.22      d.f. = 2        P-value = 0.8955


   Benchmark Dose Computation

Specified effect =           0.05

Risk Type        =      Extra risk

Confidence level =           0.95

             BMD =         7.2597

            BMDL =        5.19213
```

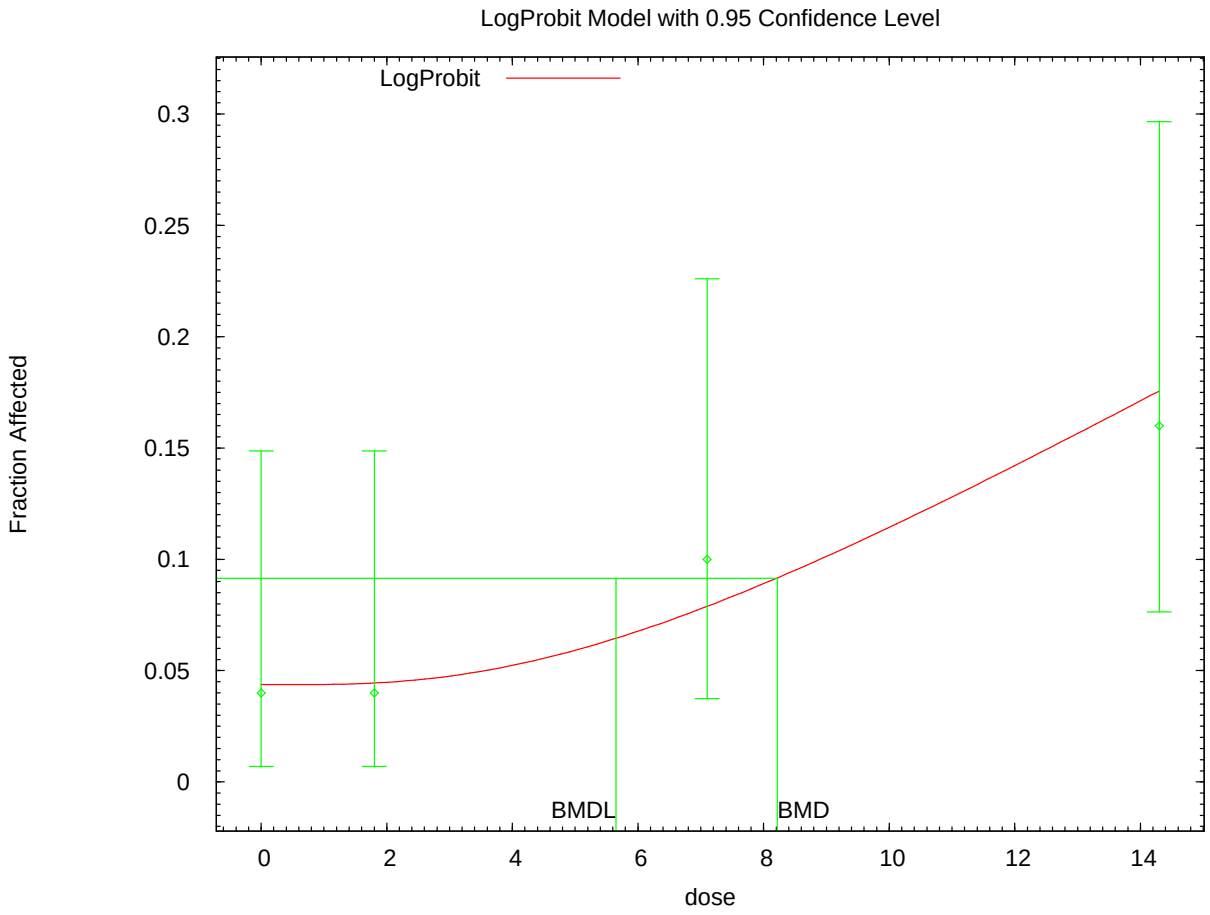

15:56 11/14 2008

```
=================================================================
        Probit Model. (Version: 3.1;  Date: 05/16/2008)
        Input Data File: C:\USEPA\BMDS2\Temp\tmp13A.(d)
        Gnuplot Plotting File:  C:\USEPA\BMDS2\Temp\tmp13A.plt
                                                Fri Nov 14 15:56:14 2008
=================================================================

BMDS Model Run
~~~~~~~~~~~~~~~~~~~~~~~~~~~~~~~~~~~~~~~~~~~~~~~~~~~~~~~~~~~~~~~~~~~~~

  The form of the probability function is:

  P[response] = Background
              + (1-Background) * CumNorm(Intercept+Slope*Log(Dose)),

  where CumNorm(.) is the cumulative normal distribution function


  Dependent variable = Response
  Independent variable = DOSE
  Slope parameter is restricted as slope >= 1

  Total number of observations = 4
  Total number of records with missing values = 0
  Maximum number of iterations = 250
  Relative Function Convergence has been set to: 1e-008
  Parameter Convergence has been set to: 1e-008


  User has chosen the log transformed model


                Default Initial (and Specified) Parameter Values
```

```
                    background =         0.04
                     intercept =     -3.50754
                         slope =            1


          Asymptotic Correlation Matrix of Parameter Estimates

          ( *** The model parameter(s)  -slope
                have been estimated at a boundary point, or have been specified by the user,
                and do not appear in the correlation matrix )

            background    intercept

background            1        -0.51

 intercept        -0.51            1


                                Parameter Estimates

                                                        95.0% Wald Confidence Interval
      Variable         Estimate        Std. Err.     Lower Conf. Limit   Upper Conf. Limit
    background        0.0436672        0.0205583          0.00337363           0.0839607
     intercept         -3.75124         0.270066            -4.28056            -3.22192
         slope                1               NA

NA - Indicates that this parameter has hit a bound
     implied by some inequality constraint and thus
     has no standard error.


                       Analysis of Deviance Table

       Model      Log(likelihood)  # Param's  Deviance  Test d.f.   P-value
     Full model        -55.0321         4
   Fitted model        -55.2386         2      0.413147      2          0.8134
  Reduced model        -58.1629         1       6.26165      3         0.09955

          AIC:         114.477

                                  Goodness  of  Fit
                                                                      Scaled
     Dose     Est._Prob.    Expected    Observed     Size       Residual
  ---------------------------------------------------------------------------
    0.0000     0.0437         2.183     2.000          50       -0.127
    1.8000     0.0444         2.221     2.000          50       -0.151
    7.1000     0.0787         3.935     5.000          50        0.559
   14.3000     0.1753         8.765     8.000          50       -0.284

 Chi^2 = 0.43      d.f. = 2        P-value = 0.8054


   Benchmark Dose Computation

Specified effect =           0.05

Risk Type        =      Extra risk

Confidence level =           0.95

             BMD =        8.21852

            BMDL =        5.64968
```

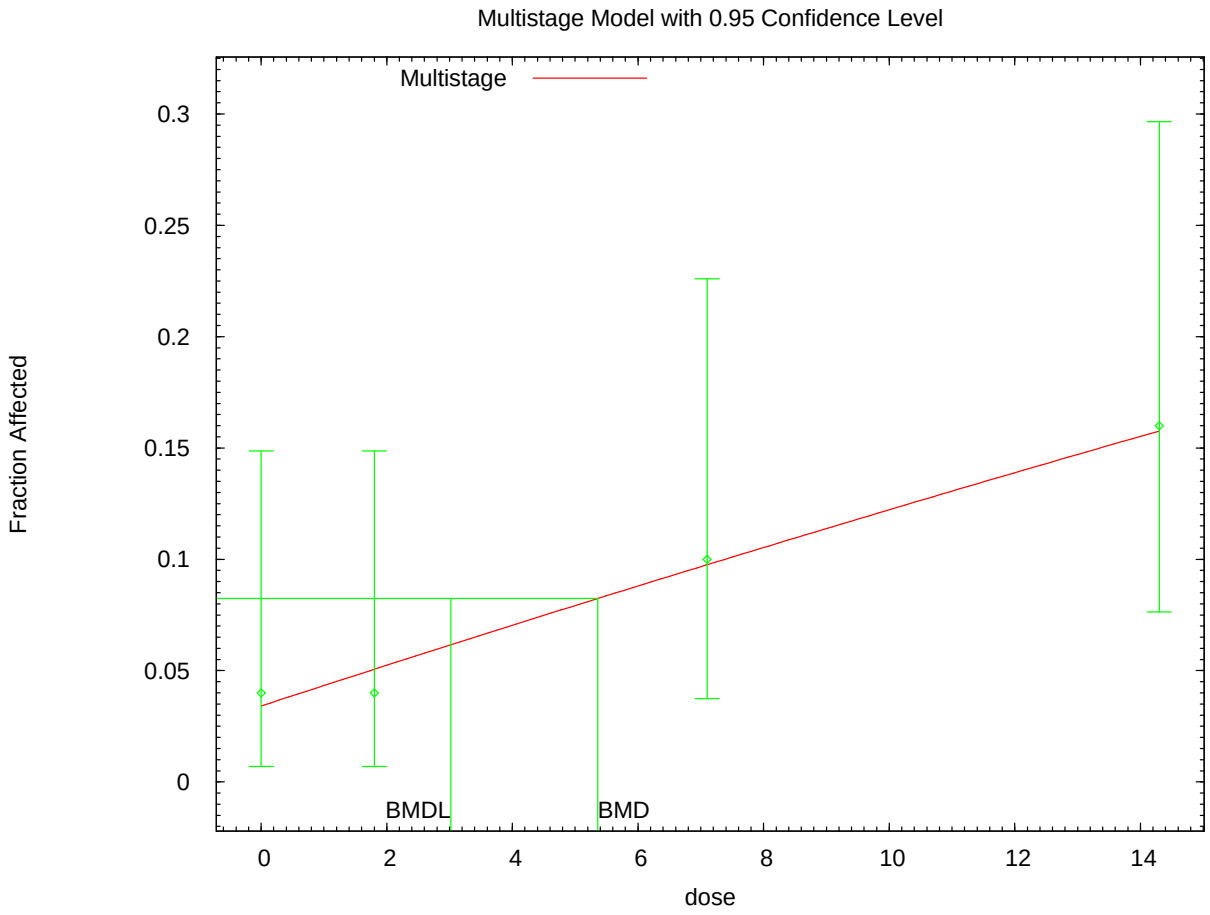

16:01 11/14 2008

```
==========================================================================
        Multistage Model. (Version: 3.0;  Date: 05/16/2008)
        Input Data File: C:\USEPA\BMDS2\Temp\tmp13D.(d)
        Gnuplot Plotting File:  C:\USEPA\BMDS2\Temp\tmp13D.plt
                                                  Fri Nov 14 16:01:58 2008
==========================================================================

BMDS Model Run
~~~~~~~~~~~~~~~~~~~~~~~~~~~~~~~~~~~~~~~~~~~~~~~~~~~~~~~~~~~~~~~~~~~~~~~~~~

  The form of the probability function is:

  P[response] = background + (1-background)*[1-EXP(
               -beta1*dose^1)]

  The parameter betas are restricted to be positive


  Dependent variable = Response
  Independent variable = DOSE

Total number of observations = 4
Total number of records with missing values = 0
Total number of parameters in model = 2
Total number of specified parameters = 0
Degree of polynomial = 1


Maximum number of iterations = 250
Relative Function Convergence has been set to: 1e-008
Parameter Convergence has been set to: 1e-008
```

Default Initial Parameter Values
Background = 0.032589
Beta(1) = 0.00986338

Asymptotic Correlation Matrix of Parameter Estimates

	Background	Beta(1)
Background	1	-0.7
Beta(1)	-0.7	1

Parameter Estimates

Variable	Estimate	Std. Err.	95.0% Wald Confidence Interval Lower Conf. Limit	Upper Conf. Limit
Background	0.0341442	*	*	*
Beta(1)	0.00957473	*	*	*

* - Indicates that this value is not calculated.

Analysis of Deviance Table

Model	Log(likelihood)	# Param's	Deviance	Test d.f.	P-value
Full model	-55.0321	4			
Fitted model	-55.1226	2	0.181118	2	0.9134
Reduced model	-58.1629	1	6.26165	3	0.09955

AIC: 114.245

Goodness of Fit

Dose	Est._Prob.	Expected	Observed	Size	Scaled Residual
0.0000	0.0341	1.707	2.000	50	0.228
1.8000	0.0506	2.532	2.000	50	-0.343
7.1000	0.0976	4.881	5.000	50	0.057
14.3000	0.1577	7.887	8.000	50	0.044

Chi^2 = 0.18 d.f. = 2 P-value = 0.9162

Benchmark Dose Computation

Specified effect = 0.05

Risk Type = Extra risk

Confidence level = 0.95

BMD = 5.35715

BMDL = 3.01931

BMDU = 16.4514

Taken together, (3.01931, 16.4514) is a 90 % two-sided confidence interval for the BMD

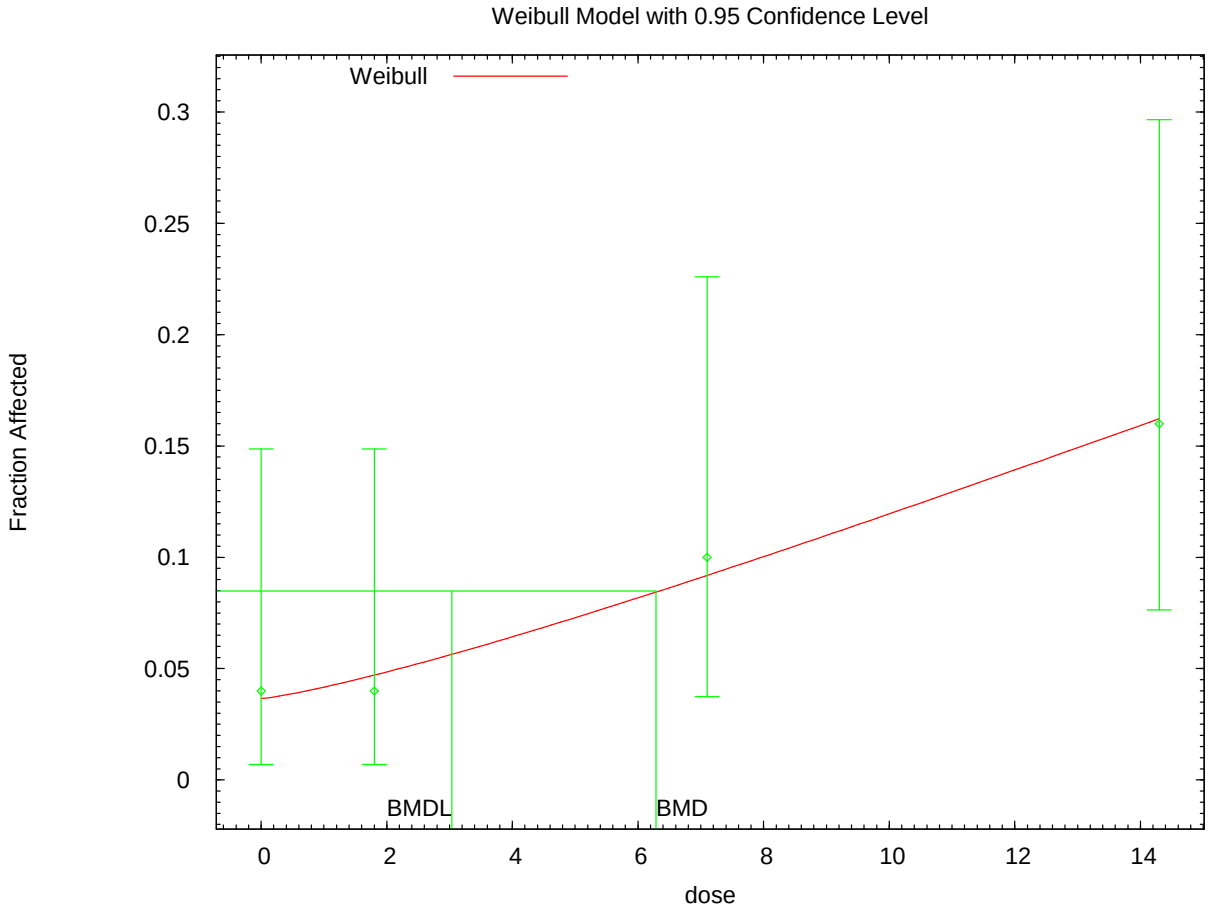

16:09 11/14 2008

```
=================================================================
        Weibull Model using Weibull Model (Version: 2.12;  Date: 05/16/2008)
        Input Data File: C:\USEPA\BMDS2\Temp\tmp143.(d)
        Gnuplot Plotting File:  C:\USEPA\BMDS2\Temp\tmp143.plt
                                                Fri Nov 14 16:09:11 2008
=================================================================

BMDS Model Run
~~~~~~~~~~~~~~~~~~~~~~~~~~~~~~~~~~~~~~~~~~~~~~~~~~~~~~~~~~~~~~~~~~~~~

  The form of the probability function is:

  P[response] = background + (1-background)*[1-EXP(-slope*dose^power)]


  Dependent variable = Response
  Independent variable = DOSE
  Power parameter is restricted as power >=1

  Total number of observations = 4
  Total number of records with missing values = 0
  Maximum number of iterations = 250
  Relative Function Convergence has been set to: 1e-008
  Parameter Convergence has been set to: 1e-008


                Default Initial (and Specified) Parameter Values
                   Background =    0.0490196
                        Slope =   0.00467913
                        Power =      1.25557


          Asymptotic Correlation Matrix of Parameter Estimates
```

	Background	Slope	Power
Background	1	-0.54	0.47
Slope	-0.54	1	-0.99
Power	0.47	-0.99	1

Parameter Estimates

Variable	Estimate	Std. Err.	95.0% Wald Confidence Interval Lower Conf. Limit	Upper Conf. Limit
Background	0.0366324	0.0230239	-0.00849362	0.0817585
Slope	0.00530377	0.0138578	-0.021857	0.0324646
Power	1.23448	1.00512	-0.735513	3.20447

Analysis of Deviance Table

Model	Log(likelihood)	# Param's	Deviance	Test d.f.	P-value
Full model	-55.0321	4			
Fitted model	-55.0891	3	0.114024	1	0.7356
Reduced model	-58.1629	1	6.26165	3	0.09955

AIC: 116.178

Goodness of Fit

Dose	Est._Prob.	Expected	Observed	Size	Scaled Residual
0.0000	0.0366	1.832	2.000	50	0.127
1.8000	0.0471	2.357	2.000	50	-0.238
7.1000	0.0924	4.620	5.000	50	0.186
14.3000	0.1638	8.188	8.000	50	-0.072

Chi^2 = 0.11 d.f. = 1 P-value = 0.7375

Benchmark Dose Computation

Specified effect = 0.05

Risk Type = Extra risk

Confidence level = 0.95

BMD = 6.28482

BMDL = 3.03737

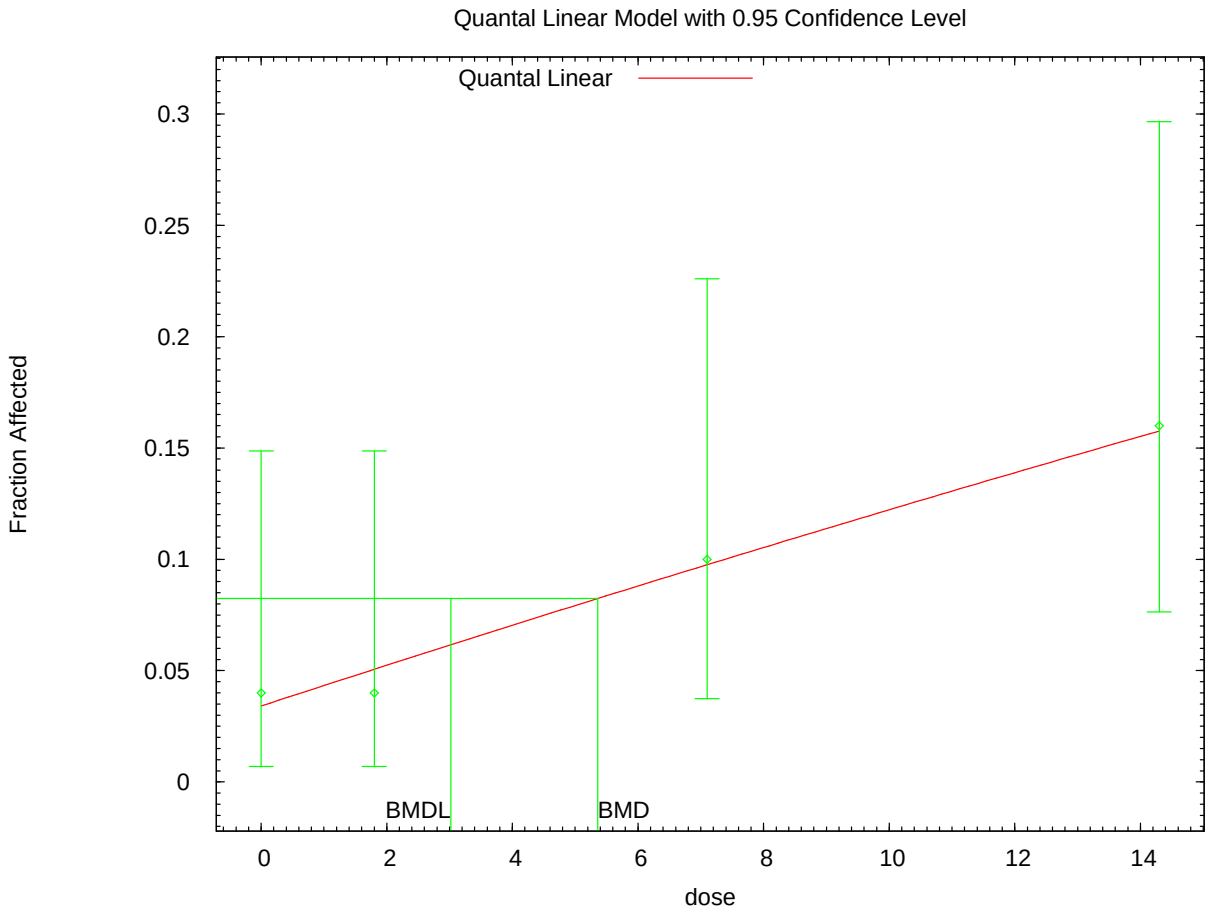

16:13 11/14 2008

```
================================================================================
        Quantal Linear Model using Weibull Model (Version: 2.12;  Date: 05/16/2008)
        Input Data File: C:\USEPA\BMDS2\Temp\tmp146.(d)
        Gnuplot Plotting File:  C:\USEPA\BMDS2\Temp\tmp146.plt
                                                  Fri Nov 14 16:13:01 2008
================================================================================

BMDS Model Run
~~~~~~~~~~~~~~~~~~~~~~~~~~~~~~~~~~~~~~~~~~~~~~~~~~~~~~~~~~~~~~~~~~~~~~~~~~~~~~~~

  The form of the probability function is:

  P[response] = background + (1-background)*[1-EXP(-slope*dose)]


  Dependent variable = Response
  Independent variable = DOSE

  Total number of observations = 4
  Total number of records with missing values = 0
  Maximum number of iterations = 250
  Relative Function Convergence has been set to: 1e-008
  Parameter Convergence has been set to: 1e-008


                 Default Initial (and Specified) Parameter Values
                    Background =    0.0490196
                         Slope =   0.00923495
                         Power =            1   Specified


          Asymptotic Correlation Matrix of Parameter Estimates
```

(*** The model parameter(s) -Power
have been estimated at a boundary point, or have been specified by the user,
and do not appear in the correlation matrix)

	Background	Slope
Background	1	-0.53
Slope	-0.53	1

Parameter Estimates

Variable	Estimate	Std. Err.	95.0% Wald Confidence Interval Lower Conf. Limit	Upper Conf. Limit
Background	0.0341442	0.0203958	-0.00583081	0.0741193
Slope	0.00957473	0.00414213	0.0014563	0.0176932

Analysis of Deviance Table

Model	Log(likelihood)	# Param's	Deviance	Test d.f.	P-value
Full model	-55.0321	4			
Fitted model	-55.1226	2	0.181118	2	0.9134
Reduced model	-58.1629	1	6.26165	3	0.09955

AIC: 114.245

Goodness of Fit

Dose	Est._Prob.	Expected	Observed	Size	Scaled Residual
0.0000	0.0341	1.707	2.000	50	0.228
1.8000	0.0506	2.532	2.000	50	-0.343
7.1000	0.0976	4.881	5.000	50	0.057
14.3000	0.1577	7.887	8.000	50	0.044

Chi^2 = 0.18 d.f. = 2 P-value = 0.9162

Benchmark Dose Computation

Specified effect = 0.05

Risk Type = Extra risk

Confidence level = 0.95

BMD = 5.35715

BMDL = 3.01931

APPENDIX B-2. NONCANCER INHALATION DOSE-RESPONSE ASSESSMENT (RfC): BMD MODELING RESULTS EMPLOYING THE INCIDENCE DATA FOR NONNEOPLASTIC NASAL LESIONS IN RATS EXPOSED TO AN BY INHALATION FOR 2 YEARS (TABLES B-6 THROUGH B-9)

For these modeling exercises, a BMR of 10% extra risk was selected due to the limited number of rats in each exposure group. BMC and BMCL refer to the model-predicted concentration and its lower 95% confidence limit, respectively, associated with a 10% extra risk for developing the lesion.

Table B-6. Incidence data for selected nasal lesions in Sprague-Dawley rats exposed by inhalation to AN for 2 years

Nasal lesion	Exposure level (ppm)	Exposure level (mg/m^3)	HEC (mg/m^3)[a]	Incidence
Hyperplasia of mucus-secreting cells in males	0	0	0	0/11 (0%)
	20	43.4	2.1	7/12 (58%)[b]
	80	173.6	8.5	8/10 (80%)[b]
Flattening of respiratory epithelium in females	0	0	0	1/11 (9%)
	20	43.4	2.1	7/10 (70%)[b]
	80	173.6	8.5	8/10 (80%)[b]

[a]HEC as per U.S. EPA (1994b) methods for a category 1 gas producing an upper respiratory effect. Sample calculation: 43.4 mg/m^3 × 6h/24h × 5d/7d × $RGDR_{ET}$ = 2.1 mg/m^3, where $RGDR_{ET}$ = 0.275 = [VE/SA_{ET}] rat ÷ [VE/SA_{ET}] human; VE = minute volume = 0.281 L/min rat; 13.8 L/min human; and SA_{ET} = extrathoracic surface area = 5 cm^2 rat, 200 cm^2 human.
[b]Statistically significantly different from control value as reported by the authors.

Source: Quast et al. (1980b).

Table B-7. A summary of BMDS (version 1.3.2) modeling results based on incidence of hyperplasia of mucus-secreting cells in male Sprague-Dawley rats exposed to AN via inhalation for 2 years

Model	χ^2 *p*-value[a]	AIC	BMC_{10}[b] (mg/m^3)	$BMCL_{10}$[c] (mg/m^3)
Gamma	0.34	30.27	0.396	0.252
Logistic	0.02	38.05	1.17	0.718
Log-logistic	**0.94**	**28.43**	**0.187**	**0.082**
Multistage	0.34	30.27	0.396	0.252
Probit	0.01	37.99	1.17	0.776
Log-probit	0.37	29.98	0.625	0.382
Weibull	0.34	30.27	0.396	0.252

[a]χ^2 *p*-value from the χ^2 test for lack of fit. Values <0.1 fail to meet conventional goodness-of-fit criteria.
[b]BMC_{10} = BMC associated with 10% extra risk for nonneoplastic nasal lesions.
[c]$BMCL_{10}$ = 95% lower confidence limit on the BMC_{10} for nonneoplastic nasal lesions.

Source: Quast et al. (1980b).

BMDS (version 1.3.2) model output for the best-fit model (i.e., log-logistic) based on incidence of hyperplasia of mucus-secreting cells in male Sprague-Dawley rats exposed to AN via inhalation for 2 years

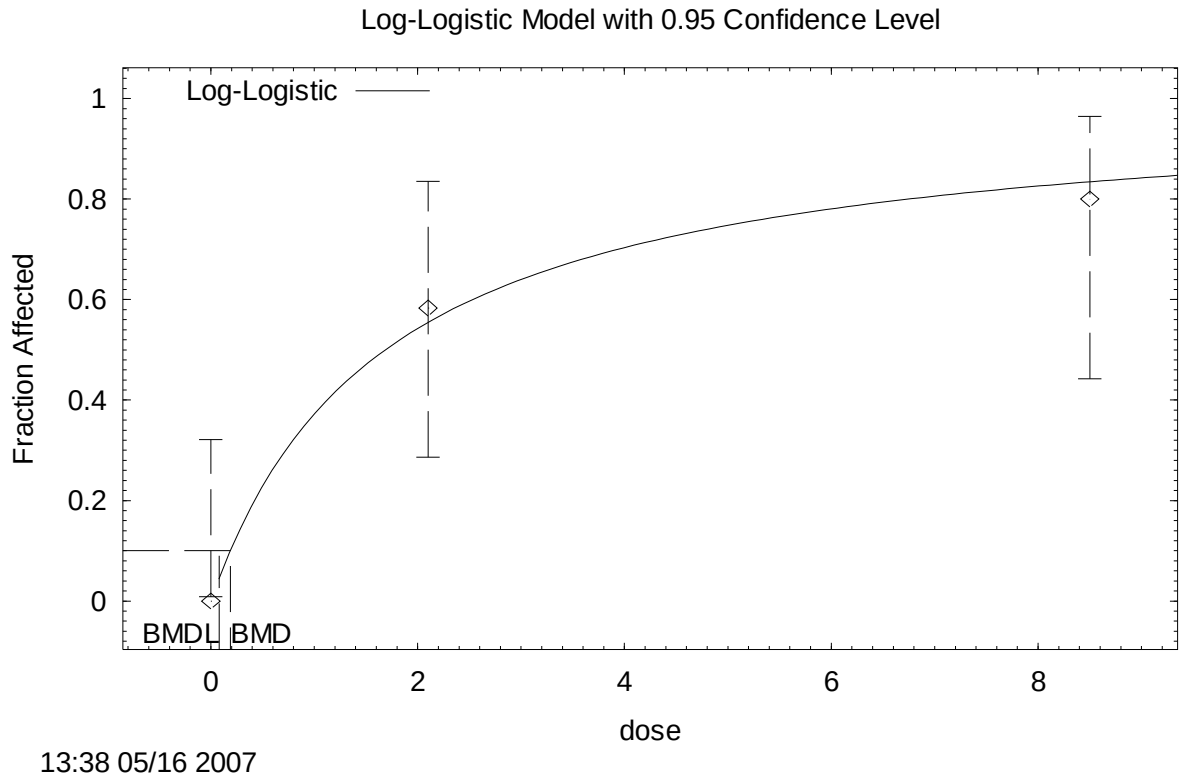


```
 ================================================================
         Logistic Model $Revision: 2.1 $ $Date: 2000/02/26 03:38:20 $
         Input Data File: G:\ACN DOSE-RESPONSE
MODELING\NONCANCER\INHALATION\SD_MALE_NASAL_INHALATION.(d)
         Gnuplot Plotting File:  G:\ACN DOSE-RESPONSE
MODELING\NONCANCER\INHALATION\SD_MALE_NASAL_INHALATION.plt
                                                  Wed May 16 13:38:57 2007
 ================================================================

 BMDS MODEL RUN
~~~~~~~~~~~~~~~~~~~~~~~~~~~~~~~~~~~~~~~~~~~~~~~~~~~~~~~~~~~~~~~~~~~~~~~~

   The form of the probability function is:

   P[response] = background+(1-background)/[1+EXP(-intercept-slope*Log(dose))]


   Dependent variable = Response
   Independent variable = Dose
   Slope parameter is restricted as slope >= 1

   Total number of observations = 3
   Total number of records with missing values = 0
   Maximum number of iterations = 250
   Relative Function Convergence has been set to: 1e-008
   Parameter Convergence has been set to: 1e-008



   User has chosen the log transformed model
```

```
                 Default Initial Parameter Values
                    background =            0
                     intercept =    -0.581093
                         slope =            1


          Asymptotic Correlation Matrix of Parameter Estimates

          ( *** The model parameter(s)  -background    -slope
                have been estimated at a boundary point, or have been specified by the user, and
do not appear in the correlation matrix )

             intercept

 intercept           1



                         Parameter Estimates

      Variable           Estimate             Std. Err.
    background                  0                   NA
     intercept          -0.522564             0.479706
         slope                  1                   NA

NA - Indicates that this parameter has hit a bound
     implied by some inequality constraint and thus
     has no standard error.



                       Analysis of Deviance Table

      Model      Log(likelihood)  Deviance  Test DF     P-value
    Full model        -13.1543
   Fitted model       -13.2153     0.121833      2          0.9409
  Reduced model       -22.7373      19.1659      2         <.0001

          AIC:         28.4305


                     Goodness  of  Fit

                                                                 Scaled
    Dose     Est._Prob.    Expected    Observed     Size       Residual
  ---------------------------------------------------------------------
   0.0000      0.0000          0.000          0           11            0
   2.1000      0.5546          6.655          7           12       0.2001
   8.5000      0.8345          8.345          8           10      -0.2931

 Chi-square =       0.13     DF = 2        P-value = 0.9390


   Benchmark Dose Computation

Specified effect =           0.1

Risk Type        =      Extra risk

Confidence level =          0.95

             BMD =       0.187372

            BMDL =     0.0818673
```

Table B-8. A summary of BMDS (version 1.3.2) modeling results based on incidence of flattening of respiratory epithelium in female Sprague-Dawley rats exposed to AN via inhalation for 2 years

Model	χ^2 *p*-value[a]	AIC	BMC_{10}[b] (mg/m^3)	$BMCL_{10}$[c] (mg/m^3)
Gamma	0.08	35.78	0.419	0.245
Logistic	0.02	38.47	1.02	0.610
Log-logistic	**0.43**	**33.50**	**0.162**	**0.059**
Multistage	0.08	35.78	0.419	0.245
Probit	0.02	38.54	1.05	0.683
Log-probit	0.08	35.53	0.616	0.340
Weibull	0.08	35.78	0.419	0.245

[a]χ^2 *p*-value from the χ^2 test for lack of fit. Values <0.1 fail to meet conventional goodness-of-fit criteria.
[b]BMC_{10} = BMC associated with 10% extra risk for nonneoplastic nasal lesions.
[c]$BMCL_{10}$ = 95% lower confidence limit on the BMC_{10} for nonneoplastic nasal lesions.

Source: Quast et al. (1980b).

BMDS (version 1.3.2) model output for the best-fit model (log-logistic) based on incidence of flattening of respiratory epithelium in female Sprague-Dawley rats exposed to AN via inhalation for 2 years

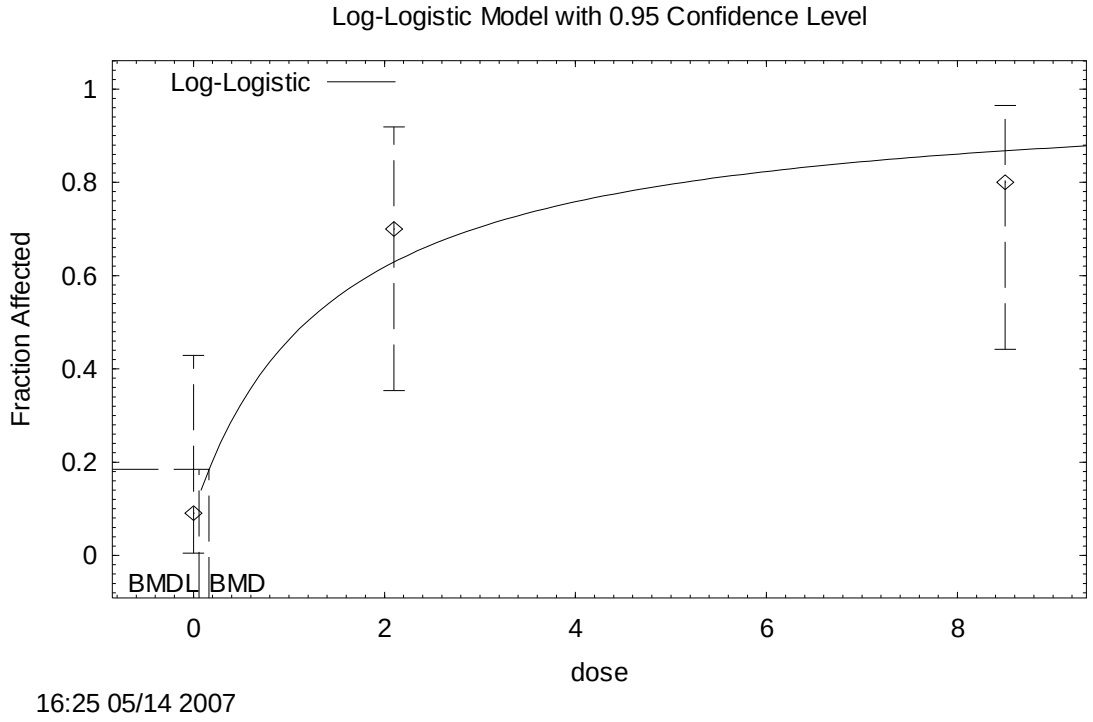


```
 ======================================================================
         Logistic Model $Revision: 2.1 $ $Date: 2000/02/26 03:38:20 $
         Input Data File: G:\ACN DOSE-RESPONSE MODELING\NONCANCER\SD_FEMALE_NASAL_INHALATION.(d)
         Gnuplot Plotting File:  G:\ACN DOSE-RESPONSE
MODELING\NONCANCER\SD_FEMALE_NASAL_INHALATION.plt
                                                    Mon May 14 16:25:24 2007
 ======================================================================

 BMDS MODEL RUN
~~~~~~~~~~~~~~~~~~~~~~~~~~~~~~~~~~~~~~~~~~~~~~~~~~~~~~~~~~~~~~~~~~~~~~~~~~~~

   The form of the probability function is:

   P[response] = background+(1-background)/[1+EXP(-intercept-slope*Log(dose))]


   Dependent variable = Response
   Independent variable = Dose
   Slope parameter is restricted as slope >= 1

   Total number of observations = 3
   Total number of records with missing values = 0
   Maximum number of iterations = 250
   Relative Function Convergence has been set to: 1e-008
   Parameter Convergence has been set to: 1e-008



   User has chosen the log transformed model


                 Default Initial Parameter Values
                    background =    0.0909091
                     intercept =    -0.457634
                         slope =            1
```

Asymptotic Correlation Matrix of Parameter Estimates

(*** The model parameter(s) -slope
have been estimated at a boundary point, or have been specified by the user,
and do not appear in the correlation matrix)

	background	intercept
background	1	-0.27
intercept	-0.27	1

Parameter Estimates

Variable	Estimate	Std. Err.
background	0.0938695	0.089458
intercept	-0.374871	0.586482
slope	1	NA

NA - Indicates that this parameter has hit a bound
implied by some inequality constraint and thus
has no standard error.

Analysis of Deviance Table

Model	Log(likelihood)	Deviance	Test DF	P-value
Full model	-14.4637			
Fitted model	-14.751	0.574692	1	0.4484
Reduced model	-21.4714	14.0155	2	0.0009048

AIC: 33.502

Goodness of Fit

Dose	Est._Prob.	Expected	Observed	Size	Scaled Residual
0.0000	0.0939	1.033	1	11	-0.03367
2.1000	0.6292	6.292	7	10	0.4637
8.5000	0.8676	8.676	8	10	-0.6305

Chi-square = 0.61 DF = 1 P-value = 0.4334

Benchmark Dose Computation

Specified effect = 0.1

Risk Type = Extra risk

Confidence level = 0.95

BMD = 0.161645

BMDL = 0.0593975

APPENDIX B-3. CANCER ORAL DOSE-RESPONSE ASSESSMENT: BMD DOSE MODELING RESULTS FOR TUMOR INCIDENCE DATA FROM RATS CHRONICALLY EXPOSED TO AN IN DRINKING WATER

As summarized in Section 4.6.1, AN is a multisite carcinogen in chronic oral rodent bioassays. Oral carcinogenicity studies of animals chronically exposed to AN include drinking water studies in two strains of rats, Sprague-Dawley (Johannsen and Levinskas, 2002a; Quast, 2002; Biodynamics, 1980a; Quast et al., 1980a) and F344 (Johannsen and Levinskas, 2002b; Biodynamics, 1980b). In Sprague-Dawley rats, significantly increased incidences of forestomach, CNS, Zymbal gland, tongue, and mammary gland (females only) tumors were found. In F344 rats, significantly increased incidences of forestomach, CNS, Zymbal gland, and mammary gland (females only) tumors were found.

Two of these chronic drinking water studies were selected for dose-response modeling using the BMD approach and derivation of oral CSFs for AN. In one study by Quast (2002), Sprague-Dawley rats were exposed to 0, 35, 100, or 300 ppm of AN in drinking water for 2 years. In the second study by Johannsen and Levinskas (2002b), F344 rats were exposed to 0, 1, 3, 10, 30, or 100 ppm of AN in drinking water for 2 years.

In this appendix, detailed results of the dose-response modeling for each of the tumor sites listed above are presented (Tables B-9 though B-26). For each tumor site, first a summary of the dose-response data is presented, followed by a table summarizing the results of the dose-response modeling. Finally, the standard output from EPA's BMDS, version 1.4.1, for the selected dose-response model for each tumor site is presented.

In general, the multistage model was fit to all of the data sets with the BMR set at 0.1 (i.e., 10% extra risk). In fitting this model, successive stages of the multistage model, starting with stage 1 and ending with the stage equal to the number of dose groups minus one, were fit to the tumor incidence data at a particular site for each rat strain and sex employing the internal dose metrics CEO in blood and AN in blood. Then, for each dose metric, all stages of the multistage model that did not show a significant lack of fit (i.e., $p > 0.1$) were compared using AIC. The stage of the multistage model with the lowest AIC was selected as the best-fit model. For most tumor sites, the one-stage model exhibited the best fit. For data sets that exhibited a significant lack of fit for all stages of the multistage model, dose groups were dropped (starting with the highest dose group) until an adequate fit was achieved.

Sprague-Dawley Rats (Quast, 2002; Quast et al., 1980a)

Tumor Site: Forestomach

Table B-9. Incidence of forestomach (nonglandular) tumors in Sprague-Dawley rats exposed to AN in drinking water for 2 years

Sex	Administered animal dose (ppm in drinking water)	Equivalent administered animal dose[a] (mg/kg-d)	Predicted internal dose metrics		Incidence of forestomach tumors[b]
			AN-AUC in blood (mg/L)	CEO-AUC in blood (mg/L)	
Male	0	0	0	0	0/80 (0%)
	35	3.42	2.06×10^{-2}	1.83×10^{-3}	2/47 (4%)
	100	8.53	5.36×10^{-2}	4.36×10^{-3}	23/48 (48%)[c]
	300	21.2	1.46×10^{-1}	9.70×10^{-3}	39/48 (81%)[c]
Female	0	0	0	0	1/80 (1%)
	35	4.36	2.37×10^{-2}	2.07×10^{-3}	1/48 (2%)
	100	10.8	6.18×10^{-2}	4.87×10^{-3}	12/48 (25%)[c]
	300	25.0	1.56×10^{-1}	1.01×10^{-2}	30/48 (62%)[c]

[a]Administered doses were averages calculated by the study authors based on animal BW and drinking water intake.
[b]Incidences for Sprague-Dawley rats do not include animals from the 6- and 12-mo sacrifices and were further adjusted to exclude (from the denominators) rats that died between 0 and 12 mos in the study.
[c]Significantly different from controls ($p < 0.05$) as calculated by the study authors.

Sources: Quast (2002); Quast et al. (1980a).

Table B-10. Summary of BMD modeling results based on incidence of forestomach (nonglandular) tumors in Sprague-Dawley rats exposed to AN in drinking water for 2 years

Dose metric	Best-fit model[a]	χ^2 *p*-value[b]	AIC	BMD_{10}[c]	$BMDL_{10}$[d]
Males					
Administered dose	2°MS[e]	0.46	86.82	3.62 mg/kg-d	2.76 mg/kg-d
CEO	2°MS[e]	0.39	87.28	1.87×10^{-3} mg/L	1.44×10^{-3} mg/L
AN	2°MS[e]	0.54	86.45	2.26×10^{-2} mg/L	1.70×10^{-2} mg/L
Females					
Administered dose	2°MS	0.17	145.97	7.76 mg/kg-d	4.81 mg/kg-d
CEO	2°MS	0.52	143.50	3.29×10^{-3} mg/L	2.38×10^{-3} mg/L
AN	2°MS	0.13	146.45	4.22×10^{-2} mg/L	2.49×10^{-2} mg/L

[a]Dose-response models were fit using BMDS, version 1.4.1. "2°MS" indicates a two-stage multistage model.
[b]*p* value from the χ^2 goodness-of-fit test. Values <0.1 indicate a significant lack of fit.
[c]BMD_{10} = BMD at 10% extra risk.
[d]$BMDL_{10}$ = 95% lower confidence limit on the BMD at 10% extra risk.
[e]Highest dose dropped prior to model fitting.

BMDS (version 1.4.1) output for forestomach tumors in Sprague-Dawley male rats employing administered dose as a dose metric

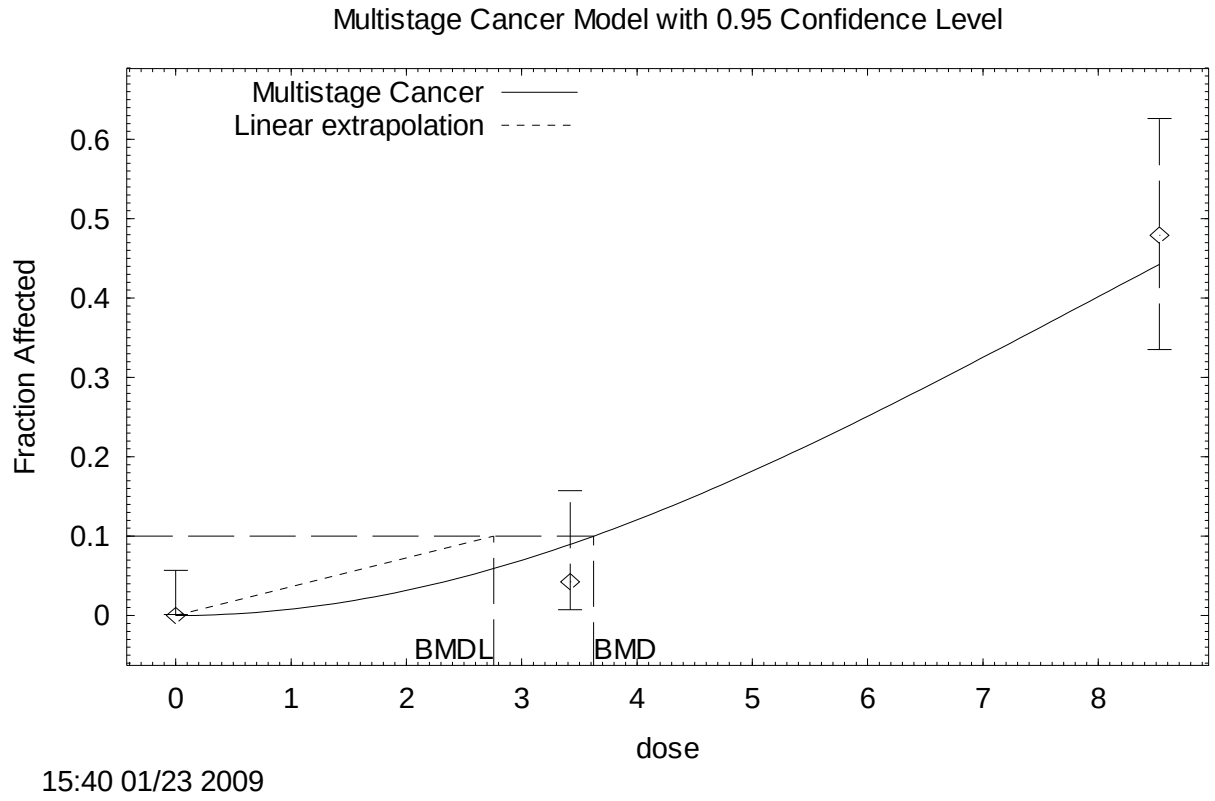


```
 ================================================================
         Multistage Cancer Model. (Version: 1.5;  Date: 02/20/2007)
         Input Data File: M:\ACN DOSE-RESPONSE MODELING\CANCER\ORAL\SD_MALE_FORESTOMACH_DW.(d)
         Gnuplot Plotting File:  M:\ACN DOSE-RESPONSE
MODELING\CANCER\ORAL\SD_MALE_FORESTOMACH_DW.plt
                                                    Fri Jan 23 15:40:45 2009
 ================================================================

 BMDS MODEL RUN
~~~~~~~~~~~~~~~~~~~~~~~~~~~~~~~~~~~~~~~~~~~~~~~~~~~~~~~~~~~~~~~~~~~~~~~~

   The form of the probability function is:

   P[response] = background + (1-background)*[1-EXP(
                -beta1*dose^1-beta2*dose^2)]

   The parameter betas are restricted to be positive


   Dependent variable = Response
   Independent variable = Dose

 Total number of observations = 3
 Total number of records with missing values = 0
 Total number of parameters in model = 3
 Total number of specified parameters = 0
 Degree of polynomial = 2


 Maximum number of iterations = 250
 Relative Function Convergence has been set to: 1e-008
 Parameter Convergence has been set to: 1e-008
```

Default Initial Parameter Values
Background = 0
Beta(1) = 0
Beta(2) = 0.00929613

Asymptotic Correlation Matrix of Parameter Estimates

(*** The model parameter(s) -Background -Beta(1)
have been estimated at a boundary point, or have been specified by the user,
and do not appear in the correlation matrix)

	Beta(2)
Beta(2)	1

Parameter Estimates

Variable	Estimate	Std. Err.	95.0% Wald Confidence Interval Lower Conf. Limit	Upper Conf. Limit
Background	0	*	*	*
Beta(1)	0	*	*	*
Beta(2)	0.00803192	*	*	*

* - Indicates that this value is not calculated.

Analysis of Deviance Table

Model	Log(likelihood)	# Param's	Deviance	Test d.f.	P-value
Full model	-41.5002	3			
Fitted model	-42.4099	1	1.81939	2	0.4026
Reduced model	-71.7704	1	60.5403	2	<.0001

AIC: 86.8198

Goodness of Fit

Dose	Est._Prob.	Expected	Observed	Size	Scaled Residual
0.0000	0.0000	0.000	0	80	0.000
3.4200	0.0897	4.214	2	47	-1.131
8.5300	0.4426	21.243	23	48	0.511

Chi^2 = 1.54 d.f. = 2 P-value = 0.4633

```
   Benchmark Dose Computation

Specified effect =            0.1

Risk Type        =      Extra risk

Confidence level =           0.95

              BMD =        3.62184

             BMDL =        2.75694

             BMDU =         4.3186

Taken together, (2.75694, 4.3186 ) is a 90     % two-sided confidence
interval for the BMD

Multistage Cancer Slope Factor =     0.0362721
```

BMDS (version 1.4.1) output for forestomach tumors in Sprague-Dawley male rats employing CEO in blood as an internal dose metric

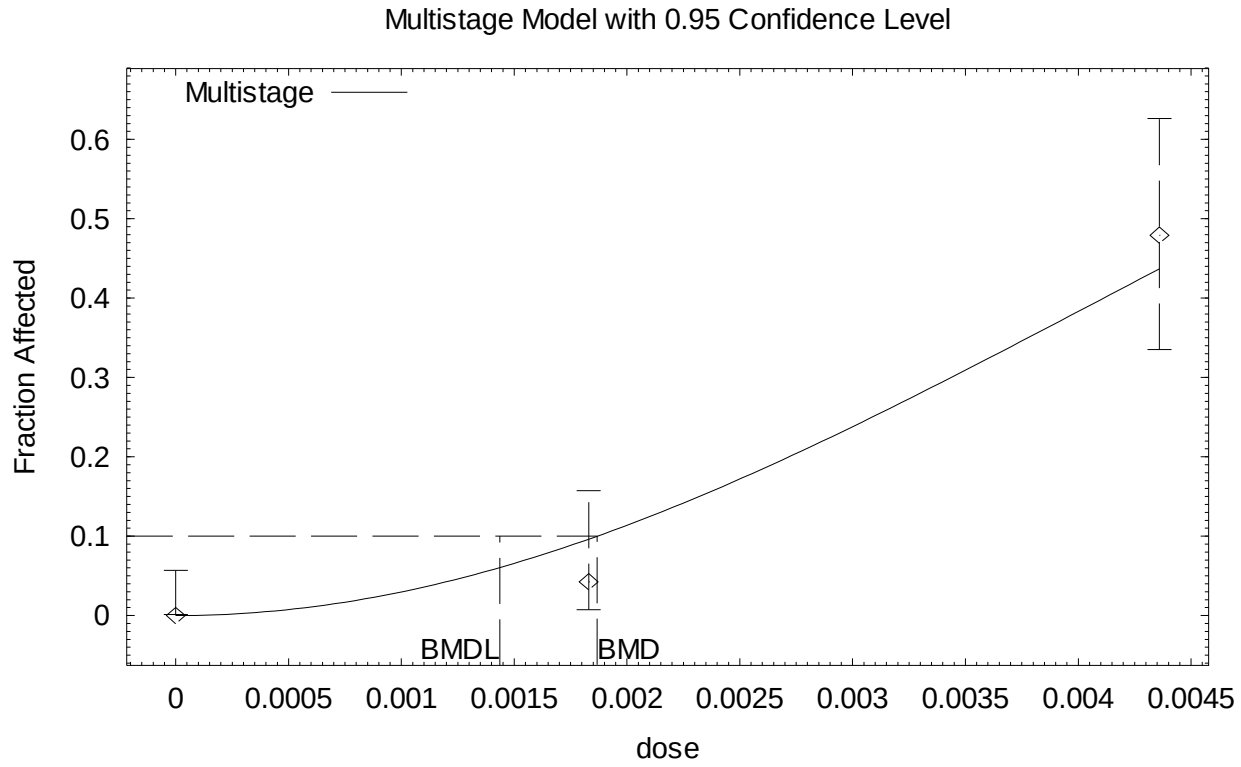

13:46 09/27 2007

```
 ======================================================================
         Multistage Model. (Version: 2.8;  Date: 02/20/2007)
         Input Data File: G:\ACN DOSE-RESPONSE
MODELING\CANCER\ORAL\SD_MALE_FORESTOMACH_BLOOD_CEO.(d)
         Gnuplot Plotting File:  G:\ACN DOSE-RESPONSE
MODELING\CANCER\ORAL\SD_MALE_FORESTOMACH_BLOOD_CEO.plt
                                                Thu Sep 27 13:46:37 2007
 ======================================================================

 BMDS MODEL RUN
~~~~~~~~~~~~~~~~~~~~~~~~~~~~~~~~~~~~~~~~~~~~~~~~~~~~~~~~~~~~~~~~~~~~~~~~

   The form of the probability function is:

   P[response] = background + (1-background)*[1-EXP(
                -beta1*dose^1-beta2*dose^2)]

   The parameter betas are restricted to be positive


   Dependent variable = Response
   Independent variable = Dose

 Total number of observations = 3
 Total number of records with missing values = 0
 Total number of parameters in model = 3
 Total number of specified parameters = 0
 Degree of polynomial = 2


 Maximum number of iterations = 250
 Relative Function Convergence has been set to: 1e-008
 Parameter Convergence has been set to: 1e-008
```

Default Initial Parameter Values
Background = 0
Beta(1) = 0
Beta(2) = 35739.1

Asymptotic Correlation Matrix of Parameter Estimates

(*** The model parameter(s) -Background -Beta(1)
have been estimated at a boundary point, or have been specified by the user, and
do not appear in the correlation matrix)

	Beta(2)
Beta(2)	1

Parameter Estimates

Variable	Estimate	Std. Err.	95.0% Wald Confidence Interval Lower Conf. Limit	Upper Conf. Limit
Background	0	*	*	*
Beta(1)	0	*	*	*
Beta(2)	30229.1	*	*	*

* - Indicates that this value is not calculated.

Analysis of Deviance Table

Model	Log(likelihood)	# Param's	Deviance	Test d.f.	P-value
Full model	-41.5002	3			
Fitted model	-42.6376	1	2.27473	2	0.3207
Reduced model	-71.7704	1	60.5403	2	<.0001

AIC: 87.2752

Goodness of Fit

Dose	Est._Prob.	Expected	Observed	Size	Scaled Residual
0.0000	0.0000	0.000	0	80	0.000
0.0018	0.0963	4.525	2	47	-1.249
0.0044	0.4371	20.981	23	48	0.588

Chi^2 = 1.90 d.f. = 2 P-value = 0.3859

Benchmark Dose Computation

Specified effect = 0.1

Risk Type = Extra risk

Confidence level = 0.95

BMD = 0.00186692

BMDL = 0.00143604

BMDU = 0.00222594

Taken together, (0.00143604, 0.00222594) is a 90 % two-sided confidence interval for the BMD

BMDS (version 1.4.1) output for forestomach tumors in Sprague-Dawley male rats employing AN in blood as an internal dose metric

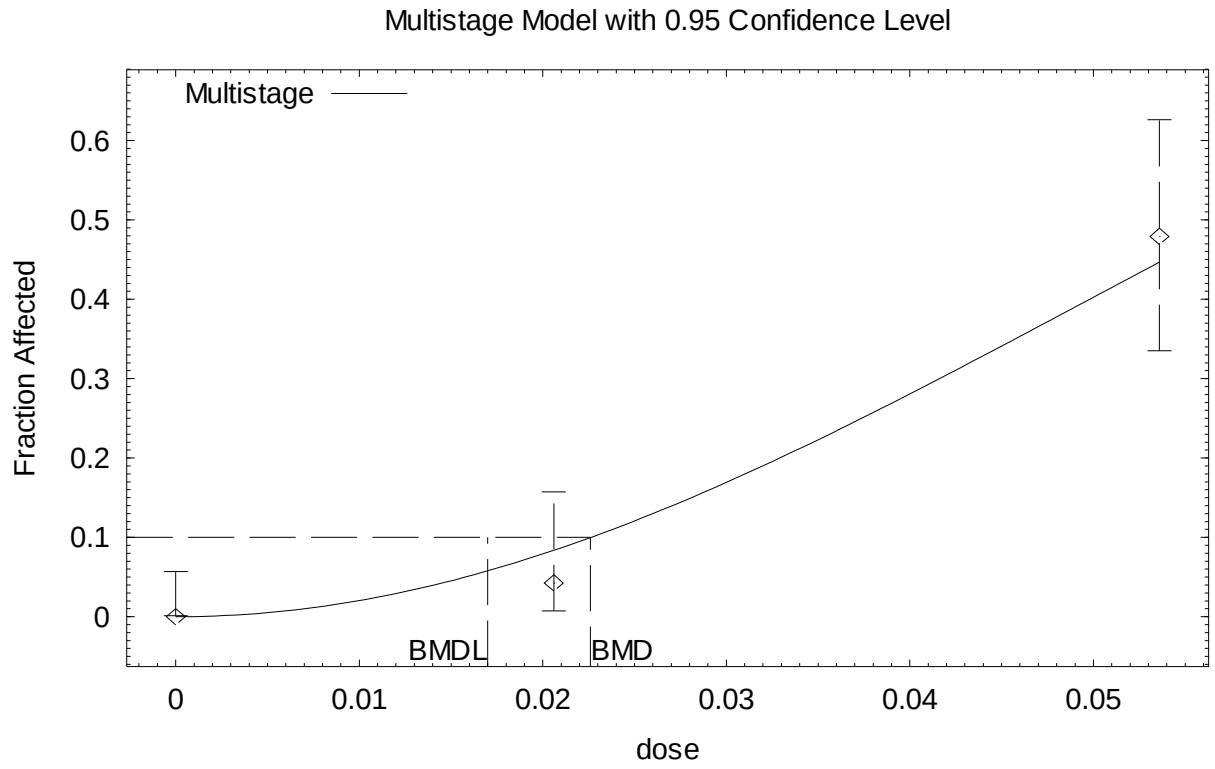

10:32 09/27 2007

```
 ======================================================================
         Multistage Model. (Version: 2.8;  Date: 02/20/2007)
         Input Data File: G:\ACN DOSE-RESPONSE
MODELING\CANCER\ORAL\SD_MALE_FORESTOMACH_BLOOD_AN.(d)
         Gnuplot Plotting File:  G:\ACN DOSE-RESPONSE
MODELING\CANCER\ORAL\SD_MALE_FORESTOMACH_BLOOD_AN.plt
                                                    Thu Sep 27 10:32:01 2007
 ======================================================================

 BMDS MODEL RUN
~~~~~~~~~~~~~~~~~~~~~~~~~~~~~~~~~~~~~~~~~~~~~~~~~~~~~~~~~~~~~~~~~~~~~~~~~~~~

   The form of the probability function is:

   P[response] = background + (1-background)*[1-EXP(
                -beta1*dose^1-beta2*dose^2)]

   The parameter betas are restricted to be positive


   Dependent variable = Response
   Independent variable = Dose

 Total number of observations = 3
 Total number of records with missing values = 0
 Total number of parameters in model = 3
 Total number of specified parameters = 0
 Degree of polynomial = 2


 Maximum number of iterations = 250
 Relative Function Convergence has been set to: 1e-008
 Parameter Convergence has been set to: 1e-008


                  Default Initial Parameter Values
```

```
                    Background =            0
                       Beta(1) =            0
                       Beta(2) =      234.473


           Asymptotic Correlation Matrix of Parameter Estimates

           ( *** The model parameter(s)  -Background    -Beta(1)
                 have been estimated at a boundary point, or have been specified by the user, and
do not appear in the correlation matrix )

                Beta(2)

   Beta(2)           1



                                Parameter Estimates

                                                          95.0% Wald Confidence Interval
      Variable         Estimate        Std. Err.     Lower Conf. Limit   Upper Conf. Limit
     Background               0            *                *                   *
        Beta(1)               0            *                *                   *
        Beta(2)          206.388           *                *                   *

* - Indicates that this value is not calculated.


                        Analysis of Deviance Table

       Model      Log(likelihood)  # Param's  Deviance  Test d.f.   P-value
     Full model        -41.5002         3
    Fitted model       -42.2261         1       1.45174      2          0.4839
  Reduced model        -71.7704         1       60.5403      2         <.0001

           AIC:         86.4522


                                 Goodness  of  Fit
                                                                      Scaled
     Dose     Est._Prob.    Expected    Observed     Size       Residual
  ---------------------------------------------------------------------------
    0.0000     0.0000         0.000         0          80        0.000
    0.0206     0.0839         3.941         2          47       -1.022
    0.0536     0.4473        21.470        23          48        0.444

 Chi^2 = 1.24      d.f. = 2        P-value = 0.5377


   Benchmark Dose Computation

Specified effect =           0.1

Risk Type        =      Extra risk

Confidence level =          0.95

              BMD =      0.0225942

             BMDL =      0.0170019

             BMDU =      0.0269423

Taken together, (0.0170019, 0.0269423) is a 90     % two-sided confidence
interval for the BMD
```

BMDS (version 1.4.1) output for forestomach tumors in Sprague-Dawley female rats employing administered dose as a dose metric

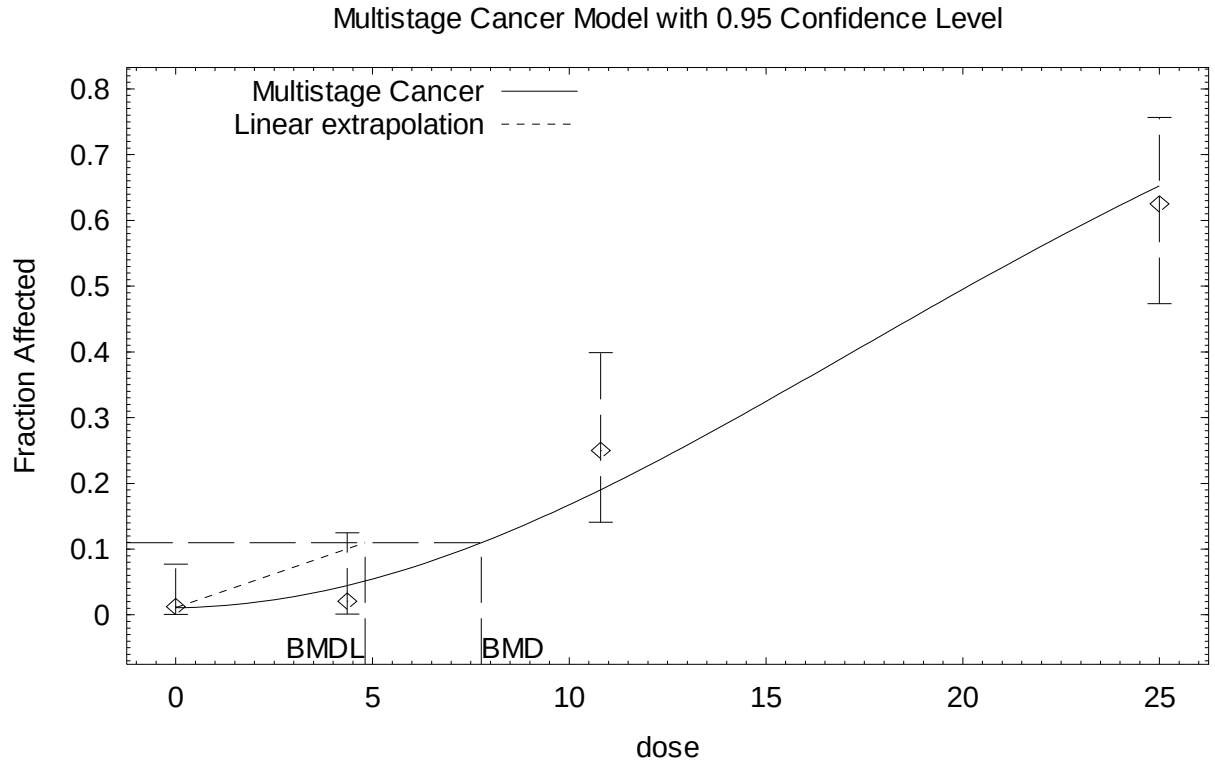


```
 ================================================================
         Multistage Cancer Model. (Version: 1.5;  Date: 02/20/2007)
         Input Data File: M:\ACN DOSE-RESPONSE MODELING\CANCER\ORAL\SD_FEMALE_FORESTOMACH_DW.(d)
         Gnuplot Plotting File:  M:\ACN DOSE-RESPONSE
MODELING\CANCER\ORAL\SD_FEMALE_FORESTOMACH_DW.plt
                                                Fri Jan 23 16:14:45 2009
 ================================================================

 BMDS MODEL RUN
~~~~~~~~~~~~~~~~~~~~~~~~~~~~~~~~~~~~~~~~~~~~~~~~~~~~~~~~~~~~~~~~~~~~

   The form of the probability function is:

   P[response] = background + (1-background)*[1-EXP(
                -beta1*dose^1-beta2*dose^2)]

   The parameter betas are restricted to be positive


   Dependent variable = Response
   Independent variable = Dose

 Total number of observations = 4
 Total number of records with missing values = 0
 Total number of parameters in model = 3
 Total number of specified parameters = 0
 Degree of polynomial = 2


 Maximum number of iterations = 250
 Relative Function Convergence has been set to: 1e-008
 Parameter Convergence has been set to: 1e-008
```

Default Initial Parameter Values
Background = 0
Beta(1) = 0.0138175
Beta(2) = 0.00104033

Asymptotic Correlation Matrix of Parameter Estimates

	Background	Beta(1)	Beta(2)
Background	1	-0.57	0.39
Beta(1)	-0.57	1	-0.93
Beta(2)	0.39	-0.93	1

Parameter Estimates

Variable	Estimate	Std. Err.	95.0% Wald Confidence Interval Lower Conf. Limit	Upper Conf. Limit
Background	0.0107986	*	*	*
Beta(1)	0.000833319	*	*	*
Beta(2)	0.00164062	*	*	*

* - Indicates that this value is not calculated.

Analysis of Deviance Table

Model	Log(likelihood)	# Param's	Deviance	Test d.f.	P-value
Full model	-68.9836	4			
Fitted model	-69.9834	3	1.99958	1	0.1573
Reduced model	-110.972	1	83.9771	3	<.0001

AIC: 145.967

Goodness of Fit

Dose	Est._Prob.	Expected	Observed	Size	Scaled Residual
0.0000	0.0108	0.864	1	80	0.147
4.3600	0.0447	2.143	1	48	-0.799
10.8000	0.1904	9.139	12	48	1.052
25.0000	0.6525	31.321	30	48	-0.401

Chi^2 = 1.93 d.f. = 1 P-value = 0.1652

```
   Benchmark Dose Computation

Specified effect =            0.1

Risk Type        =      Extra risk

Confidence level =           0.95

              BMD =        7.76379

             BMDL =        4.81488

             BMDU =        9.11082

Taken together, (4.81488, 9.11082) is a 90     % two-sided confidence
interval for the BMD

Multistage Cancer Slope Factor =     0.0207689
```

BMDS (version 1.4.1) output for forestomach tumors in Sprague-Dawley female rats employing CEO in blood as an internal dose metric

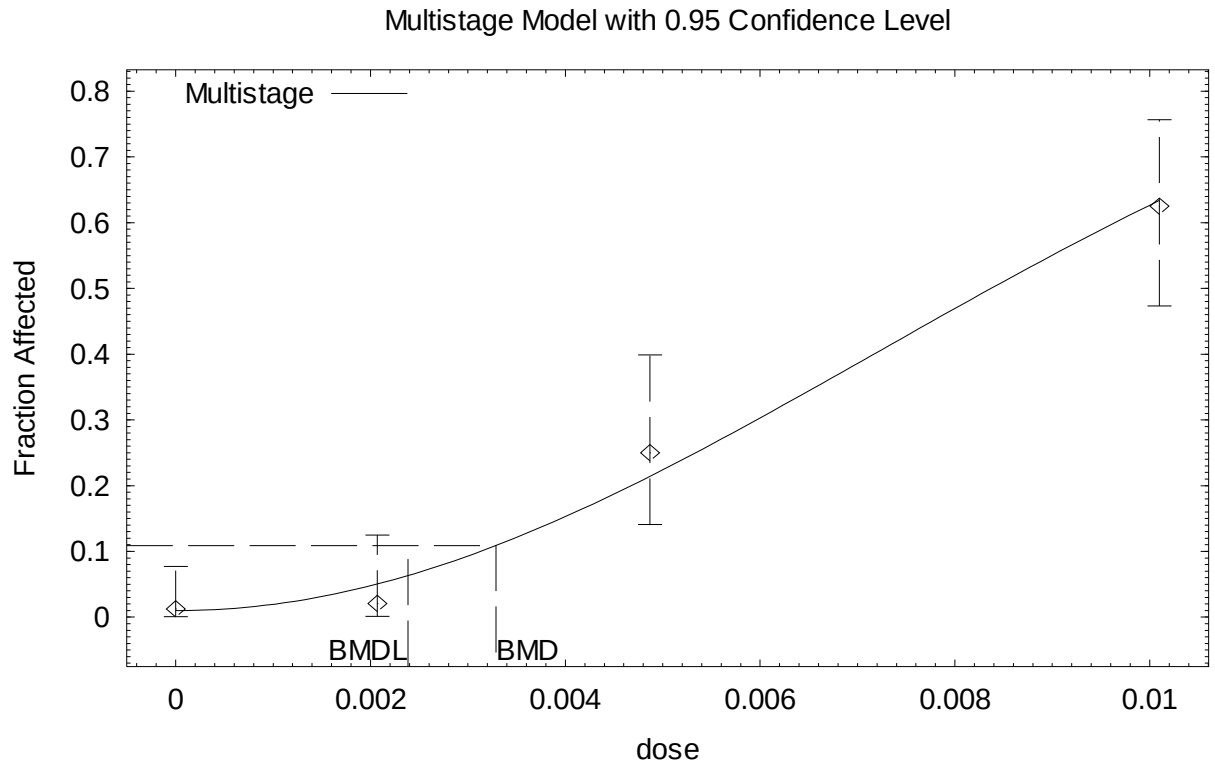


```
 ======================================================================
         Multistage Model. (Version: 2.8;  Date: 02/20/2007)
         Input Data File: G:\ACN DOSE-RESPONSE
MODELING\CANCER\ORAL\SD_FEMALE_FORESTOMACH_BLOOD_CEO.(d)
         Gnuplot Plotting File:  G:\ACN DOSE-RESPONSE
MODELING\CANCER\ORAL\SD_FEMALE_FORESTOMACH_BLOOD_CEO.plt
                                                  Thu Sep 27 14:24:06 2007
 ======================================================================

 BMDS MODEL RUN
~~~~~~~~~~~~~~~~~~~~~~~~~~~~~~~~~~~~~~~~~~~~~~~~~~~~~~~~~~~~~~~~~~~~~~~~

   The form of the probability function is:

   P[response] = background + (1-background)*[1-EXP(
                -beta1*dose^1-beta2*dose^2)]

   The parameter betas are restricted to be positive


   Dependent variable = Response
   Independent variable = Dose

 Total number of observations = 4
 Total number of records with missing values = 0
 Total number of parameters in model = 3
 Total number of specified parameters = 0
 Degree of polynomial = 2


 Maximum number of iterations = 250
 Relative Function Convergence has been set to: 1e-008
 Parameter Convergence has been set to: 1e-008


                  Default Initial Parameter Values
```

```
                    Background =           0
                       Beta(1) =     14.7147
                       Beta(2) =     8253.52


           Asymptotic Correlation Matrix of Parameter Estimates

           ( *** The model parameter(s)  -Beta(1)
                 have been estimated at a boundary point, or have been specified by the user,
                 and do not appear in the correlation matrix )

             Background      Beta(2)

Background            1        -0.48

   Beta(2)        -0.48            1



                                Parameter Estimates

                                                          95.0% Wald Confidence Interval
      Variable         Estimate        Std. Err.     Lower Conf. Limit   Upper Conf. Limit
    Background       0.00991437            *                *                   *
       Beta(1)                0            *                *                   *
       Beta(2)          9752.18            *                *                   *

* - Indicates that this value is not calculated.


                        Analysis of Deviance Table

      Model      Log(likelihood)  # Param's  Deviance  Test d.f.   P-value
    Full model        -68.9836         4
   Fitted model       -69.7499         2       1.53257      2          0.4647
  Reduced model       -110.972         1       83.9771      3         <.0001

           AIC:           143.5


                                Goodness  of  Fit
                                                                      Scaled
    Dose     Est._Prob.    Expected    Observed     Size       Residual
  ---------------------------------------------------------------------------
    0.0000     0.0099         0.793         1          80        0.233
    0.0021     0.0504         2.421         1          48       -0.937
    0.0049     0.2144        10.289        12          48        0.602
    0.0101     0.6339        30.426        30          48       -0.128

 Chi^2 = 1.31      d.f. = 2        P-value = 0.5192


   Benchmark Dose Computation

Specified effect =           0.1

Risk Type        =      Extra risk

Confidence level =          0.95

             BMD =     0.00328691

            BMDL =     0.00238295

            BMDU =      0.0037821

Taken together, (0.00238295, 0.0037821) is a 90     % two-sided confidence
interval for the BMD
```

BMDS (version 1.4.1) output for forestomach tumors in Sprague-Dawley female rats employing AN in blood as an internal dose metric

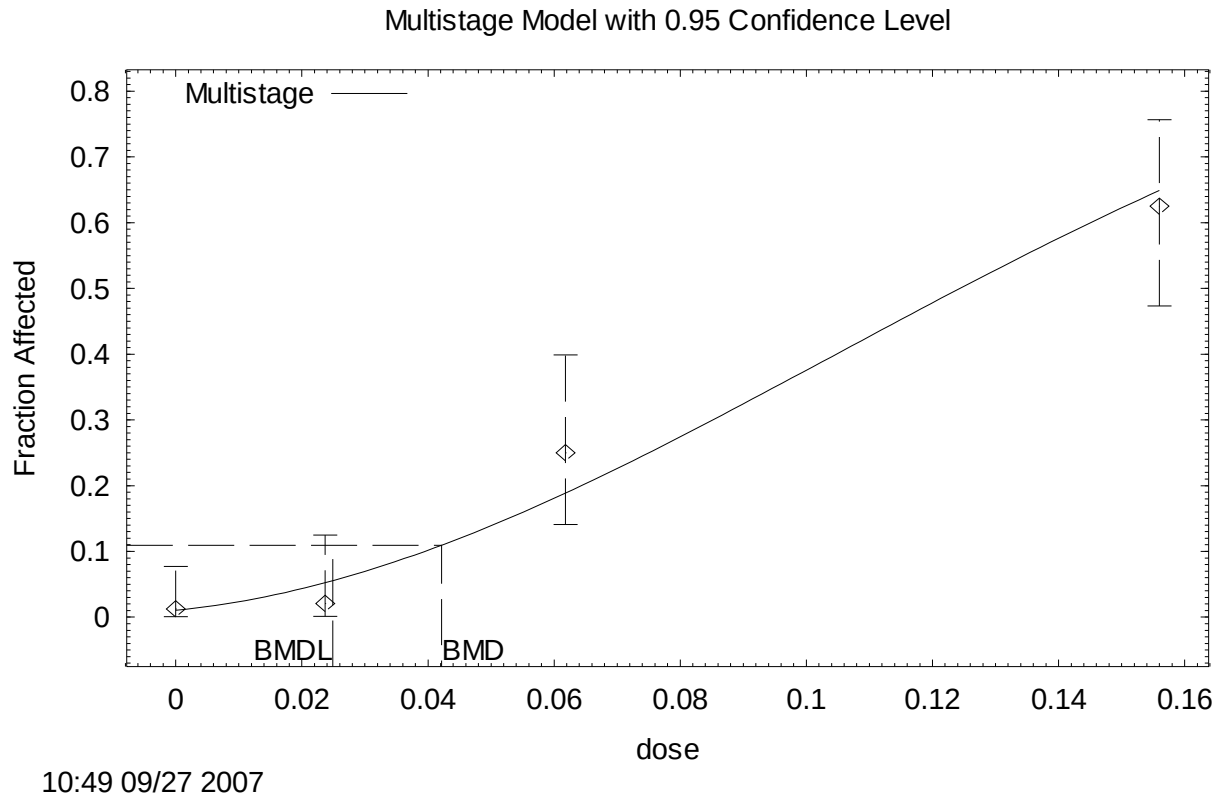


```
 ======================================================================
         Multistage Model. (Version: 2.8;  Date: 02/20/2007)
         Input Data File: G:\ACN DOSE-RESPONSE
MODELING\CANCER\ORAL\SD_FEMALE_FORESTOMACH_BLOOD_AN.(d)
         Gnuplot Plotting File:  G:\ACN DOSE-RESPONSE
MODELING\CANCER\ORAL\SD_FEMALE_FORESTOMACH_BLOOD_AN.plt
                                                  Thu Sep 27 10:49:49 2007
 ======================================================================

 BMDS MODEL RUN
~~~~~~~~~~~~~~~~~~~~~~~~~~~~~~~~~~~~~~~~~~~~~~~~~~~~~~~~~~~~~~~~~~~~~~~~

   The form of the probability function is:

   P[response] = background + (1-background)*[1-EXP(
                -beta1*dose^1-beta2*dose^2)]

   The parameter betas are restricted to be positive


   Dependent variable = Response
   Independent variable = Dose

 Total number of observations = 4
 Total number of records with missing values = 0
 Total number of parameters in model = 3
 Total number of specified parameters = 0
 Degree of polynomial = 2


 Maximum number of iterations = 250
 Relative Function Convergence has been set to: 1e-008
 Parameter Convergence has been set to: 1e-008
```

Default Initial Parameter Values
Background = 0
Beta(1) = 3.15264
Beta(2) = 20.8062

Asymptotic Correlation Matrix of Parameter Estimates

	Background	Beta(1)	Beta(2)
Background	1	-0.57	0.4
Beta(1)	-0.57	1	-0.93
Beta(2)	0.4	-0.93	1

Parameter Estimates

Variable	Estimate	Std. Err.	95.0% Wald Confidence Interval Lower Conf. Limit	Upper Conf. Limit
Background	0.0105127	*	*	*
Beta(1)	0.96299	*	*	*
Beta(2)	36.4178	*	*	*

* - Indicates that this value is not calculated.

Analysis of Deviance Table

Model	Log(likelihood)	# Param's	Deviance	Test d.f.	P-value
Full model	-68.9836	4			
Fitted model	-70.2231	3	2.47911	1	0.1154
Reduced model	-110.972	1	83.9771	3	<.0001

AIC: 146.446

Goodness of Fit

Dose	Est._Prob.	Expected	Observed	Size	Scaled Residual
0.0000	0.0105	0.841	1	80	0.174
0.0237	0.0524	2.516	1	48	-0.982
0.0618	0.1887	9.060	12	48	1.085
0.1560	0.6490	31.154	30	48	-0.349

Chi^2 = 2.29 d.f. = 1 P-value = 0.1300

Benchmark Dose Computation

Specified effect = 0.1

Risk Type = Extra risk

Confidence level = 0.95

BMD = 0.0421673

BMDL = 0.0249138

BMDU = 0.055287

Taken together, (0.0249138, 0.055287) is a 90 % two-sided confidence interval for the BMD

Tumor Site: CNS (Quast, 2002; Quast et al., 1980a)

Table B-11. Incidence of CNS tumors in Sprague-Dawley rats exposed to AN in drinking water for 2 years

Sex	Administered animal dose (ppm in drinking water)	Equivalent administered animal dose[a] (mg/kg-d)	Predicted internal dose metrics		Incidence of CNS tumors[b]
			AN-AUC in blood (mg/L)	CEO-AUC in blood (mg/L)	
Male	0	0	0	0	1/80 (1%)
	35	3.42	2.06×10^{-2}	1.83×10^{-3}	12/47 (26%)[c]
	100	8.53	5.36×10^{-2}	4.36×10^{-3}	22/48 (46%)[c]
	300	21.2	1.46×10^{-1}	9.70×10^{-3}	30/48 (62%)[c]
Female	0	0	0	0	1/80 (1%)
	35	4.36	2.37×10^{-2}	2.07×10^{-3}	20/48 (42%)[c]
	100	10.8	6.18×10^{-2}	4.87×10^{-3}	25/48 (52%)[c]
	300	25.0	1.56×10^{-1}	1.01×10^{-2}	31/48 (65%)[c]

[a]Administered doses were averages calculated by the study authors based on animal BW and drinking water intake.
[b]Incidences for Sprague-Dawley rats do not include animals from the 6- and 12-mo sacrifices and were further adjusted to exclude (from the denominators) rats that died between 0 and 12 mos in the study.
[c]Significantly different from controls ($p < 0.05$) as calculated by the study authors.

Table B-12. Summary of BMD modeling results based on incidence of CNS tumors in Sprague-Dawley rats exposed to AN in drinking water for 2 years

Dose metric	Best-fit model[a]	χ^2 *p*-value[b]	AIC	BMD_{10}[c]	$BMDL_{10}$[d]
Males					
Administered dose	1°MS	0.16	201.38	1.84 mg/kg-d	1.48 mg/kg-d
CEO	1°MS	0.37	199.81	8.87×10^{-4} mg/L	7.16×10^{-4} mg/L
AN	1°MS[e]	0.59	134.64	8.82×10^{-3} mg/L	6.64×10^{-3} mg/L
Females					
Administered dose	1°MS[e]	0.06	149.85	1.26 mg/kg-d	0.99 mg/kg-d
CEO	1°MS[e]	0.08	149.29	5.79×10^{-4} mg/L	4.51×10^{-4} mg/L
AN	1°MS[e]	0.04	150.45	7.12×10^{-3} mg/L	5.55×10^{-3} mg/L

[a]Dose-response models were fit using BMDS, version 1.4.1. "1°MS" indicates a one-stage multistage model.
[b]*p* value from the χ^2 goodness of fit test. Values <0.1 indicate a significant lack of fit.
[c]BMD_{10} = BMD at 10% extra risk.
[d]$BMDL_{10}$ = 95% lower confidence limit on the BMD at 10% extra risk.
[e]Highest dose dropped prior to model fitting.

BMDS (version 1.4.1) output for CNS tumors in Sprague-Dawley male rats employing administered dose as a dose metric

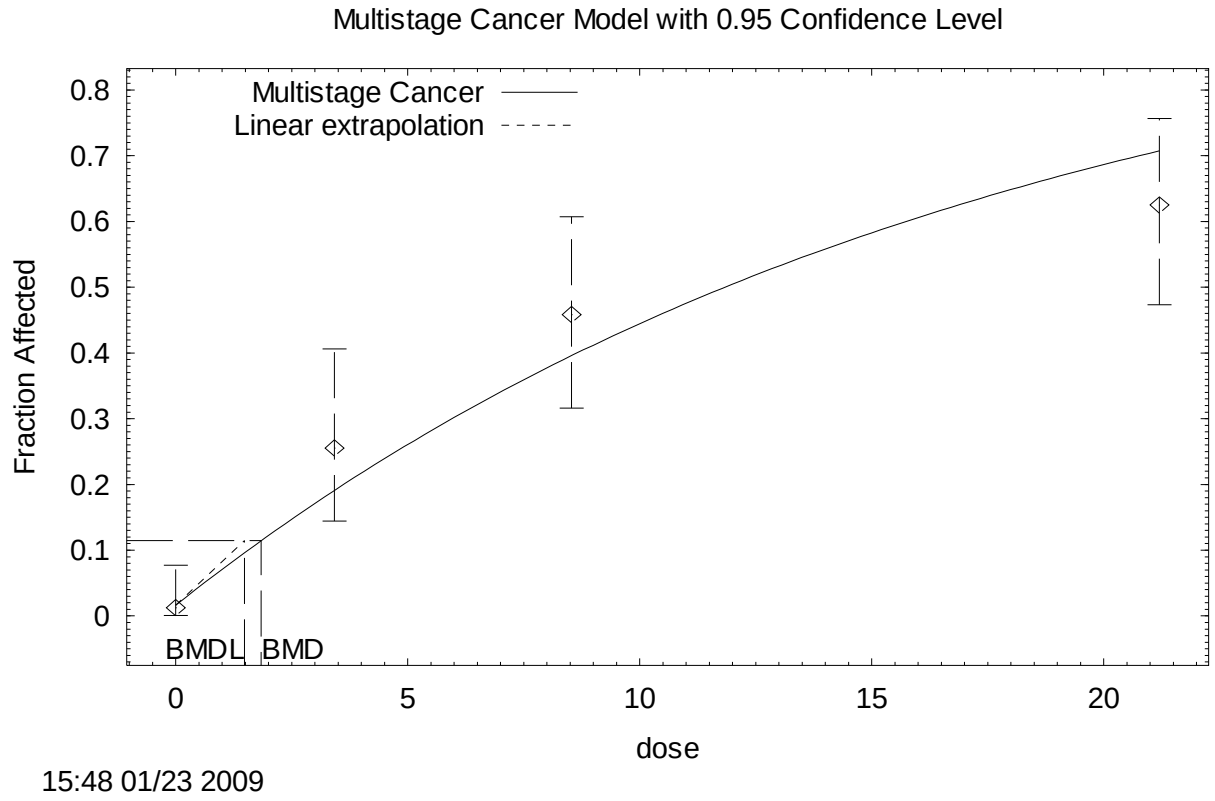


```
=================================================================
        Multistage Cancer Model. (Version: 1.5;  Date: 02/20/2007)
        Input Data File: M:\ACN DOSE-RESPONSE MODELING\CANCER\ORAL\SD_MALE_CNS_DW.(d)
        Gnuplot Plotting File:  M:\ACN DOSE-RESPONSE MODELING\CANCER\ORAL\SD_MALE_CNS_DW.plt
                                                  Fri Jan 23 15:48:14 2009
=================================================================

BMDS MODEL RUN
~~~~~~~~~~~~~~~~~~~~~~~~~~~~~~~~~~~~~~~~~~~~~~~~~~~~~~~~~~~~~~~~~~~~~

  The form of the probability function is:

  P[response] = background + (1-background)*[1-EXP(
               -beta1*dose^1)]

  The parameter betas are restricted to be positive


  Dependent variable = Response
  Independent variable = Dose

Total number of observations = 4
Total number of records with missing values = 0
Total number of parameters in model = 2
Total number of specified parameters = 0
Degree of polynomial = 1


Maximum number of iterations = 250
Relative Function Convergence has been set to: 1e-008
Parameter Convergence has been set to: 1e-008


                 Default Initial Parameter Values
```

Background = 0.108455
Beta(1) = 0.0435027

Asymptotic Correlation Matrix of Parameter Estimates

	Background	Beta(1)
Background	1	-0.62
Beta(1)	-0.62	1

Parameter Estimates

Variable	Estimate	Std. Err.	95.0% Wald Confidence Interval Lower Conf. Limit	Upper Conf. Limit
Background	0.0160781	*	*	*
Beta(1)	0.0572137	*	*	*

* - Indicates that this value is not calculated.

Analysis of Deviance Table

Model	Log(likelihood)	# Param's	Deviance	Test d.f.	P-value
Full model	-96.9359	4			
Fitted model	-98.6909	2	3.51012	2	0.1729
Reduced model	-134.574	1	75.2765	3	<.0001

AIC: 201.382

Goodness of Fit

Dose	Est._Prob.	Expected	Observed	Size	Scaled Residual
0.0000	0.0161	1.286	1	80	-0.254
3.4200	0.1909	8.974	12	47	1.123
8.5300	0.3960	19.010	22	48	0.882
21.2000	0.7075	33.958	30	48	-1.256

Chi^2 = 3.68 d.f. = 2 P-value = 0.1587

```
   Benchmark Dose Computation

Specified effect =            0.1

Risk Type        =      Extra risk

Confidence level =           0.95

              BMD =        1.84153

             BMDL =         1.4836

             BMDU =        2.34034

Taken together, (1.4836 , 2.34034) is a 90     % two-sided confidence
interval for the BMD

Multistage Cancer Slope Factor =     0.0674034
```

BMDS (version 1.4.1) output for CNS tumors in Sprague-Dawley male rats employing CEO in blood as an internal dose metric

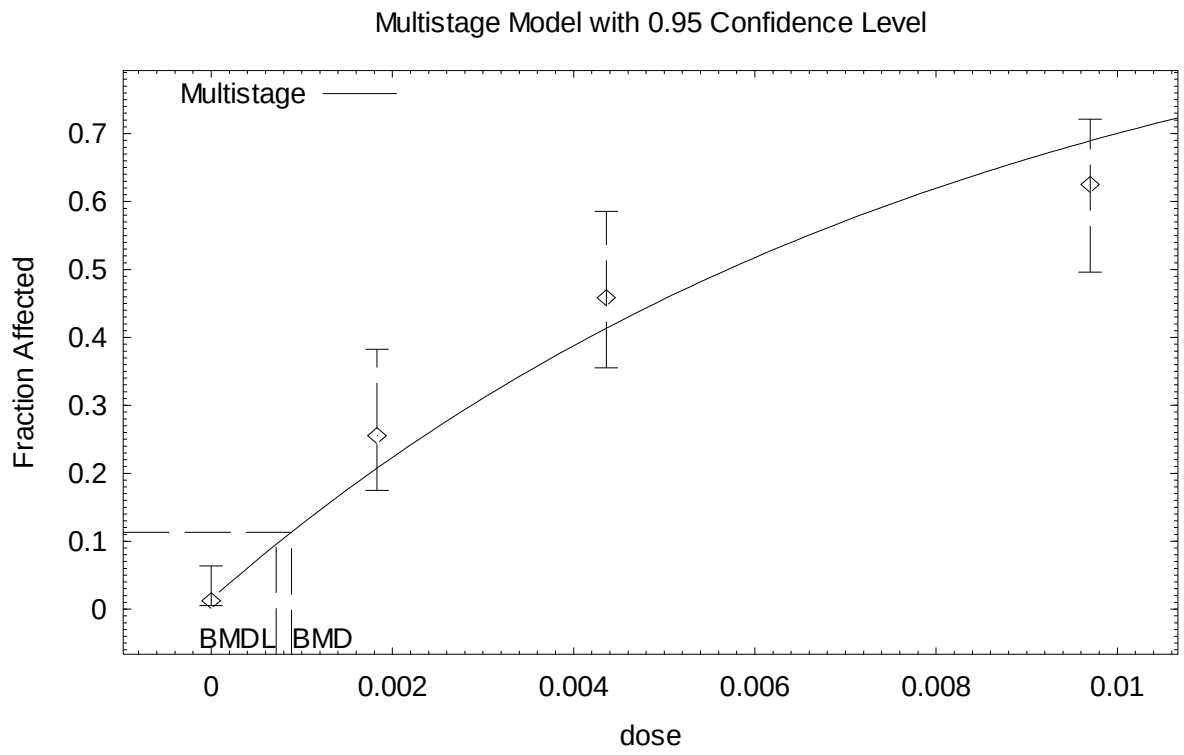

09:11 09/25 2007

```
 ======================================================================
         Multistage Model. $Revision: 2.1 $ $Date: 2000/08/21 03:38:21 $
         Input Data File: G:\ACN DOSE-RESPONSE MODELING\CANCER\ORAL\SD_MALE_CNS_BLOOD_CEO.(d)
         Gnuplot Plotting File:  G:\ACN DOSE-RESPONSE
MODELING\CANCER\ORAL\SD_MALE_CNS_BLOOD_CEO.plt
                                                    Tue Sep 25 09:11:57 2007
 ======================================================================

 BMDS MODEL RUN
~~~~~~~~~~~~~~~~~~~~~~~~~~~~~~~~~~~~~~~~~~~~~~~~~~~~~~~~~~~~~~~~~~~~~~~~~~~~

   The form of the probability function is:

   P[response] = background + (1-background)*[1-EXP(
-beta1*dose^1)]

   The parameter betas are restricted to be positive


   Dependent variable = Response
   Independent variable = Dose

 Total number of observations = 4
 Total number of records with missing values = 0
 Total number of parameters in model = 2
 Total number of specified parameters = 0
 Degree of polynomial = 1


 Maximum number of iterations = 250
 Relative Function Convergence has been set to: 1e-008
 Parameter Convergence has been set to: 1e-008


                  Default Initial Parameter Values
                     Background =    0.0859878
                        Beta(1) =      97.0212
```

```
**** WARNING:  Completion code = -3.  Optimum not found. Trying new starting point****
**** WARNING 0:  Completion code = -3 trying new start****
**** WARNING 1:  Completion code = -3 trying new start****
**** WARNING 2:  Completion code = -3 trying new start****
**** WARNING 3:  Completion code = -3 trying new start****
**** WARNING 4:  Completion code = -3 trying new start****
**** WARNING 5:  Completion code = -3 trying new start****
**** WARNING 6:  Completion code = -3 trying new start****
**** WARNING 7:  Completion code = -3 trying new start****
**** WARNING 8:  Completion code = -3 trying new start****
**** WARNING 9:  Completion code = -3 trying new start****


          Asymptotic Correlation Matrix of Parameter Estimates

            Background      Beta(1)

Background            1        -0.62

   Beta(1)        -0.62            1


                        Parameter Estimates

       Variable           Estimate            Std. Err.
     Background           0.0146577           0.100785
        Beta(1)             118.766            28.4627


                     Analysis of Deviance Table

       Model      Log(likelihood)  Deviance  Test DF     P-value
     Full model         -96.9359
   Fitted model         -97.9055       1.93933      2          0.3792
  Reduced model         -134.574       75.2765      3         <.0001

          AIC:          199.811


                    Goodness  of  Fit

     Dose     Est._Prob.    Expected    Observed     Size     Chi^2 Res.
  ------------------------------------------------------------------------
i: 1
    0.0000     0.0147         1.173         1          80      -0.149
i: 2
    0.0018     0.2071         9.736        12          47       0.293
i: 3
    0.0044     0.4129        19.820        22          48       0.187
i: 4
    0.0097     0.6886        33.055        30          48      -0.297

 Chi-square =       2.01     DF = 2        P-value = 0.3669


   Benchmark Dose Computation

Specified effect =            0.1

Risk Type        =      Extra risk

Confidence level =           0.95

             BMD =     0.00088713

            BMDL =     0.00071632
```

BMDS (version 1.4.1) output for CNS tumors in Sprague-Dawley male rats employing AN in blood as an internal dose metric

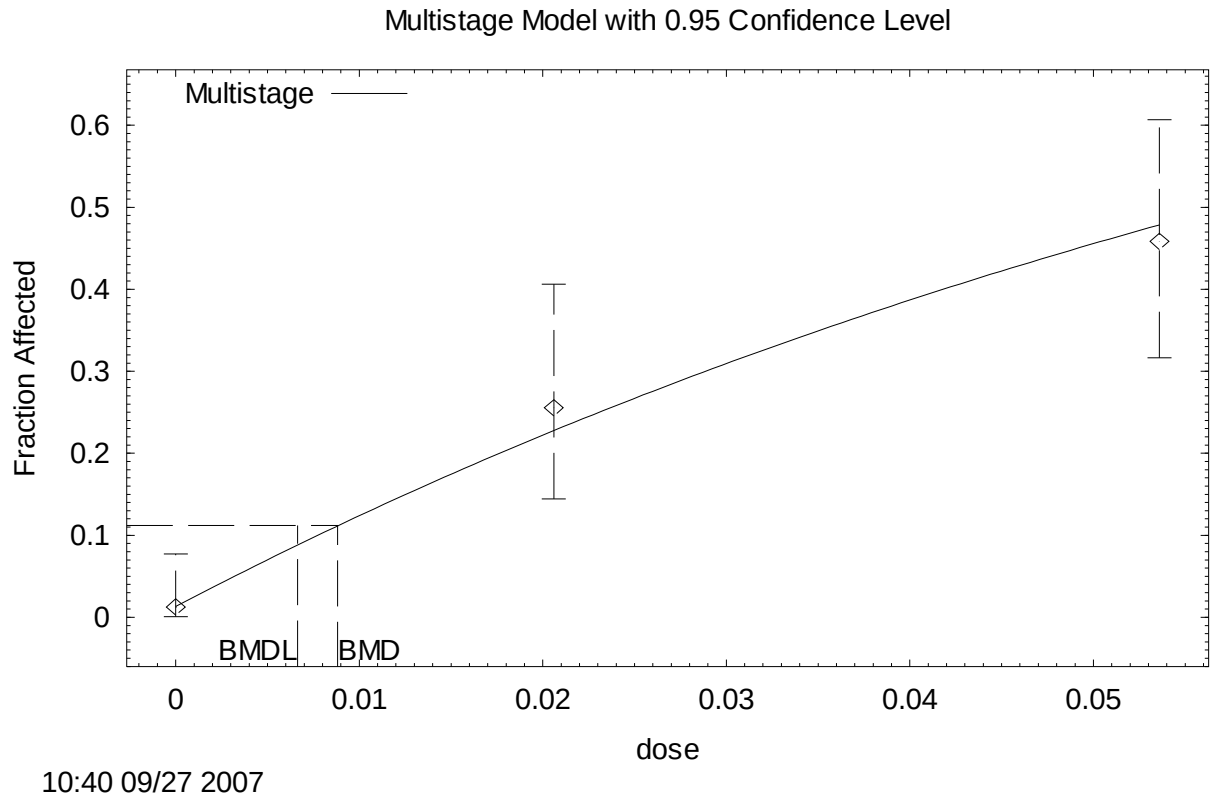


```
 ======================================================================
         Multistage Model. (Version: 2.8;  Date: 02/20/2007)
         Input Data File: G:\ACN DOSE-RESPONSE MODELING\CANCER\ORAL\SD_MALE_CNS_BLOOD_AN.(d)
         Gnuplot Plotting File:  G:\ACN DOSE-RESPONSE
MODELING\CANCER\ORAL\SD_MALE_CNS_BLOOD_AN.plt
                                                  Thu Sep 27 10:40:46 2007
 ======================================================================

 BMDS MODEL RUN
~~~~~~~~~~~~~~~~~~~~~~~~~~~~~~~~~~~~~~~~~~~~~~~~~~~~~~~~~~~~~~~~~~~~~~~~

   The form of the probability function is:

   P[response] = background + (1-background)*[1-EXP(
                -beta1*dose^1)]

   The parameter betas are restricted to be positive


   Dependent variable = Response
   Independent variable = Dose

 Total number of observations = 3
 Total number of records with missing values = 0
 Total number of parameters in model = 2
 Total number of specified parameters = 0
 Degree of polynomial = 1


 Maximum number of iterations = 250
 Relative Function Convergence has been set to: 1e-008
 Parameter Convergence has been set to: 1e-008
```

Default Initial Parameter Values
Background = 0.032766
Beta(1) = 11.0585

Asymptotic Correlation Matrix of Parameter Estimates

	Background	Beta(1)
Background	1	-0.61
Beta(1)	-0.61	1

Parameter Estimates

Variable	Estimate	Std. Err.	95.0% Wald Confidence Interval Lower Conf. Limit	Upper Conf. Limit
Background	0.0130586	*	*	*
Beta(1)	11.9435	*	*	*

* - Indicates that this value is not calculated.

Analysis of Deviance Table

Model	Log(likelihood)	# Param's	Deviance	Test d.f.	P-value
Full model	-65.1808	3			
Fitted model	-65.3204	2	0.279194	1	0.5972
Reduced model	-87.5704	1	44.7792	2	<.0001

AIC: 134.641

Goodness of Fit

Dose	Est._Prob.	Expected	Observed	Size	Scaled Residual
0.0000	0.0131	1.045	1	80	-0.044
0.0206	0.2283	10.731	12	47	0.441
0.0536	0.4797	23.025	22	48	-0.296

Chi^2 = 0.28 d.f. = 1 P-value = 0.5940

Benchmark Dose Computation

Specified effect = 0.1

Risk Type = Extra risk

Confidence level = 0.95

BMD = 0.00882158

BMDL = 0.00664413

BMDU = 0.0121508

Taken together, (0.00664413, 0.0121508) is a 90 % two-sided confidence interval for the BMD

BMDS (version 1.4.1) output for CNS tumors in Sprague-Dawley female rats employing administered dose as a dose metric

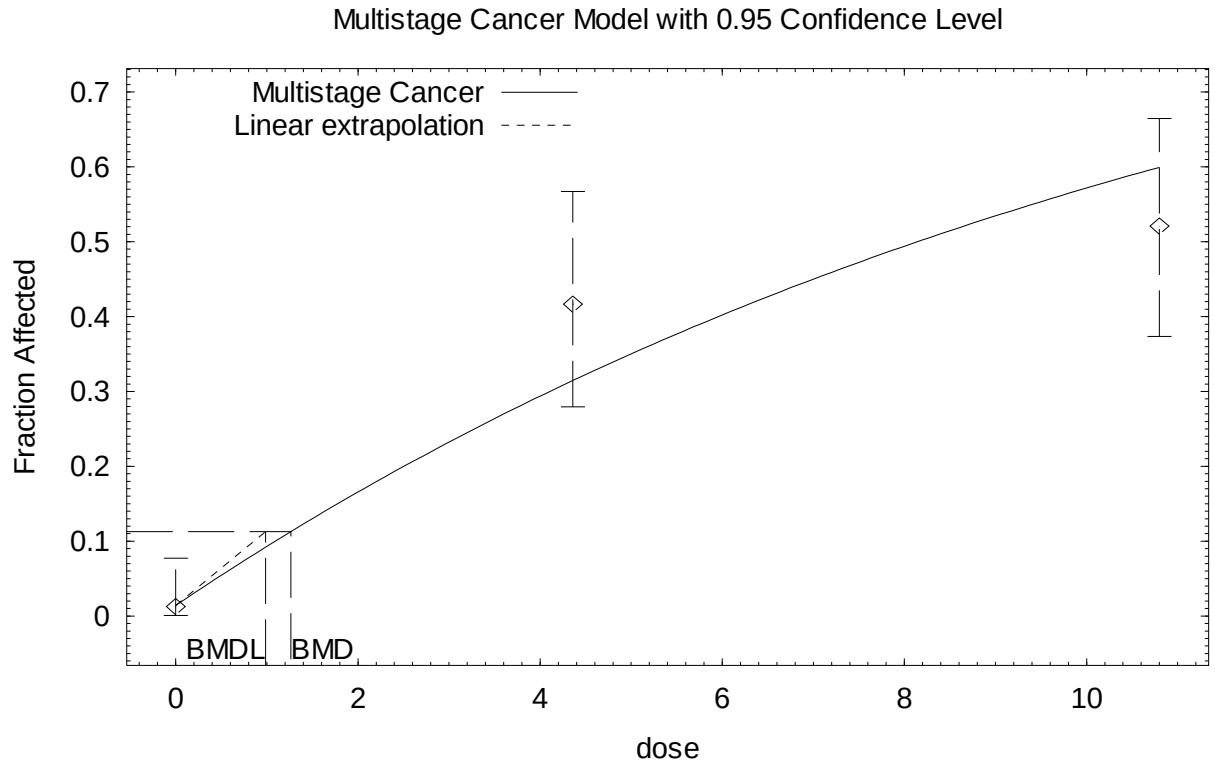


```
=================================================================
        Multistage Cancer Model. (Version: 1.5;  Date: 02/20/2007)
        Input Data File: M:\ACN DOSE-RESPONSE MODELING\CANCER\ORAL\SD_FEMALE_CNS_DW.(d)
        Gnuplot Plotting File:  M:\ACN DOSE-RESPONSE MODELING\CANCER\ORAL\SD_FEMALE_CNS_DW.plt
                                                  Fri Jan 23 16:19:26 2009
=================================================================

BMDS MODEL RUN
~~~~~~~~~~~~~~~~~~~~~~~~~~~~~~~~~~~~~~~~~~~~~~~~~~~~~~~~~~~~~~~~~~~~~

  The form of the probability function is:

  P[response] = background + (1-background)*[1-EXP(
               -beta1*dose^1)]

  The parameter betas are restricted to be positive


  Dependent variable = Response
  Independent variable = Dose

Total number of observations = 3
Total number of records with missing values = 0
Total number of parameters in model = 2
Total number of specified parameters = 0
Degree of polynomial = 1


Maximum number of iterations = 250
Relative Function Convergence has been set to: 1e-008
Parameter Convergence has been set to: 1e-008


                 Default Initial Parameter Values
```

Background = 0.0993663
Beta(1) = 0.0642026

Asymptotic Correlation Matrix of Parameter Estimates

	Background	Beta(1)
Background	1	-0.62
Beta(1)	-0.62	1

Parameter Estimates

Variable	Estimate	Std. Err.	95.0% Wald Confidence Interval Lower Conf. Limit	Upper Conf. Limit
Background	0.0141417	*	*	*
Beta(1)	0.0833707	*	*	*

* - Indicates that this value is not calculated.

Analysis of Deviance Table

Model	Log(likelihood)	# Param's	Deviance	Test d.f.	P-value
Full model	-71.2064	3			
Fitted model	-72.9251	2	3.43738	1	0.06374
Reduced model	-101.108	1	59.8036	2	<.0001

AIC: 149.85

Goodness of Fit

Dose	Est._Prob.	Expected	Observed	Size	Scaled Residual
0.0000	0.0141	1.131	1	80	-0.124
4.3600	0.3146	15.100	20	48	1.523
10.8000	0.5993	28.768	25	48	-1.110

Chi^2 = 3.57 d.f. = 1 P-value = 0.0589

```
   Benchmark Dose Computation

Specified effect =            0.1

Risk Type        =      Extra risk

Confidence level =           0.95

              BMD =        1.26376

             BMDL =       0.985061

             BMDU =        1.66456

Taken together, (0.985061, 1.66456) is a 90     % two-sided confidence
interval for the BMD

Multistage Cancer Slope Factor =      0.101517
```

BMDS (version 1.4.1) output for CNS tumors in Sprague-Dawley female rats employing CEO in blood as an internal dose metric

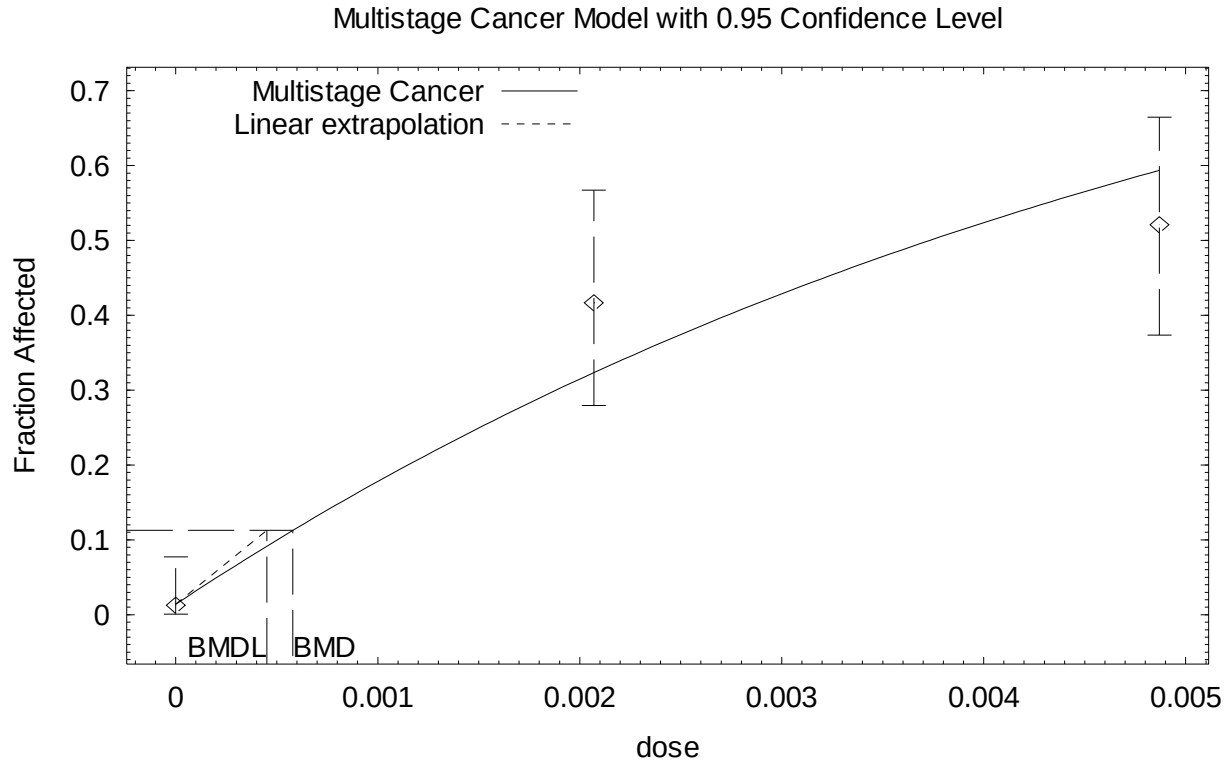


```
     09:03 12/03 2008
=====================================================================
         Multistage Cancer Model. (Version: 1.5;  Date: 02/20/2007)
         Input Data File: M:\ACN DOSE-RESPONSE MODELING\CANCER\ORAL\SD_FEMALE_CNS_BLOOD_CEO.(d)
         Gnuplot Plotting File:  M:\ACN DOSE-RESPONSE
MODELING\CANCER\ORAL\SD_FEMALE_CNS_BLOOD_CEO.plt
                                                Wed Dec 03 09:03:51 2008
 =====================================================================

 BMDS MODEL RUN
~~~~~~~~~~~~~~~~~~~~~~~~~~~~~~~~~~~~~~~~~~~~~~~~~~~~~~~~~~~~~~~~~~~~~~~

   The form of the probability function is:

   P[response] = background + (1-background)*[1-EXP(
                -beta1*dose^1)]

   The parameter betas are restricted to be positive


   Dependent variable = Response
   Independent variable = Dose

 Total number of observations = 3
 Total number of records with missing values = 0
 Total number of parameters in model = 2
 Total number of specified parameters = 0
 Degree of polynomial = 1


 Maximum number of iterations = 250
 Relative Function Convergence has been set to: 1e-008
 Parameter Convergence has been set to: 1e-008
```

Default Initial Parameter Values
Background = 0.0914603
Beta(1) = 144.025

Asymptotic Correlation Matrix of Parameter Estimates

	Background	Beta(1)
Background	1	-0.62
Beta(1)	-0.62	1

Parameter Estimates

Variable	Estimate	Std. Err.	95.0% Wald Confidence Interval Lower Conf. Limit	Upper Conf. Limit
Background	0.0138803	*	*	*
Beta(1)	182.002	*	*	*

* - Indicates that this value is not calculated.

Analysis of Deviance Table

Model	Log(likelihood)	# Param's	Deviance	Test d.f.	P-value
Full model	-71.2064	3			
Fitted model	-72.6449	2	2.87694	1	0.08986
Reduced model	-101.108	1	59.8036	2	<.0001

AIC: 149.29

Goodness of Fit

Dose	Est._Prob.	Expected	Observed	Size	Scaled Residual
0.0000	0.0139	1.110	1	80	-0.106
0.0021	0.3234	15.525	20	48	1.381
0.0049	0.5936	28.491	25	48	-1.026

Chi^2 = 2.97 d.f. = 1 P-value = 0.0848

Benchmark Dose Computation

Specified effect = 0.1

Risk Type = Extra risk

Confidence level = 0.95

BMD = 0.000578899

BMDL = 0.000451438

BMDU = 0.000761804

Taken together, (0.000451438, 0.000761804) is a 90 % two-sided confidence interval for the BMD

Multistage Cancer Slope Factor = 221.515

BMDS (version 1.4.1) output for CNS tumors in Sprague-Dawley female rats employing AN in blood as an internal dose metric

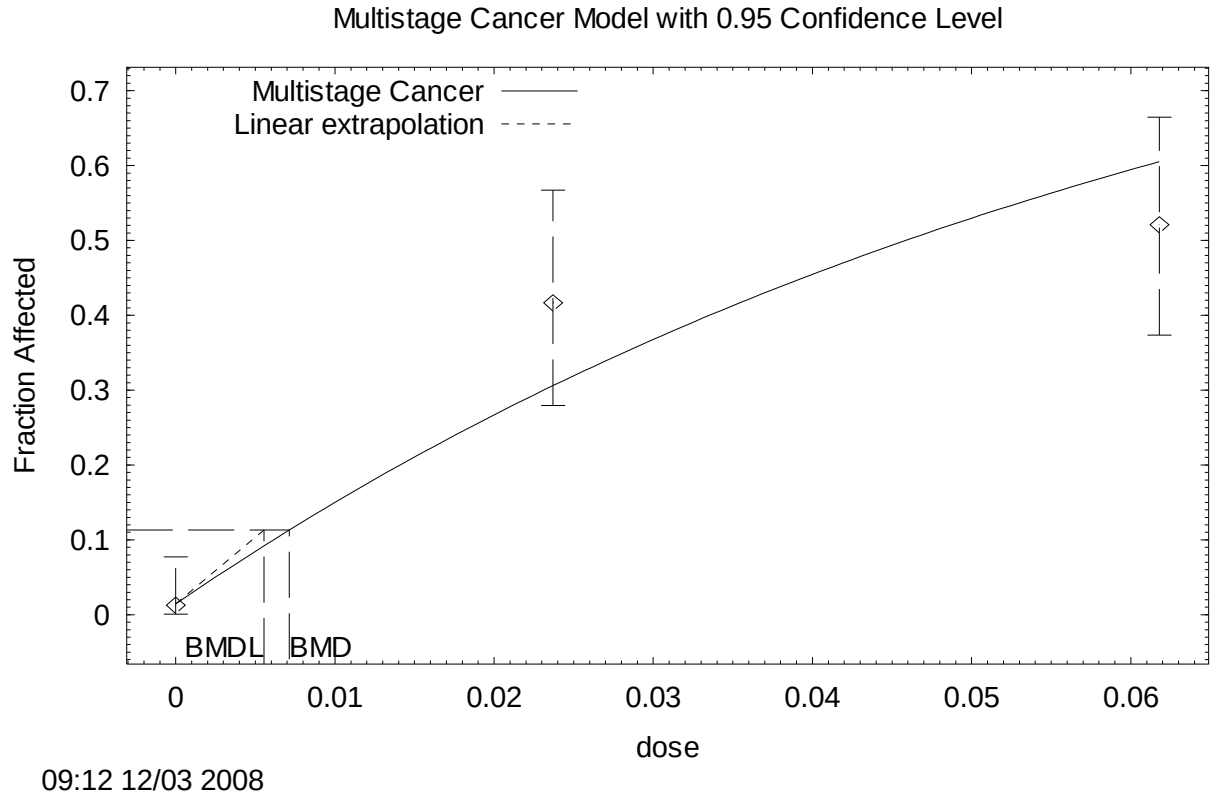


```
================================================================
         Multistage Cancer Model. (Version: 1.5;  Date: 02/20/2007)
         Input Data File: M:\ACN DOSE-RESPONSE MODELING\CANCER\ORAL\SD_FEMALE_CNS_BLOOD_AN.(d)
         Gnuplot Plotting File:  M:\ACN DOSE-RESPONSE
MODELING\CANCER\ORAL\SD_FEMALE_CNS_BLOOD_AN.plt
                                                    Wed Dec 03 09:12:32 2008
 ================================================================

 BMDS MODEL RUN
~~~~~~~~~~~~~~~~~~~~~~~~~~~~~~~~~~~~~~~~~~~~~~~~~~~~~~~~~~~~~~~~~~~~

   The form of the probability function is:

   P[response] = background + (1-background)*[1-EXP(
                -beta1*dose^1)]

   The parameter betas are restricted to be positive


   Dependent variable = Response
   Independent variable = Dose

 Total number of observations = 3
 Total number of records with missing values = 0
 Total number of parameters in model = 2
 Total number of specified parameters = 0
 Degree of polynomial = 1


 Maximum number of iterations = 250
 Relative Function Convergence has been set to: 1e-008
 Parameter Convergence has been set to: 1e-008
```

Default Initial Parameter Values
Background = 0.106975
Beta(1) = 11.0861

Asymptotic Correlation Matrix of Parameter Estimates

	Background	Beta(1)
Background	1	-0.62
Beta(1)	-0.62	1

Parameter Estimates

Variable	Estimate	Std. Err.	95.0% Wald Confidence Interval Lower Conf. Limit	Upper Conf. Limit
Background	0.0144346	*	*	*
Beta(1)	14.7901	*	*	*

* - Indicates that this value is not calculated.

Analysis of Deviance Table

Model	Log(likelihood)	# Param's	Deviance	Test d.f.	P-value
Full model	-71.2064	3			
Fitted model	-73.2271	2	4.04128	1	0.0444
Reduced model	-101.108	1	59.8036	2	<.0001

AIC: 150.454

Goodness of Fit

Dose	Est._Prob.	Expected	Observed	Size	Scaled Residual
0.0000	0.0144	1.155	1	80	-0.145
0.0237	0.3058	14.681	20	48	1.666
0.0618	0.6049	29.034	25	48	-1.191

Chi^2 = 4.22 d.f. = 1 P-value = 0.0400

Benchmark Dose Computation

Specified effect = 0.1

Risk Type = Extra risk

Confidence level = 0.95

BMD = 0.0071237

BMDL = 0.00554992

BMDU = 0.00939265

Taken together, (0.00554992, 0.00939265) is a 90 % two-sided confidence interval for the BMD

Multistage Cancer Slope Factor = 18.0183

Tumor Site: Zymbal Gland (Quast, 2002; Quast et al., 1980a)

Table B-13. Incidence of Zymbal gland tumors in Sprague-Dawley rats exposed to AN in drinking water for 2 years

Sex	Administered animal dose (ppm in drinking water)	Equivalent administered animal dose[a] (mg/kg-d)	Predicted internal dose metrics		Incidence of Zymbal gland tumors[b]
			AN-AUC in blood (mg/L)	CEO-AUC in blood (mg/L)	
Male	0	0	0	0	3/80 (4%)
	35	3.42	2.06×10^{-2}	1.83×10^{-3}	4/47 (9%)
	100	8.53	5.36×10^{-2}	4.36×10^{-3}	3/48 (6%)
	300	21.2	1.46×10^{-1}	9.70×10^{-3}	16/48 (33%)[c]
Female	0	0	0	0	1/80 (1%)
	35	4.36	2.37×10^{-2}	2.07×10^{-3}	5/48 (10%)[c]
	100	10.8	6.18×10^{-2}	4.87×10^{-3}	9/48 (19%)[c]
	300	25.0	1.56×10^{-1}	1.01×10^{-2}	18/48 (38%)[c]

[a]Administered doses were averages calculated by the study authors based on animal BW and drinking water intake.
[b]Incidences for Sprague-Dawley rats do not include animals from the 6- and 12-mo sacrifices and were further adjusted to exclude (from the denominators) rats that died between 0 and 12 mos in the study.
[c]Significantly different from controls ($p < 0.05$) as calculated by the study authors.

Table B-14. Summary of BMD modeling results based on incidence of Zymbal gland tumors in Sprague-Dawley rats exposed to AN in drinking water for 2 years

Dose metric	Best-fit model[a]	χ^2 *p*-value[b]	AIC	BMD_{10}[c]	$BMDL_{10}$[d]
Males					
Administered dose	2°MS	0.43	142.15	11.80 mg/kg-d	6.29 mg/kg-d
CEO	2°MS	0.38	142.46	5.46×10^{-3} mg/L	3.15×10^{-3} mg/L
AN	3°MS	0.28	143.58	8.94×10^{-2} mg/L	4.26×10^{-2} mg/L
Females					
Administered dose	1°MS	0.94	156.80	5.66 mg/kg-d	4.19 mg/kg-d
CEO	1°MS	0.95	156.77	2.40×10^{-3} mg/L	1.78×10^{-3} mg/L
AN	1°MS	0.85	156.98	3.41×10^{-2} mg/L	2.52×10^{-2} mg/L

[a]Dose-response models were fit using BMDS, version 1.4.1. "1°MS" indicates a one-stage multistage model, "2°MS" indicates a two-stage multistage model, and "3°MS" indicates a three-stage multistage model.
[b]*p* value from the χ^2 goodness of fit test. Values <0.1 indicate a significant lack of fit.
[c]BMD_{10} = BMD at 10% extra risk.
[d]$BMDL_{10}$ = 95% lower confidence limit on the BMD at 10% extra risk.

BMDS (version 1.4.1) output for Zymbal gland tumors in Sprague-Dawley male rats employing administered dose as a dose metric

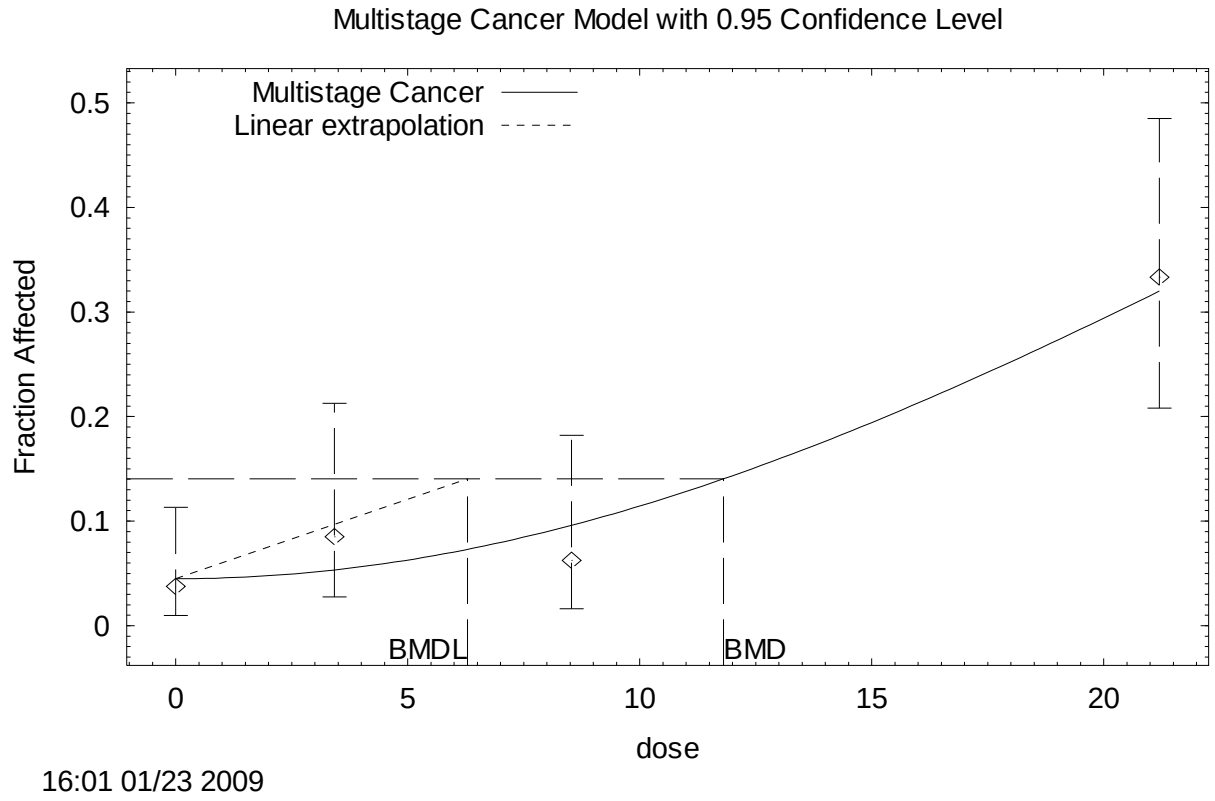


```
=====================================================================
        Multistage Cancer Model. (Version: 1.5;  Date: 02/20/2007)
        Input Data File: M:\ACN DOSE-RESPONSE MODELING\CANCER\ORAL\SD_MALE_ZYMBAL_DW.(d)
        Gnuplot Plotting File:  M:\ACN DOSE-RESPONSE MODELING\CANCER\ORAL\SD_MALE_ZYMBAL_DW.plt
                                                Fri Jan 23 16:01:39 2009
=====================================================================

BMDS MODEL RUN
~~~~~~~~~~~~~~~~~~~~~~~~~~~~~~~~~~~~~~~~~~~~~~~~~~~~~~~~~~~~~~~~~~~~~~~

  The form of the probability function is:

  P[response] = background + (1-background)*[1-EXP(
               -beta1*dose^1-beta2*dose^2)]

  The parameter betas are restricted to be positive


  Dependent variable = Response
  Independent variable = Dose

Total number of observations = 4
Total number of records with missing values = 0
Total number of parameters in model = 3
Total number of specified parameters = 0
Degree of polynomial = 2


Maximum number of iterations = 250
Relative Function Convergence has been set to: 1e-008
Parameter Convergence has been set to: 1e-008


                 Default Initial Parameter Values
```

```
                    Background =     0.042253
                       Beta(1) =            0
                       Beta(2) =   0.00079507


          Asymptotic Correlation Matrix of Parameter Estimates

          ( *** The model parameter(s)  -Beta(1)
                have been estimated at a boundary point, or have been specified by the user,
                and do not appear in the correlation matrix )

            Background      Beta(2)

Background           1        -0.49

   Beta(2)       -0.49            1


                                Parameter Estimates

                                                        95.0% Wald Confidence Interval
      Variable         Estimate        Std. Err.     Lower Conf. Limit   Upper Conf. Limit
    Background        0.0449236            *                *                   *
       Beta(1)                0            *                *                   *
       Beta(2)      0.000756128            *                *                   *

* - Indicates that this value is not calculated.


                       Analysis of Deviance Table

      Model      Log(likelihood)  # Param's  Deviance  Test d.f.   P-value
    Full model        -68.2481         4
   Fitted model       -69.0738         2       1.65141      2          0.4379
  Reduced model       -80.2977         1       24.0991      3         <.0001

          AIC:         142.148


                                 Goodness  of  Fit
                                                                      Scaled
    Dose     Est._Prob.    Expected    Observed     Size       Residual
  ---------------------------------------------------------------------------
    0.0000     0.0449         3.594         3          80       -0.321
    3.4200     0.0533         2.507         4          47        0.969
    8.5300     0.0960         4.610         3          48       -0.789
   21.2000     0.3201        15.364        16          48        0.197

 Chi^2 = 1.70      d.f. = 2        P-value = 0.4267
```

```
   Benchmark Dose Computation

Specified effect =            0.1

Risk Type        =      Extra risk

Confidence level =           0.95

              BMD =        11.8043

             BMDL =        6.28905

             BMDU =         15.532

Taken together, (6.28905, 15.532 ) is a 90     % two-sided confidence
interval for the BMD

Multistage Cancer Slope Factor =     0.0159007
```

BMDS (version 1.4.1) output for Zymbal gland tumors in Sprague-Dawley male rats employing CEO in blood as an internal dose metric

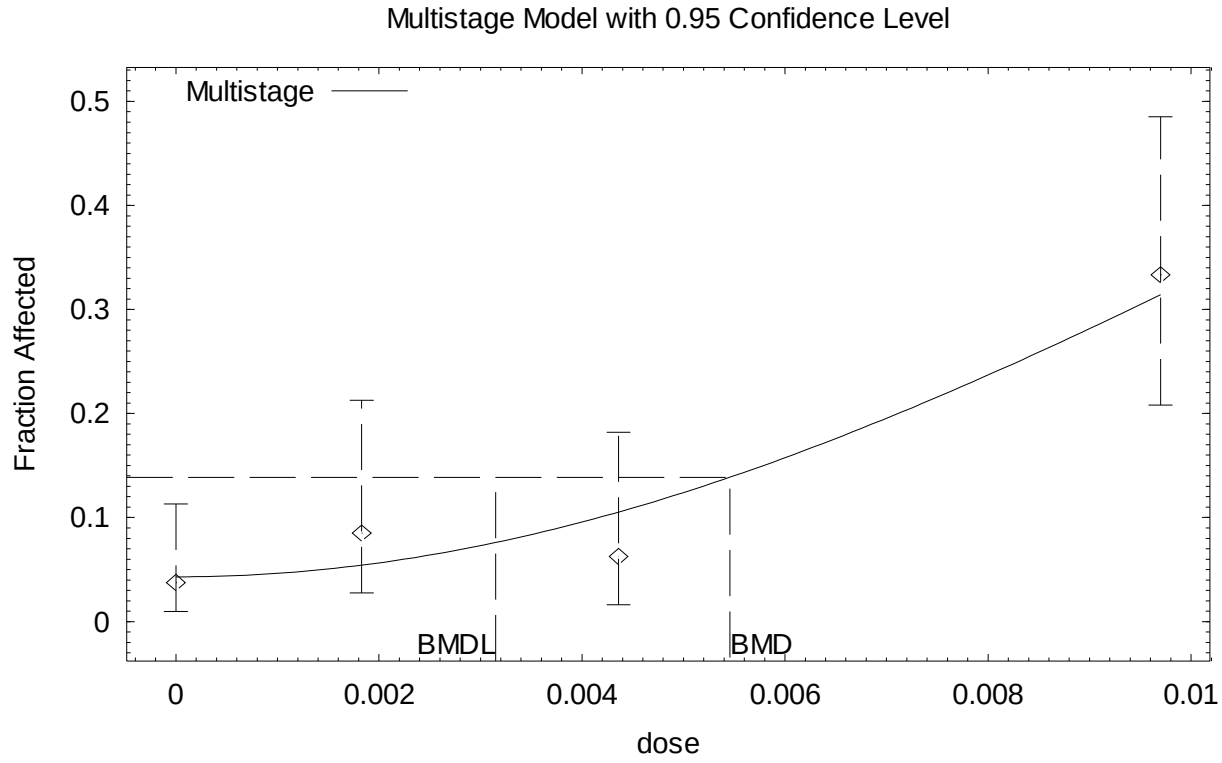


```
 ======================================================================
         Multistage Model. (Version: 2.8;  Date: 02/20/2007)
         Input Data File: G:\ACN DOSE-RESPONSE MODELING\CANCER\ORAL\SD_MALE_ZYMBAL_BLOOD_CEO.(d)
         Gnuplot Plotting File:  G:\ACN DOSE-RESPONSE
MODELING\CANCER\ORAL\SD_MALE_ZYMBAL_BLOOD_CEO.plt
                                                  Thu Sep 27 14:09:41 2007
 ======================================================================

 BMDS MODEL RUN
~~~~~~~~~~~~~~~~~~~~~~~~~~~~~~~~~~~~~~~~~~~~~~~~~~~~~~~~~~~~~~~~~~~~~~~~~~~~

   The form of the probability function is:

   P[response] = background + (1-background)*[1-EXP(
                -beta1*dose^1-beta2*dose^2)]

   The parameter betas are restricted to be positive


   Dependent variable = Response
   Independent variable = Dose

 Total number of observations = 4
 Total number of records with missing values = 0
 Total number of parameters in model = 3
 Total number of specified parameters = 0
 Degree of polynomial = 2


 Maximum number of iterations = 250
 Relative Function Convergence has been set to: 1e-008
 Parameter Convergence has been set to: 1e-008



                  Default Initial Parameter Values
                     Background =    0.0373755
```

```
                    Beta(1) =            0
                    Beta(2) =      3819.76


          Asymptotic Correlation Matrix of Parameter Estimates

          ( *** The model parameter(s)  -Beta(1)
                have been estimated at a boundary point, or have been specified by the user,
                and do not appear in the correlation matrix )

            Background      Beta(2)

Background            1        -0.51

   Beta(2)        -0.51            1



                               Parameter Estimates

                                                          95.0% Wald Confidence Interval
      Variable         Estimate        Std. Err.     Lower Conf. Limit   Upper Conf. Limit
    Background        0.0429942            *                *                   *
       Beta(1)                0            *                *                   *
       Beta(2)          3535.6             *                *                   *

* - Indicates that this value is not calculated.


                        Analysis of Deviance Table

      Model      Log(likelihood)  # Param's  Deviance  Test d.f.   P-value
    Full model        -68.2481         4
  Fitted model         -69.231         2       1.96583      2          0.3742
 Reduced model        -80.2977         1       24.0991      3         <.0001

          AIC:         142.462
```

Goodness of Fit

Dose	Est._Prob.	Expected	Observed	Size	Scaled Residual
0.0000	0.0430	3.440	3	80	-0.242
0.0018	0.0543	2.550	4	47	0.934
0.0044	0.1052	5.050	3	48	-0.964
0.0097	0.3138	15.063	16	48	0.291

Chi^2 = 1.94 d.f. = 2 P-value = 0.3781

Benchmark Dose Computation

Specified effect = 0.1

Risk Type = Extra risk

Confidence level = 0.95

BMD = 0.00545893

BMDL = 0.00315099

BMDU = 0.00717256

Taken together, (0.00315099, 0.00717256) is a 90 % two-sided confidence interval for the BMD

BMDS (version 1.4.1) output for Zymbal gland tumors in Sprague-Dawley male rats employing AN in blood as an internal dose metric

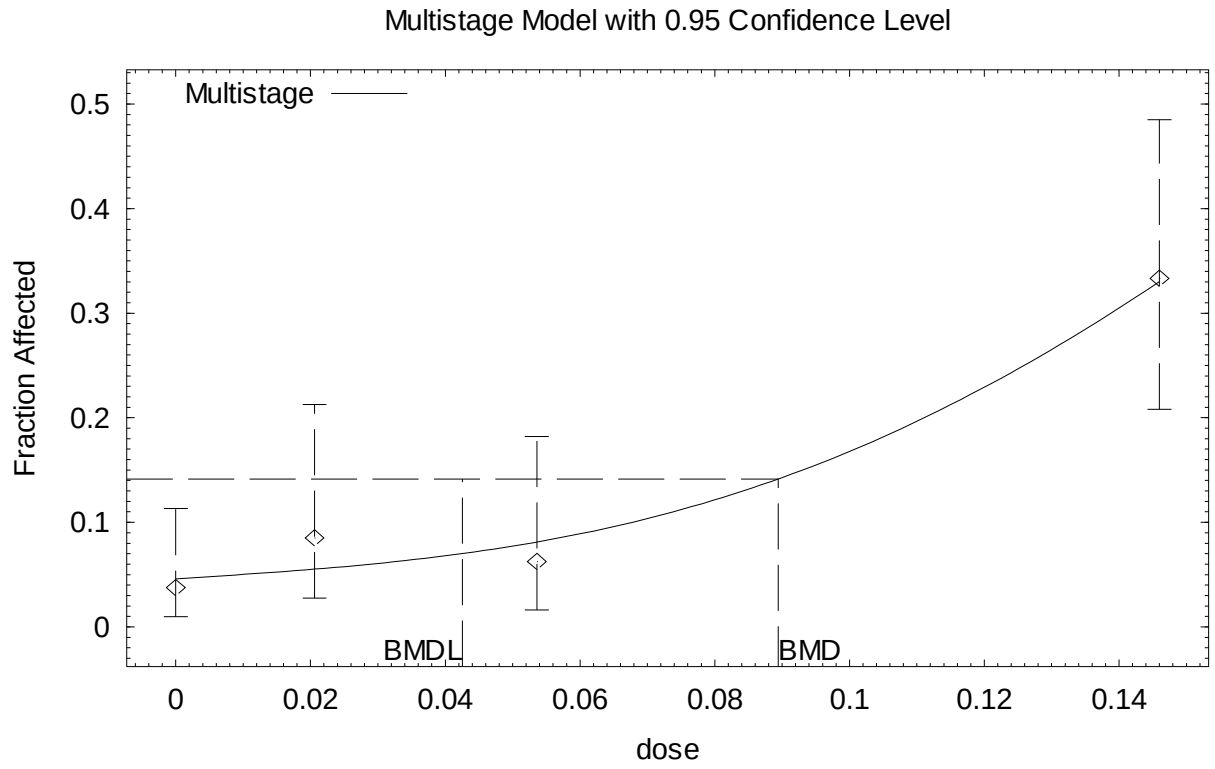


```
 ======================================================================
         Multistage Model. (Version: 2.8;  Date: 02/20/2007)
         Input Data File: G:\ACN DOSE-RESPONSE MODELING\CANCER\ORAL\SD_MALE_ZYMBAL_BLOOD_AN.(d)
         Gnuplot Plotting File:  G:\ACN DOSE-RESPONSE
MODELING\CANCER\ORAL\SD_MALE_ZYMBAL_BLOOD_AN.plt
                                                    Thu Sep 27 10:44:18 2007
 ======================================================================

 BMDS MODEL RUN
~~~~~~~~~~~~~~~~~~~~~~~~~~~~~~~~~~~~~~~~~~~~~~~~~~~~~~~~~~~~~~~~~~~~~~~~~~~~

   The form of the probability function is:

   P[response] = background + (1-background)*[1-EXP(
                -beta1*dose^1-beta2*dose^2-beta3*dose^3)]

   The parameter betas are restricted to be positive


   Dependent variable = Response
   Independent variable = Dose

 Total number of observations = 4
 Total number of records with missing values = 0
 Total number of parameters in model = 4
 Total number of specified parameters = 0
 Degree of polynomial = 3


 Maximum number of iterations = 250
 Relative Function Convergence has been set to: 1e-008
 Parameter Convergence has been set to: 1e-008

                 Default Initial Parameter Values
                    Background =    0.0542857
                       Beta(1) =    0.0987621
                       Beta(2) =            0
```

Beta(3) = 107.536

Asymptotic Correlation Matrix of Parameter Estimates

(*** The model parameter(s) -Beta(2)
have been estimated at a boundary point, or have been specified by the user,
and do not appear in the correlation matrix)

	Background	Beta(1)	Beta(3)
Background	1	-0.71	0.58
Beta(1)	-0.71	1	-0.95
Beta(3)	0.58	-0.95	1

Parameter Estimates

Variable	Estimate	Std. Err.	95.0% Wald Confidence Interval Lower Conf. Limit	Upper Conf. Limit
Background	0.0460186	*	*	*
Beta(1)	0.432974	*	*	*
Beta(2)	0	*	*	*
Beta(3)	93.2629	*	*	*

* - Indicates that this value is not calculated.

Analysis of Deviance Table

Model	Log(likelihood)	# Param's	Deviance	Test d.f.	P-value
Full model	-68.2481	4			
Fitted model	-68.7881	3	1.07988	1	0.2987
Reduced model	-80.2977	1	24.0991	3	<.0001

AIC: 143.576

Goodness of Fit

Dose	Est._Prob.	Expected	Observed	Size	Scaled Residual
0.0000	0.0460	3.681	3	80	-0.364
0.0206	0.0553	2.597	4	47	0.896
0.0536	0.0812	3.897	3	48	-0.474
0.1460	0.3301	15.843	16	48	0.048

Chi^2 = 1.16 d.f. = 1 P-value = 0.2812

Benchmark Dose Computation

Specified effect = 0.1

Risk Type = Extra risk

Confidence level = 0.95

BMD = 0.0894055

BMDL = 0.0425525

BMDU = 0.117269

Taken together, (0.0425525, 0.117269) is a 90 % two-sided confidence
interval for the BMD

BMDS (version 1.4.1) output for Zymbal gland tumors in Sprague-Dawley female rats employing administered dose as a dose metric

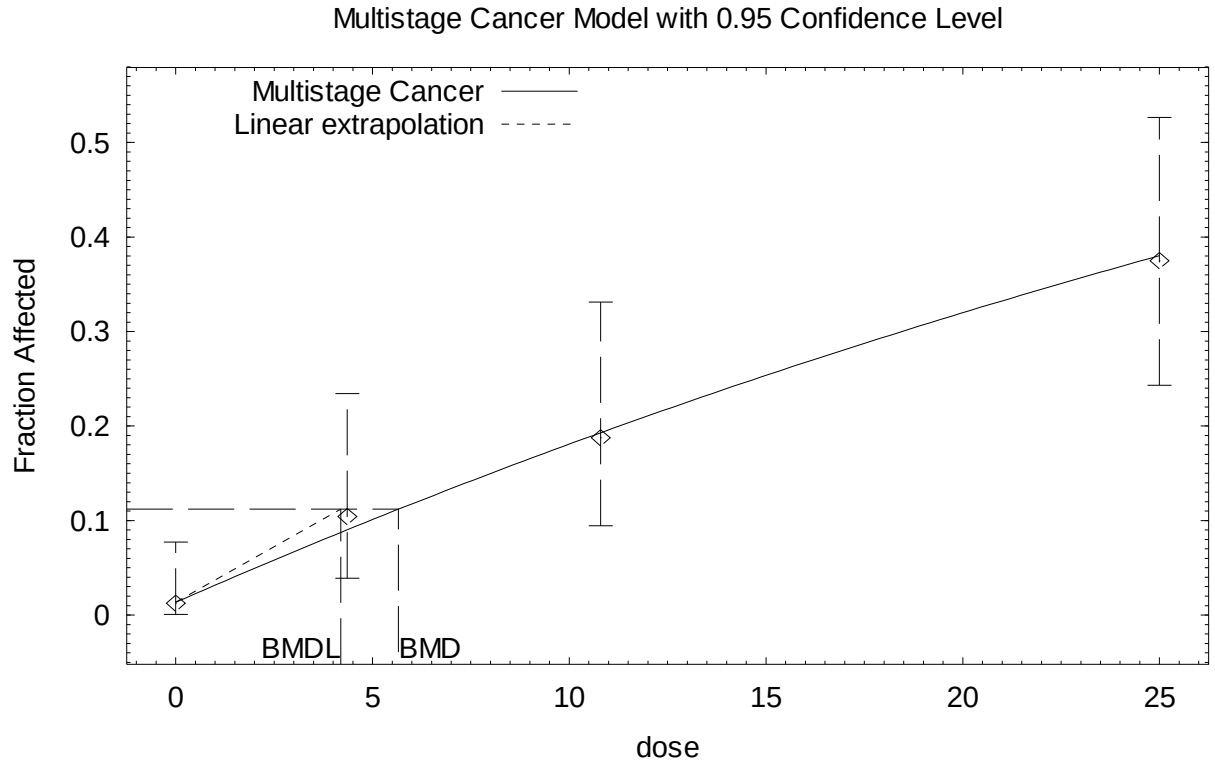


```
 ======================================================================
         Multistage Cancer Model. (Version: 1.5;  Date: 02/20/2007)
         Input Data File: M:\ACN DOSE-RESPONSE MODELING\CANCER\ORAL\SD_FEMALE_ZYMBAL_DW.(d)
         Gnuplot Plotting File:  M:\ACN DOSE-RESPONSE
MODELING\CANCER\ORAL\SD_FEMALE_ZYMBAL_DW.plt
                                                    Fri Jan 23 16:28:50 2009
 ======================================================================

 BMDS MODEL RUN
~~~~~~~~~~~~~~~~~~~~~~~~~~~~~~~~~~~~~~~~~~~~~~~~~~~~~~~~~~~~~~~~~~~~~~~~

   The form of the probability function is:

   P[response] = background + (1-background)*[1-EXP(
                -beta1*dose^1)]

   The parameter betas are restricted to be positive


   Dependent variable = Response
   Independent variable = Dose

 Total number of observations = 4
 Total number of records with missing values = 0
 Total number of parameters in model = 2
 Total number of specified parameters = 0
 Degree of polynomial = 1


 Maximum number of iterations = 250
 Relative Function Convergence has been set to: 1e-008
 Parameter Convergence has been set to: 1e-008
```

Default Initial Parameter Values
Background = 0.0190401
Beta(1) = 0.0180112

Asymptotic Correlation Matrix of Parameter Estimates

	Background	Beta(1)
Background	1	-0.64
Beta(1)	-0.64	1

Parameter Estimates

Variable	Estimate	Std. Err.	95.0% Wald Confidence Interval Lower Conf. Limit	Upper Conf. Limit
Background	0.013388	*	*	*
Beta(1)	0.0186127	*	*	*

* - Indicates that this value is not calculated.

Analysis of Deviance Table

Model	Log(likelihood)	# Param's	Deviance	Test d.f.	P-value
Full model	-76.3334	4			
Fitted model	-76.3975	2	0.128259	2	0.9379
Reduced model	-93.6397	1	34.6128	3	<.0001

AIC: 156.795

Goodness of Fit

Dose	Est._Prob.	Expected	Observed	Size	Scaled Residual
0.0000	0.0134	1.071	1	80	-0.069
4.3600	0.0903	4.334	5	48	0.335
10.8000	0.1931	9.266	9	48	-0.097
25.0000	0.3805	18.263	18	48	-0.078

Chi^2 = 0.13 d.f. = 2 P-value = 0.9357

Benchmark Dose Computation

Specified effect = 0.1

Risk Type = Extra risk

Confidence level = 0.95

BMD = 5.66068

BMDL = 4.19199

BMDU = 8.10463

Taken together, (4.19199, 8.10463) is a 90 % two-sided confidence interval for the BMD

Multistage Cancer Slope Factor = 0.023855

BMDS (version 1.4.1) output for Zymbal gland tumors in Sprague-Dawley female rats employing CEO in blood as an internal dose metric

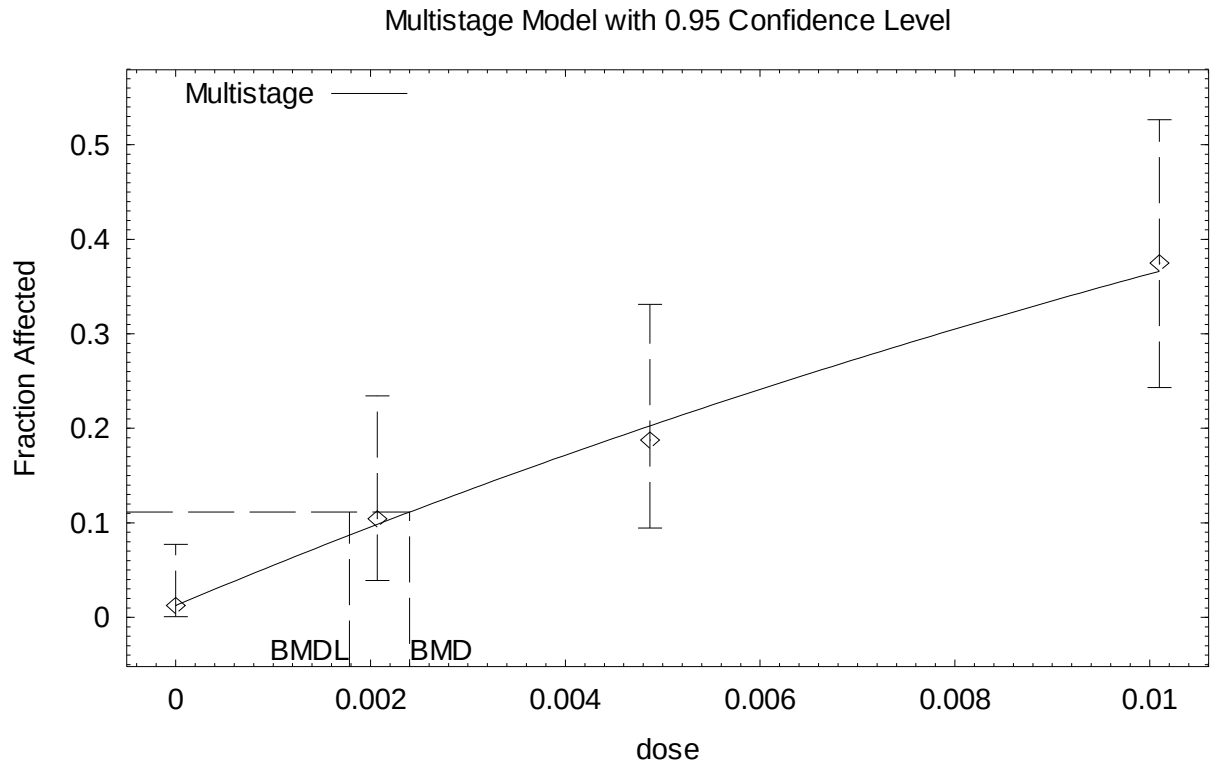


```
 ================================================================
         Multistage Model. (Version: 2.8;  Date: 02/20/2007)
         Input Data File: G:\ACN DOSE-RESPONSE
MODELING\CANCER\ORAL\SD_FEMALE_ZYMBAL_BLOOD_CEO.(d)
         Gnuplot Plotting File:  G:\ACN DOSE-RESPONSE
MODELING\CANCER\ORAL\SD_FEMALE_ZYMBAL_BLOOD_CEO.plt
                                                Thu Sep 27 14:43:02 2007
 ================================================================

 BMDS MODEL RUN
~~~~~~~~~~~~~~~~~~~~~~~~~~~~~~~~~~~~~~~~~~~~~~~~~~~~~~~~~~~~~~~~~~~~~~~

   The form of the probability function is:

   P[response] = background + (1-background)*[1-EXP(
                -beta1*dose^1)]

   The parameter betas are restricted to be positive


   Dependent variable = Response
   Independent variable = Dose

 Total number of observations = 4
 Total number of records with missing values = 0
 Total number of parameters in model = 2
 Total number of specified parameters = 0
 Degree of polynomial = 1


 Maximum number of iterations = 250
 Relative Function Convergence has been set to: 1e-008
 Parameter Convergence has been set to: 1e-008


                  Default Initial Parameter Values
```

```
                    Background =   0.00883347
                       Beta(1) =      44.8786


          Asymptotic Correlation Matrix of Parameter Estimates

            Background      Beta(1)

Background            1        -0.65

   Beta(1)        -0.65            1


                                Parameter Estimates

                                                        95.0% Wald Confidence Interval
      Variable         Estimate        Std. Err.     Lower Conf. Limit   Upper Conf. Limit
    Background        0.0125628            *                *                   *
       Beta(1)          43.9052            *                *                   *

* - Indicates that this value is not calculated.


                        Analysis of Deviance Table

       Model      Log(likelihood)  # Param's  Deviance  Test d.f.   P-value
     Full model        -76.3334         4
   Fitted model         -76.385         2      0.103357      2          0.9496
  Reduced model        -93.6397         1       34.6128      3         <.0001

           AIC:          156.77


                                Goodness  of  Fit
                                                                      Scaled
     Dose     Est._Prob.    Expected    Observed     Size       Residual
  ---------------------------------------------------------------------------
    0.0000     0.0126         1.005         1          80       -0.005
    0.0021     0.0983         4.721         5          48        0.135
    0.0049     0.2026         9.727         9          48       -0.261
    0.0101     0.3662        17.580        18          48        0.126

 Chi^2 = 0.10      d.f. = 2        P-value = 0.9501


   Benchmark Dose Computation

Specified effect =           0.1

Risk Type        =      Extra risk

Confidence level =          0.95

             BMD =     0.00239973

            BMDL =     0.00178178

            BMDU =     0.00341242

Taken together, (0.00178178, 0.00341242) is a 90     % two-sided confidence
interval for the BMD
```

BMDS (version 1.4.1) output for Zymbal gland tumors in Sprague-Dawley female rats employing AN in blood as an internal dose metric

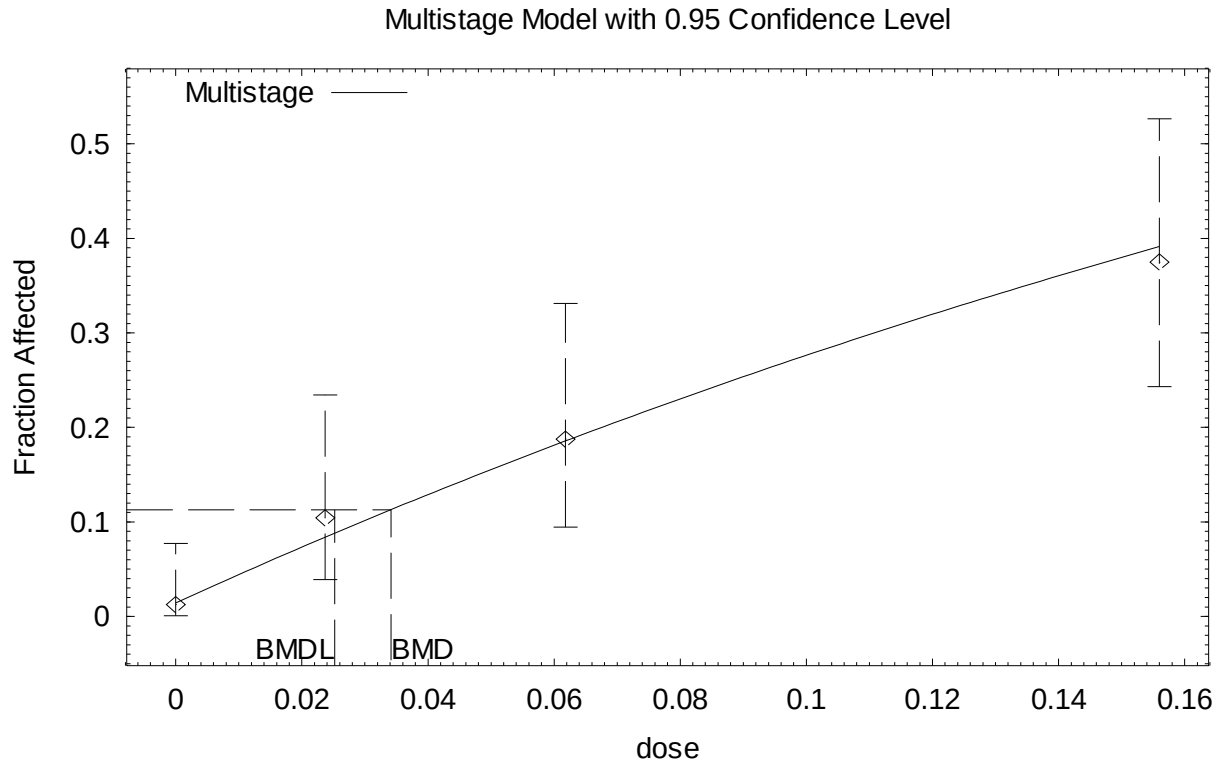

10:55 09/27 2007

```
 ======================================================================
         Multistage Model. (Version: 2.8;  Date: 02/20/2007)
         Input Data File: G:\ACN DOSE-RESPONSE
MODELING\CANCER\ORAL\SD_FEMALE_ZYMBAL_BLOOD_AN.(d)
         Gnuplot Plotting File:  G:\ACN DOSE-RESPONSE
MODELING\CANCER\ORAL\SD_FEMALE_ZYMBAL_BLOOD_AN.plt
                                                  Thu Sep 27 10:55:27 2007
 ======================================================================

 BMDS MODEL RUN
~~~~~~~~~~~~~~~~~~~~~~~~~~~~~~~~~~~~~~~~~~~~~~~~~~~~~~~~~~~~~~~~~~~~~~~~

   The form of the probability function is:

   P[response] = background + (1-background)*[1-EXP(
                -beta1*dose^1)]

   The parameter betas are restricted to be positive


   Dependent variable = Response
   Independent variable = Dose

 Total number of observations = 4
 Total number of records with missing values = 0
 Total number of parameters in model = 2
 Total number of specified parameters = 0
 Degree of polynomial = 1


 Maximum number of iterations = 250
 Relative Function Convergence has been set to: 1e-008
 Parameter Convergence has been set to: 1e-008
```

Default Initial Parameter Values
Background = 0.0269441
Beta(1) = 2.86115

Asymptotic Correlation Matrix of Parameter Estimates

	Background	Beta(1)
Background	1	-0.63
Beta(1)	-0.63	1

Parameter Estimates

Variable	Estimate	Std. Err.	95.0% Wald Confidence Interval Lower Conf. Limit	Upper Conf. Limit
Background	0.0143198	*	*	*
Beta(1)	3.08705	*	*	*

* - Indicates that this value is not calculated.

Analysis of Deviance Table

Model	Log(likelihood)	# Param's	Deviance	Test d.f.	P-value
Full model	-76.3334	4			
Fitted model	-76.4902	2	0.313733	2	0.8548
Reduced model	-93.6397	1	34.6128	3	<.0001

AIC: 156.98

Goodness of Fit

Dose	Est._Prob.	Expected	Observed	Size	Scaled Residual
0.0000	0.0143	1.146	1	80	-0.137
0.0237	0.0839	4.025	5	48	0.508
0.0618	0.1855	8.905	9	48	0.035
0.1560	0.3910	18.770	18	48	-0.228

Chi^2 = 0.33 d.f. = 2 P-value = 0.8481

Benchmark Dose Computation

Specified effect = 0.1

Risk Type = Extra risk

Confidence level = 0.95

BMD = 0.0341298

BMDL = 0.0251994

BMDU = 0.0492353

Taken together, (0.0251994, 0.0492353) is a 90 % two-sided confidence interval for the BMD

Tumor Site: Tongue (Quast, 2002; Quast et al., 1980a)

Table B-15. Incidence of tongue tumors in Sprague-Dawley rats exposed to AN in drinking water for 2 years

Sex	Administered animal dose (ppm in drinking water)	Equivalent administered animal dose[a] (mg/kg-d)	Predicted internal dose metrics		Incidence of tongue tumors[b]
			AN-AUC in blood (mg/L)	CEO-AUC in blood (mg/L)	
Male	0	0	0	0	1/80 (1%)
	35	3.42	2.06×10^{-2}	1.83×10^{-3}	2/47 (4%)
	100	8.53	5.36×10^{-2}	4.36×10^{-3}	4/48 (8%)
	300	21.2	1.46×10^{-1}	9.70×10^{-3}	5/48 (10%)[c]
Female	0	0	0	0	0/80 (0%)
	35	4.36	2.37×10^{-2}	2.07×10^{-3}	1/48 (2%)
	100	10.8	6.18×10^{-2}	4.87×10^{-3}	2/48 (4%)
	300	25.0	1.56×10^{-1}	1.01×10^{-2}	12/48 (25%)[c]

[a]Administered doses were averages calculated by the study authors based on animal BW and drinking water intake.
[b]Incidences for Sprague-Dawley rats do not include animals from the 6- and 12-mo sacrifices and were further adjusted to exclude (from the denominators) rats that died between 0 and 12 mos in the study.
[c]Significantly different from controls ($p < 0.05$) as calculated by the study authors.

Table B-16. Summary of BMD modeling results based on incidence of tongue tumors in Sprague-Dawley rats exposed to AN in drinking water for 2 years

Dose metric	Best-fit model[a]	χ^2 *p*-value[b]	AIC	BMD_{10}[c]	$BMDL_{10}$[d]
Males					
Administered dose	1°MS	0.69	91.62	18.89 mg/kg-d	10.35 mg/kg-d
CEO	1°MS	0.78	91.40	8.78×10^{-3} mg/L	4.90×10^{-3} mg/L
AN	1°MS	0.62	91.83	1.29×10^{-1} mg/L	6.97×10^{-2} mg/L
Females					
Administered dose	3°MS	0.92	84.51	15.99 mg/kg-d	10.64 mg/kg-d
CEO	3°MS	0.88	84.59	6.70×10^{-3} mg/L	4.74×10^{-3} mg/L
AN	3°MS	0.93	84.48	9.67×10^{-2} mg/L	6.10×10^{-2} mg/L

[a]Dose-response models were fit using BMDS, version 1.4.1. "1°MS" indicates a one-stage multistage model and "3°MS" indicates a three-stage multistage model.
[b]*p* value from the χ^2 goodness of fit test. Values <0.1 indicate a significant lack of fit.
[c]BMD_{10} = BMD at 10% extra risk.
[d]$BMDL_{10}$ = 95% lower confidence limit on the BMD at 10% extra risk.

BMDS (version 1.4.1) output for tongue tumors in Sprague-Dawley male rats employing administered dose as a dose metric

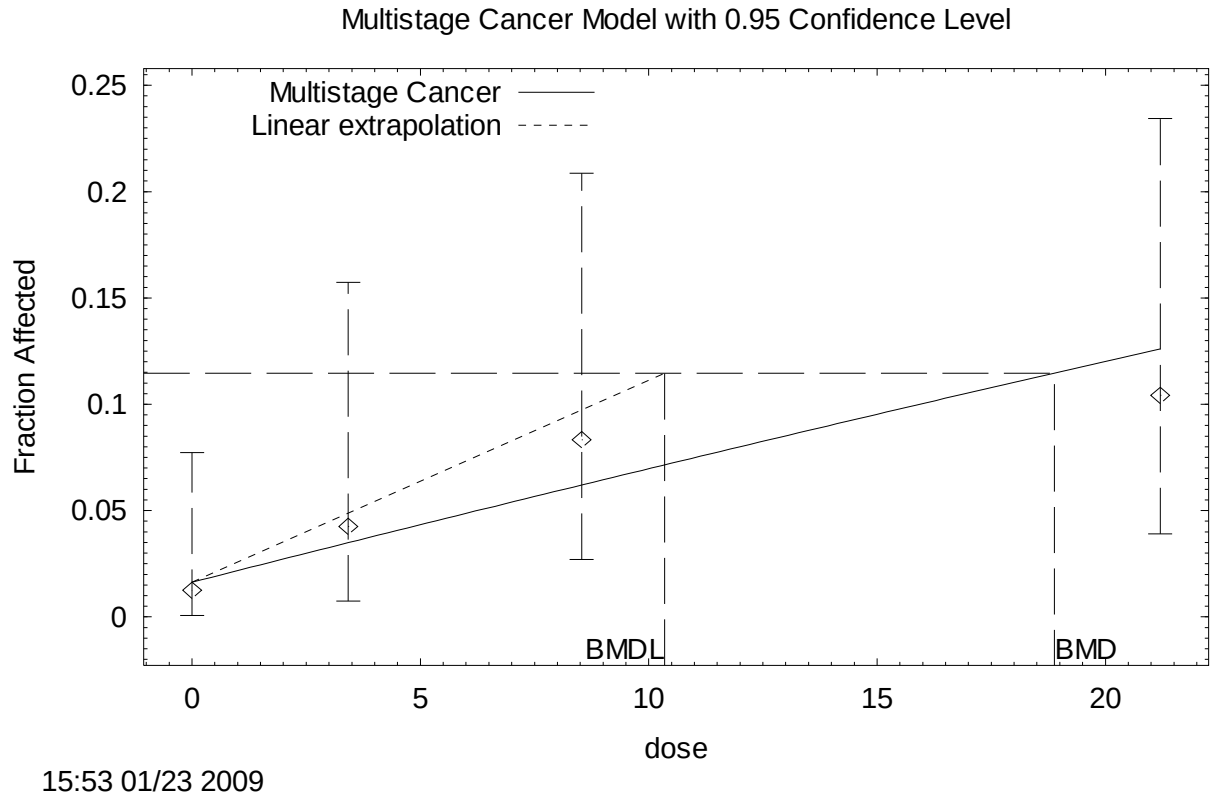


```
================================================================
        Multistage Cancer Model. (Version: 1.5;  Date: 02/20/2007)
        Input Data File: M:\ACN DOSE-RESPONSE MODELING\CANCER\ORAL\SD_MALE_TONGUE_DW.(d)
        Gnuplot Plotting File:  M:\ACN DOSE-RESPONSE MODELING\CANCER\ORAL\SD_MALE_TONGUE_DW.plt
                                                Fri Jan 23 15:53:59 2009
================================================================

BMDS MODEL RUN
~~~~~~~~~~~~~~~~~~~~~~~~~~~~~~~~~~~~~~~~~~~~~~~~~~~~~~~~~~~~~~~~~~~~~~~~

  The form of the probability function is:

  P[response] = background + (1-background)*[1-EXP(
               -beta1*dose^1)]

  The parameter betas are restricted to be positive


  Dependent variable = Response
  Independent variable = Dose

Total number of observations = 4
Total number of records with missing values = 0
Total number of parameters in model = 2
Total number of specified parameters = 0
Degree of polynomial = 1


Maximum number of iterations = 250
Relative Function Convergence has been set to: 1e-008
Parameter Convergence has been set to: 1e-008


                 Default Initial Parameter Values
```

Background = 0.0269073
Beta(1) = 0.00434306

Asymptotic Correlation Matrix of Parameter Estimates

	Background	Beta(1)
Background	1	-0.69
Beta(1)	-0.69	1

Parameter Estimates

Variable	Estimate	Std. Err.	95.0% Wald Confidence Interval Lower Conf. Limit	Upper Conf. Limit
Background	0.0162768	*	*	*
Beta(1)	0.00557883	*	*	*

* - Indicates that this value is not calculated.

Analysis of Deviance Table

Model	Log(likelihood)	# Param's	Deviance	Test d.f.	P-value
Full model	-43.4536	4			
Fitted model	-43.8112	2	0.715245	2	0.6993
Reduced model	-46.7384	1	6.56959	3	0.08696

AIC: 91.6224

Goodness of Fit

Dose	Est._Prob.	Expected	Observed	Size	Scaled Residual
0.0000	0.0163	1.302	1	80	-0.267
3.4200	0.0349	1.639	2	47	0.287
8.5300	0.0620	2.976	4	48	0.613
21.2000	0.1260	6.048	5	48	-0.456

Chi^2 = 0.74 d.f. = 2 P-value = 0.6916

```
   Benchmark Dose Computation

Specified effect =            0.1

Risk Type        =      Extra risk

Confidence level =           0.95

              BMD =        18.8858

             BMDL =        10.3512

             BMDU =        62.8005

Taken together, (10.3512, 62.8005) is a 90     % two-sided confidence
interval for the BMD

Multistage Cancer Slope Factor =    0.00966069
```

BMDS (version 1.4.1) output for tongue tumors in Sprague-Dawley male rats employing CEO in blood as an internal dose metric

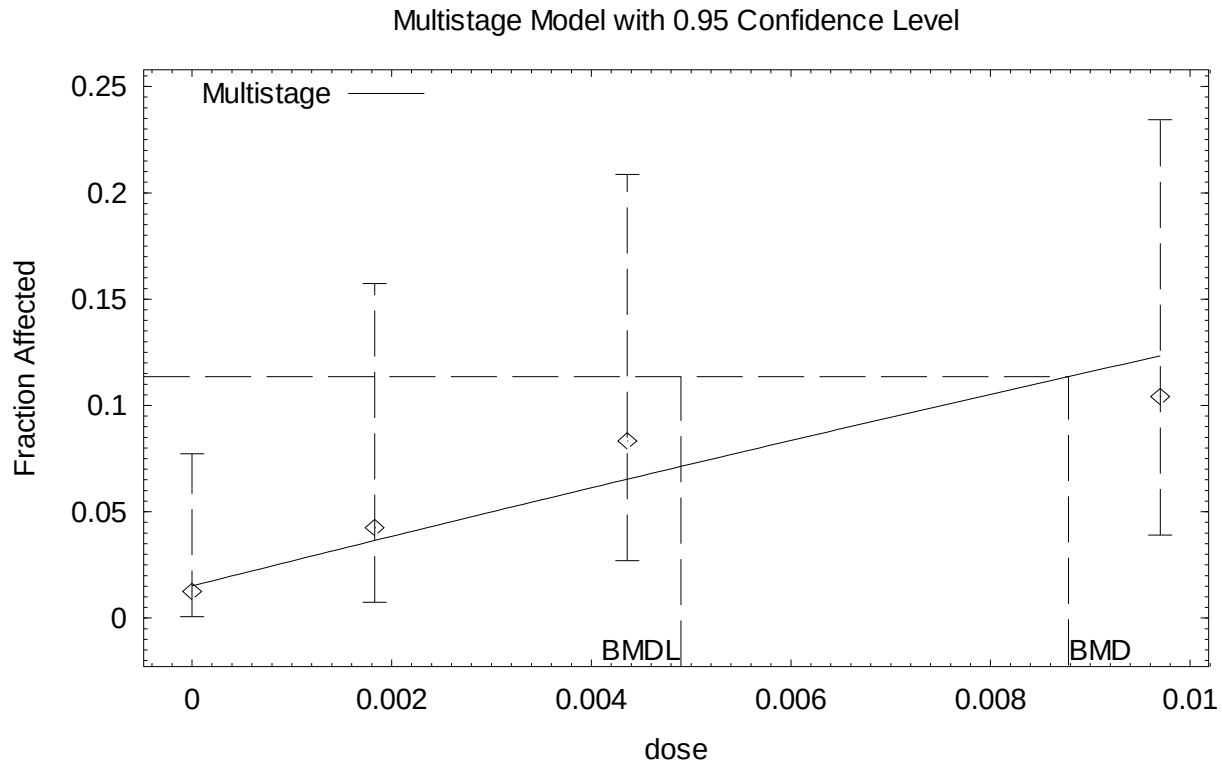


```
 ======================================================================
         Multistage Model. (Version: 2.8;  Date: 02/20/2007)
         Input Data File: G:\ACN DOSE-RESPONSE MODELING\CANCER\ORAL\SD_MALE_TONGUE_BLOOD_CEO.(d)
         Gnuplot Plotting File:  G:\ACN DOSE-RESPONSE
MODELING\CANCER\ORAL\SD_MALE_TONGUE_BLOOD_CEO.plt
                                                  Thu Sep 27 14:19:57 2007
 ======================================================================

 BMDS MODEL RUN
~~~~~~~~~~~~~~~~~~~~~~~~~~~~~~~~~~~~~~~~~~~~~~~~~~~~~~~~~~~~~~~~~~~~~~~~

   The form of the probability function is:

   P[response] = background + (1-background)*[1-EXP(
                -beta1*dose^1)]

   The parameter betas are restricted to be positive


   Dependent variable = Response
   Independent variable = Dose

 Total number of observations = 4
 Total number of records with missing values = 0
 Total number of parameters in model = 2
 Total number of specified parameters = 0
 Degree of polynomial = 1


 Maximum number of iterations = 250
 Relative Function Convergence has been set to: 1e-008
 Parameter Convergence has been set to: 1e-008
```

Default Initial Parameter Values
Background = 0.0241886
Beta(1) = 9.76289

Asymptotic Correlation Matrix of Parameter Estimates

	Background	Beta(1)
Background	1	-0.7
Beta(1)	-0.7	1

Parameter Estimates

Variable	Estimate	Std. Err.	95.0% Wald Confidence Interval Lower Conf. Limit	Upper Conf. Limit
Background	0.0150764	*	*	*
Beta(1)	11.9992	*	*	*

* - Indicates that this value is not calculated.

Analysis of Deviance Table

Model	Log(likelihood)	# Param's	Deviance	Test d.f.	P-value
Full model	-43.4536	4			
Fitted model	-43.6998	2	0.492394	2	0.7818
Reduced model	-46.7384	1	6.56959	3	0.08696

AIC: 91.3995

Goodness of Fit

Dose	Est._Prob.	Expected	Observed	Size	Scaled Residual
0.0000	0.0151	1.206	1	80	-0.189
0.0018	0.0365	1.714	2	47	0.223
0.0044	0.0653	3.133	4	48	0.506
0.0097	0.1233	5.918	5	48	-0.403

Chi^2 = 0.50 d.f. = 2 P-value = 0.7772

Benchmark Dose Computation

Specified effect = 0.1

Risk Type = Extra risk

Confidence level = 0.95

BMD = 0.00878063

BMDL = 0.00489829

BMDU = 0.0274259

Taken together, (0.00489829, 0.0274259) is a 90 % two-sided confidence interval for the BMD

BMDS (version 1.4.1) output for tongue tumors in Sprague-Dawley male rats employing AN in blood as an internal dose metric

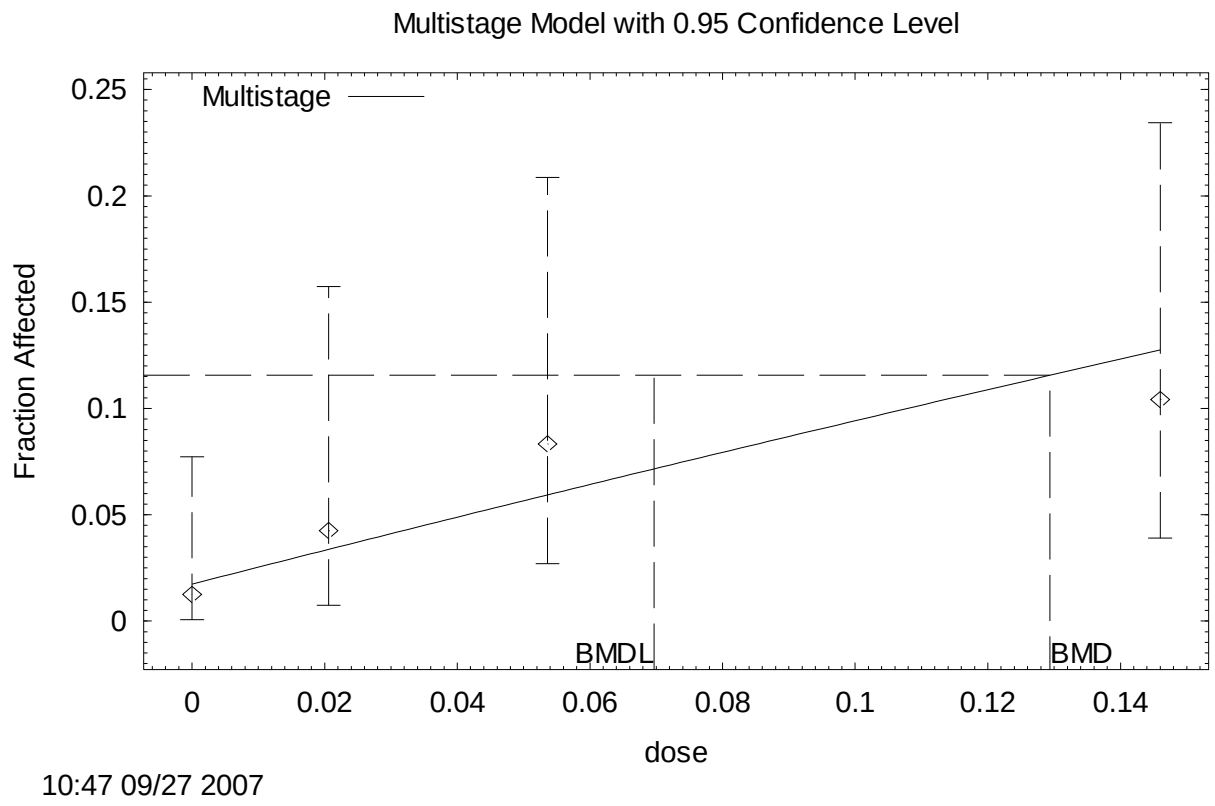


```
 ======================================================================
         Multistage Model. (Version: 2.8;  Date: 02/20/2007)
         Input Data File: G:\ACN DOSE-RESPONSE MODELING\CANCER\ORAL\SD_MALE_TONGUE_BLOOD_AN.(d)
         Gnuplot Plotting File:  G:\ACN DOSE-RESPONSE
MODELING\CANCER\ORAL\SD_MALE_TONGUE_BLOOD_AN.plt
                                                Thu Sep 27 10:47:13 2007
 ======================================================================

 BMDS MODEL RUN
~~~~~~~~~~~~~~~~~~~~~~~~~~~~~~~~~~~~~~~~~~~~~~~~~~~~~~~~~~~~~~~~~~~~~~~~

   The form of the probability function is:

   P[response] = background + (1-background)*[1-EXP(
                -beta1*dose^1)]

   The parameter betas are restricted to be positive


   Dependent variable = Response
   Independent variable = Dose

 Total number of observations = 4
 Total number of records with missing values = 0
 Total number of parameters in model = 2
 Total number of specified parameters = 0
 Degree of polynomial = 1


 Maximum number of iterations = 250
 Relative Function Convergence has been set to: 1e-008
 Parameter Convergence has been set to: 1e-008
```

Default Initial Parameter Values
Background = 0.0289604
Beta(1) = 0.615459

Asymptotic Correlation Matrix of Parameter Estimates

	Background	Beta(1)
Background	1	-0.68
Beta(1)	-0.68	1

Parameter Estimates

Variable	Estimate	Std. Err.	95.0% Wald Confidence Interval Lower Conf. Limit	Upper Conf. Limit
Background	0.0174494	*	*	*
Beta(1)	0.814352	*	*	*

* - Indicates that this value is not calculated.

Analysis of Deviance Table

Model	Log(likelihood)	# Param's	Deviance	Test d.f.	P-value
Full model	-43.4536	4			
Fitted model	-43.9131	2	0.919024	2	0.6316
Reduced model	-46.7384	1	6.56959	3	0.08696

AIC: 91.8261

Goodness of Fit

Dose	Est._Prob.	Expected	Observed	Size	Scaled Residual
0.0000	0.0174	1.396	1	80	-0.338
0.0206	0.0338	1.588	2	47	0.332
0.0536	0.0594	2.852	4	48	0.701
0.1460	0.1276	6.124	5	48	-0.486

Chi^2 = 0.95 d.f. = 2 P-value = 0.6210

Benchmark Dose Computation

Specified effect = 0.1

Risk Type = Extra risk

Confidence level = 0.95

BMD = 0.12938

BMDL = 0.0696872

BMDU = 0.4562

Taken together, (0.0696872, 0.4562) is a 90 % two-sided confidence interval for the BMD

BMDS (version 1.4.1) output for tongue tumors in Sprague-Dawley female rats employing administered dose as a dose metric

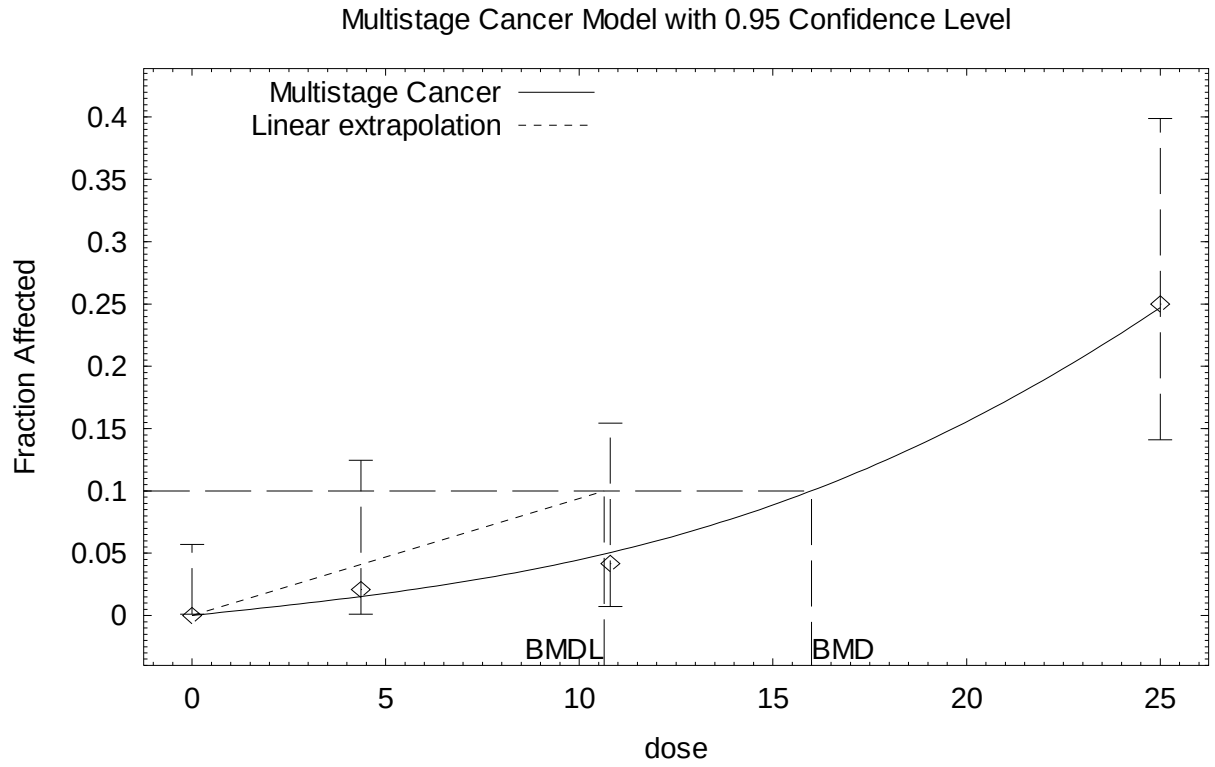


```
 ======================================================================
         Multistage Cancer Model. (Version: 1.5;  Date: 02/20/2007)
         Input Data File: M:\ACN DOSE-RESPONSE MODELING\CANCER\ORAL\SD_FEMALE_TONGUE_DW.(d)
         Gnuplot Plotting File:  M:\ACN DOSE-RESPONSE
MODELING\CANCER\ORAL\SD_FEMALE_TONGUE_DW.plt
                                                    Fri Jan 23 16:26:08 2009
 ======================================================================

 BMDS MODEL RUN
~~~~~~~~~~~~~~~~~~~~~~~~~~~~~~~~~~~~~~~~~~~~~~~~~~~~~~~~~~~~~~~~~~~~~~~~~~~~

   The form of the probability function is:

   P[response] = background + (1-background)*[1-EXP(
                -beta1*dose^1-beta2*dose^2-beta3*dose^3)]

   The parameter betas are restricted to be positive


   Dependent variable = Response
   Independent variable = Dose

 Total number of observations = 4
 Total number of records with missing values = 0
 Total number of parameters in model = 4
 Total number of specified parameters = 0
 Degree of polynomial = 3


 Maximum number of iterations = 250
 Relative Function Convergence has been set to: 1e-008
 Parameter Convergence has been set to: 1e-008
```

Default Initial Parameter Values
Background = 0.00365935
Beta(1) = 0.00218662
Beta(2) = 0
Beta(3) = 1.46642e-005

Asymptotic Correlation Matrix of Parameter Estimates

(*** The model parameter(s) -Background -Beta(2)
have been estimated at a boundary point, or have been specified by the user,
and do not appear in the correlation matrix)

	Beta(1)	Beta(3)
Beta(1)	1	-0.93
Beta(3)	-0.93	1

Parameter Estimates

Variable	Estimate	Std. Err.	95.0% Wald Confidence Interval Lower Conf. Limit	Upper Conf. Limit
Background	0	*	*	*
Beta(1)	0.00329024	*	*	*
Beta(2)	0	*	*	*
Beta(3)	1.28922e-005	*	*	*

* - Indicates that this value is not calculated.

Analysis of Deviance Table

Model	Log(likelihood)	# Param's	Deviance	Test d.f.	P-value
Full model	-40.1666	4			
Fitted model	-40.2528	2	0.172251	2	0.9175
Reduced model	-55.0401	1	29.7469	3	<.0001

AIC: 84.5055

Goodness of Fit

Dose	Est._Prob.	Expected	Observed	Size	Scaled Residual
0.0000	0.0000	0.000	0	80	0.000
4.3600	0.0153	0.734	1	48	0.313
10.8000	0.0505	2.422	2	48	-0.278
25.0000	0.2470	11.856	12	48	0.048

Chi^2 = 0.18 d.f. = 2 P-value = 0.9151

Benchmark Dose Computation

Specified effect = 0.1

Risk Type = Extra risk

Confidence level = 0.95

BMD = 15.9932

BMDL = 10.6421

BMDU = 19.9332

Taken together, (10.6421, 19.9332) is a 90 % two-sided confidence interval for the BMD

Multistage Cancer Slope Factor = 0.00939663

BMDS (version 1.4.1) output for tongue tumors in Sprague-Dawley female rats employing CEO in blood as an internal dose metric

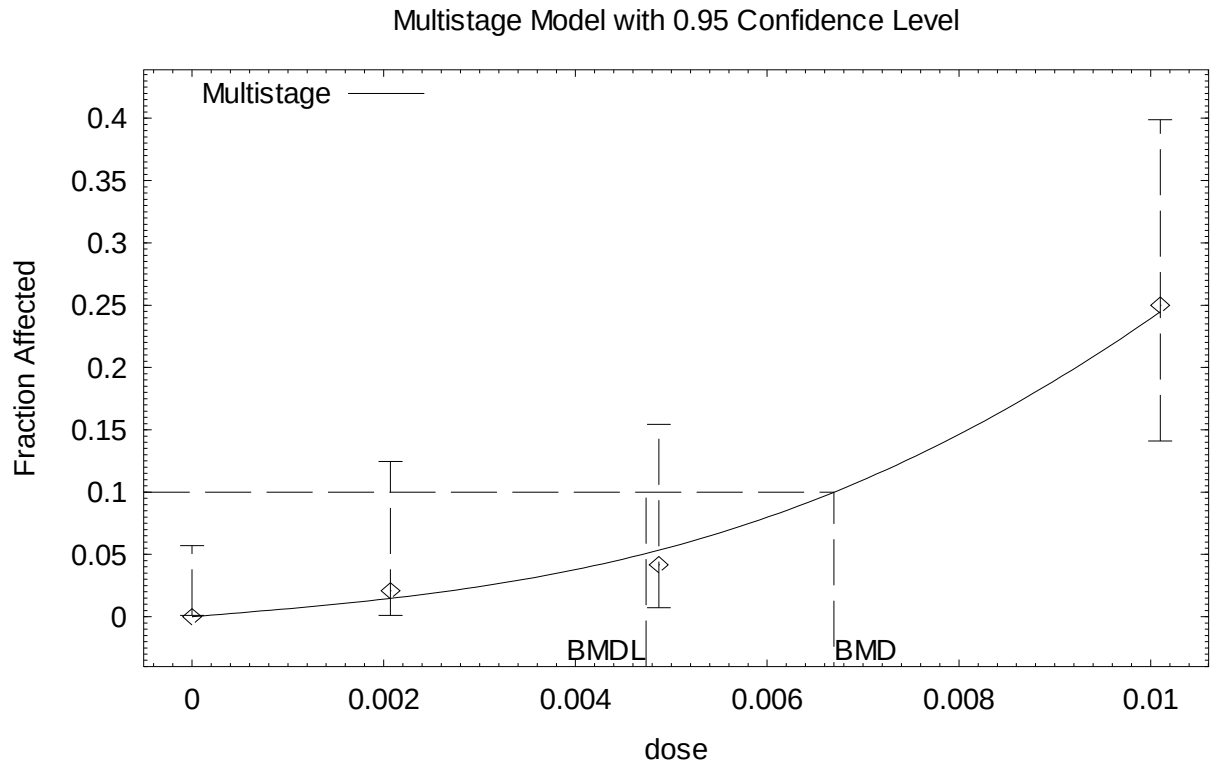


```
 ======================================================================
         Multistage Model. (Version: 2.8;  Date: 02/20/2007)
         Input Data File: G:\ACN DOSE-RESPONSE
MODELING\CANCER\ORAL\SD_FEMALE_TONGUE_BLOOD_CEO.(d)
         Gnuplot Plotting File:  G:\ACN DOSE-RESPONSE
MODELING\CANCER\ORAL\SD_FEMALE_TONGUE_BLOOD_CEO.plt
                                                  Thu Sep 27 14:49:16 2007
 ======================================================================

 BMDS MODEL RUN
~~~~~~~~~~~~~~~~~~~~~~~~~~~~~~~~~~~~~~~~~~~~~~~~~~~~~~~~~~~~~~~~~~~~~~~~

   The form of the probability function is:

   P[response] = background + (1-background)*[1-EXP(
                -beta1*dose^1-beta2*dose^2-beta3*dose^3)]

   The parameter betas are restricted to be positive

   Dependent variable = Response
   Independent variable = Dose

 Total number of observations = 4
 Total number of records with missing values = 0
 Total number of parameters in model = 4
 Total number of specified parameters = 0
 Degree of polynomial = 3

 Maximum number of iterations = 250
 Relative Function Convergence has been set to: 1e-008
 Parameter Convergence has been set to: 1e-008

                 Default Initial Parameter Values
                    Background =    0.0043768
                       Beta(1) =      2.92561
                       Beta(2) =            0
                       Beta(3) =       245868
```

Asymptotic Correlation Matrix of Parameter Estimates

(*** The model parameter(s) -Background -Beta(2)
have been estimated at a boundary point, or have been specified by the user,
and do not appear in the correlation matrix)

	Beta(1)	Beta(3)
Beta(1)	1	-0.92
Beta(3)	-0.92	1

Parameter Estimates

Variable	Estimate	Std. Err.	95.0% Wald Confidence Interval Lower Conf. Limit	Upper Conf. Limit
Background	0	*	*	*
Beta(1)	6.26329	*	*	*
Beta(2)	0	*	*	*
Beta(3)	211165	*	*	*

* - Indicates that this value is not calculated.

Analysis of Deviance Table

Model	Log(likelihood)	# Param's	Deviance	Test d.f.	P-value
Full model	-40.1666	4			
Fitted model	-40.2953	2	0.257381	2	0.8792
Reduced model	-55.0401	1	29.7469	3	<.0001

AIC: 84.5907

Goodness of Fit

Dose	Est._Prob.	Expected	Observed	Size	Scaled Residual
0.0000	0.0000	0.000	0	80	0.000
0.0021	0.0147	0.707	1	48	0.351
0.0049	0.0534	2.564	2	48	-0.362
0.0101	0.2448	11.752	12	48	0.083

Chi^2 = 0.26 d.f. = 2 P-value = 0.8776

Benchmark Dose Computation

Specified effect = 0.1

Risk Type = Extra risk

Confidence level = 0.95

BMD = 0.00669671

BMDL = 0.00473574

BMDU = 0.00818609

Taken together, (0.00473574, 0.00818609) is a 90 % two-sided confidence interval for the BMD

BMDS (version 1.4.1) output for tongue tumors in Sprague-Dawley female rats employing AN in blood as an internal dose metric

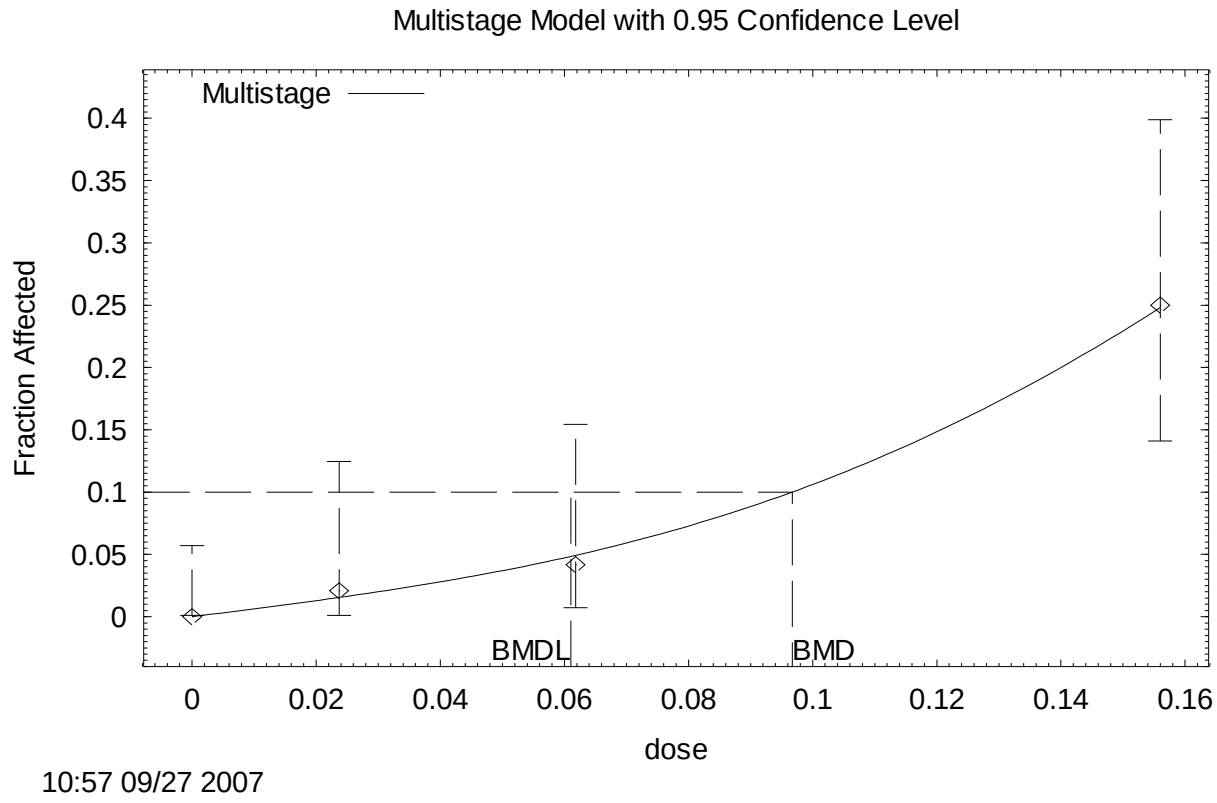


```
 ======================================================================
         Multistage Model. (Version: 2.8;  Date: 02/20/2007)
         Input Data File: G:\ACN DOSE-RESPONSE
MODELING\CANCER\ORAL\SD_FEMALE_TONGUE_BLOOD_AN.(d)
         Gnuplot Plotting File:  G:\ACN DOSE-RESPONSE
MODELING\CANCER\ORAL\SD_FEMALE_TONGUE_BLOOD_AN.plt
                                                  Thu Sep 27 10:57:41 2007
 ======================================================================

 BMDS MODEL RUN
~~~~~~~~~~~~~~~~~~~~~~~~~~~~~~~~~~~~~~~~~~~~~~~~~~~~~~~~~~~~~~~~~~~~~~~~

   The form of the probability function is:

   P[response] = background + (1-background)*[1-EXP(
                -beta1*dose^1-beta2*dose^2-beta3*dose^3)]

   The parameter betas are restricted to be positive

   Dependent variable = Response
   Independent variable = Dose

 Total number of observations = 4
 Total number of records with missing values = 0
 Total number of parameters in model = 4
 Total number of specified parameters = 0
 Degree of polynomial = 3

 Maximum number of iterations = 250
 Relative Function Convergence has been set to: 1e-008
 Parameter Convergence has been set to: 1e-008


                  Default Initial Parameter Values
                     Background =    0.0034253
                        Beta(1) =     0.462467
```

```
                    Beta(2) =            0
                    Beta(3) =      55.8325


          Asymptotic Correlation Matrix of Parameter Estimates

          ( *** The model parameter(s)  -Background    -Beta(2)
                have been estimated at a boundary point, or have been specified by the user,
                and do not appear in the correlation matrix )

               Beta(1)      Beta(3)

   Beta(1)           1        -0.93

   Beta(3)       -0.93            1


                              Parameter Estimates

                                                          95.0% Wald Confidence Interval
      Variable         Estimate        Std. Err.     Lower Conf. Limit   Upper Conf. Limit
     Background               0            *                *                   *
        Beta(1)        0.629858            *                *                   *
        Beta(2)               0            *                *                   *
        Beta(3)         49.1667            *                *                   *

* - Indicates that this value is not calculated.


                      Analysis of Deviance Table

       Model      Log(likelihood)  # Param's  Deviance  Test d.f.   P-value
     Full model        -40.1666         4
    Fitted model       -40.2395         2      0.145677      2          0.9298
   Reduced model       -55.0401         1       29.7469      3         <.0001

          AIC:          84.479


                              Goodness  of  Fit
                                                                    Scaled
     Dose     Est._Prob.    Expected    Observed     Size       Residual
  ---------------------------------------------------------------------------
    0.0000     0.0000         0.000         0          80        0.000
    0.0237     0.0155         0.742         1          48        0.302
    0.0618     0.0493         2.365         2          48       -0.244
    0.1560     0.2479        11.900        12          48        0.033

 Chi^2 = 0.15      d.f. = 2        P-value = 0.9271

   Benchmark Dose Computation

Specified effect =           0.1

Risk Type        =      Extra risk

Confidence level =          0.95

             BMD =      0.0966976

            BMDL =      0.0610292

            BMDU =       0.122886

Taken together, (0.0610292, 0.122886) is a 90     % two-sided confidence
interval for the BMD
```

Tumor Site: Mammary Gland (Quast, 2002; Quast et al., 1980a)

Table B-17. Incidence of mammary gland tumors in Sprague-Dawley rats exposed to AN in drinking water for 2 years

Sex	Administered animal dose (ppm in drinking water)	Equivalent administered animal dose[a] (mg/kg-d)	Predicted internal dose metrics		Incidence of mammary gland tumors[b]
			AN-AUC in blood (mg/L)	CEO-AUC in blood (mg/L)	
Female	0	0	0	0	58/80 (72%)
	35	4.36	2.37×10^{-2}	2.07×10^{-3}	42/47 (89%)[c]
	100	10.8	6.18×10^{-2}	4.87×10^{-3}	42/48 (88%)[c]
	300	25.0	1.56×10^{-1}	1.01×10^{-2}	35/48 (73%)

[a]Administered doses were averages calculated by the study authors based on animal BW and drinking water intake.
[b]Incidences for Sprague-Dawley rats do not include animals from the 6- and 12-mo sacrifices and were further adjusted to exclude (from the denominators) rats that died between 0 and 12 mos in the study.
[c]Significantly different from controls ($p < 0.05$) as calculated by the study authors.

Table B-18. Summary of BMD modeling results based on incidence of mammary gland tumors in Sprague-Dawley rats exposed to AN in drinking water for 2 years

Dose metric	Best-fit model[a]	χ^2 *p*-value[b]	AIC	BMD_{10}[c]	$BMDL_{10}$[d]
Females					
Administered dose	1°MS[e]	0.25	171.81	1.22 mg/kg-d	0.66 mg/kg-d
CEO	1°MS[e]	0.27	171.69	5.50×10^{-4} mg/L	2.98×10^{-4} mg/L
AN	1°MS[e]	0.24	171.93	7.05×10^{-3} mg/L	3.77×10^{-3} mg/L

[a]Dose-response models were fit using BMDS, version 1.4.1. "1°MS" indicates a one-stage multistage model.
[b]*p* value from the χ^2 goodness of fit test. Values <0.1 indicate a significant lack of fit.
[c]BMD_{10} = BMD at 10% extra risk.
[d]$BMDL_{10}$ = 95% lower confidence limit on the BMD at 10% extra risk.
[e]Highest dose dropped prior to model fitting.

BMDS (version 1.4.1) output for mammary gland tumors in Sprague-Dawley female rats employing administered dose as a dose metric

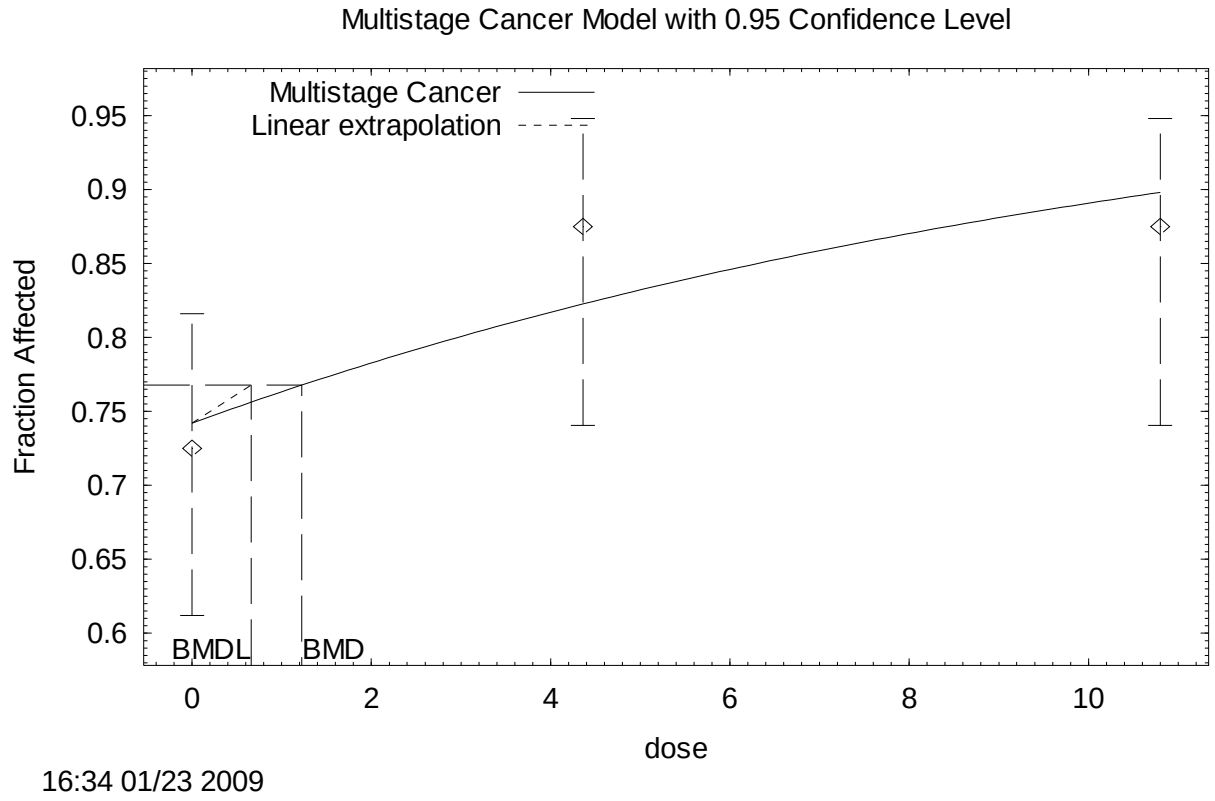


```
 ================================================================
         Multistage Cancer Model. (Version: 1.5;  Date: 02/20/2007)
         Input Data File: M:\ACN DOSE-RESPONSE MODELING\CANCER\ORAL\SD_FEMALE_MAMMARY_DW.(d)
         Gnuplot Plotting File:  M:\ACN DOSE-RESPONSE
MODELING\CANCER\ORAL\SD_FEMALE_MAMMARY_DW.plt
                                                    Fri Jan 23 16:34:25 2009
 ================================================================

 BMDS MODEL RUN
~~~~~~~~~~~~~~~~~~~~~~~~~~~~~~~~~~~~~~~~~~~~~~~~~~~~~~~~~~~~~~~~~~~~~~~~

   The form of the probability function is:

   P[response] = background + (1-background)*[1-EXP(
                -beta1*dose^1)]

   The parameter betas are restricted to be positive


   Dependent variable = Response
   Independent variable = Dose

 Total number of observations = 3
 Total number of records with missing values = 0
 Total number of parameters in model = 2
 Total number of specified parameters = 0
 Degree of polynomial = 1


 Maximum number of iterations = 250
 Relative Function Convergence has been set to: 1e-008
 Parameter Convergence has been set to: 1e-008
```

Default Initial Parameter Values
Background = 0.771359
Beta(1) = 0.0674842

Asymptotic Correlation Matrix of Parameter Estimates

	Background	Beta(1)
Background	1	-0.58
Beta(1)	-0.58	1

Parameter Estimates

Variable	Estimate	Std. Err.	95.0% Wald Confidence Interval Lower Conf. Limit	Upper Conf. Limit
Background	0.741898	*	*	*
Beta(1)	0.0860351	*	*	*

* - Indicates that this value is not calculated.

Analysis of Deviance Table

Model	Log(likelihood)	# Param's	Deviance	Test d.f.	P-value
Full model	-83.2234	3			
Fitted model	-83.9062	2	1.36543	1	0.2426
Reduced model	-86.3815	1	6.31609	2	0.04251

AIC: 171.812

Goodness of Fit

Dose	Est._Prob.	Expected	Observed	Size	Scaled Residual
0.0000	0.7419	59.352	58	80	-0.345
4.3600	0.8226	39.486	42	48	0.950
10.8000	0.8981	43.108	42	48	-0.529

Chi^2 = 1.30 d.f. = 1 P-value = 0.2540

```
   Benchmark Dose Computation

Specified effect =            0.1

Risk Type        =      Extra risk

Confidence level =           0.95

              BMD =        1.22462

             BMDL =       0.659237

             BMDU =        4.94647

Taken together, (0.659237, 4.94647) is a 90     % two-sided confidence
interval for the BMD

Multistage Cancer Slope Factor =      0.151691
```

BMDS (version 1.4.1) output for mammary gland tumors in Sprague-Dawley female rats employing CEO in blood as an internal dose metric

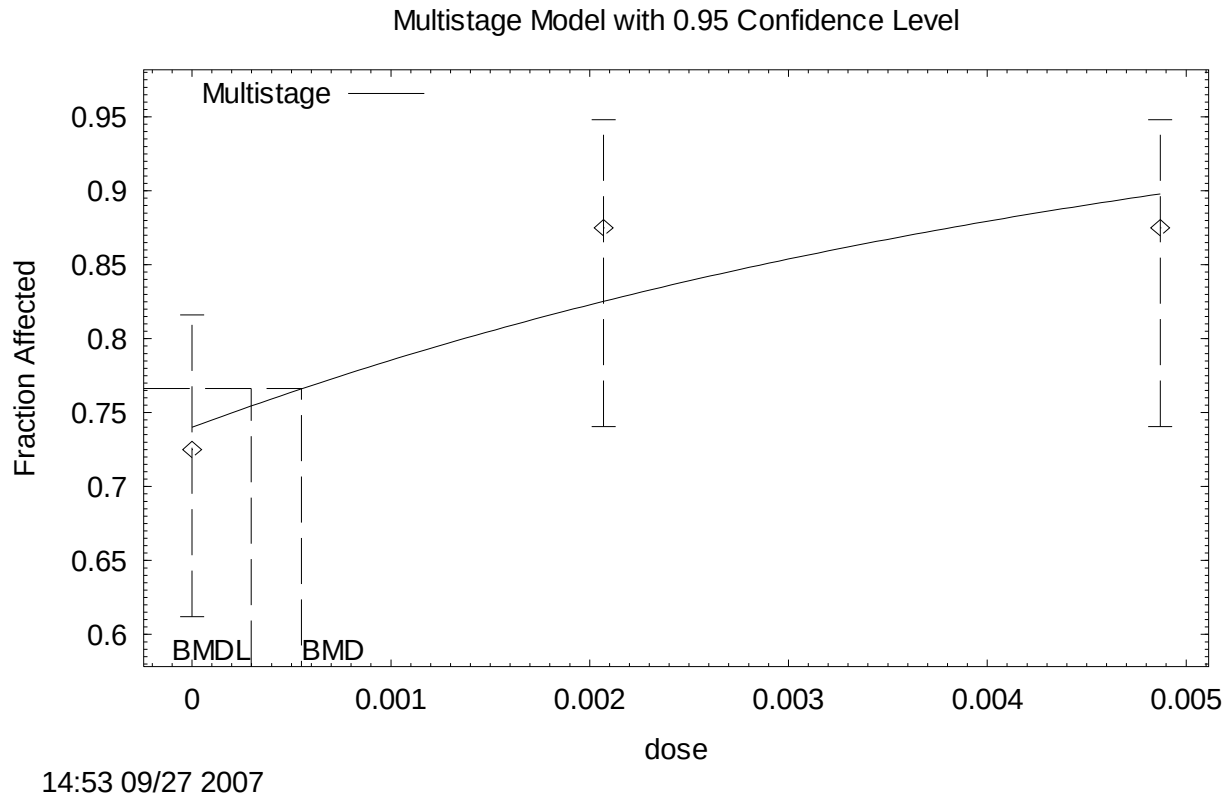


```
 ======================================================================
         Multistage Model. (Version: 2.8;  Date: 02/20/2007)
         Input Data File: G:\ACN DOSE-RESPONSE
MODELING\CANCER\ORAL\SD_FEMALE_MAMMARY_BLOOD_CEO.(d)
         Gnuplot Plotting File:  G:\ACN DOSE-RESPONSE
MODELING\CANCER\ORAL\SD_FEMALE_MAMMARY_BLOOD_CEO.plt
                                                  Thu Sep 27 14:53:05 2007
 ======================================================================

 BMDS MODEL RUN
~~~~~~~~~~~~~~~~~~~~~~~~~~~~~~~~~~~~~~~~~~~~~~~~~~~~~~~~~~~~~~~~~~~~~~~~

   The form of the probability function is:

   P[response] = background + (1-background)*[1-EXP(
                -beta1*dose^1)]

   The parameter betas are restricted to be positive


   Dependent variable = Response
   Independent variable = Dose

 Total number of observations = 3
 Total number of records with missing values = 0
 Total number of parameters in model = 2
 Total number of specified parameters = 0
 Degree of polynomial = 1


 Maximum number of iterations = 250
 Relative Function Convergence has been set to: 1e-008
 Parameter Convergence has been set to: 1e-008
```

Default Initial Parameter Values
Background = 0.768564
Beta(1) = 152.668

Asymptotic Correlation Matrix of Parameter Estimates

	Background	Beta(1)
Background	1	-0.58
Beta(1)	-0.58	1

Parameter Estimates

Variable	Estimate	Std. Err.	95.0% Wald Confidence Interval Lower Conf. Limit	Upper Conf. Limit
Background	0.740346	*	*	*
Beta(1)	191.729	*	*	*

* - Indicates that this value is not calculated.

Analysis of Deviance Table

Model	Log(likelihood)	# Param's	Deviance	Test d.f.	P-value
Full model	-83.2234	3			
Fitted model	-83.8471	2	1.24732	1	0.2641
Reduced model	-86.3815	1	6.31609	2	0.04251

AIC: 171.694

Goodness of Fit

Dose	Est._Prob.	Expected	Observed	Size	Scaled Residual
0.0000	0.7403	59.228	58	80	-0.313
0.0021	0.8254	39.619	42	48	0.905
0.0049	0.8979	43.101	42	48	-0.525

Chi^2 = 1.19 d.f. = 1 P-value = 0.2748

Benchmark Dose Computation

Specified effect = 0.1

Risk Type = Extra risk

Confidence level = 0.95

BMD = 0.000549528

BMDL = 0.000298184

BMDU = 0.00214159

Taken together, (0.000298184, 0.00214159) is a 90 % two-sided confidence interval for the BMD

BMDS (version 1.4.1) output for mammary gland tumors in Sprague-Dawley female rats employing AN in blood as an internal dose metric

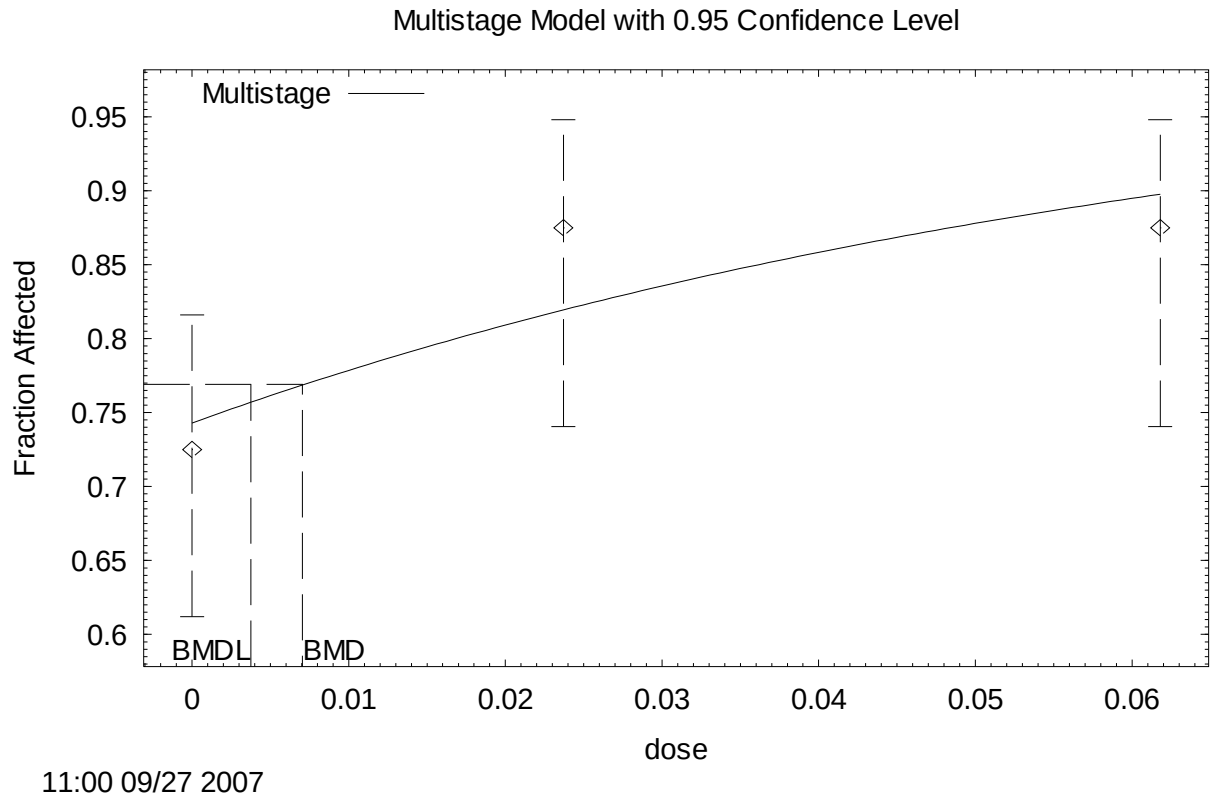


```
 ======================================================================
         Multistage Model. (Version: 2.8;  Date: 02/20/2007)
         Input Data File: G:\ACN DOSE-RESPONSE
MODELING\CANCER\ORAL\SD_FEMALE_MAMMARY_BLOOD_AN.(d)
         Gnuplot Plotting File:  G:\ACN DOSE-RESPONSE
MODELING\CANCER\ORAL\SD_FEMALE_MAMMARY_BLOOD_AN.plt
                                                  Thu Sep 27 11:00:59 2007
 ======================================================================

 BMDS MODEL RUN
~~~~~~~~~~~~~~~~~~~~~~~~~~~~~~~~~~~~~~~~~~~~~~~~~~~~~~~~~~~~~~~~~~~~~~~~

   The form of the probability function is:

   P[response] = background + (1-background)*[1-EXP(
                -beta1*dose^1)]

   The parameter betas are restricted to be positive


   Dependent variable = Response
   Independent variable = Dose

 Total number of observations = 3
 Total number of records with missing values = 0
 Total number of parameters in model = 2
 Total number of specified parameters = 0
 Degree of polynomial = 1


 Maximum number of iterations = 250
 Relative Function Convergence has been set to: 1e-008
 Parameter Convergence has been set to: 1e-008


                  Default Initial Parameter Values
```

```
                    Background =     0.773999
                       Beta(1) =      11.5581


          Asymptotic Correlation Matrix of Parameter Estimates

            Background      Beta(1)

Background            1        -0.58

   Beta(1)        -0.58            1


                               Parameter Estimates

                                                        95.0% Wald Confidence Interval
      Variable         Estimate        Std. Err.     Lower Conf. Limit   Upper Conf. Limit
    Background         0.743458            *                *                   *
       Beta(1)          14.9428            *                *                   *

* - Indicates that this value is not calculated.


                       Analysis of Deviance Table

      Model      Log(likelihood)  # Param's  Deviance  Test d.f.   P-value
    Full model        -83.2234         3
   Fitted model       -83.9649         2       1.48294      1          0.2233
  Reduced model       -86.3815         1       6.31609      2         0.04251

          AIC:          171.93


                               Goodness  of  Fit
                                                                    Scaled
    Dose     Est._Prob.    Expected    Observed     Size       Residual
  ---------------------------------------------------------------------
    0.0000     0.7435        59.477        58          80       -0.378
    0.0237     0.8200        39.358        42          48        0.992
    0.0618     0.8981        43.110        42          48       -0.529

 Chi^2 = 1.41      d.f. = 1        P-value = 0.2354


   Benchmark Dose Computation

Specified effect =           0.1

Risk Type        =      Extra risk

Confidence level =          0.95

             BMD =     0.00705091

            BMDL =     0.00376506

            BMDU =      0.0295793

Taken together, (0.00376506, 0.0295793) is a 90     % two-sided confidence
interval for the BMD
```

F344 Rats (Johannsen and Levinskas, 2002b; Biodynamics, 1980b)

Tumor Site: Forestomach

Table B-19. Incidence of forestomach (nonglandular) tumors in F344 rats exposed to AN in drinking water for 2 years

Sex	Administered animal dose (ppm in drinking water)	Equivalent administered animal dose[a] (mg/kg-d)	Predicted internal dose metrics		Incidence of forestomach tumors[b]
			AN-AUC in blood (mg/L)	CEO-AUC in blood (mg/L)	
Male	0	0	0	0	0/159 (0%)
	1	0.08	4.33×10^{-4}	4.06×10^{-5}	1/80 (1%)
	3	0.25	1.35×10^{-3}	1.27×10^{-4}	4/78 (5%)[c]
	10	0.83	4.52×10^{-3}	4.19×10^{-4}	3/80 (4%)[c]
	30	2.48	1.37×10^{-2}	1.23×10^{-3}	4/80 (5%)[c]
	100	8.37	4.85×10^{-2}	3.97×10^{-3}	1/77 (1%)
Female	0	0	0	0	0/157 (0%)
	1	0.12	5.73×10^{-4}	5.32×10^{-5}	1/80 (1%)
	3	0.36	1.72×10^{-3}	1.59×10^{-4}	2/79 (3%)
	10	1.25	6.02×10^{-3}	5.49×10^{-4}	2/77 (3%)
	30	3.65	1.79×10^{-2}	1.58×10^{-3}	4/80 (5%)[c]
	100	10.90	5.63×10^{-2}	4.46×10^{-3}	2/75 (3%)

[a]Administered doses were averages calculated by the study authors based on animal BW and drinking water intake.
[b]Incidences for F344 rats do not include animals from the 6- and 12-mo sacrifices and were further adjusted to exclude (from the denominators) rats that died between 0 and 12 mos in the study.
[c]Significantly different from controls ($p < 0.05$) as calculated by the study authors.

Table B-20. Summary of BMD modeling results based on incidence of forestomach (nonglandular) tumors in F344 rats exposed to AN in drinking water for 2 years

Dose metric	Best-fit model[a]	χ^2 *p*-value[b]	AIC	BMD_{10}[c]	$BMDL_{10}$[d]
Males					
Administered dose	1°MS[e]	0.18	74.08	1.19 mg/kg-d	0.70 mg/kg-d
CEO	1°MS[e]	0.19	74.04	6.03×10^{-4} mg/L	3.55×10^{-4} mg/L
AN	1°MS[e]	0.18	74.12	6.48×10^{-3} mg/L	3.81×10^{-3} mg/L
Females					
Administered dose	1°MS[f]	0.83	96.64	8.43 mg/kg-d	3.89 mg/kg-d
CEO	1°MS[f]	0.83	96.62	3.65×10^{-3} mg/L	1.69×10^{-3} mg/L
AN	1°MS[f]	0.82	96.65	4.13×10^{-2} mg/L	1.90×10^{-2} mg/L

[a]Dose-response models were fit using BMDS, version 1.4.1. "1°MS" indicates a one-stage multistage model.
[b]*p* value from the χ^2 goodness of fit test. Values <0.1 indicate a significant lack of fit.
[c]BMD_{10} = BMD at 10% extra risk.
[d]$BMDL_{10}$ = 95% lower confidence limit on the BMD at 10% extra risk.
[e]Two highest doses dropped prior to model fitting.
[f]Highest dose dropped prior to model fitting.

BMDS (version 1.4.1) output for forestomach tumors in F344 male rats employing administered dose as a dose metric

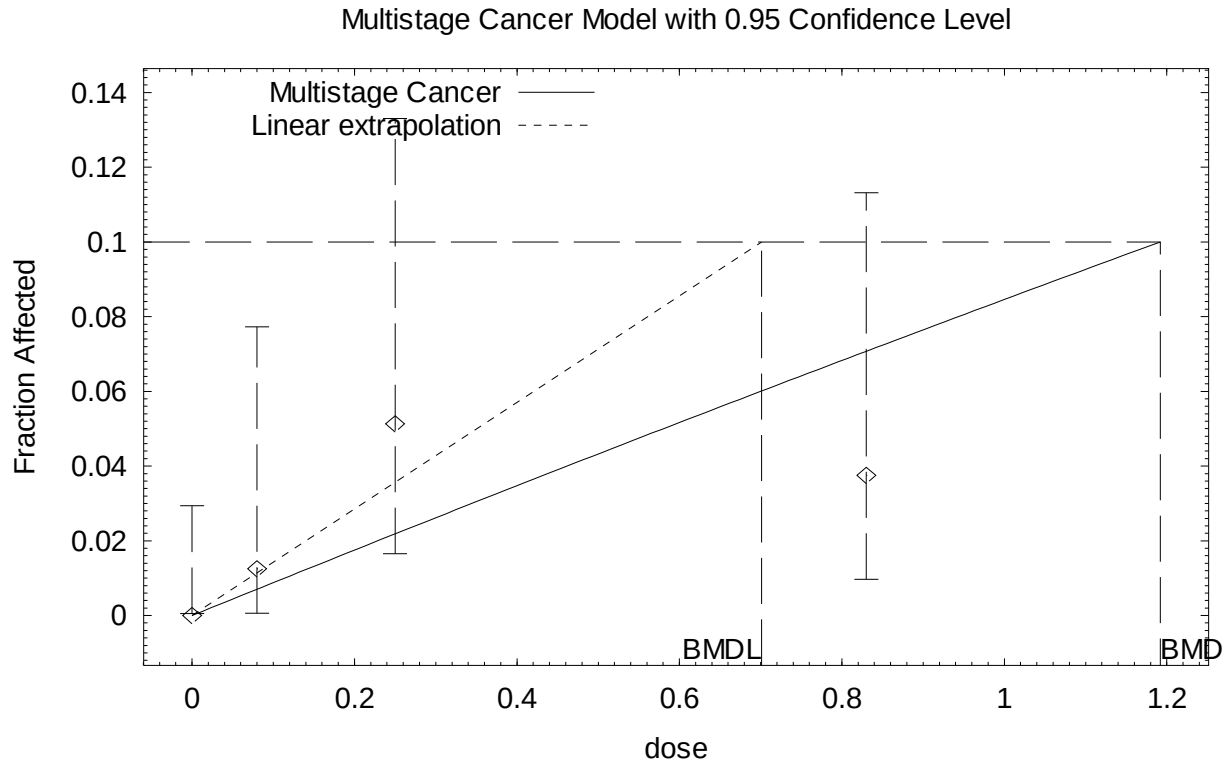


```
 ======================================================================
         Multistage Cancer Model. (Version: 1.5;  Date: 02/20/2007)
         Input Data File: M:\ACN DOSE-RESPONSE MODELING\CANCER\ORAL\F344_MALE_FORESTOMACH_DW.(d)
         Gnuplot Plotting File:  M:\ACN DOSE-RESPONSE
MODELING\CANCER\ORAL\F344_MALE_FORESTOMACH_DW.plt
                                                Mon Jan 26 14:29:05 2009
 ======================================================================

 BMDS MODEL RUN
~~~~~~~~~~~~~~~~~~~~~~~~~~~~~~~~~~~~~~~~~~~~~~~~~~~~~~~~~~~~~~~~~~~~~~~~

   The form of the probability function is:

   P[response] = background + (1-background)*[1-EXP(
                -beta1*dose^1)]

   The parameter betas are restricted to be positive


   Dependent variable = Response
   Independent variable = Dose

 Total number of observations = 4
 Total number of records with missing values = 0
 Total number of parameters in model = 2
 Total number of specified parameters = 0
 Degree of polynomial = 1


 Maximum number of iterations = 250
 Relative Function Convergence has been set to: 1e-008
 Parameter Convergence has been set to: 1e-008
```

Default Initial Parameter Values
Background = 0.0148134
Beta(1) = 0.0377128

Asymptotic Correlation Matrix of Parameter Estimates

(*** The model parameter(s) -Background
have been estimated at a boundary point, or have been specified by the user,
and do not appear in the correlation matrix)

	Beta(1)
Beta(1)	1

Parameter Estimates

Variable	Estimate	Std. Err.	95.0% Wald Confidence Interval Lower Conf. Limit	Upper Conf. Limit
Background	0	*	*	*
Beta(1)	0.0883999	*	*	*

* - Indicates that this value is not calculated.

Analysis of Deviance Table

Model	Log(likelihood)	# Param's	Deviance	Test d.f.	P-value
Full model	-33.9463	4			
Fitted model	-36.0377	1	4.18282	3	0.2424
Reduced model	-39.1548	1	10.417	3	0.01533

AIC: 74.0755

Goodness of Fit

Dose	Est._Prob.	Expected	Observed	Size	Scaled Residual
0.0000	0.0000	0.000	0	159	0.000
0.0800	0.0070	0.564	1	80	0.583
0.2500	0.0219	1.705	4	78	1.777
0.8300	0.0707	5.660	3	80	-1.160

Chi^2 = 4.84 d.f. = 3 P-value = 0.1836

```
   Benchmark Dose Computation

Specified effect =            0.1

Risk Type        =      Extra risk

Confidence level =           0.95

              BMD =        1.19186

             BMDL =       0.701326

             BMDU =        3.81474

Taken together, (0.701326, 3.81474) is a 90     % two-sided confidence
interval for the BMD

Multistage Cancer Slope Factor =      0.142587
```

BMDS (version 1.4.1) output for forestomach tumors in F344 male rats employing CEO in blood as an internal dose metric

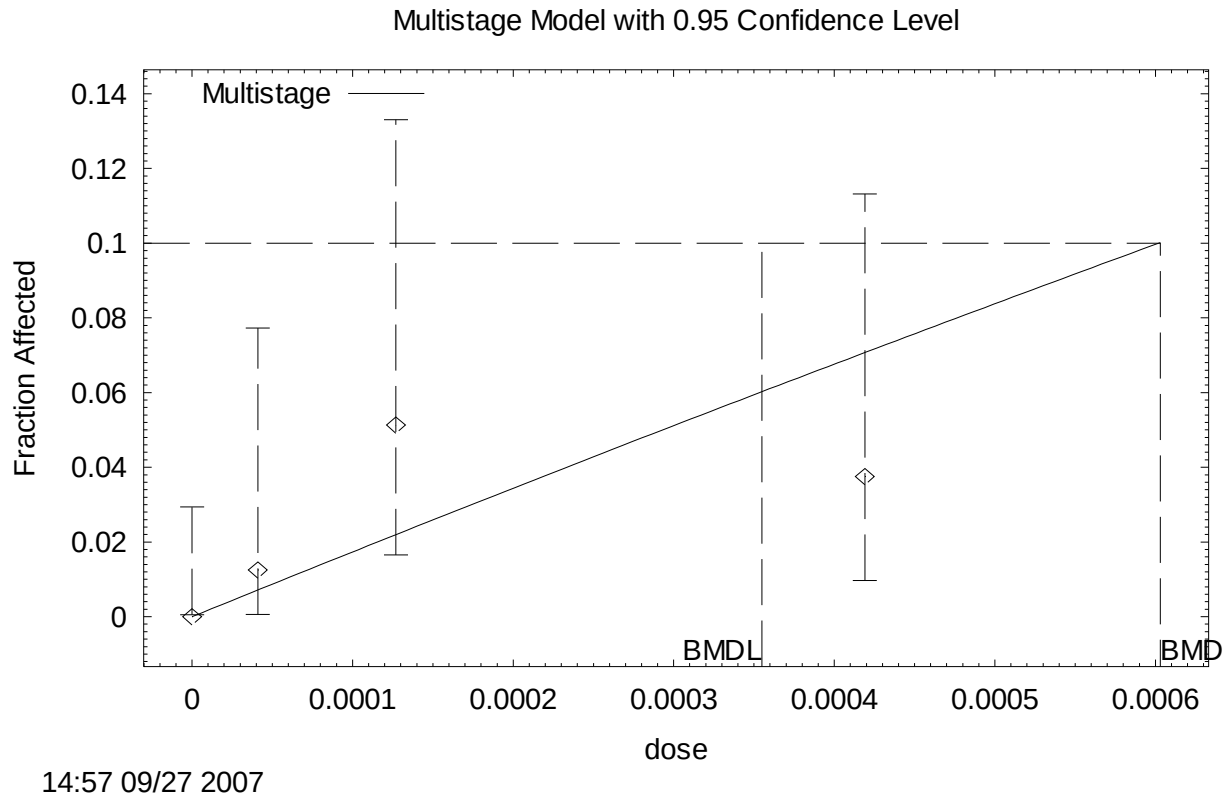


```
 ======================================================================
         Multistage Model. (Version: 2.8;  Date: 02/20/2007)
         Input Data File: G:\ACN DOSE-RESPONSE
MODELING\CANCER\ORAL\F344_MALE_FORESTOMACH_BLOOD_CEO.(d)
         Gnuplot Plotting File:  G:\ACN DOSE-RESPONSE
MODELING\CANCER\ORAL\F344_MALE_FORESTOMACH_BLOOD_CEO.plt
                                                Thu Sep 27 14:57:13 2007
 ======================================================================

 BMDS MODEL RUN
~~~~~~~~~~~~~~~~~~~~~~~~~~~~~~~~~~~~~~~~~~~~~~~~~~~~~~~~~~~~~~~~~~~~~~~~

   The form of the probability function is:

   P[response] = background + (1-background)*[1-EXP(
                -beta1*dose^1)]

   The parameter betas are restricted to be positive


   Dependent variable = Response
   Independent variable = Dose

 Total number of observations = 4
 Total number of records with missing values = 0
 Total number of parameters in model = 2
 Total number of specified parameters = 0
 Degree of polynomial = 1


 Maximum number of iterations = 250
 Relative Function Convergence has been set to: 1e-008
 Parameter Convergence has been set to: 1e-008
```

Default Initial Parameter Values
Background = 0.0147622
Beta(1) = 74.9311

Asymptotic Correlation Matrix of Parameter Estimates

(*** The model parameter(s) -Background
have been estimated at a boundary point, or have been specified by the user,
and do not appear in the correlation matrix)

	Beta(1)
Beta(1)	1

Parameter Estimates

Variable	Estimate	Std. Err.	95.0% Wald Confidence Interval Lower Conf. Limit	Upper Conf. Limit
Background	0	*	*	*
Beta(1)	174.815	*	*	*

* - Indicates that this value is not calculated.

Analysis of Deviance Table

Model	Log(likelihood)	# Param's	Deviance	Test d.f.	P-value
Full model	-33.9463	4			
Fitted model	-36.0209	1	4.14909	3	0.2458
Reduced model	-39.1548	1	10.417	3	0.01533

AIC: 74.0417

Goodness of Fit

Dose	Est._Prob.	Expected	Observed	Size	Scaled Residual
0.0000	0.0000	0.000	0	159	0.000
0.0000	0.0071	0.566	1	80	0.579
0.0001	0.0220	1.713	4	78	1.767
0.0004	0.0706	5.650	3	80	-1.157

Chi^2 = 4.80 d.f. = 3 P-value = 0.1873

Benchmark Dose Computation

Specified effect = 0.1

Risk Type = Extra risk

Confidence level = 0.95

BMD = 0.000602696

BMDL = 0.000354643

BMDU = 0.00191036

Taken together, (0.000354643, 0.00191036) is a 90 % two-sided confidence interval for the BMD

BMDS (version 1.4.1) output for forestomach tumors in F344 male rats employing AN in blood as an internal dose metric

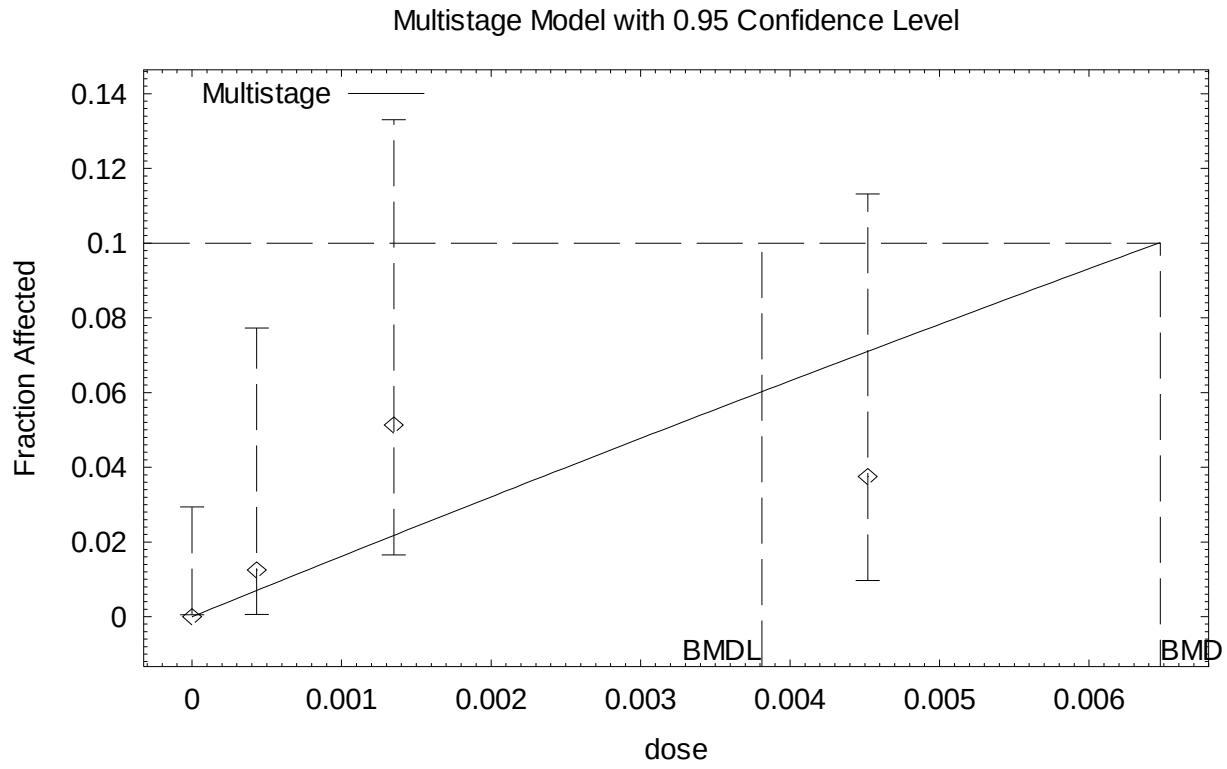


```
 ======================================================================
         Multistage Model. (Version: 2.8;  Date: 02/20/2007)
         Input Data File: G:\ACN DOSE-RESPONSE
MODELING\CANCER\ORAL\F344_MALE_FORESTOMACH_BLOOD_AN.(d)
         Gnuplot Plotting File:  G:\ACN DOSE-RESPONSE
MODELING\CANCER\ORAL\F344_MALE_FORESTOMACH_BLOOD_AN.plt
                                                    Thu Sep 27 11:04:04 2007
 ======================================================================

 BMDS MODEL RUN
~~~~~~~~~~~~~~~~~~~~~~~~~~~~~~~~~~~~~~~~~~~~~~~~~~~~~~~~~~~~~~~~~~~~~~~~~~~~

   The form of the probability function is:

   P[response] = background + (1-background)*[1-EXP(
                -beta1*dose^1)]

   The parameter betas are restricted to be positive


   Dependent variable = Response
   Independent variable = Dose

 Total number of observations = 4
 Total number of records with missing values = 0
 Total number of parameters in model = 2
 Total number of specified parameters = 0
 Degree of polynomial = 1


 Maximum number of iterations = 250
 Relative Function Convergence has been set to: 1e-008
 Parameter Convergence has been set to: 1e-008


                  Default Initial Parameter Values
```

```
                    Background =    0.0148807
                       Beta(1) =      6.89727


           Asymptotic Correlation Matrix of Parameter Estimates

           ( *** The model parameter(s)  -Background
                 have been estimated at a boundary point, or have been specified by the user,
                 and do not appear in the correlation matrix )

                Beta(1)

   Beta(1)            1
```

Parameter Estimates

Variable	Estimate	Std. Err.	95.0% Wald Confidence Interval Lower Conf. Limit	Upper Conf. Limit
Background	0	*	*	*
Beta(1)	16.2684	*	*	*

* - Indicates that this value is not calculated.

Analysis of Deviance Table

Model	Log(likelihood)	# Param's	Deviance	Test d.f.	P-value
Full model	-33.9463	4			
Fitted model	-36.0601	1	4.22747	3	0.2379
Reduced model	-39.1548	1	10.417	3	0.01533

AIC: 74.1201

Goodness of Fit

Dose	Est._Prob.	Expected	Observed	Size	Scaled Residual
0.0000	0.0000	0.000	0	159	0.000
0.0004	0.0070	0.562	1	80	0.587
0.0014	0.0217	1.694	4	78	1.791
0.0045	0.0709	5.672	3	80	-1.164

Chi^2 = 4.91 d.f. = 3 P-value = 0.1788

Benchmark Dose Computation

```
Specified effect =           0.1

Risk Type        =      Extra risk

Confidence level =          0.95

             BMD =     0.00647638

            BMDL =     0.00381089

            BMDU =      0.0209986

Taken together, (0.00381089, 0.0209986) is a 90     % two-sided confidence
interval for the BMD
```

BMDS (version 1.4.1) output for forestomach tumors in F344 female rats employing administered dose as a dose metric

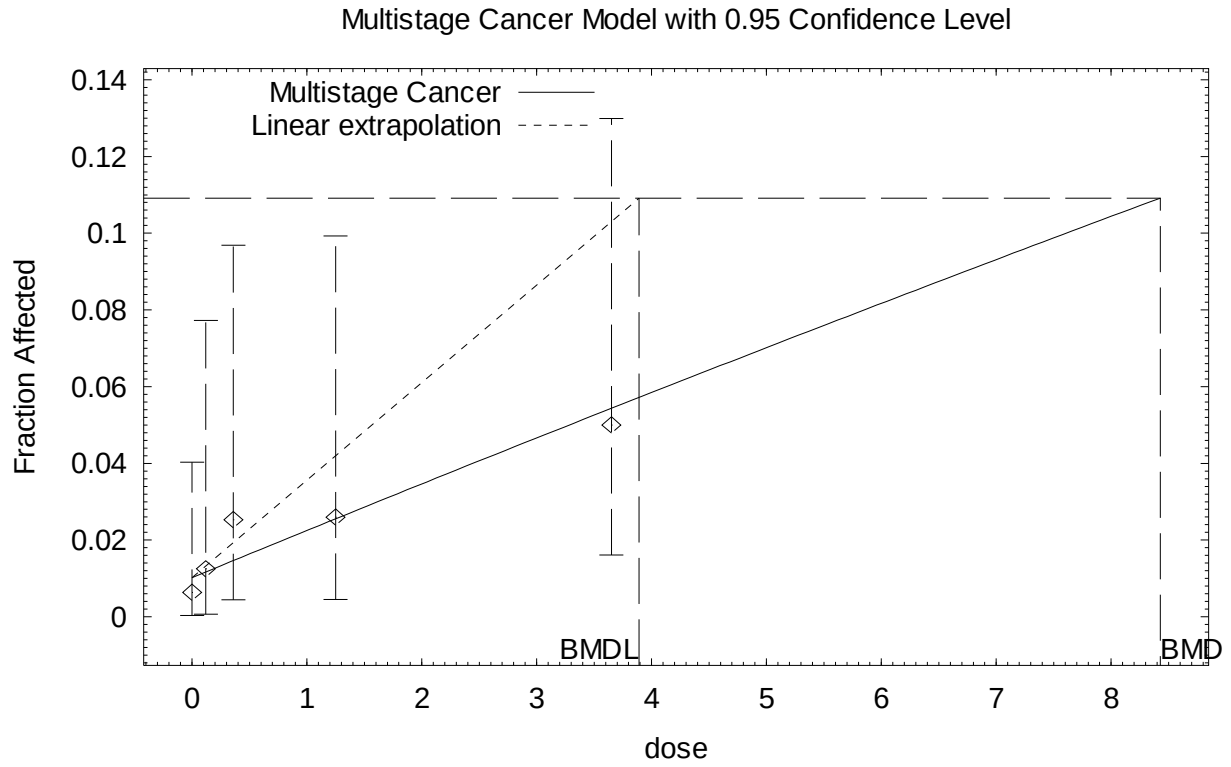


```
 ======================================================================
         Multistage Cancer Model. (Version: 1.5;  Date: 02/20/2007)
         Input Data File: M:\ACN DOSE-RESPONSE
MODELING\CANCER\ORAL\F344_FEMALE_FORESTOMACH_DW.(d)
         Gnuplot Plotting File:  M:\ACN DOSE-RESPONSE
MODELING\CANCER\ORAL\F344_FEMALE_FORESTOMACH_DW.plt
                                                Mon Jan 26 14:49:27 2009
 ======================================================================

 BMDS MODEL RUN
~~~~~~~~~~~~~~~~~~~~~~~~~~~~~~~~~~~~~~~~~~~~~~~~~~~~~~~~~~~~~~~~~~~~~~~~

   The form of the probability function is:

   P[response] = background + (1-background)*[1-EXP(
                -beta1*dose^1)]

   The parameter betas are restricted to be positive


   Dependent variable = Response
   Independent variable = Dose

 Total number of observations = 5
 Total number of records with missing values = 0
 Total number of parameters in model = 2
 Total number of specified parameters = 0
 Degree of polynomial = 1


 Maximum number of iterations = 250
 Relative Function Convergence has been set to: 1e-008
 Parameter Convergence has been set to: 1e-008
```

Default Initial Parameter Values
Background = 0.0127929
Beta(1) = 0.0107517

Asymptotic Correlation Matrix of Parameter Estimates

	Background	Beta(1)
Background	1	-0.58
Beta(1)	-0.58	1

Parameter Estimates

Variable	Estimate	Std. Err.	95.0% Wald Confidence Interval Lower Conf. Limit	Upper Conf. Limit
Background	0.0101696	*	*	*
Beta(1)	0.0125023	*	*	*

* - Indicates that this value is not calculated.

Analysis of Deviance Table

Model	Log(likelihood)	# Param's	Deviance	Test d.f.	P-value
Full model	-45.9122	5			
Fitted model	-46.3178	2	0.81118	3	0.8468
Reduced model	-48.4586	1	5.09287	4	0.2779

AIC: 96.6356

Goodness of Fit

Dose	Est._Prob.	Expected	Observed	Size	Scaled Residual
0.0000	0.0102	1.597	1	157	-0.475
0.1200	0.0117	0.932	1	80	0.071
0.3600	0.0146	1.155	2	79	0.793
1.2500	0.0255	1.965	2	77	0.025
3.6500	0.0543	4.346	4	80	-0.171

Chi^2 = 0.89 d.f. = 3 P-value = 0.8283

```
   Benchmark Dose Computation

Specified effect =            0.1

Risk Type        =      Extra risk

Confidence level =           0.95

              BMD =        8.42727

             BMDL =        3.88972

             BMDU =        48.9918

Taken together, (3.88972, 48.9918) is a 90     % two-sided confidence
interval for the BMD

Multistage Cancer Slope Factor =     0.0257088
```

BMDS (version 1.4.1) output for forestomach tumors in F344 female rats employing CEO in blood as an internal dose metric

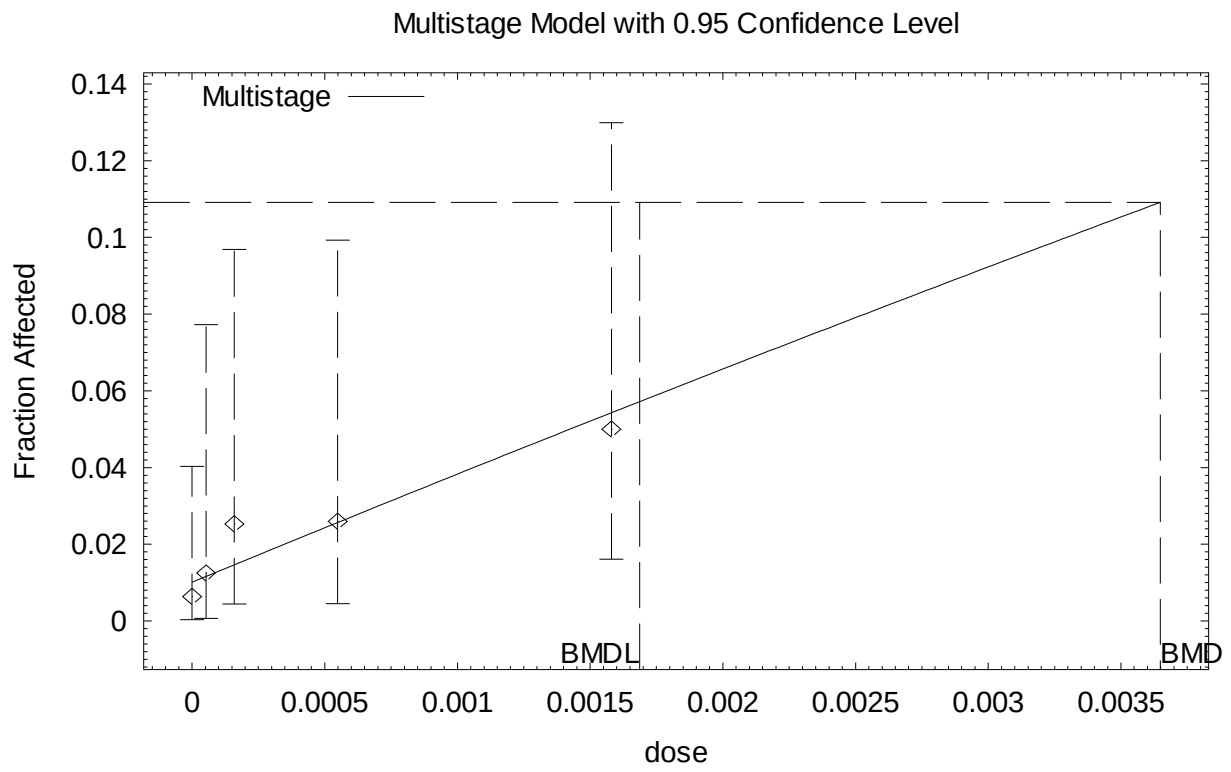


```
 ======================================================================
         Multistage Model. (Version: 2.8;  Date: 02/20/2007)
         Input Data File: G:\ACN DOSE-RESPONSE
MODELING\CANCER\ORAL\F344_FEMALE_FORESTOMACH_BLOOD_CEO.(d)
         Gnuplot Plotting File:  G:\ACN DOSE-RESPONSE
MODELING\CANCER\ORAL\F344_FEMALE_FORESTOMACH_BLOOD_CEO.plt
                                                  Thu Sep 27 15:07:15 2007
 ======================================================================

 BMDS MODEL RUN
~~~~~~~~~~~~~~~~~~~~~~~~~~~~~~~~~~~~~~~~~~~~~~~~~~~~~~~~~~~~~~~~~~~~~~~~

   The form of the probability function is:

   P[response] = background + (1-background)*[1-EXP(
                -beta1*dose^1)]

   The parameter betas are restricted to be positive


   Dependent variable = Response
   Independent variable = Dose

 Total number of observations = 5
 Total number of records with missing values = 0
 Total number of parameters in model = 2
 Total number of specified parameters = 0
 Degree of polynomial = 1


 Maximum number of iterations = 250
 Relative Function Convergence has been set to: 1e-008
 Parameter Convergence has been set to: 1e-008
```

Default Initial Parameter Values
Background = 0.0127198
Beta(1) = 24.8654

Asymptotic Correlation Matrix of Parameter Estimates

	Background	Beta(1)
Background	1	-0.58
Beta(1)	-0.58	1

Parameter Estimates

Variable	Estimate	Std. Err.	95.0% Wald Confidence Interval Lower Conf. Limit	Upper Conf. Limit
Background	0.0101112	*	*	*
Beta(1)	28.8833	*	*	*

* - Indicates that this value is not calculated.

Analysis of Deviance Table

Model	Log(likelihood)	# Param's	Deviance	Test d.f.	P-value
Full model	-45.9122	5			
Fitted model	-46.3121	2	0.799693	3	0.8495
Reduced model	-48.4586	1	5.09287	4	0.2779

AIC: 96.6241

Goodness of Fit

Dose	Est._Prob.	Expected	Observed	Size	Scaled Residual
0.0000	0.0101	1.587	1	157	-0.469
0.0001	0.0116	0.930	1	80	0.072
0.0002	0.0146	1.157	2	79	0.789
0.0005	0.0257	1.978	2	77	0.016
0.0016	0.0543	4.342	4	80	-0.169

Chi^2 = 0.88 d.f. = 3 P-value = 0.8310

Benchmark Dose Computation

Specified effect = 0.1

Risk Type = Extra risk

Confidence level = 0.95

BMD = 0.0036478

BMDL = 0.00168696

BMDU = 1361.26

Taken together, (0.00168696, 1361.26) is a 90 % two-sided confidence interval for the BMD

BMDS (version 1.4.1) output for forestomach tumors in F344 female rats employing AN in blood as an internal dose metric

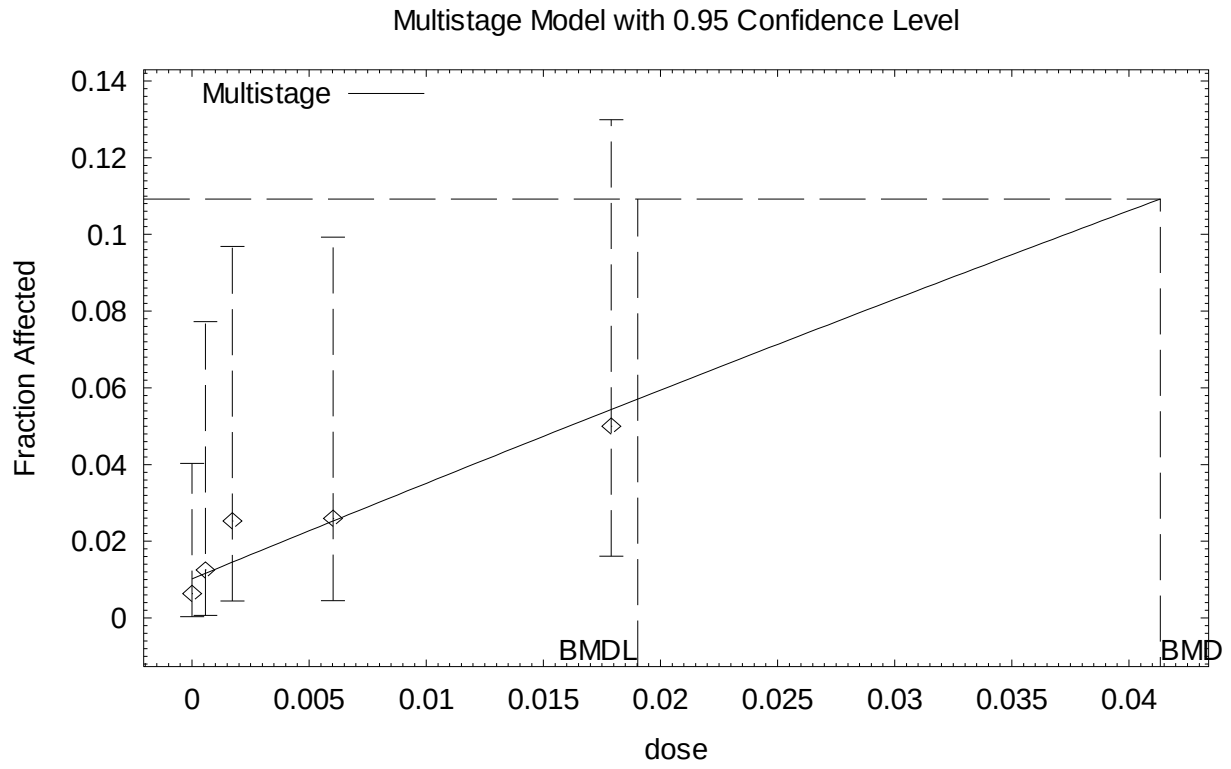


```
 ======================================================================
         Multistage Model. (Version: 2.8;  Date: 02/20/2007)
         Input Data File: G:\ACN DOSE-RESPONSE
MODELING\CANCER\ORAL\F344_FEMALE_FORESTOMACH_BLOOD_AN.(d)
         Gnuplot Plotting File:  G:\ACN DOSE-RESPONSE
MODELING\CANCER\ORAL\F344_FEMALE_FORESTOMACH_BLOOD_AN.plt
                                                  Thu Sep 27 11:30:39 2007
 ======================================================================

 BMDS MODEL RUN
~~~~~~~~~~~~~~~~~~~~~~~~~~~~~~~~~~~~~~~~~~~~~~~~~~~~~~~~~~~~~~~~~~~~~~~~

   The form of the probability function is:

   P[response] = background + (1-background)*[1-EXP(
                -beta1*dose^1)]

   The parameter betas are restricted to be positive


   Dependent variable = Response
   Independent variable = Dose

 Total number of observations = 5
 Total number of records with missing values = 0
 Total number of parameters in model = 2
 Total number of specified parameters = 0
 Degree of polynomial = 1


 Maximum number of iterations = 250
 Relative Function Convergence has been set to: 1e-008
 Parameter Convergence has been set to: 1e-008


                  Default Initial Parameter Values
```

```
                    Background =    0.0128833
                       Beta(1) =      2.18924


           Asymptotic Correlation Matrix of Parameter Estimates

             Background      Beta(1)

Background            1        -0.58

   Beta(1)        -0.58            1


                                Parameter Estimates

                                                        95.0% Wald Confidence Interval
       Variable         Estimate        Std. Err.     Lower Conf. Limit   Upper Conf. Limit
     Background        0.0102427            *                *                   *
        Beta(1)          2.54885            *                *                   *

* - Indicates that this value is not calculated.


                        Analysis of Deviance Table

       Model      Log(likelihood)  # Param's  Deviance  Test d.f.   P-value
     Full model        -45.9122         5
   Fitted model        -46.3252         2      0.826038      3          0.8432
  Reduced model        -48.4586         1       5.09287      4          0.2779

           AIC:         96.6505


                                Goodness  of  Fit
                                                                      Scaled
     Dose     Est._Prob.    Expected    Observed     Size       Residual
  ---------------------------------------------------------------------------
    0.0000     0.0102         1.608         1         157       -0.482
    0.0006     0.0117         0.935         1          80        0.068
    0.0017     0.0146         1.151         2          79        0.797
    0.0060     0.0253         1.949         2          77        0.037
    0.0179     0.0544         4.351         4          80       -0.173

 Chi^2 = 0.90      d.f. = 3        P-value = 0.8246


   Benchmark Dose Computation

Specified effect =           0.1

Risk Type        =      Extra risk

Confidence level =          0.95

             BMD =      0.0413364

            BMDL =      0.0190324

            BMDU =       0.242436

Taken together, (0.0190324, 0.242436) is a 90     % two-sided confidence
interval for the BMD
```

Tumor Site: CNS (Johannsen and Levinskas, 2002b; Biodynamics, 1980b)

Table B-21. Incidence of CNS tumors in F344 rats exposed to AN in drinking water for 2 years

Sex	Administered animal dose (ppm in drinking water)	Equivalent administered animal dose[a] (mg/kg-d)	Predicted internal dose metrics		Incidence of CNS tumors[b]
			AN-AUC in blood (mg/L)	CEO-AUC in blood (mg/L)	
Male	0	0	0	0	0/160 (0%)
	1	0.08	4.33×10^{-4}	4.06×10^{-5}	2/80 (3%)
	3	0.25	1.35×10^{-3}	1.27×10^{-4}	1/78 (1%)
	10	0.83	4.52×10^{-3}	4.19×10^{-4}	2/80 (3%)
	30	2.48	1.37×10^{-2}	1.23×10^{-3}	10/79 (13%)[c]
	100	8.37	4.85×10^{-2}	3.97×10^{-3}	25/76 (33%)[c]
Female	0	0	0	0	1/157 (1%)
	1	0.12	5.73×10^{-4}	5.32×10^{-5}	1/80 (1%)
	3	0.36	1.72×10^{-3}	1.59×10^{-4}	2/80 (3%)
	10	1.25	6.02×10^{-3}	5.49×10^{-4}	5/75 (7%)
	30	3.65	1.79×10^{-2}	1.58×10^{-3}	6/80 (8%)[c]
	100	10.90	5.63×10^{-2}	4.46×10^{-3}	24/76 (32%)[c]

[a]Administered doses were averages calculated by the study authors based on animal BW and drinking water intake.
[b]Incidences for F344 rats do not include animals from the 6- and 12-mo sacrifices and were further adjusted to exclude (from the denominators) rats that died between 0 and 12 mos in the study.
[c]Significantly different from controls ($p < 0.01$) as calculated by the study authors.

Table B-22. Summary of BMD modeling results based on incidence of CNS tumors in F344 rats exposed to AN in drinking water for 2 years

Dose metric	Best-fit model[a]	χ^2 *p*-value[b]	AIC	BMD_{10}[c]	$BMDL_{10}$[d]
Males					
Administered dose	1°MS	0.73	240.57	2.41 mg/kg-d	1.81 mg/kg-d
CEO	1°MS	0.70	240.75	1.16×10^{-3} mg/L	8.74×10^{-4} mg/L
AN	1°MS	0.74	240.44	1.37×10^{-2} mg/L	1.03×10^{-2} mg/L
Females					
Administered dose	1°MS	0.68	222.13	3.34 mg/kg-d	2.52 mg/kg-d
CEO	1°MS	0.66	222.30	1.39×10^{-3} mg/L	1.05×10^{-3} mg/L
AN	1°MS	0.68	222.04	1.70×10^{-2} mg/L	1.28×10^{-2} mg/L

[a]Dose-response models were fit using BMDS, version 1.4.1. "1°MS" indicates a one-stage multistage model.
[b]*p* value from the χ^2 goodness of fit test. Values <0.1 indicate a significant lack of fit.
[c]BMD_{10} = BMD at 10% extra risk.
[d]$BMDL_{10}$ = 95% lower confidence limit on the BMD at 10% extra risk.

BMDS (version 1.4.1) output for CNS tumors in F344 male rats employing administered dose as a dose metric

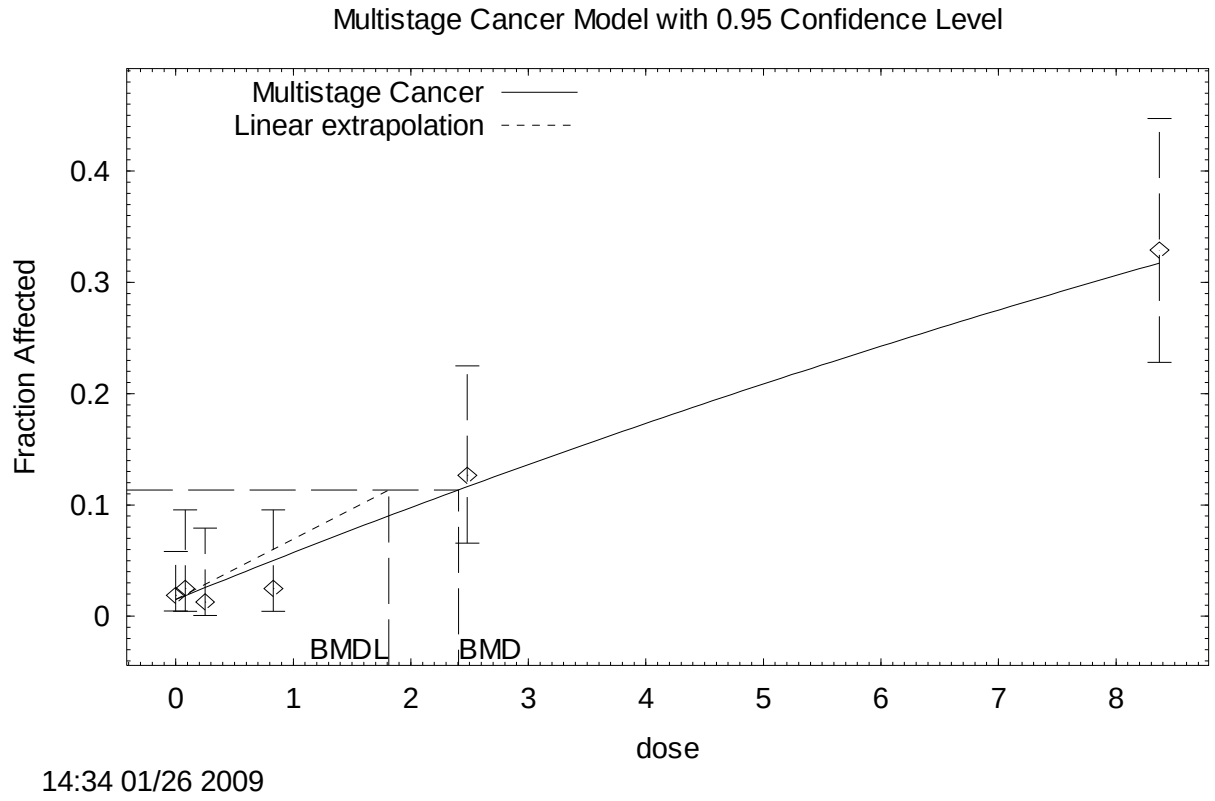


```
=================================================================
        Multistage Cancer Model. (Version: 1.5;  Date: 02/20/2007)
        Input Data File: M:\ACN DOSE-RESPONSE MODELING\CANCER\ORAL\F344_MALE_CNS_DW.(d)
        Gnuplot Plotting File:  M:\ACN DOSE-RESPONSE MODELING\CANCER\ORAL\F344_MALE_CNS_DW.plt
                                                  Mon Jan 26 14:34:10 2009
=================================================================

BMDS MODEL RUN
~~~~~~~~~~~~~~~~~~~~~~~~~~~~~~~~~~~~~~~~~~~~~~~~~~~~~~~~~~~~~~~~~~~~~

  The form of the probability function is:

  P[response] = background + (1-background)*[1-EXP(
               -beta1*dose^1)]

  The parameter betas are restricted to be positive


  Dependent variable = Response
  Independent variable = Dose

Total number of observations = 6
Total number of records with missing values = 0
Total number of parameters in model = 2
Total number of specified parameters = 0
Degree of polynomial = 1


Maximum number of iterations = 250
Relative Function Convergence has been set to: 1e-008
Parameter Convergence has been set to: 1e-008


                 Default Initial Parameter Values
```

Background = 0.00946328
Beta(1) = 0.0466

Asymptotic Correlation Matrix of Parameter Estimates

	Background	Beta(1)
Background	1	-0.47
Beta(1)	-0.47	1

Parameter Estimates

Variable	Estimate	Std. Err.	95.0% Wald Confidence Interval Lower Conf. Limit	Upper Conf. Limit
Background	0.0149509	*	*	*
Beta(1)	0.0437933	*	*	*

* - Indicates that this value is not calculated.

Analysis of Deviance Table

Model	Log(likelihood)	# Param's	Deviance	Test d.f.	P-value
Full model	-117.105	6			
Fitted model	-118.287	2	2.36443	4	0.6691
Reduced model	-151.112	1	68.0145	5	<.0001

AIC: 240.574

Goodness of Fit

Dose	Est._Prob.	Expected	Observed	Size	Scaled Residual
0.0000	0.0150	2.392	3	160	0.396
0.0800	0.0184	1.472	2	80	0.440
0.2500	0.0257	2.003	1	78	-0.718
0.8300	0.0501	4.009	2	80	-1.030
2.4800	0.1163	9.190	10	79	0.284
8.3700	0.3172	24.110	25	76	0.219

Chi^2 = 2.05 d.f. = 4 P-value = 0.7258

```
   Benchmark Dose Computation

Specified effect =            0.1

Risk Type        =      Extra risk

Confidence level =           0.95

              BMD =        2.40586

             BMDL =         1.8134

             BMDU =        3.32187

Taken together, (1.8134 , 3.32187) is a 90     % two-sided confidence
interval for the BMD

Multistage Cancer Slope Factor =     0.0551449
```

BMDS (version 1.4.1) output for CNS tumors in F344 male rats employing CEO in blood as an internal dose metric

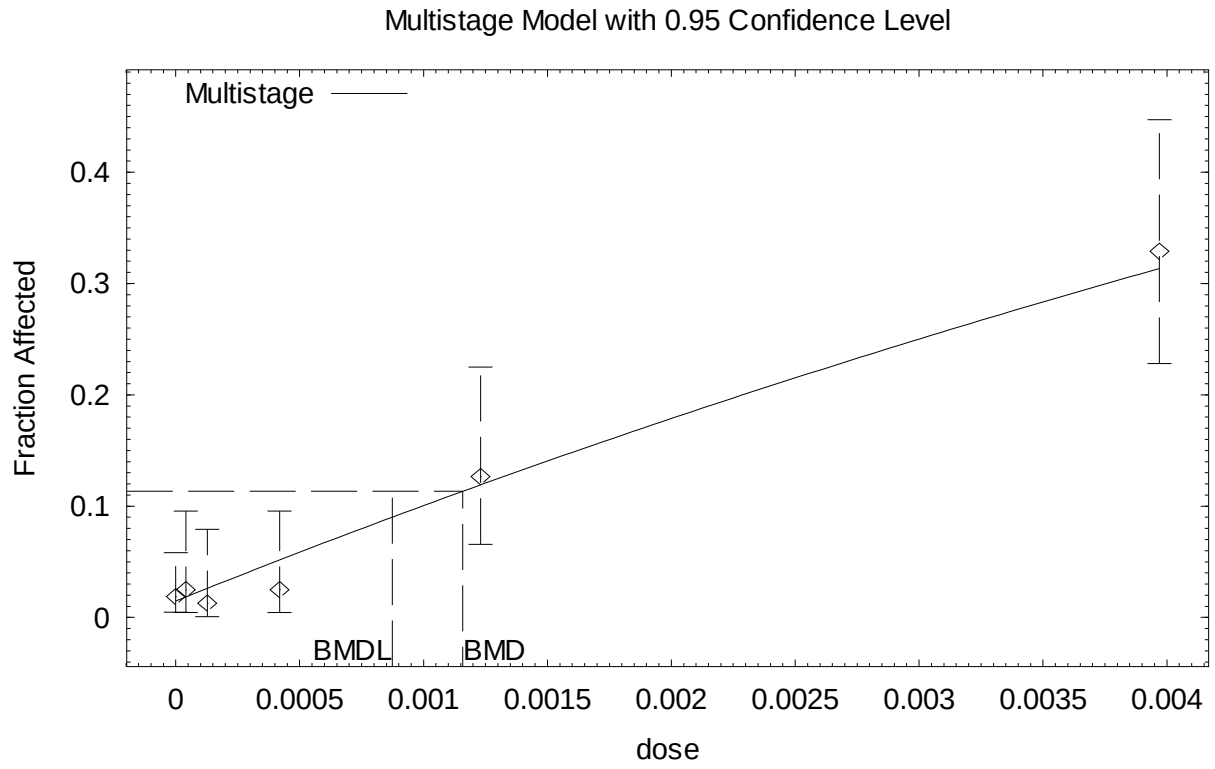


```
 ================================================================
         Multistage Model. (Version: 2.8;  Date: 02/20/2007)
         Input Data File: G:\ACN DOSE-RESPONSE MODELING\CANCER\ORAL\F344_MALE_CNS_BLOOD_CEO.(d)
         Gnuplot Plotting File:  G:\ACN DOSE-RESPONSE
MODELING\CANCER\ORAL\F344_MALE_CNS_BLOOD_CEO.plt
                                                  Thu Sep 27 15:00:12 2007
 ================================================================

 BMDS MODEL RUN
~~~~~~~~~~~~~~~~~~~~~~~~~~~~~~~~~~~~~~~~~~~~~~~~~~~~~~~~~~~~~~~~~~~~~~~~

   The form of the probability function is:

   P[response] = background + (1-background)*[1-EXP(
                -beta1*dose^1)]

   The parameter betas are restricted to be positive


   Dependent variable = Response
   Independent variable = Dose

 Total number of observations = 6
 Total number of records with missing values = 0
 Total number of parameters in model = 2
 Total number of specified parameters = 0
 Degree of polynomial = 1


 Maximum number of iterations = 250
 Relative Function Convergence has been set to: 1e-008
 Parameter Convergence has been set to: 1e-008



                  Default Initial Parameter Values
```

Background = 0.00793445
Beta(1) = 98.3167

Asymptotic Correlation Matrix of Parameter Estimates

	Background	Beta(1)
Background	1	-0.47
Beta(1)	-0.47	1

Parameter Estimates

Variable	Estimate	Std. Err.	95.0% Wald Confidence Interval Lower Conf. Limit	Upper Conf. Limit
Background	0.0147547	*	*	*
Beta(1)	90.9591	*	*	*

* - Indicates that this value is not calculated.

Analysis of Deviance Table

Model	Log(likelihood)	# Param's	Deviance	Test d.f.	P-value
Full model	-117.105	6			
Fitted model	-118.375	2	2.54113	4	0.6373
Reduced model	-151.112	1	68.0145	5	<.0001

AIC: 240.75

Goodness of Fit

Dose	Est._Prob.	Expected	Observed	Size	Scaled Residual
0.0000	0.0148	2.361	3	160	0.419
0.0000	0.0184	1.471	2	80	0.440
0.0001	0.0261	2.034	1	78	-0.734
0.0004	0.0516	4.128	2	80	-1.075
0.0012	0.1190	9.404	10	79	0.207
0.0040	0.3134	23.817	25	76	0.293

Chi^2 = 2.19 d.f. = 4 P-value = 0.7002

Benchmark Dose Computation

Specified effect = 0.1

Risk Type = Extra risk

Confidence level = 0.95

BMD = 0.00115833

BMDL = 0.000873641

BMDU = 0.00159795

Taken together, (0.000873641, 0.00159795) is a 90 % two-sided confidence interval for the BMD

BMDS (version 1.4.1) output for CNS tumors in F344 male rats employing AN in blood as an internal dose metric

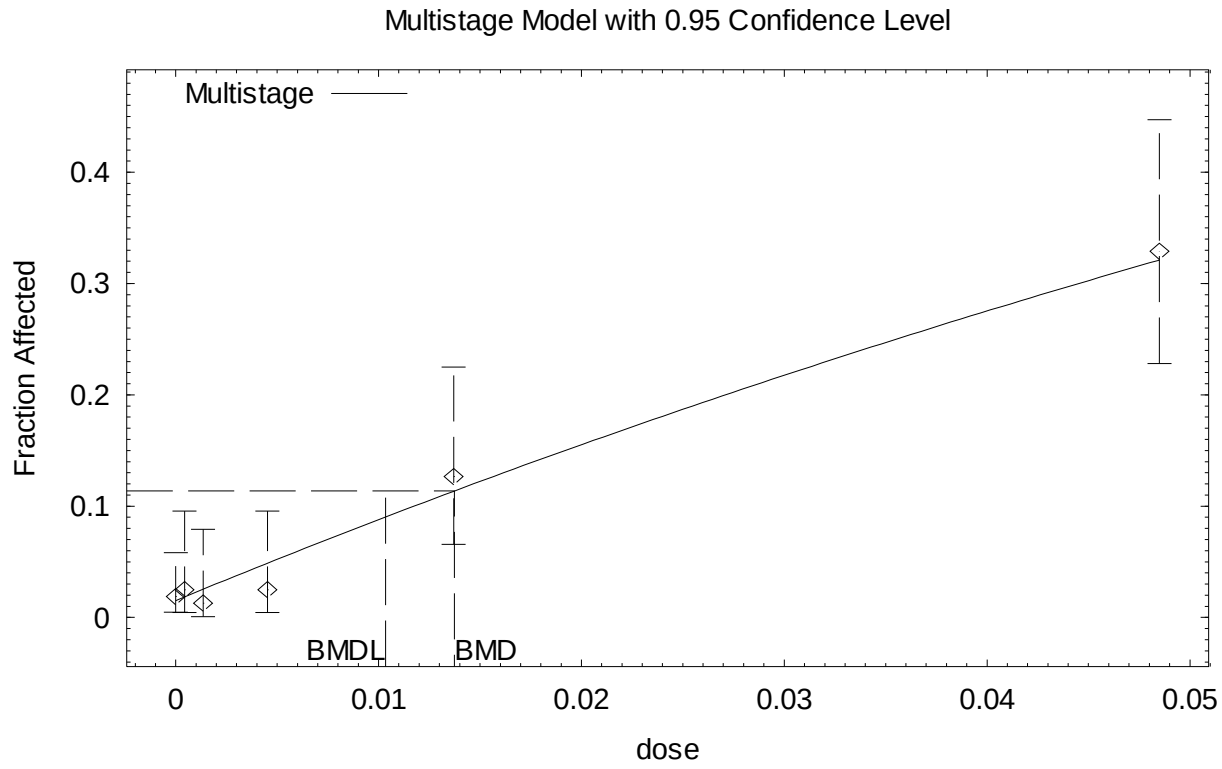


```
 ======================================================================
         Multistage Model. (Version: 2.8;  Date: 02/20/2007)
         Input Data File: G:\ACN DOSE-RESPONSE MODELING\CANCER\ORAL\F344_MALE_CNS_BLOOD_AN.(d)
         Gnuplot Plotting File:  G:\ACN DOSE-RESPONSE
MODELING\CANCER\ORAL\F344_MALE_CNS_BLOOD_AN.plt
                                                    Thu Sep 27 11:07:15 2007
 ======================================================================

 BMDS MODEL RUN
~~~~~~~~~~~~~~~~~~~~~~~~~~~~~~~~~~~~~~~~~~~~~~~~~~~~~~~~~~~~~~~~~~~~~~~~~~~~

   The form of the probability function is:

   P[response] = background + (1-background)*[1-EXP(
                -beta1*dose^1)]

   The parameter betas are restricted to be positive


   Dependent variable = Response
   Independent variable = Dose

 Total number of observations = 6
 Total number of records with missing values = 0
 Total number of parameters in model = 2
 Total number of specified parameters = 0
 Degree of polynomial = 1


 Maximum number of iterations = 250
 Relative Function Convergence has been set to: 1e-008
 Parameter Convergence has been set to: 1e-008



                  Default Initial Parameter Values
```

Background = 0.0109984
Beta(1) = 8.0341

Asymptotic Correlation Matrix of Parameter Estimates

	Background	Beta(1)
Background	1	-0.46
Beta(1)	-0.46	1

Parameter Estimates

Variable	Estimate	Std. Err.	95.0% Wald Confidence Interval Lower Conf. Limit	Upper Conf. Limit
Background	0.0151616	*	*	*
Beta(1)	7.67068	*	*	*

* - Indicates that this value is not calculated.

Analysis of Deviance Table

Model	Log(likelihood)	# Param's	Deviance	Test d.f.	P-value
Full model	-117.105	6			
Fitted model	-118.218	2	2.22757	4	0.694
Reduced model	-151.112	1	68.0145	5	<.0001

AIC: 240.437

Goodness of Fit

Dose	Est._Prob.	Expected	Observed	Size	Scaled Residual
0.0000	0.0152	2.426	3	160	0.371
0.0004	0.0184	1.474	2	80	0.437
0.0014	0.0253	1.974	1	78	-0.702
0.0045	0.0487	3.898	2	80	-0.986
0.0137	0.1134	8.959	10	79	0.369
0.0485	0.3211	24.405	25	76	0.146

Chi^2 = 1.95 d.f. = 4 P-value = 0.7447

Benchmark Dose Computation

Specified effect = 0.1

Risk Type = Extra risk

Confidence level = 0.95

BMD = 0.0137355

BMDL = 0.0103458

BMDU = 0.0189838

Taken together, (0.0103458, 0.0189838) is a 90 % two-sided confidence interval for the BMD

BMDS (version 1.4.1) output for CNS tumors in F344 female rats employing administered dose as a dose metric

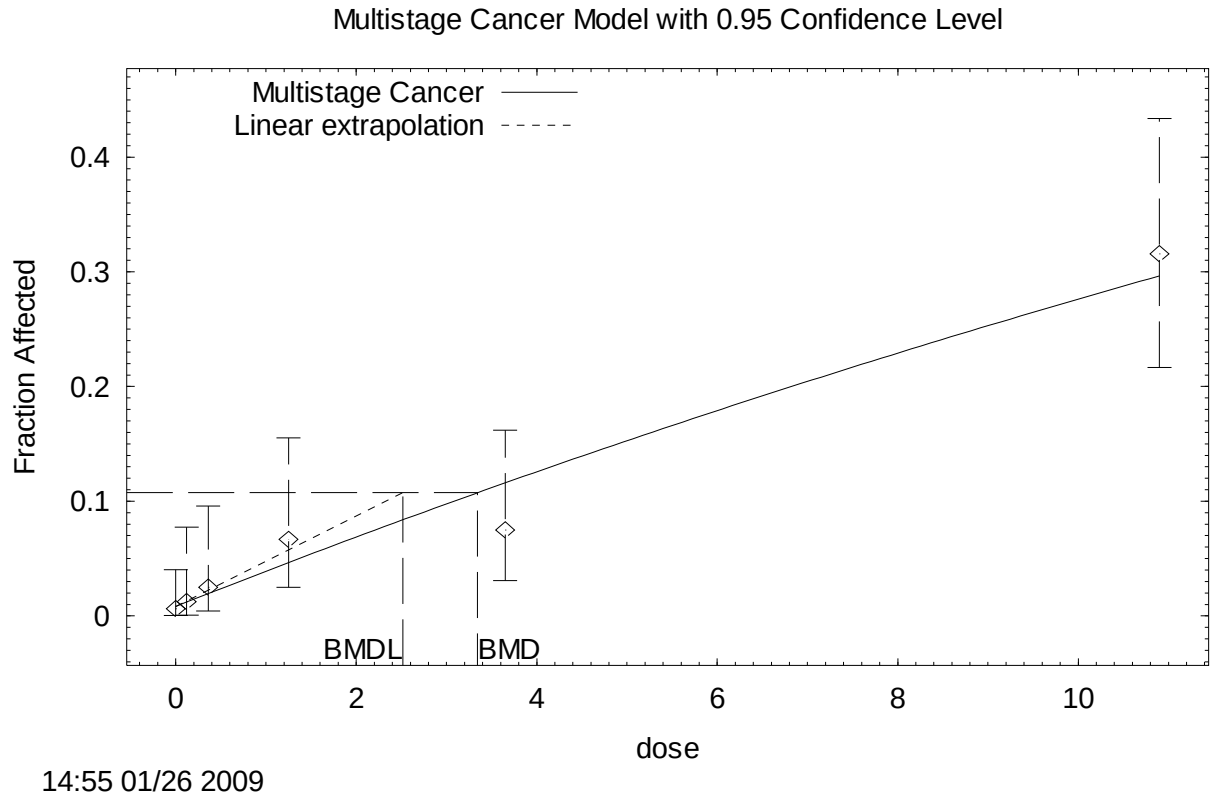


```
 ================================================================
         Multistage Cancer Model. (Version: 1.5;  Date: 02/20/2007)
         Input Data File: M:\ACN DOSE-RESPONSE MODELING\CANCER\ORAL\F344_FEMALE_CNS_DW.(d)
         Gnuplot Plotting File:  M:\ACN DOSE-RESPONSE
MODELING\CANCER\ORAL\F344_FEMALE_CNS_DW.plt
                                                    Mon Jan 26 14:55:28 2009
 ================================================================

 BMDS MODEL RUN
~~~~~~~~~~~~~~~~~~~~~~~~~~~~~~~~~~~~~~~~~~~~~~~~~~~~~~~~~~~~~~~~~~~~~~~~

   The form of the probability function is:

   P[response] = background + (1-background)*[1-EXP(
                -beta1*dose^1)]

   The parameter betas are restricted to be positive


   Dependent variable = Response
   Independent variable = Dose

 Total number of observations = 6
 Total number of records with missing values = 0
 Total number of parameters in model = 2
 Total number of specified parameters = 0
 Degree of polynomial = 1


 Maximum number of iterations = 250
 Relative Function Convergence has been set to: 1e-008
 Parameter Convergence has been set to: 1e-008
```

Default Initial Parameter Values
Background = 0.00525608
Beta(1) = 0.0331149

Asymptotic Correlation Matrix of Parameter Estimates

	Background	Beta(1)
Background	1	-0.49
Beta(1)	-0.49	1

Parameter Estimates

Variable	Estimate	Std. Err.	95.0% Wald Confidence Interval Lower Conf. Limit	Upper Conf. Limit
Background	0.00823648	*	*	*
Beta(1)	0.0315054	*	*	*

* - Indicates that this value is not calculated.

Analysis of Deviance Table

Model	Log(likelihood)	# Param's	Deviance	Test d.f.	P-value
Full model	-107.86	6			
Fitted model	-109.065	2	2.41059	4	0.6607
Reduced model	-140.644	1	65.5686	5	<.0001

AIC: 222.13

Goodness of Fit

Dose	Est._Prob.	Expected	Observed	Size	Scaled Residual
0.0000	0.0082	1.293	1	157	-0.259
0.1200	0.0120	0.958	1	80	0.043
0.3600	0.0194	1.554	2	80	0.362
1.2500	0.0465	3.490	5	75	0.828
3.6500	0.1160	9.278	6	80	-1.144
10.9000	0.2965	22.534	24	76	0.368

Chi^2 = 2.33 d.f. = 4 P-value = 0.6753

```
   Benchmark Dose Computation

Specified effect =            0.1

Risk Type        =      Extra risk

Confidence level =           0.95

              BMD =        3.34421

             BMDL =        2.51554

             BMDU =        4.64166

Taken together, (2.51554, 4.64166) is a 90     % two-sided confidence
interval for the BMD

Multistage Cancer Slope Factor =     0.0397529
```

BMDS (version 1.4.1) output for CNS tumors in F344 female rats employing CEO in blood as an internal dose metric

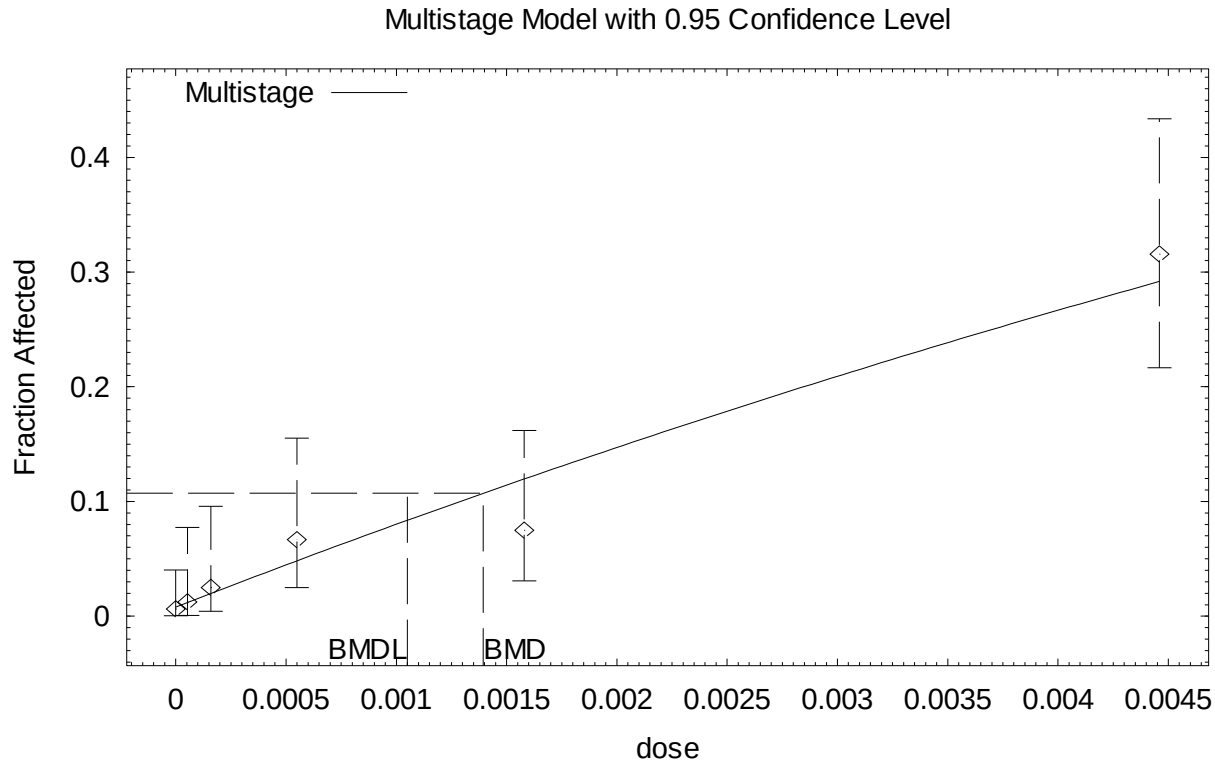


```
    15:10 09/27 2007
 ======================================================================
         Multistage Model. (Version: 2.8;  Date: 02/20/2007)
         Input Data File: G:\ACN DOSE-RESPONSE
MODELING\CANCER\ORAL\F344_FEMALE_CNS_BLOOD_CEO.(d)
         Gnuplot Plotting File:  G:\ACN DOSE-RESPONSE
MODELING\CANCER\ORAL\F344_FEMALE_CNS_BLOOD_CEO.plt
                                                Thu Sep 27 15:10:31 2007
 ======================================================================

 BMDS MODEL RUN
~~~~~~~~~~~~~~~~~~~~~~~~~~~~~~~~~~~~~~~~~~~~~~~~~~~~~~~~~~~~~~~~~~~~~~~~

   The form of the probability function is:

   P[response] = background + (1-background)*[1-EXP(
                -beta1*dose^1)]

   The parameter betas are restricted to be positive


   Dependent variable = Response
   Independent variable = Dose

 Total number of observations = 6
 Total number of records with missing values = 0
 Total number of parameters in model = 2
 Total number of specified parameters = 0
 Degree of polynomial = 1


 Maximum number of iterations = 250
 Relative Function Convergence has been set to: 1e-008
 Parameter Convergence has been set to: 1e-008
```

Default Initial Parameter Values
Background = 0.00362563
Beta(1) = 80.7118

Asymptotic Correlation Matrix of Parameter Estimates

	Background	Beta(1)
Background	1	-0.5
Beta(1)	-0.5	1

Parameter Estimates

Variable	Estimate	Std. Err.	95.0% Wald Confidence Interval Lower Conf. Limit	Upper Conf. Limit
Background	0.00790184	*	*	*
Beta(1)	75.5979	*	*	*

* - Indicates that this value is not calculated.

Analysis of Deviance Table

Model	Log(likelihood)	# Param's	Deviance	Test d.f.	P-value
Full model	-107.86	6			
Fitted model	-109.148	2	2.57752	4	0.6308
Reduced model	-140.644	1	65.5686	5	<.0001

AIC: 222.297

Goodness of Fit

Dose	Est._Prob.	Expected	Observed	Size	Scaled Residual
0.0000	0.0079	1.241	1	157	-0.217
0.0001	0.0119	0.951	1	80	0.051
0.0002	0.0198	1.580	2	80	0.337
0.0005	0.0482	3.618	5	75	0.745
0.0016	0.1196	9.568	6	80	-1.229
0.0045	0.2919	22.181	24	76	0.459

Chi^2 = 2.44 d.f. = 4 P-value = 0.6554

Benchmark Dose Computation

Specified effect = 0.1

Risk Type = Extra risk

Confidence level = 0.95

BMD = 0.0013937

BMDL = 0.00104985

BMDU = 0.00193063

Taken together, (0.00104985, 0.00193063) is a 90 % two-sided confidence interval for the BMD

BMDS (version 1.4.1) output for CNS tumors in F344 female rats employing AN in blood as an internal dose metric

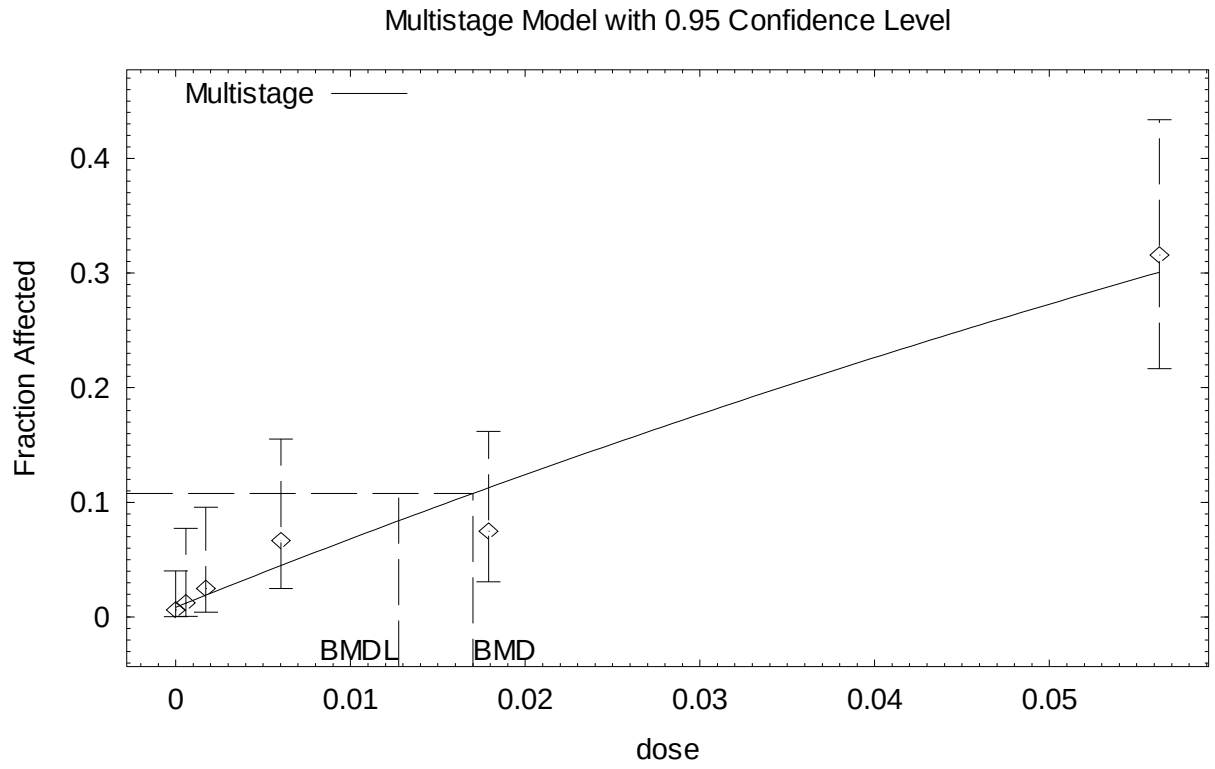


```
 ================================================================
         Multistage Model. (Version: 2.8;  Date: 02/20/2007)
         Input Data File: G:\ACN DOSE-RESPONSE MODELING\CANCER\ORAL\F344_FEMALE_CNS_BLOOD_AN.(d)
         Gnuplot Plotting File:  G:\ACN DOSE-RESPONSE
MODELING\CANCER\ORAL\F344_FEMALE_CNS_BLOOD_AN.plt
                                                  Thu Sep 27 11:34:20 2007
 ================================================================

 BMDS MODEL RUN
~~~~~~~~~~~~~~~~~~~~~~~~~~~~~~~~~~~~~~~~~~~~~~~~~~~~~~~~~~~~~~~~~~~~~~~~

   The form of the probability function is:

   P[response] = background + (1-background)*[1-EXP(
                -beta1*dose^1)]

   The parameter betas are restricted to be positive


   Dependent variable = Response
   Independent variable = Dose

 Total number of observations = 6
 Total number of records with missing values = 0
 Total number of parameters in model = 2
 Total number of specified parameters = 0
 Degree of polynomial = 1


 Maximum number of iterations = 250
 Relative Function Convergence has been set to: 1e-008
 Parameter Convergence has been set to: 1e-008



                  Default Initial Parameter Values
```

Background = 0.00679319
Beta(1) = 6.4212

Asymptotic Correlation Matrix of Parameter Estimates

	Background	Beta(1)
Background	1	-0.49
Beta(1)	-0.49	1

Parameter Estimates

Variable	Estimate	Std. Err.	95.0% Wald Confidence Interval Lower Conf. Limit	Upper Conf. Limit
Background	0.00859669	*	*	*
Beta(1)	6.19715	*	*	*

* - Indicates that this value is not calculated.

Analysis of Deviance Table

Model	Log(likelihood)	# Param's	Deviance	Test d.f.	P-value
Full model	-107.86	6			
Fitted model	-109.017	2	2.31525	4	0.678
Reduced model	-140.644	1	65.5686	5	<.0001

AIC: 222.035

Goodness of Fit

Dose	Est._Prob.	Expected	Observed	Size	Scaled Residual
0.0000	0.0086	1.350	1	157	-0.302
0.0006	0.0121	0.969	1	80	0.032
0.0017	0.0191	1.529	2	80	0.385
0.0060	0.0449	3.368	5	75	0.910
0.0179	0.1127	9.015	6	80	-1.066
0.0563	0.3006	22.846	24	76	0.289

Chi^2 = 2.29 d.f. = 4 P-value = 0.6828

Benchmark Dose Computation

Specified effect = 0.1

Risk Type = Extra risk

Confidence level = 0.95

BMD = 0.0170014

BMDL = 0.0127694

BMDU = 0.0236456

Taken together, (0.0127694, 0.0236456) is a 90 % two-sided confidence interval for the BMD

Tumor Site: Zymbal's Gland (Johannsen and Levinskas, 2002b; Biodynamics, 1980b)

Table B-23. Incidence of Zymbal gland tumors in F344 rats exposed to AN in drinking water for 2 years

Sex	Administered animal dose (ppm in drinking water)	Equivalent administered animal dose[a] (mg/kg-d)	Predicted internal dose metrics		Incidence of Zymbal's gland tumors[b]
			AN-AUC in blood (mg/L)	CEO-AUC in blood (mg/L)	
Male	0	0	0	0	1/147 (1%)
	1	0.08	4.33×10^{-4}	4.06×10^{-5}	1/76 (1%)
	3	0.25	1.35×10^{-3}	1.27×10^{-4}	0/73 (0%)
	10	0.83	4.52×10^{-3}	4.19×10^{-4}	0/67 (0%)
	30	2.48	1.37×10^{-2}	1.23×10^{-3}	2/71 (3%)[c]
	100	8.37	4.85×10^{-2}	3.97×10^{-3}	14/68 (21%)[c]
Female	0	0	0	0	0/157 (0%)
	1	0.12	5.73×10^{-4}	5.32×10^{-5}	0/73 (0%)
	3	0.36	1.72×10^{-3}	1.59×10^{-4}	0/73 (0%)
	10	1.25	6.02×10^{-3}	5.49×10^{-4}	0/70 (0%)
	30	3.65	1.79×10^{-2}	1.58×10^{-3}	2/73 (3%)[c]
	100	10.90	5.63×10^{-2}	4.46×10^{-3}	8/62 (13%)[c]

[a]Administered doses were averages calculated by the study authors based on animal BW and drinking water intake.
[b]Incidences for F344 rats do not include animals from the 6- and 12-mo sacrifices and were further adjusted to exclude (from the denominators) rats that died between 0 and 12 mos in the study.
[c]Significantly different from controls ($p < 0.01$) as calculated by the study authors.

Table B-24. Summary of BMD modeling results based on incidence of Zymbal gland tumors in F344 rats exposed to AN in drinking water for 2 years

Dose metric	Best-fit model[a]	χ^2 *p*-value[b]	AIC	BMD_{10}[c]	$BMDL_{10}$[d]
Males					
Administered dose	2°MS	0.78	116.51	5.73 mg/kg-d	4.55 mg/kg-d
CEO	2°MS	0.77	116.53	2.73×10^{-3} mg/L	2.19×10^{-3} mg/L
AN	2°MS	0.78	116.52	3.31×10^{-2} mg/L	2.59×10^{-2} mg/L
Females					
Administered dose	2°MS	0.95	70.80	9.16 mg/kg-d	7.17 mg/kg-d
CEO	2°MS	0.99	68.68	3.78×10^{-3} mg/L	2.97×10^{-3} mg/L
AN	1°MS	0.89	70.82	5.41×10^{-2} mg/L	3.35×10^{-2} mg/L

[a]Dose-response models were fit using BMDS, version 1.4.1. "1°MS" indicates a one-stage multistage model and "2°MS" indicates a two-stage multistage model.
[b]*p* value from the χ^2 goodness of fit test. Values <0.1 indicate a significant lack of fit.
[c]BMD_{10} = BMD at 10% extra risk.
[d]$BMDL_{10}$ = 95% lower confidence limit on the BMD at 10% extra risk.

BMDS (version 1.4.1) output for Zymbal gland tumors in F344 male rats employing administered dose as a dose metric

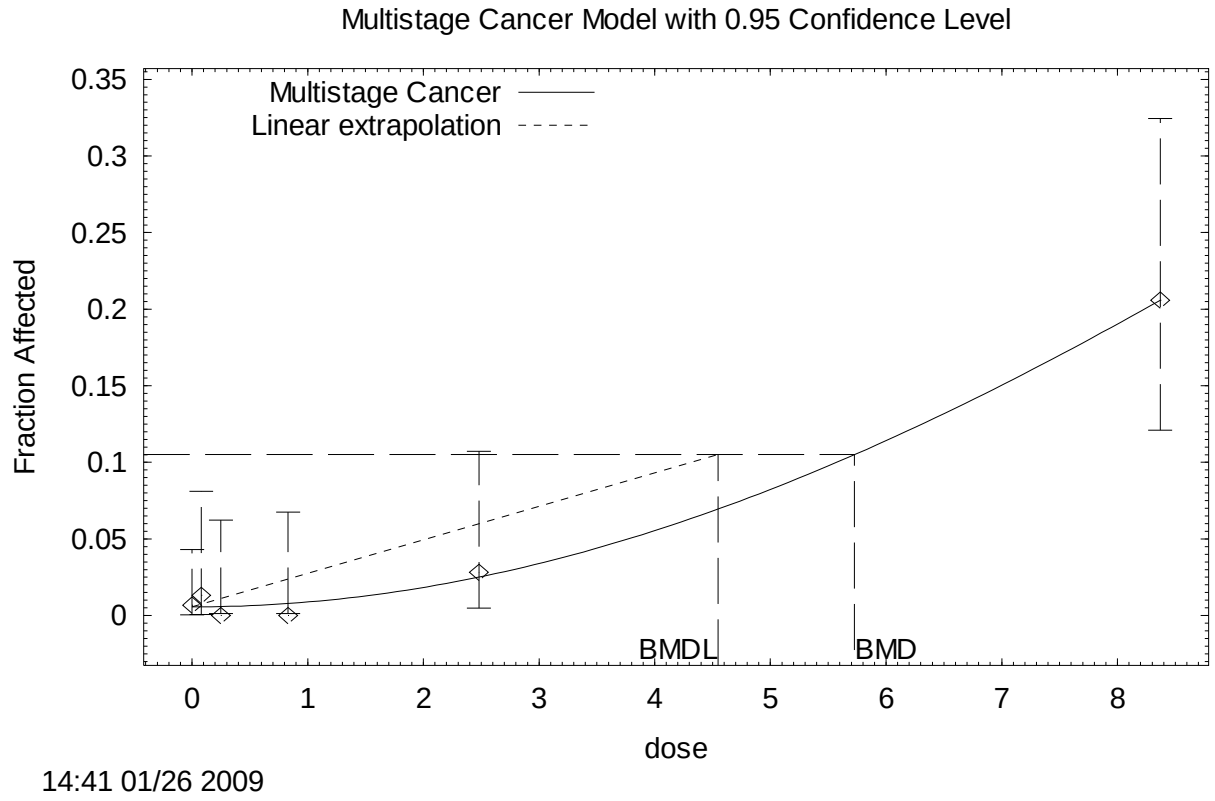


```
 ======================================================================
         Multistage Cancer Model. (Version: 1.5;  Date: 02/20/2007)
         Input Data File: M:\ACN DOSE-RESPONSE MODELING\CANCER\ORAL\F344_MALE_ZYMBAL_DW.(d)
         Gnuplot Plotting File:  M:\ACN DOSE-RESPONSE
MODELING\CANCER\ORAL\F344_MALE_ZYMBAL_DW.plt
                                                    Mon Jan 26 14:41:15 2009
 ======================================================================

 BMDS MODEL RUN
~~~~~~~~~~~~~~~~~~~~~~~~~~~~~~~~~~~~~~~~~~~~~~~~~~~~~~~~~~~~~~~~~~~~~~~~~~~~

   The form of the probability function is:

   P[response] = background + (1-background)*[1-EXP(
                -beta1*dose^1-beta2*dose^2)]

   The parameter betas are restricted to be positive


   Dependent variable = Response
   Independent variable = Dose

 Total number of observations = 6
 Total number of records with missing values = 0
 Total number of parameters in model = 3
 Total number of specified parameters = 0
 Degree of polynomial = 2


 Maximum number of iterations = 250
 Relative Function Convergence has been set to: 1e-008
 Parameter Convergence has been set to: 1e-008
```

Default Initial Parameter Values
Background = 0.00522088
Beta(1) = 0
Beta(2) = 0.00321913

Asymptotic Correlation Matrix of Parameter Estimates

(*** The model parameter(s) -Beta(1)
have been estimated at a boundary point, or have been specified by the user,
and do not appear in the correlation matrix)

	Background	Beta(2)
Background	1	-0.37
Beta(2)	-0.37	1

Parameter Estimates

Variable	Estimate	Std. Err.	95.0% Wald Confidence Interval Lower Conf. Limit	Upper Conf. Limit
Background	0.00563419	*	*	*
Beta(1)	0	*	*	*
Beta(2)	0.00321262	*	*	*

* - Indicates that this value is not calculated.

Analysis of Deviance Table

Model	Log(likelihood)	# Param's	Deviance	Test d.f.	P-value
Full model	-54.9964	6			
Fitted model	-56.2568	2	2.52093	4	0.6409
Reduced model	-77.5815	1	45.1702	5	<.0001

AIC: 116.514

Goodness of Fit

Dose	Est._Prob.	Expected	Observed	Size	Scaled Residual
0.0000	0.0056	0.828	1	147	0.189
0.0800	0.0057	0.430	1	76	0.872
0.2500	0.0058	0.426	0	73	-0.654
0.8300	0.0078	0.525	0	67	-0.727
2.4800	0.0251	1.781	2	71	0.166
8.3700	0.2060	14.010	14	68	-0.003

Chi^2 = 1.78 d.f. = 4 P-value = 0.7758

```
   Benchmark Dose Computation

Specified effect =            0.1

Risk Type        =      Extra risk

Confidence level =           0.95

              BMD =        5.72676

             BMDL =        4.54678

             BMDU =        7.26717

Taken together, (4.54678, 7.26717) is a 90     % two-sided confidence
interval for the BMD

Multistage Cancer Slope Factor =     0.0219936
```

BMDS (version 1.4.1) output for Zymbal gland tumors in F344 male rats employing CEO in blood as an internal dose metric

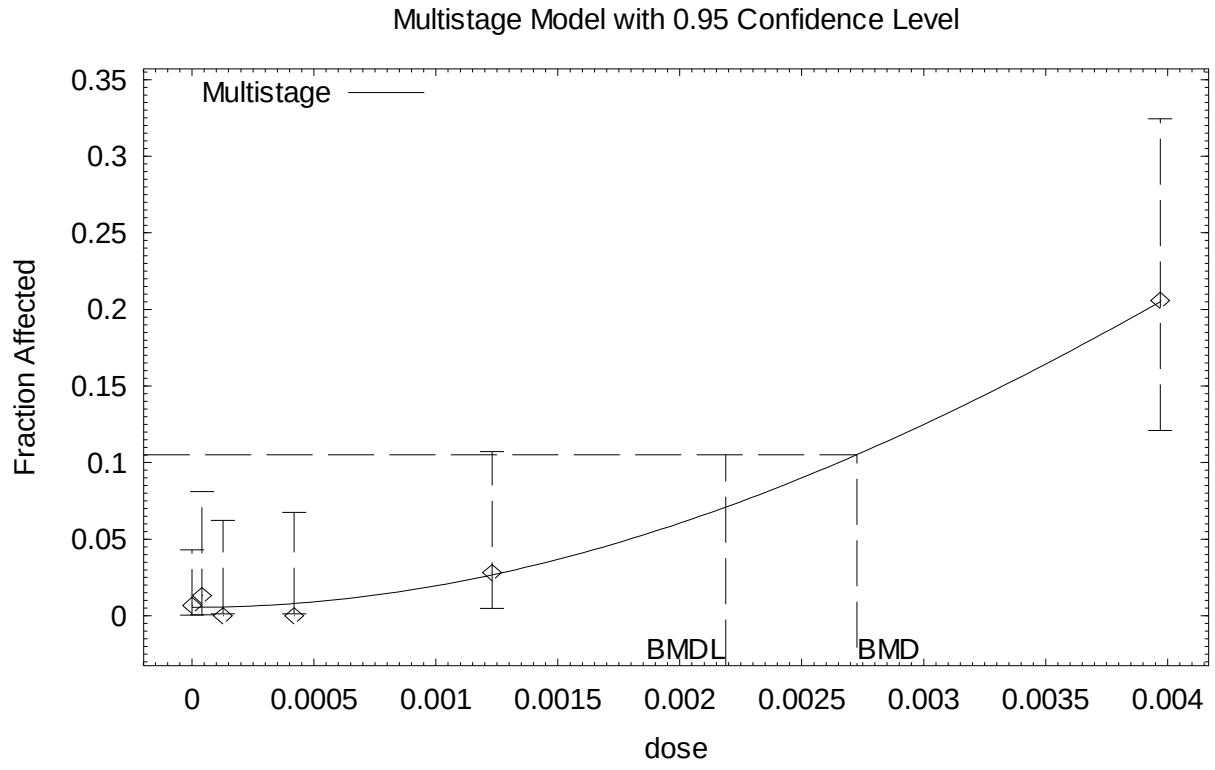


```
 ================================================================
         Multistage Model. (Version: 2.8;  Date: 02/20/2007)
         Input Data File: G:\ACN DOSE-RESPONSE
MODELING\CANCER\ORAL\F344_MALE_ZYMBAL_BLOOD_CEO.(d)
         Gnuplot Plotting File:  G:\ACN DOSE-RESPONSE
MODELING\CANCER\ORAL\F344_MALE_ZYMBAL_BLOOD_CEO.plt
                                                Thu Sep 27 15:02:53 2007
 ================================================================

 BMDS MODEL RUN
~~~~~~~~~~~~~~~~~~~~~~~~~~~~~~~~~~~~~~~~~~~~~~~~~~~~~~~~~~~~~~~~~~~~~~~~

   The form of the probability function is:

   P[response] = background + (1-background)*[1-EXP(
                -beta1*dose^1-beta2*dose^2)]

   The parameter betas are restricted to be positive


   Dependent variable = Response
   Independent variable = Dose

 Total number of observations = 6
 Total number of records with missing values = 0
 Total number of parameters in model = 3
 Total number of specified parameters = 0
 Degree of polynomial = 2


 Maximum number of iterations = 250
 Relative Function Convergence has been set to: 1e-008
 Parameter Convergence has been set to: 1e-008
```

Default Initial Parameter Values
Background = 0.00480523
Beta(1) = 0
Beta(2) = 14327.9

Asymptotic Correlation Matrix of Parameter Estimates

(*** The model parameter(s) -Beta(1)
have been estimated at a boundary point, or have been specified by the user,
and do not appear in the correlation matrix)

	Background	Beta(2)
Background	1	-0.38
Beta(2)	-0.38	1

Parameter Estimates

Variable	Estimate	Std. Err.	95.0% Wald Confidence Interval Lower Conf. Limit	Upper Conf. Limit
Background	0.00556639	*	*	*
Beta(1)	0	*	*	*
Beta(2)	14170.3	*	*	*

* - Indicates that this value is not calculated.

Analysis of Deviance Table

Model	Log(likelihood)	# Param's	Deviance	Test d.f.	P-value
Full model	-54.9964	6			
Fitted model	-56.2667	2	2.54061	4	0.6374
Reduced model	-77.5815	1	45.1702	5	<.0001

AIC: 116.533

Goodness of Fit

Dose	Est._Prob.	Expected	Observed	Size	Scaled Residual
0.0000	0.0056	0.818	1	147	0.201
0.0000	0.0056	0.425	1	76	0.885
0.0001	0.0058	0.423	0	73	-0.652
0.0004	0.0080	0.538	0	67	-0.737
0.0012	0.0267	1.893	2	71	0.079
0.0040	0.2046	13.913	14	68	0.026

Chi^2 = 1.80 d.f. = 4 P-value = 0.7727

Benchmark Dose Computation

Specified effect = 0.1

Risk Type = Extra risk

Confidence level = 0.95

BMD = 0.00272678

BMDL = 0.00218772

BMDU = 0.00345798

Taken together, (0.00218772, 0.00345798) is a 90 % two-sided confidence
interval for the BMD

BMDS (version 1.4.1) output for Zymbal gland tumors in F344 male rats employing AN in blood as an internal dose metric

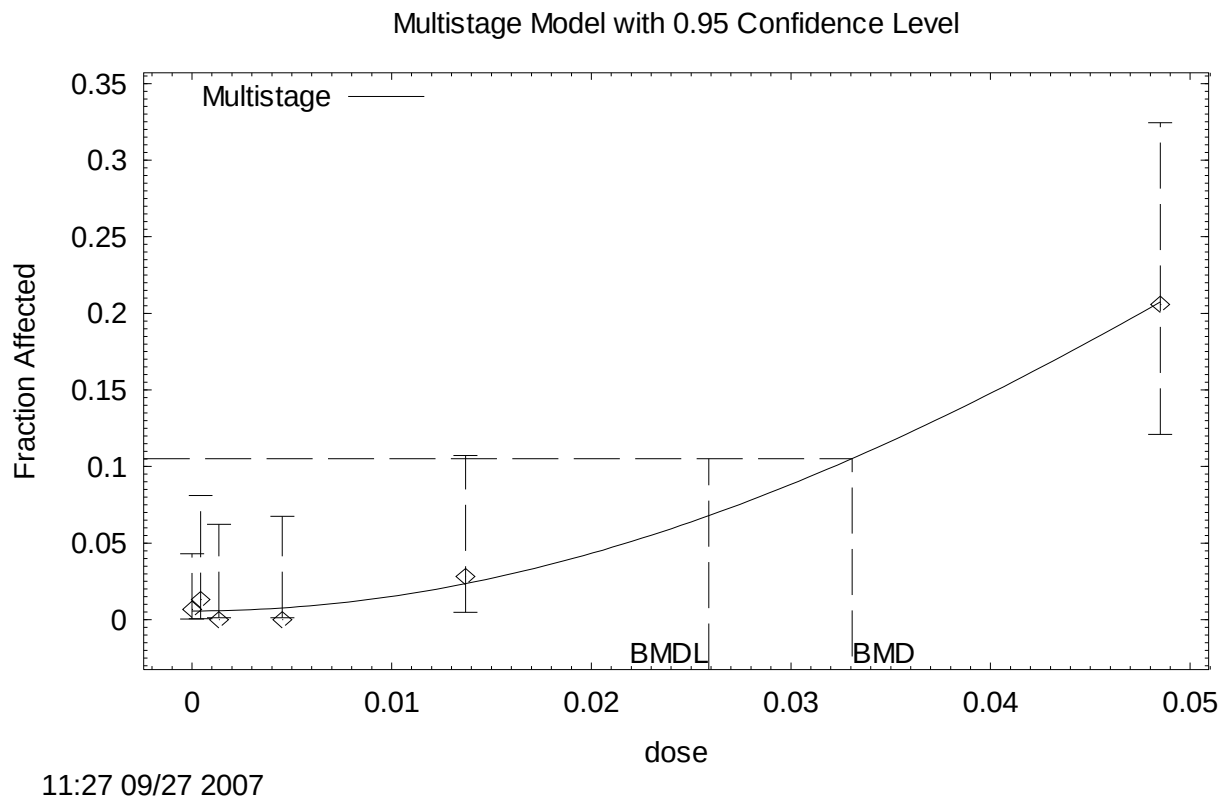


```
 ======================================================================
         Multistage Model. (Version: 2.8;  Date: 02/20/2007)
         Input Data File: G:\ACN DOSE-RESPONSE
MODELING\CANCER\ORAL\F344_MALE_ZYMBAL_BLOOD_AN.(d)
         Gnuplot Plotting File:  G:\ACN DOSE-RESPONSE
MODELING\CANCER\ORAL\F344_MALE_ZYMBAL_BLOOD_AN.plt
                                                Thu Sep 27 11:27:02 2007
 ======================================================================

 BMDS MODEL RUN
~~~~~~~~~~~~~~~~~~~~~~~~~~~~~~~~~~~~~~~~~~~~~~~~~~~~~~~~~~~~~~~~~~~~~~~~

   The form of the probability function is:

   P[response] = background + (1-background)*[1-EXP(
                -beta1*dose^1-beta2*dose^2)]

   The parameter betas are restricted to be positive

   Dependent variable = Response
   Independent variable = Dose

 Total number of observations = 6
 Total number of records with missing values = 0
 Total number of parameters in model = 3
 Total number of specified parameters = 0
 Degree of polynomial = 2


 Maximum number of iterations = 250
 Relative Function Convergence has been set to: 1e-008
 Parameter Convergence has been set to: 1e-008

                  Default Initial Parameter Values
                     Background =   0.00503997
                        Beta(1) =     0.191539
```

Beta(2) = 91.9968

Asymptotic Correlation Matrix of Parameter Estimates

(*** The model parameter(s) -Beta(1)
have been estimated at a boundary point, or have been specified by the user,
and do not appear in the correlation matrix)

	Background	Beta(2)
Background	1	-0.37
Beta(2)	-0.37	1

Parameter Estimates

Variable	Estimate	Std. Err.	95.0% Wald Confidence Interval Lower Conf. Limit	Upper Conf. Limit
Background	0.00571347	*	*	*
Beta(1)	0	*	*	*
Beta(2)	96.3581	*	*	*

* - Indicates that this value is not calculated.

Analysis of Deviance Table

Model	Log(likelihood)	# Param's	Deviance	Test d.f.	P-value
Full model	-54.9964	6			
Fitted model	-56.2582	2	2.52365	4	0.6404
Reduced model	-77.5815	1	45.1702	5	<.0001

AIC: 116.516

Goodness of Fit

Dose	Est._Prob.	Expected	Observed	Size	Scaled Residual
0.0000	0.0057	0.840	1	147	0.175
0.0004	0.0057	0.436	1	76	0.858
0.0014	0.0059	0.430	0	73	-0.658
0.0045	0.0077	0.514	0	67	-0.720
0.0137	0.0235	1.671	2	71	0.258
0.0485	0.2074	14.101	14	68	-0.030

Chi^2 = 1.78 d.f. = 4 P-value = 0.7755

Benchmark Dose Computation

Specified effect = 0.1

Risk Type = Extra risk

Confidence level = 0.95

BMD = 0.033067

BMDL = 0.0258907

BMDU = 0.0419928

Taken together, (0.0258907, 0.0419928) is a 90 % two-sided confidence interval for the BMD

BMDS (version 1.4.1) output for Zymbal gland tumors in F344 female rats employing administered dose as a dose metric

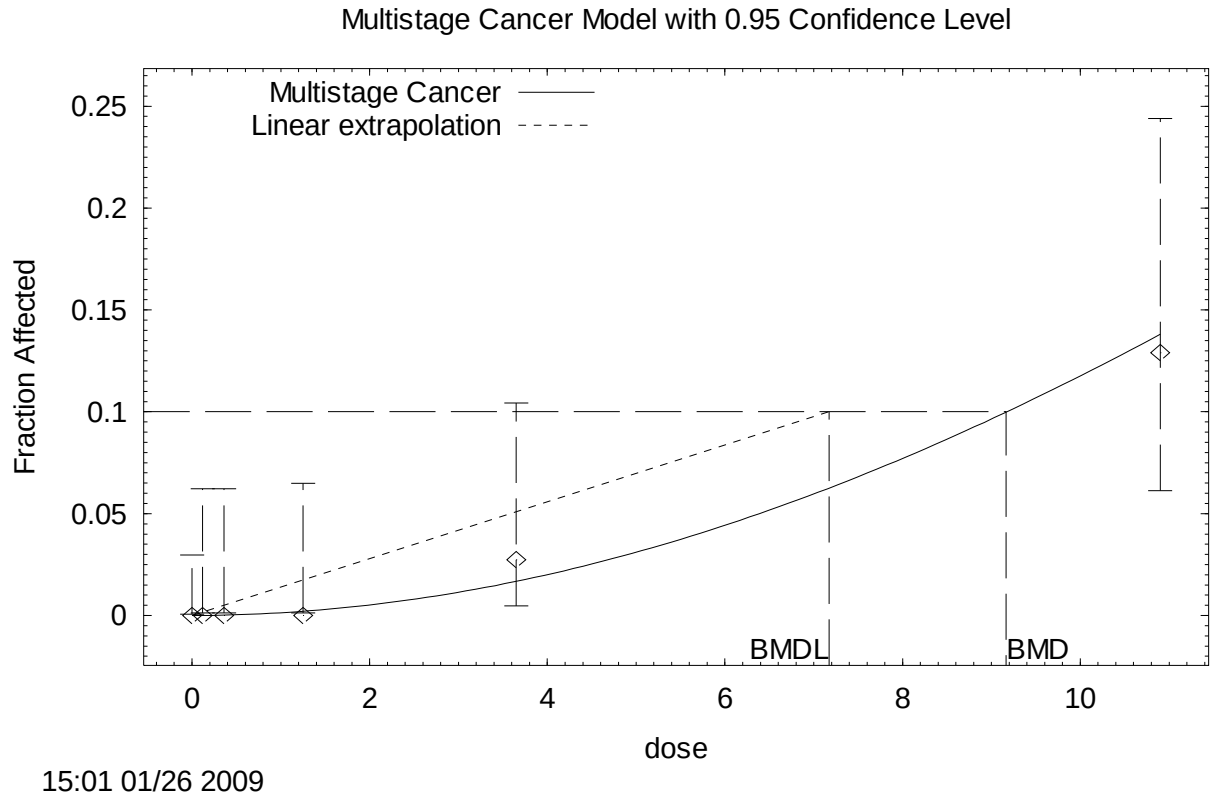


```
 ======================================================================
         Multistage Cancer Model. (Version: 1.5;  Date: 02/20/2007)
         Input Data File: M:\ACN DOSE-RESPONSE MODELING\CANCER\ORAL\F344_FEMALE_ZYMBAL_DW.(d)
         Gnuplot Plotting File:  M:\ACN DOSE-RESPONSE
MODELING\CANCER\ORAL\F344_FEMALE_ZYMBAL_DW.plt
                                                    Mon Jan 26 15:01:22 2009
 ======================================================================

 BMDS MODEL RUN
~~~~~~~~~~~~~~~~~~~~~~~~~~~~~~~~~~~~~~~~~~~~~~~~~~~~~~~~~~~~~~~~~~~~~~~~~~~~

   The form of the probability function is:

   P[response] = background + (1-background)*[1-EXP(
                -beta1*dose^1-beta2*dose^2)]

   The parameter betas are restricted to be positive


   Dependent variable = Response
   Independent variable = Dose

 Total number of observations = 6
 Total number of records with missing values = 0
 Total number of parameters in model = 3
 Total number of specified parameters = 0
 Degree of polynomial = 2


 Maximum number of iterations = 250
 Relative Function Convergence has been set to: 1e-008
 Parameter Convergence has been set to: 1e-008
```

Default Initial Parameter Values
Background = 0
Beta(1) = 0.00476273
Beta(2) = 0.000742952

Asymptotic Correlation Matrix of Parameter Estimates

(*** The model parameter(s) -Background
have been estimated at a boundary point, or have been specified by the user,
and do not appear in the correlation matrix)

	Beta(1)	Beta(2)
Beta(1)	1	-0.95
Beta(2)	-0.95	1

Parameter Estimates

Variable	Estimate	Std. Err.	95.0% Wald Confidence Interval Lower Conf. Limit	Upper Conf. Limit
Background	0	*	*	*
Beta(1)	0.000111429	*	*	*
Beta(2)	0.00124232	*	*	*

* - Indicates that this value is not calculated.

Analysis of Deviance Table

Model	Log(likelihood)	# Param's	Deviance	Test d.f.	P-value
Full model	-33.0086	6			
Fitted model	-33.4019	2	0.786523	4	0.9402
Reduced model	-49.1799	1	32.3425	5	<.0001

AIC: 70.8038

Goodness of Fit

Dose	Est._Prob.	Expected	Observed	Size	Scaled Residual
0.0000	0.0000	0.000	0	157	0.000
0.1200	0.0000	0.002	0	73	-0.048
0.3600	0.0002	0.015	0	73	-0.121
1.2500	0.0021	0.145	0	70	-0.382
3.6500	0.0168	1.227	2	73	0.703
10.9000	0.1383	8.573	8	62	-0.211

Chi^2 = 0.70 d.f. = 4 P-value = 0.9511

```
   Benchmark Dose Computation

Specified effect =            0.1

Risk Type        =      Extra risk

Confidence level =           0.95

              BMD =        9.16446

             BMDL =        7.17181

             BMDU =        13.5889

Taken together, (7.17181, 13.5889) is a 90     % two-sided confidence
interval for the BMD

Multistage Cancer Slope Factor =     0.0139435
```

BMDS (version 1.4.1) output for Zymbal gland tumors in F344 female rats employing CEO in blood as an internal dose metric

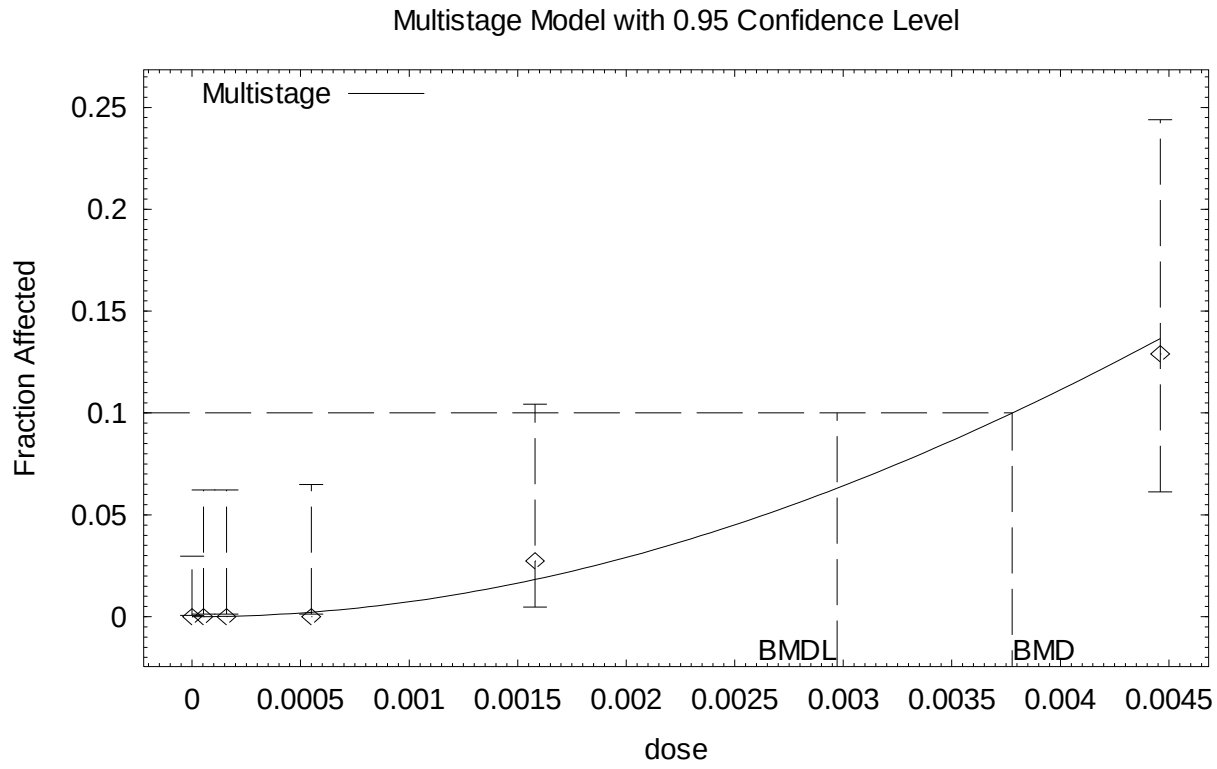


```
 ======================================================================
         Multistage Model. (Version: 2.8;  Date: 02/20/2007)
         Input Data File: G:\ACN DOSE-RESPONSE
MODELING\CANCER\ORAL\F344_FEMALE_ZYMBAL_BLOOD_CEO.(d)
         Gnuplot Plotting File:  G:\ACN DOSE-RESPONSE
MODELING\CANCER\ORAL\F344_FEMALE_ZYMBAL_BLOOD_CEO.plt
                                                  Thu Sep 27 15:13:27 2007
 ======================================================================

 BMDS MODEL RUN
~~~~~~~~~~~~~~~~~~~~~~~~~~~~~~~~~~~~~~~~~~~~~~~~~~~~~~~~~~~~~~~~~~~~~~~~

   The form of the probability function is:

   P[response] = background + (1-background)*[1-EXP(
                -beta1*dose^1-beta2*dose^2)]

   The parameter betas are restricted to be positive


   Dependent variable = Response
   Independent variable = Dose

 Total number of observations = 6
 Total number of records with missing values = 0
 Total number of parameters in model = 3
 Total number of specified parameters = 0
 Degree of polynomial = 2


 Maximum number of iterations = 250
 Relative Function Convergence has been set to: 1e-008
 Parameter Convergence has been set to: 1e-008
```

Default Initial Parameter Values
Background = 0
Beta(1) = 9.4165
Beta(2) = 4928.95

Asymptotic Correlation Matrix of Parameter Estimates

(*** The model parameter(s) -Background -Beta(1)
have been estimated at a boundary point, or have been specified by the user,
and do not appear in the correlation matrix)

	Beta(2)
Beta(2)	1

Parameter Estimates

Variable	Estimate	Std. Err.	95.0% Wald Confidence Interval Lower Conf. Limit	Upper Conf. Limit
Background	0	*	*	*
Beta(1)	0	*	*	*
Beta(2)	7382.1	*	*	*

* - Indicates that this value is not calculated.

Analysis of Deviance Table

Model	Log(likelihood)	# Param's	Deviance	Test d.f.	P-value
Full model	-33.0086	6			
Fitted model	-33.3423	1	0.667255	5	0.9847
Reduced model	-49.1799	1	32.3425	5	<.0001

AIC: 68.6845

Goodness of Fit

Dose	Est._Prob.	Expected	Observed	Size	Scaled Residual
0.0000	0.0000	0.000	0	157	0.000
0.0001	0.0000	0.002	0	73	-0.039
0.0002	0.0002	0.014	0	73	-0.117
0.0005	0.0022	0.156	0	70	-0.395
0.0016	0.0183	1.333	2	73	0.583
0.0045	0.1366	8.467	8	62	-0.173

Chi^2 = 0.54 d.f. = 5 P-value = 0.9905

Benchmark Dose Computation

Specified effect = 0.1

Risk Type = Extra risk

Confidence level = 0.95

BMD = 0.00377789

BMDL = 0.00297198

BMDU = 0.00541558

Taken together, (0.00297198, 0.00541558) is a 90 % two-sided confidence interval for the BMD

BMDS (version 1.4.1) output for Zymbal gland tumors in F344 female rats employing AN in blood as an internal dose metric

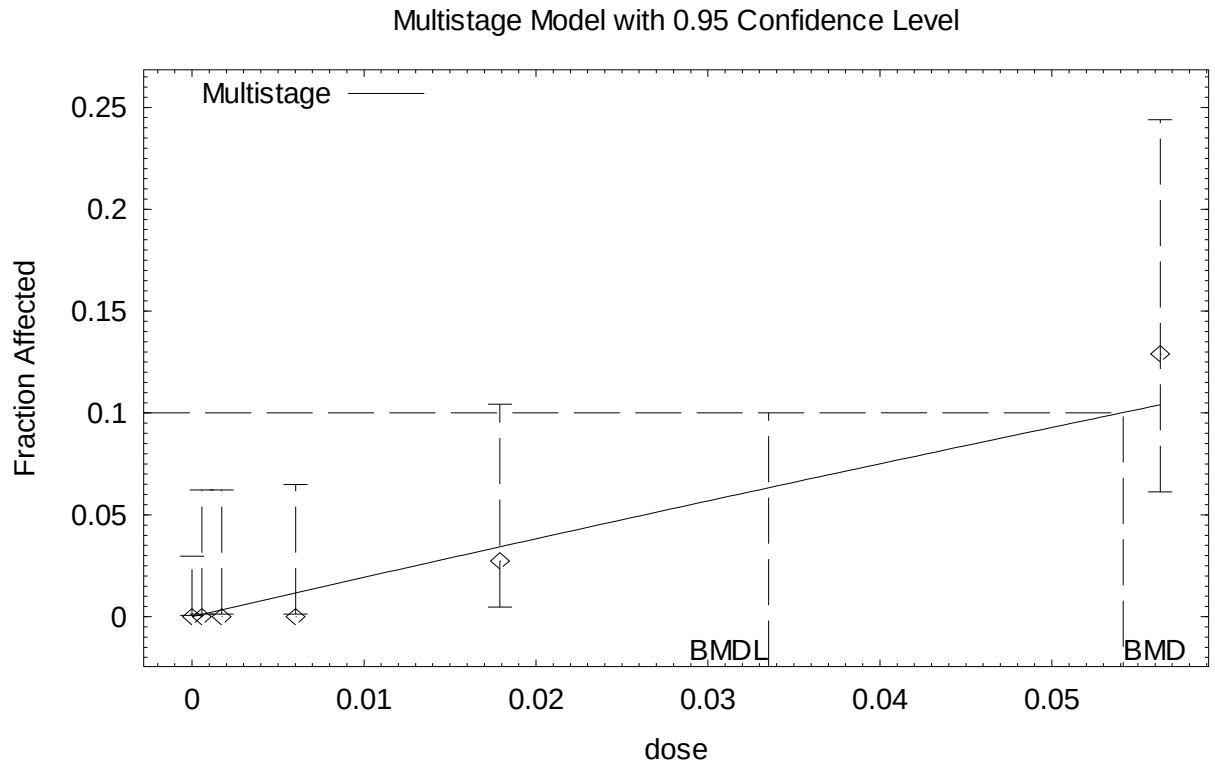


```
 ======================================================================
         Multistage Model. (Version: 2.8;  Date: 02/20/2007)
         Input Data File: G:\ACN DOSE-RESPONSE
MODELING\CANCER\ORAL\F344_FEMALE_ZYMBAL_BLOOD_AN.(d)
         Gnuplot Plotting File:  G:\ACN DOSE-RESPONSE
MODELING\CANCER\ORAL\F344_FEMALE_ZYMBAL_BLOOD_AN.plt
                                                  Thu Sep 27 11:37:11 2007
 ======================================================================

 BMDS MODEL RUN
~~~~~~~~~~~~~~~~~~~~~~~~~~~~~~~~~~~~~~~~~~~~~~~~~~~~~~~~~~~~~~~~~~~~~~~~

   The form of the probability function is:

   P[response] = background + (1-background)*[1-EXP(
                -beta1*dose^1)]

   The parameter betas are restricted to be positive


   Dependent variable = Response
   Independent variable = Dose

 Total number of observations = 6
 Total number of records with missing values = 0
 Total number of parameters in model = 2
 Total number of specified parameters = 0
 Degree of polynomial = 1


 Maximum number of iterations = 250
 Relative Function Convergence has been set to: 1e-008
 Parameter Convergence has been set to: 1e-008
```

Default Initial Parameter Values
Background = 0
Beta(1) = 2.5025

Asymptotic Correlation Matrix of Parameter Estimates

(*** The model parameter(s) -Background
have been estimated at a boundary point, or have been specified by the user,
and do not appear in the correlation matrix)

	Beta(1)
Beta(1)	1

Parameter Estimates

Variable	Estimate	Std. Err.	95.0% Wald Confidence Interval Lower Conf. Limit	Upper Conf. Limit
Background	0	*	*	*
Beta(1)	1.94599	*	*	*

* - Indicates that this value is not calculated.

Analysis of Deviance Table

Model	Log(likelihood)	# Param's	Deviance	Test d.f.	P-value
Full model	-33.0086	6			
Fitted model	-34.4088	1	2.80031	5	0.7307
Reduced model	-49.1799	1	32.3425	5	<.0001

AIC: 70.8176

Goodness of Fit

Dose	Est._Prob.	Expected	Observed	Size	Scaled Residual
0.0000	0.0000	0.000	0	157	0.000
0.0006	0.0011	0.081	0	73	-0.285
0.0017	0.0033	0.244	0	73	-0.495
0.0060	0.0116	0.815	0	70	-0.908
0.0179	0.0342	2.499	2	73	-0.321
0.0563	0.1038	6.434	8	62	0.652

Chi^2 = 1.68 d.f. = 5 P-value = 0.8915

Benchmark Dose Computation

Specified effect = 0.1

Risk Type = Extra risk

Confidence level = 0.95

BMD = 0.0541423

BMDL = 0.0335374

BMDU = 0.0957005

Taken together, (0.0335374, 0.0957005) is a 90 % two-sided confidence
interval for the BMD

Tumor Site: Mammary Gland (Johannsen and Levinskas, 2002b; Biodynamics, 1980b)

Table B-25. Incidence of mammary gland tumors in F344 rats exposed to AN in drinking water for 2 years

Sex	Administered animal dose (ppm in drinking water)	Equivalent administered animal dose[a] (mg/kg-d)	Predicted internal dose metrics		Incidence of mammary gland tumors[b]
			AN-AUC in blood (mg/L)	CEO-AUC in blood (mg/L)	
Female	0	0	0	0	14/156 (9%)
	1	0.12	5.73×10^{-4}	5.32×10^{-5}	8/80 (10%)
	3	0.36	1.72×10^{-3}	1.59×10^{-4}	6/80 (8%)
	10	1.25	6.02×10^{-3}	5.49×10^{-4}	9/80 (11%)
	30	3.65	1.79×10^{-2}	1.58×10^{-3}	12/80 (15%)
	100	10.90	5.63×10^{-2}	4.46×10^{-3}	14/73 (19%)

[a]Administered doses were averages calculated by the study authors based on animal BW and drinking water intake.
[b]Incidences for F344 rats do not include animals from the 6- and 12-mo sacrifices and were further adjusted to exclude (from the denominators) rats that died between 0 and 12 mos in the study.

Table B-26. Summary of BMD modeling results based on incidence of mammary gland tumors in F344 rats exposed to AN in drinking water for 2 years

Dose metric	Best-fit model[a]	χ^2 *p*-value[b]	AIC	BMD_{10}[c]	$BMDL_{10}$[d]
Females					
Administered dose	1°MS	0.94	388.94	8.73 mg/kg-d	4.77 mg/kg-d
CEO	1°MS	0.94	388.88	3.58×10^{-3} mg/L	1.97×10^{-3} mg/L
AN	1°MS	0.93	389.00	4.51×10^{-2} mg/L	2.45×10^{-2} mg/L

[a]Dose-response models were fit using BMDS, version 1.4.1. "1°MS" indicates a one-stage multistage model.
[b]*p* value from the χ^2 goodness of fit test. Values <0.1 indicate a significant lack of fit.
[c]BMD_{10} = BMD at 10% extra risk.
[d]$BMDL_{10}$ = 95% lower confidence limit on the BMD at 10% extra risk.

BMDS (version 1.4.1) output for mammary gland tumors in F344 female rats employing administered dose as a dose metric

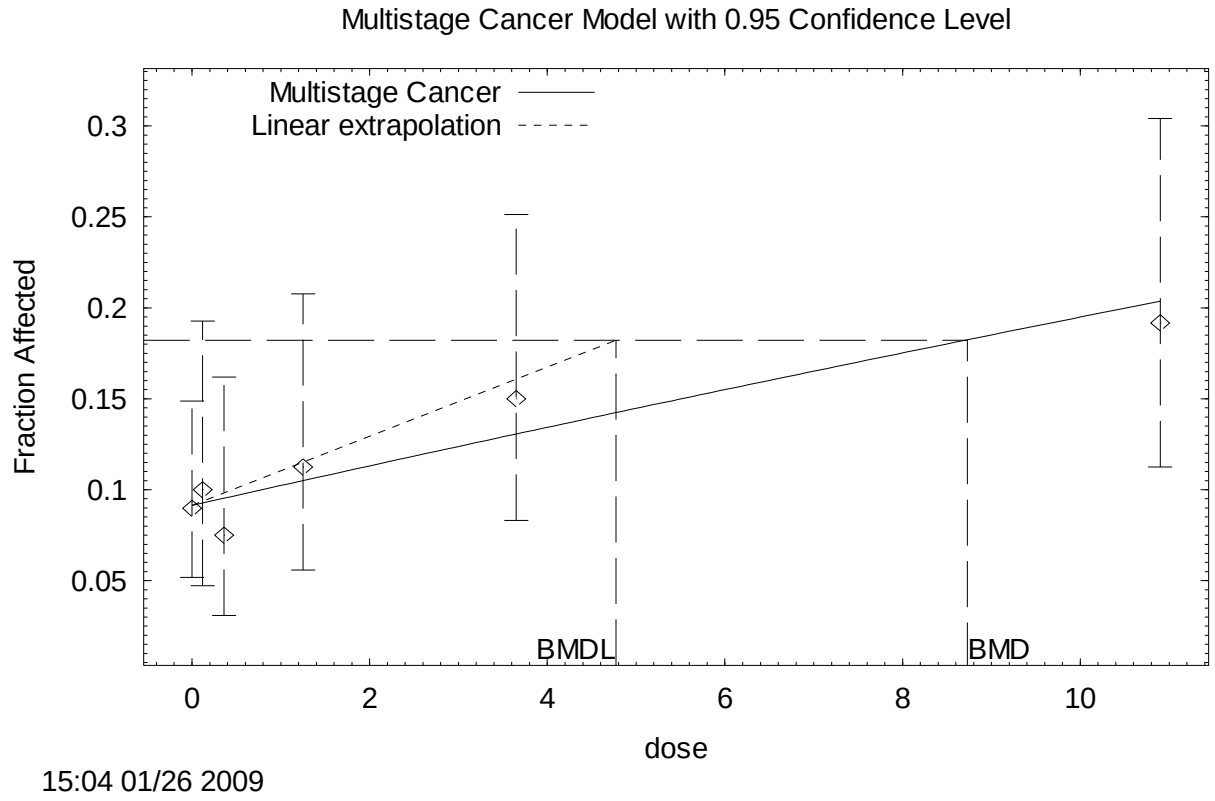


```
 ================================================================
         Multistage Cancer Model. (Version: 1.5;  Date: 02/20/2007)
         Input Data File: M:\ACN DOSE-RESPONSE MODELING\CANCER\ORAL\F344_FEMALE_MAMMARY_DW.(d)
         Gnuplot Plotting File:  M:\ACN DOSE-RESPONSE
MODELING\CANCER\ORAL\F344_FEMALE_MAMMARY_DW.plt
                                                    Mon Jan 26 15:04:09 2009
 ================================================================

 BMDS MODEL RUN
~~~~~~~~~~~~~~~~~~~~~~~~~~~~~~~~~~~~~~~~~~~~~~~~~~~~~~~~~~~~~~~~~~~~~~~~

   The form of the probability function is:

   P[response] = background + (1-background)*[1-EXP(
                -beta1*dose^1)]

   The parameter betas are restricted to be positive


   Dependent variable = Response
   Independent variable = Dose

 Total number of observations = 6
 Total number of records with missing values = 0
 Total number of parameters in model = 2
 Total number of specified parameters = 0
 Degree of polynomial = 1


 Maximum number of iterations = 250
 Relative Function Convergence has been set to: 1e-008
 Parameter Convergence has been set to: 1e-008
```

Default Initial Parameter Values
Background = 0.093497
Beta(1) = 0.0112514

Asymptotic Correlation Matrix of Parameter Estimates

	Background	Beta(1)
Background	1	-0.52
Beta(1)	-0.52	1

Parameter Estimates

Variable	Estimate	Std. Err.	95.0% Wald Confidence Interval Lower Conf. Limit	Upper Conf. Limit
Background	0.0913697	*	*	*
Beta(1)	0.0120689	*	*	*

* - Indicates that this value is not calculated.

Analysis of Deviance Table

Model	Log(likelihood)	# Param's	Deviance	Test d.f.	P-value
Full model	-192.056	6			
Fitted model	-192.471	2	0.830208	4	0.9344
Reduced model	-195.631	1	7.14977	5	0.2097

AIC: 388.943

Goodness of Fit

Dose	Est._Prob.	Expected	Observed	Size	Scaled Residual
0.0000	0.0914	14.254	14	156	-0.070
0.1200	0.0927	7.415	8	80	0.226
0.3600	0.0953	7.625	6	80	-0.619
1.2500	0.1050	8.398	9	80	0.220
3.6500	0.1305	10.442	12	80	0.517
10.9000	0.2034	14.846	14	73	-0.246

Chi^2 = 0.81 d.f. = 4 P-value = 0.9365

```
   Benchmark Dose Computation

Specified effect =            0.1

Risk Type        =      Extra risk

Confidence level =           0.95

              BMD =        8.72994

             BMDL =        4.77219

             BMDU =        27.9615

Taken together, (4.77219, 27.9615) is a 90     % two-sided confidence
interval for the BMD

Multistage Cancer Slope Factor =     0.0209547
```

BMDS (version 1.4.1) output for mammary gland tumors in F344 female rats employing CEO in blood as an internal dose metric

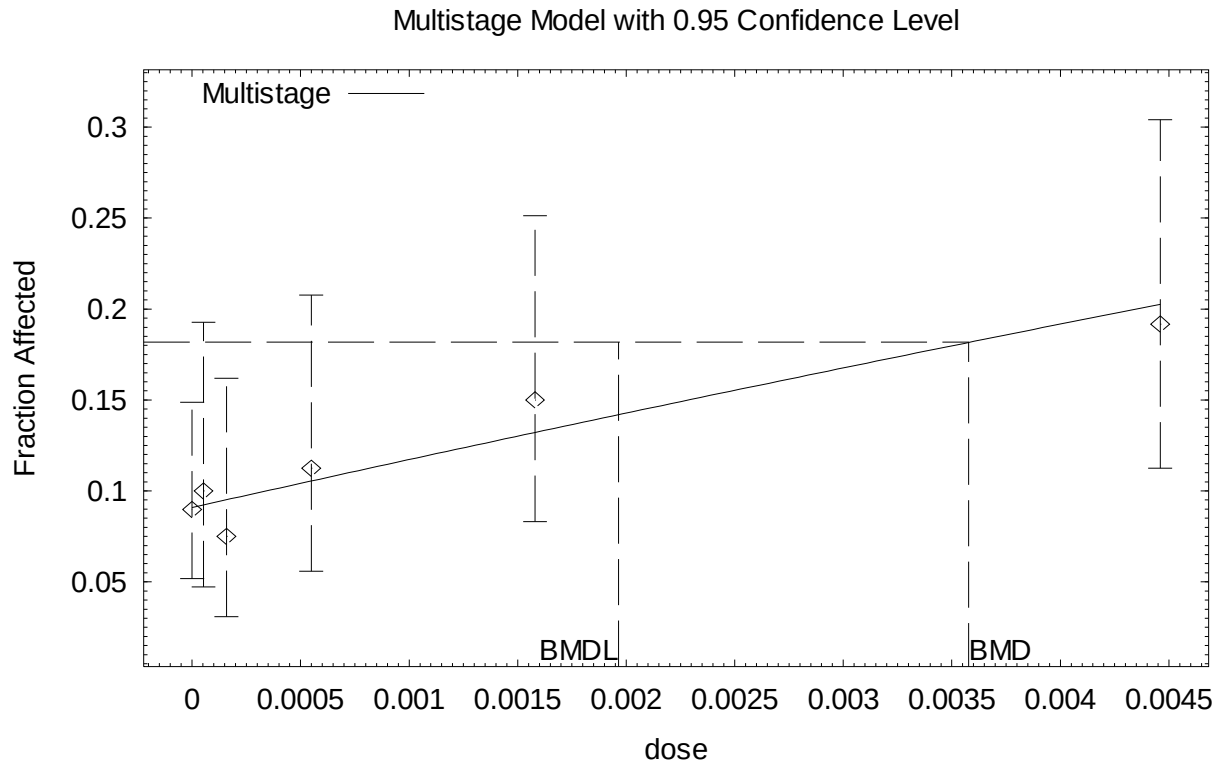


```
 ======================================================================
         Multistage Model. (Version: 2.8;  Date: 02/20/2007)
         Input Data File: G:\ACN DOSE-RESPONSE
MODELING\CANCER\ORAL\F344_FEMALE_MAMMARY_BLOOD_CEO.(d)
         Gnuplot Plotting File:  G:\ACN DOSE-RESPONSE
MODELING\CANCER\ORAL\F344_FEMALE_MAMMARY_BLOOD_CEO.plt
                                                Thu Sep 27 15:16:49 2007
 ======================================================================

 BMDS MODEL RUN
~~~~~~~~~~~~~~~~~~~~~~~~~~~~~~~~~~~~~~~~~~~~~~~~~~~~~~~~~~~~~~~~~~~~~~~~

   The form of the probability function is:

   P[response] = background + (1-background)*[1-EXP(
                -beta1*dose^1)]

   The parameter betas are restricted to be positive


   Dependent variable = Response
   Independent variable = Dose

 Total number of observations = 6
 Total number of records with missing values = 0
 Total number of parameters in model = 2
 Total number of specified parameters = 0
 Degree of polynomial = 1


 Maximum number of iterations = 250
 Relative Function Convergence has been set to: 1e-008
 Parameter Convergence has been set to: 1e-008
```

Default Initial Parameter Values
Background = 0.0927789
Beta(1) = 27.631

Asymptotic Correlation Matrix of Parameter Estimates

	Background	Beta(1)
Background	1	-0.53
Beta(1)	-0.53	1

Parameter Estimates

Variable	Estimate	Std. Err.	95.0% Wald Confidence Interval Lower Conf. Limit	Upper Conf. Limit
Background	0.0908696	*	*	*
Beta(1)	29.4458	*	*	*

* - Indicates that this value is not calculated.

Analysis of Deviance Table

Model	Log(likelihood)	# Param's	Deviance	Test d.f.	P-value
Full model	-192.056	6			
Fitted model	-192.441	2	0.770201	4	0.9424
Reduced model	-195.631	1	7.14977	5	0.2097

AIC: 388.883

Goodness of Fit

Dose	Est._Prob.	Expected	Observed	Size	Scaled Residual
0.0000	0.0909	14.176	14	156	-0.049
0.0001	0.0923	7.383	8	80	0.238
0.0002	0.0951	7.609	6	80	-0.613
0.0005	0.1054	8.436	9	80	0.205
0.0016	0.1322	10.576	12	80	0.470
0.0045	0.2028	14.801	14	73	-0.233

Chi^2 = 0.75 d.f. = 4 P-value = 0.9447

Benchmark Dose Computation

Specified effect = 0.1

Risk Type = Extra risk

Confidence level = 0.95

BMD = 0.00357812

BMDL = 0.00196521

BMDU = 0.011322

Taken together, (0.00196521, 0.011322) is a 90 % two-sided confidence interval for the BMD

BMDS (version 1.4.1) output for mammary gland tumors in F344 female rats employing AN in blood as an internal dose metric

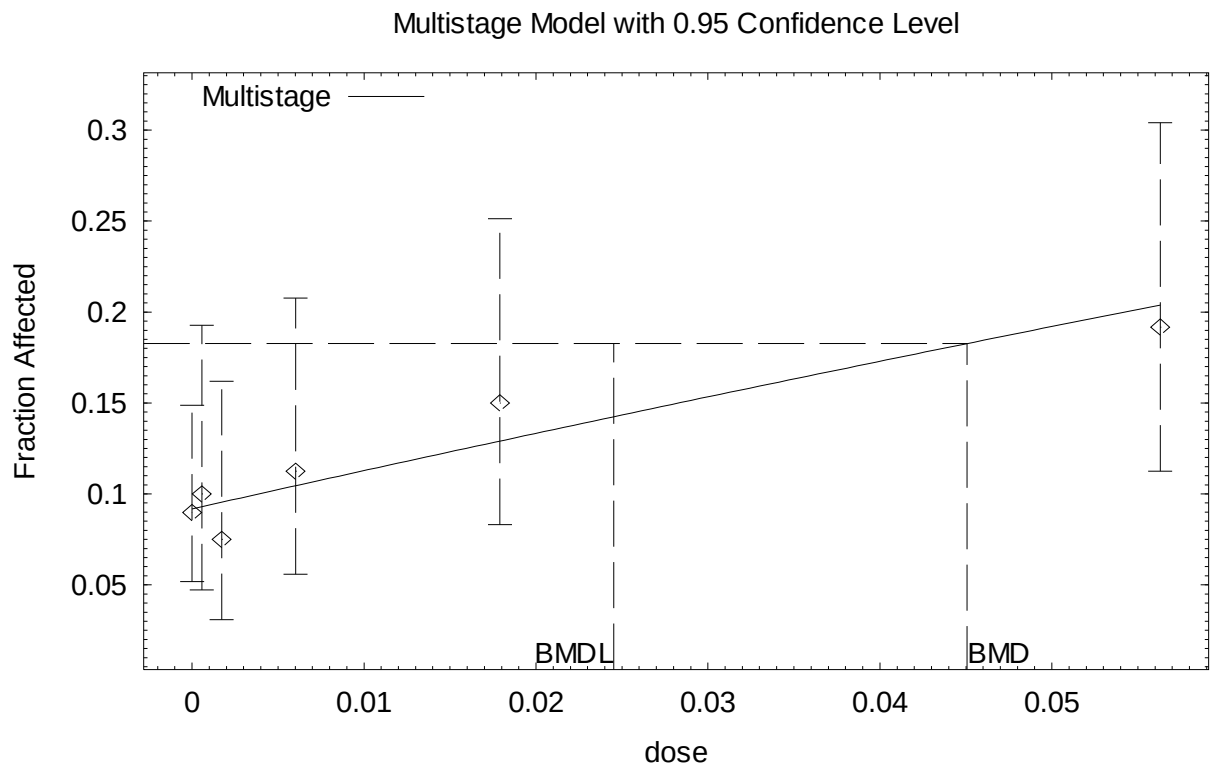


```
 ======================================================================
         Multistage Model. (Version: 2.8;  Date: 02/20/2007)
         Input Data File: G:\ACN DOSE-RESPONSE
MODELING\CANCER\ORAL\F344_FEMALE_MAMMARY_BLOOD_AN.(d)
         Gnuplot Plotting File:  G:\ACN DOSE-RESPONSE
MODELING\CANCER\ORAL\F344_FEMALE_MAMMARY_BLOOD_AN.plt
                                                  Thu Sep 27 11:39:30 2007
 ======================================================================

 BMDS MODEL RUN
~~~~~~~~~~~~~~~~~~~~~~~~~~~~~~~~~~~~~~~~~~~~~~~~~~~~~~~~~~~~~~~~~~~~~~~~

   The form of the probability function is:

   P[response] = background + (1-background)*[1-EXP(
                -beta1*dose^1)]

   The parameter betas are restricted to be positive


   Dependent variable = Response
   Independent variable = Dose

 Total number of observations = 6
 Total number of records with missing values = 0
 Total number of parameters in model = 2
 Total number of specified parameters = 0
 Degree of polynomial = 1


 Maximum number of iterations = 250
 Relative Function Convergence has been set to: 1e-008
 Parameter Convergence has been set to: 1e-008


                  Default Initial Parameter Values
```

Background = 0.0941503
Beta(1) = 2.16751

Asymptotic Correlation Matrix of Parameter Estimates

	Background	Beta(1)
Background	1	-0.52
Beta(1)	-0.52	1

Parameter Estimates

Variable	Estimate	Std. Err.	95.0% Wald Confidence Interval Lower Conf. Limit	Upper Conf. Limit
Background	0.0918429	*	*	*
Beta(1)	2.33757	*	*	*

* - Indicates that this value is not calculated.

Analysis of Deviance Table

Model	Log(likelihood)	# Param's	Deviance	Test d.f.	P-value
Full model	-192.056	6			
Fitted model	-192.5	2	0.887943	4	0.9263
Reduced model	-195.631	1	7.14977	5	0.2097

AIC: 389.001

Goodness of Fit

Dose	Est._Prob.	Expected	Observed	Size	Scaled Residual
0.0000	0.0918	14.327	14	156	-0.091
0.0006	0.0931	7.445	8	80	0.214
0.0017	0.0955	7.639	6	80	-0.624
0.0060	0.1045	8.363	9	80	0.233
0.0179	0.1291	10.325	12	80	0.559
0.0563	0.2038	14.880	14	73	-0.256

Chi^2 = 0.87 d.f. = 4 P-value = 0.9282

Benchmark Dose Computation

Specified effect = 0.1

Risk Type = Extra risk

Confidence level = 0.95

BMD = 0.0450726

BMDL = 0.0245301

BMDU = 0.146059

Taken together, (0.0245301, 0.146059) is a 90 % two-sided confidence interval for the BMD

APPENDIX B-4. CANCER INHALATION DOSE-RESPONSE ASSESSMENT: BMD MODELING RESULTS FOR TUMOR INCIDENCE DATA FROM RATS CHRONICALLY EXPOSED TO AN VIA INHALATION

As summarized in Section 4.6.2, AN is a multisite carcinogen in chronic rodent bioassays. Data from the only available chronic inhalation cancer bioassay with multiple exposure levels to AN were used for dose-response assessment (Dow Chemical Co., 1992a; Quast et al., 1980b). In this study, male and female Sprague-Dawley rats were exposed to AN in air at concentrations of 0, 20, or 80 ppm 6 hours/day, 5 days/week for 2 years. At 80 ppm, significantly increased incidences of CNS tumors (i.e., astrocytomas and glial cell proliferation) and Zymbal's gland tumors were observed in males and females. Also at this concentration, significantly increased incidences of malignant mammary gland tumors (i.e., adenocarcinomas) in females, as well as intestinal and tongue tumors in males, were seen. At 20 ppm, male and female rats exhibited increased incidences (although nonsignificant) of CNS tumors (i.e., astrocytomas and glial cell proliferation) and Zymbal's gland tumors.

In this appendix, detailed results of the dose-response modeling for each of the tumor sites listed above are presented (Tables B-27 through B-36). For each tumor site, first a summary of the dose-response data is presented, followed by a table summarizing the results of the dose-response modeling. Finally, the standard output from EPA's BMDS, version 1.4.1, for the selected dose-response model for each tumor site is presented.

In general, the multistage model was fit to all of the data sets with the BMR set at 0.1 (i.e., 10% extra risk). In fitting this model, successive stages of the multistage model, starting with stage 1 and ending with the stage equal to the number of dose groups minus one, were fit to the tumor incidence data at a particular site for each rat sex employing either administered dose or the internal dose metric CEO in blood. Then, for each dose metric, all stages of the multistage model that did not show a significant lack of fit (i.e., $p > 0.1$) were compared using AIC. The stage of the multistage model with the lowest AIC was selected as the best-fit model. For most tumor sites, the one-stage model exhibited the best fit. For data sets that exhibited a significant lack of fit for all stages of the multistage model, dose groups were dropped (starting with the highest dose group) until an adequate fit was achieved.

Sprague-Dawley Rats (Dow Chemical Co., 1992a; Quast et al., 1980b)

Tumor Site: Intestine

Table B-27. Incidence of intestinal tumors in Sprague-Dawley rats exposed to AN in air for 2 years

Sex	Administered AN concentration (ppm in air)	Predicted CEO-AUC in blood (mg/L)	Incidence of intestinal tumors[a]
Male	0	0	4/96 (4%)
	20	2.17×10^{-3}	3/93 (3%)
	80	8.20×10^{-3}	17/82 (21%)[b]

[a]Incidences for Sprague-Dawley rats do not include animals from the 6- and 12-mo sacrifices and were further adjusted to exclude (from the denominators) rats that died between 0 and 12 mos in the study.
[b]Significantly different from controls ($p < 0.05$) as calculated by the study authors.

Table B-28. Summary of BMD modeling results based on incidence of intestinal tumors in Sprague-Dawley rats exposed to AN in air for 2 years

Dose metric	Best-fit model[a]	χ^2 *p* value[b]	AIC	BMD_{10}[c]	$BMDL_{10}$[d]
Males					
Administered dose	2°MS	0.45	148.05	59.04 ppm	42.68 ppm
CEO	2°MS	0.42	148.13	6.06×10^{-3} mg/L	4.47×10^{-3} mg/L

[a]Dose-response models were fit using BMDS, version 1.4.1. "2°MS" indicates a two-stage multistage model
[b]*p* value from the χ^2 goodness of fit test. Values <0.1 indicate a significant lack of fit.
[c]BMD_{10} = BMD at 10% extra risk.
[d]$BMDL_{10}$ = 95% lower confidence limit on the BMD at 10% extra risk.

BMDS (version 1.4.1) output for intestinal tumors in Sprague-Dawley male rats employing administered dose as a dose metric

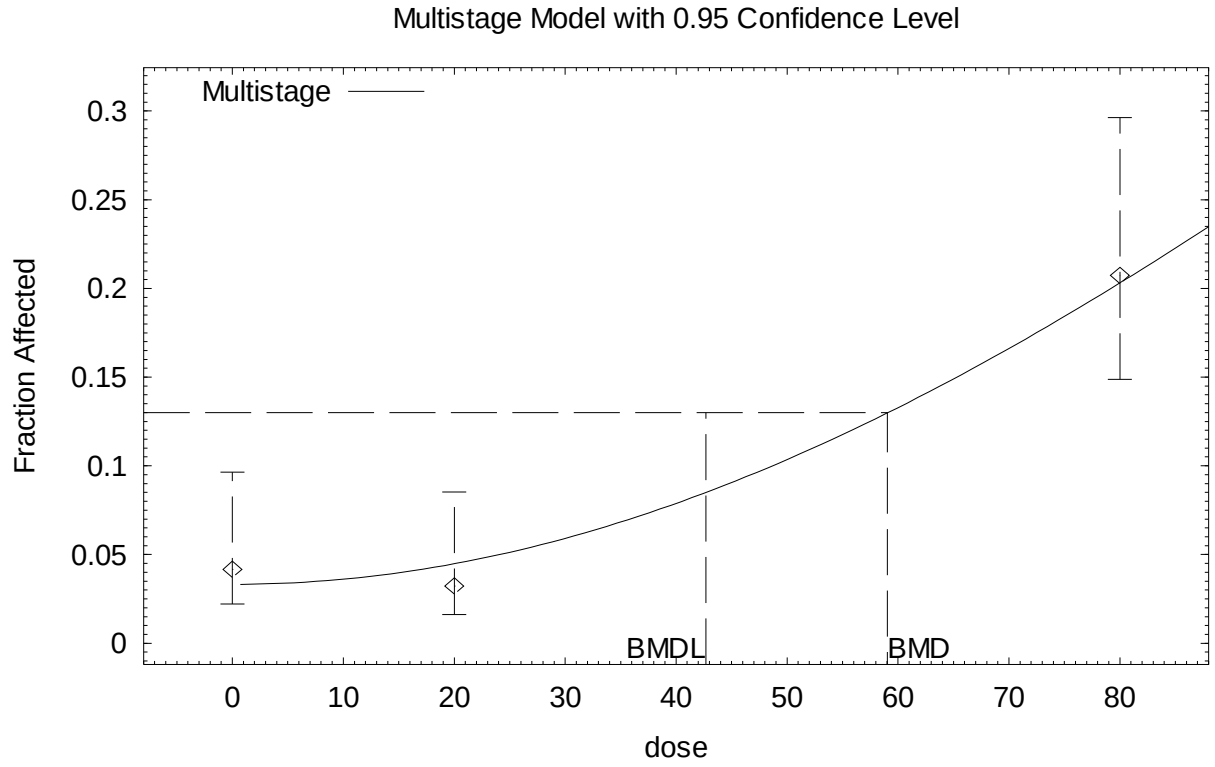


```
    13:10 04/13 2007
 ======================================================================
         Multistage Model. $Revision: 2.1 $ $Date: 2000/08/21 03:38:21 $
         Input Data File: G:\ACN DOSE-RESPONSE
MODELING\CANCER\INHALATION\SD_MALE_INTESTINE_INHALE_PPM.(d)
         Gnuplot Plotting File:  G:\ACN DOSE-RESPONSE
MODELING\CANCER\INHALATION\SD_MALE_INTESTINE_INHALE_PPM.plt
                                                Fri Apr 13 13:10:33 2007
 ======================================================================

 BMDS MODEL RUN
~~~~~~~~~~~~~~~~~~~~~~~~~~~~~~~~~~~~~~~~~~~~~~~~~~~~~~~~~~~~~~~~~~~~~~~~

   The form of the probability function is:

   P[response] = background + (1-background)*[1-EXP(
-beta1*dose^1-beta2*dose^2)]

   The parameter betas are restricted to be positive


   Dependent variable = Response
   Independent variable = Dose

 Total number of observations = 3
 Total number of records with missing values = 0
 Total number of parameters in model = 3
 Total number of specified parameters = 0
 Degree of polynomial = 2


 Maximum number of iterations = 250
 Relative Function Convergence has been set to: 1e-008
 Parameter Convergence has been set to: 1e-008
```

Default Initial Parameter Values
Background = 0.0312892
Beta(1) = 0
Beta(2) = 3.12226e-005

Asymptotic Correlation Matrix of Parameter Estimates

(*** The model parameter(s) -Beta(1)
have been estimated at a boundary point, or have been specified by the user,
and do not appear in the correlation matrix)

	Background	Beta(2)
Background	1	-0.55
Beta(2)	-0.55	1

Parameter Estimates

Variable	Estimate	Std. Err.
Background	0.033209	0.0736218
Beta(1)	0	NA
Beta(2)	3.02304e-005	2.28675e-005

NA - Indicates that this parameter has hit a bound
implied by some inequality constraint and thus
has no standard error.

Analysis of Deviance Table

Model	Log(likelihood)	Deviance	Test DF	P-value
Full model	-71.7319			
Fitted model	-72.0247	0.585523	1	0.4442
Reduced model	-81.082	18.7001	2	<.0001

AIC: 148.049

Goodness of Fit

Dose	Est._Prob.	Expected	Observed	Size	Chi^2 Res.
i: 1					
0.0000	0.0332	3.188	4	96	0.263
i: 2					
20.0000	0.0448	4.169	3	93	-0.294
i: 3					
80.0000	0.2033	16.669	17	82	0.025

Chi-square = 0.57 DF = 1 P-value = 0.4521

Benchmark Dose Computation

Specified effect = 0.1

Risk Type = Extra risk

Confidence level = 0.95

BMD = 59.036

BMDL = 42.6779

BMDS (version 1.4.1) output for intestinal tumors in Sprague-Dawley male rats employing CEO in blood as an internal dose metric

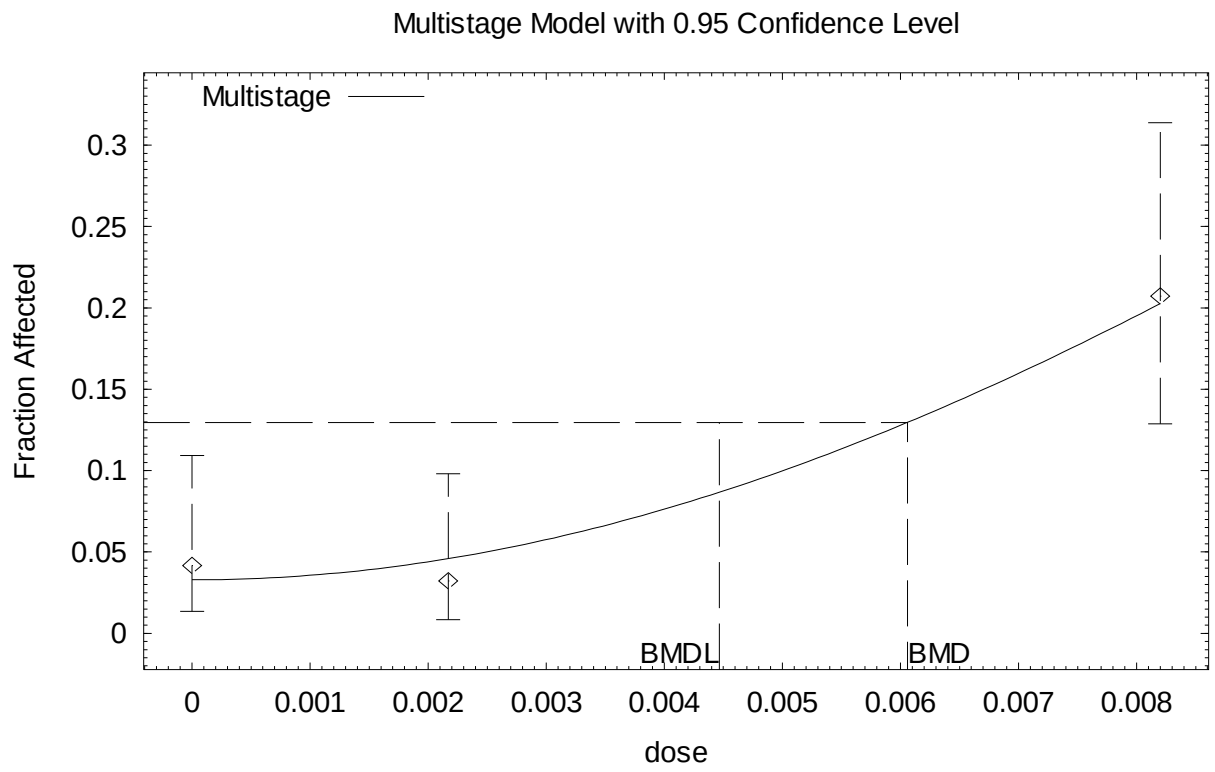


```
 ======================================================================
         Multistage Model. (Version: 2.8;  Date: 02/20/2007)
         Input Data File: G:\ACN DOSE-RESPONSE
MODELING\CANCER\INHALATION\SD_MALE_INTESTINE_INHALE_BLOOD_CEO.(d)
         Gnuplot Plotting File:  G:\ACN DOSE-RESPONSE
MODELING\CANCER\INHALATION\SD_MALE_INTESTINE_INHALE_BLOOD_CEO.plt
                                                  Thu Sep 27 15:20:06 2007
 ======================================================================

 BMDS MODEL RUN
~~~~~~~~~~~~~~~~~~~~~~~~~~~~~~~~~~~~~~~~~~~~~~~~~~~~~~~~~~~~~~~~~~~~~~~~

   The form of the probability function is:

   P[response] = background + (1-background)*[1-EXP(
                -beta1*dose^1-beta2*dose^2)]

   The parameter betas are restricted to be positive


   Dependent variable = Response
   Independent variable = Dose

 Total number of observations = 3
 Total number of records with missing values = 0
 Total number of parameters in model = 3
 Total number of specified parameters = 0
 Degree of polynomial = 2


 Maximum number of iterations = 250
 Relative Function Convergence has been set to: 1e-008
 Parameter Convergence has been set to: 1e-008


                  Default Initial Parameter Values
```

```
                    Background =    0.0306135
                       Beta(1) =            0
                       Beta(2) =      2979.81


           Asymptotic Correlation Matrix of Parameter Estimates

           ( *** The model parameter(s)  -Beta(1)
                 have been estimated at a boundary point, or have been specified by the user,
                 and do not appear in the correlation matrix )

             Background      Beta(2)

Background            1        -0.55

   Beta(2)        -0.55            1


                                Parameter Estimates

                                                        95.0% Wald Confidence Interval
      Variable         Estimate        Std. Err.     Lower Conf. Limit   Upper Conf. Limit
     Background        0.0328821           *                *                   *
        Beta(1)                0           *                *                   *
        Beta(2)          2868.6            *                *                   *

* - Indicates that this value is not calculated.


                        Analysis of Deviance Table

       Model      Log(likelihood)  # Param's  Deviance  Test d.f.   P-value
     Full model        -71.7319         3
    Fitted model       -72.0636         2      0.663417      1          0.4154
  Reduced model         -81.082         1       18.7001      2         <.0001

           AIC:         148.127

                                Goodness  of  Fit
                                                                      Scaled
     Dose     Est._Prob.    Expected    Observed     Size       Residual
  ---------------------------------------------------------------------------
    0.0000     0.0329         3.157         4          96        0.483
    0.0022     0.0459         4.265         3          93       -0.627
    0.0082     0.2025        16.609        17          82        0.107

 Chi^2 = 0.64      d.f. = 1        P-value = 0.4246


   Benchmark Dose Computation

Specified effect =           0.1

Risk Type        =      Extra risk

Confidence level =          0.95

              BMD =     0.00606044

             BMDL =       0.004465

             BMDU =     0.00809222

Taken together, (0.004465, 0.00809222) is a 90     % two-sided confidence
interval for the BMD
```

Tumor Site: CNS (Dow Chemical Co., 1992a; Quast et al., 1980b)

Table B-29. Incidence of CNS tumors in Sprague-Dawley rats exposed to AN in air for 2 years

Sex	Administered AN concentration (ppm in air)	Predicted CEO-AUC in blood (mg/L)	Incidence of CNS tumors[a]
Male	0	0	0/96 (0%)
	20	2.17×10^{-3}	4/93 (4%)
	80	8.20×10^{-3}	22/82 (27%)[b]
Female	0	0	0/93 (0%)
	20	2.18×10^{-3}	8/99 (8%)[b]
	80	8.24×10^{-3}	20/89 (22%)[b]

[a]Incidences for Sprague-Dawley rats do not include animals from the 6- and 12-mo sacrifices and were further adjusted to exclude (from the denominators) rats that died between 0 and 12 mos in the study.
[b]Significantly different from controls ($p < 0.05$) as calculated by the study authors.

Table B-30. Summary of BMD modeling results based on incidence of CNS tumors in Sprague-Dawley rats exposed to AN in air for 2 years

Dose metric	Best-fit model[a]	χ^2 *p*-value[b]	AIC	BMD_{10}[c]	$BMDL_{10}$[d]
Males					
Administered dose	1°MS	0.56	131.64	30.22 ppm	22.23 ppm
CEO	1°MS	0.50	131.92	3.14×10^{-3} mg/L	2.31×10^{-3} mg/L
Females					
Administered dose	1°MS	0.80	152.86	30.79 ppm	22.89 ppm
CEO	1°MS	0.87	152.70	3.21×10^{-3} mg/L	2.39×10^{-3} mg/L

[a]Dose-response models were fit using BMDS, version 1.4.1. "1°MS" indicates a one-stage multistage model.
[b]*p* value from the χ^2 goodness of fit test. Values <0.1 indicate a significant lack of fit.
[c]BMD_{10} = BMD at 10% extra risk.
[d]$BMDL_{10}$ = 95% lower confidence limit on the BMD at 10% extra risk.

BMDS (version 1.4.1) output for CNS tumors in Sprague-Dawley male rats employing administered dose as a dose metric

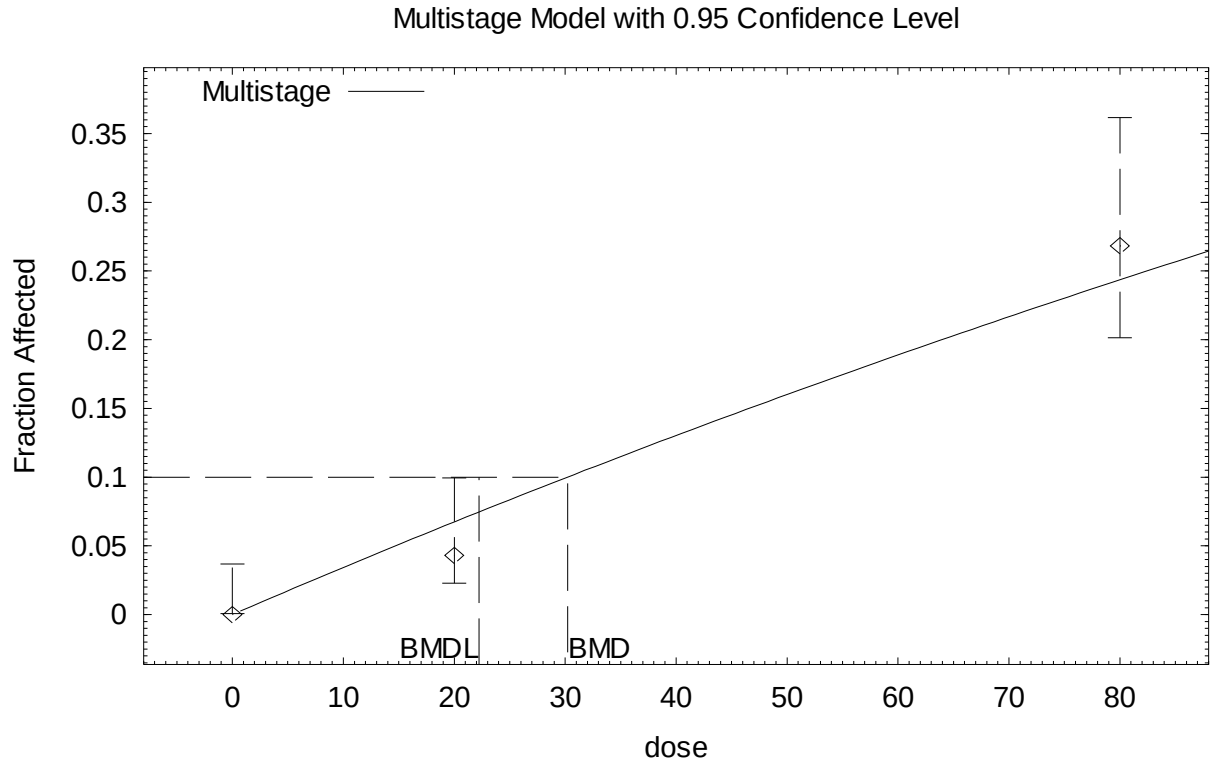


```
13:18 04/13 2007
 ======================================================================
         Multistage Model. $Revision: 2.1 $ $Date: 2000/08/21 03:38:21 $
         Input Data File: G:\ACN DOSE-RESPONSE
MODELING\CANCER\INHALATION\SD_MALE_CNS_INHALE_PPM.(d)
         Gnuplot Plotting File:  G:\ACN DOSE-RESPONSE
MODELING\CANCER\INHALATION\SD_MALE_CNS_INHALE_PPM.plt
                                                Fri Apr 13 13:18:45 2007
 ======================================================================

 BMDS MODEL RUN
~~~~~~~~~~~~~~~~~~~~~~~~~~~~~~~~~~~~~~~~~~~~~~~~~~~~~~~~~~~~~~~~~~~~~~~~

   The form of the probability function is:

   P[response] = background + (1-background)*[1-EXP(
-beta1*dose^1)]

   The parameter betas are restricted to be positive


   Dependent variable = Response
   Independent variable = Dose

 Total number of observations = 3
 Total number of records with missing values = 0
 Total number of parameters in model = 2
 Total number of specified parameters = 0
 Degree of polynomial = 1


 Maximum number of iterations = 250
 Relative Function Convergence has been set to: 1e-008
 Parameter Convergence has been set to: 1e-008
```

```
                 Default Initial Parameter Values
                    Background =            0
                       Beta(1) =   0.00403595


          Asymptotic Correlation Matrix of Parameter Estimates

          ( *** The model parameter(s)  -Background
                have been estimated at a boundary point, or have been specified by the user,
                and do not appear in the correlation matrix )

                    Beta(1)

   Beta(1)            1




                         Parameter Estimates

       Variable           Estimate             Std. Err.
     Background                  0                 NA
        Beta(1)          0.00348587          0.00147454

NA - Indicates that this parameter has hit a bound
     implied by some inequality constraint and thus
     has no standard error.


                       Analysis of Deviance Table

       Model      Log(likelihood)  Deviance  Test DF     P-value
     Full model        -64.1853
   Fitted model        -64.8194       1.26826      2          0.5304
  Reduced model        -85.6554       42.9402      2         <.0001

          AIC:         131.639

                     Goodness  of  Fit

     Dose     Est._Prob.    Expected    Observed     Size     Chi^2 Res.
  ----------------------------------------------------------------------
i: 1
    0.0000     0.0000         0.000         0          96       0.000
i: 2
   20.0000     0.0673         6.263         4          93      -0.387
i: 3
   80.0000     0.2434        19.956        22          82       0.135

 Chi-square =       1.15     DF = 2        P-value = 0.5617


   Benchmark Dose Computation

Specified effect =            0.1

Risk Type        =      Extra risk

Confidence level =           0.95

             BMD =         30.225

            BMDL =        22.2323
```

BMDS (version 1.4.1) output for CNS tumors in Sprague-Dawley male rats employing CEO in blood as an internal dose metric

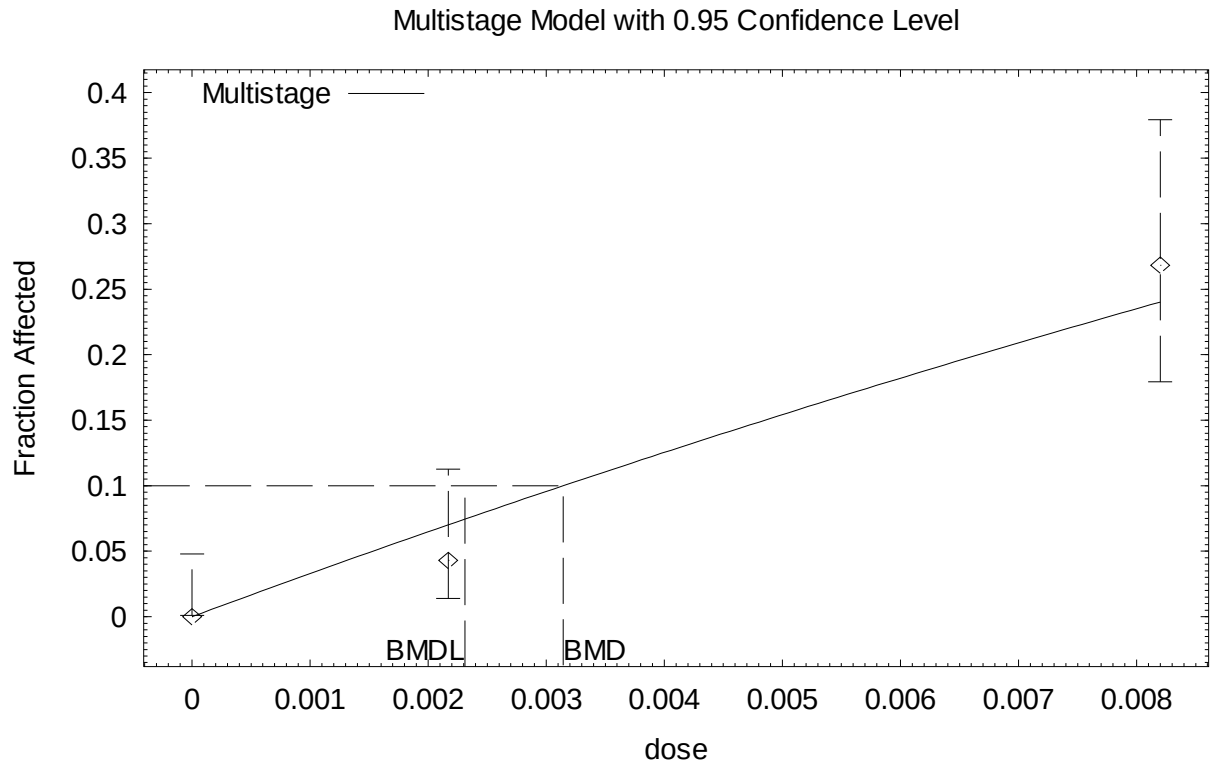


```
 ======================================================================
         Multistage Model. (Version: 2.8;  Date: 02/20/2007)
         Input Data File: G:\ACN DOSE-RESPONSE
MODELING\CANCER\INHALATION\SD_MALE_CNS_INHALE_BLOOD_CEO.(d)
         Gnuplot Plotting File:  G:\ACN DOSE-RESPONSE
MODELING\CANCER\INHALATION\SD_MALE_CNS_INHALE_BLOOD_CEO.plt
                                                  Thu Sep 27 15:22:30 2007
 ======================================================================

 BMDS MODEL RUN
~~~~~~~~~~~~~~~~~~~~~~~~~~~~~~~~~~~~~~~~~~~~~~~~~~~~~~~~~~~~~~~~~~~~~~~~

   The form of the probability function is:

   P[response] = background + (1-background)*[1-EXP(
                -beta1*dose^1)]

   The parameter betas are restricted to be positive


   Dependent variable = Response
   Independent variable = Dose

 Total number of observations = 3
 Total number of records with missing values = 0
 Total number of parameters in model = 2
 Total number of specified parameters = 0
 Degree of polynomial = 1


 Maximum number of iterations = 250
 Relative Function Convergence has been set to: 1e-008
 Parameter Convergence has been set to: 1e-008


                  Default Initial Parameter Values
```

```
                    Background =            0
                       Beta(1) =      39.4721


           Asymptotic Correlation Matrix of Parameter Estimates

           ( *** The model parameter(s)  -Background
                 have been estimated at a boundary point, or have been specified by the user,
                 and do not appear in the correlation matrix )

                Beta(1)

   Beta(1)            1



                                Parameter Estimates

                                                          95.0% Wald Confidence Interval
      Variable         Estimate        Std. Err.     Lower Conf. Limit   Upper Conf. Limit
     Background               0            *                *                   *
        Beta(1)          33.5271            *                *                   *

* - Indicates that this value is not calculated.


                       Analysis of Deviance Table

       Model      Log(likelihood)  # Param's  Deviance  Test d.f.   P-value
     Full model        -64.1853         3
    Fitted model       -64.9602         1       1.54975      2          0.4608
   Reduced model       -85.6554         1       42.9402      2         <.0001

           AIC:          131.92


                                Goodness  of  Fit
                                                                      Scaled
     Dose     Est._Prob.    Expected    Observed     Size       Residual
  ---------------------------------------------------------------------------
    0.0000     0.0000         0.000         0          96        0.000
    0.0022     0.0702         6.525         4          93       -1.025
    0.0082     0.2404        19.711        22          82        0.592

 Chi^2 = 1.40      d.f. = 2        P-value = 0.4963


   Benchmark Dose Computation

Specified effect =            0.1

Risk Type        =      Extra risk

Confidence level =           0.95

              BMD =     0.00314255

             BMDL =     0.00231159

             BMDU =     0.00442253

Taken together, (0.00231159, 0.00442253) is a 90     % two-sided confidence
interval for the BMD
```

BMDS (version 1.4.1) output for CNS tumors in Sprague-Dawley female rats employing administered dose as a dose metric

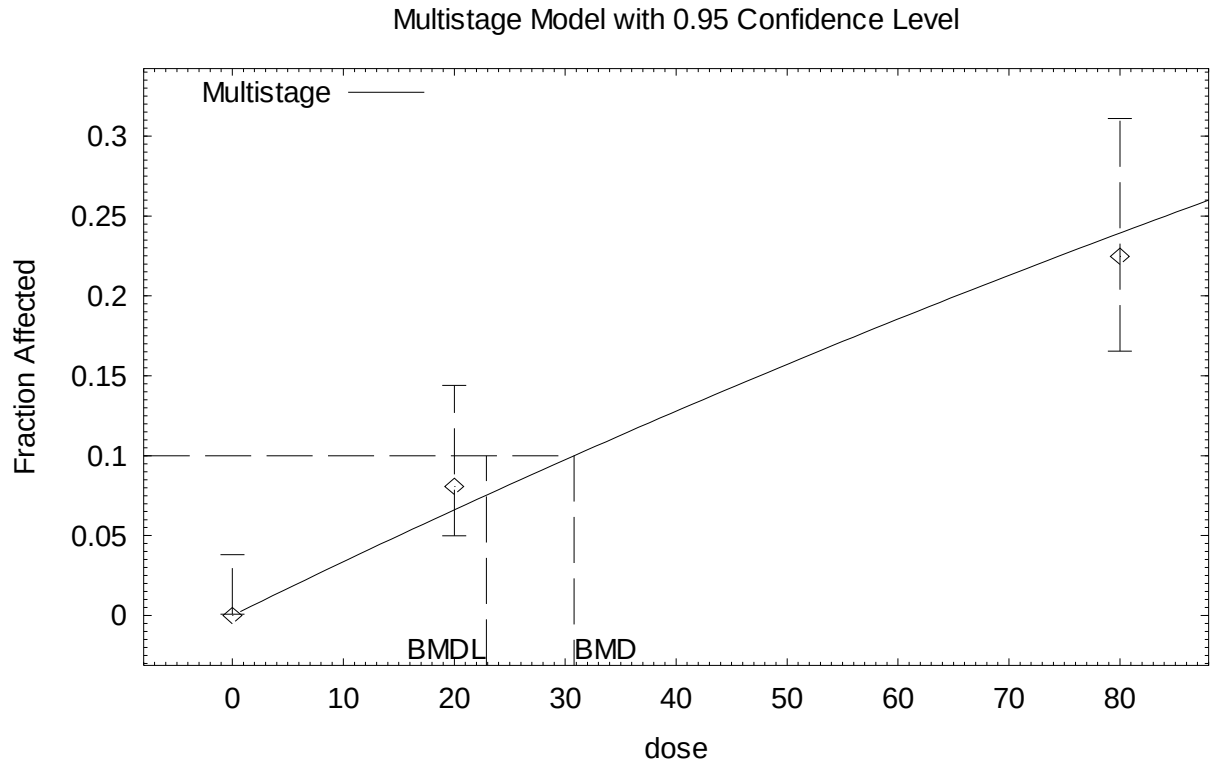


```
 ======================================================================
         Multistage Model. $Revision: 2.1 $ $Date: 2000/08/21 03:38:21 $
         Input Data File: G:\ACN DOSE-RESPONSE
MODELING\CANCER\INHALATION\SD_FEMALE_CNS_INHALE_PPM.(d)
         Gnuplot Plotting File:  G:\ACN DOSE-RESPONSE
MODELING\CANCER\INHALATION\SD_FEMALE_CNS_INHALE_PPM.plt
                                                Fri Apr 13 13:31:42 2007
 ======================================================================

 BMDS MODEL RUN
~~~~~~~~~~~~~~~~~~~~~~~~~~~~~~~~~~~~~~~~~~~~~~~~~~~~~~~~~~~~~~~~~~~~~~~~

   The form of the probability function is:

   P[response] = background + (1-background)*[1-EXP(
-beta1*dose^1)]

   The parameter betas are restricted to be positive


   Dependent variable = Response
   Independent variable = Dose

 Total number of observations = 3
 Total number of records with missing values = 0
 Total number of parameters in model = 2
 Total number of specified parameters = 0
 Degree of polynomial = 1


 Maximum number of iterations = 250
 Relative Function Convergence has been set to: 1e-008
 Parameter Convergence has been set to: 1e-008
```

```
                 Default Initial Parameter Values
                    Background =   0.00947538
                       Beta(1) =   0.00310229


          Asymptotic Correlation Matrix of Parameter Estimates

          ( *** The model parameter(s)  -Background
                have been estimated at a boundary point, or have been specified by the user,
                and do not appear in the correlation matrix )

                Beta(1)

   Beta(1)            1



                         Parameter Estimates

       Variable           Estimate             Std. Err.
     Background                  0                   NA
        Beta(1)          0.00342189          0.00148795

NA - Indicates that this parameter has hit a bound
     implied by some inequality constraint and thus
     has no standard error.

                       Analysis of Deviance Table

       Model      Log(likelihood)  Deviance  Test DF     P-value
     Full model        -75.2138
   Fitted model        -75.4293      0.431111      2          0.8061
  Reduced model        -91.1284       31.8293      2         <.0001

          AIC:         152.859


                     Goodness  of  Fit

     Dose     Est._Prob.    Expected    Observed     Size     Chi^2 Res.
  ----------------------------------------------------------------------
i: 1
    0.0000     0.0000         0.000         0          93       0.000
i: 2
   20.0000     0.0661         6.549         8          99       0.237
i: 3
   80.0000     0.2395        21.314        20          89      -0.081

 Chi-square =       0.45     DF = 2        P-value = 0.7982


   Benchmark Dose Computation

Specified effect =            0.1

Risk Type        =      Extra risk

Confidence level =           0.95

             BMD =        30.7901

            BMDL =        22.8938
```

BMDS (version 1.4.1) output for CNS tumors in Sprague-Dawley female rats employing CEO in blood as an internal dose metric

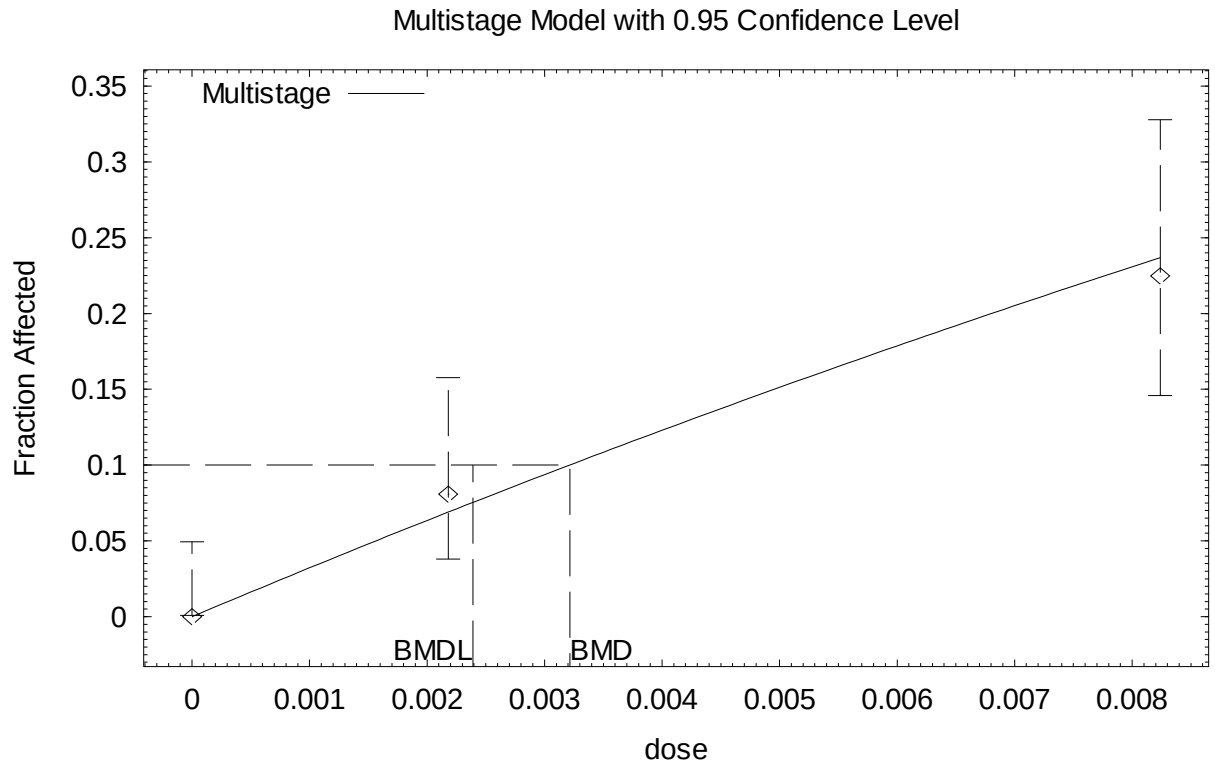


```
 ======================================================================
         Multistage Model. (Version: 2.8;  Date: 02/20/2007)
         Input Data File: G:\ACN DOSE-RESPONSE
MODELING\CANCER\INHALATION\SD_FEMALE_CNS_INHALE_BLOOD_CEO.(d)
         Gnuplot Plotting File:  G:\ACN DOSE-RESPONSE
MODELING\CANCER\INHALATION\SD_FEMALE_CNS_INHALE_BLOOD_CEO.plt
                                                  Thu Sep 27 15:38:25 2007
 ======================================================================

 BMDS MODEL RUN
~~~~~~~~~~~~~~~~~~~~~~~~~~~~~~~~~~~~~~~~~~~~~~~~~~~~~~~~~~~~~~~~~~~~~~~~

   The form of the probability function is:

   P[response] = background + (1-background)*[1-EXP(
                -beta1*dose^1)]

   The parameter betas are restricted to be positive


   Dependent variable = Response
   Independent variable = Dose

 Total number of observations = 3
 Total number of records with missing values = 0
 Total number of parameters in model = 2
 Total number of specified parameters = 0
 Degree of polynomial = 1


 Maximum number of iterations = 250
 Relative Function Convergence has been set to: 1e-008
 Parameter Convergence has been set to: 1e-008
```

Default Initial Parameter Values
Background = 0.00769725
Beta(1) = 30.2917

Asymptotic Correlation Matrix of Parameter Estimates

(*** The model parameter(s) -Background
have been estimated at a boundary point, or have been specified by the user,
and do not appear in the correlation matrix)

	Beta(1)
Beta(1)	1

Parameter Estimates

Variable	Estimate	Std. Err.	95.0% Wald Confidence Interval Lower Conf. Limit	Upper Conf. Limit
Background	0	*	*	*
Beta(1)	32.7805	*	*	*

* - Indicates that this value is not calculated.

Analysis of Deviance Table

Model	Log(likelihood)	# Param's	Deviance	Test d.f.	P-value
Full model	-75.2138	3			
Fitted model	-75.3524	1	0.277338	2	0.8705
Reduced model	-91.1284	1	31.8293	2	<.0001

AIC: 152.705

Goodness of Fit

Dose	Est._Prob.	Expected	Observed	Size	Scaled Residual
0.0000	0.0000	0.000	0	93	0.000
0.0022	0.0690	6.827	8	99	0.465
0.0082	0.2367	21.065	20	89	-0.266

Chi^2 = 0.29 d.f. = 2 P-value = 0.8663

Benchmark Dose Computation

Specified effect = 0.1

Risk Type = Extra risk

Confidence level = 0.95

BMD = 0.00321413

BMDL = 0.00238988

BMDU = 0.00446381

Taken together, (0.00238988, 0.00446381) is a 90 % two-sided confidence interval for the BMD

Tumor Site: Zymbal Gland (Dow Chemical Co., 1992a; Quast et al., 1980b)

Table B-31. Incidence of Zymbal gland tumors in Sprague-Dawley rats exposed to AN in air for 2 years

Sex	Administered AN concentration (ppm in air)	Predicted CEO-AUC in blood (mg/L)	Incidence of Zymbal gland tumors[a]
Male	0	0	2/96 (2%)
	20	2.17×10^{-3}	4/93 (4%)
	80	8.20×10^{-3}	11/82 (13%)[b]
Female	0	0	0/93 (0%)
	20	2.18×10^{-3}	1/98 (1%)
	80	8.24×10^{-3}	11/89 (12%)[b]

[a]Incidences for Sprague-Dawley rats do not include animals from the 6- and 12-mo sacrifices and were further adjusted to exclude (from the denominators) rats that died between 0 and 12 mos in the study.
[b]Significantly different from controls ($p < 0.05$) as calculated by the study authors.

Table B-32. Summary of BMD modeling results based on incidence of Zymbal's gland tumors in Sprague-Dawley rats exposed to AN in air for 2 years

Dose metric	Best-fit model[a]	χ^2 *p*-value[b]	AIC	BMD_{10}[c]	$BMDL_{10}$[d]
Males					
Administered dose	1°MS	0.78	121.17	70.29 ppm	42.53 ppm
CEO	1°MS	0.73	121.21	7.26×10^{-3} mg/L	4.40×10^{-3} mg/L
Females					
Administered dose	1°MS	0.50	81.47	75.70 ppm	48.74 ppm
CEO	1°MS	0.46	81.67	7.90×10^{-3} mg/L	5.09×10^{-3} mg/L

[a]Dose-response models were fit using BMDS, version 1.4.1. "1°MS" indicates a one-stage multistage model.
[b]*p* value from the χ^2 goodness of fit test. Values <0.1 indicate a significant lack of fit.
[c]BMD_{10} = BMD at 10% extra risk.
[d]$BMDL_{10}$ = 95% lower confidence limit on the BMD at 10% extra risk.

BMDS (version 1.4.1) output for Zymbal gland tumors in Sprague-Dawley male rats employing administered dose as a dose metric

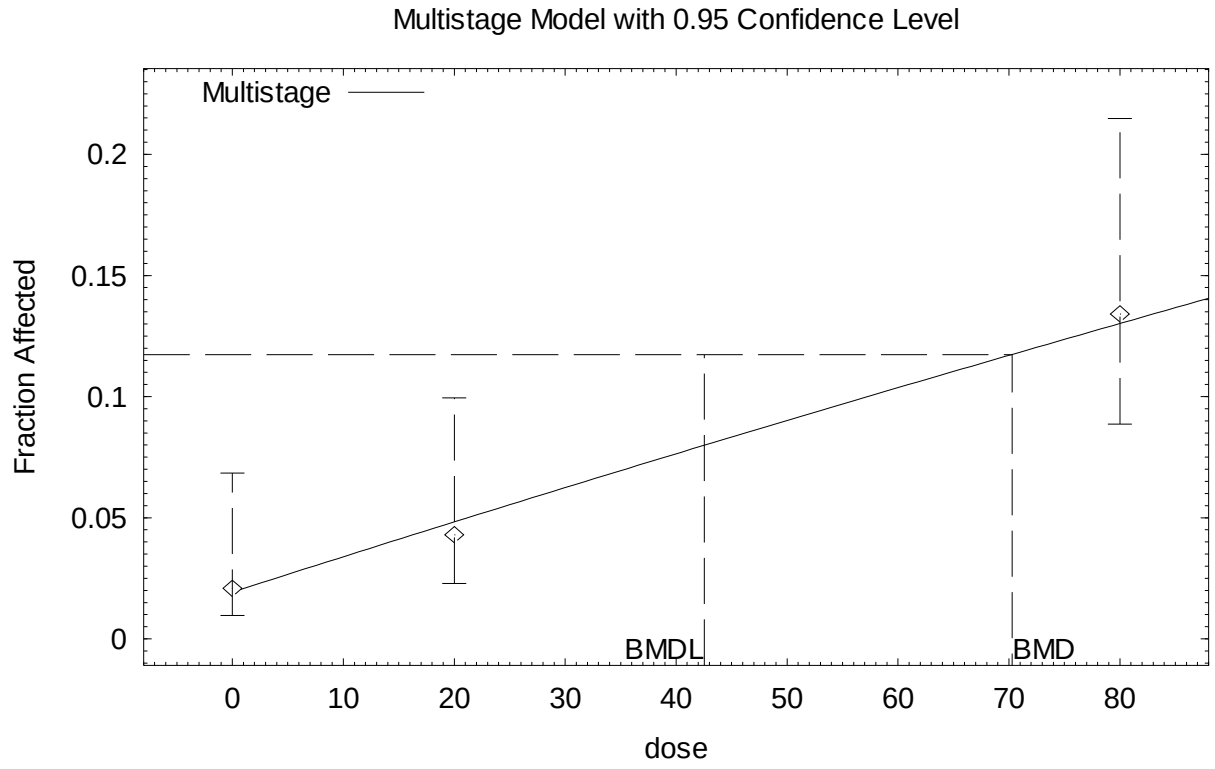

13:22 04/13 2007

```
 ================================================================
         Multistage Model. $Revision: 2.1 $ $Date: 2000/08/21 03:38:21 $
         Input Data File: G:\ACN DOSE-RESPONSE
MODELING\CANCER\INHALATION\SD_MALE_ZYMBAL_INHALE_PPM.(d)
         Gnuplot Plotting File:  G:\ACN DOSE-RESPONSE
MODELING\CANCER\INHALATION\SD_MALE_ZYMBAL_INHALE_PPM.plt
                                                Fri Apr 13 13:22:06 2007
 ================================================================

 BMDS MODEL RUN
~~~~~~~~~~~~~~~~~~~~~~~~~~~~~~~~~~~~~~~~~~~~~~~~~~~~~~~~~~~~~~~~~~~~~~~~

   The form of the probability function is:

   P[response] = background + (1-background)*[1-EXP(
-beta1*dose^1)]

   The parameter betas are restricted to be positive


   Dependent variable = Response
   Independent variable = Dose

 Total number of observations = 3
 Total number of records with missing values = 0
 Total number of parameters in model = 2
 Total number of specified parameters = 0
 Degree of polynomial = 1


 Maximum number of iterations = 250
 Relative Function Convergence has been set to: 1e-008
 Parameter Convergence has been set to: 1e-008
```

Default Initial Parameter Values
Background = 0.0172853
Beta(1) = 0.00156747

Asymptotic Correlation Matrix of Parameter Estimates

	Background	Beta(1)
Background	1	-0.66
Beta(1)	-0.66	1

Parameter Estimates

Variable	Estimate	Std. Err.
Background	0.0193054	0.0819561
Beta(1)	0.00149893	0.00187956

Analysis of Deviance Table

Model	Log(likelihood)	Deviance	Test DF	P-value
Full model	-58.5432			
Fitted model	-58.5838	0.0811571	1	0.7757
Reduced model	-63.5267	9.9669	2	0.00685

AIC: 121.168

Goodness of Fit

Dose	Est._Prob.	Expected	Observed	Size	Chi^2 Res.
i: 1					
0.0000	0.0193	1.853	2	96	0.081
i: 2					
20.0000	0.0483	4.489	4	93	-0.114
i: 3					
80.0000	0.1301	10.670	11	82	0.036

Chi-square = 0.08 DF = 1 P-value = 0.7780

```
   Benchmark Dose Computation

Specified effect =            0.1

Risk Type        =      Extra risk

Confidence level =           0.95

             BMD =        70.2907

            BMDL =        42.5347
```

BMDS (version 1.4.1) output for Zymbal gland tumors in Sprague-Dawley male rats employing CEO in blood as an internal dose metric

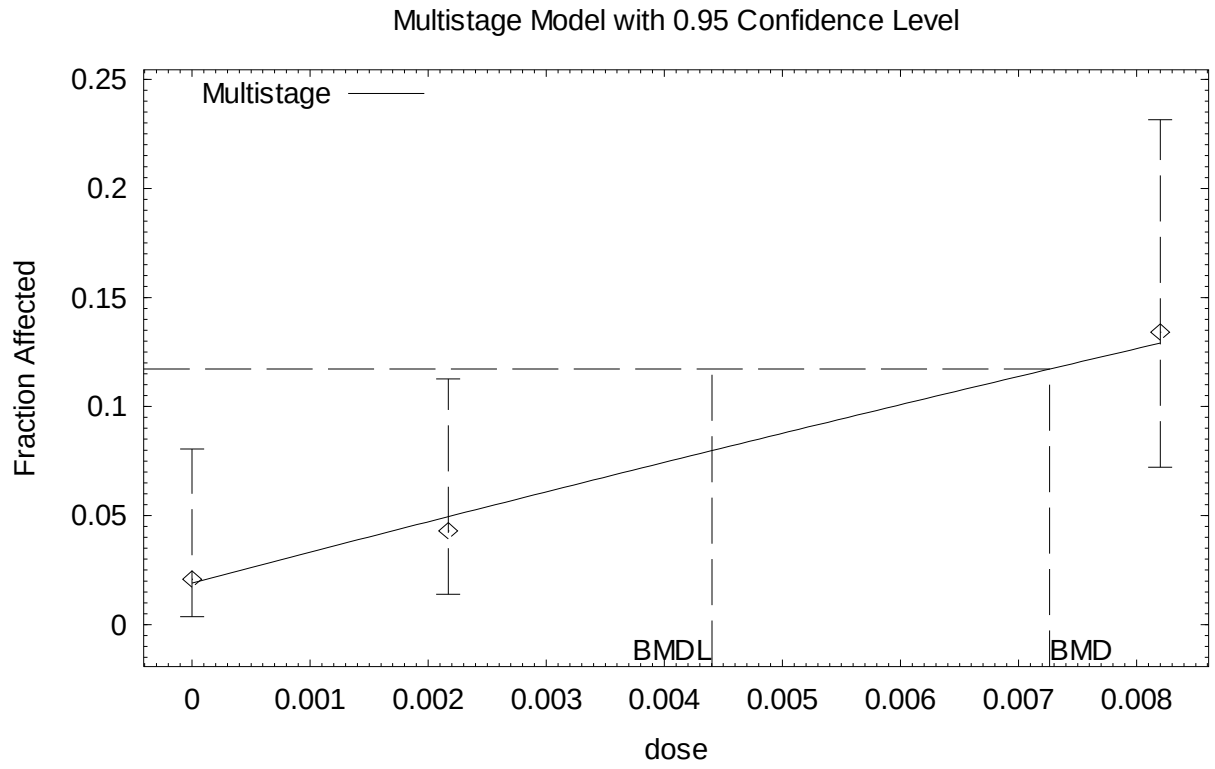


```
 ======================================================================
         Multistage Model. (Version: 2.8;  Date: 02/20/2007)
         Input Data File: G:\ACN DOSE-RESPONSE
MODELING\CANCER\INHALATION\SD_MALE_ZYMBAL_INHALE_BLOOD_CEO.(d)
         Gnuplot Plotting File:  G:\ACN DOSE-RESPONSE
MODELING\CANCER\INHALATION\SD_MALE_ZYMBAL_INHALE_BLOOD_CEO.plt
                                                  Thu Sep 27 15:25:06 2007
 ======================================================================

 BMDS MODEL RUN
~~~~~~~~~~~~~~~~~~~~~~~~~~~~~~~~~~~~~~~~~~~~~~~~~~~~~~~~~~~~~~~~~~~~~~~~

   The form of the probability function is:

   P[response] = background + (1-background)*[1-EXP(
                -beta1*dose^1)]

   The parameter betas are restricted to be positive


   Dependent variable = Response
   Independent variable = Dose

 Total number of observations = 3
 Total number of records with missing values = 0
 Total number of parameters in model = 2
 Total number of specified parameters = 0
 Degree of polynomial = 1


 Maximum number of iterations = 250
 Relative Function Convergence has been set to: 1e-008
 Parameter Convergence has been set to: 1e-008
```

Default Initial Parameter Values
Background = 0.0165179
Beta(1) = 15.3411

Asymptotic Correlation Matrix of Parameter Estimates

	Background	Beta(1)
Background	1	-0.66
Beta(1)	-0.66	1

Parameter Estimates

Variable	Estimate	Std. Err.	95.0% Wald Confidence Interval Lower Conf. Limit	Upper Conf. Limit
Background	0.0190621	*	*	*
Beta(1)	14.5086	*	*	*

* - Indicates that this value is not calculated.

Analysis of Deviance Table

Model	Log(likelihood)	# Param's	Deviance	Test d.f.	P-value
Full model	-58.5432	3			
Fitted model	-58.6032	2	0.120008	1	0.729
Reduced model	-63.5267	1	9.9669	2	0.00685

AIC: 121.206

Goodness of Fit

Dose	Est._Prob.	Expected	Observed	Size	Scaled Residual
0.0000	0.0191	1.830	2	96	0.127
0.0022	0.0495	4.600	4	93	-0.287
0.0082	0.1291	10.586	11	82	0.136

Chi^2 = 0.12 d.f. = 1 P-value = 0.7323

Benchmark Dose Computation

Specified effect = 0.1

Risk Type = Extra risk

Confidence level = 0.95

BMD = 0.00726195

BMDL = 0.00440461

BMDU = 0.0159076

Taken together, (0.00440461, 0.0159076) is a 90 % two-sided confidence interval for the BMD

BMDS (version 1.4.1) output for Zymbal gland tumors in Sprague-Dawley female rats employing administered dose as a dose metric

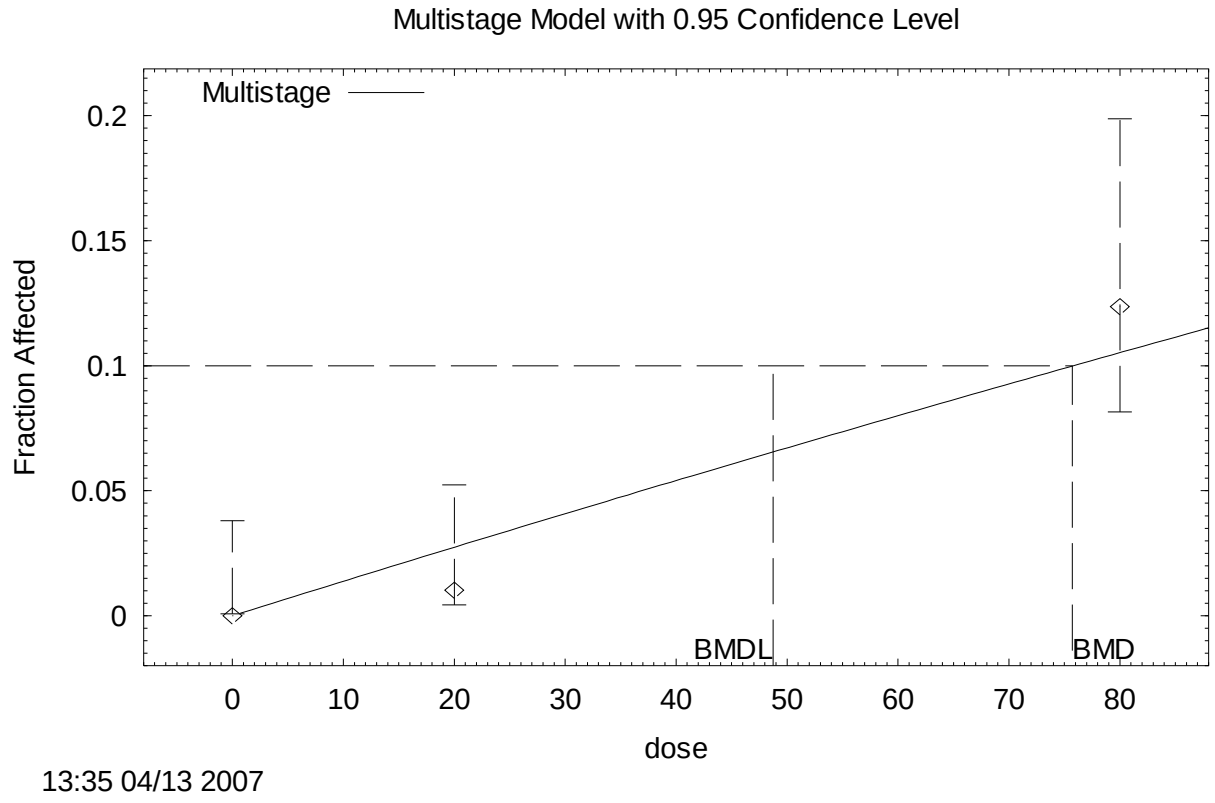


```
 ======================================================================
         Multistage Model. $Revision: 2.1 $ $Date: 2000/08/21 03:38:21 $
         Input Data File: G:\ACN DOSE-RESPONSE
MODELING\CANCER\INHALATION\SD_FEMALE_ZYMBAL_INHALE_PPM.(d)
         Gnuplot Plotting File:  G:\ACN DOSE-RESPONSE
MODELING\CANCER\INHALATION\SD_FEMALE_ZYMBAL_INHALE_PPM.plt
                                                  Fri Apr 13 13:35:30 2007
 ======================================================================

 BMDS MODEL RUN
~~~~~~~~~~~~~~~~~~~~~~~~~~~~~~~~~~~~~~~~~~~~~~~~~~~~~~~~~~~~~~~~~~~~~~~~

   The form of the probability function is:

   P[response] = background + (1-background)*[1-EXP(
-beta1*dose^1)]

   The parameter betas are restricted to be positive


   Dependent variable = Response
   Independent variable = Dose

 Total number of observations = 3
 Total number of records with missing values = 0
 Total number of parameters in model = 2
 Total number of specified parameters = 0
 Degree of polynomial = 1


 Maximum number of iterations = 250
 Relative Function Convergence has been set to: 1e-008
 Parameter Convergence has been set to: 1e-008
```

```
                 Default Initial Parameter Values
                    Background =            0
                       Beta(1) =    0.0017365


          Asymptotic Correlation Matrix of Parameter Estimates

          ( *** The model parameter(s)  -Background
                have been estimated at a boundary point, or have been specified by the user,
                and do not appear in the correlation matrix )

                    Beta(1)

   Beta(1)            1



                         Parameter Estimates

       Variable           Estimate             Std. Err.
     Background                  0                   NA
        Beta(1)          0.00139182          0.00127839

NA - Indicates that this parameter has hit a bound
     implied by some inequality constraint and thus
     has no standard error.

                       Analysis of Deviance Table

       Model      Log(likelihood)  Deviance  Test DF     P-value
     Full model        -38.8683
   Fitted model        -39.7334       1.73007      2           0.421
  Reduced model        -49.5377       21.3387      2         <.0001

          AIC:         81.4668


                     Goodness  of  Fit

     Dose     Est._Prob.    Expected    Observed     Size     Chi^2 Res.
  ----------------------------------------------------------------------
i: 1
    0.0000     0.0000         0.000         0          93       0.000
i: 2
   20.0000     0.0275         2.690         1          98      -0.646
i: 3
   80.0000     0.1054         9.378        11          89       0.193

 Chi-square =       1.41     DF = 2        P-value = 0.4952


   Benchmark Dose Computation

Specified effect =            0.1

Risk Type        =      Extra risk

Confidence level =           0.95

             BMD =        75.6997

            BMDL =        48.7384
```

BMDS (version 1.4.1) output for Zymbal gland tumors in Sprague-Dawley female rats employing CEO in blood as an internal dose metric

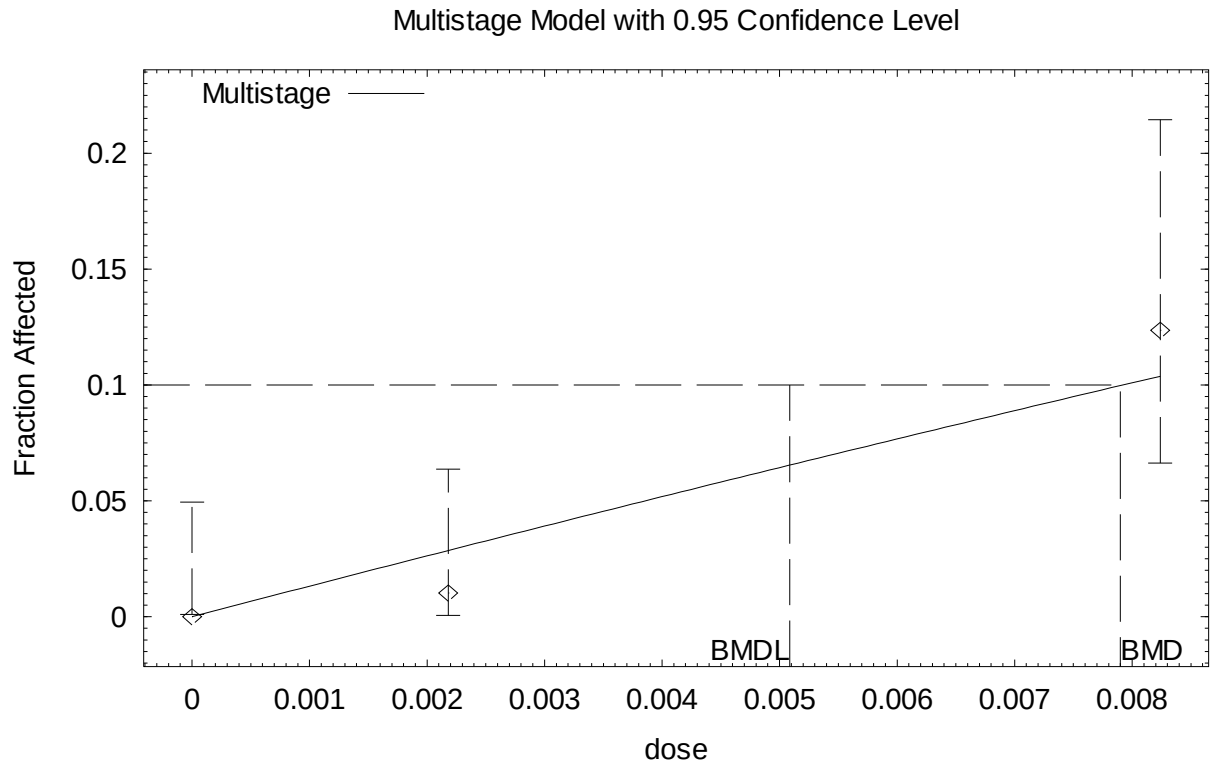

15:41 09/27 2007

```
 ======================================================================
         Multistage Model. (Version: 2.8;  Date: 02/20/2007)
         Input Data File: G:\ACN DOSE-RESPONSE
MODELING\CANCER\INHALATION\SD_FEMALE_ZYMBAL_INHALE_BLOOD_CEO.(d)
         Gnuplot Plotting File:  G:\ACN DOSE-RESPONSE
MODELING\CANCER\INHALATION\SD_FEMALE_ZYMBAL_INHALE_BLOOD_CEO.plt
                                                  Thu Sep 27 15:41:40 2007
 ======================================================================

 BMDS MODEL RUN
~~~~~~~~~~~~~~~~~~~~~~~~~~~~~~~~~~~~~~~~~~~~~~~~~~~~~~~~~~~~~~~~~~~~~~~~

   The form of the probability function is:

   P[response] = background + (1-background)*[1-EXP(
                -beta1*dose^1)]

   The parameter betas are restricted to be positive


   Dependent variable = Response
   Independent variable = Dose

 Total number of observations = 3
 Total number of records with missing values = 0
 Total number of parameters in model = 2
 Total number of specified parameters = 0
 Degree of polynomial = 1


 Maximum number of iterations = 250
 Relative Function Convergence has been set to: 1e-008
 Parameter Convergence has been set to: 1e-008


                  Default Initial Parameter Values
```

```
                    Background =           0
                       Beta(1) =     16.8864


           Asymptotic Correlation Matrix of Parameter Estimates

           ( *** The model parameter(s)  -Background
                 have been estimated at a boundary point, or have been specified by the user,
                 and do not appear in the correlation matrix )

                Beta(1)

   Beta(1)           1
```

Parameter Estimates

Variable	Estimate	Std. Err.	95.0% Wald Confidence Interval Lower Conf. Limit	Upper Conf. Limit
Background	0	*	*	*
Beta(1)	13.3383	*	*	*

* - Indicates that this value is not calculated.

Analysis of Deviance Table

Model	Log(likelihood)	# Param's	Deviance	Test d.f.	P-value
Full model	-38.8683	3			
Fitted model	-39.8337	1	1.93077	2	0.3808
Reduced model	-49.5377	1	21.3387	2	<.0001

AIC: 81.6675

Goodness of Fit

Dose	Est._Prob.	Expected	Observed	Size	Scaled Residual
0.0000	0.0000	0.000	0	93	0.000
0.0022	0.0287	2.808	1	98	-1.095
0.0082	0.1041	9.263	11	89	0.603

Chi^2 = 1.56 d.f. = 2 P-value = 0.4579

Benchmark Dose Computation

```
Specified effect =           0.1

Risk Type        =      Extra risk

Confidence level =          0.95

             BMD =     0.00789912

            BMDL =     0.00508579

            BMDU =      0.0132303

Taken together, (0.00508579, 0.0132303) is a 90     % two-sided confidence
interval for the BMD
```

Tumor Site: Tongue (Dow Chemical Co., 1992a; Quast et al., 1980b)

Table B-33. Incidence of tongue tumors in Sprague-Dawley rats exposed to AN in air for 2 years

Sex	Administered AN concentration (ppm in air)	Predicted CEO-AUC in blood (mg/L)	Incidence of tongue tumors[a]
Male	0	0	1/95 (1%)
	20	2.17×10^{-3}	0/14 (0%)
	80	8.20×10^{-3}	7/82 (9%)[b]

[a]Incidences for Sprague-Dawley rats do not include animals from the 6- and 12-mo sacrifices and were further adjusted to exclude (from the denominators) rats that died between 0 and 12 mos in the study.
[b]Significantly different from controls ($p < 0.05$) as calculated by the study authors.

Table B-34. Summary of BMD modeling results based on incidence of tongue tumors in Sprague-Dawley rats exposed to AN in air for 2 years

Dose metric	Best-fit model[a]	χ^2 *p*-value[b]	AIC	BMD_{10}[c]	$BMDL_{10}$[d]
Males					
Administered dose	1°MS	0.51	63.76	111.06 ppm	59.41 ppm
CEO	2°MS	0.63	63.37	9.48×10^{-3} mg/L	6.39×10^{-3} mg/L

[a]Dose-response models were fit using BMDS, version 1.4.1. "1°MS" indicates a one-stage multistage model. "2°MS" indicates a two-stage multistage model.
[b]*p* value from the χ^2 goodness of fit test. Values <0.1 indicate a significant lack of fit.
[c]BMD_{10} = BMD at 10% extra risk.
[d]$BMDL_{10}$ = 95% lower confidence limit on the BMD at 10% extra risk.

BMDS (version 1.4.1) output for tongue tumors in Sprague-Dawley male rats employing administered dose as a dose metric

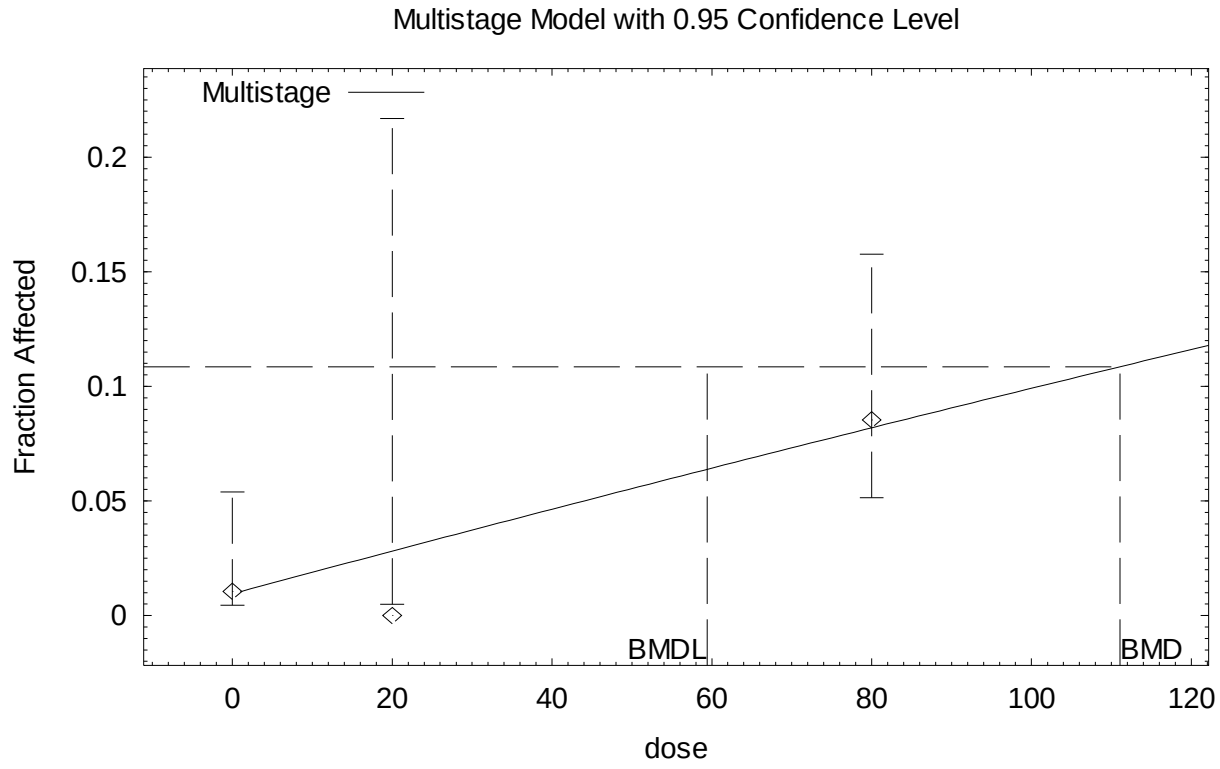


```
13:25 04/13 2007
 ======================================================================
         Multistage Model. $Revision: 2.1 $ $Date: 2000/08/21 03:38:21 $
         Input Data File: G:\ACN DOSE-RESPONSE
MODELING\CANCER\INHALATION\SD_MALE_TONGUE_INHALE_PPM.(d)
         Gnuplot Plotting File:  G:\ACN DOSE-RESPONSE
MODELING\CANCER\INHALATION\SD_MALE_TONGUE_INHALE_PPM.plt
                                                Fri Apr 13 13:25:25 2007
 ======================================================================

 BMDS MODEL RUN
~~~~~~~~~~~~~~~~~~~~~~~~~~~~~~~~~~~~~~~~~~~~~~~~~~~~~~~~~~~~~~~~~~~~~~~~

   The form of the probability function is:

   P[response] = background + (1-background)*[1-EXP(
-beta1*dose^1)]

   The parameter betas are restricted to be positive


   Dependent variable = Response
   Independent variable = Dose

 Total number of observations = 3
 Total number of records with missing values = 0
 Total number of parameters in model = 2
 Total number of specified parameters = 0
 Degree of polynomial = 1


 Maximum number of iterations = 250
 Relative Function Convergence has been set to: 1e-008
 Parameter Convergence has been set to: 1e-008
```

Default Initial Parameter Values
Background = 0
Beta(1) = 0.00109944

Asymptotic Correlation Matrix of Parameter Estimates

	Background	Beta(1)
Background	1	-0.65
Beta(1)	-0.65	1

Parameter Estimates

Variable	Estimate	Std. Err.
Background	0.00947867	0.0968926
Beta(1)	0.000948673	0.00186696

Analysis of Deviance Table

Model	Log(likelihood)	Deviance	Test DF	P-value
Full model	-29.4666			
Fitted model	-29.8775	0.821799	1	0.3647
Reduced model	-33.2127	7.49227	2	0.02361

AIC: 63.755

Goodness of Fit

Dose	Est._Prob.	Expected	Observed	Size	Chi^2 Res.
i: 1					
0.0000	0.0095	0.900	1	95	0.112
i: 2					
20.0000	0.0281	0.393	0	14	-1.029
i: 3					
80.0000	0.0819	6.713	7	82	0.046

Chi-square = 0.43 DF = 1 P-value = 0.5124

```
   Benchmark Dose Computation

Specified effect =            0.1

Risk Type        =      Extra risk

Confidence level =           0.95

             BMD =        111.061

            BMDL =        59.4126
```

BMDS (version 1.4.1) output for tongue tumors in Sprague-Dawley male rats employing CEO in blood as an internal dose metric

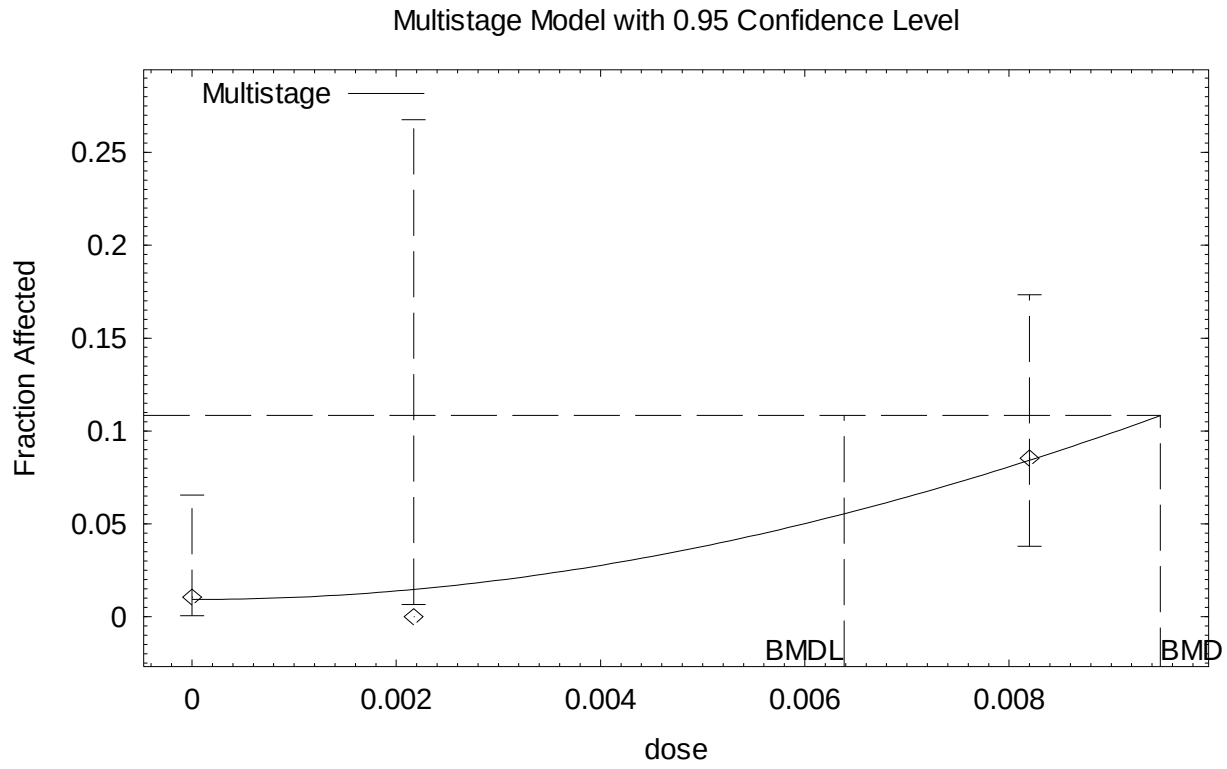


```
 ======================================================================
         Multistage Model. (Version: 2.8;  Date: 02/20/2007)
         Input Data File: G:\ACN DOSE-RESPONSE
MODELING\CANCER\INHALATION\SD_MALE_TONGUE_INHALE_BLOOD_CEO.(d)
         Gnuplot Plotting File:  G:\ACN DOSE-RESPONSE
MODELING\CANCER\INHALATION\SD_MALE_TONGUE_INHALE_BLOOD_CEO.plt
                                                  Thu Sep 27 15:28:11 2007
 ======================================================================

 BMDS MODEL RUN
~~~~~~~~~~~~~~~~~~~~~~~~~~~~~~~~~~~~~~~~~~~~~~~~~~~~~~~~~~~~~~~~~~~~~~~~

   The form of the probability function is:

   P[response] = background + (1-background)*[1-EXP(
                -beta1*dose^1-beta2*dose^2)]

   The parameter betas are restricted to be positive


   Dependent variable = Response
   Independent variable = Dose

 Total number of observations = 3
 Total number of records with missing values = 0
 Total number of parameters in model = 3
 Total number of specified parameters = 0
 Degree of polynomial = 2


 Maximum number of iterations = 250
 Relative Function Convergence has been set to: 1e-008
 Parameter Convergence has been set to: 1e-008


                  Default Initial Parameter Values
```

```
                    Background =   0.00257667
                       Beta(1) =            0
                       Beta(2) =      1279.63


           Asymptotic Correlation Matrix of Parameter Estimates

           ( *** The model parameter(s)  -Beta(1)
                 have been estimated at a boundary point, or have been specified by the user,
                 and do not appear in the correlation matrix )

             Background      Beta(2)

Background            1        -0.64

   Beta(2)        -0.64            1

                                Parameter Estimates

                                                          95.0% Wald Confidence Interval
      Variable         Estimate        Std. Err.     Lower Conf. Limit   Upper Conf. Limit
     Background       0.00925756            *                 *                   *
        Beta(1)                0            *                 *                   *
        Beta(2)          1172.26            *                 *                   *

* - Indicates that this value is not calculated.


                        Analysis of Deviance Table

       Model      Log(likelihood)  # Param's  Deviance  Test d.f.   P-value
     Full model        -29.4666         3
    Fitted model       -29.6826         2      0.431994      1           0.511
  Reduced model        -33.2127         1       7.49227      2         0.02361

           AIC:         63.3652


                                 Goodness  of  Fit
                                                                      Scaled
     Dose     Est._Prob.    Expected    Observed     Size       Residual
  ---------------------------------------------------------------------------
    0.0000     0.0093         0.879         1          95        0.129
    0.0022     0.0147         0.206         0          14       -0.457
    0.0082     0.0844         6.917         7          82        0.033

 Chi^2 = 0.23      d.f. = 1        P-value = 0.6339


   Benchmark Dose Computation

Specified effect =           0.1

Risk Type        =      Extra risk

Confidence level =          0.95

              BMD =      0.0094804

             BMDL =     0.00638558

             BMDU =      0.0279407

Taken together, (0.00638558, 0.0279407) is a 90     % two-sided confidence
interval for the BMD
```

Tumor Site: Mammary Gland (Dow Chemical Co., 1992a; Quast et al., 1980b)

Table B-35. Incidence of mammary gland tumors in Sprague-Dawley rats exposed to AN in air for 2 years

Sex	Administered AN concentration (ppm in air)	Predicted CEO-AUC in blood (mg/L)	Incidence of mammary gland tumors[a]
Female	0	0	9/93 (10%)
	20	2.18×10^{-3}	8/98 (8%)
	80	8.24×10^{-3}	20/99 (20%)[b]

[a]Incidences for Sprague-Dawley rats do not include animals from the 6- and 12-mo sacrifices and were further adjusted to exclude (from the denominators) rats that died between 0 and 12 mos in the study.
[b]Significantly different from controls ($p < 0.05$) as calculated by the study authors.

Table B-36. Summary of BMD modeling results based on incidence of mammary gland tumors in Sprague-Dawley rats exposed to AN in air for 2 years

Dose metric	Best-fit model[a]	χ^2 *p*-value[b]	AIC	BMD_{10}[c]	$BMDL_{10}$[d]
Females					
Administered dose	1°MS	0.28	219.42	66.48 ppm	37.82 ppm
CEO	2°MS	0.57	218.52	7.31×10^{-3} mg/L	4.33×10^{-3} mg/L

[a]Dose-response models were fit using BMDS, version 1.4.1. "1°MS" indicates a one-stage multistage model. "2°MS" indicates a two-stage multistage model.
[b]*p* value from the χ^2 goodness of fit test. Values <0.1 indicate a significant lack of fit.
[c]BMD_{10} = BMD at 10% extra risk.
[d]$BMDL_{10}$ = 95% lower confidence limit on the BMD at 10% extra risk.

BMDS (version 1.4.1) output for mammary gland tumors in Sprague-Dawley female rats employing administered dose as a dose metric

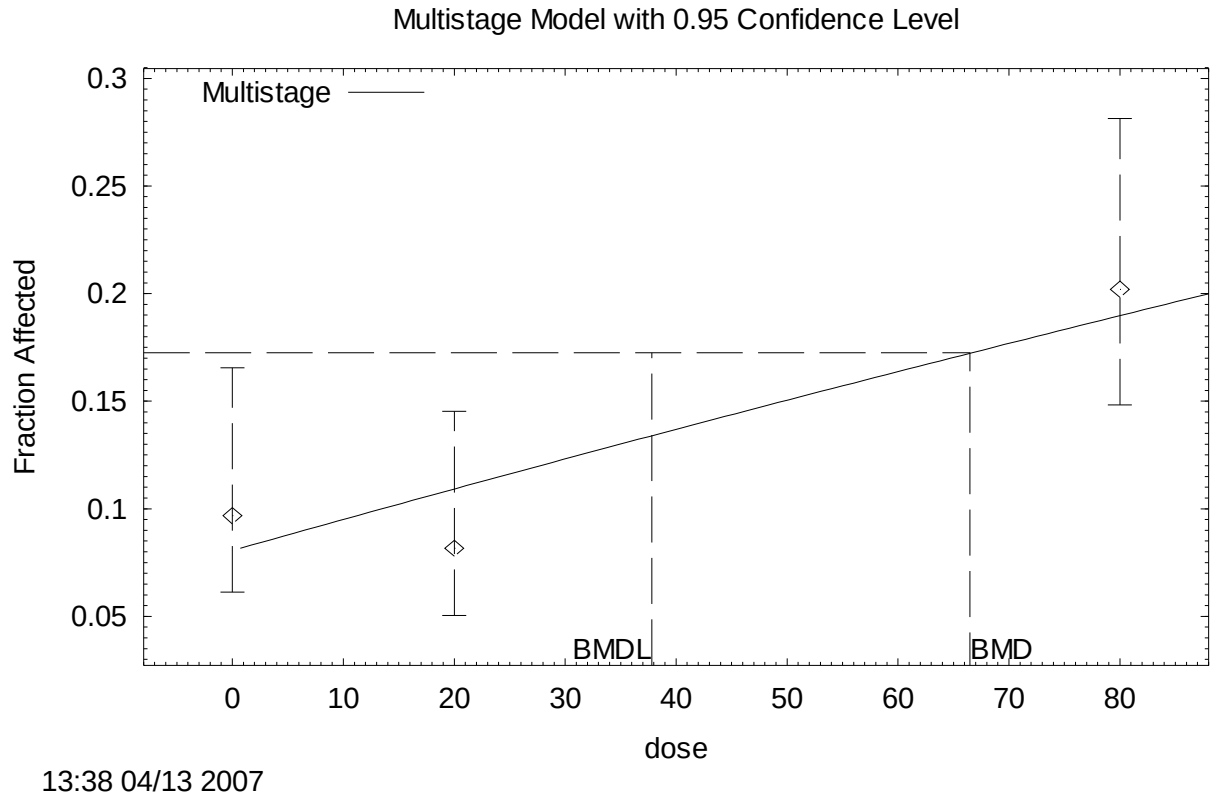


```
 ======================================================================
         Multistage Model. $Revision: 2.1 $ $Date: 2000/08/21 03:38:21 $
         Input Data File: G:\ACN DOSE-RESPONSE
MODELING\CANCER\INHALATION\SD_FEMALE_MAMMARY_INHALE_PPM.(d)
         Gnuplot Plotting File:  G:\ACN DOSE-RESPONSE
MODELING\CANCER\INHALATION\SD_FEMALE_MAMMARY_INHALE_PPM.plt
                                                  Fri Apr 13 13:38:03 2007
 ======================================================================

 BMDS MODEL RUN
~~~~~~~~~~~~~~~~~~~~~~~~~~~~~~~~~~~~~~~~~~~~~~~~~~~~~~~~~~~~~~~~~~~~~~~~

   The form of the probability function is:

   P[response] = background + (1-background)*[1-EXP(
-beta1*dose^1)]

   The parameter betas are restricted to be positive


   Dependent variable = Response
   Independent variable = Dose

 Total number of observations = 3
 Total number of records with missing values = 0
 Total number of parameters in model = 2
 Total number of specified parameters = 0
 Degree of polynomial = 1


 Maximum number of iterations = 250
 Relative Function Convergence has been set to: 1e-008
 Parameter Convergence has been set to: 1e-008
```

Default Initial Parameter Values
Background = 0.0767126
Beta(1) = 0.00173168

Asymptotic Correlation Matrix of Parameter Estimates

	Background	Beta(1)
Background	1	-0.68
Beta(1)	-0.68	1

Parameter Estimates

Variable	Estimate	Std. Err.
Background	0.0806351	0.0783644
Beta(1)	0.00158474	0.00179372

Analysis of Deviance Table

Model	Log(likelihood)	Deviance	Test DF	P-value
Full model	-107.092			
Fitted model	-107.71	1.23579	1	0.2663
Reduced model	-110.714	7.24319	2	0.02674

AIC: 219.421

Goodness of Fit

Dose	Est._Prob.	Expected	Observed	Size	Chi^2 Res.
i: 1					
0.0000	0.0806	7.499	9	93	0.218
i: 2					
20.0000	0.1093	10.713	8	98	-0.284
i: 3					
80.0000	0.1901	18.820	20	99	0.077

Chi-square = 1.19 DF = 1 P-value = 0.2754

Benchmark Dose Computation

Specified effect = 0.1

Risk Type = Extra risk

Confidence level = 0.95

BMD = 66.4843

BMDL = 37.8172

BMDS (version 1.4.1) output for mammary gland tumors in Sprague-Dawley female rats employing CEO in blood as an internal dose metric

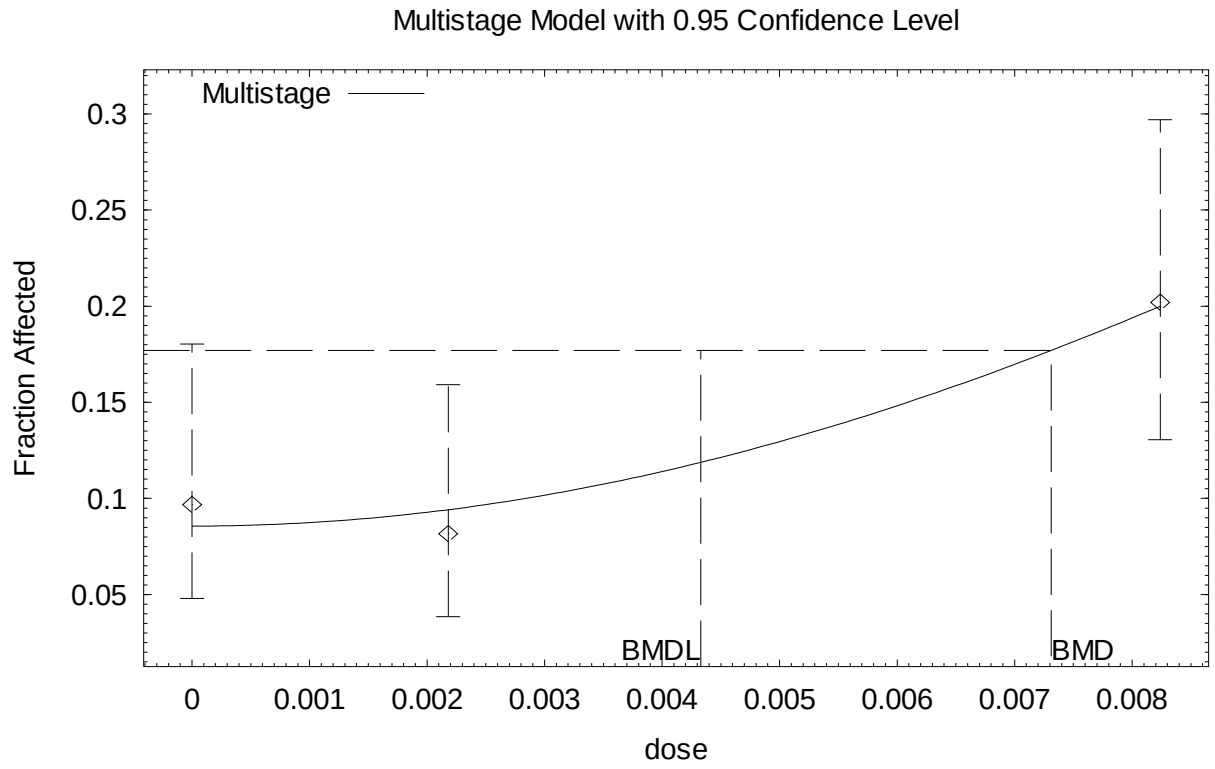

15:44 09/27 2007

```
 ================================================================
         Multistage Model. (Version: 2.8;  Date: 02/20/2007)
         Input Data File: G:\ACN DOSE-RESPONSE
MODELING\CANCER\INHALATION\SD_FEMALE_MAMMARY_INHALE_BLOOD_CEO.(d)
         Gnuplot Plotting File:  G:\ACN DOSE-RESPONSE
MODELING\CANCER\INHALATION\SD_FEMALE_MAMMARY_INHALE_BLOOD_CEO.plt
                                                  Thu Sep 27 15:44:26 2007
 ================================================================

 BMDS MODEL RUN
~~~~~~~~~~~~~~~~~~~~~~~~~~~~~~~~~~~~~~~~~~~~~~~~~~~~~~~~~~~~~~~~~~~~~~~~

   The form of the probability function is:

   P[response] = background + (1-background)*[1-EXP(
                -beta1*dose^1-beta2*dose^2)]

   The parameter betas are restricted to be positive


   Dependent variable = Response
   Independent variable = Dose

 Total number of observations = 3
 Total number of records with missing values = 0
 Total number of parameters in model = 3
 Total number of specified parameters = 0
 Degree of polynomial = 2


 Maximum number of iterations = 250
 Relative Function Convergence has been set to: 1e-008
 Parameter Convergence has been set to: 1e-008


                  Default Initial Parameter Values
```

```
                    Background =    0.0853385
                       Beta(1) =            0
                       Beta(2) =      1996.34


           Asymptotic Correlation Matrix of Parameter Estimates

           ( *** The model parameter(s)  -Beta(1)
                 have been estimated at a boundary point, or have been specified by the user,
                 and do not appear in the correlation matrix )

             Background      Beta(2)

Background            1         -0.6

   Beta(2)         -0.6            1

                                Parameter Estimates

                                                        95.0% Wald Confidence Interval
      Variable         Estimate        Std. Err.     Lower Conf. Limit   Upper Conf. Limit
     Background        0.0856208            *                *                   *
        Beta(1)              0              *                *                   *
        Beta(2)          1971.76            *                *                   *

* - Indicates that this value is not calculated.


                        Analysis of Deviance Table

       Model      Log(likelihood)  # Param's  Deviance  Test d.f.   P-value
     Full model        -107.092         3
    Fitted model       -107.258         2      0.332027      1          0.5645
  Reduced model        -110.714         1       7.24319      2         0.02674

           AIC:         218.517


                                Goodness  of  Fit
                                                                      Scaled
     Dose     Est._Prob.    Expected    Observed     Size       Residual
  ---------------------------------------------------------------------------
    0.0000     0.0856         7.963         9          93        0.384
    0.0022     0.0941         9.226         8          98       -0.424
    0.0082     0.2002        19.818        20          99        0.046

 Chi^2 = 0.33      d.f. = 1        P-value = 0.5658


   Benchmark Dose Computation

Specified effect =           0.1

Risk Type        =      Extra risk

Confidence level =          0.95

              BMD =     0.00730992

             BMDL =     0.00432882

             BMDU =      0.0152838

Taken together, (0.00432882, 0.0152838) is a 90     % two-sided confidence
interval for the BMD
```

APPENDIX B-5. ANALYSIS TO ASSESS COMBINING TUMOR INCIDENCE DATA FROM TWO CANCER BIOASSAYS EMPLOYING SPRAGUE-DAWLEY RATS

A statistical analysis was conducted to determine whether tumor dose-response data from two 2-year drinking water bioassays in Sprague-Dawley rats were similar enough to be combined. The first study employed AN drinking water concentrations of 0, 35, 100, and 300 ppm (Quast, 2002; Quast et al., 1980a), while the second study used AN drinking water concentrations of 0, 1, and 100 ppm (Johannsen and Levinskas, 2002a). To conduct the analysis, the multistage model in BMDS (version 1.3.2) was fit to the tumor incidence data from three sites (forestomach, CNS, and Zymbal gland) in each sex across both studies, using administered animal dose expressed in mg/kg-day. Using the best-fit model, a statistical test described by Stiteler et al. (1993), which employs a maximum likelihood ratio statistic distributed as a χ^2, was then used to test the null hypothesis that the corresponding data sets from the two studies are compatible with a common dose-response model. If the null hypothesis is not rejected, this analysis provides evidence that the results from the two studies may be pooled.

The results of this analysis showed that forestomach and Zymbal gland tumors in male and female Sprague-Dawley rats were not compatible with a common dose-response model, while CNS tumors in male and female Sprague-Dawley rats were compatible with a common dose-response model. Because of these conflicting results, it was decided that the results from the two Sprague-Dawley drinking water studies would not be pooled. Therefore, the final dose-response analysis for deriving the oral slope factor for AN focused on the two rat drinking water studies containing the most dose groups (i.e., the Sprague-Dawley rat bioassay reported by Quast [2002] and the F344 rat bioassay reported by Johannsen and Levinskas [2002b]). For each tumor site, summaries of the results of the statistical tests for compatibility are shown below.

Test 1: Forestomach tumors in male Sprague-Dawley rats

Tumor incidence data (Johannsen and Levinskas, 2002a):

- 0 ppm (0 mg/kg-day): 3/78
- 1 ppm (0.085 mg/kg-day): 3/78
- 100 ppm (8.53 mg/kg-day): 11/77

Best-fit model: 1-stage multistage
Log (likelihood) = –57.0113

Tumor incidence data (Quast, 2002):

- 0 ppm (0 mg/kg-day): 0/80
- 35 ppm (3.42 mg/kg-day): 2/47

- 100 ppm (8.53 mg/kg-day): 23/48
- 300 ppm (21.20 mg/kg-day): 39/48

Best-fit model: 2-stage multistage (highest dose group dropped)
Log (likelihood) = –42.4099

Tumor incidence data (combined):
- 0 ppm (0 mg/kg-day): 3/158
- 1 ppm (0.085 mg/kg-day): 3/78
- 35 ppm (3.42 mg/kg-day): 2/47
- 100 ppm (8.53 mg/kg-day): 34/125
- 300 ppm (21.20 mg/kg-day): 39/48

Best-fit model: 2-stage multistage
Log (likelihood) = –132.865

Conclusion: Based on the likelihood ratio test statistic, $-2 \ln \Lambda = 2[132.865 - (42.4099 + 57.0113)] = 2 \times 33.4438 = 66.89$, the data sets are not compatible with a common dose-response model at $p < 0.0001$.

Test 2: Forestomach tumors in female Sprague-Dawley rats

Tumor incidence data (Johannsen and Levinskas, 2002a):
- 0 ppm (0 mg/kg-day): 1/80
- 1 ppm (0.11 mg/kg-day): 4/79
- 100 ppm (10.80 mg/kg-day): 7/79

Best-fit model: 1-stage multistage
Log (likelihood) = –45.8328

Tumor incidence data (Quast, 2002):
- 0 ppm (0 mg/kg-day): 1/80
- 35 ppm (4.36 mg/kg-day): 1/48
- 100 ppm (10.80 mg/kg-day): 12/48
- 300 ppm (25.00 mg/kg-day): 30/48

Best-fit model: 2-stage multistage
Log (likelihood) = –69.9834

Tumor incidence data (combined):

- 0 ppm (0 mg/kg-day): 2/160
- 1 ppm (0.11 mg/kg-day): 4/79
- 35 ppm (4.36 mg/kg-day): 1/48
- 100 ppm (10.80 mg/kg-day): 19/127
- 300 ppm (25.00 mg/kg-day): 30/48

Best-fit model: 2-stage multistage
Log (likelihood) = –119.054

Conclusion: Based on the likelihood ratio test statistic, $-2 \ln \Lambda = 2[119.054 - (69.9834 + 45.8328)] = 2 \times 3.2378 = 6.48$, the data sets are not compatible with a common dose-response model at $p = 0.011$.

Test 3: CNS tumors in male Sprague-Dawley rats

Tumor incidence data (Johannsen and Levinskas, 2002a):

- 0 ppm (0 mg/kg-day): 2/78
- 1 ppm (0.085 mg/kg-day): 3/75
- 100 ppm (8.53 mg/kg-day): 23/77

Best-fit model: 1-stage multistage
Log (likelihood) = –68.9254

Tumor incidence data (Quast, 2002):

- 0 ppm (0 mg/kg-day): 1/80
- 35 ppm (3.42 mg/kg-day): 12/47
- 100 ppm (8.53 mg/kg-day): 22/48
- 300 ppm (21.20 mg/kg-day): 30/48

Best-fit model: 1-stage multistage
Log (likelihood) = –98.6909

Tumor incidence data (combined):

- 0 ppm (0 mg/kg-day): 3/158
- 1 ppm (0.085 mg/kg-day): 3/75

- 35 ppm (3.42 mg/kg-day): 12/47
- 100 ppm (8.53 mg/kg-day): 45/125
- 300 ppm (21.20 mg/kg-day): 30/48

Best-fit model: 1-stage multistage
Log (likelihood) = –168.873

Conclusion: Based on the likelihood ratio test statistic, $-2 \ln \Lambda = 2[168.873 - (98.6909 + 68.9254)] = 2 \times 1.2567 = 2.51$, the data sets are compatible with a common dose-response model at $p = 0.113$.

Test 4: CNS Tumors in female Sprague-Dawley rats

Tumor incidence data (Johannsen and Levinskas, 2002a):
- 0 ppm (0 mg/kg-day): 0/79
- 1 ppm (0.11 mg/kg-day): 1/80
- 100 ppm (10.80 mg/kg-day): 39/78

Best-fit model: 1-stage multistage
Log (likelihood) = –59.5775

Tumor incidence data (Quast, 2002):
- 0 ppm (0 mg/kg-day): 1/80
- 35 ppm (4.36 mg/kg-day): 20/48
- 100 ppm (10.80 mg/kg-day): 25/48
- 300 ppm (25.00 mg/kg-day): 31/48

Best-fit model: Log-logistic
Log (likelihood) = –104.123

Tumor incidence data (combined):
- 0 ppm (0 mg/kg-day): 1/159
- 1 ppm (0.11 mg/kg-day): 1/80
- 35 ppm (4.36 mg/kg-day): 20/48
- 100 ppm (10.80 mg/kg-day): 64/126
- 300 ppm (25.00 mg/kg-day): 31/48

Best-fit model: Log-logistic

Log (likelihood) = –164.485

Conclusion: Based on the likelihood ratio test statistic, $-2 \ln \Lambda = 2[164.485 - (104.123 + 59.5775)] = 2 \times 0.7845 = 1.57$, the data sets are compatible with a common dose-response model at $p = 0.210$.

Test 5: Zymbal gland tumors in male Sprague-Dawley rats

Tumor incidence data (Johannsen and Levinskas, 2002a):

- 0 ppm (0 mg/kg-day): 1/80
- 1 ppm (0.085 mg/kg-day): 0/71
- 100 ppm (8.53 mg/kg-day): 17/73

Best-fit model: 1-stage multistage
Log (likelihood) = –45.815

Tumor incidence data (Quast, 2002):

- 0 ppm (0 mg/kg-day): 3/80
- 35 ppm (3.42 mg/kg-day): 4/47
- 100 ppm (8.53 mg/kg-day): 3/48
- 300 ppm (21.20 mg/kg-day): 16/48

Best-fit model: 1-stage multistage
Log (likelihood) = –70.1142

Tumor incidence data (combined):

- 0 ppm (0 mg/kg-day): 4/160
- 1 ppm (0.085 mg/kg-day): 0/71
- 35 ppm (3.42 mg/kg-day): 4/47
- 100 ppm (8.53 mg/kg-day): 20/121
- 300 ppm (21.20 mg/kg-day): 16/48

Best-fit model: 1-stage multistage
Log (likelihood) = –118.806

Conclusion: Based on the likelihood ratio test statistic, $-2 \ln \Lambda = 2[118.806 - (70.1142 + 45.815)] = 2 \times 2.8768 = 5.75$, the data sets are not compatible with a common dose-response model at $p = 0.016$.

Test 6: Zymbal gland tumors in female Sprague-Dawley rats

Tumor incidence data (Johannsen and Levinskas, 2002a):

- 0 ppm (0 mg/kg-day): 1/79
- 1 ppm (0.11 mg/kg-day): 0/75
- 100 ppm (10.80 mg/kg-day): 12/78

Best-fit model: 1-stage multistage
Log (likelihood) = –39.6428

Tumor incidence data (Quast, 2002):

- 0 ppm (0 mg/kg-day): 1/80
- 35 ppm (4.36 mg/kg-day): 5/48
- 100 ppm (10.80 mg/kg-day): 9/48
- 300 ppm (25.00 mg/kg-day): 18/48

Best-fit model: 1-stage multistage
Log (likelihood) = –76.3975

Tumor incidence data (combined):

- 0 ppm (0 mg/kg-day): 1/159
- 1 ppm (0.11 mg/kg-day): 0/75
- 35 ppm (4.36 mg/kg-day): 5/48
- 100 ppm (10.80 mg/kg-day): 21/126
- 300 ppm (25.00 mg/kg-day): 18/48

Best-fit model: 1-stage multistage
Log (likelihood) = –111.439

Conclusion: Based on the likelihood ratio test statistic, $-2 \ln \Lambda = 2[111.439 - (76.3975 + 39.6428)] = 2 \times (-4.6013) = -9.20 = 9.20$, the data sets are not compatible with a common dose-response model at $p = 0.002$.

APPENDIX B-6. ESTIMATION OF COMPOSITE CANCER RISK FROM EXPOSURE TO AN BY COMBINING RISK ESTIMATES ACROSS MULTIPLE TUMOR SITES

Increased tumor incidences were observed at multiple sites in male and female rats following exposure to AN both orally and by inhalation. With this multiplicity of tumors, the concern is that a potency or risk estimate based solely on one tumor site (e.g., the most sensitive site) may underestimate the overall cancer risk associated with exposure to this chemical. The most recent EPA cancer guidelines (U.S. EPA, 2005a) identified two ways to approach this issue: 1) analyze the incidence of tumor-bearing animals, or 2) combine the potencies associated with significantly elevated tumors at each site. The NRC (1994) concluded that an approach based on counts of animals with one or more tumors would tend to underestimate overall risk when tumor types occur independently, and thus an approach based on combining the risk estimates from each separate tumor type should be used.

Because potencies are typically upper bound estimates, summing such upper bound estimates across tumor sites is likely to overstate the overall risk. Therefore, following the recommendations of the NRC (1994) and the *Guidelines for Carcinogen Risk Assessment* (U.S. EPA, 2005a), a statistically valid upper bound on combined risk was derived in order to gain some understanding of the overall risk resulting from tumors occurring at multiple sites. It is important to note that this estimate of overall potency describes the risk of developing tumors at any combination of the sites considered and is not the risk of developing tumors at all three sites simultaneously.

For modeling individual tumor data, the multistage model is specified as follows:

$$(1)\ P(d) = 1 - exp[-(q_0 + q_1 d + q_2 d^2 + ... + q_m d^m)].$$

The model for the combined (or composite) tumor risk is still multistage, with a functional form that has the sum of stage-specific multistage coefficients as the corresponding multistage coefficient.

$$(2)\ P_c(d) = 1 - exp[-(\Sigma q_{0i} + d\Sigma q_{1i} + d^2\Sigma q_{2i} + ... + d^m\Sigma q_{mi})], \text{ for i=1,…, k,}$$
$$\text{where k = total number of sites}$$

The resulting equation for fixed extra risk (BMR) is polynomial in dose (when logarithms of both sides are taken) and can be straightforwardly solved for the combined BMD. However, confidence bounds for this BMD are not able to be estimated by the current version of BMDS.

Therefore, a Bayesian approach to finding confidence bounds on the combined BMD was implemented using WinBugs (Spiegelhalter et al., 2003). WinBugs software is freely available and implements Markov chain Monte Carlo (MCMC) computations. Use of WinBugs has been

demonstrated for derivation of a distribution of BMDs for a single multistage model (Kopylev et al., 2007) and can be straightforwardly generalized to derive the distribution of BMDs for the combined tumor load, following the NRC (1994) methodology described above. The advantage of a Bayesian approach is that it produces a distribution of BMDs that allows better characterization of statistical uncertainty. For the current analysis, a diffuse (high variance or low tolerance) Gaussian prior restricted to be nonnegative was used. The posterior distribution was based on three chains with 50,000 burn-in (i.e., the initial 50,000 simulations were dropped) and a thinning rate of 20, resulting in 150,000 simulations total. The median and 5^{th} percentile of the posterior distribution provided the BMD_{10} (central estimate) and $BMDL_{10}$ (lower bound) for combined tumor load, respectively.

The methodology above was applied to the dose-response data for the male and female Sprague-Dawley (Quast, 2002) and F344 (Johannsen and Levinskas, 2002b) rat drinking water studies, as well as to the data from male and female Sprague-Dawley rats in the Quast et al. (1980b) inhalation study. As with the risk estimates generated for individual tumor sites, the combined analysis used the internal dose metric CEO in blood (see Appendices B-3 and B-4). The human equivalent PODs are presented in Tables B-37 (episodic oral exposure) and B-38 (continuous inhalation exposure). Estimates of composite risk were estimated by dividing the BMR of 10% extra risk by the composite $BMDL_{10}$s ($0.1/BMDL_{10}$). Human equivalent composite CSFs are presented in Table B-39, and composite unit risks are presented in Table B-40. The slopes derived from the composite BMD_{10}s ($0.1/ BMD_{10}$) are also included in these tables for comparison.

Table B-37. Summary of PODs for composite cancer risk associated with episodic oral exposure to AN, using CEO-AUC levels in blood as dose metric and multiple tumor incidence data in rats

Rat strain, sex **Tumor site**	**PODs based on rat dose-response using internal dose metric CEO-AUC in blood (mg/L)**		**Human equivalent PODs[a] (mg/kg-d)**	
	BMD_{10}	**$BMDL_{10}$**	**BMD_{10}**	**$BMDL_{10}$**
Sprague-Dawley, male Forestomach, CNS, Zymbal gland, tongue	4.2×10^{-4}	3.6×10^{-4}	0.042	0.036
Sprague-Dawley, female Forestomach, CNS, Zymbal gland, tongue, mammary gland	2.6×10^{-4}	2.0×10^{-4}	0.026	0.020
F344, male Forestomach, CNS, Zymbal gland	4.6×10^{-4}	3.3×10^{-4}	0.046	0.033
F344, female Forestomach, CNS, Zymbal gland, mammary gland	6.7×10^{-4}	5.2×10^{-4}	0.066	0.051

[a]Converted using human PBPK model.

Table B-38. Summary of PODs for composite cancer risk associated with inhalation exposure to AN, based on multiple tumor incidence data in rats and CEO-AUC levels in blood

Rat strain, sex **Tumor site**	**PODs for rat dose-response in terms of CEO-AUC in blood (mg/L)**		**Human equivalent PODs: AN in air[a] (mg/m^3)**	
	BMC_{10}	**$BMCL_{10}$**	**BMC_{10}**	**$BMCL_{10}$**
Sprague-Dawley, male Intestine, CNS, Zymbal gland, tongue	1.4×10^{-3}	1.1×10^{-3}	1.9	1.5
Sprague-Dawley, female CNS, Zymbal gland, mammary gland	1.7×10^{-3}	1.3×10^{-3}	2.3	1.8

[a]Converted using human PBPK model.

Table B-39. Estimated human oral CSFs for AN based on multiple tumor incidence data in rats and CEO-AUC levels in blood

Rat strain, sex **Tumor site**	**Slope derived from composite BMD_{10}[a] $(mg/kg\text{-}d)^{-1}$**	**Composite CSF[b] $(mg/kg\text{-}d)^{-1}$**
Sprague-Dawley, male Forestomach, CNS, Zymbal gland, tongue	2.4	2.8
Sprague-Dawley, female Forestomach, CNS, Zymbal gland, tongue, mammary gland	3.8	5.0
F344, male Forestomach, CNS, Zymbal gland	2.2	3.1
F344, female Forestomach, CNS, Zymbal gland, mammary gland	1.5	1.9

[a]Slope estimated by $0.1/BMD_{10}$.
[b]$CSF = 0.1/BMDL_{10}$.

Table B-40. Estimated human IURs for AN based on multiple tumor incidence data in rats and CEO-AUC levels in blood

Rat strain, sex **Tumor site**	**Slope to background from overall BMC_{10}[a] $(mg/m^3)^{-1}$**	**Overall IUR[b] $(mg/m^3)^{-1}$**
Sprague-Dawley, male Intestine, CNS, Zymbal gland, tongue	5.4×10^{-2}	6.8×10^{-2}
Sprague-Dawley, female CNS, Zymbal gland, mammary gland	4.4×10^{-2}	5.7×10^{-2}

[a]Slope estimated by $0.1/BMD_{10}$.
[b]$IUR = 0.1/BMDL_{10}$.

APPENDIX B-7. STATISTICAL ANALYSIS OF BLAIR ET AL. (1998)

The Data

The data used in this analysis came from the best available epidemiological study (see Section 5.4.1) by Blair et al. (1998). The raw data from the study were provided to EPA courtesy of NCI. The process of data collection is described in Blair et al. (1998) and in more detail in Stewart et al. (1998). The full raw data set contains 363 variables on 25,460 subjects. The variables include demographic information, employment information, vital status, and various measures of exposure per study year (1942–1983), including maximum and minimum estimates, "best estimate," frequency of peaks, and several other ways of measuring exposure. The raw data provided by NCI did not include the smoking data that were collected for approximately 10% of the subjects. Therefore, smoking information was not part of the EPA's statistical analysis. The uncertainty connected to lack of smoking information is discussed in Section 5.4.5.2. The data on dates of exposure and corresponding exposure amounts, dates of mortality due to lung cancer and other causes, a plant worked, and the birth year were retained for the statistical analysis. Biological age was chosen as a time scale. Data handling and statistical analysis were performed using S-Plus™ statistical software.

The Statistical Model

The semi-parametric Cox proportional hazards model (Cox, 1972) is a widely used model in hazard regression. The Cox model with time-dependent covariates was chosen to model the data for to two main reasons. Primarily, it allows taking into account individual covariate history, allowing utilization of the extensive exposure data collected by Blair et al. (1998). Additionally, the Cox model uses internal controls. Internal controls constitute an appropriate comparison group, given the healthy worker effect observed by Blair et al. (1998) and further demonstrated by Marsh et al. (2001).

In the Cox model, the conditional hazard function, given the covariate process Z(t), is assumed to have the form:

$$\lambda(t|Z(t)) = \lambda_0(t)\exp(\beta^T Z(t))$$

where β is the vector of regression coefficients and $\lambda_0(t)$ denotes the baseline hazard function. No particular shape is assumed for the baseline hazard; it is estimated nonparametrically. The contributions of covariates to the hazard are multiplicative. When $\beta^T Z(t)$ is small and Z(t) represents exposure, the Cox proportional model is consistent with linearity of dose-response for low doses. When no time-dependent covariates are present, the cumulative hazard function $\Lambda_0(t)$ is estimated using a Breslow (Breslow, 1974) estimator:

$$\hat{\Lambda}_0 = \sum_{\{i:ti\le t\}} \frac{d_i}{\sum_{j\in R(ti)} \exp(\hat{\beta}^T Z_j)}$$

where Z_j is the (time-independent) covariate vector of the j^{th} individual at age t_i, $\hat{\beta}$ is an estimate of β from the Cox model, d_i is the number of deaths at the age t_i, and $R(t_i)$ is the risk set at age t_i. Risk set is defined as all the individuals who are under observation and at risk of death at age t_i. The Breslow estimator is piecewise constant with discrete jumps at times of death. The corresponding estimate of the baseline hazard function is the size of the jump of the cumulative hazard at ages of death and zero otherwise. The survival function $S(t) = \exp(-\Lambda(t))$ is estimated by plugging in the Breslow estimator:

$$\hat{S}(t) = \exp(-\hat{\Lambda}(t))$$

The cumulative probability of death $R(t) = 1-S(t)$ is estimated by:

$$\hat{R}(t) = 1 - \hat{S}(t)$$

With time-dependent covariates, EPA followed the suggestion by Starr (2004) of a modified Breslow estimator:

$$\sum_{\{i:ti\le t\}} \frac{d_i}{\sum_{j\in R(ti)} \exp(\hat{\beta}^T Z_j(t_i))}$$

The survival function and cumulative probability of death are then estimated using the modified cumulative hazard estimator. The modified estimator only approximates the true cumulative hazard since a covariate path is not encountered in the estimator. Therneau and Grambsch (2000) discuss clinical examples when this estimator could lead to inappropriate results, but the occupational case is very different from clinical examples, since at the baseline, not all workers are exposed and exposure is nondecreasing and often ends well before death.

Calculations of Excess Risk

Following Starr et al. (2004), EPA defined hazard functions for lung cancer mortality $\lambda^{lc}(t)$ and other causes of death $\lambda^{oc}(t)$, with the corresponding cause-specific cumulative hazard functions, $\Lambda^{lc}(t)$ and $\Lambda^{oc}(t)$. The sum of $\Lambda^{lc}(t)$ and $\Lambda^{oc}(t)$ is the all-causes mortality hazard $\Lambda^{ac}(t)$ with corresponding survival function $S^{ac}(t)$. Then, the cumulative risk of lung cancer mortality by age t, given covariate path Z(t)=z(t) is:

$$R^{lc}(t|z(t)) = \sum_{u \le t} \lambda^{lc}(u|z(t)) S^{ac}(u|z(t))$$

The cumulative risk of lung cancer mortality by age t in the absence of exposure:

$$R^{lc}(t|Z(t)=0) = \sum_{u \le t} \lambda^{lc}(u|Z(t)=0) S^{ac}(u|Z(t)=0)$$

Excess risk, given covariate path Z(t)=z(t), is calculated by:

$$\frac{R^{lc}(t|Z(t)=z(t)) - R^{lc}(t|Z(t)=0)}{1 - R^{lc}(t|Z(t)=0)}$$

When $z(t)^T \beta^{lc} << 1$ and $\beta^{oc} \approx 0$, the first order expansion of the numerator simplifies into approximately:

$$\beta^{lc} \sum_{u \le t} \lambda^{lc}(u|z(t)=0) S^{ac}(u|z(t)=0) \left\{ z(u) - \sum_{v \le u} z(v) \lambda^{lc}(v|z(t)=0) \right\}$$

Plugging in estimates of β, hazard rate, and survival function into the equation above, an estimate of excess risk is obtained. Using estimated UCL on β instead of β results in the upper confidence bound on the estimated risk.

Results

Model Choice. There were not enough lung cancer deaths in other than white males sex-race groups, so sex and race were not included as covariates. Including time-independent covariates, such as duration and average exposure, was investigated, but time-dependent cumulative exposure was used since it allows taking into account individual exposure history. Neither the birth year (p = 0.77) nor the plant worked on (p = 0.061) was significant, so cumulative AN exposure was the only (time-dependent) covariate used in the model.

Mortality and Risk Estimates. The *coxph* function of S-Plus™ was used to obtain estimates of β. The estimate of β^{lc} was equal to $1.24 \times 10^{-3}$with the standard error of 2.47×10^{-2} ($p = 0.61$). The estimate of β^{oc} was equal to 6.7×10^{-4} with a standard error of 9.66×10^{-4} ($p = 0.49$). The estimates, covariates, and event times were then used to construct estimates of cumulative hazard and risks, as described in the previous section. The exposures corresponding to excess risks were divided by 2 to account for differences in volume of air inhaled during a working day and during a whole day (10 vs. 20 m^3/day). Resulting exposure estimates (by age 80): EC_{01} = 0.992 ppm and LEC_{01} = 0.238 ppm. The corresponding unit risk was calculated to equal 4.2×10^{-2} ppm^{-1}.

Limitations of the Statistical Approach

The statistical approach followed the approach of Starr et al. (2004), and it shares the limitations and uncertainties described there. The limitations and uncertainties include the following:

- The Cox model fit the data adequately, but it was an empirical model fit rather than a biologically based model.
- The estimator of the cumulative hazard does not account for the covariate path and hence, is only an approximation.
- The estimate of risk is obtained using the first-order "linearized" approximation. However, the results are consistent with assumptions of the first-order approximation validity.
- The Cox model uses internal controls and hence, it is much more vulnerable than SMR computation to contamination of pool of workers who are free of lung cancer by lung cancer cases. That is caused by misdiagnosis of lung cancer as not a lung cancer. Selikoff and Seidman (1992) showed based on histopathological analysis of a comparably large industrial cohort (17,800 asbestos workers) that as much as 13.7% of lung cancer cases are misdiagnosed on death certificates, both as neoplasms and nonmalignant diseases, with about 3% as asbestos only diseases (mesothelioma and asbestosis). Therefore, the Blair cohort may have as much as 10% of internal controls that are actually lung cancers. That would cause a strong bias against finding a statistically significant relationship.

APPENDIX C. PBPK MODEL DESCRIPTIONS AND SOURCE CODE

Model Description

The PBPK models used to calculate rat and human internal doses for the development of candidate RfDs, oral CSFs, and IURs were those revised from Kedderis et al. (1996) (rat, with EH activity towards CEO added and other parameters revised) and Sweeney et al. (2003) (human). Both models are flow limited, lumped compartment models that predict amounts and concentrations of AN and its metabolite of toxicological interest, CEO, in blood and seven tissues: lung, brain, fat, stomach, liver, and rapidly and slowly perfused tissues. Both models include portals of entry for oral, inhalation, and i.v. routes of exposure. Drinking water is modeled as a continuous infusion to the GI lumen. (The model code allows one to define episodic oral exposure as a series of boluses up to 6 times/day, but the simpler approach of treating the exposure as continuous was chosen.) For rats, the infusion rate is set such that the total amount consumed equals the average total amount ingested during the bioassays as determined from water consumption and administered AN concentration. Inhalation duration and frequency can be explicitly defined. Simulated metabolism of AN and CEO occur only in the liver. Elimination of both compounds is accomplished via second-order GSH conjugation in various tissues, saturable hepatic metabolism, and pulmonary excretion into exhaled air.

The rat and human models are based on the same structural framework but have two primary differences: (1) physiological and metabolic parameters for each are species specific, and (2) the human model simulates saturable, enzyme-mediated hydrolysis of CEO, a metabolic process not observed in rats. In the absence of human in vivo data for metabolism, human metabolic parameters were estimated from in vitro values extrapolated to in vivo values by using in vitro/in vivo ratios in rats, which is described fully in Sweeney et al. (2003). In the Sweeney et al. (2003) model, a conversion factor for in vitro to in vivo extrapolation of human metabolic constants is implicitly defined in the calculation of V_{max} values for AN oxidation and CEO hydrolysis. Model parameter values used for both species are given in Table C-1.

The acslXtreme model code as used to calculate the various dose metrics, followed by the corresponding Matlab model code used to perform the optimizations for fitting of the revised parameters, are given at the end of this appendix. The Matlab code is divided into three .m files: the top-level “optACN2.m” file, a secondary “RunACN.m” file that is called by the opt file and returns the value of the objective function, and an “EqACN.m” file that defines the set of differential equations.

Table C-1. Rat and human PBPK model parameter values

Parameter	Rat value[a]		Human value[a]	
Total BW (kg)	0.25		70	
Percentage of BW				
Liver	4		2.57	
Brain	0.6		2.00	
Stomach	0.63		0.21	
Fat	7		21.42	
Rapidly perfused	3.77		5.22	
Slowly perfused	75		58.58	
Venous blood	3.9		4.35	
Arterial blood	2.1		2.74	
Blood flows (L/h/kg$^{0.74}$)				
Cardiac output	14.0		13.4	
Alveolar ventilation	14.0		12.9	
Percentage of cardiac output				
Liver	25		21.4	
Brain	2.4		11.4	
Stomach	1.3		1.3	
Fat	9		5.2	
Rapidly perfused	47.3		32.5	
Slowly perfused	15		28.2	
GSH content (mmol/L)				
Liver	8.53		5.63	
Brain	2.00		2.99	
Stomach	4.59		3.61	
Rapidly perfused	2.65		2.59	
Slowly perfused	0.75		1.13	
PCs	**AN**	**CEO**	**AN**	**CEO**
Blood:air	512	1,658	154	1,658
Liver:blood	0.46	0.274	1.51	0.274
Brain:blood	0.40	1.407	1.34	1.407
Stomach:blood	0.46	0.274	1.51	0.274
Fat:blood	0.28	0.785	0.94	0.785
Rapidly perfused:blood	0.46	0.274	1.51	0.274
Slowly perfused:blood	0.35	1.853	1.16	1.853
Blood binding (h^{-1})				
Hb (k_{BC}, k_{BC2})	1.245 (*3.66*)	1.134 (*3.33*)	1.245 (*3.66*)	1.134 (*3.33*)
Blood sulfhydryls (k_{FBC}, k_{FBC2})	2.54	0.68	0.0008	0.84
AN oxidation				
V_{maxC} (mg/h/kg$^{0.7}$)	5.0 (*7.1*)		15.6 (*22.1*)	
K_m (mg/L)	1.5 (*2.76*)		0.8	

Table C-1. Rat and human PBPK model parameter values

Parameter	Rat value[a]	Human value[a]
CEO hydrolysis		
V_{maxcC2} (mg/h/kg$^{0.7}$)	---	841 (---)
K_{m2} (mg/L)	---	113 (---)
k_{EHC} (L/h/kg$^{0.7}$)	--- *(3.92)*	--- (*2.20*)
AN-GSH conjugation		
Enzymatic: k_{FC} (h/kg$^{0.3}$)$^{-1}$	73 (*50*)	113 (*77*)
Spontaneous: k_{SO} (mmol/h)$^{-1}$	0.2584	0.2584
CEO-GSH conjugation		
Liver: k_{FC2} (h/kg$^{0.3}$)$^{-1}$	500	197
Brain/liver (k_{FBRC}/k_{FC2})	0.0234	0.0531
Stomach/liver (k_{FSTC}/k_{FC2})	0.0538	0.0641
Rapidly perfused/liver (k_{FRC}/k_{FC2})	0.0311	0.0460
Slowly perfused/liver (k_{FSC}/k_{FC2})	0.00879	0.0201
Oral absorption: Ka (h^{-1})	8.0 *(4.2)*	8.0 *(4.2)*

[a]Revised values used in this assessment are italicized in parentheses.

Sources: Sweeney et al. (2003); Kedderis et al. (1996).

Estimation of Internal Doses Corresponding to Bioassay Exposures

The model code from Sweeney et al. (2003) was modified to enable the explicit definition of desired daily oral intake of AN either as a continuous infusion or in an episodic pattern of up to six episodes (or both continuous and episodic). The continuous-infusion oral exposure rate (STDOSE) is simply calculated as being equal to the total daily exposure (STEADYODOSE*BW, by continuous oral dosing) divided by 24 hours. The episodic exposure is calculated as the drinking water concentration (DRCONC) times the standard drinking water volume (DRVOL, based on BW) times the ratio of actual water consumption to standard consumption (FRACVOL) times the fraction of daily water consumed at episode "I" (DRP(I)), with that quantity added as a bolus to the GI lumen compartment at episode time "I" (DRT(I)). The first episodic exposure time is assumed to be TIME = 0, the same time at which a daily gavage dose (ODOSE*BW) is also administered.

To simulate inhalation exposures as described in Quast (1980b), the model was run to provide 6-hour continuous inhalation exposures, repeating every 24 hours (by setting model variable TCHNG1 = 6.0) for 5 days/week (by setting model variable TCHNG2 = 120, the number of hours in 5 days). Inhalation simulations were run for 800 continuous simulated hours so that the effect of the 5 day/week exposures would be included in the calculation of average lifetime daily AUCs. Study-specific rat BWs were used. In this way the PBPK model accounted for the dynamics of concentration rise at the beginning of each exposure and clearance at the end

of each exposure. The resulting internal dose metrics for inhalation exposure of the rat are listed in Table 5-16.

Rat to Human Extrapolations

For inhalation and oral cancer and oral noncancer effects, similar approaches were used to extrapolate PODs from rats to humans. Following derivation of PODs for noncancer and cancer endpoints, as weekly average concentrations of AN and CEO in rat blood tissue ($C_{I,tissue,rat}(BMCL_{10})$ in mg/L), HECs were then calculated using the human PBPK model and a standard human BW of 70 kg, as the blood or brain concentration, assuming steady-state exposure for a set of predefined exposure levels and that equal internal metrics in rats and humans are associated with the same degree of response. The relationship between exposure level and internal metric as predicted by the human PBPK model was then plotted in Excel and a second-order polynomial of the form, $HEC = a \times C_I^2 + b \times C_I$, where C_I is the internal dose metric, was fit to the relationship for each metric (blood and brain AN and CEO).

Inhalation Exposure

The relationship between inhalation exposure level and internal metric as predicted by the human PBPK model is shown in Figures C-1 and C-2 for AN and CEO, respectively. This polynomial form gave an excellent fit and was fit over a range of concentrations that bracketed the range of $C_{I,tissue,rat}(BMCL_{10})$ for various cases. The resulting polynomials were then used to convert the rat C_I values to human equivalent exposures, reported in Chapter 5 for each toxicity value.

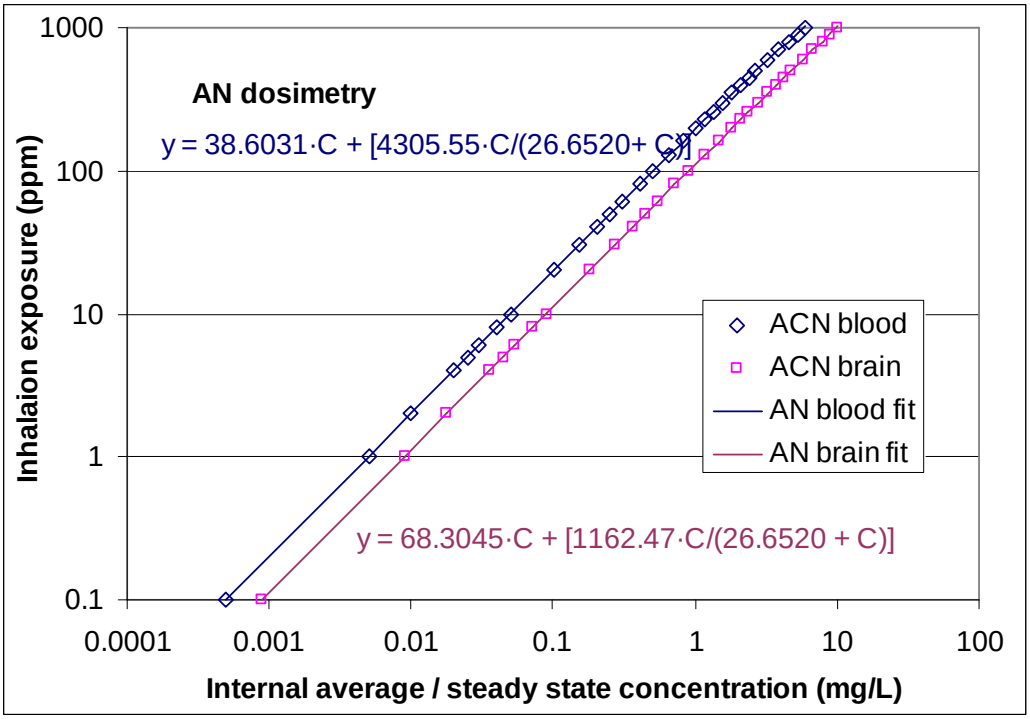

Points are steady-state internal AN concentrations predicted by the human PBPK model for given inhalation exposure concentrations. Curves are polynomial regressions.

Figure C-1. Human inhalation exposure level vs. internal AN concentration.

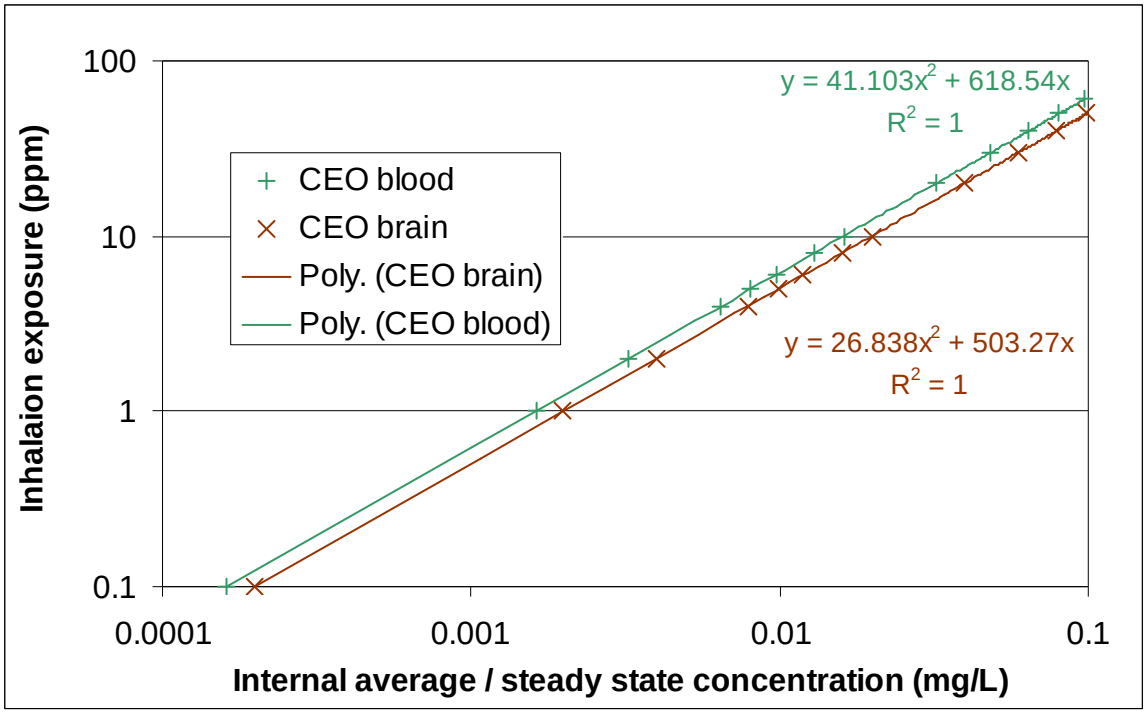

Points are steady-state internal CEO concentrations predicted by the human PBPK model for given inhalation exposure concentrations. Curves are polynomial regressions.

Figure C-2. Human inhalation exposure level vs. internal CEO concentrations.

Oral Cancer Risks

For extrapolation of oral cancer risks from exposure in drinking water, the exact pattern of ingestion of drinking water by the rats in the bioassay was not measured and will be variable among humans. Therefore, the rat PBPK model was used to estimate the internal doses of AN and CEO at the exposure levels of the PODs as determined above (in mg/kg-day ingested), while assuming two distinct exposure patterns that are expected to bound the truth: continuous ingestion and ingestion in six boluses ("episodic").

The continuous pattern is simply described as continuous infusion to the stomach lumen compartment (i.e., 24 hours/day) at a rate equal to the total daily ingestion (at the $BMDL_{10}$). This pattern leads to the lowest predicted peak concentration of any possible pattern that would have the same total ingestion and, therefore, the least saturation of metabolism. The episodic pattern assumes that rats consume their drinking water in six boluses, spaced at 4-hour intervals during each day. The fraction of their total daily ingestion at each of these events is 23.3, 10, 10, 10, 23.3, and 23.4%, respectively. For continuous exposures, the steady-state blood and brain concentrations of AN and CEO were calculated as internal dose metrics, while for the episodic pattern, the daily average concentrations were determined.

Stricker et al. (2003) measured water and food intake by Sprague-Dawley rats on diets containing normal (1%) and high (8%) levels of NaCl. On days 5 and 10 of control exposure, the rats were observed to consume water in 15.9 ± 2.0 and 19.3 ± 2.4 bouts, with amount consumed per bout being 2.1 ± 0.3 and 1.8 ± 0.3 mL, respectively. Thus, actual consumption by rats occurs in many more than six bouts, and the amount consumed per bout is much more uniform than the episodic pattern. The data also show that most of the consumption occurs during the 12-hour dark/waking period (represented by the first and final two boluses in the EPA's pattern), with much less consumed during the light/sleeping period (represented by the second to fourth boluses). Further, data on water consumption relative to controlled meal delivery showed that drinking bouts can last as long as 80 seconds, rather than occurring in an instantaneous bolus. Thus, actual consumption lies between an assumed continuous pattern and the idealized episodic pattern. Because episodic consumption will lead to model prediction of the greatest metabolic saturation, to obtain the desired prediction that represents an upper bound of that behavior (including the possibility that water consumption in the bioassays, which included F344 as well as Sprague-Dawley rats, may have differed from those observed by Stricker at al. [2003]), this idealized episodic pattern rather than one designed to more closely match that reported by Stricker et al. (2003) was chosen. The results of the PBPK simulations for continuous oral infusion vs. an idealized episodic ingestion pattern for various oral BMDL values differed by no more than 7%, indicating that for the rat internal dose metrics, the exact exposure pattern was not significant.

To calculate the HEDs, similarly two alternate assumptions of continuous and episodic exposure to the corresponding rat metrics were applied. For the episodic pattern, it was again assumed that this occurred in six bolus doses but occurring at 0, 3, 5, 8, 11, and 15 hours computation time (i.e., from the time of first ingestion in the morning, assumed to occur at breakfast), with the amount consumed in each bolus being 25, 10, 25, 10, 25, and 5% of the total daily intake, respectively. As with the inhalation extrapolation, the human PBPK model was run using a range of fixed input dose rates (using both continuous and episodic regimens), the resulting internal doses calculated, and then an empirical regression performed in Excel to interpolate between those doses. The resulting simulation values (points) and regressions (lines) are shown in Figures C-3 to C-6.

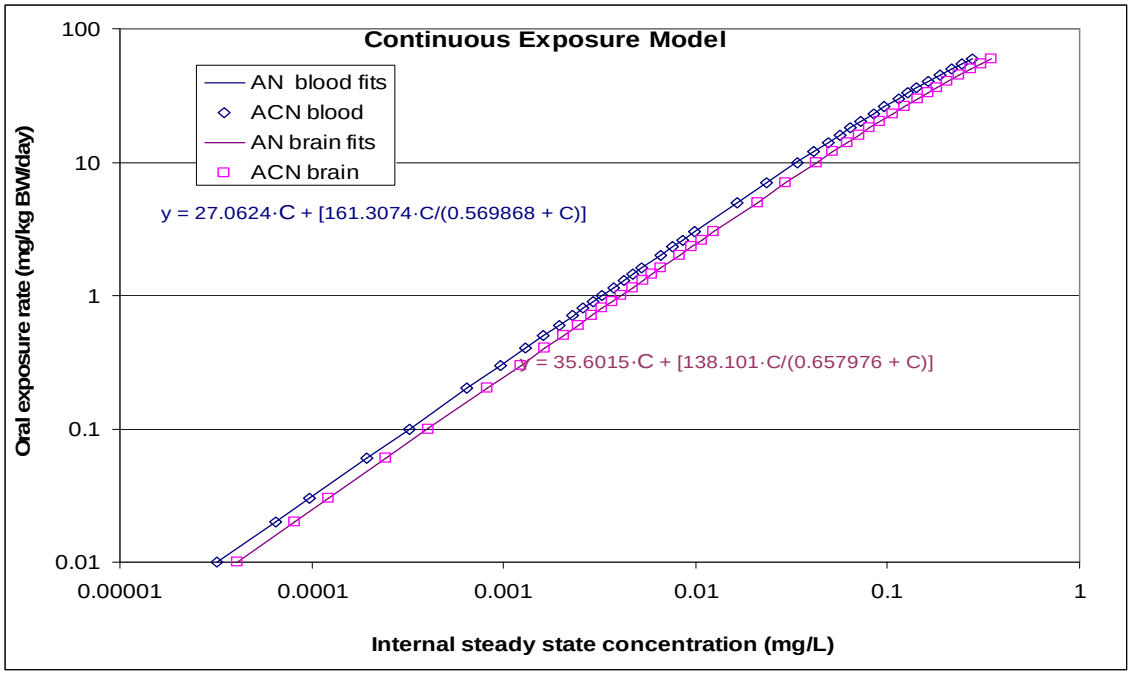

Points are PBPK model predictions; curves are polynomial regressions.

Figure C-3. Human oral exposure level vs. internal AN concentration for continuous exposure.

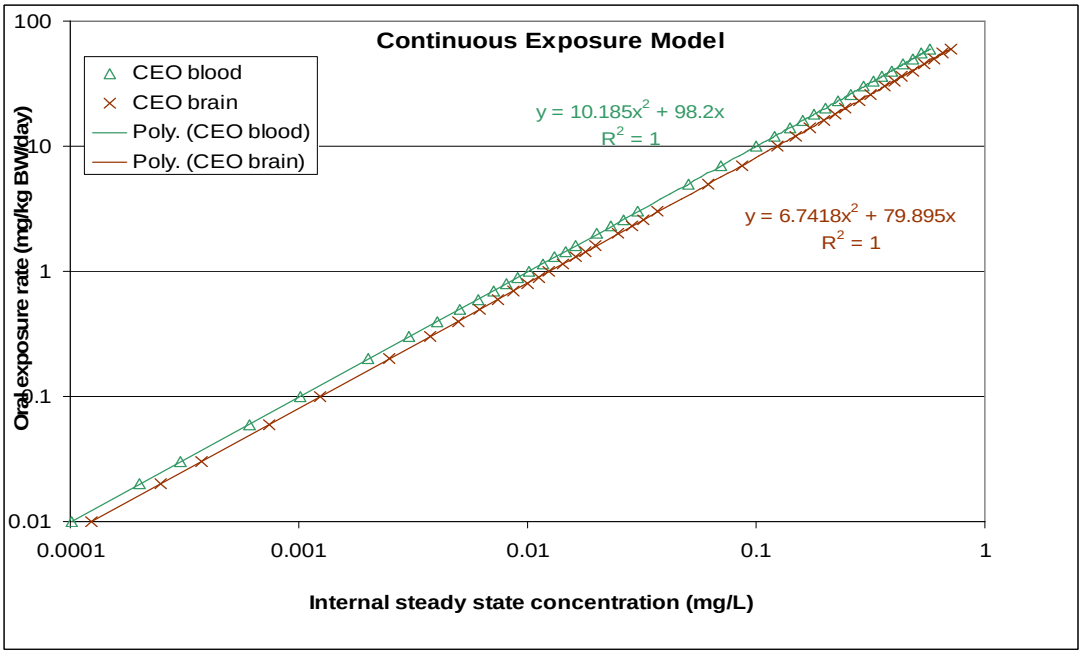

Points are PBPK model predictions; curves are polynomial regressions.

Figure C-4. Human oral exposure level vs. internal CEO concentration for continuous exposure.

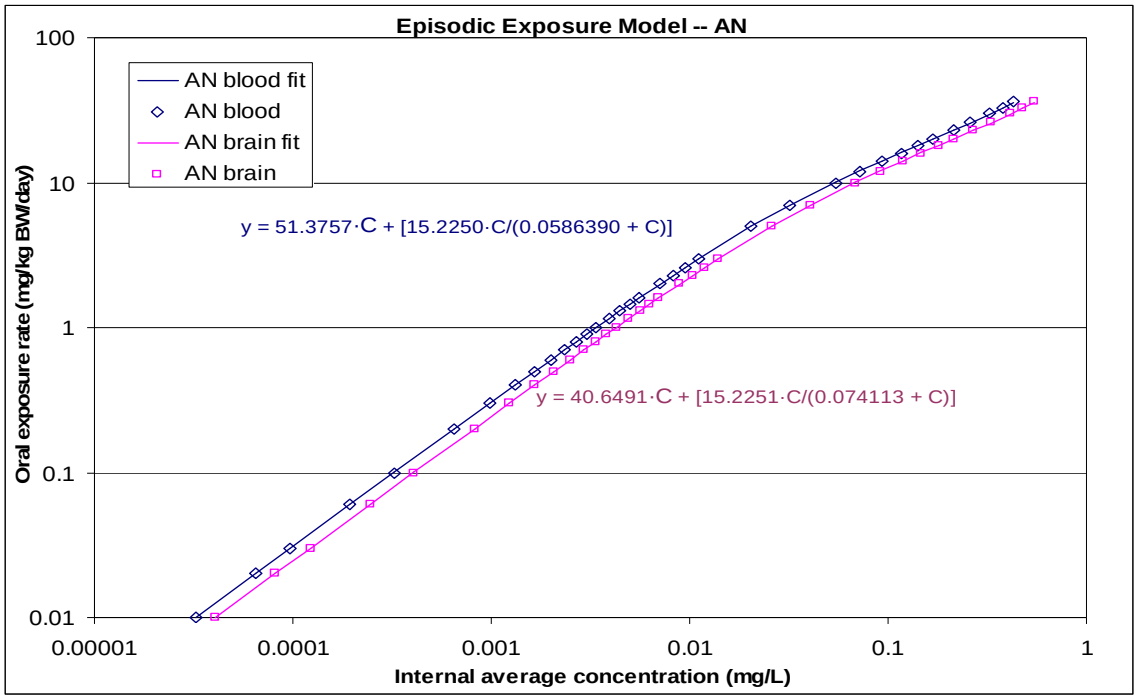

Points are PBPK model predictions; curves are nonlinear regressions.

Figure C-5. Human oral exposure level vs. internal AN concentration for episodic exposure.

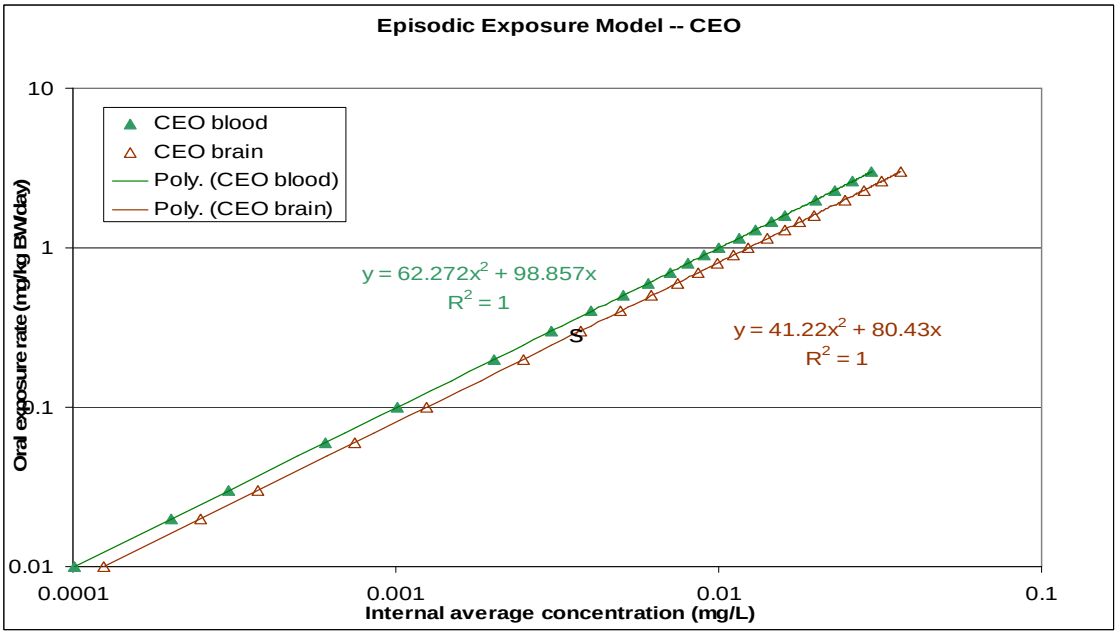

Points are PBPK model predictions; curves are polynomial regressions.

Figure C-6. Human oral exposure level vs. internal CEO concentration for episodic exposure.

acslXtreme Model Source Code

```
PROGRAM
! ACRYLONITRILE and CYANOETHYLENE OXIDE MODEL w/ 1st order epoxide hydrolase
      ! Model of ACN administration and CEO production!
      ! Revised model of G.L. Kedderis!
      ! Original by M.L. Gargas 10/9/89, revised 5/6/92!
      ! Revised 2/21/94 by G.L. Kedderis!
      ! Refined 6/28-7/12/95, 8/8/95 by G.L. Kedderis!
! Modified by SMH - 5/2/97!
! Modified for continuous oral dose by LMS 3/7/00!
!pst2, pr2, and pb2 revised to Kedderis et al 1996 values!
!periodic drinking water reinstated!
!modified for revised human scaling by LMS 7/26/01!
!built blood flow mass balance into equations LMS 7/27/01!
!built blood mass balance into equations, made blood binding!
!rates equal in venous and arterial blood LMS 7/31/01!
!modified to explicitly define DW conc. and daily ACN intake MHL 08/05!
!statement added to calculate daily ACN intake (mg/kg/day) ml 08/05!
! Modified 05/05/06 by Paul Schlosser and Allan Marcus to include!
! Linear-range approximation to epoxide hydrolase model of ACN to CEO!
!and to simplify the oral dosing calculations -- to avoid divide-by-zero!
!errors and allow for either or both continuous and/or periodic exposure!
! June '06 - Jan '07: Other modifications by P. Schlosser to allow both
!continuous and episodic drinking water dosing, and to update default
!parameters for rat

INTEGER I   !counter for drinking water arrays!
REAL DRT(6), DRP(6)     !store drink water times, percents in array!
DIMENSION   A0(16)      !Set of zeros to force values to be >/= 0!
CONSTANT   A0 = 0,0,0,0,0,0,0,0,0,0,0,0,0,0,0,0
CONSTANT   QPC = 14.    ! Alveolar ventilation rate (L/hr)!
CONSTANT   QCC = 14.    ! Cardiac output (L/hr)!
CONSTANT   QLC = 0.25   ! Fractional blood flow to liver!
CONSTANT   QFC = 0.09   ! Fractional blood flow to fat!
CONSTANT   QBRC = 0.024 ! Fractional blood flow to brain!
CONSTANT   QSTC = 0.013 ! Fractional blood flow to the stomach!
CONSTANT   QSC = 0.15   ! Fractional blood flow to slowly perfused tissue

CONSTANT   BW = 0.523   ! Body weight (kg) male rat!
CONSTANT   VLC = 0.04   ! Fraction of liver tissue to total body!
CONSTANT   VRC = 0.0377 ! Fraction of richly perfused tissue to total!
CONSTANT   VSC = 0.75   ! Fraction of slowly perfused tissue to total!
CONSTANT   VBRC = 0.006 ! Fraction of brain tissue!
CONSTANT   VFC = 0.07   ! Fraction of fat tissue!
CONSTANT   VSTC = 0.0063! Fraction of stomach tissue!
CONSTANT   BVC = 0.06   ! Fraction of blood volume!
CONSTANT   VVBC = 0.65  ! Fraction of venous blood volume!

CONSTANT   PBR = 0.40   ! AN brain/blood partition coefficient!
CONSTANT   PBR2 = 1.407 ! CEO brain/blood partition coefficient!
CONSTANT   PL = 0.46    ! AN liver/blood partition coefficient!
CONSTANT   PL2 = 0.274  ! CEO liver/blood partition coefficient!
CONSTANT   PST = 0.46   ! AN stomach/blood partition coefficient!
CONSTANT   PST2 = 0.274 ! CEO stomach/blood partition coefficient!
CONSTANT   PF = 0.28    ! AN fat/blood partition coefficient!
CONSTANT   PF2 = 0.785  ! CEO fat/blood partition coefficient!
CONSTANT   PS = 0.35    ! AN slowly perfused tissue/blood partition!
CONSTANT   PS2 = 1.853  ! CEO slowly perfused tissue/blood partition!
```

```
CONSTANT   PR = 0.46    ! AN rapidly perfused tissue/blood partition!
CONSTANT   PR2 = 0.274  ! CEO rapidly perfused tissue/blood partition!
CONSTANT   PB = 512     ! AN blood/air partition coefficient!
CONSTANT   PB2 = 1658   ! CEO blood/air partition coefficient!

CONSTANT   MW = 53.06   ! ACN molecular weight (g/mol)!
CONSTANT   MW2 = 69.05  ! CEO molecular weight (g/mol)!

CONSTANT   KEHC = 3.92  ! Effective 1st-order EH rate, liter/hr/kg^0.7
CONSTANT   VMAXC = 7.1  ! Maximum velocity of metabolism (mg/hr-1kg)!
CONSTANT   VMAXC2 = 0.0 ! Maximum velocity of metabolism, CEO (mg/hr-1kg)!
CONSTANT   KM = 2.76    ! Michaelis-Menten constant (mg/L)!
CONSTANT   KM2 = 113.   ! Michaelis-Menten constant, CEO (mg/L)!
CONSTANT   KFC = 50     ! ACN first order metabolism rate const (/hr-1kg)!
CONSTANT   KFC2 = 500   ! CEO first order metabolism rate const (/hr-1kg)!
CONSTANT   KSO = 0.2584 ! ACN second order reaction with GSH (L/mMol/hr)!

CONSTANT   GSHL = 8.53  ! Liver GSH conc (mMol/L)!
CONSTANT   GSHBR = 2.   ! Brain GSH (mMol/L)!
CONSTANT   GSHST = 4.59 ! Stomach GSH (mMol/L)!
CONSTANT   GSHS = 0.75  ! Slowly perfused (muscle) GSH (mMol/L)!
CONSTANT   GSHR = 2.65  ! Rapidly perfused GSH (mMol/L)!

CONSTANT   KBC = 3.66   ! ACN 1ST order binding to blood hb (/hr)!
CONSTANT   KBC2 = 3.33  ! CEO 1ST order binding to blood hb (/hr)!
CONSTANT   KFBC = 2.54  ! ACN 1ST order binding to blood RSH (/hr)!
CONSTANT   KFBC2 = 0.68 ! CEO 1ST order binding to blood RSH (/hr)!
CONSTANT   KA = 4.2     ! Oral uptake rate (/hr)!

CONSTANT   IVDOSE = 0.  ! IV dose (mg/kg)!
CONSTANT   CONC = 0.    ! Inhaled concentration (ppm) ACN!
CONSTANT   CONC2 = 0.   ! Inhaled concentration (ppm) CEO!
CONSTANT   ODOSE= 0. ! Oral dose in mg/kg-day, assumed given at t=0, 24, etc.

     ! Timing commands!
CONSTANT   TCHNG1 = 24.0      ! Length of exposure (hrs)!
CONSTANT   TCHNG2 = 120.0     ! Allows for 5 day/week exposure!
CONSTANT   TINF = .003        ! Length of IV infusion (hrs)!

CONSTANT    STEADYODOSE = 0
!daily dose mg/kg-day, if assuming continuous oral infusion

!periodic drinking water section!
CONSTANT DRCONC=0.0           ! Conc. of ACN in drinking water (mg/L)
CONSTANT DRT=0,2,4,6,8,10
      ! Times for multiple oral drinks/day *after* 0
      ! Must be ascending, 0 <= times < 24 hr
      ! DRTIME(1) assumed = 0 and not used
CONSTANT DRP=1,0,0,0,0,0      !Percent consumed by drinking at those times
      ! Bolus of ODOSE*BW + DRPCT(1)*DRDOSE will be given at t=0,24,48, etc.
CONSTANT FRACVOL = 1.0
      ! Actual daily water consumption / nominal or control volume
      ! used when calculating DRDOSE

INITIAL
       DRVOL = 0.102*BW**0.7  ! Water consumption (L/d)
            ! 2L/d water consumption for a 70kg human
      DRDOSE = DRCONC*DRVOL*FRACVOL
   DAYDOSE = ODOSE*BW + DRP(1)*DRDOSE
            ! Once daily oral dose; given at t=0 via initial condition
```

```
      STDOSE = STEADYODOSE*BW/24    ! Steady oral dosing rate in mg/hr
         IVR = IVDOSE*BW/TINF
      NEWDAY = 0; I = 2 ! First dose given as initial condition

      SCHEDULE ORALDOSE.AT.DRT(2)

      ! Scaled parameters!

       QC = QCC*BW**0.74
       QP = QPC*BW**0.74
       QL = QLC*QC
       QF = QFC*QC
      QBR = QBRC*QC
      QST = QSTC*QC
       QS = QSC*QC
       QR = QC-QL-QF-QBR-QS-QST
       VL = VLC*BW
       VF = VFC*BW
      VBR = VBRC*BW
      VST = VSTC*BW
       VS = VSC*BW
       VR = VRC*BW
       BV = BVC*BW
      VAB = BV*(1-VVBC)       !volume arterial blood!
      VVB = BV*VVBC
    GSHRB = GSHBR/GSHL        !ratio of brain GSH to liver GSH!
   GSHRST = GSHST/GSHL        !ratio of stomach GSH to liver GSH!
    GSHRS = GSHS/GSHL         !ratio of slowly perfused GSH to liver GSH!
    GSHRR = GSHR/GSHL         !ratio of richly perfused GSH to liver GSH!
     VMAX = VMAXC*BW**0.7     ! Liver P450 ACN to CEO!
    VMAX2 = VMAXC2*BW**0.7    ! Liver CEO Hydrolysis!
       KF = KFC/BW**0.3       ! Liver ACN-GSH rate!
      KF2 = KFC2/BW**0.3      ! Liver CEO-GSH/RSH rate!
        KEH = KEHC*BW**0.7    ! Approx. first-order rate in liver!
    KFBRC = KFC2*.1*GSHRB     ! CEO brain reaction - 10% GSH ratio!
    KFSTC = KFC2*.1*GSHRST    ! CEO stomach reaction - 10% GSH ratio!
     KFSC = KFC2*.1*GSHRS     ! CEO slowly perfused reaction - 10% GSH ratio!
     KFRC = KFC2*.1*GSHRR     ! CEO richly perfused reaction - 10% GSH ratio!
     KFBR = KFBRC/BW**.3      ! CEO brain RSH rate!
     KFST = KFSTC/BW**.3      ! CEO stomach RSH rate!
      KFS = KFSC/BW**.3       ! CEO SPT RSH rate!
      KFR = KFRC/BW**.3       ! CEO RPT RSH rate!
      KFB = KFBC
     KFB2 = KFBC2
        KB = KBC
      KB2 = KBC2

DAILYDOSE = ODOSE+STEADYODOSE+(DRDOSE/BW)+(AI/BW/(TSTOP/24))
      !daily dose mg/kg-day via oral and/or inhalation routes!

END   !of INITIAL

DYNAMIC
      ALGORITHM IALG = 2      !Gear method for stiff systems!
      MAXTERVAL MAXT = 1.0e-3
      MINTERVAL MINT = 1.0e-9
      CINTERVAL CINT = 0.5

DERIVATIVE
```

```
!-----------------------------------!
!---------  ACRYLONITRILE  ---------!
!-----------------------------------!

      ! CI = Concentration in inhaled air (mg/L)!
   CIZONE = PULSE(0.0,24.0,TCHNG1) * PULSE(0.0,168.0,TCHNG2)
       CI = CIZONE*CONC*MW/24450.

      ! AI = Amount inhaled (mg)!
      RAI = QP*CI
       AI = INTEG(RAI,0)

      ! MR = Amount in stomach lumen (mg)!
            RMR = STDOSE - KA*MR
            AMR = INTEG(RMR,DAYDOSE)
             MR = MAX(AMR, A0(1))   !no negative values!

     ! CAL = Concentration in arterial lung blood (mg/L)!
      CAL = (QC*CVB+QP*CI)/(QC+(QP/PB))

      ! CA = Conc. in systemic arterial blood (mg/l)!
      RAB = QC*(CAL-CA)-(KB+KFB)*AB
       AB = INTEG(RAB,A0(2))
       CA = AB/VAB

      ! AX = Amount exhaled (mg)!
       CX = CAL/PB
    CXPPM = (0.7*CX+0.3*CI)*24450./MW
      RAX = QP*CX
       AX = INTEG(RAX,A0(3))

     ! AST = Amount in stomach tissue (mg)!
     RAST = QST*(CA-CVST) - STGSH + KA*MR
      AST = INTEG(RAST,A0(4))
     CVST = AST/(VST*PST)
      CST = AST/VST
    STGSH = KSO*CVST*GSHST*VST
     ASTG = INTEG(STGSH,A0(5))

      ! AS = Amount in slowly perfused tissues (mg)!
      RAS = QS*(CA-CVS) - SGSH
       AS = INTEG(RAS,A0(6))
      CVS = AS/(VS*PS)
       CS = AS/VS
     SGSH = KSO*CVS*GSHS*VS
      ASG = INTEG(SGSH,A0(7))

      ! AR = Amount in rapidly perfused tissues (mg)!
      RAR = QR*(CA-CVR) - RGSH
       AR = INTEG(RAR,A0(8))
      CVR = AR/(VR*PR)
       CR = AR/VR
     RGSH = KSO*CVR*GSHR*VR
      ARG = INTEG(RGSH,A0(9))

      ! AF = Amount in fat tissue (mg)!
      RAF = QF*(CA-CVF)
       AF = INTEG(RAF,A0(10))
      CVF = AF/(VF*PF)
       CF = AF/VF
```

```
      ! ABR = Amount in brain tissue (mg)!
      RABR = QBR*(CA-CVBR) - BRGSH
       ABR = INTEG(RABR,A0(11))
      CVBR = ABR/(VBR*PBR)
       CBR = ABR/VBR
     BRGSH = KSO*CVBR*GSHBR*VBR
      ABRG = INTEG(BRGSH,A0(12))

    ! AL = Amount in liver tissue (mg)
       RAL = QL*CA + QST*CVST - (QL+QST)*CVL - RAM1 - RAM2 - LGSH
        AL = INTEG(RAL,A0(13))
       CVL = AL/(VL*PL)
        CL = AL/VL
      AUCL = INTEG(CL,0.)
      LGSH = KSO*CVL*GSHL*VL
       ALG = INTEG((LGSH+RAM2+(KB*CVB*VVB)+(KFB*CVB*VVB)),A0(14))

      ! AM1 = Amount metabolized, saturable (P450) and linear pathways (mg)!
      RAM1 = VMAX*CVL/(KM+CVL)
     RAM1M = RAM1*1000/MW
       AM1 = INTEG(RAM1,A0(15))

      ! AM2 = Amount metabolized, first-order pathway (GST) (mg)!
      RAM2 = KF*CVL*VL
       AM2 = INTEG(RAM2,0)

       ! CV = Mixed venous blood concentration (mg/L)!
         IV = IVR*(T<=TINF) ! PULSE(0,24,TINF)
        CV = (QF*CVF + (QL+QST)*CVL + QS*CVS + QR*CVR + QBR*CVBR + IV)/QC

       ! CVB = Mixed venous ACN conc. after binding (mg/L)!
       RVB = QC*(CV-CVB) - (KB+KFB)*VB
        VB = INTEG(RVB,A0(16))
       CVB = VB/VVB

    ! TMASS = mass balance (mg)!
     TMASS = ABR+AF+AL+AS+AR+AST+AM1+AM2+AX+MR+ASTG+ASG+ARG+ABRG+ALG

!---------------------------------------!
!----------------  CEO  ----------------!
!---------------------------------------!

       ! CI2 = Concentration in inhaled air (mg/L)!
            CI2 = CIZONE*CONC2*MW2/24450.

       ! CAL2 = Concentration in arterial lung blood (mg/L)!
        CAL2 = (QC*CVB2+QP*CI2)/(QC+(QP/PB2))

        ! CA2 = Conc. in systemic arterial blood (mg/l)!
        RAB2 = QC*(CAL2-CA2)-(KB2+KFB2)*AB2
         AB2 = INTEG(RAB2,0.)
         CA2 = AB2/VAB

       ! AS2 = Amount in slowly perfused tissues (mg)!
       RAS2 = QS*(CA2-CVS2) - KFS*CVS2*VS
        AS2 = INTEG(RAS2,0.)
       CVS2 = AS2/(VS*PS2)
        CS2 = AS2/VS
```

```
       ! AR2 = Amount in rapidly perfused tissues (mg)!
       RAR2 = QR*(CA2-CVR2) - KFR*CVR2*VR
        AR2 = INTEG(RAR2,0.)
       CVR2 = AR2/(VR*PR2)
        CR2 = AR2/VR

      ! AST2 = Amount in stomach (mg)!
      RAST2 = QST*(CA2-CVST2) - KFST*CVST2*VST
       AST2 = INTEG(RAST2,0.)
      CVST2 = AST2/(VST*PST2)
       CST2 = AST2/VST

       ! AF2 = Amount in fat tissue (mg)!
       RAF2 = QF*(CA2-CVF2)
        AF2 = INTEG(RAF2,0.)
       CVF2 = AF2/(VF*PF2)
        CF2 = AF2/VF

      ! ABR2 = Amount in brain tissue (mg)!
      RABR2 = QBR*(CA2-CVBR2) - KFBR*CVBR2*VBR
       ABR2 = INTEG(RABR2,0.)
      CVBR2 = ABR2/(VBR*PBR2)
       CBR2 = ABR2/VBR

       ! CEO Hydrolysis!
       ! VMAX2 = maximum velocity of metabolism (mg/hr-1kg)!
       ! KM2 = Michaelis-Menten constant (mg/L)!
       ! KEH is parameter for linear metabolism in liver to replace saturable
       ! AL2 = Amount CEO in liver tissue (mg)!
            RAM = RAM1M*MW2/1000.
            RAL2ADD = QL*CA2 + QST*CVST2 + RAM
            RAL2M = VMAX2*CVL2/(KM2+CVL2) + KEH*CVL2
          RAL2 = RAL2ADD - (QL+QST)*CVL2 - KF2*CVL2*VL - RAL2M
        AL2 = INTEG(RAL2,0.)
            CVL2 = AL2/(VL*PL2)
        CL2 = AL2/VL

       ! CV2 = Mixed venous blood concentration (mg/L)!
       CV2 = (QF*CVF2 + (QL+QST)*CVL2 + QS*CVS2 + QR*CVR2 + QBR*CVBR2)/QC

       ! CVB2 = Mixed venous CEO conc. after binding!
            RVB2 = QC*(CV2-CVB2) - (KB2+KFB2)*VB2
            VB2 = INTEG(RVB2,0.)
            CVB2 = VB2/VVB

      ! Calculation of the AUC for ACN and CEO in the brain and blood!
            AUCBR = INTEG(CBR,0.)   ! AUC for ACN brain conc.!
            AUCBR2 = INTEG(CBR2,0.) ! AUC for CEO brain conc.!
            AUCB = INTEG(CVB,0.)    ! AUC for ACN blood conc.!
            AUCB2 = INTEG(CVB2,0.)  ! AUC for CEO blood conc.!
            DAILYSTAUC = INTEG(CST,0.)/(TSTOP/24)     !Mean daily stomach AN
            DAILYST2AUC = INTEG(CST2,0.)/(TSTOP/24)   !Mean daily stomach CEO

     END     ! Derivative
       ! Code that is executed once at each communication interval goes here
CONSTANT   TSTOP = 24.0    ! Length of experiment (hrs)!
TERMT(T.GE.TSTOP, 'checked on communication interval: REACHED TSTOP')

DISCRETE ORALDOSE
      IF (I.EQ.1) THEN
```

```
            AMR = AMR + DAYDOSE     ! Initial dose of day/daily dose
        ELSE
            AMR = AMR + DRP(I)*DRDOSE  ! Drinking percent
        END IF
        I = MOD((I+1),6)
        IF (I.EQ.1) THEN
            SCHEDULE ORALDOSE.AT.NEWDAY     ! Go to start of the next day
            NEWDAY = NEWDAY + 24
        ELSE
            SCHEDULE ORALDOSE.AT.(NEWDAY+DRT(I)) ! Go to next drink time
        END IF

END     ! DISCRETE ORALDOSE

END     ! Dynamic

        TERMINAL    ! Metrics calculated below!
         DAILYBRAUC = AUCBR/(TSTOP/24)      ! Mean daily stomach ACN
        DAILYBR2AUC = AUCBR2/(TSTOP/24)     ! Mean daily stomach CEO
          DAILYBAUC = AUCB/(TSTOP/24)       ! Mean daily blood ACN
         DAILYB2AUC = AUCB2/(TSTOP/24)      ! Mean daily blood CEO

        PEAKPBR = MAX(0, CBR)   ! Peak conc. parent compound in brain!
         PEAKPB = MAX(0, CV)    ! Peak conc. parent compound in blood!
        PEAKMBR = MAX(0, CBR2)  ! Peak conc. metabolite in brain!
         PEAKMB = MAX(0, CV2)   ! Peak conc. metabolite in blood!

        ! Calc. of the avg. values of ACN and CEO in the brain and blood!
        AVEBR = AUCBR/TSTOP     ! Average of ACN brain conc.!
        AVEBR2 = AUCBR2/TSTOP   ! Average of CEO brain conc.!
        AVEB = AUCB/TSTOP       ! Average of ACN blood conc.!
        AVEB2 = AUCB2/TSTOP     ! Average of CEO blood conc.!

        END   ! TERMINAL

END     ! PROGRAM
```

Matlab source code – 3 programs (.m files)

```
% ACN / CEO PBPK model optimization file
%
% Main program, or SHELL for PBPK model.
%
%                   P = optACN2(pin, pvn, datfilename, switch)
%
% swtch = optimization choice (see below)
% pin = values of *all* parameters (input)
% pvn = cell-vector of parameter names TO BE VARIED
% datfilename = name of data file (.csv) to use
% P = values of the output parameters (optimized)
%
% where pin is the vector of paramters to input and swtch determines whether
% to run the  simulation (swtch = 0), or to optimize (swtch = 1 neld2
search).
%
% pvn = {'name1' ; 'name2' ; ... }  Note: use curly brackets and semi-colons

%-------------------------------------------------------------------------
-
function P = optACN(pin,pvn,dfn,sw)
format long
%----------------------------------globalize data sets---------------------
-
global quan phys prs Ypt pv yname itr datfile pvar pbl j1 jf ncv tsp pex
global ICs Ccafpt Ccafc nv Cost C0 ps MW MW2 nv
%-------------------load dat set---------------------
quan.dat=load([dfn,'.csv']);
swtch=sw;
%close all
% The sequence of columns in the data sets are as follows:
% tspan, CVB, CL, CBR, CVB2, CL2, CBR2, ODOSE(initial), IVDOSE(initial) ...
%   % AN-GSH in urine, % CEO-GSH in urine, % Hb-bound material
yname={'CVB';'CL';'CBR';'CVB2';'CL2';'CBR2';'AGSHU';'CGSHU';'PBH';'MassBal'};
ncv=32;
%-------------------------find indeces of parameters to be varied----------
-

pname={'VmaxC';'Km';'VmaxC2';'Km2';'kEHC';'kFC';'kFC2';'kA';'gammA';'gammC';'
kH';'kH2'};
%prs = [5.0;    1;  1.e-18;  113.;  3.9;  73.;  500.;  8.;   1;      1];
%prs = [3.27;.000425;  1.e-18;  113.;  3.9; 95.7; 500.;  8.; .0107;  1];
prs = [.102; 2.76;  1.e-18;  113.;  0.98; 82.3; 14.1; 4.94; .0107;  0.941;
1.245; 1.134];
prs = [2.24; 2.76;  1.e-18;  113.;  0.98; 82.3; 14.1; 4.94; .0107;  0.941;
1.245; 1.134];
%prs = [1.86; 1.5; 1.e-18; 113.;  3.9; 15.7; 2240.;  8.;   .425;  1.10];
%those above are default values
pbl={', ';', ';', ';', ';', ';', ';', ';', ';', ';', ';', ';', ';', '};
% KEHC =     %Effective 1st-order EH rate, liter/hr/kg^0.7
% VMAXC =     %Maximum velocity of metabolism (mg/hr-1kg)%
% VMAXC2 =  %Max. vel. of metabolism, CEO (mg/hr-1kg)%
% KM =       %Michaelis-Menten constant (mg/L)%
% KM2 =     %Michaelis-Menten constant, CEO (mg/L)%
% KFC =      %ACN first order metab rate const (/hr-1kg)%
% KFC2 =    %CEO first order metab rate const (/hr-1kg)%
% KA =       %Oral uptake rate (/hr)%
```

```
fname='EqACN';  % file with set of model equations to use is fname.m
runfn='RunACN';  % Run file runfn.m
quan.ns = length(pname); pv = 1:quan.ns; pvar = pname;
if length(pin)>quan.ns
   error('input parameter vector is too long')
end
if sum(pin) % if pin =[], then no optimization, use default params
    popt=reshape(log(pin),length(pin),1);
    if strmatch('all',pvn,'exact')
        if length(pin)~=quan.ns
            error('length of pin is wrong; must be ',num2str(quan.ns),' to
match pvn =  all')
        end
        prs=pin;
    else
        pvar =  pvn;
        quan.ns = length(pvn);
        pv = zeros(1,quan.ns);
        if (length(pin)~=quan.ns)&(length(pin)~=length(pname))
            error(['Length of pin is wrong; must be ',num2str(quan.ns),...
                ' to match pvn or ',num2str(length(pname)),' to match
pname.'])
        else
            for i = 1:quan.ns
                if strmatch(pvn(i),pname,'exact')
                    pv(i) = strmatch(pvn(i),pname,'exact');
                else
                    error([char(pvn{i}),' is not in the named list of
parameters.'])
                end
            end
        end
        if length(pin)==length(pname)
            prs=pin; popt=popt(pv);
        end
    end
else
    popt=log(prs); swtch=0; 'No pin so running simulation only with default
params.'
end

save pv pv
%-------------------------find indeces of start times---------------
quan.t = quan.dat(:,1);
tci = (quan.t > 0);
datc=quan.dat(:,[2:7,12:14]);   % data columns used for fitting
nv = size(datc,2);   % number of variables to plot, etc
Ccafc=zeros(length(quan.t),(nv+1));
nplt=0;
for i=1:6
    quan.ic{i} = find((datc(:,i)>0) & tci);
    quan.datc{i} = datc(quan.ic{i},i);
    if quan.datc{i}
        nplt=nplt+1;
    end
    quan.tc{i} = quan.t(quan.ic{i});
    quan.nc(i) = sum((datc(:,i)>0) & tci);
end
nplt2=0;
for i=7:nv
```

```
    quan.ic{i} = find((datc(:,i)>0) & tci);
    quan.datc{i} = datc(quan.ic{i},i);
    if quan.datc{i}
        nplt2=nplt2+1;
    end
    quan.tc{i} = quan.t(quan.ic{i});
    quan.nc(i) = sum((datc(:,i)>0) & tci);
end

C0=sum(quan.nc)*(log(2*pi)+1);
quan.mc=datc>0;
sz=length(quan.t);
quan.yc=0*[datc,datc(:,1)];
quan.jt = find(quan.t == 0);
% jt = vector of indeces of rows in data file starting with "0"
quan.idf= length(quan.jt);
quan.jt = [quan.jt;(sz+1)];
% add a pseudo-index to mark the end of the data file
%-----------------------constant parameters---------------------------
ps.KSO = 0.2584;  %ACN second order rxn with GSH (L/mMol/hr)%
ps.GSHL = 8.53;   %Liver GSH conc (mMol/L)%
ps.GSHBR = 2.;    %Brain GSH (mMol/L)%
ps.GSHST = 4.59;  %Stomach GSH (mMol/L)%
ps.GSHS = 0.75;   %Slowly perfused (muscle) GSH (mMol/L)%
ps.GSHR = 2.65;   %Rapidly perfused GSH (mMol/L)%

%ps.KB = 1.245 + 2.54;     %ACN 1ST order binding to blood hb + RSH (/hr)%
ps.KB0 = 2.54;     %ACN 1ST order binding to blood hb + RSH (/hr)%
ps.KB0
%ps.KH = 1.245;
ps.KFB = 2.54;
%ps.KB2 = 1.134 + 0.68 + 0.413;
ps.KB20 = 0.68 + 0.413;
%ps.KH2 = 1.134;
phys.KHR = 1.134/1.245;
ps.KFB2 = 0.68;
    %CEO 1ST order binding to blood hb + RSH + chem. hydrol. (/hr)%

ps.tinf=.003; %blood infusion time (hr)
% ACN PCs
phys.PL = 0.46;     % liver:blood PC
phys.PST = 0.46;    % stomach tissue:blood PC, also used for GI
phys.PBR = 0.40;    % brain tissue:blood PC
phys.PF = 0.28;    % fat tissue:blood PC
phys.PS = 0.35;    % slowly tissue:blood PC
phys.PR = 0.46;     % richly tissue:blodd PC
phys.PB = 512;     % blood tissue:blodd PC

%CEO PCs
phys.PL2 = 0.274;     % liver:blood PC
phys.PST2 = 0.274;    % stomach tissue:blood PC, also used for GI
phys.PBR2 = 1.407;    % brain tissue:blood PC
phys.PF2 = 0.785;    % fat tissue:blood PC
phys.PS2 = 1.853;    % slowly tissue:blood PC
phys.PR2 = 0.274;     % richly tissue:blodd PC
phys.PB2 = 1658;     % blood tissue:blodd PC

QPC = 14.;  %Alveolar ventilation rate (L/hr)%
QCC = 14.;  %Cardiac output (L/hr)%
```

```
QBRC = 0.024;   % blood flow to brain
QSTC = 0.013;   % Blood flow rate for stomach tissue (portal vein)
QFC = 0.09;     % blood flow to fat tissue
QLC = 0.25;     % Blood flow rate for liver )
QSC = 0.15;     % Blood flow rate for slowly

phys.BW=0.25; %body weight
VLC = 0.04;     %Fraction of liver tissue to total body%
VRC = 0.0377;   %Fraction of richly perf tiss to total%
VSC = 0.75;     %Fraction of sloly perf tiss to total%
VBRC = 0.006;   %Fraction of brain tissue%
VFC = 0.07;     %Fraction of fat tissue%
VSTC = 0.0063;  %Fraction of stomach tissue%
BV = 0.06*phys.BW;   %Blood vol%
VVBC = 0.65;    %Fraction of venous blood vol%

MW = 53.06;    %ACN molecular weight (g/mol)%
MW2 = 69.05;   %CEO molecular weight (g/mol)%

%---------------- preset varying parameters --------------------------
phys.QC = QCC*phys.BW^0.74;
phys.QP = QPC*phys.BW^0.74;
phys.QBR = QBRC*phys.QC;    % blood flow to brain
phys.QST = QSTC*phys.QC;    % Blood flow rate for stomach tissue (portal
vein)
phys.QS = QSC*phys.QC;  % Blood flow rate for slowly
phys.QL = QLC*phys.QC;  % Blood flow rate for liver (hepatic artery)
phys.QF = QFC*phys.QC;  % blood flow to fat
phys.QR = phys.QC-phys.QL-phys.QF-phys.QBR-phys.QS-phys.QST;
phys.VBR = VBRC*phys.BW;     % brain volume (L)
phys.VST = VSTC*phys.BW;     % GI volume (use RP density)
phys.VL = VLC*phys.BW;
phys.VF = VFC*phys.BW;
phys.VBR = VBRC*phys.BW;
phys.VST = VSTC*phys.BW;
phys.VS = VSC*phys.BW;
phys.VR = VRC*phys.BW;
phys.VAB = BV*(1-VVBC);       %volume arterial blood%
phys.VVB = BV*VVBC;
phys.GSHRB = 0.1*ps.GSHBR/ps.GSHL;    %ratio of brain GSH*GST to liver GSH%
phys.GSHRST = 0.1*ps.GSHST/ps.GSHL;   %ratio of stomach GSH*GST to liver GSH%
phys.GSHRS = 0.1*ps.GSHS/ps.GSHL;     %ratio of spt GSH*GST to liver GSH%
phys.GSHRR = 0.1*ps.GSHR/ps.GSHL     %ratio of rpt GSH*GST to liver GSH%

ICs=[];
for i=1:quan.idf  % idf is the number of simulations/initial conditions in
    j1(i) = quan.jt(i); % index of initial data row for this
experiment/simulation
    jf(i) = quan.jt(i+1)-1; % index of final data row for this
expt./simulation
    tsp{i} = quan.t(j1(i):jf(i));
    oral0=quan.dat(j1(i),8)*phys.BW;
    ps.blood0(i)=quan.dat(j1(i),9)*phys.BW/ps.tinf;
    ps.cinh(i)=quan.dat(j1(i),10)*MW/24450; ps.tinh(i)=quan.dat(j1(i),11);
    ICs=[ICs;[oral0,zeros(1,ncv-1)]]; % initial conditions
end
save ICs ICs

%----------call simulation or optimization procedure-----------------
```

```
quan.pt=0; itr=0; P=prs;
if swtch==0
    quan.pt=1;
    y=eval([runfn,'(popt)']);
elseif swtch==1
    pnew = exp(neld2(popt, runfn, 1e-6, 1000, 50000));
else
   options = optimset('MaxFunEvals',8000,'MaxIter',8000);
   pnew = exp(fminsearch(runfn,popt,options));
end

if swtch>0
    P(pv) = pnew(1:quan.ns);
   'Initial Parameter Values, Jinit ='
   Cst=eval([runfn,'(popt)']);
   'Final Parameters, Jopt ='
   quan.pt=1;
   Cst=eval([runfn,'(log(P(pv)))']);
end

%----------------- final results/plots -------------------
co =
['rbkgmcrbkgmcrbkgmcrbkgmcrbkgmcrbkgmcrbkgmcrbkgmcrbkgmcrbkgmcrbkgmcrbkgmcrbk
gmcrbkgmcrbkgmcrbkgmc'];
%co = ['kkkkkkkkkkkkkkkkkkkkkkkkkkkkkkkkkkkkkkkkkkkkk'];
pc =
['+o*xsd^v<>ph+o*xsd^v<>ph+o*xsd^v<>ph+o*xsd^v<>ph+o*xsd^v<>ph+o*xsd^v<>ph+o*
xsd^v<>ph+o*xsd^v<>ph'];
linet = ['- ';'--';': ';'-.';'- ';'--';': ';'-.';'- ';'--';': ';'-.';...
    '- ';'--';': ';'-.';'- ';'--';': ';'-.';'- ';'--';': ';'-.';...
    '- ';'--';': ';'-.';'- ';'--';': ';'-.';'- ';'--';': ';'-.';...
    '- ';'--';': ';'-.';'- ';'--';': ';'-.';'- ';'--';': ';'-.';...
    '- ';'--';': ';'-.';'- ';'--';': ';'-.';'- ';'--';': ';'-.';...
    '- ';'--';': ';'-.';'- ';'--';': ';'-.';'- ';'--';': ';'-.';...
    '- ';'--';': ';'-.';'- ';'--';': ';'-.';'- ';'--';': ';'-.';...
    '- ';'--';': ';'-.';'- ';'--';': ';'-.';'- ';'--';': ';'-.'];
np=min(quan.idf,96);
quan.jtp = [find(quan.tp == 0);(length(quan.tp)+1)];
% jt = vector of indeces of rows in data file starting with "0"; plus one
%close all
kf0=30;
kf=1+kf0;
figure(kf)
rows=ceil(nplt/2);
set(kf,'Units','inches','Position',[0.1, 0.5, 6.3, (0.1+2.5*rows)]);
set(gcf,'DefaultTextFontSize',10,'DefaultAxesFontSize',12,'DefaultTextFontNam
e','Arial');
npt = -1;
for k = 1:6
   if quan.datc{k}
       npt=npt+2;
       pos=mod(npt,(rows*2))+(npt>(rows*2));
       h=subplot(rows,2,pos);
       set(h,'Units','inches','Position',[(3.5-
2.95*mod(pos,2)),(0.45+2.35*(rows-ceil(pos/2))),2.7,2.1])
       box on
       j1=quan.jt(1);
       j2=quan.jt(2)-1;
       p1=quan.jtp(1);
       p2=quan.jtp(2)-1;
```

```
        dt=quan.t(j1:j2);
        dp = datc(j1:j2,k);
        dj = find(dp > 0);
        dk=find(datc(:,k)>0);
        xm=ceil(1.01*max(quan.t( dk ))*10)/10;
        xl=floor(0.99*min(quan.t( dk )*10)-1)/10;
        if xl<0
            xl = - round(2.5*xm)/100;
        end
        ym=max(log10(1.1*[Ccafpt(find(Ccafpt(:,k)>0),k);datc(dk,k)]));
        if (10^ceil(ym))/(10^ym) > 2
            ym = (10^ceil(ym))/2;
        else
            ym = 10^ceil(ym);
        end
        set(gca,'YScale','log')
         if k==1
            axis([xl,xm,.03,ym])
         end
         if k==2
            axis([xl,xm,.01,ym])
         end
         if k==3
            axis([xl,xm,.01,ym])
         end
         if k==4
            axis([xl,xm,.001,ym])
         end
         if k==5
            axis([xl,xm,.001,ym])
         end
         if k==6
            axis([xl,xm,.001,ym])
         end
         hold on
         if dj
            plot(dt(dj),dp(dj),['k',pc(1)]); %,[co(1),pc(1)])
            plot(quan.tp(p1:p2),Ccafpt(p1:p2,k),['k',linet(1,:)]);
%[co(1),linet(1,:)]);
         end
         if np > 1
            for i = 2:np
                j1=quan.jt(i);
                j2=quan.jt(i+1)-1;
                dt=quan.t(j1:j2);
                p1=quan.jtp(i);
                p2=quan.jtp(i+1)-1;
                dp = datc(j1:j2,k);
                dj = find(dp > 0);
                if dj
                    plot(dt(dj),dp(dj),['k',pc(i)]); %,[co(1),pc(1)])
                    plot(quan.tp(p1:p2),Ccafpt(p1:p2,k),['k',linet(i,:)]);
%[co(1),linet(1,:)]);
                end
            end
         end
        yl=0.1*get(gca,'YLim');
        title(yname(k),'Position',[mean(get(gca,'XLim')),yl(2)],'FontSize',14,
...
            'EdgeColor','k','BackgroundColor','w','Fontname','Arial');
```

```
       if k==2
           legend('show')
       end
       hold off
   end
end

kf=2+kf0;
if quan.datc{7}
    figure(kf);
    set(kf,'Units','inches','Position',[0.1, 0.5, 3.3, 7.6]);

set(gcf,'DefaultTextFontSize',14,'DefaultAxesFontSize',12,'DefaultTextFontNam
e','Arial');
    for k = 7:9
       h=subplot(3,1,k-6);
       set(h,'Units','inches','Position',[.55,(0.45+2.35*(9-k)),2.7,2.1])
       box on; hold on
       dk=find(datc(:,k)>0);
       plot(quan.dat(dk-1,8),datc(dk,k),['k',pc(k-6)]); %,[co(1),pc(1)])
       plot(quan.dat(dk-1,8),Ccafc(dk,k),['k',linet(k-6,:)]);
%[co(1),linet(1,:)]);
       yl=0.3*get(gca,'YLim');
       title(yname(k),'Position',[mean(get(gca,'XLim')),yl(2)],'FontSize',14,
...
           'EdgeColor','k','BackgroundColor','w','Fontname','Arial');
       hold off
   end
end


k=nv+1; % show mass balance
figure(k)
set(k,'Units','inches','Position',[1,1,4.1,4.1]);
hold on
title(yname(k));
p1=quan.jtp(1);
p2=quan.jtp(2)-1;
plot(quan.tp(p1:p2),Ccafpt(p1:p2,k),[co(1),linet(1,:)]);
for i = 2:np
    p1=quan.jtp(i);
    p2=quan.jtp(i+1)-1;
    plot(quan.tp(p1:p2),Ccafpt(p1:p2,k),[co(i),linet(i,:)]);
end

if swtch>0
'optimized params = '
[num2str([1:length(P)]'),char(pbl),char(pname),char(pbl),num2str(P)]
end
```

```
%RunACN file to return value of objective function, given input parameters
function Cost = RunACN(popt)
%-----------------------------globals-------------------------
global phys prs yname quan itr pv pvar pbl j1 jf ian ICs ncv tsp Ccafpt C0
global Cost Ccafc MW MW2 VMAX VMAX2 KF KF2 KEH KFBRC KFSTC KFSC KFRC KFBR
global KFST KFS KFR KA KM KM2 Ccafpt nv ps
tol=1.e-8;
options = odeset('RelTol',tol,'AbsTol',tol);
itr=itr+1;
```

```
comp=0;
p = reshape(exp(popt),length(popt),1);
pu=prs;
pu(pv)=p;
save ptemp pu
[num2str(pv'),char(pbl(pv)),char(pvar),char(pbl(pv)),num2str(p)]
%quan.gam(1:5)=2./exp(exp(-popt((quan.ns+1):(quan.ns+5)) ));
%quan.gam(6:11)=quan.gam(5);
%quan.gam(1:5)
% display current values of parameters being valued (retransformed)
Ccafpt=[];Ccafw=[];
quan.tp=[];
comp=comp+1;

VMAXC = pu(1); %Max. vel. of metabolism, CEO (mg/hr-kg^0.7)%
KM = pu(2);     %Michaelis-Menten constant (mg/L)%
VMAXC2=pu(3);   %Max. vel of metabolism, CEO (mg/hr-jg^0.7)
KM2=pu(4);      %CEO M-M constant (mg/L)
KEHC = pu(5);   %Effective 1st-order EH rate, liter/hr/kg^0.7
KFC = pu(6);    %ACN first order metab rate const (/hr-1kg)%
KFC2 = pu(7);   %CEO first order metab rate const (/hr-1kg)%
KA = pu(8);     %Oral uptake rate (/hr)%
gA = min(pu(9),2);     % gammA
gC = min(pu(10),2);    % gammC
ps.KH = pu(11);
ps.KHR2 = pu(12);
ps.KB = ps.KH + ps.KB0;     %ACN 1ST order binding to blood hb + RSH (/hr)%
ps.KH2 = ps.KH*phys.KHR*ps.KHR2;
ps.KB2 = ps.KH2 + ps.KB20
%    VMAX = VMAXC*(phys.BW^0.7);   %Liver P450 ACN to CEO%
    VMAX2 = VMAXC2*(phys.BW^0.7);  %Liver CEO Hydrolysis%
       KF = KFC/(phys.BW^0.3);     %Liver ACN-GSH rate%
      KF2 = KFC2/(phys.BW^0.3);    %Liver CEO-GSH/RSH rate%
      KEH = KEHC*(phys.BW^0.7);    % Approx. first-order rate in liver %
    %CEO rxn rates%
     KFBR = KF2*phys.GSHRB;     %CEO brain RSH rate%
     KFST = KF2*phys.GSHRST;    %CEO stomach RSH rate%
      KFS = KF2*phys.GSHRS;     %CEO SPT RSH rate%
      KFR = KF2*phys.GSHRR;     %CEO RPT RSH rate%

%-------------------------------loop for running equations-------------------
-
% figure(15)
% set(15,'Units','inches','Position',[1,1,4.1,4.1]);
% hold on
% title('RAM1');
for i=1:quan.idf  % idf is the number of simulations/initial conditions in
             % the data file this was computed in optACN.m
ian=i;

tsc = [0:1050]'*quan.t(jf(i))/1000;
%ICs(i,[1,16])
[ts,Ys] = ode15s(@EqACN2,tsc,ICs(i,:),options); %
%[ts(1:4),Ys(1:4,1:16)]'
%[Ys(1:10,13),VMAX*Ys(1:10,13)./(KM+Ys(1:10,13)),(Ys(2:11,15)-Ys(1:10,15))]
massb=sum(Ys(:,1:16),2);
% plot(ts,Ys(:,15)); %VMAX*Ys(:,13)./(KM+Ys(:,13)));

% The sequence of columns in the data sets are as follows:
```

```
% tspan, CVB, CL, CBR, CVB2, CL2, CBR2, ODOSE(initial), IVDOSE(initial)
Yp=[Ys(:,16)/phys.VVB, Ys(:,13)/phys.VL, Ys(:,11)/phys.VBR, ...
    Ys(:,24)/phys.VVB, Ys(:,23)/phys.VL, Ys(:,22)/phys.VBR, ...
    Ys(:,30:32)/phys.BW, massb];

Ccafc(j1(i):jf(i),:)=interp1(ts,Yp,tsp{i});
quan.tp=[quan.tp;ts];
Ccafpt=[Ccafpt;Yp];
Ccafw=[Ccafw;[tsp{i},Ccafc(j1(i):jf(i),:)]];
%--------------------------------end loop---------------------------------
end
%--------------------------------------------------------------------------
-
if quan.pt==1
     yname = {'AN in blood'; 'AN in liver'; 'AN in brain'; ...
         'CEO in blood'; 'CEO in liver'; 'CEO in brain'; ...
         'AN-GSH in urine'; 'CEO-GSH in urine'; 'Hb binding'; 'mass
balance'};
     fid=fopen(['ACN.txt'],'w');
     fprintf(fid,['time','\t','CVB','\t','CL','\t','CBR','\t',...
             'CVB2','\t','CL2','\t','CBR2','\t','mball','\r']);
     fprintf(fid,'%g\t%g\t%g\t%g\t%g\t%g\t%g\t%g\r',Ccafw');
%[quan.tp,Ccafpt]');
    status=fclose(fid);
end
%Ccafpt=Ccafc;quan.tp=quan.t; % uncomment this line to plot only the fitted
%values
%--------------------------------cost function----------------------------
-
Cost=C0+max(0,pu(9)-2)+max(0,pu(10)-2);gamm=[gA gA gA gC gC gC gC gC gC];
for i=1:nv
    if quan.datc{i}
        Cost = Cost + gamm(i)*sum(quan.datc{i}) + ...
        quan.nc(i)*log( sum( ((quan.datc{i} - Ccafc(quan.ic{i},i)).^2)./...
        (Ccafc(quan.ic{i},i).^gamm(i)) )/quan.nc(i) );
    end
end

['itr = ',num2str(itr),';  Cost = ',num2str(Cost)]
```

```
% ACN PBPK model equation file -- returns derivatve dx = dx/dt, given
% state variable x and parameters passed through global statements
%
%-----------------------------function defined--------------------------
function dx = eqs(t,x)
%-----------------------------globals----------------------------
global prs  phys ICs quan ps ian MW2 MW CINH TINH
global VMAX VMAX2 KF KF2 KEH KFBRC KFSTC KFSC KFRC KFBR KFST KFS KFR KA KM
KM2

%--------------------------assign parameters to names----------------------
dx=zeros(size(x));
% "dx" = dx/dt, where x is the state vector

%-----------------------------------!
%---------  ACRYLONITRILE  ---------!
%-----------------------------------!
```

```
% MR = x(1);  %MR = Amount in stomach lumen (mg)!
% AB = x(2);  %Amount in systemic arterial blood (mg)!
    CA = x(2)/phys.VAB; %concentration
%AX = x(3);  % ACN exhaled (mg)!
%AST = x(4); % ACN in stomach tissue tissue (mg)!
    CST = x(4)/phys.VST; CVST = CST/phys.PST; % tissue/venous concn's
%ASTG = x(5); % ACN GSH conjugated in stomach tissue (mg)
%AS = x(6); % ACN in slowly perfused (mg)
    CVS = x(6)/(phys.VS*phys.PS); % venous concentration
%ASG = x(7); % ACN-GSH conjugated in slowly (mg)
%AR = x(8); % ACN in richly (mg)
    CVR = x(8)/(phys.VR*phys.PR); % venous concentration
%ARG = x(9); % ACN-GSH conjugated in richly
%AF = x(10); % ACN in fat (mg)
    CVF = x(10)/(phys.VF*phys.PF); % venous concentration
%ABR = x(11); % ACN in brain (mg)
    CBR = x(11)/phys.VBR; CVBR = CBR/phys.PBR; % tissue/venous concn's
%ABRG = x(12); % ACN-GSH conjugated in brain
%AL = x(13); % ACN in liver (mg)
    CL = x(13)/phys.VL; CVL = CL/phys.PL; % tissue/venous concn's
% ALG = x(14); ACN-GSH conjugated in liver (mg)
% AM1 = x(15); ACN metabolized by P450 in liver (mg)
% AVB = x(16); ACN in mixed venous blood (mg)
    CVB = x(16)/phys.VVB; % concentration

RMR = KA*x(1); % rate of absorption from stomach
CI=ps.cinh(ian)*(t<=ps.tinh(ian)); %Inhaled concentration
CAL = (phys.QC*CVB+phys.QP*CI)/(phys.QC+(phys.QP/phys.PB));
    %CAL = Concentration in arterial lung blood (mg/L)!
%CX = CAL/phys.PB; % concentration in exiting pulmonary air
% CXPPM = (0.7*CX+0.3*CI)*24450./ps.MW
%RAB = ps.KB*x(2)CA*phys.VAB; % ACN binding in arterial blood
STGSH = ps.KSO*CVST*ps.GSHST*phys.VST; % stomach GSH conjugation of ACN
SGSH = ps.KSO*CVS*ps.GSHS*phys.VS; % slowly GSH conjugation of ACN
RGSH = ps.KSO*CVR*ps.GSHR*phys.VR; % richly GSH conjugation of ACN
BRGSH = ps.KSO*CVBR*ps.GSHBR*phys.VBR; % brain GSH conjugation of ACN
LGSH = ps.KSO*CVL*ps.GSHL*phys.VL; % liver GSH conjugation of ACN
% ACN metabolized,saturable (P450) and linear pathways (mg)!
     RAM1 = VMAX*CVL/(KM+CVL); % (mg/hr)
     %VMAX,KM,RAM1
%ACN metabolized,first-order pathway (GST) (mg)!
     RAM2 = KF*CVL*phys.VL; % (mg/hr)
RTV =
phys.QF*CVF+(phys.QL+phys.QST)*CVL+phys.QS*CVS+phys.QR*CVR+phys.QBR*CVBR;
    % mixed venous blood concentration
%RVB = ps.KB*CV*phys.VVB; % ACN binding in venous blood
 %[t,CVB/(RTV/phys.QC),CAL/CVB,CA/CAL,x(1),RMR]
 dx(1) = - RMR; % ACN stomach lumen
 dx(2) = phys.QC*(CAL - CA) - ps.KB*x(2); % ACN arterial blood after binding
 dx(3) = phys.QP*CAL/phys.PB; % ACN exiting pulmonary air
 dx(4) = phys.QST*(CA-CVST) - STGSH + RMR; % ACN stomach tissue
 dx(5) = STGSH; % ACN-GSH conjugated in stomach tissue
 dx(6) = phys.QS*(CA-CVS) - SGSH; % ACN slowly
 dx(7) = SGSH; % ACN-GSH conjugated in slowly
 dx(8) = phys.QR*(CA-CVR) - RGSH; % ACN in richly (mg)
 dx(9) = RGSH; % ACN-GSH conjugated in richly
dx(10) = phys.QF*(CA-CVF); % ACN in fat (mg)!
dx(11) = phys.QBR*(CA-CVBR) - BRGSH; % ACN in brain (mg)!
```

```
dx(12) = BRGSH; % ACN-GSH conjugated in brain
dx(13) = phys.QL*CA + phys.QST*CVST -(phys.QL+phys.QST)*CVL -RAM1 -RAM2 -
LGSH;
dx(14) = LGSH + RAM2 + ps.KB*(x(2)+x(16));
    % ACN-GSH conjugated in liver + bound in blood
dx(15) = RAM1; % ACN metabolized by P450 in liver
dx(16) = RTV - phys.QC*CVB - ps.KB*x(16) + ps.blood0(ian)*(t<=ps.tinf);
    %Mixed ven. ACN conc after binding (mg/L)
dx(30) = STGSH + SGSH + RGSH + BRGSH + LGSH + RAM2 + ps.KFB*(x(2)+x(16));
    % amount of AN binding to GSH
 % [x(1:16),dx(1:16)]'
%---------------------------------------!
%----------------  CEO  ----------------!
%---------------------------------------!

%AB2 = x(17); % CEO in arterial blood (mg)
    CA2 = x(17)/phys.VAB; % concentration
%AS2 = x(18); % CEO in slowly perfused (mg)
    CVS2 = x(18)/(phys.VS*phys.PS2); % venous concn
    SGSH2 = KFS*CVS2*phys.VS;
%AR2 = x(19); % CEO in richly (mg)
    CVR2 = x(19)/(phys.VR*phys.PR2); % venous concn
    RGSH2 = KFR*CVR2*phys.VR;
%AST2 = x(20); % CEO in stomach tissue tissue (mg)!
    CST2 = x(20)/phys.VST; CVST2 = CST2/phys.PST2; % tissue/venous concn's
    STGSH2 = KFST*CVST2*phys.VST;
%AF2 = x(21); % CEO in fat (mg)
    CVF2 = x(21)/(phys.VF*phys.PF2); % venous concn
%ABR2 = x(22); % CEO in brain (mg)
    CBR2 = x(22)/phys.VBR; CVBR2 = CBR2/phys.PBR2; % tissue/venous concn's
    BRGSH2 = KFBR*CVBR2*phys.VBR;
%AL2 = x(23); % CEO in liver (mg)
    CL2 = x(23)/phys.VL; CVL2 = CL2/phys.PL2; % tissue/venous concn's
% AVB2 = x(24); % Mixed ven. CEO conc after binding!
    CVB2 = x(24)/phys.VVB; % concentration

RALG2 = (VMAX2*CVL2/(KM2+CVL2)) + KF2*CVL2*phys.VL;
    % CEO hydrolysis, saturable + linear terms
    % For fitting, either saturable or linear is set to zero
CV2 = (phys.QF*CVF2 + (phys.QL+phys.QST)*CVL2 + phys.QS*CVS2 + phys.QR*CVR2
...
    + phys.QBR*CVBR2)/phys.QC; % CEO mixed venous blood conc. (mg/L)

CAL2 = (phys.QC*CVB2)/(phys.QC+(phys.QP/phys.PB2)); % CEO in arterial lung
blood (mg/L)!

dx(17) = (phys.QC*CAL2)-(phys.QC*CA2)-(ps.KB2*x(17));
    % CEO in systemic arterial after binding
dx(18) = phys.QS*(CA2-CVS2) - SGSH2; % CEO in slowly perfused tissues (mg)!
dx(19) = phys.QR*(CA2-CVR2) - RGSH2; % CEO in rapidly perfused tissues (mg)!
dx(20) = phys.QST*(CA2-CVST2) - STGSH2; % CEO in stomach (mg)!
dx(21) = phys.QF*(CA2-CVF2); % CEO in fat tissue (mg)!
dx(22) = phys.QBR*(CA2-CVBR2) - BRGSH2; % CEO in brain tissue (mg)!
dx(23) = phys.QL*(CA2-CVL2) + phys.QST*(CVST2-CVL2) - KEH*CVL2*phys.VL + ...
    (RAM1*MW2/MW) - RALG2;
dx(24) = phys.QC*CV2 - phys.QC*CVB2 - ps.KB2*x(24);
    % CEO mixed venous after binding

%Calculation of the AUC for ACN and CEO in liver, brain, and blood!
```

```
dx(25) = CL;   % AUC for ACN liver concentration
dx(26) = CBR;  % AUC for ACN brain conc.!
dx(27) = CBR2; % AUC for CEO brain conc.!
dx(28) = CVB;  % AUC for ACN blood conc.!
dx(29) = CVB2; % AUC for CEO blood conc.!

dx(31) = STGSH2 + SGSH2 + RGSH2 + BRGSH2 + RALG2 + ps.KFB2*(x(17)+x(24));
    % amount of CEO binding to GSH

dx(32) = (ps.KH*(x(2)+x(16))) + (ps.KH2*(x(17)+x(24)));


% had problems with state variables going < 0 at one point (stiff system);
% the following is a fix for this.

%dx=(dx.*(x>=0))+(abs(dx).*(x<0));
```

APPENDIX D. UNCERTAINTIES ASSOCIATED WITH CHEMICAL-SPECIFIC PARAMETERS EMPLOYED IN THE PBPK MODEL FOR AN DOSIMETRY IN HUMANS

PBPK models are computational tools used to predict chemical/drug disposition. Models are comprised of three distinct types of information: physiological, physicochemical, and biochemical. The physiological data are chemically independent and describe such parameters as organ volumes and blood flows. Physicochemical parameters are chemical specific and specify parameters, such as PCs or permeability. Biochemical parameters define the rates of chemical transformation or binding. In Appendix D, the EPA evaluates uncertainties in the chemical-specific parameters employed in the PBPK model used to predict AN dosimetry in humans, which is adapted from that of Sweeney et al. (2003). Only a small number of (metabolic) parameters were changed in the EPA's adaptation, which will be noted below. Otherwise, it should be understood that any discussion of the model of Sweeney et al. (2003) applies to the one used in this assessment.

PCs

PCs describe the extent of distribution of chemical into the body, including target tissues such as the brain and lungs. PCs employed in the model of Sweeney et al. (2003) were derived from rat tissue:air PCs and human blood:air PC for AN or CEO in the following way:

$$P_{tissue:blood}(human) = P_{tissue:air}(rat)/ P_{blood:air}(human)$$

This equation assumes that the relative difference in PCs between tissues is the same in rats as in humans. The systematic difference between the two is accounted for by the blood:air PC; for humans, the experimentally determined value for AN (154) differed from the value for the rat (512) by threefold. Due to the absence of experimental data, Sweeney et al. (2003) set the human blood:air PC for CEO equal to the rat value (1,658).

It may be asked whether the estimates produced by the above equation are reasonable considering the chemical characteristics of AN and CEO and the distribution of AN- and CEO-soluble components in human tissue. To address these issues, the method of Poulin and Theil (2002) was used to estimate the $P_{tissue:blood}$(human). The method is based on the additive solubilities of a chemical in lipid and water, and the relative distribution of these substances in tissues. Sensitivity analysis conducted by Sweeney et al. (2003) identified the $P_{stomach:blood}$ and $P_{brain:blood}$ for AN as influential on AN-related dose metrics and the $P_{brain:blood}$ for CEO as influential on CEO-related dose metrics. Table D-1 provides estimates of PCs for AN and CEO. Note that the critical PCs, the $P_{stomach:blood}$ for AN and the $P_{brain:blood}$ for AN and CEO, as predicted by the method of Poulin and Theil were within a factor of about 1.5 of the values employed by Sweeney et al. (2003).

Table D-1. Tissue:blood PCs

PCs for AN				PCs for CEO			
	Comp[a]	**Exp[b]**	**Exp:comp ratio**		**Comp[a]**	**Exp[b]**	**Exp:comp ratio**
Adipose tissue	0.30	0.94	3.11	Adipose tissue	0.22	0.79	3.52
Brain	1.12	1.34	1.19	Brain	0.99	1.40	1.41
Stomach	1.00	1.51	1.52	Stomach	0.89	0.27	0.31
Liver	1.02	1.51	1.48	Liver	0.94	0.27	0.31
Muscle	0.98	1.16	1.19	Muscle	0.83	1.84	1.97
Richly perfused	1.00	1.51	1.51	Richly perfused	0.97	0.27	0.28

[a]Computationally derived by Poulin and Theil (2002).
[b]Experimentally obtained/reported by Sweeney et al. (2003).

To evaluate the influence of the PC in the model, the revised human PBPK model was implemented with both sets of PCs (Table D-1, with $P_{blood:air}$ as measured for AN using human blood and for CEO using rat blood). For three different exposure scenarios, the peak AN and CEO did not change by more than 30% of initial value (Table D-2). This finding may be explained by consistency between both estimates of PC and a general lack of sensitivity to the PC (see Sweeney et al., 2003). Indeed, the only PCs with normalized sensitivity coefficients that exceeded 0.2 were the $P_{stomach:blood}$ (AN), $P_{brain:blood}$ (AN), and the $P_{brain:blood}$ (CEO). Consistent with these results, Table D-2 shows a greater impact of changing the PC in the brain than the blood (an averaged effect of other PCs). All of the predicted concentration in brain tended to decrease when the model was implemented with PC as per the method of Poulin and Theil (2002).

Table D-2. Impact of method of estimation of PCs on the peak AN and CEO model predictions

Exposure	PC method[a]	Peak AN (μg/L)		Peak CEO (μg/L)	
		Blood	Brain	Blood	Brain
Inhalation 2 ppm, 8 h	S	4.87	11.4	0.998	1.23
	PT	4.87	9.56	0.998	0.863
		0.0%	-16.4%	0.0%	-29.6%
Inhalation 0.4 ppm, 1 wk	S	0.975	2.29	0.200	0.245
	PT	0.975	1.91	0.200	0.173
		0%	-16.4%	0%	-29.6%
Oral 6 pulses in 24 h, 0.2 mg/kg total	S	2.50	3.11	8.36	10.14
	PT	2.68	2.77	8.64	7.44
		7.3%	-10.9%	3.4%	-26.7%

[a]S = PCs as estimated by Sweeney et al. (2003) (listed in Appendix C); PT = PCs estimated using the method of Poulin and Theil (2002). AN and CEO are from model simulations using other human parameters as listed in Appendix C.

Parameters of metabolic clearance

Sweeney et al. (2003) developed a PBPK model of AN and CEO disposition in humans based on human in vitro data and the rat model of Kedderis et al. (1996). Human in vivo pharmacokinetic data were not available for model development; therefore, the authors proposed a rodent-human parallelogram approach to consider uncertainties in the scaling of in vitro metabolism data. Critical metabolic pathways included the oxidation of AN to CEO, the conjugation of AN and CEO, and the hydrolysis of CEO.

With the exception of the latter, the scaling of in vitro rate constants for these pathways was first investigated by Kedderis et al. (1996), who observed that the scaled rate constants (rat model) derived from rat liver microsomes, did not match those constants fit from in vivo rat data. Sweeney et al. (2003) employed both in vitro and in vivo data to derive an empirical correction factor (CF) to account for uncertainties in scaling (rat). The scaling constant was assumed to be constant across species; thus, the preexisting rat model, the empirical CF, and human in vitro data were employed to specify a human PBPK model.

Because EPA altered a number of the rat metabolic parameters to accommodate the rate constant for AN hydrolysis extrapolated from in vitro data and to obtain parameters in a way that was computationally reproducible, while following the same approach as Sweeney et al. (2003) for metabolic parameter extrapolation, the EPA obtained different values for humans. First, we describe the derivation of the human V_{maxC} for the oxidation of AN to CEO in the following equations. The ratio of rates determined by human in vitro data and rat in vitro data is considered (Kedderis et al. 1993c), as well as the allometrically scaled in vivo rate constant for oxidation of AN in the rat.

$$\underset{\text{in vivo}}{V_{max\,C}(\text{human})\ (mg/h/kg^{0.7})} = \underset{\text{in vivo}}{V_{max\,C}(\text{rat})\ (mg/h/kg^{0.7})} \times \left(\frac{BW_{human}}{BW_{rat}}\right)^{0.3} \times \left(\frac{[mgMSP/g\ liver]_{human}}{[mgMSP/g\ liver]_{rat}}\right) \times \left(\frac{VLC_{human}}{VLC_{rat}}\right) \times \left(\frac{V_{max,human}}{V_{max,human}}\right)_{\text{in vitro}}$$

$$22.1 = 7.1 \times 5.422 \times 1.4225 \times 0.6425 \times 0.626$$

Next, the value (and calculations) of the empirical CF = 5.785 is shown. This value represents what is not accounted for in the in vitro to in vivo scaling in the rat.

$$CF_{in\ vivo\ /\ in\ vitro} = \underset{in\ vivo}{V_{max\,C}(rat)\ (mg/h/kg^{0.7})} \Big/ \left(\underset{in\ vitro}{V_{max\,C}(rat)\ (mg/h/kg^{0.7})} \times [mgMSP/g\ liver]_{rat} \times \frac{10^3 g}{kg} \times VLC_{rat} \times BW_{rat}{}^{0.3}\right)$$

$$5.785 = 7.1 / (0.001164 \times 40 \times 1000 \times 0.04 \times 0.659)$$

The allometrically scaled in vivo rate constant for human pseudo first-order GSH conjugation of AN and CEO was calculated in the same way (not shown).

The parallelogram method was applied differently to estimate the rate constant for enzymatic hydrolysis by EH in humans. Because the EPA extrapolated the EH rate constant in rats from in vitro to in vivo without use of an adjustment factor, the same was done for humans. Kedderis and Batra (1993) determined a V_{max} and K_m EH-mediated hydrolysis of CEO using liver microsome samples from six individual humans. The lowest estimated K_m in the group was 600 μM, so the EPA chose to describe the metabolism as first-order since in vivo concentrations are expected to stay well below that value, using the ratio of V_{max}/K_m. The ratio of V_{max}/K_m was first calculated for each individual since V_{max} and K_m tend to be statistically correlated due to the way they are estimated, and an average value for the ratio was then determined to be 7.02×10^{-6} L/minute/mg MP. We can then apply the value of 56.9 mg MP/g liver from Lipscomb et al. (2003), the liver fraction of 25.7 g/kg BW, and the standard value of 70 kg BW for a human. The rate constant for a standard human is then k_{EH} = (7.02×10^{-6} L/minute/mg EH) × (56.9 mg MP/g liver) × (25.7 g liver/kg BW) × (70 kg BW) × (60 minutes/hour) = 43.1 L/hour, and assuming it also scales as $BW^{0.7}$ (because it represents V_{max}/K_m, with K_m assumed constant), $k_{EHC} = k_{EH} \div (0.70\ kg)^{0.7}$ = 2.20 L/hour-$kg^{0.7}$.

The parallelogram approach described by Sweeney et al. (2003) is provocative, considering that human in vivo pharmacokinetic data are sparse for many compounds. What special assurances are required in using this approach?

First, what is the basis of the empirical CF? It is the basis to account for: (1) artifacts of microsomes that may bias the estimation of rate constants (as suggested by Kedderis et al., 1996) or (2) decay in activity due to handling and storage. An analysis by Lipscomb et al. (1998) compared the in vivo V_{max} that would be obtained by directly extrapolating the in vitro metabolism of trichloroethylene to the value obtained by fitting in vivo data and found that the

in-vitro-derived value came out to about one half of an in-vivo-fitted value. Thus, it appears that a CF is appropriate to account for either or both of these factors. Sweeney et al. (2003) applied the same approach to the enzyme-catalyzed GSH conjugation (cytosolic in origin). One concern that had existed is that Sweeney et al. (2003) had been forced to assume that the same factor holds for distinct enzymes (P450 and EH) that are membrane bound, because EH activity in the rat was taken to be zero in the original model of Kedderis et al. (1996), but that assumption is no longer required since the EPA was able to extrapolate the EH-mediated activity without adjustment. The EPA must still assume that the factors for P450 and GST hold across species, but, given that the in-vitro enzyme preparations and measurements of activity were made in the same way for both animals and humans, this seems a reasonable assumption. Nevertheless, it does represent a source of uncertainty.

The human PBPK model (with the EPA's revised parameters) can be tested by comparing the data of Jakubowski et al. (1987) with mass-balance calculations from the PBPK model (Table D-3). Unfortunately, there are some significant discrepancies between the data of Jakubowski et al. (1987) and these simulations. The respiratory retention (nominally in the lung) of AN from subjects exposed through a face mask ranged from 44 to 58%, with an average of 51.8%. The PBPK model predicts 99% uptake of AN inhaled to the pulmonary region. Recognizing that ~30% of inhaled air only enters the conducting airways (so-called “dead space”), the PBPK model effectively predicts a retention of 69%, which is considerably higher than measured. The respiration rates of the subjects in the Jakubowski et al. (1987) experiment ranged from 366 to 625 L/hour, with an average of 508 L/hour, which corresponds to an alveolar ventilation rate of 356 L/hour, while the PBPK model utilized a rate of 300 L/hour (for a 70-kg person), but increasing the respiration rate in the model by this amount (while holding all other parameters constant) only decreases the alveolar uptake fraction from 98.7 to 98.5%. A possible explanation is that AN is subject to a considerable “wash-in/wash-out” effect, where some of the material inhaled deposits temporarily in the conducting airways and then desorbs on expiration, which is not accounted for in the model.

Table D-3. PBPK mass balance predictions for an 8-hour human exposure to 2 ppm AN

Parameter	Metric	Amount (mg)	Percent
AI	AN mass inhaled	10.389	
AX	AN mass exhaled	0.133	1.3
ATi	AN final tissue mass (including blood)	0.725	7.0
AMt	AN metabolized by …	5.102	49.1
AMo	AN oxidized	3.904	37.6
AMgt	AN enzymatically conjugated (in liver)	0.280	2.7
AMgn	AN non-enzymatically conjugated	0.918	8.8
	Metabolic mass balance (AMo + AMgt + AMgn)/AMt	*100.00%*	
ABD	AN bound to Hb and sulfhydrils	4.429	42.6
	Total AN mass balance (AX + ATi + AMt + ABD)/AI	*100.00%*	
CMo	CEO formed from AN oxidation[a]	5.080	
CX	CEO mass exhaled	0.001	0.0
CTi	CEO final tissue mass	0.097	1.9
CEH	CEO hydrolyzed	1.128	22.2
CCl	CEO conjugated in liver	2.596	51.1
Ccti	CEO conjugated in other tissues	0.283	5.6
CBD	CEO bound to Hb and sulfhydrils	0.975	19.2
	CEO mass balance (Cti + CEH + CCl + Ccti + CBD)/CMo	*100.00%*	

[a]$CMo = AMo \times MW_{CEO} \div MW_{AN}$.

The subjects of Jakubowski et al. (1987) were then exposed in a chamber for 8 hours to an average of 10.8 or 5.6 mg/m^3 (5 or 2.6 ppm), and the total excretion of CEO in the urine was found to be an average of 26.4 or 16.3% of the retained dose (portion not exhaled) at those respective exposure levels. The PBPK model predicts that 38% of the retained AN is oxidized to CEO and that 22% of that CEO is hydrolyzed, with these fractions being fairly constant at ≤8 ppm. Assuming that all the hydrolysis product was excreted in the urine, that the acid-extraction method of Jakubowski et al. (1987) would have reversed the hydrolysis, and that the extraction/HPLC technique would have separated that product from the GSH conjugates and other metabolites, the predicted urinary excretion of "CEO" would then be 8.4% of the retained dose. Alternately, if it is assumed that all CEO conjugated with GSH was excreted in the urine and that the method of Jakubowski et al. (1987) had cleaved the GSH conjugates, then the total CEO predicted in the urine would be 79% of the CEO formed or 30% of the retained AN. Therefore, the measured CEO excretion as a fraction of the retained dose is bracketed by the predicted levels, depending on what is assumed about the assay method. These results indicate that the model predictions of AN and CEO metabolism in humans subsequent to absorption are at least in the right range.

Kedderis et al. (1996) suggest that the overestimation of CEO by the rat model at the early time points (which also occurs in the EPA's revision) may be due to an intrahepatic first

pass effects, as occurs with other epoxides formed in situ from their parent olefins (Filser and Bolt, 1984). The introduction of such a structure ("privileged access" as coined by Kohn and Melnick, 2000) would contribute to the efficient clearance of CEO; however, whether the needed differential reduction of CEO levels in the early phase would also be accomplished is not clear. The issue is that the model predicts a very rapid rise for CEO in blood to peak/plateau levels (Figure 3-5a, top panels), while the data show a gradual rise over the first ~10 minutes. It is not evident that a privileged access model would account for this dynamic difference since the current model allows for reaction of AN with GSH in stomach tissue and liver before reaching the general circulation. Further, the same lack-of-fit occurs vs. the CEO i.v.-exposure data shown in Figure 3-3, which could not be explained by a first-pass effect from GI absorption.

An alternate explanation is that the model currently assumes constant GSH levels, while GSH may be depleted during the early part of the exposure. A model that includes this depletion could predict that at very short times when GSH is near control levels, relatively little AN would remain unconjugated for conversion to CEO, but, as the depletion occurs, more and more AN would be available for oxidative conversion to CEO, hence the gradual rise. To accurately calibrate parameters that accomplish intrahepatic clearance would require a description of GSH kinetics.

Thus, the inability to fit the rat blood CEO levels over the entire time course and the lack of understanding of the biological basis for those kinetics indicate a level of uncertainty in the model that could be addressed through further research. While the model's overprediction of AN absorption in humans indicates that the description of gas uptake could be improved, this discrepancy is only 10–30% (much less than the apparent 3- to 10-fold overprediction of blood and brain CEO levels in rats and [likely] in humans by the oral route). However the model does predict AN and CEO blood and tissue levels from inhalation exposure in rats at the lowest concentration measured (186 ppm) quite well (Figure 3-4a), indicating that the gas-uptake description is adequate for prediction of rat dosimetry, and an adjustment of the description in humans would lower the predicted uptake and hence the extrapolated risk. Therefore, the use of the model to predict CEO levels after AN inhalation in humans should be adequately protective. For oral exposures, however, the greater accuracy of the AN predictions vs. CEO (Figure 3-5b vs. 3-5a), suggests greater certainty in the use of AN, although the mode of action suggests that CEO is the active metabolite.

Sensitivity and Uncertainty Analysis

Sensitivity and uncertainty analyses were performed to investigate the dependence of PBPK model predictions for AN and CEO on specific model parameters and to estimate the overall uncertainty in those predictions, given estimates of uncertainty in specific model parameters.

The first step was to perform a sensitivity analysis on PBPK model predictions to identify the degree to which model dose metric predictions depend on model parameters. For this purpose, normalized sensitivity coefficients were calculated. For example, the sensitivity of a model prediction of concentration (e.g., AN concentration in blood) to parameter P (e.g., metabolic V_{maxC} for AN oxidation), the normalized sensitivity coefficient is:

$$S = (dC/dP) \times (P/C)$$

The first term is the derivative of C with respect to P. (C is generally a function of time, so this derivative will also depend on time.) This derivative is approximated by alternately increasing and decreasing P by a small fraction, ΔP (taken to be 1% of P here) and calculating $[C(P + \Delta P) – C(P – \Delta P)] \div (2 \times \Delta P)$. The second term normalizes the sensitivity with respect to the value of C at the normal value of P and with respect to P, essentially yielding the percent change in C given a 1% change in P. These sensitivities typically vary between ±1, where values near 1 show high sensitivity and values near 0 show low sensitivity.

Sensitivities were determined for four dose metrics, the blood and brain concentrations of AN and CEO, under an inhalation and an oral exposure scenario for the human PBPK model. For simplicity, the EPA considered continuous exposures to either 0.4 ppm AN by inhalation or an oral absorption rate equal to 1 mg/kg-day and analyzed the values of these metrics at 24 hours, by which time, the human body is predicted to reach steady state. Under such conditions, the AUC for each metric is just 24 hours times the steady-state concentration (subsequent to reaching steady state), and hence, the sensitivity of the AUC is identical to the sensitivity of the concentration, given that the coefficients are normalized as described above. Since these concentrations are in the linear range of the model, they apply across the low-dose, linear range of concentrations. The sensitivity coefficients for each parameter for which at least one coefficient had absolute value greater than 0.1 are listed in Tables D-4 and D-5 for the inhalation and oral scenarios, respectively.

Table D-4. Sensitivity of AN and CEO metrics for continuous inhalation exposure

Parameter	Dose metrics[a] (concentrations)			
	AN in blood	AN in brain	CEO in blood	CEO in brain
Q_{CC}	**-0.49**	**-0.57**	**0.51**	**0.64**
Q_{PC}	**0.99**	**0.99**	**0.99**	**0.98**
V_{LC}	-0.01	-0.01	**-0.64**	**-0.64**
V_{BRC}	-0.01	-0.04	-0.04	*-0.14*
V_{SC}	*-0.14*	*-0.10*	**-0.28**	**-0.28**
V_{ABC}	-0.07	-0.07	*-0.12*	*-0.15*
V_{VBC}	*-0.12*	-0.08	**-0.20**	**-0.20**
Q_{LC}	**-0.76**	**-0.53**	**0.65**	**0.65**
Q_{BRC}	0.00	0.03	0.00	*0.10*
Q_{SC}	-0.02	-0.01	*-0.10*	*-0.10*
GSH_L	0.00	0.00	**0.27**	**0.38**
GSH_{BR}	-0.01	-0.04	-0.04	*-0.14*
GSH_S	*-0.13*	-0.09	**-0.27**	**-0.27**
V_{maxC}	-0.09	-0.06	*0.11*	*0.11*
K_m	0.09	0.06	*-0.11*	*-0.11*
k_{FC2}	0.00	0.00	**-0.86**	**-0.96**
k_{EHC}	0.00	0.00	**-0.25**	**-0.25**
k_{BC}	*-0.19*	*-0.16*	*-0.16*	*-0.16*
k_{BC2}	0.00	0.00	*-0.13*	*-0.15*
P_{BR}	0.00	**0.97**	0.00	0.00
P_{BR2}	0.00	0.00	0.00	**1.00**

[a]Values are normalized sensitivity coefficients (i.e., $(dC/dP) \times (P/C)$, for sensitivity of concentration C to parameter P) for steady state blood and brain concentrations predicted for humans during an exposure to 0.4 ppm AN. Sensitivities are approximated by increasing and decreasing each parameter by 1% of its default value. Values of 0.2 or greater are indicated in bold and values between 0.1 and 0.2 in italics. Parameters for which all coefficients are less than 0.1 are omitted.

Table D-5. Sensitivity of AN and CEO metrics for continuous oral exposure

Parameter	Dose metrics[a] (concentrations)			
	AN in blood	**AN in brain**	**CEO in blood**	**CEO in brain**
BW	**0.21**	**0.20**	**0.24**	**0.24**
Q_{CC}	**0.30**	**0.36**	**0.27**	**0.39**
V_{LC}	-0.07	-0.07	**-0.64**	**-0.64**
V_{BRC}	-0.01	-0.04	-0.03	*-0.13*
V_{SC}	*-0.10*	*-0.10*	*-0.19*	*-0.19*
V_{VBC}	*-0.12*	*-0.12*	*-0.13*	*-0.13*
Q_{LC}	**0.29**	**0.29**	**0.35**	**0.35**
GSH_L	0.00	0.00	**0.27**	**0.38**
GSH_{BR}	-0.01	-0.04	-0.03	*-0.13*
GSH_S	-0.09	-0.09	*-0.18*	*-0.18*
V_{maxC}	**-0.89**	**-0.89**	*0.11*	*0.11*
K_m	**0.89**	**0.89**	*-0.11*	*-0.11*
k_{FC2}	0.00	0.00	**-0.86**	**-0.96**
k_{EHC}	0.00	0.00	**-0.25**	**-0.25**
k_{BC}	*-0.17*	*-0.19*	-0.01	-0.01
k_{BC2}	0.00	0.00	*-0.13*	*-0.15*
P_{BR}	0.00	**0.97**	0.00	0.00
P_{BR2}	0.00	0.00	0.00	**1.00**

[a]Values are normalized sensitivity coefficients (i.e., $(dC/dP) \times (P/C)$, for sensitivity of concentration C to parameter P), for steady state blood and brain concentrations predicted for humans during a continuous oral infusion equal to 1 mg/kg-d. Sensitivities are approximated by increasing and decreasing each parameter by 1% of its default value. Values of 0.2 or greater are indicated in bold, and values between 0.1 and 0.2 in italics. Parameters for which all coefficients are less than 0.1 are omitted.

The EPA's results can be compared to those of Sweeney et al. (2003), derived for the original model, with previous parameter values. For the inhalation scenario (Table D-4), the EPA's results for AN are essentially identical to those of Sweeney et al. (2003), and those for CEO show the same qualitative pattern and only have a few notable differences. The sensitivity to the rate constant for CEO hydrolysis (k_{EHC} in the EPA's model; V_{maxC2} in Sweeney et al., 2003) is -0.25 in the revised model and −0.5 in their previous model, indicating somewhat less importance for this parameter now. On the other hand, the sensitivity to CEO-GSH conjugation in the liver parameterized by k_{FC2} increased from ~0.6−0.7 for Sweeney et al. (2003) to ~0.9 with the revised model, showing more significance now. Thus, there is a shift in the relative importance of these two parameters and the rate constant for GSH conjugation in humans is an especially important factor in the EPA's predictions, while the exact rate of CEO hydrolysis is less influential, though still somewhat important.

Important factors in comparing the EPA's results for an oral exposure to those of Sweeney et al. (2003) are that the EPA held the dose in mg/kg-day constant, so that it varied in proportion to BW when that parameter was varied, while Sweeney et al. (2003) held the dose in mg/day constant, and they calculated sensitivities of the AUC and peak concentrations for only the AN metrics, while the EPA used steady-state concentrations of AN and CEO. Thus, it is not surprising that Sweeney et al. (2003) had a negative sensitivity to BW, since the same total dose given to a larger body would result in a lower concentration, while the EPA's is positive, reflecting that a proportionately higher dose is expected to yield higher-than-proportional concentrations because the rates of metabolic elimination scale as $BW^{0.7}$.

It is interesting to note that the liver volume (fraction), which effects the rates of first- and second-order reactions in the model, and the rate constants for CEO removal but not CEO production (V_{maxC}) significantly affect the CEO metrics (absolute values from Sweeney et al. (2003) are about 0.17–0.18 for sensitivity of CEO metrics to V_{max} and K_m). The EPA's lack of significant dependence on blood flow rates to stomach (Q_{StC}) and slowly-perfused tissues (Q_{SC}) is due to the fact that the EPA is analyzing a continuous infusion, as these do significantly affect the peak concentration after a bolus exposure. Thus, these are only important for specific dosing scenarios.

Likewise the rate of absorption (k_A) from the stomach significantly affects the peak concentration (verified but not shown for the revised model) but has a much smaller affect on the AUC. These results for absorption are not surprising, since changes in k_A do not alter the fact that the entirety of an oral bolus is predicted to be absorbed. Whether or not there is an impact on the steady-state concentrations depends on what one believes about oral absorption. In particular, if one assumes 100% absorption, where the rate of absorption increases with the amount in the GI tract, then at steady state, the rate of absorption must equal the rate of ingestion and the exact rate of absorption is unimportant. It is only if orally ingested material may be eliminated in the feces or otherwise transformed in the gut without absorption that the exact rate constant for absorption would be important.

Finally, uncertainty in these steady-state model predictions was estimated using the equation of Sweeney et al. (2003) for the approximate coefficient of variation (CV):

$$CV_m = \sqrt{\sum_i \left(S_{mi}^{\ 2} \cdot CV_i \right)}$$

where CV_m is the estimated CV for metric "m," S_{mi} is the sensitivity coefficient of metric "m" to parameter p_i, as tabulated above, and CV_i is the CV of p_i. For this calculation, the EPA decided to use the individual parameter CV values as estimated and used by Sweeney et al. (2003, see Table 3-5 in that paper). The CVs for physiological parameters (e.g., blood flow rates, tissue fractions) would indeed be identical, and, while the EPA reestimated some metabolic parameters

and k_A, the underlying in vitro data on which the human extrapolation is based are the same, and hence, they are expected to be approximately the same.

The resulting CV values for the EPA's four metrics under the two exposure scenarios are listed in Table D-6.

Table D-6. Estimated CVs for AN and CEO metrics

Exposure scenario	Dose metrics (concentrations)			
	AN in blood	AN in brain	CEO in blood	CEO in brain
0.4 ppm inhalation	0.620	0.656	0.893	1.15
1 mg/kg-d oral	0.790	0.873	0.711	1.01

The overall CVs in Table D-6 are interesting in themselves, in that they indicate the overall level of confidence in the model's prediction of those dose metrics. But even more interesting is the contribution of the individual parameters to each of these metrics, as listed in Tables D-7 and D-8. What those contributions show is that the vast majority of the uncertainty arises from a small number of parameters and that most of those parameters are physiological values—alveolar ventilation (Q_{CC}), cardiac output (Q_{PC}), and blood flow to the liver (V_{LC})—and the brain:blood PC in the case of the brain metrics.

Table D-7. Parameter contributions to overall CVs for inhalation exposure

Parameter	Dose metrics[a] (concentrations)			
	AN in blood	**AN in brain**	**CEO in blood**	**CEO in brain**
Q_{CC}	**9.3**	**11.5**	**5.0**	4.6
Q_{PC}	**37.9**	**33.9**	**18.2**	**11.0**
V_{LC}	0.0	0.0	**7.7**	4.6
V_{BRC}	0.0	0.1	0.1	0.5
V_{SC}	0.7	0.3	1.4	0.9
V_{ABC}	0.4	0.4	0.6	0.5
V_{VBC}	1.1	0.5	1.5	0.9
Q_{LC}	**44.4**	**19.8**	**15.9**	**9.6**
Q_{BRC}	0.0	0.1	0.0	0.2
Q_{SC}	0.0	0.0	0.4	0.2
GSH_L	0.0	0.0	1.1	1.3
GSH_{BR}	0.0	0.2	0.1	0.7
GSH_S	0.9	0.4	1.8	1.1
V_{maxC}	1.1	0.5	0.7	0.4
K_m	0.4	0.2	0.3	0.2
k_{FC2}	0.0	0.0	**39.2**	**29.8**
k_{EHC}	0.0	0.0	3.4	2.1
k_{BC}	2.9	1.8	1.0	0.6
k_{BC2}	0.0	0.0	0.7	0.5
P_{BR}	0.0	**30.0**	0.0	0.0
P_{BR2}	0.0	0.0	0.0	**29.9**

[a]Values are $100 \times S_{mk}^2 \times CV_k / \Sigma(S_{mi}^2 \times CV_i)$. Values >5 (i.e., 5% contribution) are in bold.

Table D-8. Parameter contributions to overall CVs for oral exposure

Parameter	Dose metrics[a] (concentrations)			
	AN in blood	**AN in brain**	**CEO in blood**	**CEO in brain**
BW	1.1	0.8	1.7	0.8
Q_{CC}	2.2	2.5	2.1	2.3
V_{LC}	0.1	0.1	**12.1**	6.0
V_{BRC}	0.0	0.1	0.1	0.5
V_{SC}	0.2	0.2	1.0	0.5
V_{VBC}	0.7	0.5	0.9	0.5
Q_{LC}	4.1	3.4	**7.1**	3.5
GSH_L	0.0	0.0	1.8	1.7
GSH_{BR}	0.0	0.1	0.1	0.8
GSH_S	0.3	0.2	1.3	0.6
V_{maxC}	**66.1**	**54.1**	1.2	0.6
K_m	**23.1**	**18.9**	0.4	0.2
k_{FC2}	0.0	0.0	**61.9**	**38.6**
k_{EHC}	0.0	0.0	**5.4**	2.7
k_{BC}	1.4	1.5	0.0	0.0
k_{BC2}	0.0	0.0	1.0	0.7
P_{BR}	0.0	**16.9**	0.0	0.0
P_{BR2}	0.0	0.0	0.0	**38.7**

[a]Values are $100 \times S_{mk}^2 \times CV_k / \Sigma(S_{mi}^2 \times CV_i)$. Values >5 (i.e., 5% contribution) are in bold.

Since the PCs are expected to be similar in rats and humans, and the extrapolation really depends on the rat:human ratio of those, the true resulting uncertainty is likely to be very small. The nominal uncertainty in cardiac ventilation and blood flows is expected to be a composite of uncertainty and inter-individual variability. And the only metabolic parameter to contribute significantly to the uncertainty for inhalation exposure is the CEO-GSH conjugation rate. Thus, a significant improvement in the overall uncertainty can be gained by further investigation of only a small number of parameters, half of which are applicable to every PBPK model that might be considered for gases.

The distribution of parameter influence for the oral simulation scenario, as shown in Table D-8, is similar to that for inhalation in that most of the influence is distributed among a few parameters, with the brain:blood PCs strongly influencing brain concentrations. Also similar is that the CEO-GSH conjugation rate (k_{FC2}) is a significant factor for the CEO metrics. Unlike the inhalation case, alveolar ventilation (Q_{PC}) has negligible influence, which is to be expected, but also cardiac output (Q_{CC}) has only small influence. This later case occurs because of the strong first-pass effect for AN as it is absorbed through the liver, which also explains the very high influence of the oxidation parameters, V_{maxC} and K_m, on the AN metrics.

These results for oral exposure are quite similar to the results obtained by Sweeney et al. (2003), except that their results indicate somewhat higher influence by blood flow to the liver (i.e., 8–12% on AN metrics), liver GSH (6%), and a much higher influence of CEO hydrolysis (k_{EHC} here, parameterized by a V_{max} and K_m with influence of 12–30%) on CEO metrics. The shift of influence from hydrolysis to GSH conjugation for CEO metrics between Sweeney et al. (2003) and the EPA's results arises from the shift in the relative rates through those two pathways, but in both, the rate of CEO removal is a strong determinant of the CEO metric.